



Lake Superior North and Lake Superior South Basins

Watershed Model Development - Draft Report

Appendices A, B, and C

Prepared for
Minnesota Pollution Control Agency

Prepared by



One Park Drive, Suite 200 • PO Box 14409
Research Triangle Park, NC 27709

May 27, 2016

(This page left intentionally blank.)

Appendix A. Detailed Snow Calibration Results

WEATHER REGION 1

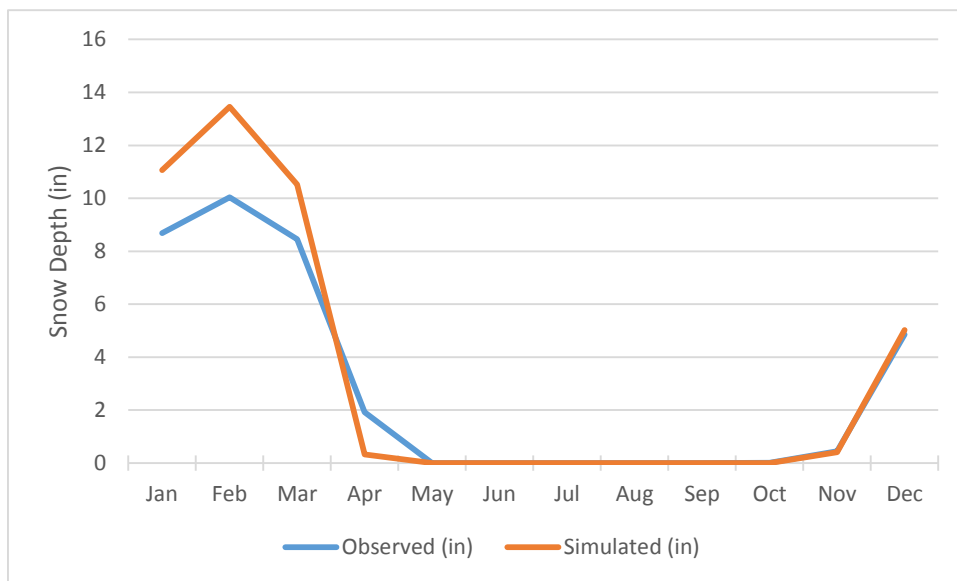


Figure 1. Mean monthly snow depth for weather region 1

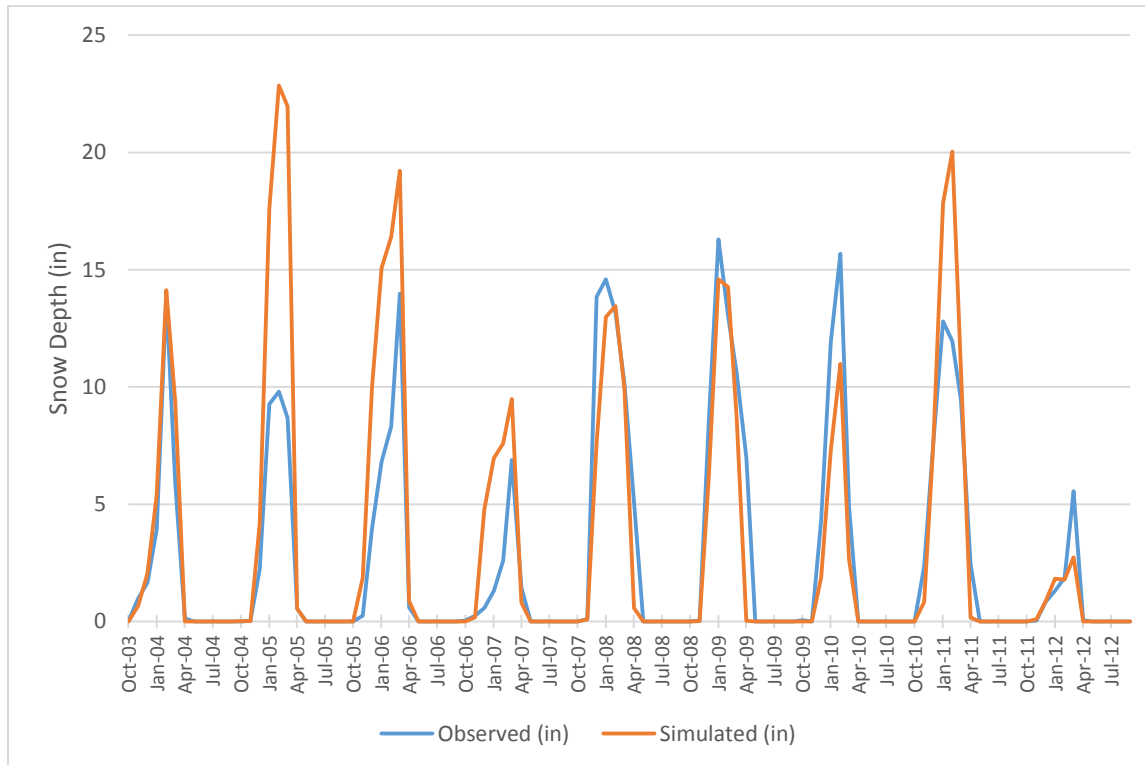


Figure 2. Mean monthly snow depth time-series for weather region 1

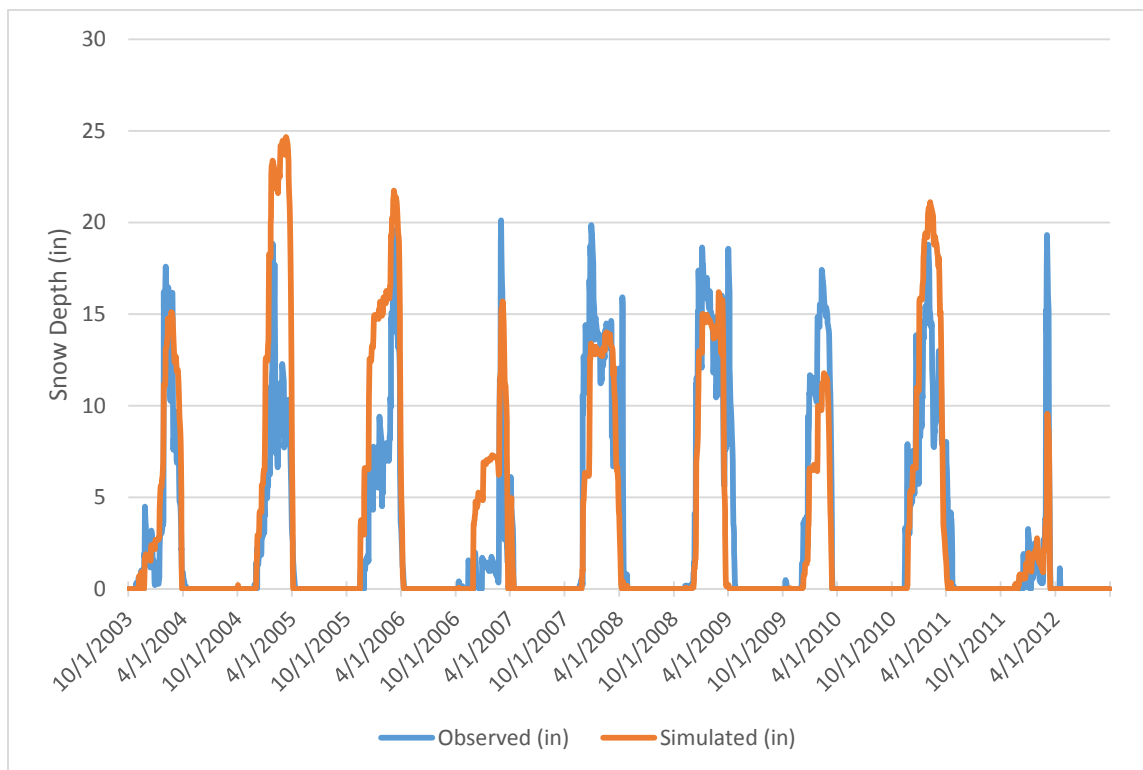


Figure 3. Mean daily snow depth time-series for weather region 1

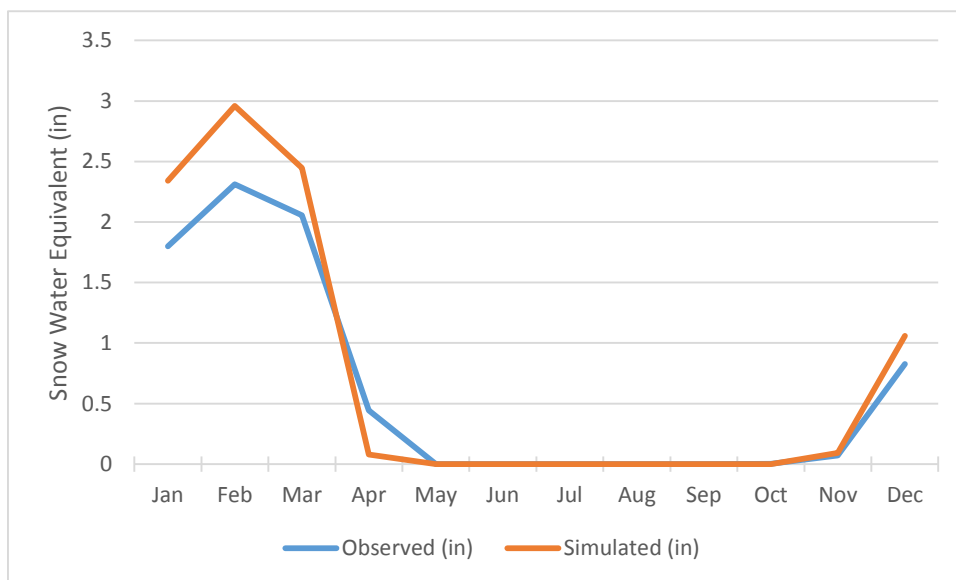


Figure 4. Mean monthly snow water equivalent for weather region 1

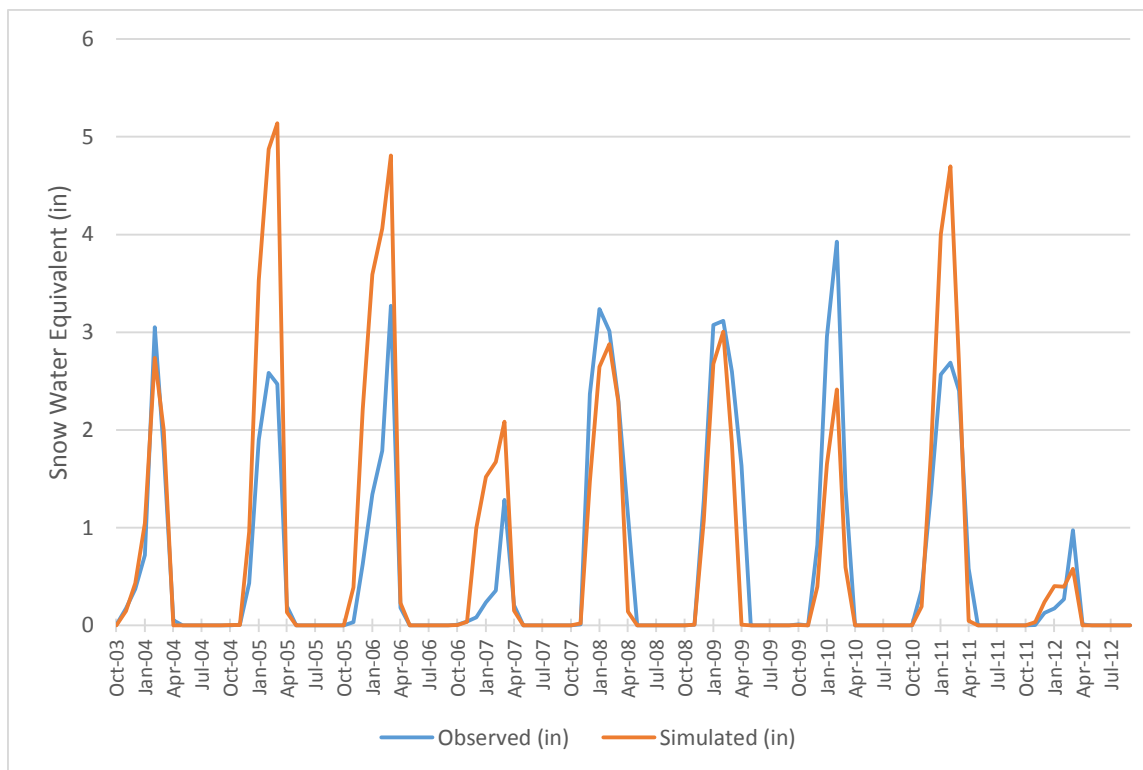


Figure 5. Mean monthly snow water equivalent time-series for weather region 1

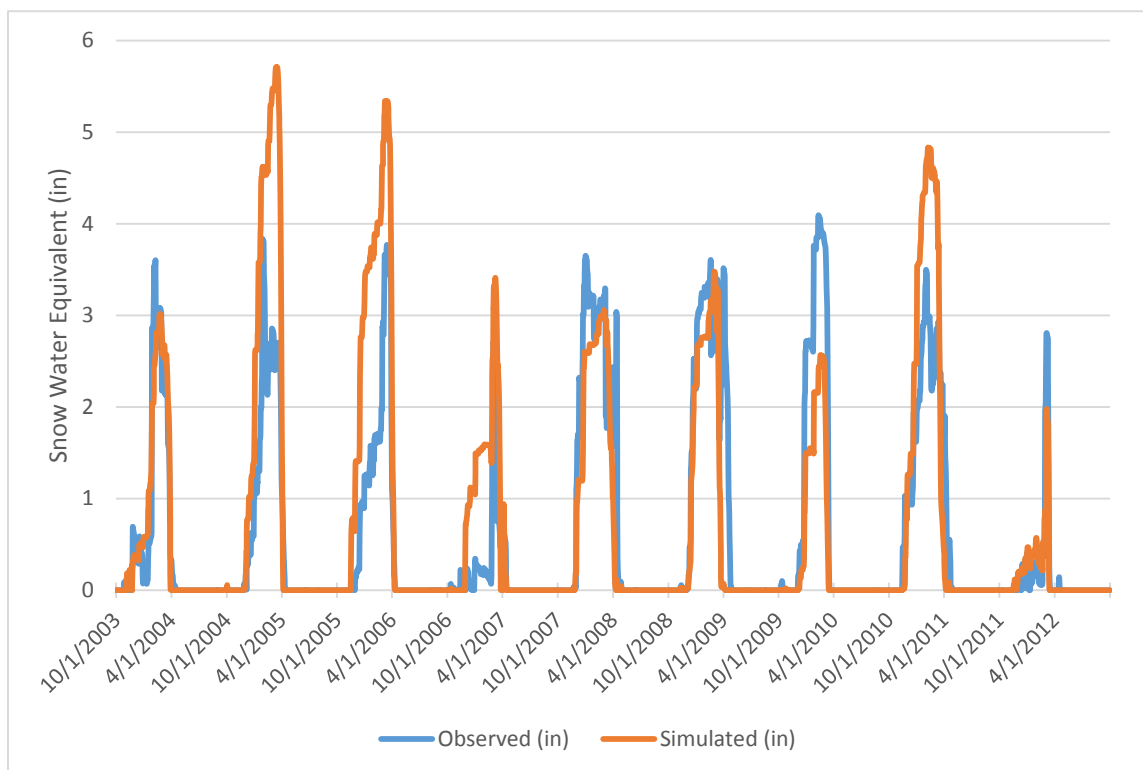


Figure 6. Mean daily snow water equivalent time-series for weather region 1

WEATHER REGION 2

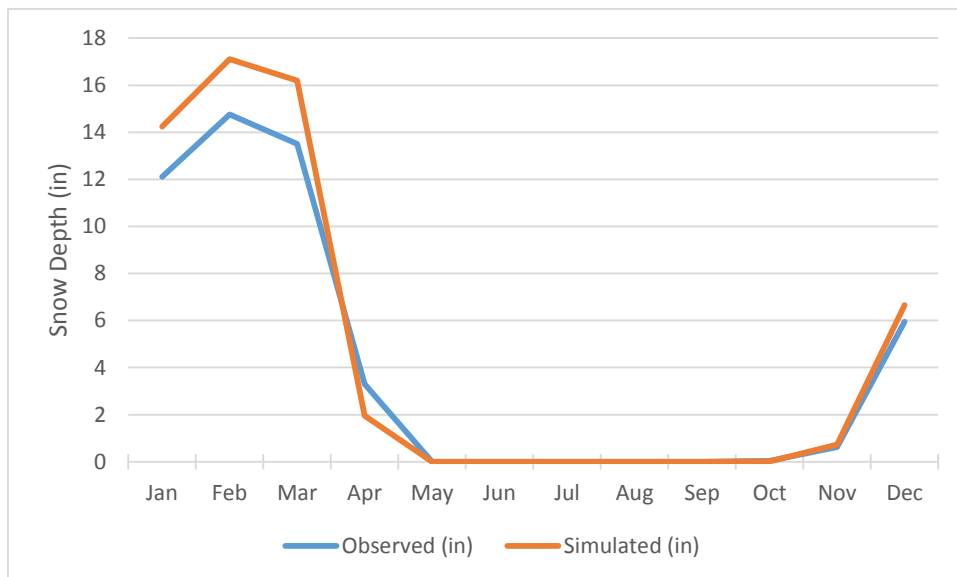


Figure 7. Mean monthly snow depth for weather region 2

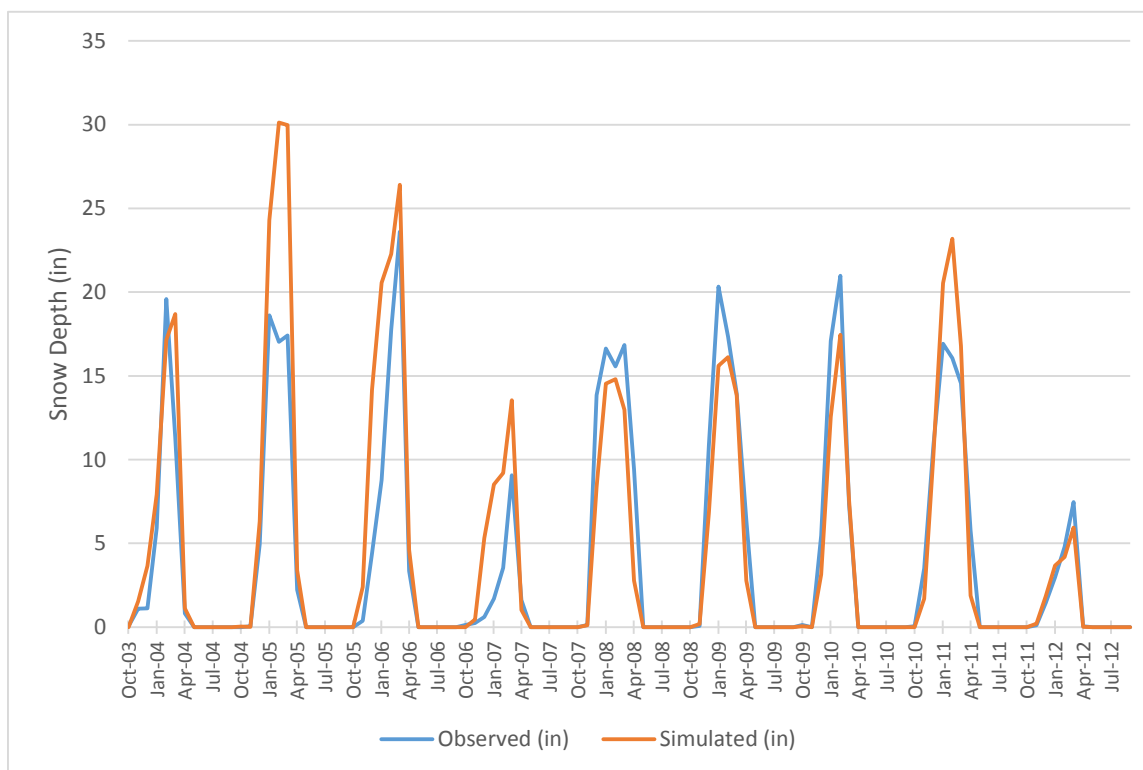


Figure 8. Mean monthly snow depth time-series for weather region 2

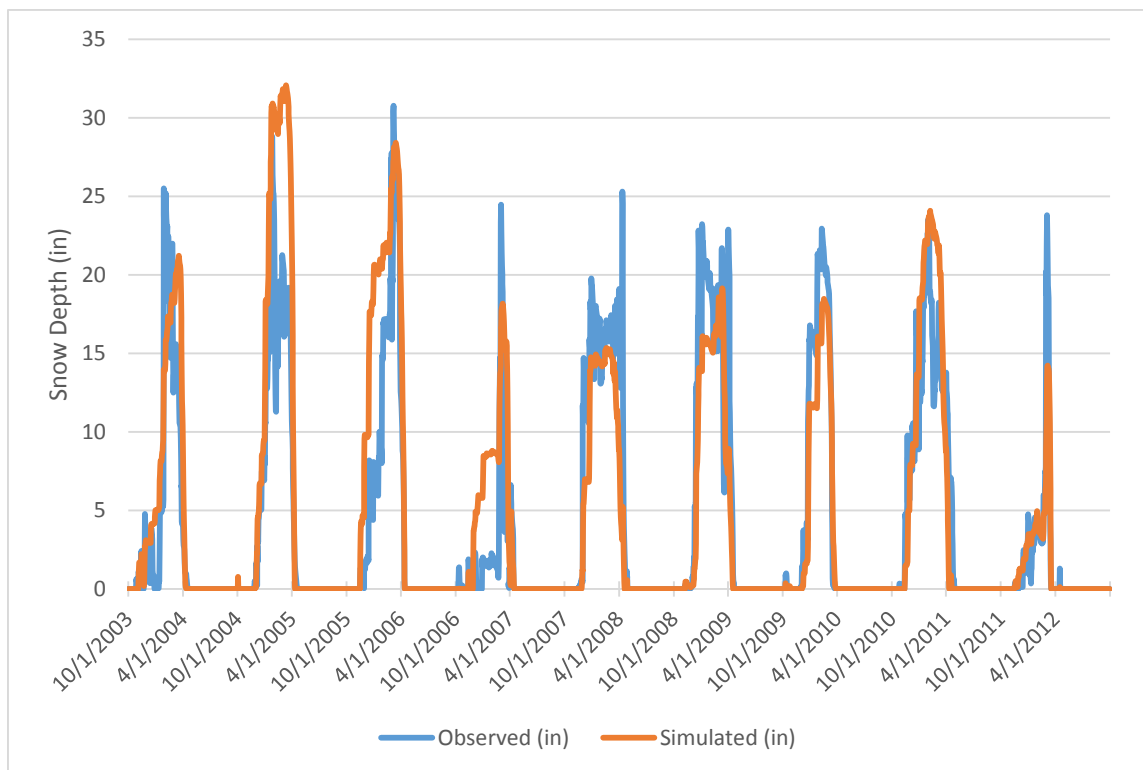


Figure 9. Mean daily snow depth time-series for weather region 2

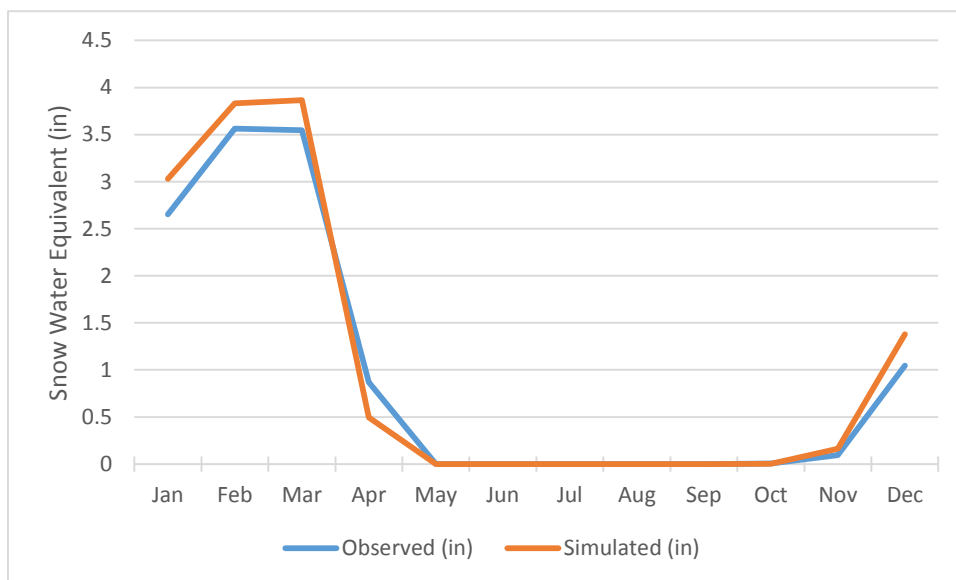


Figure 10. Mean monthly snow water equivalent for weather region 2

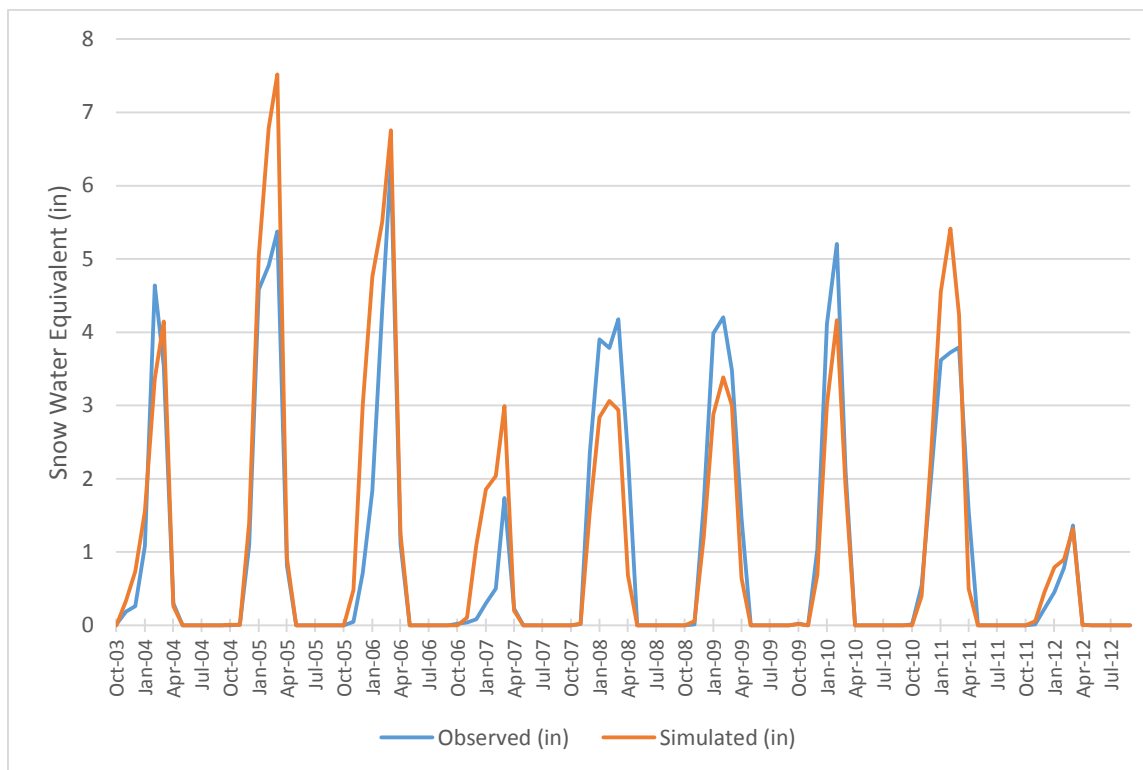


Figure 11. Mean monthly snow water equivalent time-series for weather region 2

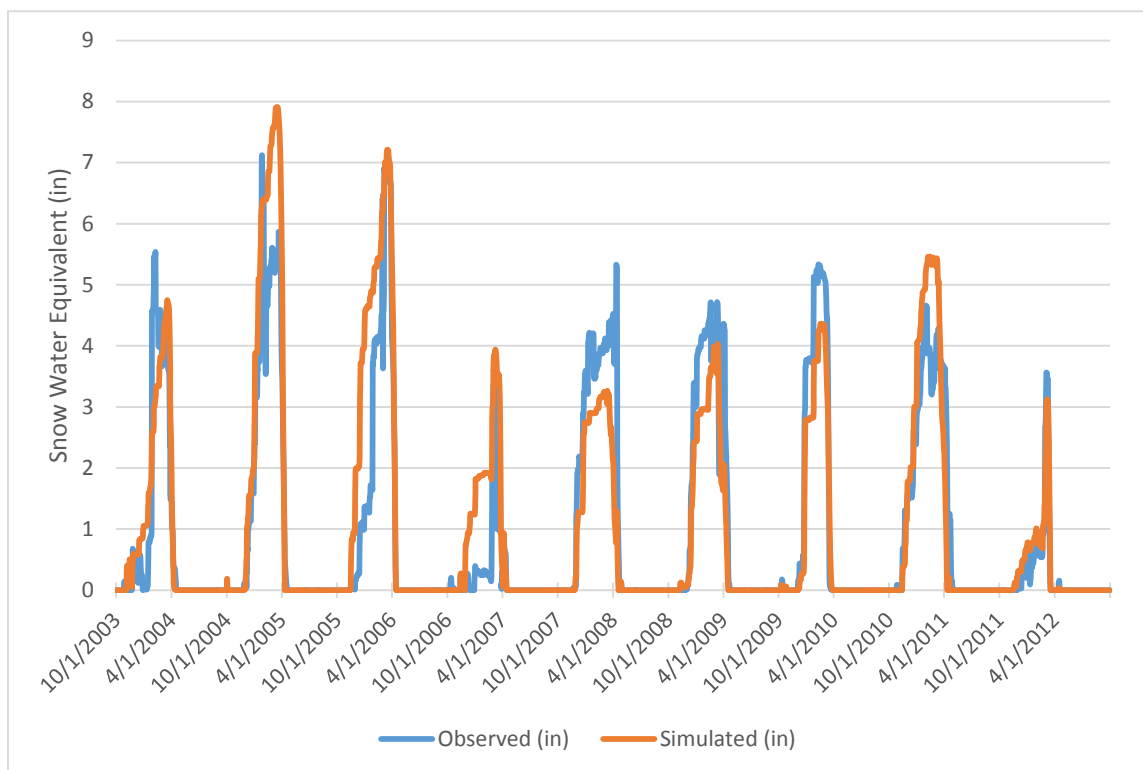


Figure 12. Mean daily snow water equivalent time-series for weather region 2

WEATHER REGION 3

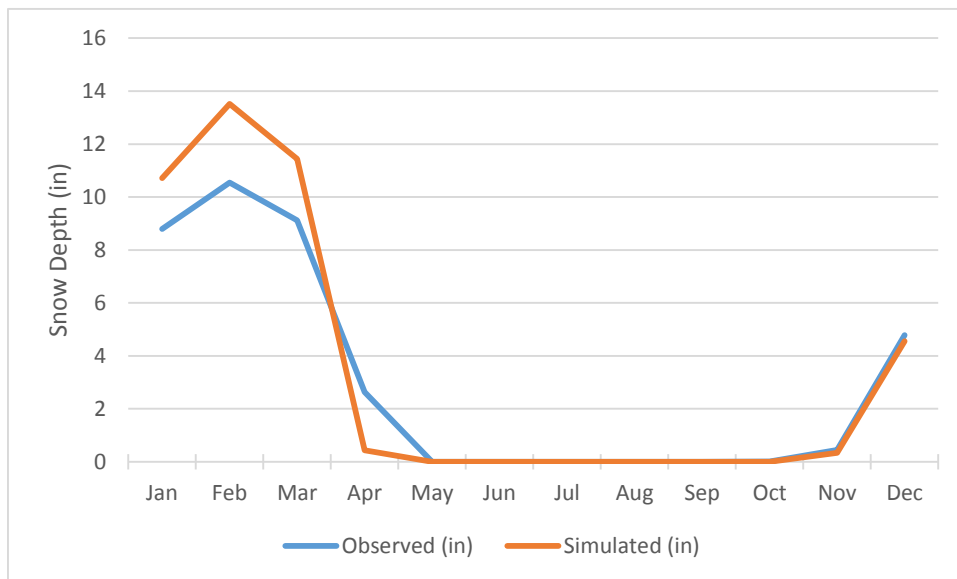


Figure 13. Mean monthly snow depth for weather region 3

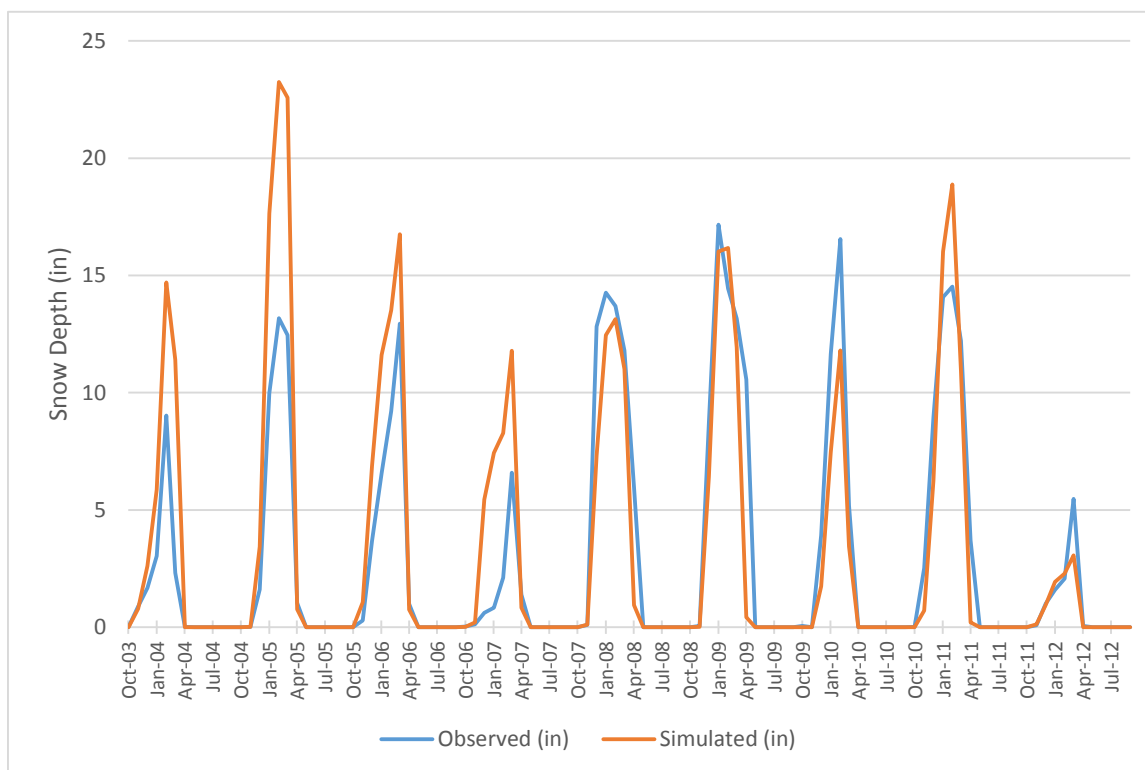


Figure 14. Mean monthly snow depth time-series for weather region 3

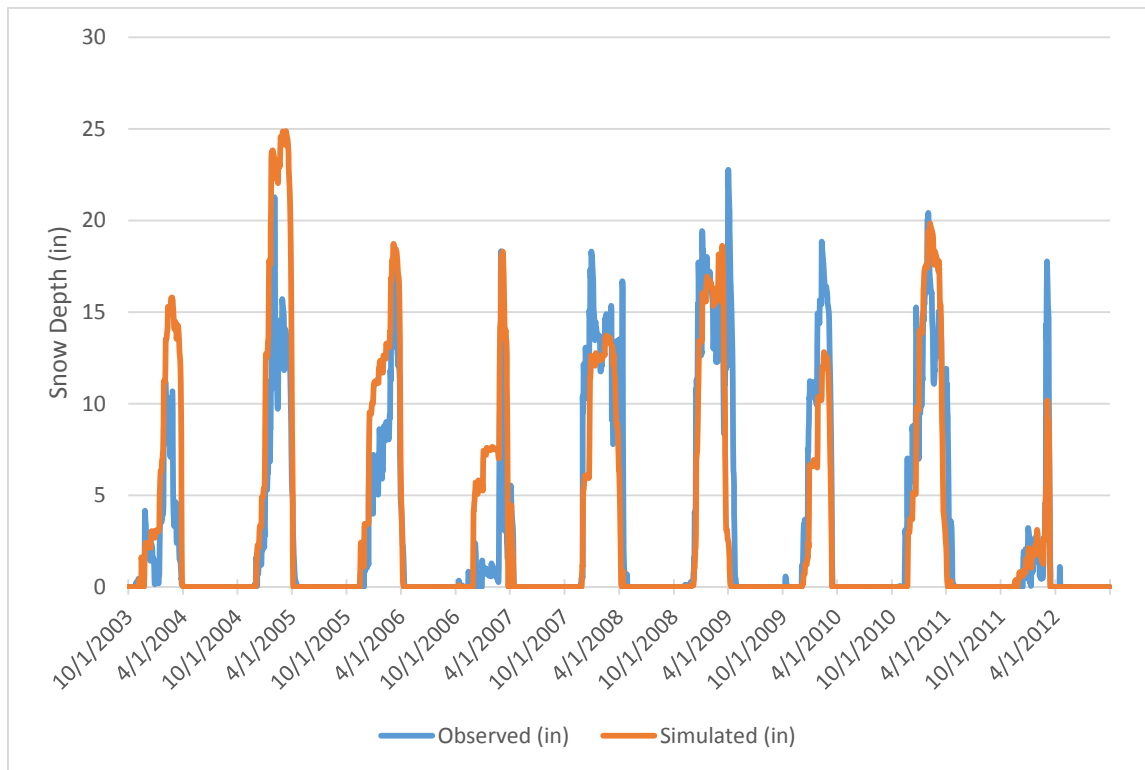


Figure 15. Mean daily snow depth time-series for weather region 3

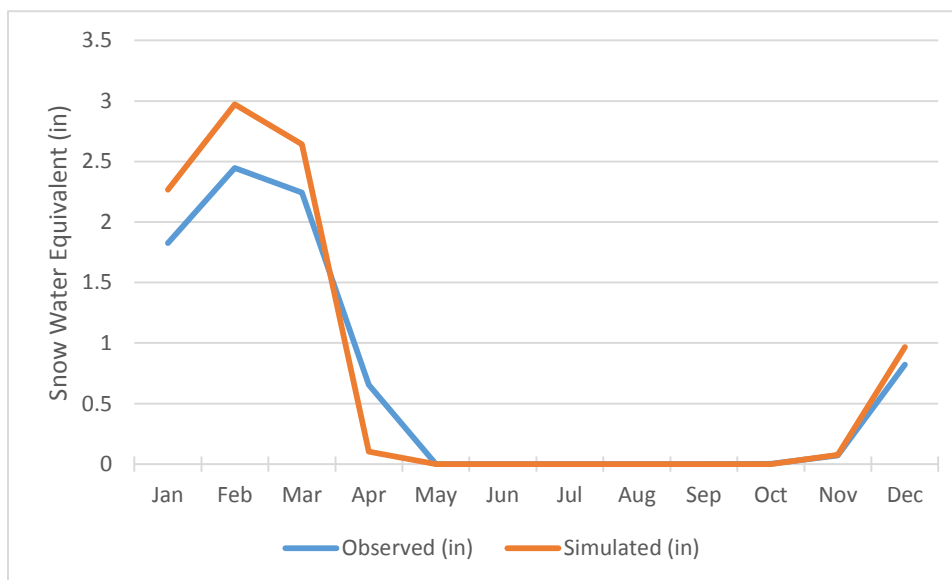


Figure 16. Mean monthly snow water equivalent for weather region 3

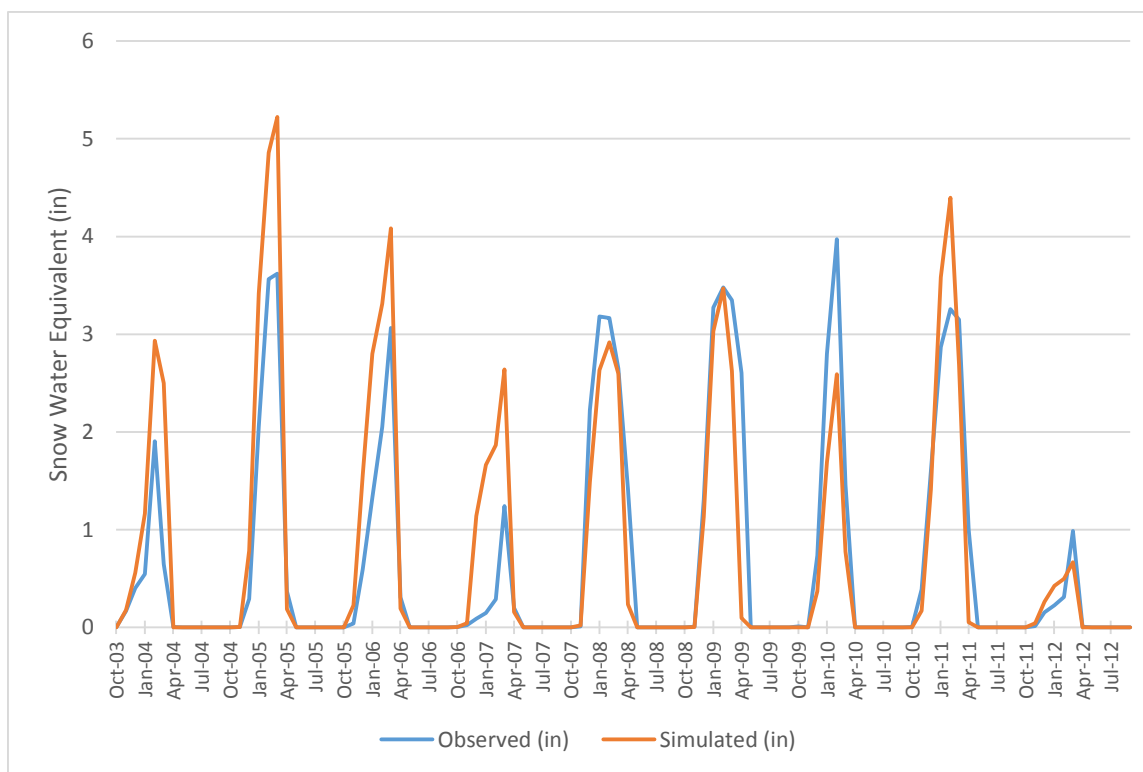


Figure 17. Mean monthly snow water equivalent time-series for weather region 3

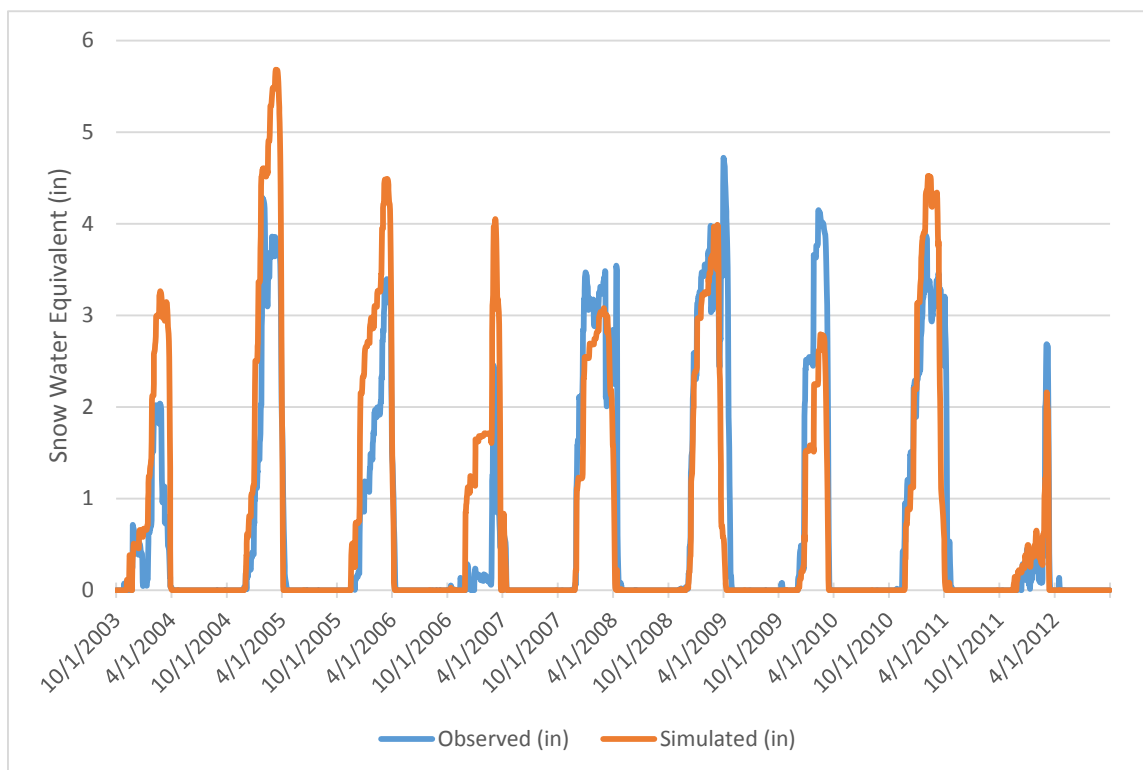


Figure 18. Mean daily snow water equivalent time-series for weather region 3

WEATHER REGION 4

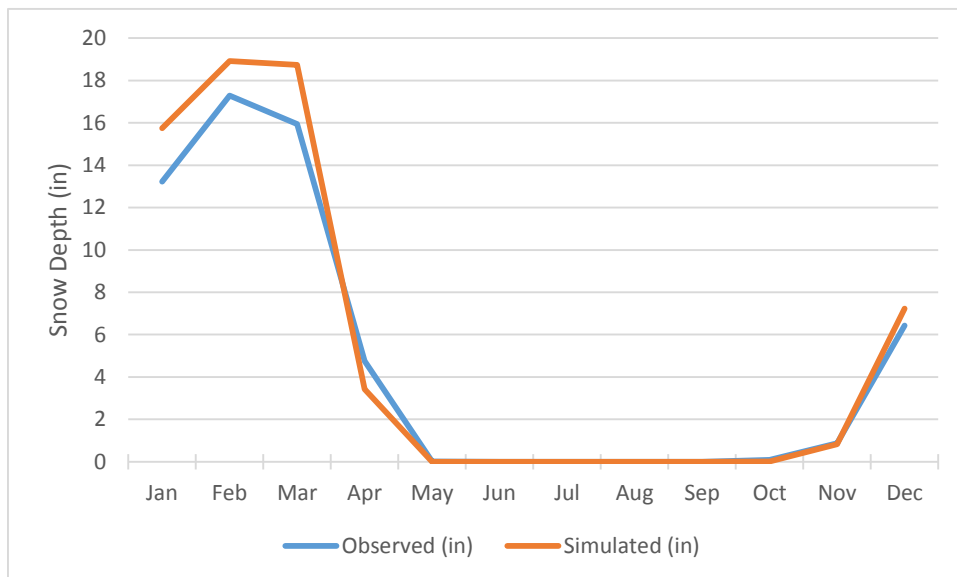


Figure 19. Mean monthly snow depth for weather region 4

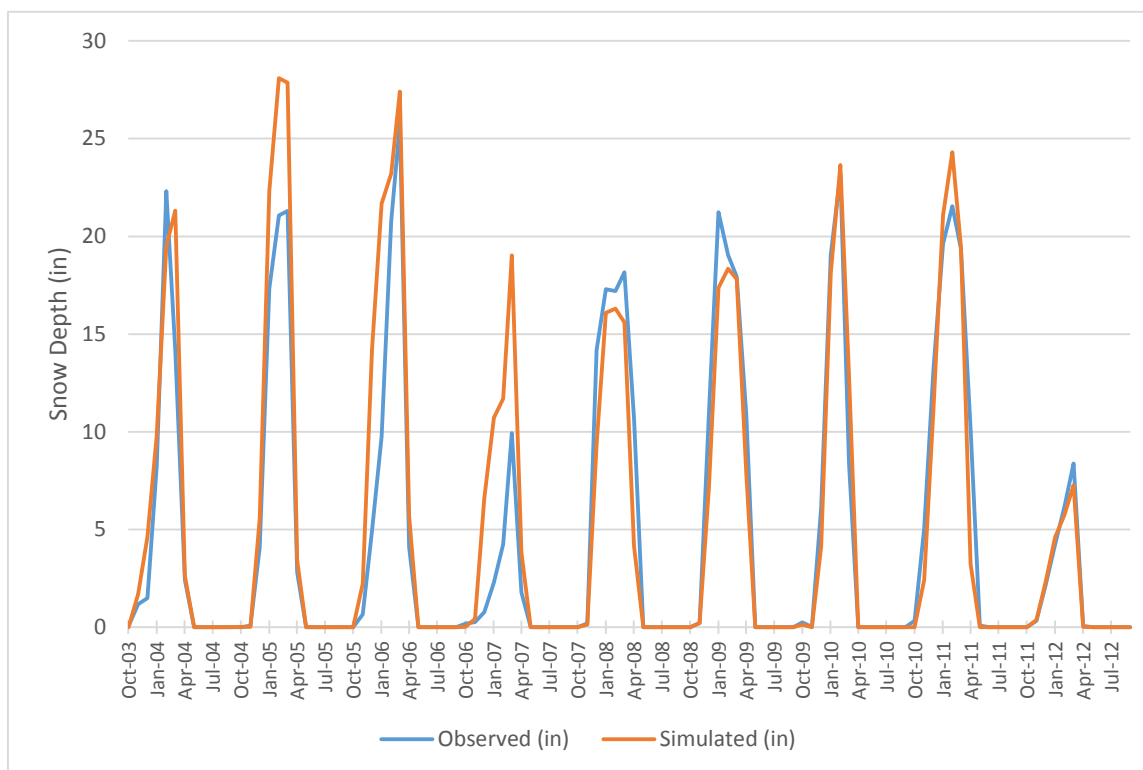


Figure 20. Mean monthly snow depth time-series for weather region 4

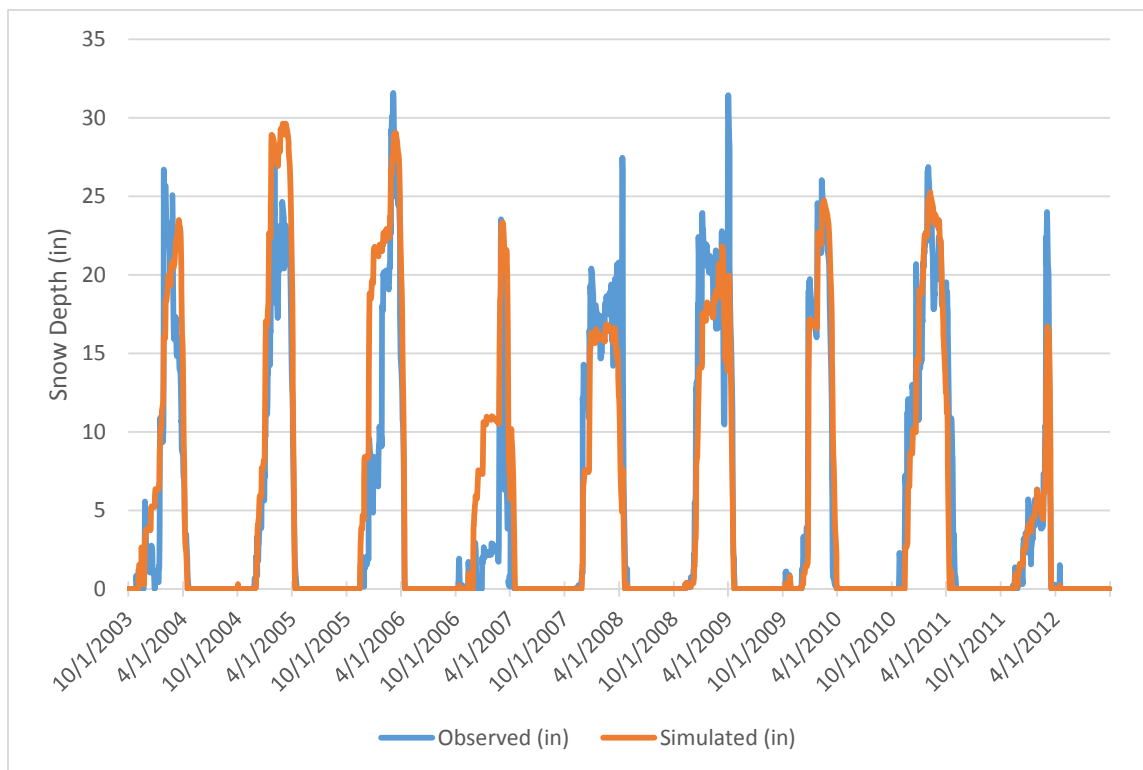


Figure 21. Mean daily snow depth time-series for weather region 4

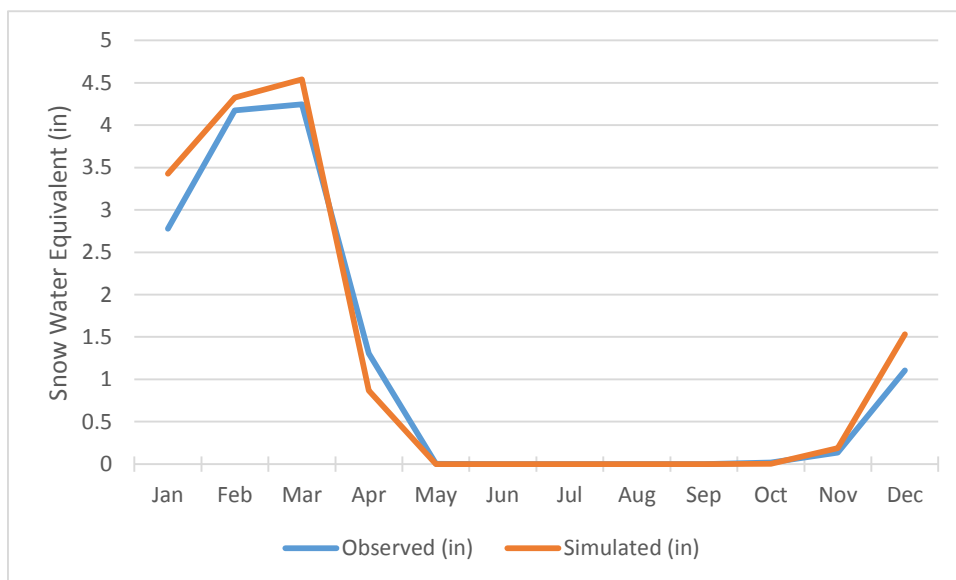


Figure 22. Mean monthly snow water equivalent for weather region 4

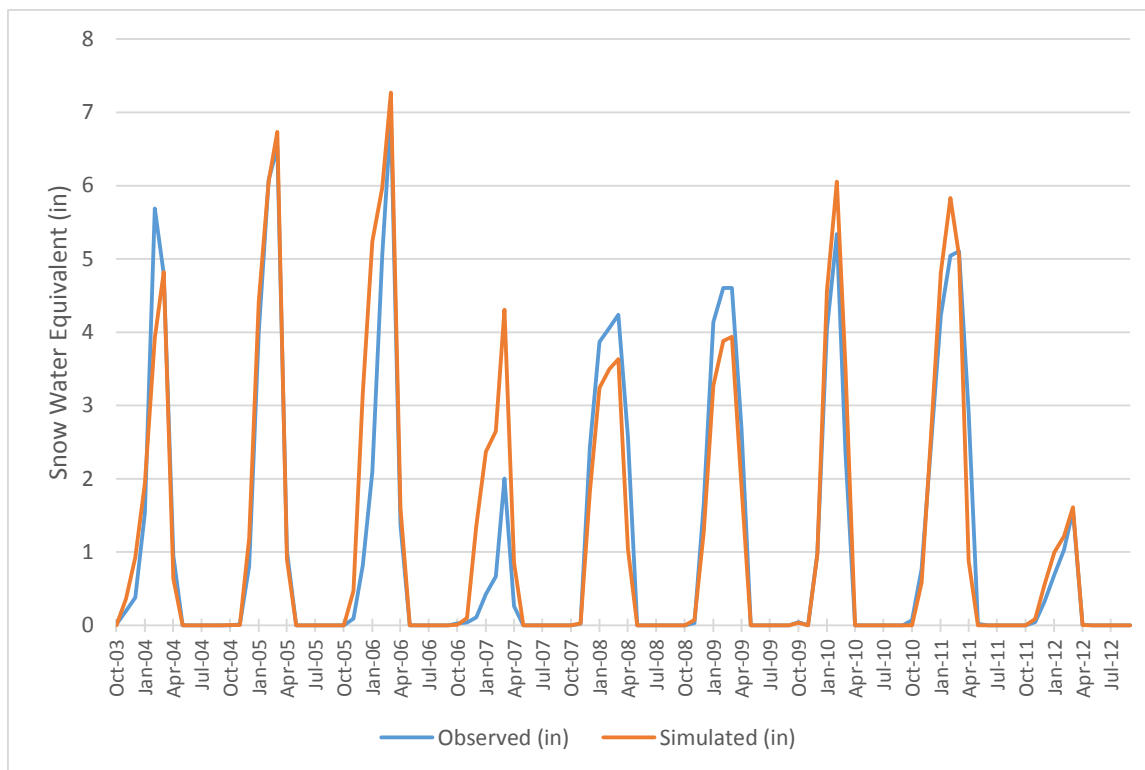


Figure 23. Mean monthly snow water equivalent time-series for weather region 4

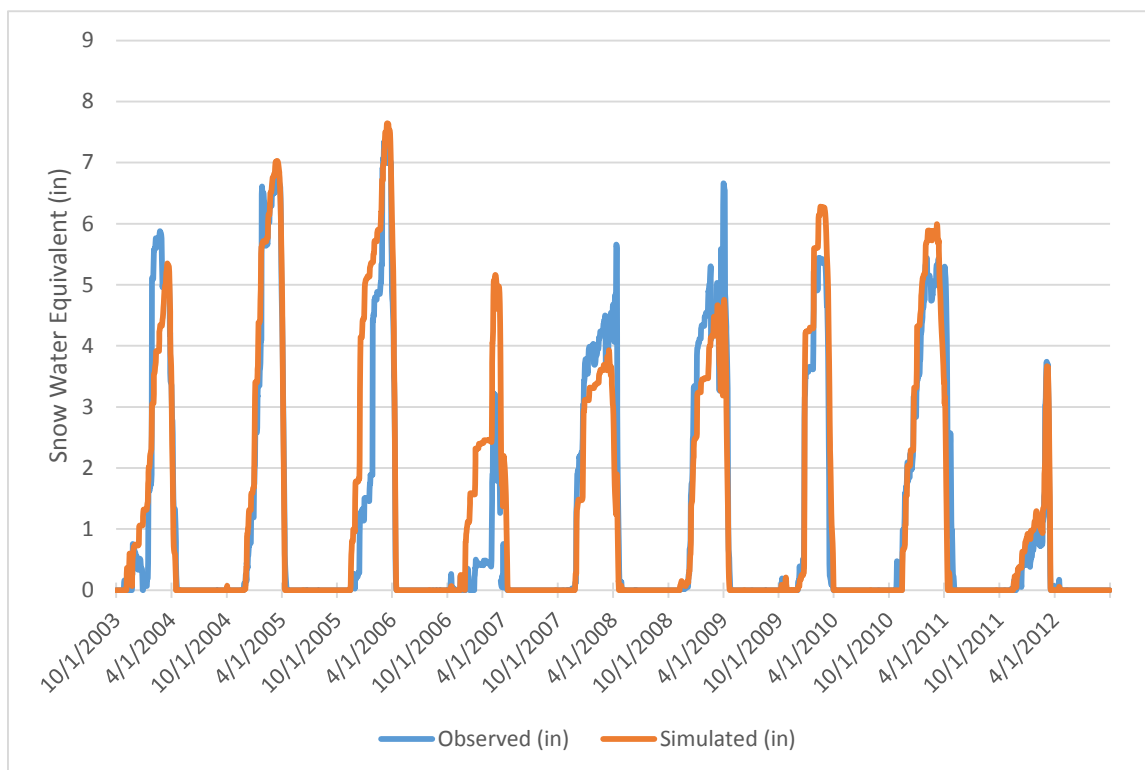


Figure 24. Mean daily snow water equivalent time-series for weather region 4

WEATHER REGION 5

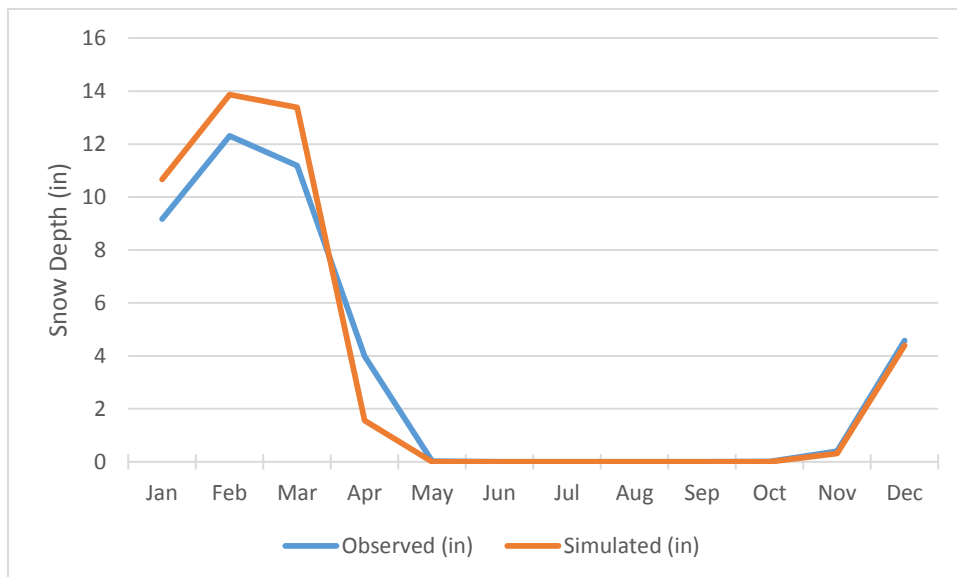


Figure 25. Mean monthly snow depth for weather region 5

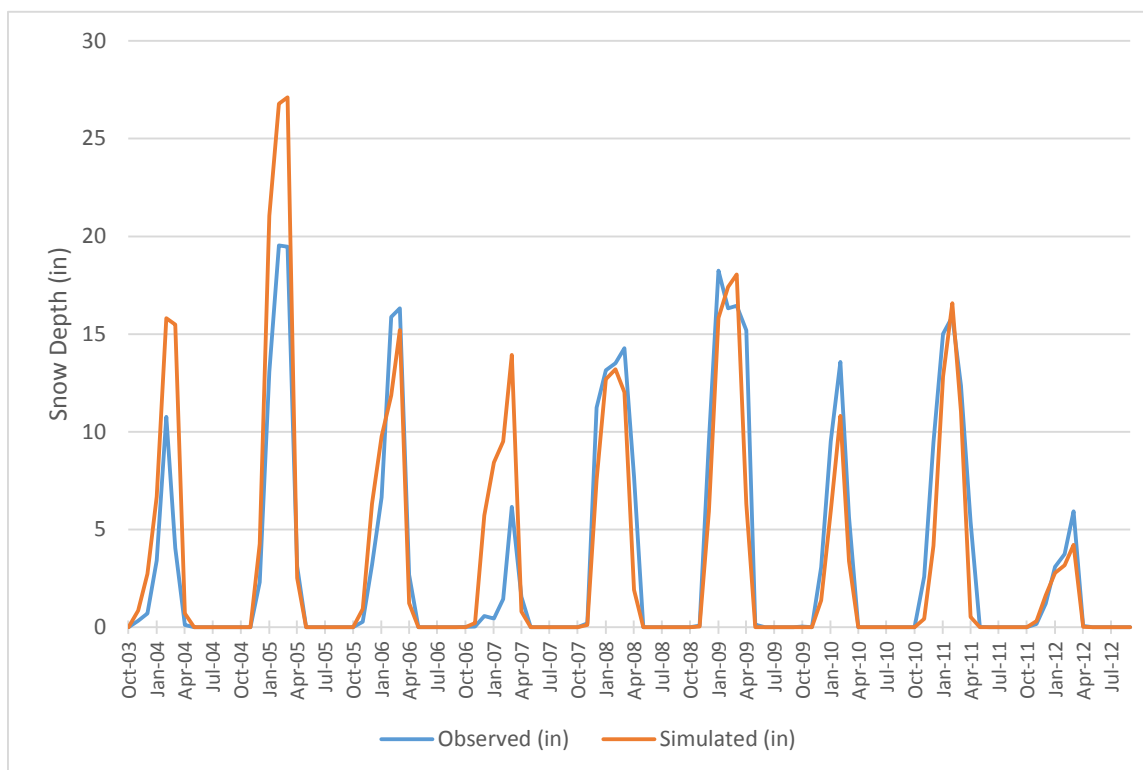


Figure 26. Mean monthly snow depth time-series for weather region 5

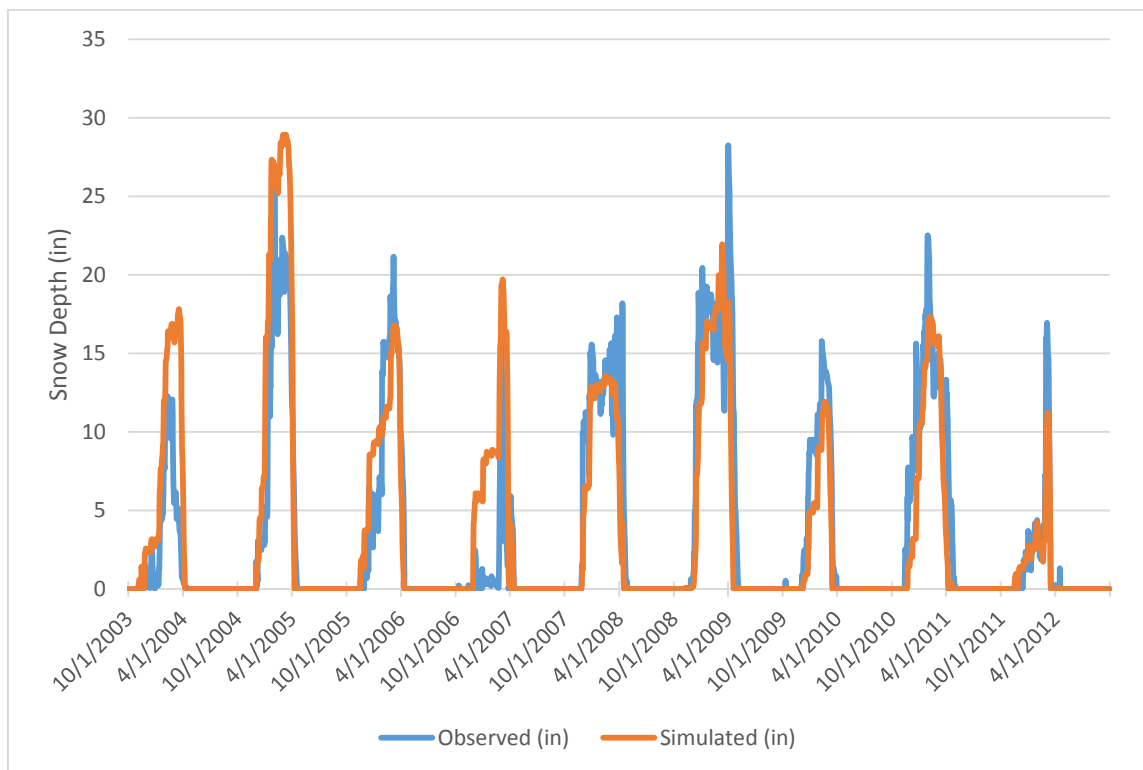


Figure 27. Mean daily snow depth time-series for weather region 5

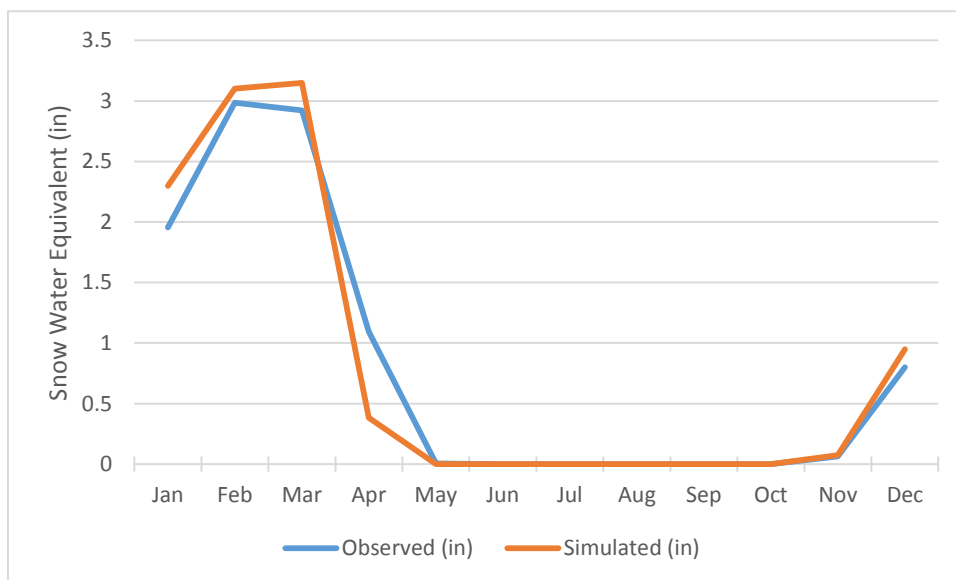


Figure 28. Mean monthly snow water equivalent for weather region 5

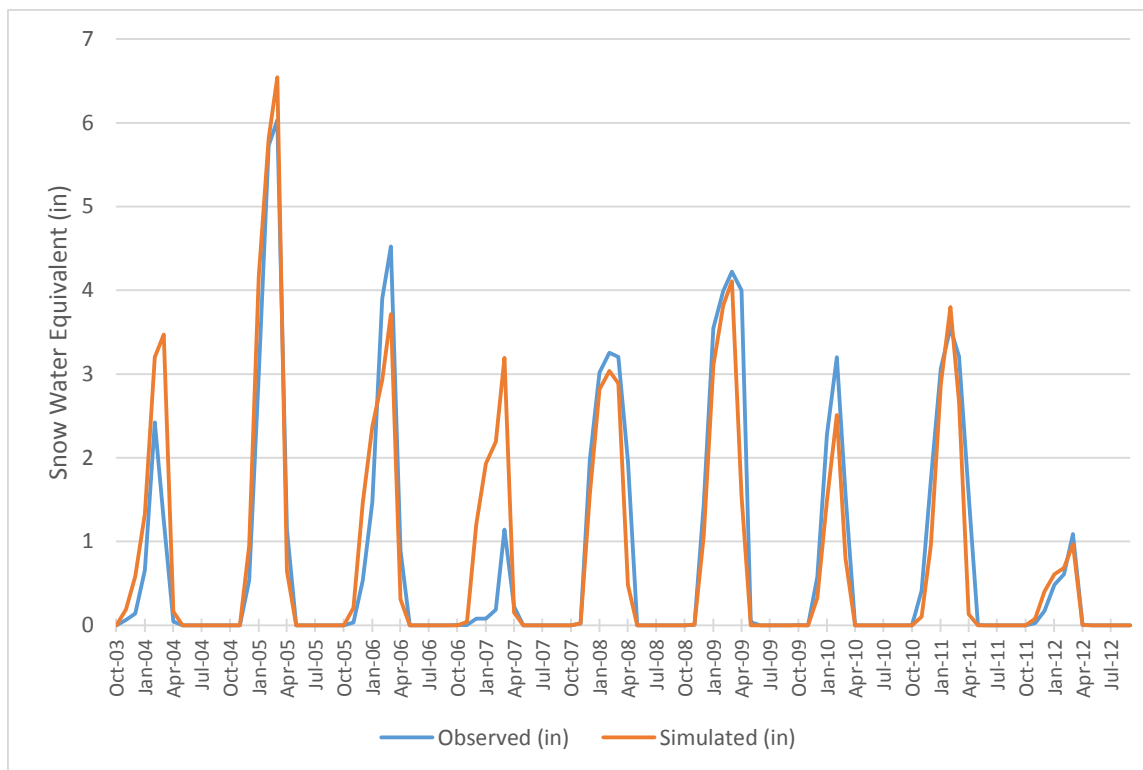


Figure 29. Mean monthly snow water equivalent time-series for weather region 5

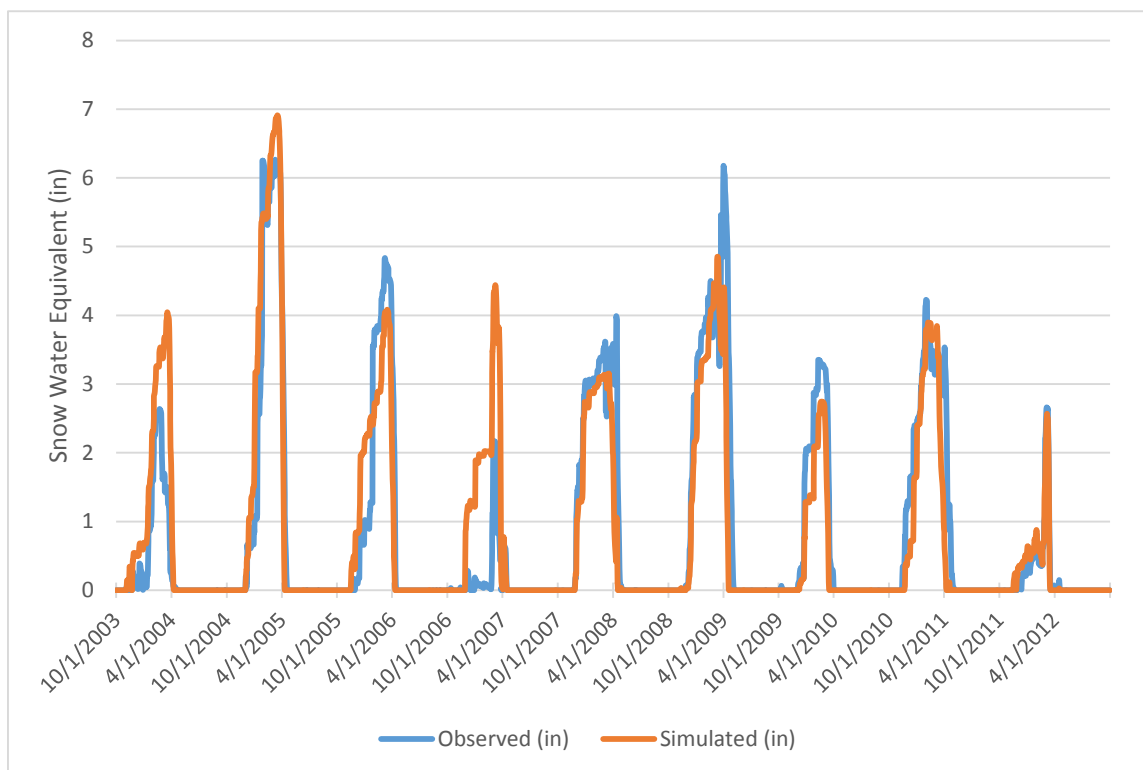


Figure 30. Mean daily snow water equivalent time-series for weather region 5

WEATHER REGION 6

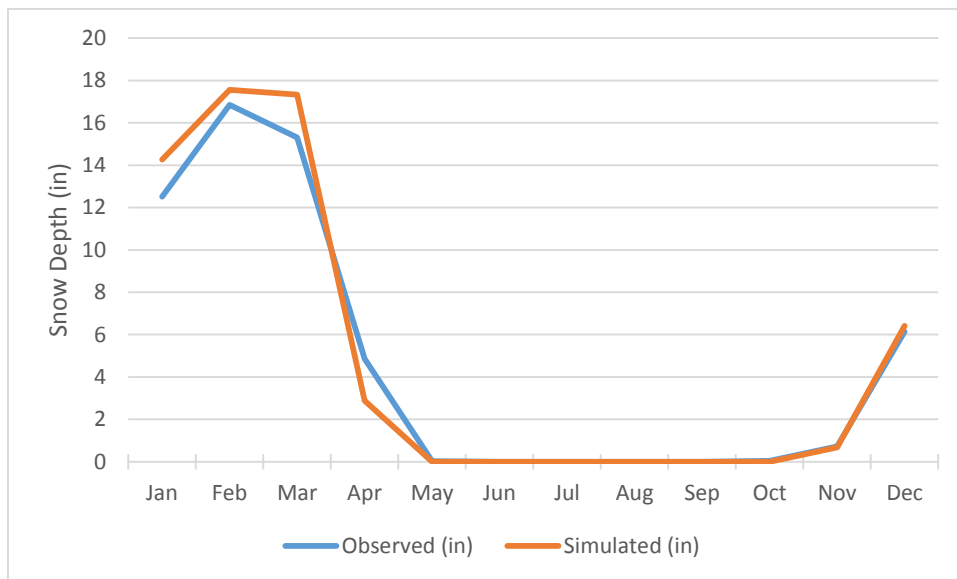


Figure 31. Mean monthly snow depth for weather region 6

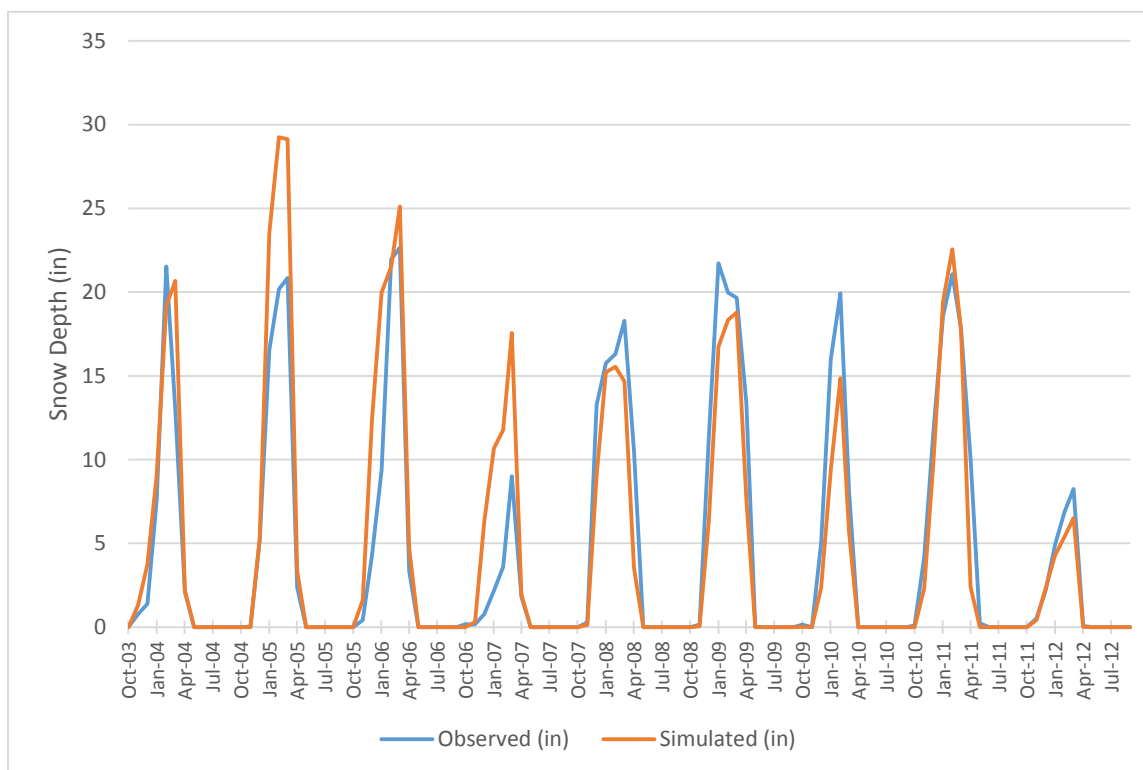


Figure 32. Mean monthly snow depth time-series for weather region 6

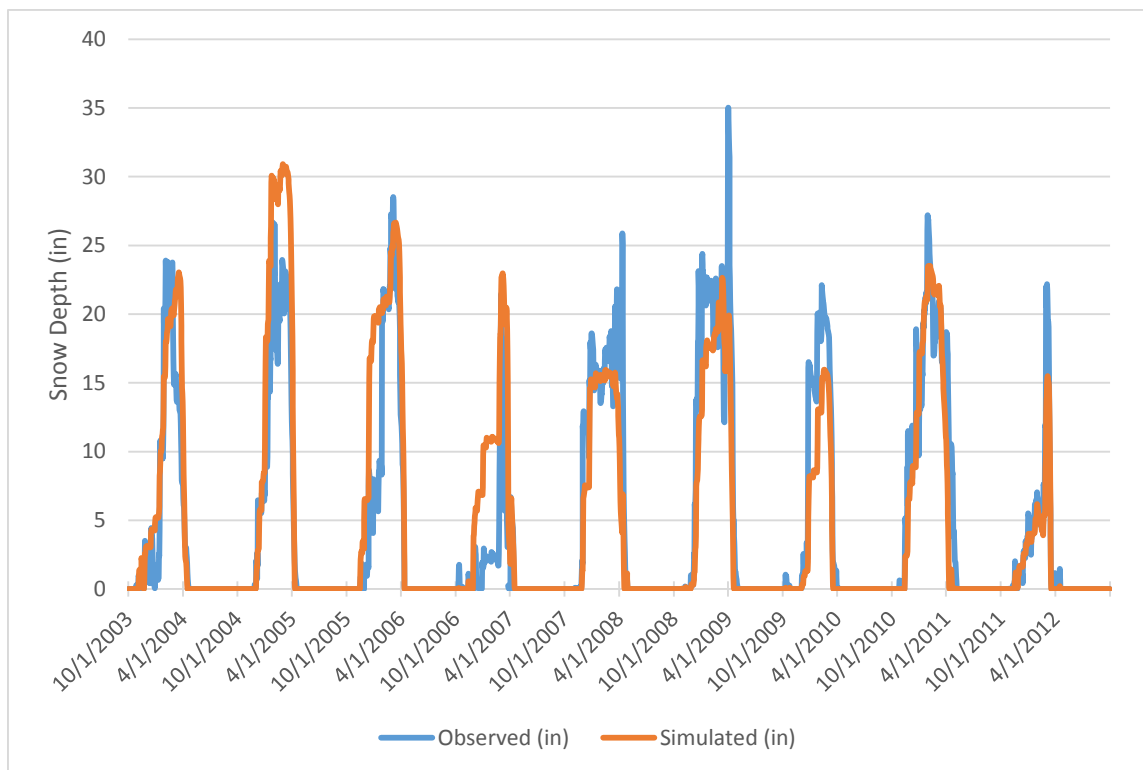


Figure 33. Mean daily snow depth time-series for weather region 6

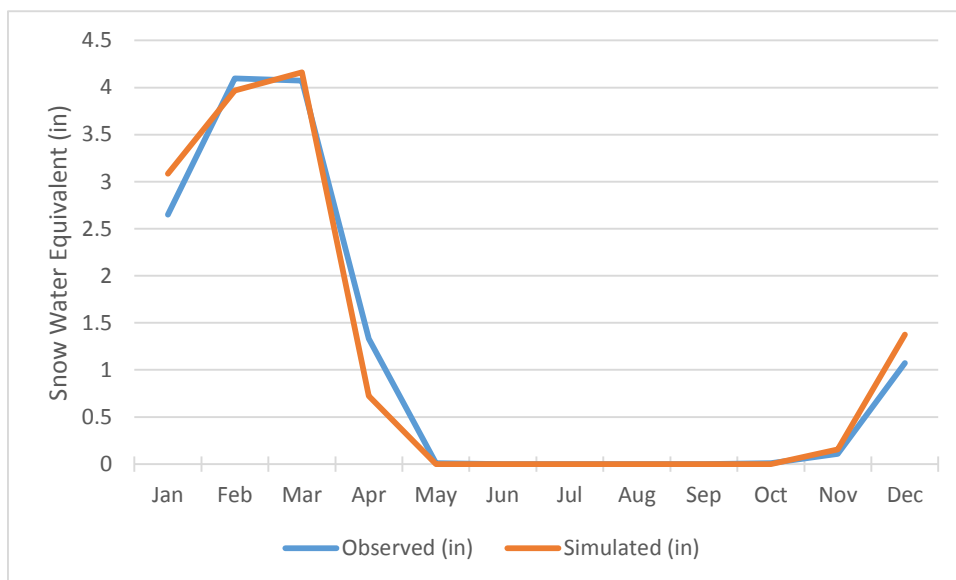


Figure 34. Mean monthly snow water equivalent for weather region 6

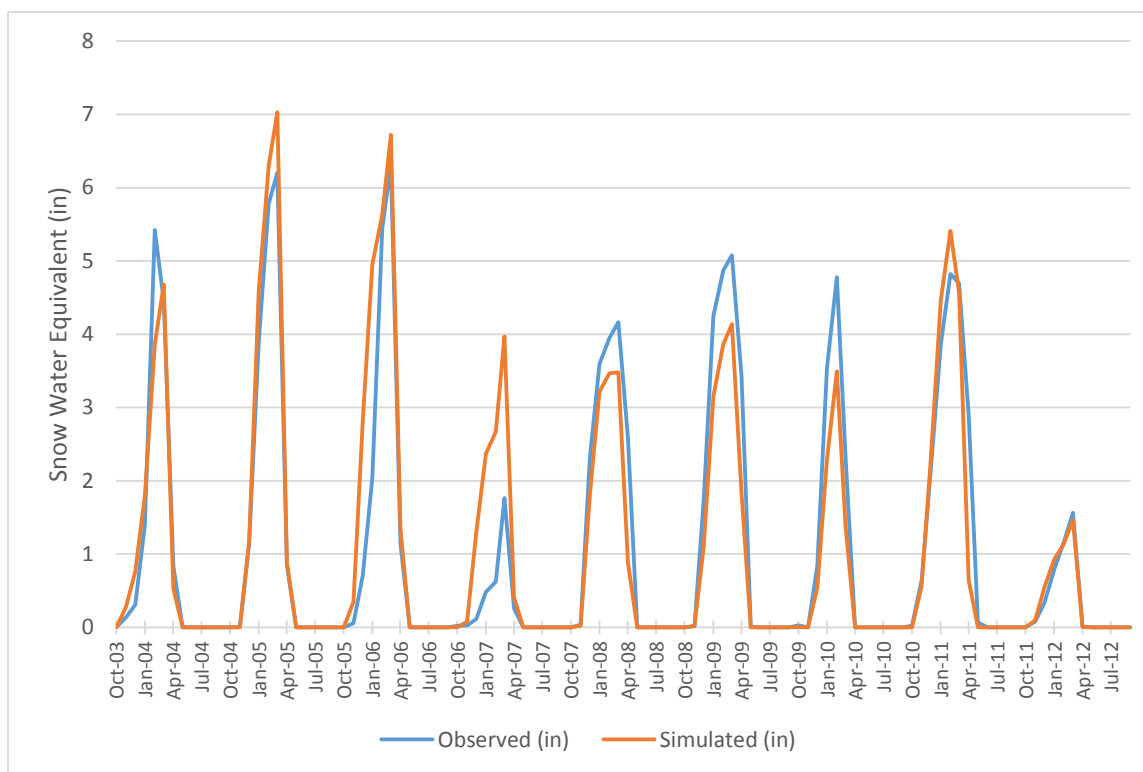


Figure 35. Mean monthly snow water equivalent time-series for weather region 6

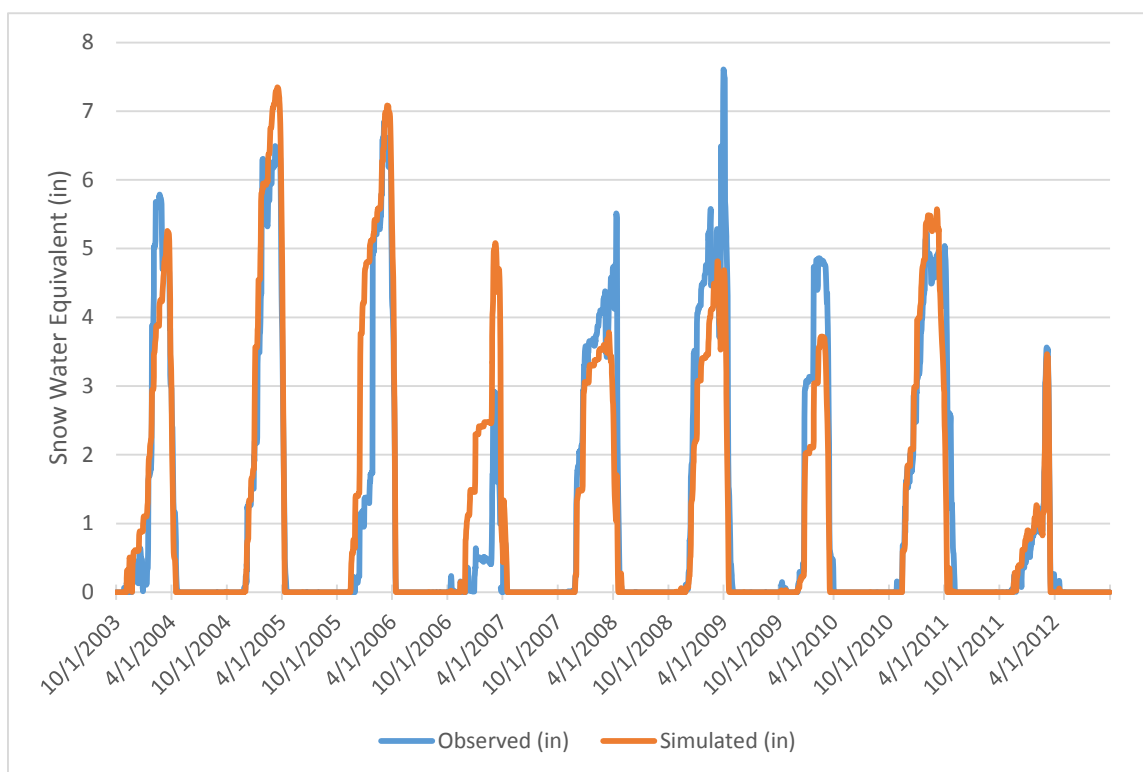


Figure 36. Mean daily snow water equivalent time-series for weather region 6

WEATHER REGION 7

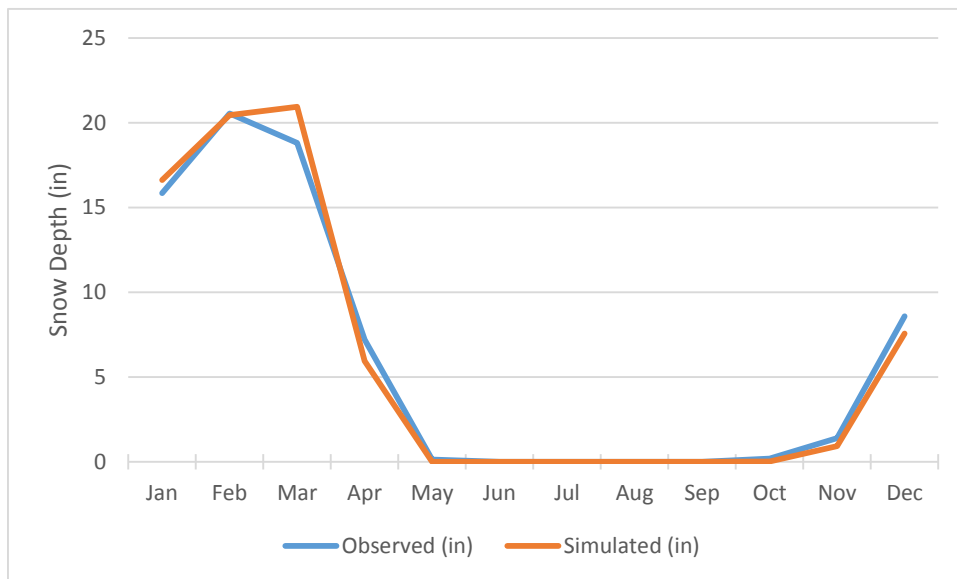


Figure 37. Mean monthly snow depth for weather region 7

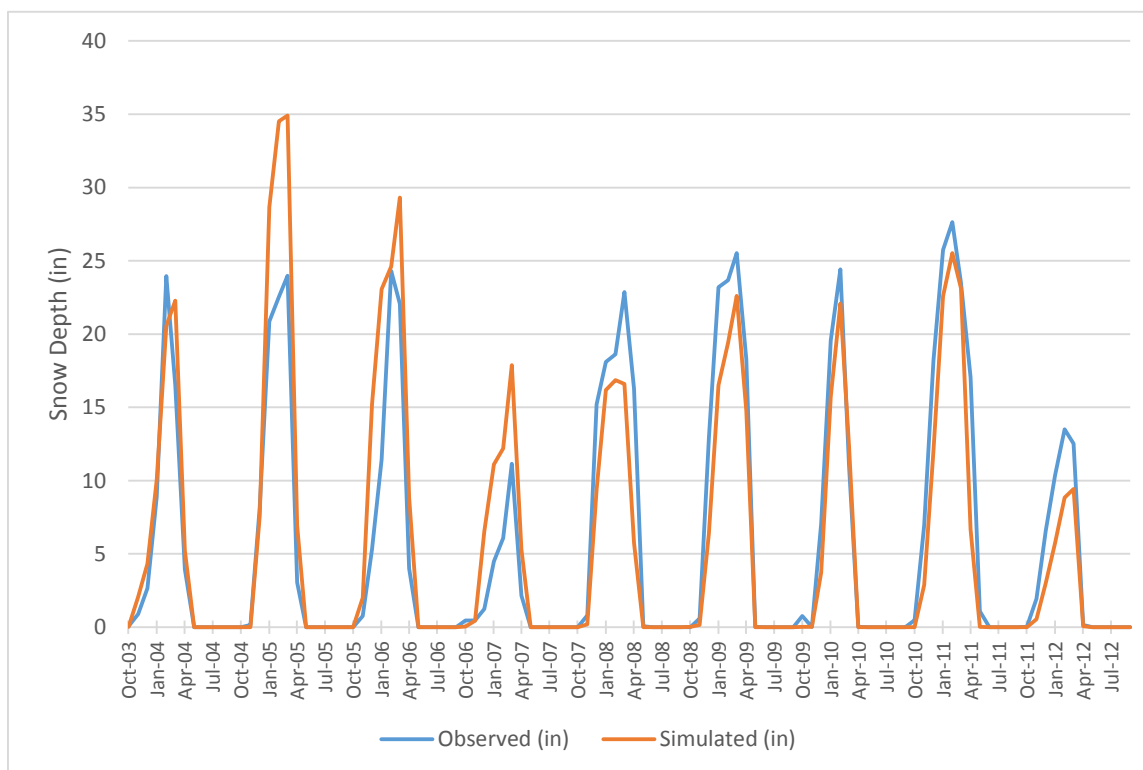


Figure 38. Mean monthly snow depth time-series for weather region 7

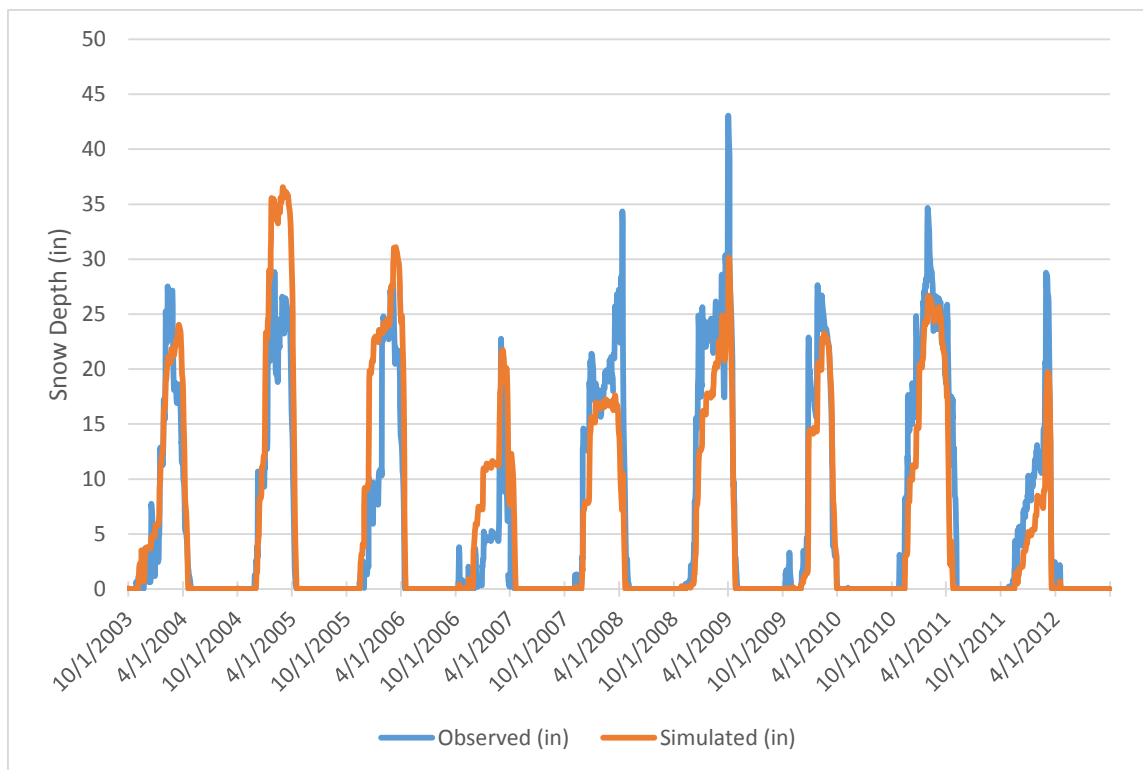


Figure 39. Mean daily snow depth time-series for weather region 7

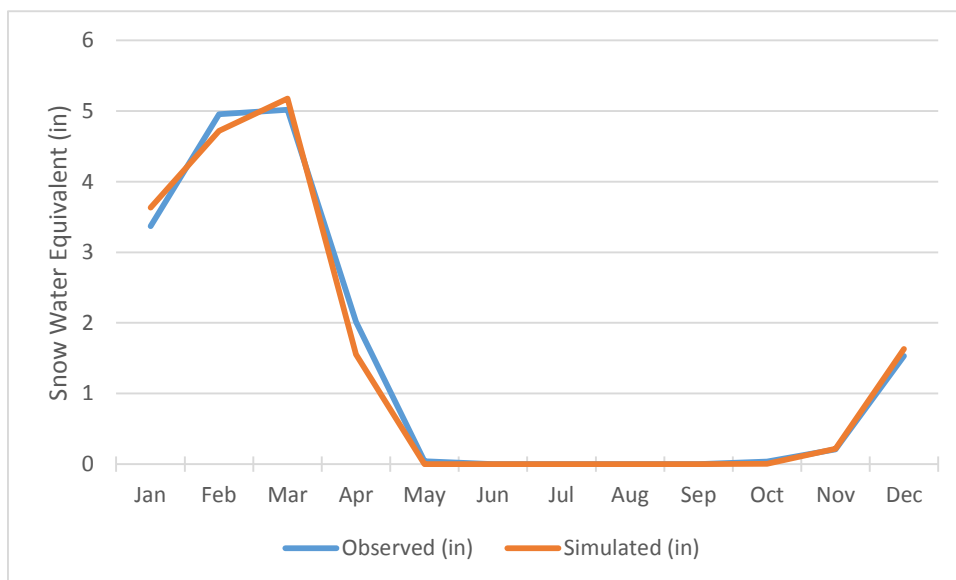


Figure 40. Mean monthly snow water equivalent for weather region 7

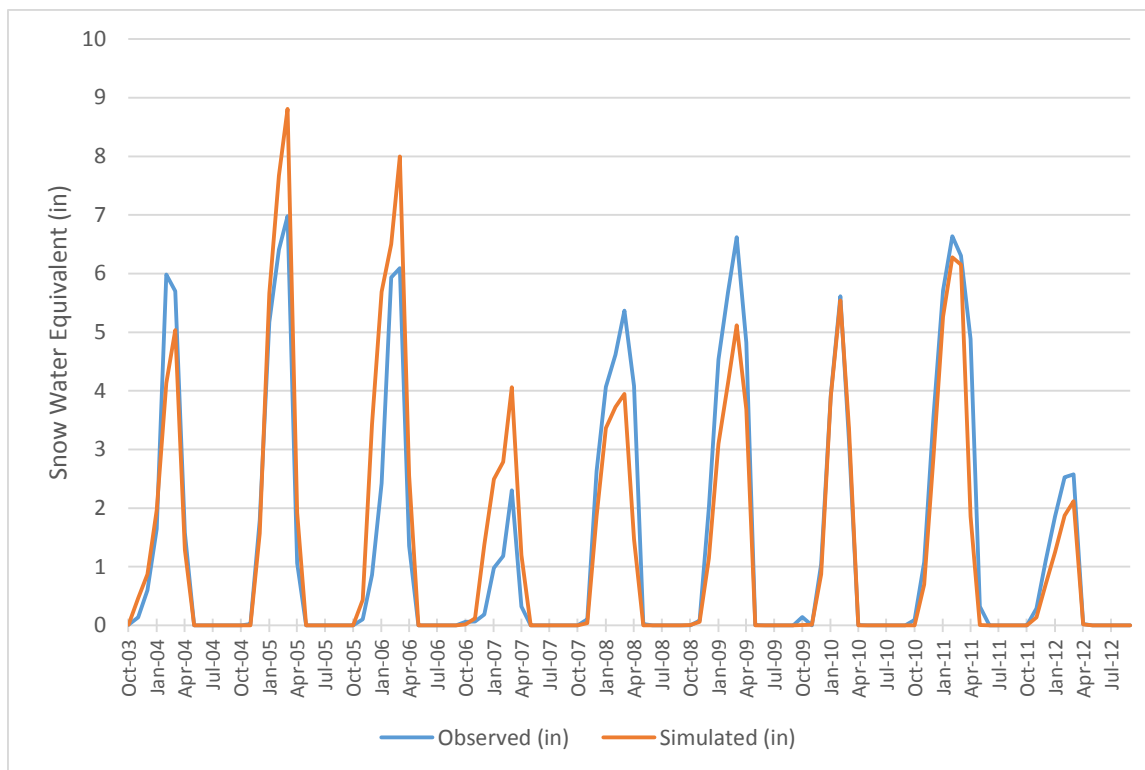


Figure 41. Mean monthly snow water equivalent time-series for weather region 7

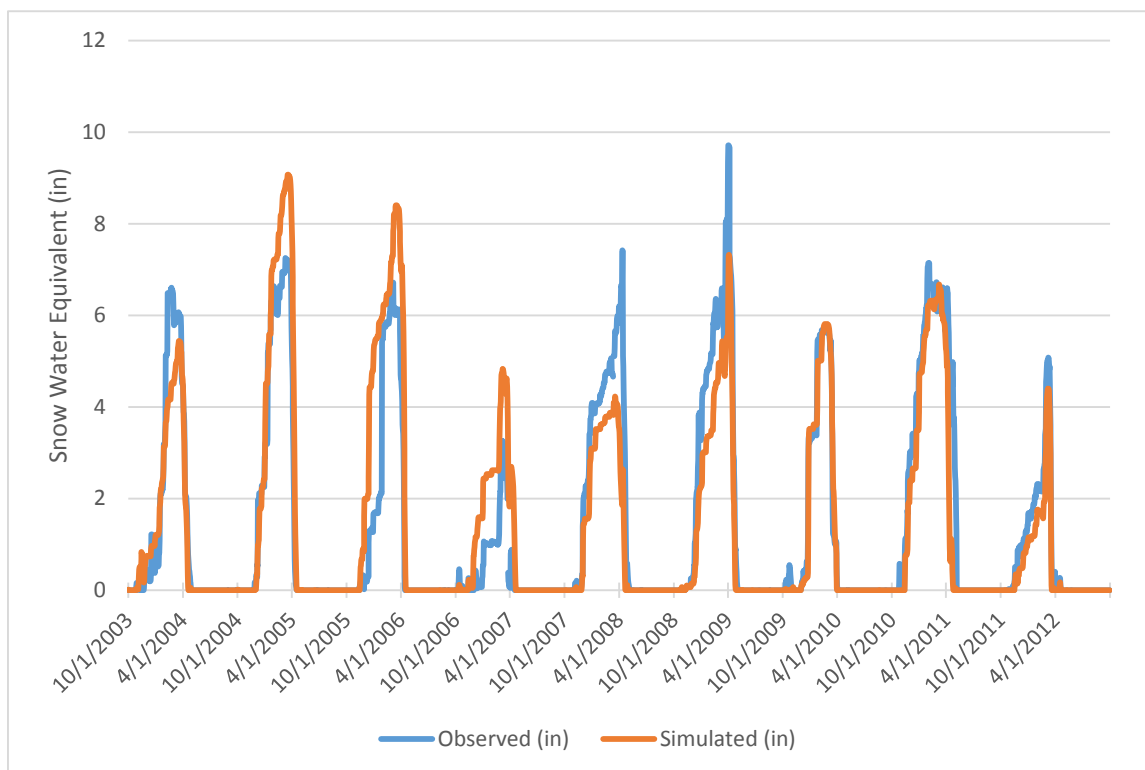


Figure 42. Mean daily snow water equivalent time-series for weather region 7

WEATHER REGION 8

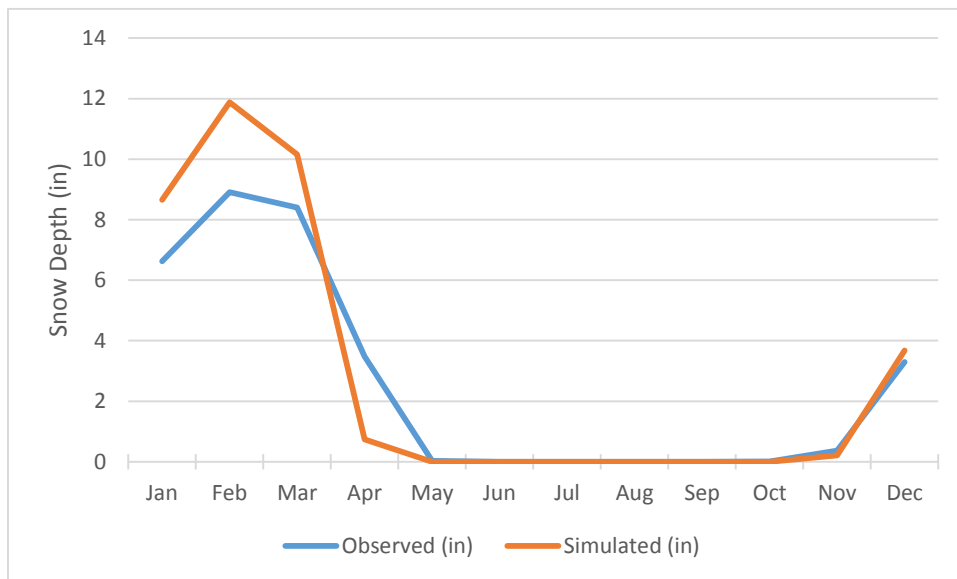


Figure 43. Mean monthly snow depth for weather region 8

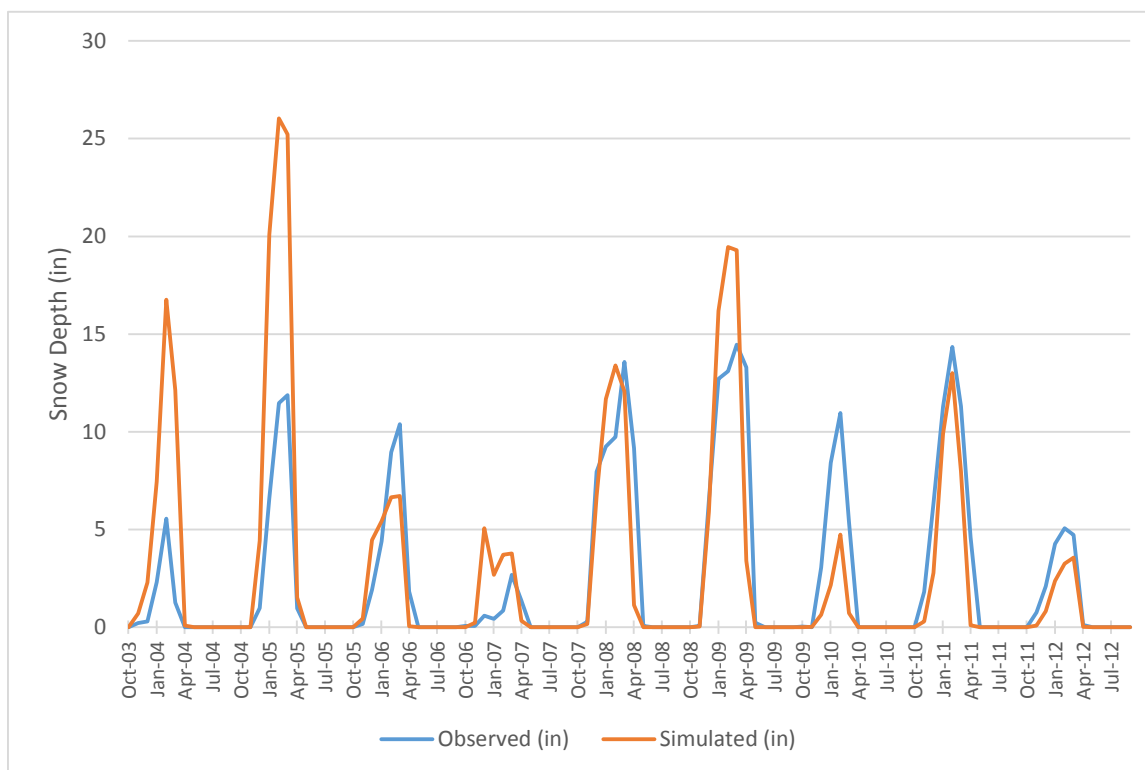


Figure 44. Mean monthly snow depth time-series for weather region 8

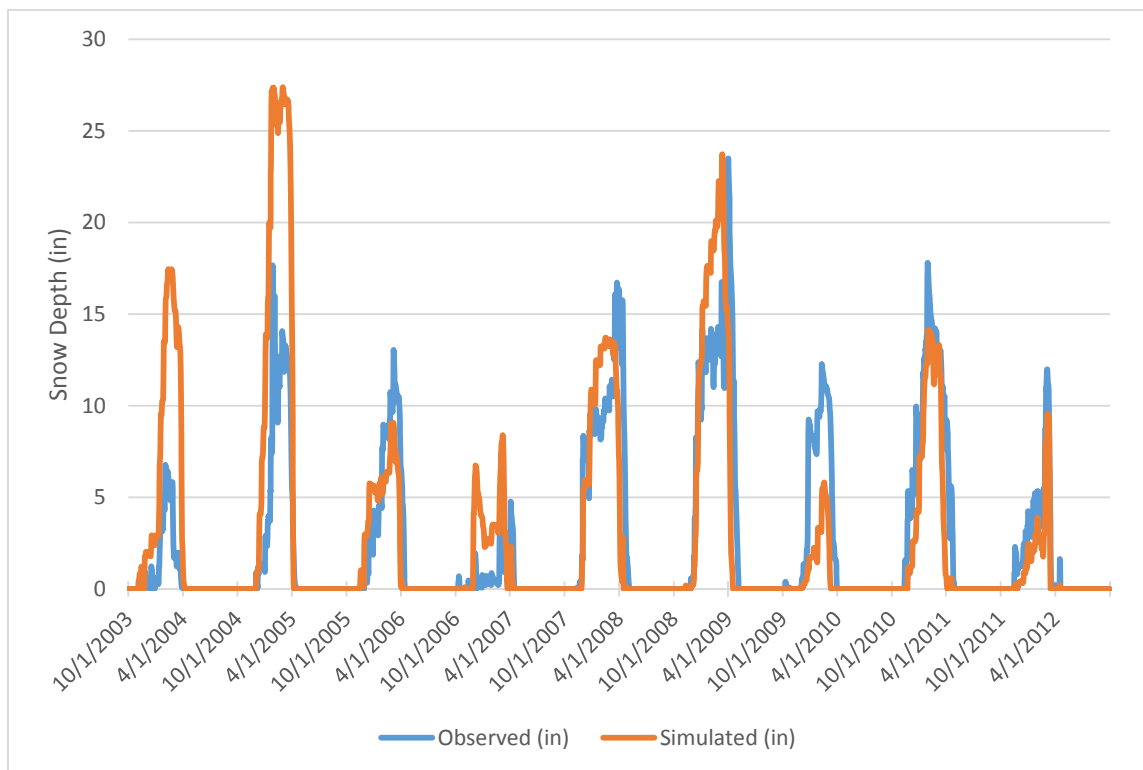


Figure 45. Mean daily snow depth time-series for weather region 8

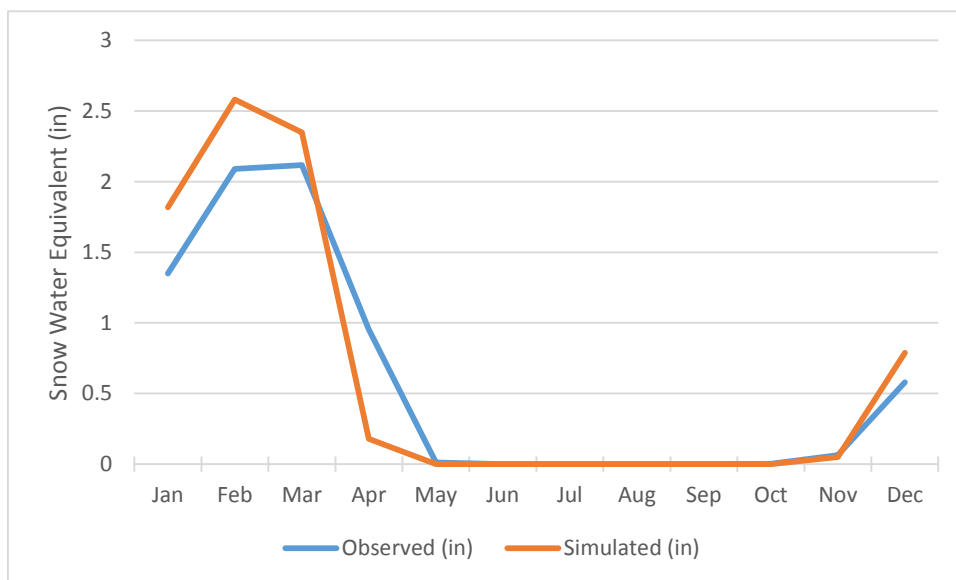


Figure 46. Mean monthly snow water equivalent for weather region 8

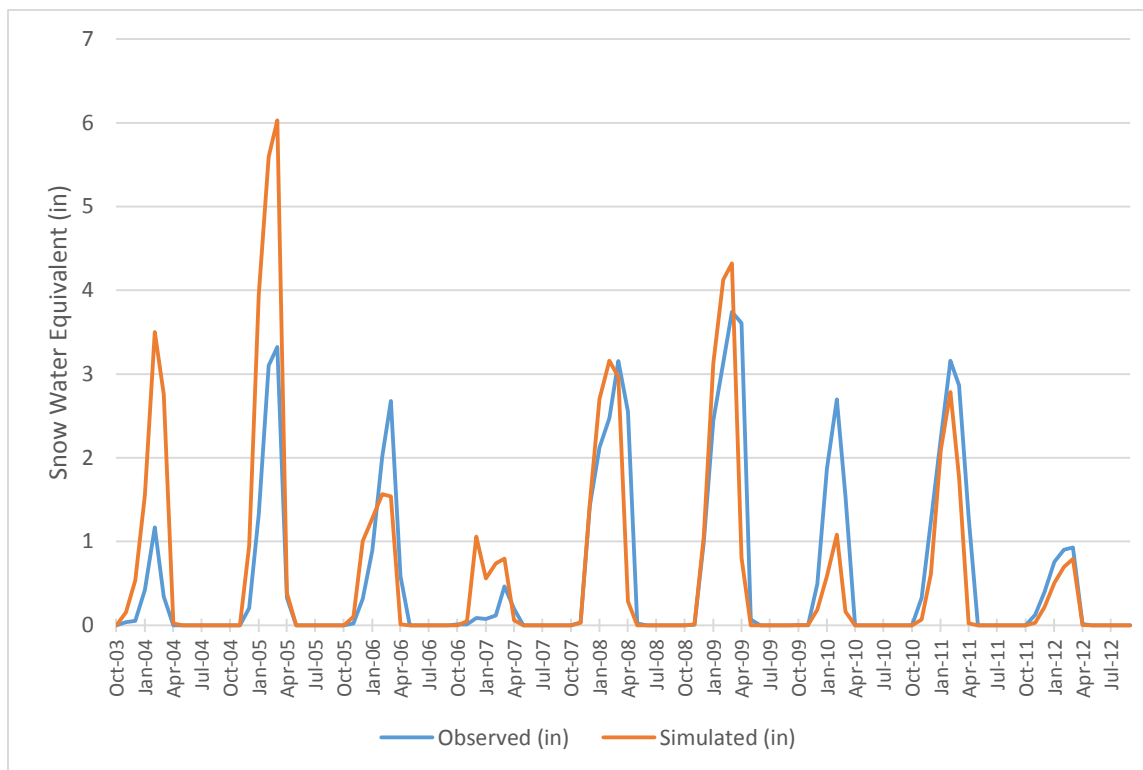


Figure 47. Mean monthly snow water equivalent time-series for weather region 8

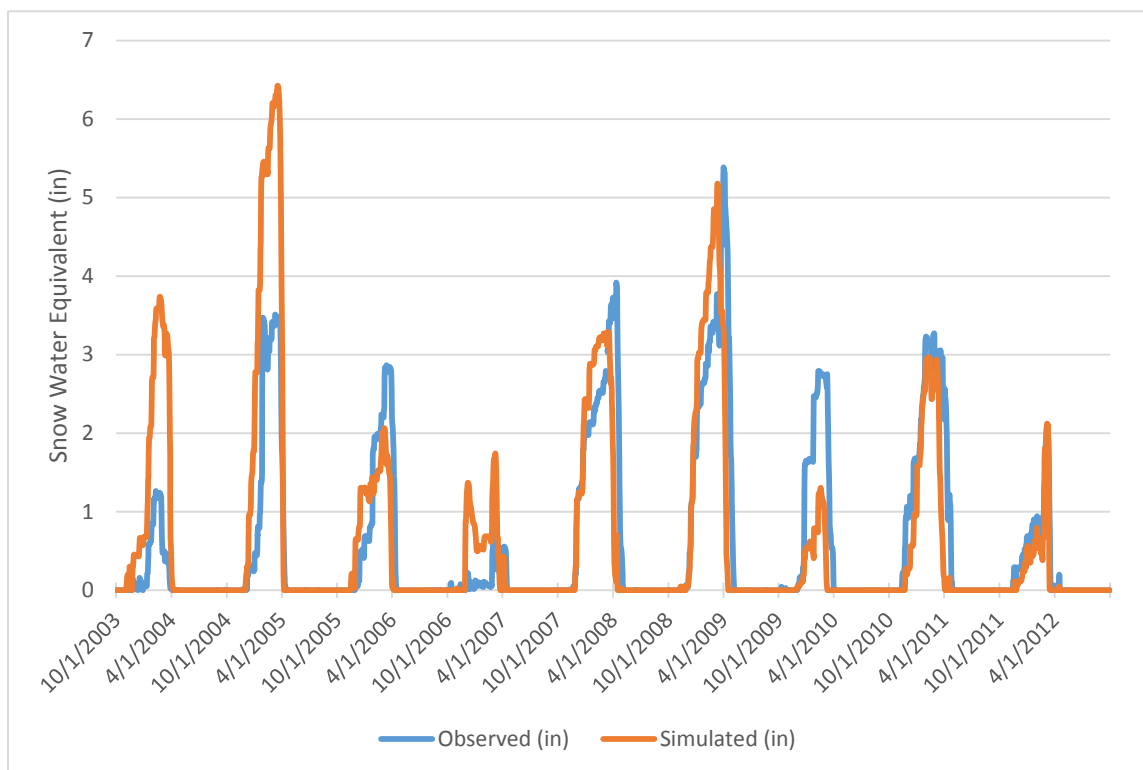


Figure 48. Mean daily snow water equivalent time-series for weather region 8

WEATHER REGION 9

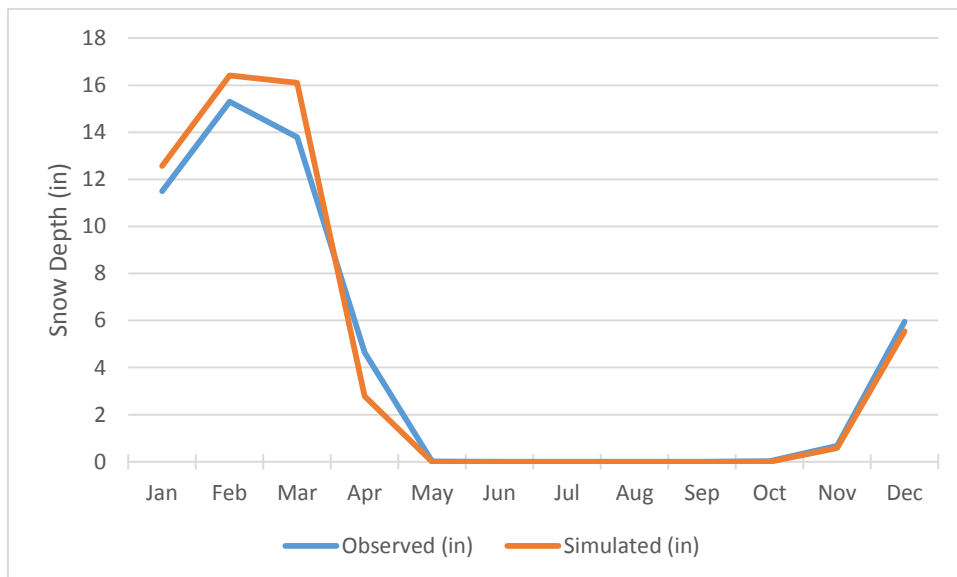


Figure 49. Mean monthly snow depth for weather region 9

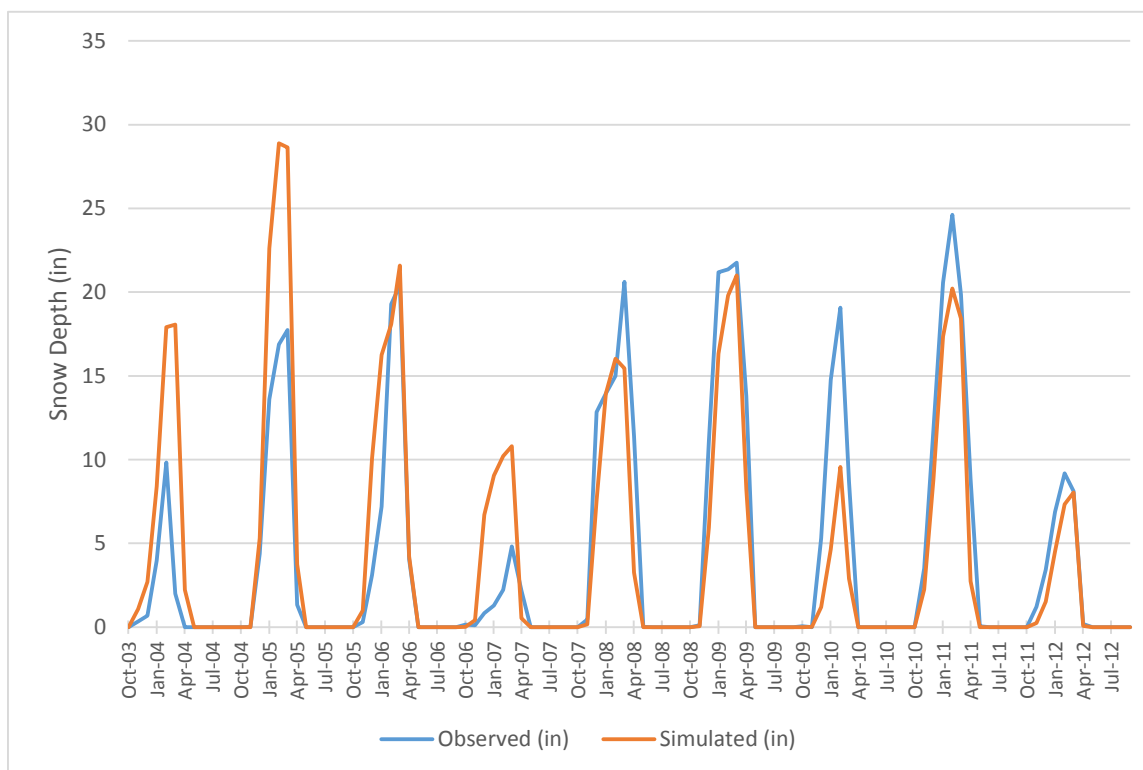


Figure 50. Mean monthly snow depth time-series for weather region 9

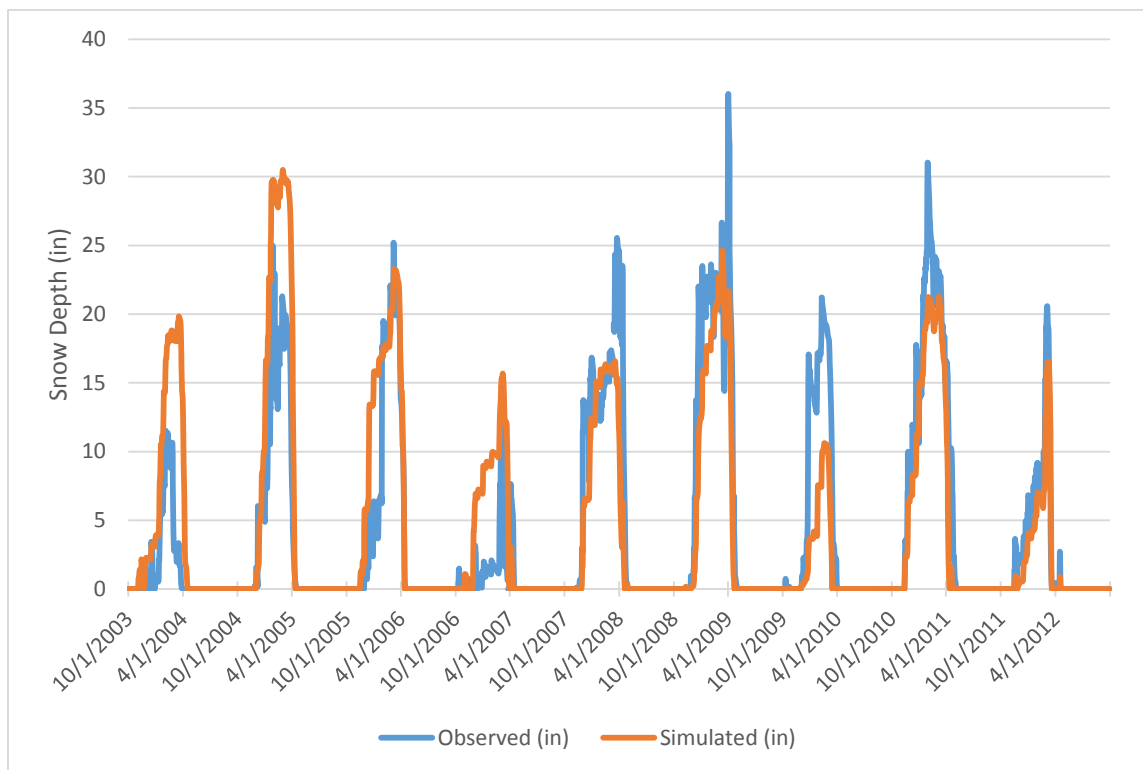


Figure 51. Mean daily snow depth time-series for weather region 9

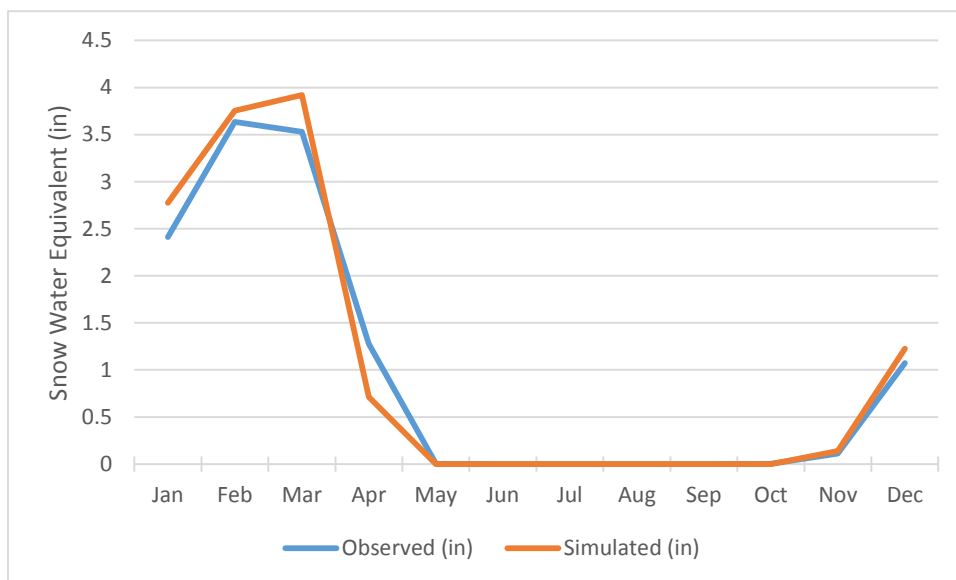


Figure 52. Mean monthly snow water equivalent for weather region 9

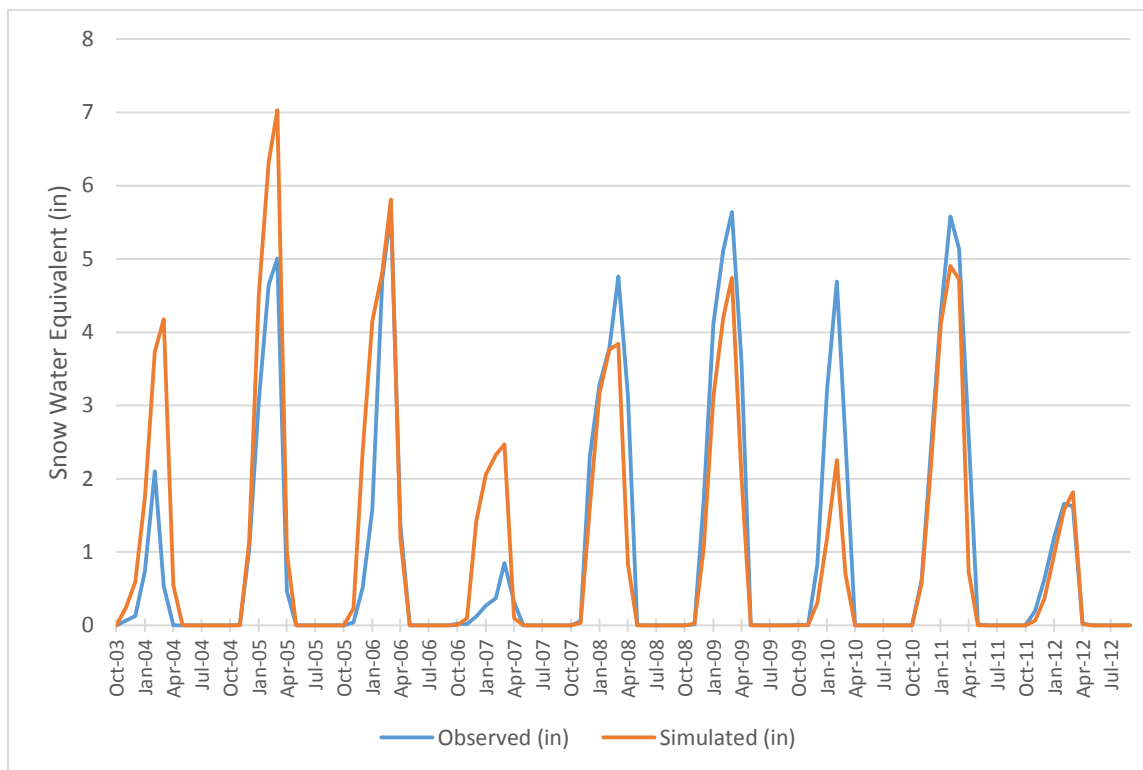


Figure 53. Mean monthly snow water equivalent time-series for weather region 9

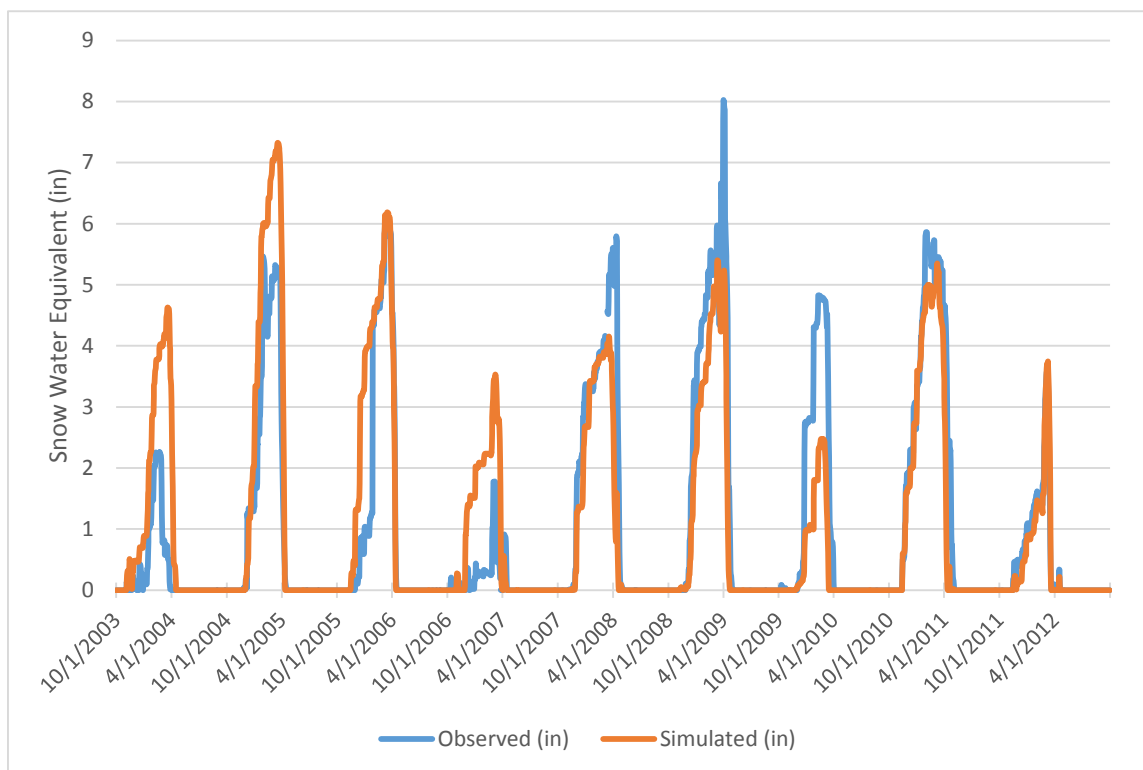


Figure 54. Mean daily snow water equivalent time-series for weather region 9

WEATHER REGION 10

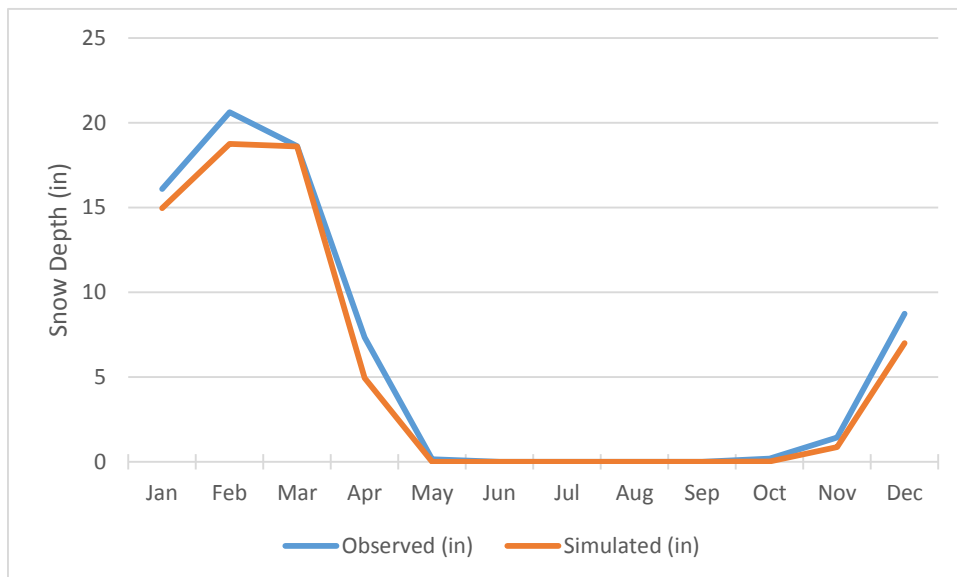


Figure 55. Mean monthly snow depth for weather region 10

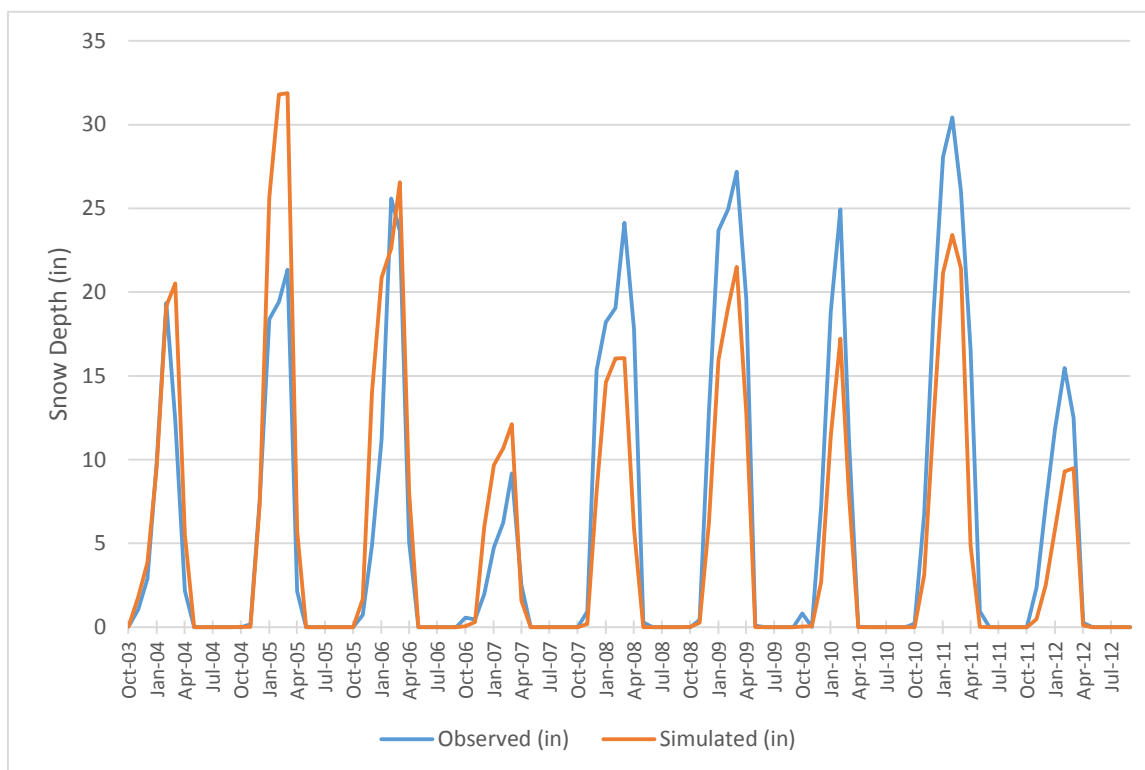


Figure 56. Mean monthly snow depth time-series for weather region 10

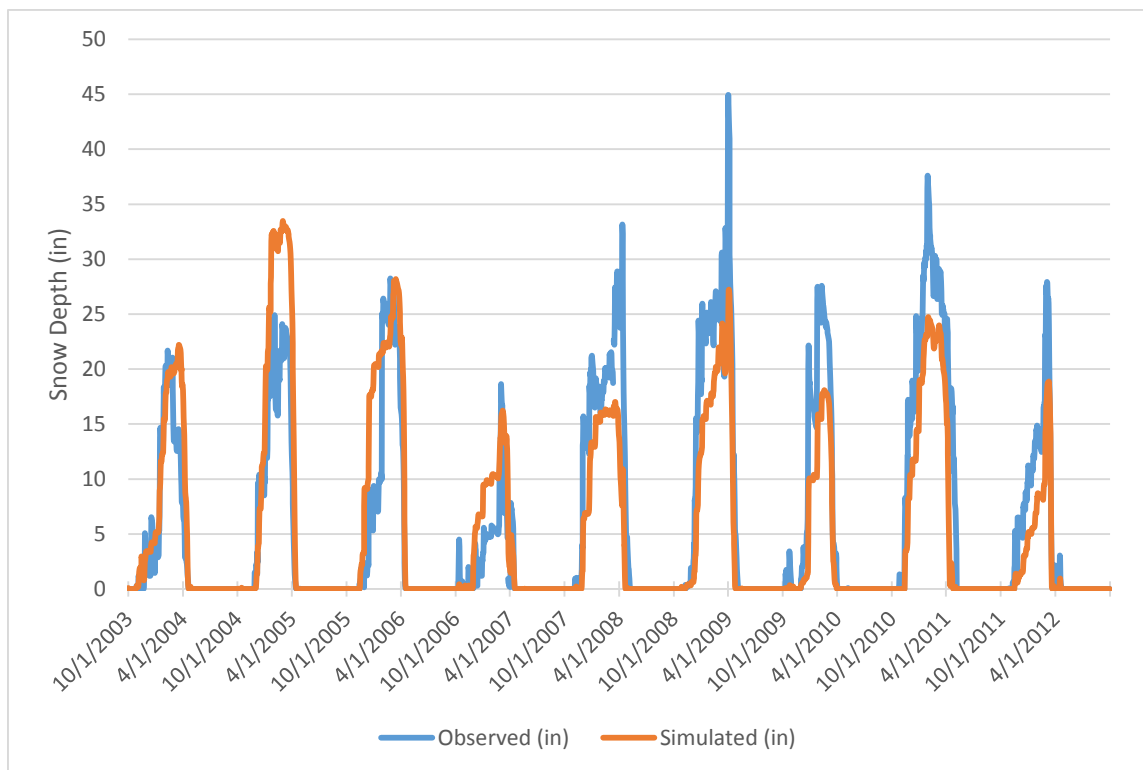


Figure 57. Mean daily snow depth time-series for weather region 10

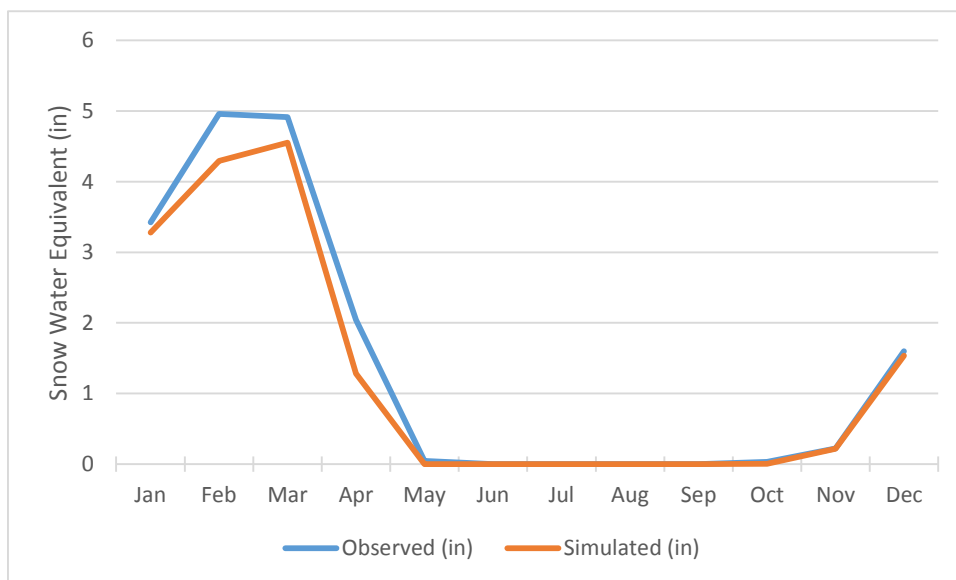


Figure 58. Mean monthly snow water equivalent for weather region 10

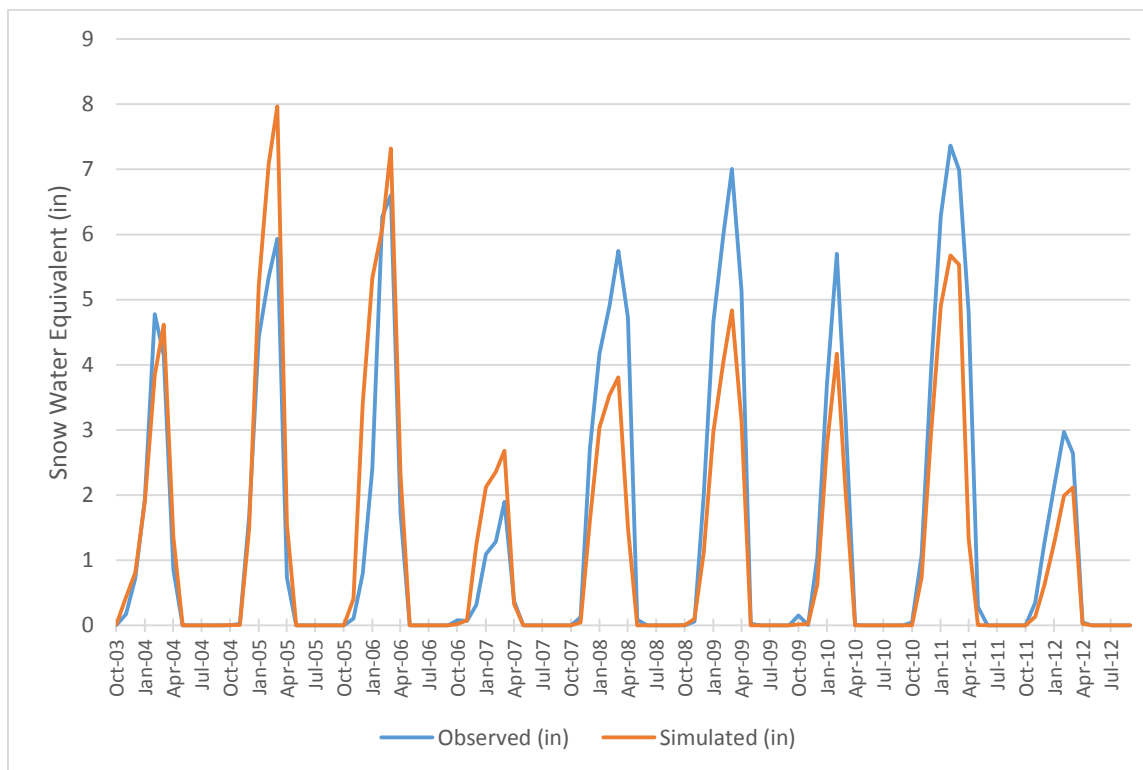


Figure 59. Mean monthly snow water equivalent time-series for weather region 10

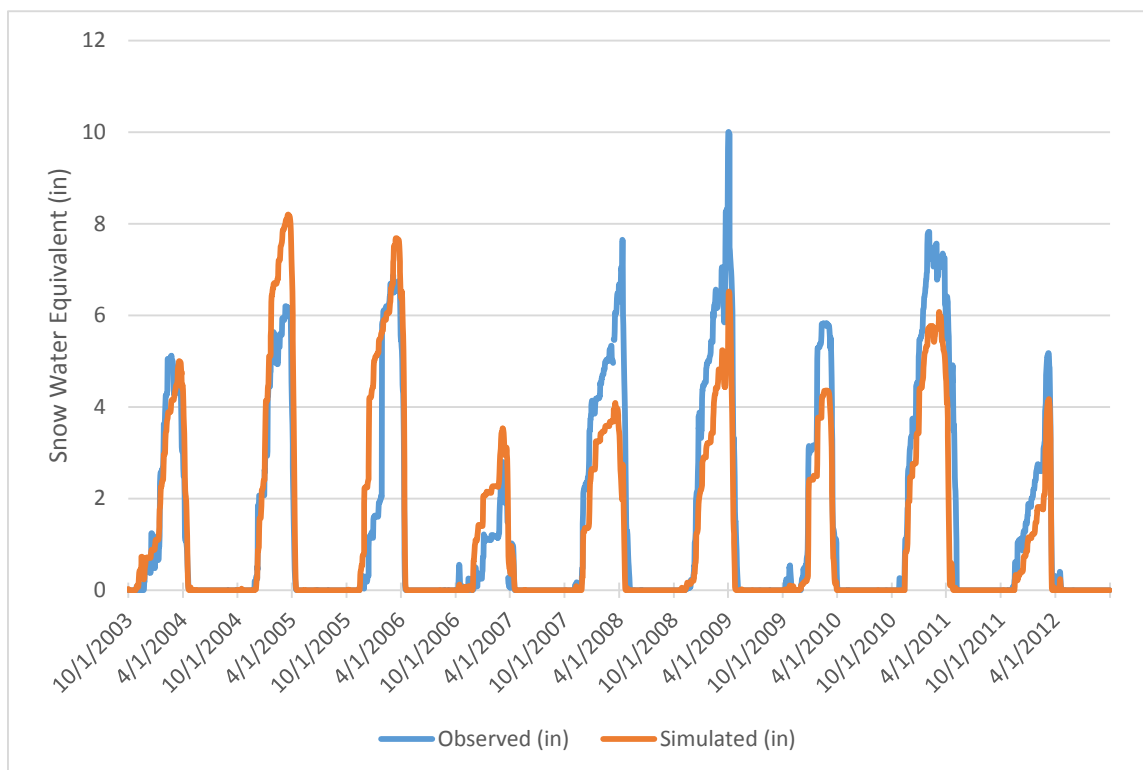


Figure 60. Mean daily snow water equivalent time-series for weather region 10

WEATHER REGION 11

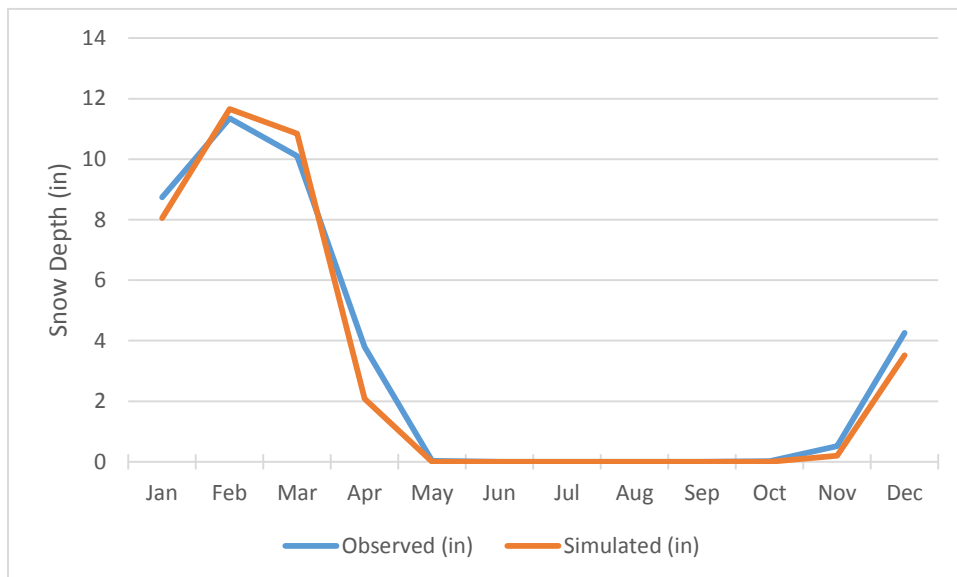


Figure 61. Mean monthly snow depth for weather region 11

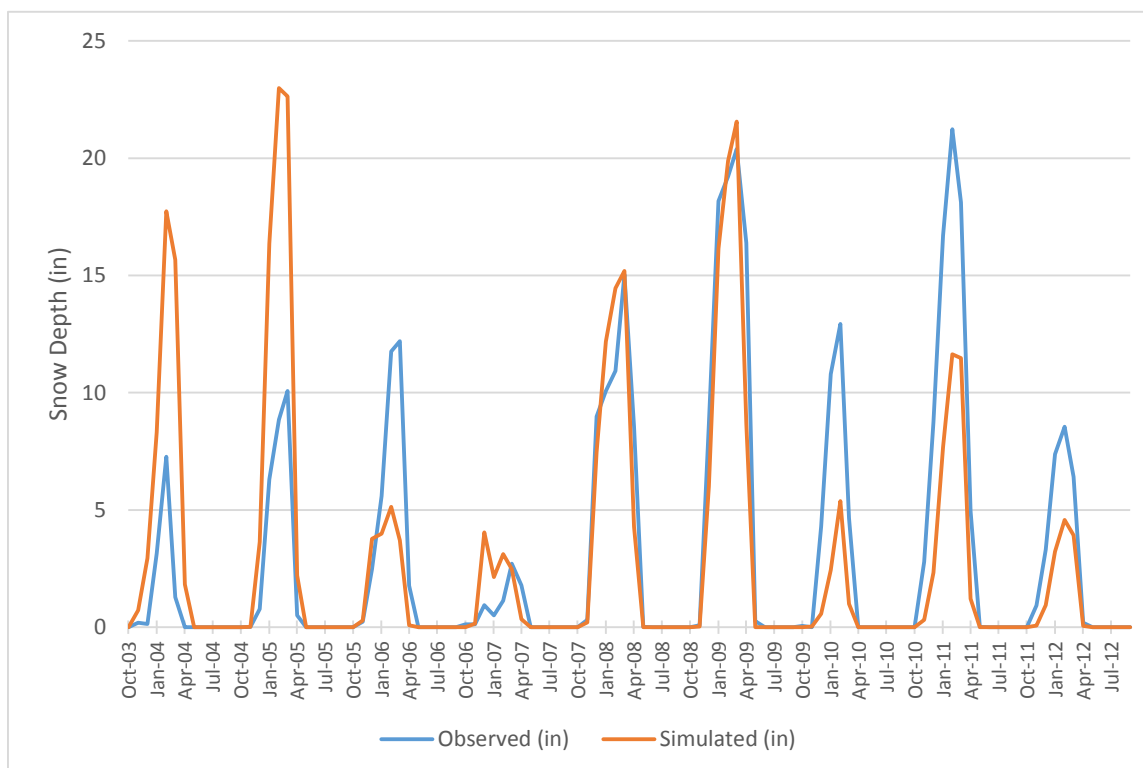


Figure 62. Mean monthly snow depth time-series for weather region 11

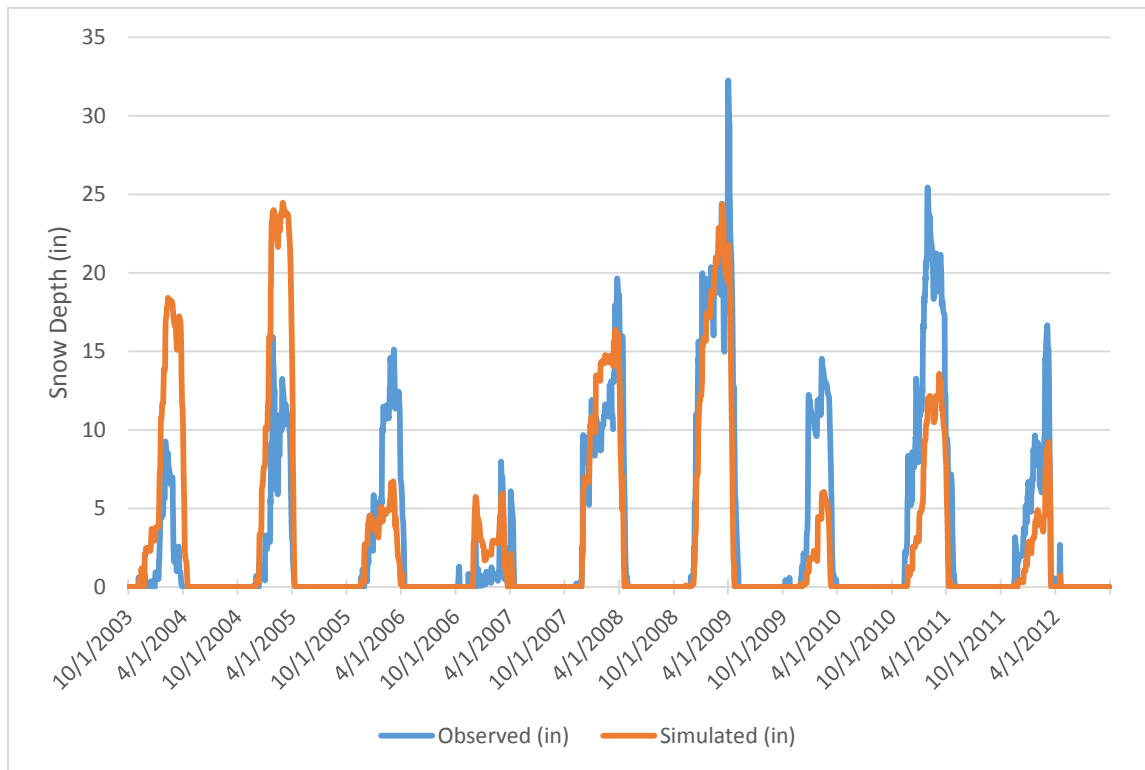


Figure 63. Mean daily snow depth time-series for weather region 11

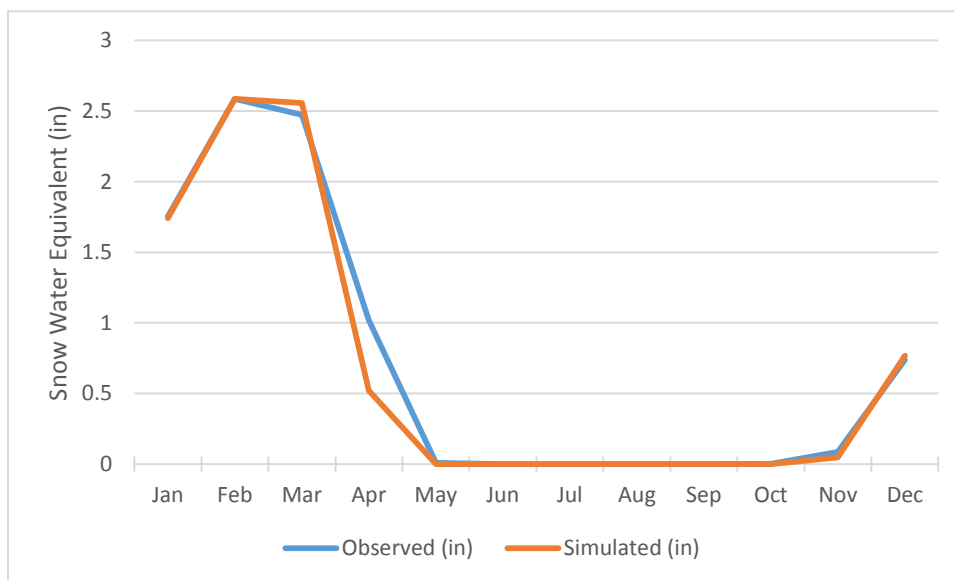


Figure 64. Mean monthly snow water equivalent for weather region 11

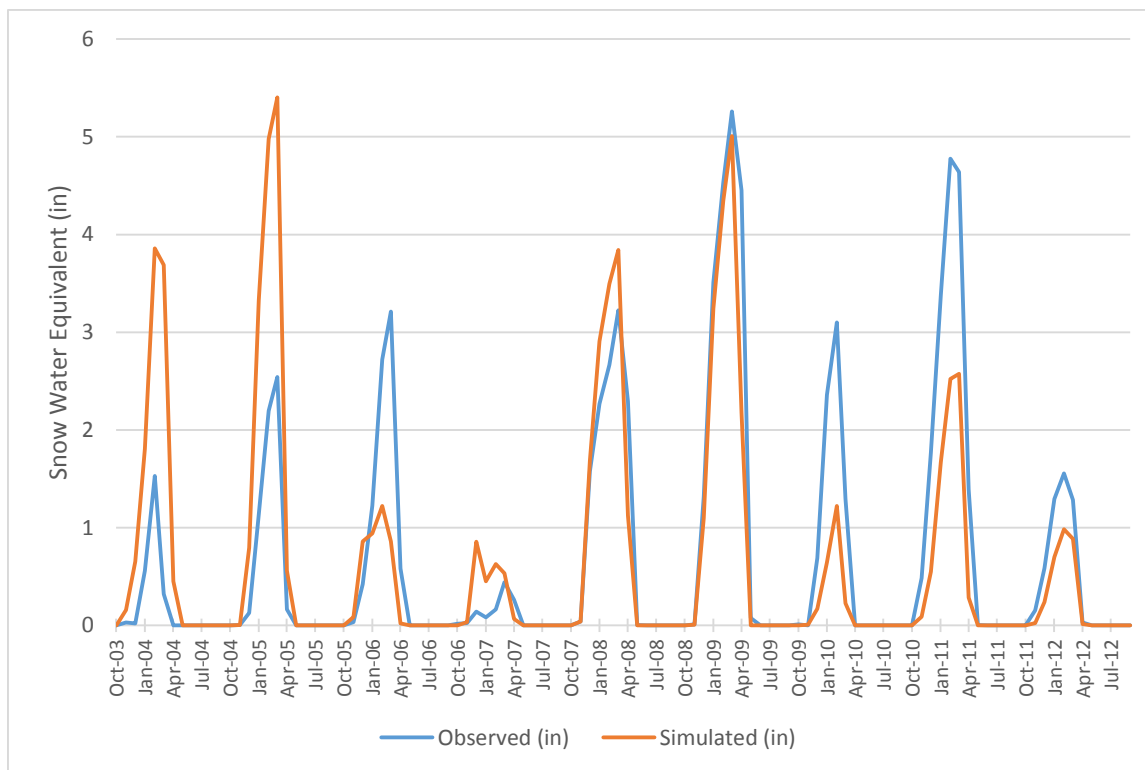


Figure 65. Mean monthly snow water equivalent time-series for weather region 11

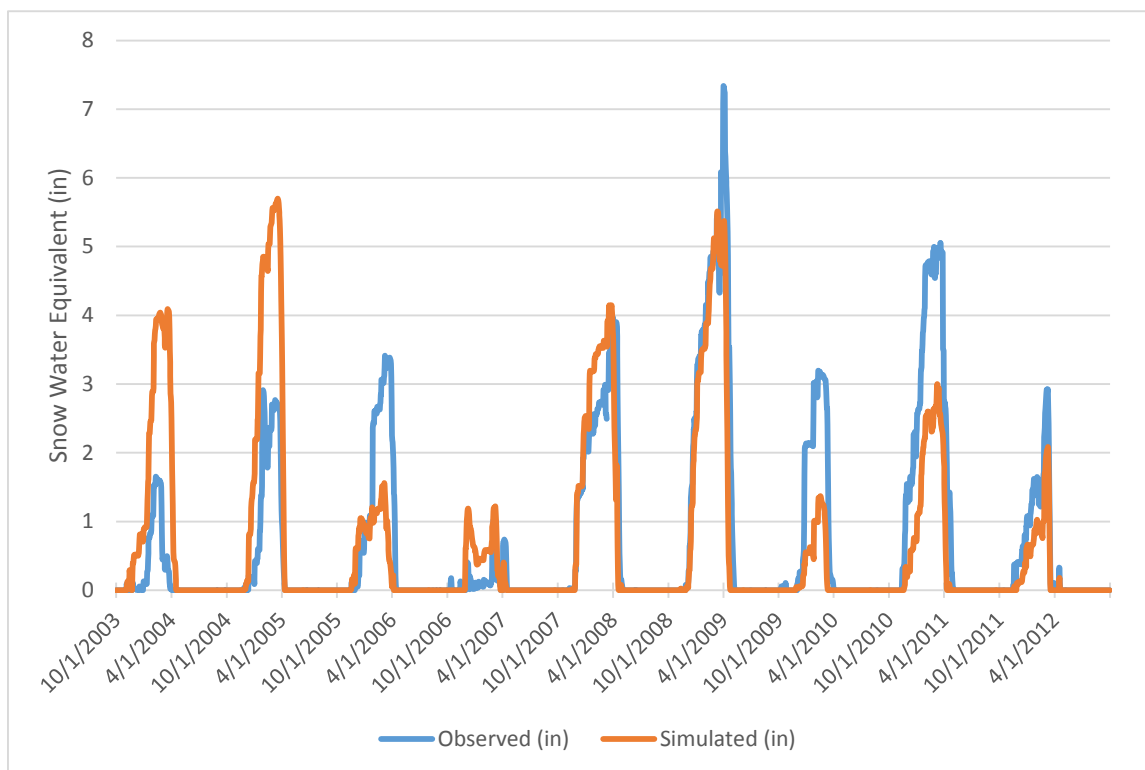


Figure 66. Mean daily snow water equivalent time-series for weather region 11

WEATHER REGION 12

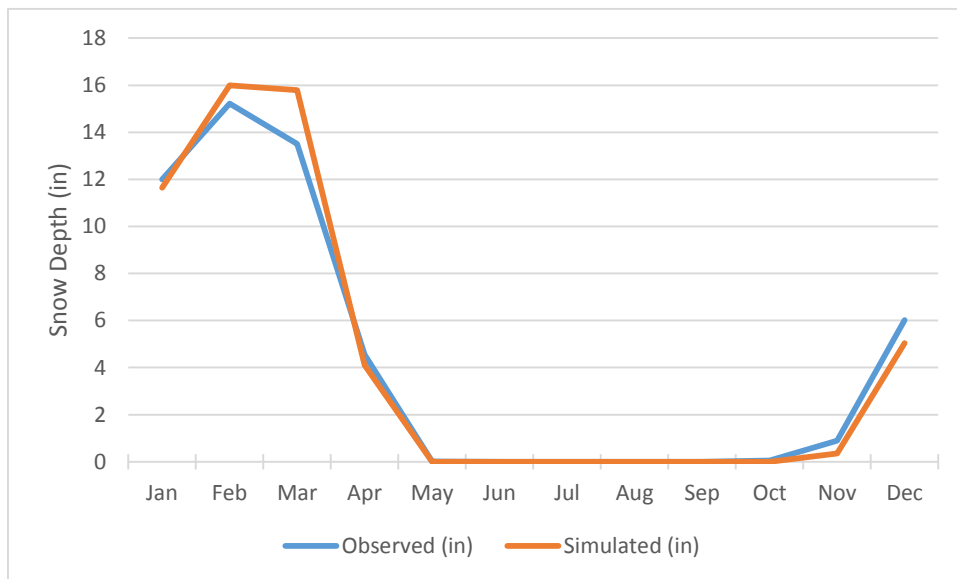


Figure 67. Mean monthly snow depth for weather region 12

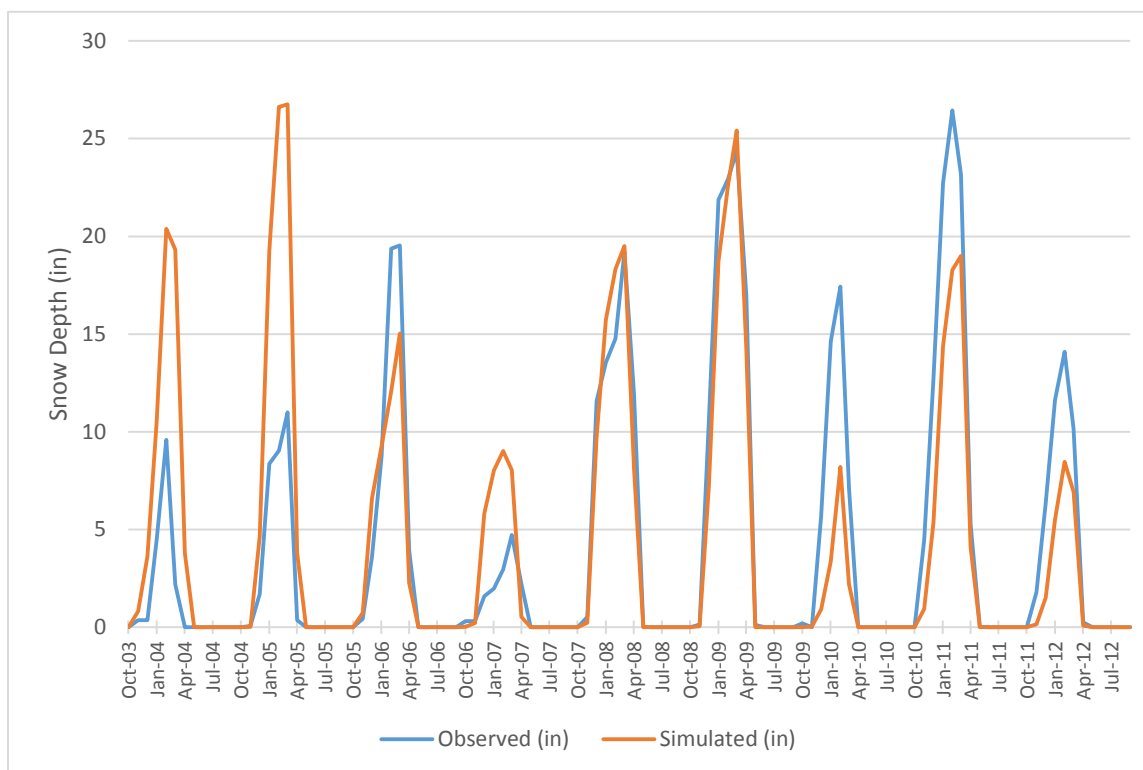


Figure 68. Mean monthly snow depth time-series for weather region 12

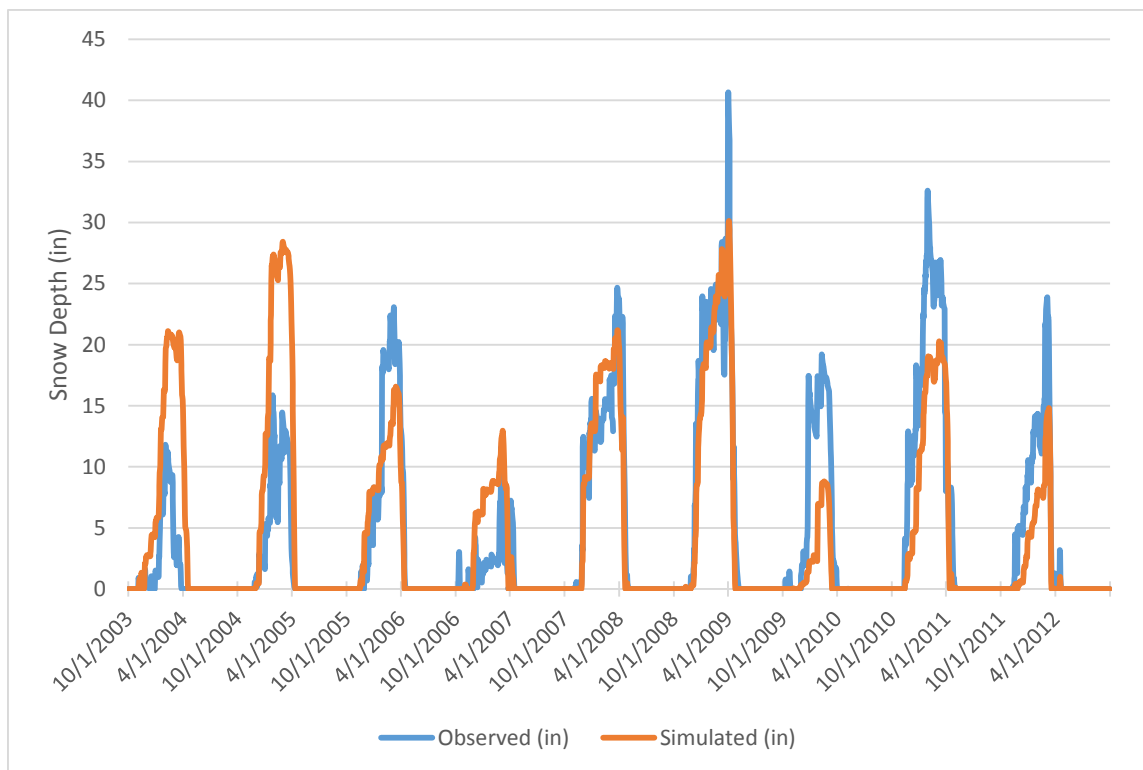


Figure 69. Mean daily snow depth time-series for weather region 12

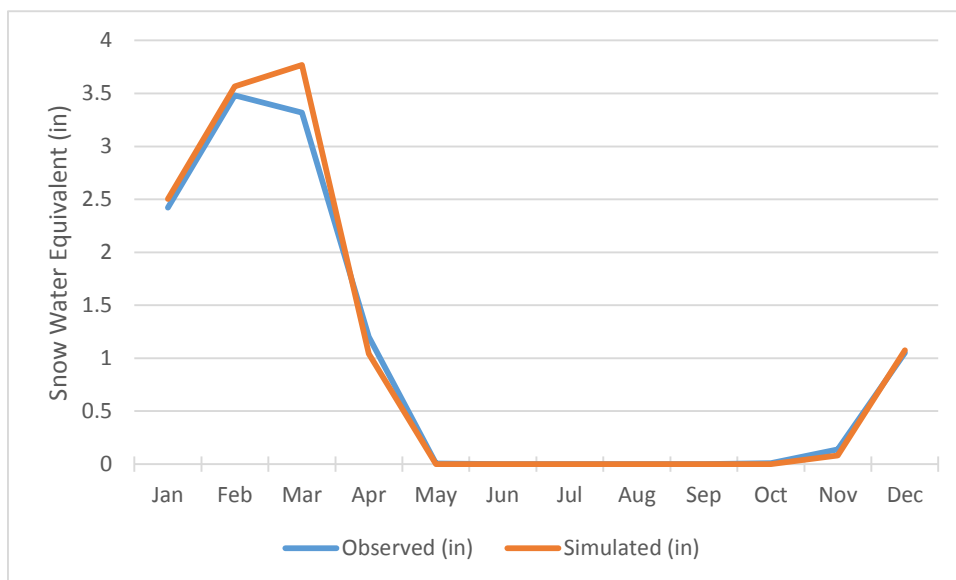


Figure 70. Mean monthly snow water equivalent for weather region 12

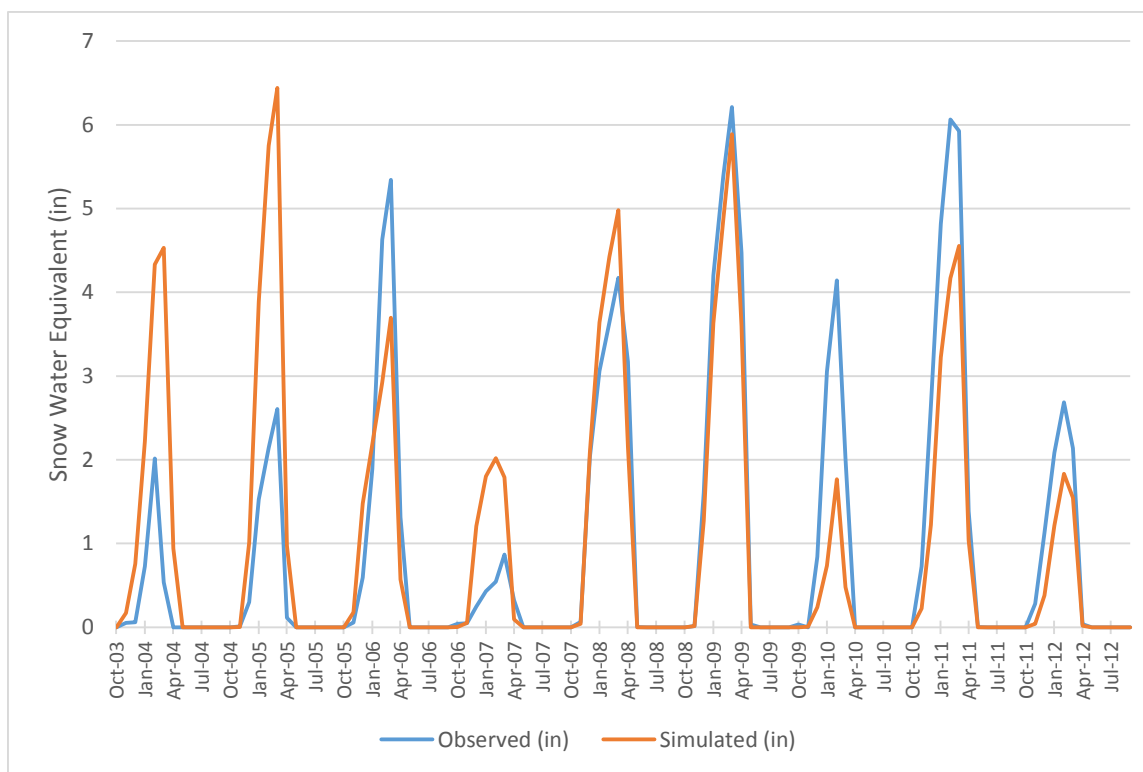


Figure 71. Mean monthly snow water equivalent time-series for weather region 12

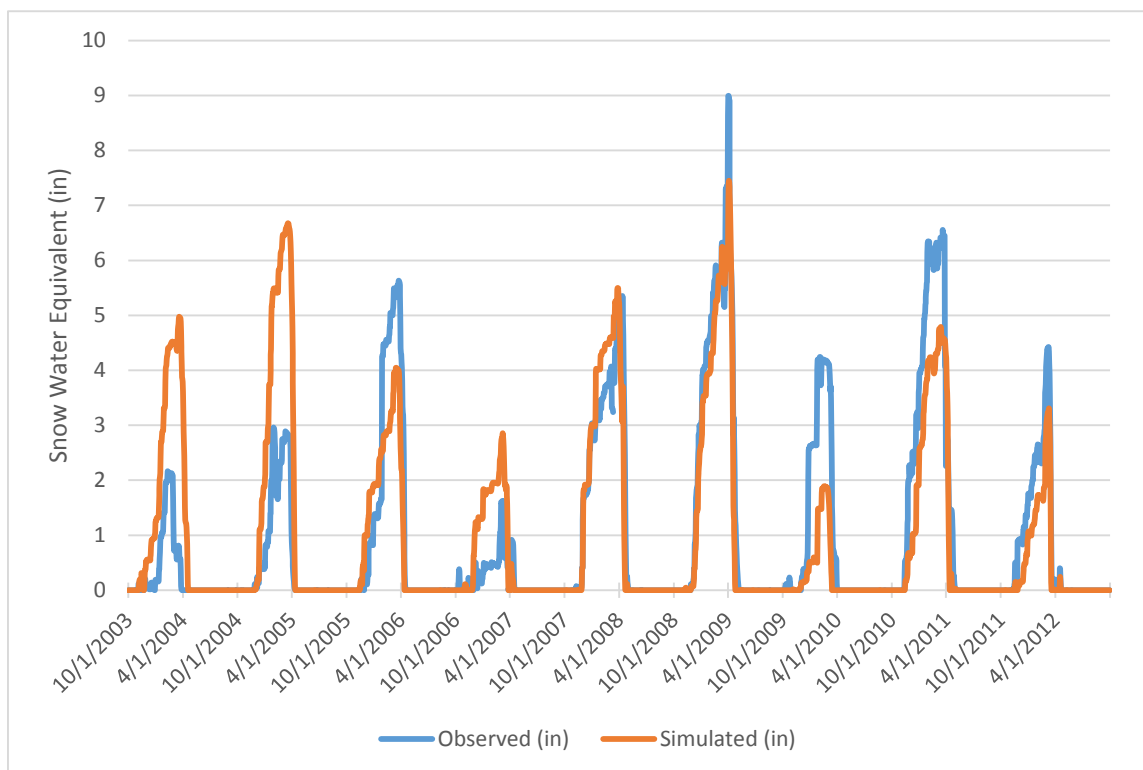


Figure 72. Mean daily snow water equivalent time-series for weather region 12

WEATHER REGION 13

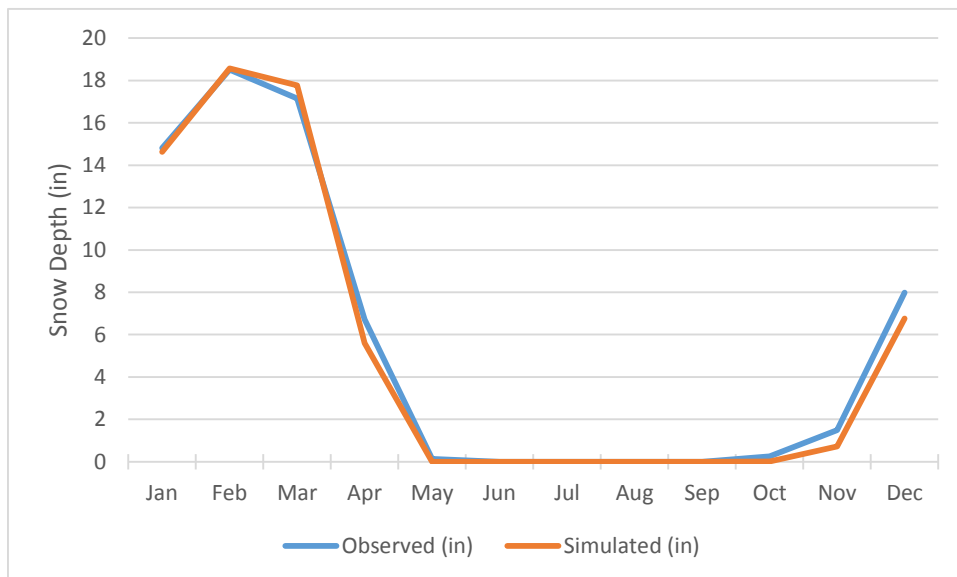


Figure 73. Mean monthly snow depth for weather region 13

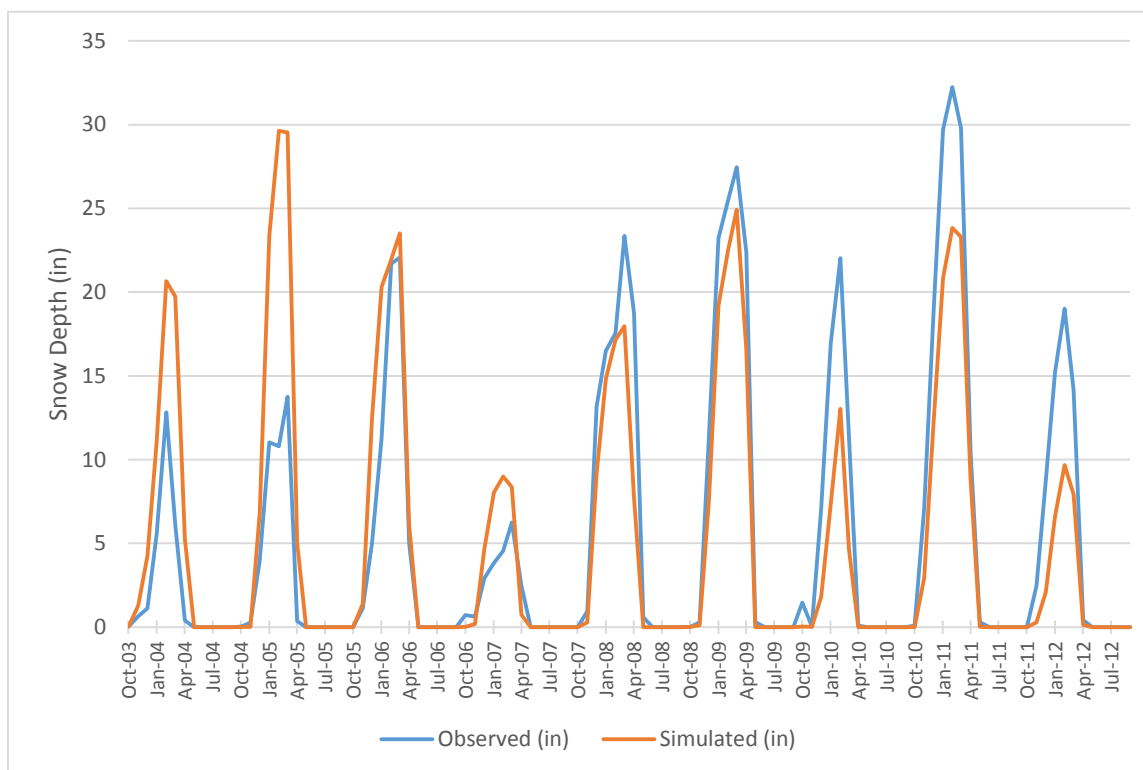


Figure 74. Mean monthly snow depth time-series for weather region 13

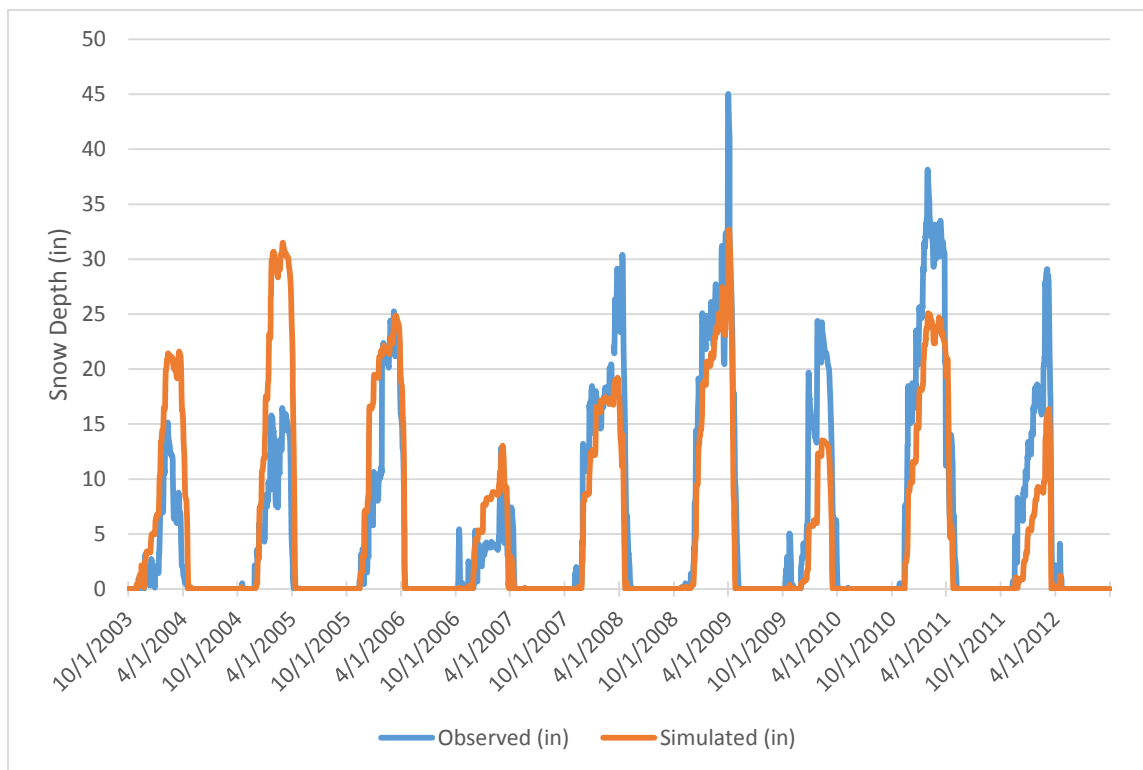


Figure 75. Mean daily snow depth time-series for weather region 13

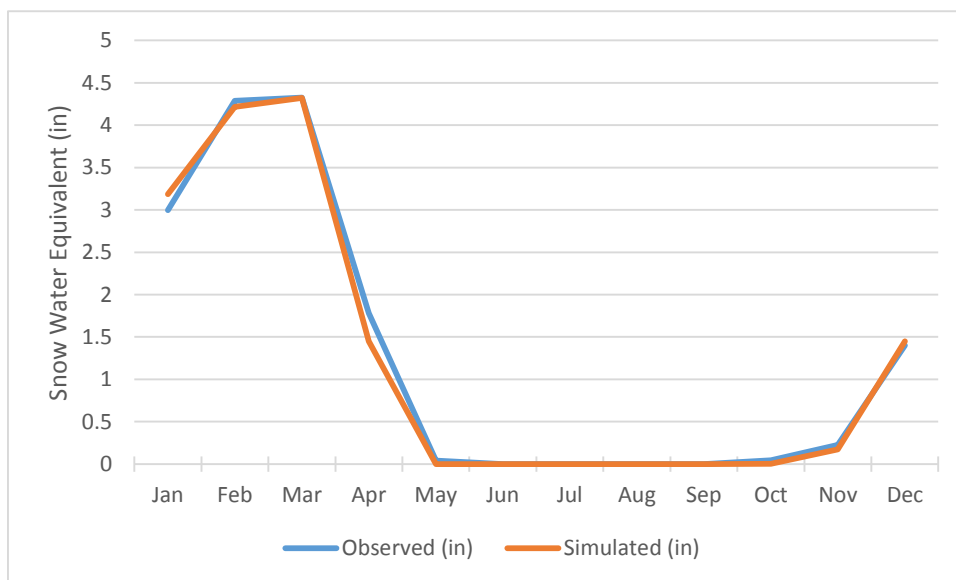


Figure 76. Mean monthly snow water equivalent for weather region 13

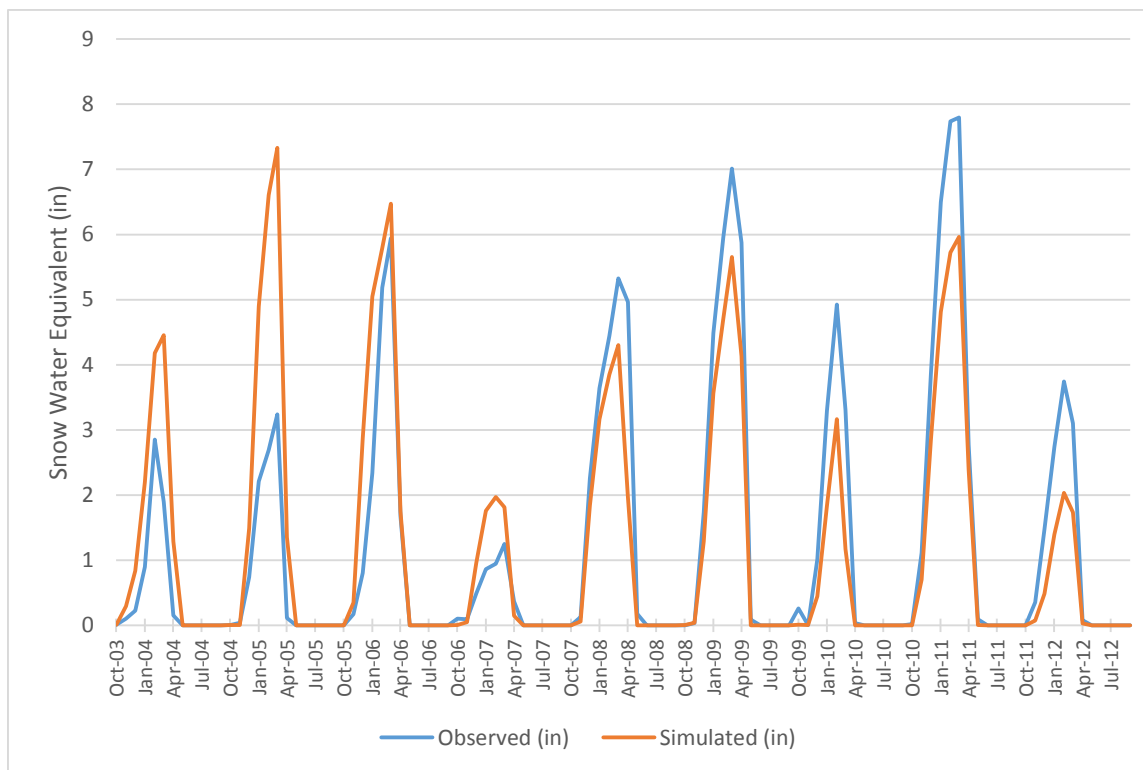


Figure 77. Mean monthly snow water equivalent time-series for weather region 13

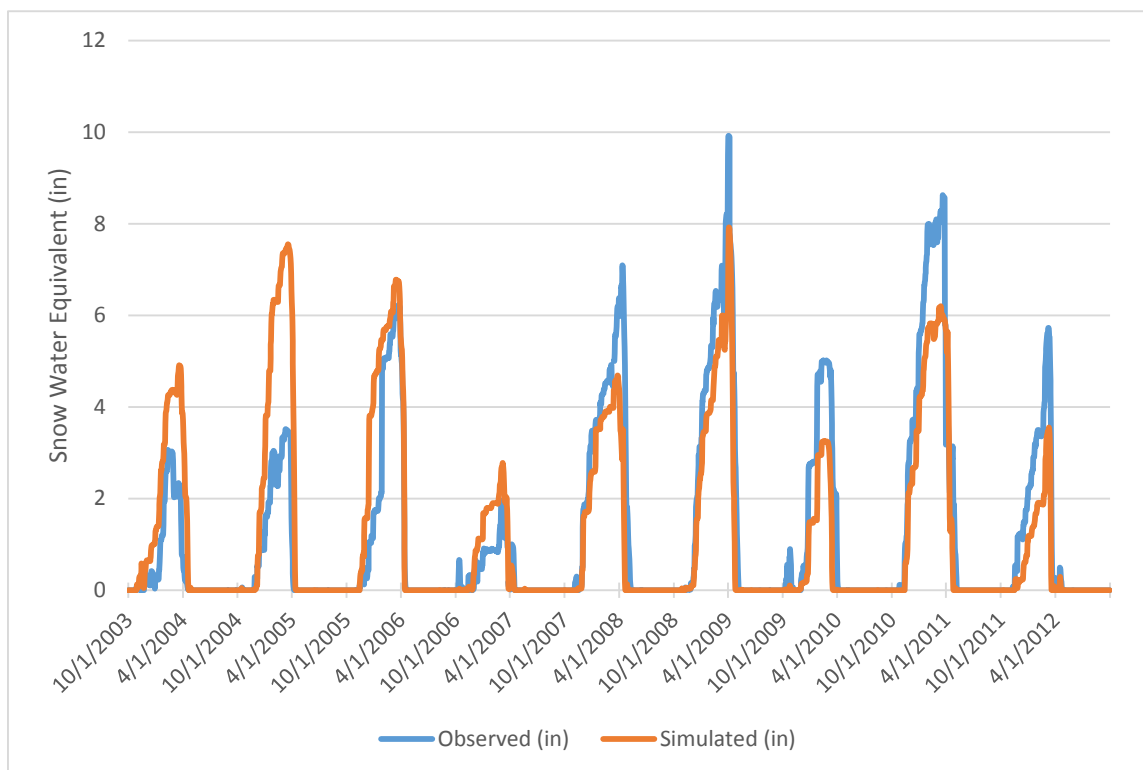


Figure 78. Mean daily snow water equivalent time-series for weather region 13

WEATHER REGION 14

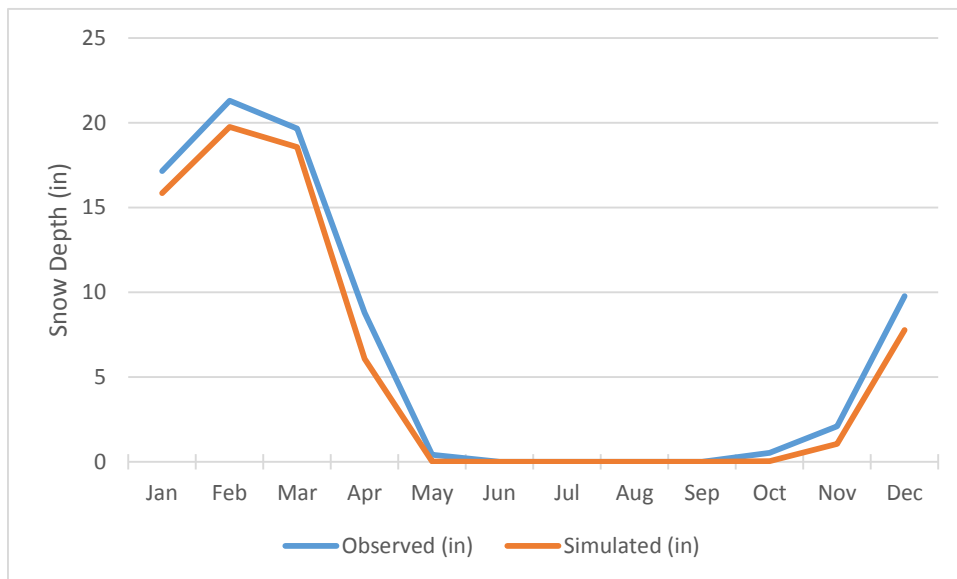


Figure 79. Mean monthly snow depth for weather region 14

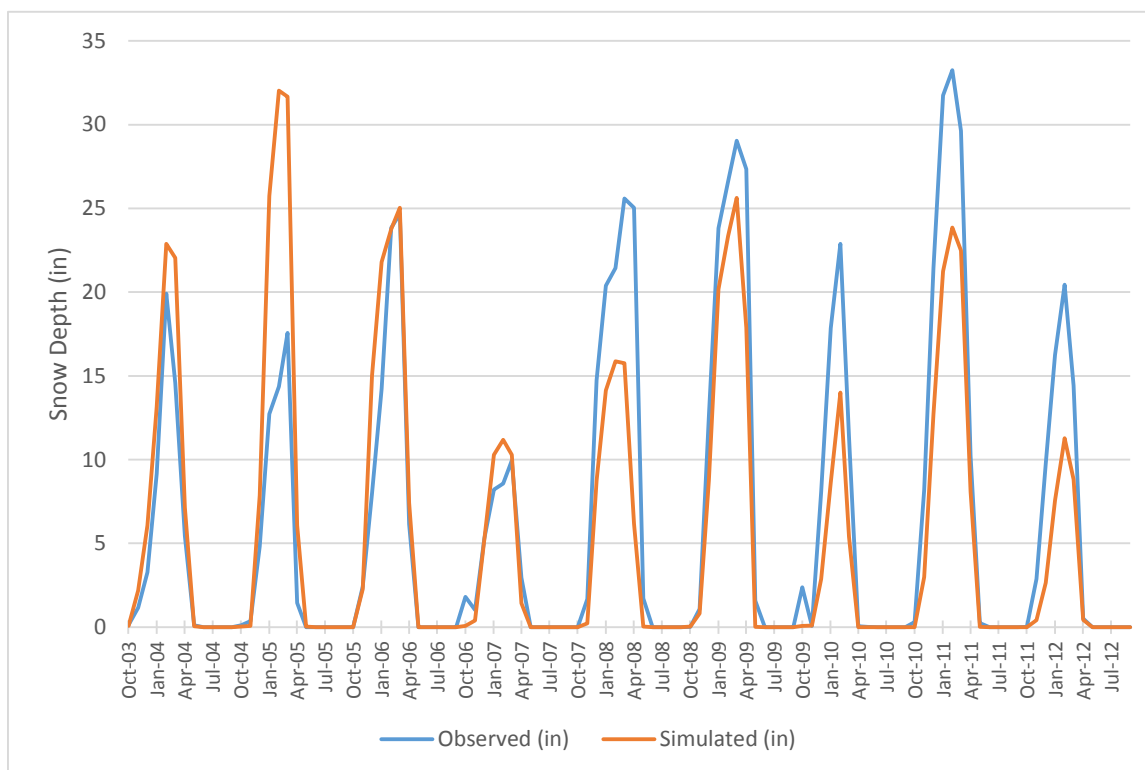


Figure 80. Mean monthly snow depth time-series for weather region 14

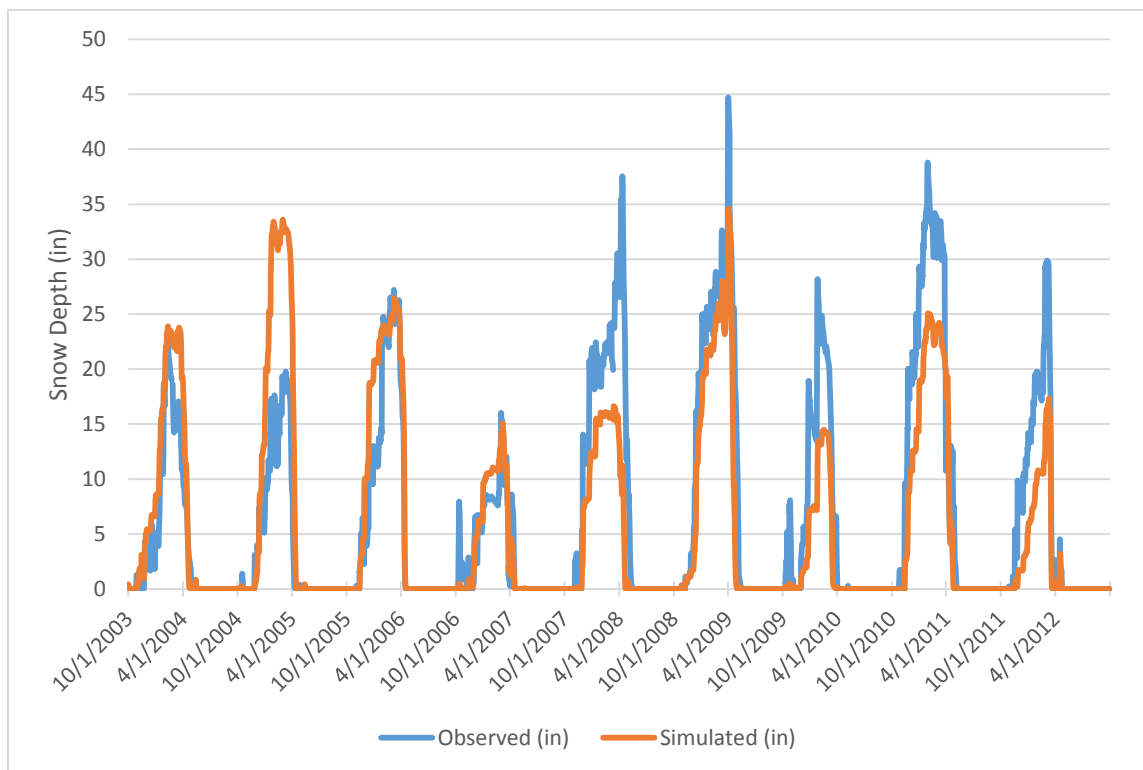


Figure 81. Mean daily snow depth time-series for weather region 14

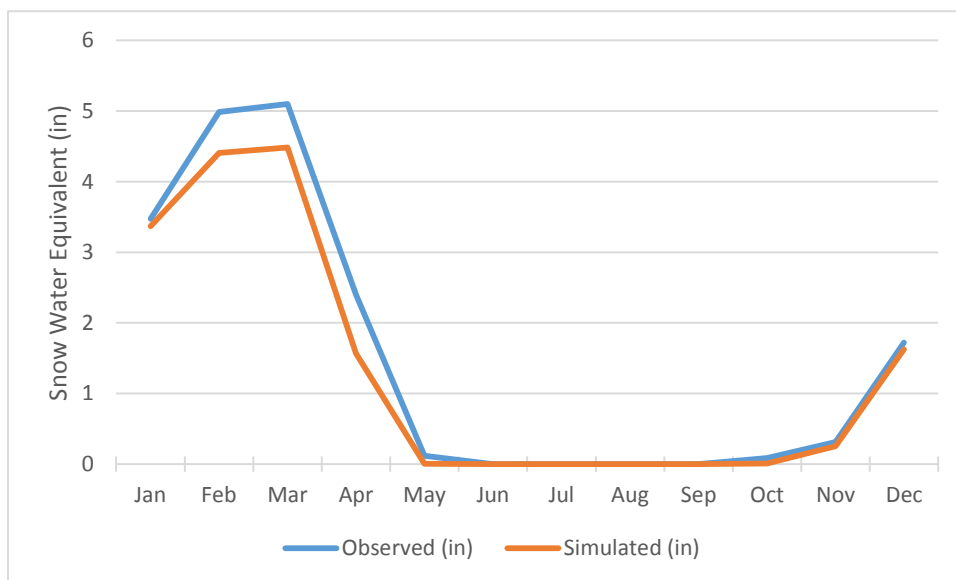


Figure 82. Mean monthly snow water equivalent for weather region 14

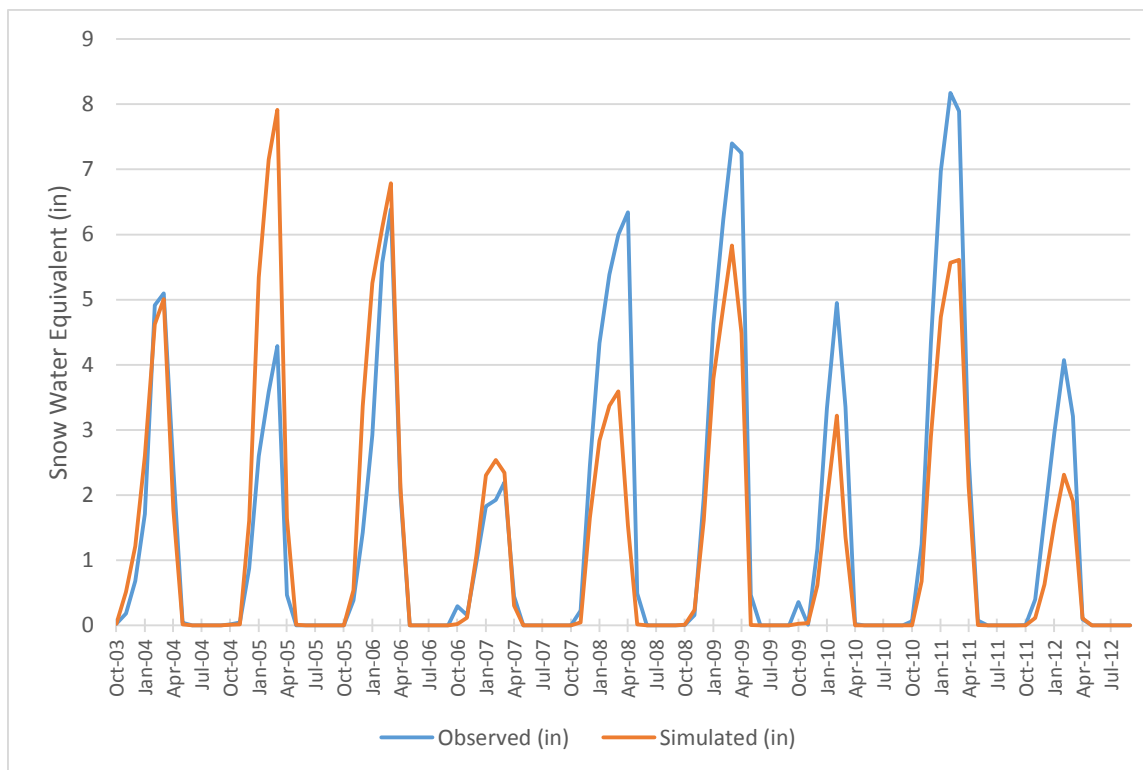


Figure 83. Mean monthly snow water equivalent time-series for weather region 14

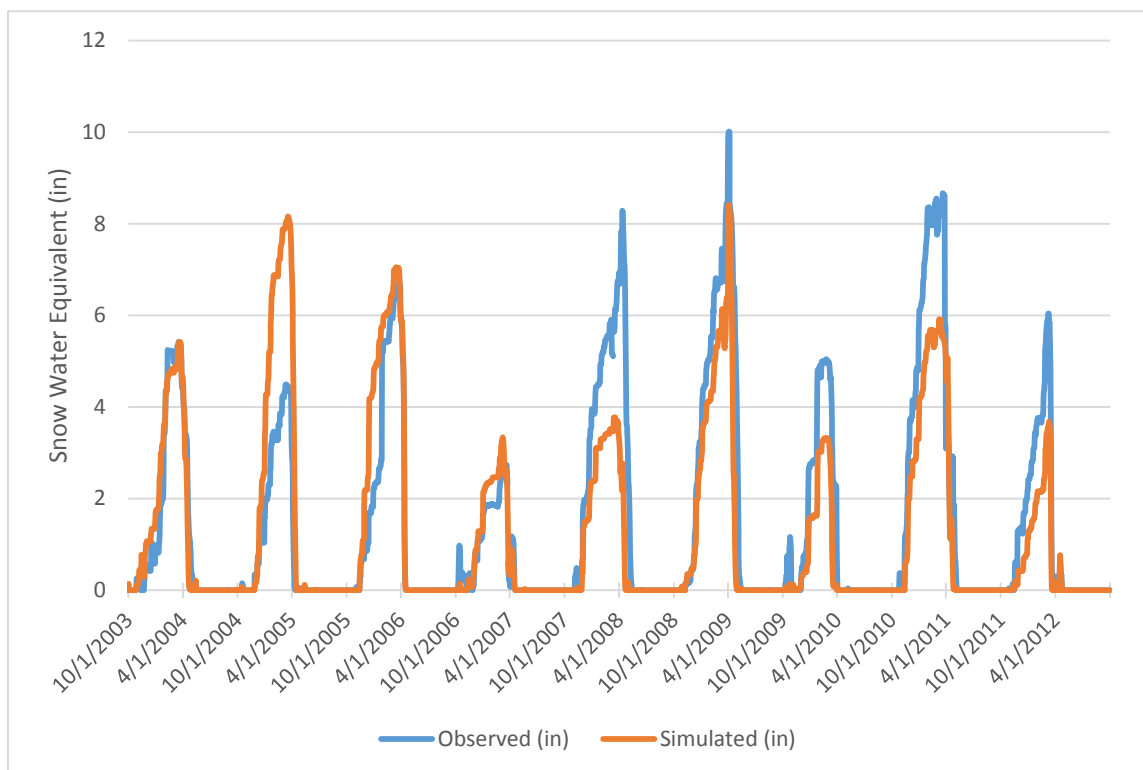


Figure 84. Mean daily snow water equivalent time-series for weather region 14

WEATHER REGION 15

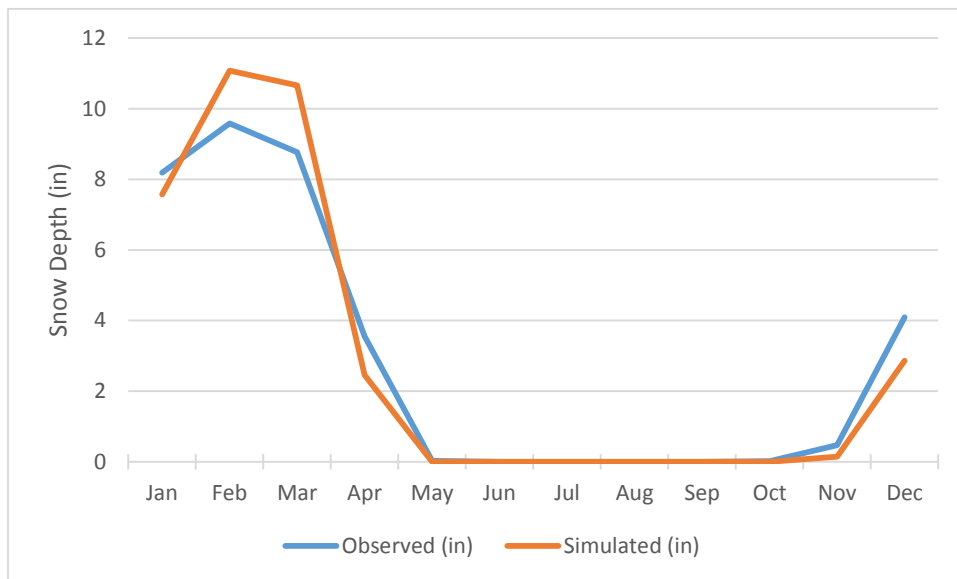


Figure 85. Mean monthly snow depth for weather region 15

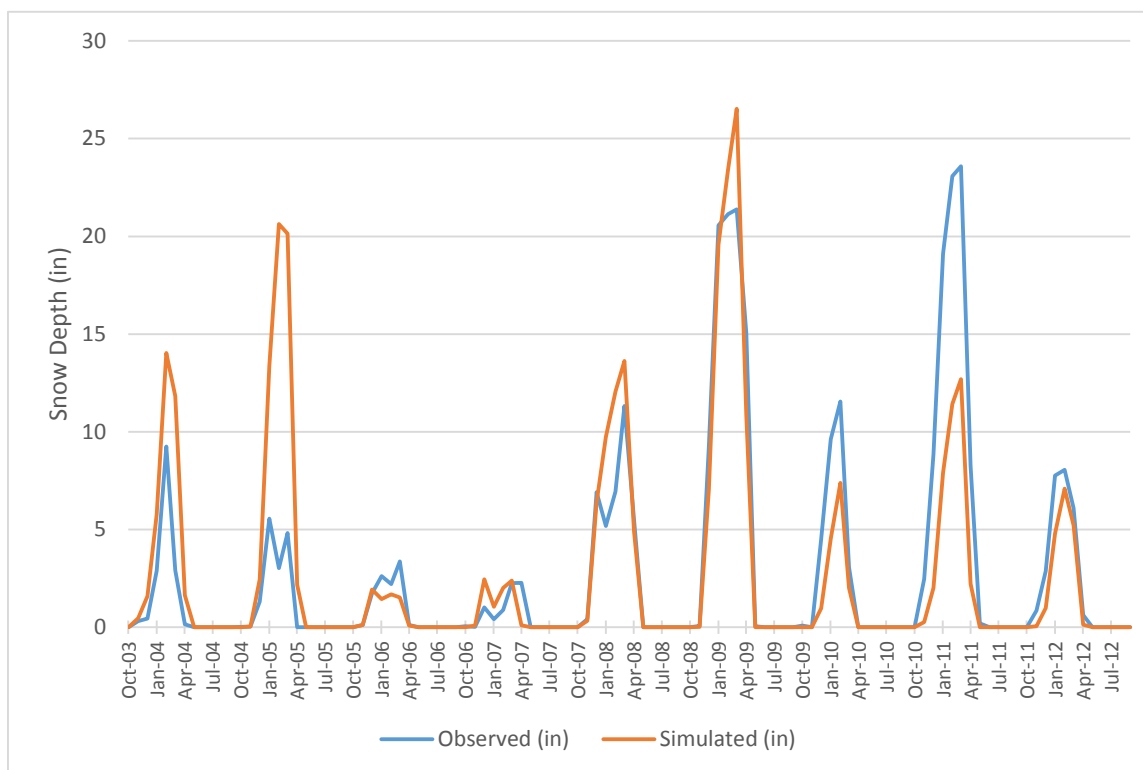


Figure 86. Mean monthly snow depth time-series for weather region 15

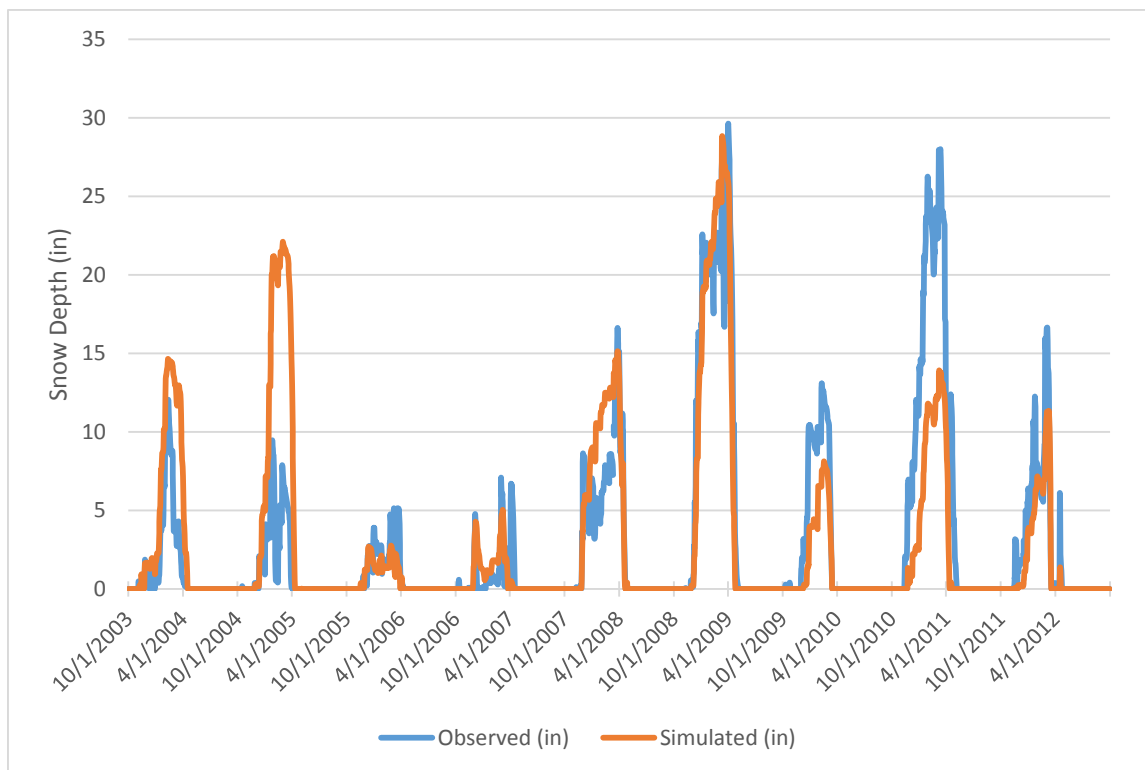


Figure 87. Mean daily snow depth time-series for weather region 15

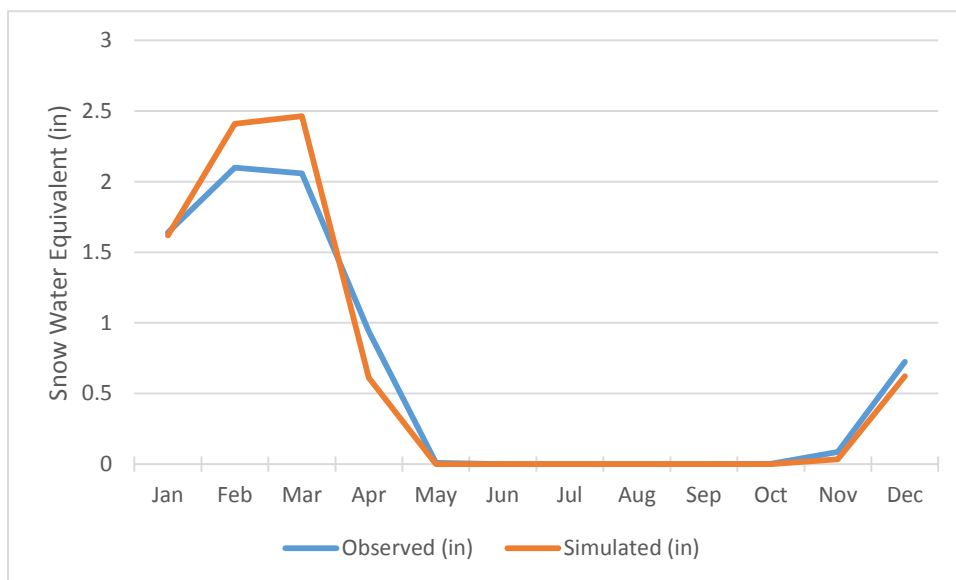


Figure 88. Mean monthly snow water equivalent for weather region 15

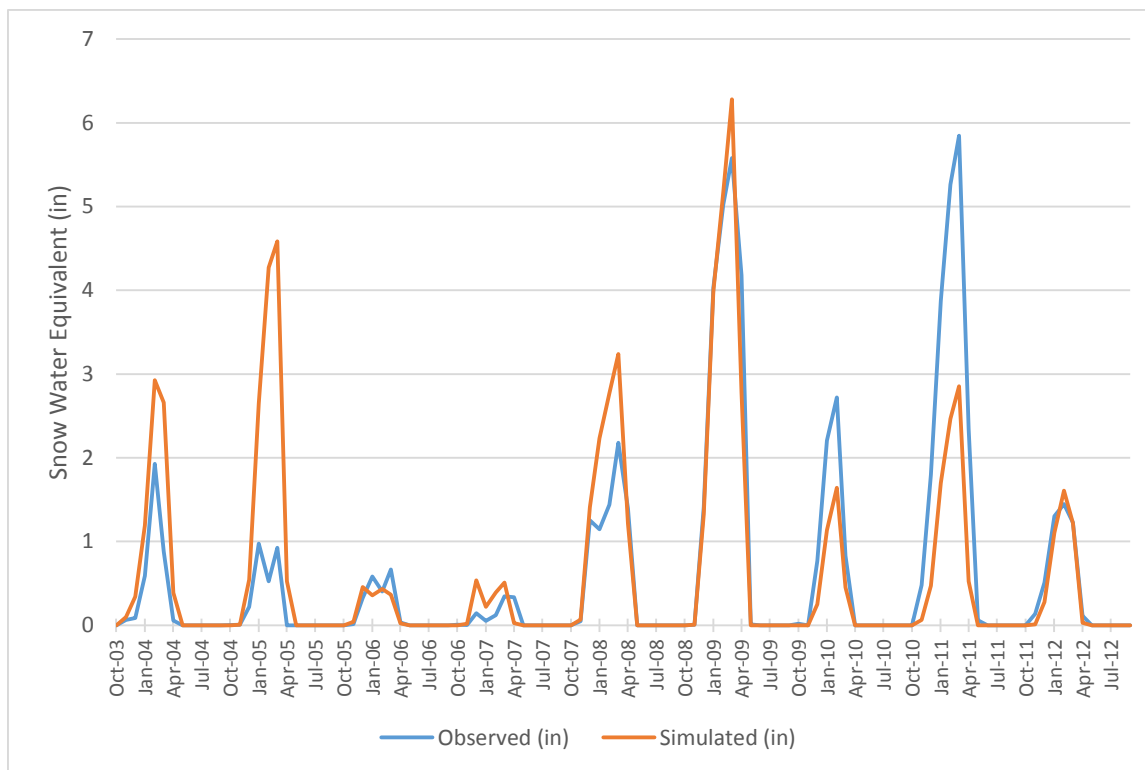


Figure 89. Mean monthly snow water equivalent time-series for weather region 15

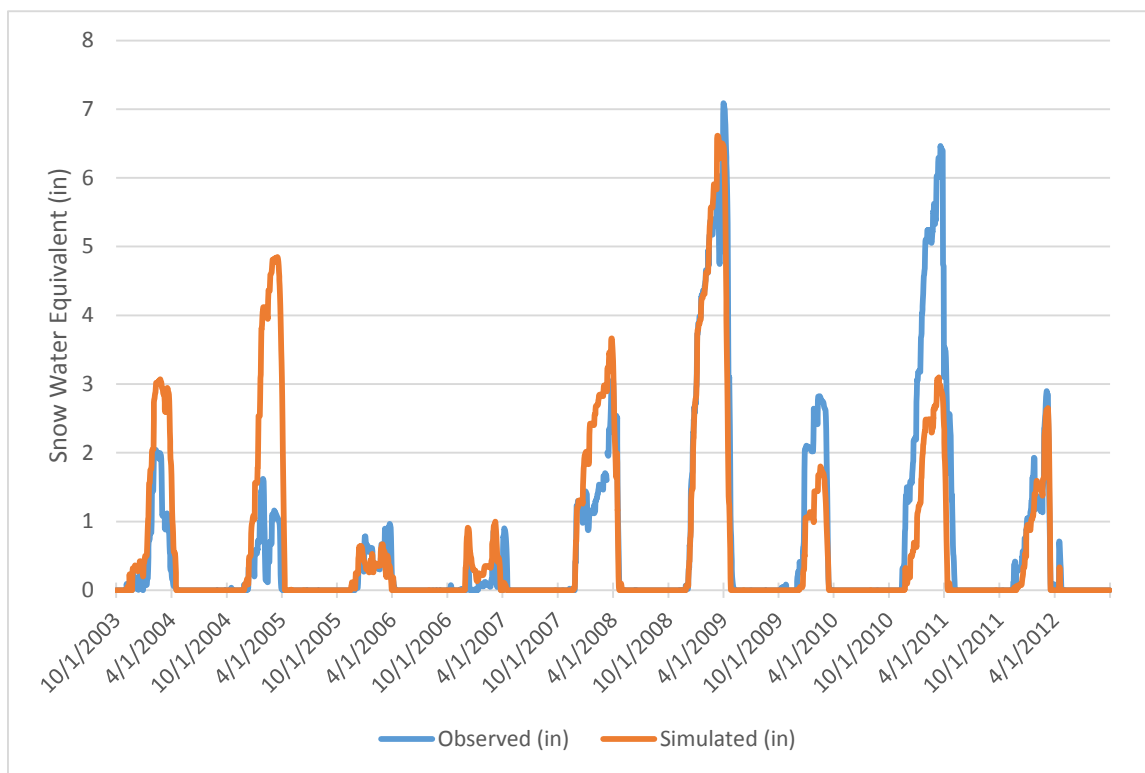


Figure 90. Mean daily snow water equivalent time-series for weather region 15

WEATHER REGION 16

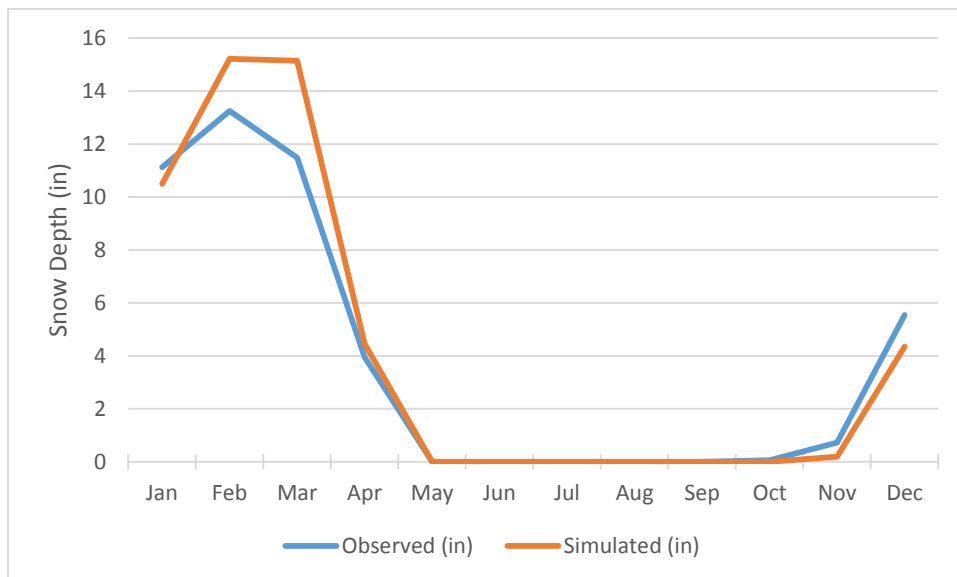


Figure 91. Mean monthly snow depth for weather region 16

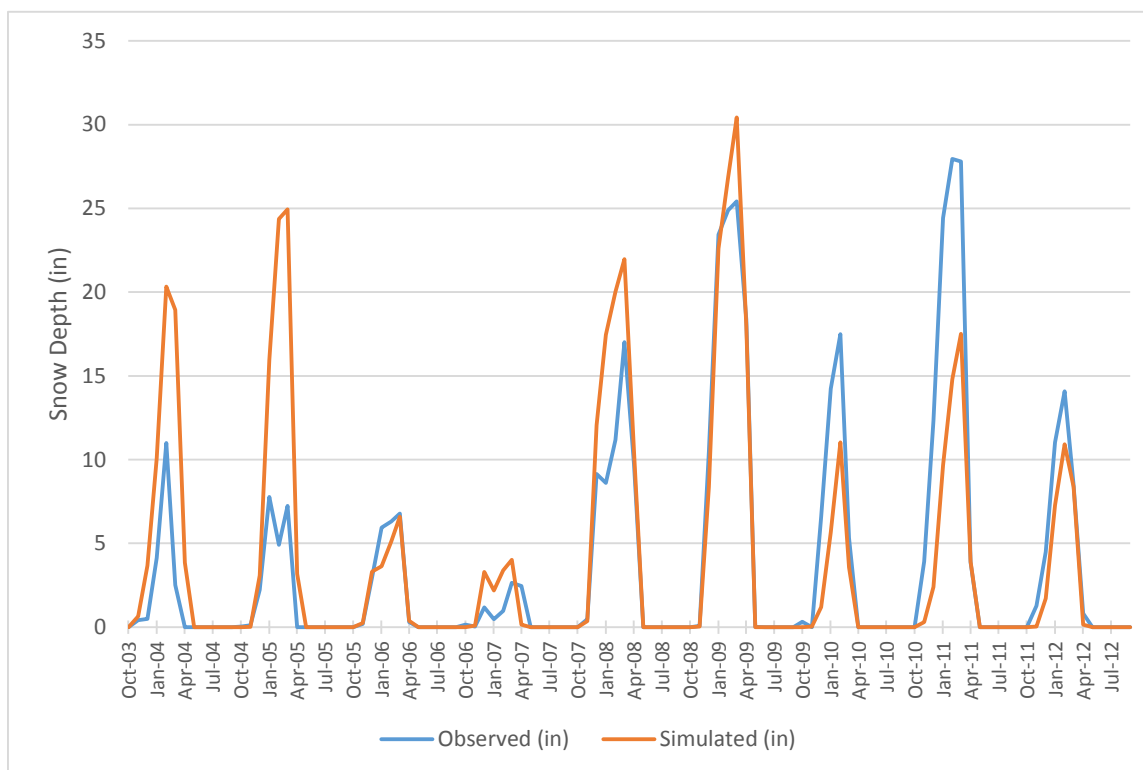


Figure 92. Mean monthly snow depth time-series for weather region 16

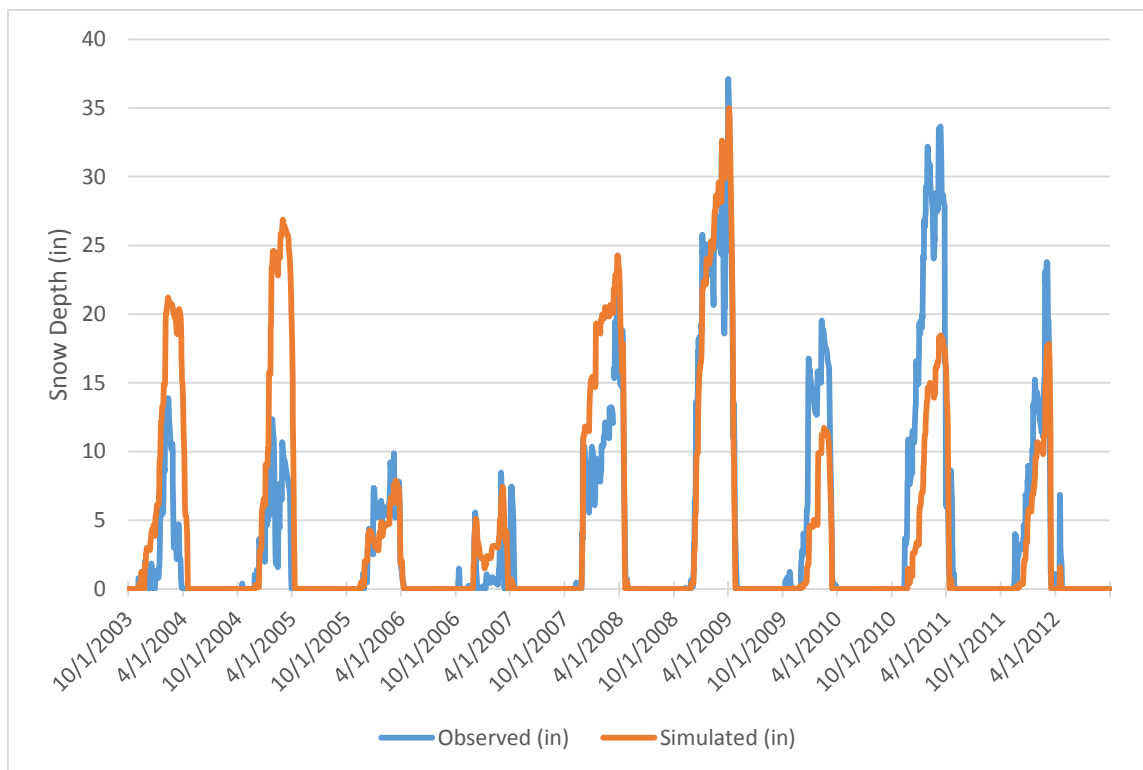


Figure 93. Mean daily snow depth time-series for weather region 16

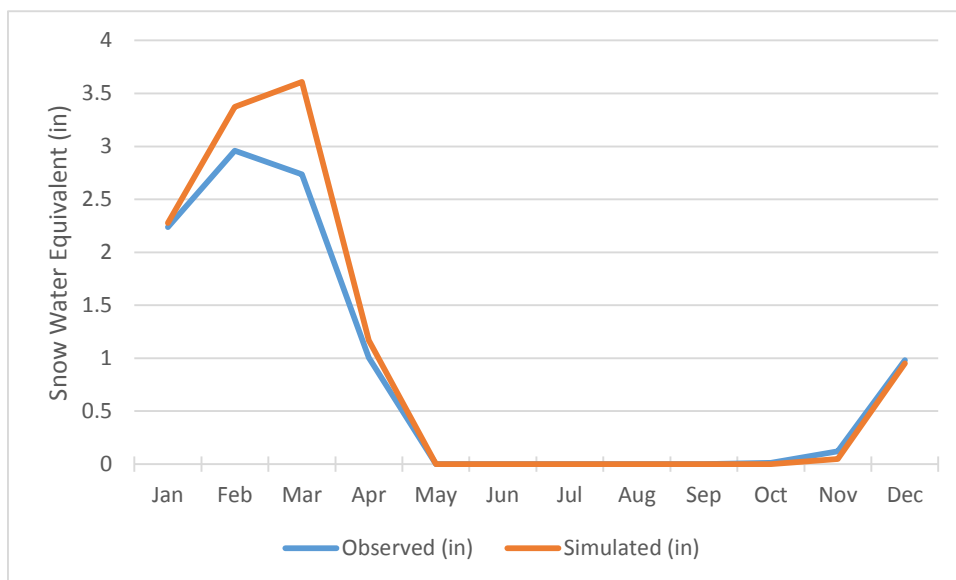


Figure 94. Mean monthly snow water equivalent for weather region 16

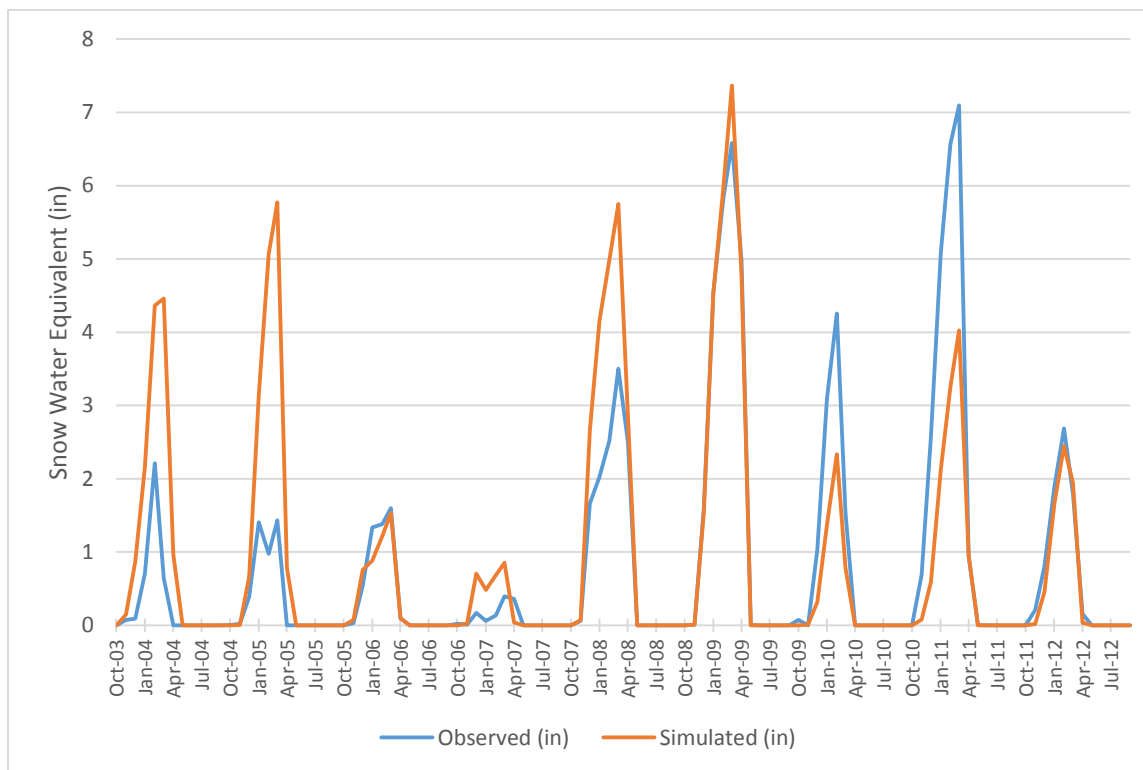


Figure 95. Mean monthly snow water equivalent time-series for weather region 16

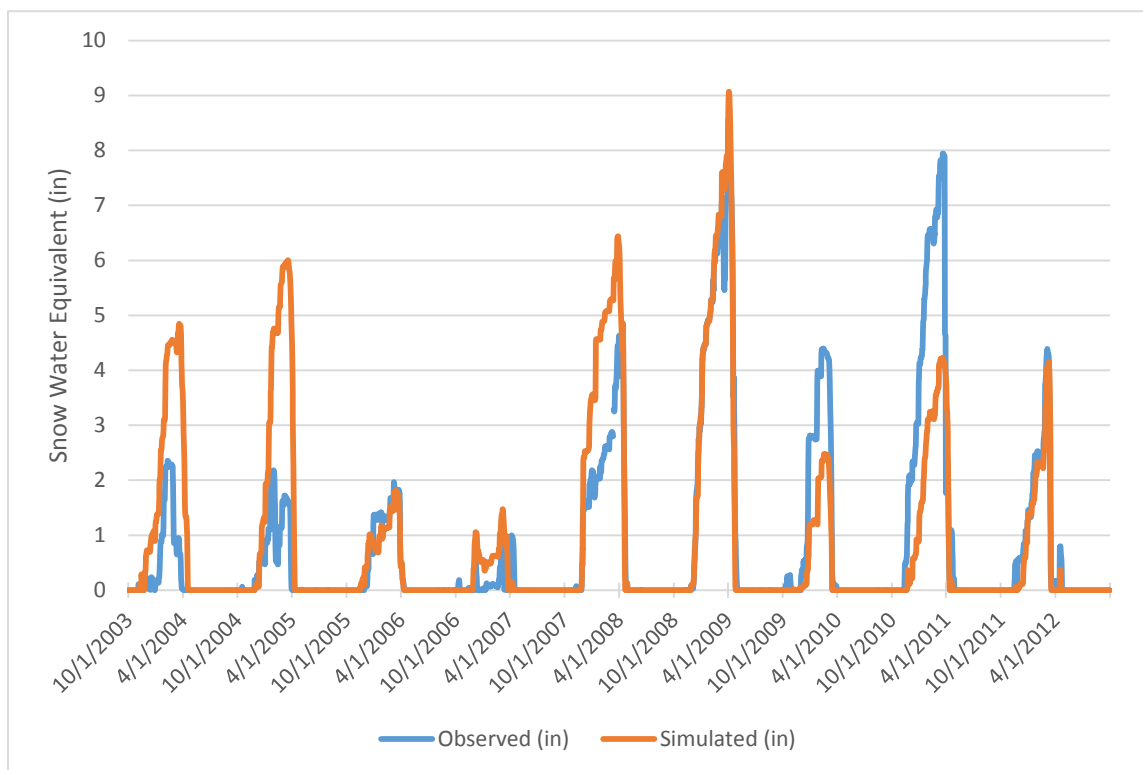


Figure 96. Mean daily snow water equivalent time-series for weather region 16

WEATHER REGION 17

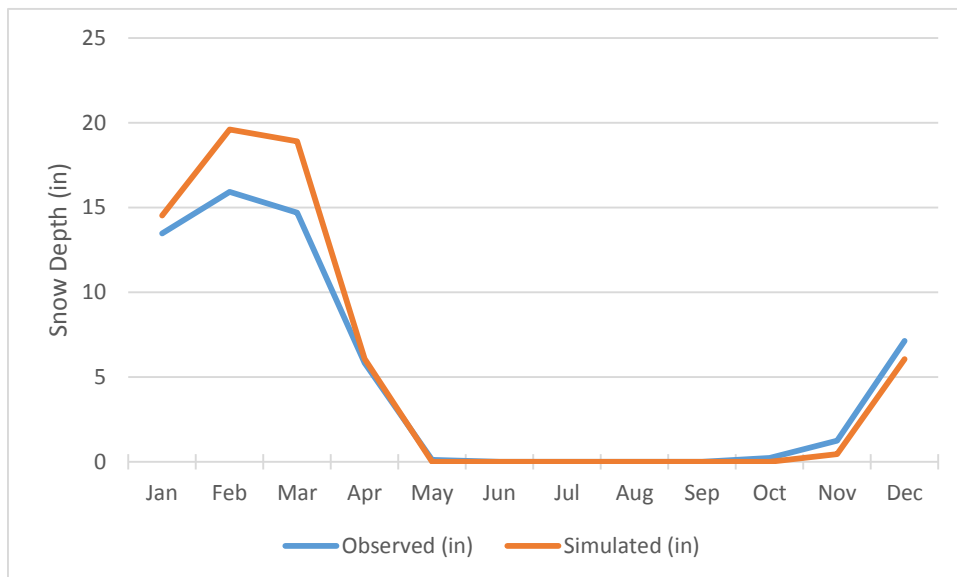


Figure 97. Mean monthly snow depth for weather region 17

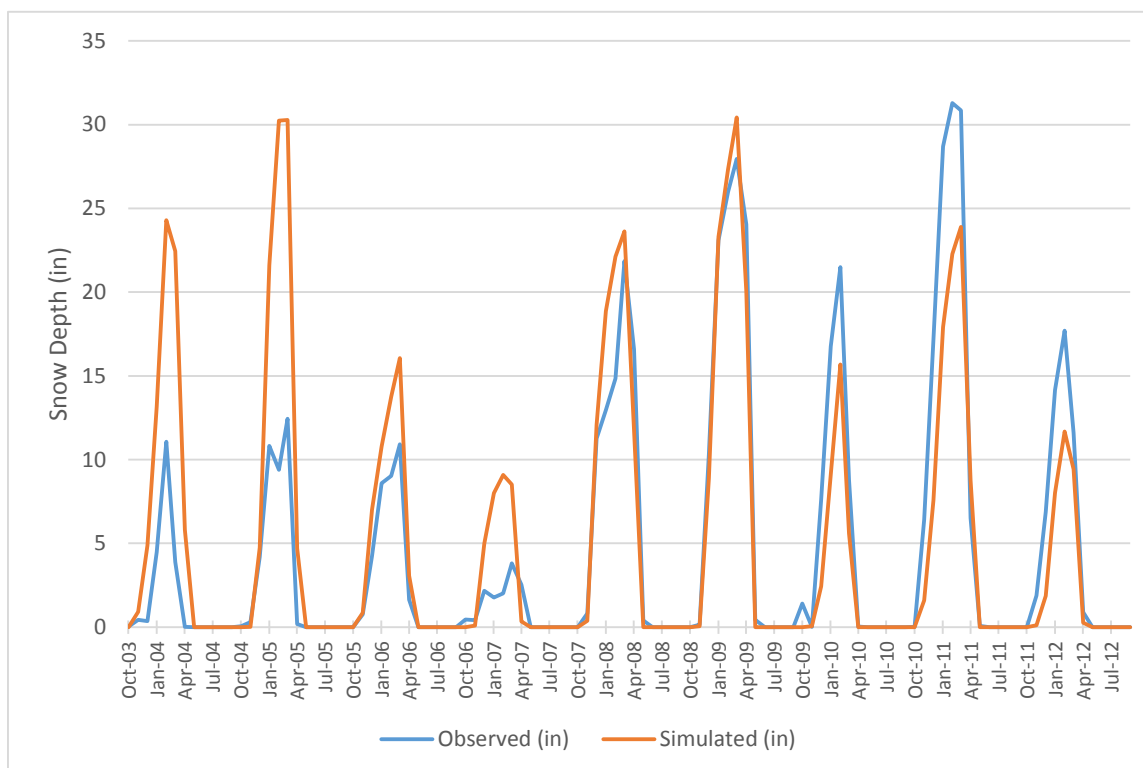


Figure 98. Mean monthly snow depth time-series for weather region 17

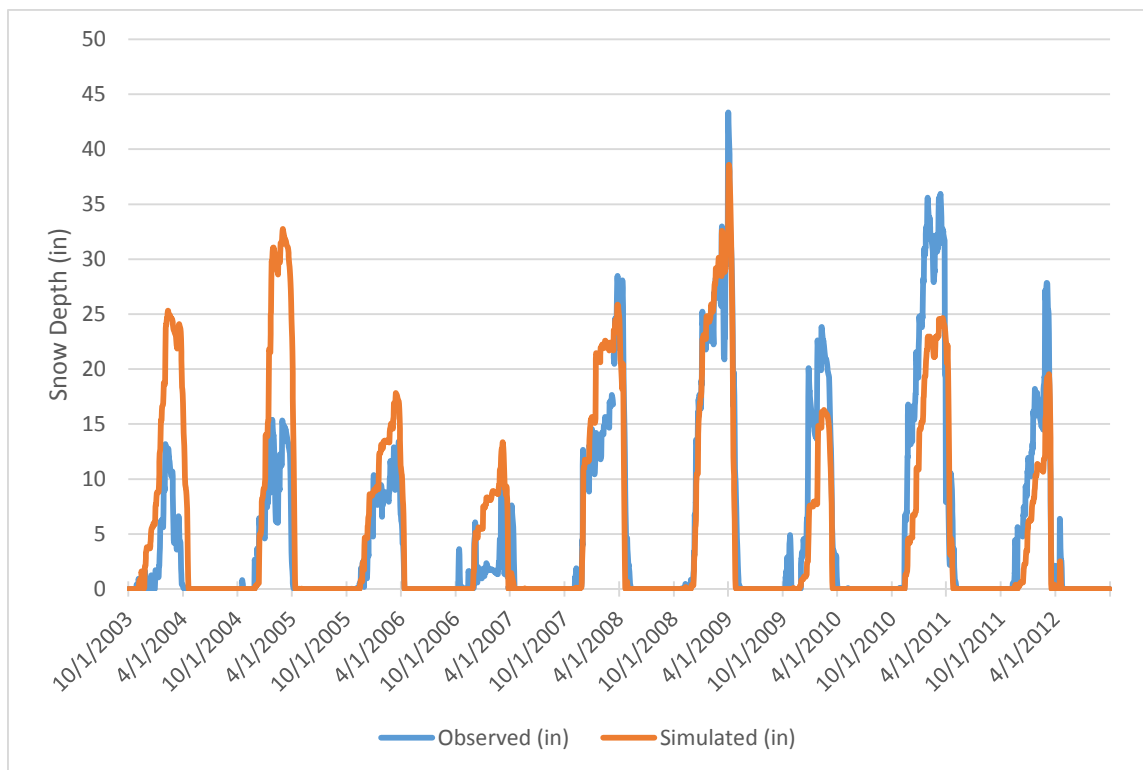


Figure 99. Mean daily snow depth time-series for weather region 17

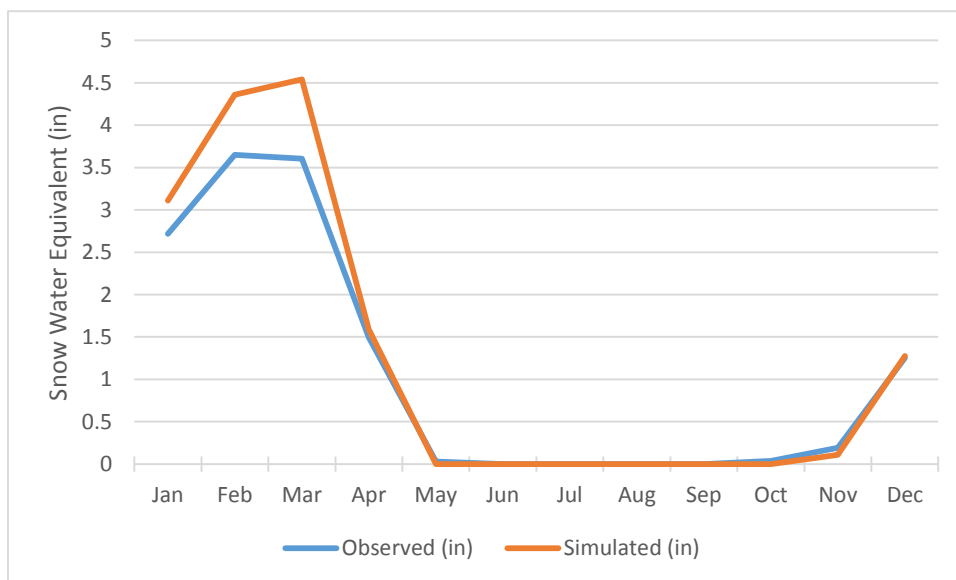


Figure 100. Mean monthly snow water equivalent for weather region 17

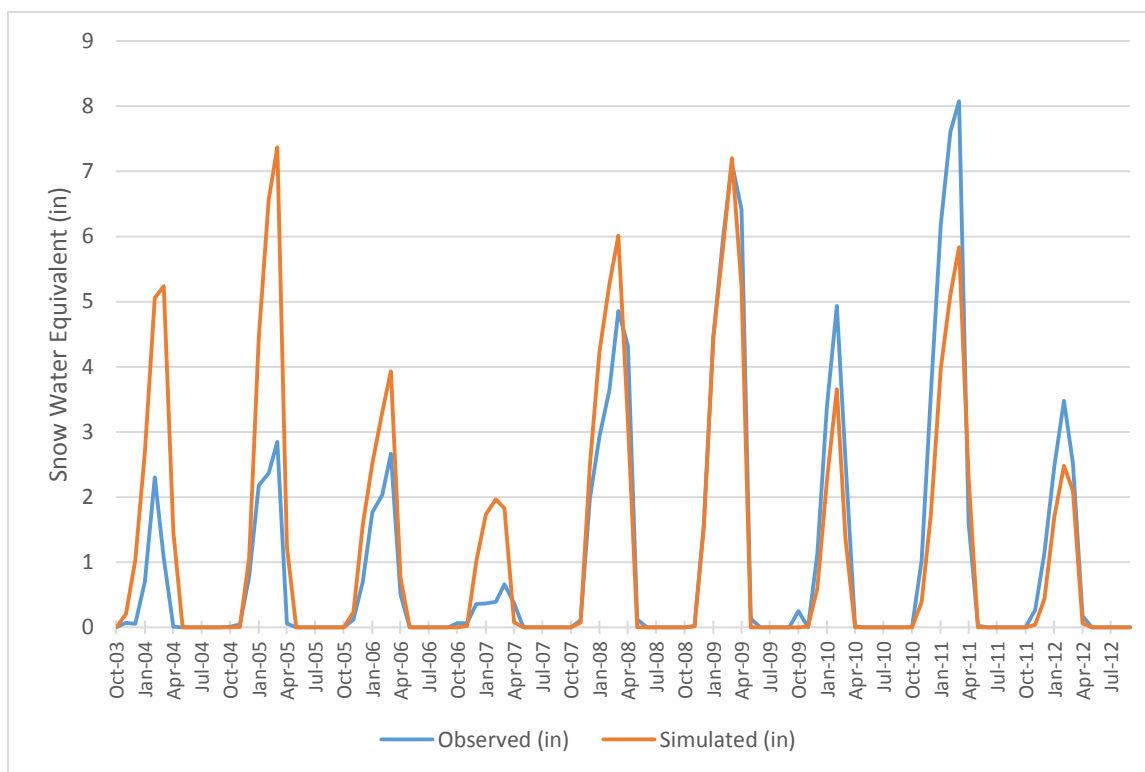


Figure 101. Mean monthly snow water equivalent time-series for weather region 17

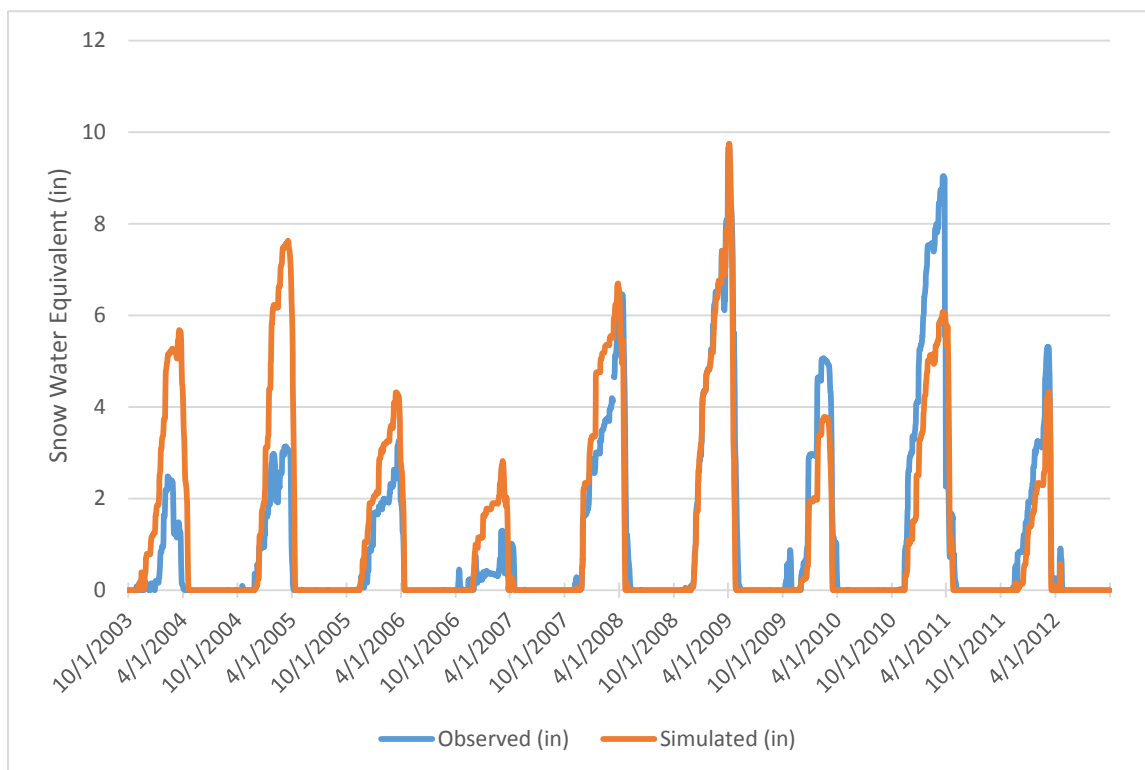


Figure 102. Mean daily snow water equivalent time-series for weather region 17

WEATHER REGION 18

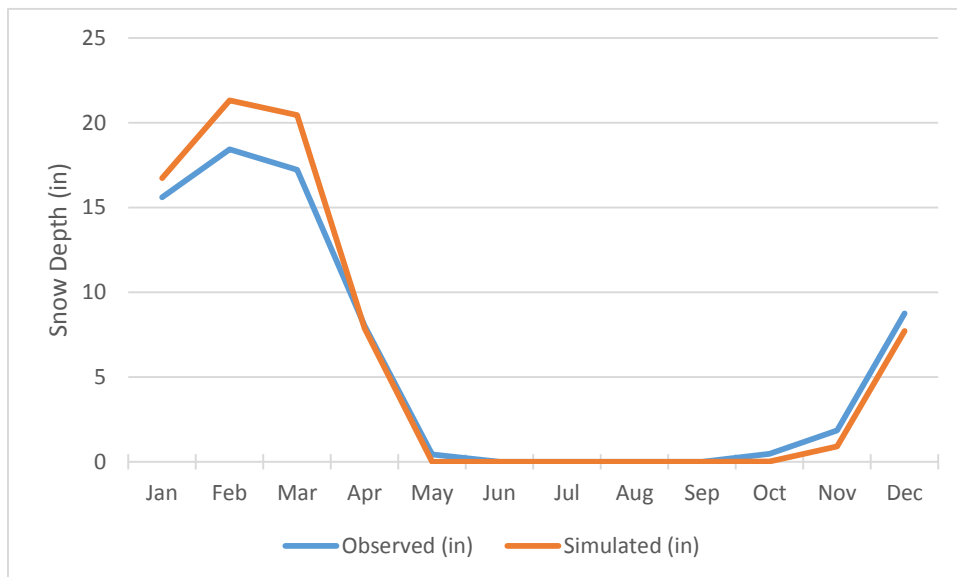


Figure 103. Mean monthly snow depth for weather region 18

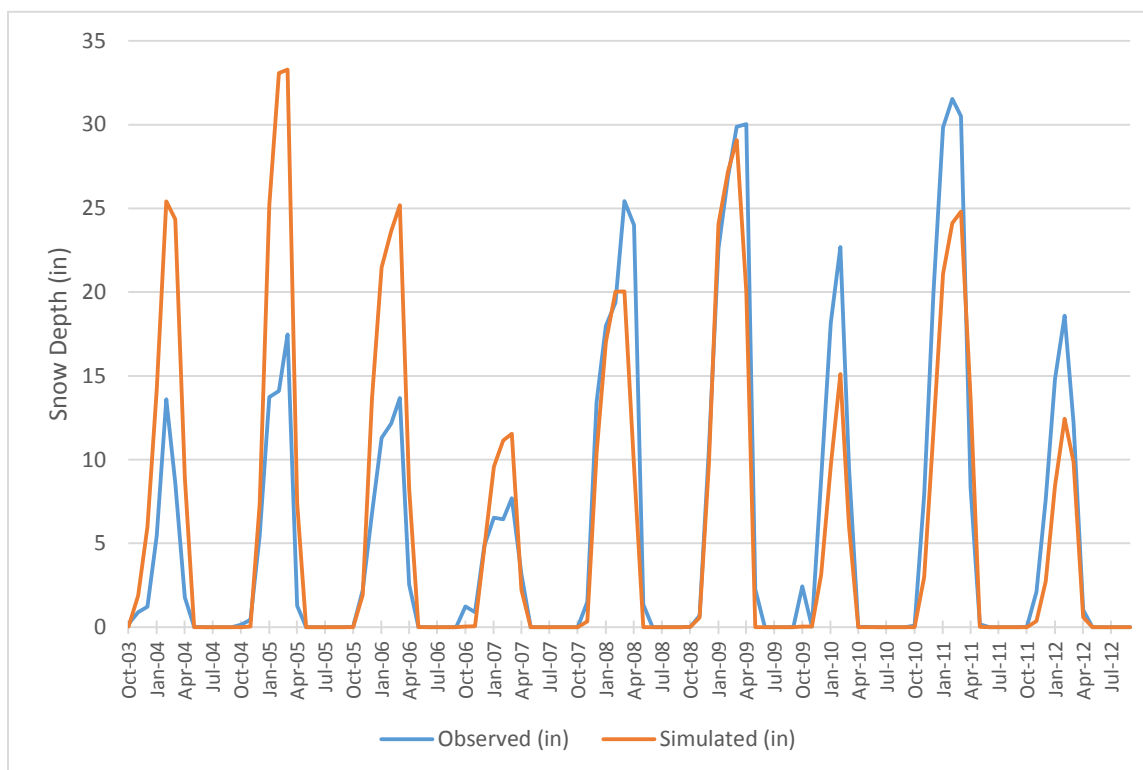


Figure 104. Mean monthly snow depth time-series for weather region 18

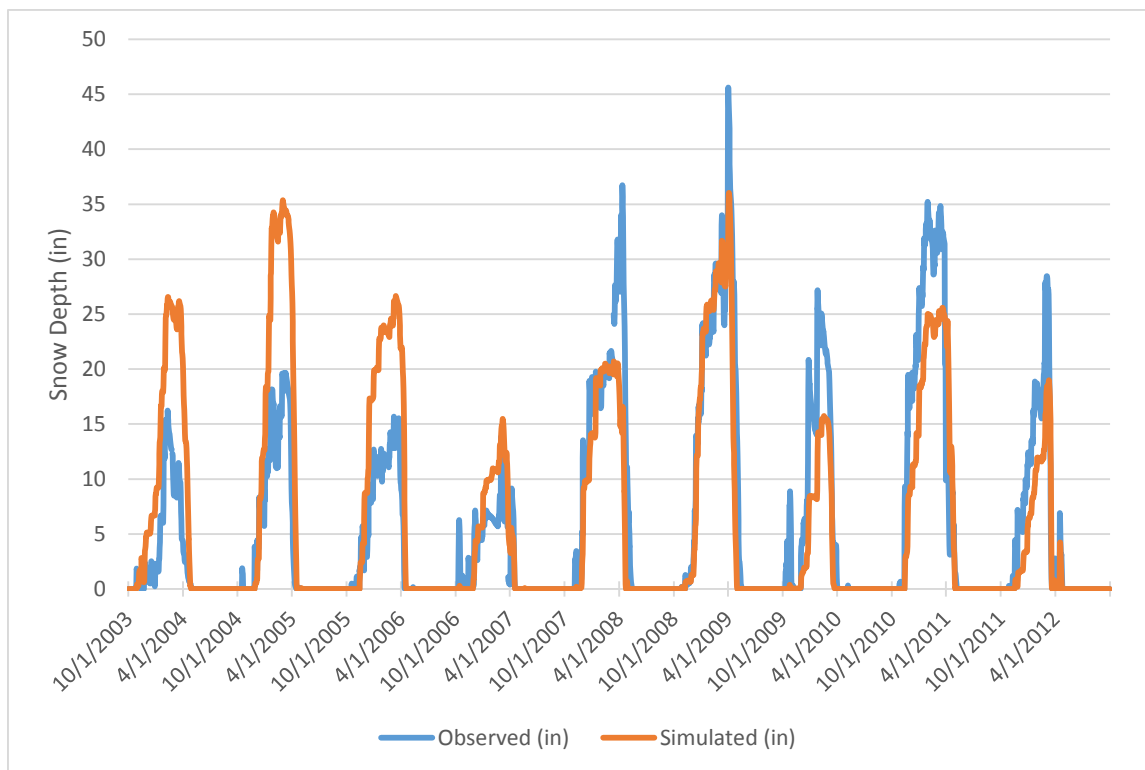


Figure 105. Mean daily snow depth time-series for weather region 18

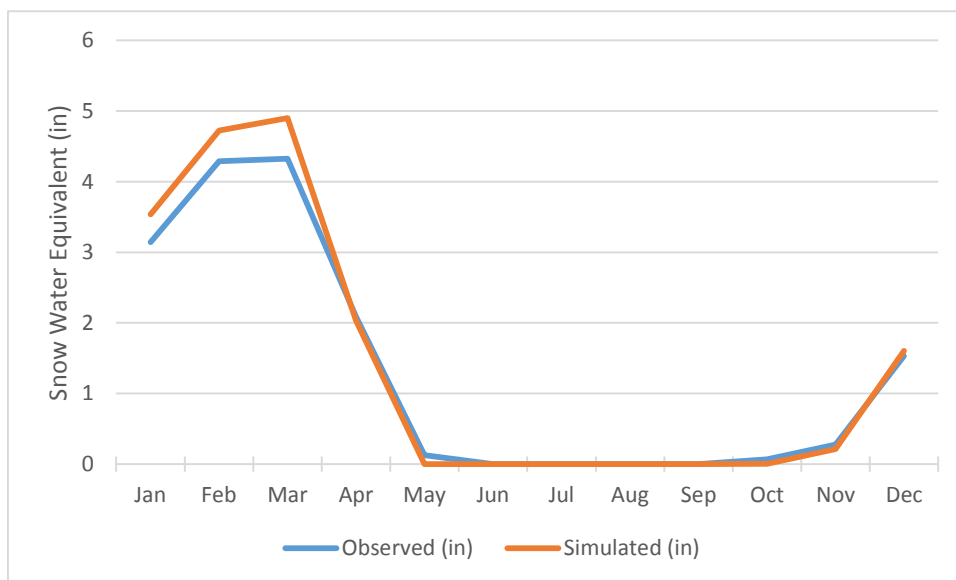


Figure 106. Mean monthly snow water equivalent for weather region 18

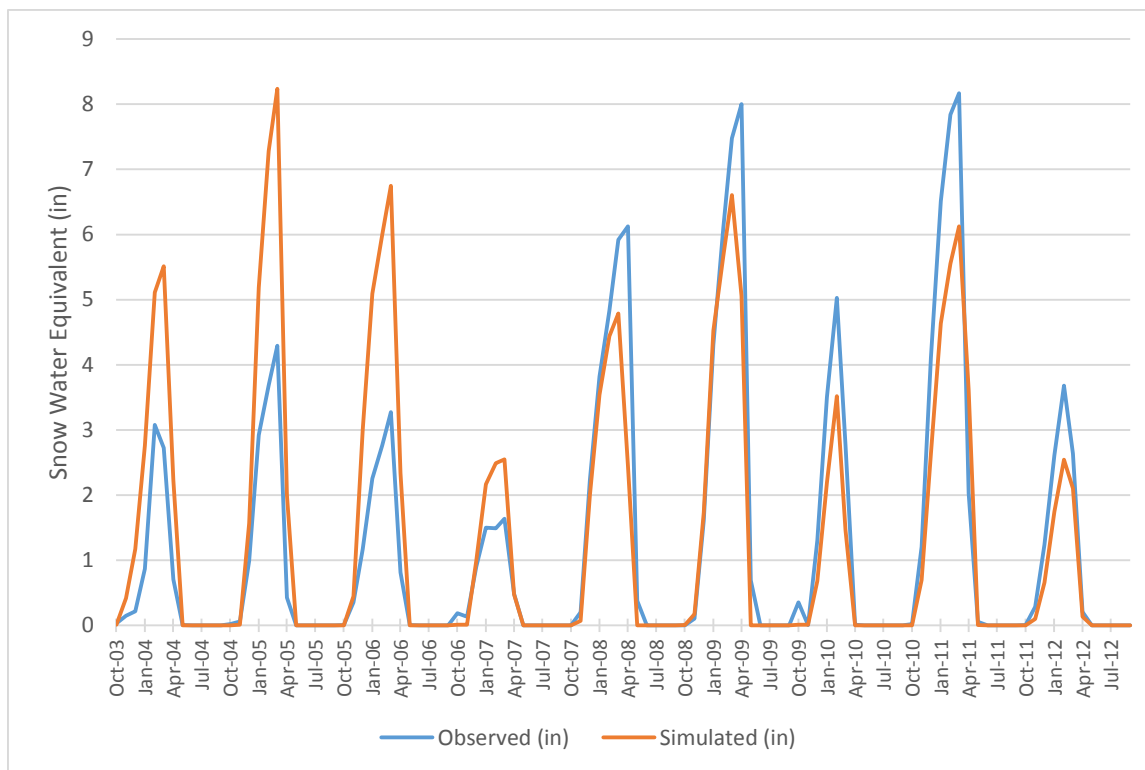


Figure 107. Mean monthly snow water equivalent time-series for weather region 18

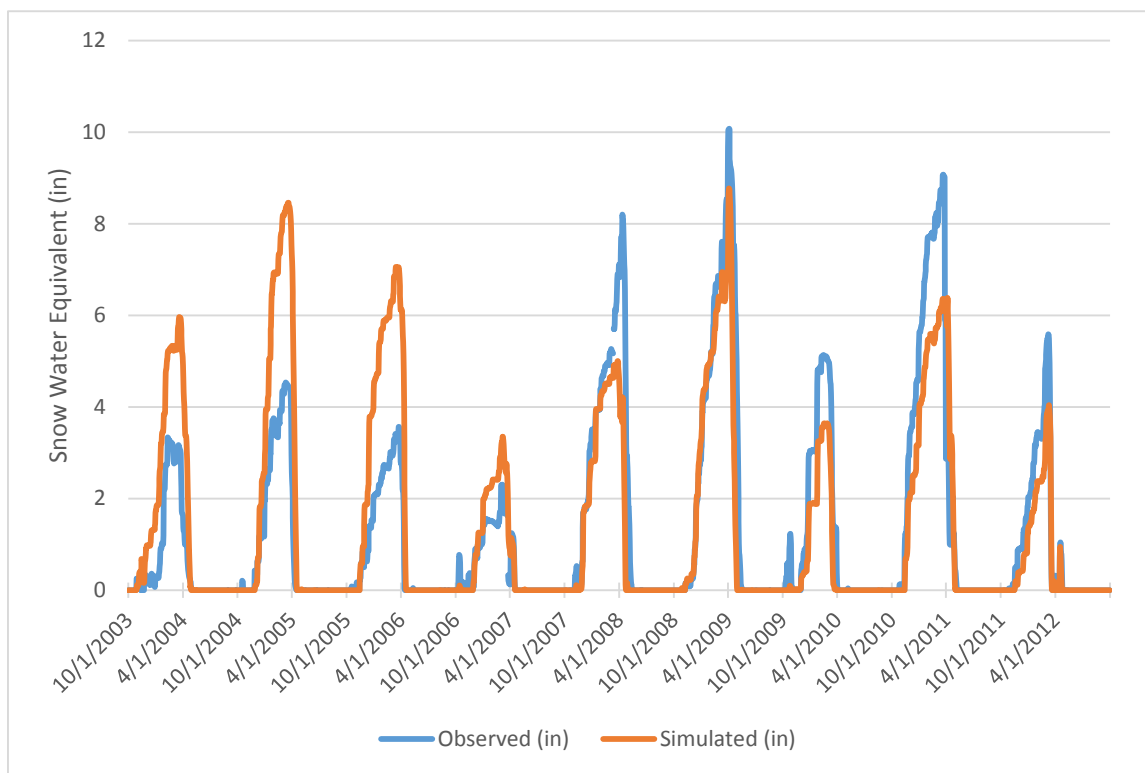


Figure 108. Mean daily snow water equivalent time-series for weather region 18

(This page left intentionally blank.)

(This page left intentionally blank.)

Appendix B. Detailed Flow Calibration Results

EAST BRANCH AMITY CREEK AT DULUTH (HYDSTRA 02037005)

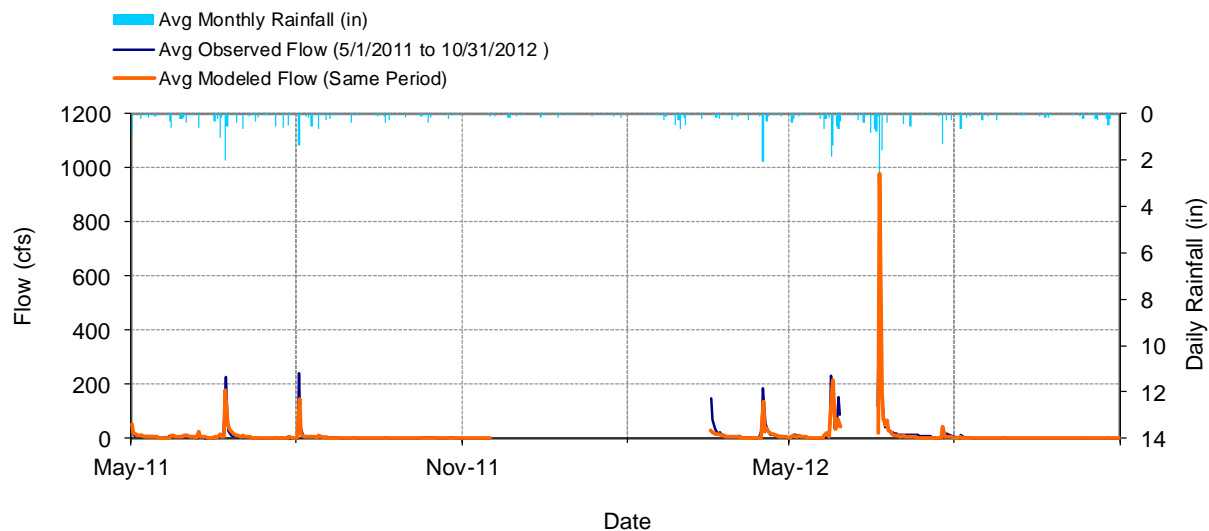


Figure 109. Mean daily flow at East Branch Amity Creek at Duluth

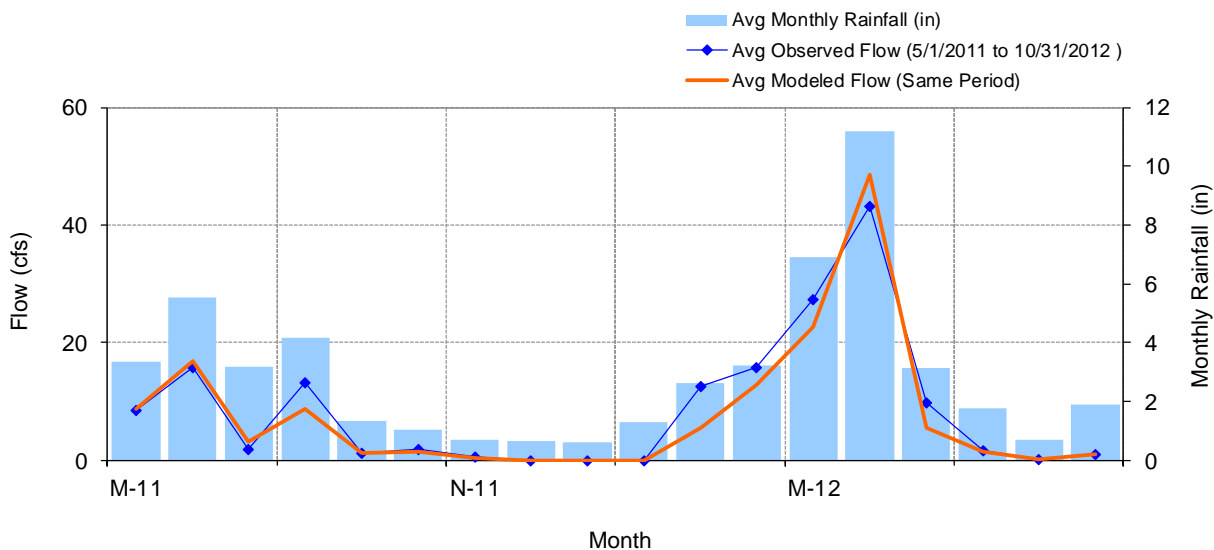


Figure 110. Mean monthly flow at East Branch Amity Creek at Duluth

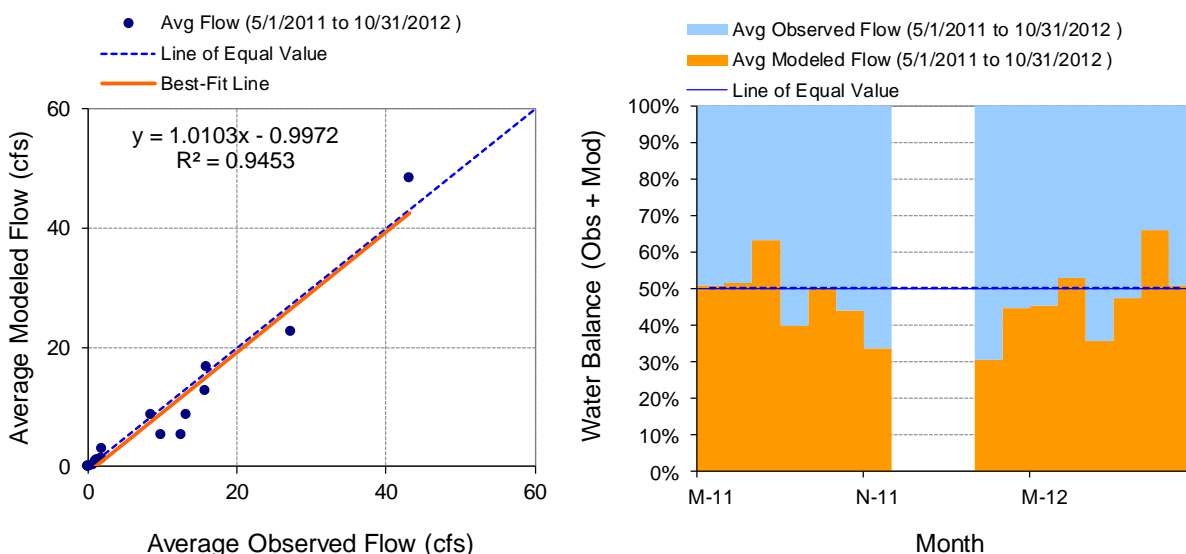


Figure 111. Monthly flow regression and temporal variation at East Branch Amity Creek at Duluth

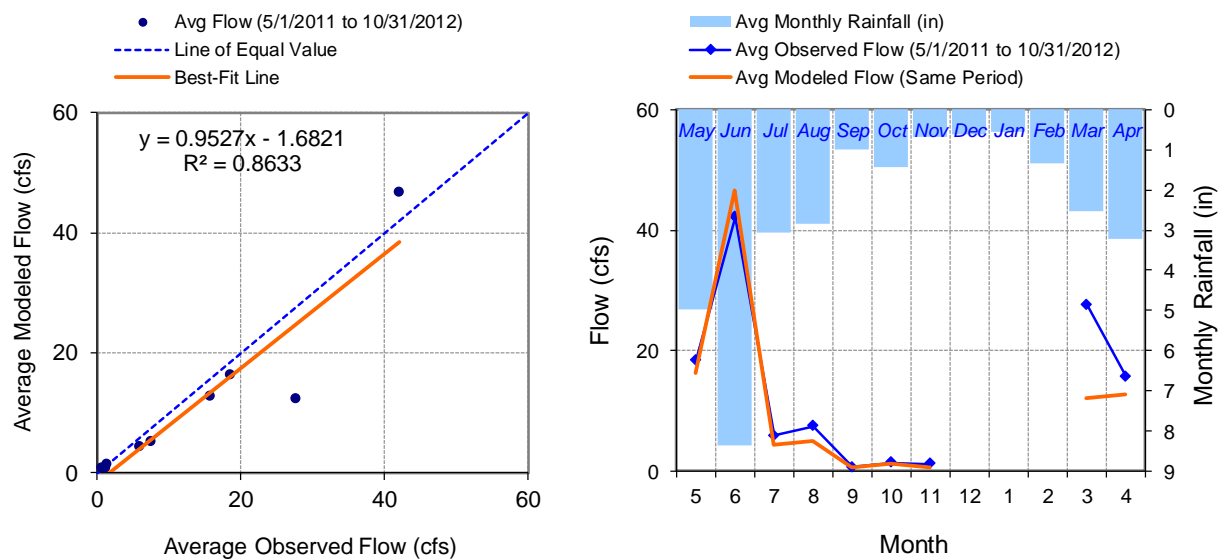


Figure 112. Seasonal regression and temporal aggregate at East Branch Amity Creek at Duluth

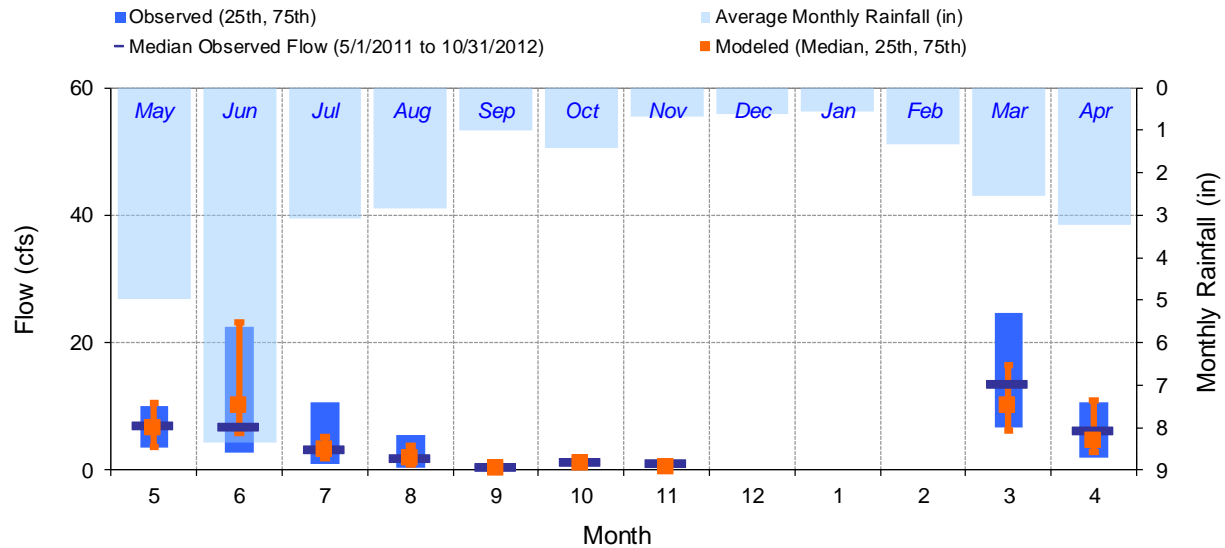


Figure 113. Seasonal medians and ranges at East Branch Amity Creek at Duluth

Table 1. Seasonal summary at East Branch Amity Creek at Duluth

MONTH	OBSERVED FLOW (CFS)				MODELED FLOW (CFS)			
	MEAN	MEDIAN	25TH	75TH	MEAN	MEDIAN	25TH	75TH
May	18.46	6.90	3.58	10.00	16.22	6.54	3.69	10.56
Jun	42.11	6.85	2.75	22.50	46.62	10.15	5.79	23.14
Jul	5.84	3.25	0.91	10.75	4.29	3.15	1.95	5.26
Aug	7.39	1.80	0.33	5.50	5.06	1.80	0.83	3.74
Sep	0.61	0.44	0.08	1.03	0.65	0.31	0.14	1.02
Oct	1.38	1.30	1.10	1.60	1.21	0.99	0.52	1.68
Nov	1.13	1.10	1.10	1.20	0.57	0.53	0.40	0.77
Dec	0.00	0.00	0.00	0.00	0.00	0.00	0.00	0.00
Jan	0.00	0.00	0.00	0.00	0.00	0.00	0.00	0.00
Feb	0.00	0.00	0.00	0.00	0.00	0.00	0.00	0.00
Mar	27.61	13.50	6.65	24.75	12.11	10.20	6.30	16.41
Apr	15.73	6.30	1.93	10.75	12.69	4.60	2.85	10.88

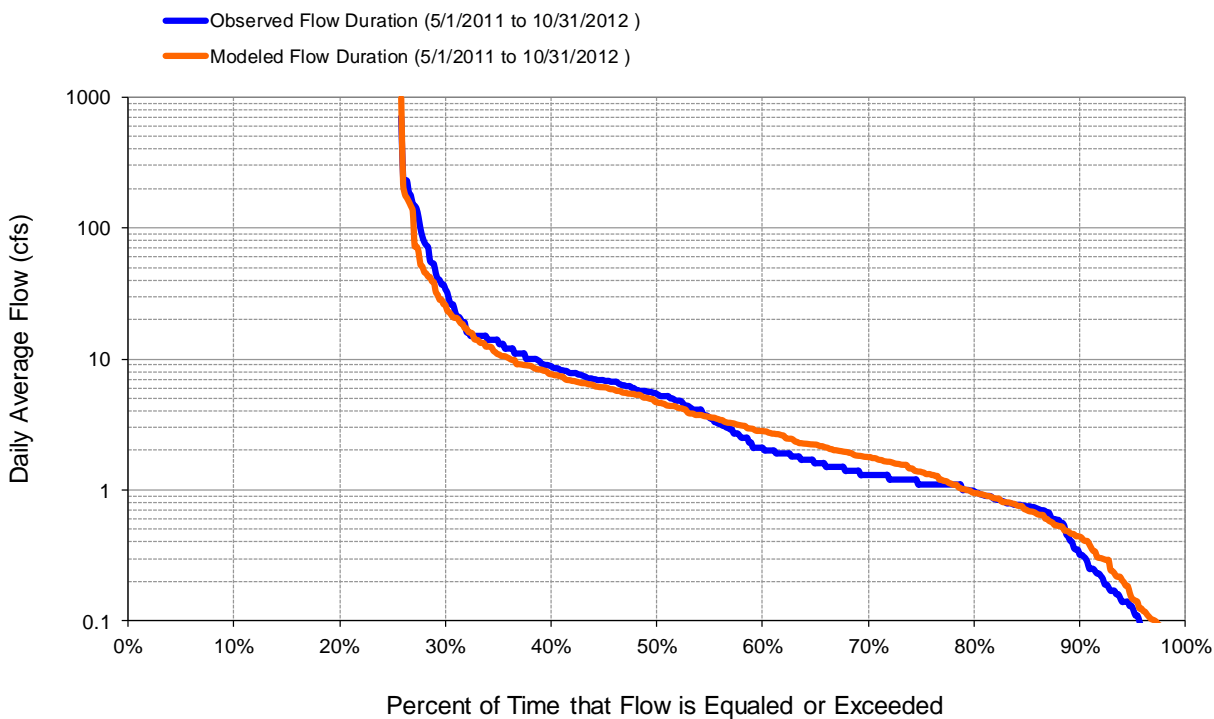


Figure 114. Flow exceedance at East Branch Amity Creek at Duluth

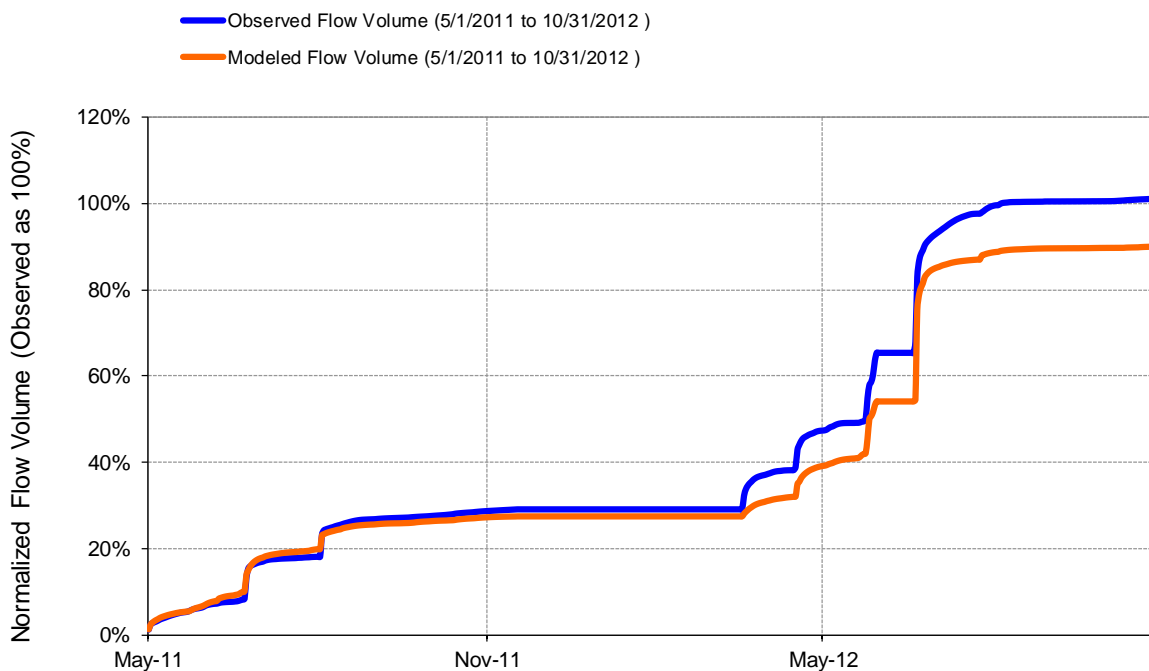


Figure 115. Flow accumulation at East Branch Amity Creek at Duluth

Table 2. Summary statistics at East Branch Amity Creek at Duluth

HSPF Simulated Flow		Observed Flow Gage	
REACH OUTFLOW FROM DSN 110 1.51-Year Analysis Period: 5/1/2011 - 10/31/2012 Flow volumes are (inches/year) for upstream drainage area		East Branch Amity Creek at Duluth, 1.8 mi DS of CSAH Manually Entered Data Drainage Area (sq-mi): 8.12	
Total Simulated In-stream Flow:	12.73	Total Observed In-stream Flow:	14.28
Total of simulated highest 10% flows:	9.26	Total of Observed highest 10% flows:	10.62
Total of Simulated lowest 50% flows:	0.63	Total of Observed Lowest 50% flows:	0.53
Simulated Summer Flow Volume (months 7-9):	1.88	Observed Summer Flow Volume (7-9):	2.61
Simulated Fall Flow Volume (months 10-12):	0.26	Observed Fall Flow Volume (10-12):	0.32
Simulated Winter Flow Volume (months 1-3):	0.52	Observed Winter Flow Volume (1-3):	1.18
Simulated Spring Flow Volume (months 4-6):	10.07	Observed Spring Flow Volume (4-6):	10.18
Total Simulated Storm Volume:	7.23	Total Observed Storm Volume:	7.50
Simulated Summer Storm Volume (7-9):	0.81	Observed Summer Storm Volume (7-9):	1.17
<i>Errors (Simulated-Observed)</i>	<i>Error Statistics</i>	<i>Recommended Criteria</i>	
Error in total volume:	-10.87	10	
Error in 50% lowest flows:	20.75	10	
Error in 10% highest flows:	-12.88	15	
Seasonal volume error - Summer:	-27.75	30	
Seasonal volume error - Fall:	-18.62	30	
Seasonal volume error - Winter:	-56.14	30	
Seasonal volume error - Spring:	-1.08	30	
Error in storm volumes:	-3.55	20	
Error in summer storm volumes:	-31.43	50	
Nash-Sutcliffe Coefficient of Efficiency, E:	0.820	Model accuracy increases	
Baseline adjusted coefficient (Garrick), E':	0.678		
Monthly NSE	0.930		

AMITY CREEK AT DULUTH (HYDSTRA 02038001)

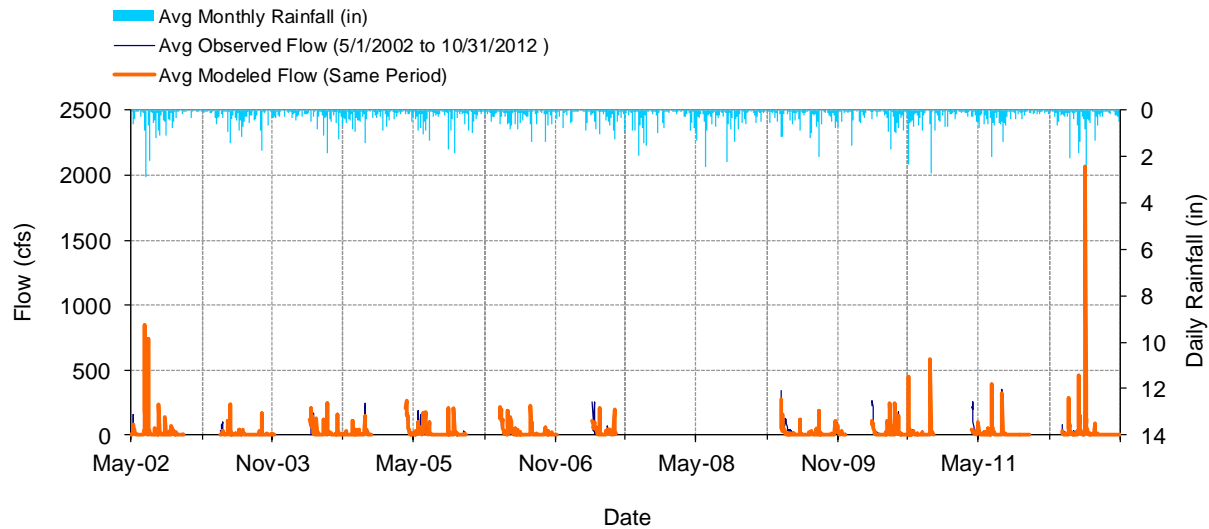


Figure 116. Mean daily flow at Amity Creek at Duluth

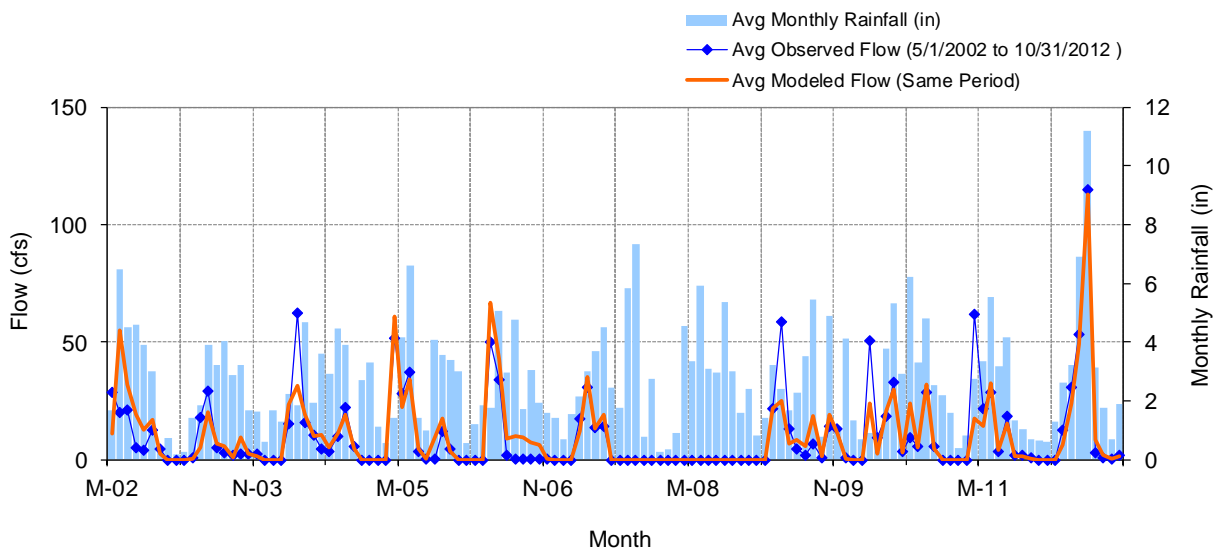


Figure 117. Mean monthly flow at Amity Creek at Duluth

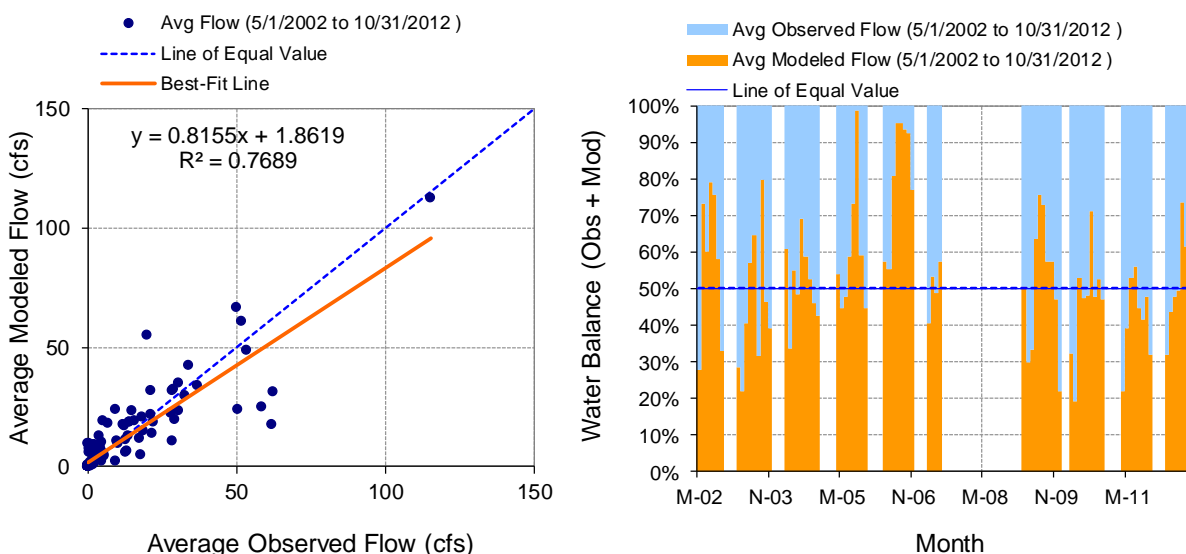


Figure 118. Monthly flow regression and temporal variation at Amity Creek at Duluth

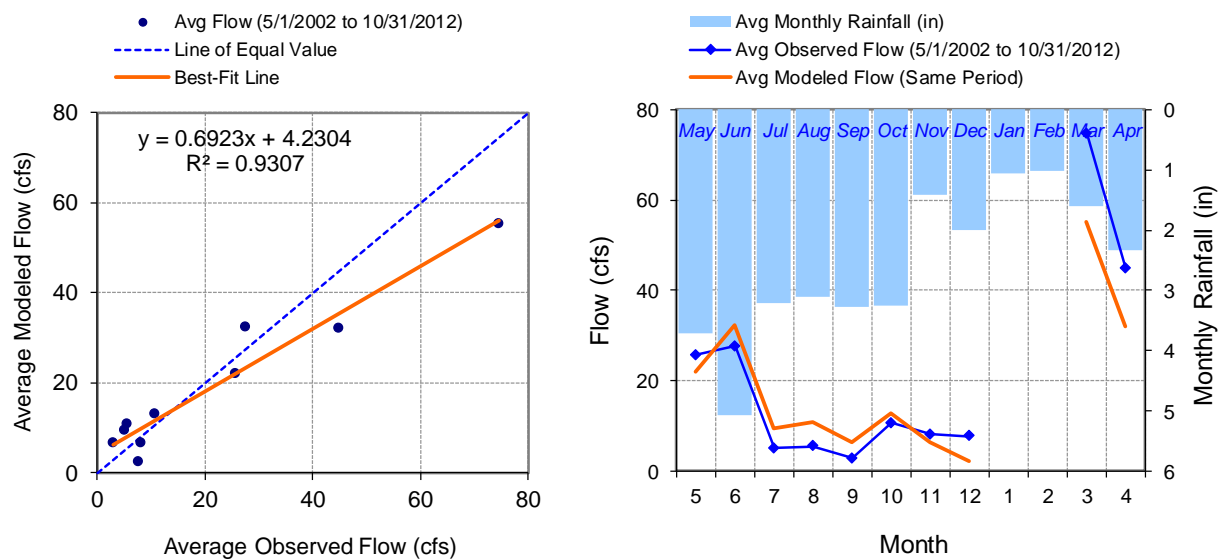


Figure 119. Seasonal regression and temporal aggregate at Amity Creek at Duluth

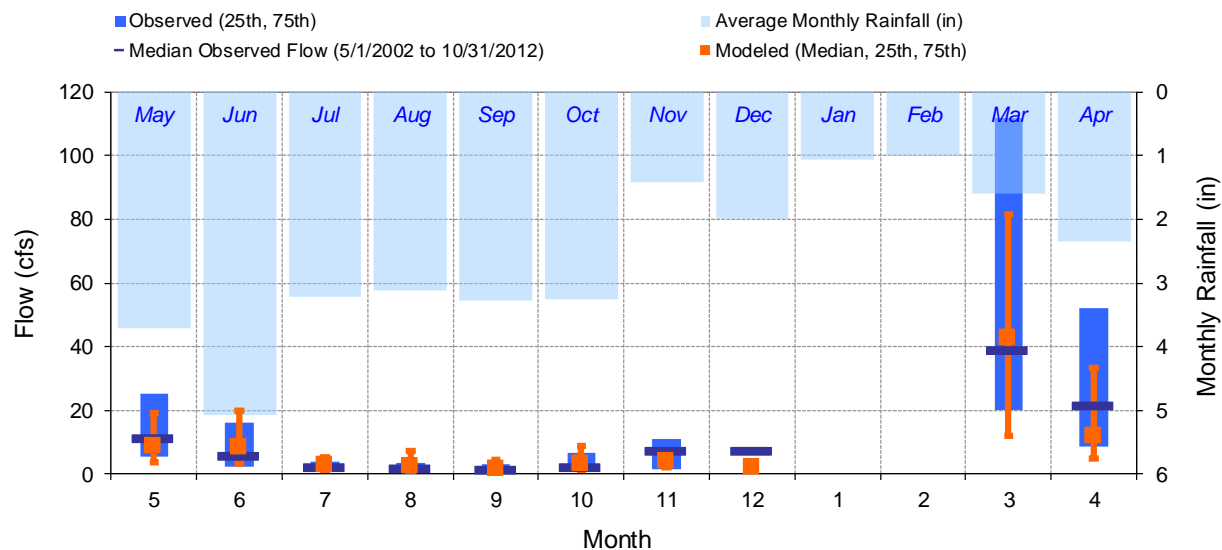


Figure 120. Seasonal medians and ranges at Amity Creek at Duluth

Table 3. Seasonal summary at Amity Creek at Duluth

MONTH	OBSERVED FLOW (CFS)				MODELED FLOW (CFS)			
	MEAN	MEDIAN	25TH	75TH	MEAN	MEDIAN	25TH	75TH
May	25.67	11.32	5.54	25.23	21.84	8.79	3.91	19.01
Jun	27.59	5.71	2.53	16.00	32.34	8.48	3.27	20.02
Jul	4.99	2.02	1.09	3.83	9.39	2.81	1.29	5.38
Aug	5.42	1.83	0.48	3.69	10.72	2.44	0.96	7.42
Sep	2.83	1.40	0.38	3.05	6.43	1.72	0.30	4.38
Oct	10.66	2.30	1.35	6.50	12.86	3.49	1.30	8.91
Nov	8.11	7.10	1.50	11.00	6.39	4.02	2.01	6.78
Dec	7.73	7.40	7.08	8.05	2.16	2.14	1.96	2.34
Jan	0.00	0.00	0.00	0.00	0.00	0.00	0.00	0.00
Feb	0.00	0.00	0.00	0.00	0.00	0.00	0.00	0.00
Mar	74.68	39.00	20.00	111.71	55.21	42.93	11.98	81.51
Apr	44.78	21.50	8.55	51.93	32.04	12.03	5.06	33.36

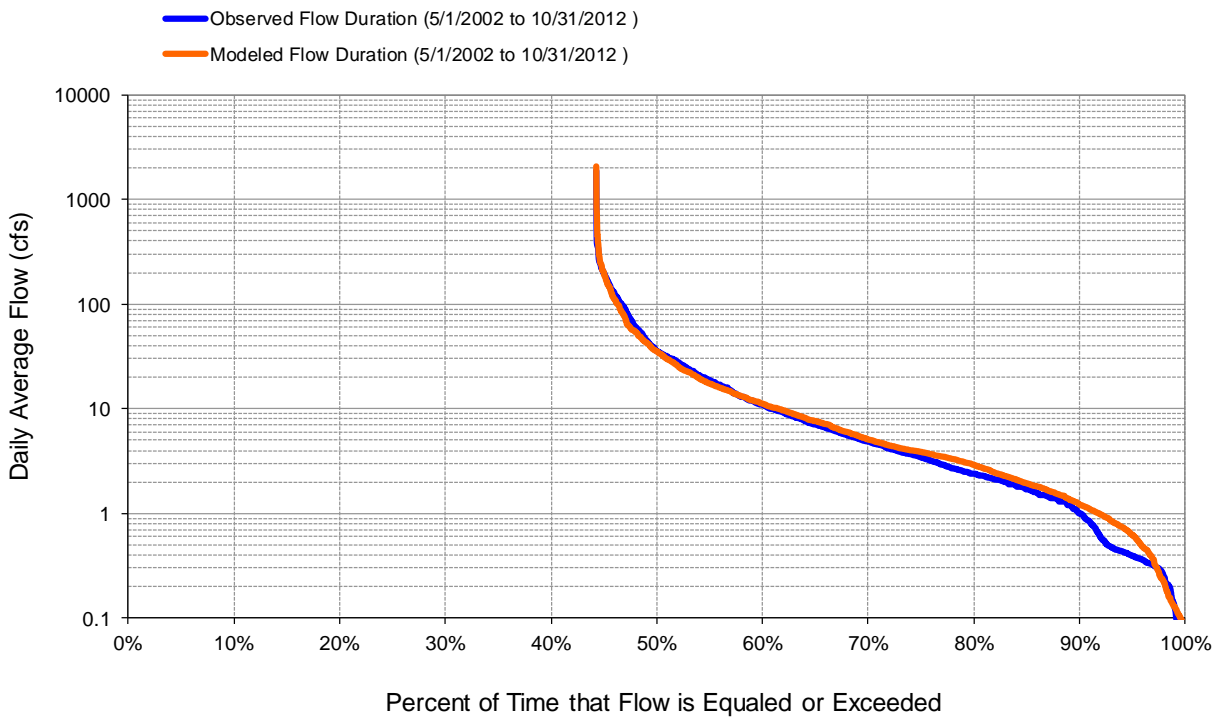


Figure 121. Flow exceedance at Amity Creek at Duluth

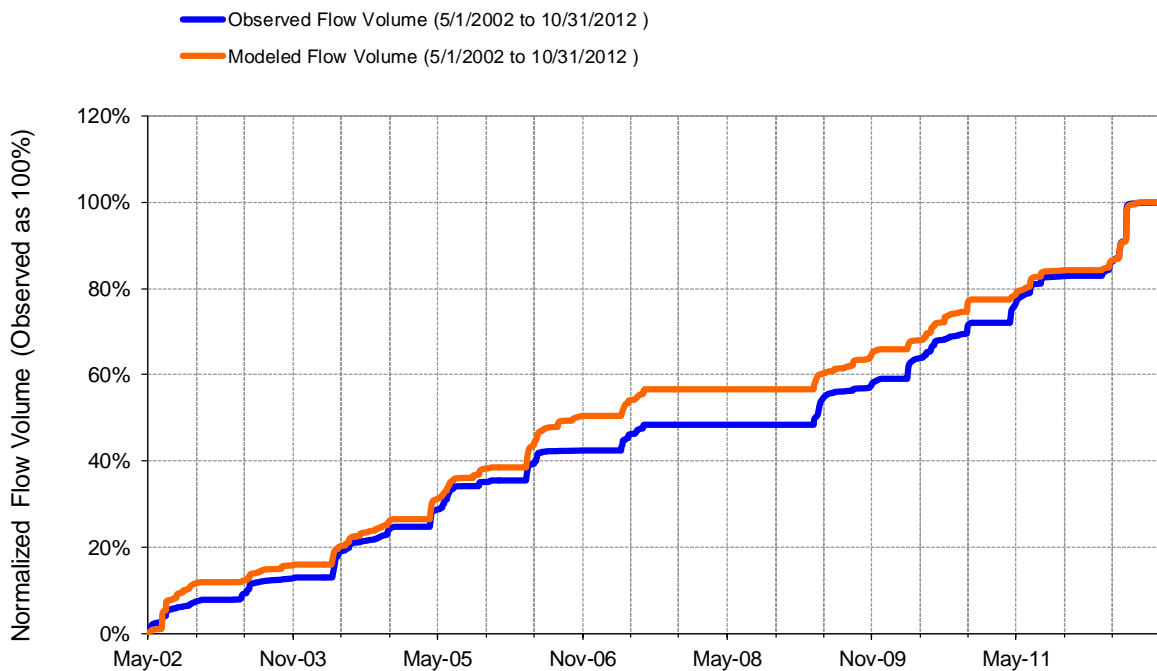


Figure 122. Flow accumulation at Amity Creek at Duluth

Table 4. Summary statistics at Amity Creek at Duluth

HSPF Simulated Flow		Observed Flow Gage	
REACH OUTFLOW FROM DSN 10 10.51-Year Analysis Period: 5/1/2002 - 10/31/2012 Flow volumes are (inches/year) for upstream drainage area		Amity Creek at Duluth, Occidental Blvd. Manually Entered Data Drainage Area (sq-mi): 16.7	
Total Simulated In-stream Flow:	8.20	Total Observed In-stream Flow:	8.19
Total of simulated highest 10% flows:	5.43	Total of Observed highest 10% flows:	5.45
Total of Simulated lowest 50% flows:	0.45	Total of Observed Lowest 50% flows:	0.38
Simulated Summer Flow Volume (months 7-9):	1.53	Observed Summer Flow Volume (7-9):	0.77
Simulated Fall Flow Volume (months 10-12):	0.95	Observed Fall Flow Volume (10-12):	0.87
Simulated Winter Flow Volume (months 1-3):	0.57	Observed Winter Flow Volume (1-3):	0.78
Simulated Spring Flow Volume (months 4-6):	5.15	Observed Spring Flow Volume (4-6):	5.78
Total Simulated Storm Volume:	4.04	Total Observed Storm Volume:	3.49
Simulated Summer Storm Volume (7-9):	0.95	Observed Summer Storm Volume (7-9):	0.40
<i>Errors (Simulated-Observed)</i>	<i>Error Statistics</i>	<i>Recommended Criteria</i>	
Error in total volume:	0.13	10	
Error in 50% lowest flows:	17.69	10	
Error in 10% highest flows:	-0.42	15	
Seasonal volume error - Summer:	100.29	30	
Seasonal volume error - Fall:	8.69	30	
Seasonal volume error - Winter:	-26.07	30	
Seasonal volume error - Spring:	-10.92	30	
Error in storm volumes:	15.95	20	
Error in summer storm volumes:	140.35	50	
Nash-Sutcliffe Coefficient of Efficiency, E:	0.653	Model accuracy increases	
Baseline adjusted coefficient (Garrick), E':	0.488		
Monthly NSE	0.712		

TALMADGE RIVER NEAR DULUTH (HYDSTRA 02035001)

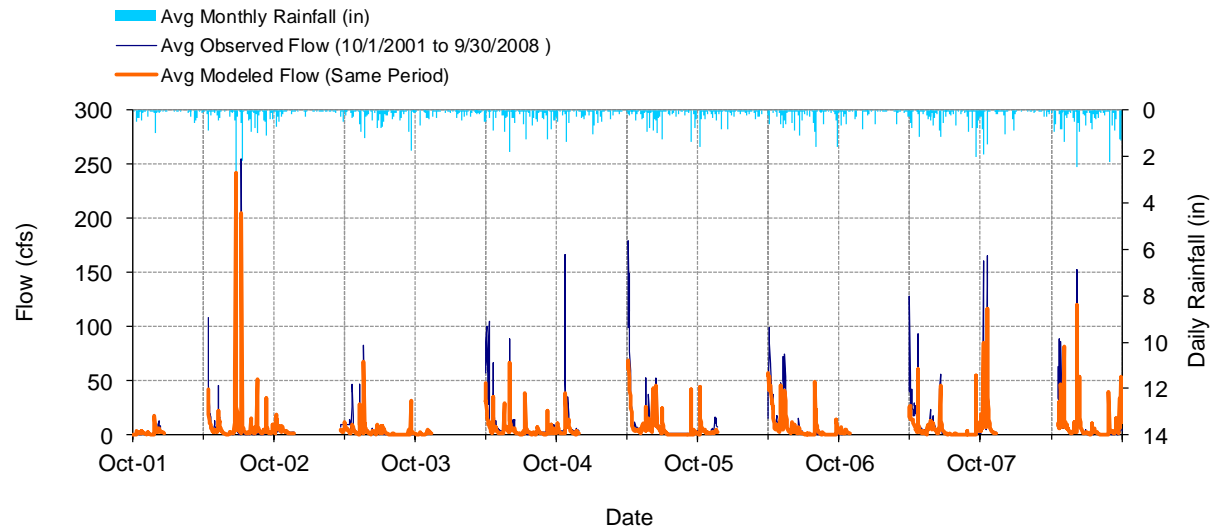


Figure 123. Mean daily flow at Talmadge River near Duluth

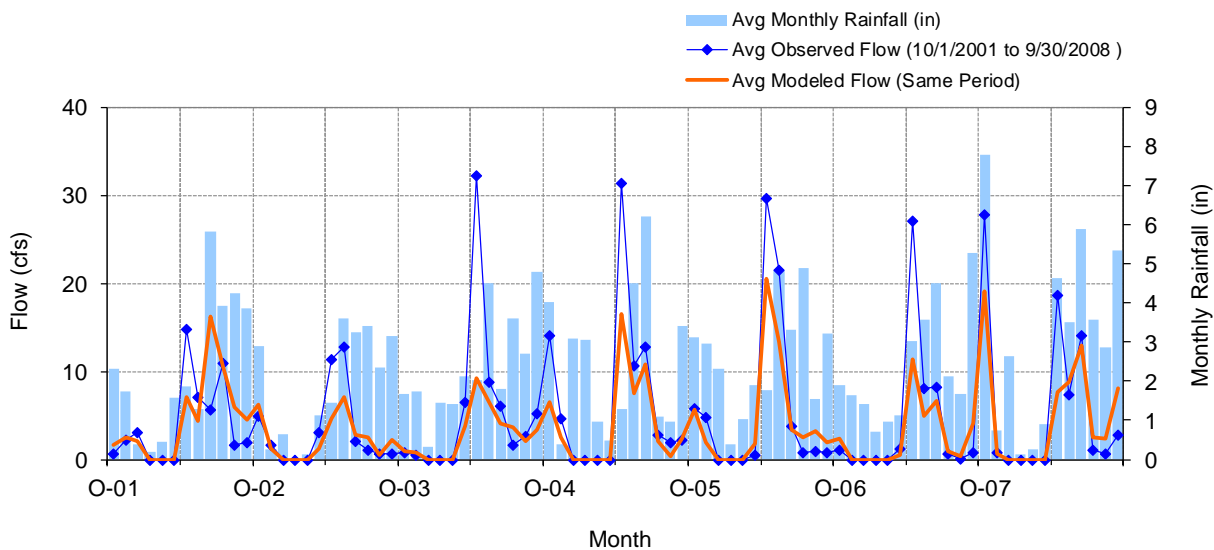


Figure 124. Mean monthly flow at Talmadge River near Duluth

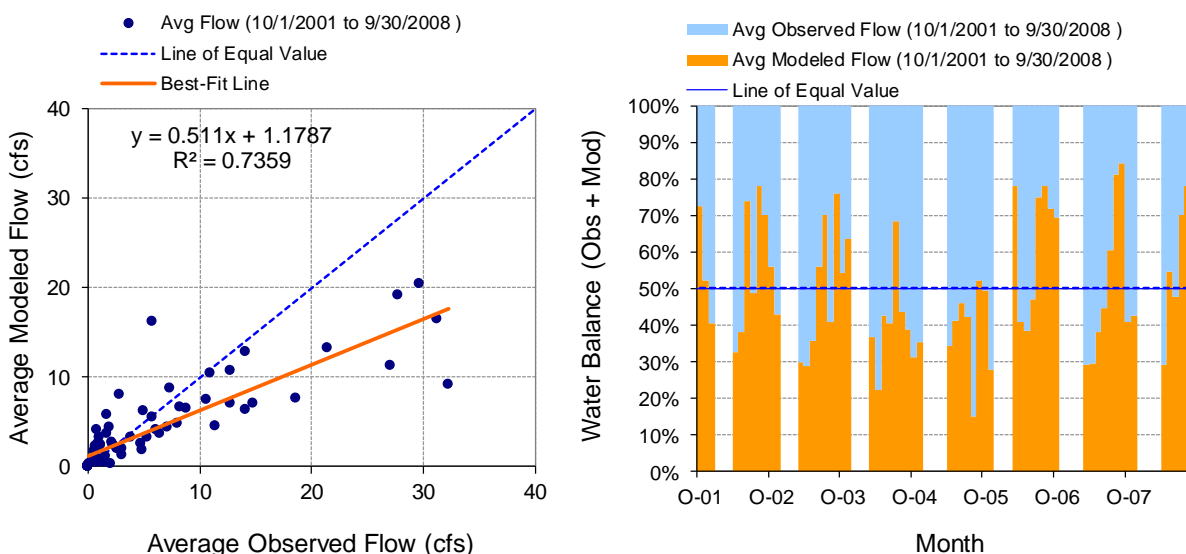


Figure 125. Monthly flow regression and temporal variation at Talmadge River near Duluth

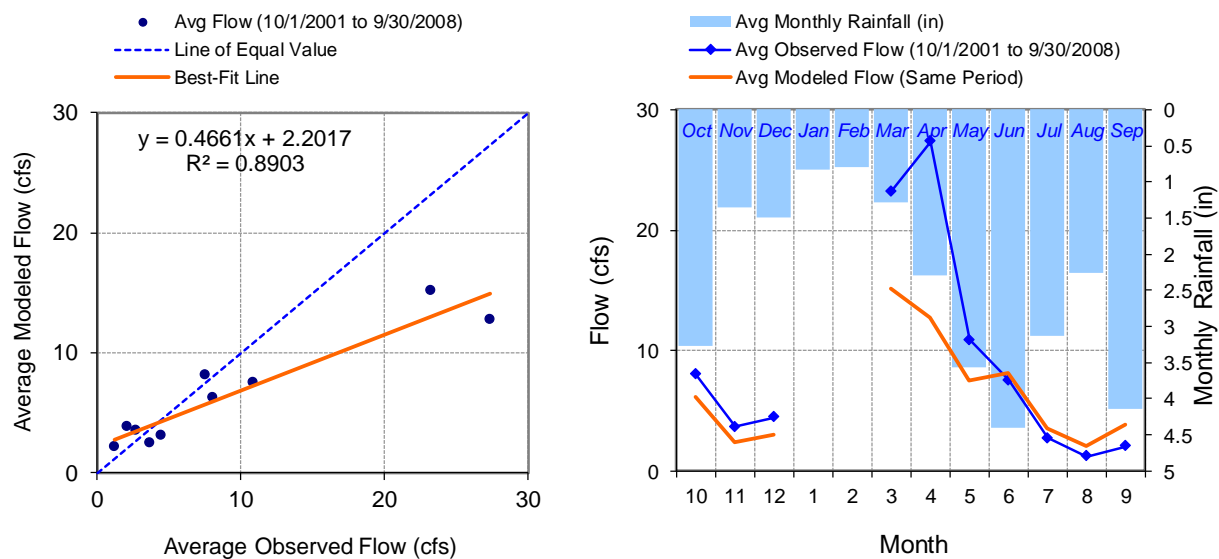


Figure 126. Seasonal regression and temporal aggregate at Talmadge River near Duluth

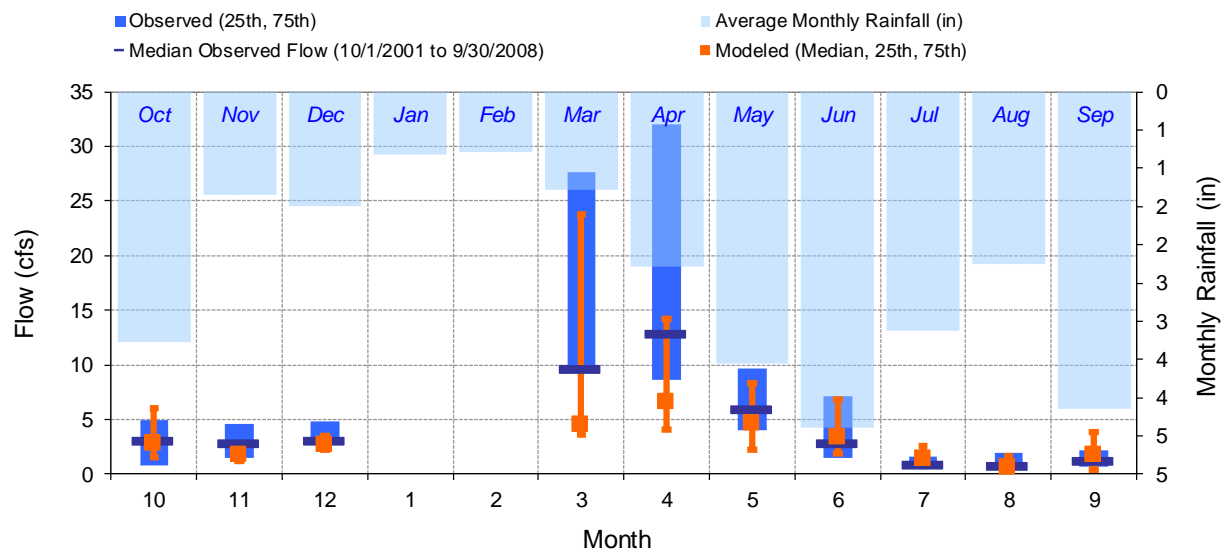


Figure 127. Seasonal medians and ranges at Talmadge River near Duluth

Table 5. Seasonal summary at Talmadge River near Duluth

MONTH	OBSERVED FLOW (CFS)				MODELED FLOW (CFS)			
	MEAN	MEDIAN	25TH	75TH	MEAN	MEDIAN	25TH	75TH
Oct	8.01	3.03	0.82	4.98	6.18	2.80	1.49	6.09
Nov	3.68	2.77	1.47	4.65	2.39	1.81	1.24	2.72
Dec	4.44	3.04	2.87	4.87	3.02	2.67	2.19	3.52
Jan	0.00	0.00	0.00	0.00	0.00	0.00	0.00	0.00
Feb	0.00	0.00	0.00	0.00	0.00	0.00	0.00	0.00
Mar	23.24	9.58	9.58	27.66	15.12	4.54	3.67	23.78
Apr	27.35	12.85	8.68	32.00	12.74	6.61	4.11	14.19
May	10.86	5.90	4.04	9.64	7.50	4.64	2.26	8.32
Jun	7.51	2.86	1.50	7.15	8.10	3.44	1.84	6.88
Jul	2.72	0.88	0.62	1.61	3.52	1.45	0.75	2.60
Aug	1.23	0.70	0.59	1.95	2.10	0.64	0.29	1.69
Sep	2.05	1.20	0.64	2.13	3.81	1.78	0.35	3.85

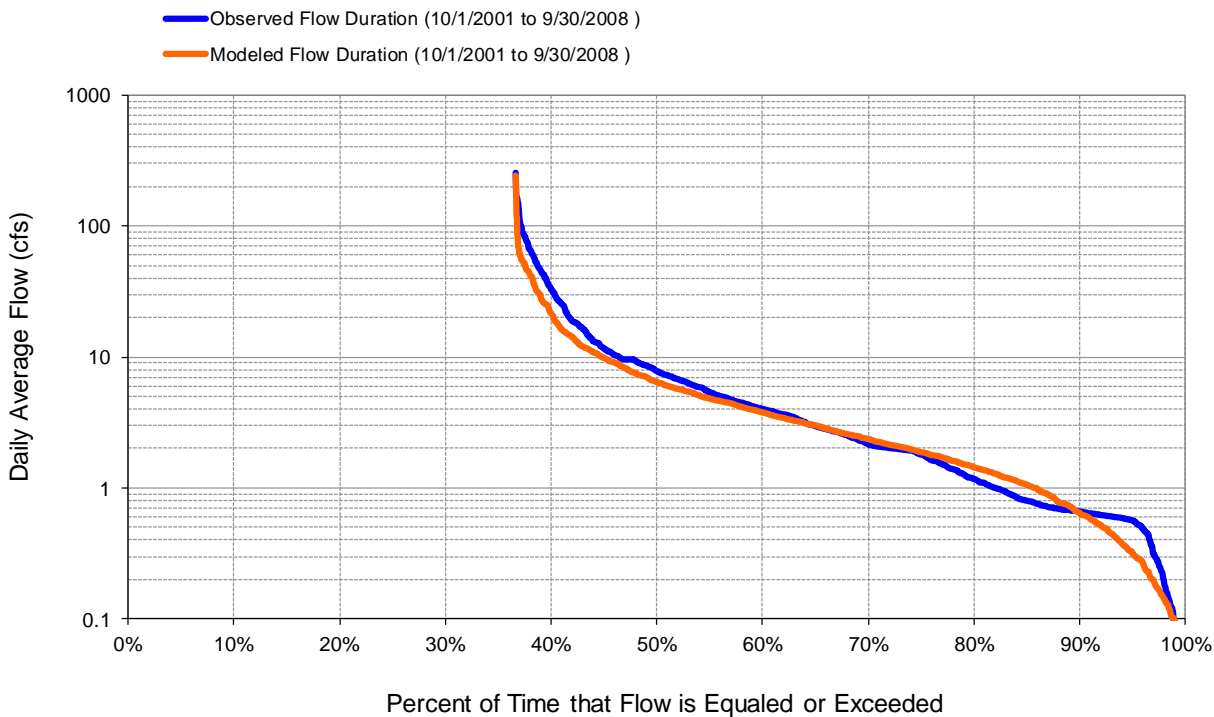


Figure 128. Flow exceedance at Talmadge River near Duluth

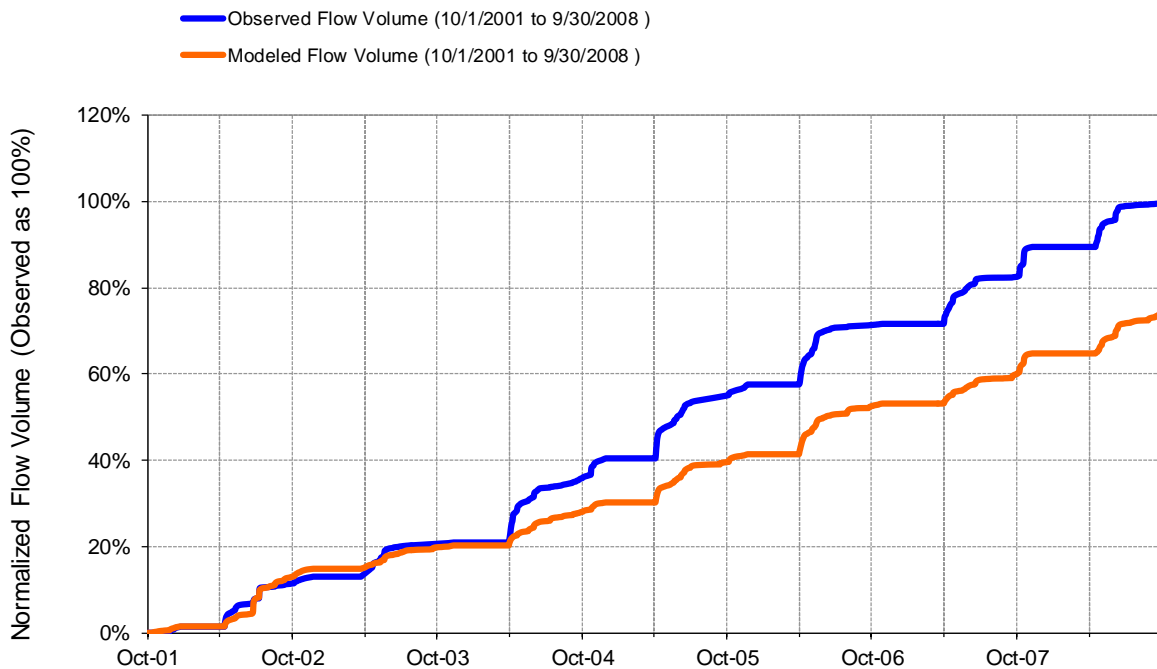


Figure 129. Flow accumulation at Talmadge River near Duluth

Table 6. Summary statistics at Talmadge River near Duluth

HSPF Simulated Flow		Observed Flow Gage	
REACH OUTFLOW FROM DSN 20 7-Year Analysis Period: 10/1/2001 - 9/30/2008 Flow volumes are (inches/year) for upstream drainage area		Talmadge River near Duluth, CR281 Manually Entered Data Drainage Area (sq-mi): 5.38	
Total Simulated In-stream Flow:	9.43	Total Observed In-stream Flow:	12.60
Total of simulated highest 10% flows:	5.05	Total of Observed highest 10% flows:	7.77
Total of Simulated lowest 50% flows:	0.93	Total of Observed Lowest 50% flows:	0.86
Simulated Summer Flow Volume (months 7-9):	1.99	Observed Summer Flow Volume (7-9):	1.27
Simulated Fall Flow Volume (months 10-12):	1.64	Observed Fall Flow Volume (10-12):	2.21
Simulated Winter Flow Volume (months 1-3):	0.22	Observed Winter Flow Volume (1-3):	0.34
Simulated Spring Flow Volume (months 4-6):	5.56	Observed Spring Flow Volume (4-6):	8.77
Total Simulated Storm Volume:	3.47	Total Observed Storm Volume:	4.61
Simulated Summer Storm Volume (7-9):	0.98	Observed Summer Storm Volume (7-9):	0.51
<i>Errors (Simulated-Observed)</i>	<i>Error Statistics</i>	<i>Recommended Criteria</i>	
Error in total volume:	-25.18	10	
Error in 50% lowest flows:	7.85	10	
Error in 10% highest flows:	-35.04	15	
Seasonal volume error - Summer:	56.66	30	
Seasonal volume error - Fall:	-25.56	30	
Seasonal volume error - Winter:	-34.96	30	
Seasonal volume error - Spring:	-36.58	30	
Error in storm volumes:	-24.82	20	
Error in summer storm volumes:	92.07	50	
Nash-Sutcliffe Coefficient of Efficiency, E:	0.533	Model accuracy increases	
Baseline adjusted coefficient (Garrick), E':	0.502		
Monthly NSE	0.569		

SUCKER RIVER NEAR PALMERS (HYDSTRA 02031001)

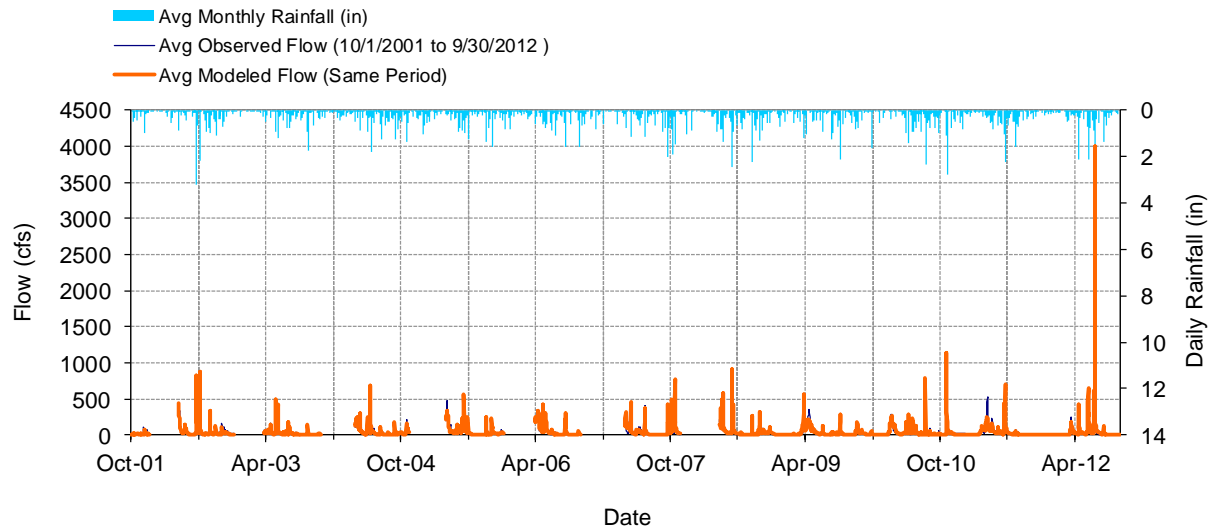


Figure 130. Mean daily flow at Sucker River near Palmers

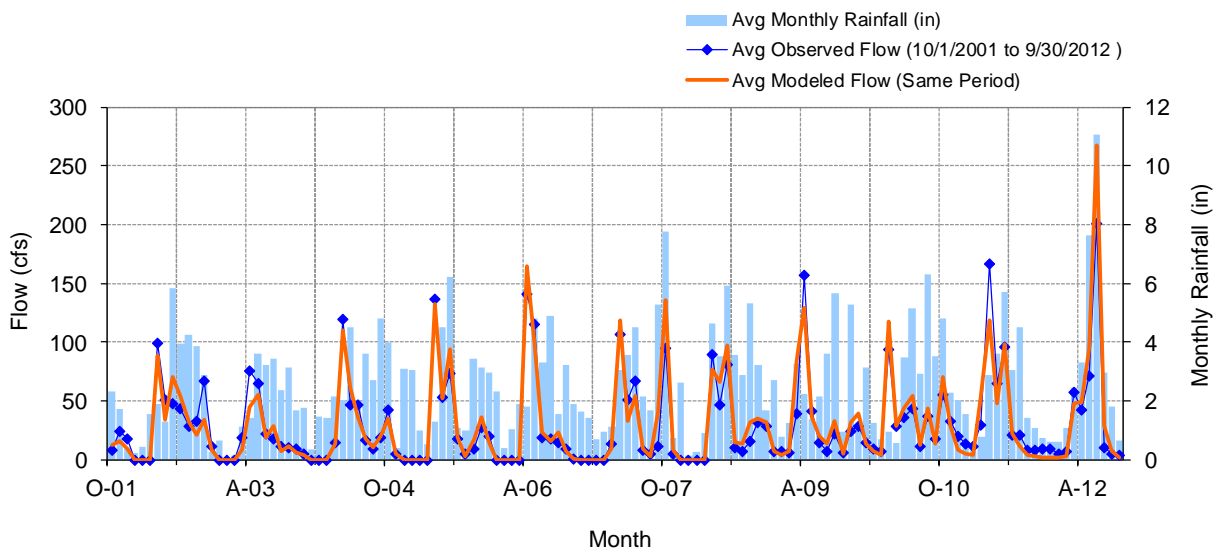


Figure 131. Mean monthly flow at Sucker River near Palmers

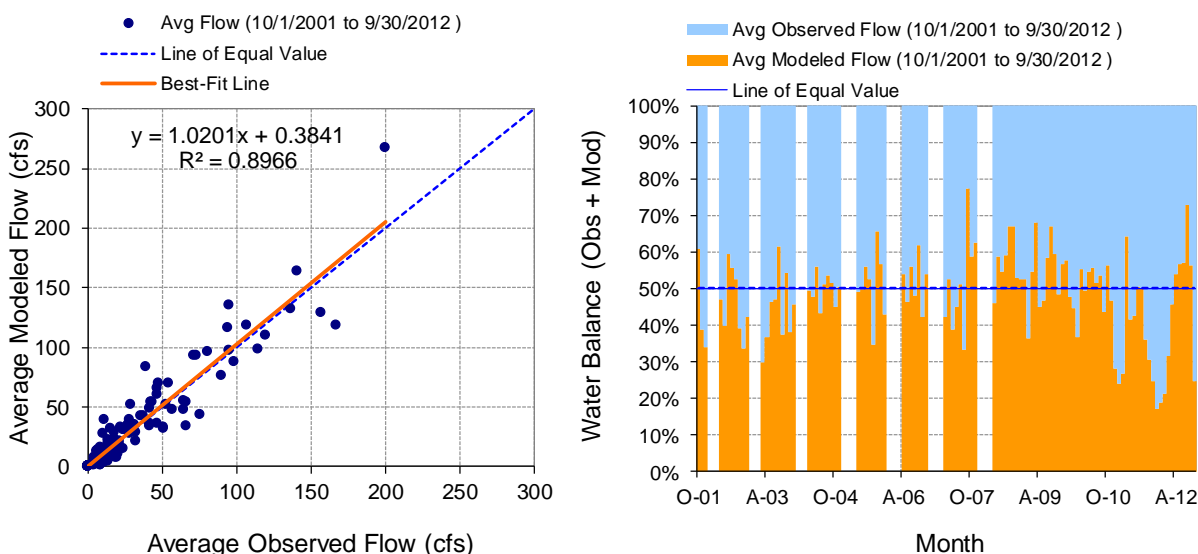


Figure 132. Monthly flow regression and temporal variation at Sucker River near Palmers

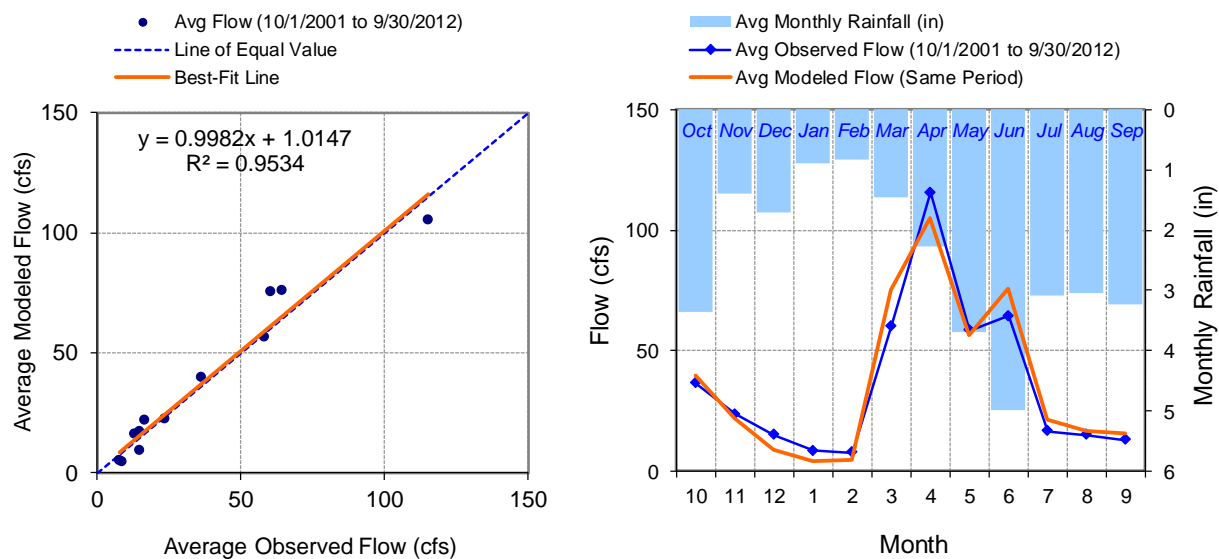


Figure 133. Seasonal regression and temporal aggregate at Sucker River near Palmers

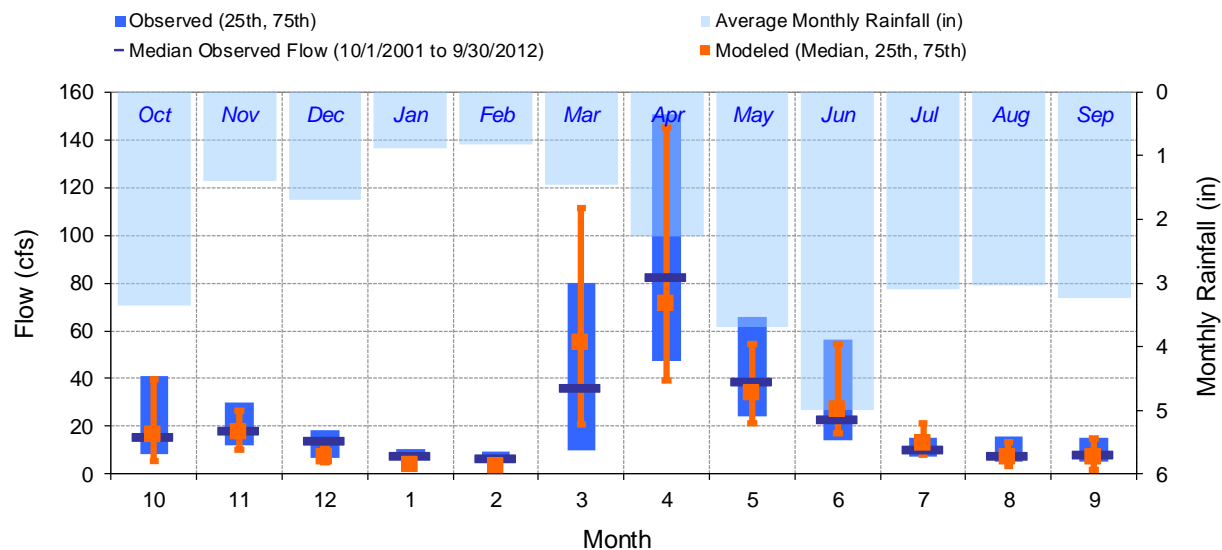


Figure 134. Seasonal medians and ranges at Sucker River near Palmers

Table 7. Seasonal summary at Sucker River near Palmers

MONTH	OBSERVED FLOW (CFS)				MODELED FLOW (CFS)			
	MEAN	MEDIAN	25TH	75TH	MEAN	MEDIAN	25TH	75TH
Oct	36.46	15.61	8.65	41.05	39.50	16.31	5.56	39.54
Nov	23.49	18.00	12.32	29.99	21.86	17.59	10.28	26.45
Dec	14.91	14.00	7.00	18.40	8.77	7.04	5.17	10.65
Jan	8.48	7.80	6.18	10.54	4.14	3.95	2.77	4.97
Feb	7.62	6.50	5.30	9.60	4.59	3.41	2.96	5.08
Mar	60.19	36.00	10.00	80.00	75.39	55.07	20.87	111.24
Apr	115.47	82.61	47.40	150.73	105.07	71.44	39.37	145.26
May	58.30	38.52	24.00	65.85	56.34	33.69	21.42	54.41
Jun	64.44	22.89	13.96	56.57	75.74	27.28	16.90	54.66
Jul	16.58	10.00	7.30	15.26	21.41	13.00	8.11	21.12
Aug	14.93	7.83	5.30	16.00	16.77	7.08	3.39	13.59
Sep	12.92	8.23	5.31	15.16	15.61	7.00	2.02	15.04

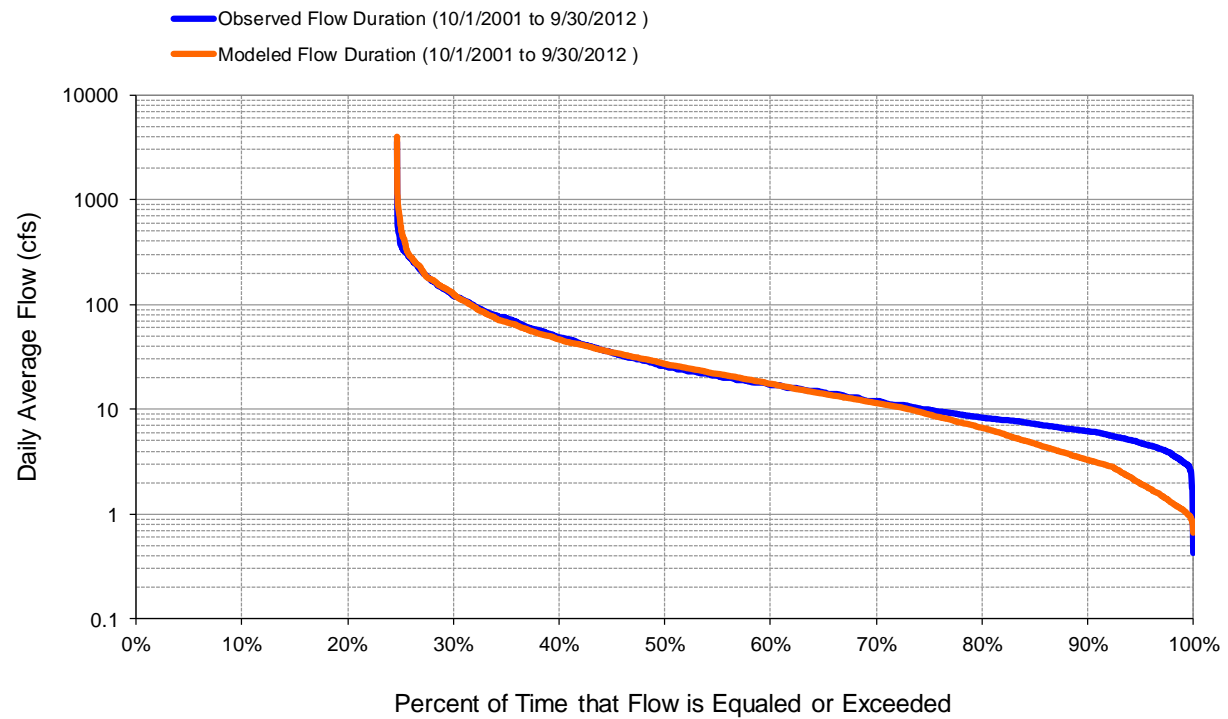


Figure 135. Flow exceedance at Sucker River near Palmers

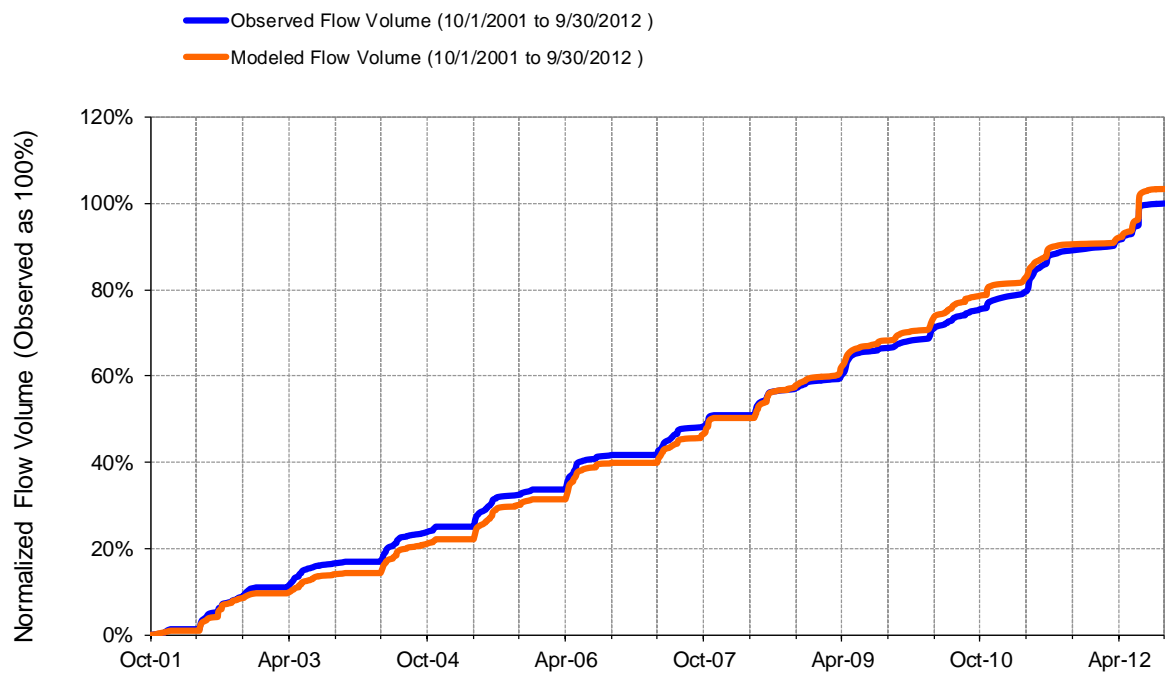


Figure 136. Flow accumulation at Sucker River near Palmers

Table 8. Summary statistics at Sucker River near Palmers

HSPF Simulated Flow		Observed Flow Gage	
REACH OUTFLOW FROM DSN 30 11-Year Analysis Period: 10/1/2001 - 9/30/2012 Flow volumes are (inches/year) for upstream drainage area Run 6h		Sucker River - 02031001 Manually Entered Data Drainage Area (sq-mi): 39.1	
Total Simulated In-stream Flow:	10.70	Total Observed In-stream Flow:	10.35
Total of simulated highest 10% flows:	5.92	Total of Observed highest 10% flows:	5.28
Total of Simulated lowest 50% flows:	0.91	Total of Observed Lowest 50% flows:	1.13
Simulated Summer Flow Volume (months 7-9):	1.57	Observed Summer Flow Volume (7-9):	1.30
Simulated Fall Flow Volume (months 10-12):	1.58	Observed Fall Flow Volume (10-12):	1.60
Simulated Winter Flow Volume (months 1-3):	0.98	Observed Winter Flow Volume (1-3):	0.88
Simulated Spring Flow Volume (months 4-6):	6.57	Observed Spring Flow Volume (4-6):	6.57
Total Simulated Storm Volume:	4.58	Total Observed Storm Volume:	3.94
Simulated Summer Storm Volume (7-9):	0.77	Observed Summer Storm Volume (7-9):	0.51
<i>Errors (Simulated-Observed)</i>	<i>Error Statistics</i>	<i>Recommended Criteria</i>	
Error in total volume:	3.35	10	
Error in 50% lowest flows:	-19.39	10	
Error in 10% highest flows:	12.11	15	
Seasonal volume error - Summer:	21.08	30	
Seasonal volume error - Fall:	-1.44	30	
Seasonal volume error - Winter:	11.82	30	
Seasonal volume error - Spring:	-0.11	30	
Error in storm volumes:	16.21	20	
Error in summer storm volumes:	51.78	50	
Nash-Sutcliffe Coefficient of Efficiency, E:	0.747	Model accuracy increases	
Baseline adjusted coefficient (Garrick), E':	0.570		
Monthly NSE	0.871		

KNIFE RIVER AT NAPPA ROAD (HYDSTRA 02021001)

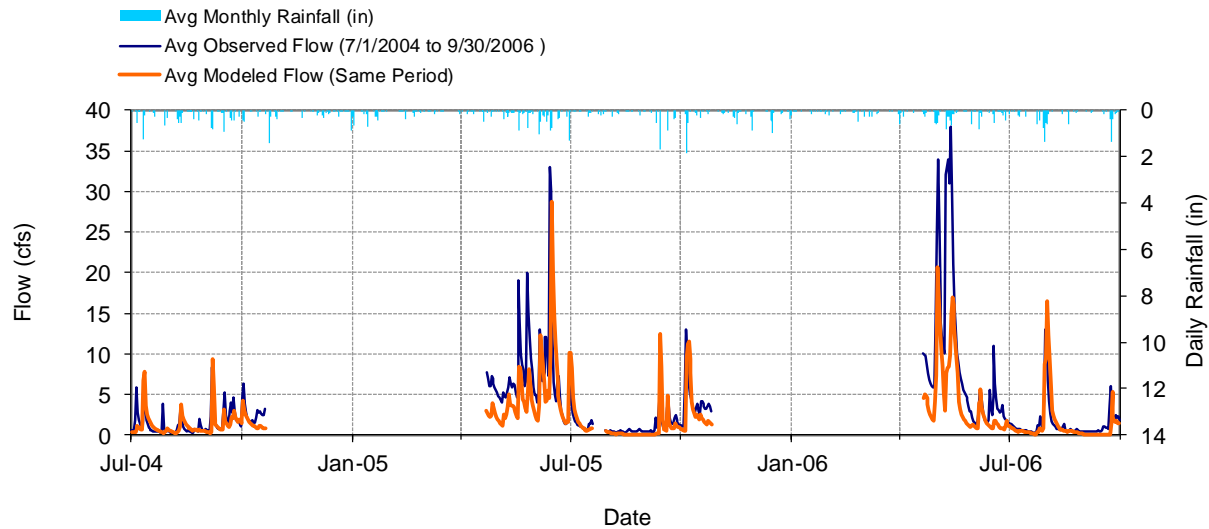


Figure 137. Mean daily flow at Knife River at Nappa Road

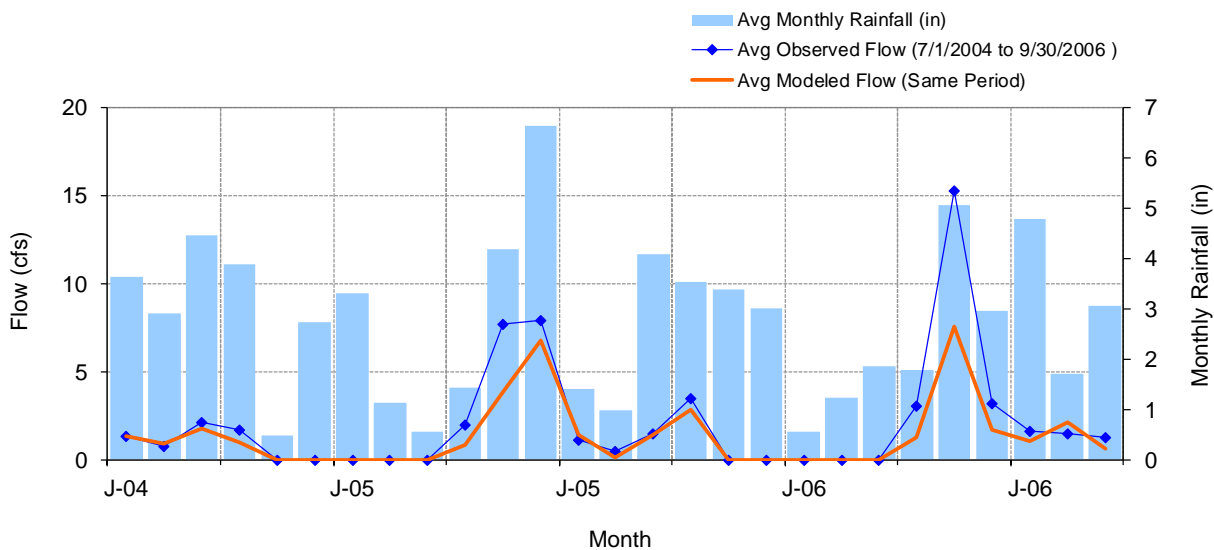


Figure 138. Mean monthly flow at Knife River at Nappa Road

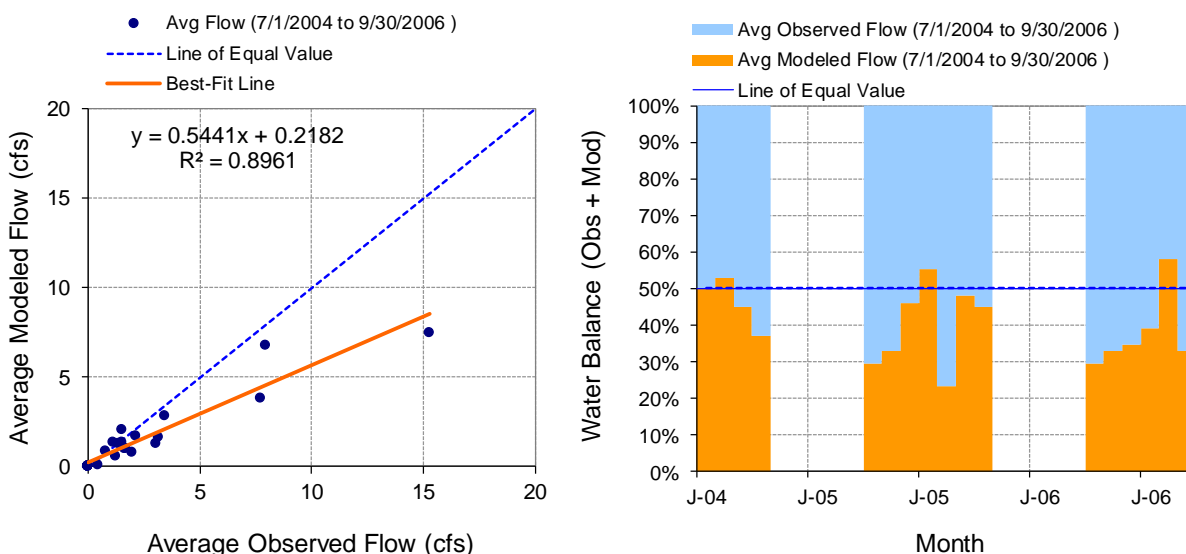


Figure 139. Monthly flow regression and temporal variation at Knife River at Nappa Road

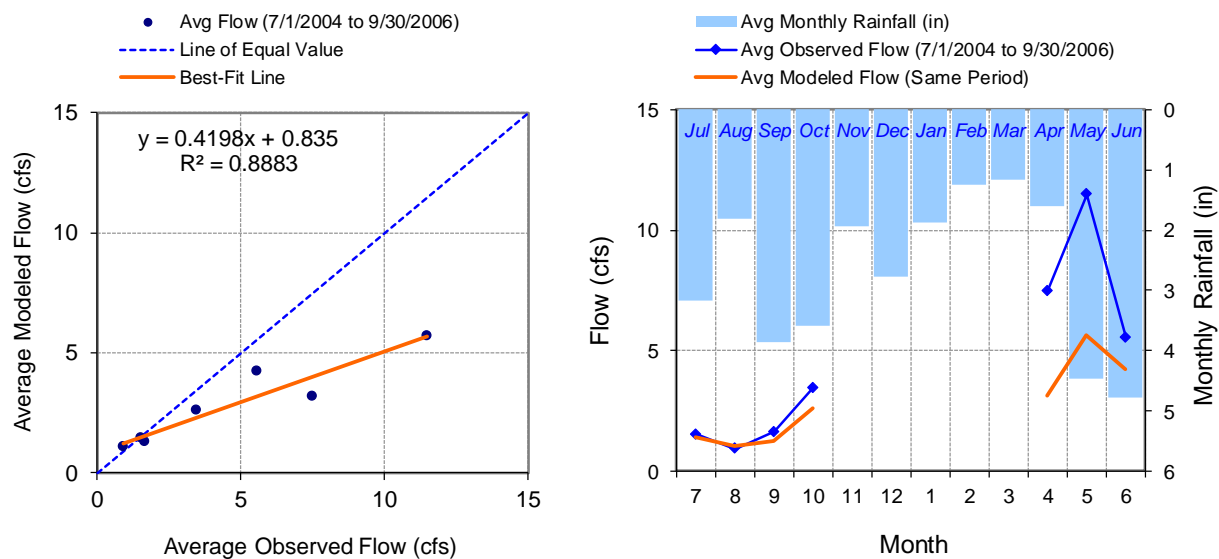


Figure 140. Seasonal regression and temporal aggregate at Knife River at Nappa Road

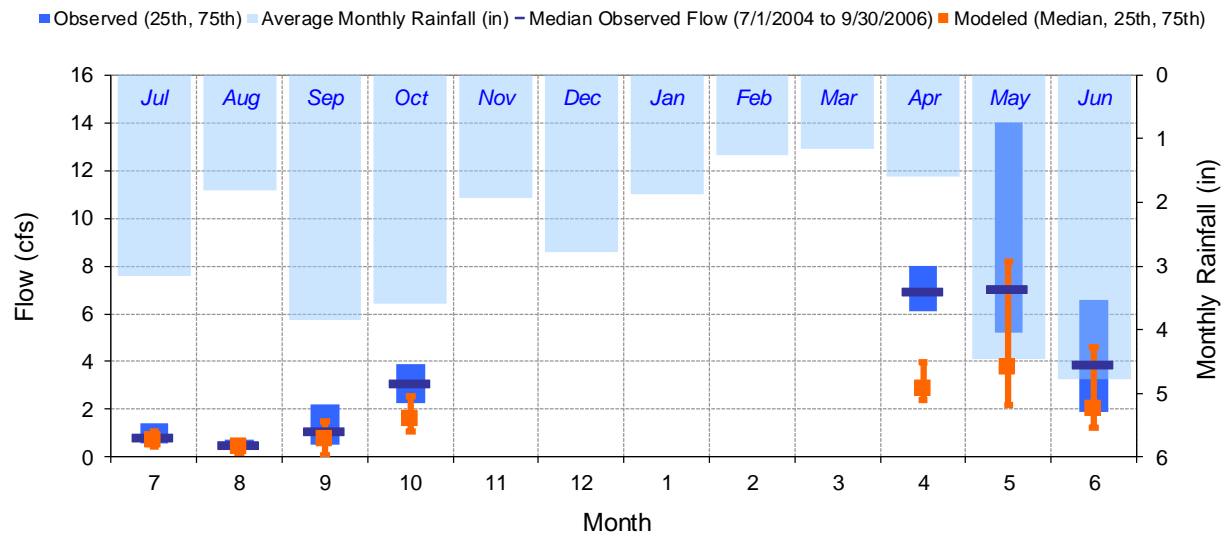


Figure 141. Seasonal medians and ranges at Knife River at Nappa Road

Table 9. Seasonal summary at Knife River at Nappa Road

MONTH	OBSERVED FLOW (CFS)				MODELED FLOW (CFS)			
	MEAN	MEDIAN	25TH	75TH	MEAN	MEDIAN	25TH	75TH
Jul	1.52	0.81	0.56	1.40	1.41	0.68	0.44	1.05
Aug	0.91	0.52	0.41	0.74	1.03	0.44	0.16	0.68
Sep	1.63	1.10	0.54	2.20	1.25	0.75	0.08	1.50
Oct	3.47	3.10	2.25	3.90	2.58	1.62	1.08	2.54
Nov	0.00	0.00	0.00	0.00	0.00	0.00	0.00	0.00
Dec	0.00	0.00	0.00	0.00	0.00	0.00	0.00	0.00
Jan	0.00	0.00	0.00	0.00	0.00	0.00	0.00	0.00
Feb	0.00	0.00	0.00	0.00	0.00	0.00	0.00	0.00
Mar	0.00	0.00	0.00	0.00	0.00	0.00	0.00	0.00
Apr	7.48	6.90	6.10	8.00	3.15	2.84	2.39	3.96
May	11.48	7.05	5.23	14.00	5.66	3.75	2.17	8.18
Jun	5.55	3.85	1.90	6.60	4.22	2.02	1.22	4.61

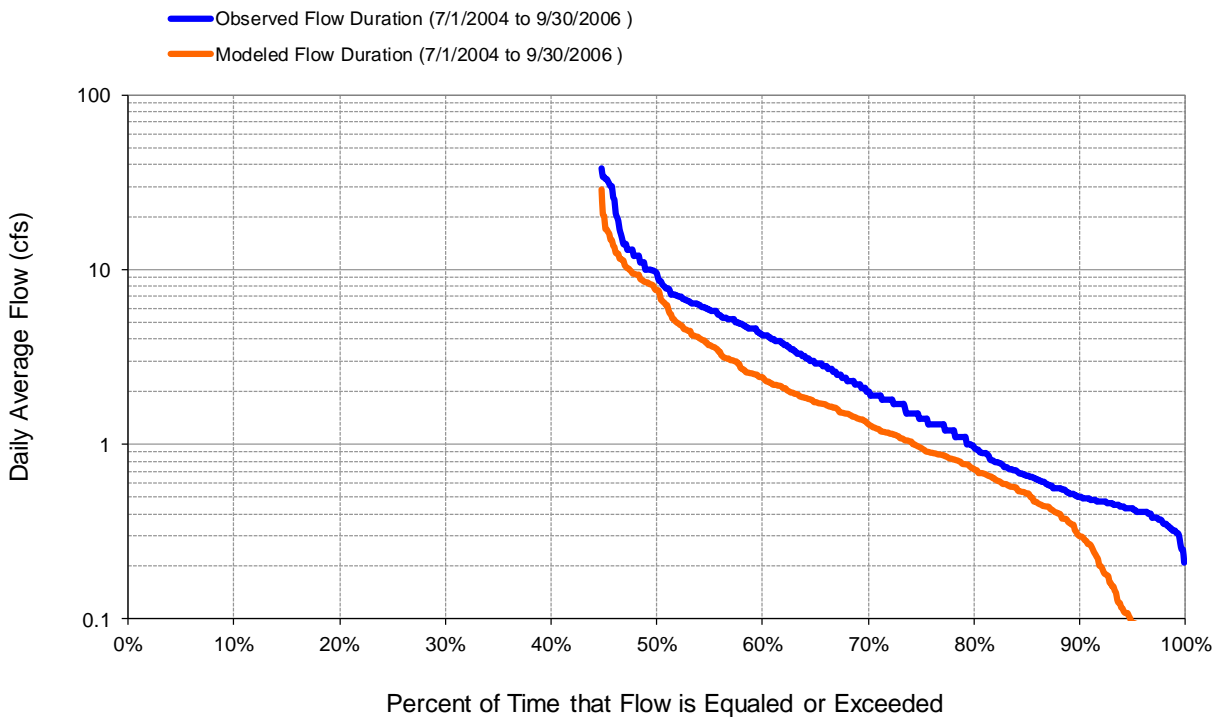


Figure 142. Flow exceedance at Knife River at Nappa Road

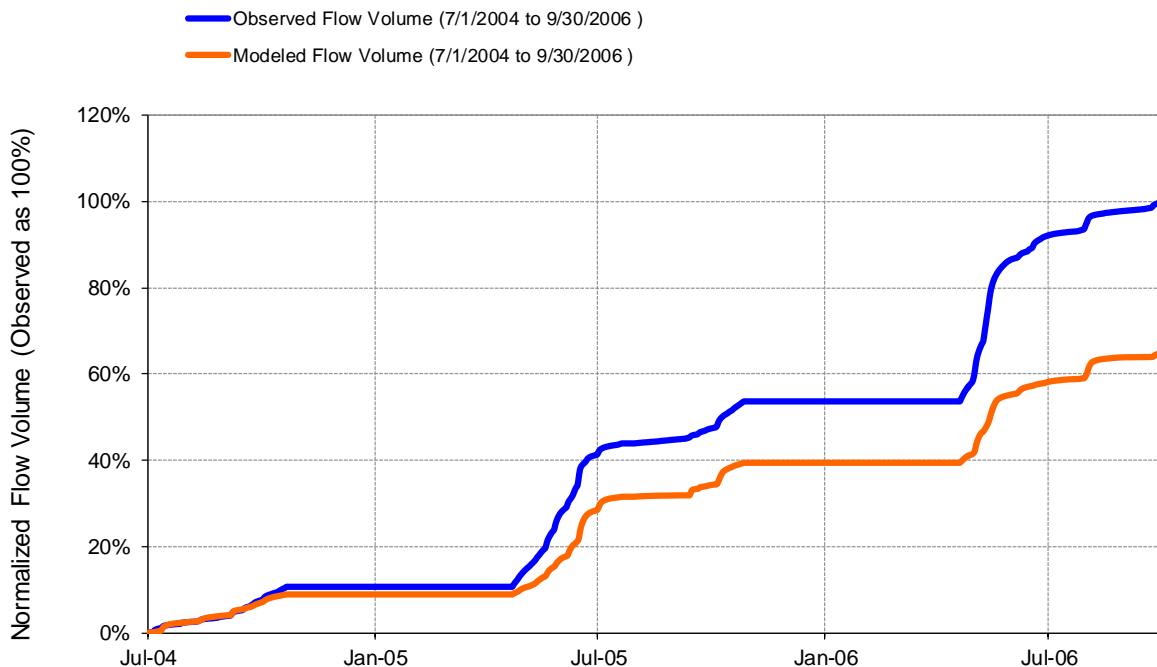


Figure 143. Flow accumulation at Knife River at Nappa Road

Table 10. Summary statistics at Knife River at Nappa Road

HSPF Simulated Flow		Observed Flow Gage	
REACH OUTFLOW FROM DSN 120 2.25-Year Analysis Period: 7/1/2004 - 9/30/2006 Flow volumes are (inches/year) for upstream drainage area		Knife River near Two Harbors, Nappa Rd Manually Entered Data Drainage Area (sq-mi): 2.71	
Total Simulated In-stream Flow:	6.78	Total Observed In-stream Flow:	10.44
Total of simulated highest 10% flows:	3.20	Total of Observed highest 10% flows:	4.76
Total of Simulated lowest 50% flows:	0.68	Total of Observed Lowest 50% flows:	1.07
Simulated Summer Flow Volume (months 7-9):	1.99	Observed Summer Flow Volume (7-9):	2.18
Simulated Fall Flow Volume (months 10-12):	0.72	Observed Fall Flow Volume (10-12):	0.97
Simulated Winter Flow Volume (months 1-3):	0.00	Observed Winter Flow Volume (1-3):	0.00
Simulated Spring Flow Volume (months 4-6):	4.07	Observed Spring Flow Volume (4-6):	7.28
Total Simulated Storm Volume:	1.99	Total Observed Storm Volume:	2.69
Simulated Summer Storm Volume (7-9):	0.71	Observed Summer Storm Volume (7-9):	0.69
<i>Errors (Simulated-Observed)</i>	<i>Error Statistics</i>	<i>Recommended Criteria</i>	
Error in total volume:	-35.08	10	
Error in 50% lowest flows:	-36.85	10	
Error in 10% highest flows:	-32.86	15	
Seasonal volume error - Summer:	-9.00	30	
Seasonal volume error - Fall:	-25.56	30	
Seasonal volume error - Winter:	0.00	30	
Seasonal volume error - Spring:	-44.17	30	
Error in storm volumes:	-26.21	20	
Error in summer storm volumes:	2.67	50	
Nash-Sutcliffe Coefficient of Efficiency, E:	0.524	Model accuracy increases	
Baseline adjusted coefficient (Garrick), E':	0.452		
Monthly NSE	0.662		

KNIFE RIVER AT AIRPORT ROAD (HYDSTRA 02009001)

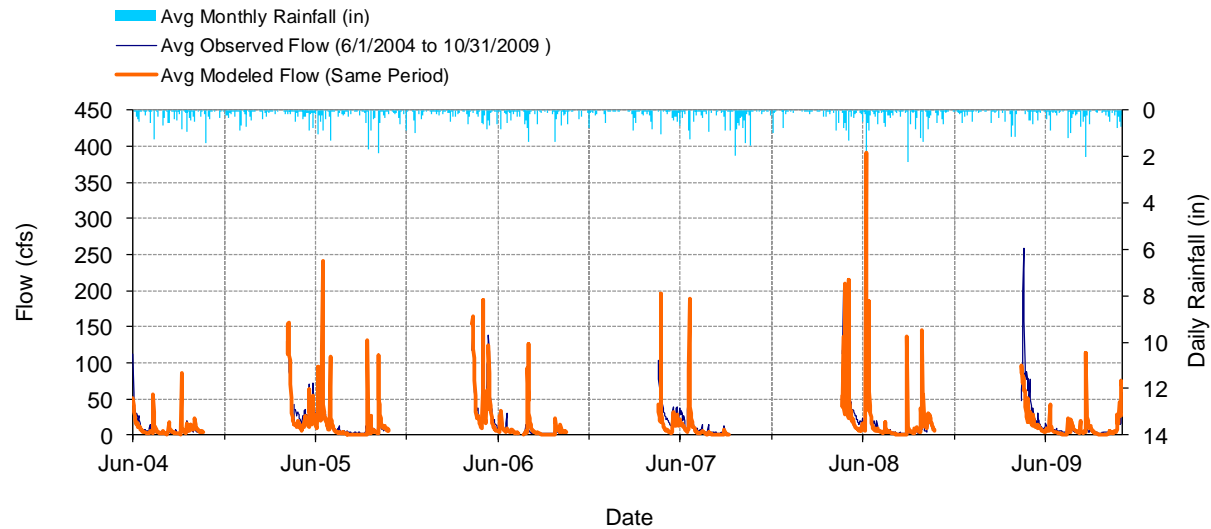


Figure 144. Mean daily flow at Knife River at Airport Road

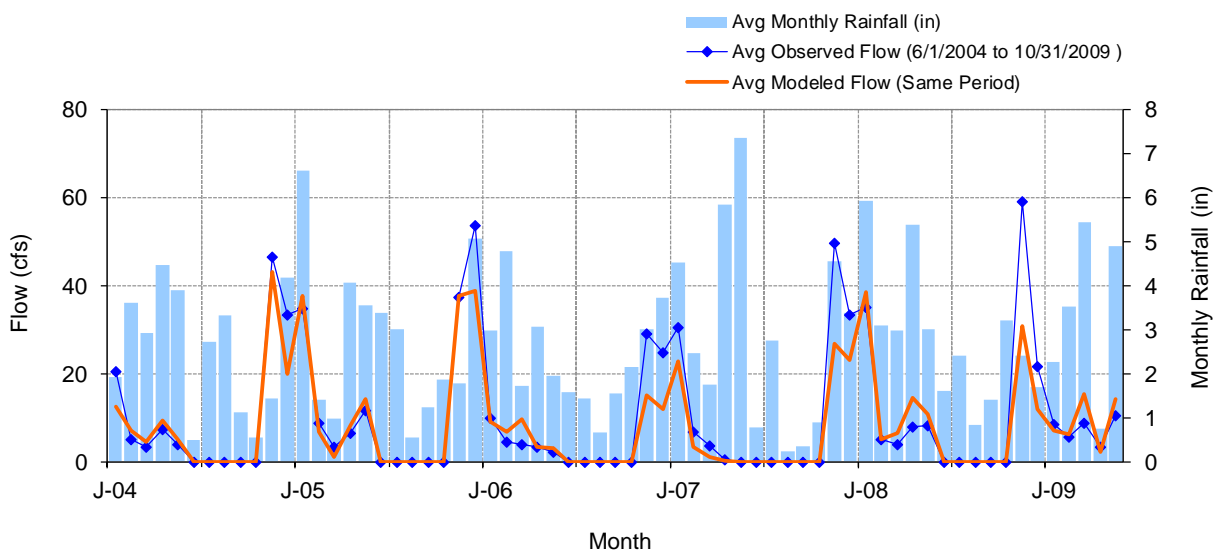


Figure 145. Mean monthly flow at Knife River at Airport Road

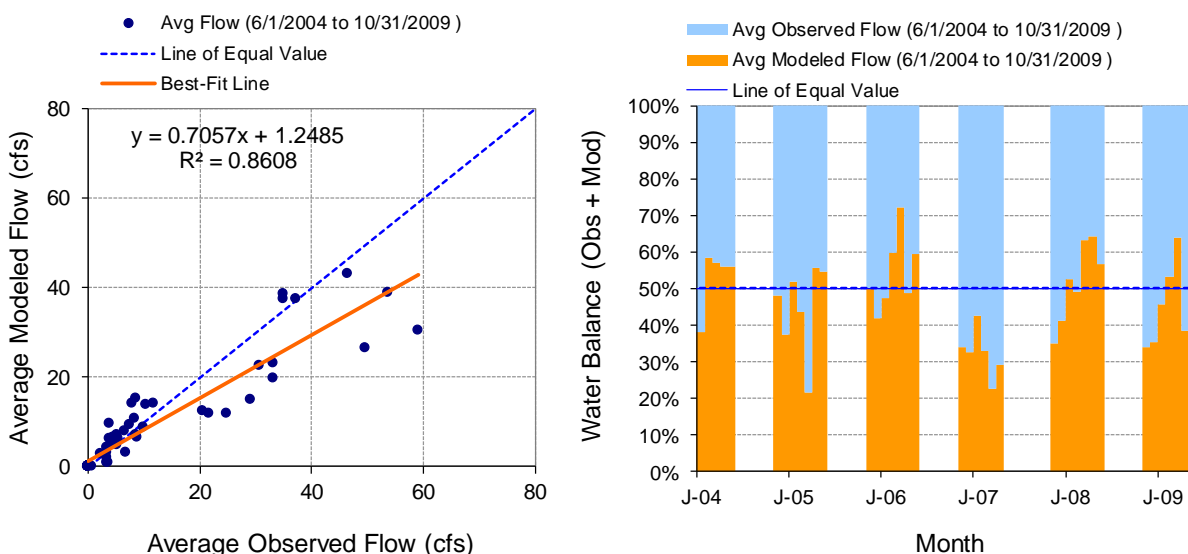


Figure 146. Monthly flow regression and temporal variation at Knife River at Airport Road

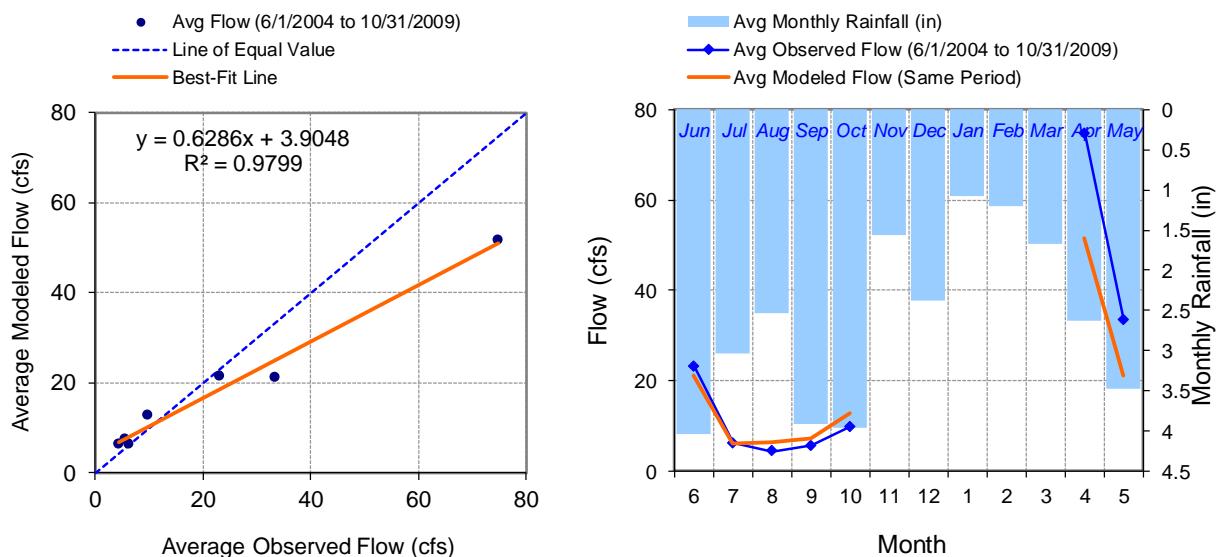


Figure 147. Seasonal regression and temporal aggregate at Knife River at Airport Road

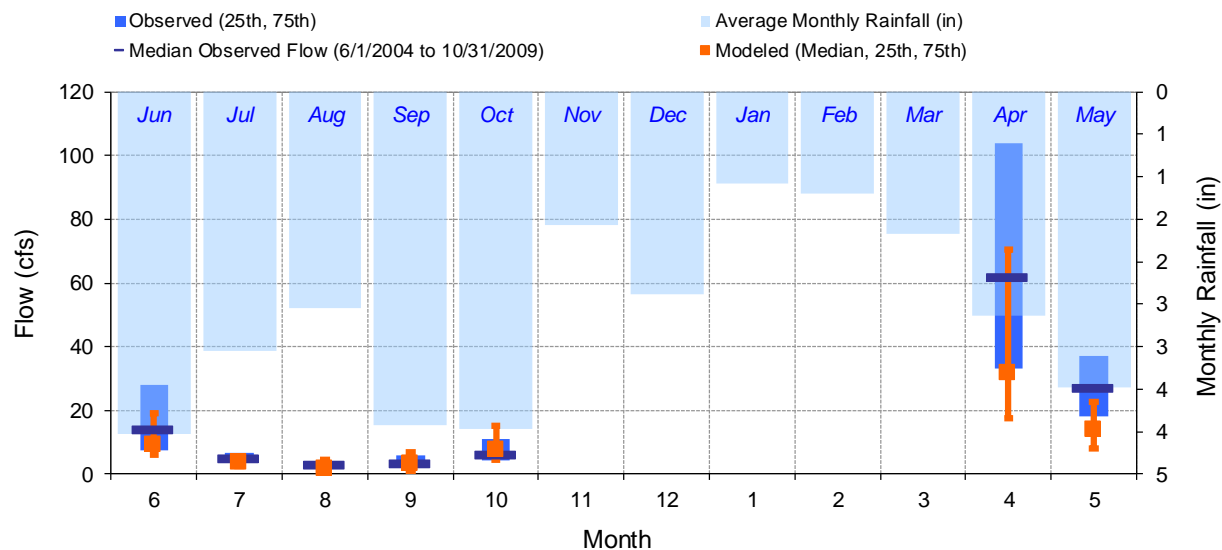


Figure 148. Seasonal medians and ranges at Knife River at Airport Road

Table 11. Seasonal summary at Knife River at Airport Road

MONTH	OBSERVED FLOW (CFS)				MODELED FLOW (CFS)			
	MEAN	MEDIAN	25TH	75TH	MEAN	MEDIAN	25TH	75TH
Jun	23.20	14.00	7.50	28.00	21.24	9.12	5.90	19.19
Jul	6.17	5.10	3.90	6.78	6.07	3.66	2.57	5.45
Aug	4.38	3.10	2.50	4.00	6.29	1.74	0.79	4.37
Sep	5.57	3.50	2.80	5.83	7.18	3.29	0.78	7.00
Oct	9.78	6.00	4.45	11.00	12.67	7.79	4.48	15.19
Nov	0.00	0.00	0.00	0.00	0.00	0.00	0.00	0.00
Dec	0.00	0.00	0.00	0.00	0.00	0.00	0.00	0.00
Jan	0.00	0.00	0.00	0.00	0.00	0.00	0.00	0.00
Feb	0.00	0.00	0.00	0.00	0.00	0.00	0.00	0.00
Mar	0.00	0.00	0.00	0.00	0.00	0.00	0.00	0.00
Apr	74.73	62.00	33.00	104.00	51.51	31.92	17.70	70.58
May	33.29	27.00	18.00	37.00	21.14	13.93	7.96	22.59

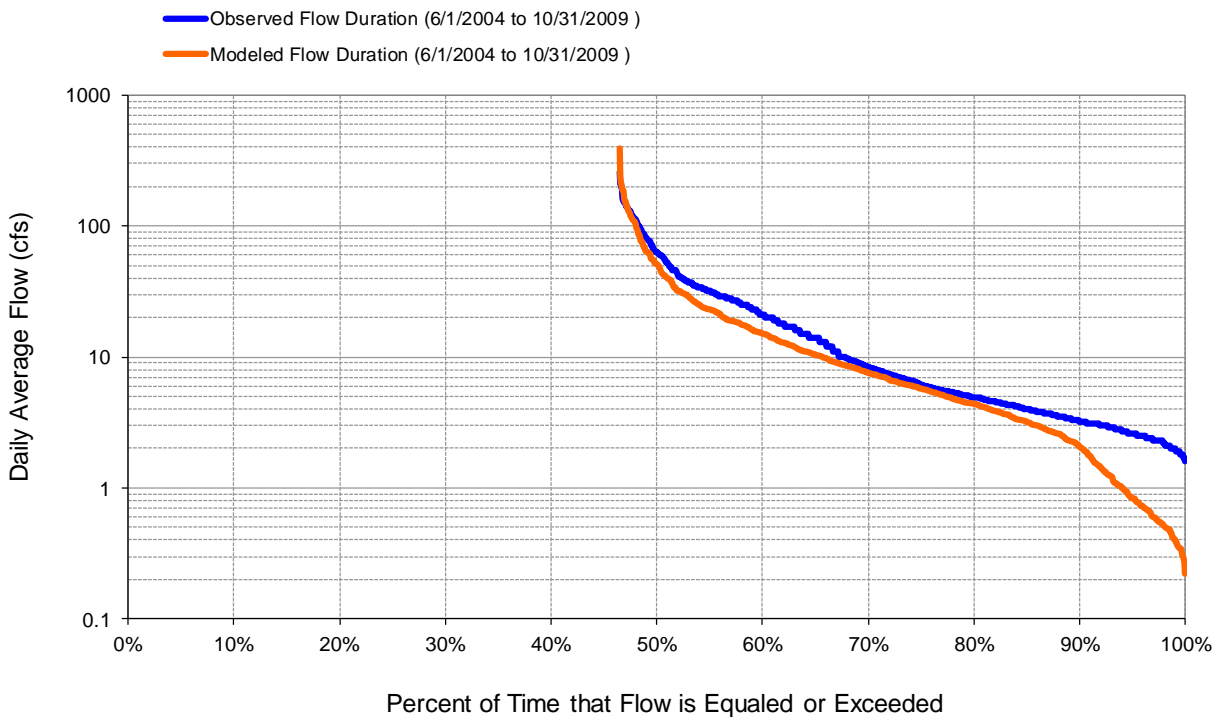


Figure 149. Flow exceedance at Knife River at Airport Road

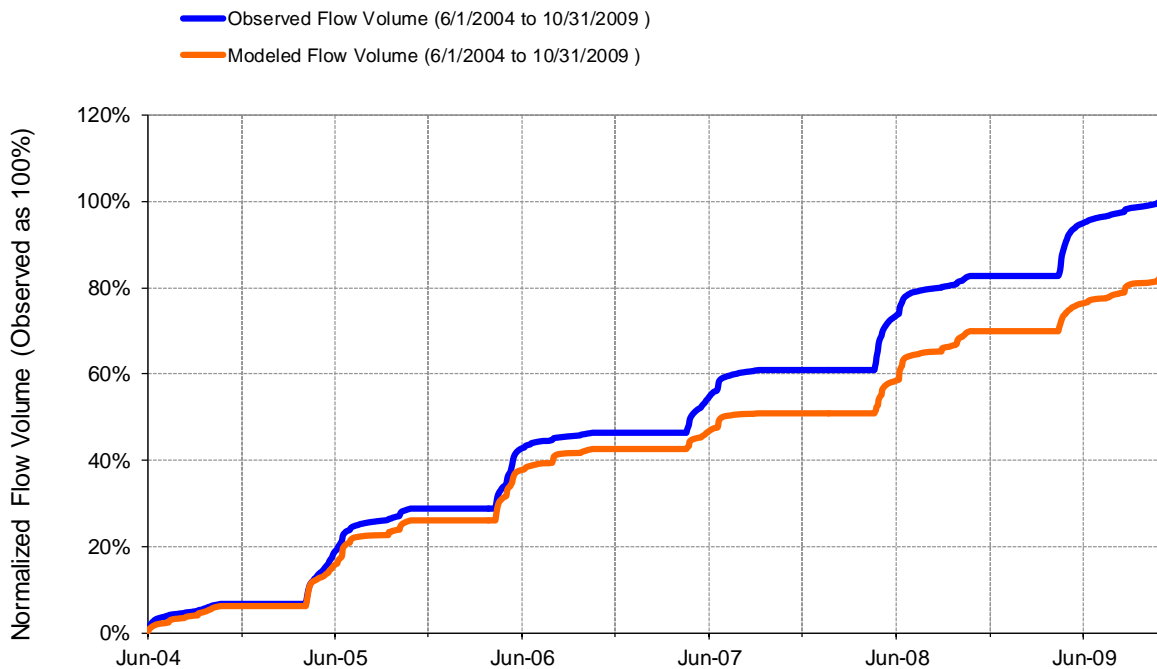


Figure 150. Flow accumulation at Knife River at Airport Road

Table 12. Summary statistics at Knife River at Airport Road

HSPF Simulated Flow		Observed Flow Gage	
REACH OUTFLOW FROM DSN 130 5.42-Year Analysis Period: 6/1/2004 - 10/31/2009 Flow volumes are (inches/year) for upstream drainage area		Knife River near Two Harbors, Airport Rd Manually Entered Data Drainage Area (sq-mi): 14.5	
Total Simulated In-stream Flow:	7.82	Total Observed In-stream Flow:	9.42
Total of simulated highest 10% flows:	4.21	Total of Observed highest 10% flows:	4.60
Total of Simulated lowest 50% flows:	0.73	Total of Observed Lowest 50% flows:	0.99
Simulated Summer Flow Volume (months 7-9):	1.60	Observed Summer Flow Volume (7-9):	1.32
Simulated Fall Flow Volume (months 10-12):	0.69	Observed Fall Flow Volume (10-12):	0.53
Simulated Winter Flow Volume (months 1-3):	0.00	Observed Winter Flow Volume (1-3):	0.00
Simulated Spring Flow Volume (months 4-6):	5.53	Observed Spring Flow Volume (4-6):	7.57
Total Simulated Storm Volume:	2.68	Total Observed Storm Volume:	2.17
Simulated Summer Storm Volume (7-9):	0.69	Observed Summer Storm Volume (7-9):	0.34
<i>Errors (Simulated-Observed)</i>	<i>Error Statistics</i>	<i>Recommended Criteria</i>	
Error in total volume:	-17.00	10	
Error in 50% lowest flows:	-26.45	10	
Error in 10% highest flows:	-8.39	15	
Seasonal volume error - Summer:	21.14	30	
Seasonal volume error - Fall:	29.57	30	
Seasonal volume error - Winter:	0.00	30	
Seasonal volume error - Spring:	-26.92	30	
Error in storm volumes:	23.28	20	
Error in summer storm volumes:	99.76	50	
Nash-Sutcliffe Coefficient of Efficiency, E:	0.579	Model accuracy increases	
Baseline adjusted coefficient (Garrick), E':	0.518		
Monthly NSE	0.749		

KNIFE RIVER NEAR TWO HARBORS (HYDSTRA 02026001/USGS 04015330)

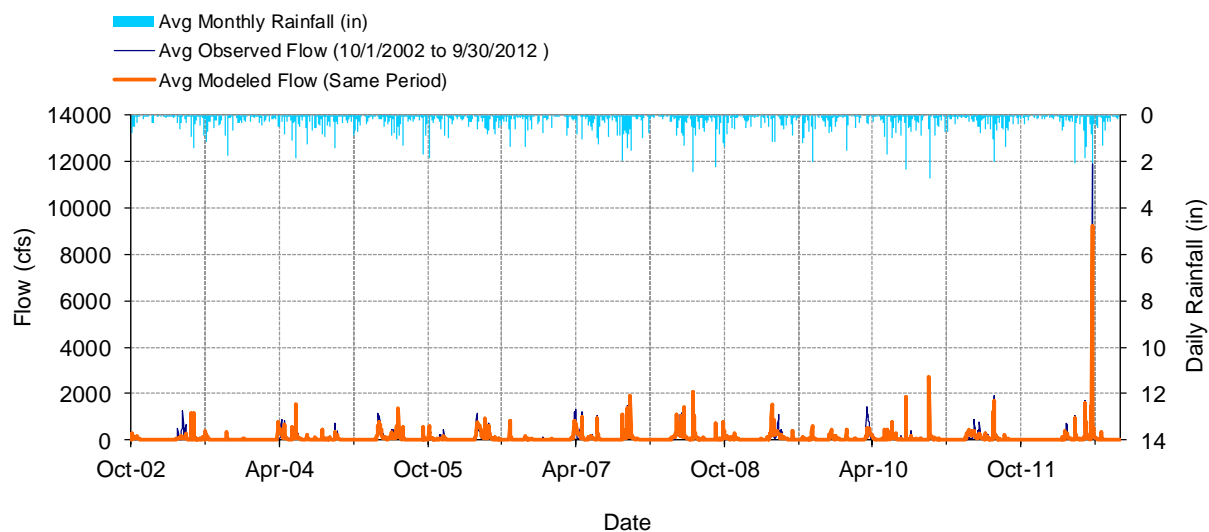


Figure 151. Mean daily flow at Knife River near Two Harbors

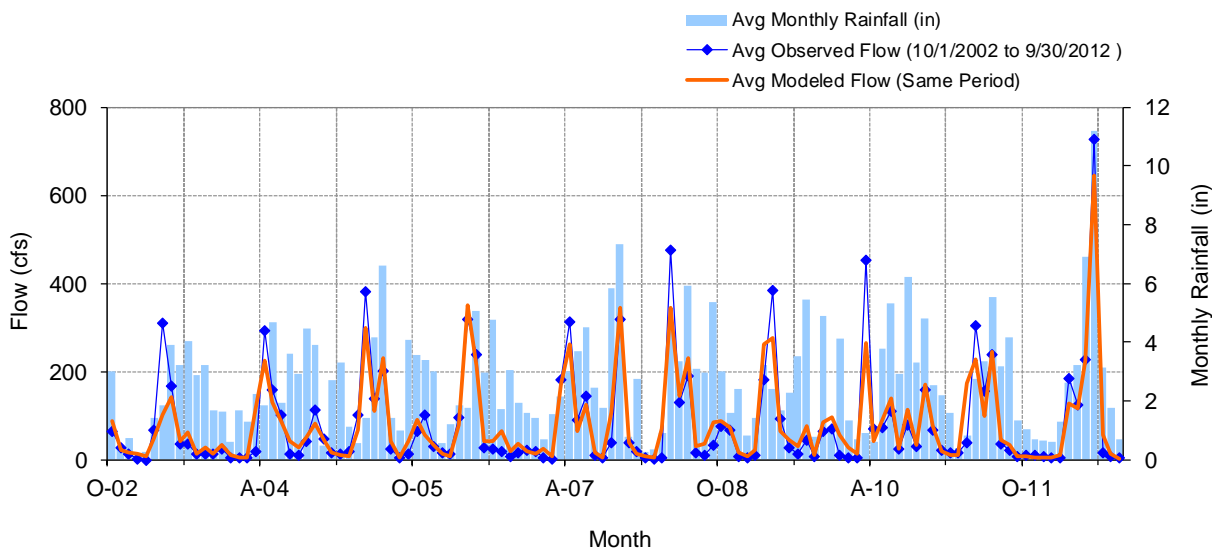


Figure 152. Mean monthly flow at Knife River near Two Harbors

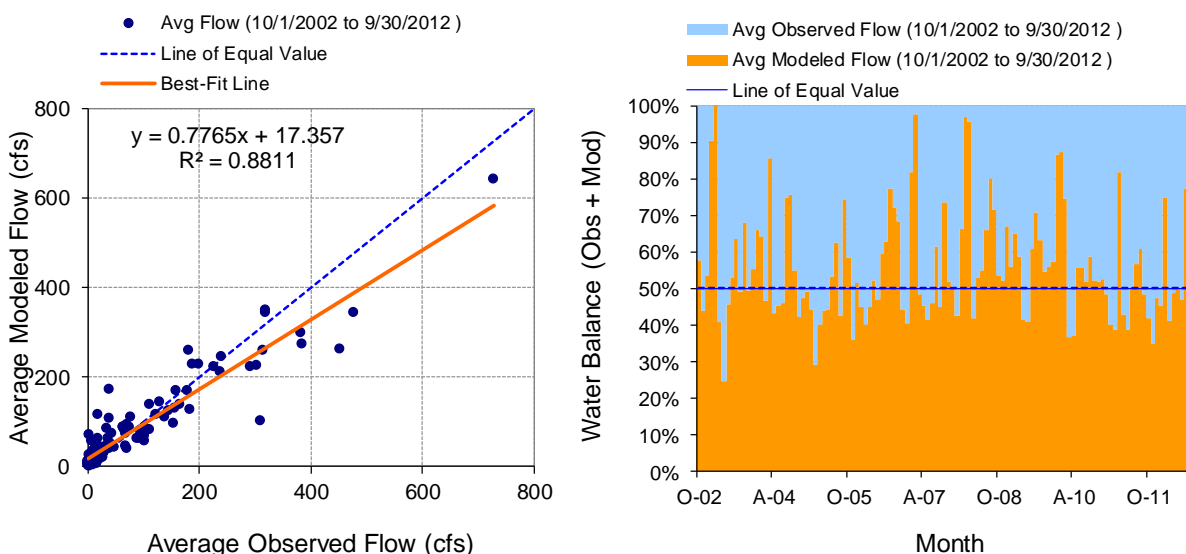


Figure 153. Monthly flow regression and temporal variation at Knife River near Two Harbors

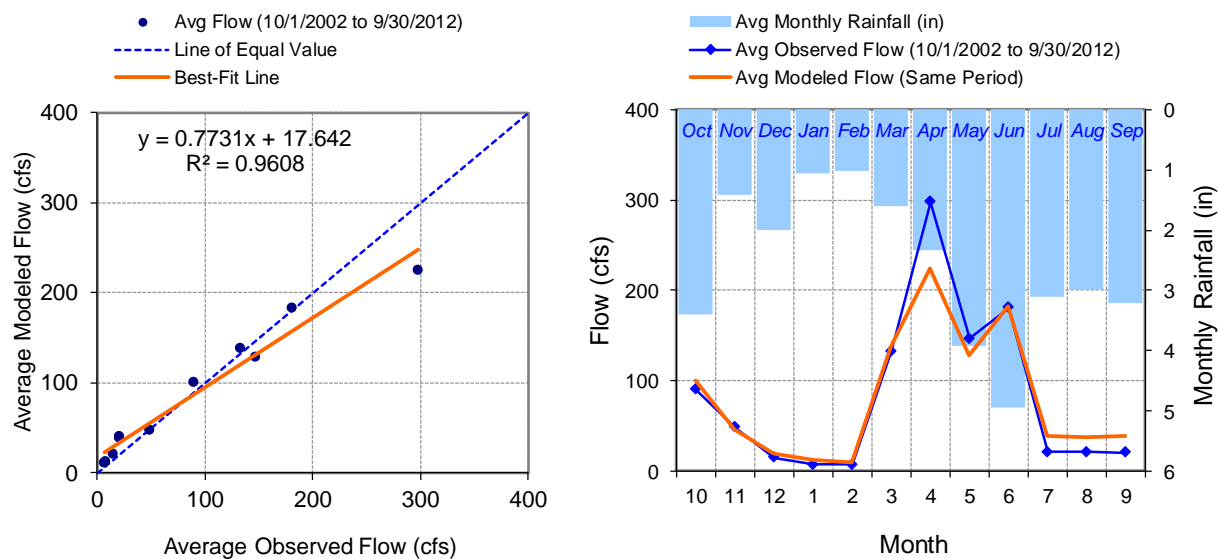


Figure 154. Seasonal regression and temporal aggregate at Knife River near Two Harbors

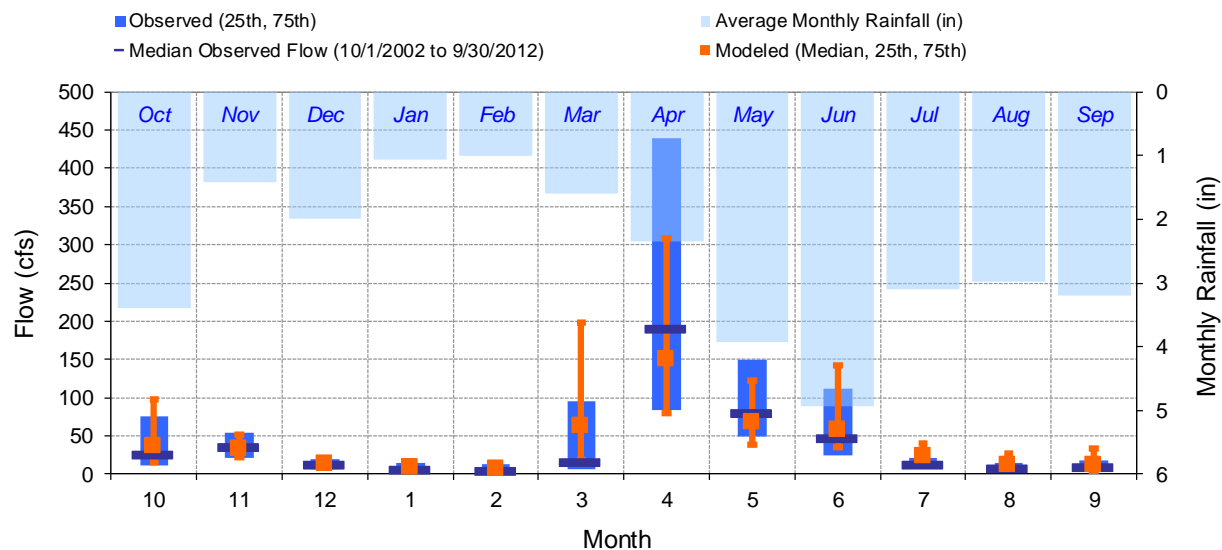


Figure 155. Seasonal medians and ranges at Knife River near Two Harbors

Table 13. Seasonal summary at Knife River near Two Harbors

MONTH	OBSERVED FLOW (CFS)				MODELED FLOW (CFS)			
	MEAN	MEDIAN	25TH	75TH	MEAN	MEDIAN	25TH	75TH
Oct	89.75	25.00	12.00	75.00	99.96	37.21	14.73	98.61
Nov	48.11	35.00	22.00	55.00	46.19	33.96	21.58	51.59
Dec	14.70	13.00	6.50	19.00	19.78	13.61	10.09	19.12
Jan	7.32	5.20	3.10	14.00	12.01	9.04	6.20	13.43
Feb	7.07	3.90	0.19	13.00	9.38	7.39	5.70	10.56
Mar	132.51	15.50	6.50	95.25	137.63	63.99	18.58	198.51
Apr	297.71	190.00	84.00	439.25	223.87	151.11	80.04	307.76
May	146.75	79.00	49.00	150.00	128.08	68.56	38.68	122.13
Jun	180.91	47.00	25.00	112.00	182.45	59.03	35.65	141.47
Jul	21.15	13.00	8.93	21.00	39.01	23.55	13.74	39.77
Aug	20.97	7.20	5.40	15.00	37.91	12.83	5.05	27.14
Sep	20.04	8.20	5.30	18.00	38.48	12.17	2.73	33.54

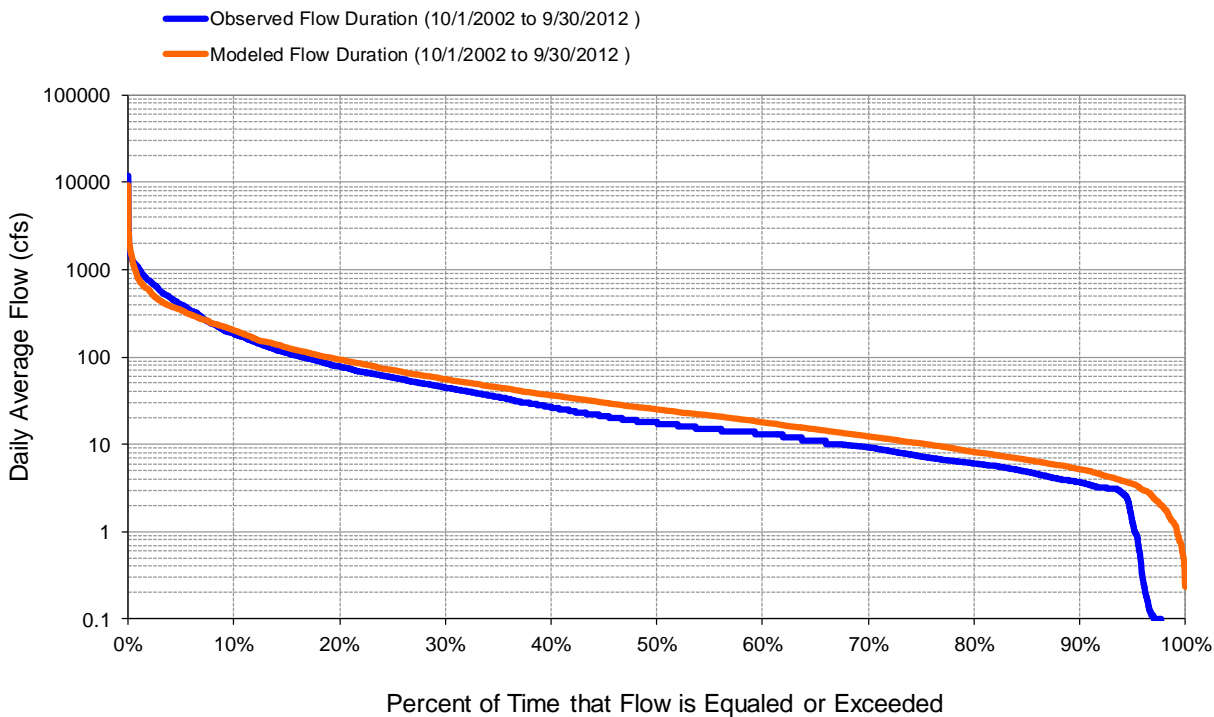


Figure 156. Flow exceedance at Knife River near Two Harbors

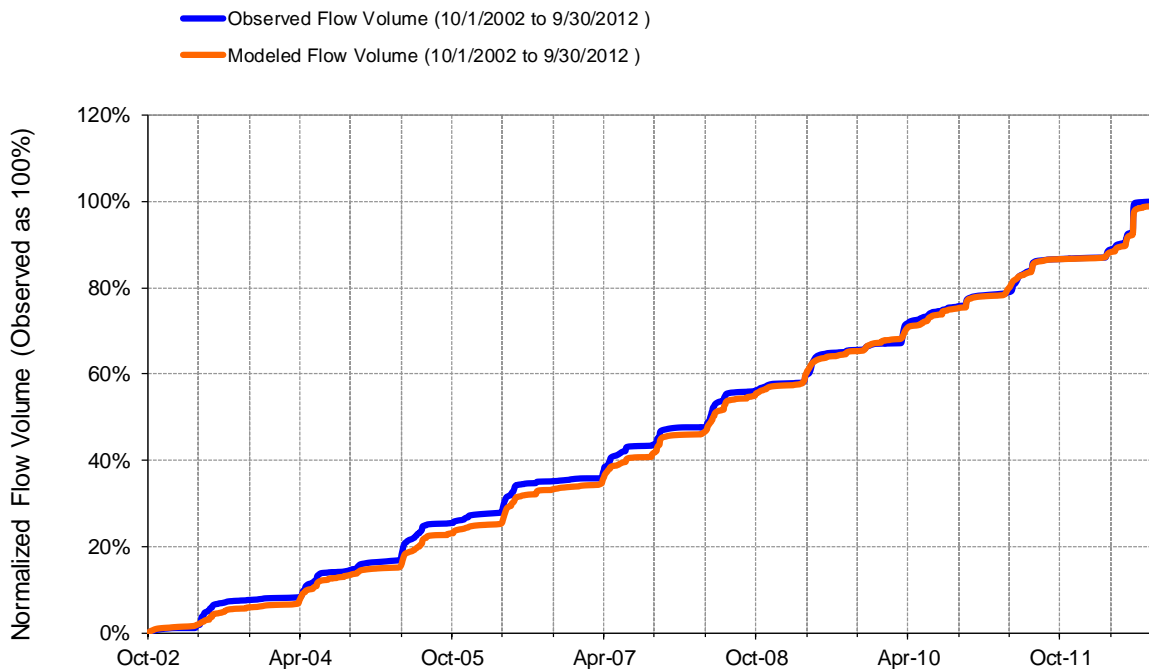


Figure 157. Flow accumulation at Knife River near Two Harbors

Table 14. Summary statistics at Knife River near Two Harbors

HSPF Simulated Flow		Observed Flow Gage	
REACH OUTFLOW FROM DSN 40 10-Year Analysis Period: 10/1/2002 - 9/30/2012 Flow volumes are (inches/year) for upstream drainage area Run 6a		Knife River near Two Harbors, MN61 Manually Entered Data Drainage Area (sq-mi): 83.6	
Total Simulated In-stream Flow:	13.21	Total Observed In-stream Flow:	13.36
Total of simulated highest 10% flows:	7.72	Total of Observed highest 10% flows:	8.92
Total of Simulated lowest 50% flows:	0.92	Total of Observed Lowest 50% flows:	0.65
Simulated Summer Flow Volume (months 7-9):	1.57	Observed Summer Flow Volume (7-9):	0.85
Simulated Fall Flow Volume (months 10-12):	2.27	Observed Fall Flow Volume (10-12):	2.08
Simulated Winter Flow Volume (months 1-3):	2.18	Observed Winter Flow Volume (1-3):	2.02
Simulated Spring Flow Volume (months 4-6):	7.19	Observed Spring Flow Volume (4-6):	8.41
Total Simulated Storm Volume:	5.75	Total Observed Storm Volume:	6.47
Simulated Summer Storm Volume (7-9):	0.83	Observed Summer Storm Volume (7-9):	0.41
<i>Errors (Simulated-Observed)</i>	<i>Error Statistics</i>	<i>Recommended Criteria</i>	
Error in total volume:	-1.10	10	
Error in 50% lowest flows:	40.79	10	
Error in 10% highest flows:	-13.45	15	
Seasonal volume error - Summer:	85.56	30	
Seasonal volume error - Fall:	8.89	30	
Seasonal volume error - Winter:	8.15	30	
Seasonal volume error - Spring:	-14.53	30	
Error in storm volumes:	-11.03	20	
Error in summer storm volumes:	104.80	50	
Nash-Sutcliffe Coefficient of Efficiency, E:	0.787	Model accuracy increases	
Baseline adjusted coefficient (Garrick), E':	0.577		
Monthly NSE	0.868		

GOOSEBERRY RIVER NEAR CASTLE DANGER (HYDSTRA 02012004)

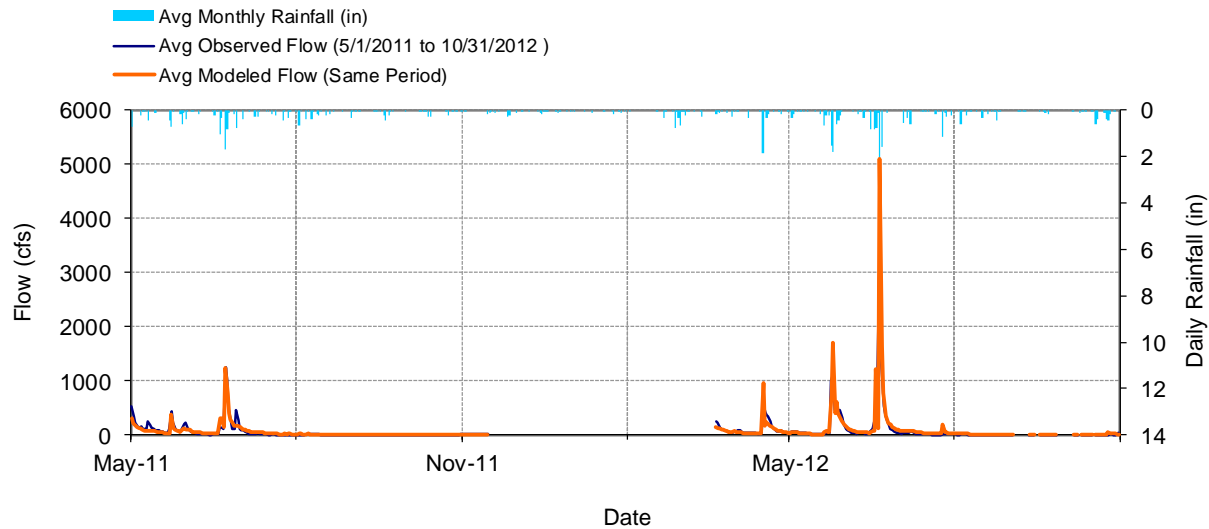


Figure 158. Mean daily flow at Gooseberry River near Castle Danger

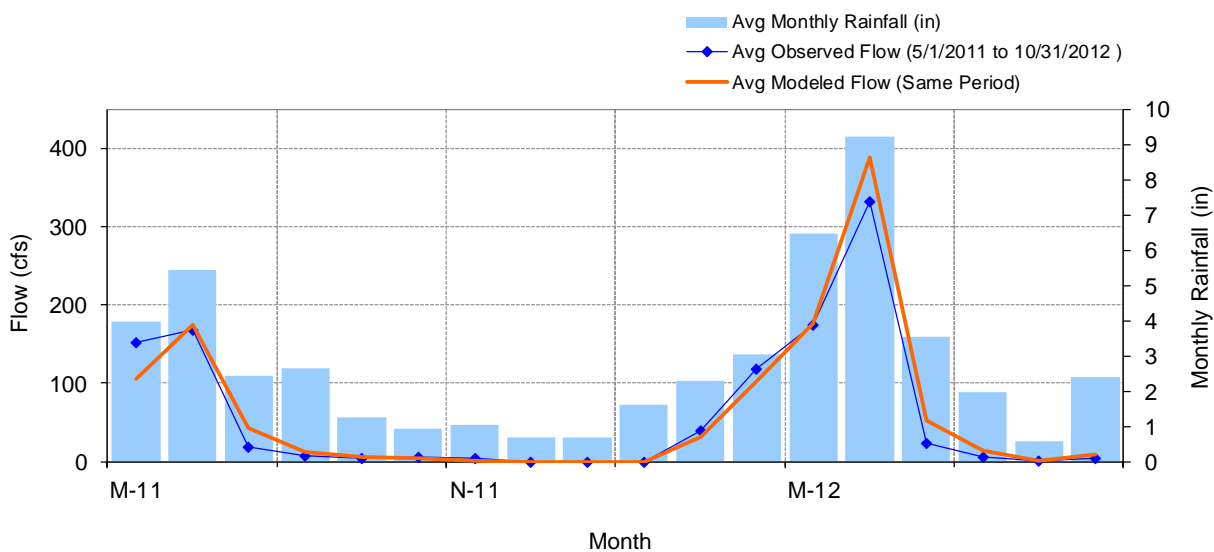


Figure 159. Mean monthly flow at Gooseberry River near Castle Danger

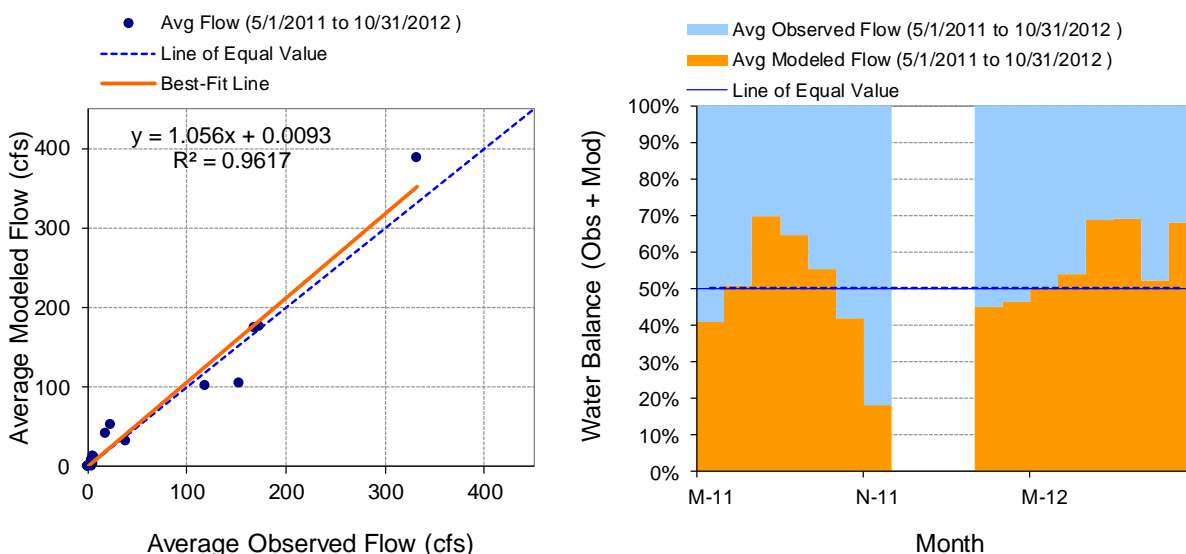


Figure 160. Monthly flow regression and temporal variation at Gooseberry River near Castle Danger

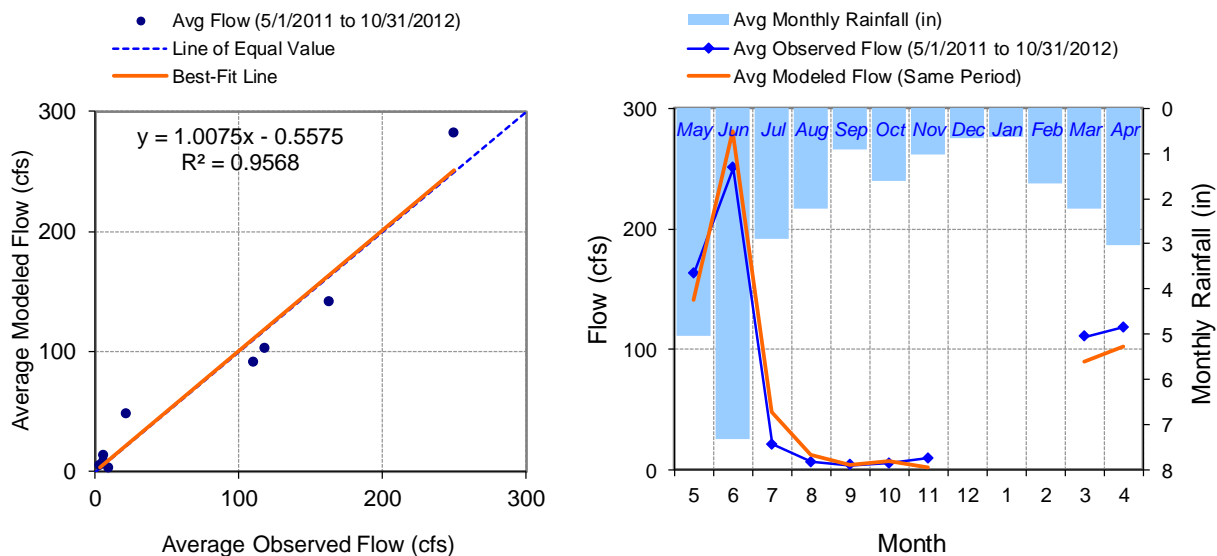


Figure 161. Seasonal regression and temporal aggregate at Gooseberry River near Castle Danger

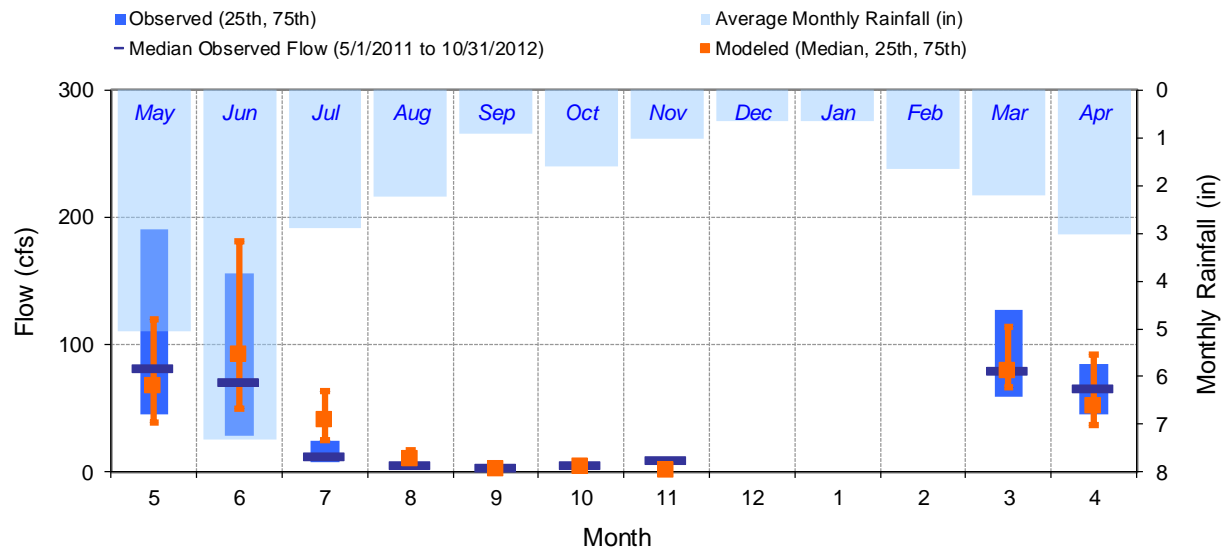


Figure 162. Seasonal medians and ranges at Gooseberry River near Castle Danger

Table 15. Seasonal summary at Gooseberry River near Castle Danger

MONTH	OBSERVED FLOW (CFS)				MODELED FLOW (CFS)			
	MEAN	MEDIAN	25TH	75TH	MEAN	MEDIAN	25TH	75TH
May	163.06	81.50	45.25	190.25	140.53	67.65	38.74	119.98
Jun	250.32	70.50	28.50	155.75	281.12	92.69	50.08	180.92
Jul	21.17	12.00	7.40	24.75	47.61	41.21	24.84	63.26
Aug	6.21	5.70	4.43	7.38	12.54	10.72	7.20	17.50
Sep	3.51	3.20	2.60	4.75	4.26	2.87	1.90	5.99
Oct	5.55	4.90	3.55	6.55	7.17	4.49	1.96	7.46
Nov	9.41	9.30	9.10	9.75	2.10	1.89	1.61	2.48
Dec	0.00	0.00	0.00	0.00	0.00	0.00	0.00	0.00
Jan	0.00	0.00	0.00	0.00	0.00	0.00	0.00	0.00
Feb	0.00	0.00	0.00	0.00	0.00	0.00	0.00	0.00
Mar	110.18	79.00	59.00	127.00	90.03	79.25	66.83	114.08
Apr	118.27	66.00	45.75	84.50	102.46	51.34	36.91	92.11

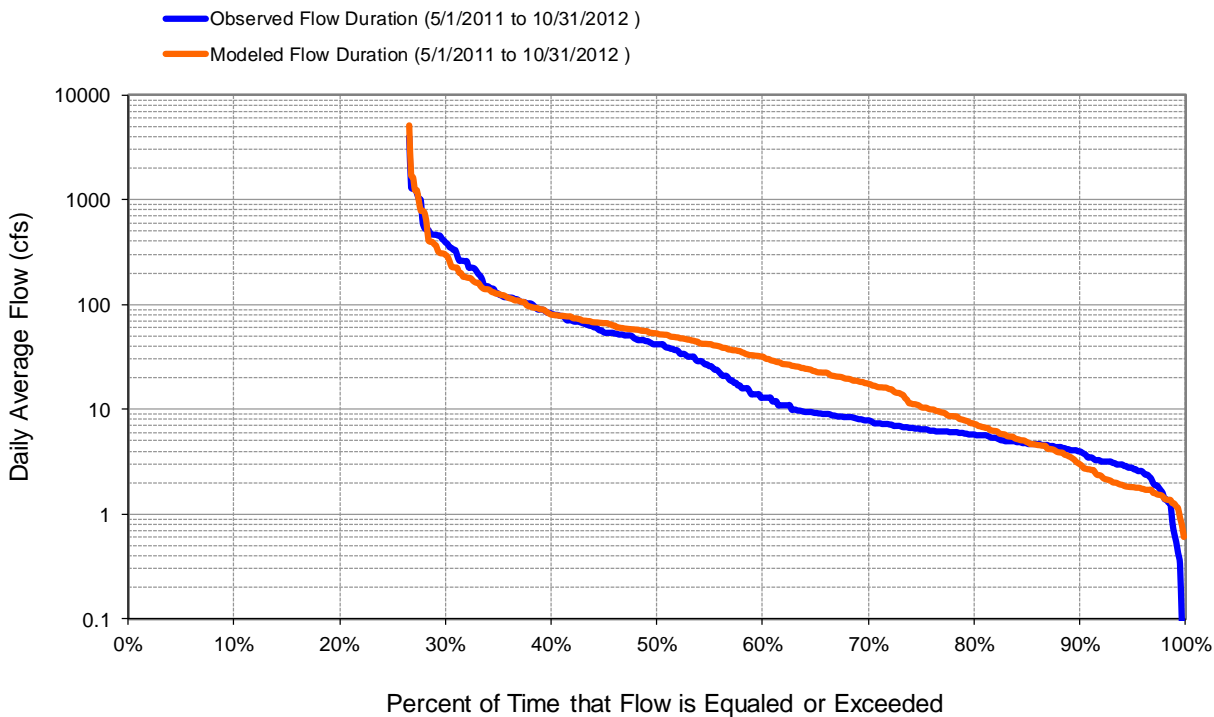


Figure 163. Flow exceedance at Gooseberry River near Castle Danger

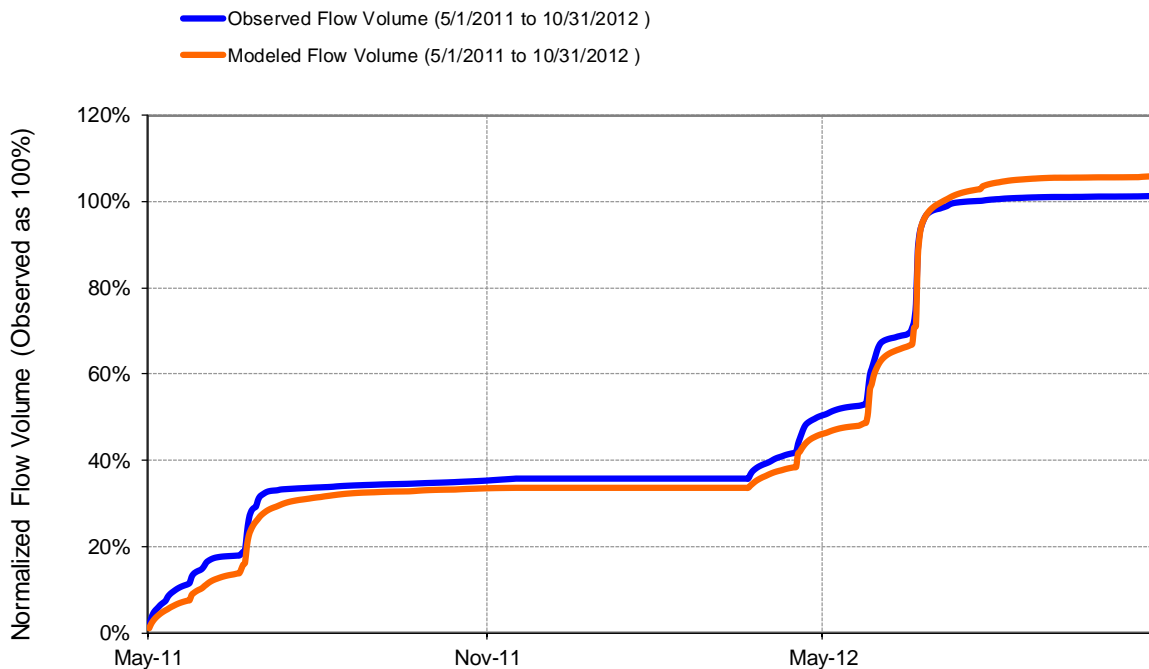
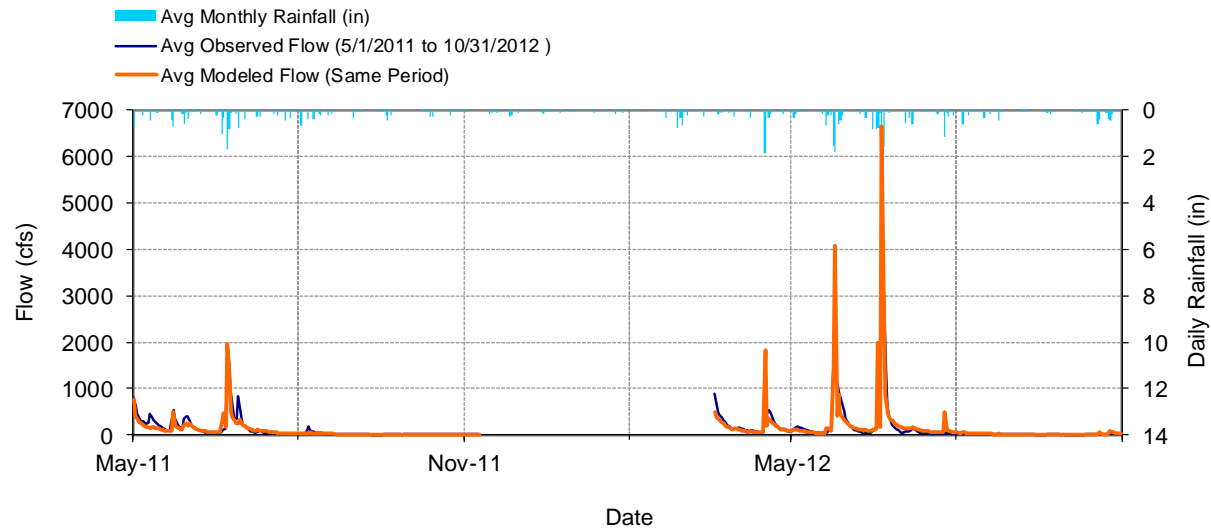
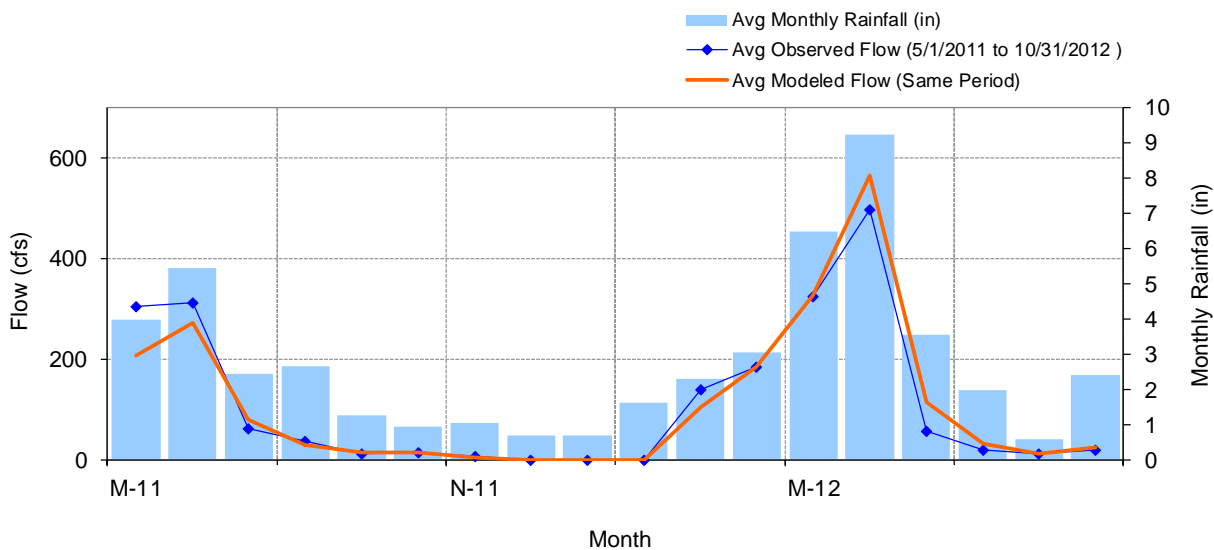


Figure 164. Flow accumulation at Gooseberry River near Castle Danger

Table 16. Summary statistics at Gooseberry River near Castle Danger

HSPF Simulated Flow		Observed Flow Gage	
REACH OUTFLOW FROM DSN 50 1.51-Year Analysis Period: 5/1/2011 - 10/31/2012 Flow volumes are (inches/year) for upstream drainage area		Gooseberry River nr Castle Danger, 0.34 mi us of MN61 Manually Entered Data Drainage Area (sq-mi): 74.8	
Total Simulated In-stream Flow:	11.23	Total Observed In-stream Flow:	10.63
Total of simulated highest 10% flows:	7.34	Total of Observed highest 10% flows:	7.44
Total of Simulated lowest 50% flows:	0.60	Total of Observed Lowest 50% flows:	0.36
Simulated Summer Flow Volume (months 7-9):	1.30	Observed Summer Flow Volume (7-9):	0.62
Simulated Fall Flow Volume (months 10-12):	0.14	Observed Fall Flow Volume (10-12):	0.15
Simulated Winter Flow Volume (months 1-3):	0.33	Observed Winter Flow Volume (1-3):	0.40
Simulated Spring Flow Volume (months 4-6):	9.46	Observed Spring Flow Volume (4-6):	9.47
Total Simulated Storm Volume:	6.24	Total Observed Storm Volume:	6.18
Simulated Summer Storm Volume (7-9):	0.26	Observed Summer Storm Volume (7-9):	0.19
<i>Errors (Simulated-Observed)</i>	<i>Error Statistics</i>	<i>Recommended Criteria</i>	
Error in total volume:	5.59	10	
Error in 50% lowest flows:	65.79	10	
Error in 10% highest flows:	-1.37	15	
Seasonal volume error - Summer:	110.98	30	
Seasonal volume error - Fall:	-4.59	30	
Seasonal volume error - Winter:	-18.29	30	
Seasonal volume error - Spring:	-0.08	30	
Error in storm volumes:	1.06	20	
Error in summer storm volumes:	37.25	50	
Nash-Sutcliffe Coefficient of Efficiency, E:	0.830	Model accuracy increases	
Baseline adjusted coefficient (Garrick), E':	0.669		
Monthly NSE	0.949		

BEAVER RIVER NEAR BEAVER BAY (HYDSTRA 02006003)**Figure 165. Mean daily flow at Beaver River near Beaver Bay****Figure 166. Mean monthly flow at Beaver River near Beaver Bay**

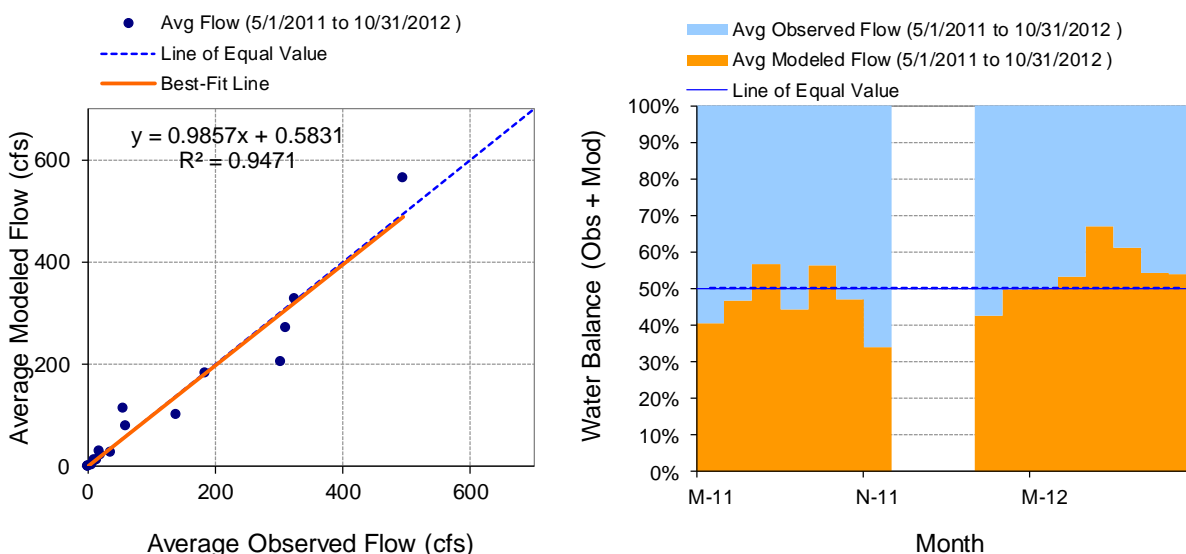


Figure 167. Monthly flow regression and temporal variation at Beaver River near Beaver Bay

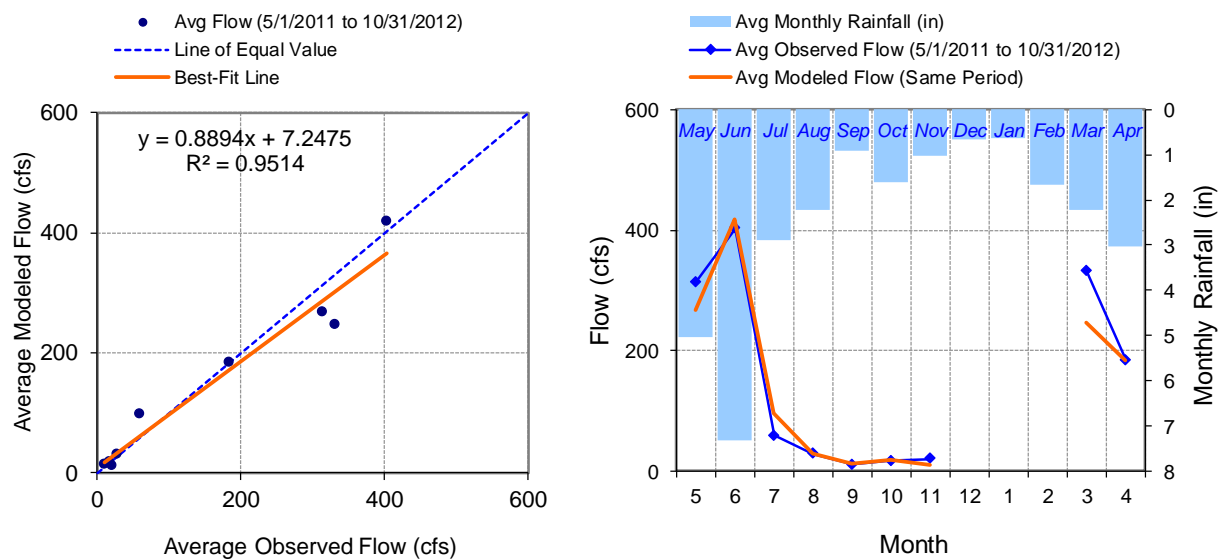


Figure 168. Seasonal regression and temporal aggregate at Beaver River near Beaver Bay

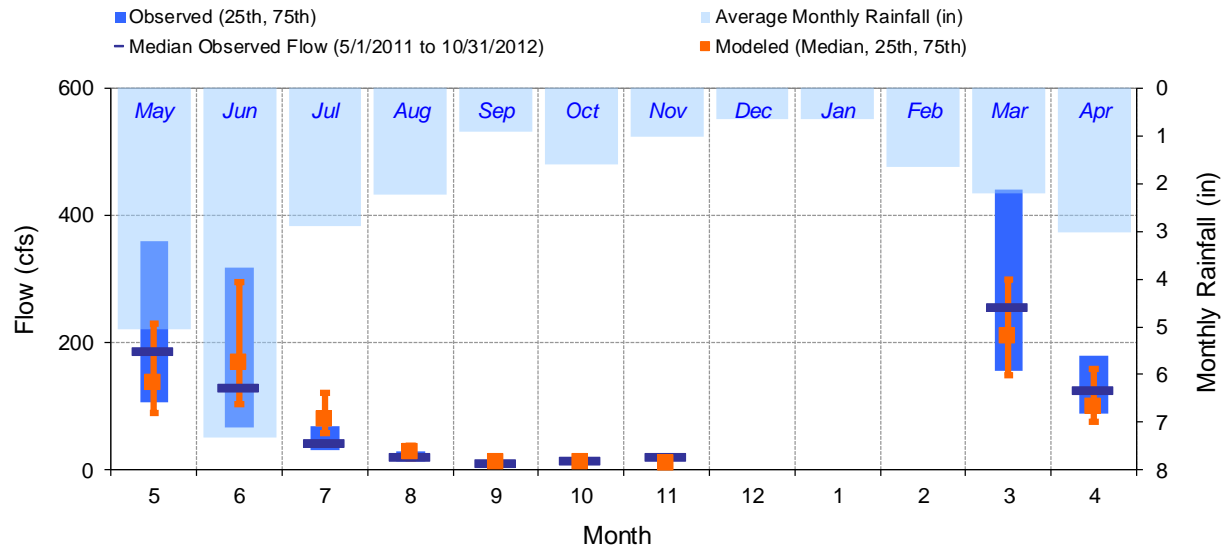
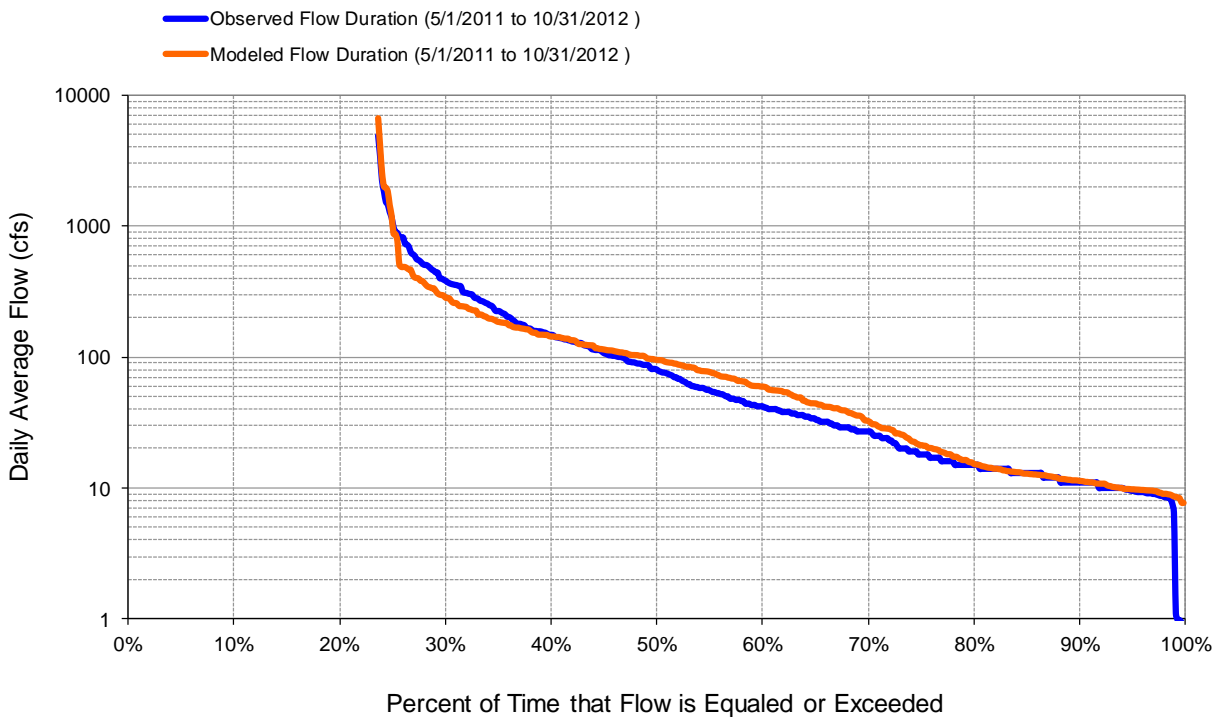
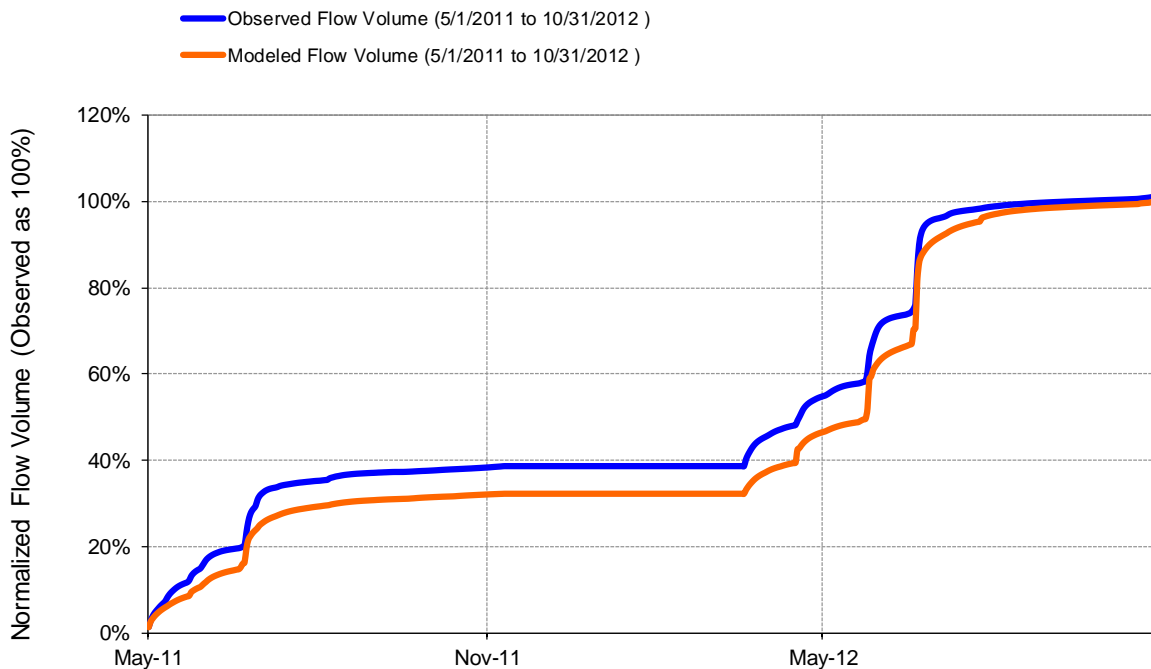


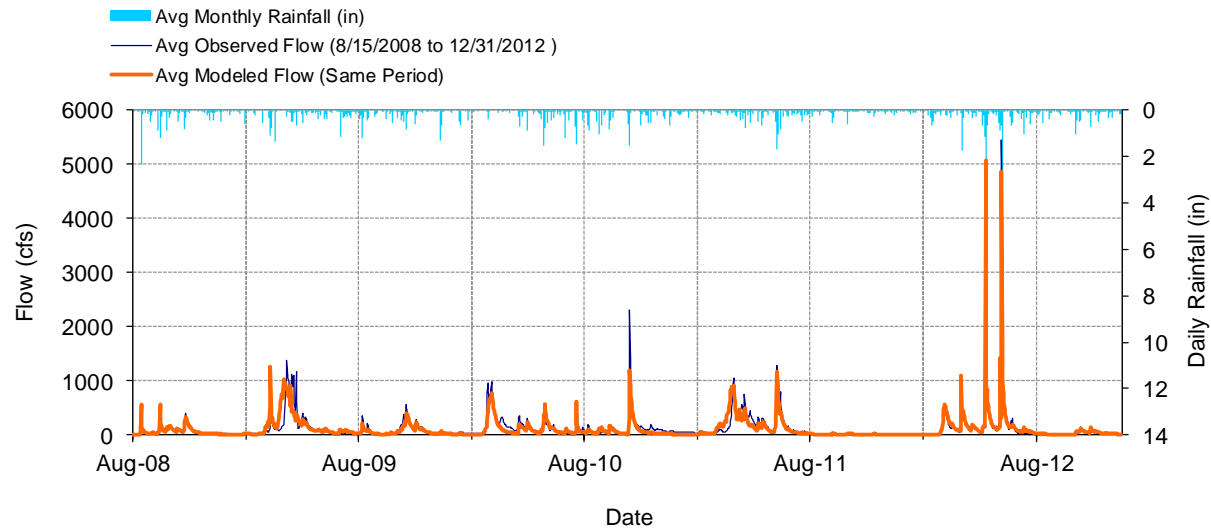
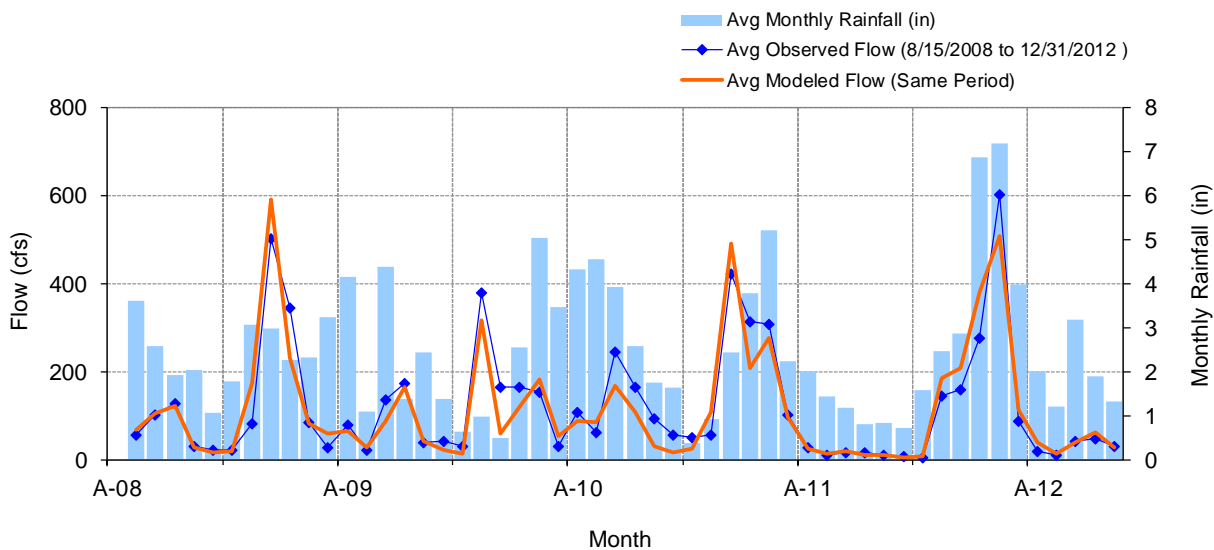
Figure 169. Seasonal medians and ranges at Beaver River near Beaver Bay

Table 17. Seasonal summary at Beaver River near Beaver Bay

MONTH	OBSERVED FLOW (CFS)				MODELED FLOW (CFS)			
	MEAN	MEDIAN	25TH	75TH	MEAN	MEDIAN	25TH	75TH
May	313.85	186.00	107.00	360.25	266.28	137.84	89.20	230.09
Jun	402.87	129.50	66.50	318.00	418.15	167.76	103.09	295.13
Jul	58.42	42.50	32.25	68.75	96.57	80.69	57.29	120.92
Aug	28.00	20.00	14.00	30.00	29.91	27.62	19.34	37.96
Sep	10.16	11.00	9.35	11.25	12.60	11.90	10.78	13.95
Oct	17.17	14.00	11.00	17.00	18.06	12.42	9.82	19.00
Nov	20.33	20.00	18.00	23.00	10.43	10.15	9.69	11.04
Dec	0.00	0.00	0.00	0.00	0.00	0.00	0.00	0.00
Jan	0.00	0.00	0.00	0.00	0.00	0.00	0.00	0.00
Feb	0.00	0.00	0.00	0.00	0.00	0.00	0.00	0.00
Mar	332.00	255.00	156.00	440.00	245.88	210.74	148.61	299.12
Apr	184.47	125.00	89.25	179.50	183.40	98.77	75.51	158.07

**Figure 170. Flow exceedance at Beaver River near Beaver Bay****Figure 171. Flow accumulation at Beaver River near Beaver Bay****Table 18. Summary statistics at Beaver River near Beaver Bay**

HSPF Simulated Flow		Observed Flow Gage	
REACH OUTFLOW FROM DSN 60 1.51-Year Analysis Period: 5/1/2011 - 10/31/2012 Flow volumes are (inches/year) for upstream drainage area		Beaver River nr Beaver Bay, 1.2mi us of MN61 Manually Entered Data Drainage Area (sq-mi): 121.6	
Total Simulated In-stream Flow:	12.21	Total Observed In-stream Flow:	12.33
Total of simulated highest 10% flows:	7.25	Total of Observed highest 10% flows:	7.52
Total of Simulated lowest 50% flows:	0.91	Total of Observed Lowest 50% flows:	0.76
Simulated Summer Flow Volume (months 7-9):	1.75	Observed Summer Flow Volume (7-9):	1.21
Simulated Fall Flow Volume (months 10-12):	0.25	Observed Fall Flow Volume (10-12):	0.25
Simulated Winter Flow Volume (months 1-3):	0.65	Observed Winter Flow Volume (1-3):	0.88
Simulated Spring Flow Volume (months 4-6):	9.57	Observed Spring Flow Volume (4-6):	9.99
Total Simulated Storm Volume:	6.16	Total Observed Storm Volume:	6.07
Simulated Summer Storm Volume (7-9):	0.31	Observed Summer Storm Volume (7-9):	0.32
<i>Errors (Simulated-Observed)</i>	<i>Error Statistics</i>	<i>Recommended Criteria</i>	
Error in total volume:	-0.97	10	
Error in 50% lowest flows:	20.05	10	
Error in 10% highest flows:	-3.57	15	
Seasonal volume error - Summer:	44.08	30	
Seasonal volume error - Fall:	-2.71	30	
Seasonal volume error - Winter:	-25.94	30	Clear
Seasonal volume error - Spring:	-4.20	30	
Error in storm volumes:	1.47	20	
Error in summer storm volumes:	-1.37	50	
Nash-Sutcliffe Coefficient of Efficiency, E:	0.735	Model accuracy increases	
Baseline adjusted coefficient (Garrick), E':	0.645		
Monthly NSE	0.941		

BAPTISM RIVER NEAR BEAVER BAY (HYDSTRA 01092001)**Figure 172. Mean daily flow at Baptism River near Beaver Bay****Figure 173. Mean monthly flow at Baptism River near Beaver Bay**

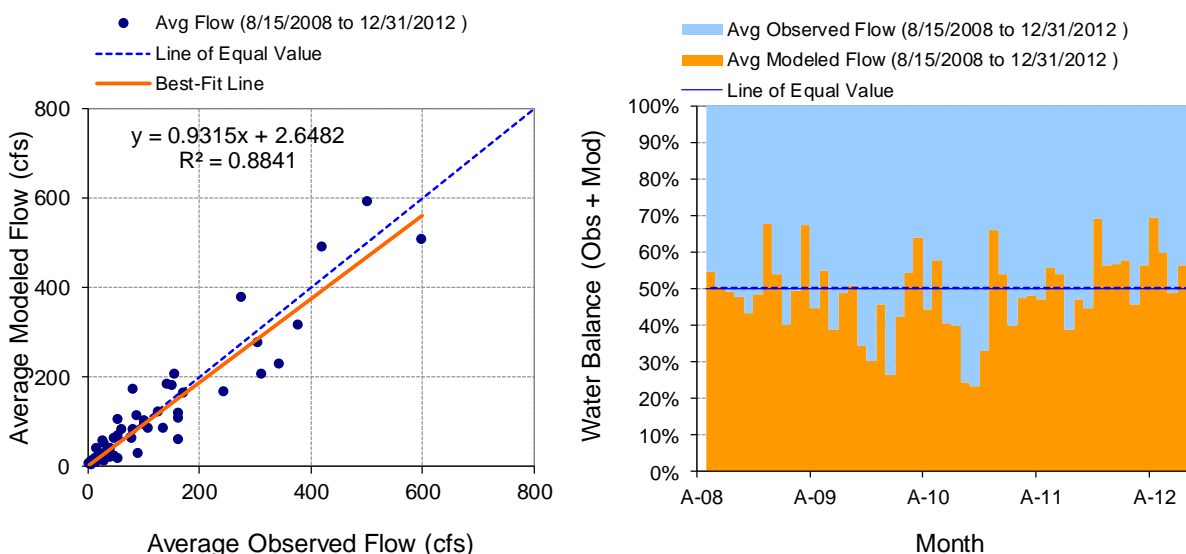


Figure 174. Monthly flow regression and temporal variation at Baptism River near Beaver Bay

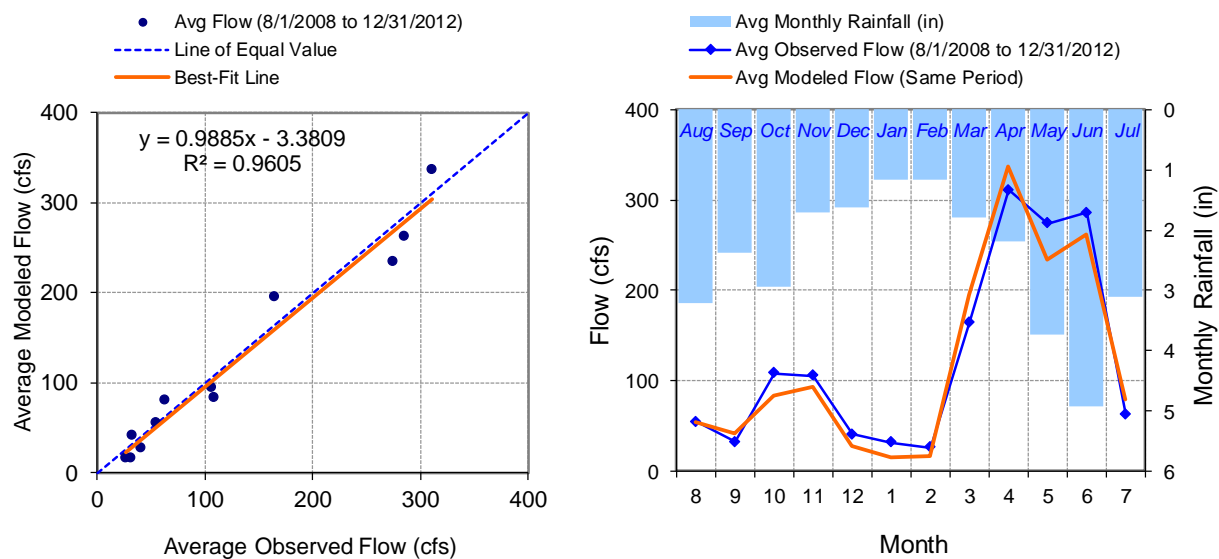


Figure 175. Seasonal regression and temporal aggregate at Baptism River near Beaver Bay

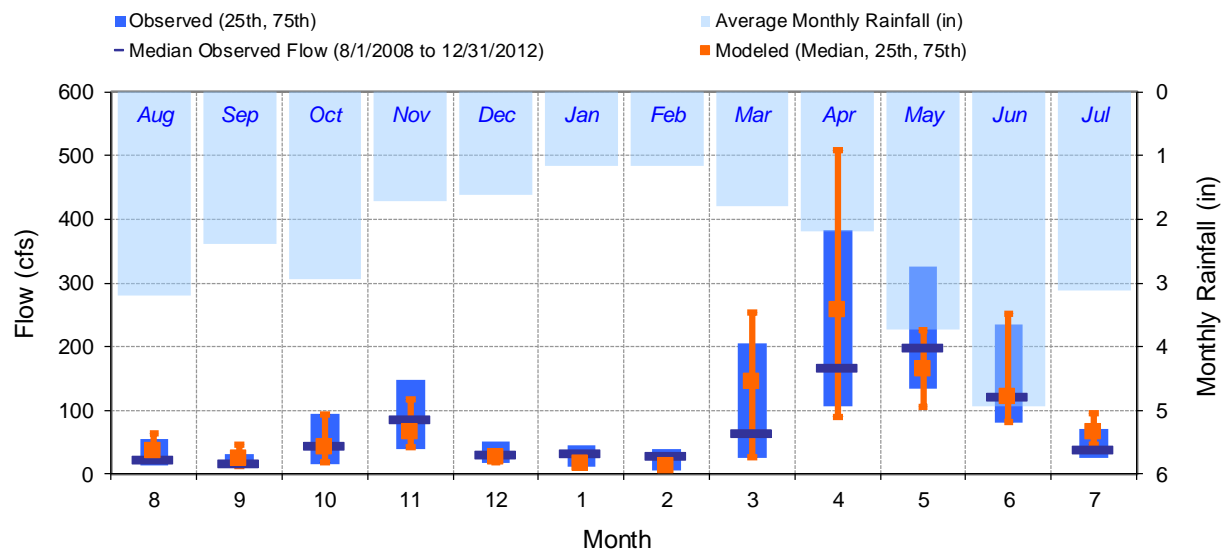


Figure 176. Seasonal medians and ranges at Baptism River near Beaver Bay

Table 19. Seasonal summary at Baptism River near Beaver Bay

MONTH	OBSERVED FLOW (CFS)				MODELED FLOW (CFS)			
	MEAN	MEDIAN	25TH	75TH	MEAN	MEDIAN	25TH	75TH
Aug	54.70	23.00	13.00	55.00	54.80	36.84	22.35	64.21
Sep	32.09	16.00	10.25	30.75	41.20	24.76	13.30	46.23
Oct	107.87	45.00	16.50	95.50	82.95	42.78	18.61	94.49
Nov	105.55	85.00	39.00	148.50	93.38	65.47	42.95	117.42
Dec	40.75	31.00	18.58	51.50	27.14	26.27	19.44	34.23
Jan	31.28	33.00	11.75	46.10	15.07	16.33	11.49	18.57
Feb	25.99	27.73	6.60	39.27	16.06	12.76	11.27	17.61
Mar	164.42	63.97	25.75	205.75	194.74	144.89	25.69	252.88
Apr	311.19	167.00	105.75	383.25	336.87	258.52	89.43	509.08
May	274.31	197.50	133.50	325.25	234.31	164.48	104.55	226.67
Jun	285.70	121.00	81.00	234.00	261.91	121.35	82.46	251.14
Jul	62.25	37.50	24.75	71.75	79.81	65.94	46.55	95.10

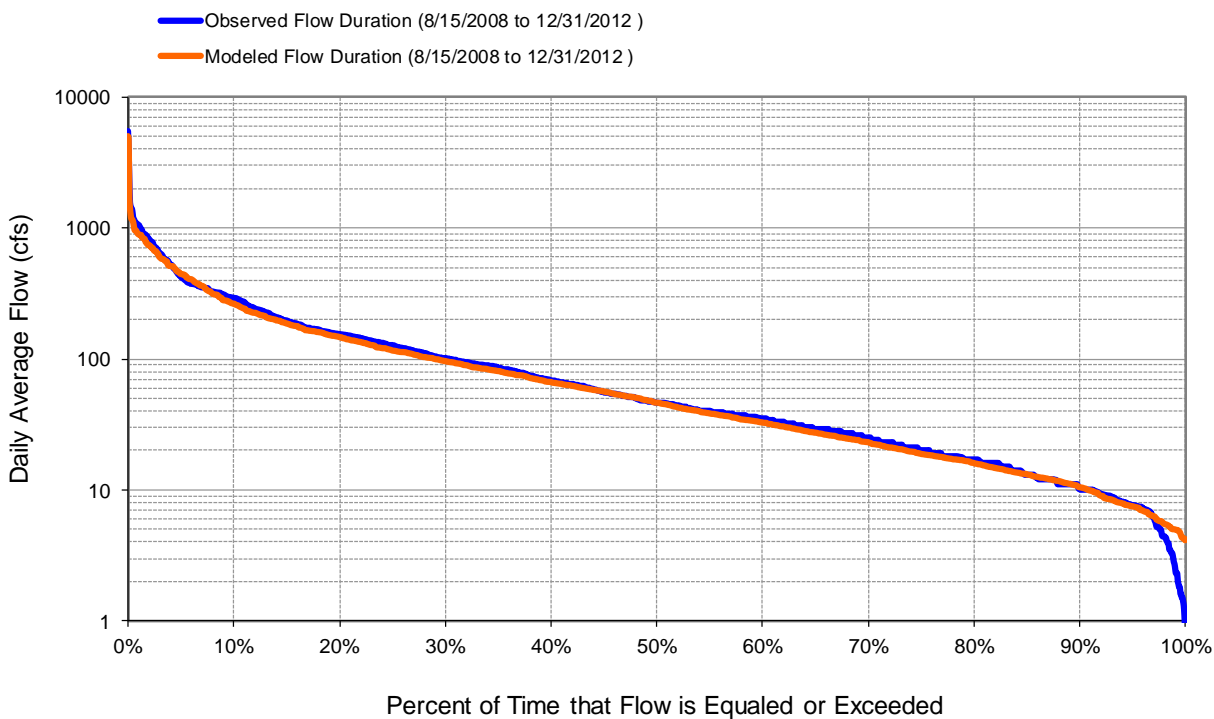


Figure 177. Flow exceedance at Baptism River near Beaver Bay

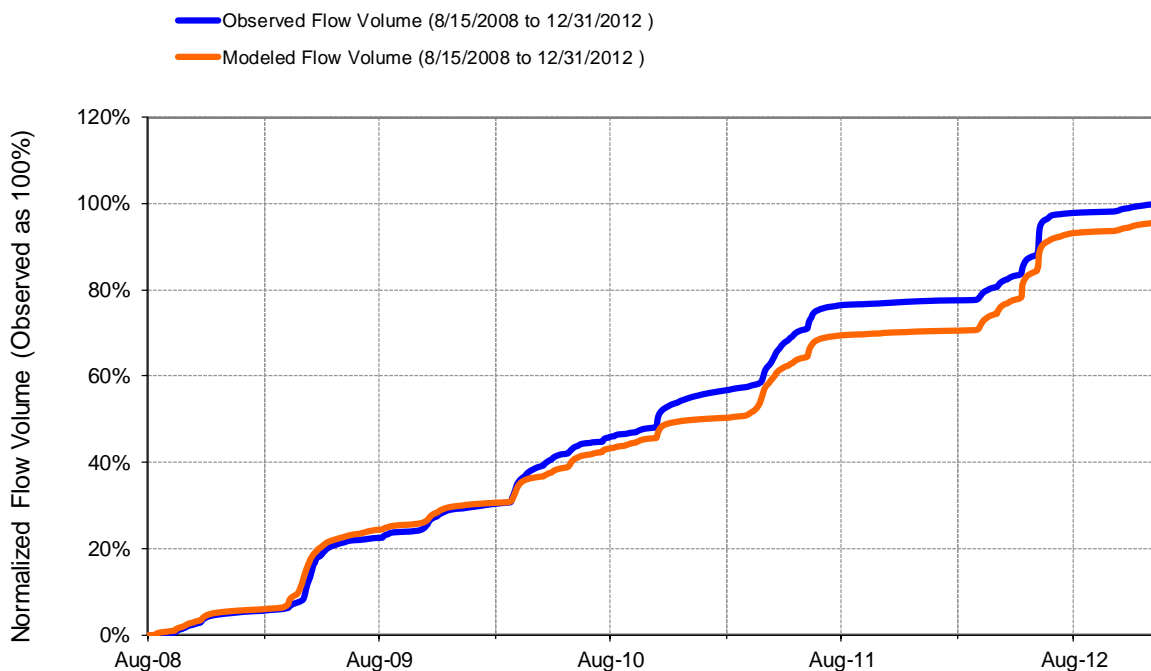
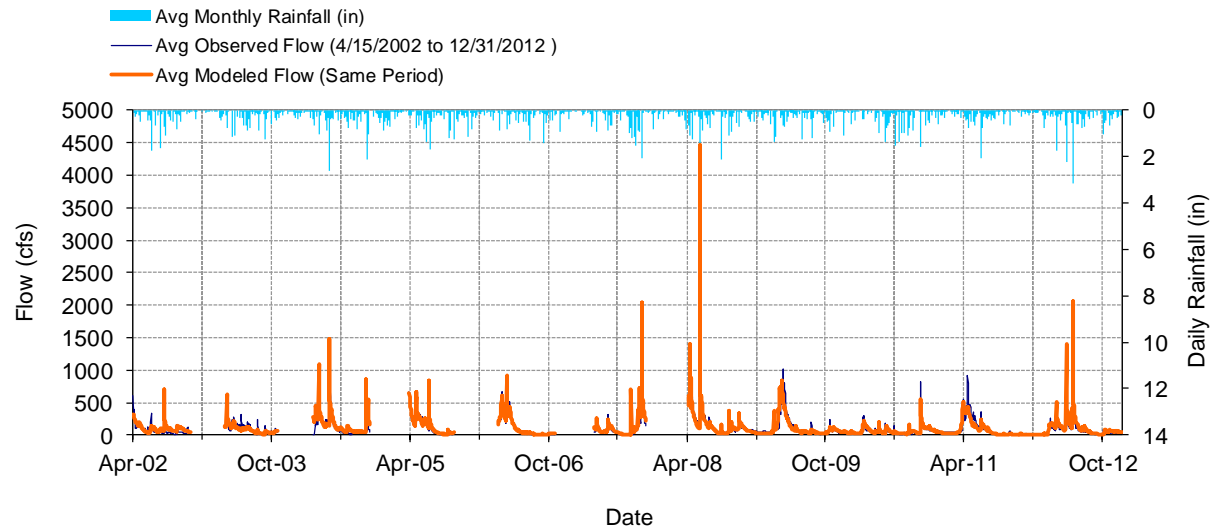
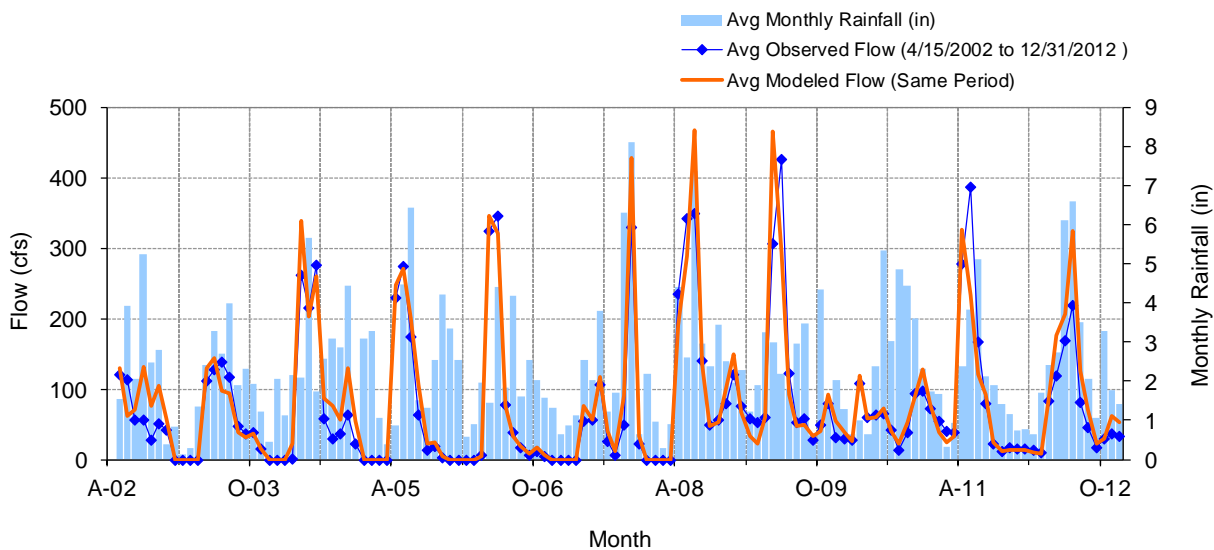


Figure 178. Flow accumulation at Baptism River near Beaver Bay

Table 20. Summary statistics at Baptism River near Beaver Bay

HSPF Simulated Flow		Observed Flow Gage		
REACH OUTFLOW FROM DSN 70 4.38-Year Analysis Period: 8/1/2008 - 12/31/2012 Flow volumes are (inches/year) for upstream drainage area Run 6h		Baptism River near Beaver Bay Manually Entered Data Drainage Area (sq-mi): 140		
Total Simulated In-stream Flow:	11.13	Total Observed In-stream Flow:	11.64	
Total of simulated highest 10% flows:	5.75	Total of Observed highest 10% flows:	6.00	
Total of Simulated lowest 50% flows:	1.04	Total of Observed Lowest 50% flows:	1.08	
Simulated Summer Flow Volume (months 7-9):	1.44	Observed Summer Flow Volume (7-9):	1.23	
Simulated Fall Flow Volume (months 10-12):	1.88	Observed Fall Flow Volume (10-12):	2.36	
Simulated Winter Flow Volume (months 1-3):	1.69	Observed Winter Flow Volume (1-3):	1.65	
Simulated Spring Flow Volume (months 4-6):	6.12	Observed Spring Flow Volume (4-6):	6.41	
Total Simulated Storm Volume:	3.54	Total Observed Storm Volume:	3.96	
Simulated Summer Storm Volume (7-9):	0.41	Observed Summer Storm Volume (7-9):	0.49	
<i>Errors (Simulated-Observed)</i>	<i>Error Statistics</i>	<i>Recommended Criteria</i>	<i>Run (n-1)</i>	<i>Run (n-2)</i>
Error in total volume:	-4.35	10	-6.22	
Error in 50% lowest flows:	-3.76	10	-3.76	
Error in 10% highest flows:	-4.16	15	-7.84	
Seasonal volume error - Summer:	17.58	30	17.58	
Seasonal volume error - Fall:	-20.06	30	-20.06	
Seasonal volume error - Winter:	2.31	30	2.31	
Seasonal volume error - Spring:	-4.48	30	-7.92	
Error in storm volumes:	-10.43	20	-16.21	
Error in summer storm volumes:	-15.44	50	-15.44	
Nash-Sutcliffe Coefficient of Efficiency, E:	0.647	Model accuracy increases	0.765	
Baseline adjusted coefficient (Garrick), E':	0.599		0.613	
Monthly NSE	0.881		0.890	

Note: Run (n-1) shows the model performance when some large observed peaks that are labeled as poor or unreliable are removed.

POPLAR RIVER NEAR LUTSEN (HYDSTRA 01063003)**Figure 179. Mean daily flow at Poplar River near Lutsen****Figure 180. Mean monthly flow at Poplar River near Lutsen**

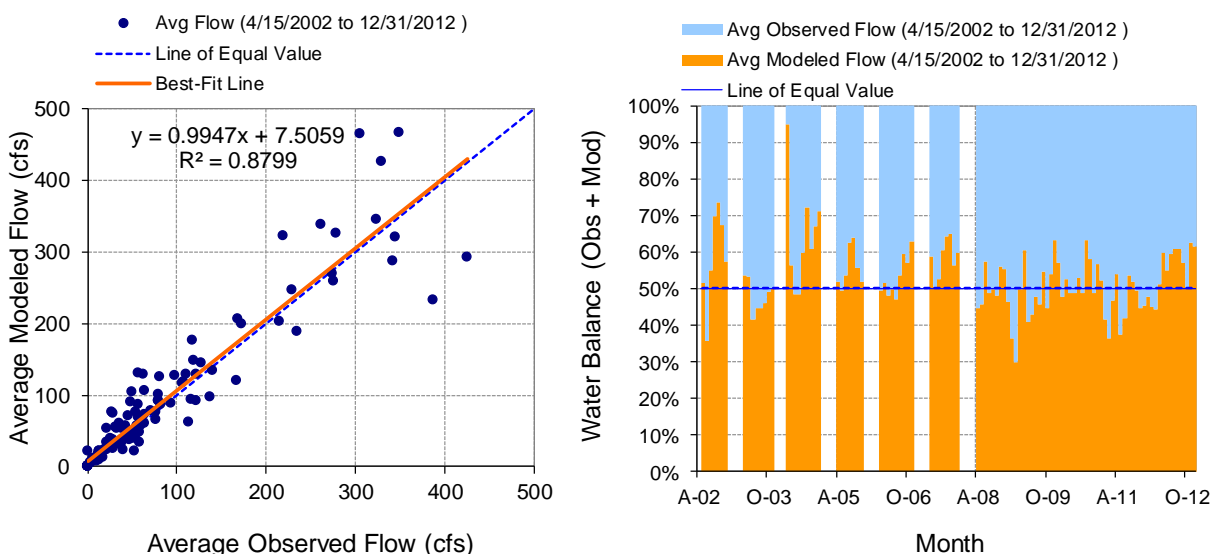


Figure 181. Monthly flow regression and temporal variation at Poplar River near Lutsen

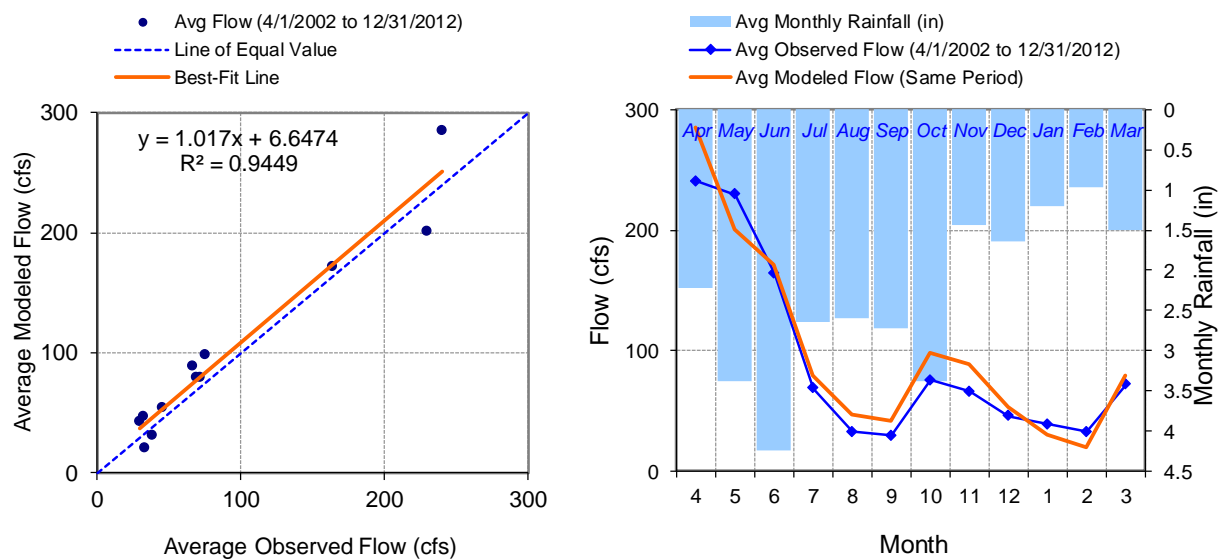


Figure 182. Seasonal regression and temporal aggregate at Poplar River near Lutsen

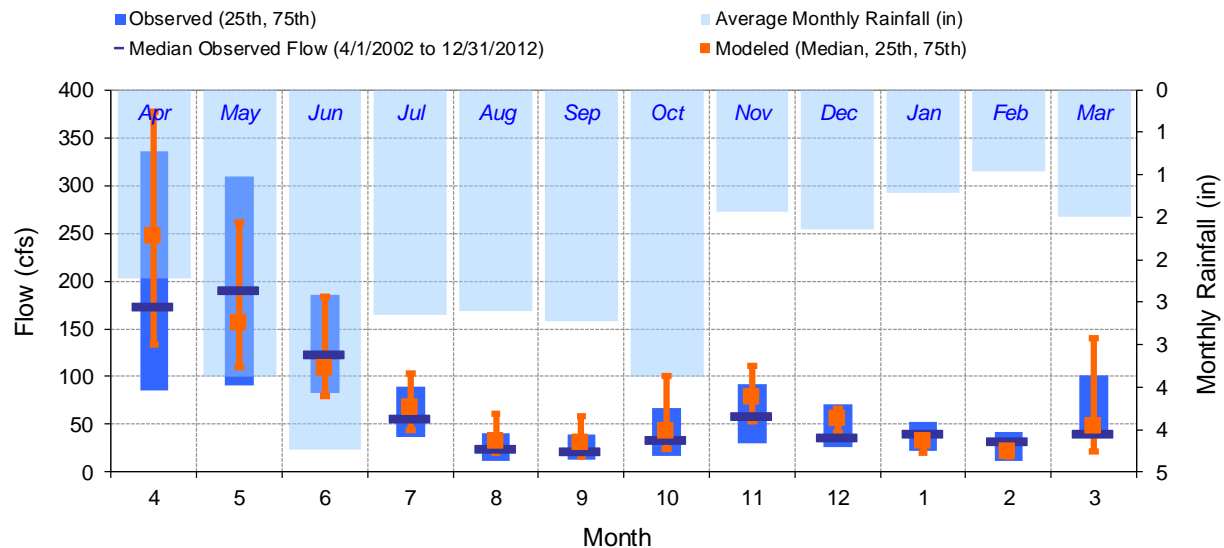


Figure 183. Seasonal medians and ranges at Poplar River near Lutsen

Table 21. Seasonal summary at Poplar River near Lutsen

MONTH	OBSERVED FLOW (CFS)				MODELED FLOW (CFS)			
	MEAN	MEDIAN	25TH	75TH	MEAN	MEDIAN	25TH	75TH
Apr	240.46	172.64	85.00	335.82	284.82	246.30	134.14	377.38
May	229.60	190.24	91.41	310.00	200.49	156.33	110.42	261.01
Jun	164.13	122.65	83.00	185.54	171.62	108.88	79.98	183.80
Jul	68.61	56.00	36.92	89.53	79.19	68.23	44.42	103.44
Aug	32.32	24.00	12.00	40.15	46.43	32.43	19.65	60.51
Sep	29.61	21.00	13.00	39.71	41.83	31.13	15.95	58.28
Oct	75.58	34.00	16.50	67.02	97.80	42.26	24.04	100.14
Nov	66.15	58.78	30.18	91.84	88.72	78.71	52.68	111.52
Dec	45.72	36.00	26.71	71.29	53.44	56.47	41.89	66.69
Jan	38.57	40.50	22.64	52.16	30.18	32.12	19.94	39.96
Feb	32.70	32.00	12.00	41.96	19.86	21.24	16.68	25.12
Mar	71.76	40.00	38.36	101.00	79.27	47.89	22.16	139.90

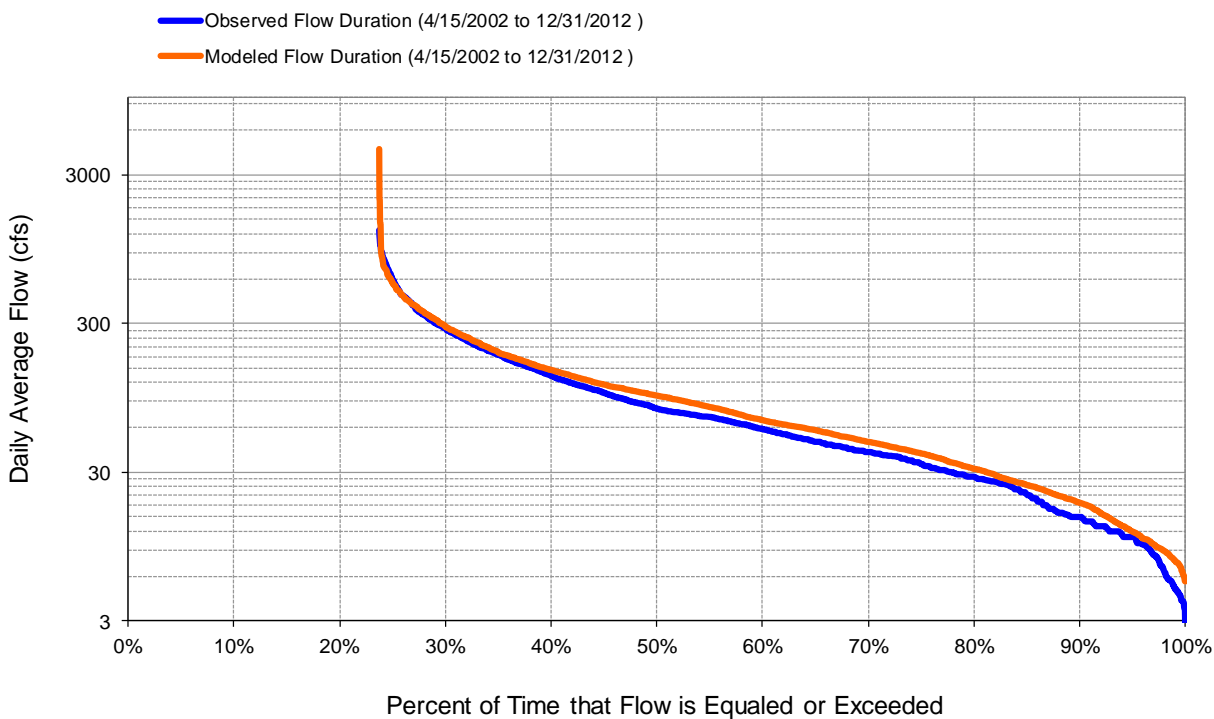


Figure 184. Flow exceedance at Poplar River near Lutsen

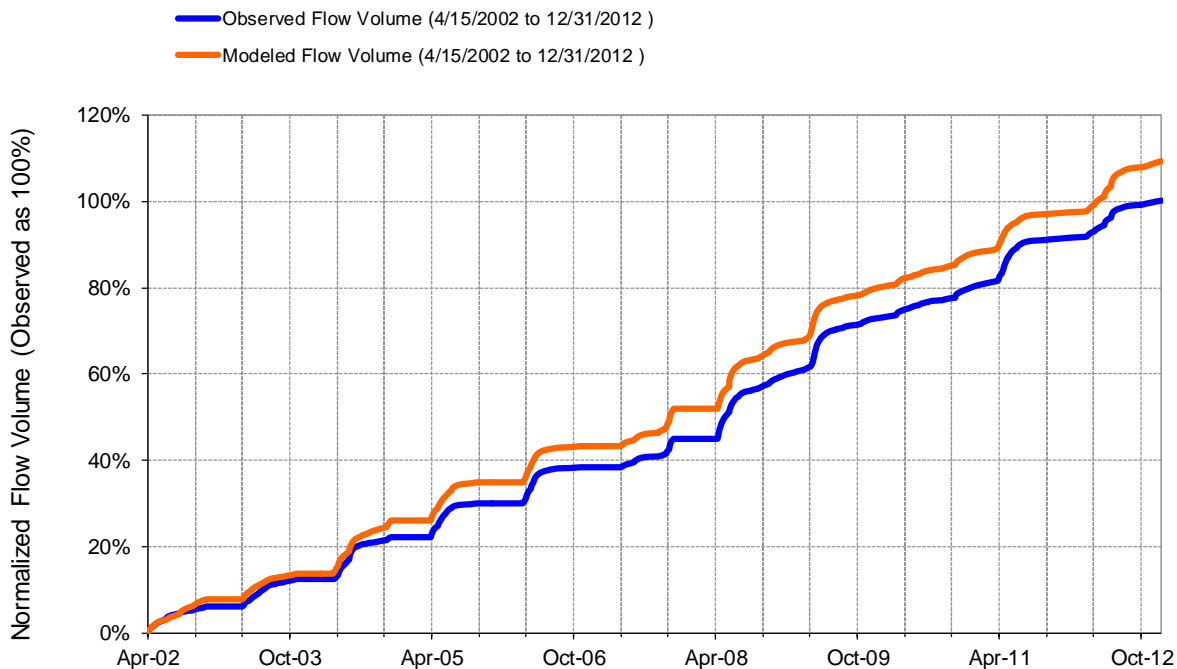
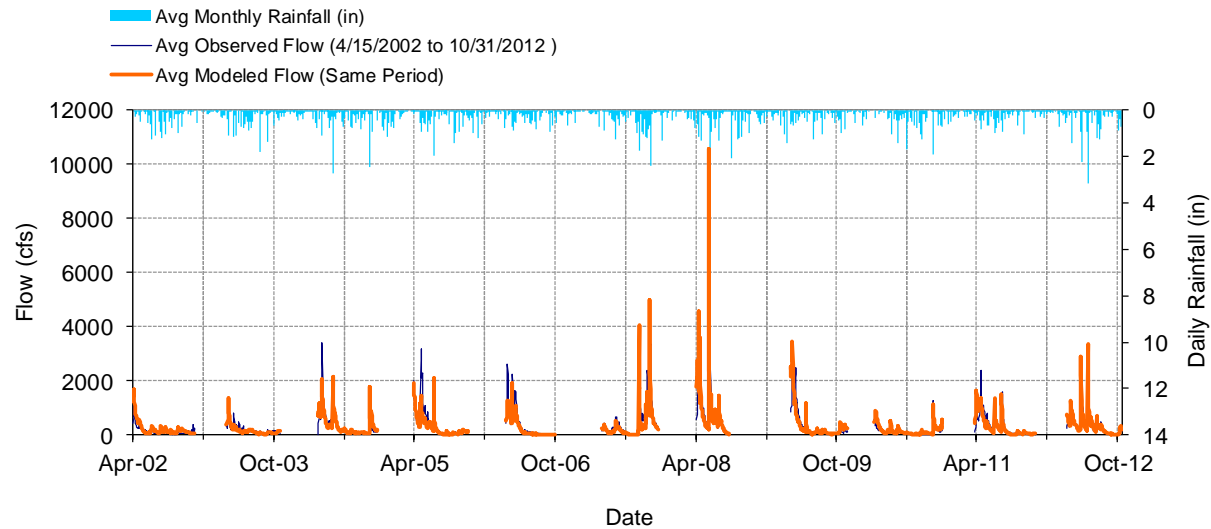
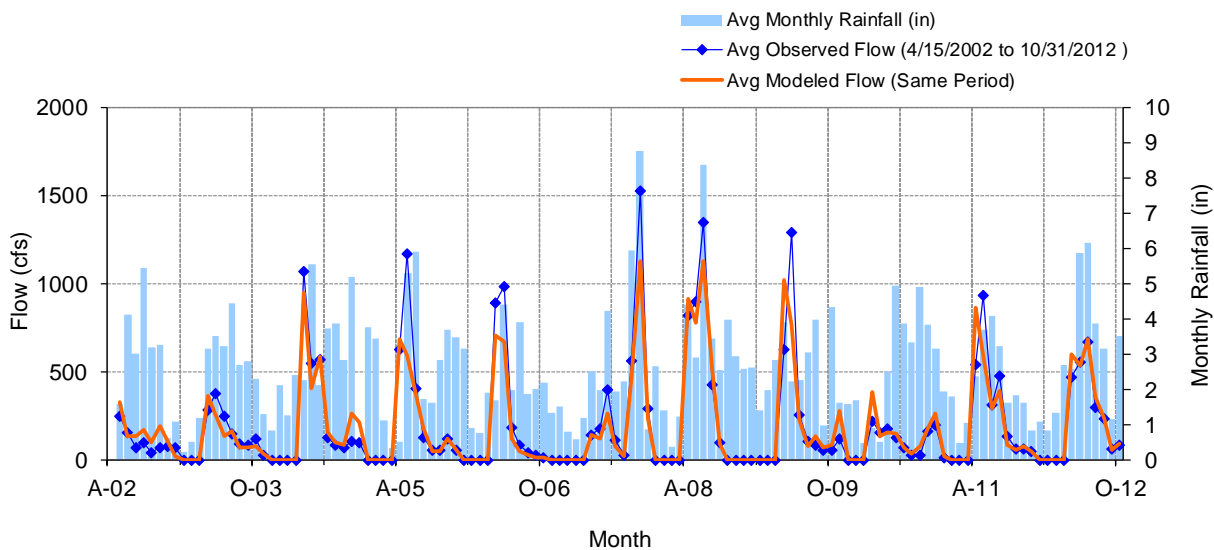


Figure 185. Flow accumulation at Poplar River near Lutsen

Table 22. Summary statistics at Poplar River near Lutsen

HSPF Simulated Flow		Observed Flow Gage		
REACH OUTFLOW FROM DSN 80 10.72-Year Analysis Period: 4/1/2002 - 12/31/2012 Flow volumes are (inches/year) for upstream drainage area		Poplar River near Lutsen, 0.2 mi us of MN61 Manually Entered Data Drainage Area (sq-mi): 114		
Total Simulated In-stream Flow:	10.03	Total Observed In-stream Flow:	9.18	
Total of simulated highest 10% flows:	4.08	Total of Observed highest 10% flows:	3.91	
Total of Simulated lowest 50% flows:	1.46	Total of Observed Lowest 50% flows:	1.24	
Simulated Summer Flow Volume (months 7-9):	1.72	Observed Summer Flow Volume (7-9):	1.35	
Simulated Fall Flow Volume (months 10-12):	1.75	Observed Fall Flow Volume (10-12):	1.36	
Simulated Winter Flow Volume (months 1-3):	0.49	Observed Winter Flow Volume (1-3):	0.54	
Simulated Spring Flow Volume (months 4-6):	6.07	Observed Spring Flow Volume (4-6):	5.94	
Total Simulated Storm Volume:	1.93	Total Observed Storm Volume:	1.99	
Simulated Summer Storm Volume (7-9):	0.29	Observed Summer Storm Volume (7-9):	0.31	
<i>Errors (Simulated-Observed)</i>	<i>Error Statistics</i>	<i>Recommended Criteria</i>	<i>Run (n-1)</i>	<i>Run (n-2)</i>
Error in total volume:	9.25	10	8.11	
Error in 50% lowest flows:	17.97	10	17.97	
Error in 10% highest flows:	4.39	15	1.68	
Seasonal volume error - Summer:	28.19	30	28.19	
Seasonal volume error - Fall:	28.85	30	28.85	
Seasonal volume error - Winter:	-8.67	30	-8.67	
Seasonal volume error - Spring:	2.11	30	0.32	
Error in storm volumes:	-3.07	20	-8.63	
Error in summer storm volumes:	-5.11	50	-5.11	
Nash-Sutcliffe Coefficient of Efficiency, E:	0.499	Model accuracy increases	0.720	
Baseline adjusted coefficient (Garrick), E':	0.598		0.609	
Monthly NSE	0.837		0.848	

Note: Run (n-1) shows the model performance when some large observed peaks that are labeled as poor or unreliable are removed.

BRULE RIVER NEAR HOVLAND (HYDSTRA 01022001)**Figure 186. Mean daily flow at Brule River near Hovland****Figure 187. Mean monthly flow at Brule River near Hovland**

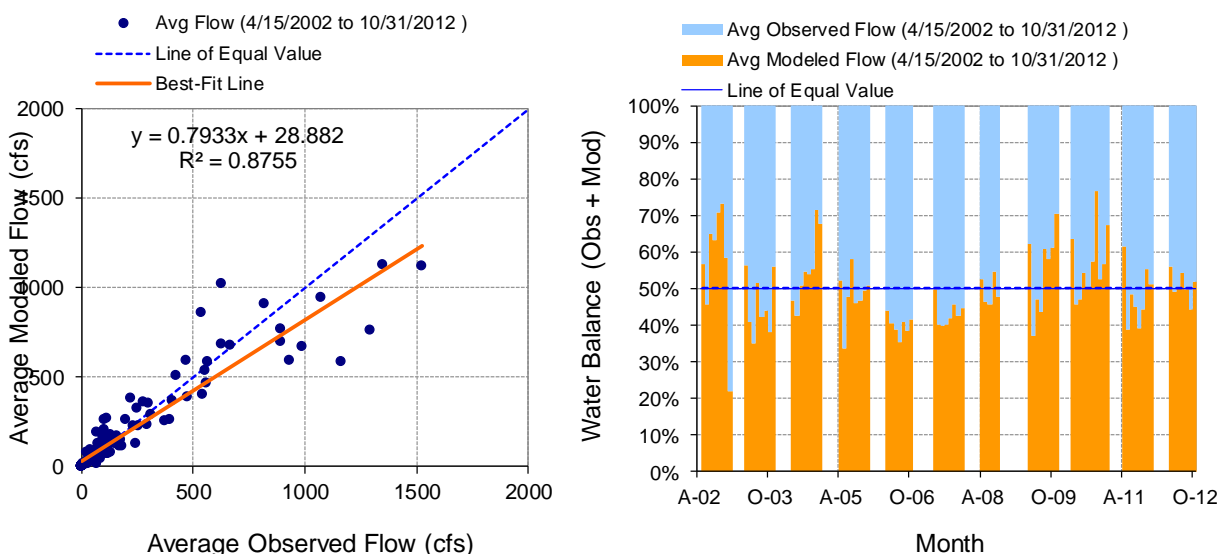


Figure 188. Monthly flow regression and temporal variation at Brule River near Hovland

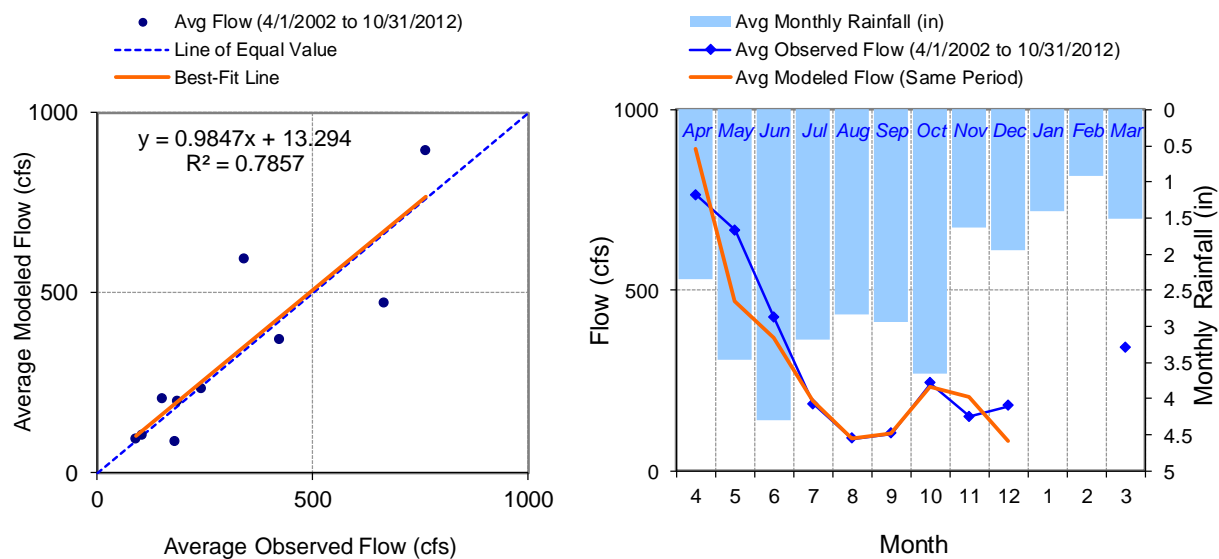


Figure 189. Seasonal regression and temporal aggregate at Brule River near Hovland

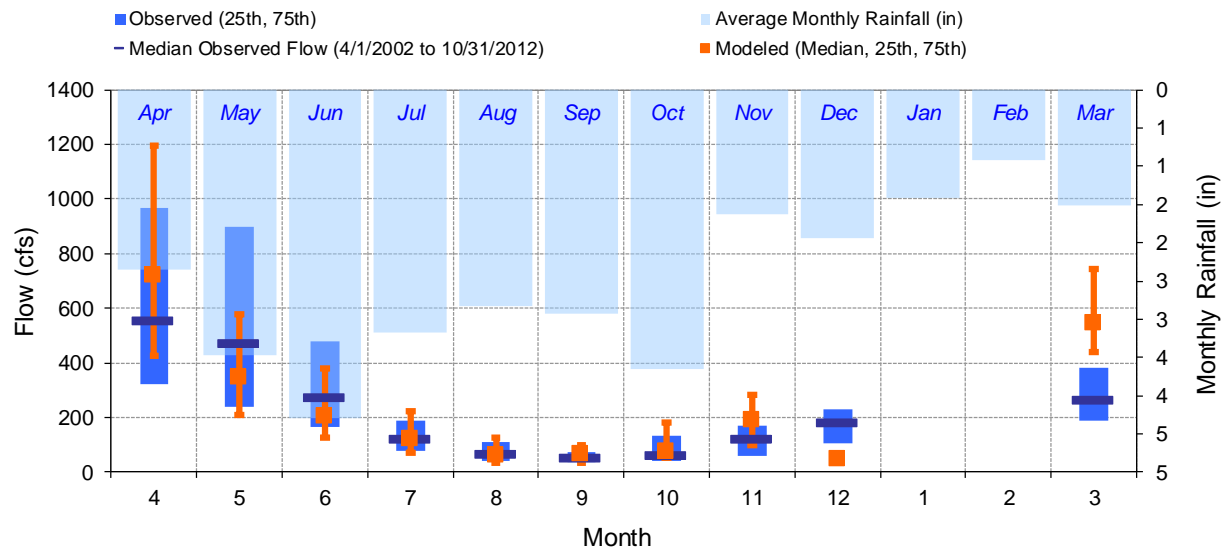


Figure 190. Seasonal medians and ranges at Brule River near Hovland

Table 23. Seasonal summary at Brule River near Hovland

MONTH	OBSERVED FLOW (CFS)				MODELED FLOW (CFS)			
	MEAN	MEDIAN	25TH	75TH	MEAN	MEDIAN	25TH	75TH
Apr	763.84	553.59	324.45	969.50	891.77	719.28	428.06	1196.93
May	666.44	471.75	239.34	900.00	469.85	348.86	209.65	577.55
Jun	422.87	272.42	167.00	479.97	369.34	205.06	125.76	381.14
Jul	185.21	119.93	79.00	188.00	194.92	121.28	71.99	224.23
Aug	88.33	68.29	39.33	112.11	91.18	61.54	32.51	125.64
Sep	103.25	52.00	37.50	71.17	102.90	64.46	34.22	96.47
Oct	242.36	63.73	42.00	134.52	231.26	77.58	52.46	183.85
Nov	150.83	120.93	60.14	171.84	203.47	191.32	100.26	280.87
Dec	180.38	182.11	106.76	230.46	82.94	50.20	45.45	55.68
Jan	0.00	0.00	0.00	0.00	0.00	0.00	0.00	0.00
Feb	0.00	0.00	0.00	0.00	0.00	0.00	0.00	0.00
Mar	340.05	262.50	190.75	380.00	590.78	544.47	438.57	746.23

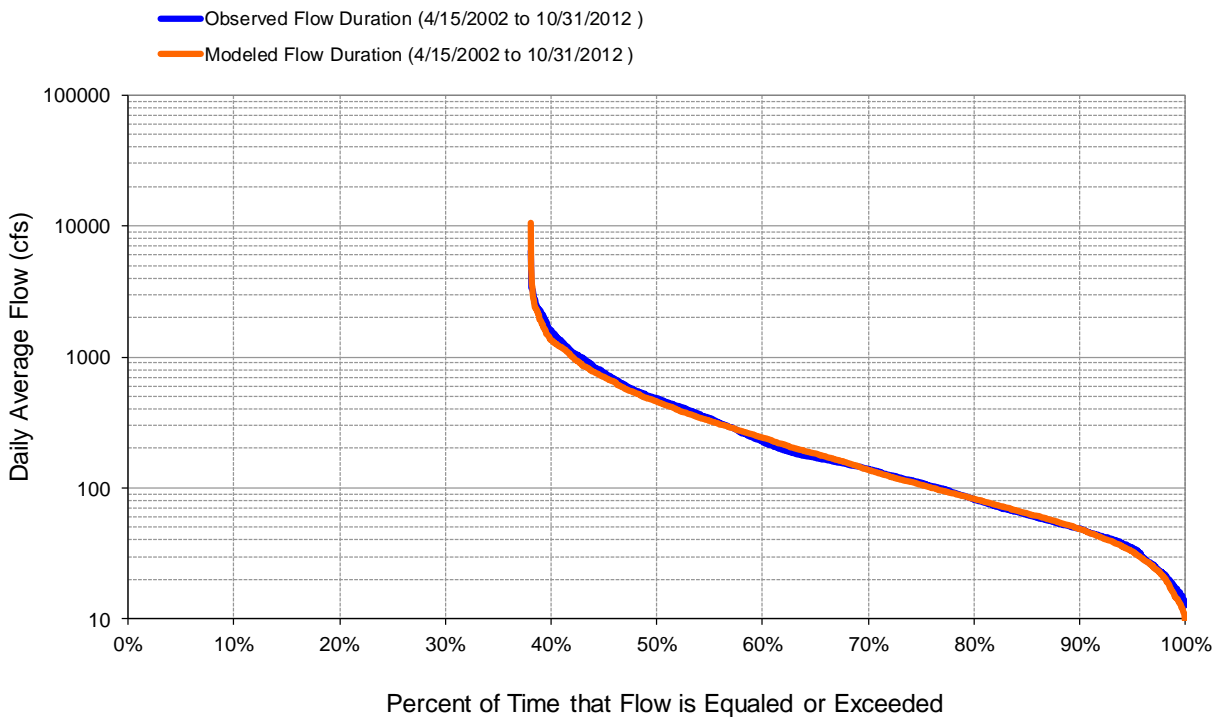


Figure 191. Flow exceedance at Brule River near Hovland

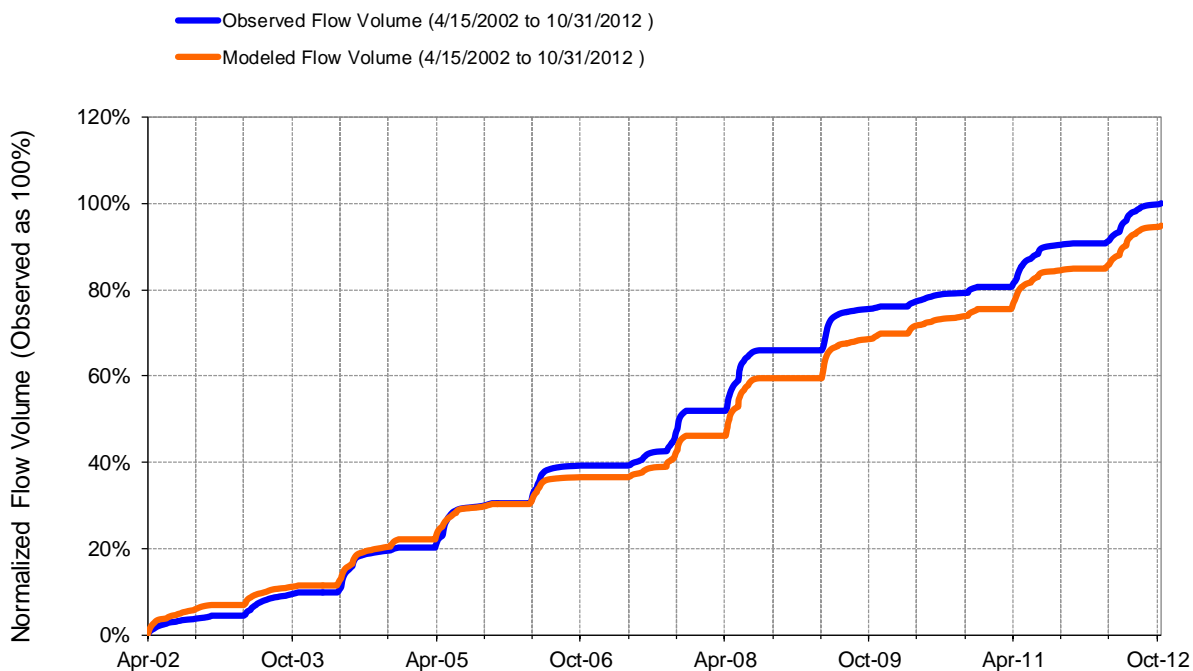


Figure 192. Flow accumulation at Brule River near Hovland

Table 24. Summary statistics at Brule River near Hovland

HSPF Simulated Flow		Observed Flow Gage	
REACH OUTFLOW FROM DSN 90 10.55-Year Analysis Period: 4/1/2002 - 10/31/2012 Flow volumes are (inches/year) for upstream drainage area		Brule River near Hovland, MN61 Manually Entered Data Drainage Area (sq-mi): 264	
Total Simulated In-stream Flow:	9.81	Total Observed In-stream Flow:	10.35
Total of simulated highest 10% flows:	4.40	Total of Observed highest 10% flows:	4.82
Total of Simulated lowest 50% flows:	1.12	Total of Observed Lowest 50% flows:	1.13
Simulated Summer Flow Volume (months 7-9):	1.71	Observed Summer Flow Volume (7-9):	1.65
Simulated Fall Flow Volume (months 10-12):	1.41	Observed Fall Flow Volume (10-12):	1.35
Simulated Winter Flow Volume (months 1-3):	0.16	Observed Winter Flow Volume (1-3):	0.09
Simulated Spring Flow Volume (months 4-6):	6.53	Observed Spring Flow Volume (4-6):	7.26
Total Simulated Storm Volume:	2.93	Total Observed Storm Volume:	3.17
Simulated Summer Storm Volume (7-9):	0.53	Observed Summer Storm Volume (7-9):	0.44
<i>Errors (Simulated-Observed)</i>	<i>Error Statistics</i>	<i>Recommended Criteria</i>	
Error in total volume:	-5.28	10	
Error in 50% lowest flows:	-1.28	10	
Error in 10% highest flows:	-8.81	15	
Seasonal volume error - Summer:	3.36	30	
Seasonal volume error - Fall:	4.84	30	
Seasonal volume error - Winter:	73.73	30	Clear
Seasonal volume error - Spring:	-10.11	30	
Error in storm volumes:	-7.52	20	
Error in summer storm volumes:	19.98	50	
Nash-Sutcliffe Coefficient of Efficiency, E:	0.520	Model accuracy increases	
Baseline adjusted coefficient (Garrick), E':	0.572		
Monthly NSE	0.827		

Appendix C. Detailed Flow Validation Results

KNIFE RIVER NEAR TWO HARBORS (HYDSTRA 02026001//USGS 04015330)

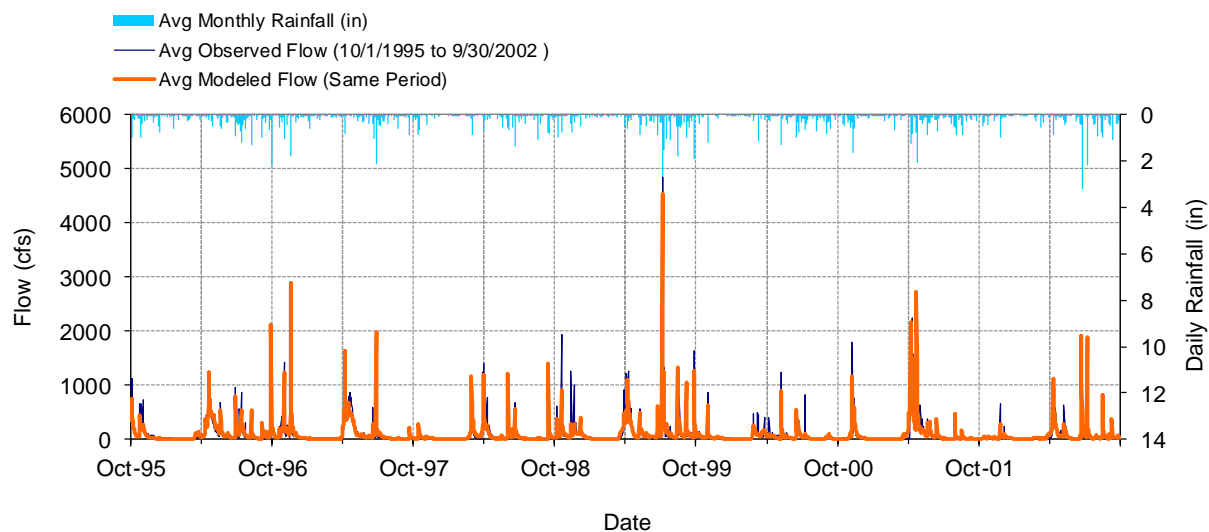


Figure 193. Mean daily flow at Knife River near Two Harbors

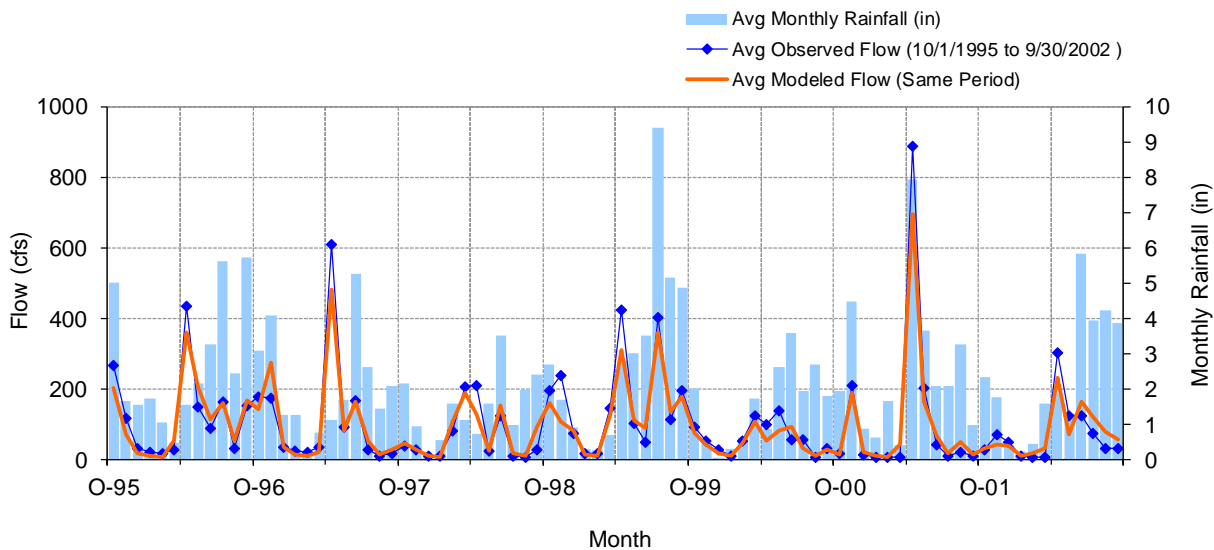


Figure 194. Mean monthly flow at Knife River near Two Harbors

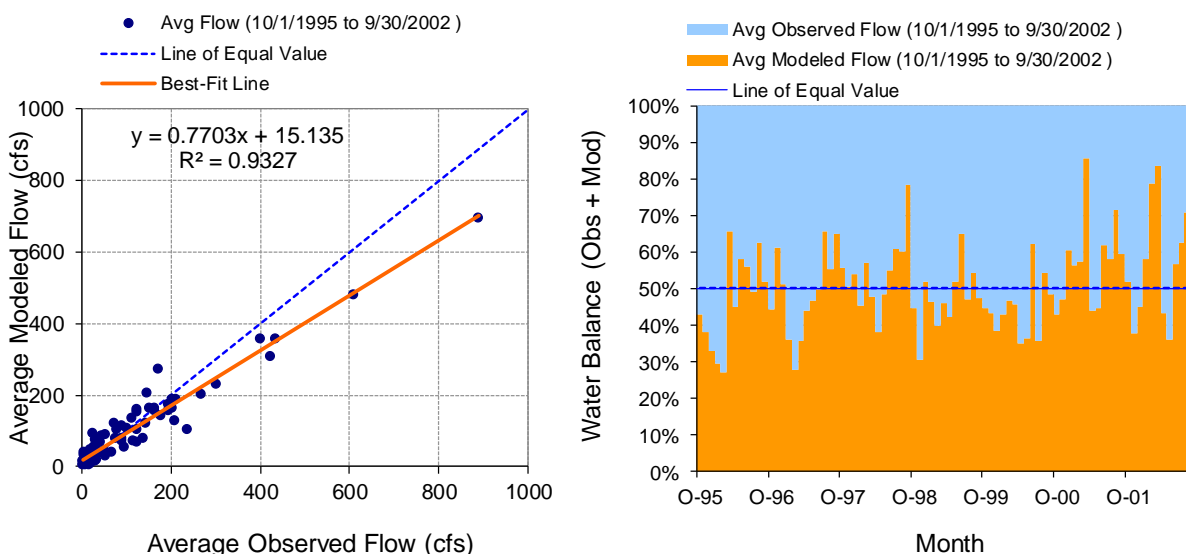


Figure 195. Monthly flow regression and temporal variation at Knife River near Two Harbors

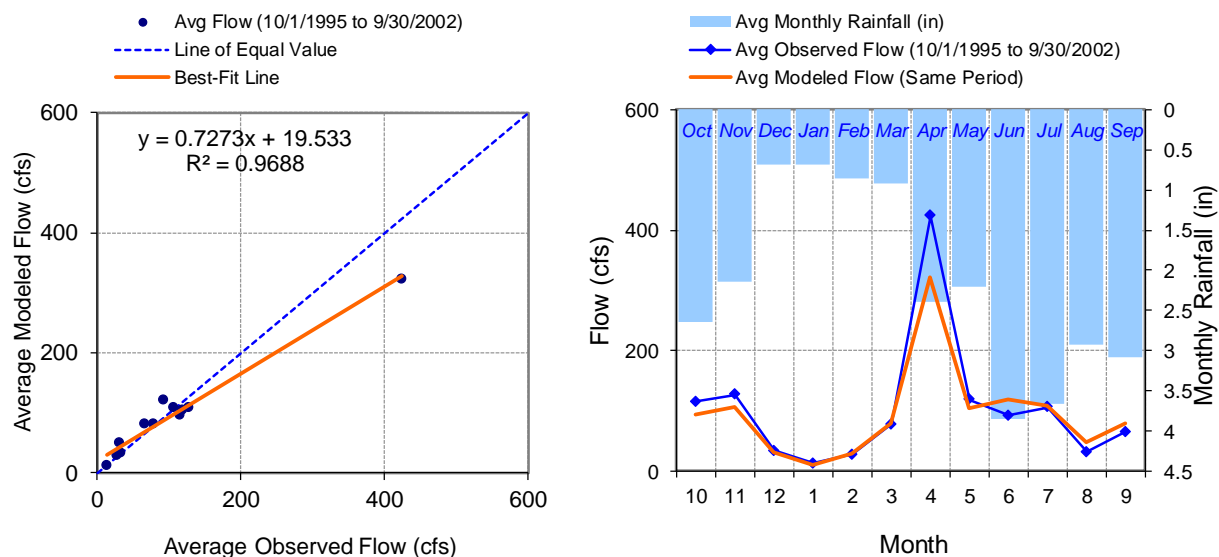


Figure 196. Seasonal regression and temporal aggregate at Knife River near Two Harbors

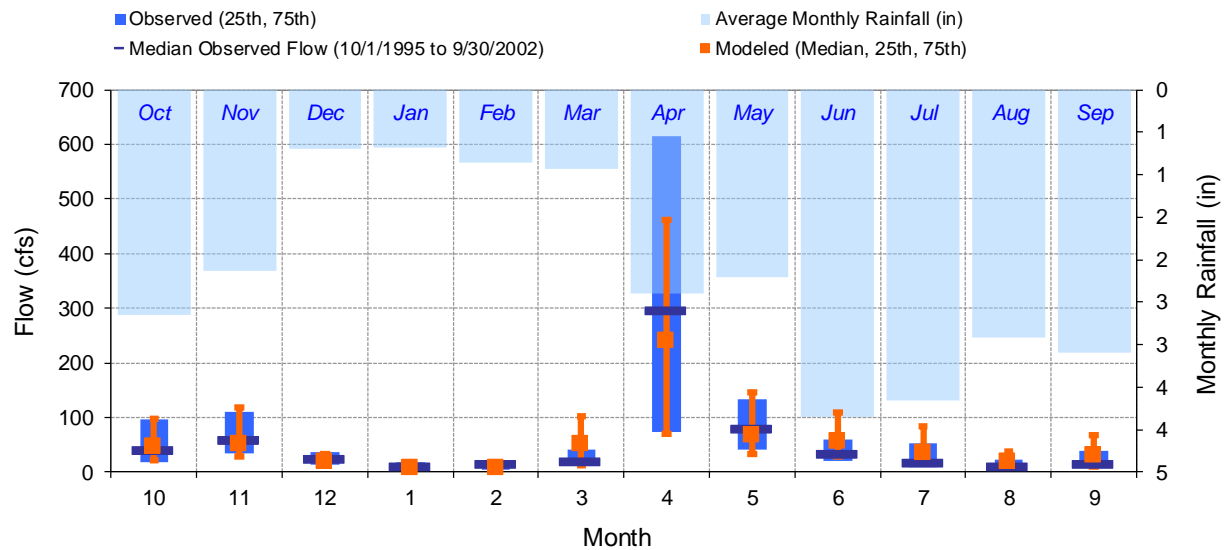


Figure 197. Seasonal medians and ranges at Knife River near Two Harbors

Table 25. Seasonal summary at Knife River near Two Harbors

MONTH	OBSERVED FLOW (CFS)				MODELED FLOW (CFS)			
	MEAN	MEDIAN	25TH	75TH	MEAN	MEDIAN	25TH	75TH
Oct	115.60	41.00	18.00	97.00	94.25	46.10	21.18	97.70
Nov	126.61	58.00	34.00	111.50	106.79	51.44	28.02	117.42
Dec	33.49	25.00	14.00	36.00	30.88	19.66	12.10	33.92
Jan	13.09	10.00	7.40	19.00	9.72	8.77	7.30	11.82
Feb	27.47	14.00	4.83	17.00	27.97	7.74	5.64	11.52
Mar	77.82	20.00	11.00	42.00	79.35	51.45	12.95	102.89
Apr	423.60	296.00	74.25	614.75	321.64	240.32	69.25	462.18
May	118.22	79.00	41.00	134.00	104.00	66.96	34.29	146.01
Jun	92.14	33.50	21.00	60.75	119.09	57.33	29.27	108.43
Jul	105.90	18.00	10.00	52.00	107.36	36.46	18.15	83.82
Aug	31.07	11.00	7.10	22.00	48.60	19.69	9.13	37.76
Sep	65.14	15.00	8.63	38.00	79.44	30.53	10.99	66.87

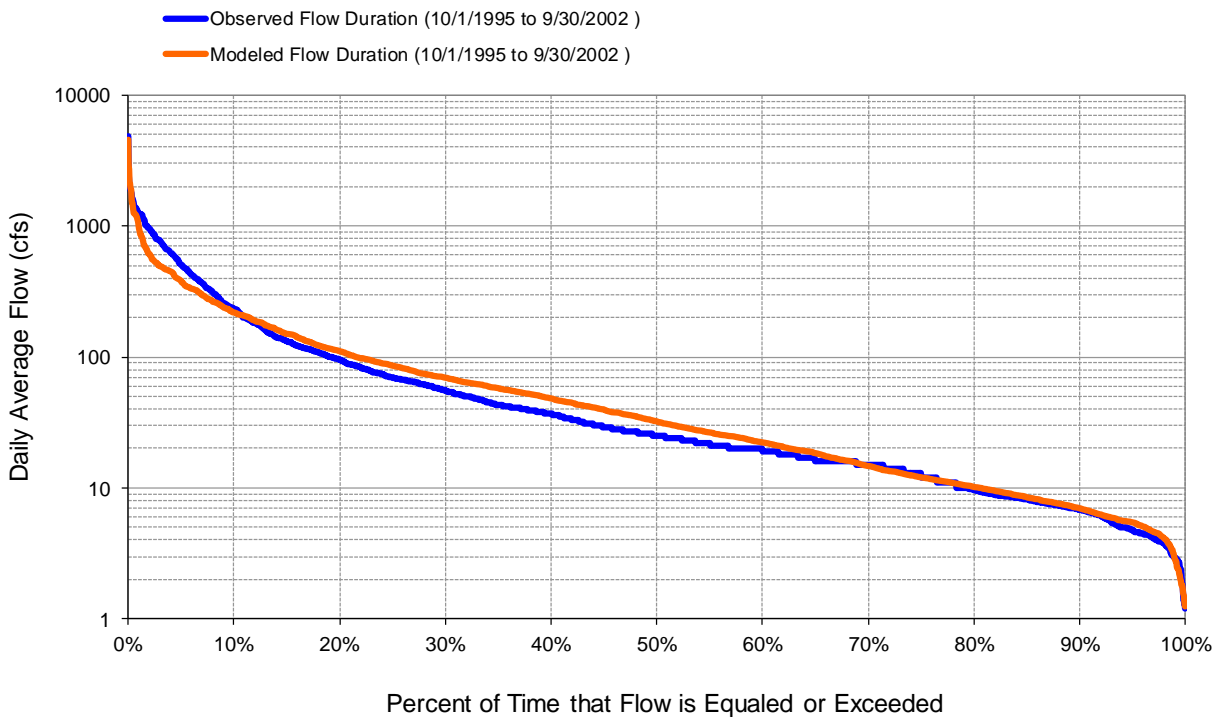


Figure 198. Flow exceedance at Knife River near Two Harbors

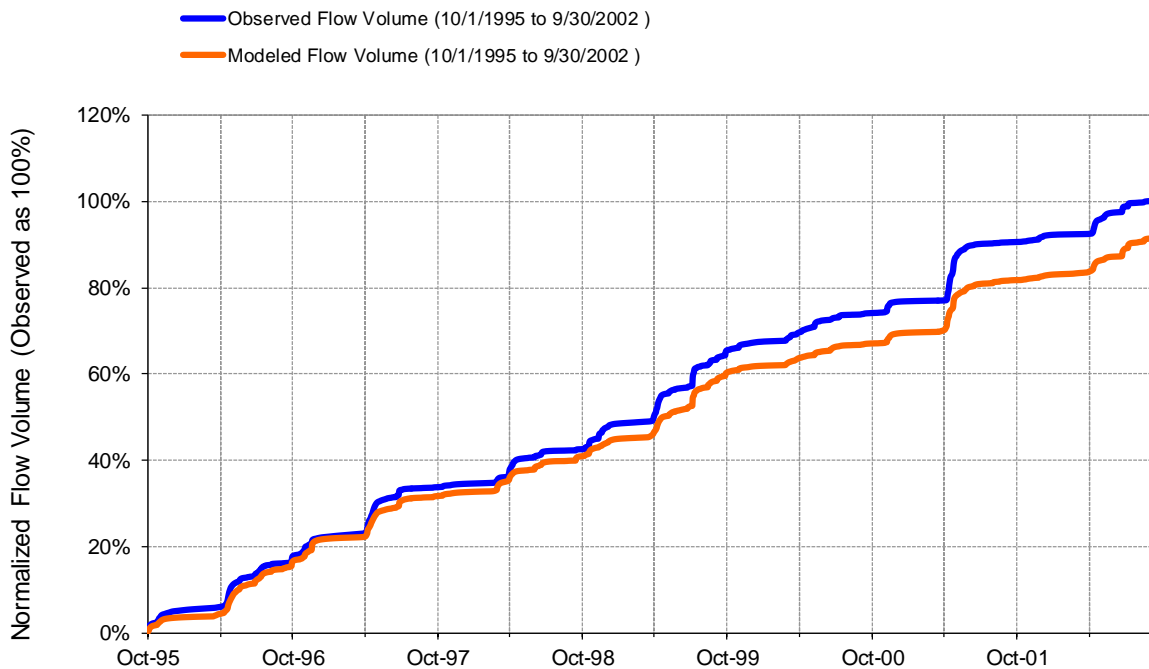


Figure 199. Flow accumulation at Knife River near Two Harbors

Table 26. Summary statistics at Knife River near Two Harbors

HSPF Simulated Flow		Observed Flow Gage	
REACH OUTFLOW FROM DSN 40 7-Year Analysis Period: 10/1/1995 - 9/30/2002 Flow volumes are (inches/year) for upstream drainage area Run 6a		Knife River near Two Harbors, MN61 Manually Entered Data Drainage Area (sq-mi): 83.6	
Total Simulated In-stream Flow:	15.26	Total Observed In-stream Flow:	16.62
Total of simulated highest 10% flows:	8.59	Total of Observed highest 10% flows:	10.90
Total of Simulated lowest 50% flows:	1.15	Total of Observed Lowest 50% flows:	1.04
Simulated Summer Flow Volume (months 7-9):	3.21	Observed Summer Flow Volume (7-9):	2.76
Simulated Fall Flow Volume (months 10-12):	3.15	Observed Fall Flow Volume (10-12):	3.75
Simulated Winter Flow Volume (months 1-3):	1.58	Observed Winter Flow Volume (1-3):	1.60
Simulated Spring Flow Volume (months 4-6):	7.32	Observed Spring Flow Volume (4-6):	8.51
Total Simulated Storm Volume:	6.57	Total Observed Storm Volume:	8.34
Simulated Summer Storm Volume (7-9):	1.83	Observed Summer Storm Volume (7-9):	1.91
<i>Errors (Simulated-Observed)</i>	<i>Error Statistics</i>	<i>Recommended Criteria</i>	
Error in total volume:	-8.17	10	
Error in 50% lowest flows:	10.73	10	
Error in 10% highest flows:	-21.20	15	
Seasonal volume error - Summer:	16.42	30	
Seasonal volume error - Fall:	-15.88	30	
Seasonal volume error - Winter:	-1.20	30	
Seasonal volume error - Spring:	-14.06	30	
Error in storm volumes:	-21.17	20	
Error in summer storm volumes:	-4.54	50	
Nash-Sutcliffe Coefficient of Efficiency, E:	0.747	Model accuracy increases	
Baseline adjusted coefficient (Garrick), E':	0.615		
Monthly NSE	0.782		



Lake Superior North and Lake Superior South Basins

Watershed Model Development Report

Appendix D

Suspended Sediment and Water Quality Calibration and Validation for Lake Superior North and South Watersheds

Prepared for
Minnesota Pollution Control Agency

Prepared by



One Park Drive, Suite 200 • PO Box 14409
Research Triangle Park, NC 27709

June 30, 2016

(This page left intentionally blank.)

Amity Creek at Duluth (HYDSTRA 02038001)

Total Suspended Solids (TSS)

Table 1. Total Suspended Solids (TSS) statistics

Count	142
Concentration Average Error	3.20%
Concentration Median Error	7.12%
Load Average Error	68.77%
Load Median Error	1.28%
Paired t concentration	0.86
Paired t load	0.07

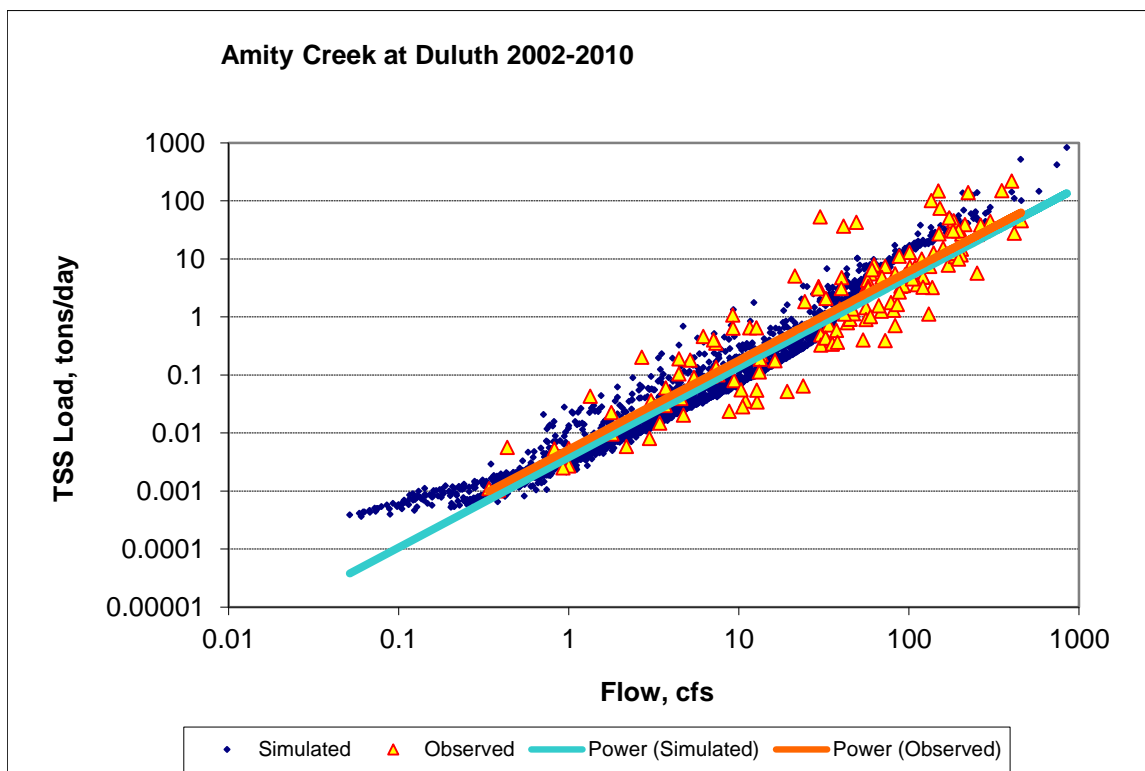


Figure 1. Power plot of simulated and observed Total Suspended Solids (TSS) load vs flow at Amity Creek at Duluth

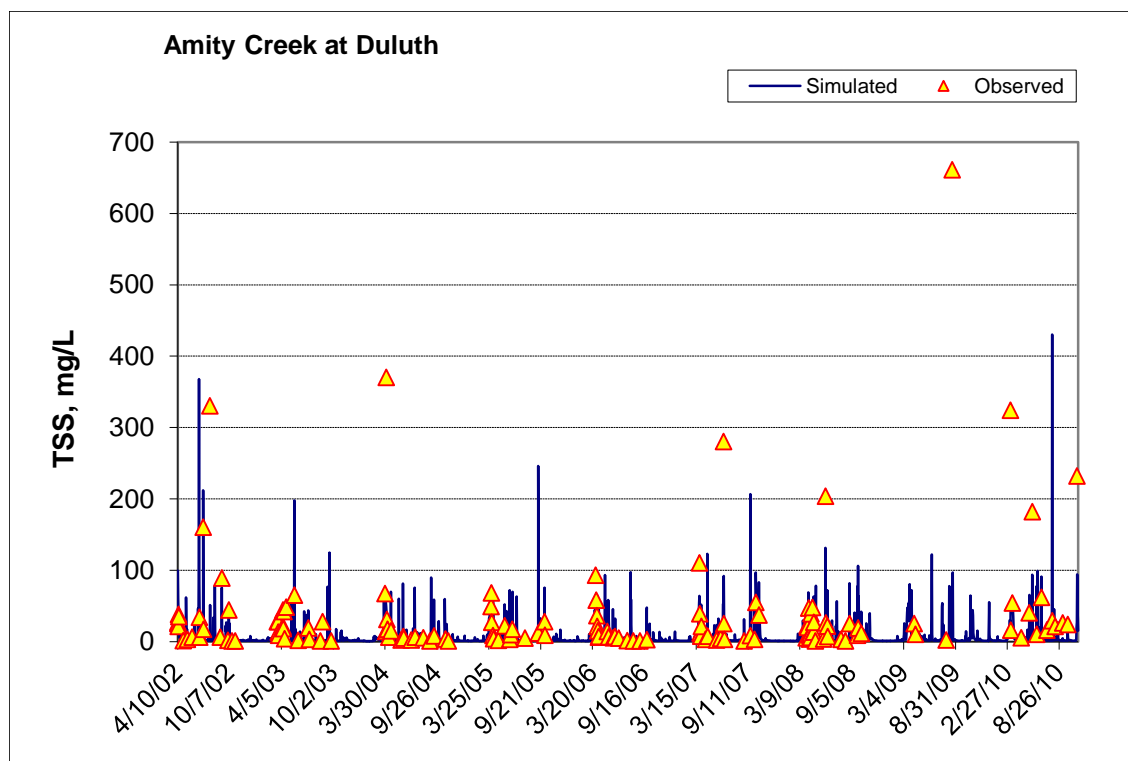


Figure 2. Time series of observed and simulated Total Suspended Solids (TSS) concentration at Amity Creek at Duluth

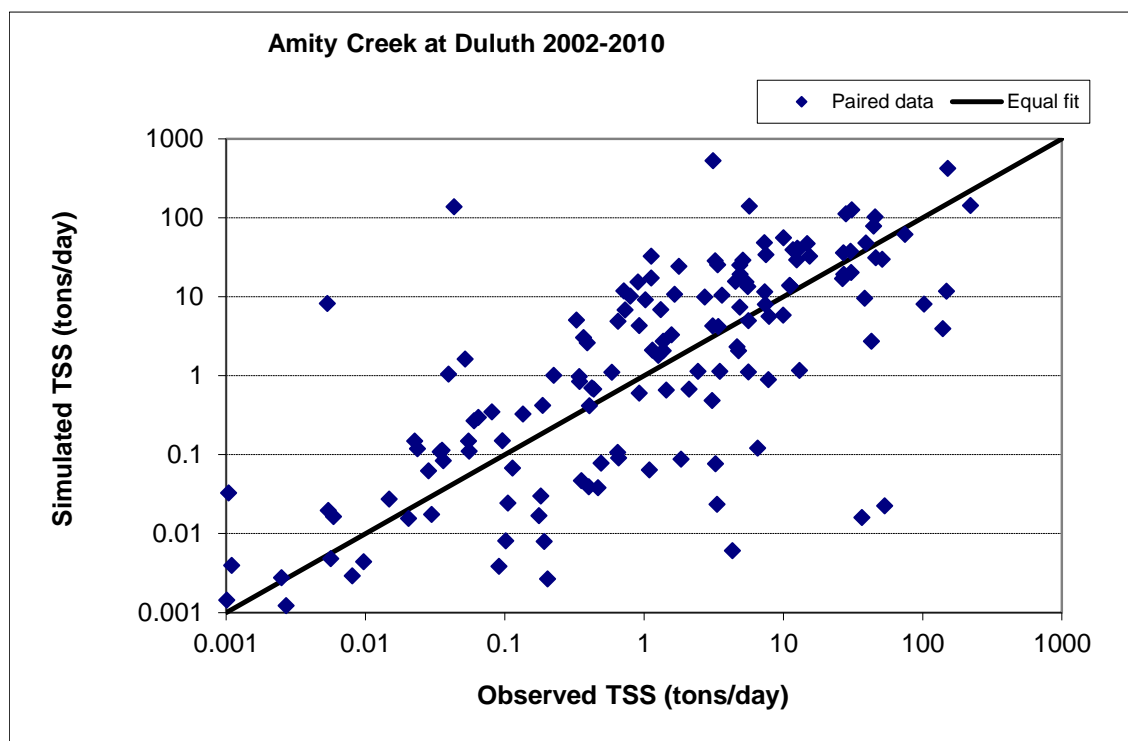


Figure 3. Paired simulated vs. observed Total Suspended Solids (TSS) load at Amity Creek at Duluth

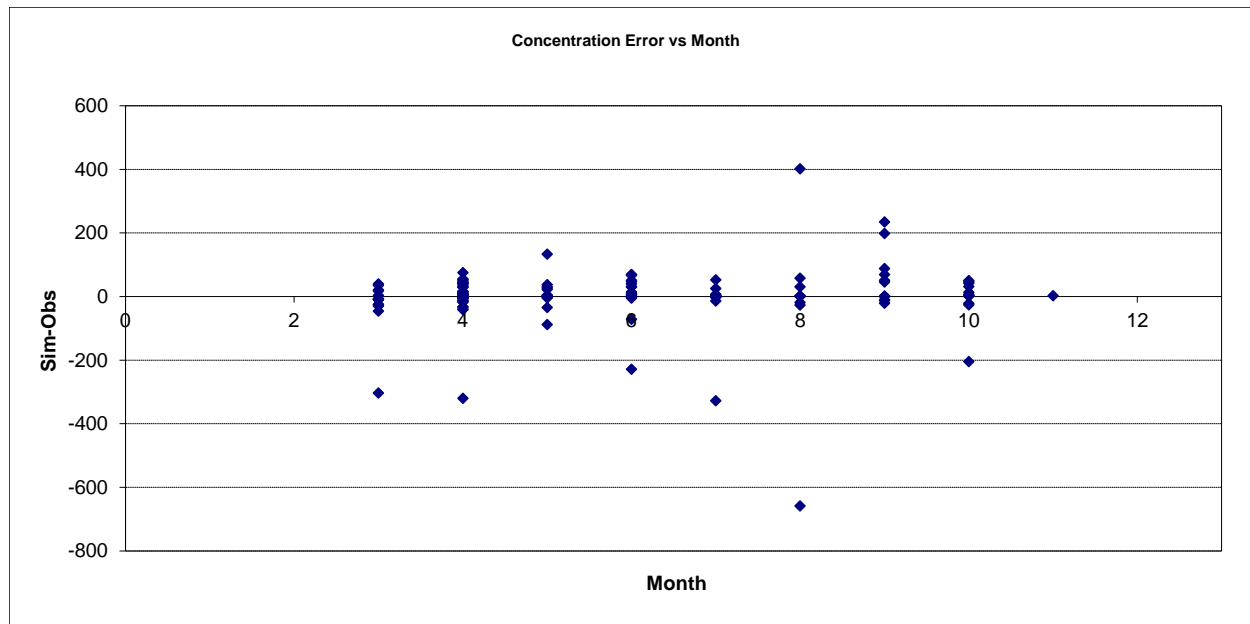


Figure 4. Residual (Simulated - Observed) vs. Month Total Suspended Solids (TSS) at Amity Creek at Duluth

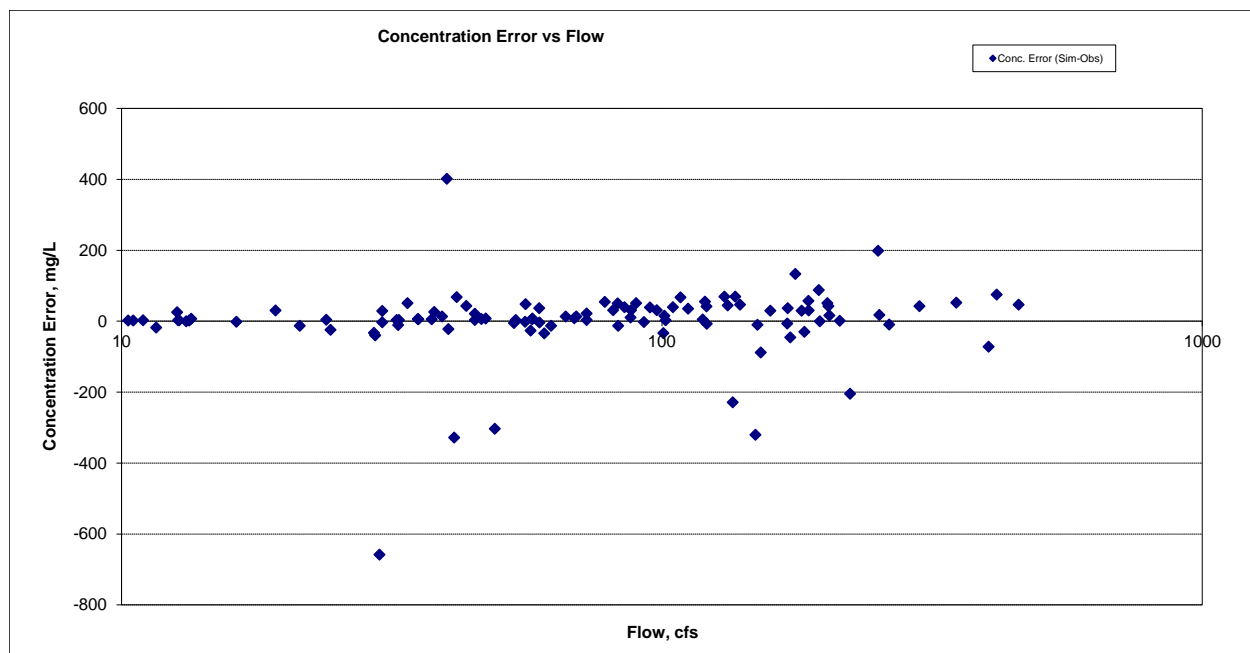


Figure 5. Residual (Simulated - Observed) vs. Flow Total Suspended Solids (TSS) at Amity Creek at Duluth

Ammonia Nitrogen (NH₃)

Table 2. Ammonia Nitrogen (NH₃) statistics

Count	12
Concentration Average Error	102.43%
Concentration Median Error	127.71%
Load Average Error	138.97%
Load Median Error	30.53%
Paired t concentration	0.06
Paired t load	0.08

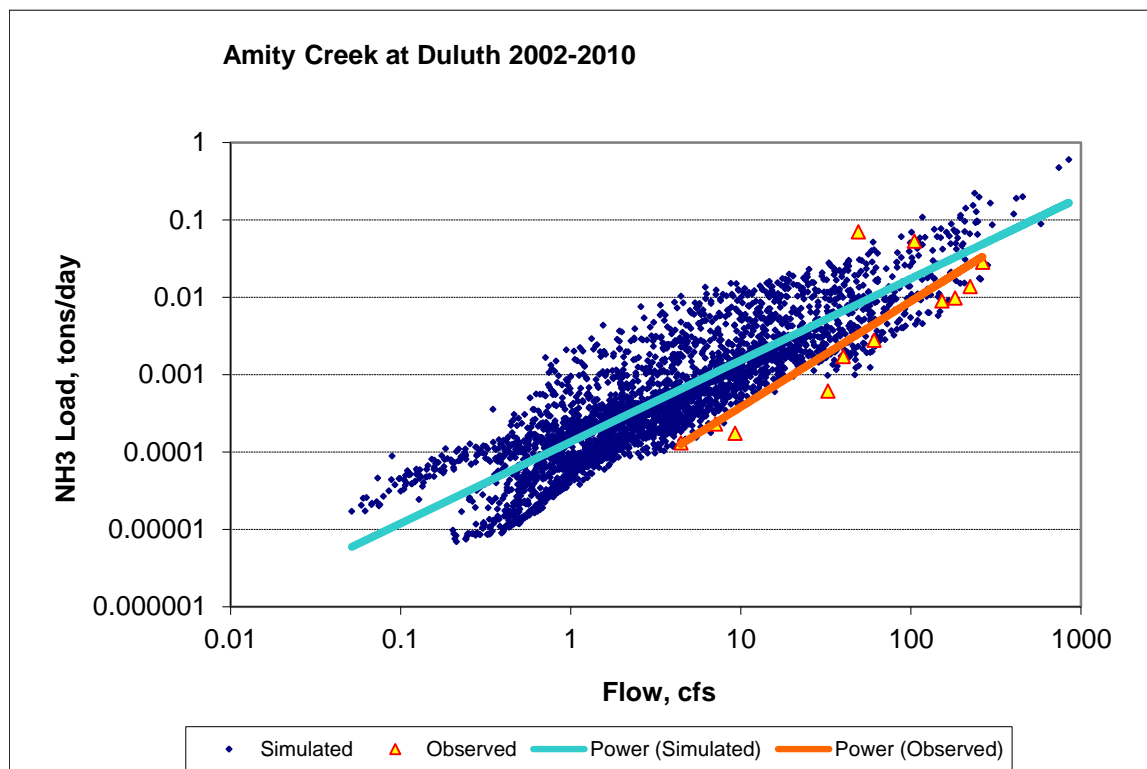


Figure 6. Power plot of simulated and observed Ammonia Nitrogen (NH₃) load vs flow at Amity Creek at Duluth

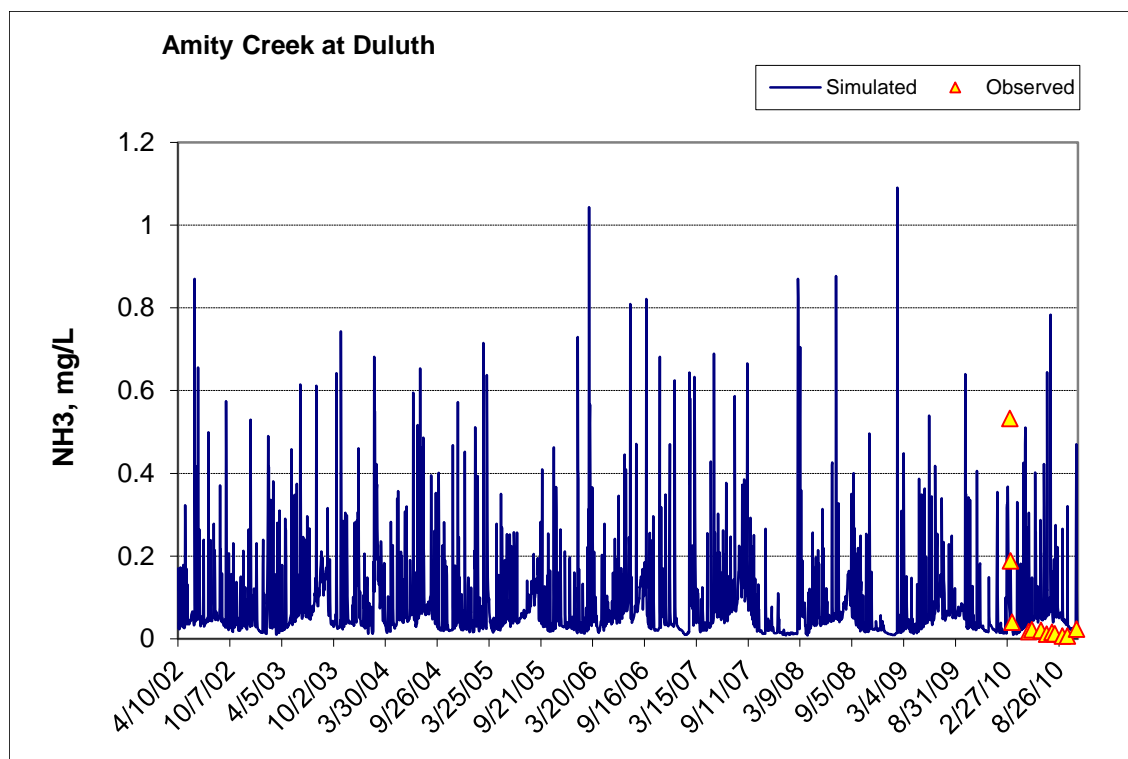


Figure 7. Time series of observed and simulated Ammonia Nitrogen (NH₃) concentration at Amity Creek at Duluth

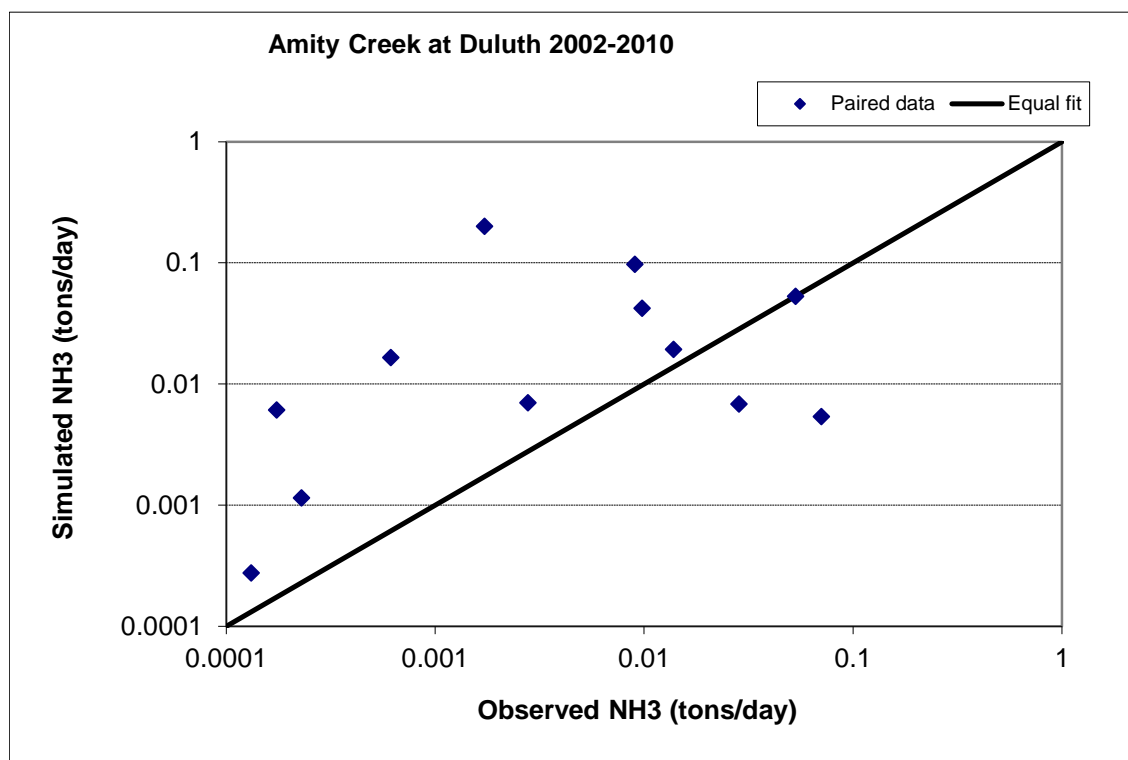


Figure 8. Paired simulated vs. observed Ammonia Nitrogen (NH₃) load at Amity Creek at Duluth

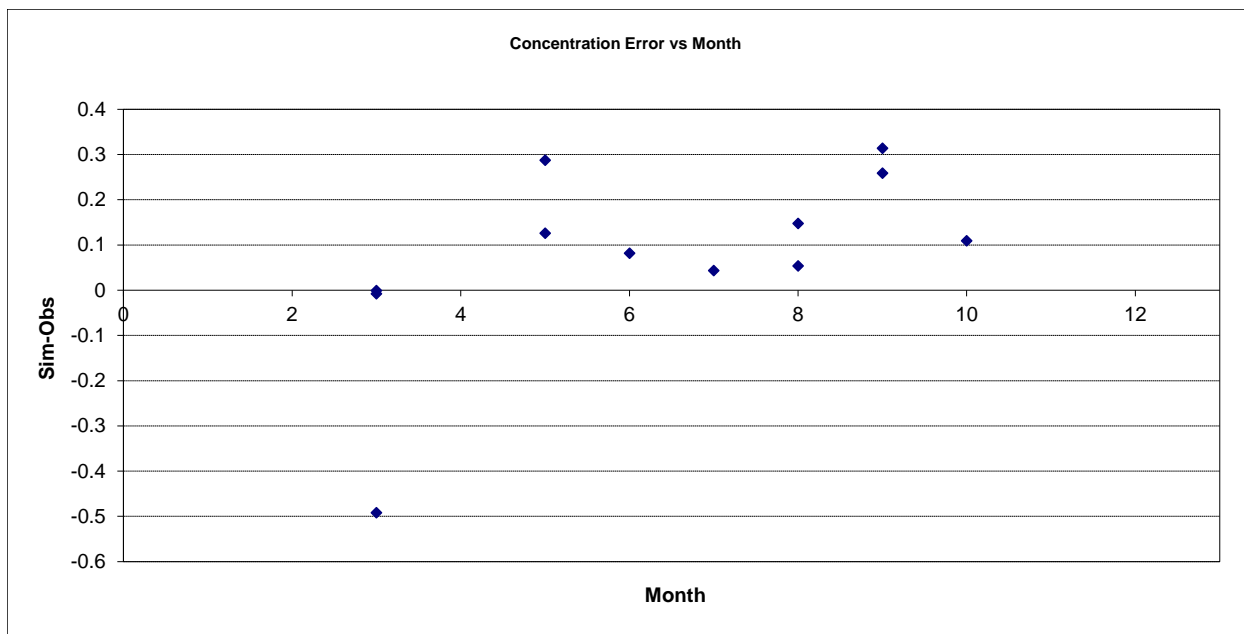


Figure 9. Residual (Simulated - Observed) vs. Month Ammonia Nitrogen (NH3) at Amity Creek at Duluth

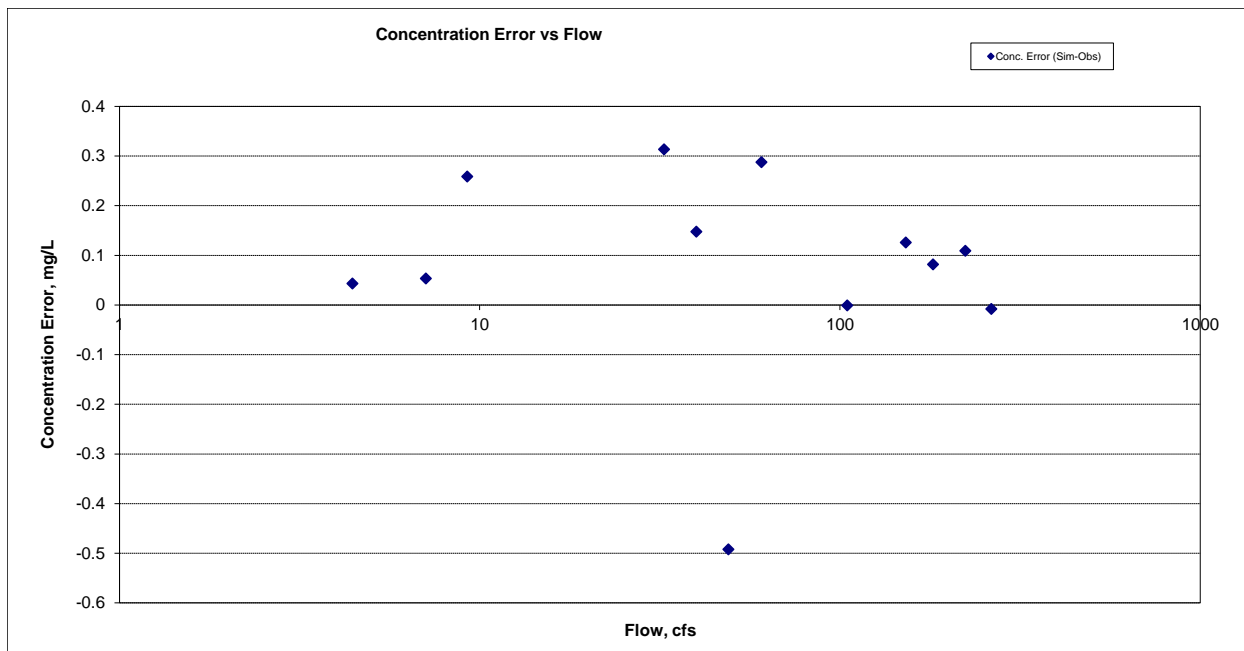


Figure 10. Residual (Simulated - Observed) vs. Flow Ammonia Nitrogen (NH3) at Amity Creek at Duluth

Total Kjeldahl Nitrogen (TKN)

Table 3. Total Kjeldahl Nitrogen (TKN) statistics

Count	59
Concentration Average Error	-7.62%
Concentration Median Error	-3.39%
Load Average Error	20.55%
Load Median Error	-0.73%
Paired t concentration	0.97
Paired t load	0.49

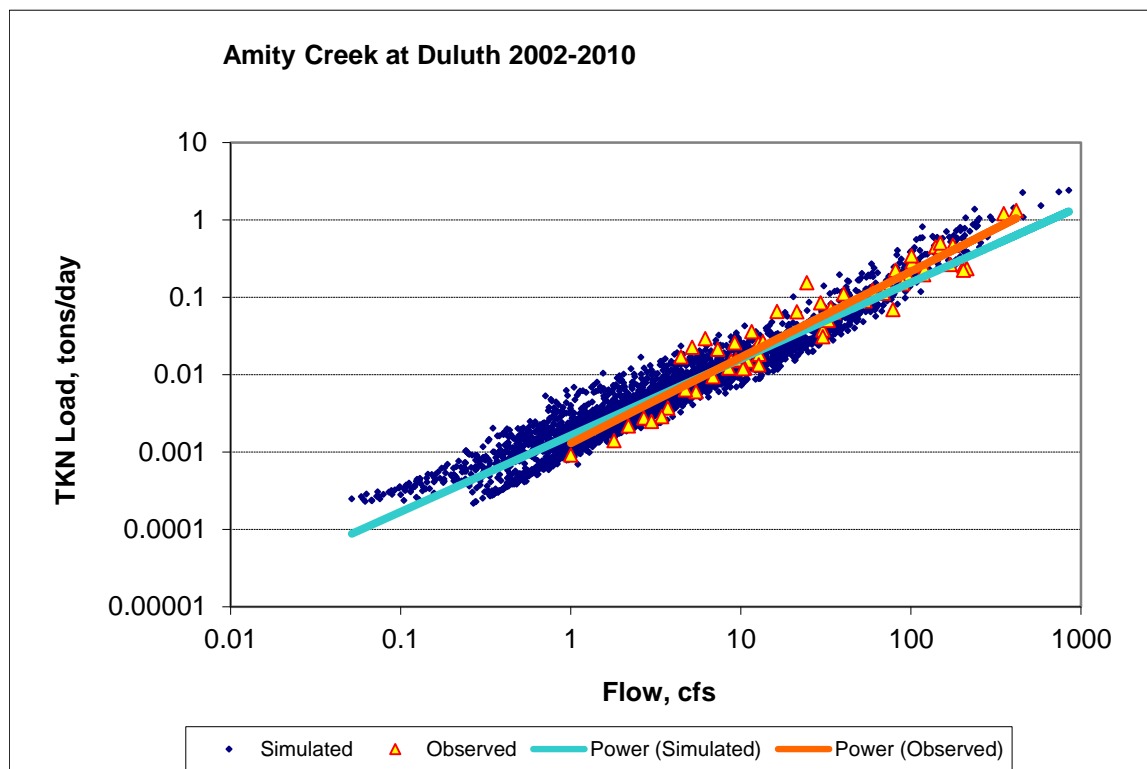


Figure 11. Power plot of simulated and observed Total Kjeldahl Nitrogen (TKN) load vs flow at Amity Creek at Duluth

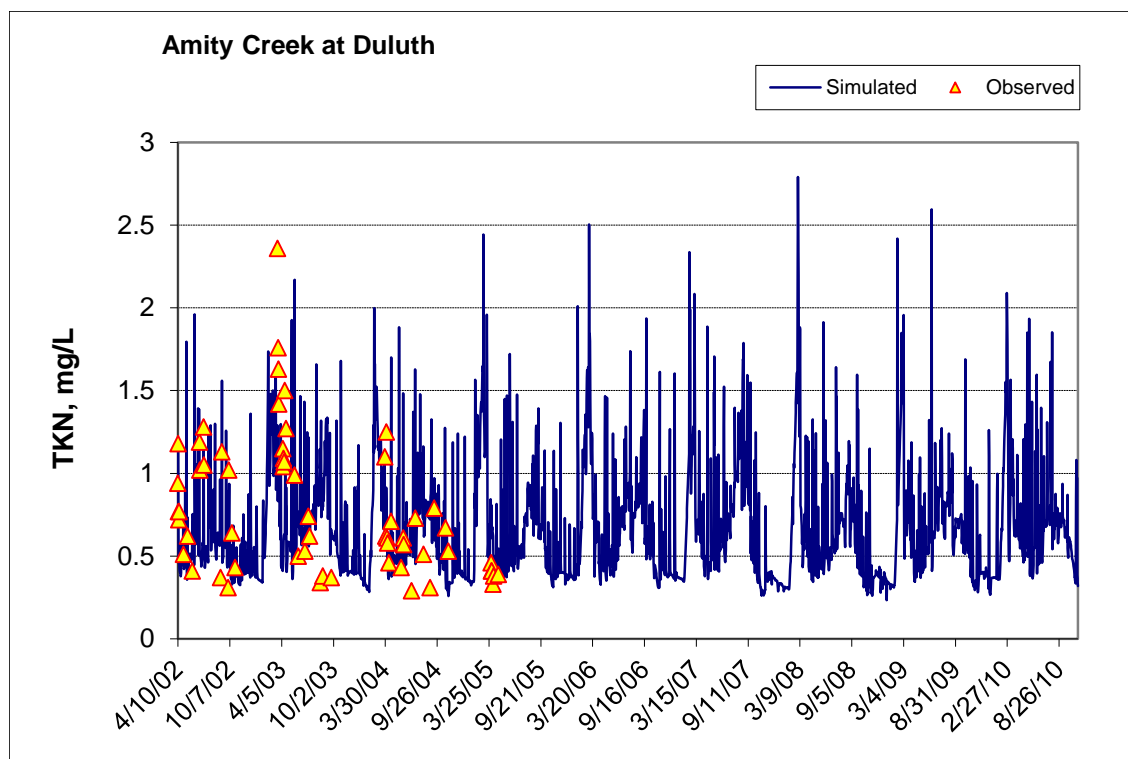


Figure 12. Time series of observed and simulated Total Kjeldahl Nitrogen (TKN) concentration at Amity Creek at Duluth

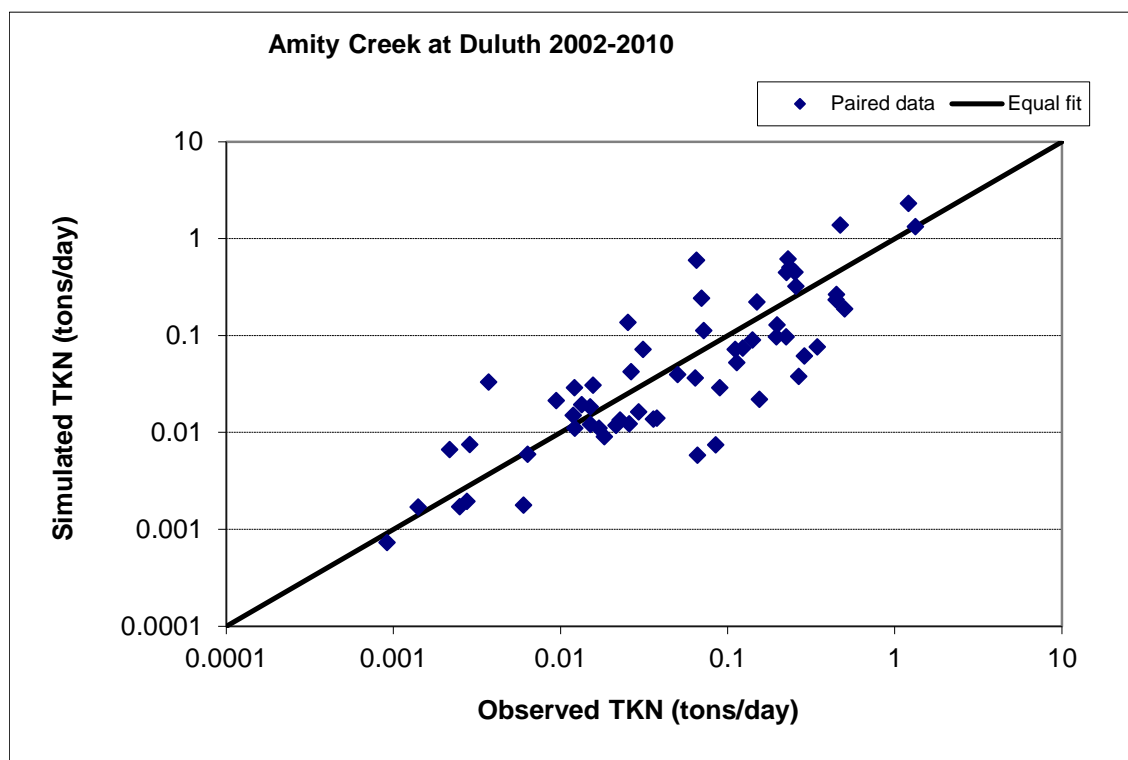


Figure 13. Paired simulated vs. observed Total Kjeldahl Nitrogen (TKN) load at Amity Creek at Duluth

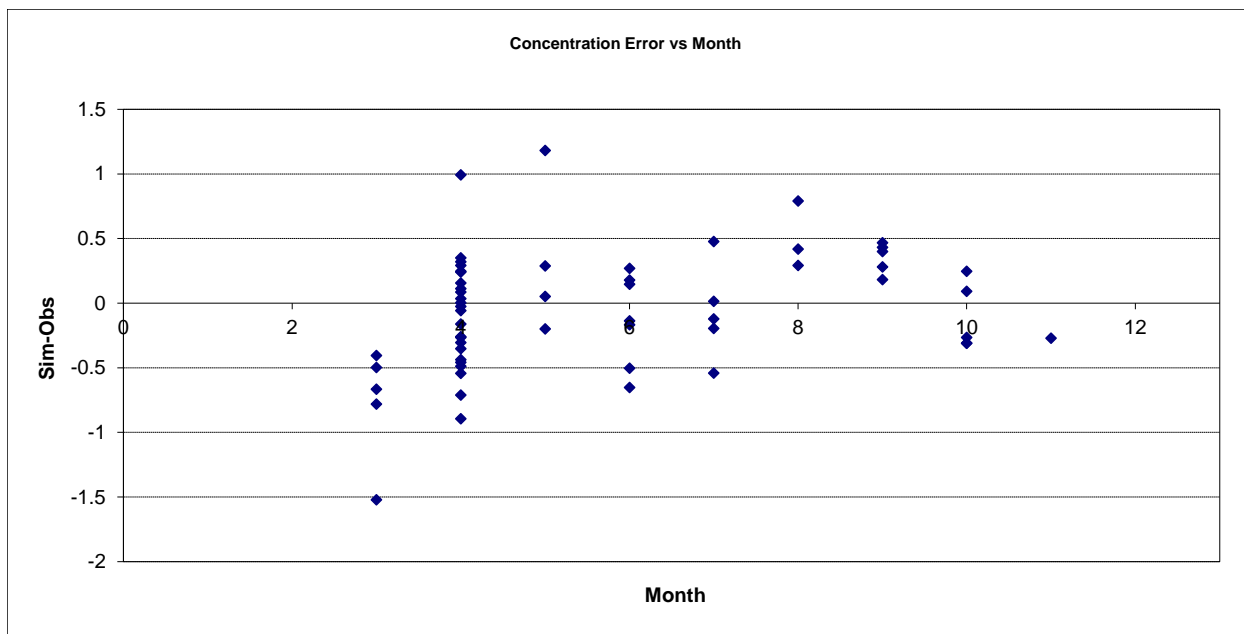


Figure 14. Residual (Simulated - Observed) vs. Month Total Kjeldahl Nitrogen (TKN) at Amity Creek at Duluth

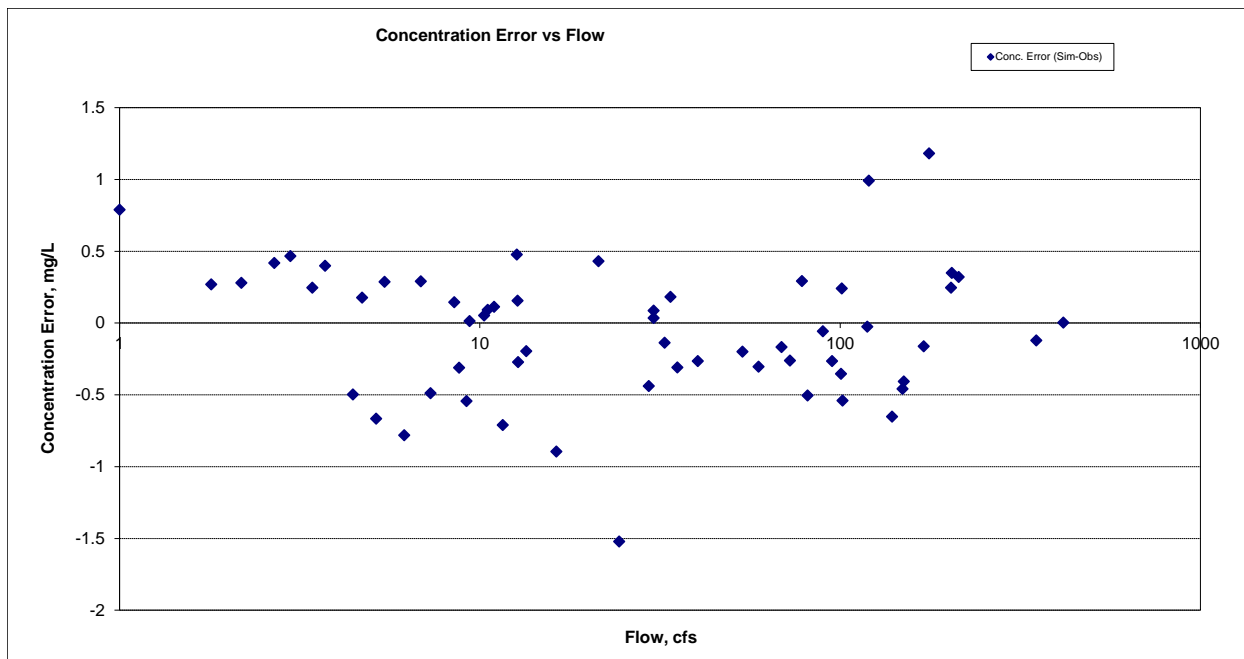


Figure 15. Residual (Simulated - Observed) vs. Flow Total Kjeldahl Nitrogen (TKN) at Amity Creek at Duluth

Nitrite+ Nitrate Nitrogen (NOx)

Table 4. Nitrite+ Nitrate Nitrogen (NOx) statistics

Count	71
Concentration Average Error	13.95%
Concentration Median Error	2.23%
Load Average Error	-2.60%
Load Median Error	0.31%
Paired t concentration	0.73
Paired t load	0.81

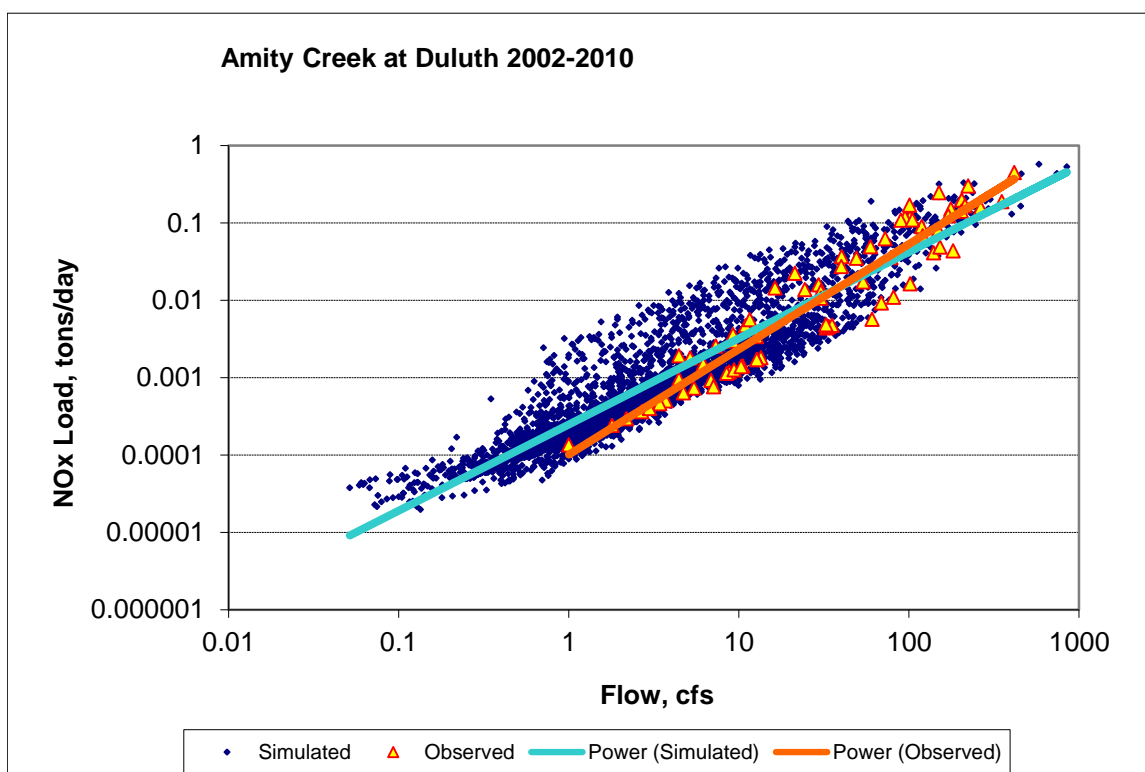


Figure 16. Power plot of simulated and observed Nitrite+ Nitrate Nitrogen (NOx) load vs flow at Amity Creek at Duluth

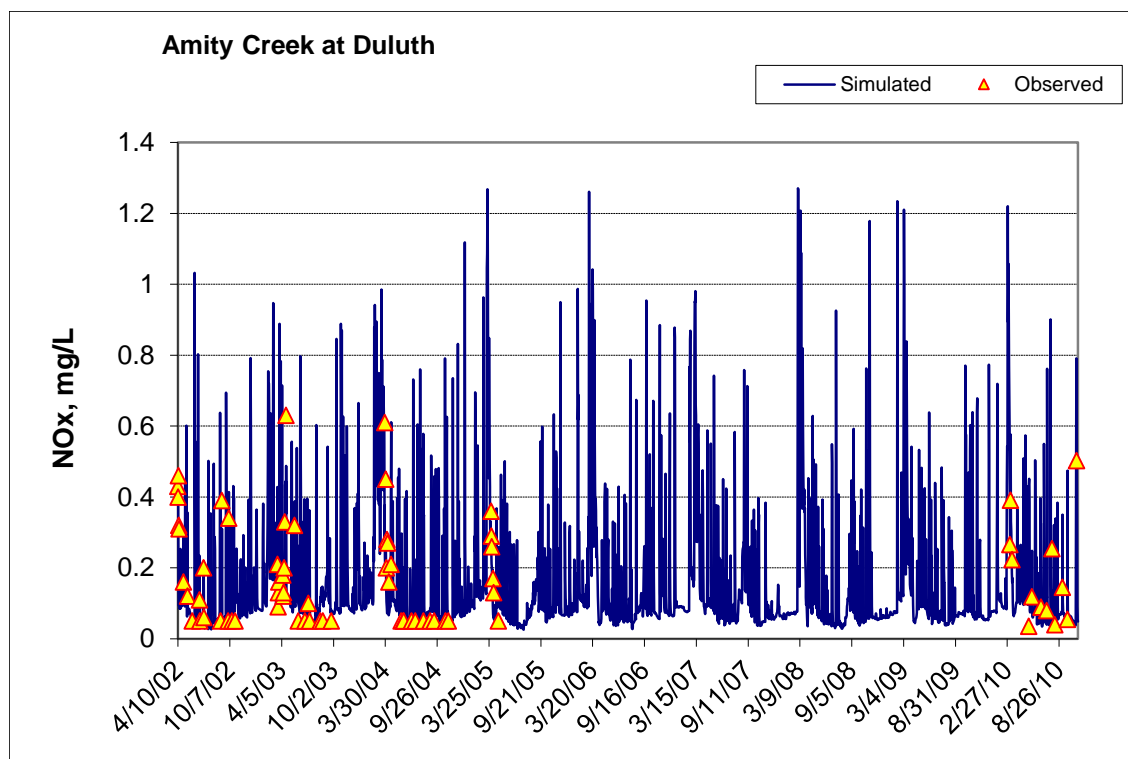


Figure 17. Time series of observed and simulated Nitrite+ Nitrate Nitrogen (NOx) concentration at Amity Creek at Duluth

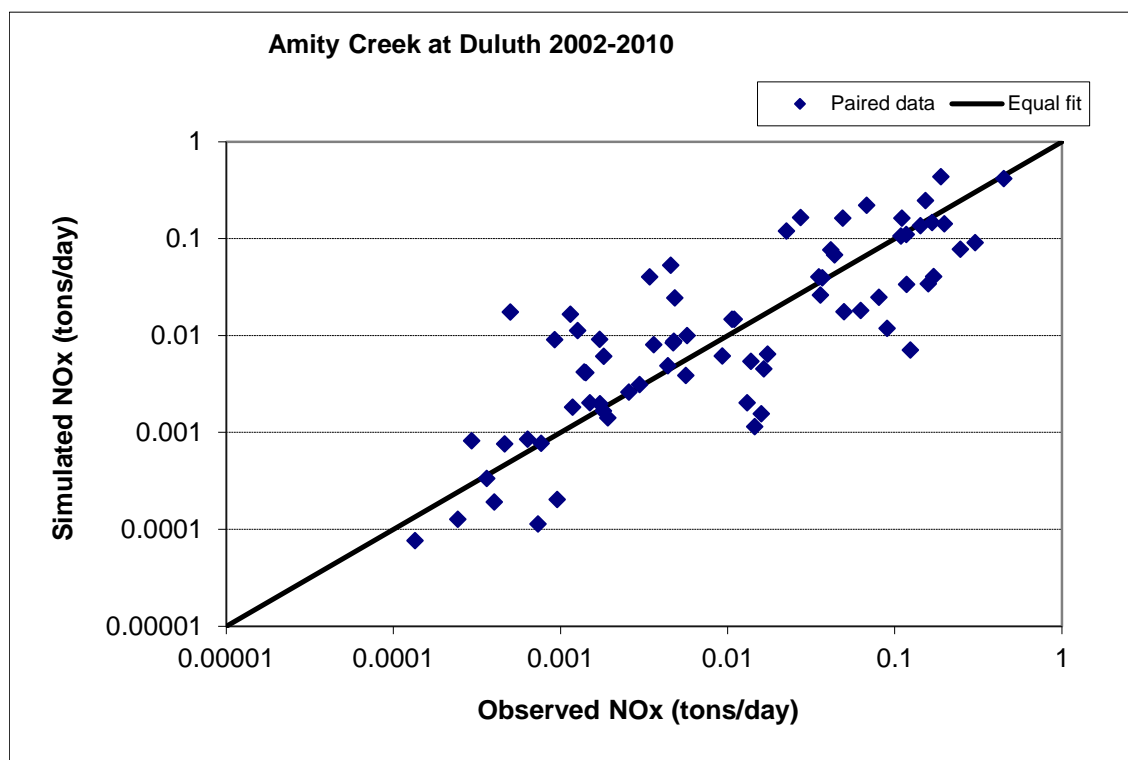


Figure 18. Paired simulated vs. observed Nitrite+ Nitrate Nitrogen (NOx) load at Amity Creek at Duluth

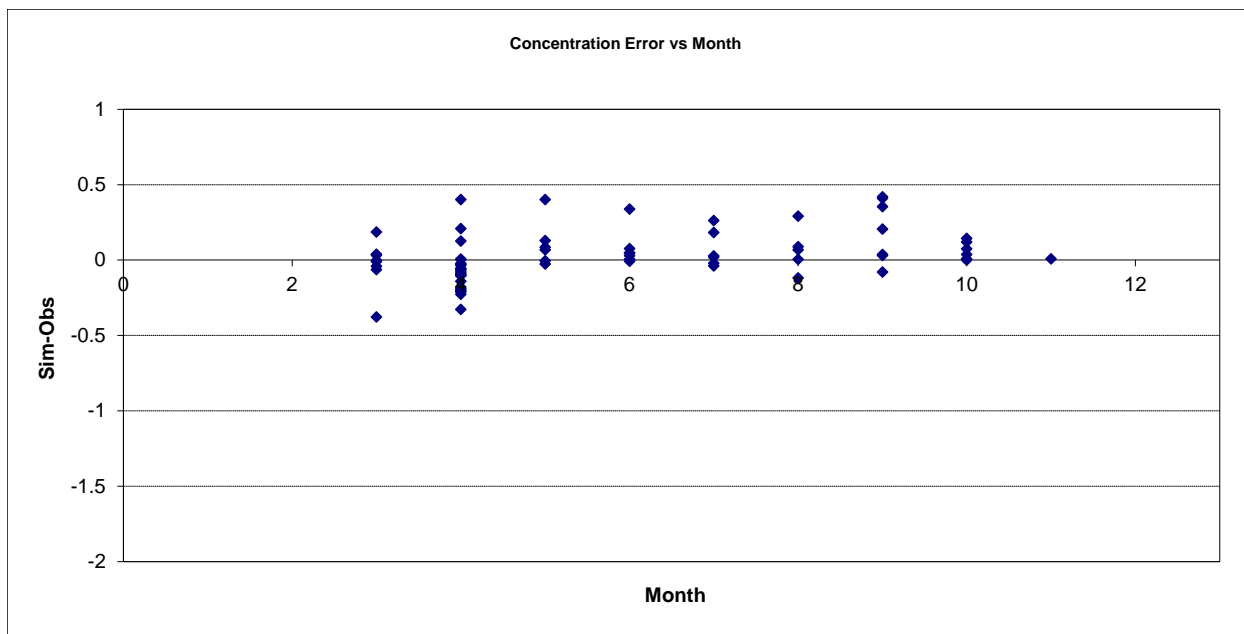


Figure 19. Residual (Simulated - Observed) vs. Month Nitrite+ Nitrate Nitrogen (NOx) at Amity Creek at Duluth

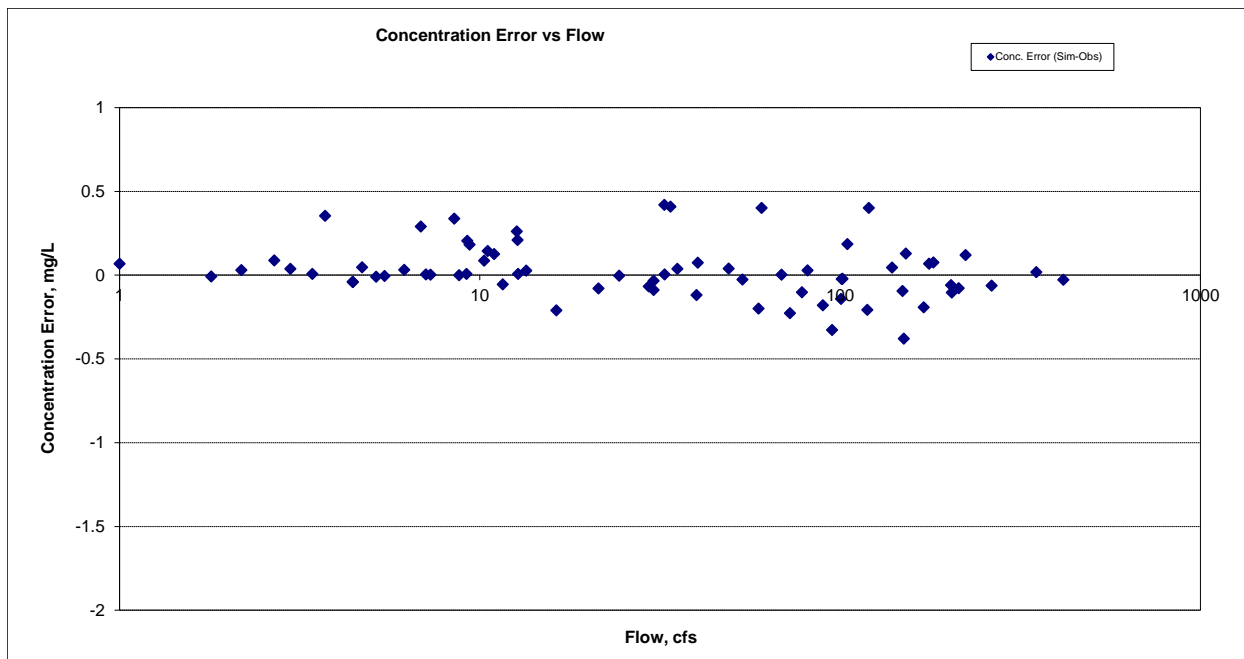


Figure 20. Residual (Simulated - Observed) vs. Flow Nitrite+ Nitrate Nitrogen (NOx) at Amity Creek at Duluth

Total Nitrogen (TN)

Table 5. Total Nitrogen (TN) statistics

Count	59
Concentration Average Error	-5.49%
Concentration Median Error	-10.85%
Load Average Error	14.55%
Load Median Error	-1.21%
Paired t concentration	0.99
Paired t load	0.58

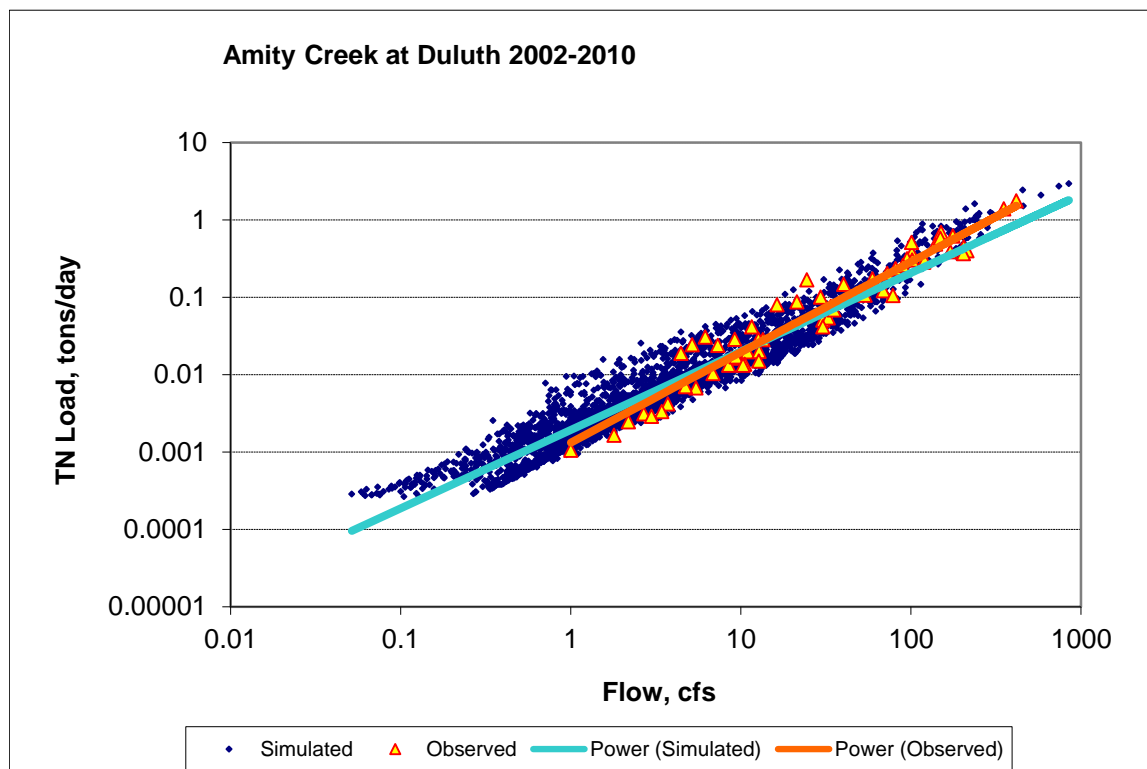


Figure 21. Power plot of simulated and observed Total Nitrogen (TN) load vs flow at Amity Creek at Duluth

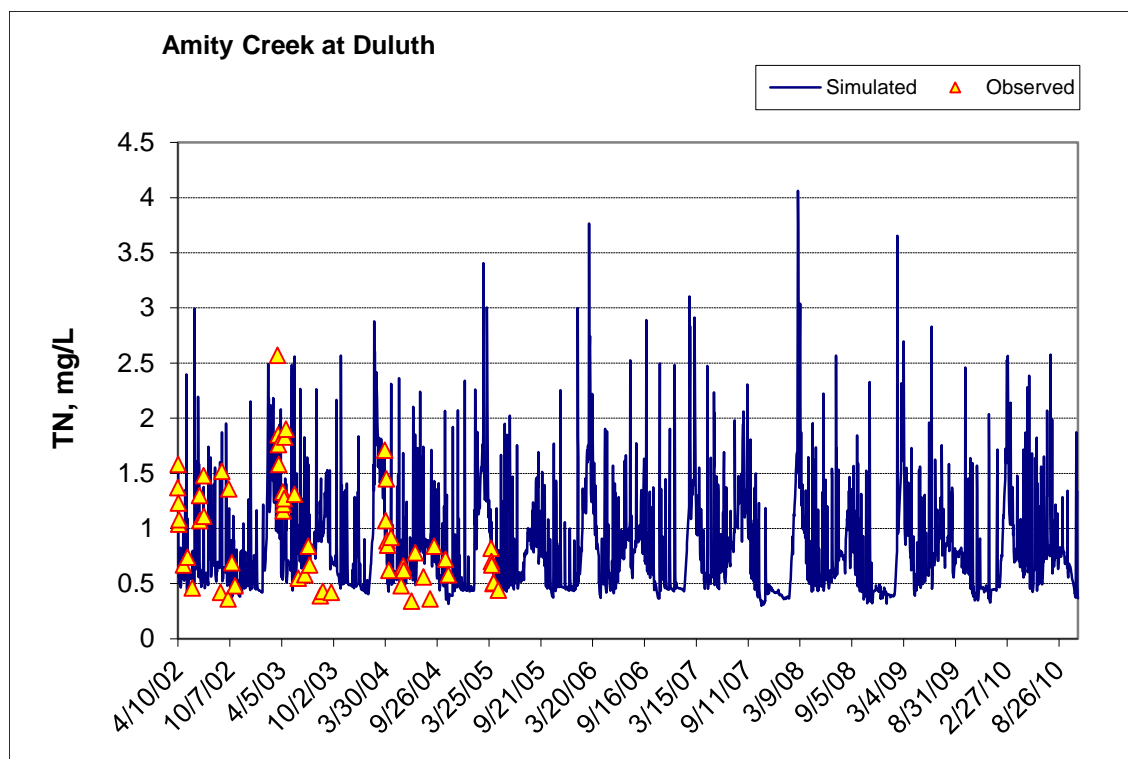


Figure 22. Time series of observed and simulated Total Nitrogen (TN) concentration at Amity Creek at Duluth

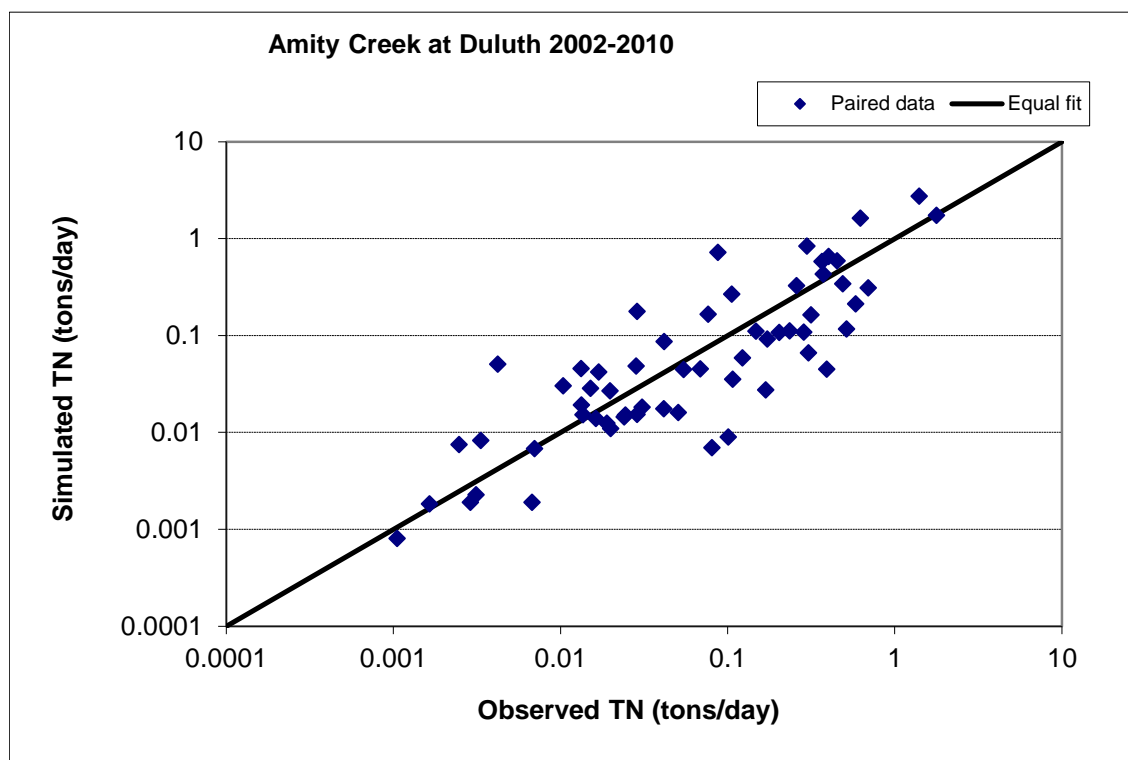


Figure 23. Paired simulated vs. observed Total Nitrogen (TN) load at Amity Creek at Duluth

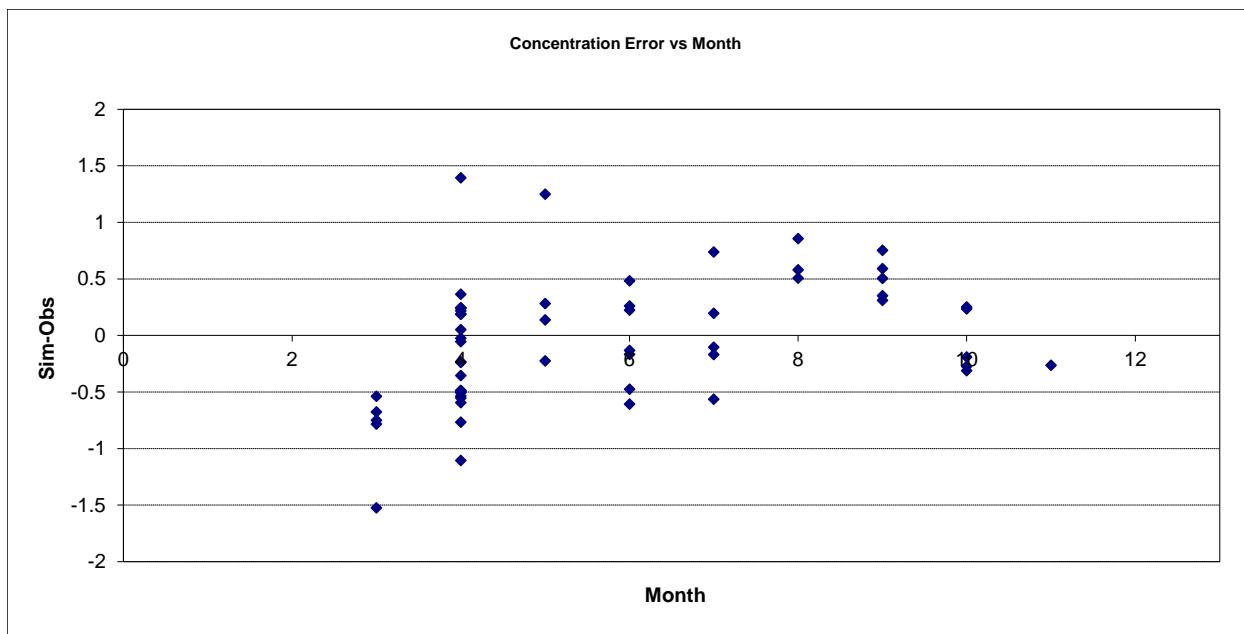


Figure 24. Residual (Simulated - Observed) vs. Month Total Nitrogen (TN) at Amity Creek at Duluth

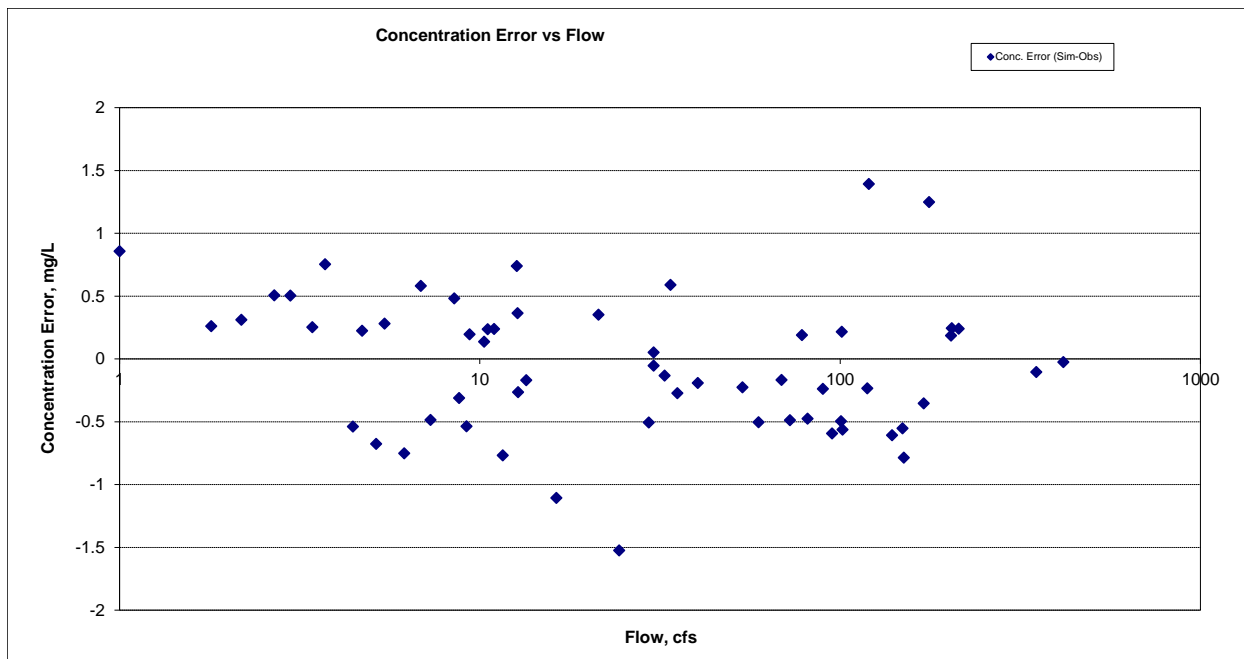


Figure 25. Residual (Simulated - Observed) vs. Flow Total Nitrogen (TN) at Amity Creek at Duluth

Soluble Reactive Phosphorus (SRP)

Table 6. Soluble Reactive Phosphorus (SRP) statistics

Count	53
Concentration Average Error	-19.54%
Concentration Median Error	5.67%
Load Average Error	21.14%
Load Median Error	-0.13%
Paired t concentration	0.52
Paired t load	0.49

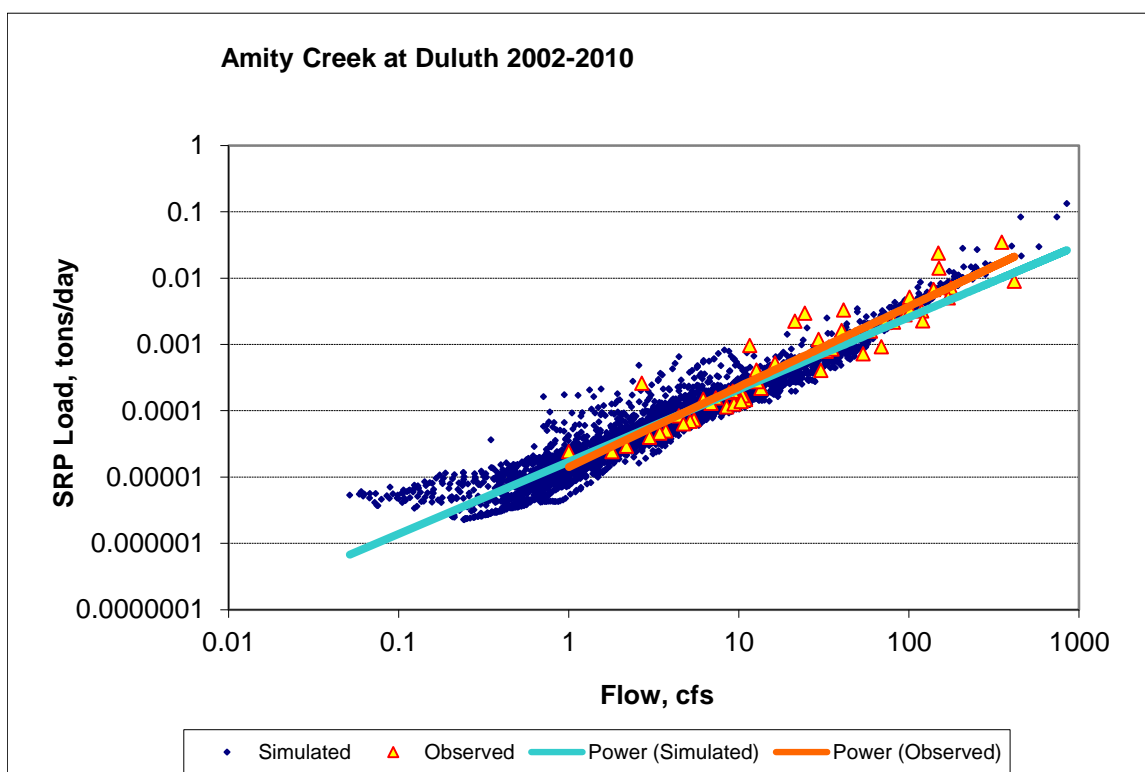


Figure 26. Power plot of simulated and observed Soluble Reactive Phosphorus (SRP) load vs flow at Amity Creek at Duluth

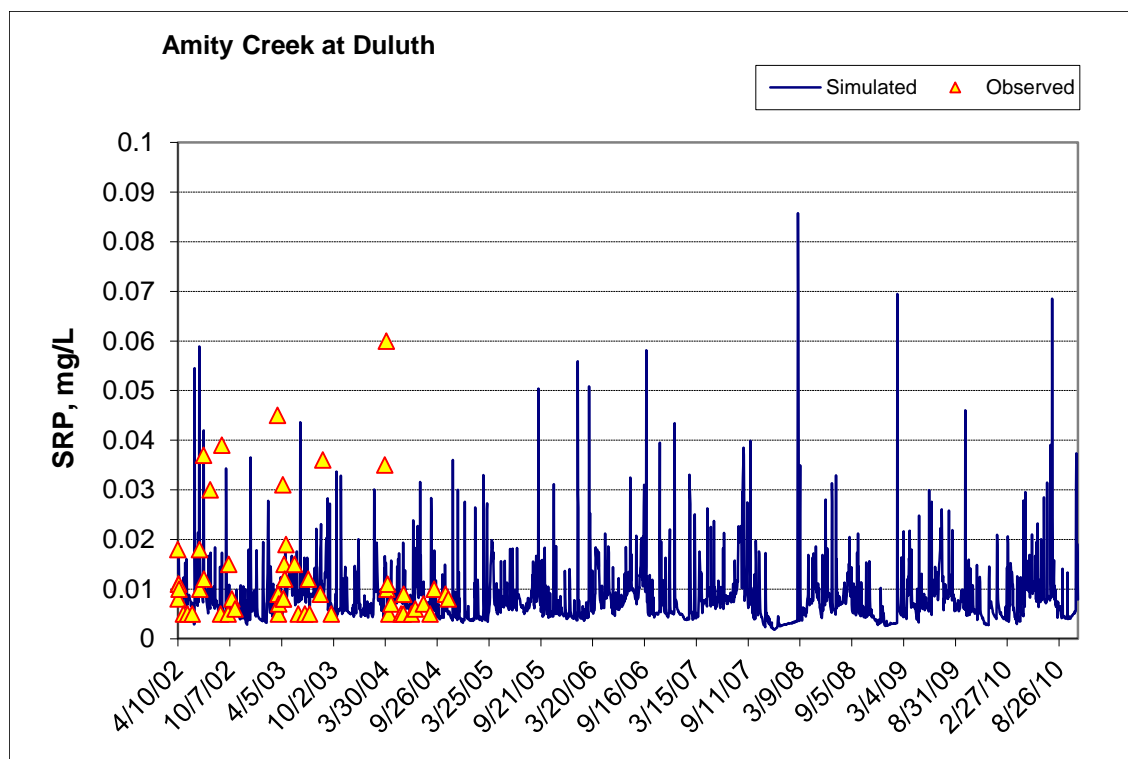


Figure 27. Time series of observed and simulated Soluble Reactive Phosphorus (SRP) concentration at Amity Creek at Duluth

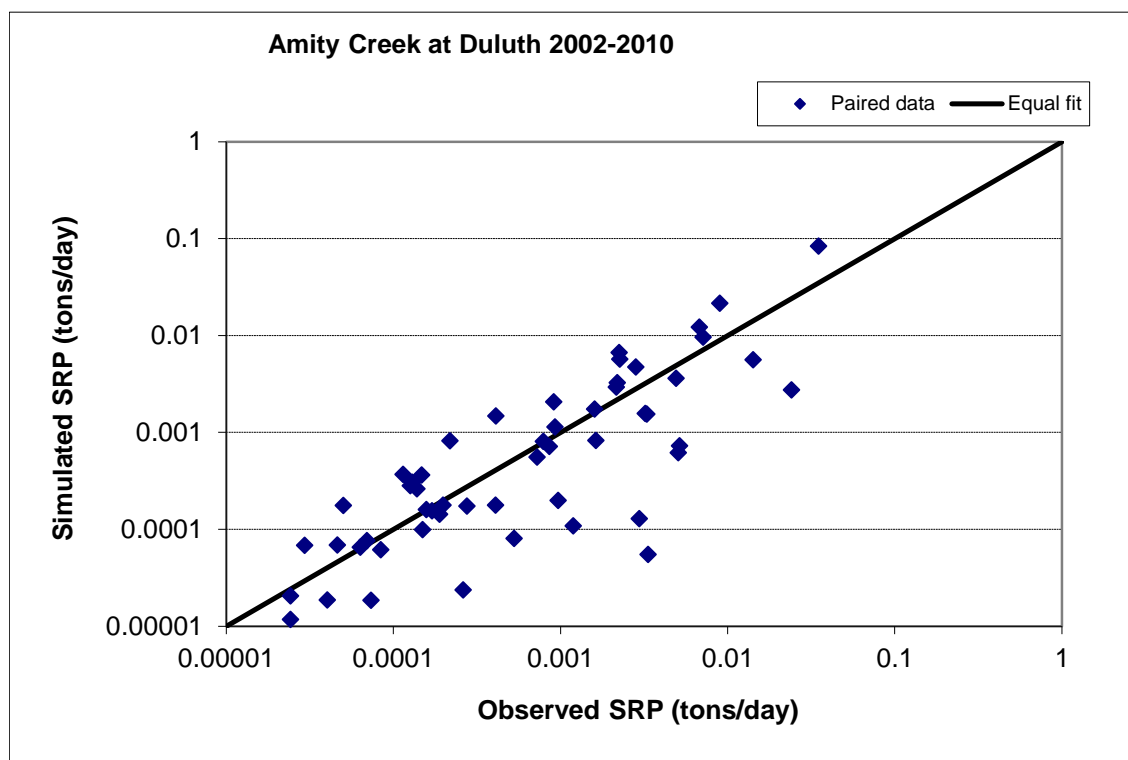


Figure 28. Paired simulated vs. observed Soluble Reactive Phosphorus (SRP) load at Amity Creek at Duluth

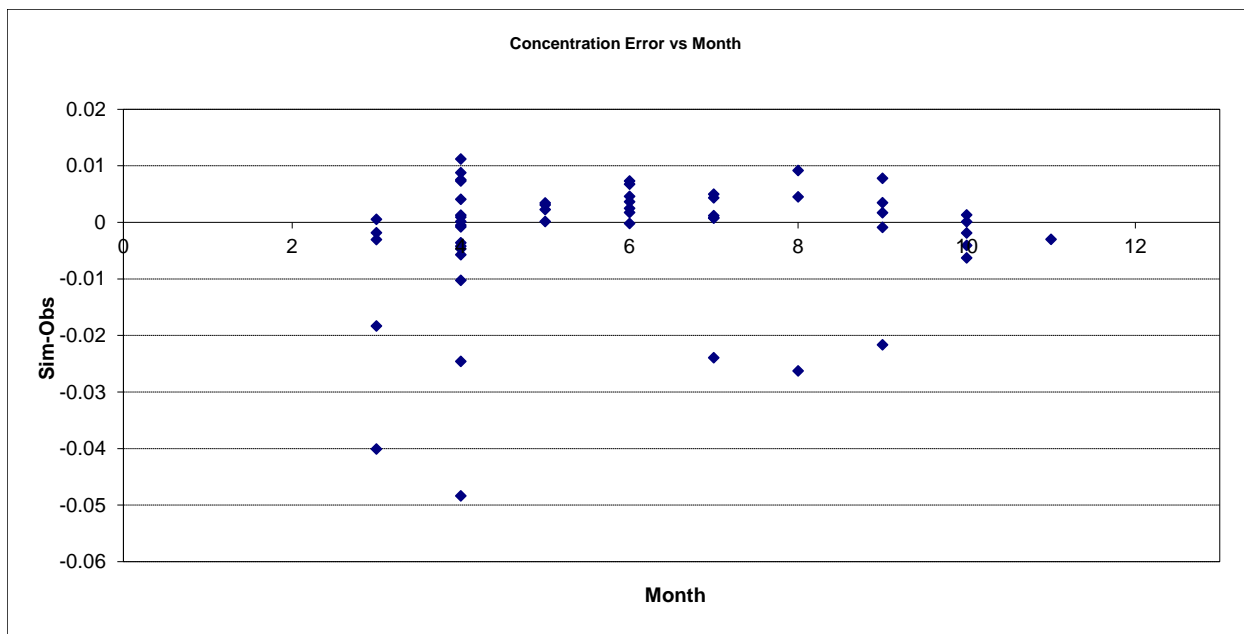


Figure 29. Residual (Simulated - Observed) vs. Month Soluble Reactive Phosphorus (SRP) at Amity Creek at Duluth

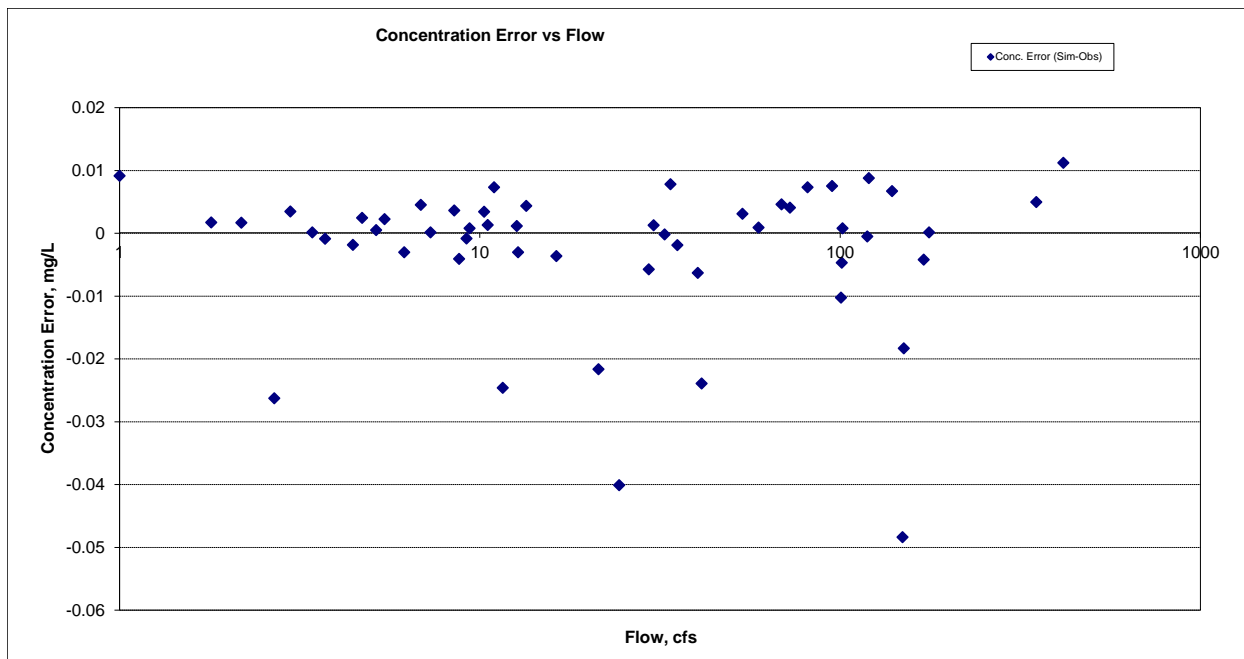


Figure 30. Residual (Simulated - Observed) vs. Flow Soluble Reactive Phosphorus (SRP) at Amity Creek at Duluth

Organic Phosphorus (OrgP)

Table 7. Organic Phosphorus (OrgP) statistics

Count	51
Concentration Average Error	-53.25%
Concentration Median Error	-19.15%
Load Average Error	-26.02%
Load Median Error	-6.65%
Paired t concentration	0.00
Paired t load	0.42

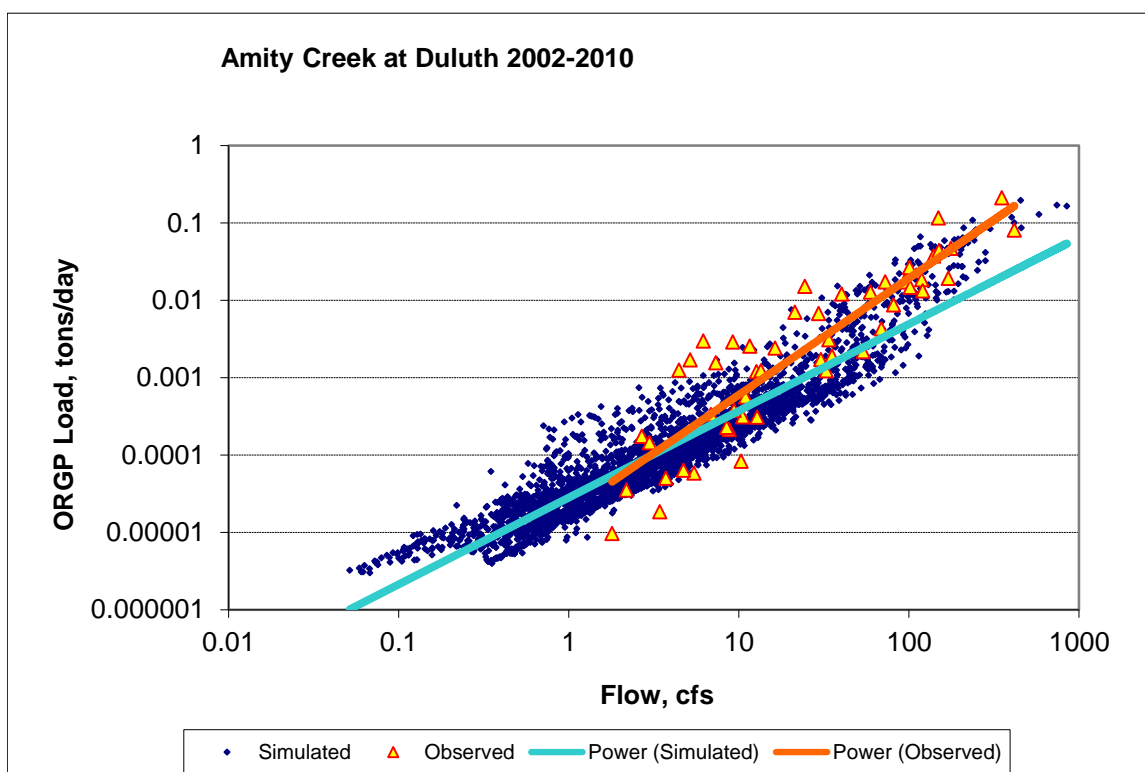


Figure 31. Power plot of simulated and observed Organic Phosphorus (OrgP) load vs flow at Amity Creek at Duluth

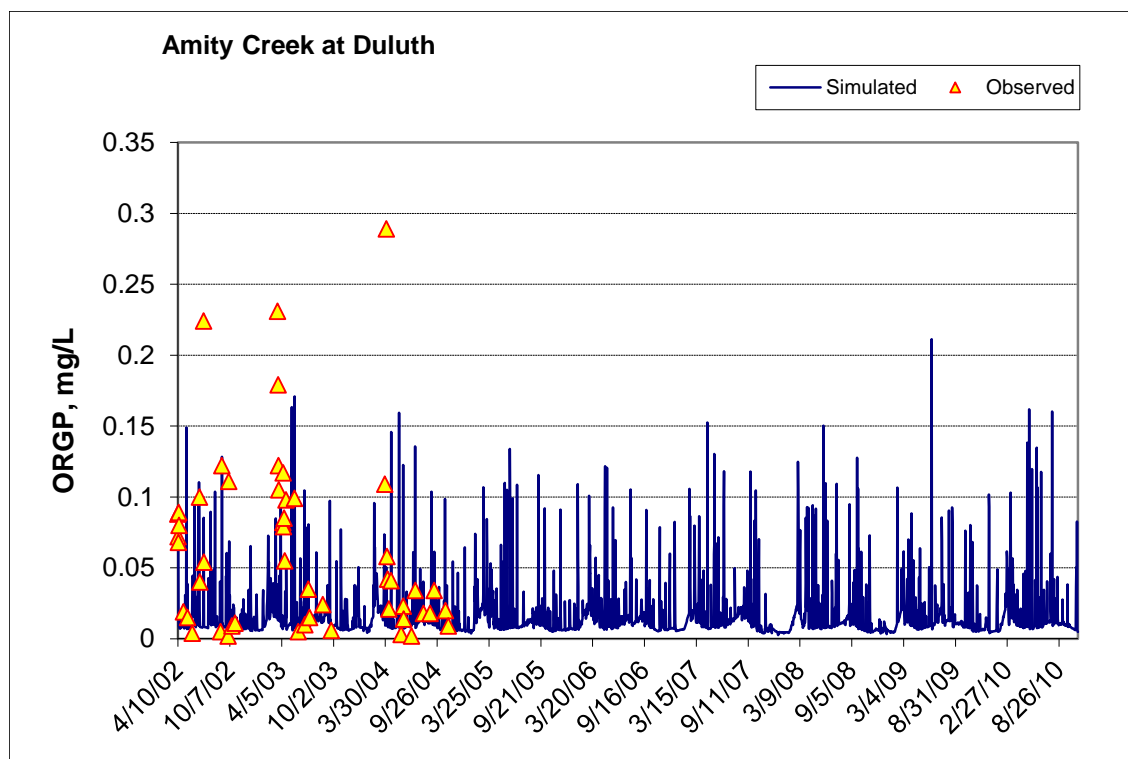


Figure 32. Time series of observed and simulated Organic Phosphorus (OrgP) concentration at Amity Creek at Duluth

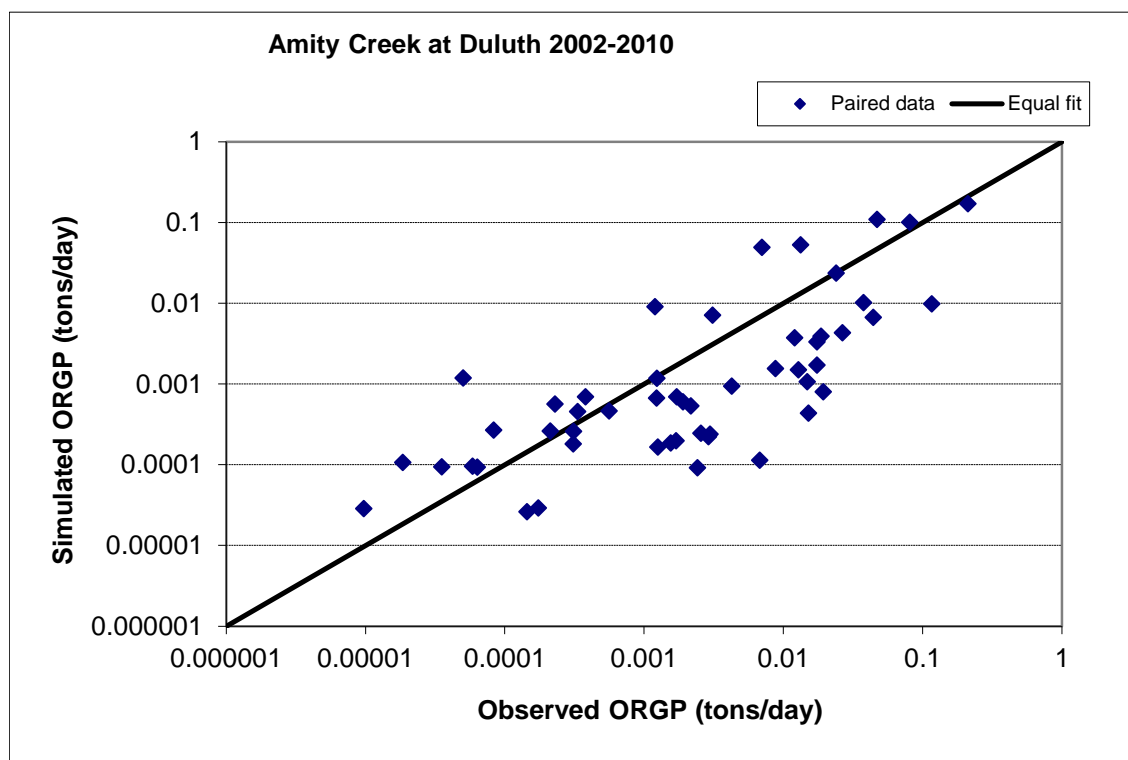


Figure 33. Paired simulated vs. observed Organic Phosphorus (OrgP) load at Amity Creek at Duluth

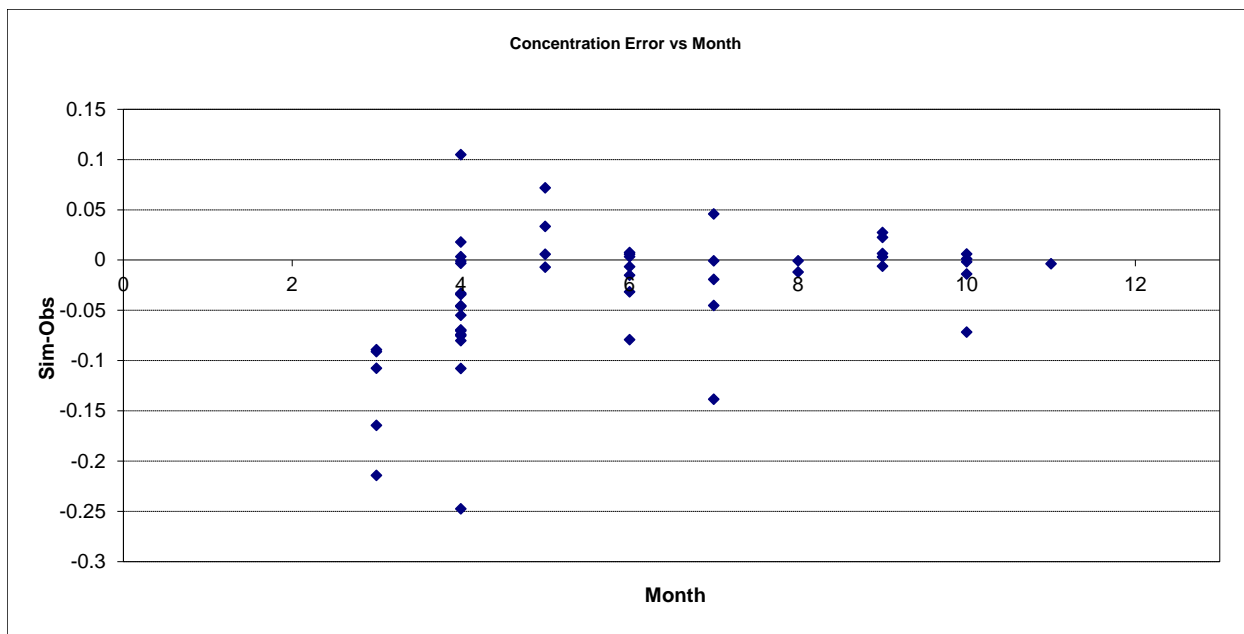


Figure 34. Residual (Simulated - Observed) vs. Month Organic Phosphorus (OrgP) at Amity Creek at Duluth

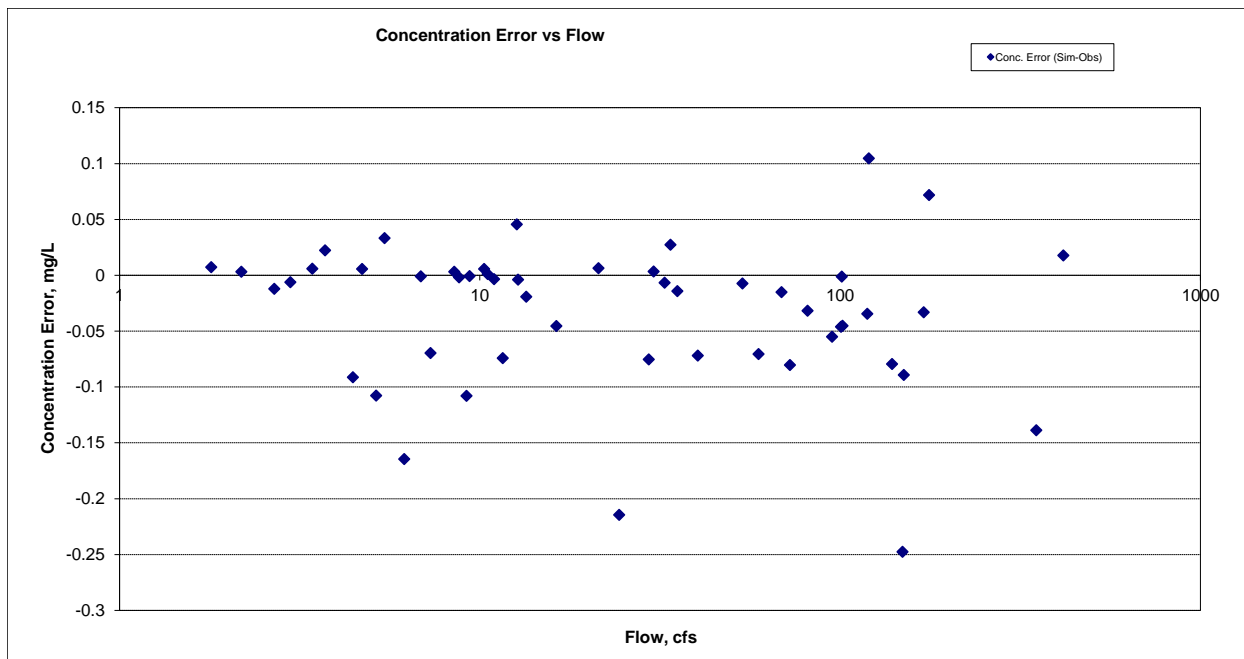


Figure 35. Residual (Simulated - Observed) vs. Flow Organic Phosphorus (OrgP) at Amity Creek at Duluth

Total Phosphorus (TP)

Table 8. Total Phosphorus (TP) statistics

Count	127
Concentration Average Error	-27.28%
Concentration Median Error	-9.56%
Load Average Error	-6.24%
Load Median Error	-0.62%
Paired t concentration	0.17
Paired t load	0.80

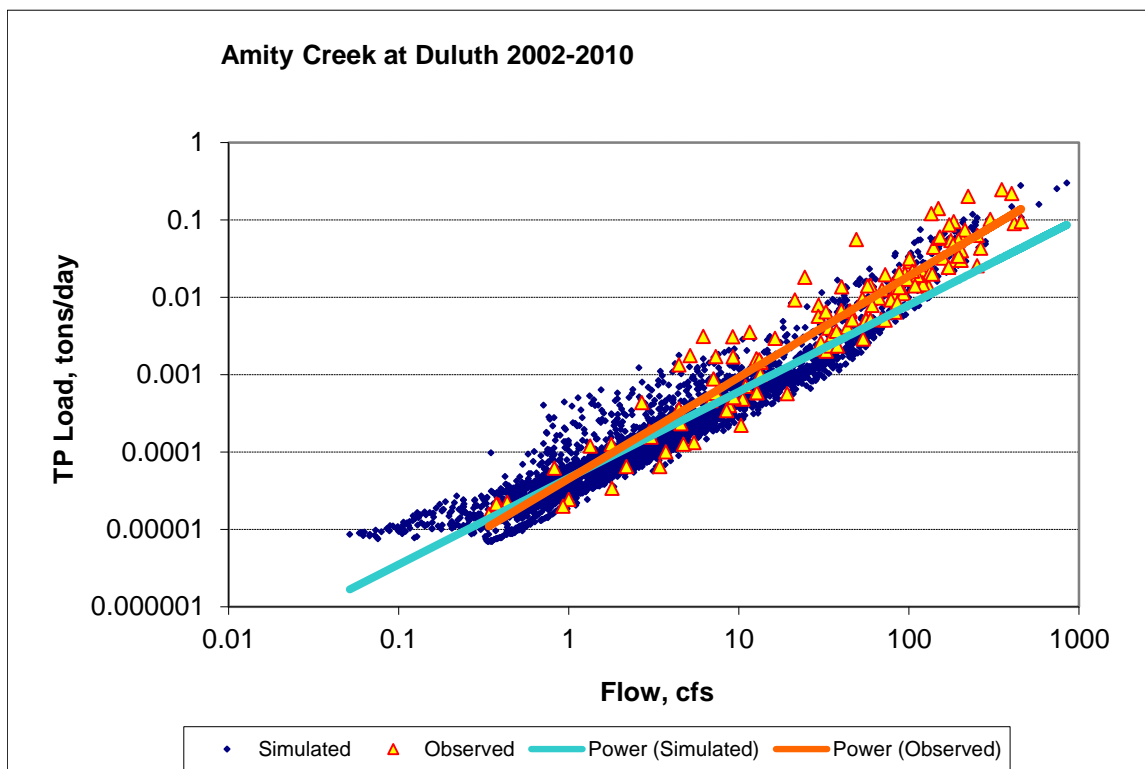


Figure 36. Power plot of simulated and observed Total Phosphorus (TP) load vs flow at Amity Creek at Duluth

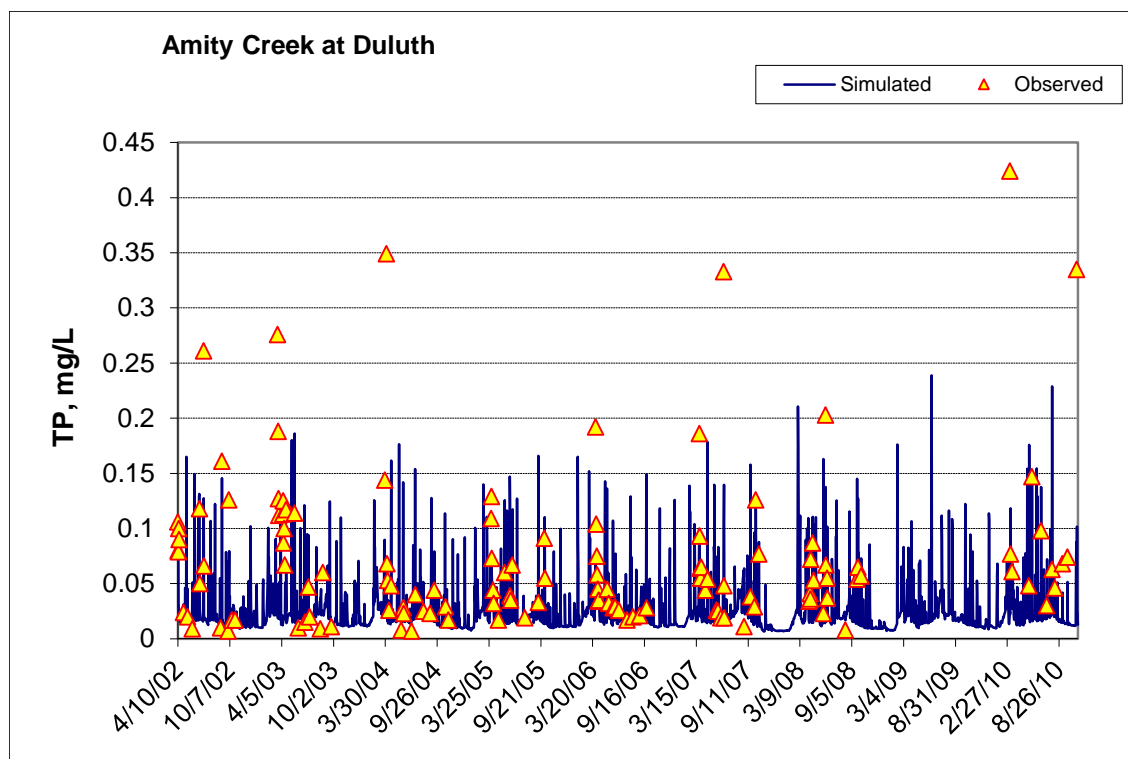


Figure 37. Time series of observed and simulated Total Phosphorus (TP) concentration at Amity Creek at Duluth

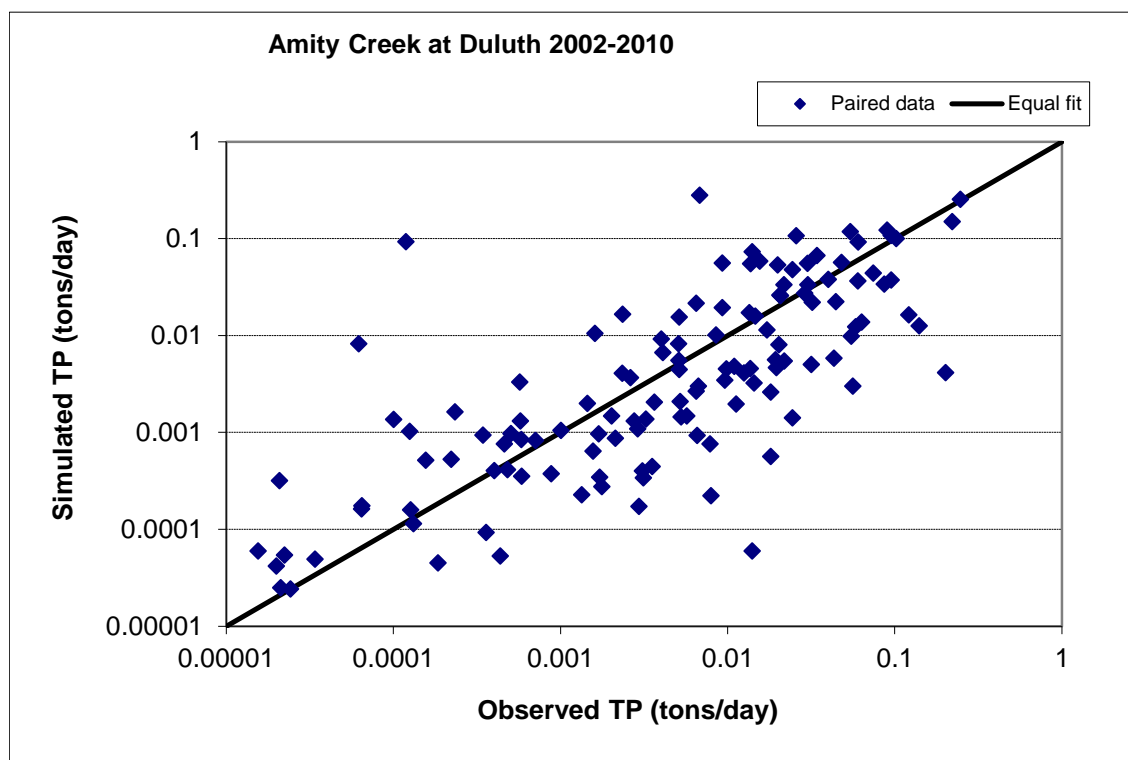


Figure 38. Paired simulated vs. observed Total Phosphorus (TP) load at Amity Creek at Duluth

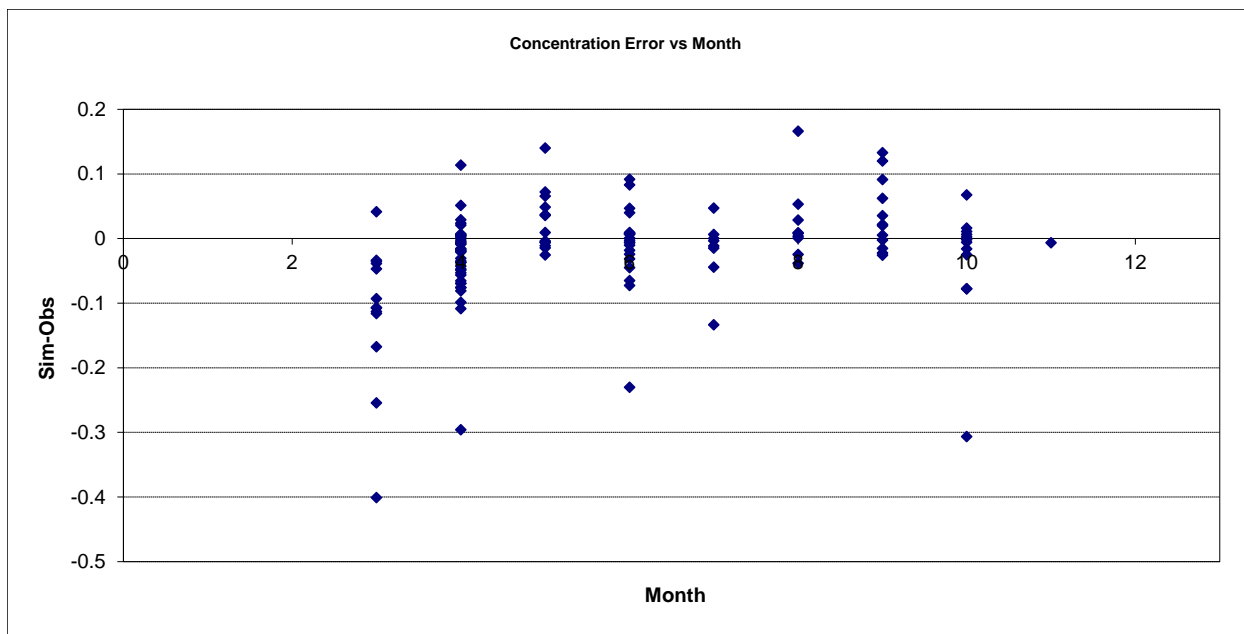


Figure 39. Residual (Simulated - Observed) vs. Month Total Phosphorus (TP) at Amity Creek at Duluth

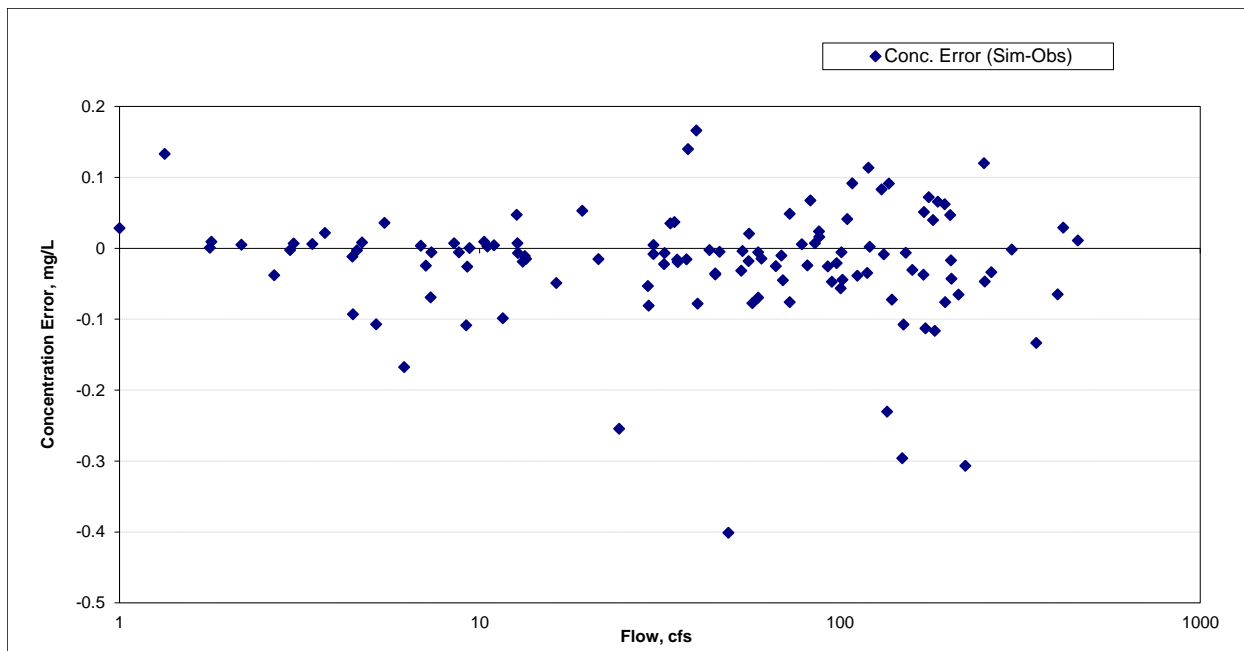


Figure 40. Residual (Simulated - Observed) vs. Flow Total Phosphorus (TP) at Amity Creek at Duluth

Talmadge River near Duluth (HYDSTRA 02035001)

Total Suspended Solids (TSS)

Table 9. Total Suspended Solids (TSS) statistics

Count	114
Concentration Average Error	23.53%
Concentration Median Error	0.06%
Load Average Error	-16.39%
Load Median Error	-0.03%
Paired t concentration	0.44
Paired t load	0.54

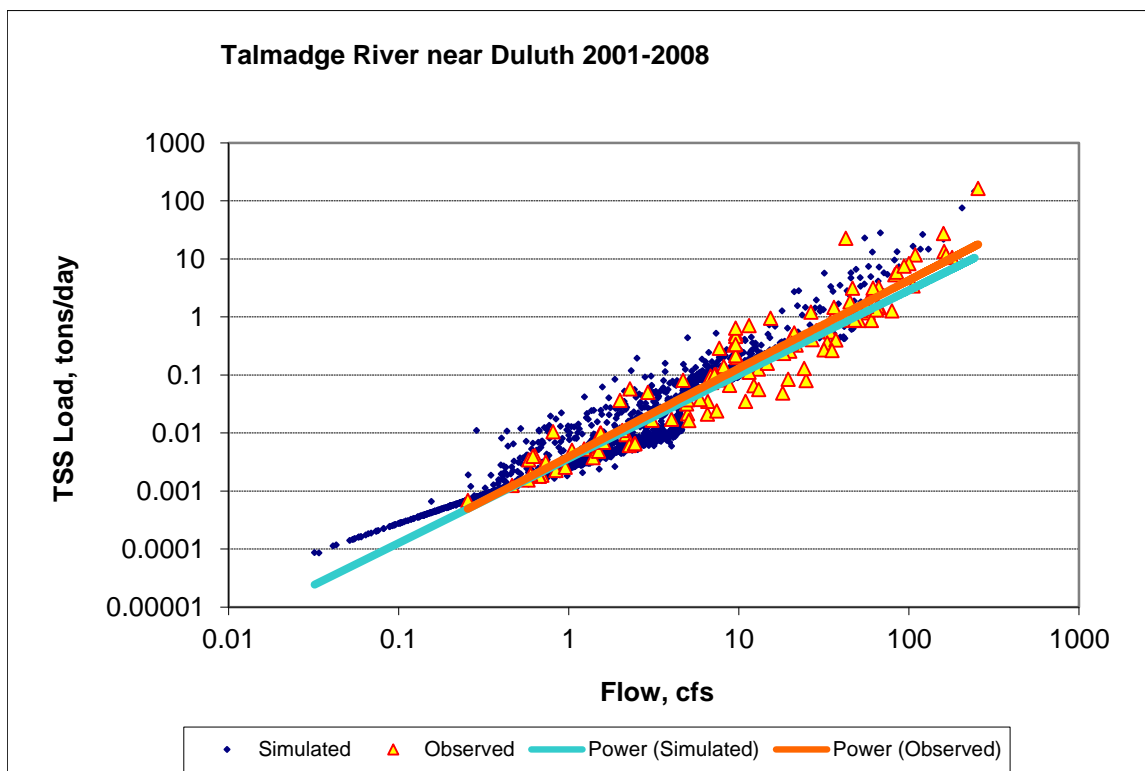


Figure 41. Power plot of simulated and observed Total Suspended Solids (TSS) load vs flow at Talmadge River near Duluth

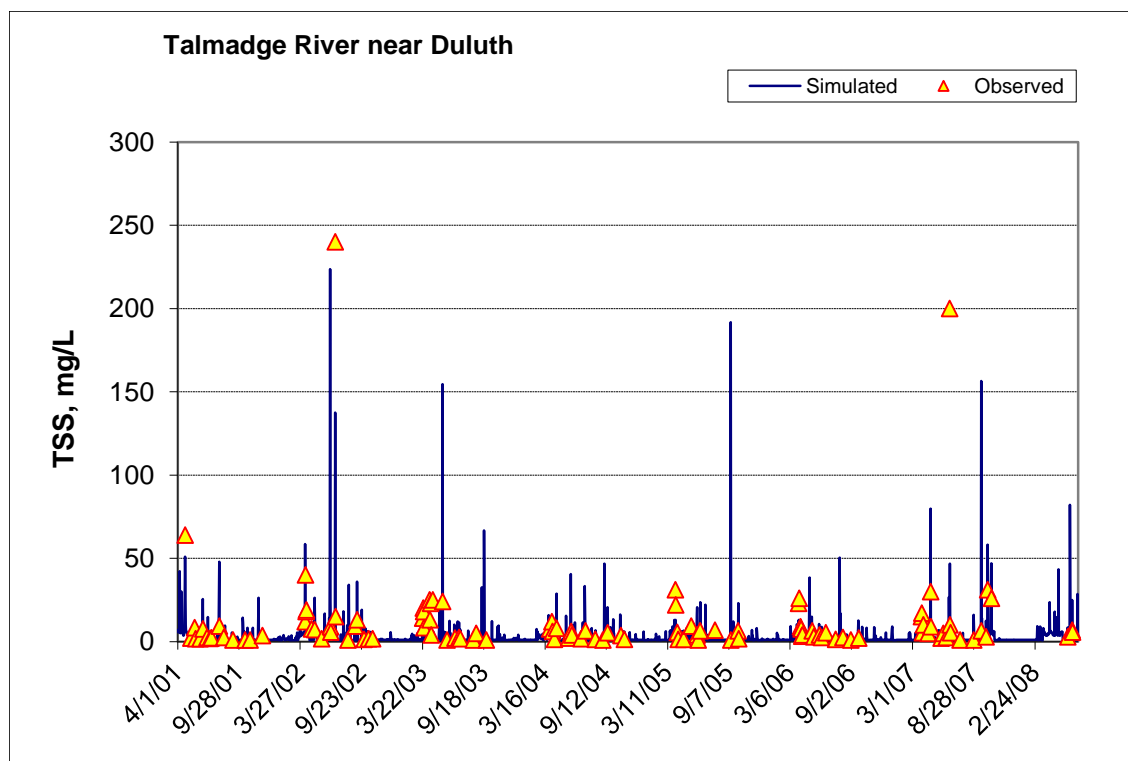


Figure 42. Time series of observed and simulated Total Suspended Solids (TSS) concentration at Talmadge River near Duluth

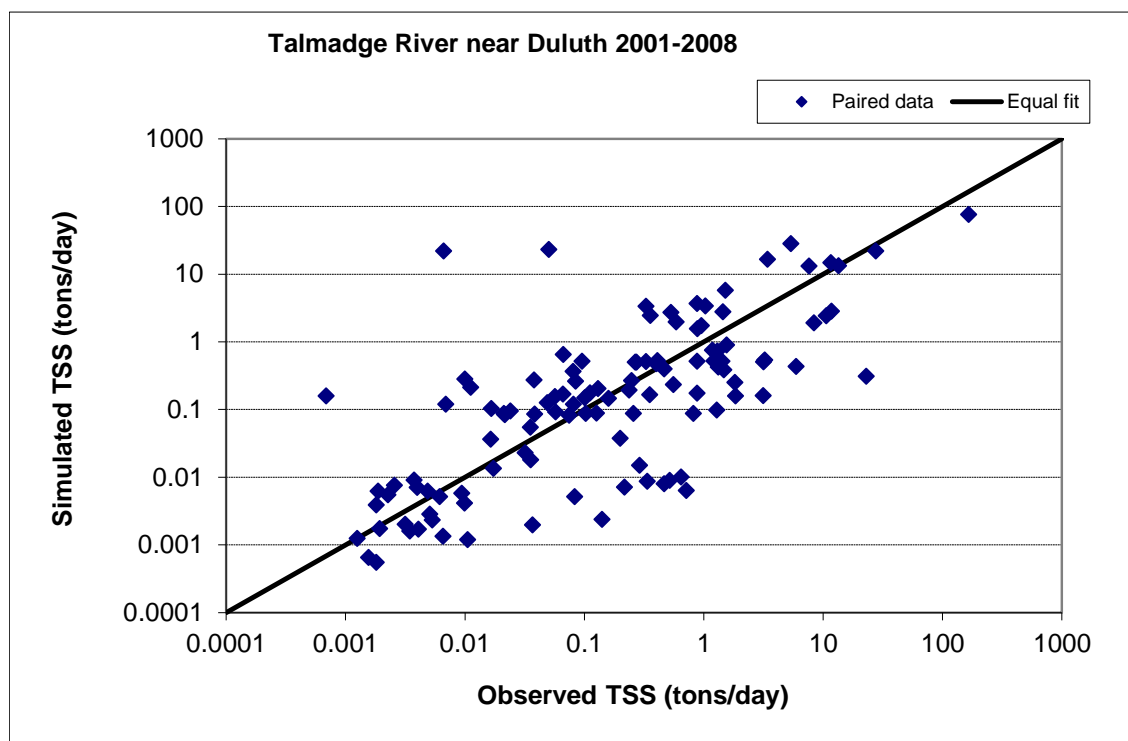


Figure 43. Paired simulated vs. observed Total Suspended Solids (TSS) load at Talmadge River near Duluth

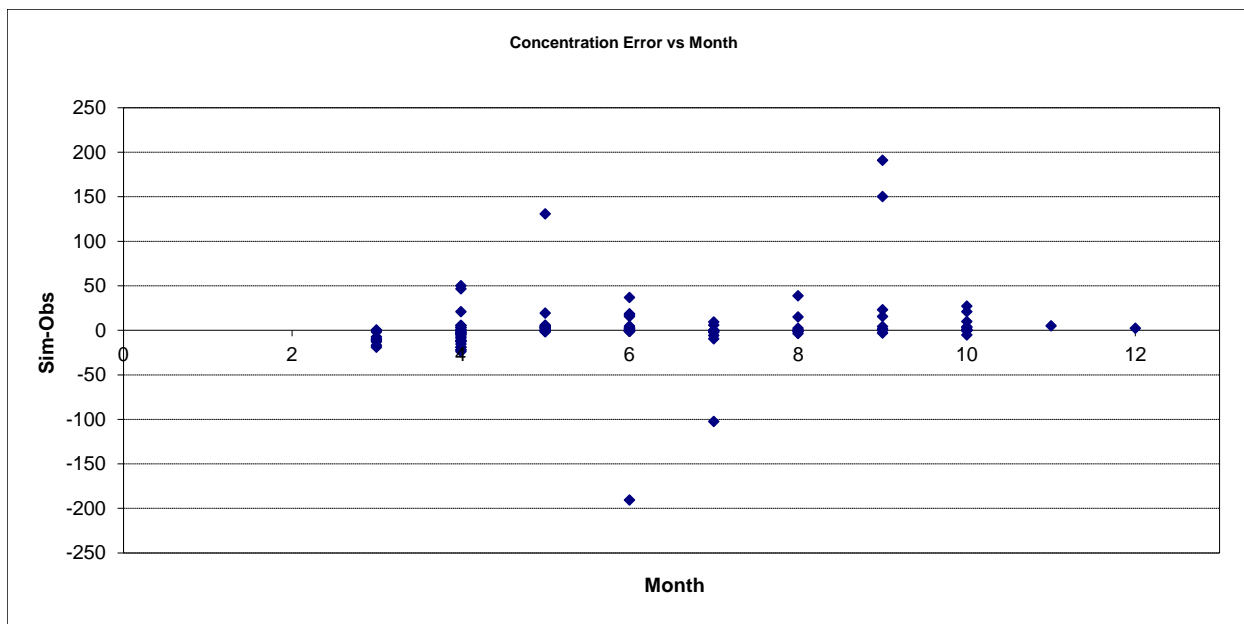


Figure 44. Residual (Simulated - Observed) vs. Month Total Suspended Solids (TSS) at Talmadge River near Duluth

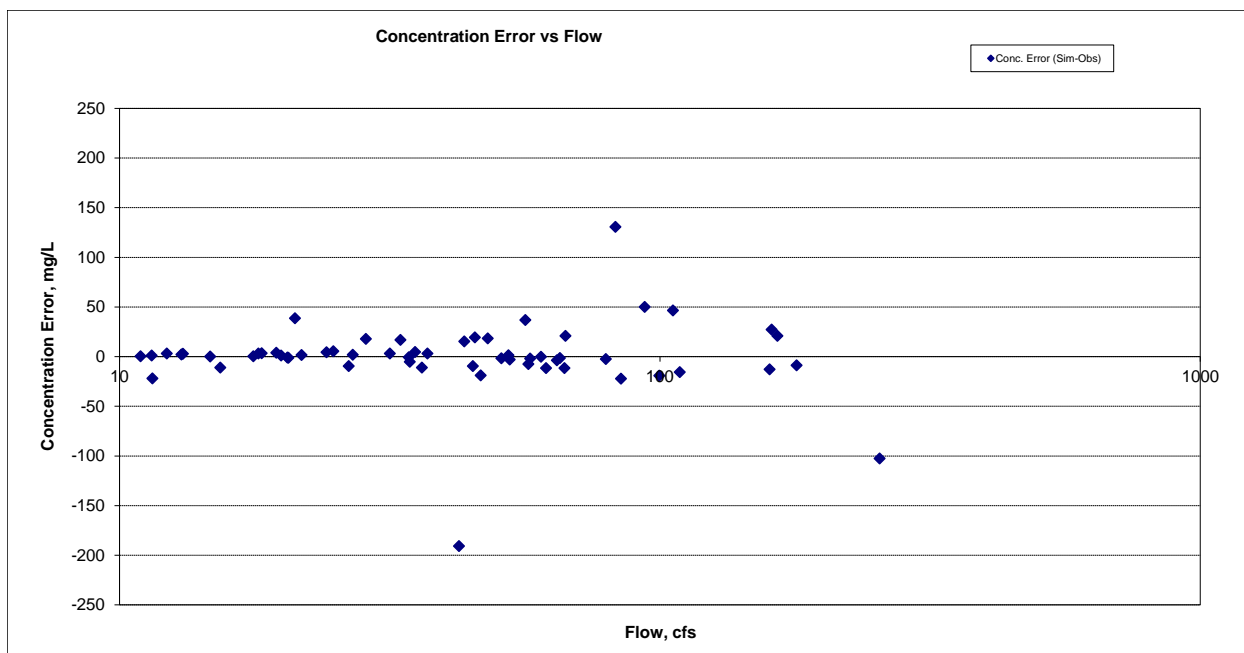


Figure 45. Residual (Simulated - Observed) vs. Flow Total Suspended Solids (TSS) at Talmadge River near Duluth

Total Kjeldahl Nitrogen (TKN)

Table 10. Total Kjeldahl Nitrogen (TKN) statistics

Count	70
Concentration Average Error	-12.88%
Concentration Median Error	-20.60%
Load Average Error	-20.19%
Load Median Error	-3.03%
Paired t concentration	0.87
Paired t load	0.50

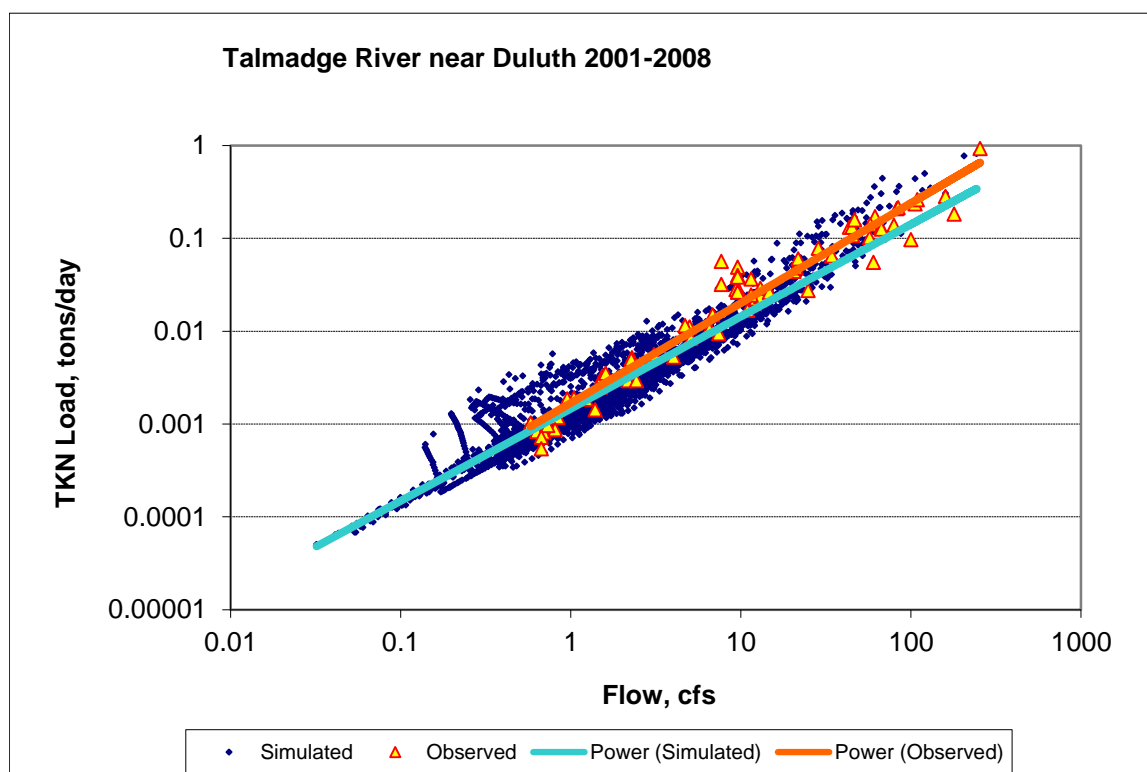


Figure 46. Power plot of simulated and observed Total Kjeldahl Nitrogen (TKN) load vs flow at Talmadge River near Duluth

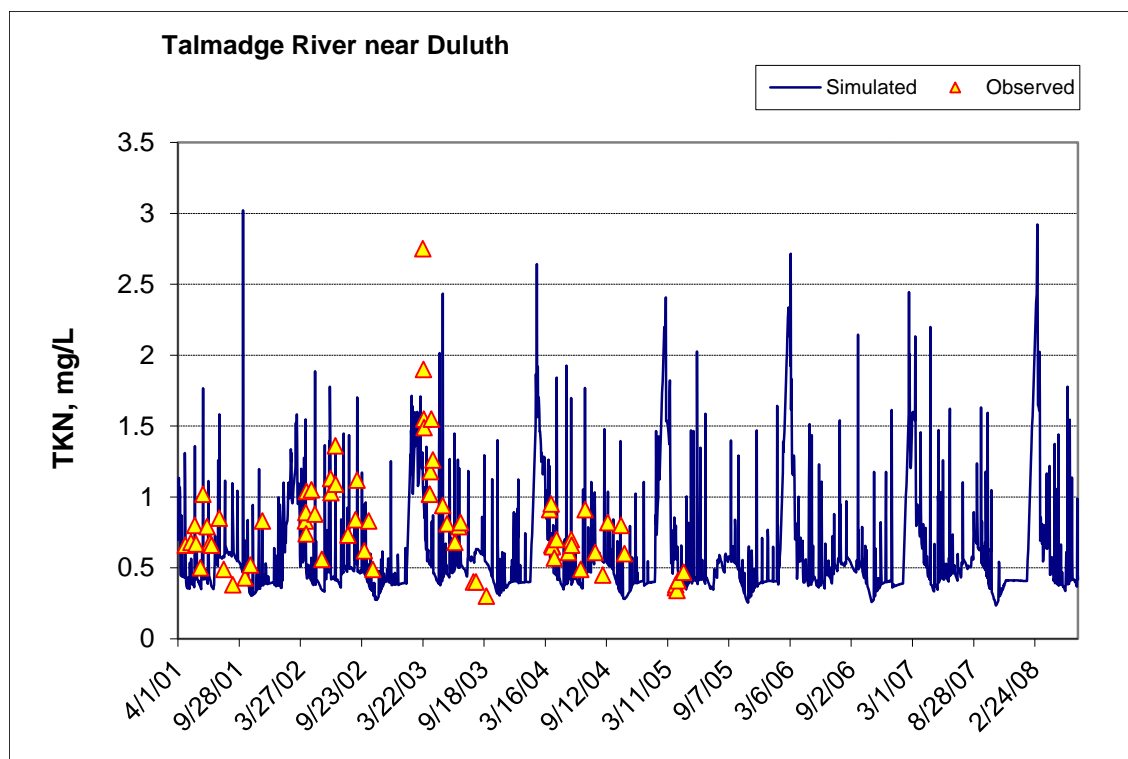


Figure 47. Time series of observed and simulated Total Kjeldahl Nitrogen (TKN) concentration at Talmadge River near Duluth

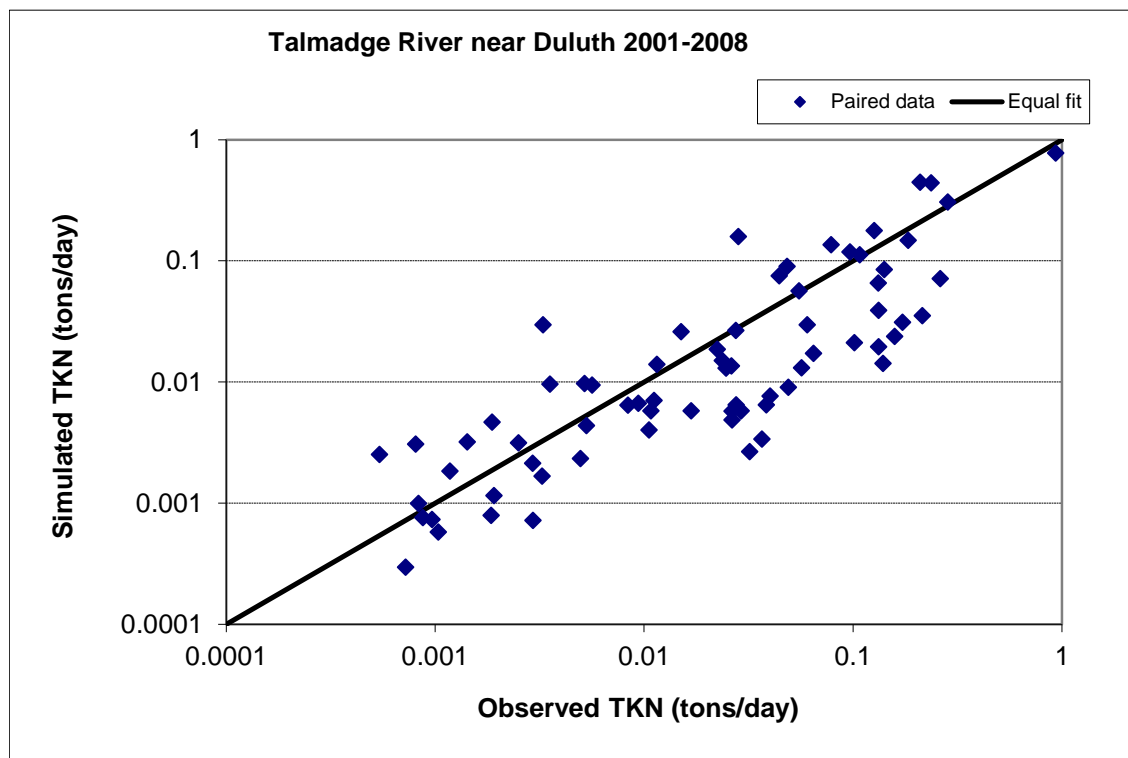


Figure 48. Paired simulated vs. observed Total Kjeldahl Nitrogen (TKN) load at Talmadge River near Duluth

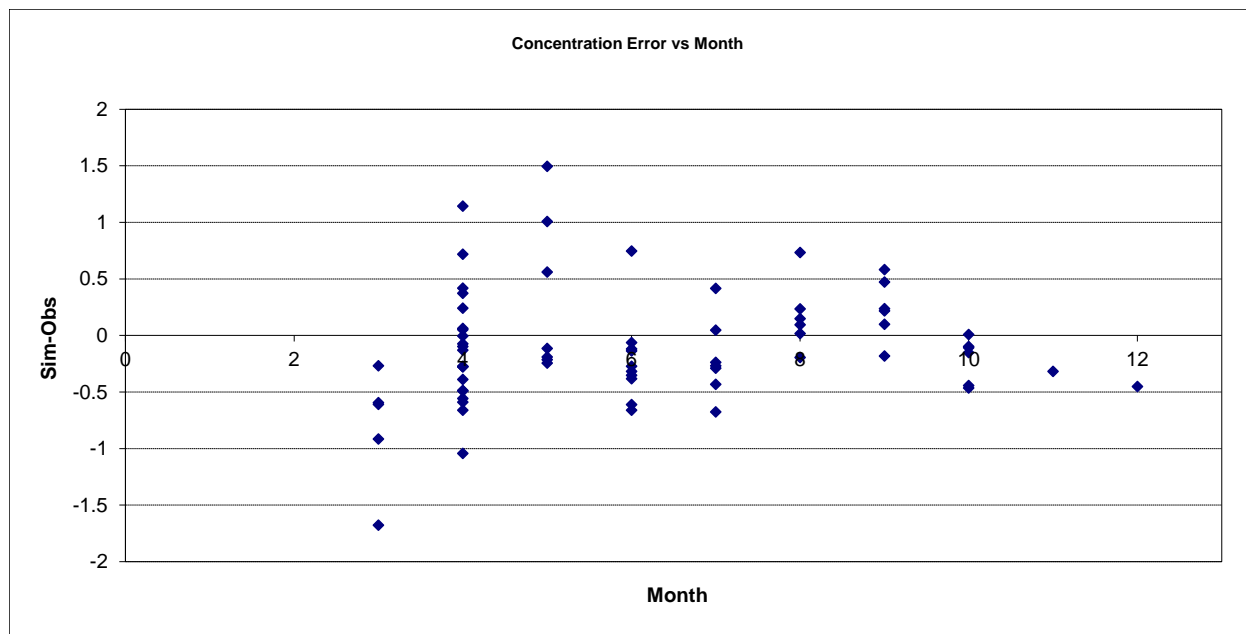


Figure 49. Residual (Simulated - Observed) vs. Month Total Kjeldahl Nitrogen (TKN) at Talmadge River near Duluth

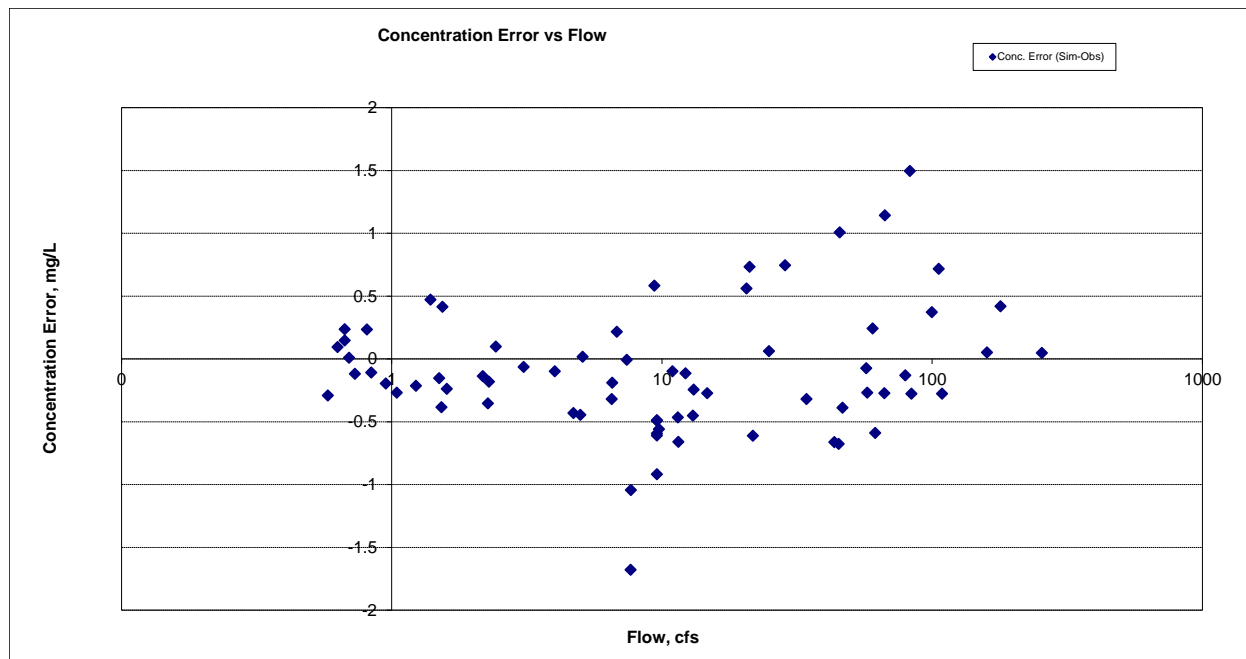


Figure 50. Residual (Simulated - Observed) vs. Flow Total Kjeldahl Nitrogen (TKN) at Talmadge River near Duluth

Nitrite+ Nitrate Nitrogen (NO_x)

Table 11. Nitrite+ Nitrate Nitrogen (NO_x) statistics

Count	70
Concentration Average Error	-7.02%
Concentration Median Error	-4.06%
Load Average Error	-39.41%
Load Median Error	-0.63%
Paired t concentration	0.88
Paired t load	0.16

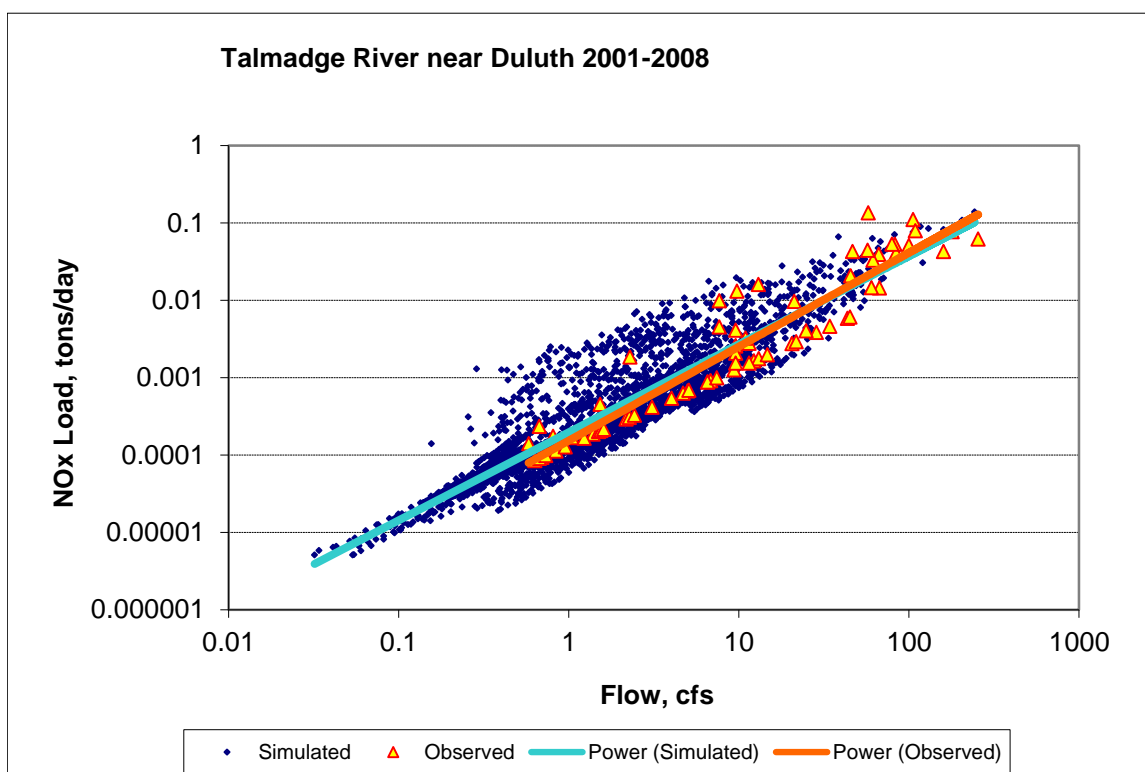


Figure 51. Power plot of simulated and observed Nitrite+ Nitrate Nitrogen (NO_x) load vs flow at Talmadge River near Duluth

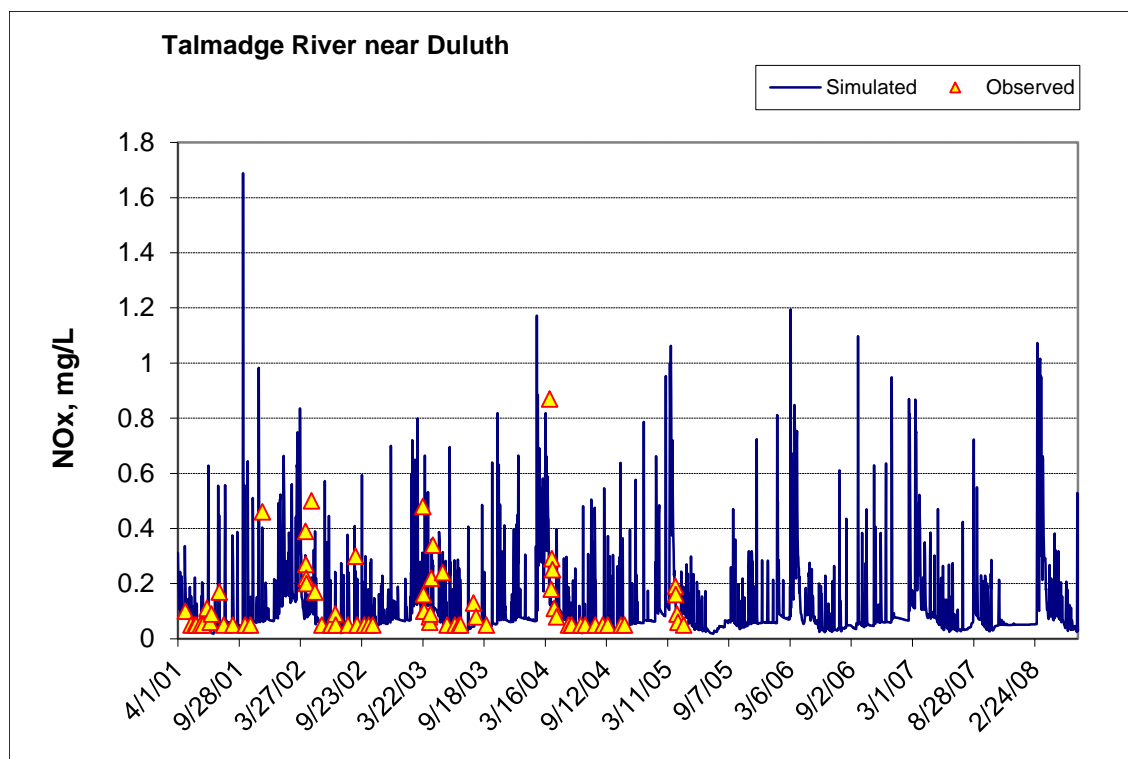


Figure 52. Time series of observed and simulated Nitrite+ Nitrate Nitrogen (NOx) concentration at Talmadge River near Duluth

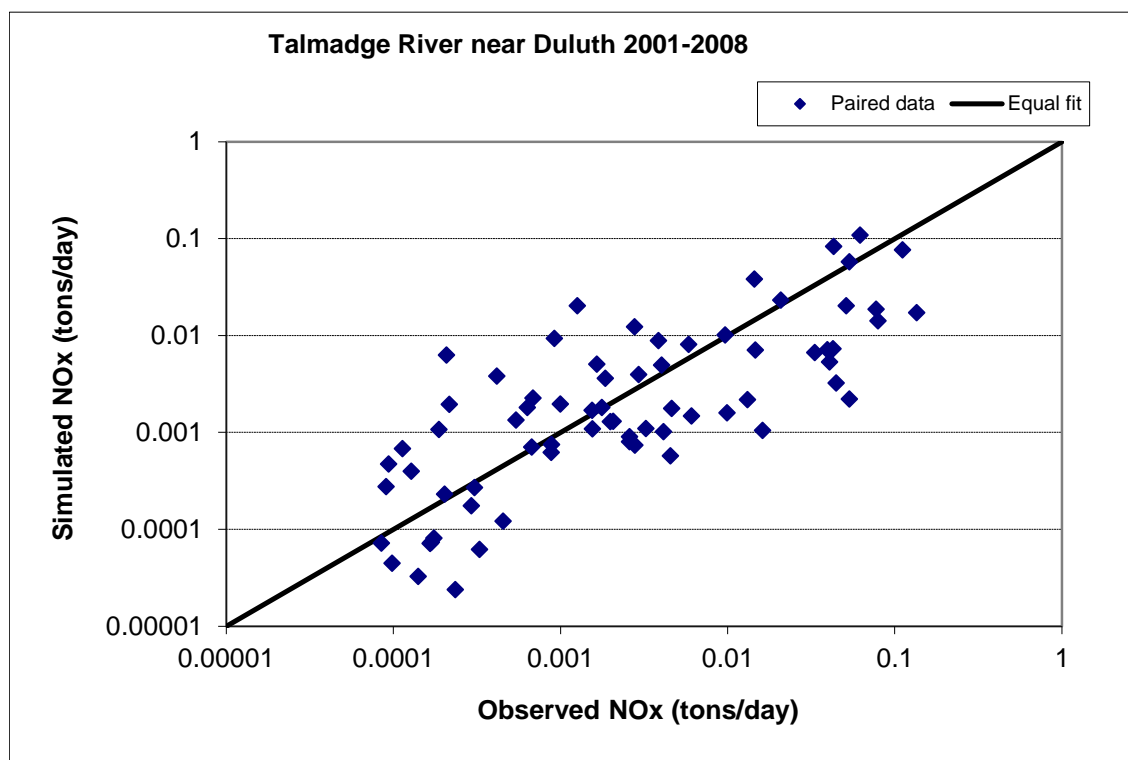


Figure 53. Paired simulated vs. observed Nitrite+ Nitrate Nitrogen (NOx) load at Talmadge River near Duluth

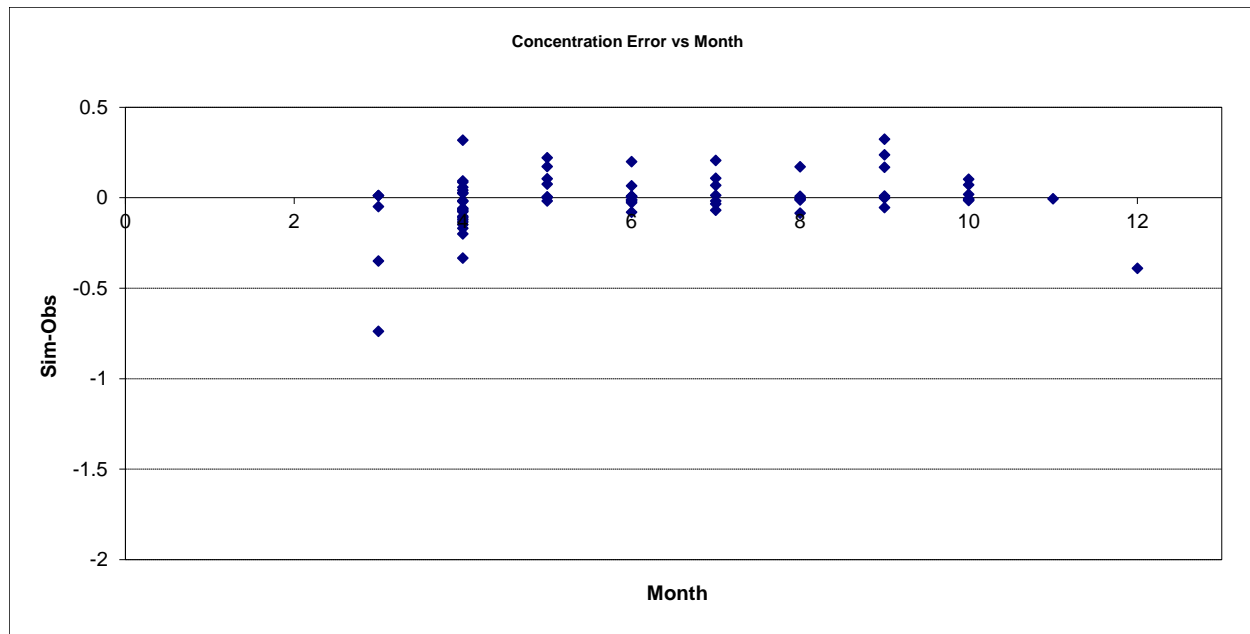


Figure 54. Residual (Simulated - Observed) vs. Month Nitrite+ Nitrate Nitrogen (NOx) at Talmadge River near Duluth

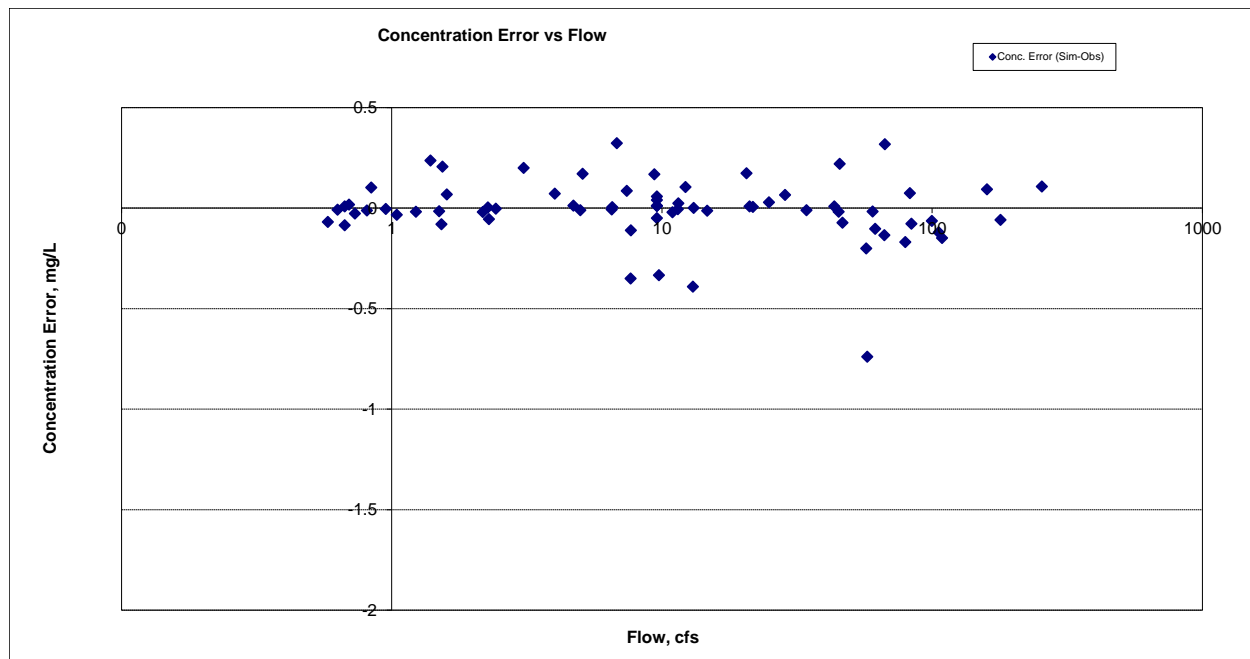


Figure 55. Residual (Simulated - Observed) vs. Flow Nitrite+ Nitrate Nitrogen (NOx) at Talmadge River near Duluth

Total Nitrogen (TN)

Table 12. Total Nitrogen (TN) statistics

Count	70
Concentration Average Error	-12.07%
Concentration Median Error	-20.40%
Load Average Error	-23.62%
Load Median Error	-2.65%
Paired t concentration	0.90
Paired t load	0.43

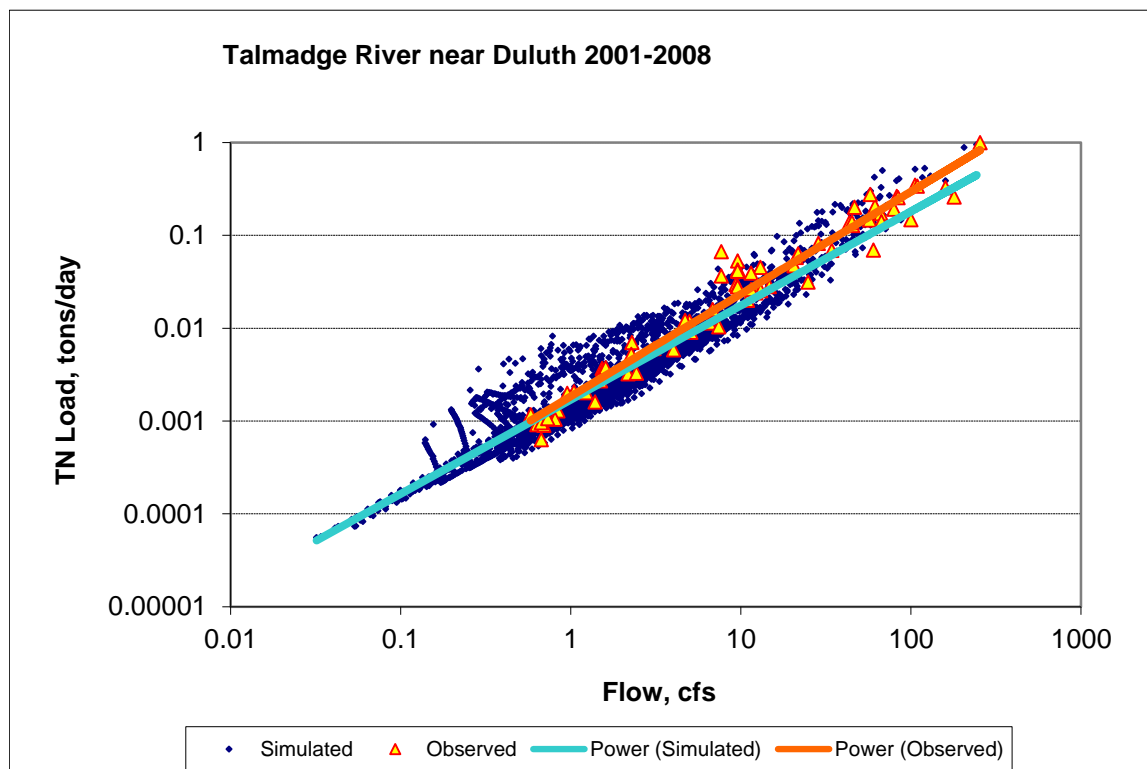


Figure 56. Power plot of simulated and observed Total Nitrogen (TN) load vs flow at Talmadge River near Duluth

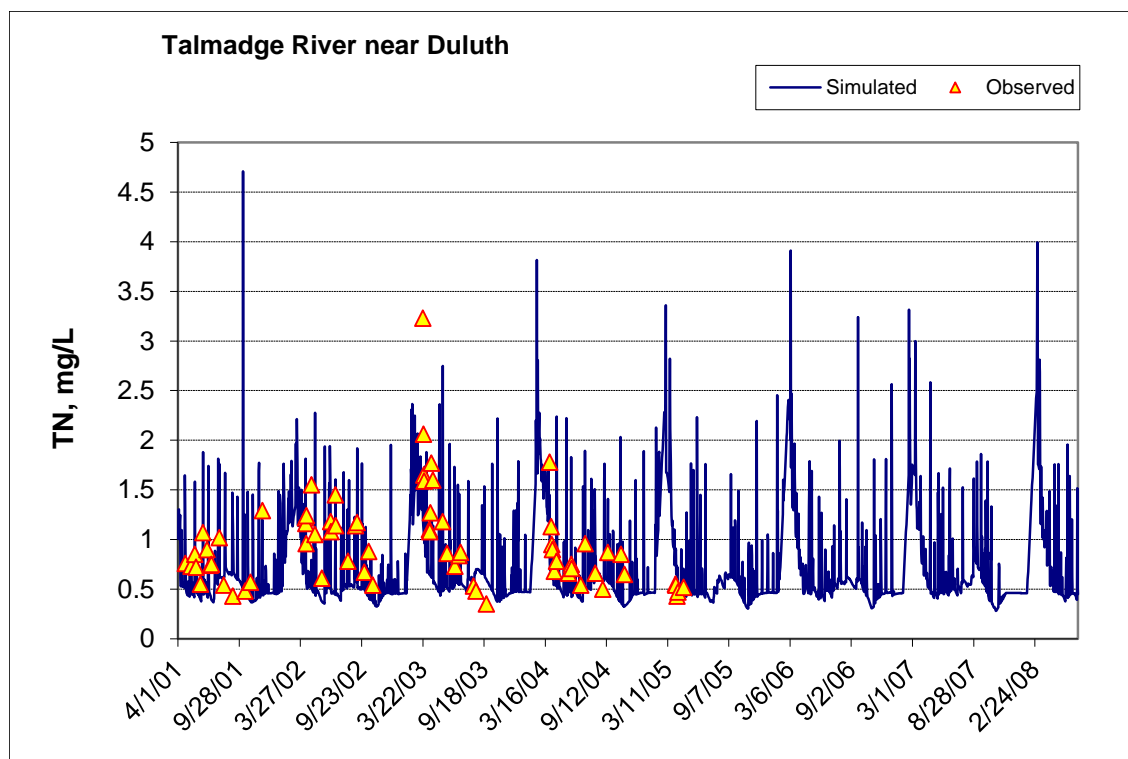


Figure 57. Time series of observed and simulated Total Nitrogen (TN) concentration at Talmadge River near Duluth

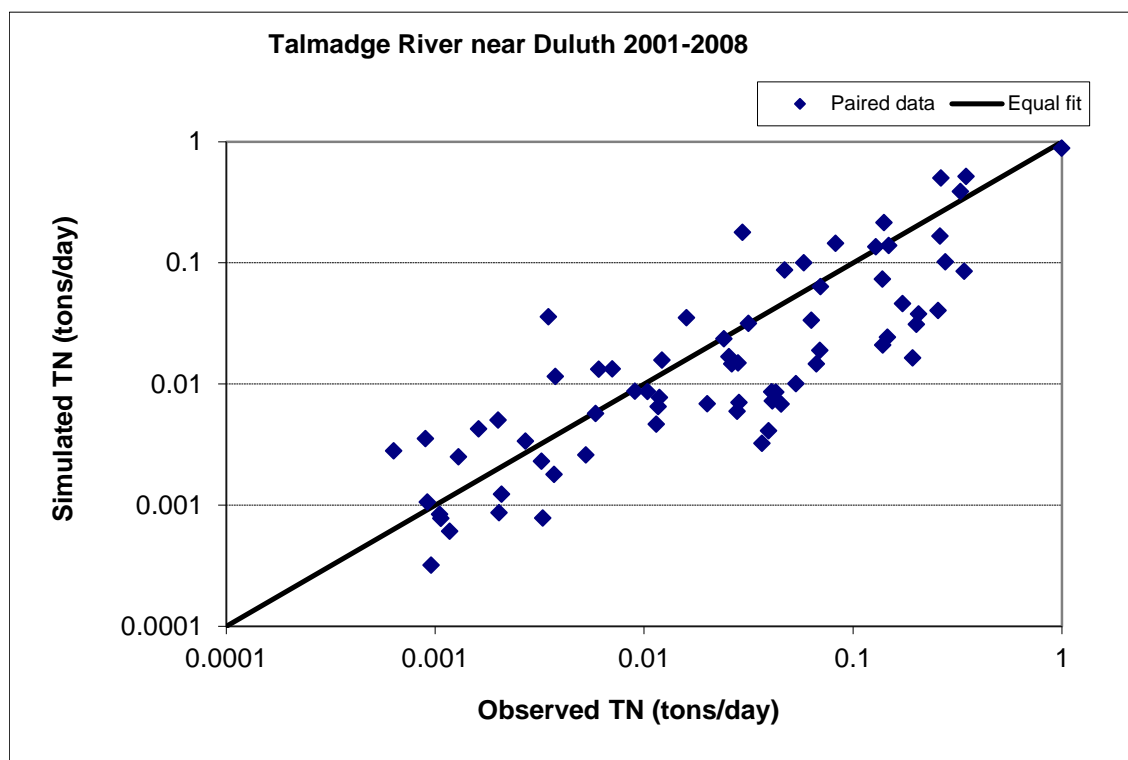


Figure 58. Paired simulated vs. observed Total Nitrogen (TN) load at Talmadge River near Duluth

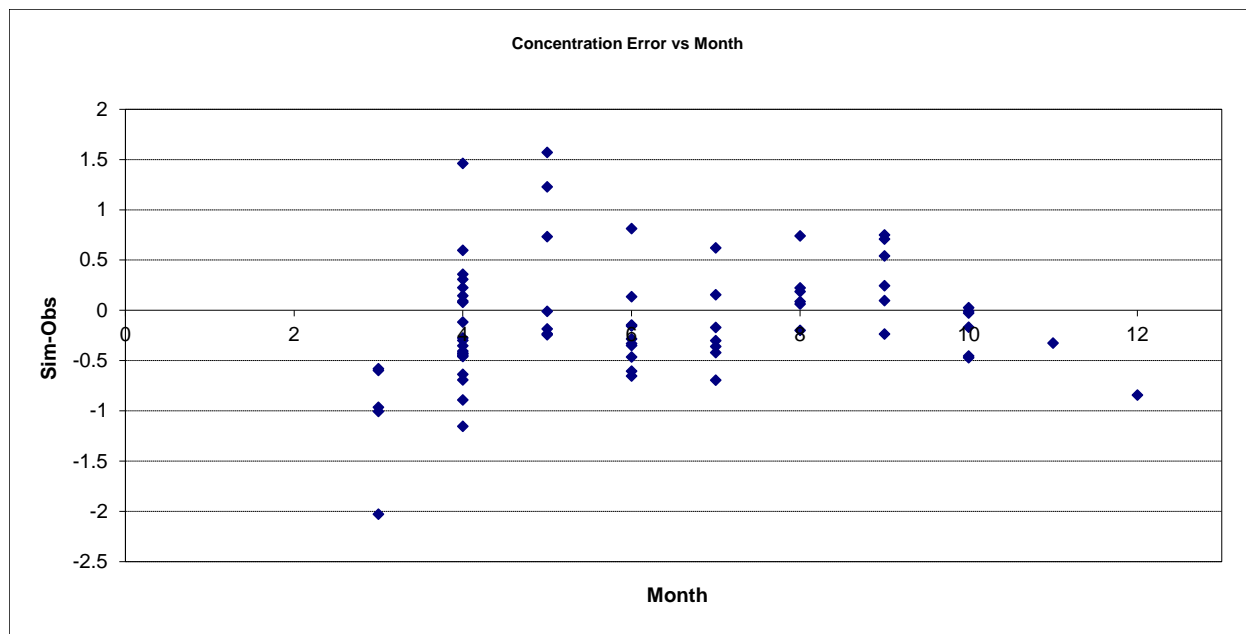


Figure 59. Residual (Simulated - Observed) vs. Month Total Nitrogen (TN) at Talmadge River near Duluth

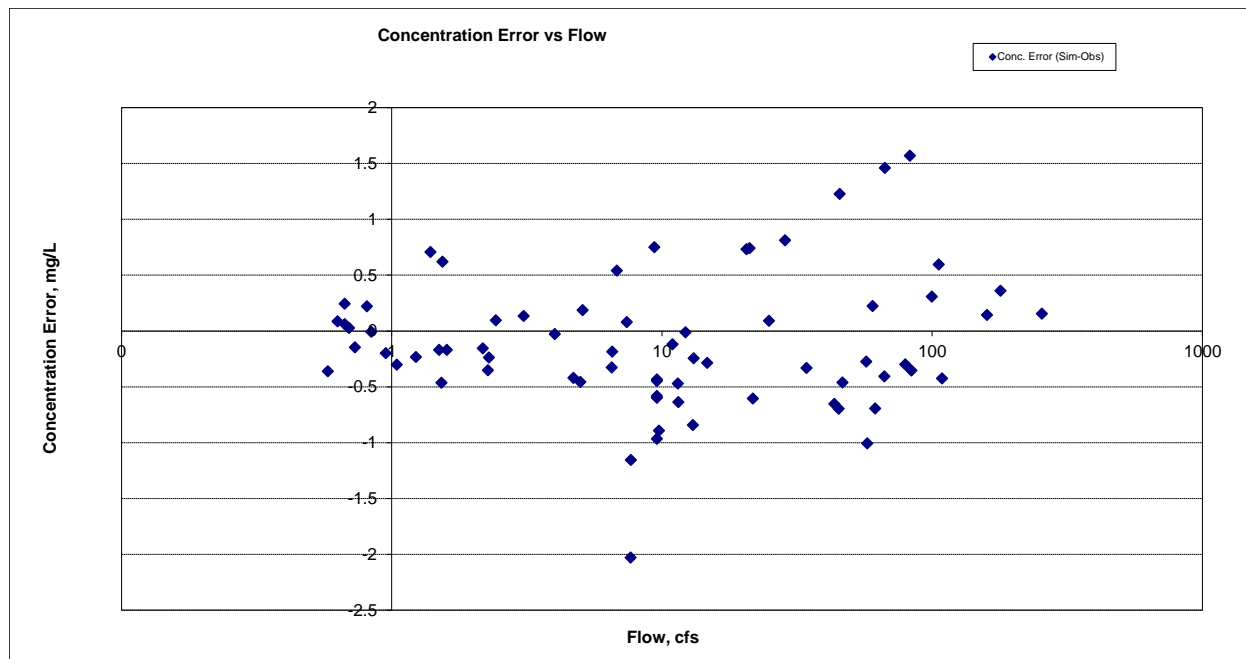


Figure 60. Residual (Simulated - Observed) vs. Flow Total Nitrogen (TN) at Talmadge River near Duluth

Soluble Reactive Phosphorus (SRP)

Table 13. Soluble Reactive Phosphorus (SRP) statistics

Count	65
Concentration Average Error	5.08%
Concentration Median Error	17.91%
Load Average Error	-25.02%
Load Median Error	-0.22%
Paired t concentration	0.95
Paired t load	0.45

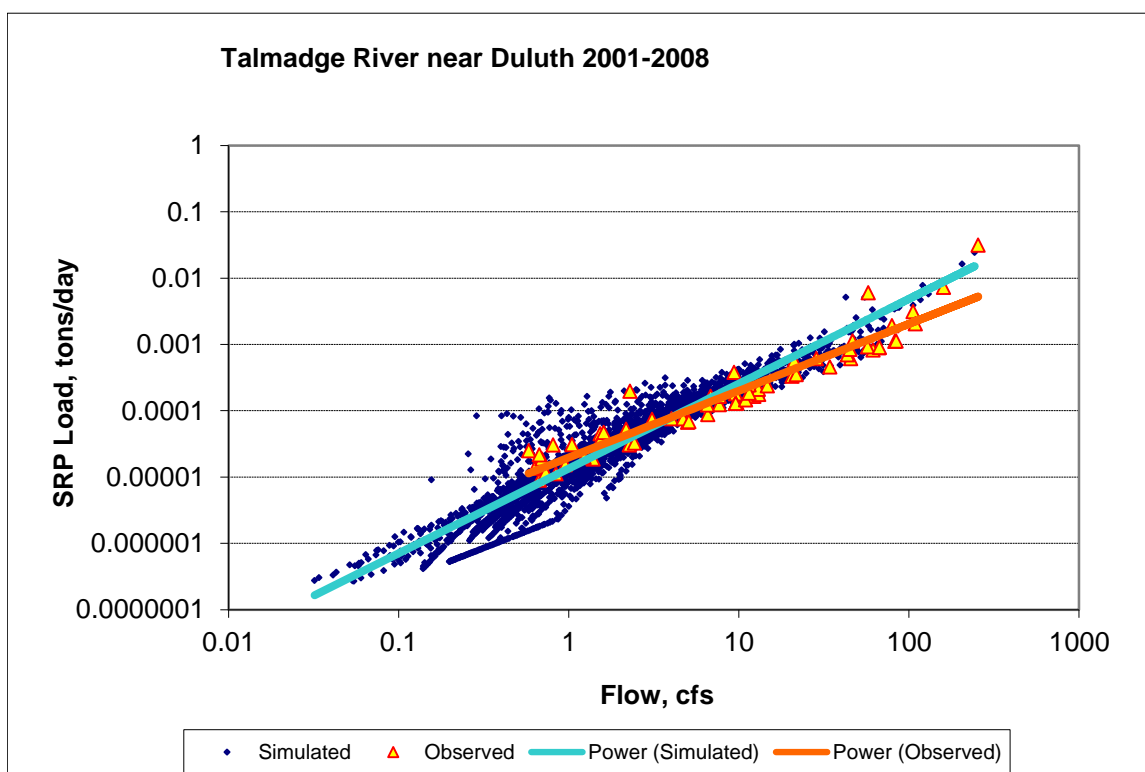


Figure 61. Power plot of simulated and observed Soluble Reactive Phosphorus (SRP) load vs flow at Talmadge River near Duluth

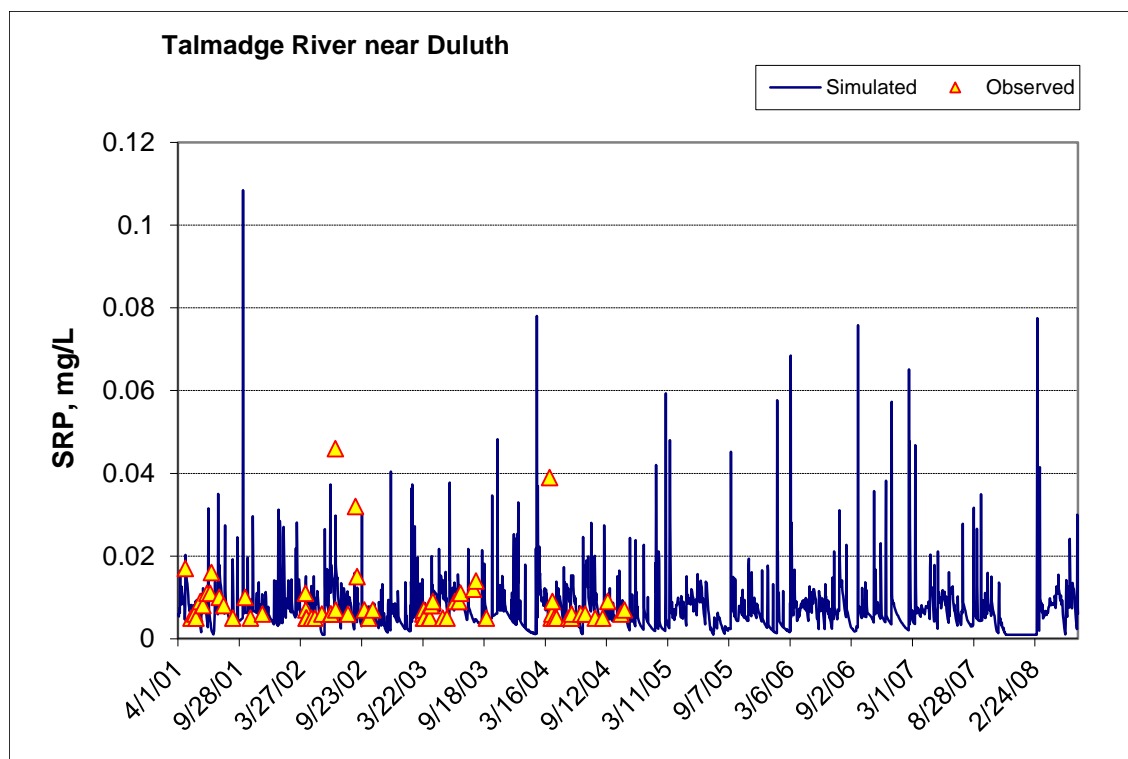


Figure 62. Time series of observed and simulated Soluble Reactive Phosphorus (SRP) concentration at Talmadge River near Duluth

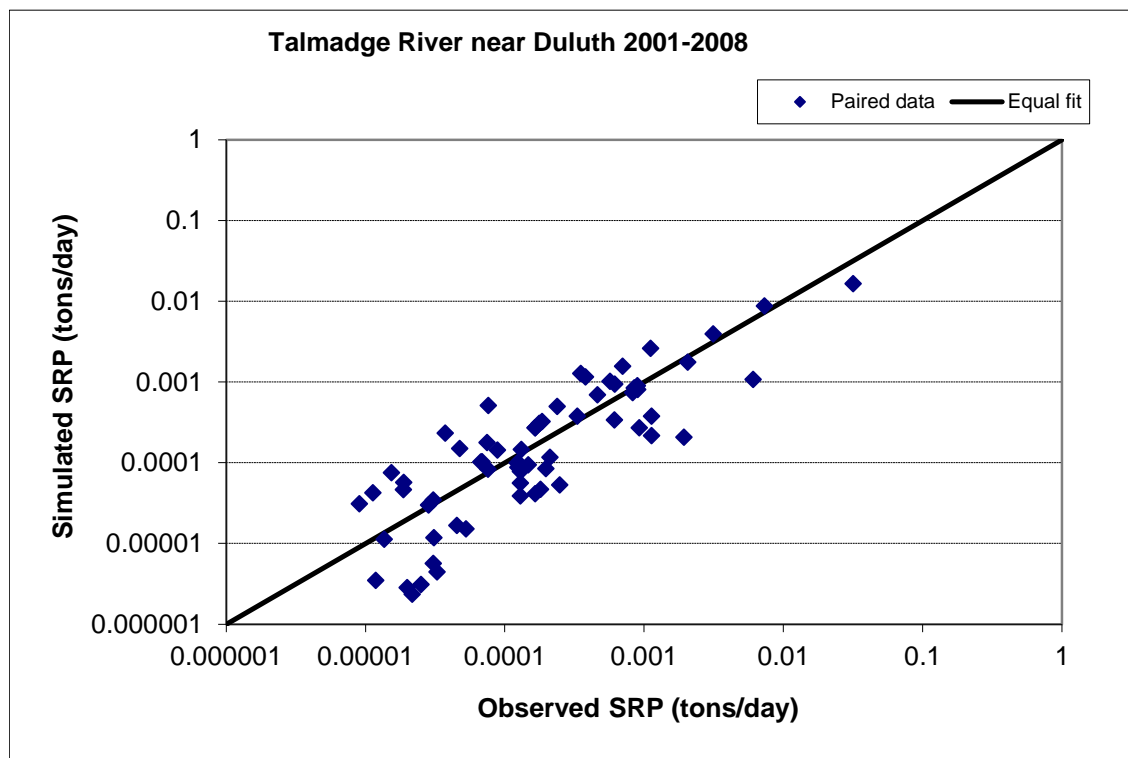


Figure 63. Paired simulated vs. observed Soluble Reactive Phosphorus (SRP) load at Talmadge River near Duluth

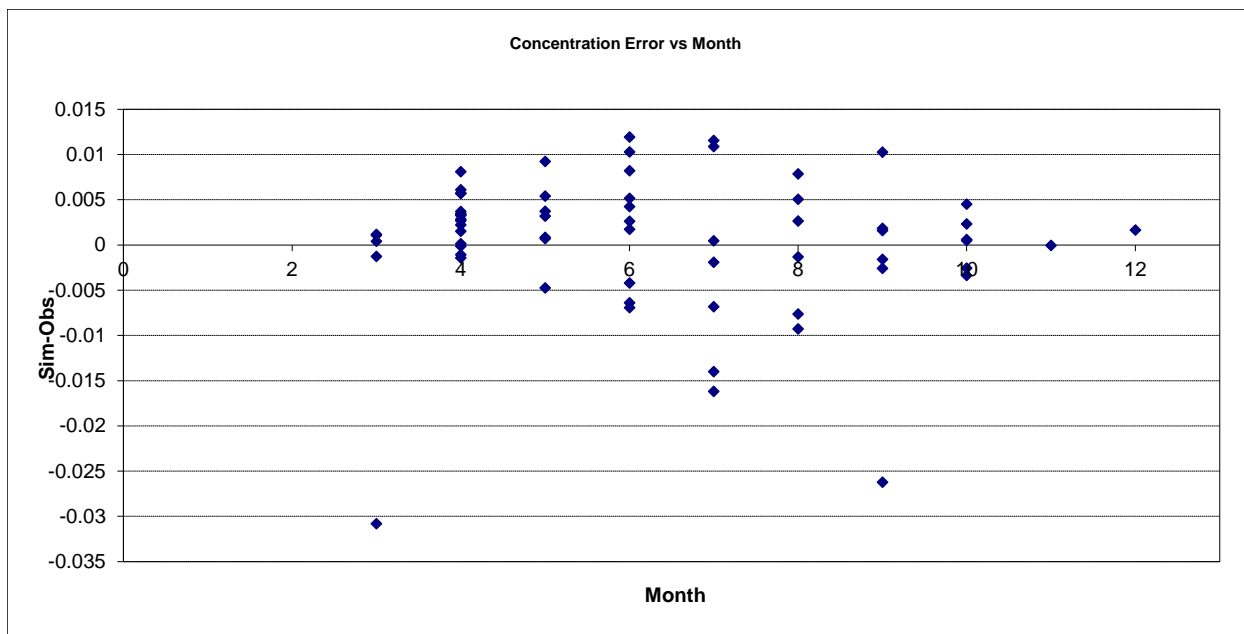


Figure 64. Residual (Simulated - Observed) vs. Month Soluble Reactive Phosphorus (SRP) at Talmadge River near Duluth

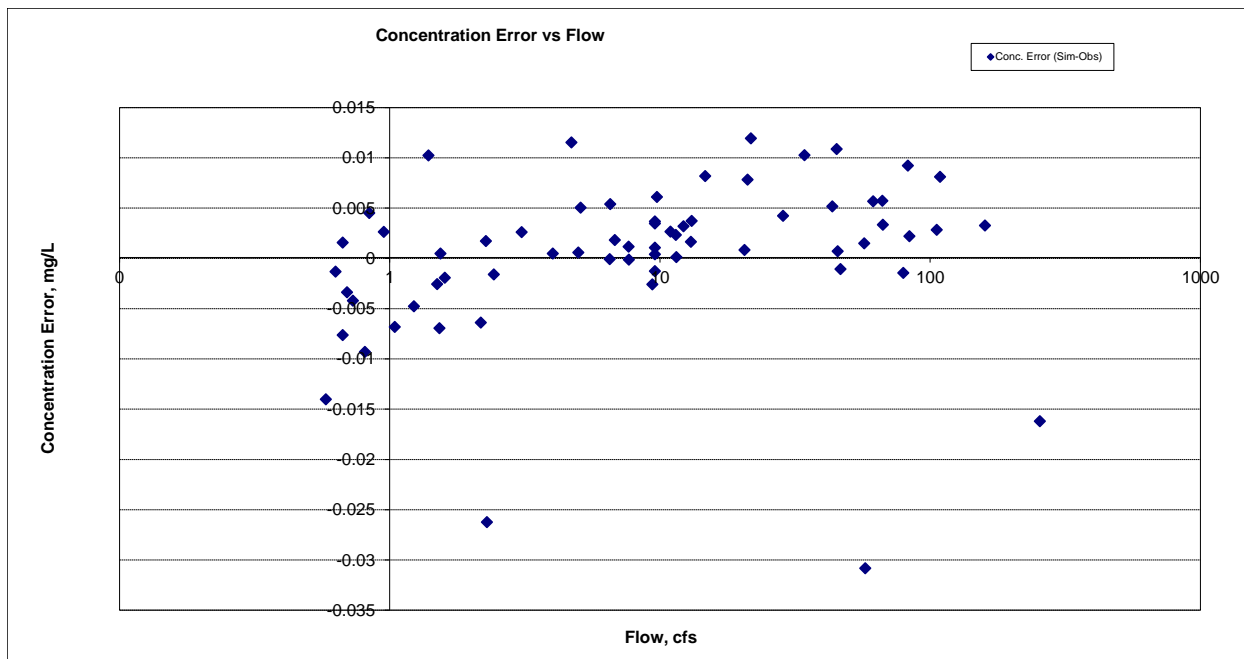


Figure 65. Residual (Simulated - Observed) vs. Flow Soluble Reactive Phosphorus (SRP) at Talmadge River near Duluth

Organic Phosphorus (OrgP)

Table 14. Organic Phosphorus (OrgP) statistics

Count	63
Concentration Average Error	-35.31%
Concentration Median Error	-28.81%
Load Average Error	-47.16%
Load Median Error	-1.52%
Paired t concentration	0.11
Paired t load	0.22

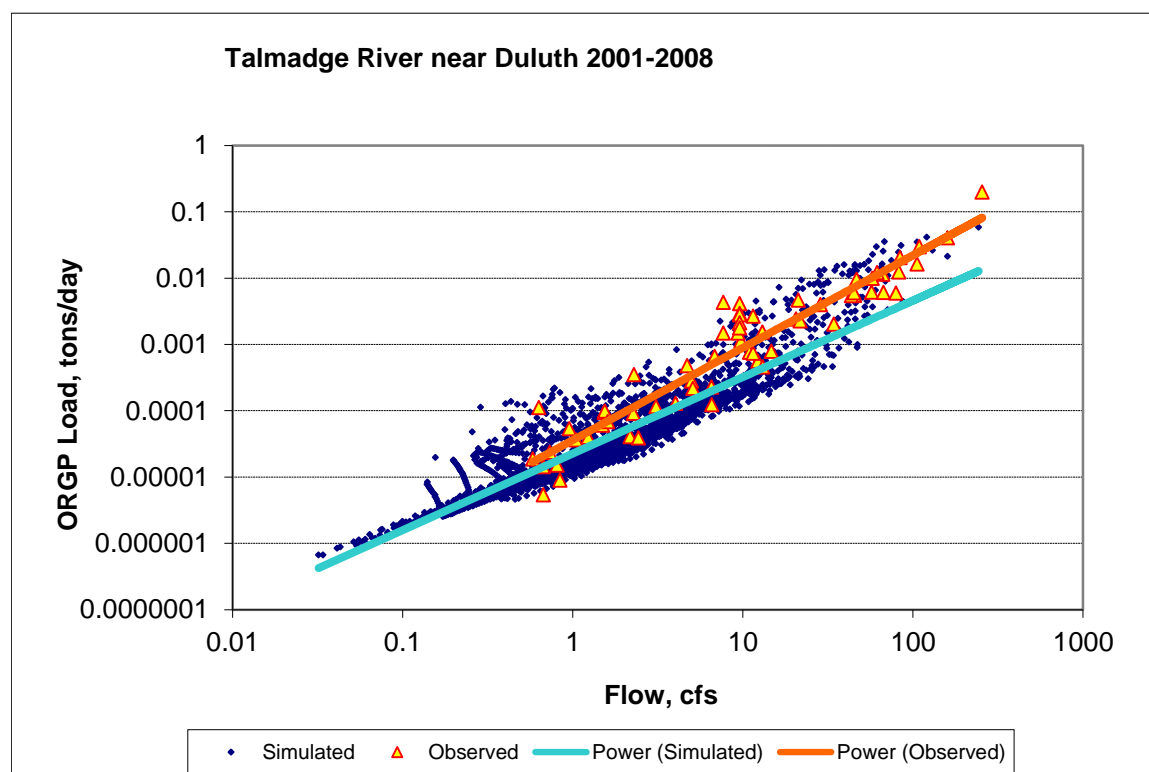


Figure 66. Power plot of simulated and observed Organic Phosphorus (OrgP) load vs flow at Talmadge River near Duluth

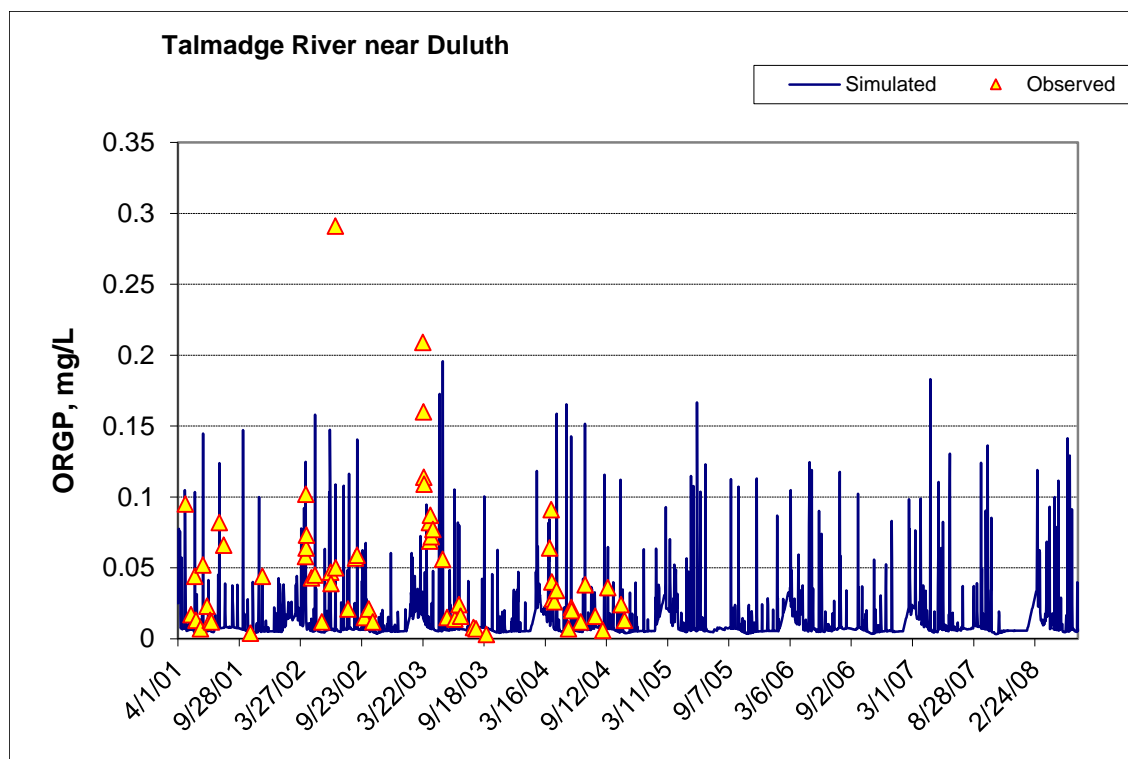


Figure 67. Time series of observed and simulated Organic Phosphorus (OrgP) concentration at Talmadge River near Duluth

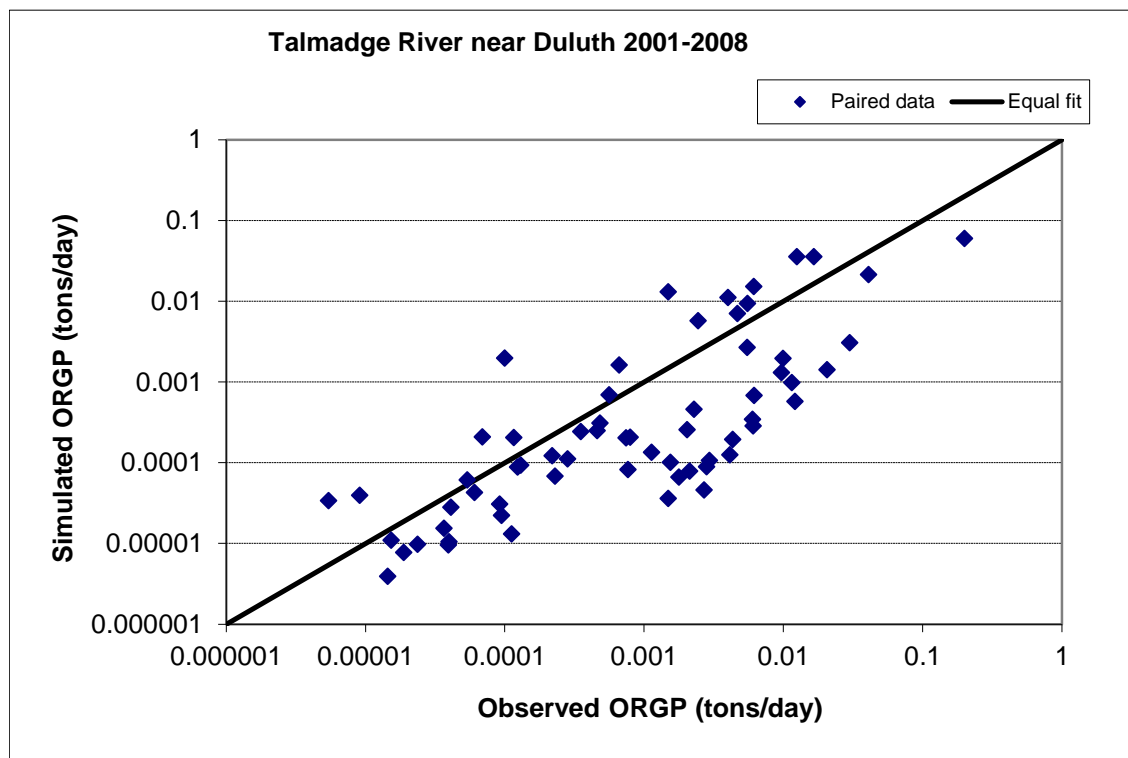


Figure 68. Paired simulated vs. observed Organic Phosphorus (OrgP) load at Talmadge River near Duluth

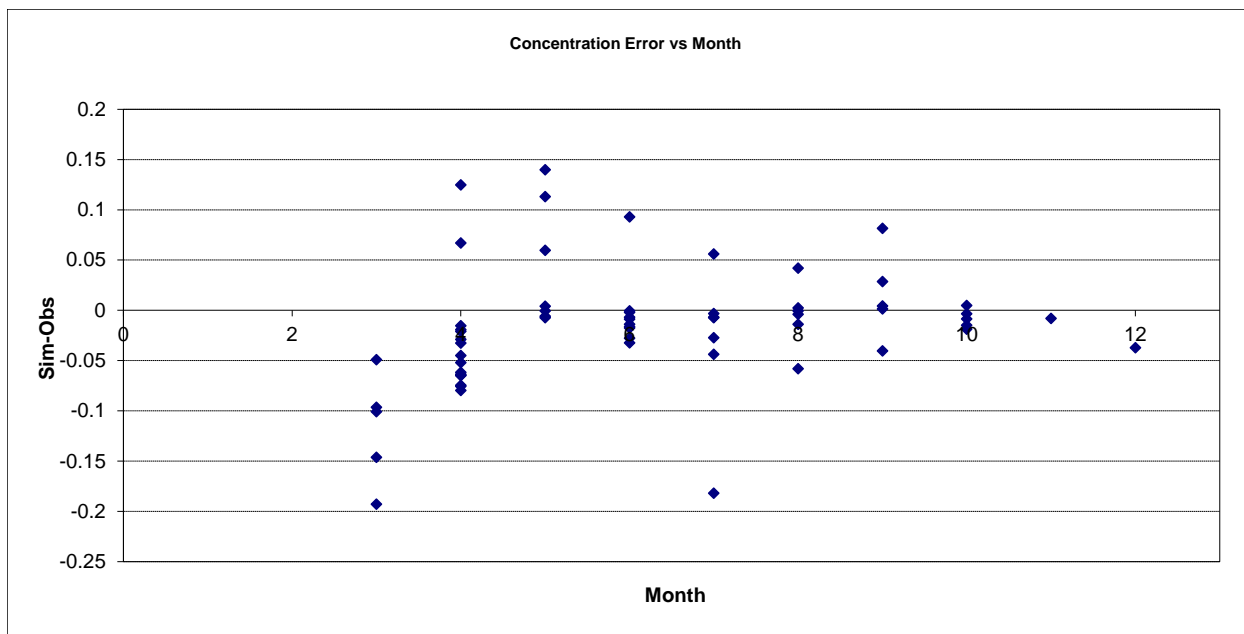


Figure 69. Residual (Simulated - Observed) vs. Month Organic Phosphorus (OrgP) at Talmadge River near Duluth

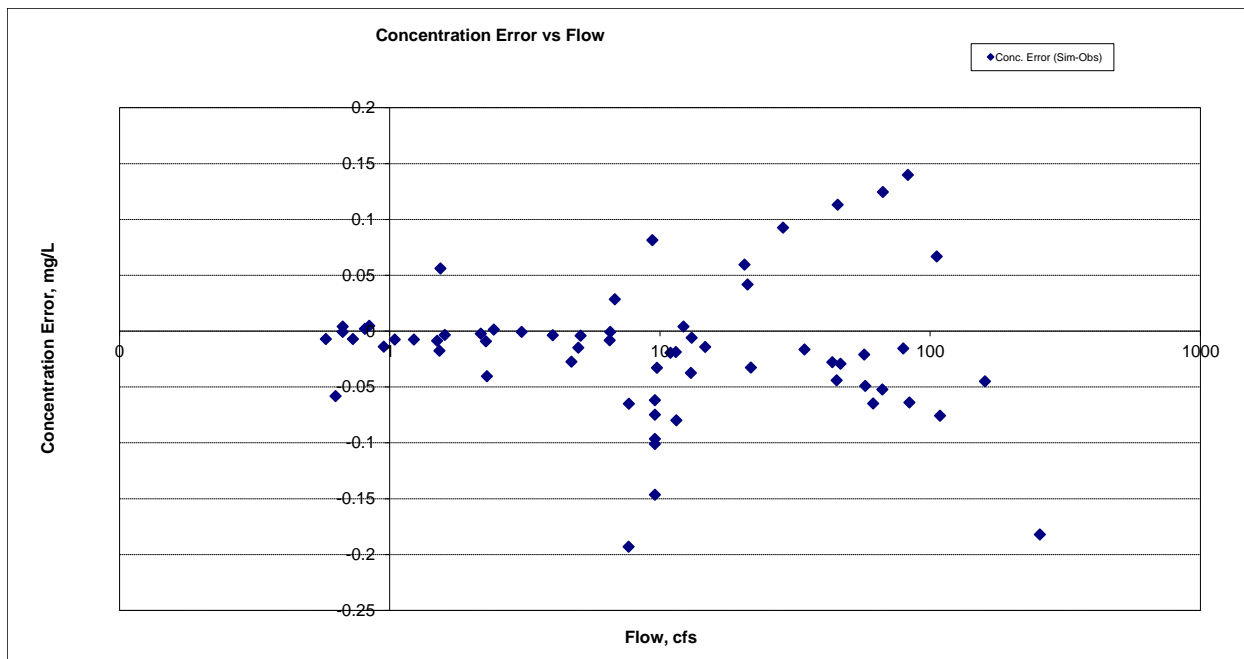


Figure 70. Residual (Simulated - Observed) vs. Flow Organic Phosphorus (OrgP) at Talmadge River near Duluth

Total Phosphorus (TP)

Table 15. Total Phosphorus (TP) statistics

Count	108
Concentration Average Error	-14.20%
Concentration Median Error	-20.08%
Load Average Error	-33.01%
Load Median Error	-1.49%
Paired t concentration	0.75
Paired t load	0.29

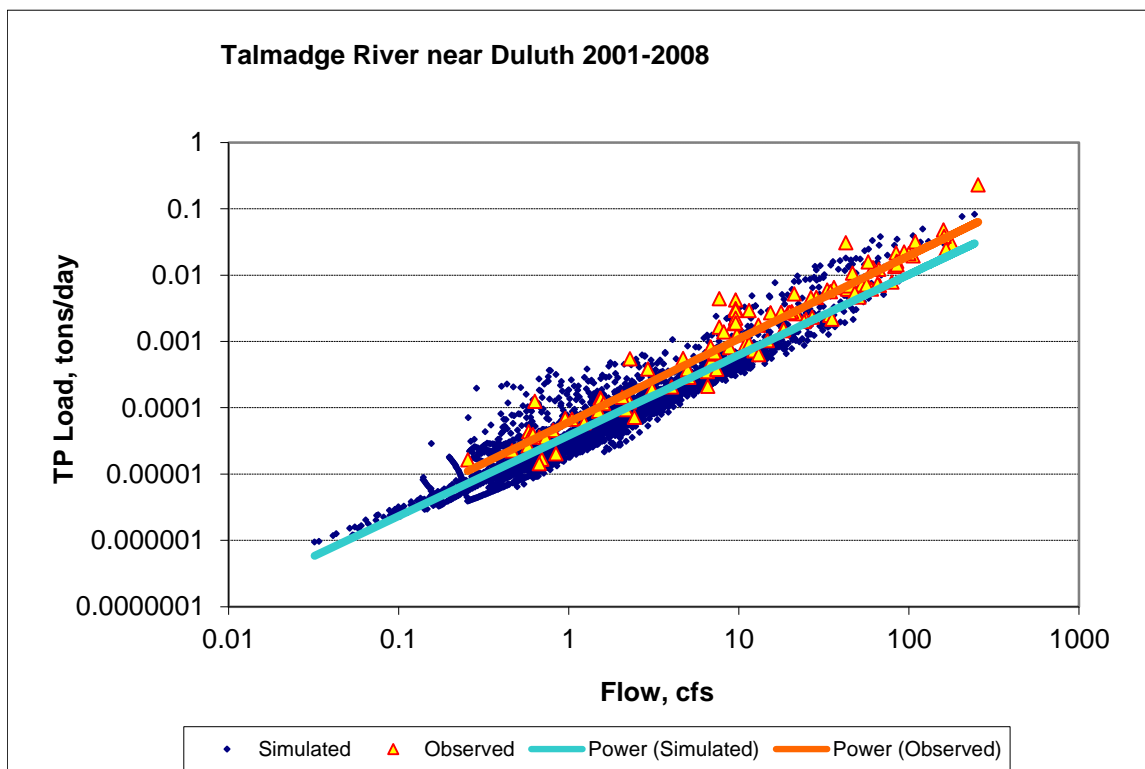


Figure 71. Power plot of simulated and observed Total Phosphorus (TP) load vs flow at Talmadge River near Duluth

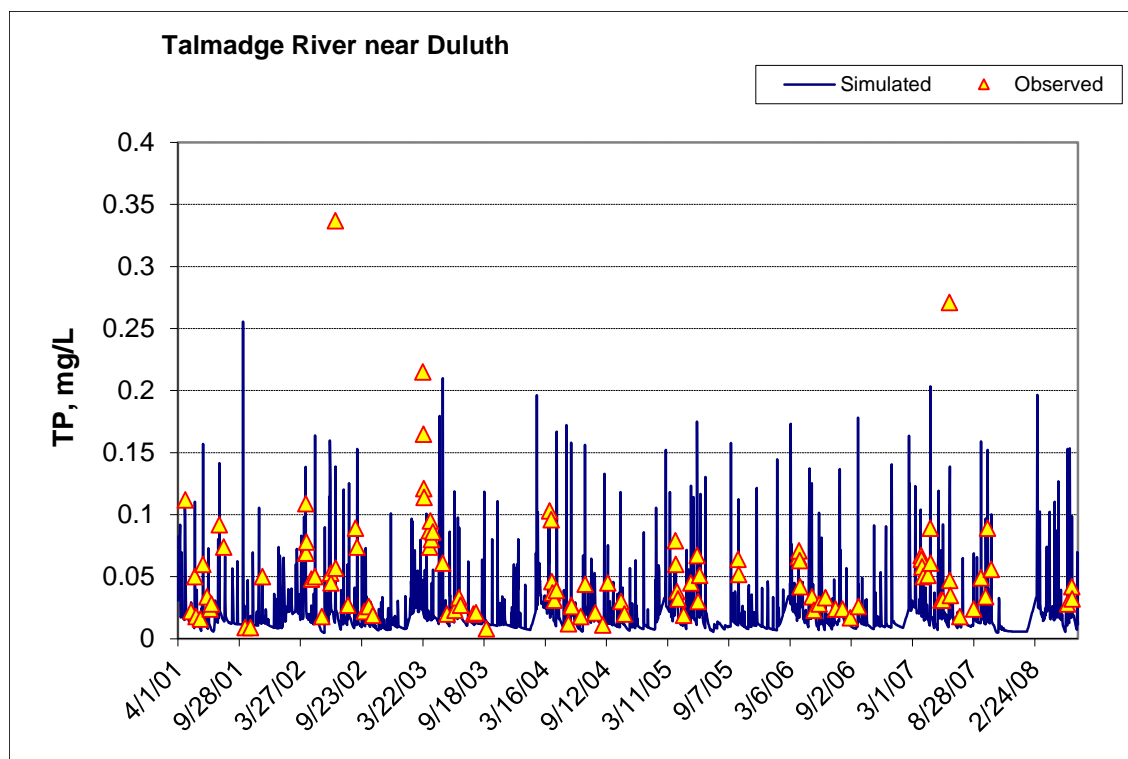


Figure 72. Time series of observed and simulated Total Phosphorus (TP) concentration at Talmadge River near Duluth

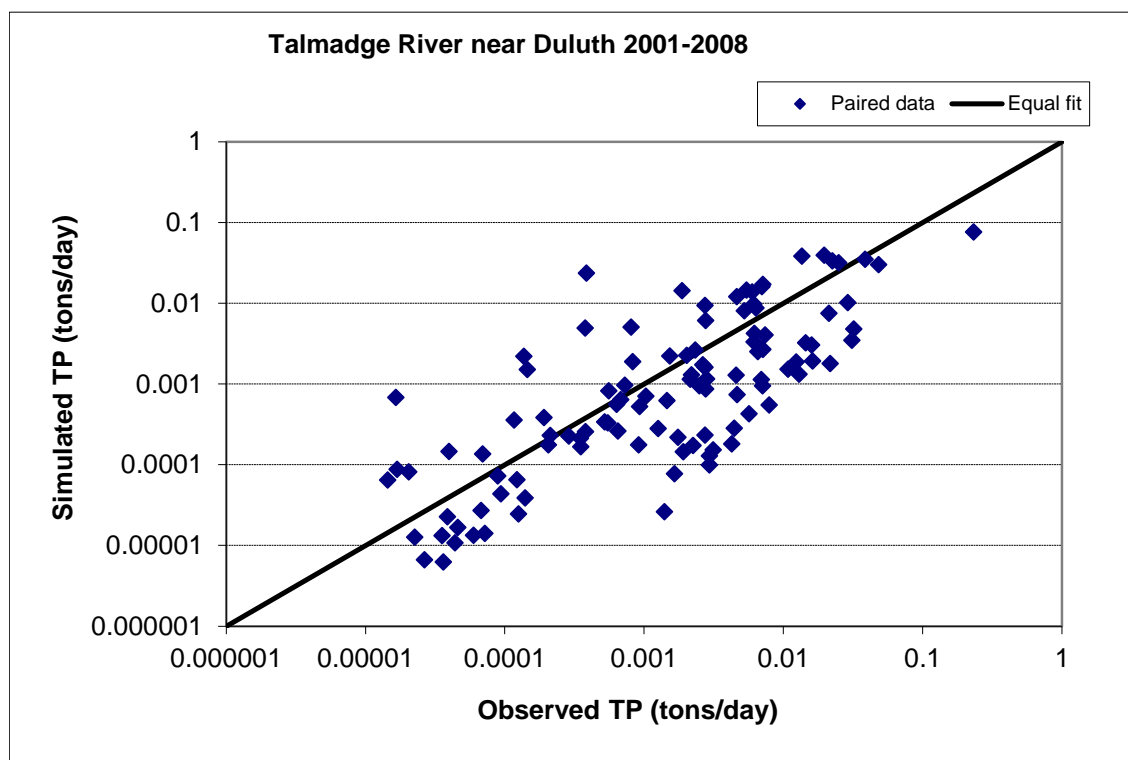


Figure 73. Paired simulated vs. observed Total Phosphorus (TP) load at Talmadge River near Duluth

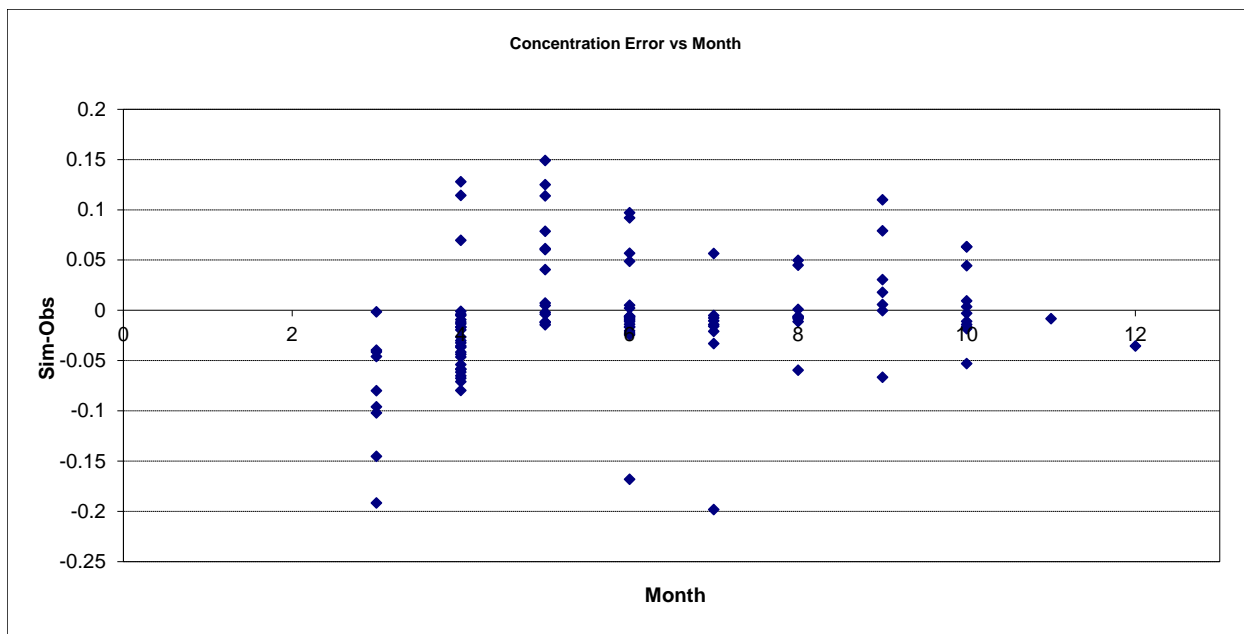


Figure 74. Residual (Simulated - Observed) vs. Month Total Phosphorus (TP) at Talmadge River near Duluth

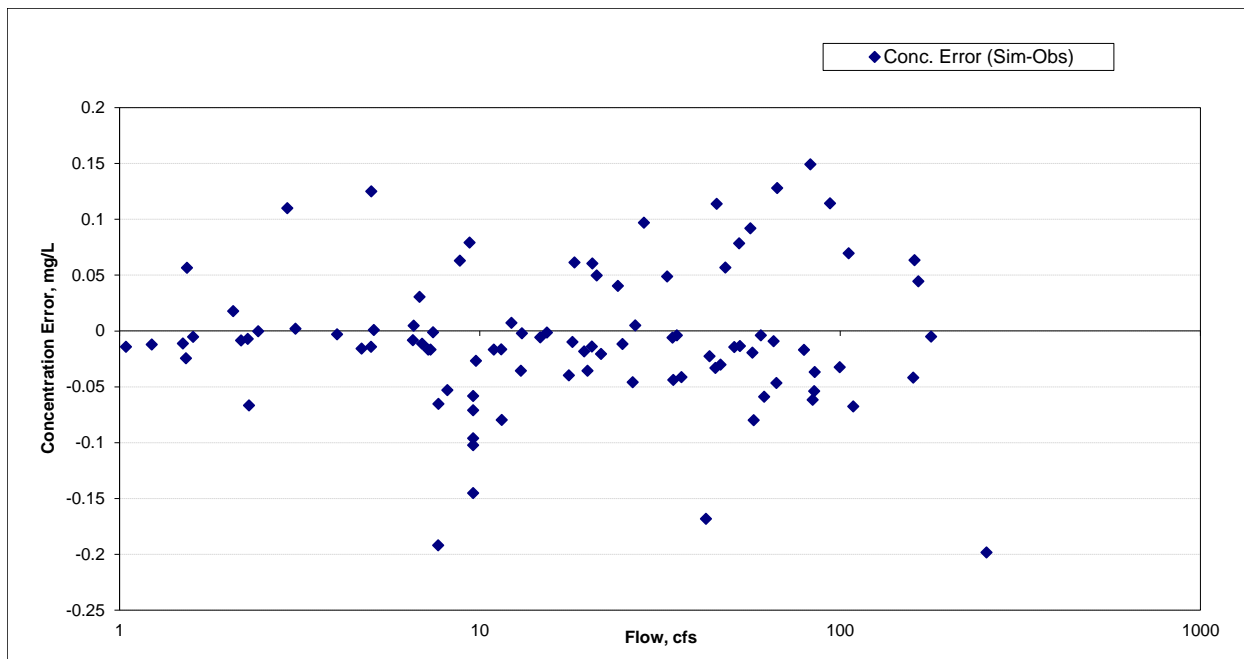


Figure 75. Residual (Simulated - Observed) vs. Flow Total Phosphorus (TP) at Talmadge River near Duluth

French River (EQUIS S001-754)

Total Suspended Solids (TSS)

Table 16. Total Suspended Solids (TSS) statistics

Count	114
Concentration Average Error	39.18%
Concentration Median Error	10.99%
Load Average Error	8.59%
Load Median Error	0.54%
Paired t concentration	0.12
Paired t load	0.63

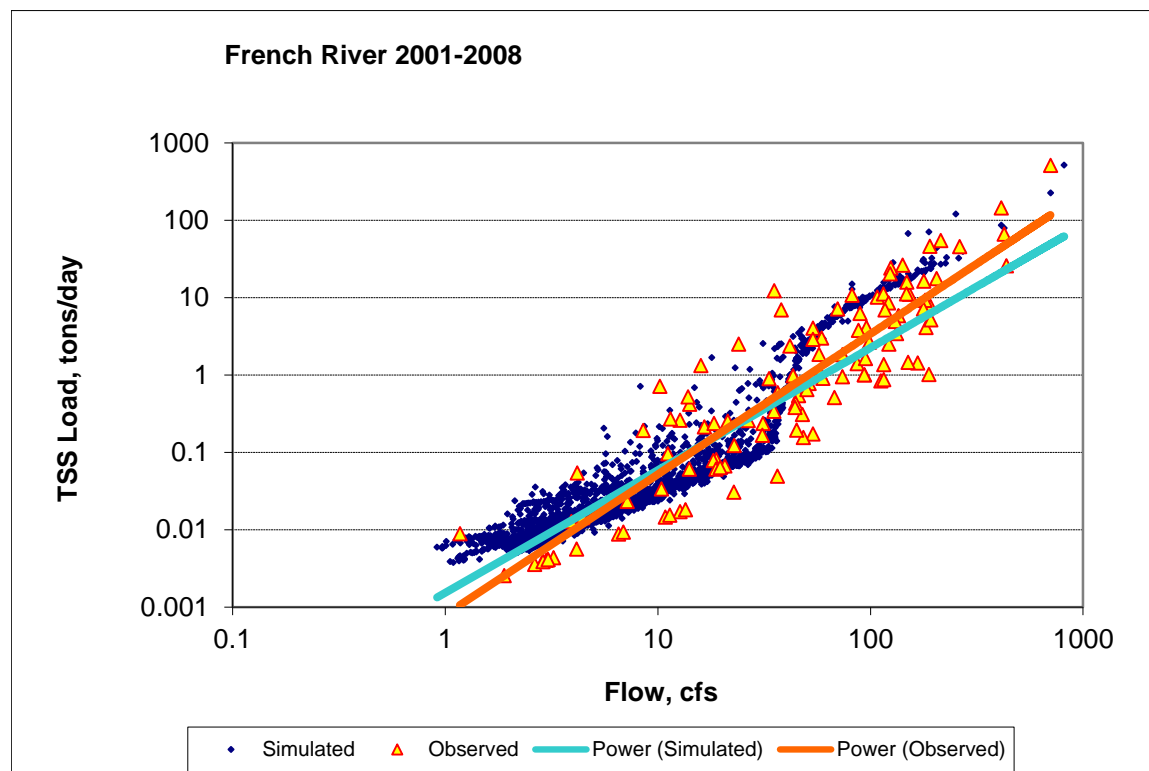


Figure 76. Power plot of simulated and observed Total Suspended Solids (TSS) load vs flow at French River

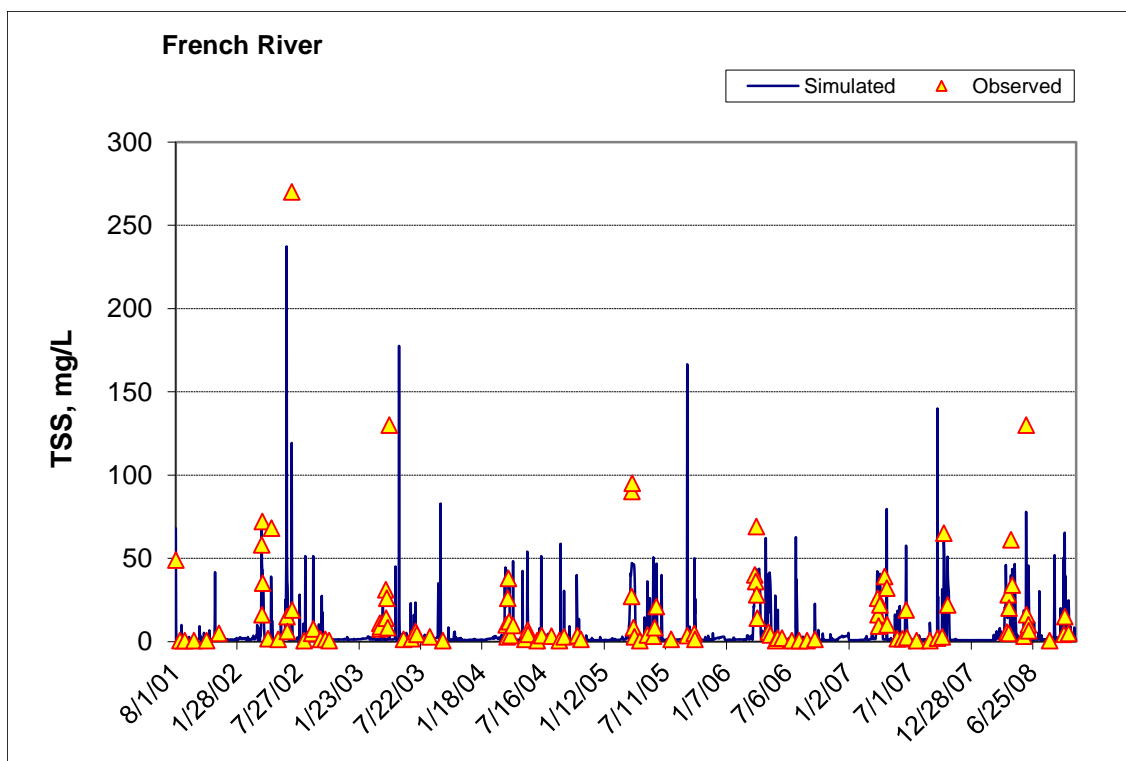


Figure 77. Time series of observed and simulated Total Suspended Solids (TSS) concentration at French River

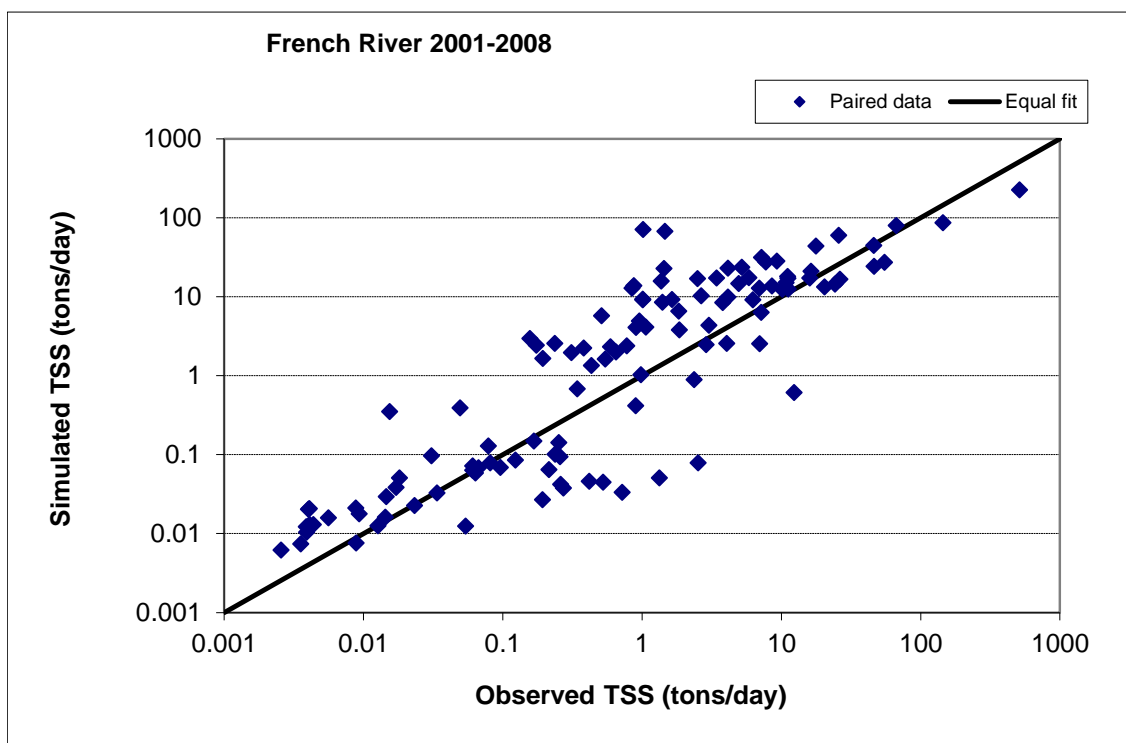


Figure 78. Paired simulated vs. observed Total Suspended Solids (TSS) load at French River

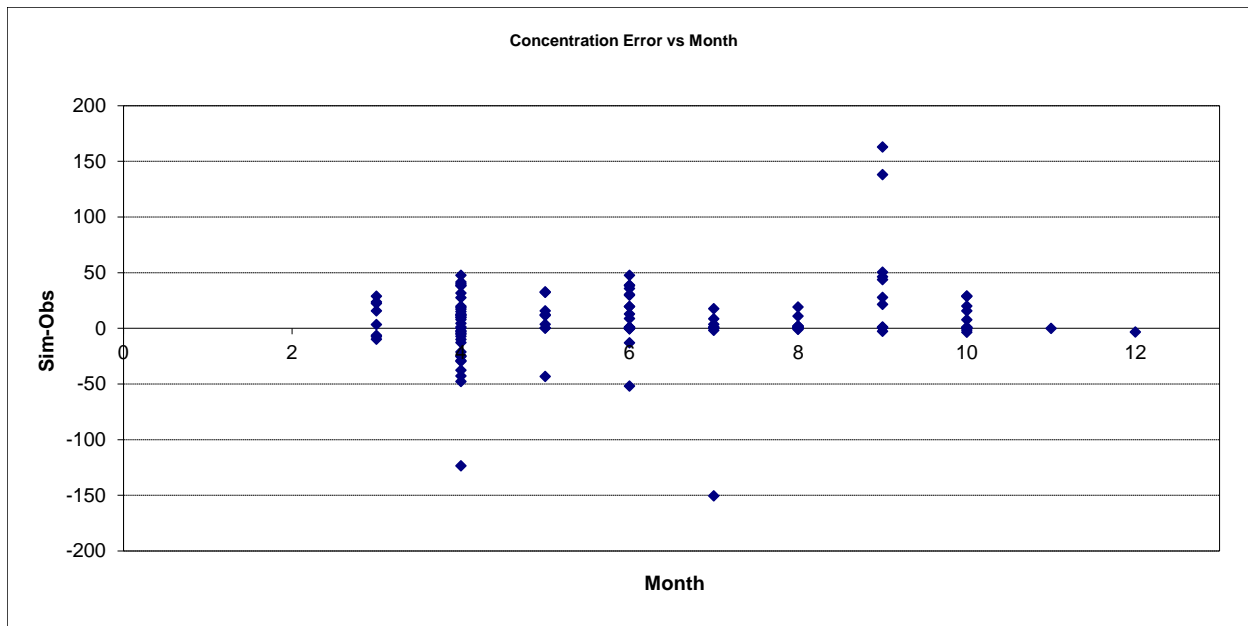


Figure 79. Residual (Simulated - Observed) vs. Month Total Suspended Solids (TSS) at French River

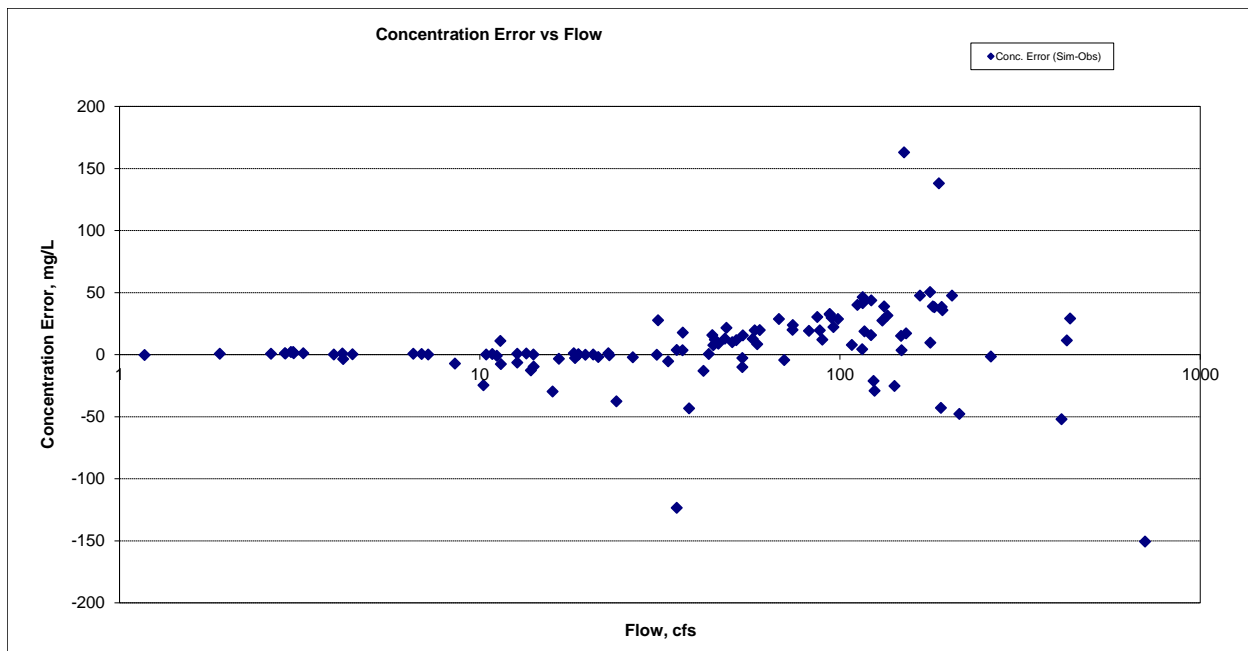


Figure 80. Residual (Simulated - Observed) vs. Flow Total Suspended Solids (TSS) at French River

Nitrite+ Nitrate Nitrogen (NOx)

Table 17. Nitrite+ Nitrate Nitrogen (NOx) statistics

Count	61
Concentration Average Error	-5.15%
Concentration Median Error	-3.46%
Load Average Error	-13.54%
Load Median Error	-0.68%
Paired t concentration	0.90
Paired t load	0.59

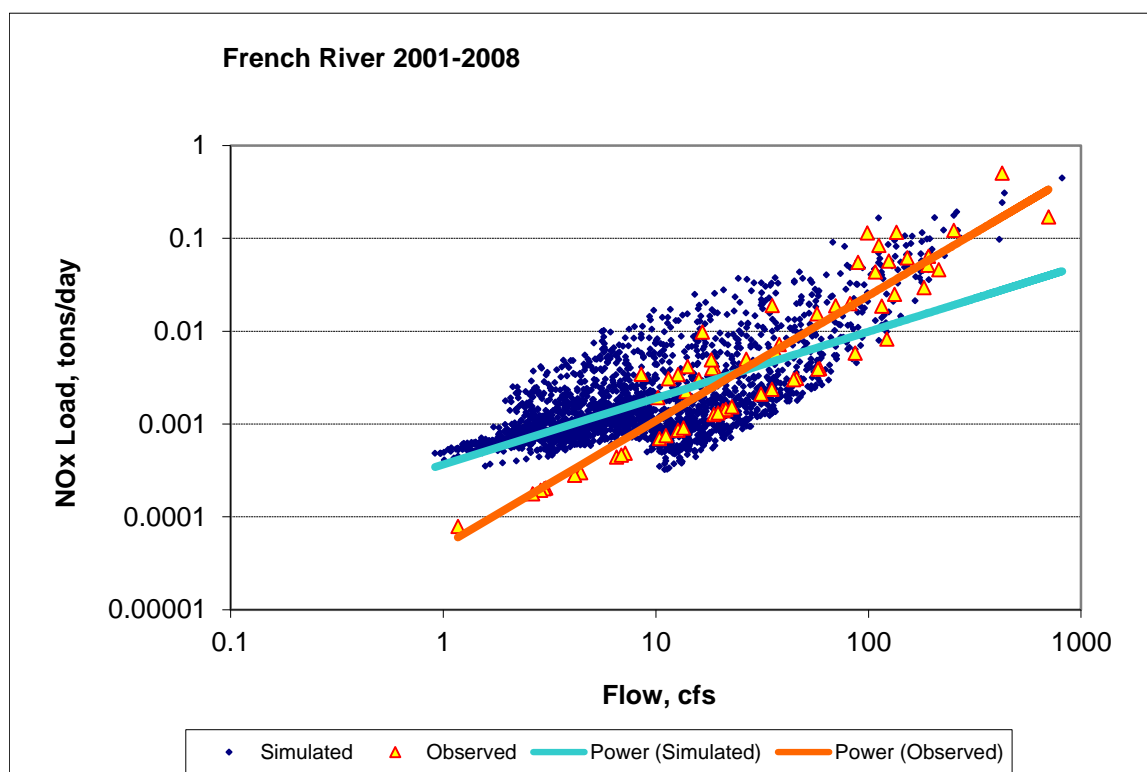


Figure 81. Power plot of simulated and observed Nitrite+ Nitrate Nitrogen (NOx) load vs flow at French River

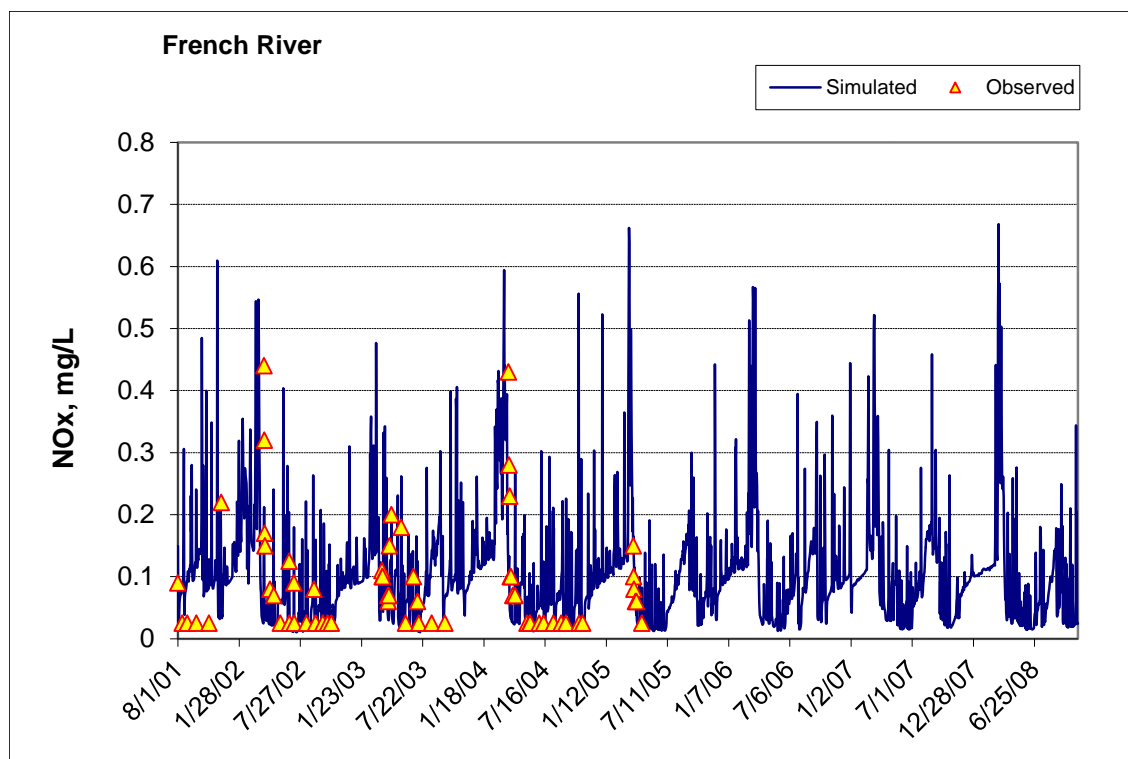


Figure 82. Time series of observed and simulated Nitrite+ Nitrate Nitrogen (NOx) concentration at French River

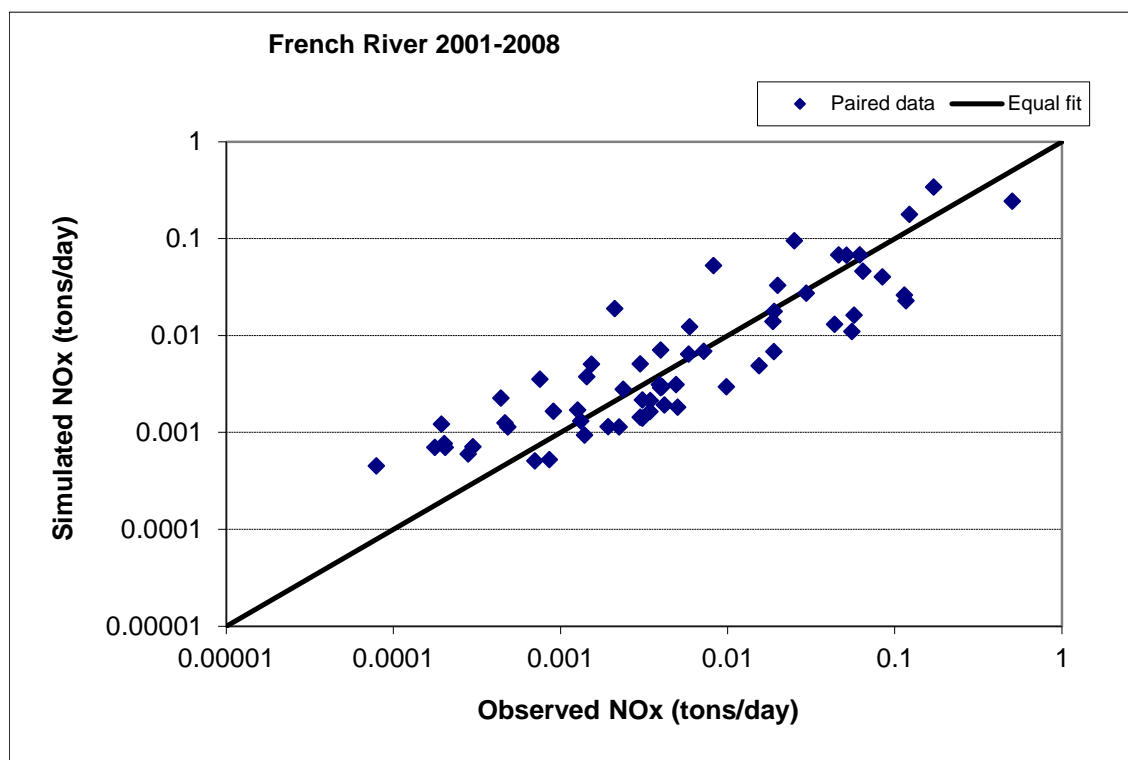


Figure 83. Paired simulated vs. observed Nitrite+ Nitrate Nitrogen (NOx) load at French River

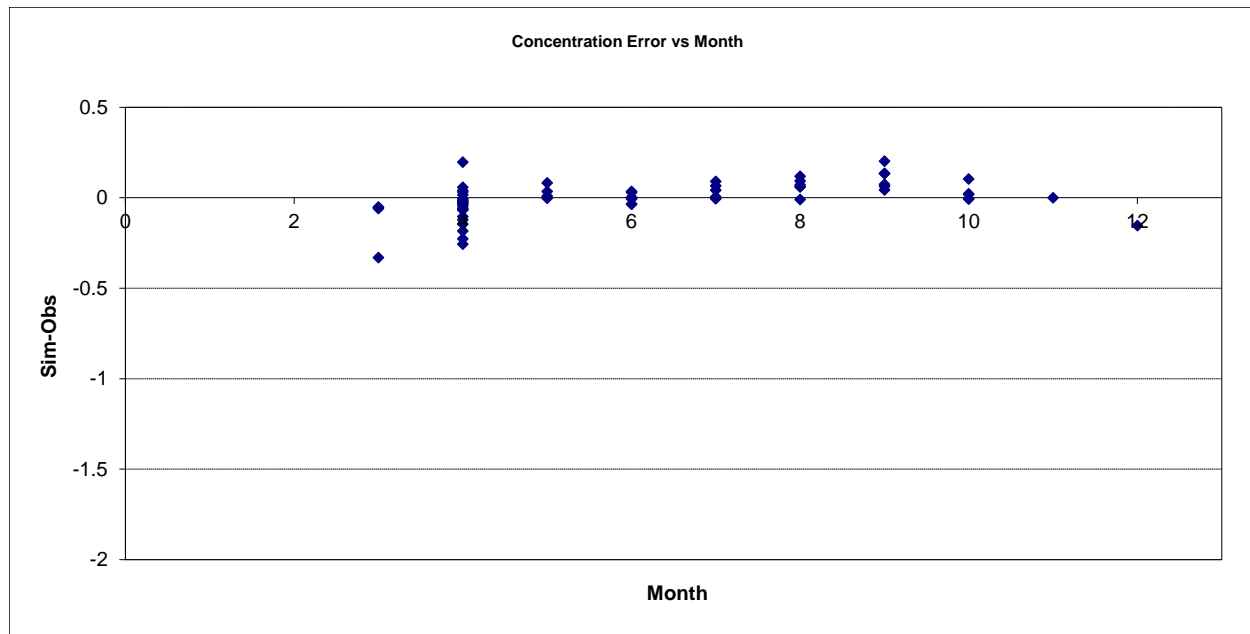


Figure 84. Residual (Simulated - Observed) vs. Month Nitrite+ Nitrate Nitrogen (NOx) at French River

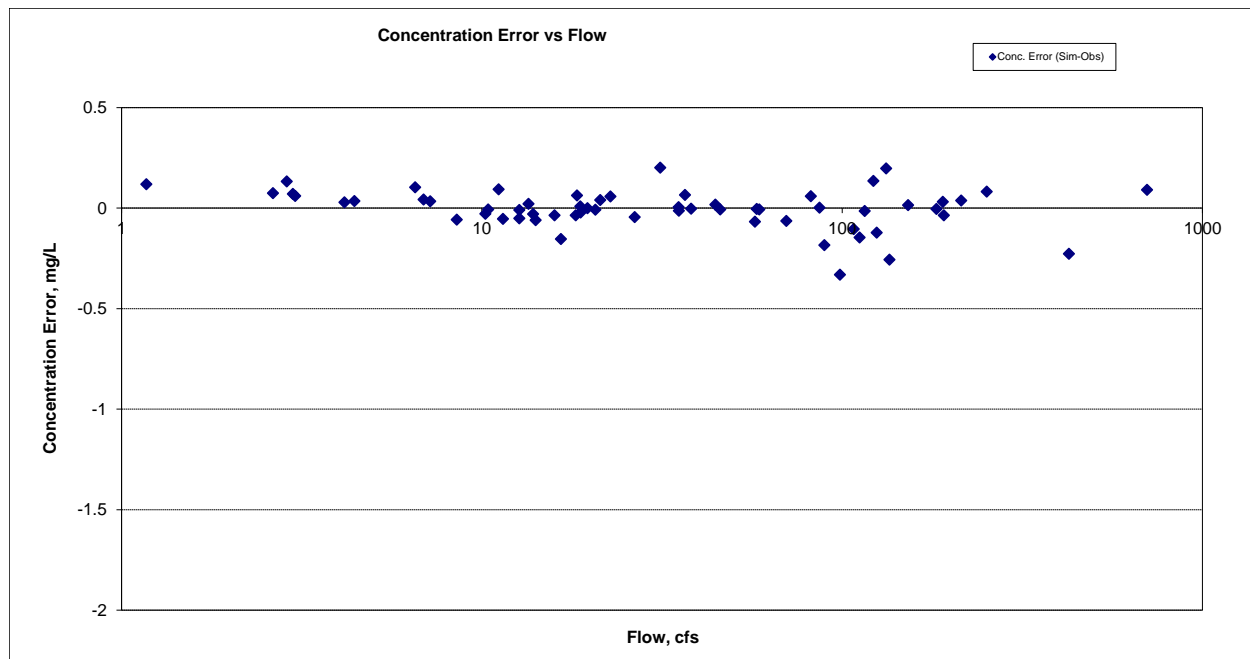


Figure 85. Residual (Simulated - Observed) vs. Flow Nitrite+ Nitrate Nitrogen (NOx) at French River

Total Phosphorus (TP)

Table 18. Total Phosphorus (TP) statistics

Count	114
Concentration Average Error	35.69%
Concentration Median Error	4.00%
Load Average Error	15.10%
Load Median Error	0.74%
Paired t concentration	0.07
Paired t load	0.57

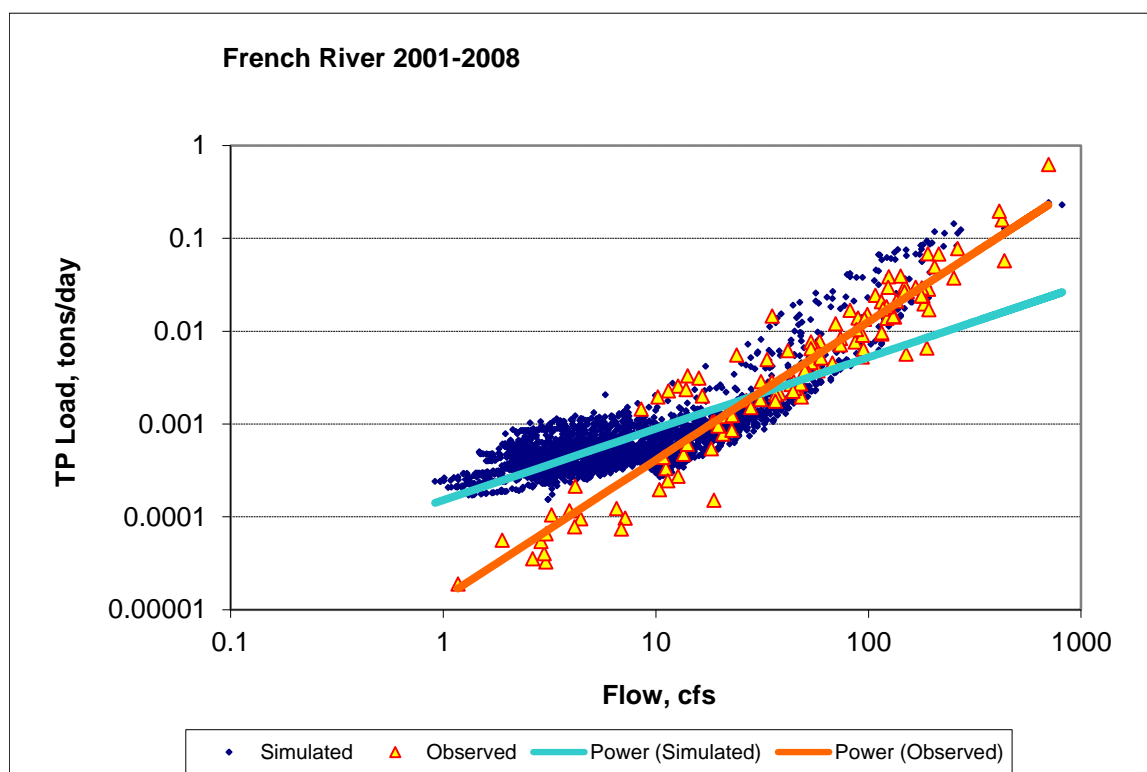


Figure 86. Power plot of simulated and observed Total Phosphorus (TP) load vs flow at French River

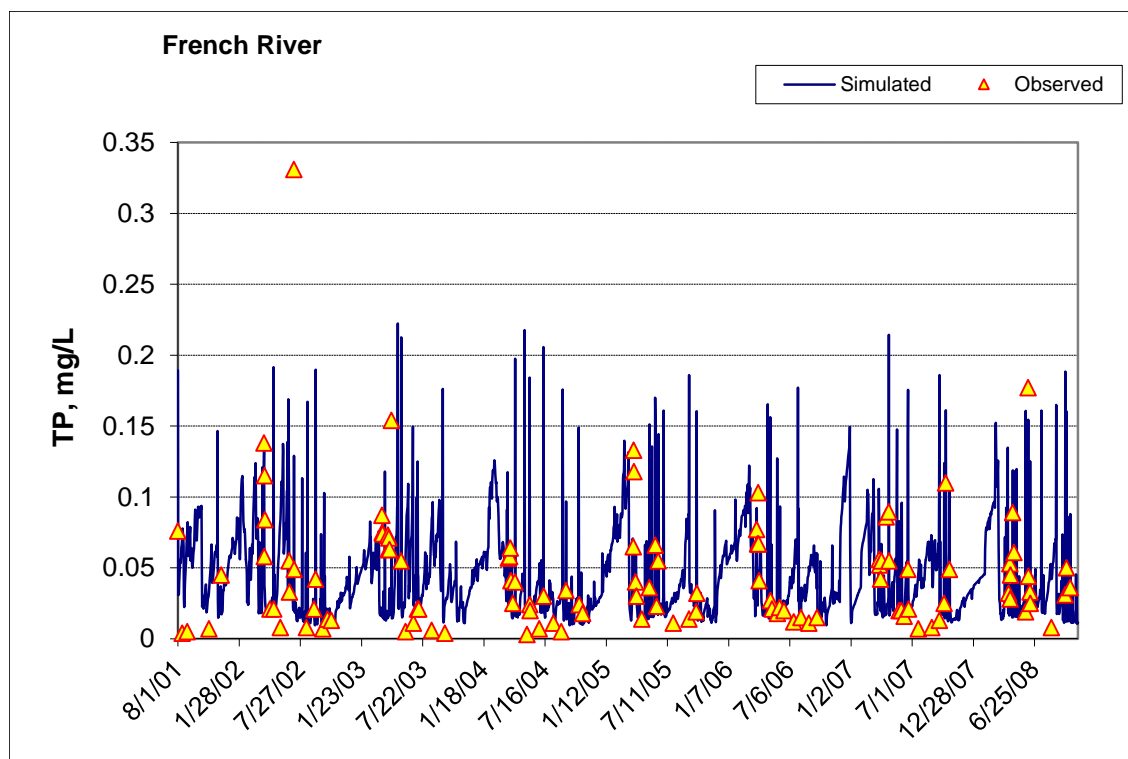


Figure 87. Time series of observed and simulated Total Phosphorus (TP) concentration at French River

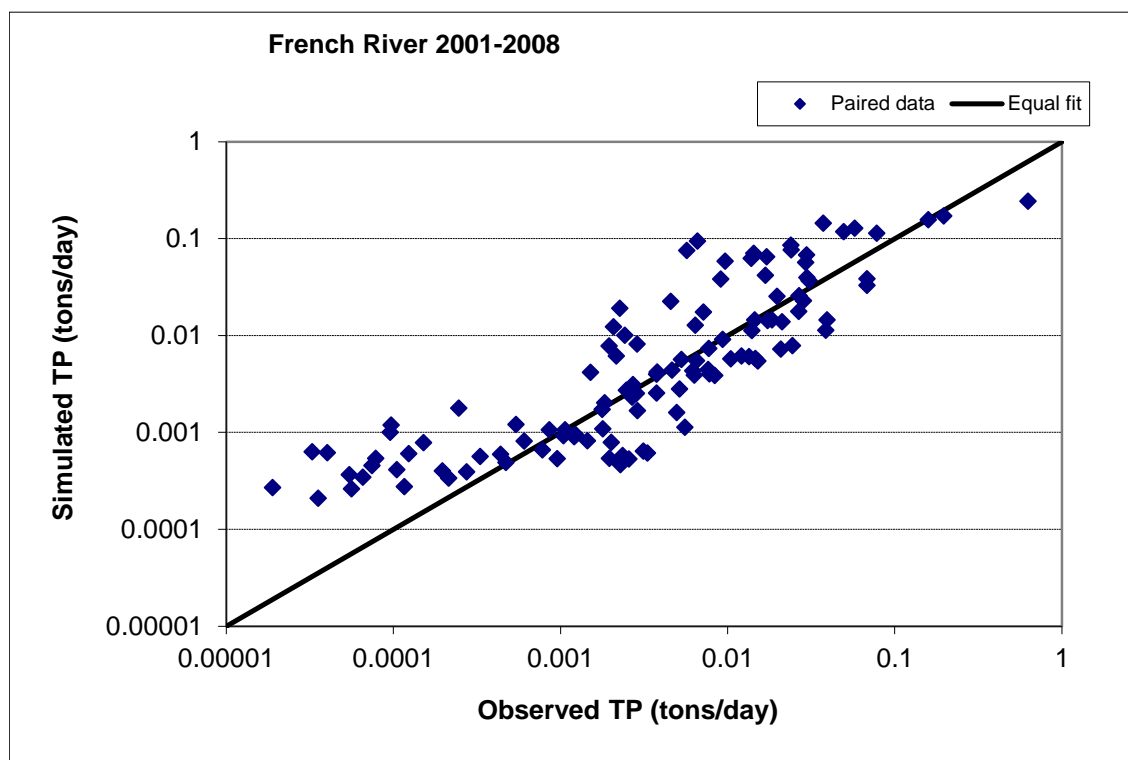


Figure 88. Paired simulated vs. observed Total Phosphorus (TP) load at French River

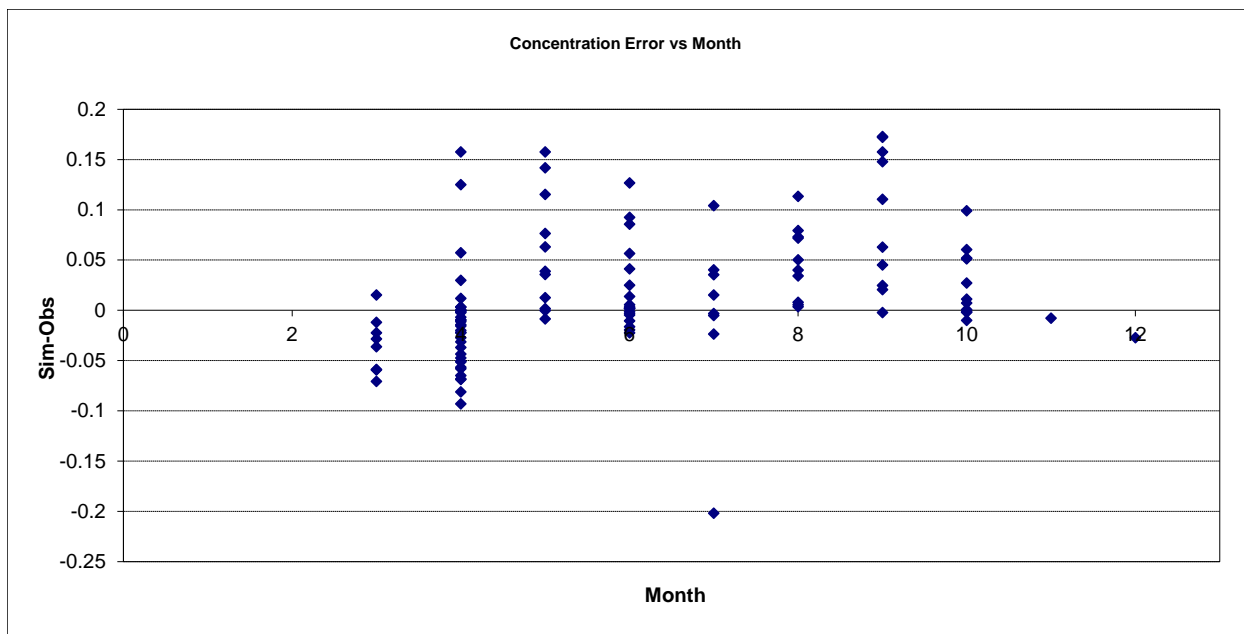


Figure 89. Residual (Simulated - Observed) vs. Month Total Phosphorus (TP) at French River

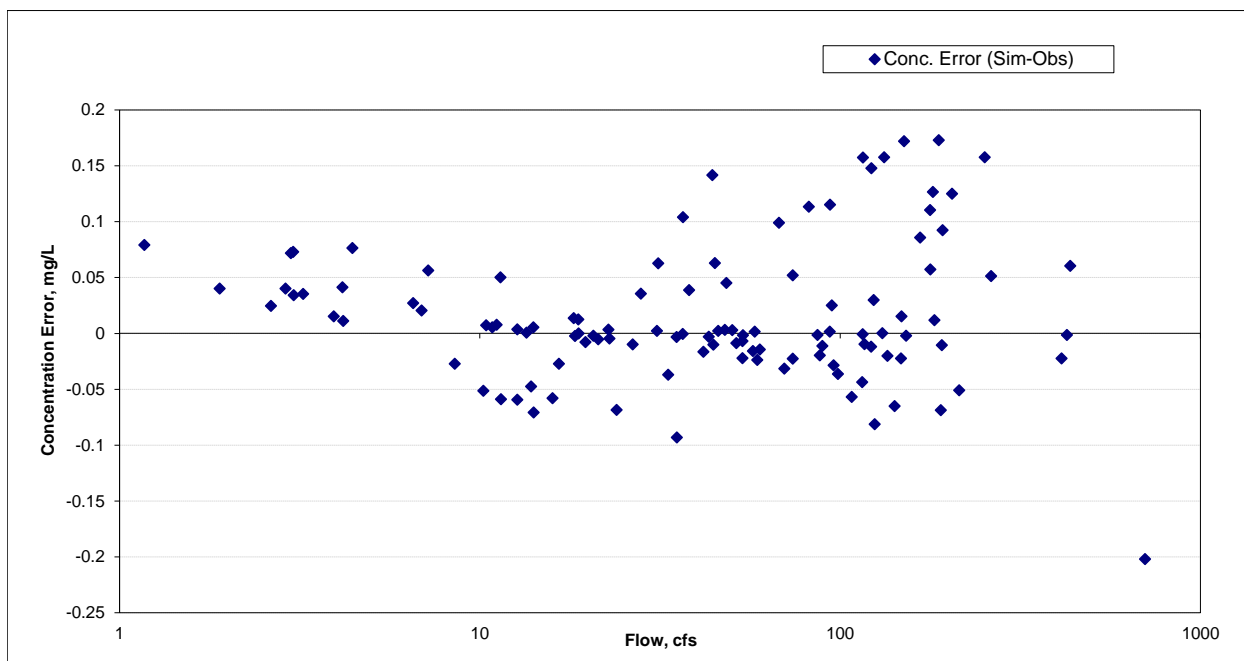


Figure 90. Residual (Simulated - Observed) vs. Flow Total Phosphorus (TP) at French River

Sucker River near Palmers (HYDSTRA 02031001)

Total Suspended Solids (TSS)

Table 19. Total Suspended Solids (TSS) statistics

Count	231
Concentration Average Error	-11.69%
Concentration Median Error	-2.83%
Load Average Error	-29.17%
Load Median Error	-0.13%
Paired t concentration	0.78
Paired t load	0.33

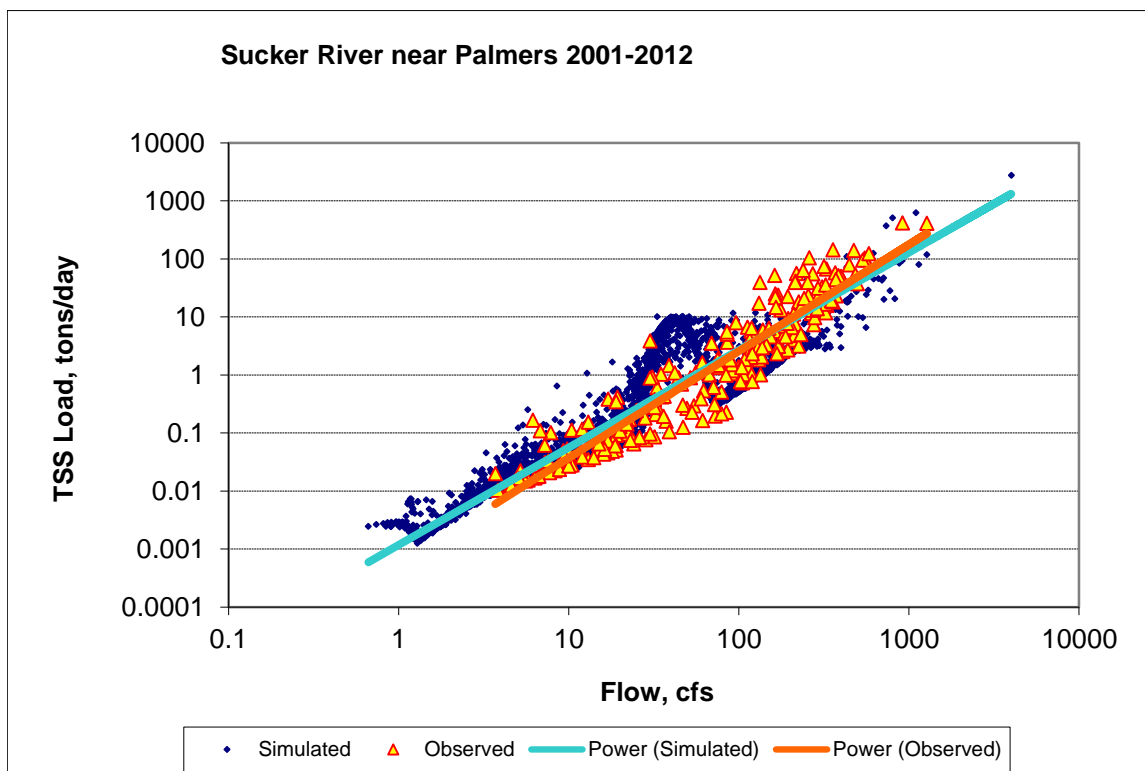


Figure 91. Power plot of simulated and observed Total Suspended Solids (TSS) load vs flow at Sucker River near Palmers

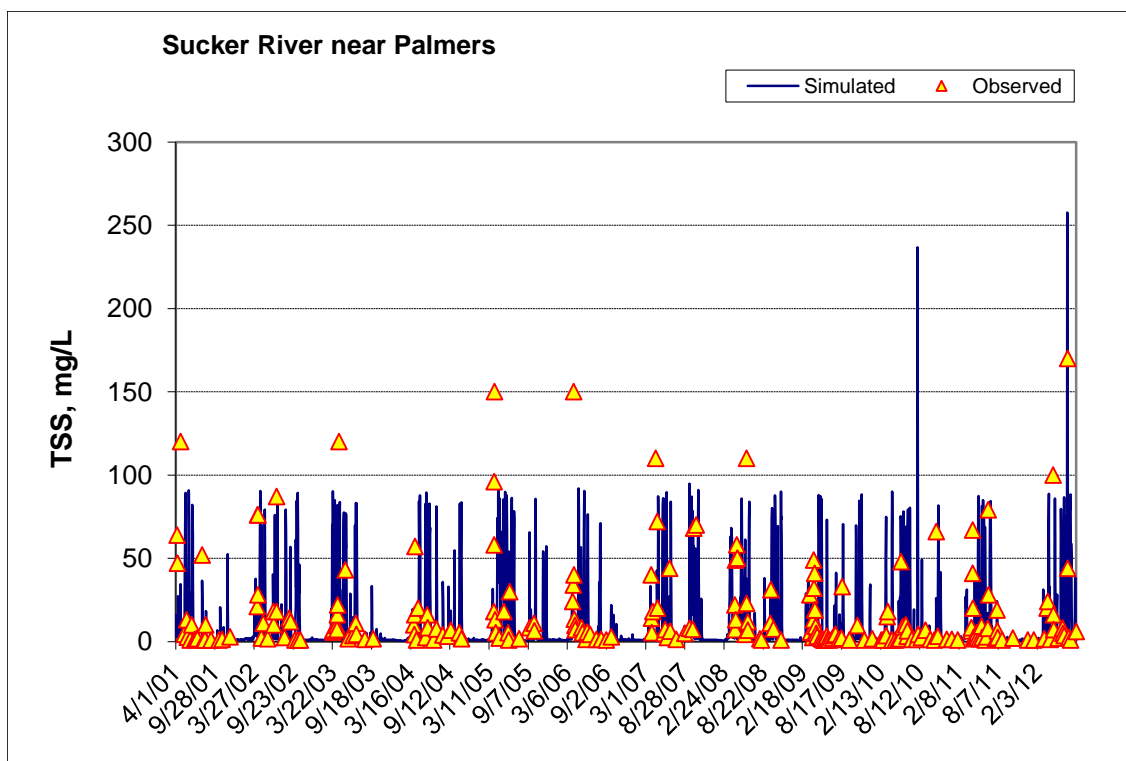


Figure 92. Time series of observed and simulated Total Suspended Solids (TSS) concentration at Sucker River near Palmers

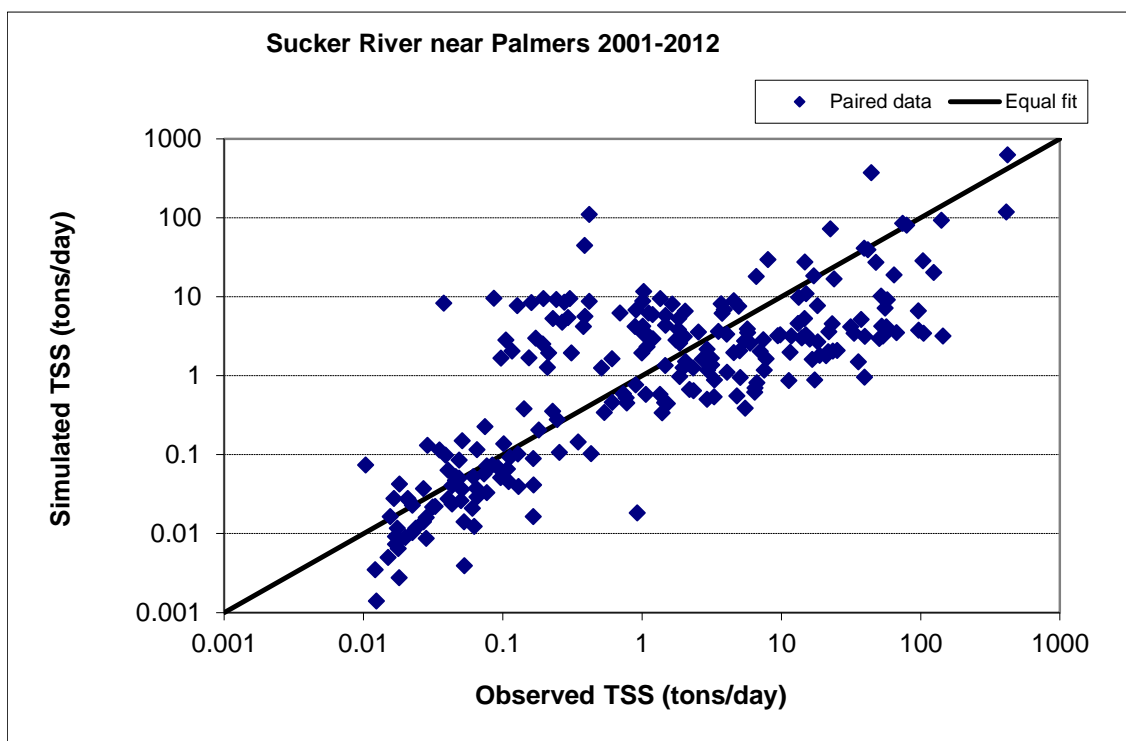


Figure 93. Paired simulated vs. observed Total Suspended Solids (TSS) load at Sucker River near Palmers

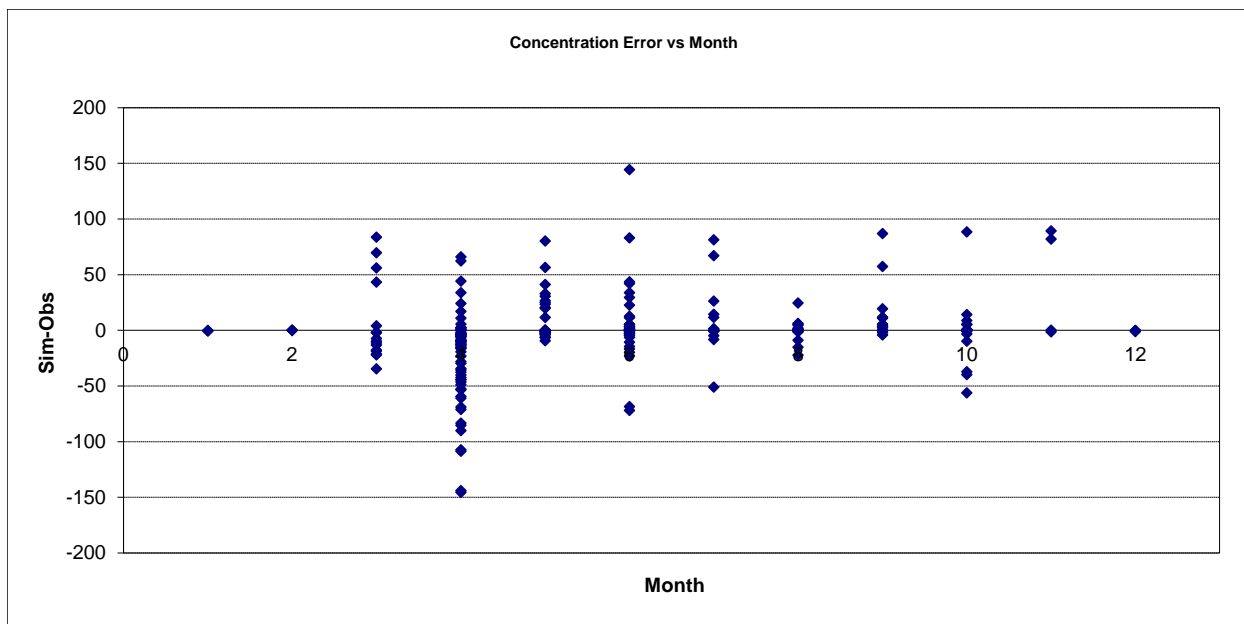


Figure 94. Residual (Simulated - Observed) vs. Month Total Suspended Solids (TSS) at Sucker River near Palmers

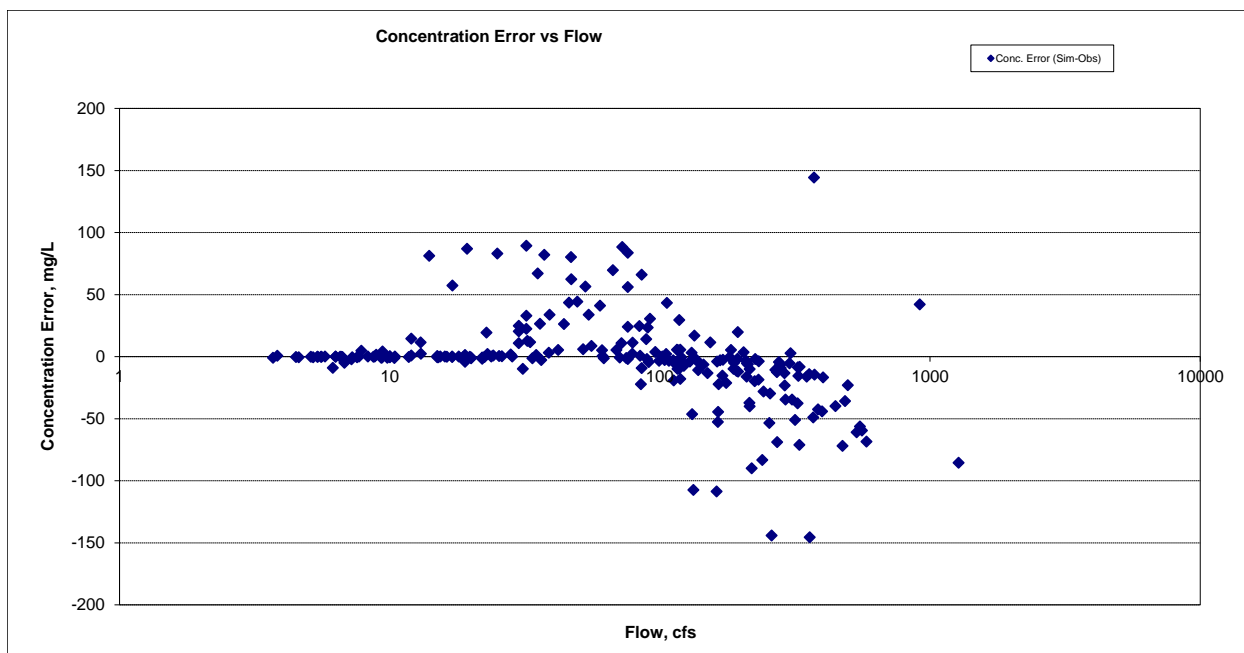


Figure 95. Residual (Simulated - Observed) vs. Flow Total Suspended Solids (TSS) at Sucker River near Palmers

Ammonia Nitrogen (NH₃)

Table 20. Ammonia Nitrogen (NH₃) statistics

Count	20
Concentration Average Error	-57.50%
Concentration Median Error	-73.36%
Load Average Error	-69.26%
Load Median Error	-50.61%
Paired t concentration	0.00
Paired t load	0.00

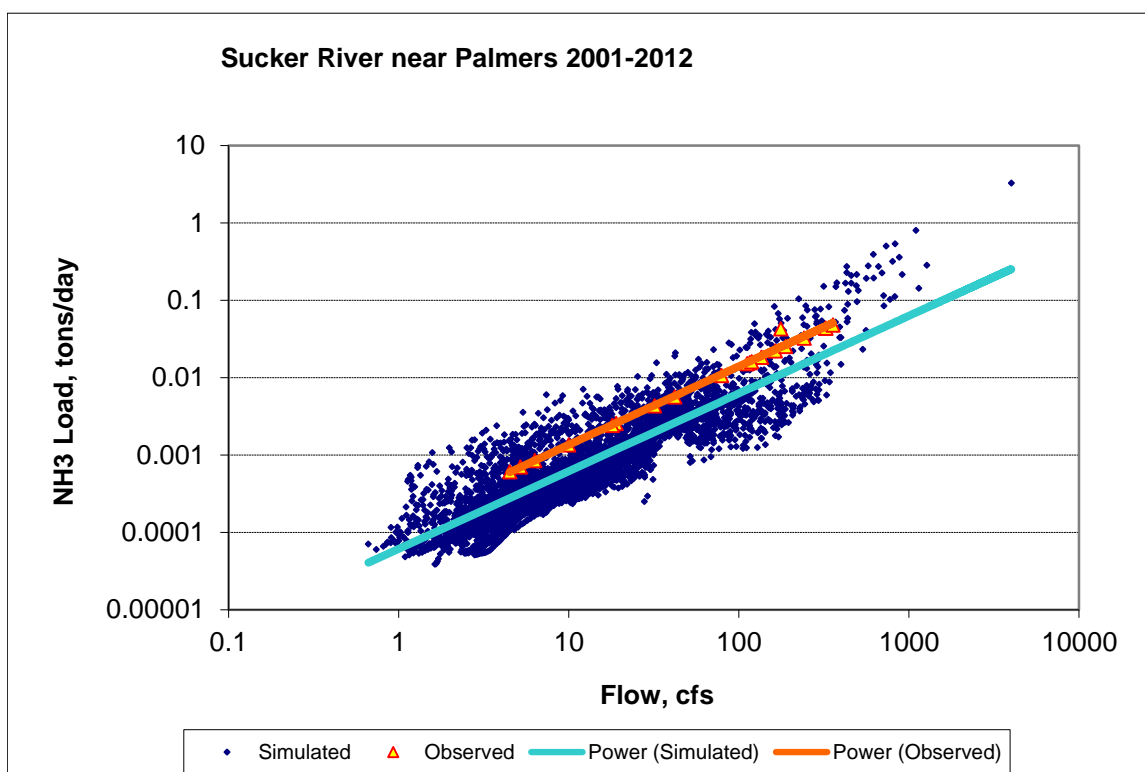


Figure 96. Power plot of simulated and observed Ammonia Nitrogen (NH₃) load vs flow at Sucker River near Palmers

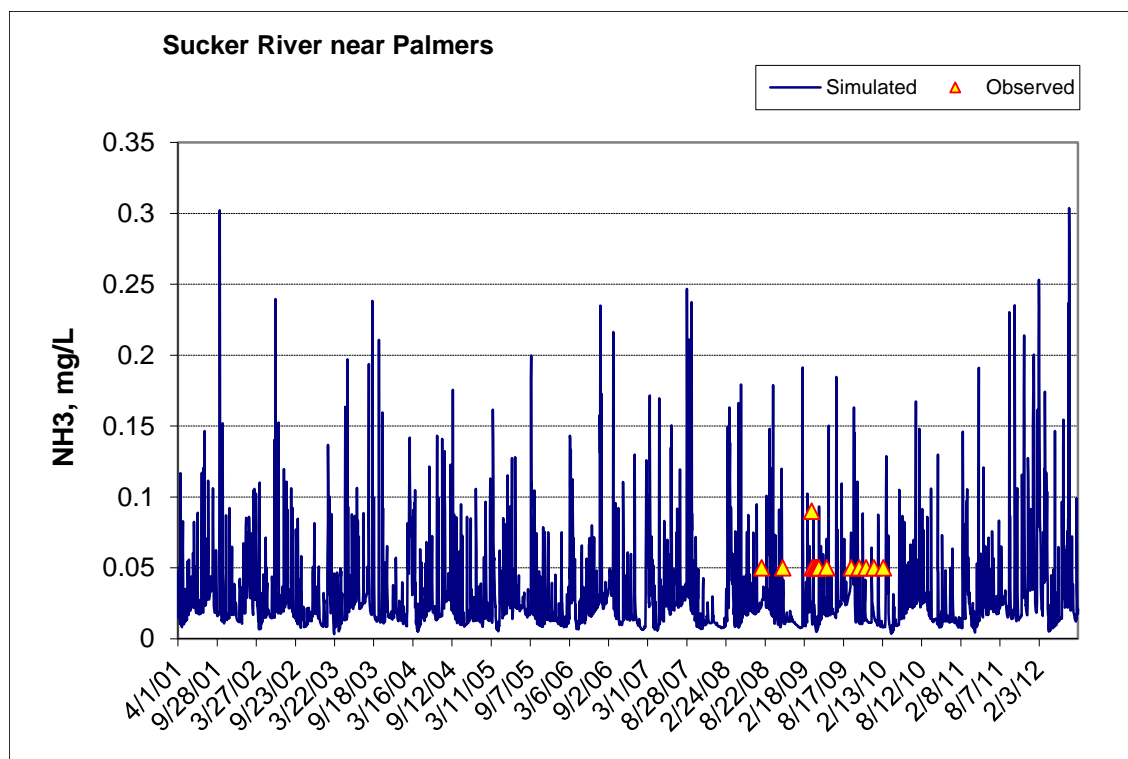


Figure 97. Time series of observed and simulated Ammonia Nitrogen (NH₃) concentration at Sucker River near Palmers

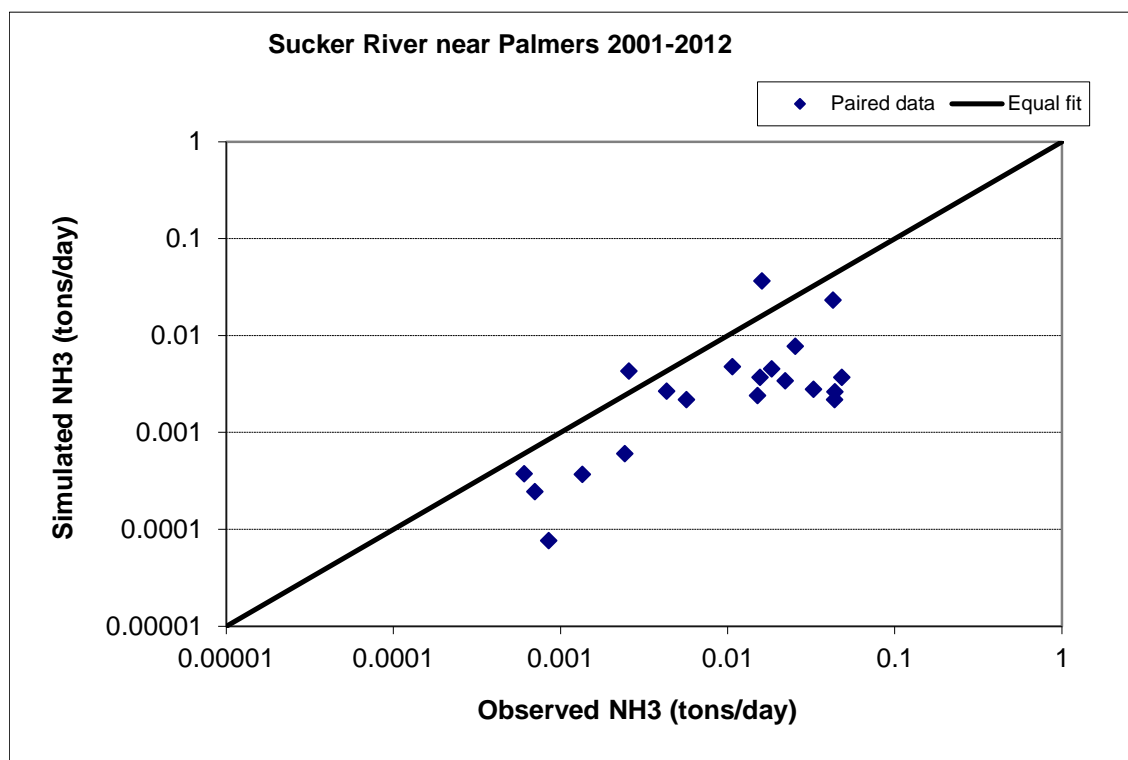


Figure 98. Paired simulated vs. observed Ammonia Nitrogen (NH₃) load at Sucker River near Palmers

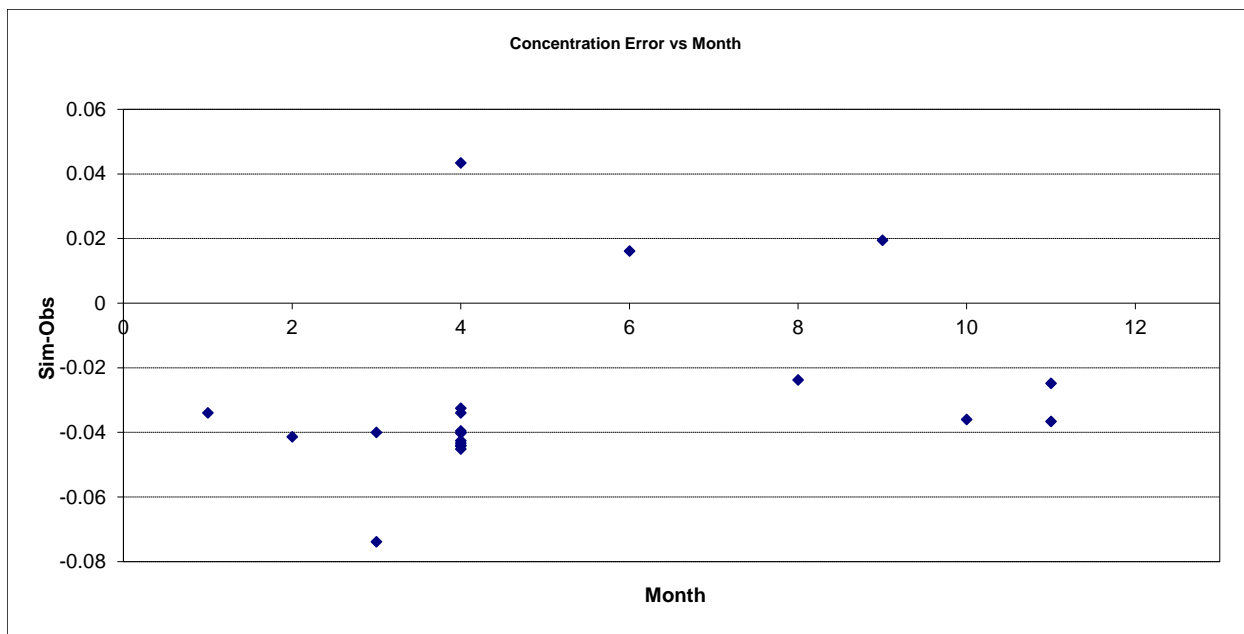


Figure 99. Residual (Simulated - Observed) vs. Month Ammonia Nitrogen (NH3) at Sucker River near Palmers

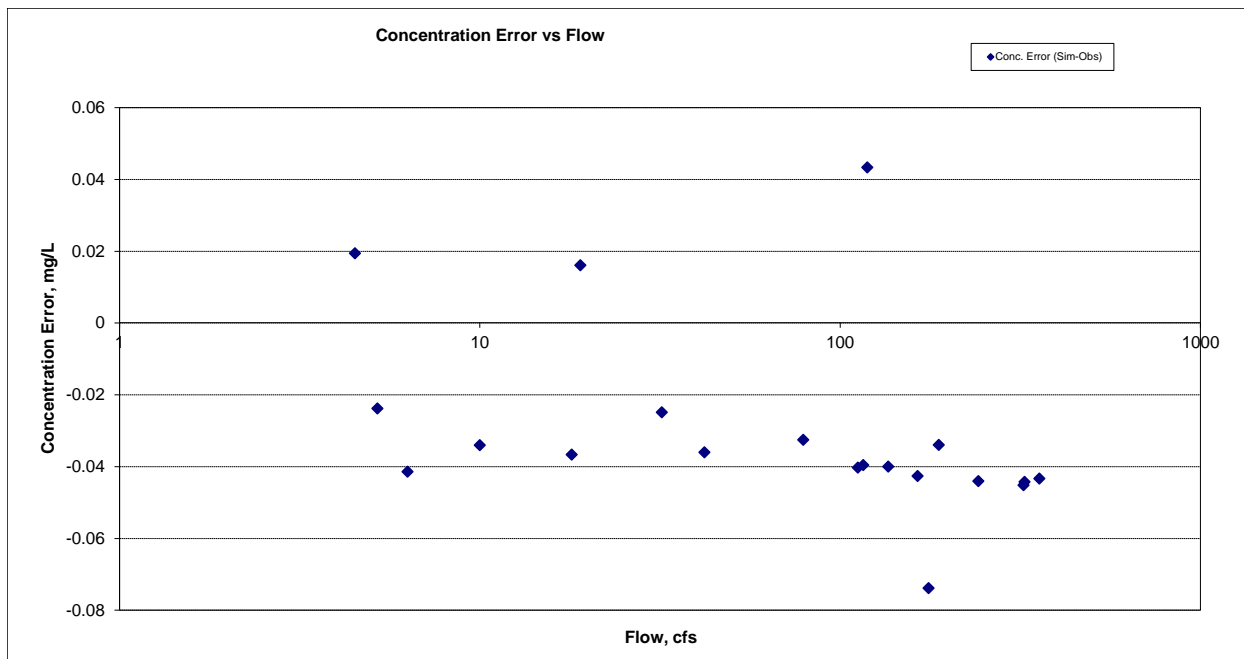


Figure 100. Residual (Simulated - Observed) vs. Flow Ammonia Nitrogen (NH3) at Sucker River near Palmers

Organic Nitrogen (OrgN)

Table 21. Organic Nitrogen (OrgN) statistics

Count	20
Concentration Average Error	1.42%
Concentration Median Error	-14.39%
Load Average Error	25.62%
Load Median Error	-3.91%
Paired t concentration	0.94
Paired t load	0.43

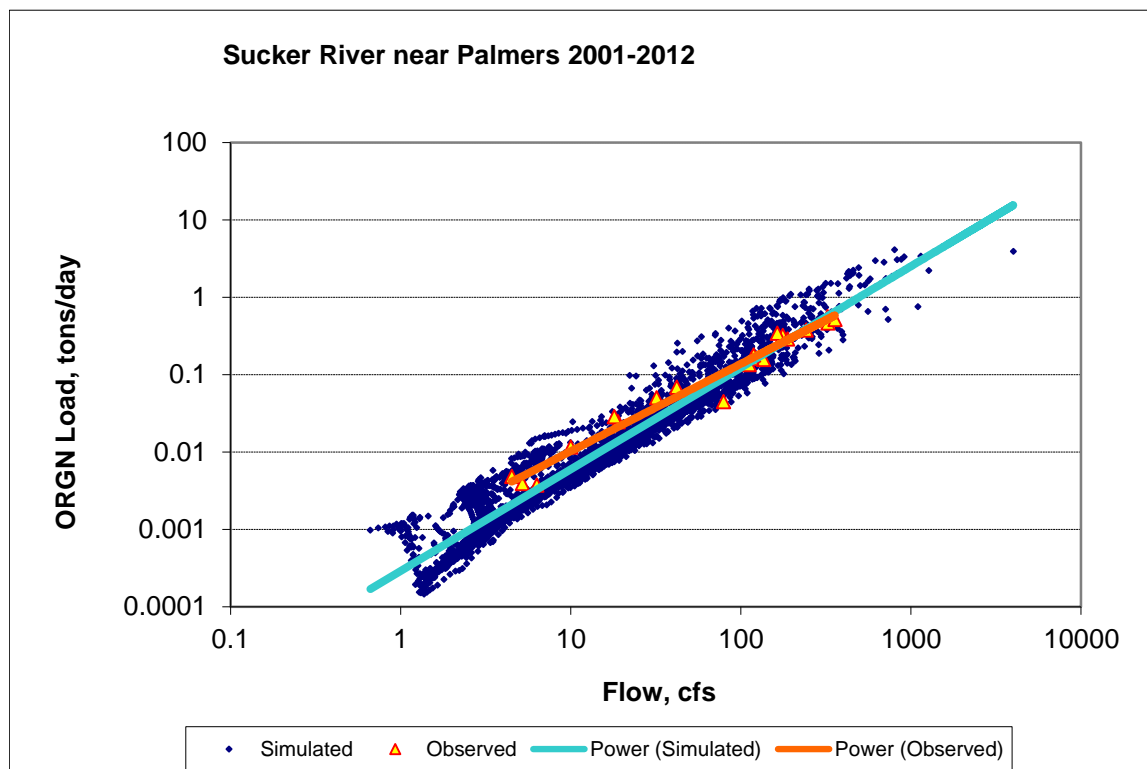


Figure 101. Power plot of simulated and observed Organic Nitrogen (OrgN) load vs flow at Sucker River near Palmers

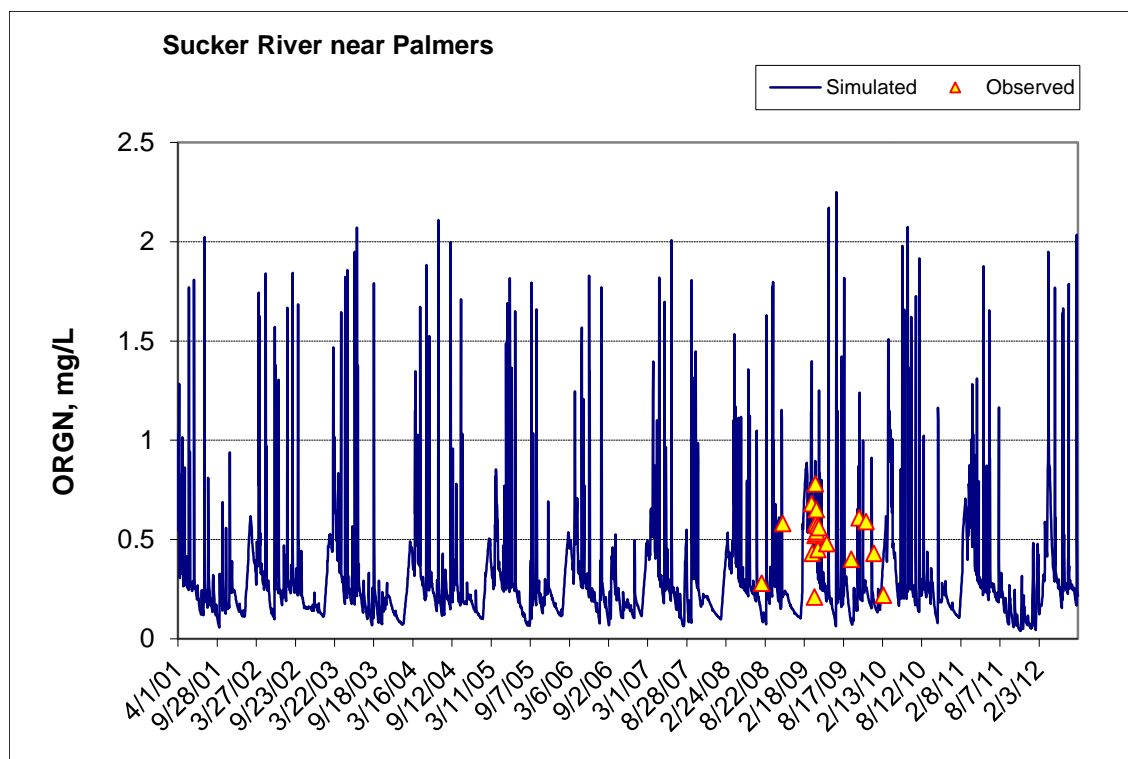


Figure 102. Time series of observed and simulated Organic Nitrogen (OrgN) concentration at Sucker River near Palmers

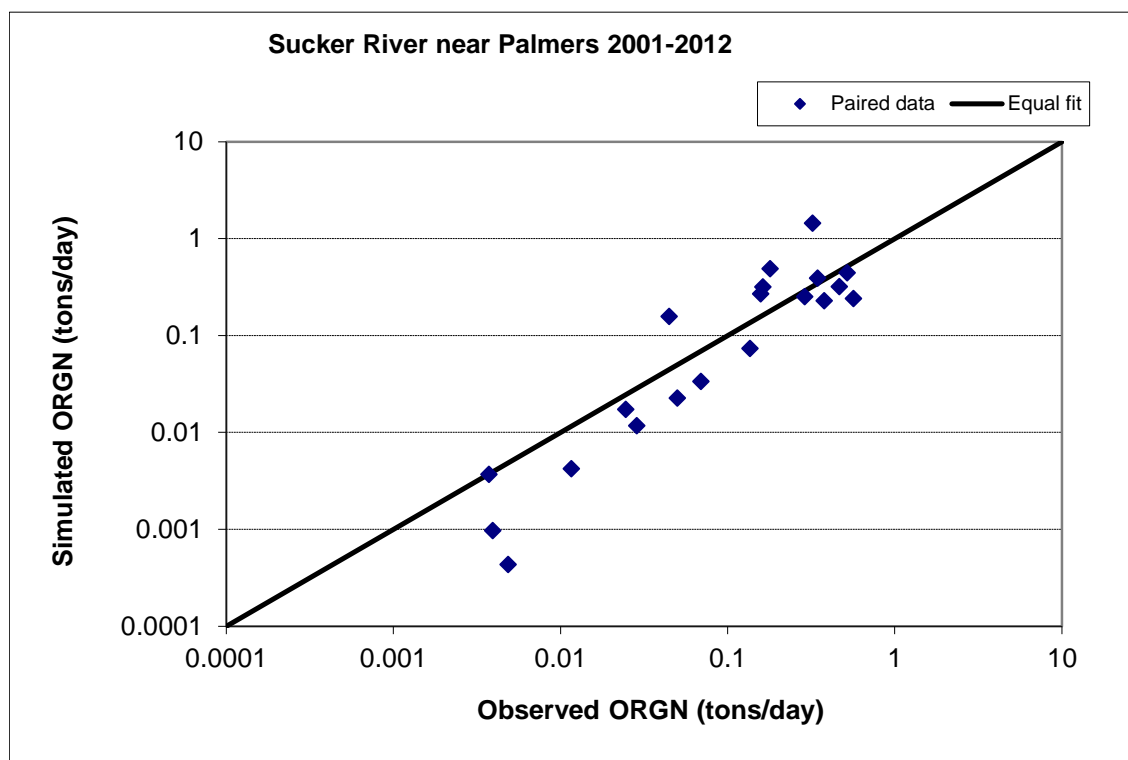


Figure 103. Paired simulated vs. observed Organic Nitrogen (OrgN) load at Sucker River near Palmers



Figure 104. Residual (Simulated - Observed) vs. Month Organic Nitrogen (OrgN) at Sucker River near Palmers

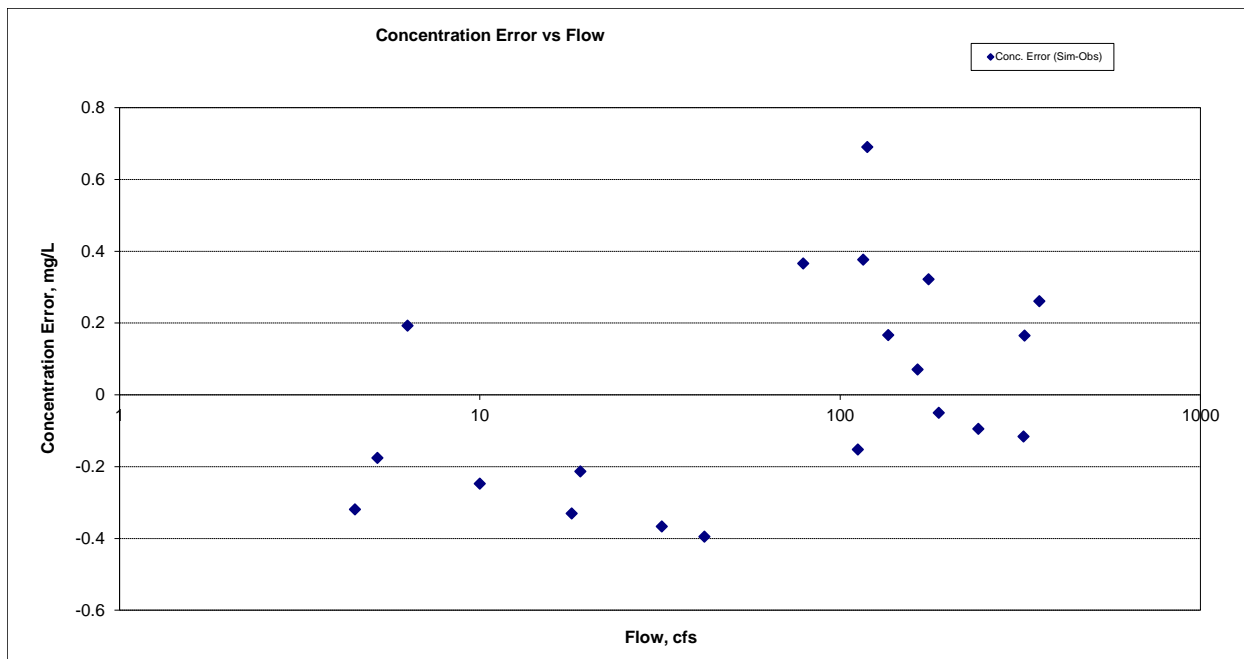


Figure 105. Residual (Simulated - Observed) vs. Flow Organic Nitrogen (OrgN) at Sucker River near Palmers

Total Kjeldahl Nitrogen (TKN)

Table 22. Total Kjeldahl Nitrogen (TKN) statistics

Count	175
Concentration Average Error	-16.68%
Concentration Median Error	-34.49%
Load Average Error	12.00%
Load Median Error	-5.08%
Paired t concentration	0.77
Paired t load	0.71

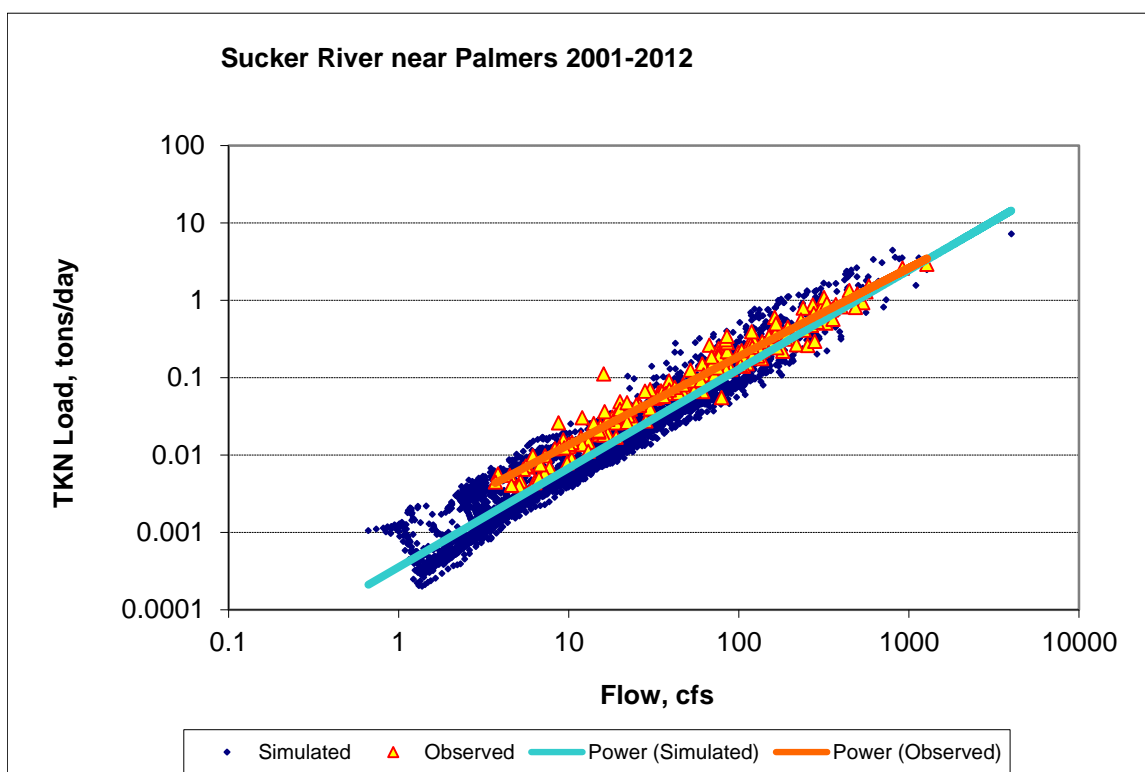


Figure 106. Power plot of simulated and observed Total Kjeldahl Nitrogen (TKN) load vs flow at Sucker River near Palmers

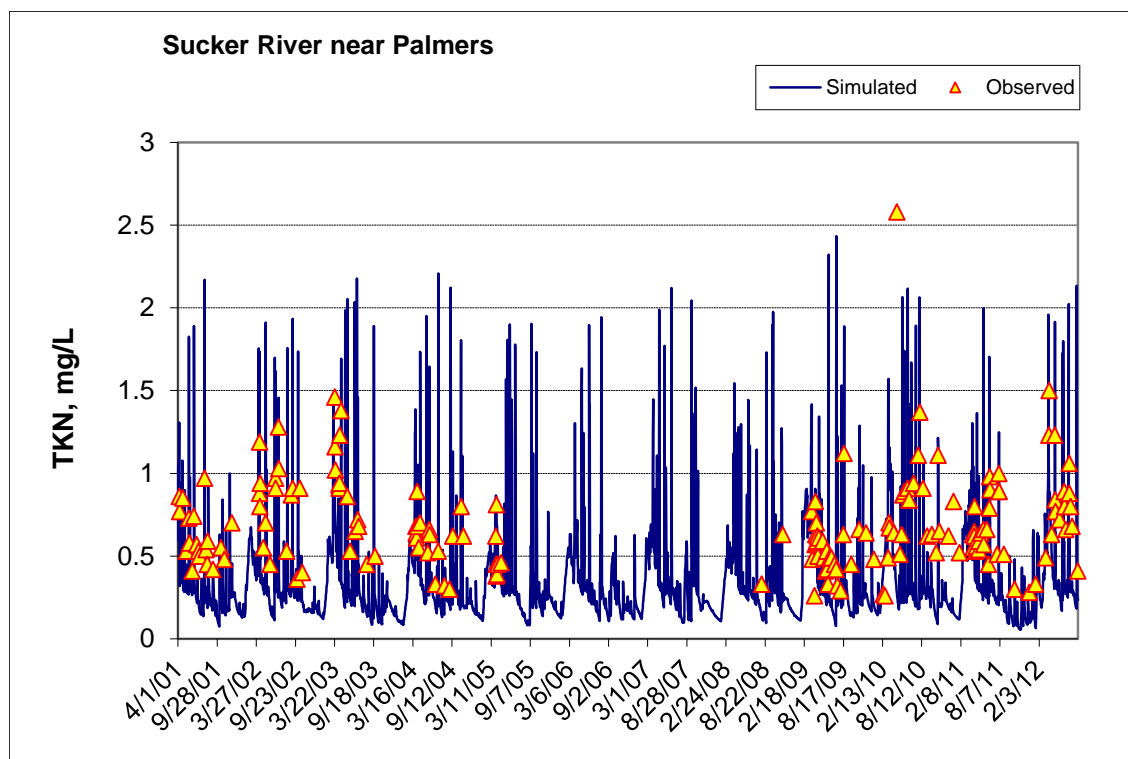


Figure 107. Time series of observed and simulated Total Kjeldahl Nitrogen (TKN) concentration at Sucker River near Palmers

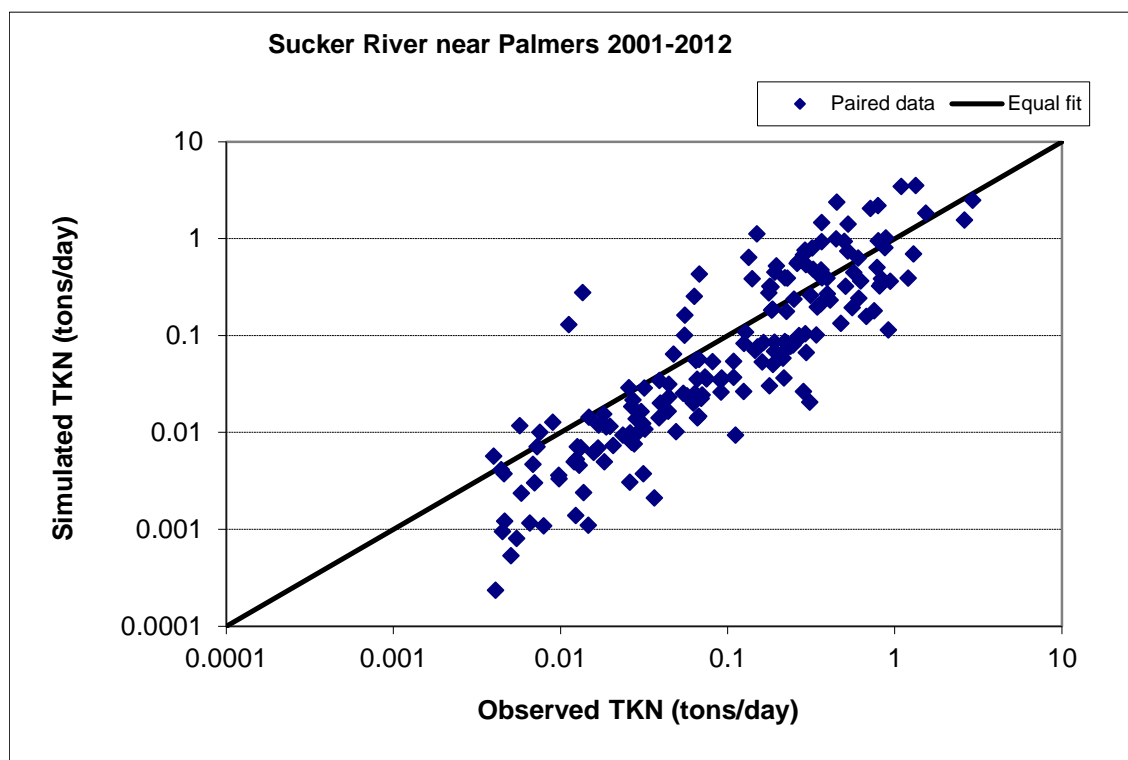


Figure 108. Paired simulated vs. observed Total Kjeldahl Nitrogen (TKN) load at Sucker River near Palmers

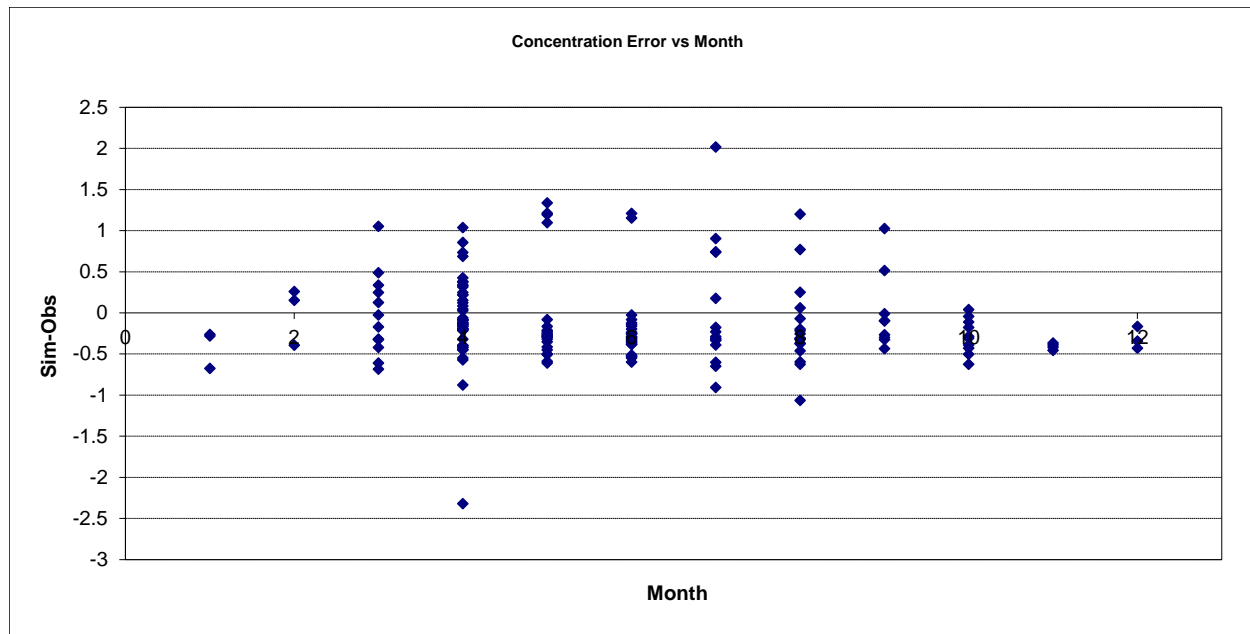


Figure 109. Residual (Simulated - Observed) vs. Month Total Kjeldahl Nitrogen (TKN) at Sucker River near Palmers

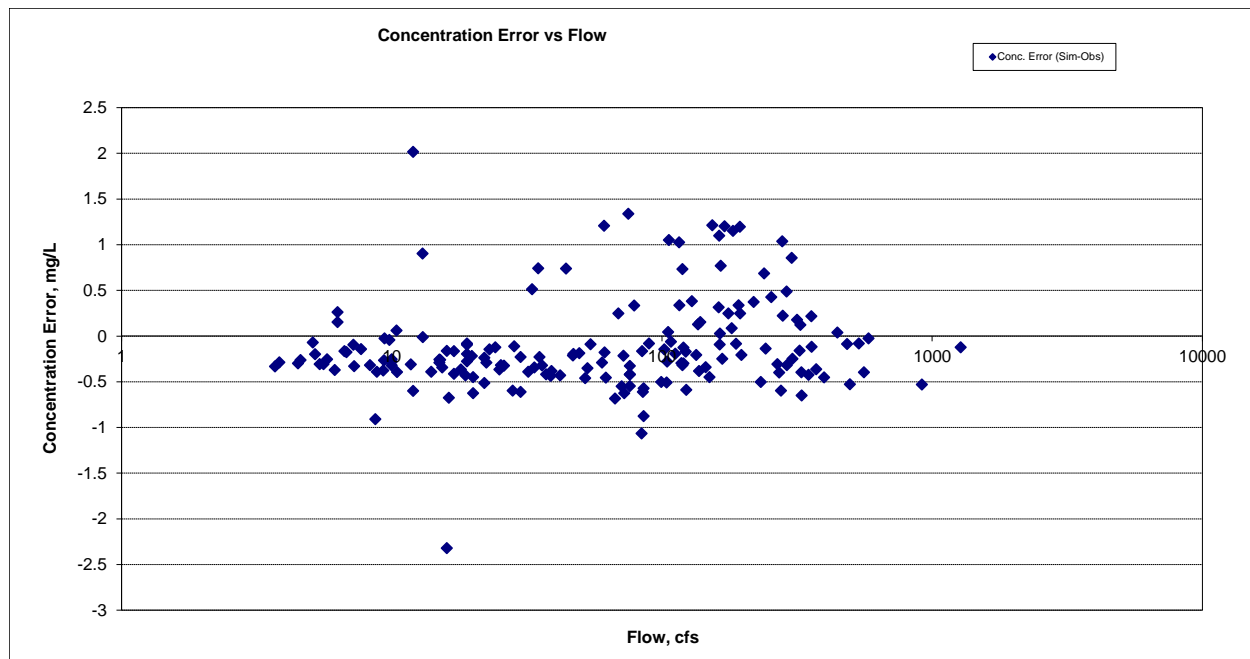


Figure 110. Residual (Simulated - Observed) vs. Flow Total Kjeldahl Nitrogen (TKN) at Sucker River near Palmers

Nitrite+ Nitrate Nitrogen (NO_x)

Table 23. Nitrite+ Nitrate Nitrogen (NO_x) statistics

Count	175
Concentration Average Error	-29.71%
Concentration Median Error	-26.18%
Load Average Error	-15.88%
Load Median Error	-4.81%
Paired t concentration	0.04
Paired t load	0.61

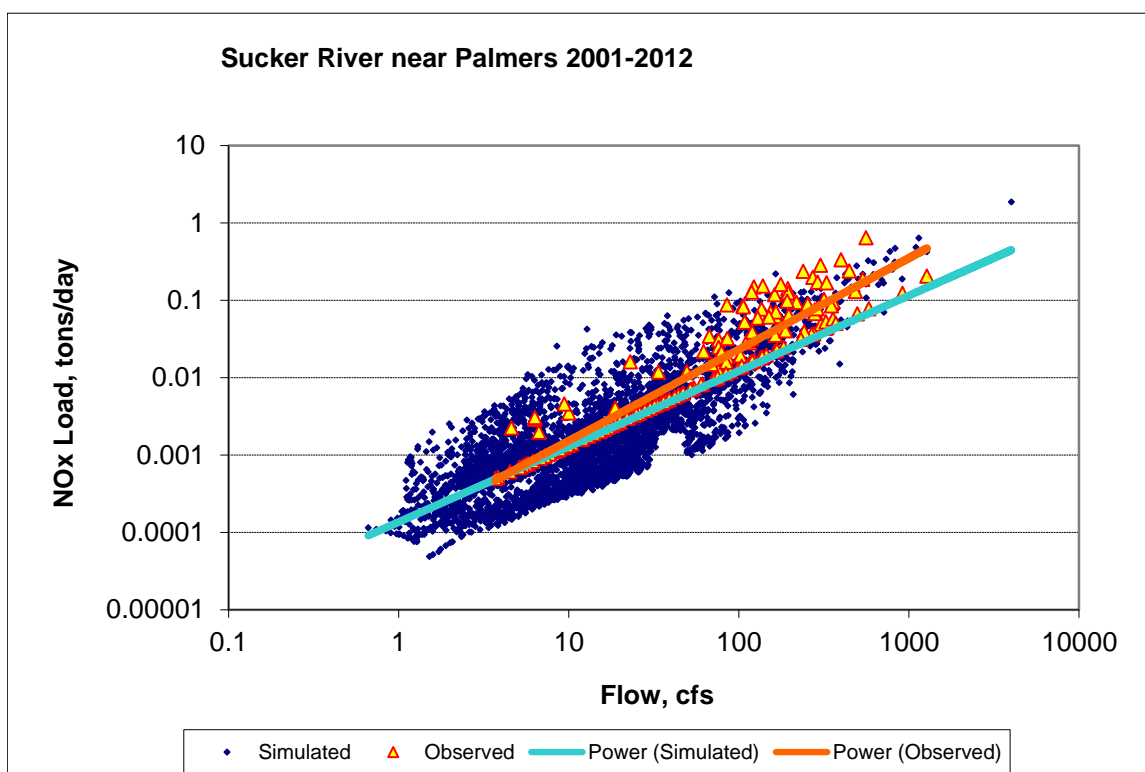


Figure 111. Power plot of simulated and observed Nitrite+ Nitrate Nitrogen (NO_x) load vs flow at Sucker River near Palmers

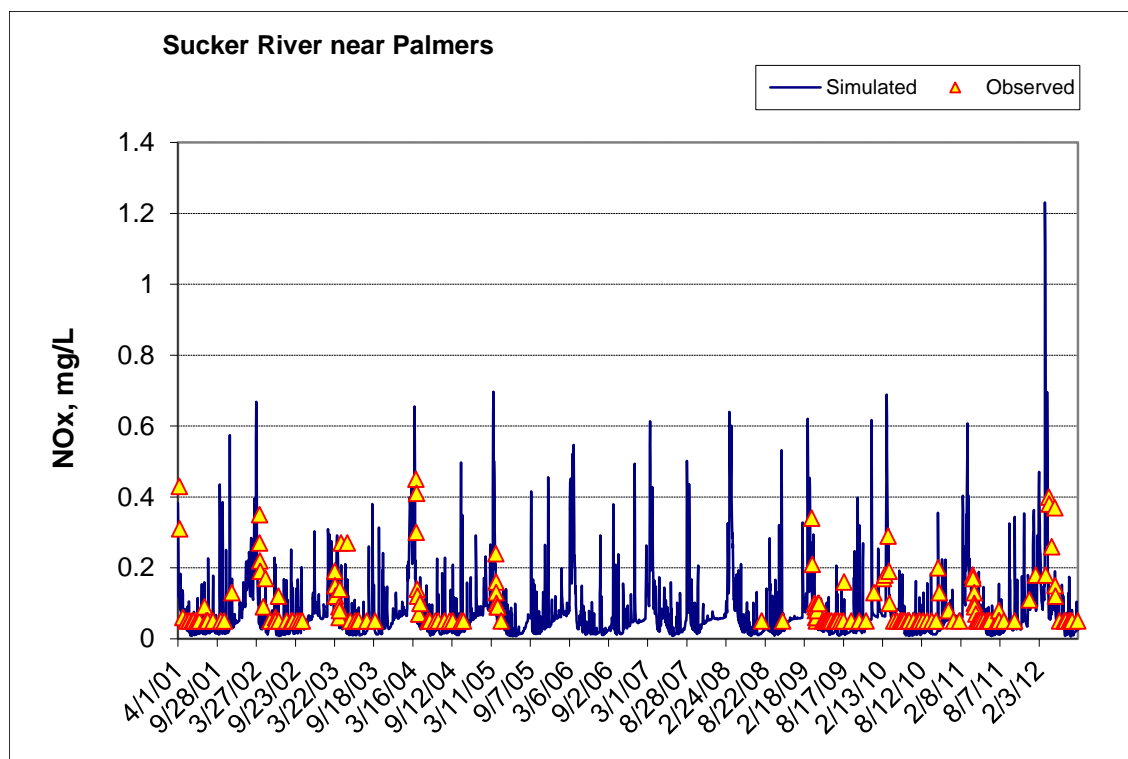


Figure 112. Time series of observed and simulated Nitrite+ Nitrate Nitrogen (NOx) concentration at Sucker River near Palmers

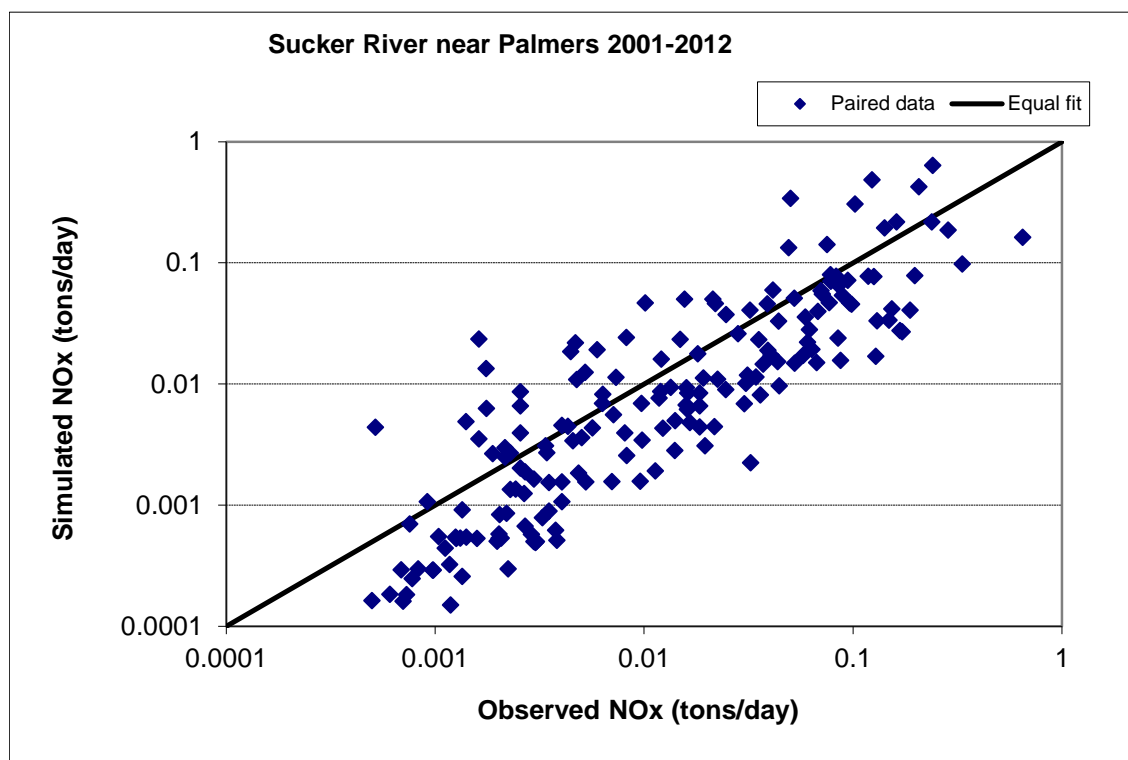


Figure 113. Paired simulated vs. observed Nitrite+ Nitrate Nitrogen (NOx) load at Sucker River near Palmers

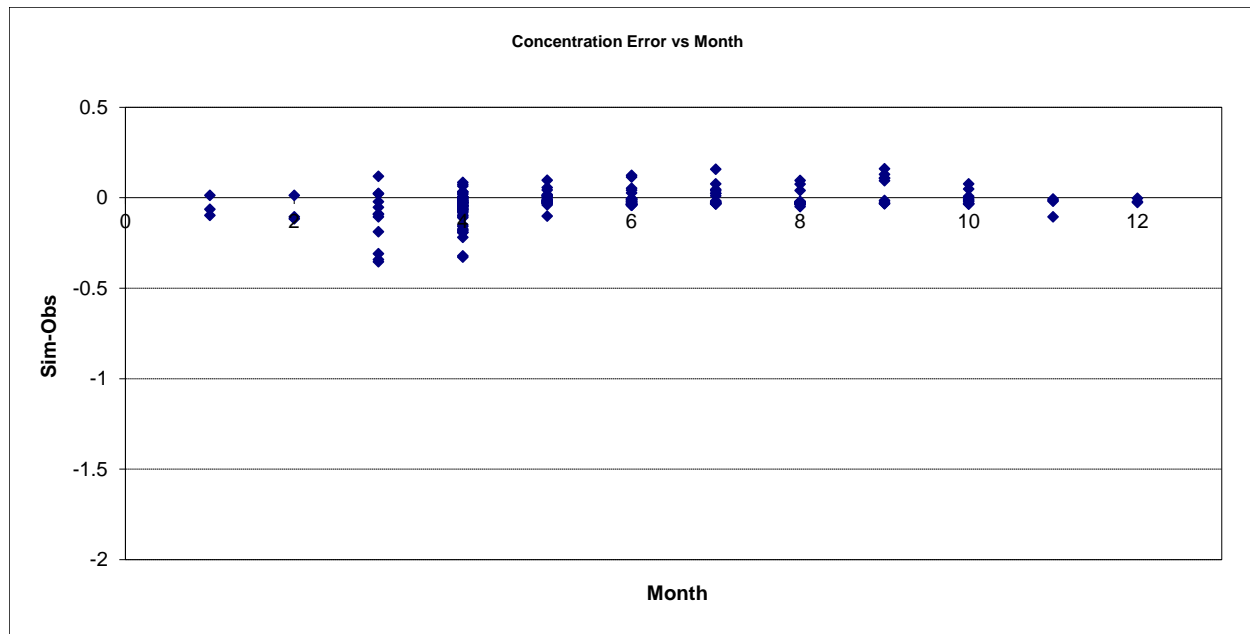


Figure 114. Residual (Simulated - Observed) vs. Month Nitrite+ Nitrate Nitrogen (NOx) at Sucker River near Palmers

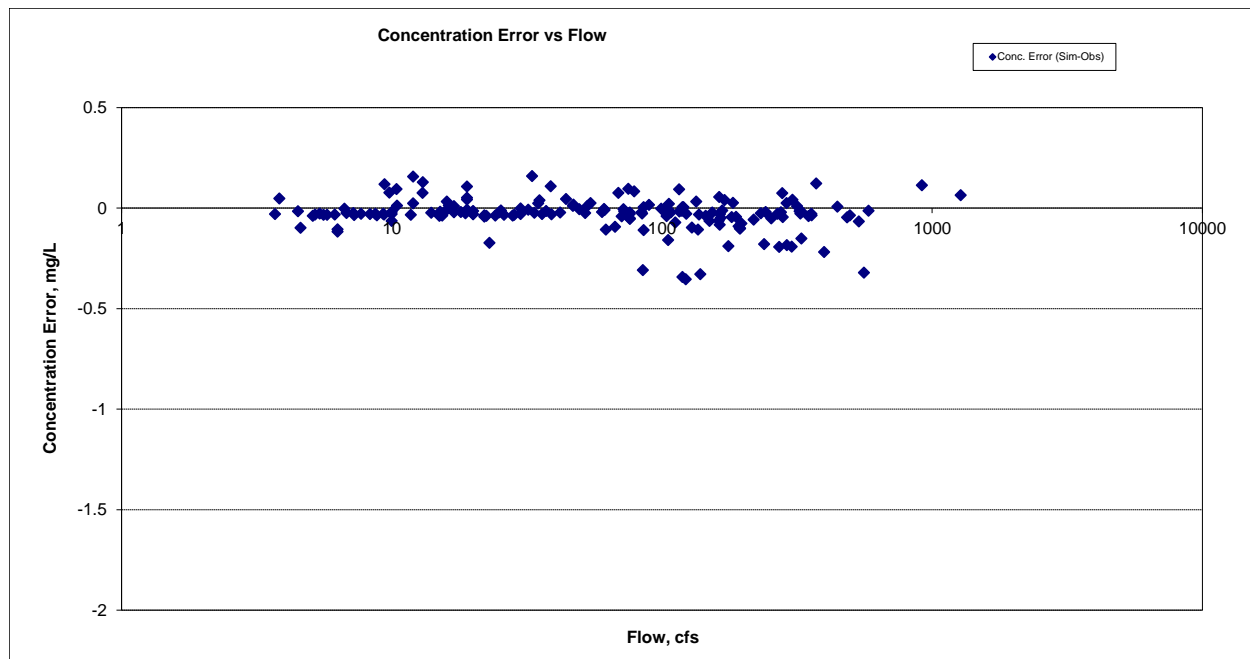


Figure 115. Residual (Simulated - Observed) vs. Flow Nitrite+ Nitrate Nitrogen (NOx) at Sucker River near Palmers

Total Nitrogen (TN)

Table 24. Total Nitrogen (TN) statistics

Count	175
Concentration Average Error	-18.31%
Concentration Median Error	-33.29%
Load Average Error	8.23%
Load Median Error	-4.82%
Paired t concentration	0.65
Paired t load	0.80

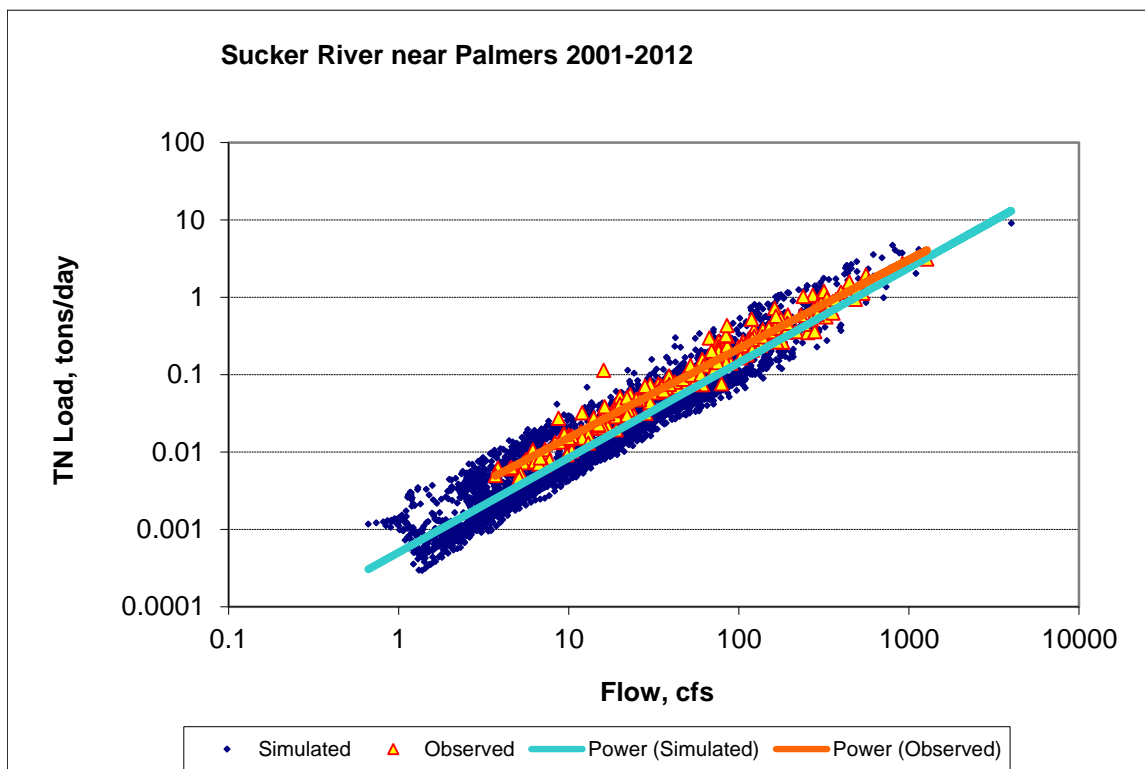


Figure 116. Power plot of simulated and observed Total Nitrogen (TN) load vs flow at Sucker River near Palmers

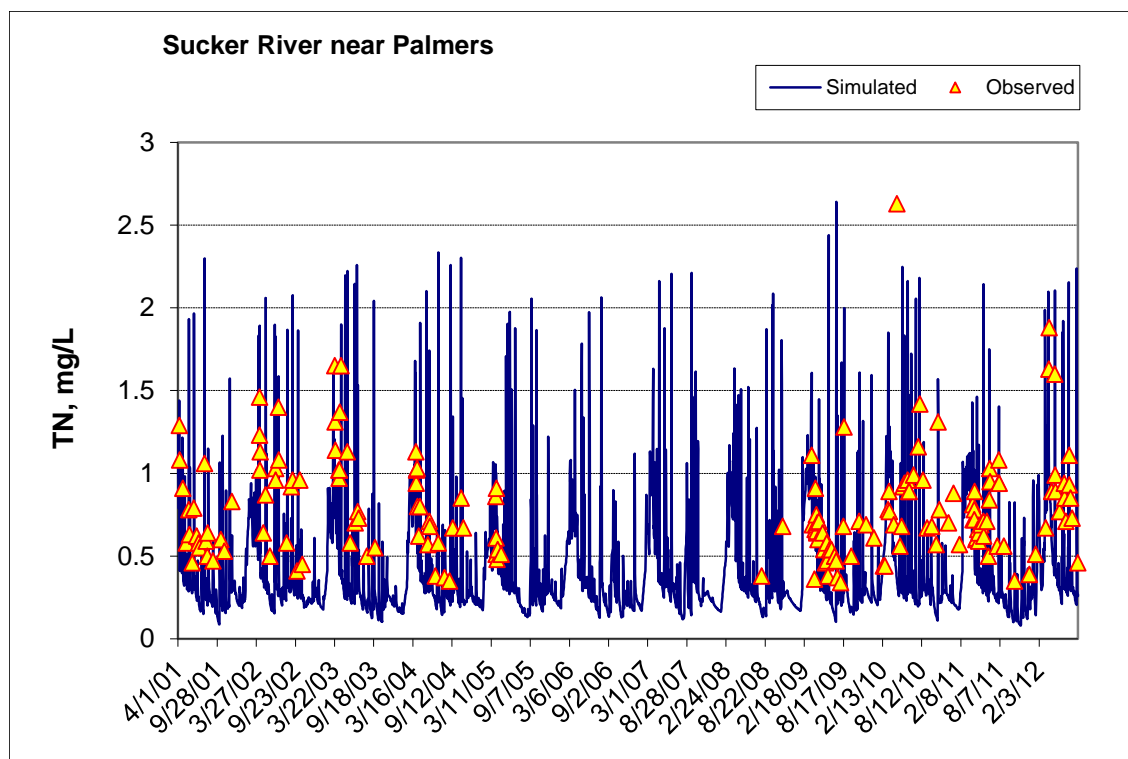


Figure 117. Time series of observed and simulated Total Nitrogen (TN) concentration at Sucker River near Palmers

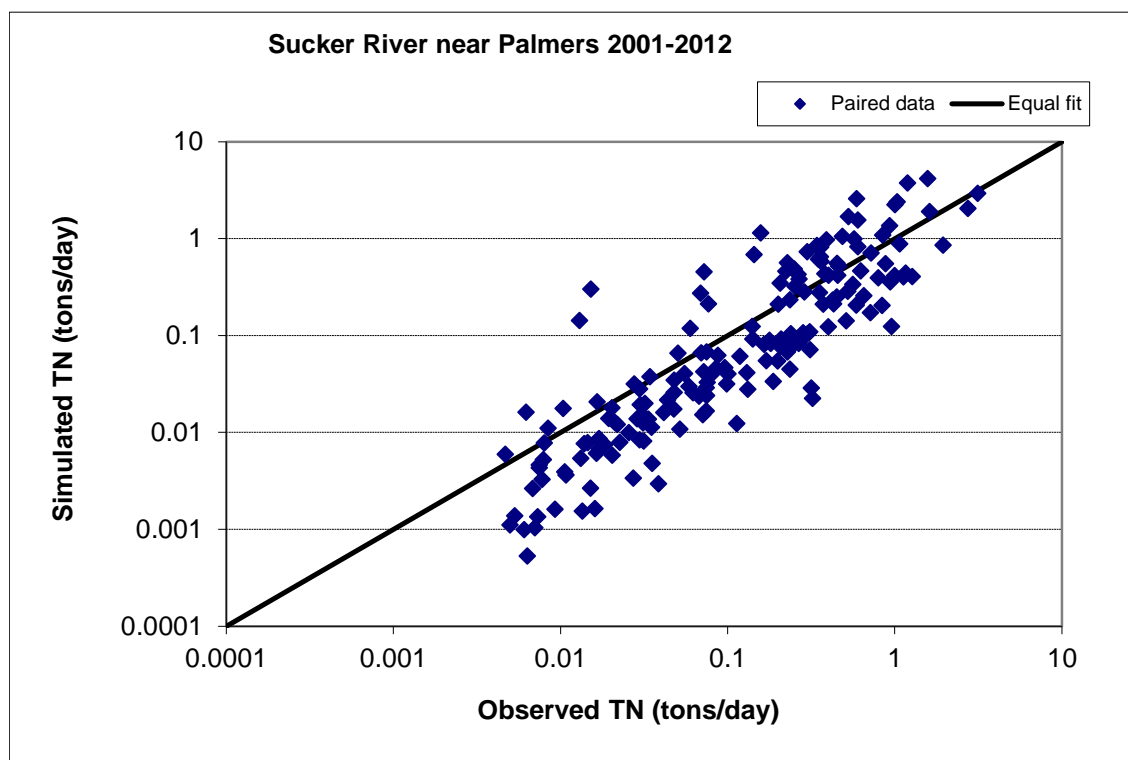


Figure 118. Paired simulated vs. observed Total Nitrogen (TN) load at Sucker River near Palmers

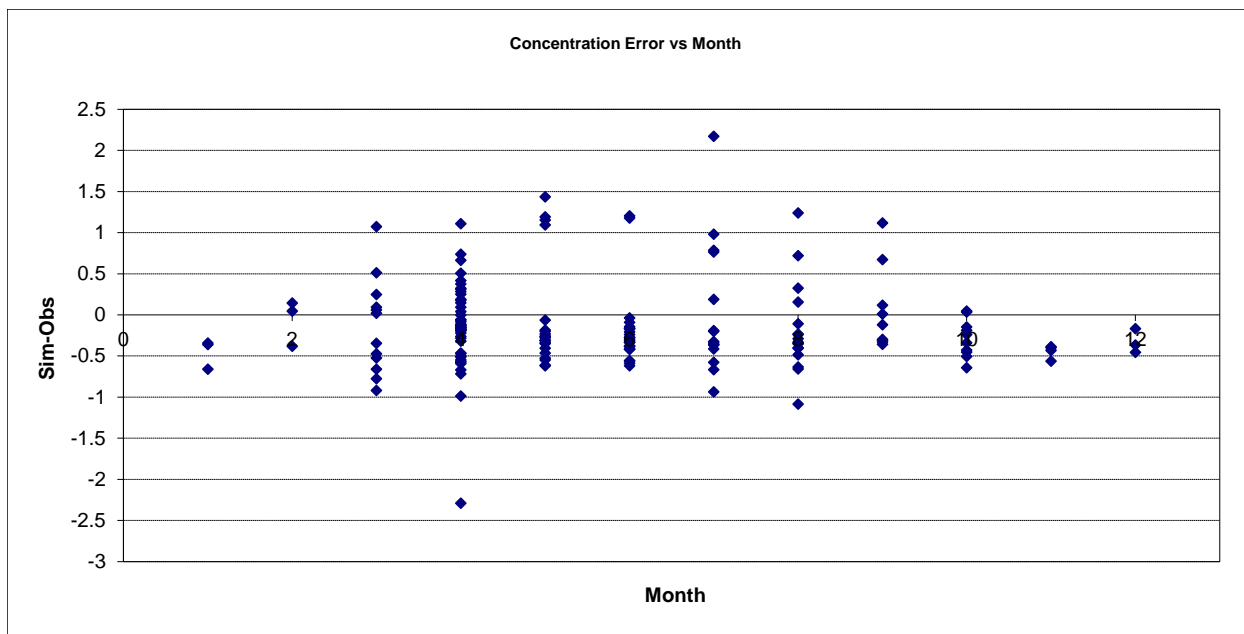


Figure 119. Residual (Simulated - Observed) vs. Month Total Nitrogen (TN) at Sucker River near Palmers

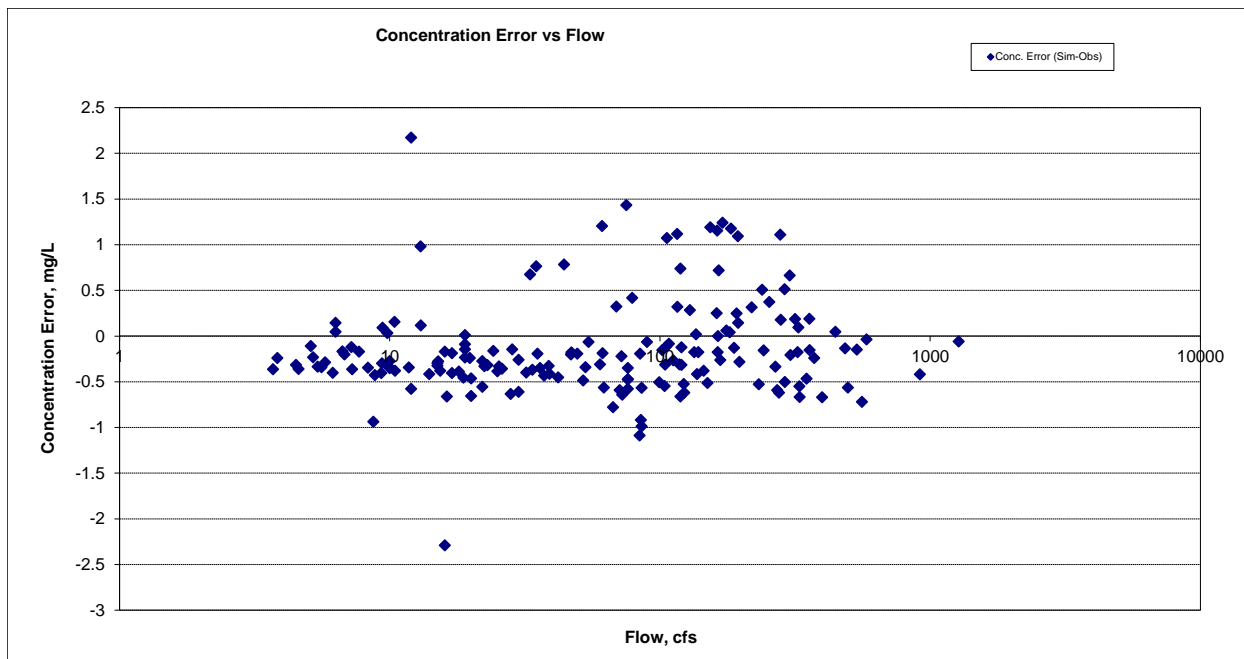


Figure 120. Residual (Simulated - Observed) vs. Flow Total Nitrogen (TN) at Sucker River near Palmers

Soluble Reactive Phosphorus (SRP)

Table 25. Soluble Reactive Phosphorus (SRP) statistics

Count	168
Concentration Average Error	-5.32%
Concentration Median Error	-18.81%
Load Average Error	-35.09%
Load Median Error	-2.09%
Paired t concentration	0.98
Paired t load	0.22

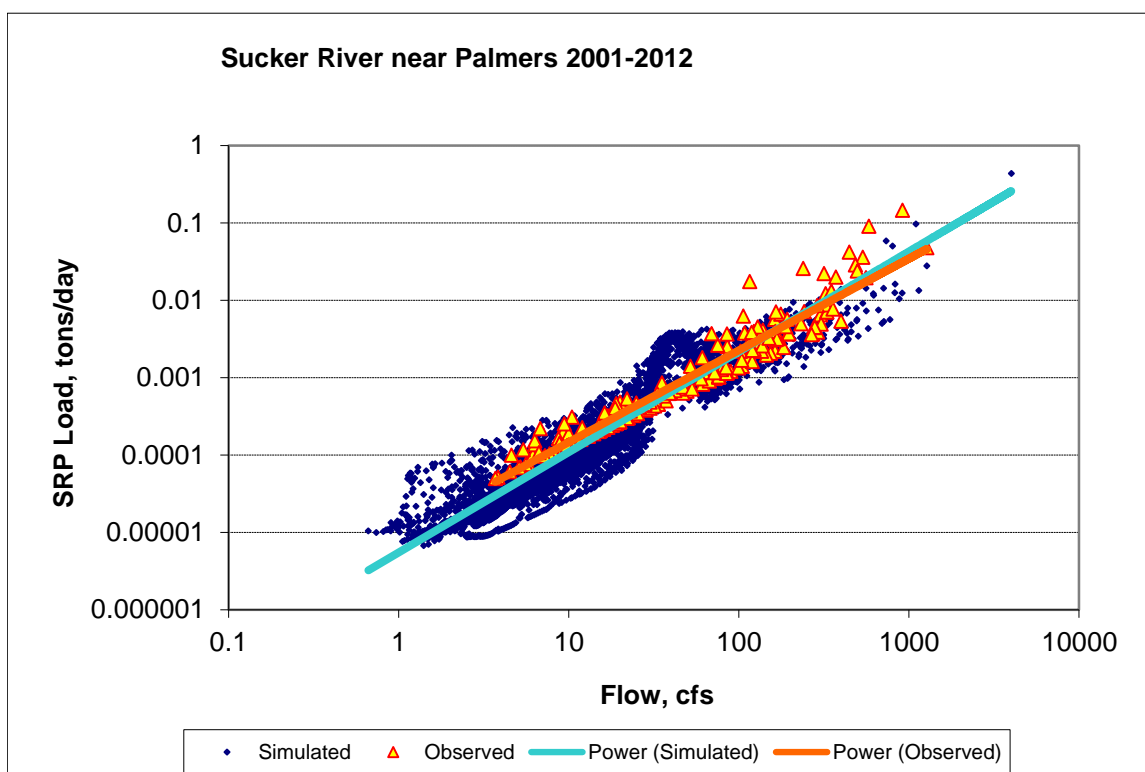


Figure 121. Power plot of simulated and observed Soluble Reactive Phosphorus (SRP) load vs flow at Sucker River near Palmers

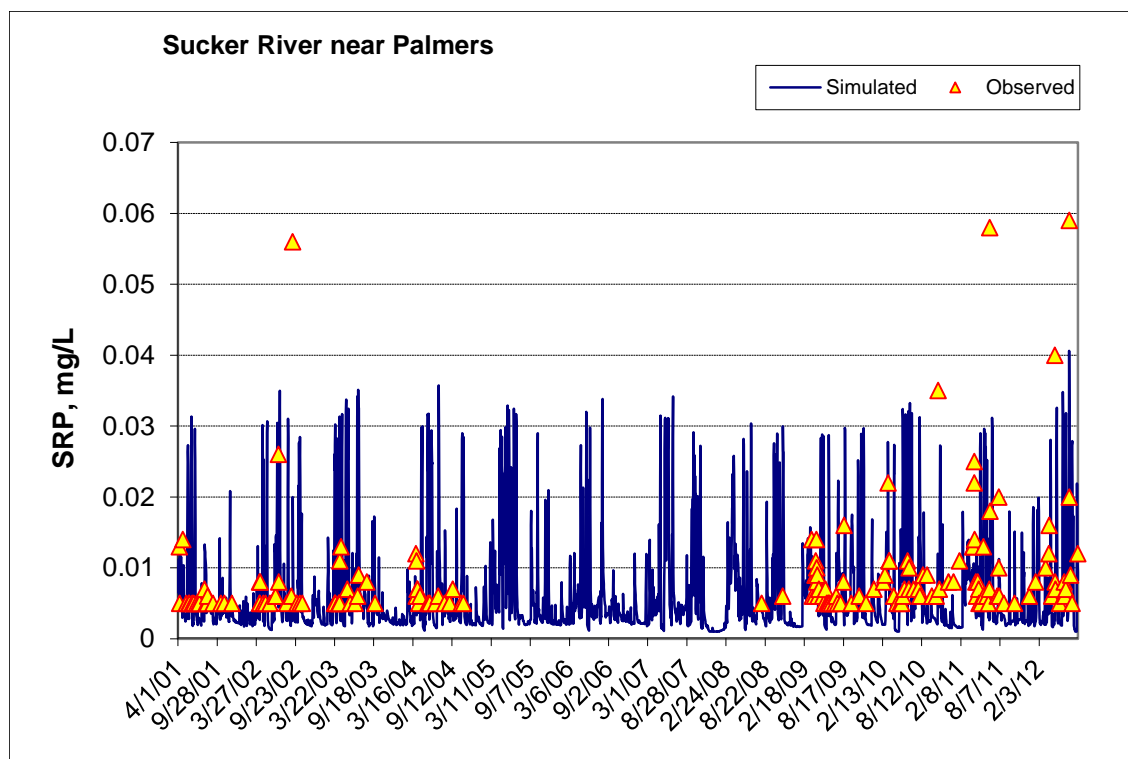


Figure 122. Time series of observed and simulated Soluble Reactive Phosphorus (SRP) concentration at Sucker River near Palmers

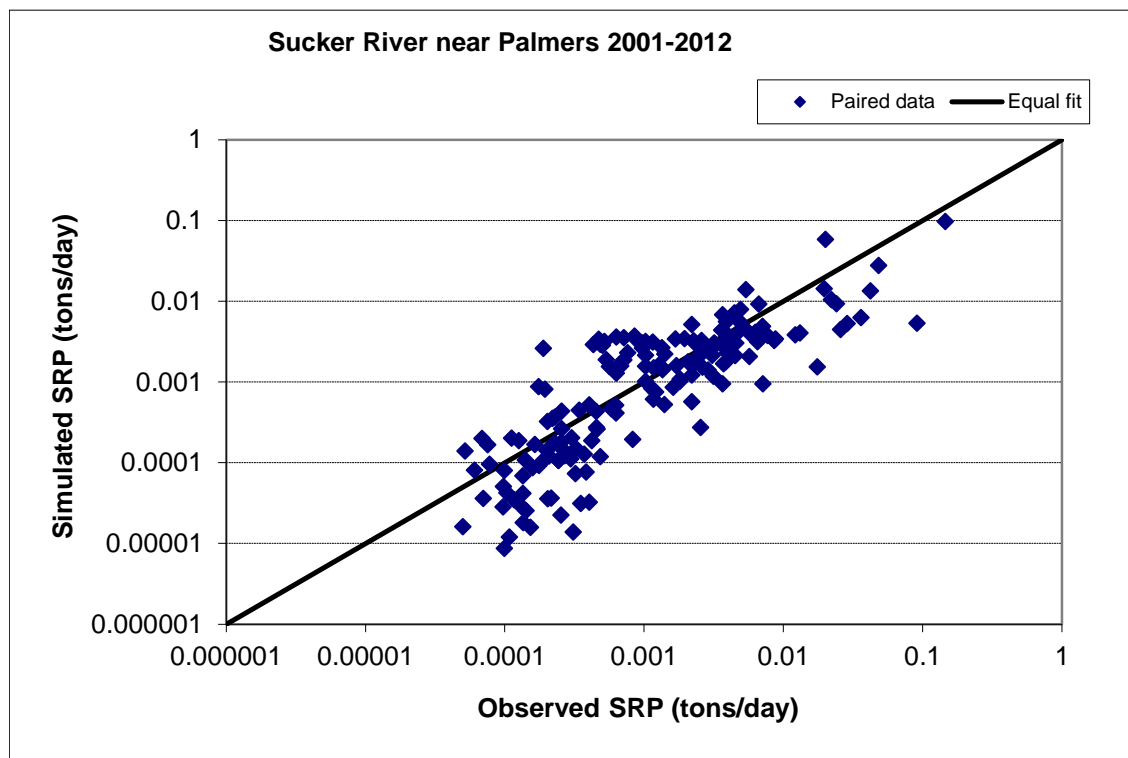


Figure 123. Paired simulated vs. observed Soluble Reactive Phosphorus (SRP) load at Sucker River near Palmers

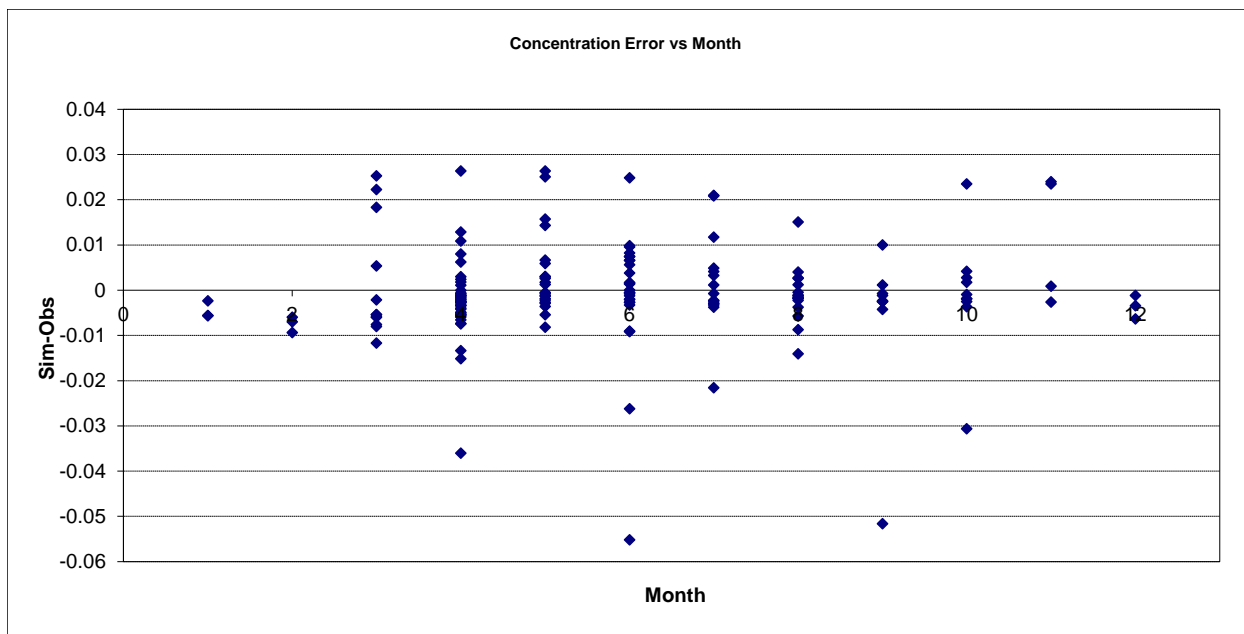


Figure 124. Residual (Simulated - Observed) vs. Month Soluble Reactive Phosphorus (SRP) at Sucker River near Palmers

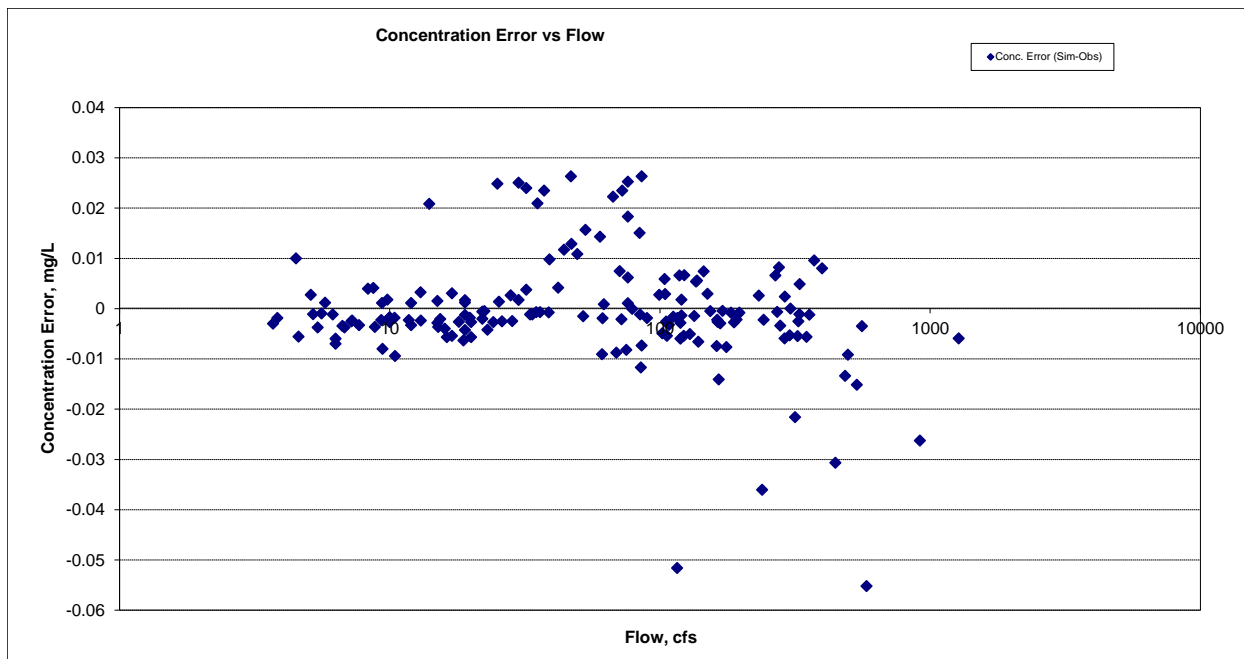


Figure 125. Residual (Simulated - Observed) vs. Flow Soluble Reactive Phosphorus (SRP) at Sucker River near Palmers

Organic Phosphorus (OrgP)

Table 26. Organic Phosphorus (OrgP) statistics

Count	166
Concentration Average Error	11.37%
Concentration Median Error	-12.68%
Load Average Error	10.69%
Load Median Error	-1.26%
Paired t concentration	0.78
Paired t load	0.67

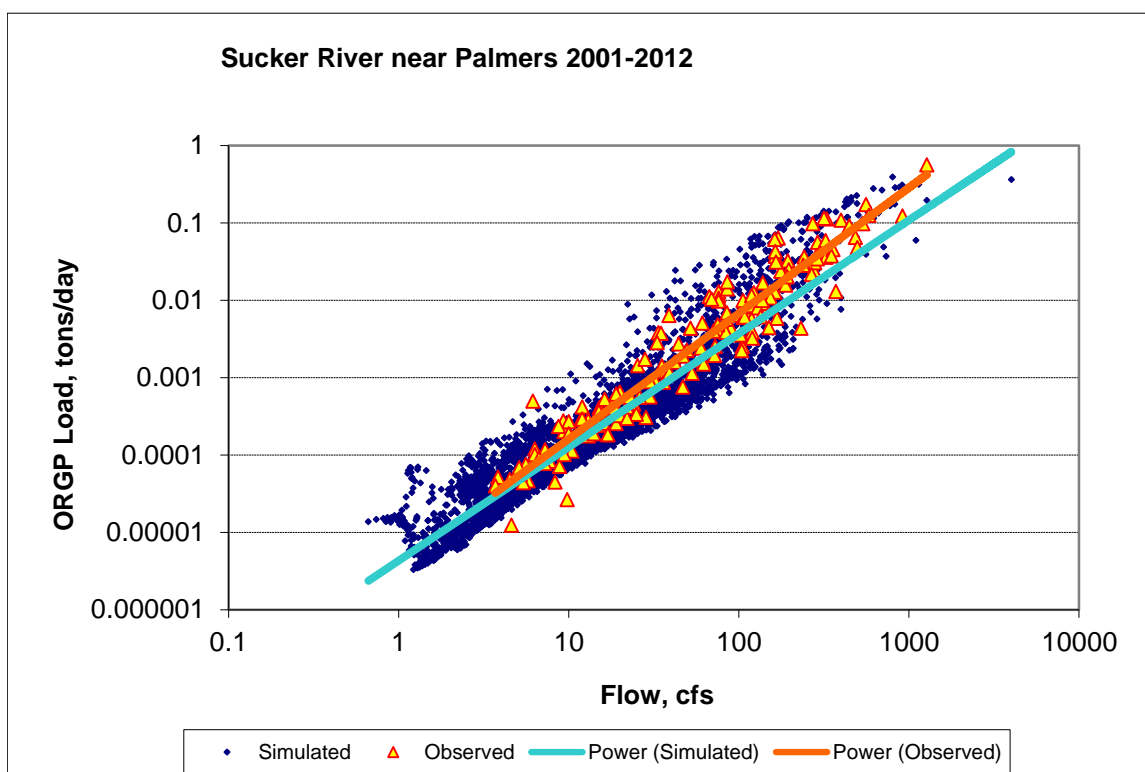


Figure 126. Power plot of simulated and observed Organic Phosphorus (OrgP) load vs flow at Sucker River near Palmers

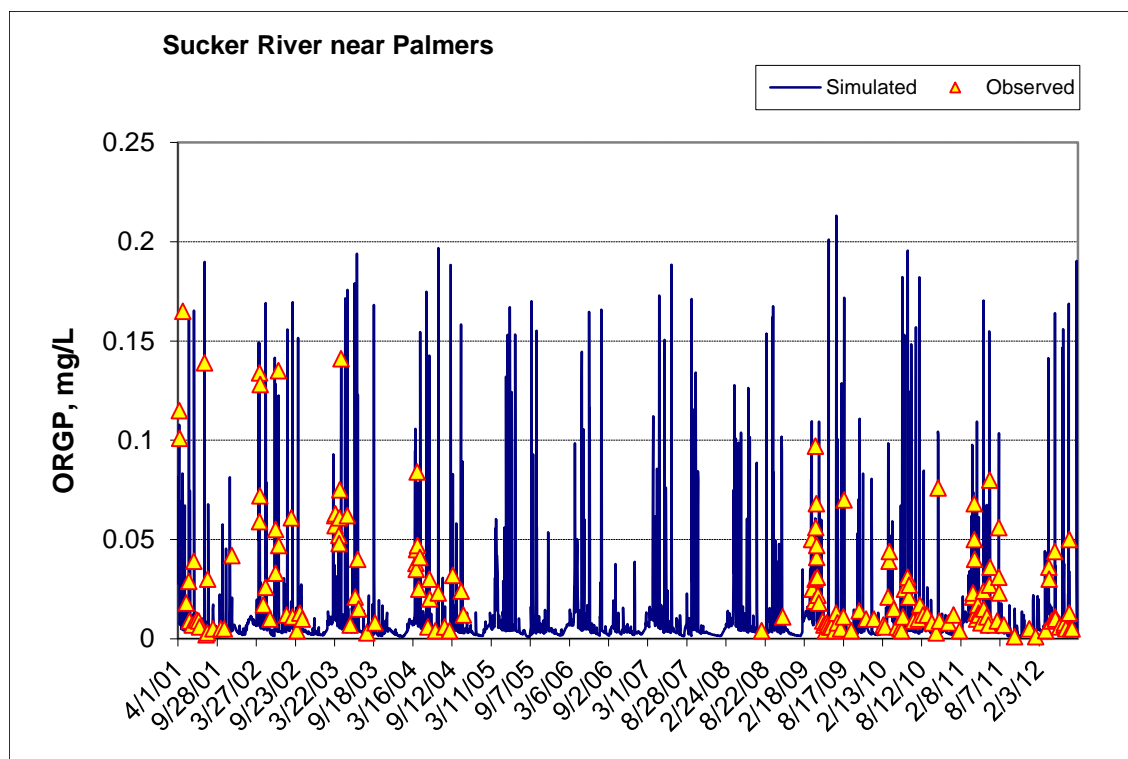


Figure 127. Time series of observed and simulated Organic Phosphorus (OrgP) concentration at Sucker River near Palmers

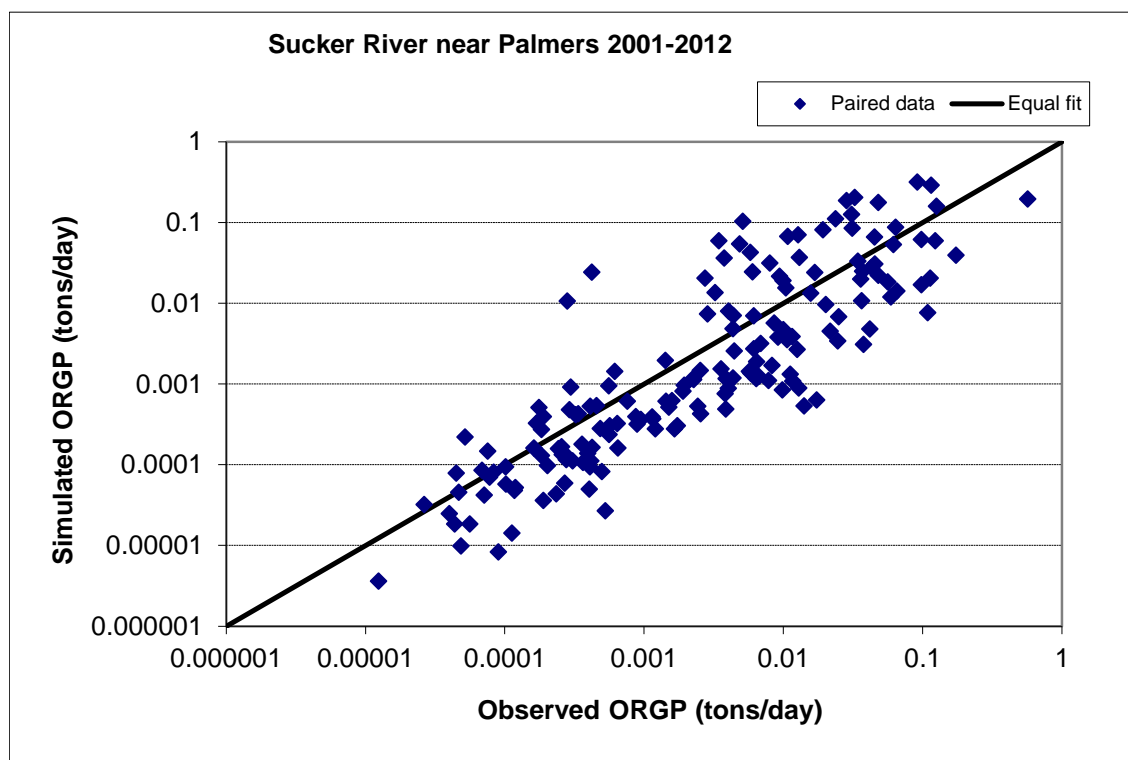


Figure 128. Paired simulated vs. observed Organic Phosphorus (OrgP) load at Sucker River near Palmers

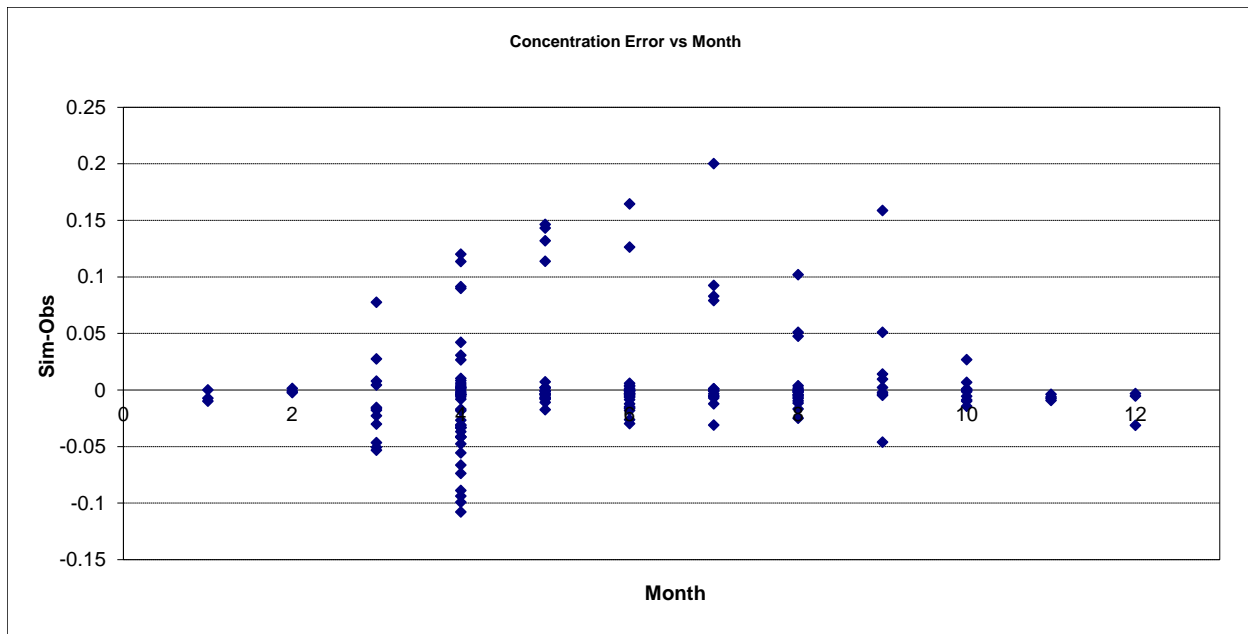


Figure 129. Residual (Simulated - Observed) vs. Month Organic Phosphorus (OrgP) at Sucker River near Palmers

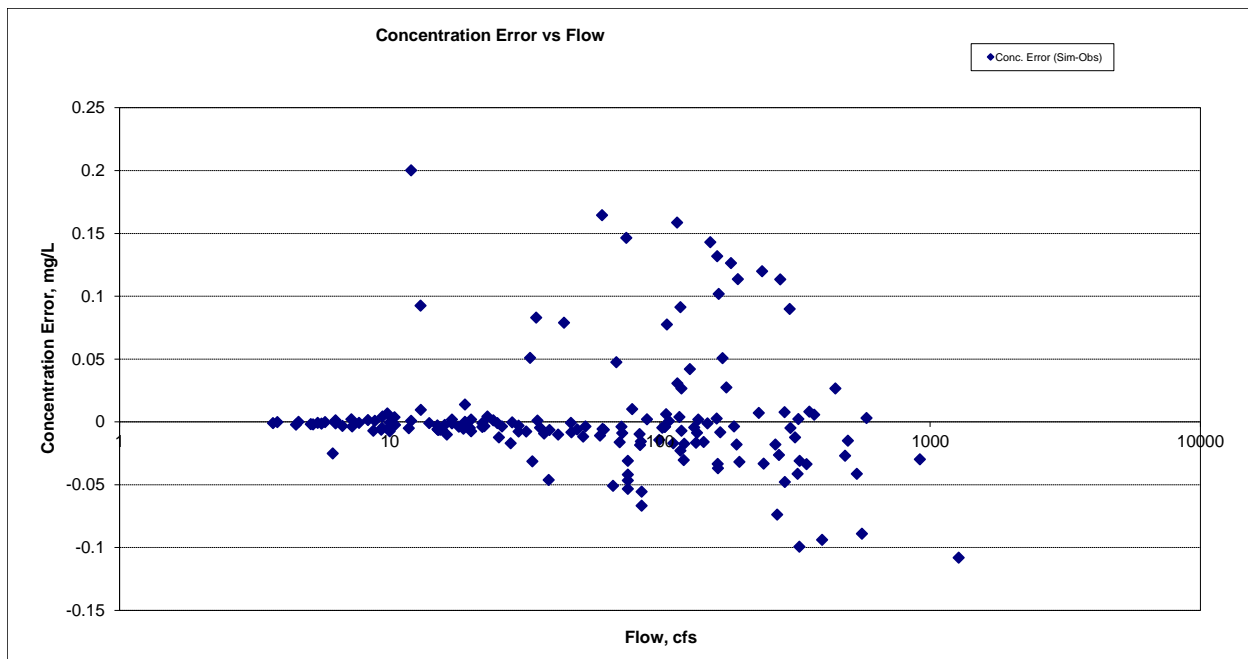


Figure 130. Residual (Simulated - Observed) vs. Flow Organic Phosphorus (OrgP) at Sucker River near Palmers

Total Phosphorus (TP)

Table 27. Total Phosphorus (TP) statistics

Count	232
Concentration Average Error	5.14%
Concentration Median Error	-9.19%
Load Ave Error	9.67%
Load Median Error	-0.58%
Paired t concentration	0.98
Paired t load	0.77

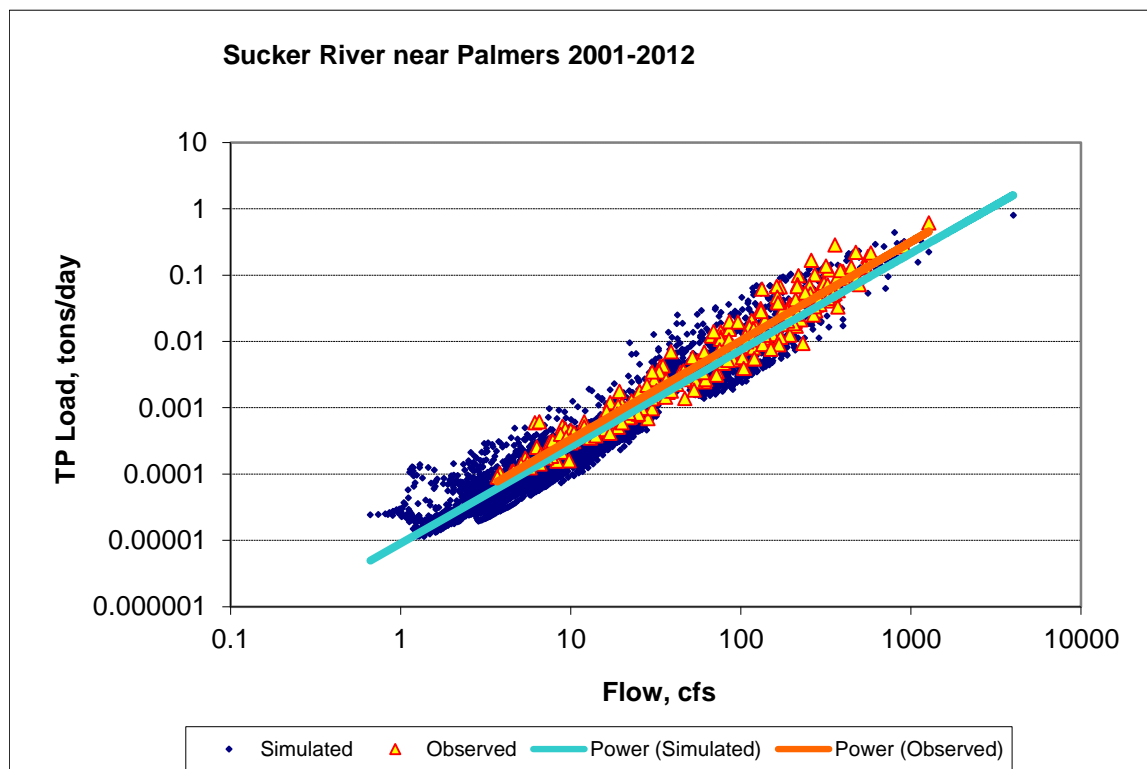


Figure 131. Power plot of simulated and observed Total Phosphorus (TP) load vs flow at Sucker River near Palmers

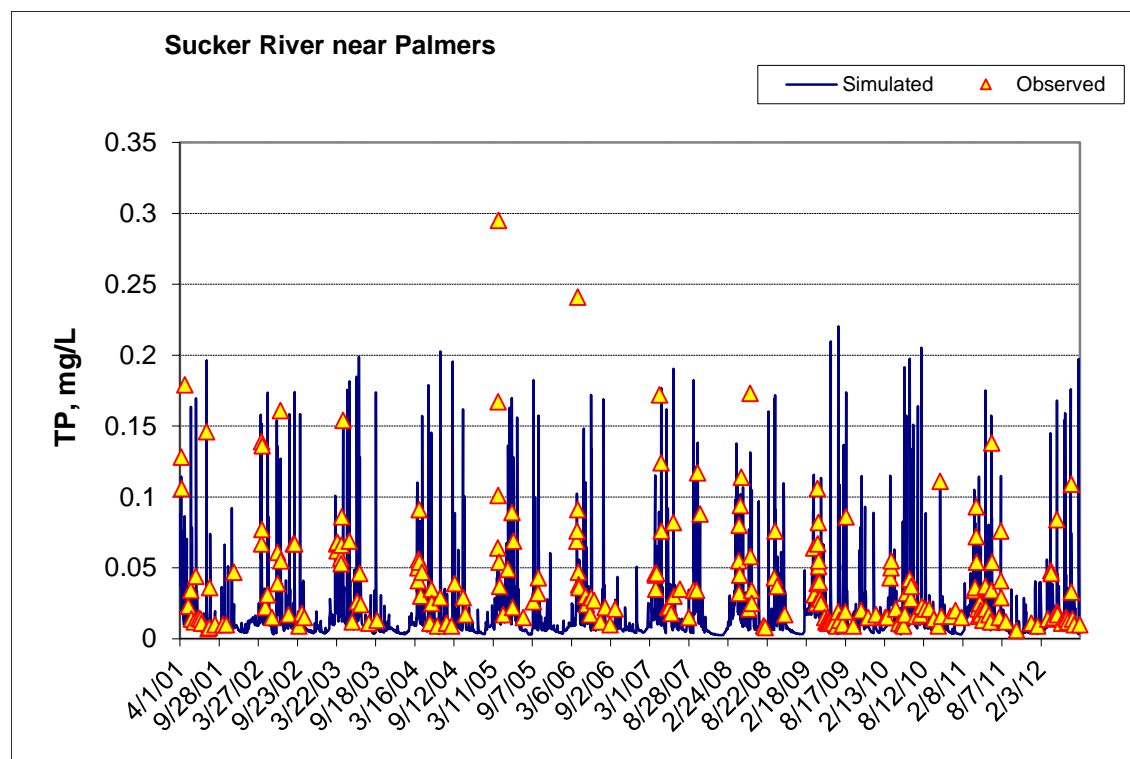


Figure 132. Time series of observed and simulated Total Phosphorus (TP) concentration at Sucker River near Palmers

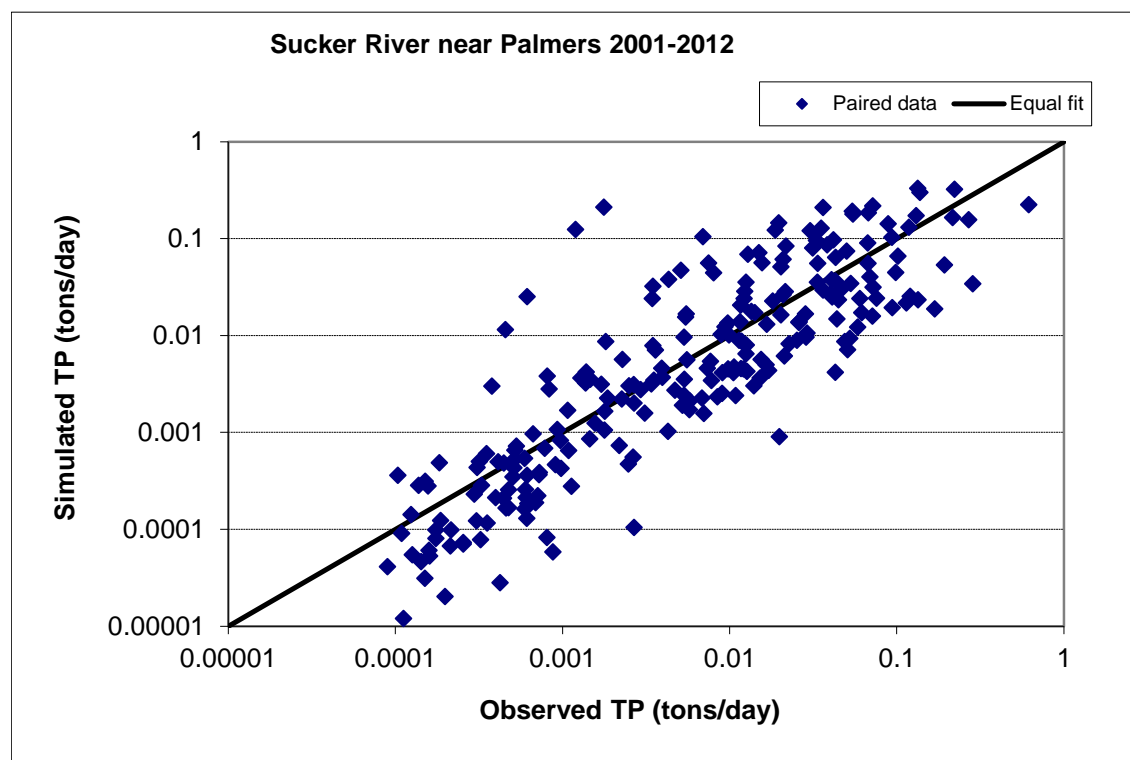


Figure 133. Paired simulated vs. observed Total Phosphorus (TP) load at Sucker River near Palmers

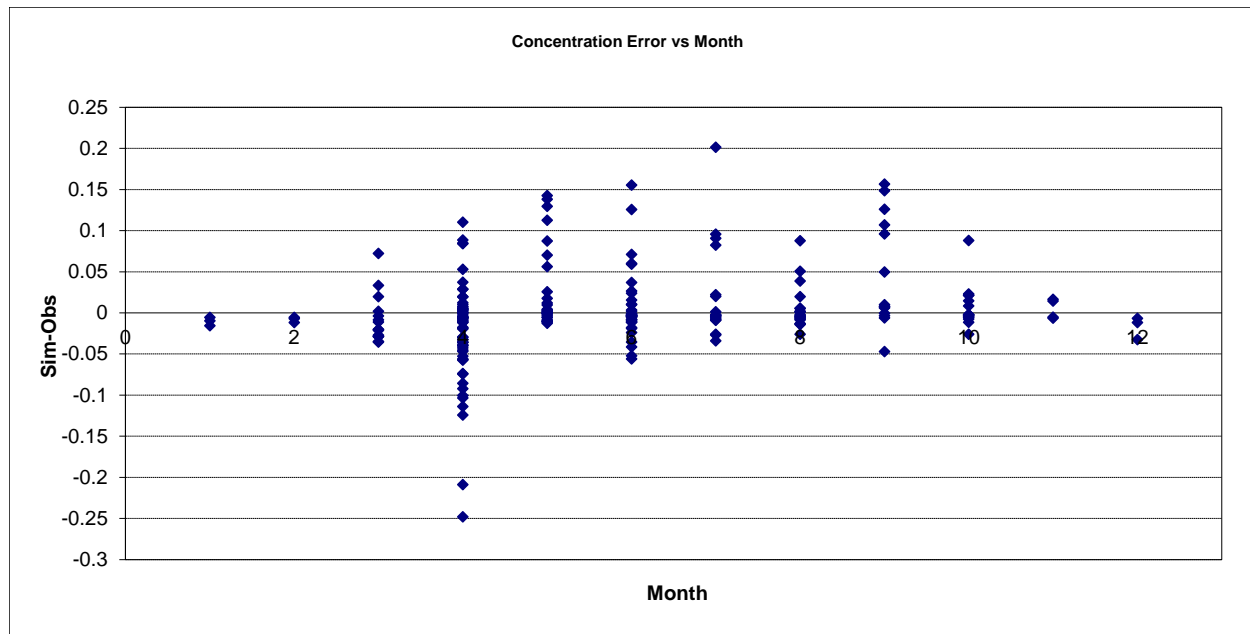


Figure 134. Residual (Simulated - Observed) vs. Month Total Phosphorus (TP) at Sucker River near Palmers

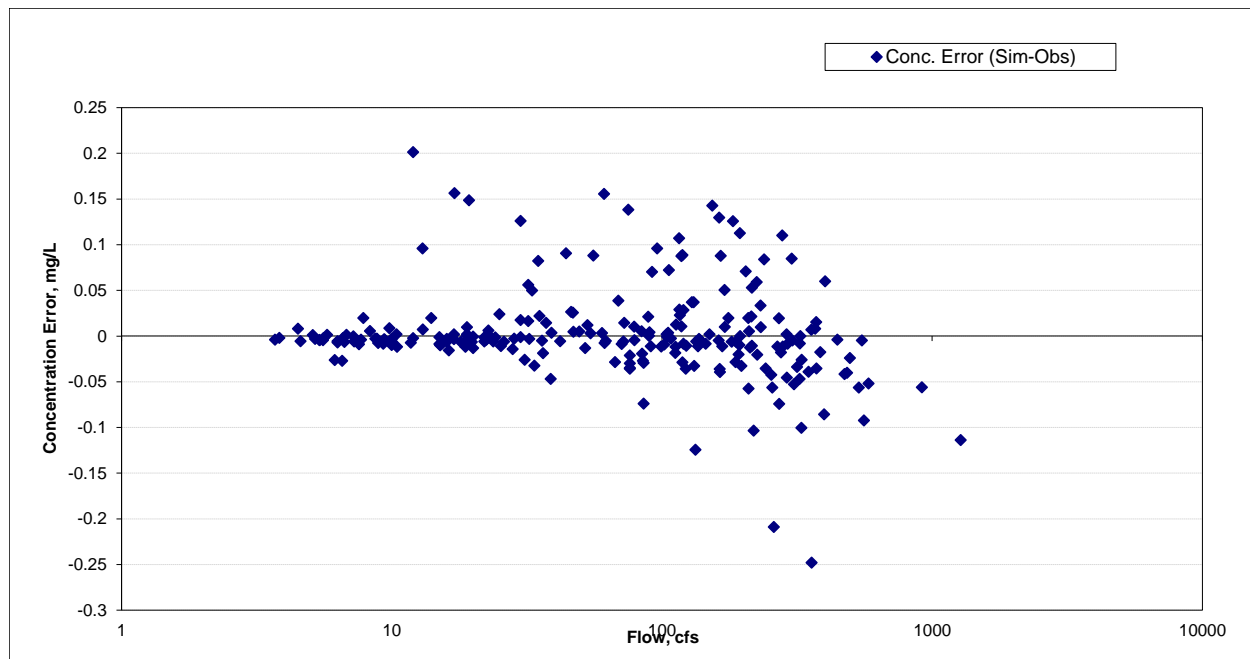


Figure 135. Residual (Simulated - Observed) vs. Flow Total Phosphorus (TP) at Sucker River near Palmers

Knife River near Two Harbors (HYDSTRA 02026001)

Total Suspended Solids (TSS)

Table 28. Total Suspended Solids (TSS) statistics

Count	231
Concentration Average Error	-11.69%
Concentration Median Error	-2.83%
Load Average Error	-29.17%
Load Median Error	-0.13%
Paired t concentration	0.78
Paired t load	0.33

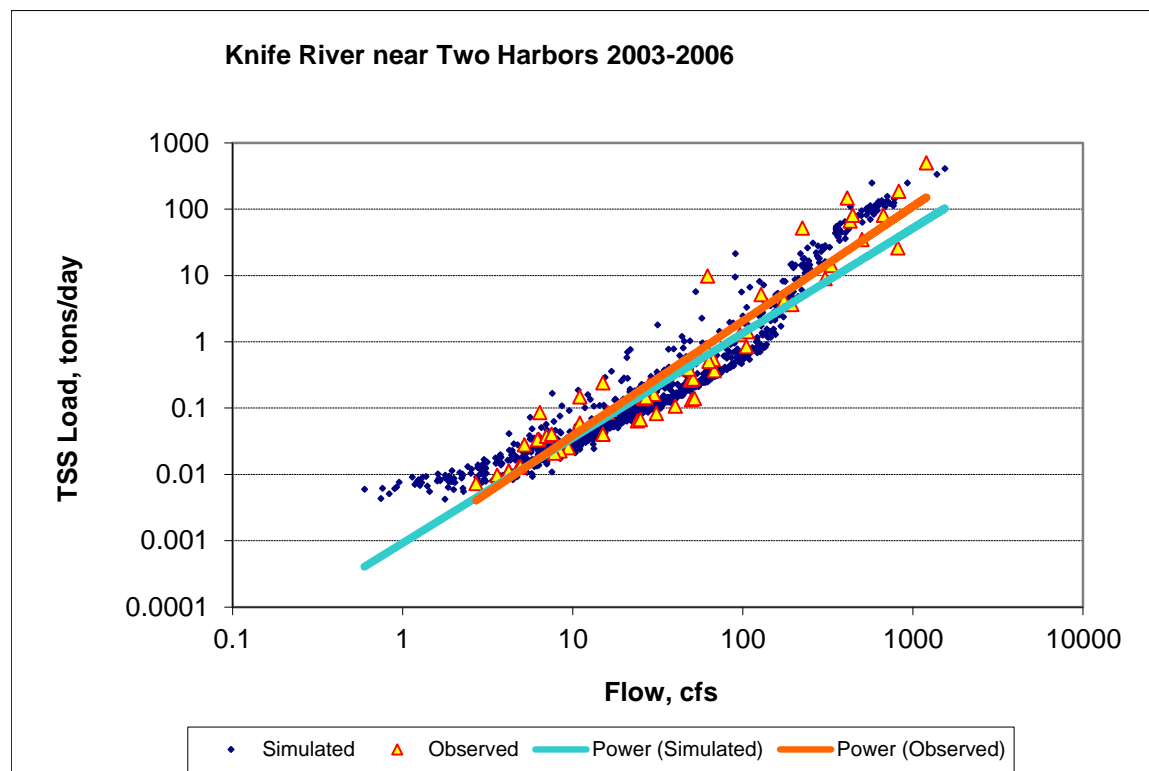


Figure 136. Power plot of simulated and observed Total Suspended Solids (TSS) load vs flow at Knife River near Two Harbors

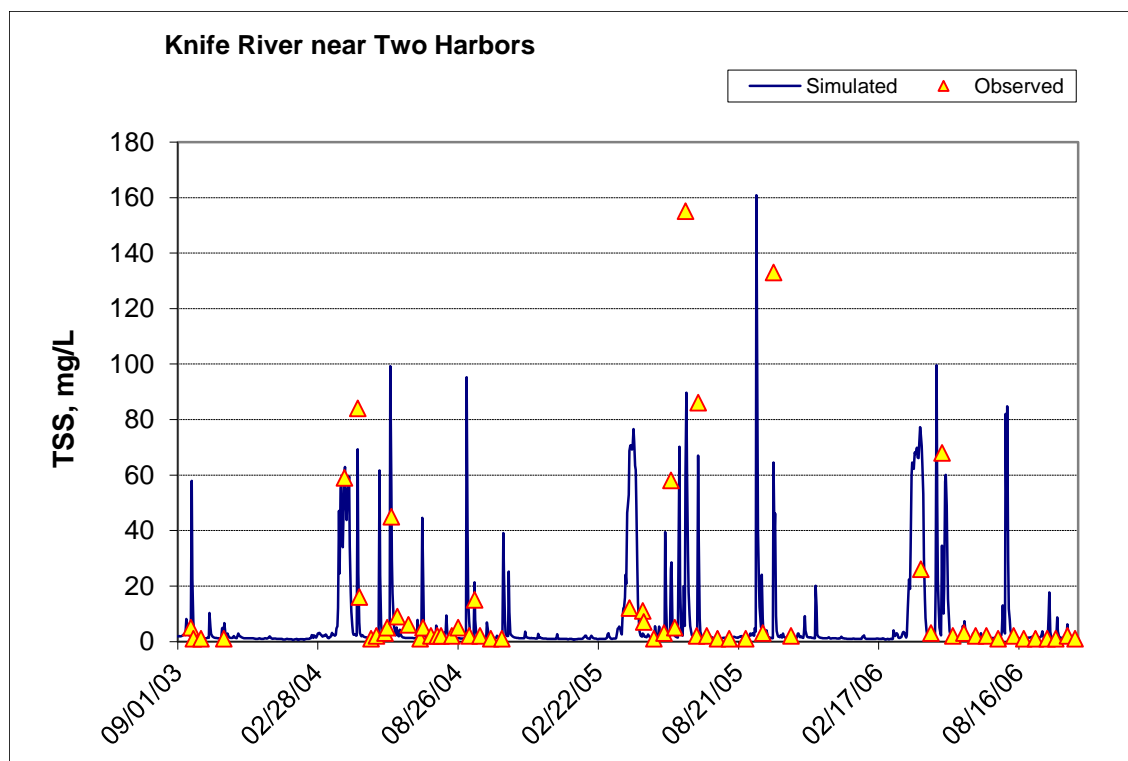


Figure 137. Time series of observed and simulated Total Suspended Solids (TSS) concentration at Knife River near Two Harbors

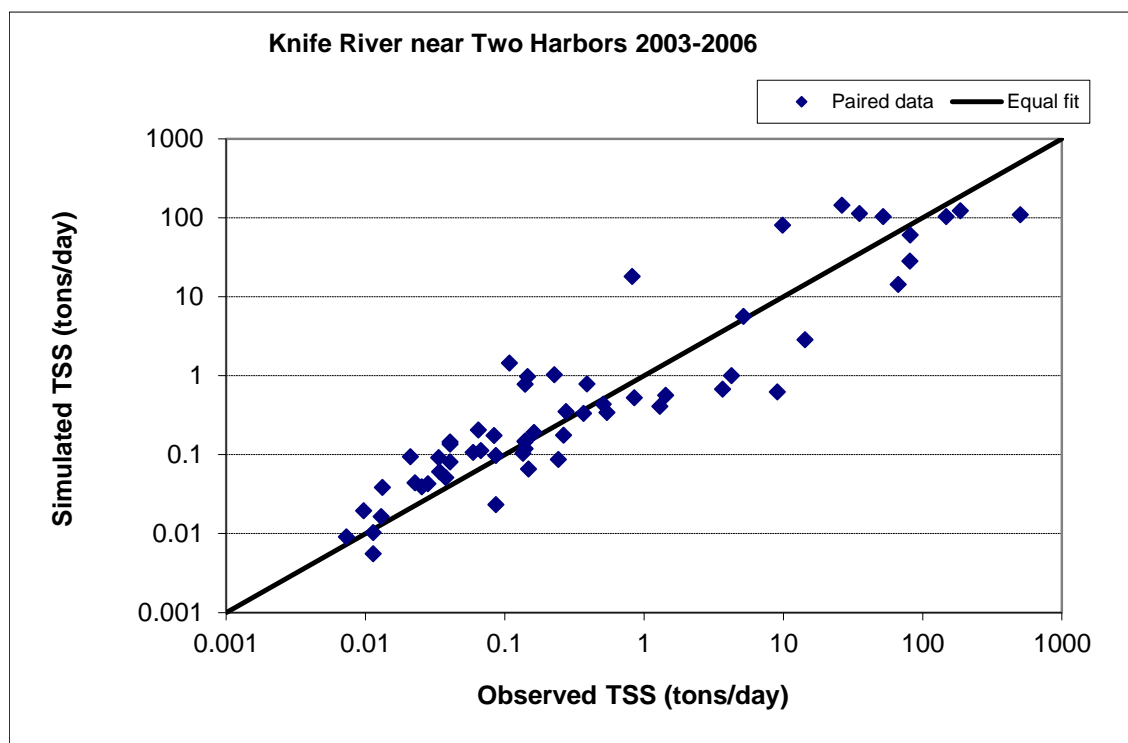


Figure 138. Paired simulated vs. observed Total Suspended Solids (TSS) load at Knife River near Two Harbors

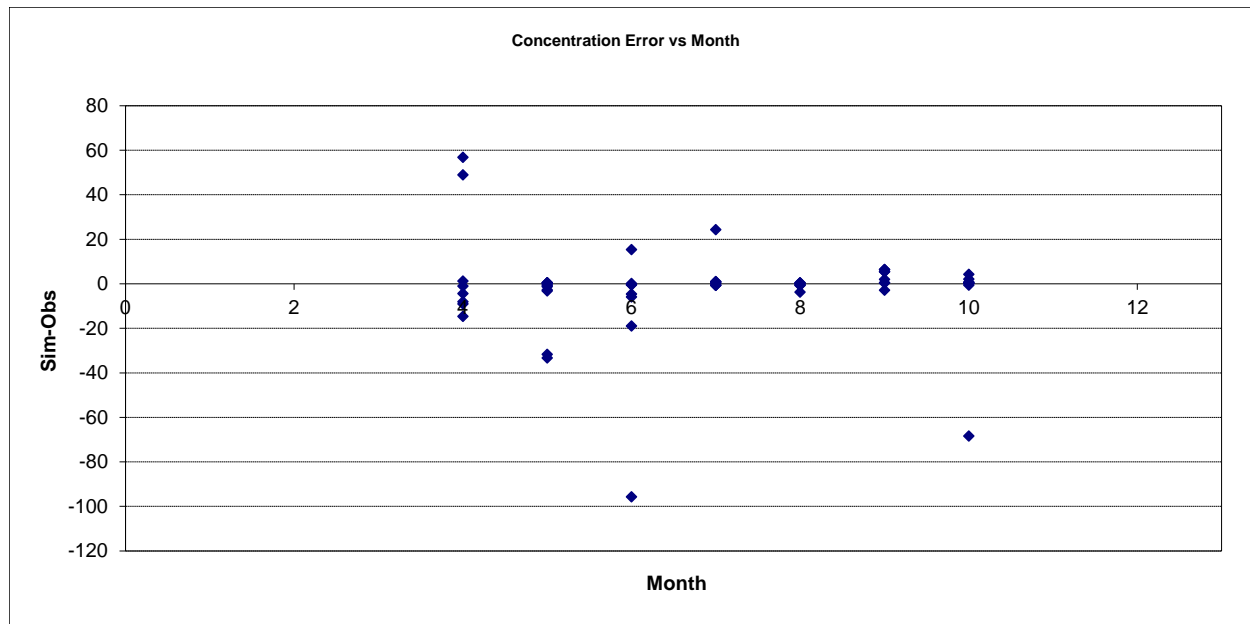


Figure 139. Residual (Simulated - Observed) vs. Month Total Suspended Solids (TSS) at Knife River near Two Harbors

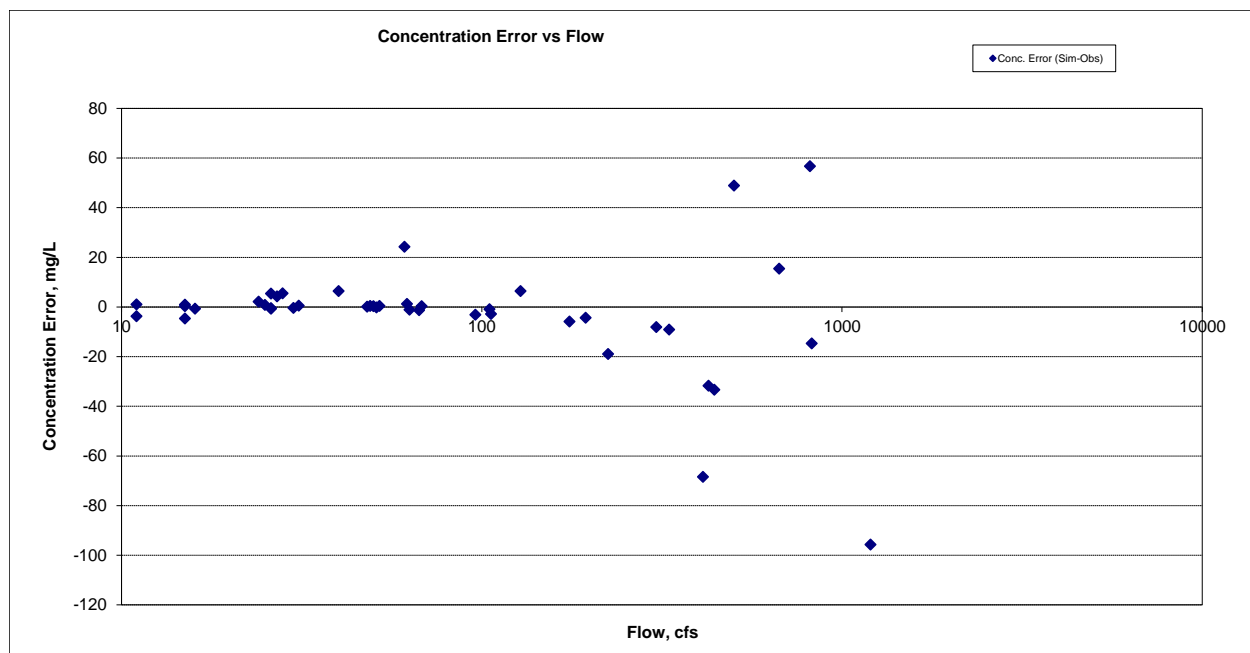


Figure 140. Residual (Simulated - Observed) vs. Flow Total Suspended Solids (TSS) at Knife River near Two Harbors

Knife River near Two Harbors (EQUIS S000-257)

Total Suspended Solids (TSS)

Table 29. Total Suspended Solids (TSS) statistics

Count	86	21
Concentration Average Error	-21.65%	5.42%
Concentration Median Error	1.07%	16.98%
Load Ave Error	-64.01%	119.29%
Load Median Error	0.01%	4.88%
Paired t concentration	0.47	0.70
Paired t load	0.22	0.09

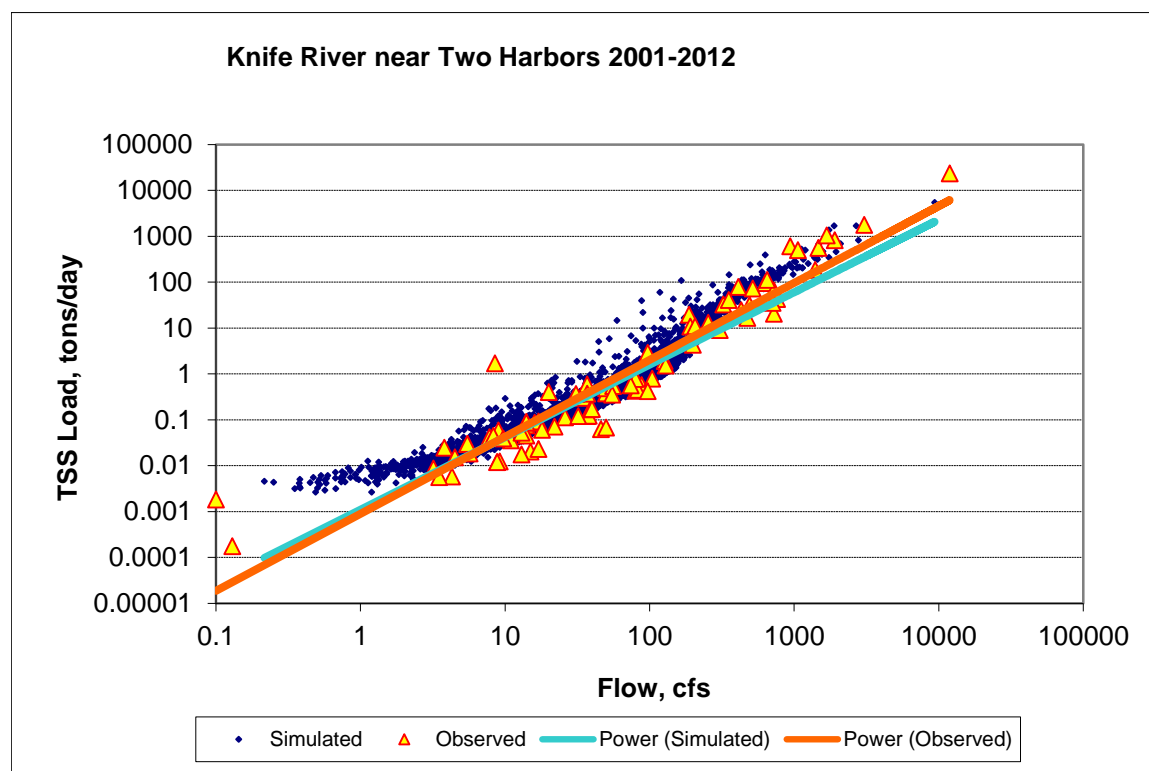


Figure 141. Power plot of simulated and observed Total Suspended Solids (TSS) load vs flow at Knife River near Two Harbors (calibration period)

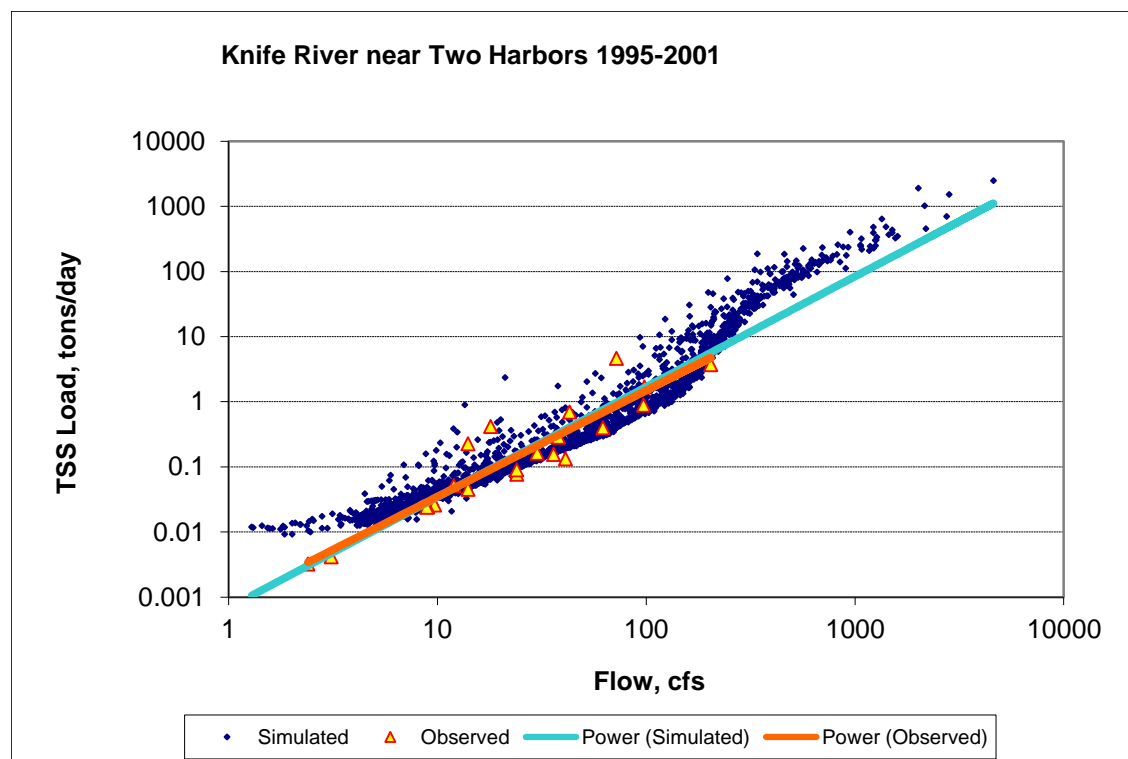


Figure 142. Power plot of simulated and observed Total Suspended Solids (TSS) load vs flow at Knife River near Two Harbors (validation period)

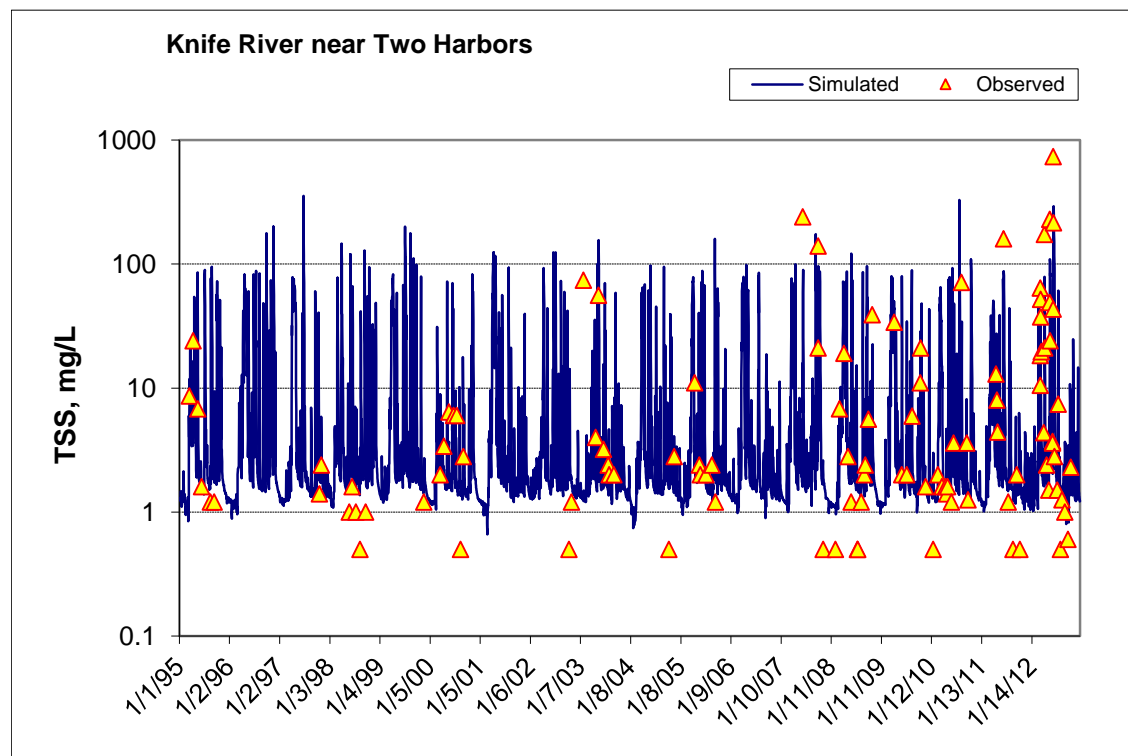


Figure 143. Time series of observed and simulated Total Suspended Solids (TSS) concentration at Knife River near Two Harbors (calibration period)

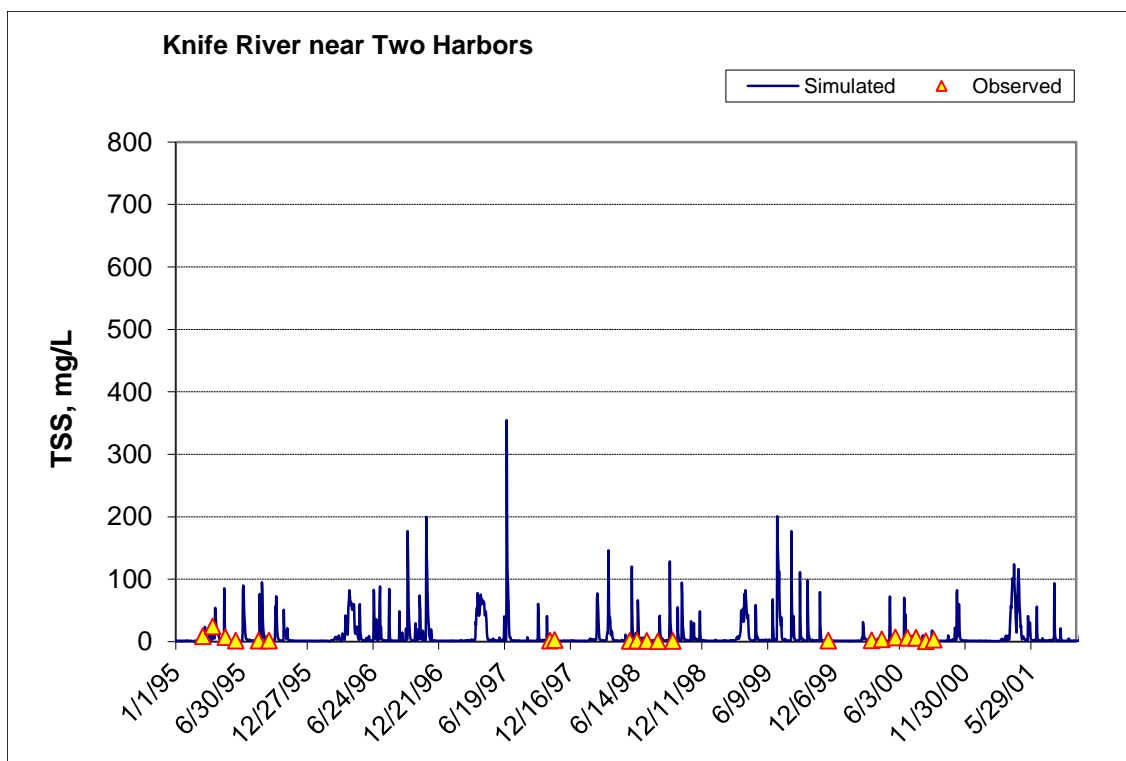


Figure 144. Time series of observed and simulated Total Suspended Solids (TSS) concentration at Knife River near Two Harbors (validation period)

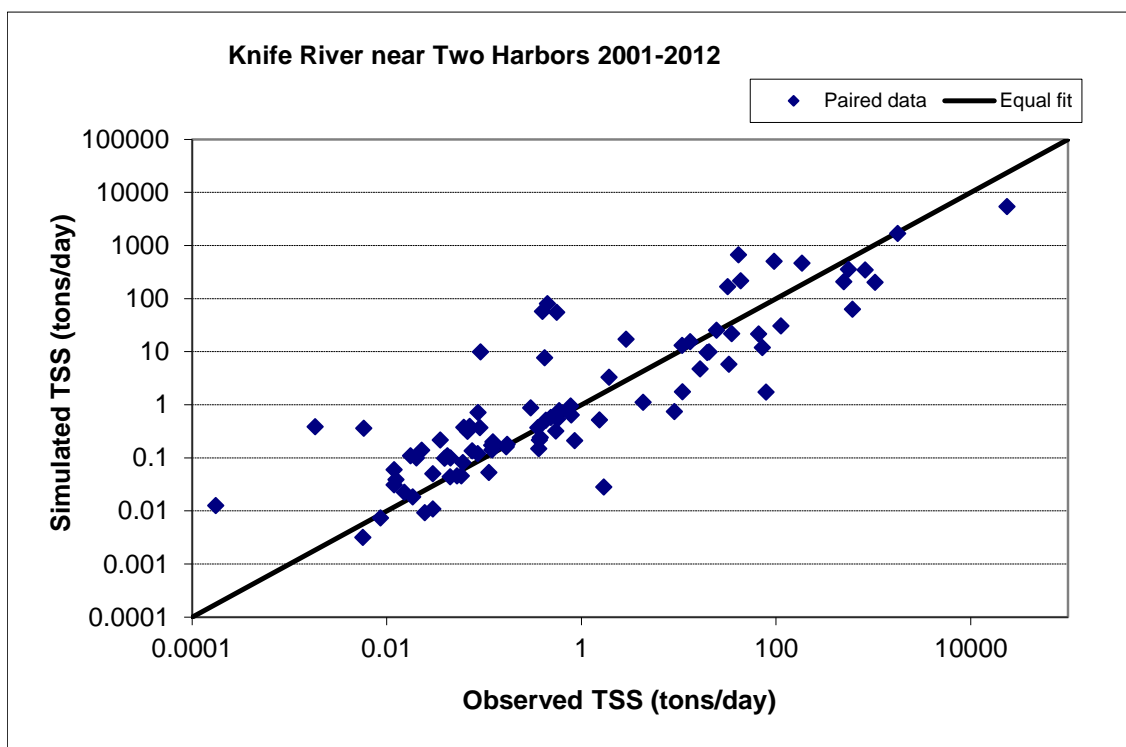


Figure 145. Paired simulated vs. observed Total Suspended Solids (TSS) load at Knife River near Two Harbors (calibration period)

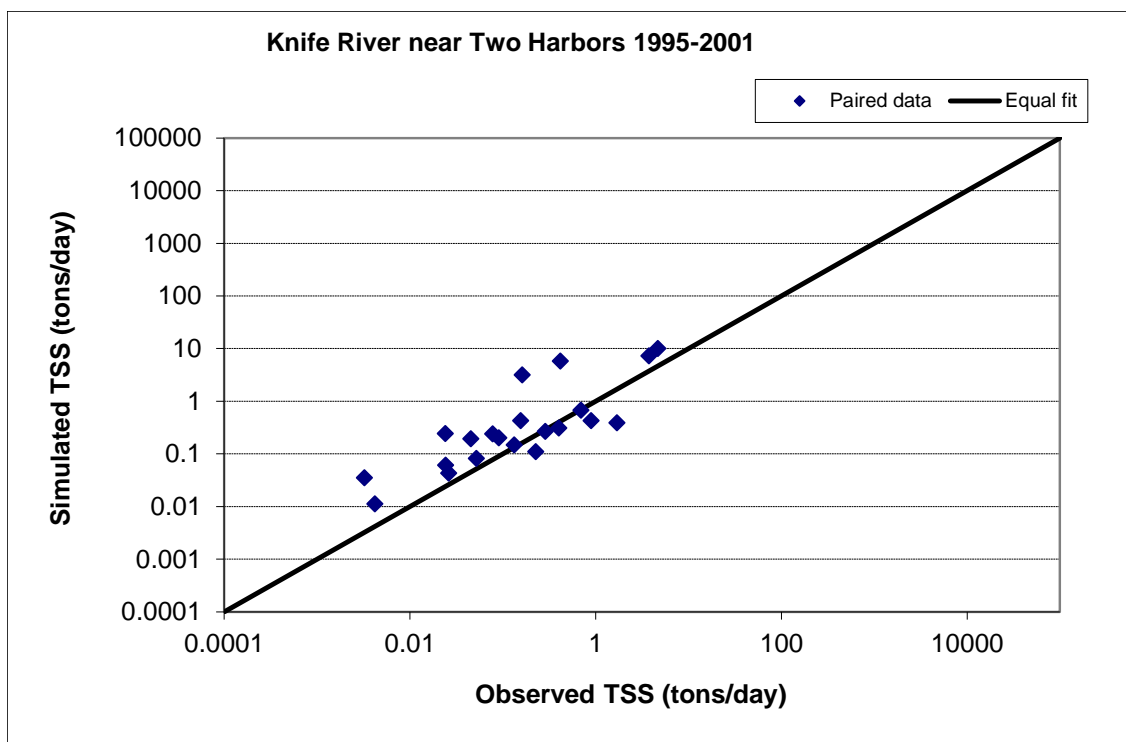


Figure 146. Paired simulated vs. observed Total Suspended Solids (TSS) load at Knife River near Two Harbors (validation period)

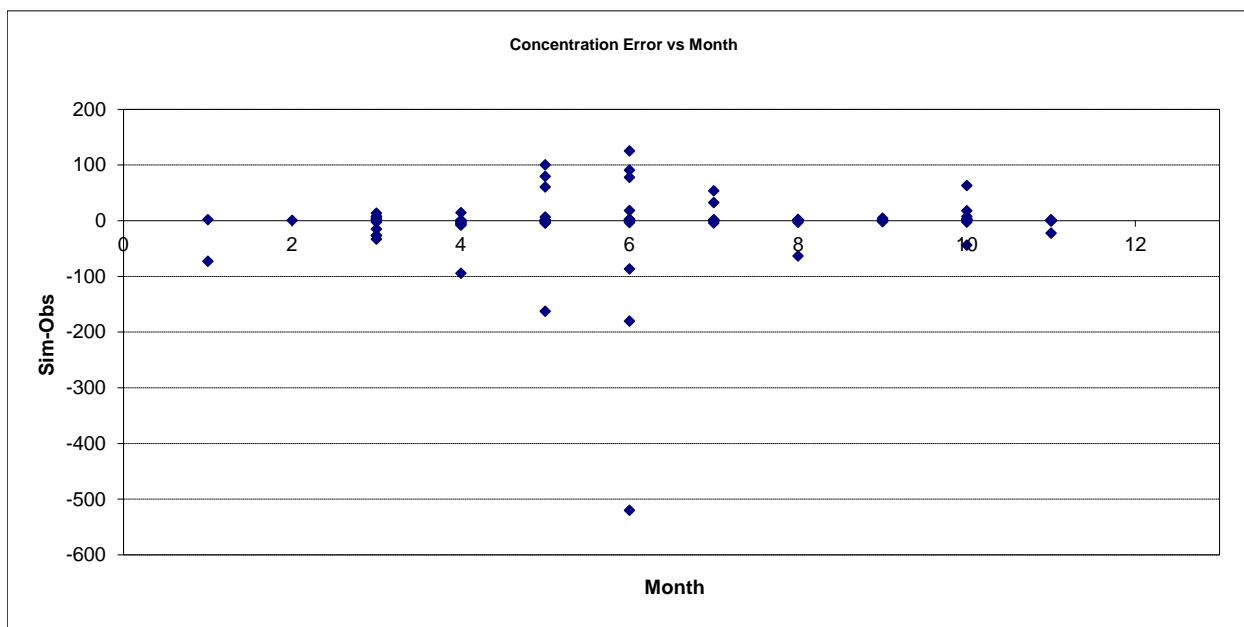


Figure 147. Residual (Simulated - Observed) vs. Month Total Suspended Solids (TSS) at Knife River near Two Harbors

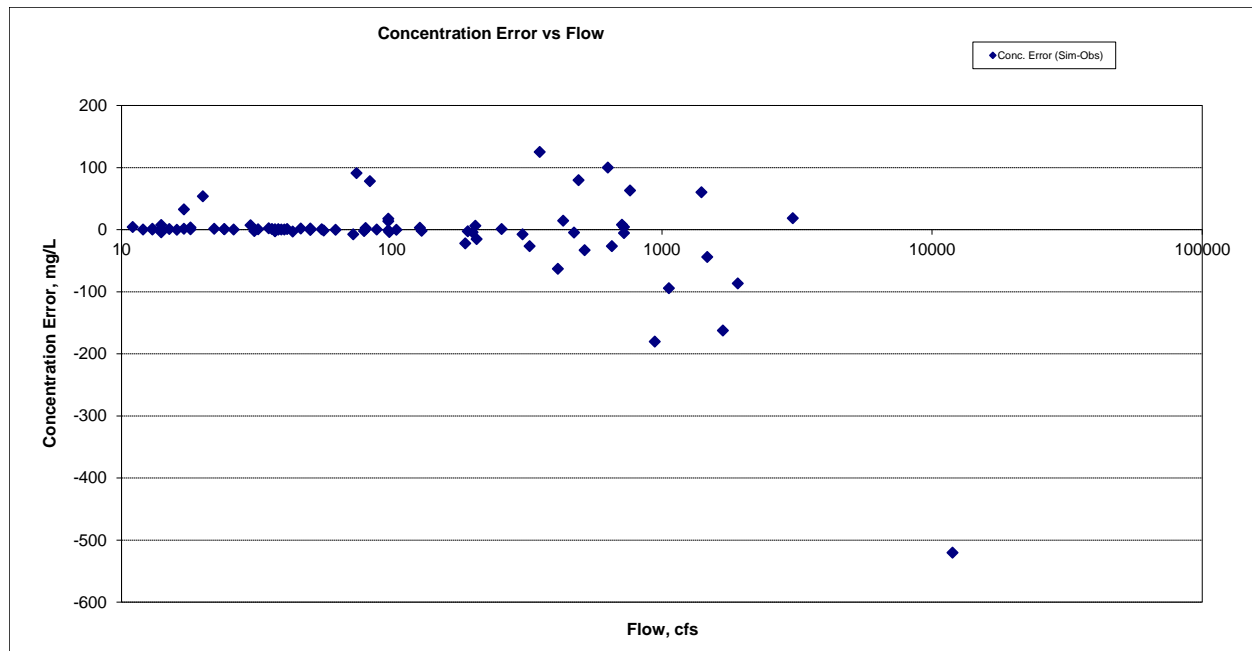


Figure 148. Residual (Simulated - Observed) vs. Flow Total Suspended Solids (TSS) at Knife River near Two Harbors

Ammonia Nitrogen (NH₃)

Table 30. Ammonia Nitrogen (NH₃) statistics

Count	36	28
Concentration Average Error	15.19%	80.64%
Concentration Median Error	21.20%	87.62%
Load Ave Error	318.68%	224.87%
Load Median Error	1.14%	131.23%
Paired t concentration	0.57	0.01
Paired t load	0.06	0.00

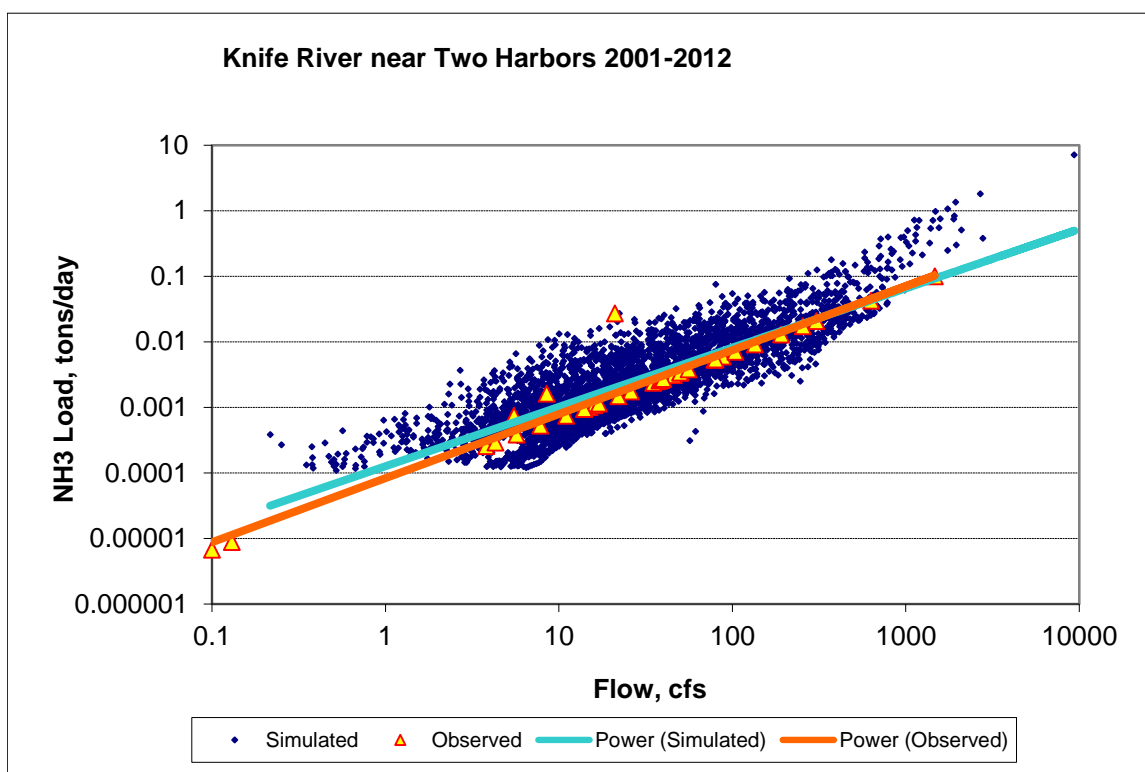


Figure 149. Power plot of simulated and observed Ammonia Nitrogen (NH₃) load vs flow at Knife River near Two Harbors (calibration period)

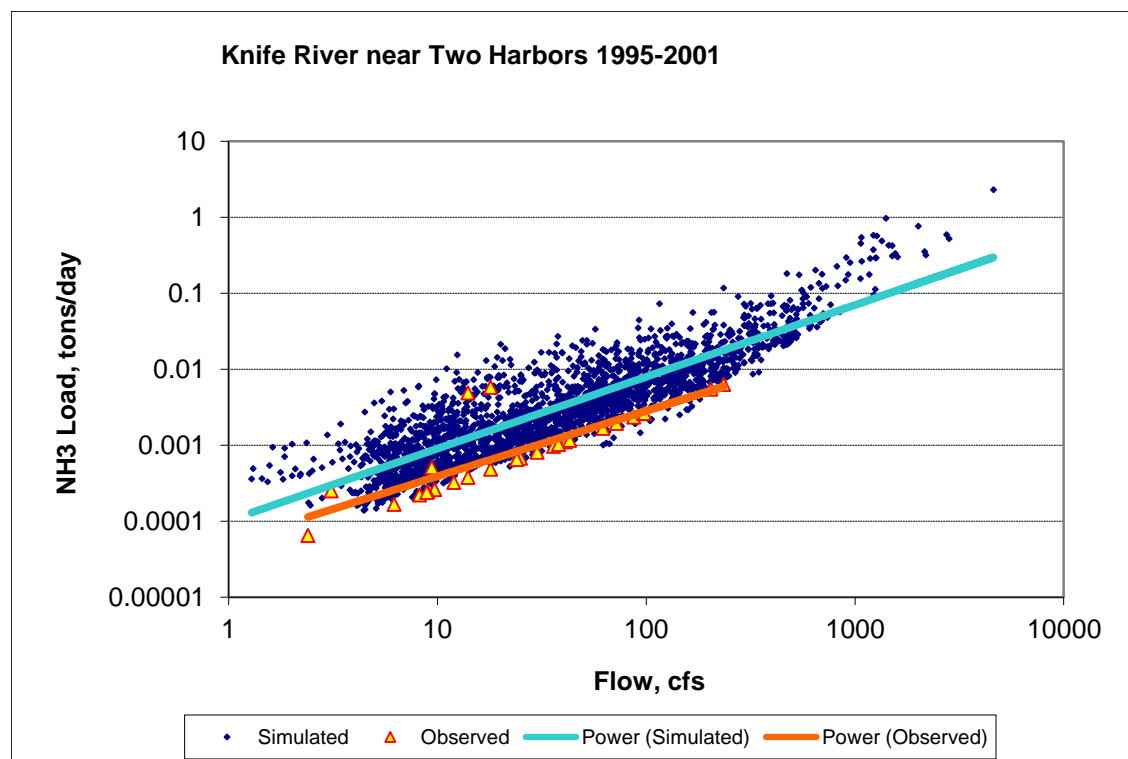


Figure 150. Power plot of simulated and observed Ammonia Nitrogen (NH₃) load vs flow at Knife River near Two Harbors (validation period)

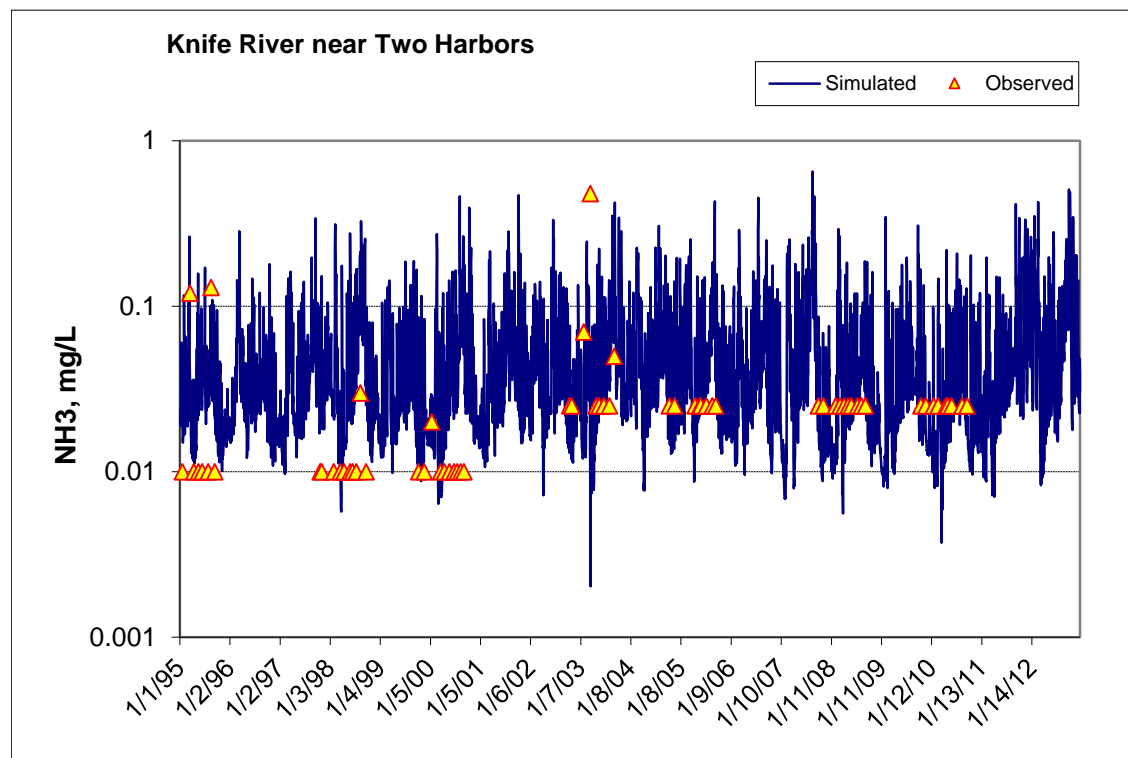


Figure 151. Time series of observed and simulated Ammonia Nitrogen (NH₃) concentration at Knife River near Two Harbors (calibration period)

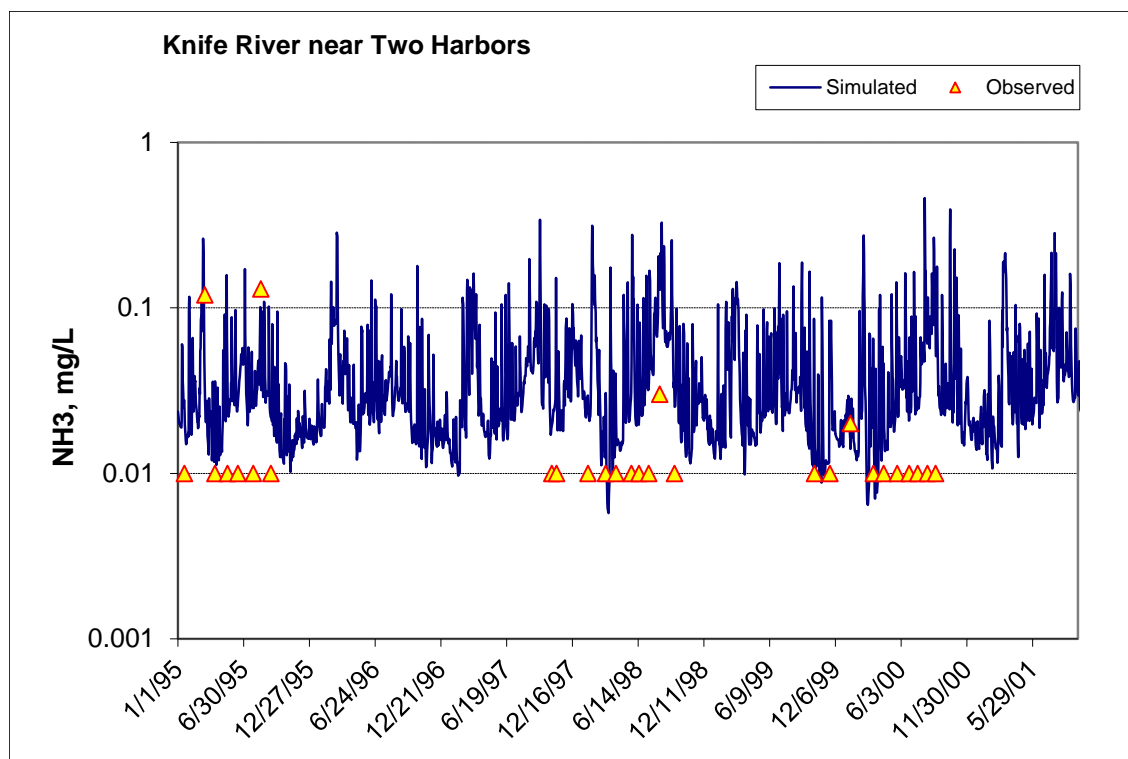


Figure 152. Time series of observed and simulated Ammonia Nitrogen (NH₃) concentration at Knife River near Two Harbors (validation period)

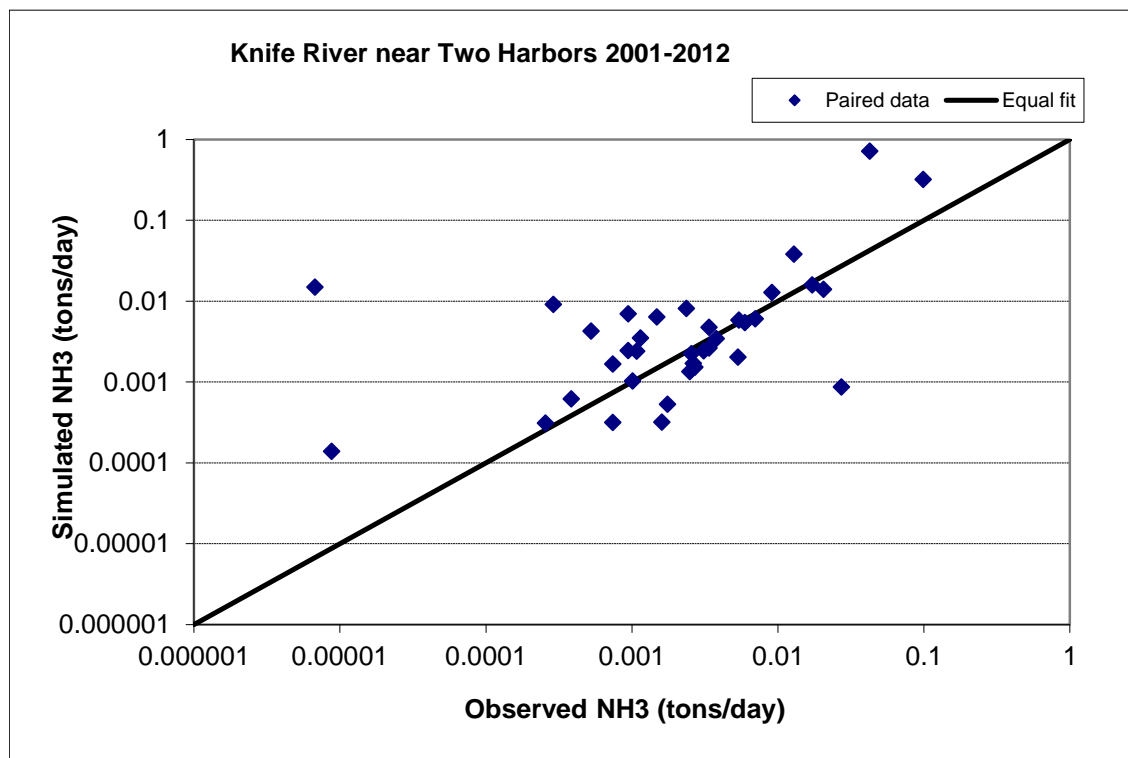


Figure 153. Paired simulated vs. observed Ammonia Nitrogen (NH₃) load at Knife River near Two Harbors (calibration period)

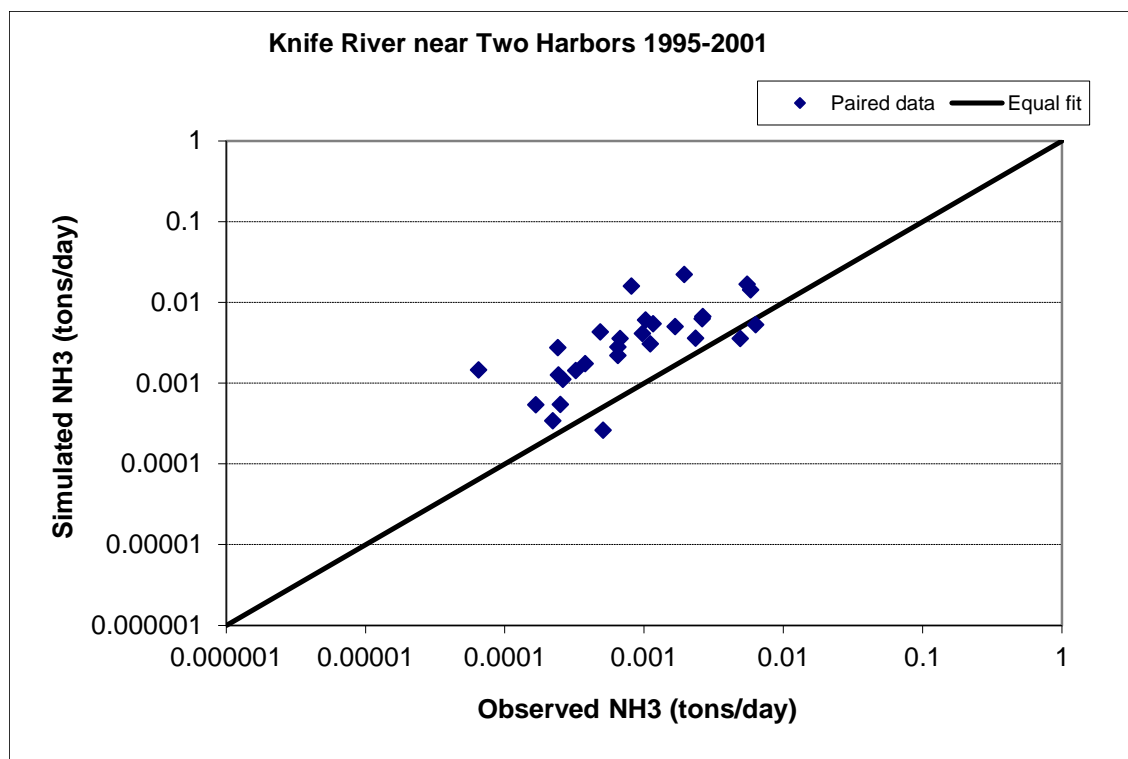


Figure 154. Paired simulated vs. observed Ammonia Nitrogen (NH₃) load at Knife River near Two Harbors (validation period)

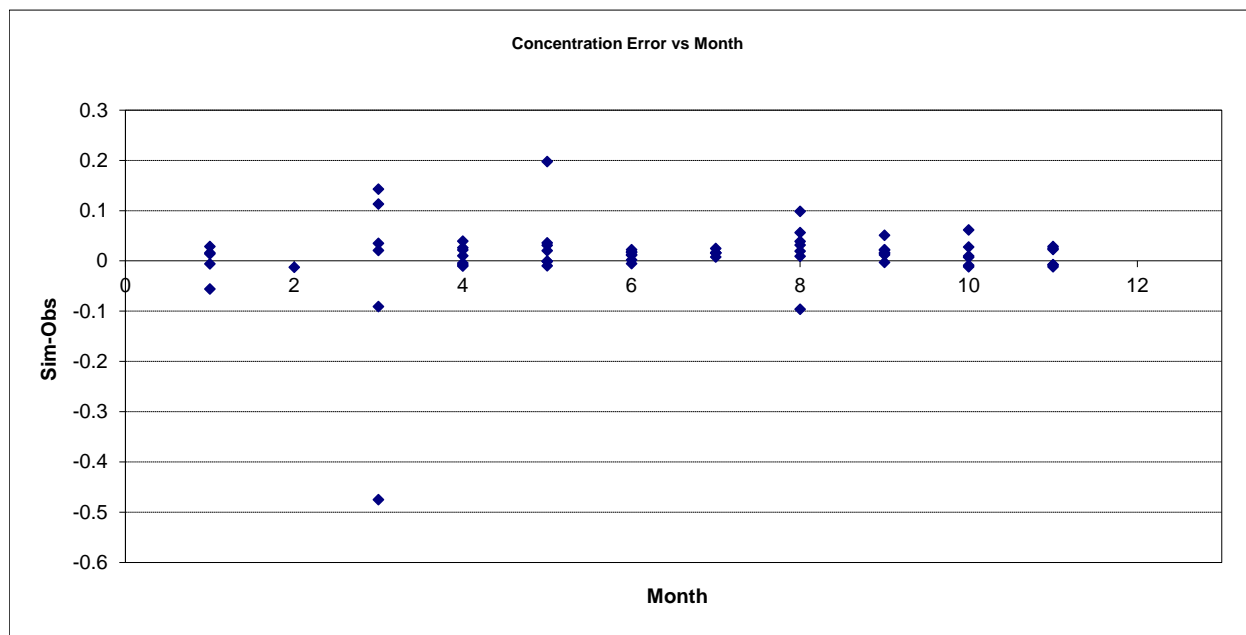


Figure 155. Residual (Simulated - Observed) vs. Month Ammonia Nitrogen (NH₃) at Knife River near Two Harbors

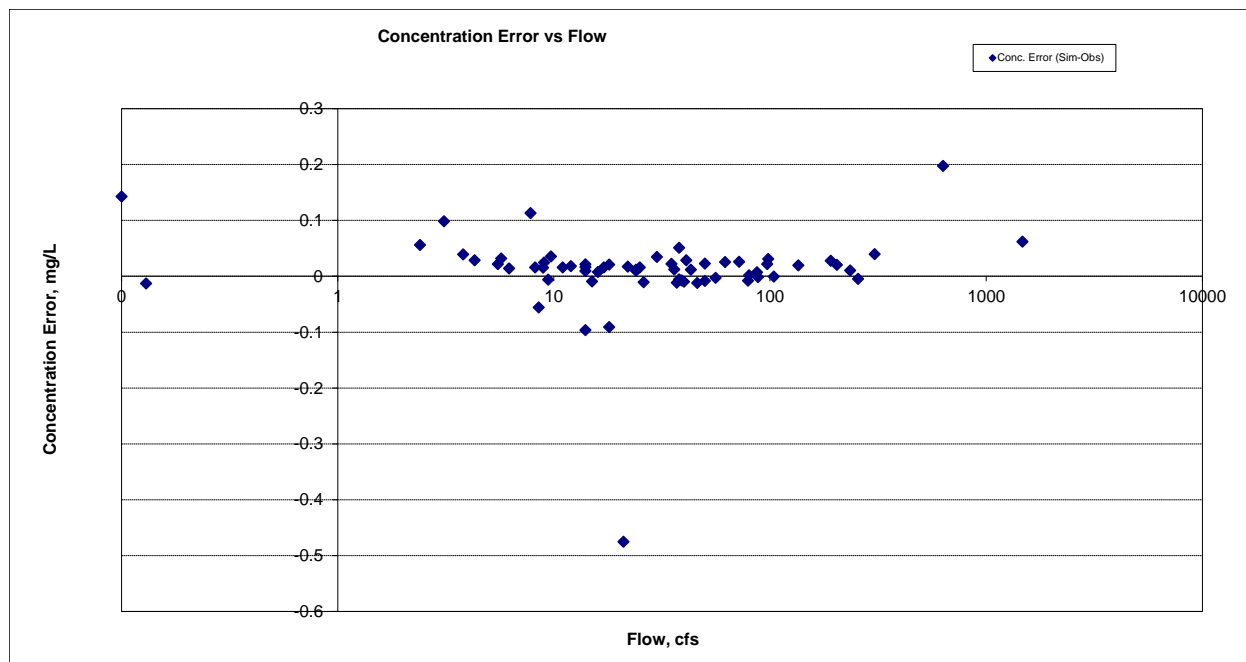


Figure 156. Residual (Simulated - Observed) vs. Flow Ammonia Nitrogen (NH₃) at Knife River near Two Harbors

Nitrite+ Nitrate Nitrogen (NO_x)

Table 31. Nitrite+ Nitrate Nitrogen (NO_x) statistics

Count	56	28
Concentration Average Error	27.92%	-14.05%
Concentration Median Error	13.35%	8.31%
Load Ave Error	280.83%	4.15%
Load Median Error	21.07%	0.48%
Paired t concentration	0.39	0.64
Paired t load	0.01	0.66

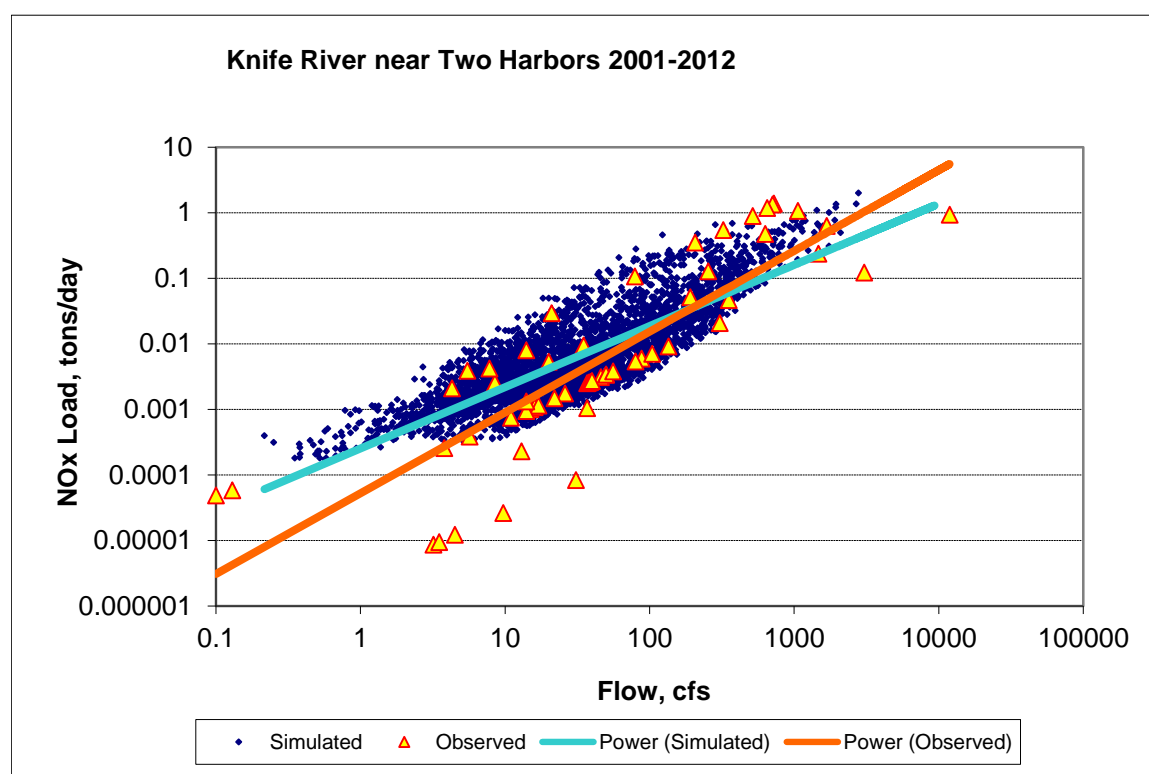


Figure 157. Power plot of simulated and observed Nitrite+ Nitrate Nitrogen (NO_x) load vs flow at Knife River near Two Harbors (calibration period)

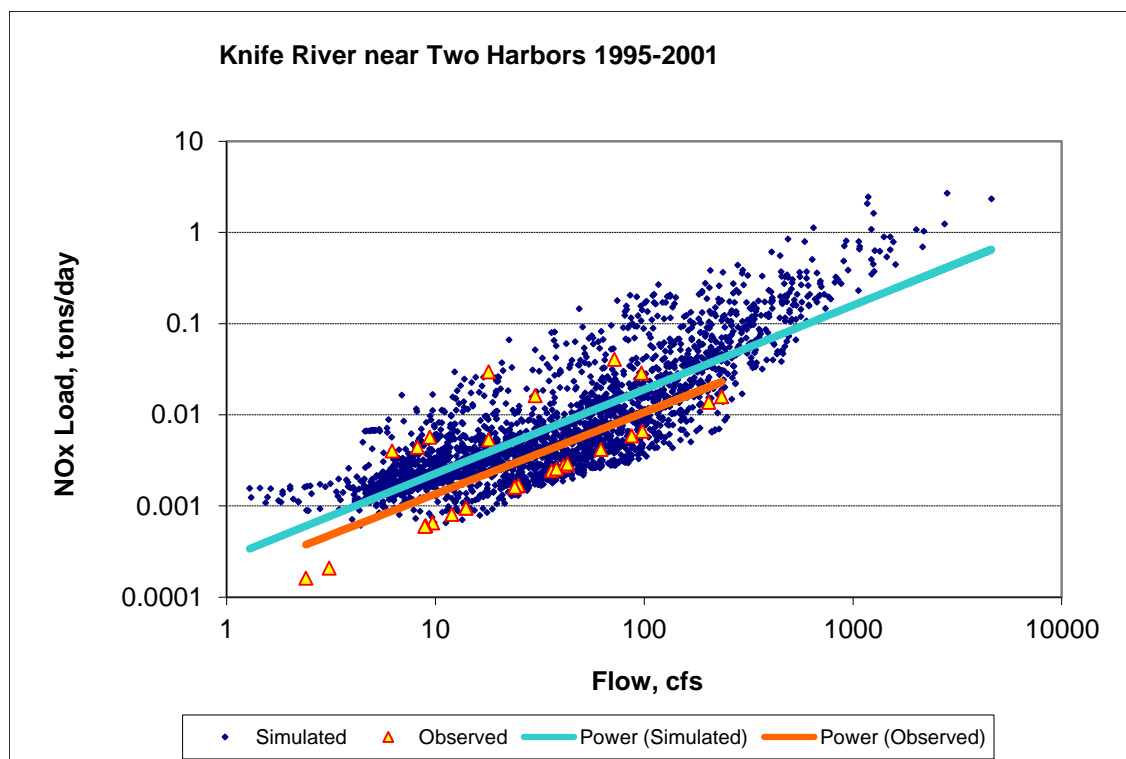


Figure 158. Power plot of simulated and observed Nitrite+ Nitrate Nitrogen (NOx) load vs flow at Knife River near Two Harbors (validation period)

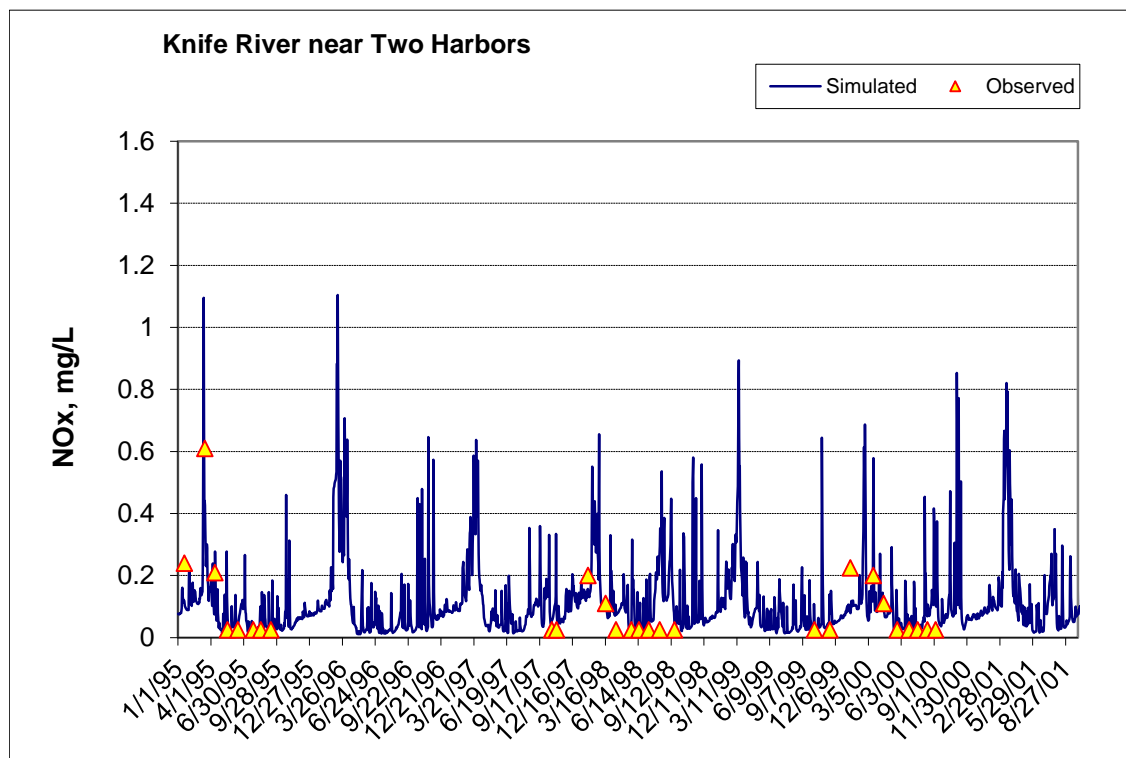


Figure 159. Time series of observed and simulated Nitrite+ Nitrate Nitrogen (NOx) concentration at Knife River near Two Harbors (calibration period)

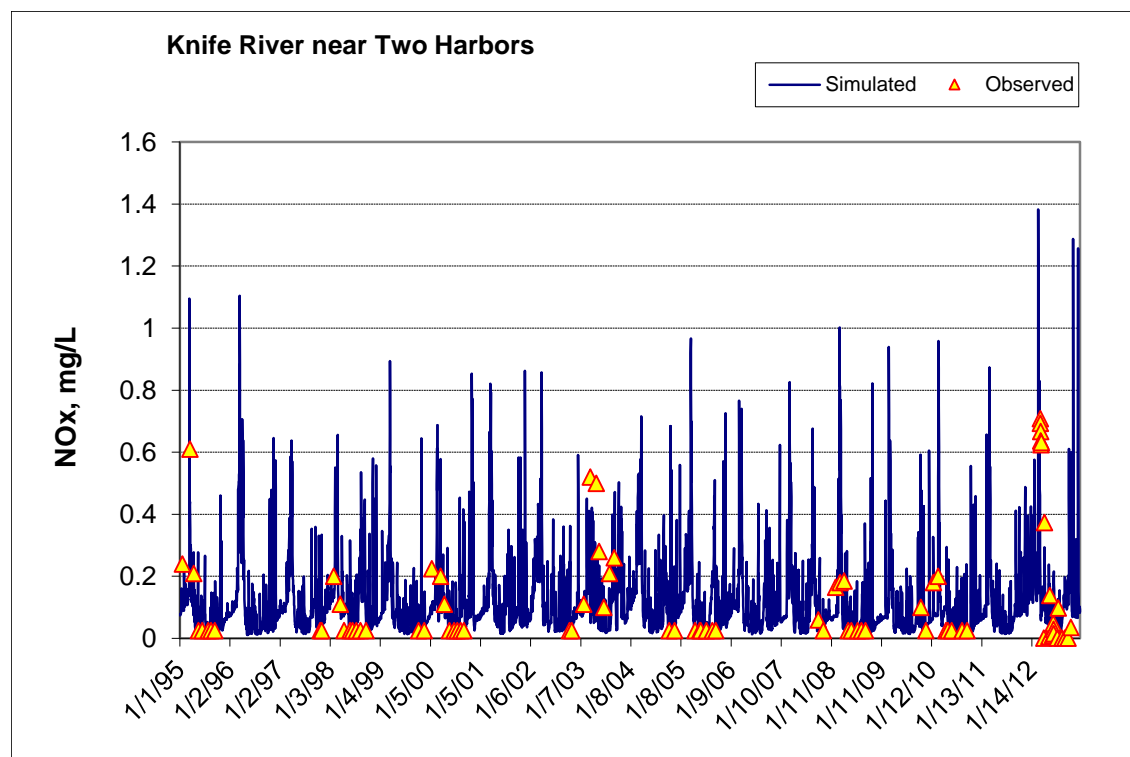


Figure 160. Time series of observed and simulated Nitrite+ Nitrate Nitrogen (NOx) concentration at Knife River near Two Harbors (validation period)

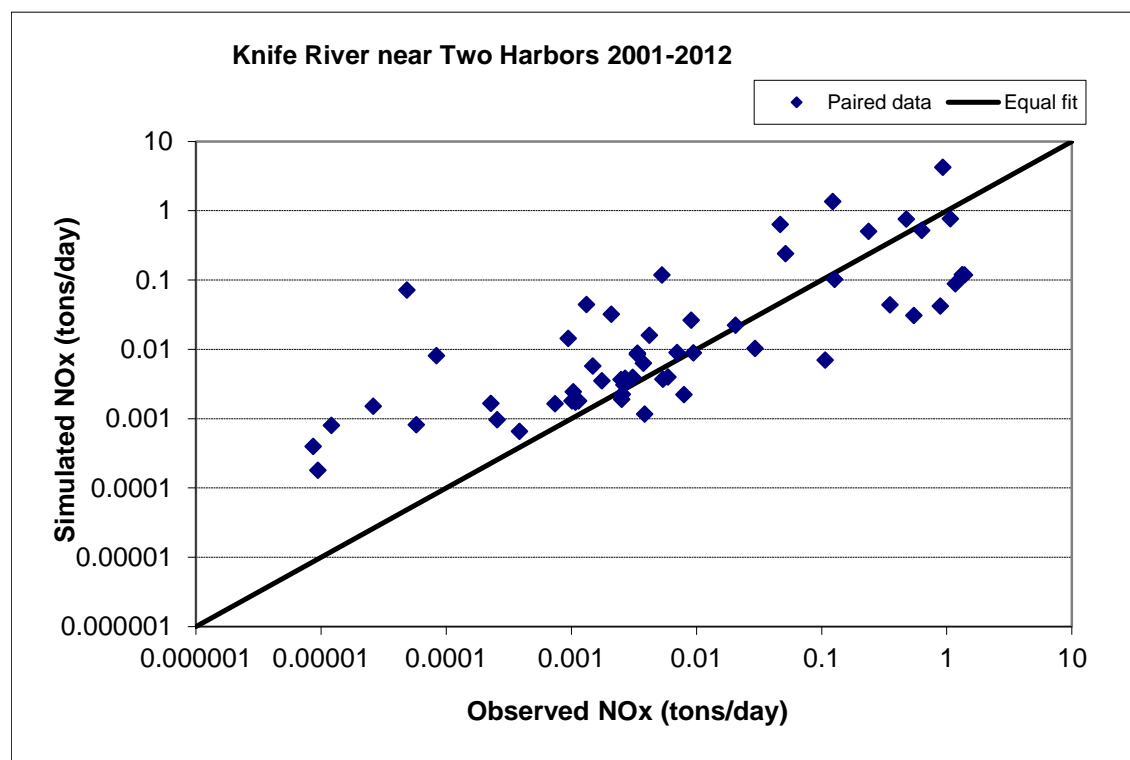


Figure 161. Paired simulated vs. observed Nitrite+ Nitrate Nitrogen (NOx) load at Knife River near Two Harbors (calibration period)

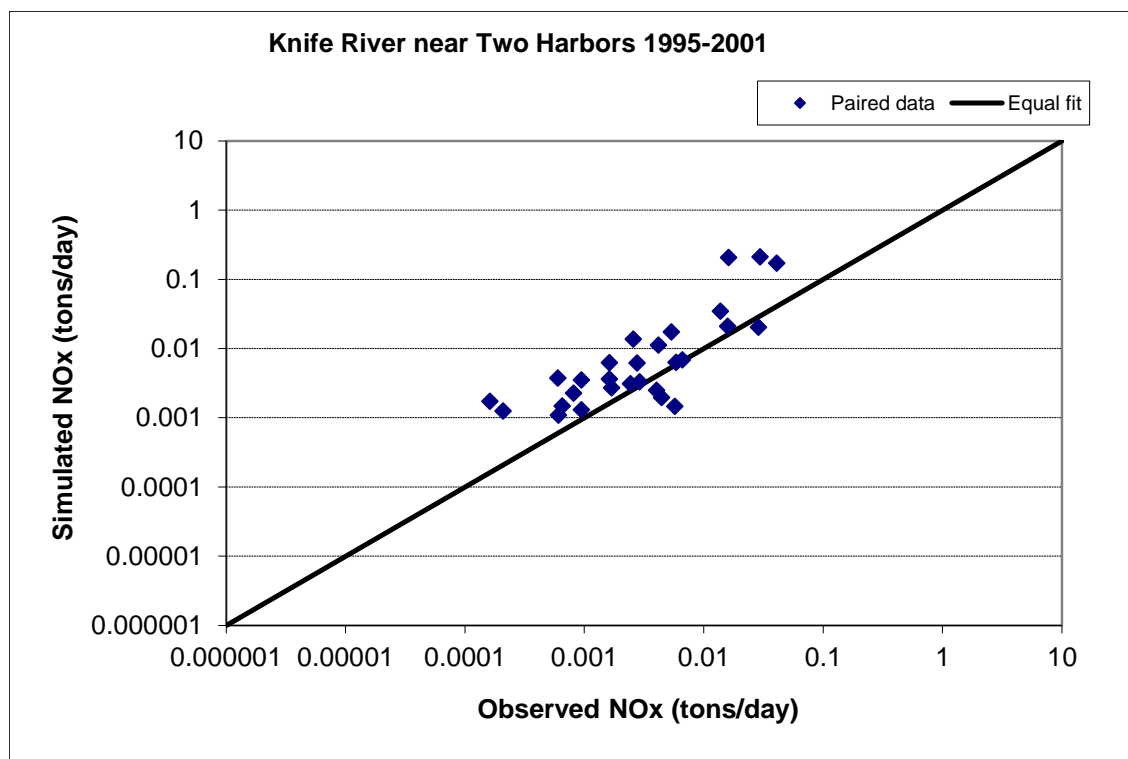


Figure 162. Paired simulated vs. observed Nitrite+ Nitrate Nitrogen (NOx) load at Knife River near Two Harbors (validation period)

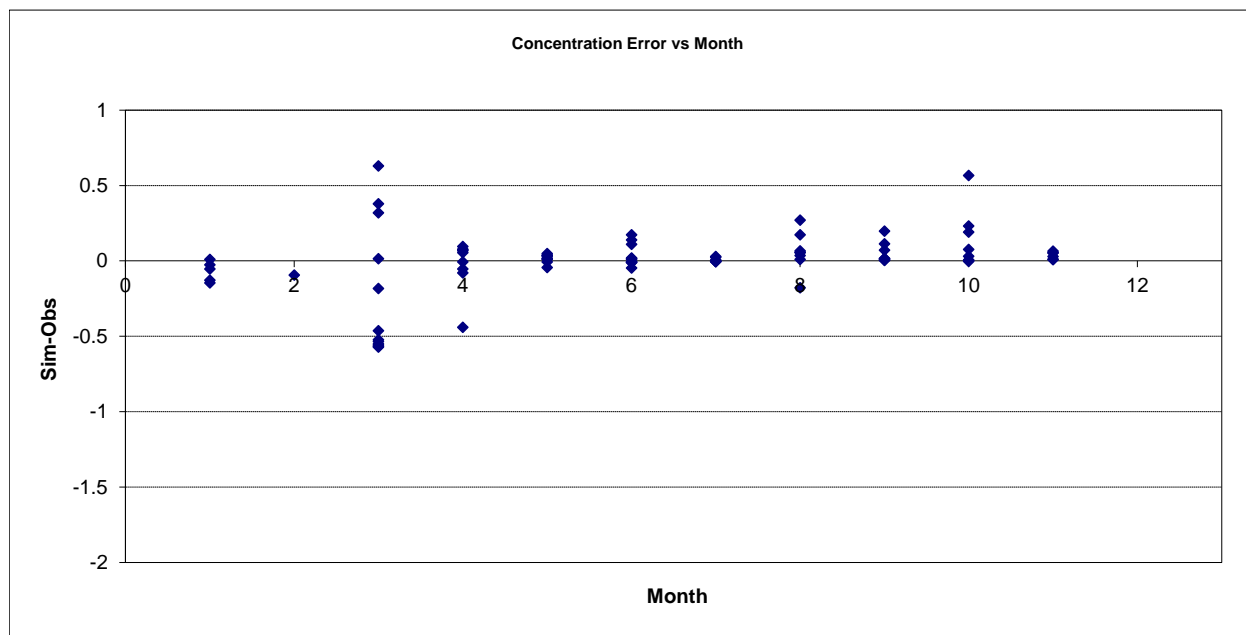


Figure 163. Residual (Simulated - Observed) vs. Month Nitrite+ Nitrate Nitrogen (NOx) at Knife River near Two Harbors

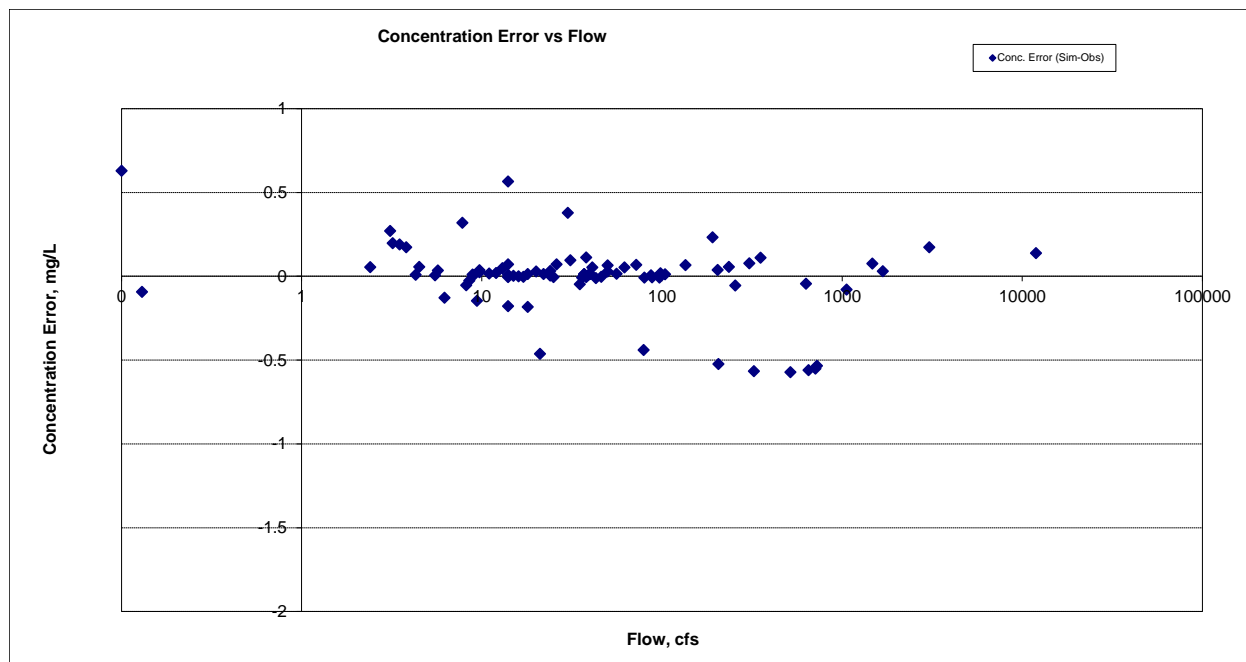


Figure 164. Residual (Simulated - Observed) vs. Flow Nitrite+ Nitrate Nitrogen (NOx) at Knife River near Two Harbors

Soluble Reactive Phosphorus (SRP)

Table 32. Soluble Reactive Phosphorus (SRP) statistics

Count	20
Concentration Average Error	97.92%
Concentration Median Error	44.24%
Load Ave Error	149.57%
Load Median Error	0.10%
Paired t concentration	0.01
Paired t load	0.14

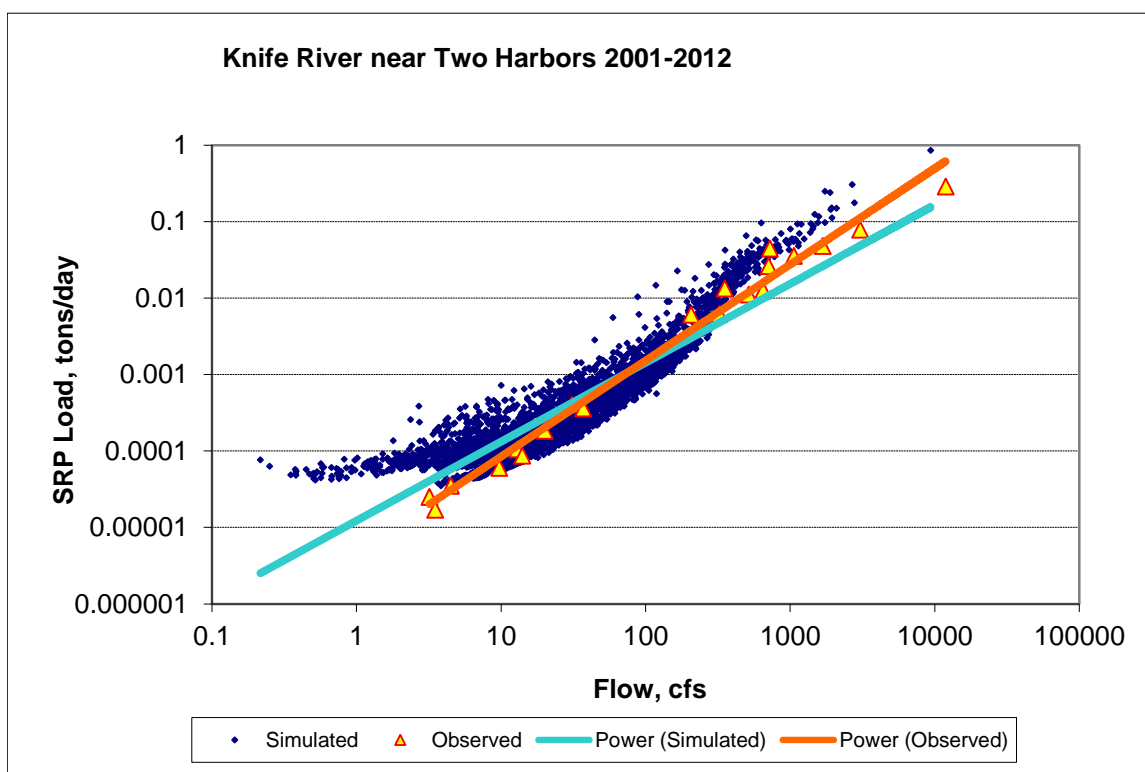


Figure 165. Power plot of simulated and observed Soluble Reactive Phosphorus (SRP) load vs flow at Knife River near Two Harbors (calibration period)

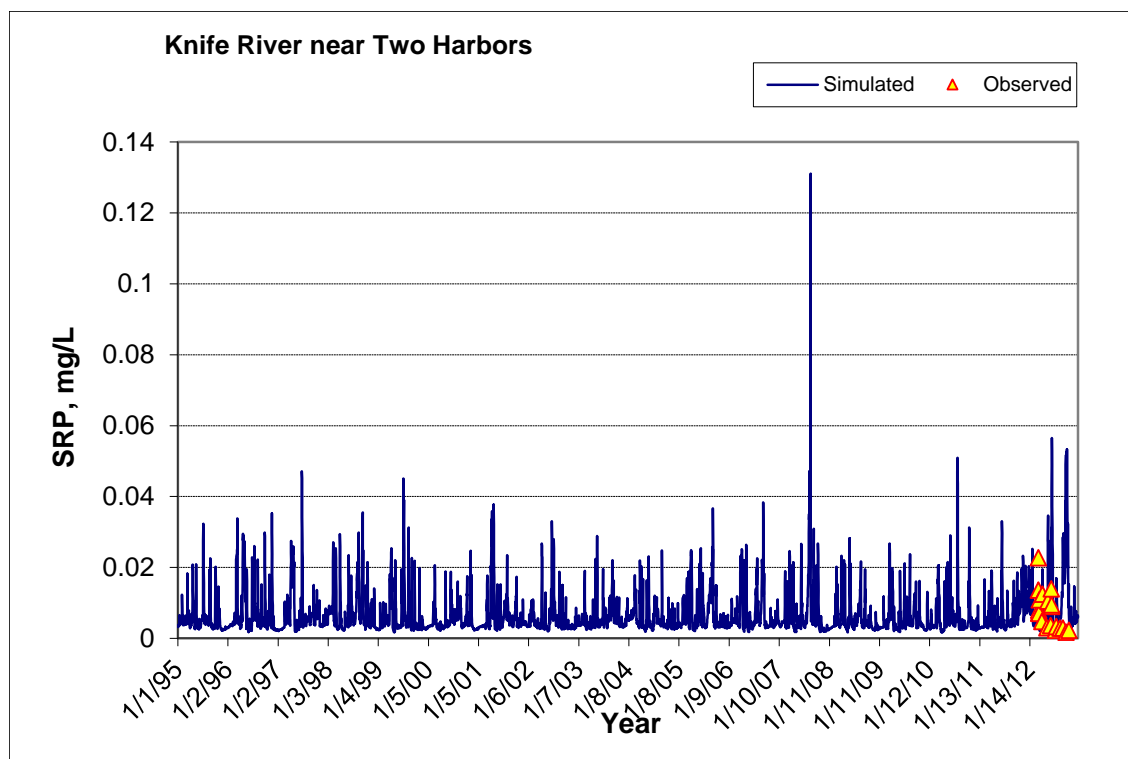


Figure 166. Time series of observed and simulated Soluble Reactive Phosphorus (SRP) concentration at Knife River near Two Harbors (calibration period)

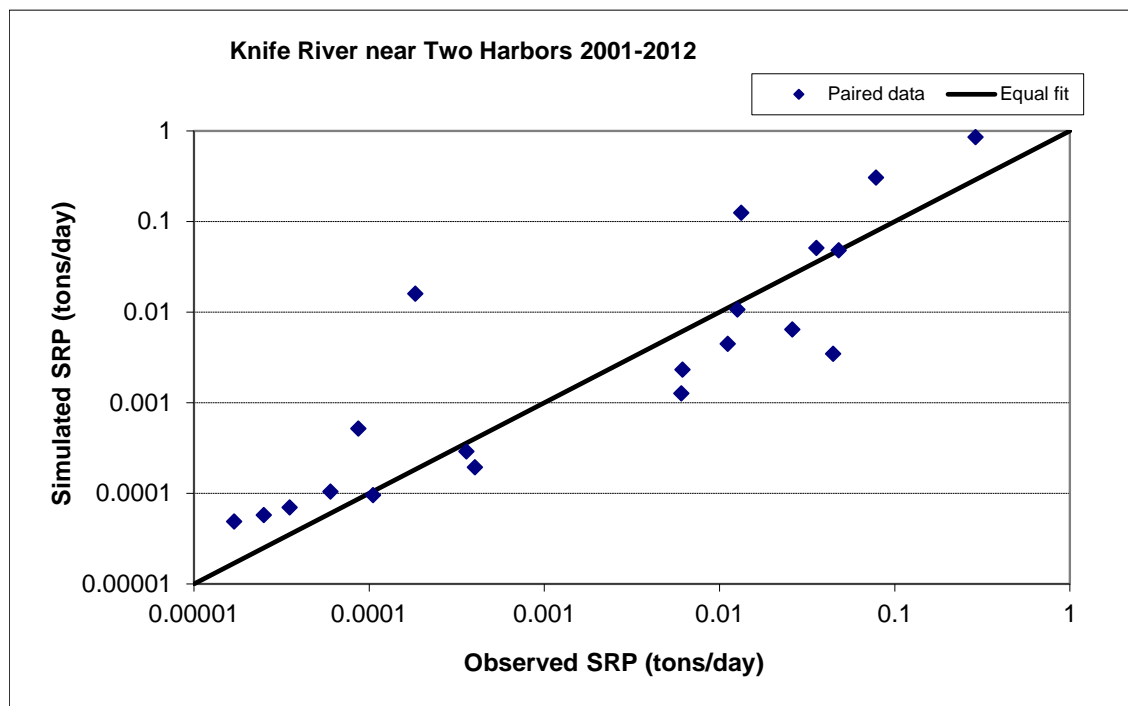


Figure 167. Paired simulated vs. observed Soluble Reactive Phosphorus (SRP) load at Knife River near Two Harbors (calibration period)

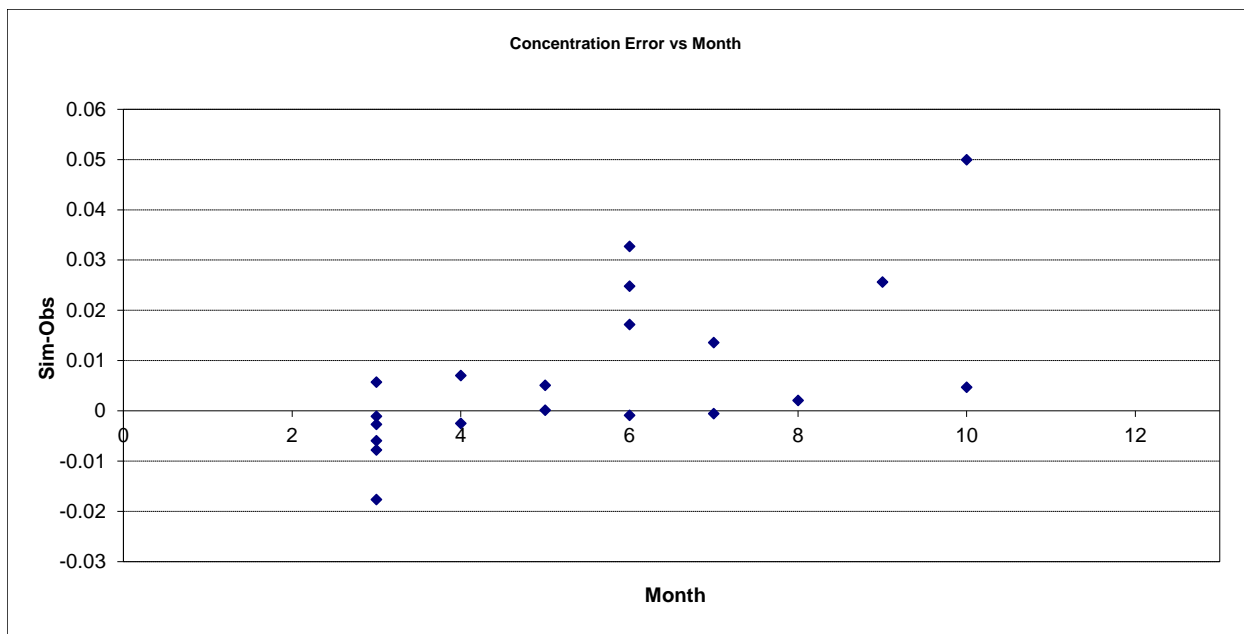


Figure 168. Residual (Simulated - Observed) vs. Month Soluble Reactive Phosphorus (SRP) at Knife River near Two Harbors

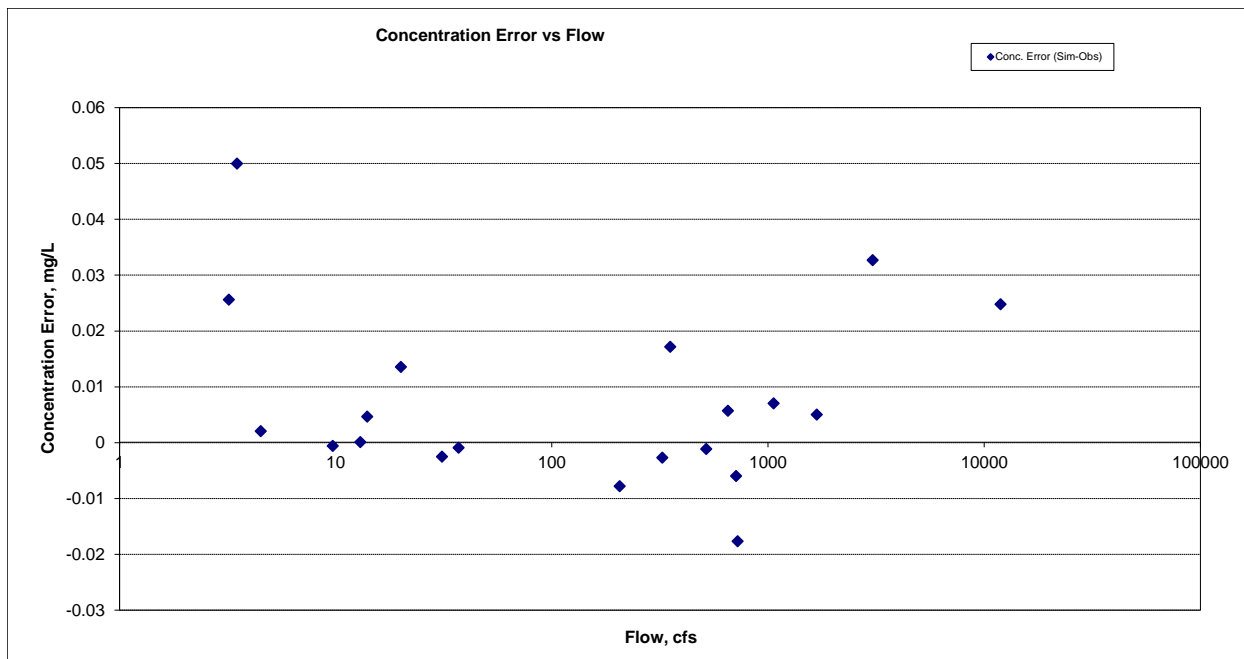


Figure 169. Residual (Simulated - Observed) vs. Flow Soluble Reactive Phosphorus (SRP) at Knife River near Two Harbors

Organic Phosphorus (OrgP)

Table 33. Organic Phosphorus (OrgP) statistics

Count	20
Concentration Average Error	-13.25%
Concentration Median Error	-2.48%
Load Ave Error	-75.60%
Load Median Error	-0.10%
Paired t concentration	0.60
Paired t load	0.18

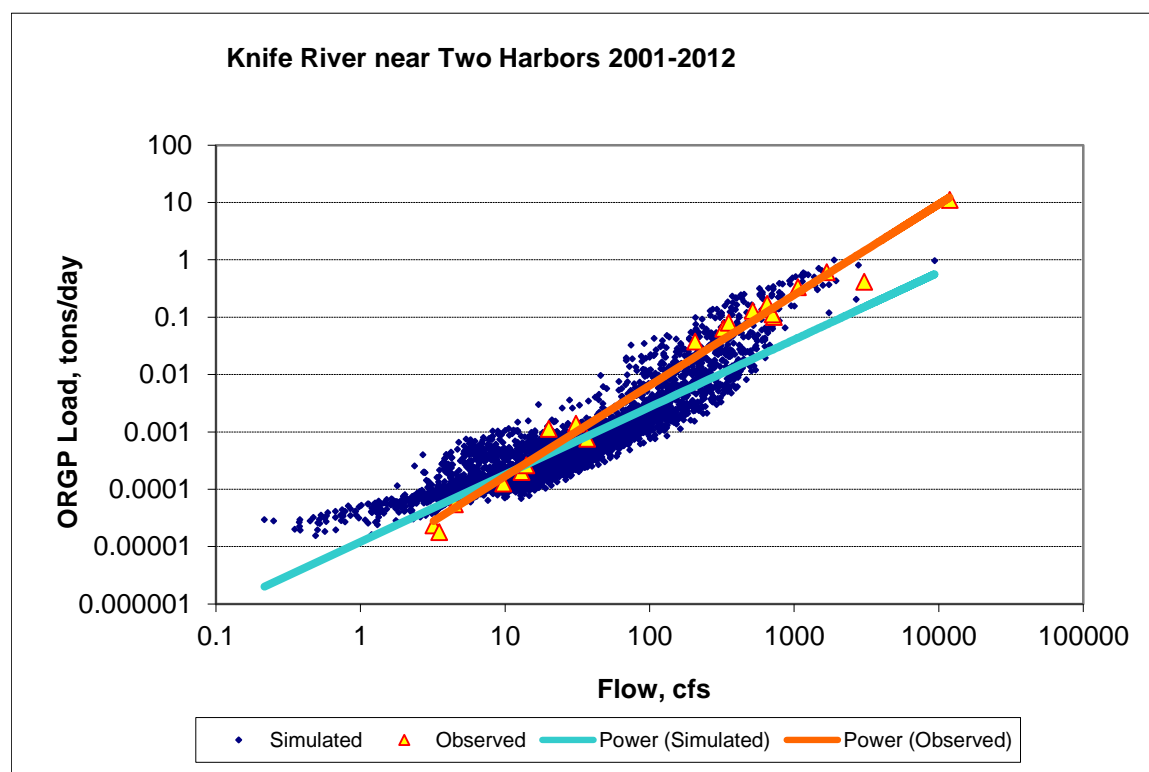


Figure 170. Power plot of simulated and observed Organic Phosphorus (OrgP) load vs flow at Knife River near Two Harbors (calibration period)

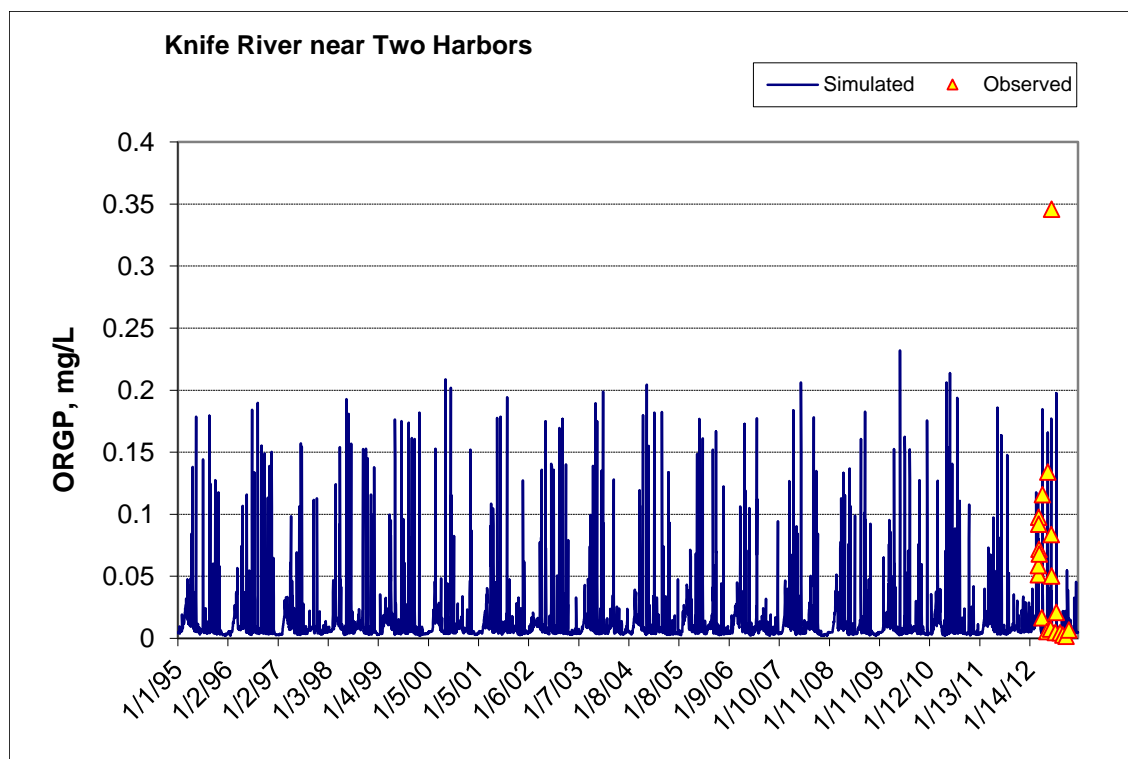


Figure 171. Time series of observed and simulated Organic Phosphorus (OrgP) concentration at Knife River near Two Harbors (calibration period)

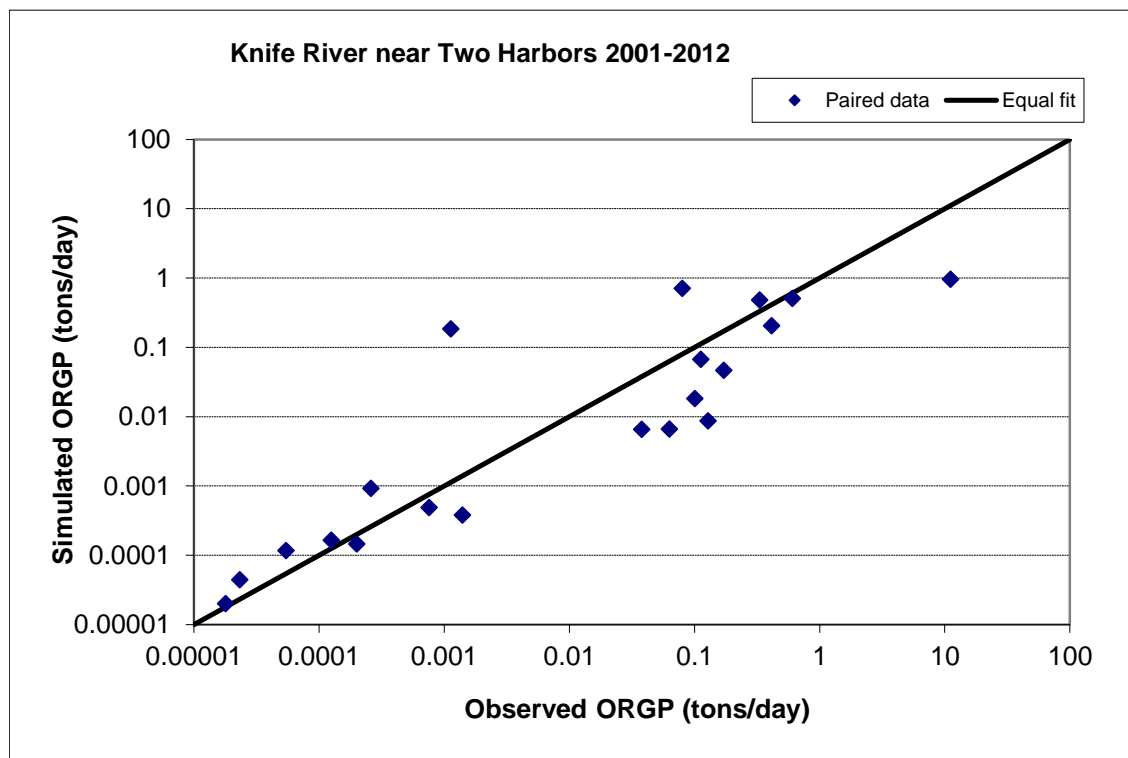


Figure 172. Paired simulated vs. observed Organic Phosphorus (OrgP) load at Knife River near Two Harbors (calibration period)

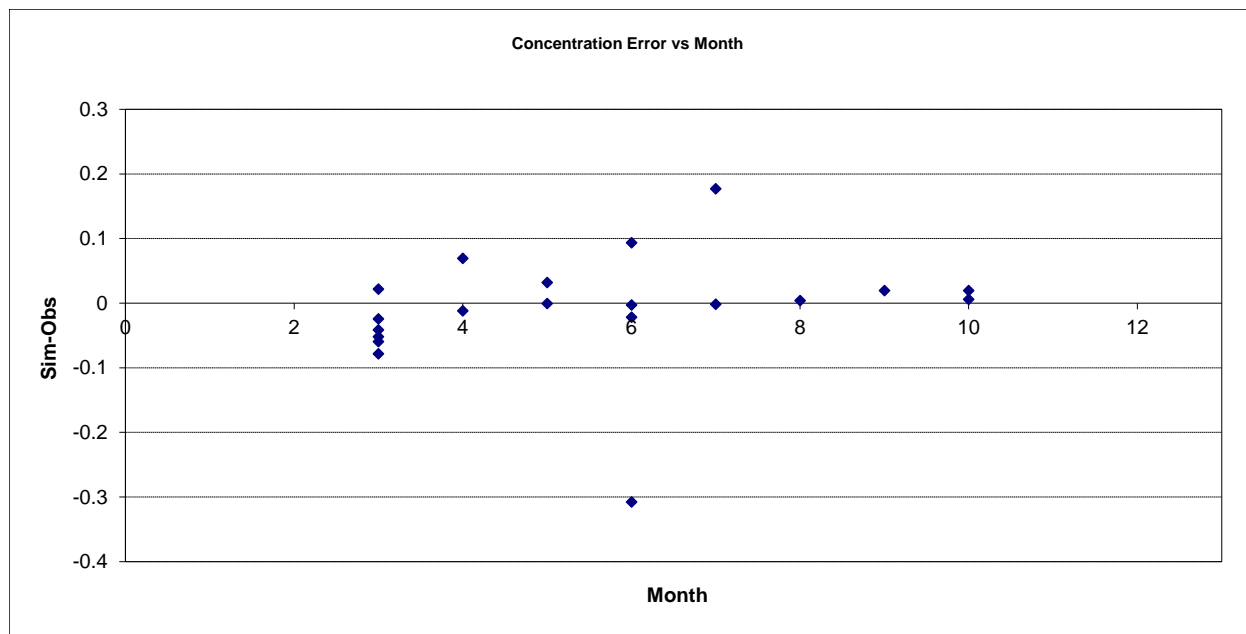


Figure 173. Residual (Simulated - Observed) vs. Month Organic Phosphorus (OrgP) at Knife River near Two Harbors

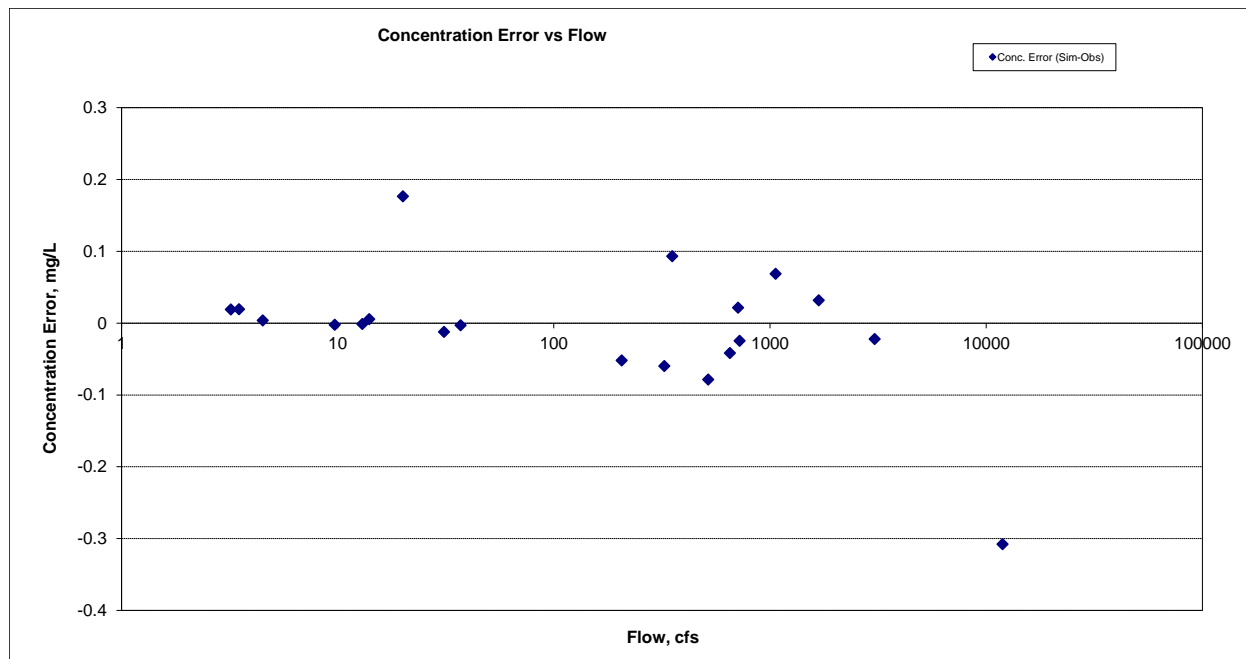


Figure 174. Residual (Simulated - Observed) vs. Flow Organic Phosphorus (OrgP) at Knife River near Two Harbors

Total Phosphorus (TP)

Table 34. Total Phosphorus (TP) statistics

Count	57	21
Concentration Average Error	-63.06%	-17.79%
Concentration Median Error	-24.45%	-14.98%
Load Ave Error	3.31%	-59.57%
Load Median Error	-4.27%	-0.18%
Paired t concentration	0.06	0.55
Paired t load	0.65	0.24

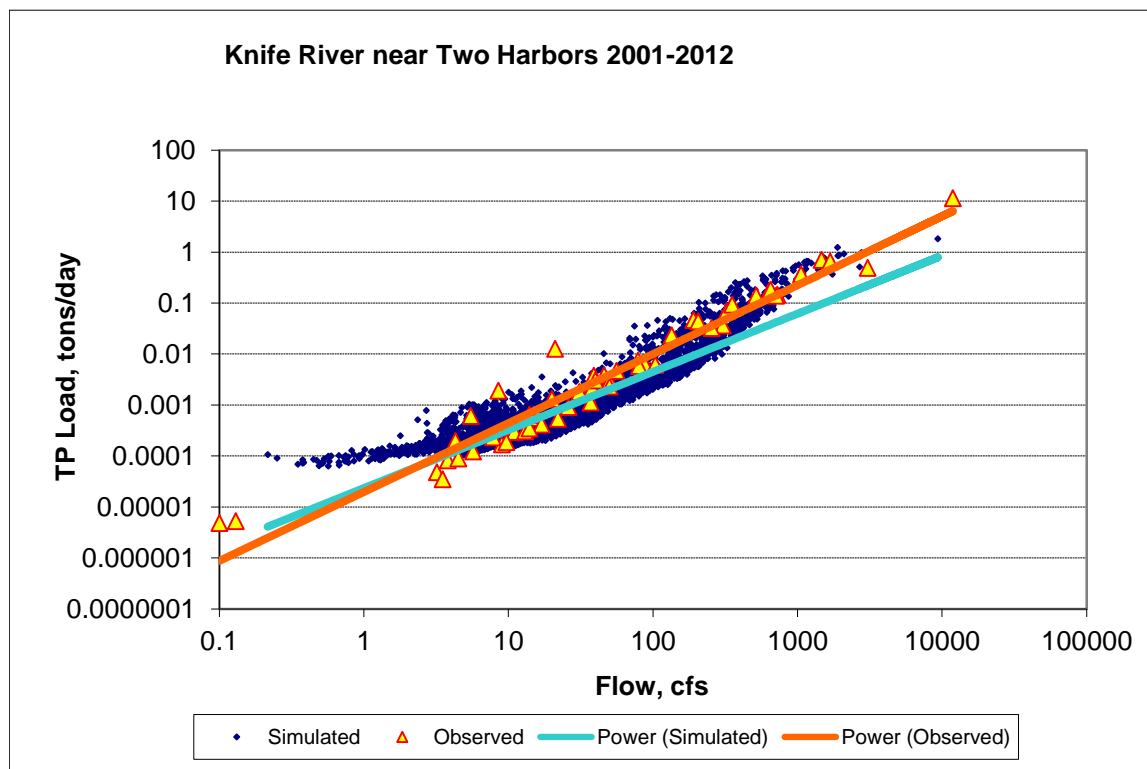


Figure 175. Power plot of simulated and observed Total Phosphorus (TP) load vs flow at Knife River near Two Harbors (calibration period)

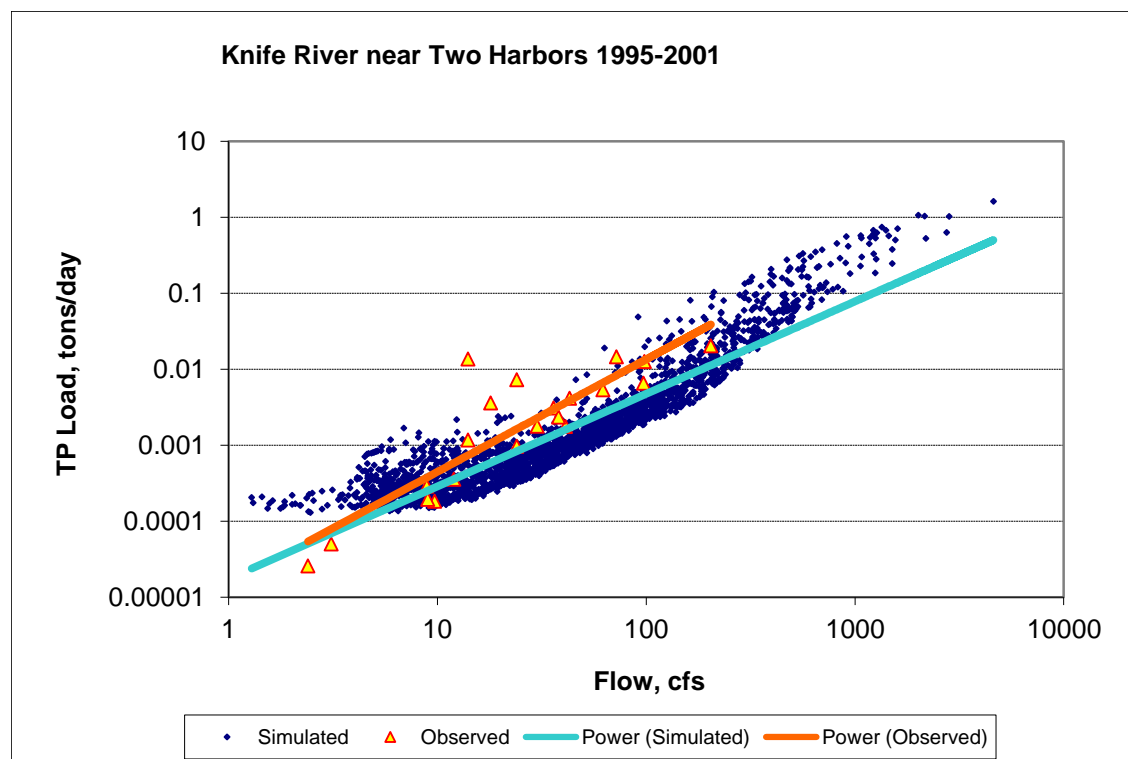


Figure 176. Power plot of simulated and observed Total Phosphorus (TP) load vs flow at Knife River near Two Harbors (validation period)

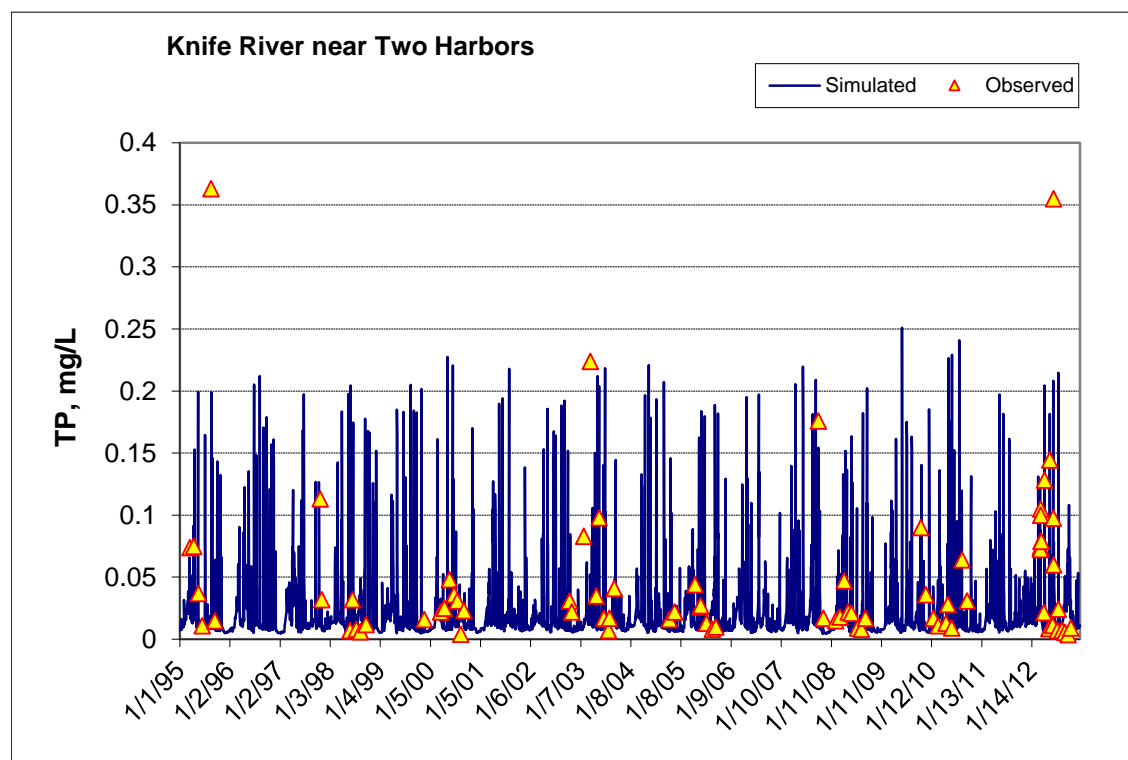


Figure 177. Time series of observed and simulated Total Phosphorus (TP) concentration at Knife River near Two Harbors (calibration period)

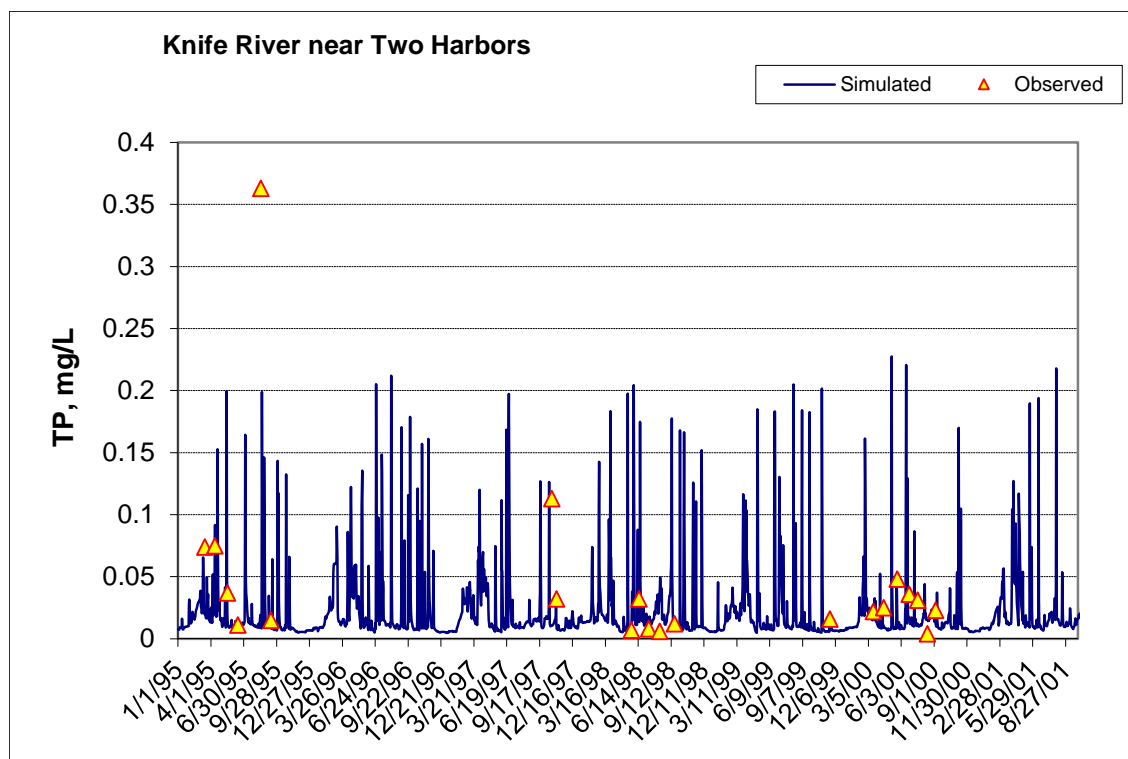


Figure 178. Time series of observed and simulated Total Phosphorus (TP) concentration at Knife River near Two Harbors (validation period)

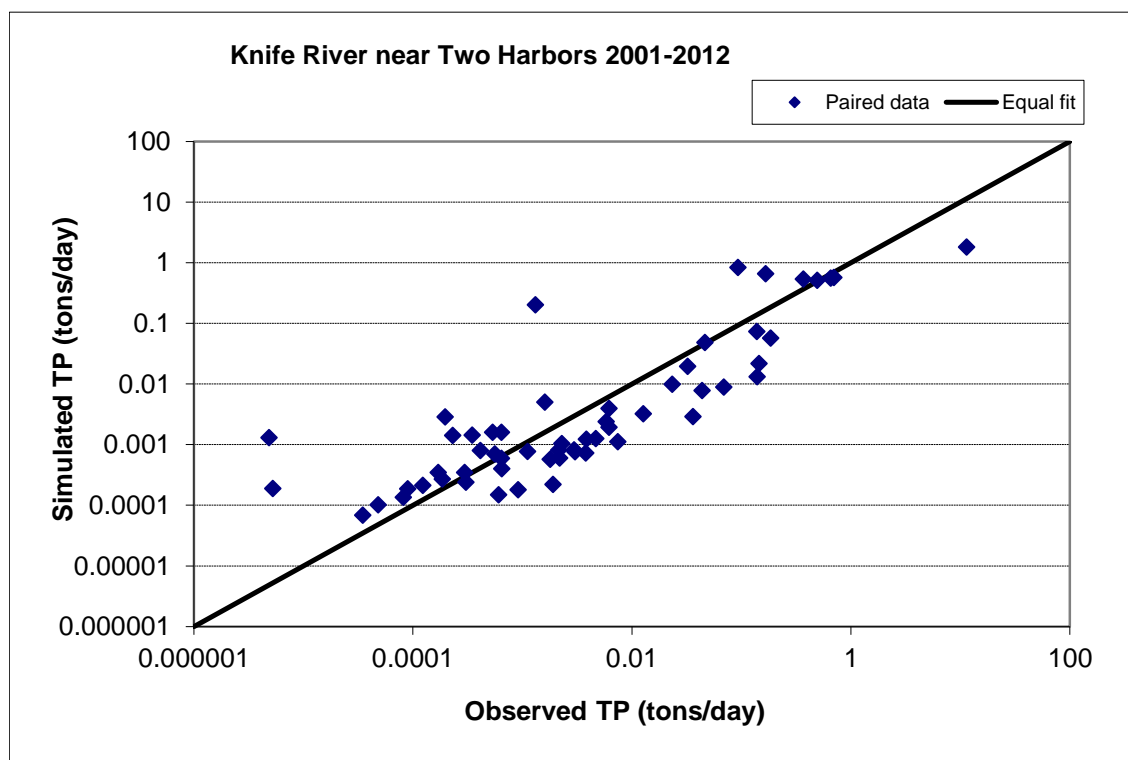


Figure 179. Paired simulated vs. observed Total Phosphorus (TP) load at Knife River near Two Harbors (calibration period)

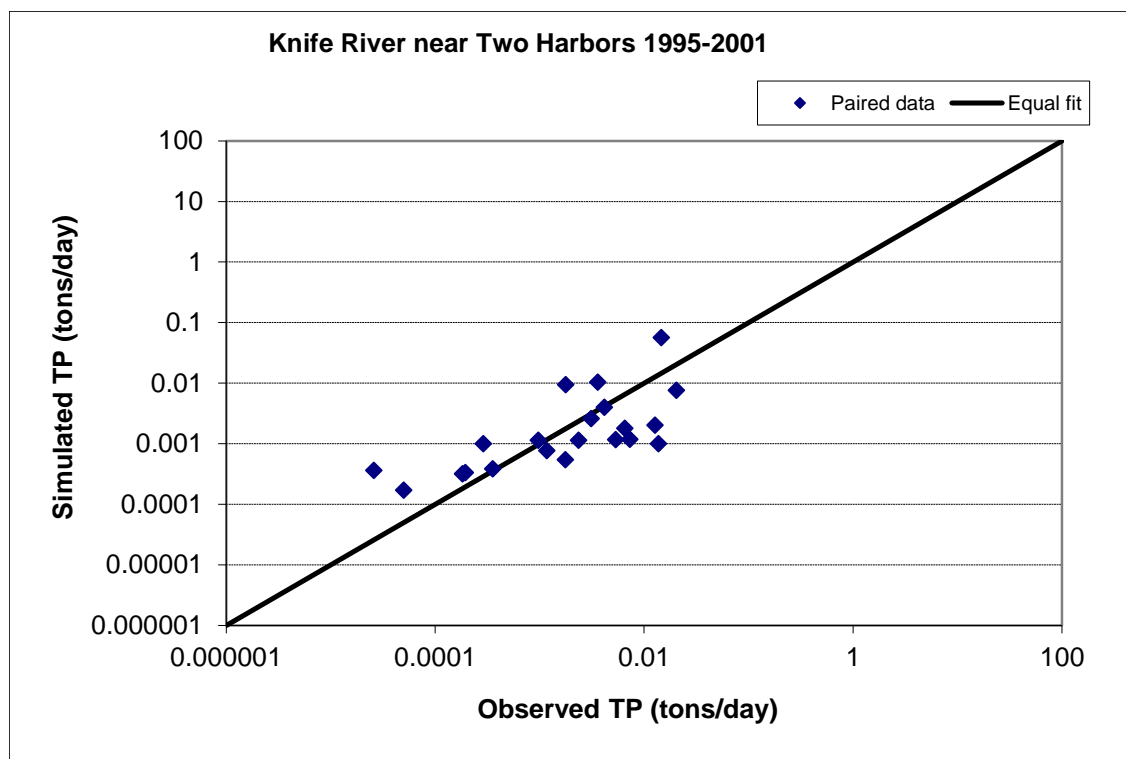


Figure 180. Paired simulated vs. observed Total Phosphorus (TP) load at Knife River near Two Harbors (validation period)

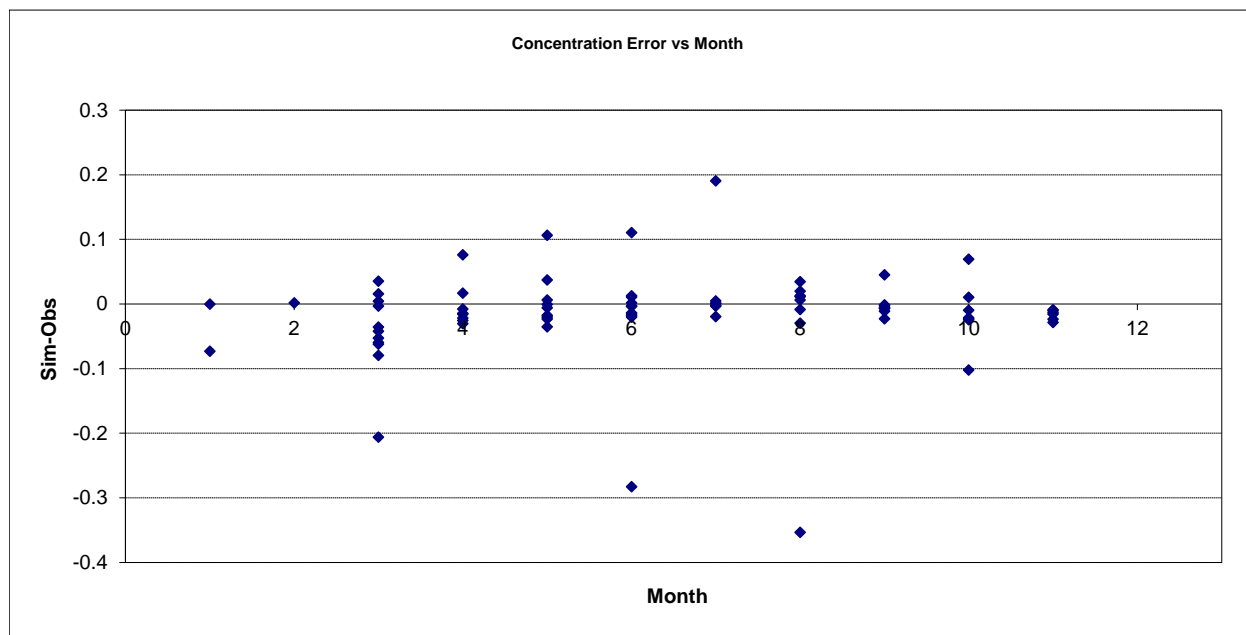


Figure 181. Residual (Simulated - Observed) vs. Month Total Phosphorus (TP) at Knife River near Two Harbors

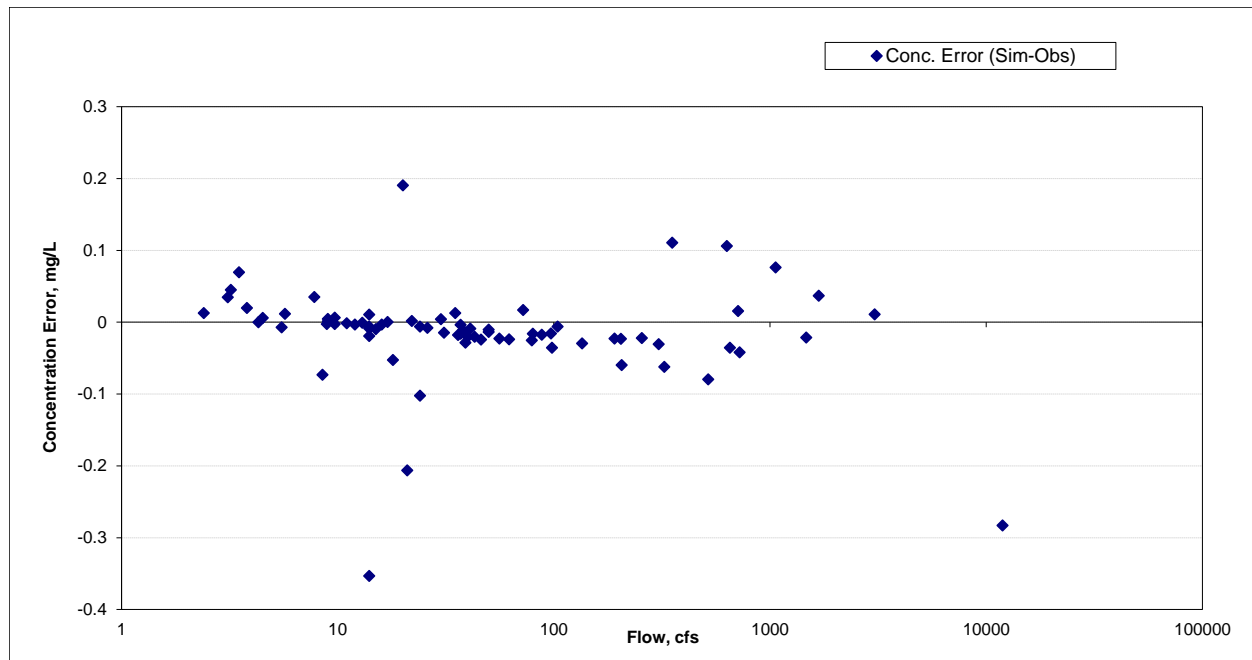


Figure 182. Residual (Simulated - Observed) vs. Flow Total Phosphorus (TP) at Knife River near Two Harbors

Split Rock River (EQUIS S000-263 and S006-235)

Total Suspended Solids (TSS)

Table 35. Total Suspended Solids (TSS) statistics

Count	29
Concentration Average Error	-40.23%
Concentration Median Error	-2.71%
Load Average Error	-36.73%
Load Median Error	-0.08%
Paired t concentration	0.27
Paired t load	0.40

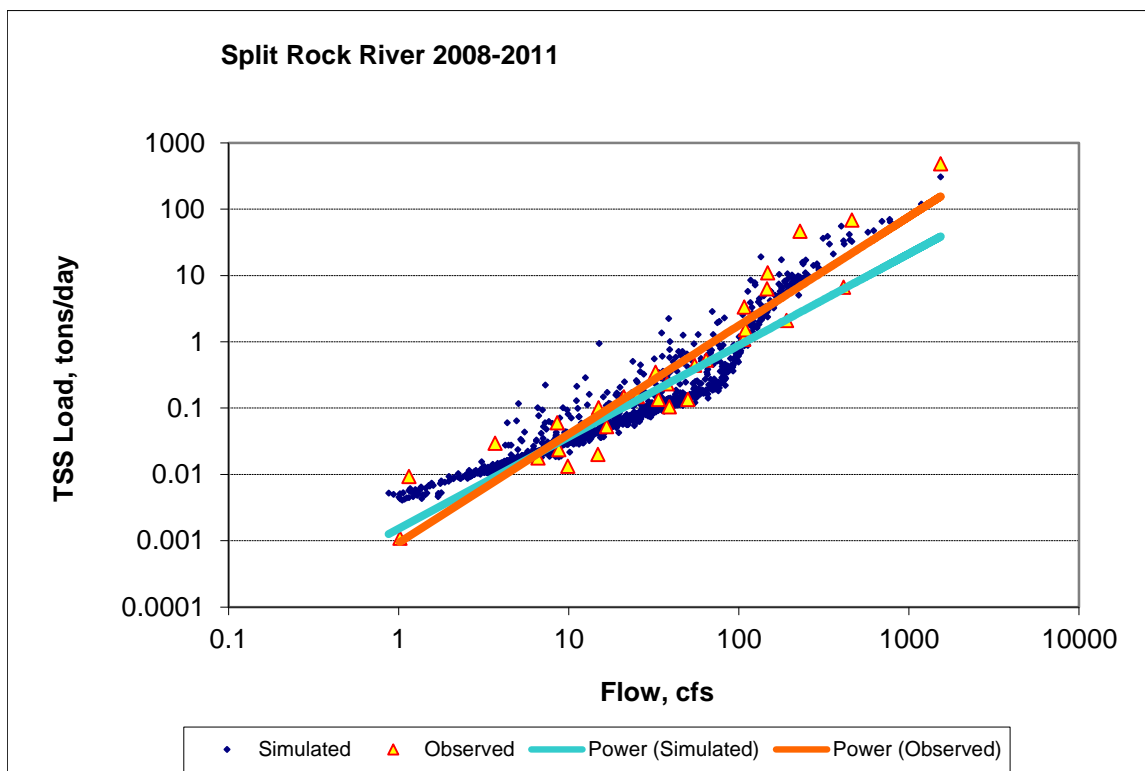


Figure 183. Power plot of simulated and observed Total Suspended Solids (TSS) load vs flow at Split Rock River

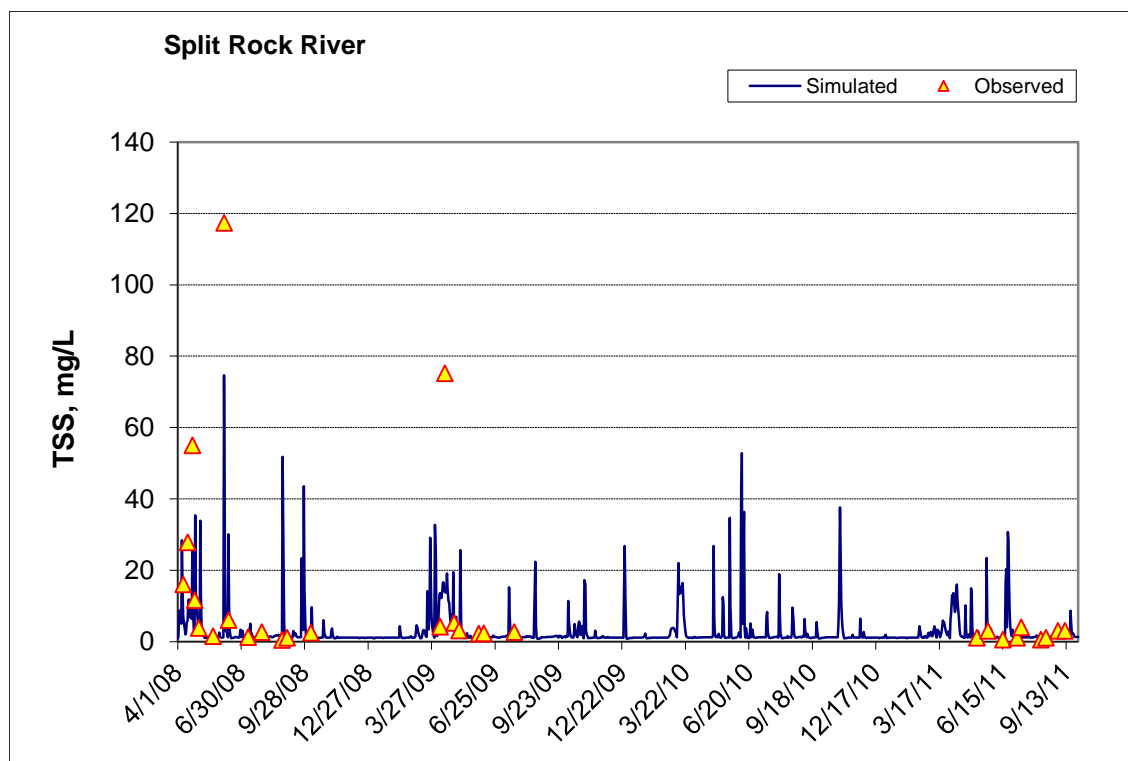


Figure 184. Time series of observed and simulated Total Suspended Solids (TSS) concentration at Split Rock River

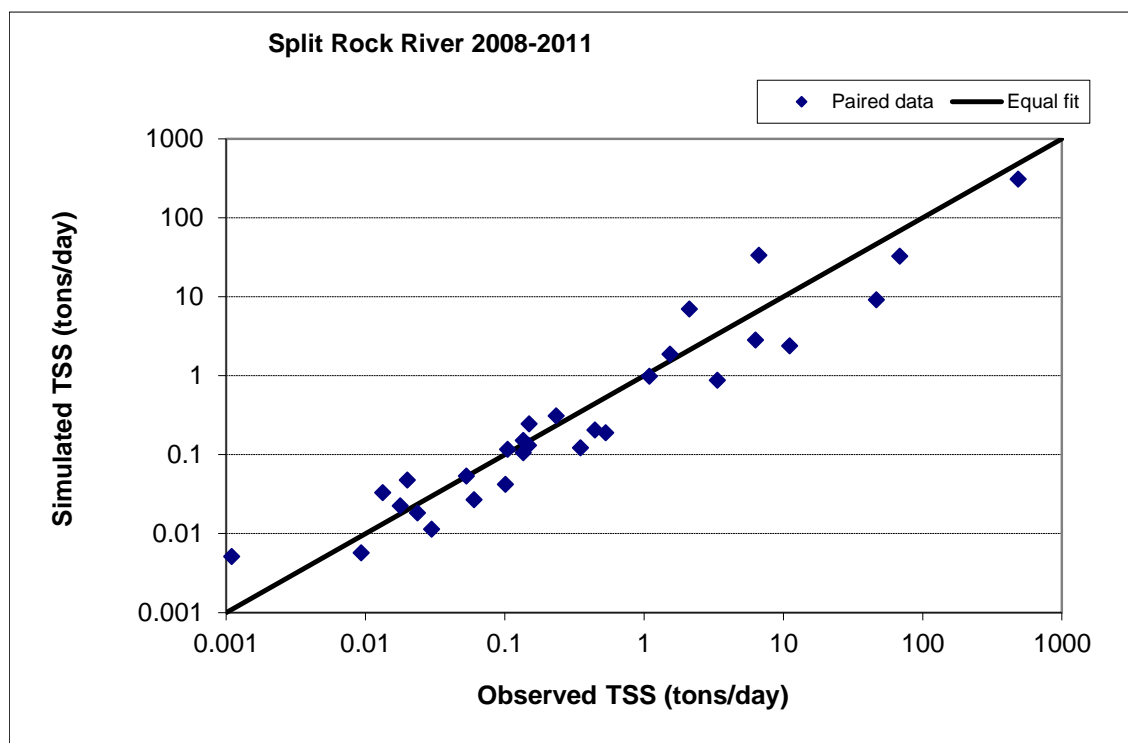


Figure 185. Paired simulated vs. observed Total Suspended Solids (TSS) load at Split Rock River

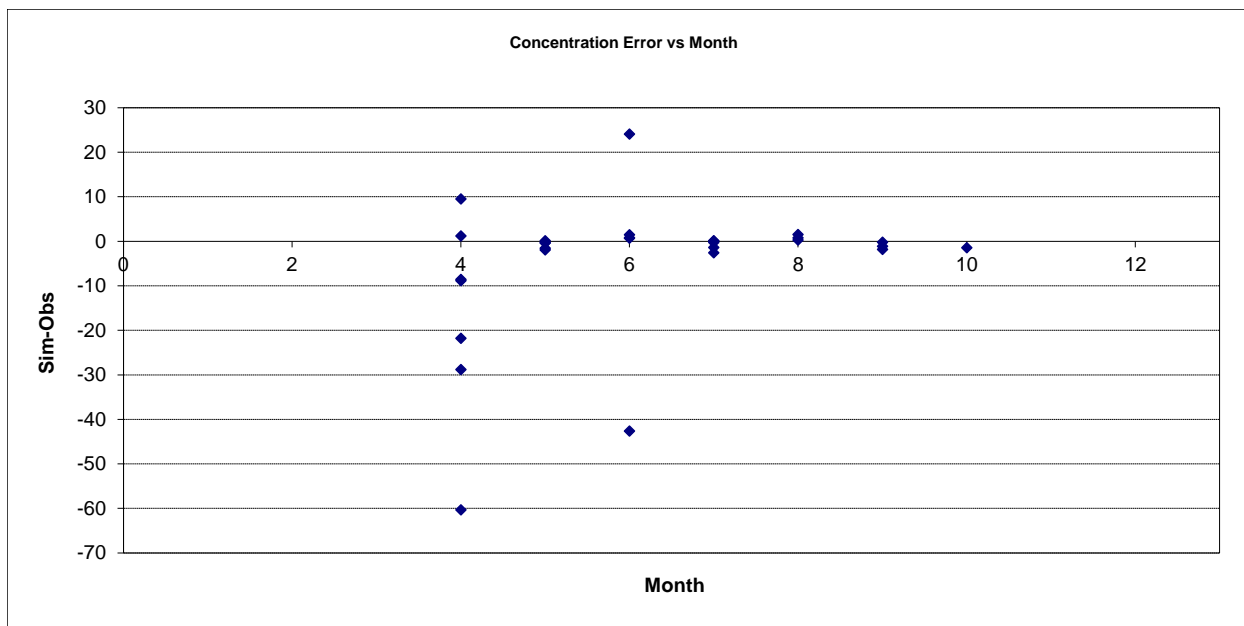


Figure 186. Residual (Simulated - Observed) vs. Month Total Suspended Solids (TSS) at Split Rock River

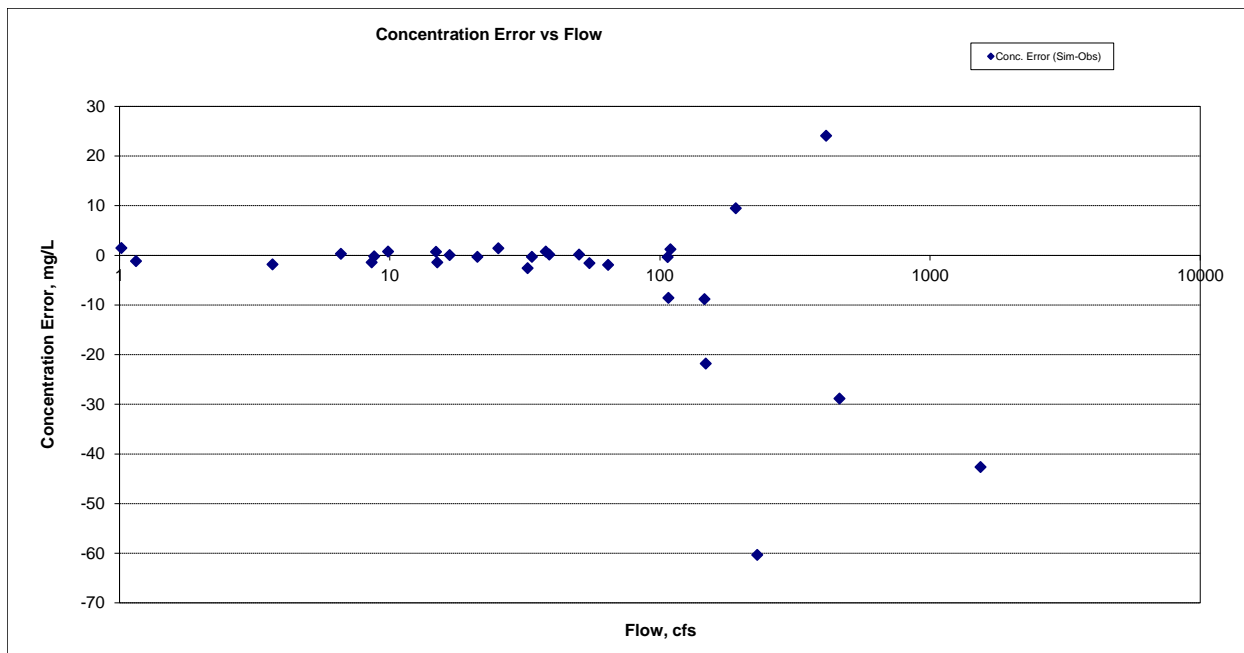


Figure 187. Residual (Simulated - Observed) vs. Flow Total Suspended Solids (TSS) at Split Rock River

Nitrite+ Nitrate Nitrogen (NO_x)

Table 36. Nitrite+ Nitrate Nitrogen (NO_x) statistics

Count	30
Concentration Average Error	-67.83%
Concentration Median Error	2.24%
Load Average Error	-35.33%
Load Median Error	0.21%
Paired t concentration	0.13
Paired t load	0.34

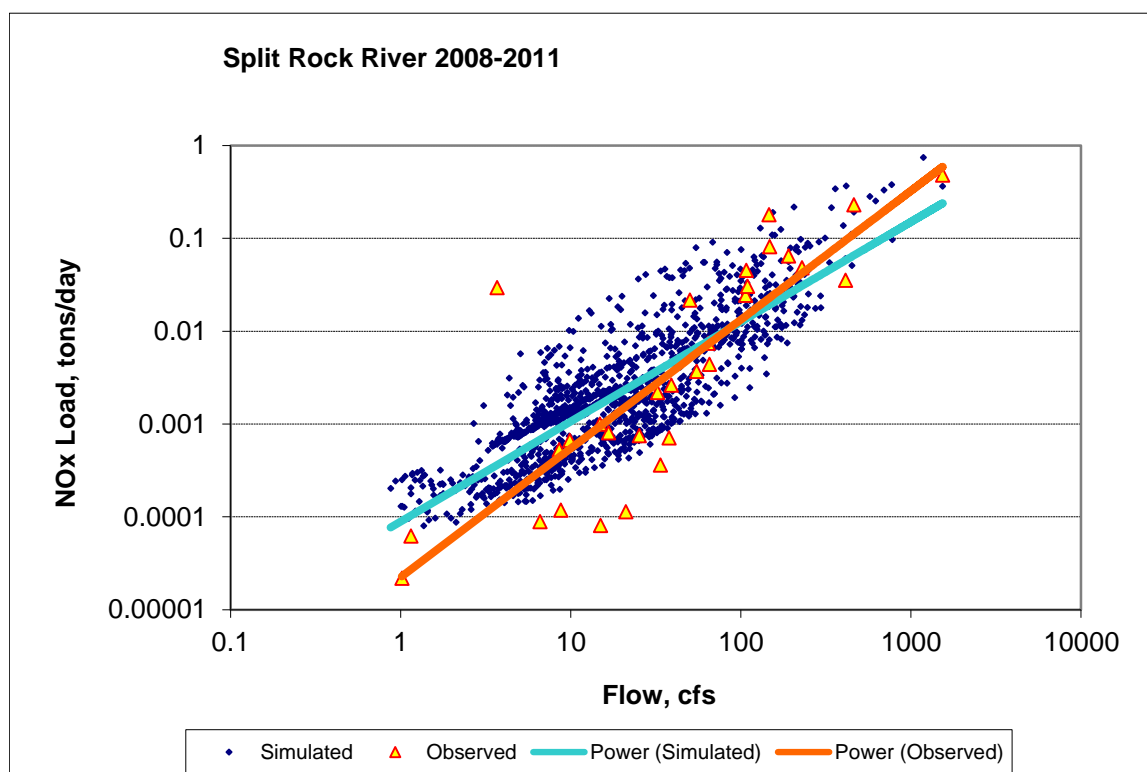


Figure 188. Power plot of simulated and observed Nitrite+ Nitrate Nitrogen (NO_x) load vs flow at Split Rock River

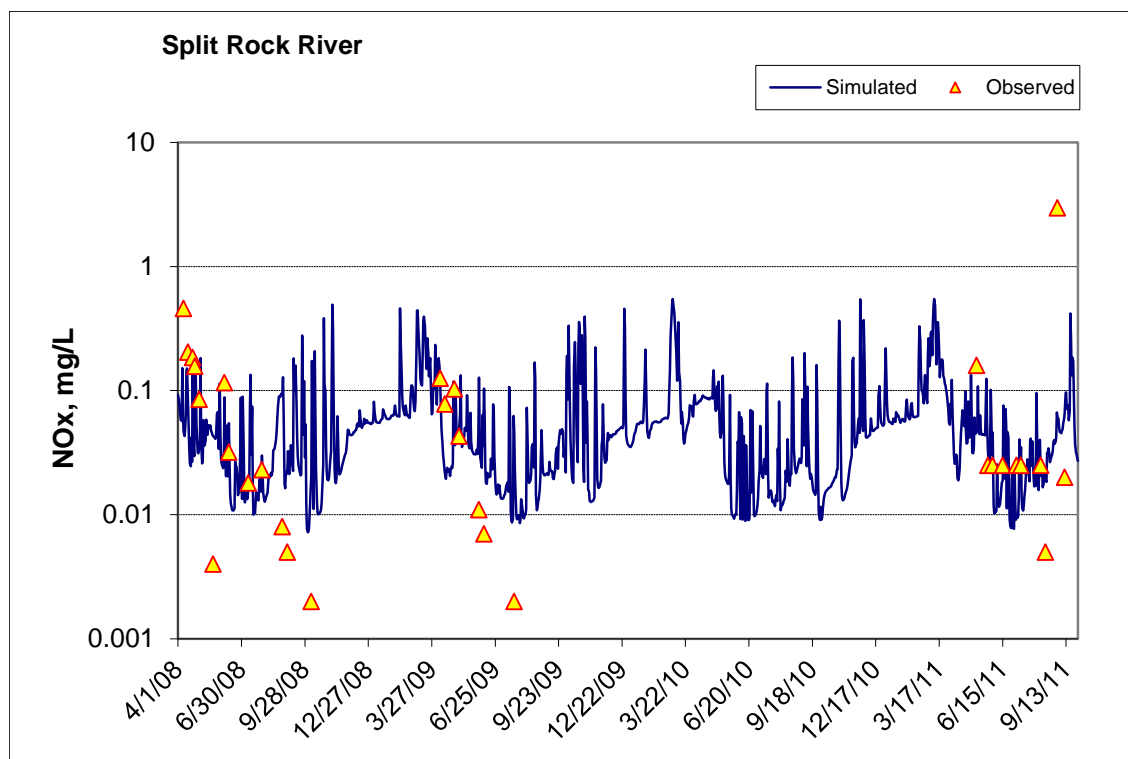


Figure 189. Time series of observed and simulated Nitrite+ Nitrate Nitrogen (NOx) concentration at Split Rock River

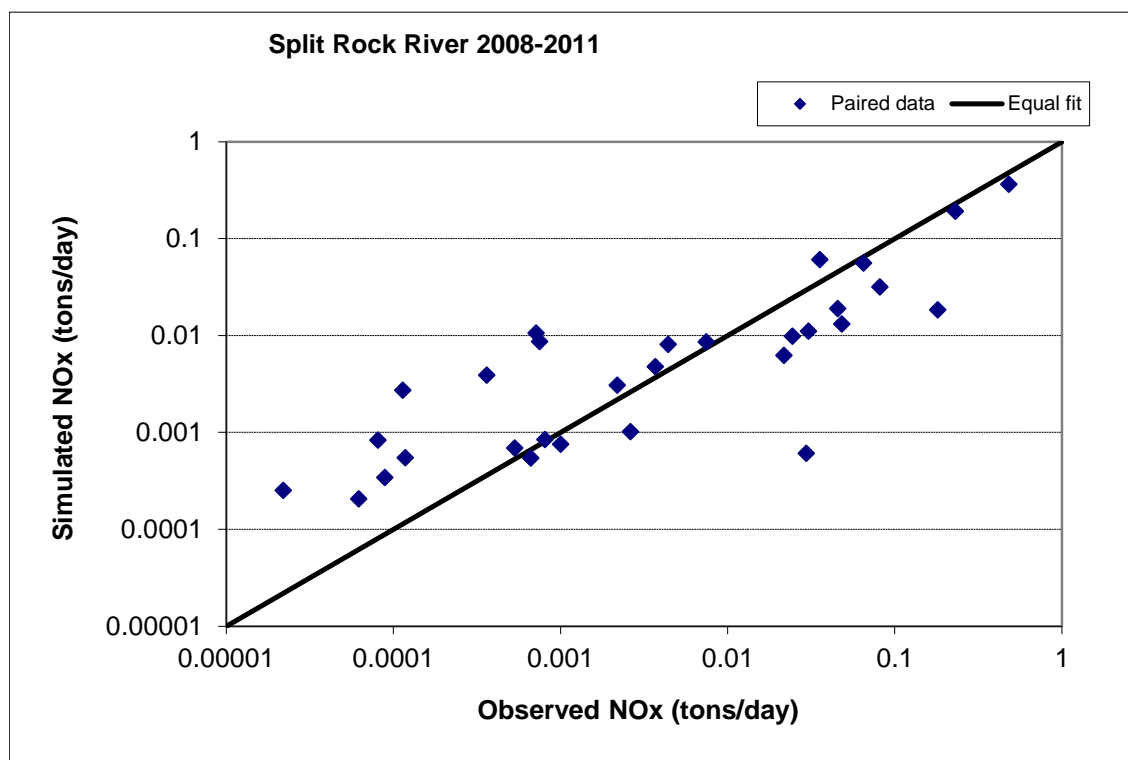


Figure 190. Paired simulated vs. observed Nitrite+ Nitrate Nitrogen (NOx) load at Split Rock River



Figure 191. Residual (Simulated - Observed) vs. Month Nitrite+ Nitrate Nitrogen (NOx) at Split Rock River

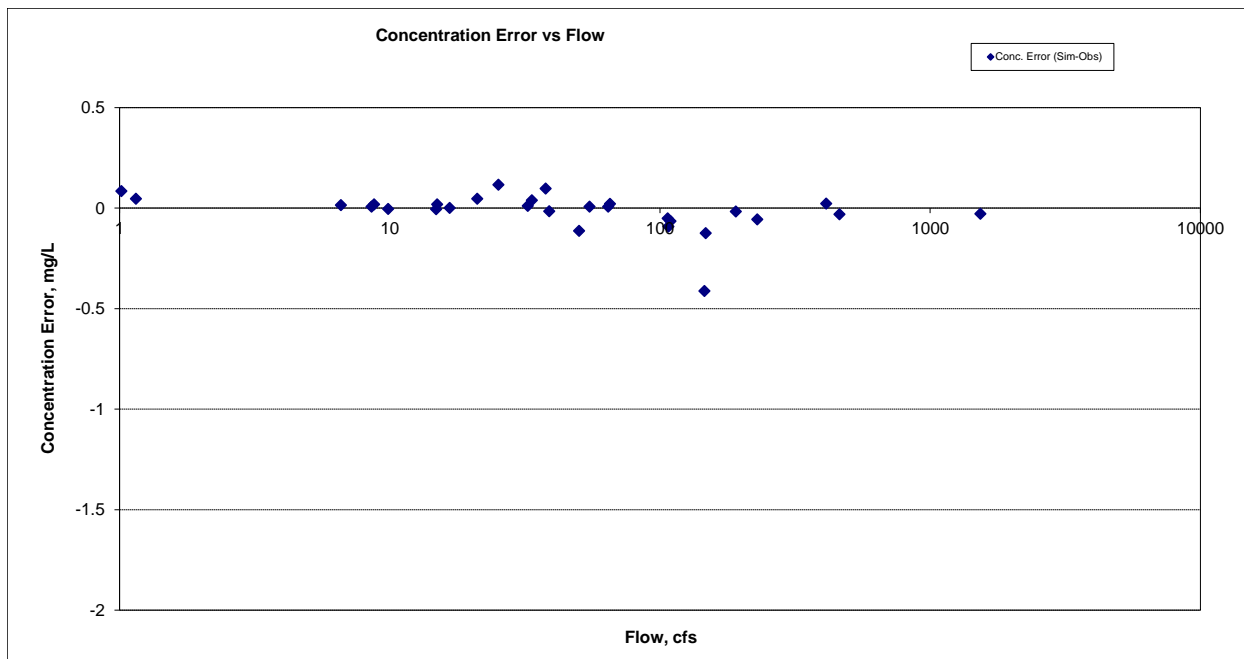


Figure 192. Residual (Simulated - Observed) vs. Flow Nitrite+ Nitrate Nitrogen (NOx) at Split Rock River

Total Phosphorus (TP)

Table 37. Total Phosphorus (TP) statistics

Count	30
Concentration Average Error	21.01%
Concentration Median Error	-7.68%
Load Average Error	35.76%
Load Median Error	-0.35%
Paired t concentration	0.48
Paired t load	0.41

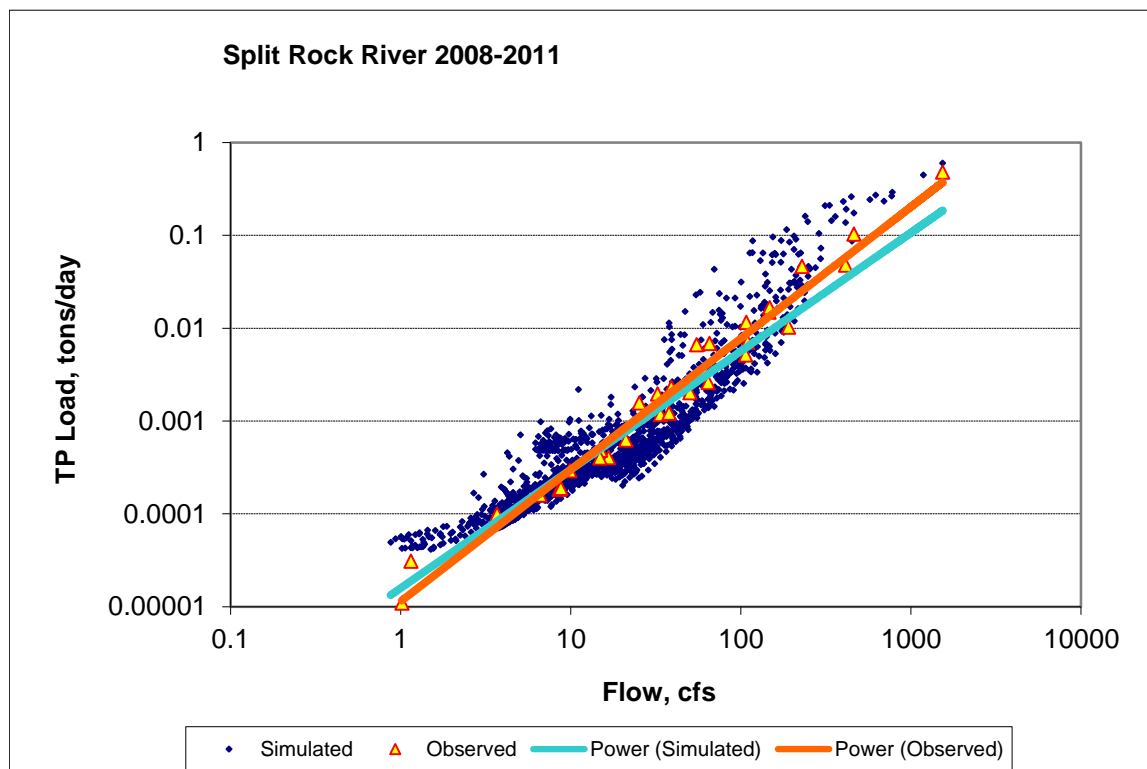


Figure 193. Power plot of simulated and observed Total Phosphorus (TP) load vs flow at Split Rock River

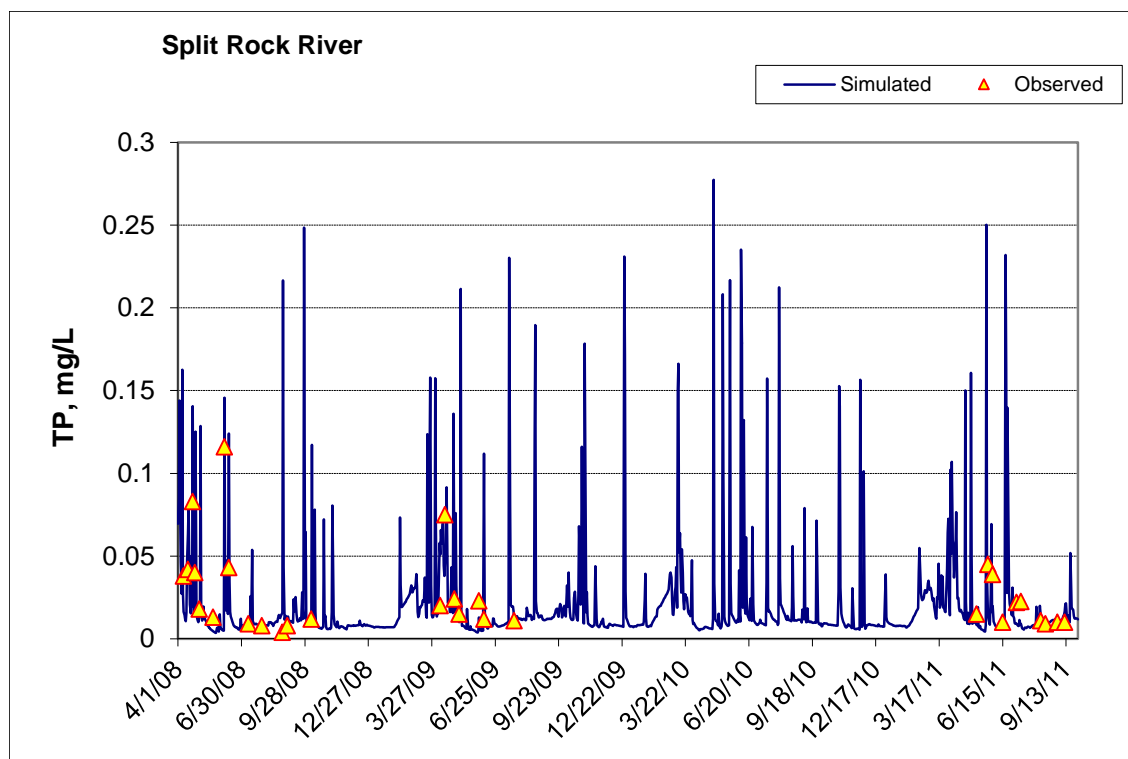


Figure 194. Time series of observed and simulated Total Phosphorus (TP) concentration at Split Rock River

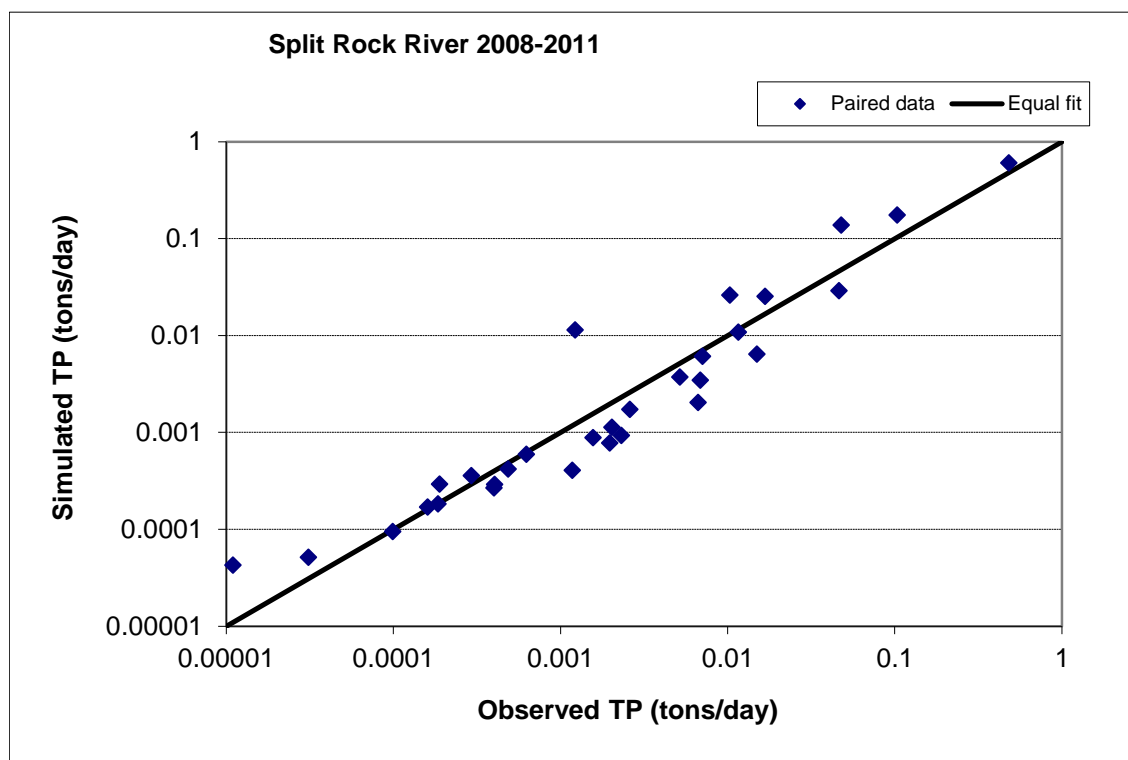
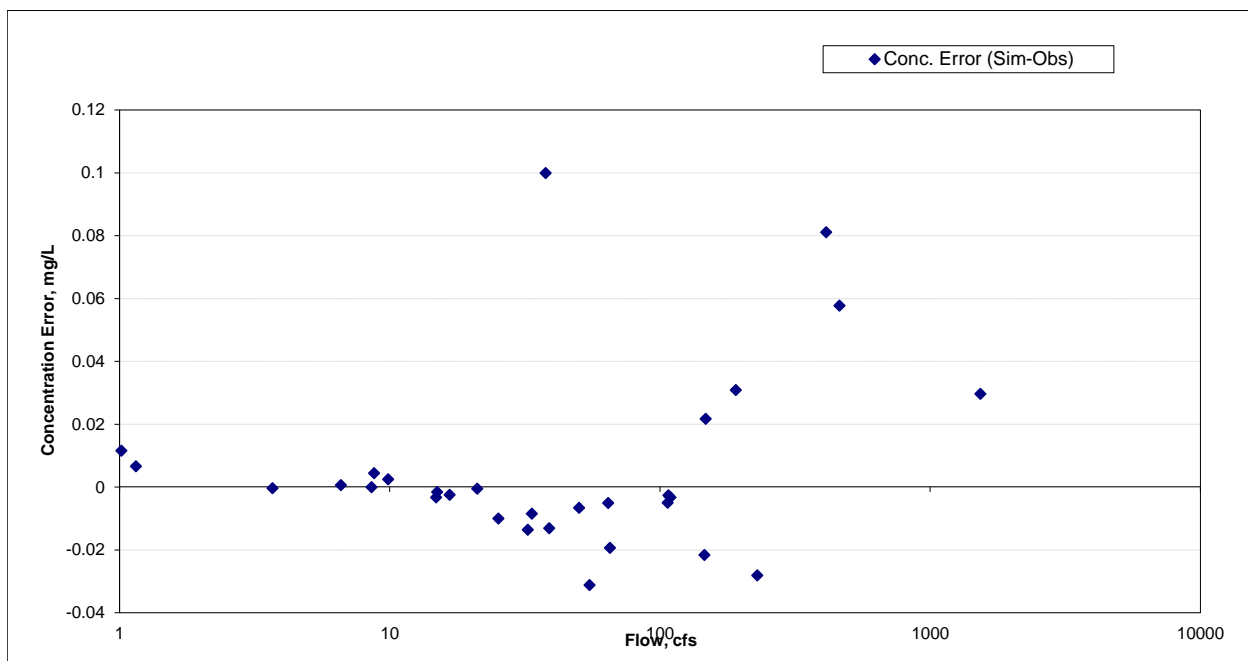
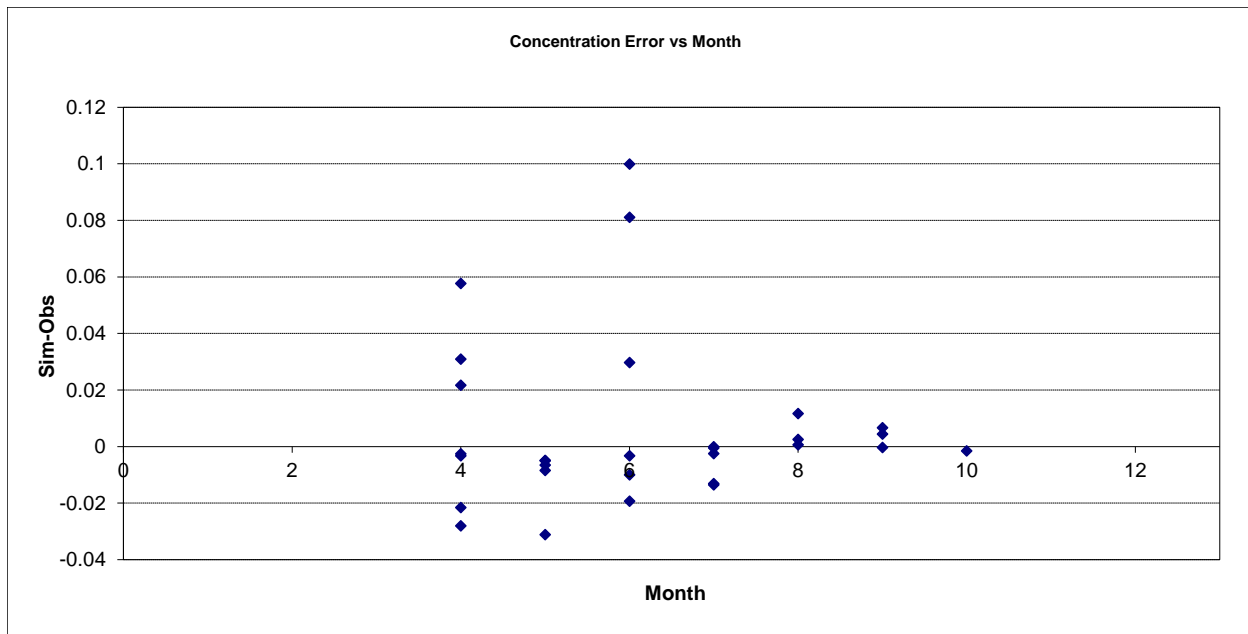


Figure 195. Paired simulated vs. observed Total Phosphorus (TP) load at Split Rock River



Gooseberry River (EQUIS S000-256)

Total Suspended Solids (TSS)

Table 38. Total Suspended Solids (TSS) statistics

Count	30
Concentration Average Error	-83.40%
Concentration Median Error	-6.84%
Load Average Error	-84.34%
Load Median Error	-0.32%
Paired t concentration	0.02
Paired t load	0.13

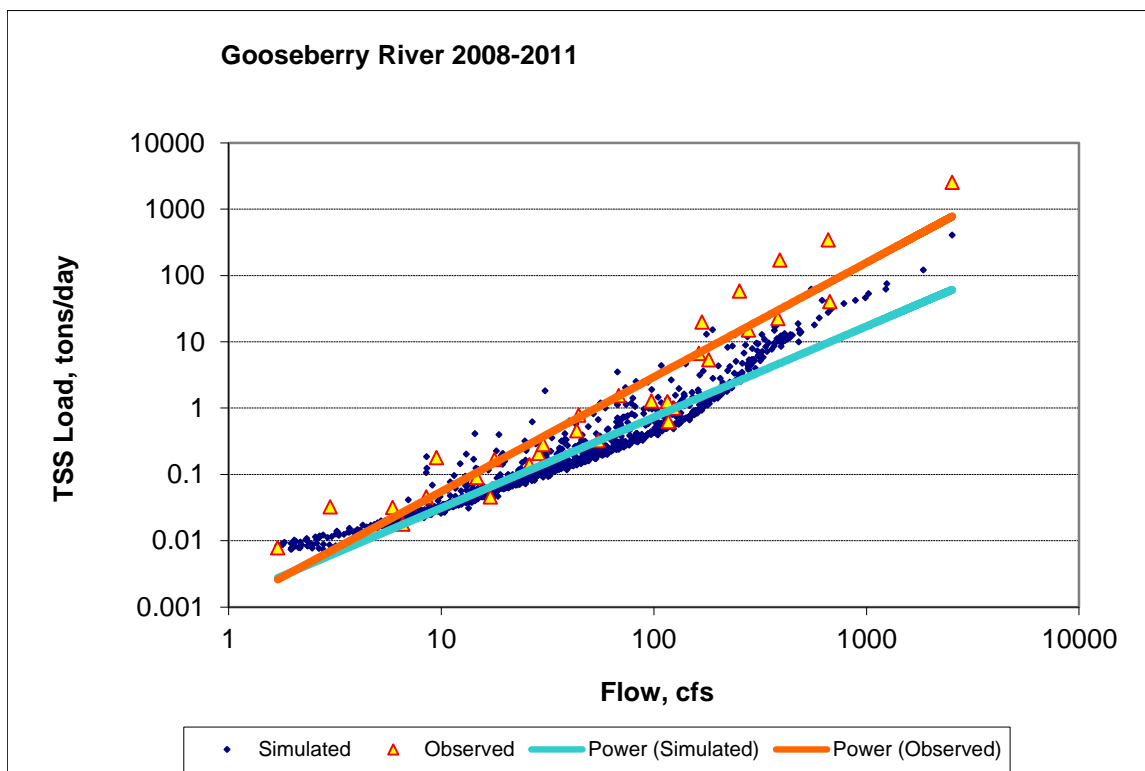


Figure 198. Power plot of simulated and observed Total Suspended Solids (TSS) load vs flow at Gooseberry River

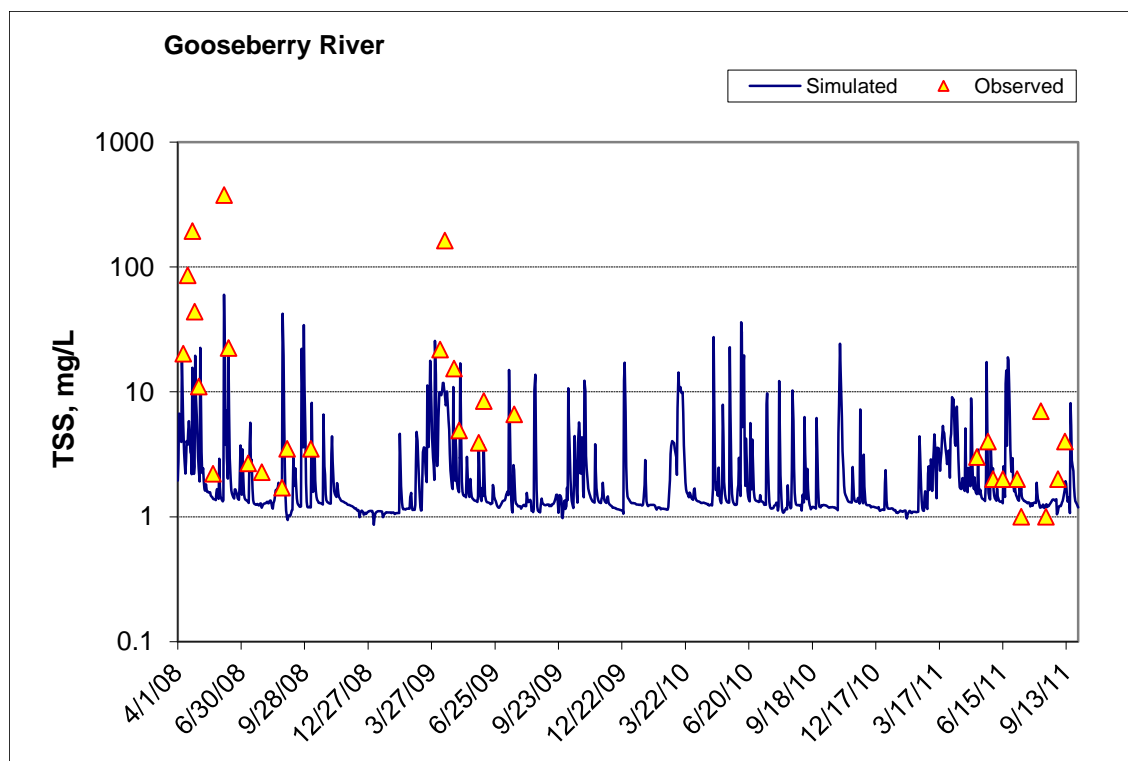


Figure 199. Time series of observed and simulated Total Suspended Solids (TSS) concentration at Gooseberry River

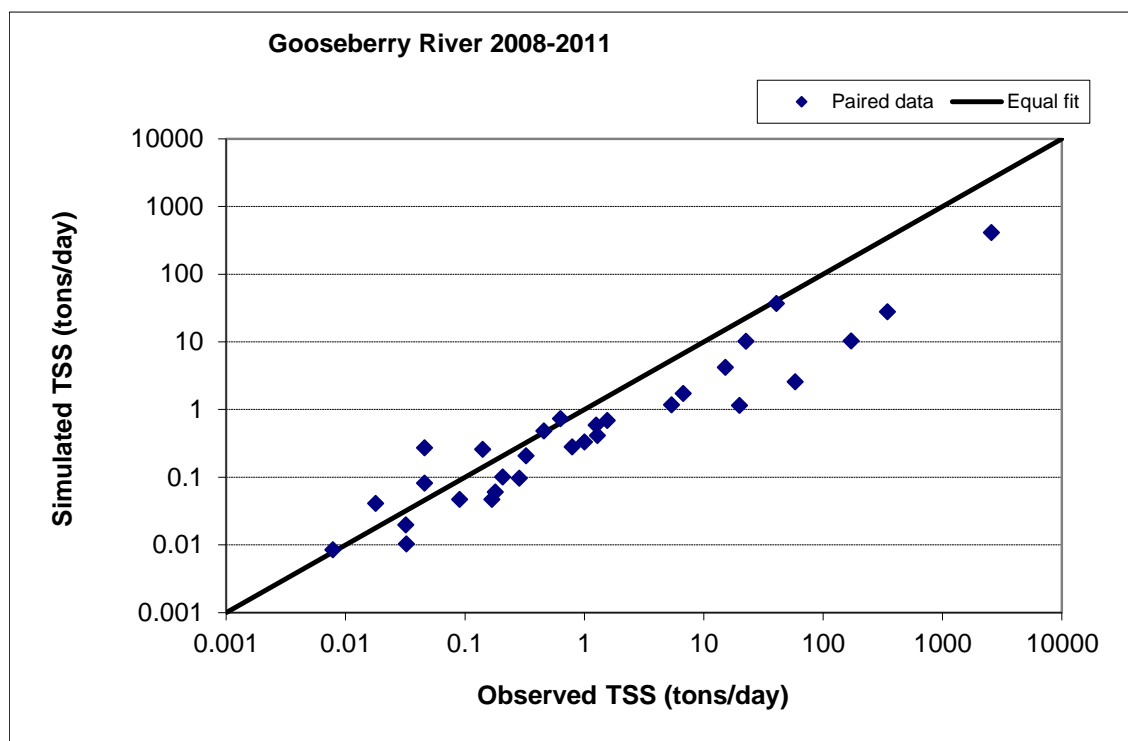


Figure 200. Paired simulated vs. observed Total Suspended Solids (TSS) load at Gooseberry River

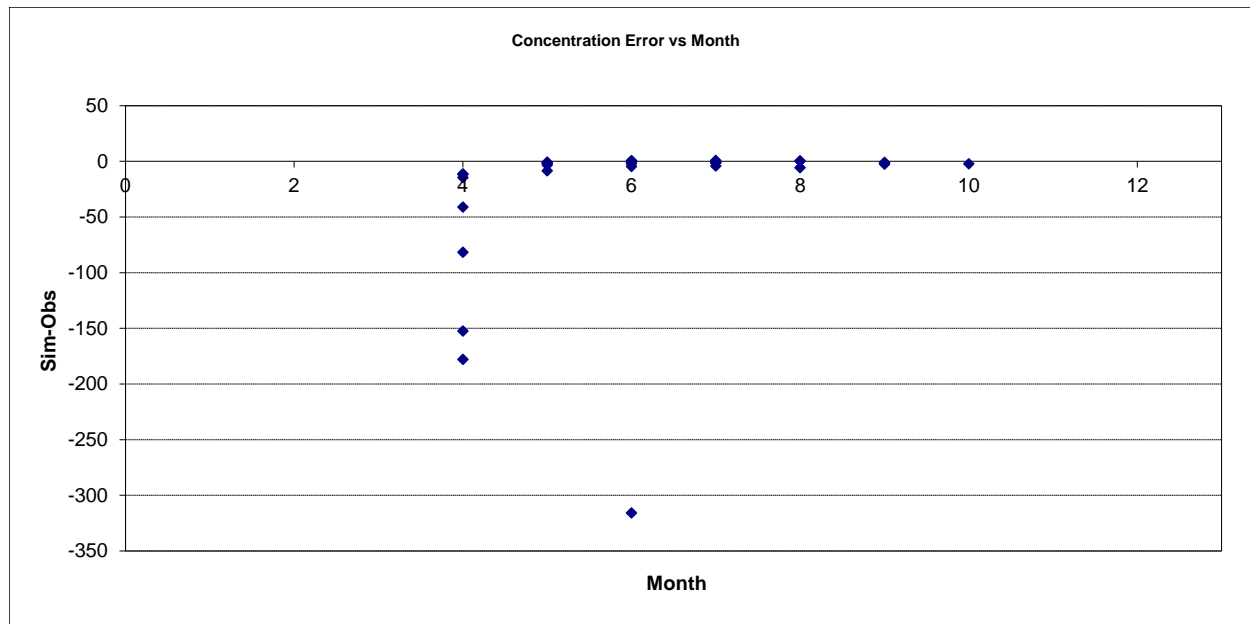


Figure 201. Residual (Simulated - Observed) vs. Month Total Suspended Solids (TSS) at Gooseberry River

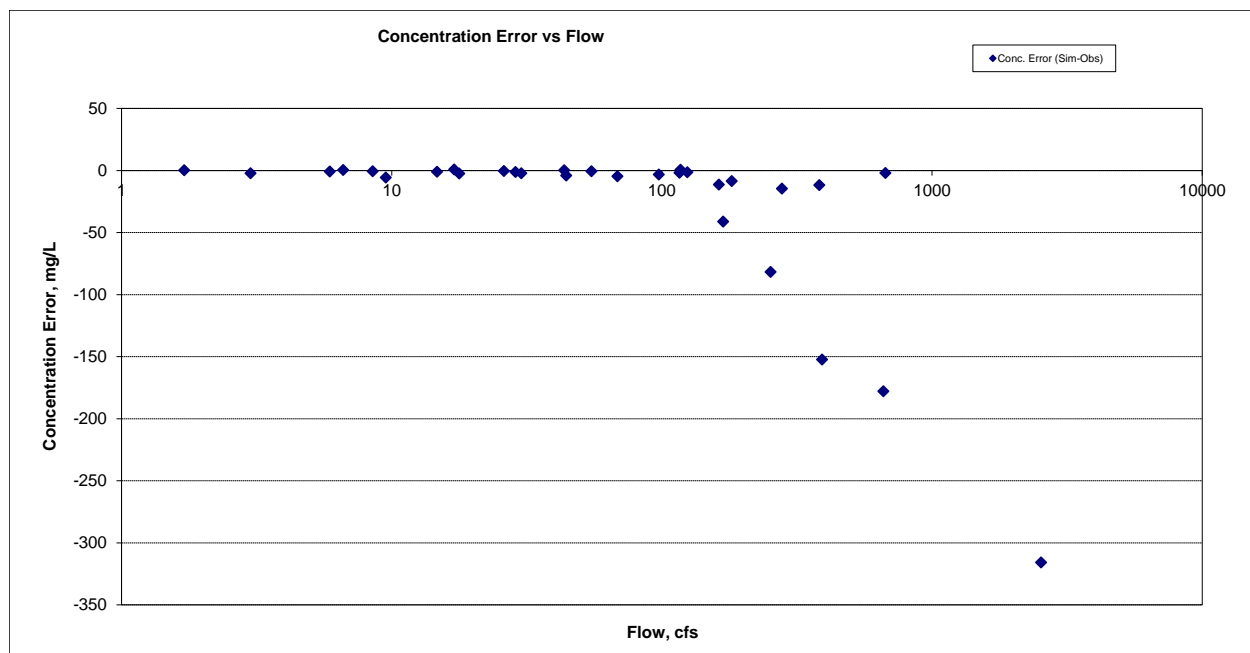


Figure 202. Residual (Simulated - Observed) vs. Flow Total Suspended Solids (TSS) at Gooseberry River

Nitrite+ Nitrate Nitrogen (NO_x)

Table 39. Nitrite+ Nitrate Nitrogen (NO_x) statistics

Count	20
Concentration Average Error	-0.62%
Concentration Median Error	12.36%
Load Average Error	-18.58%
Load Median Error	0.58%
Paired t concentration	0.81
Paired t load	0.51

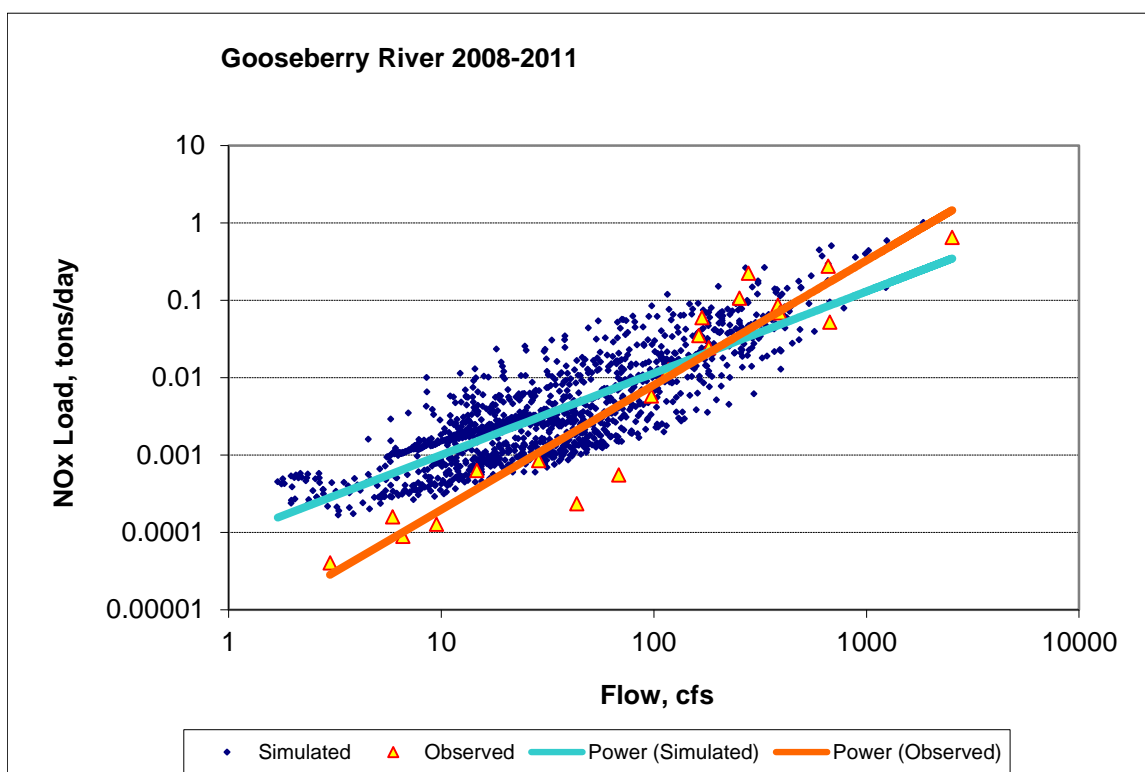


Figure 203. Power plot of simulated and observed Nitrite+ Nitrate Nitrogen (NO_x) load vs flow at Gooseberry River

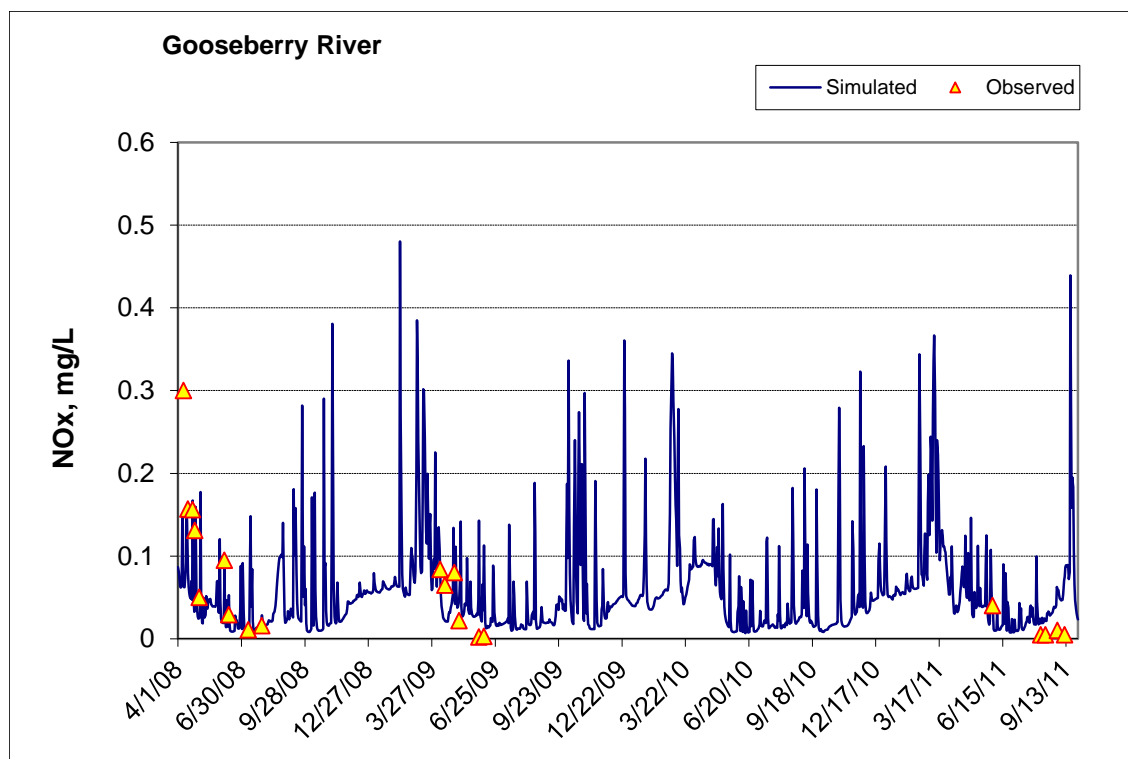


Figure 204. Time series of observed and simulated Nitrite+ Nitrate Nitrogen (NOx) concentration at Gooseberry River

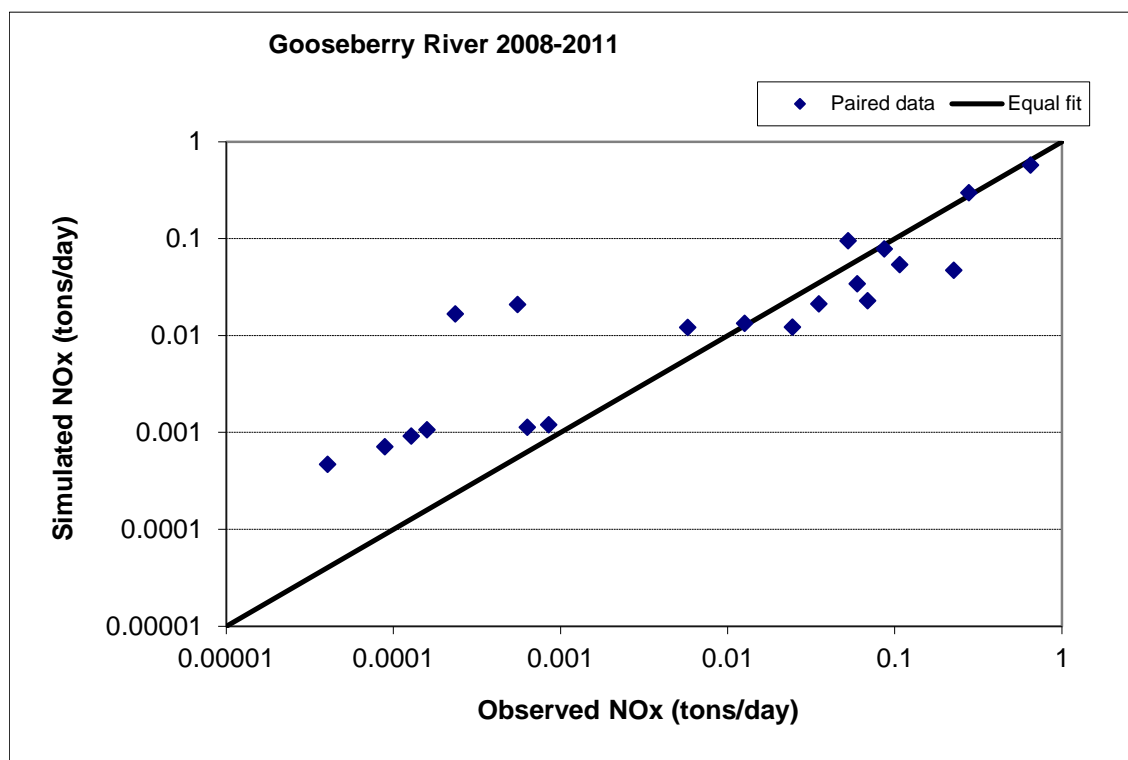


Figure 205. Paired simulated vs. observed Nitrite+ Nitrate Nitrogen (NOx) load at Gooseberry River



Figure 206. Residual (Simulated - Observed) vs. Month Nitrite+ Nitrate Nitrogen (NOx) at Gooseberry River

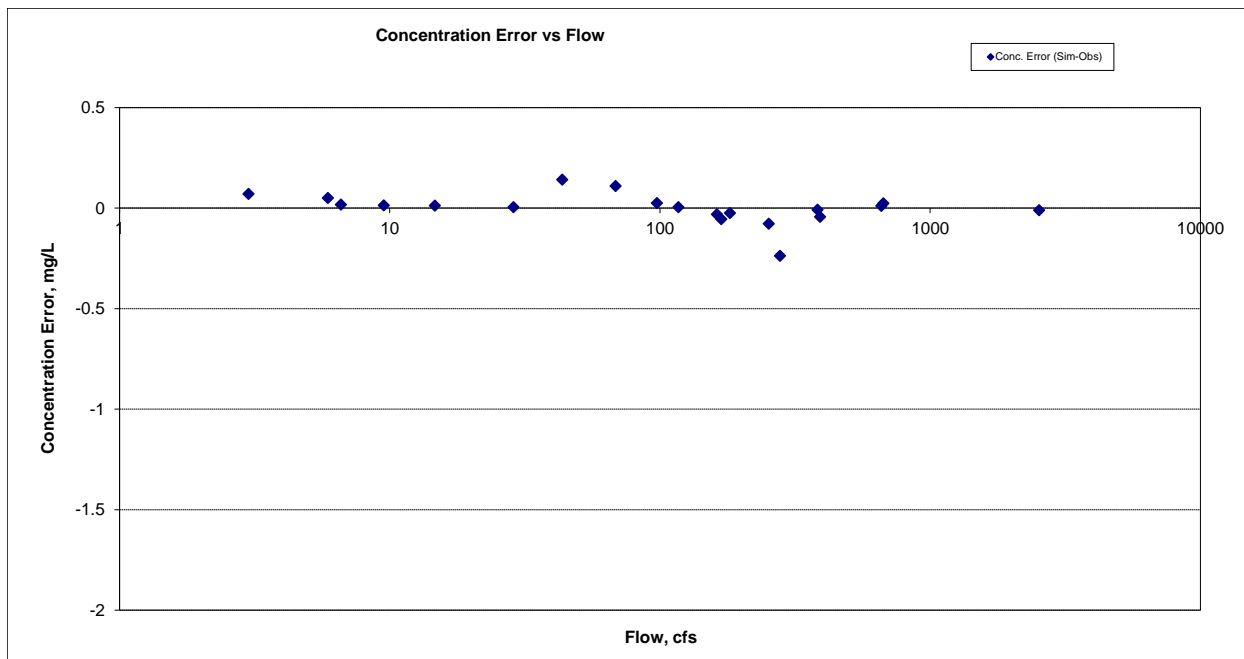


Figure 207. Residual (Simulated - Observed) vs. Flow Nitrite+ Nitrate Nitrogen (NOx) at Gooseberry River

Total Phosphorus (TP)

Table 40. Total Phosphorus (TP) statistics

Count	30
Concentration Average Error	-26.83%
Concentration Median Error	-15.49%
Load Ave Error	-13.20%
Load Median Error	-0.53%
Paired t concentration	0.37
Paired t load	0.55

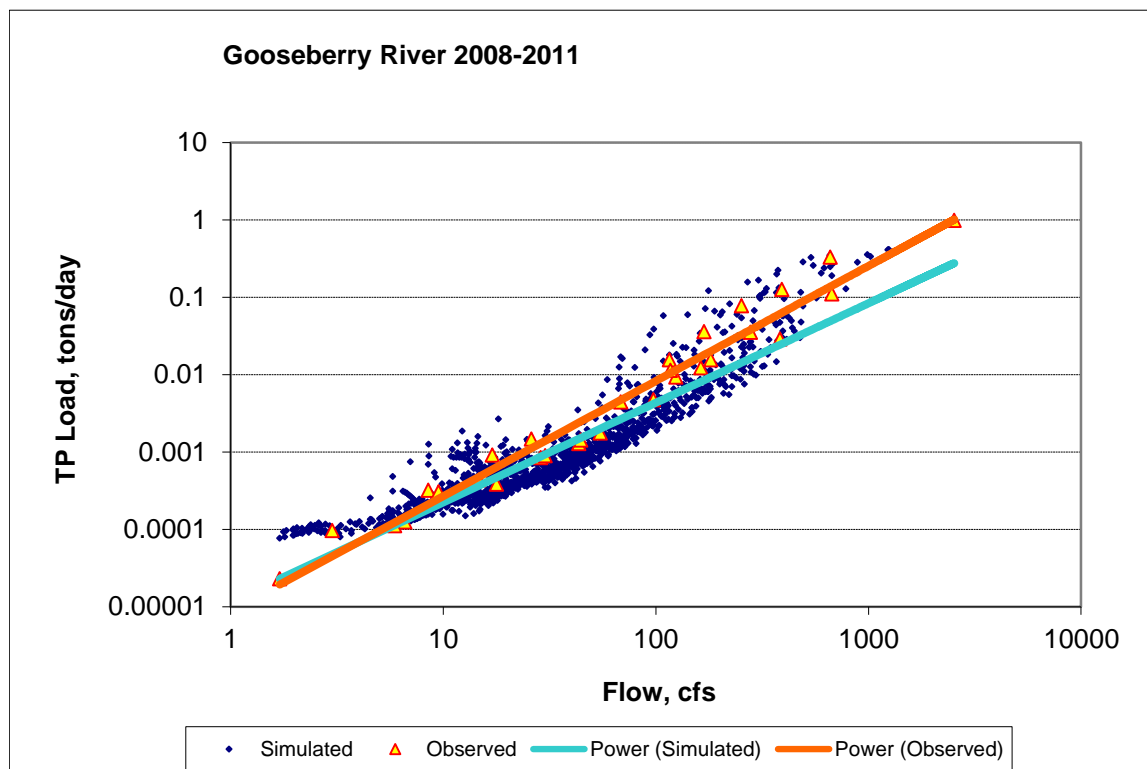


Figure 208. Power plot of simulated and observed Total Phosphorus (TP) load vs flow at Gooseberry River

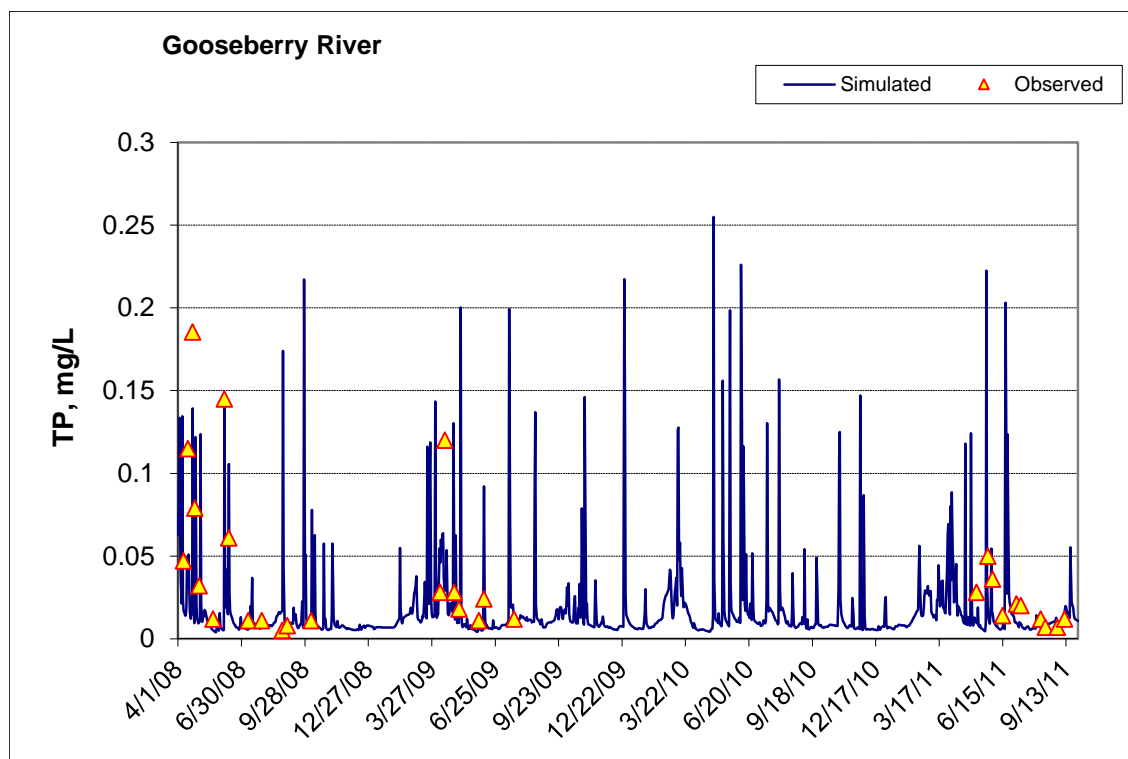


Figure 209. Time series of observed and simulated Total Phosphorus (TP) concentration at Gooseberry River

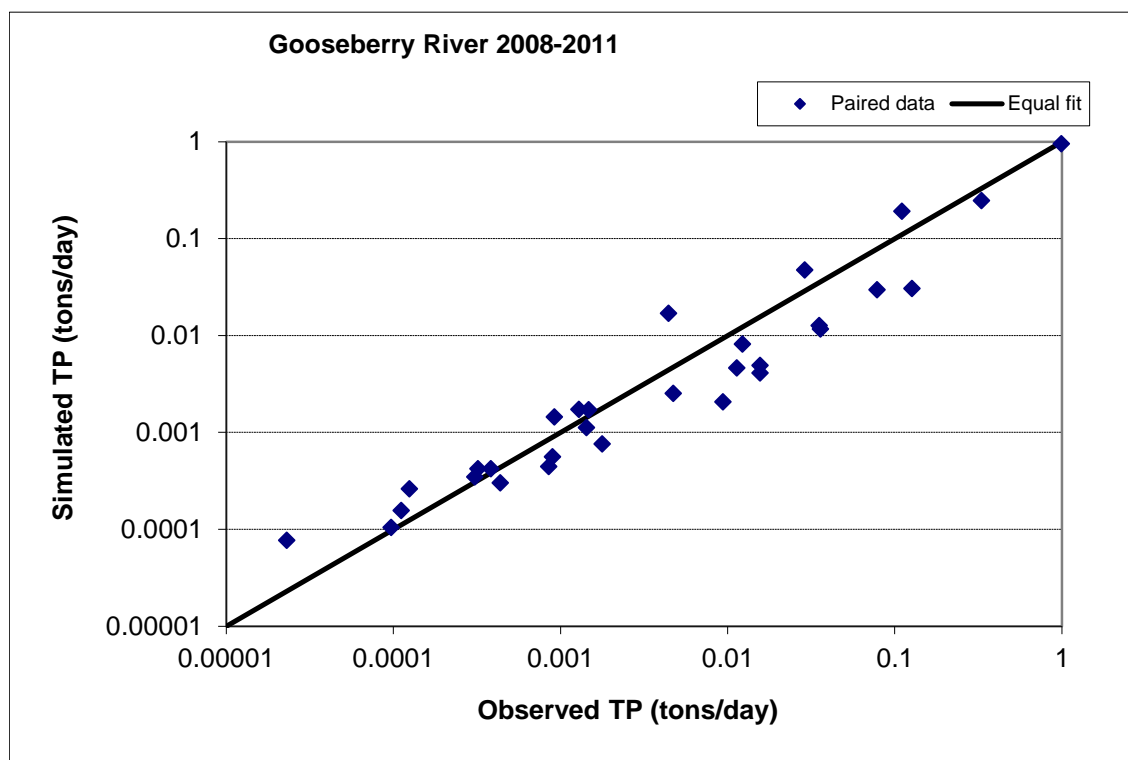


Figure 210. Paired simulated vs. observed Total Phosphorus (TP) load at Gooseberry River

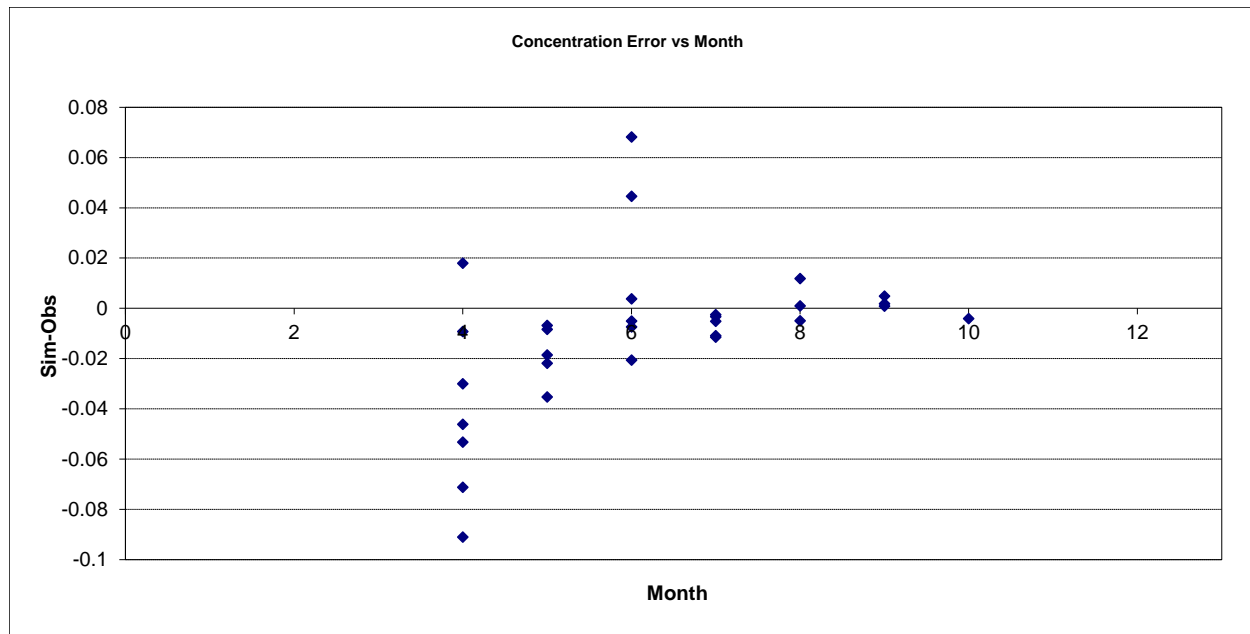


Figure 211. Residual (Simulated - Observed) vs. Month Total Phosphorus (TP) at Gooseberry River

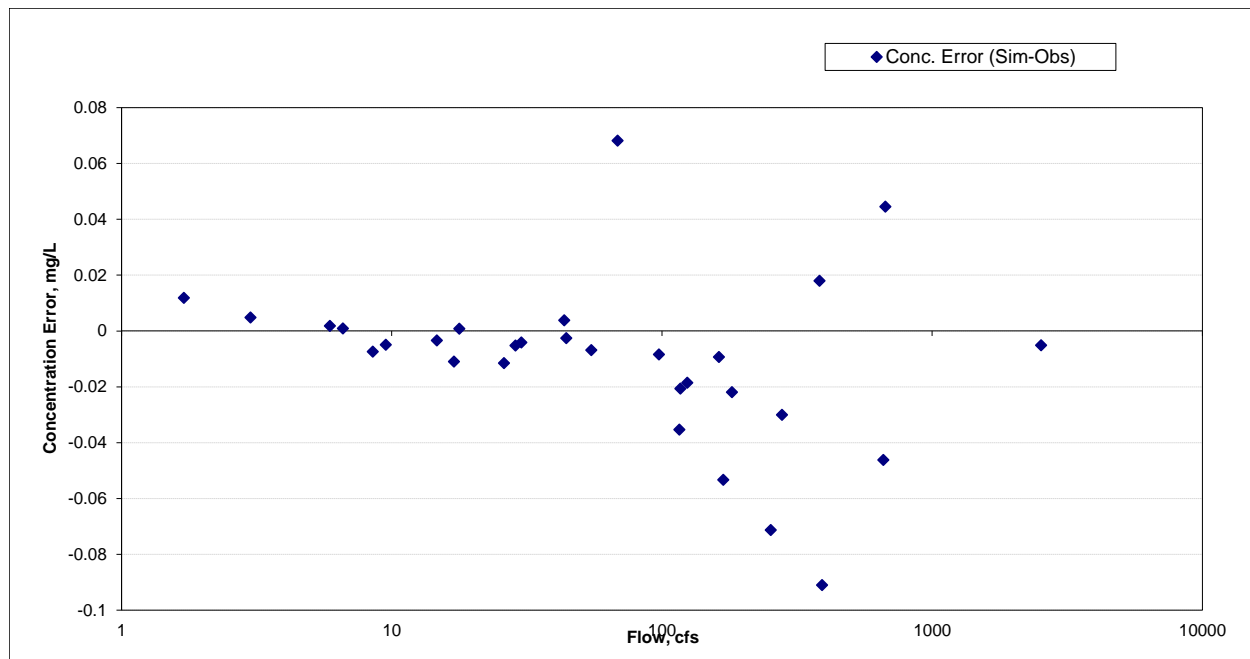


Figure 212. Residual (Simulated - Observed) vs. Flow Total Phosphorus (TP) at Gooseberry River

Baptism River near Beaver Bay (HYDSTRA 01092001)

Total Suspended Solids (TSS)

Table 41. Total Suspended Solids (TSS) statistics

Count	105
Concentration Average Error	-5.16%
Concentration Median Error	12.79%
Load Ave Error	-30.31%
Load Median Error	0.96%
Paired t concentration	0.83
Paired t load	0.34

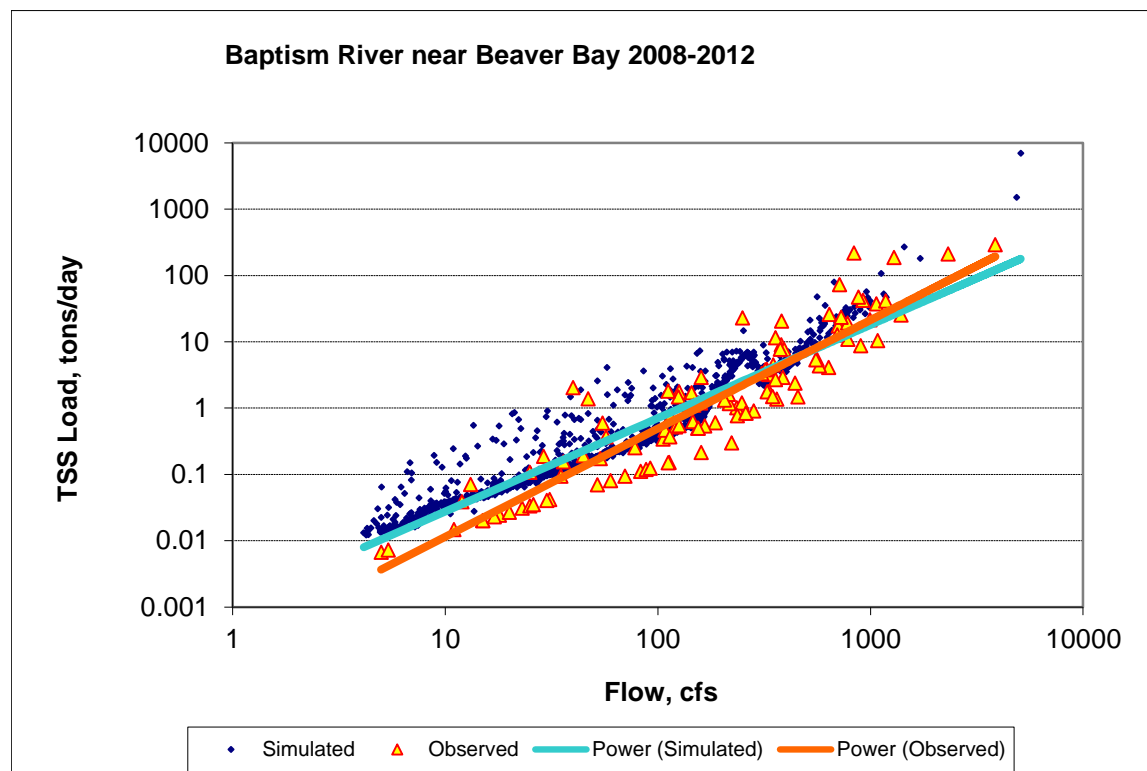


Figure 213. Power plot of simulated and observed Total Suspended Solids (TSS) load vs flow at Baptism River near Beaver Bay

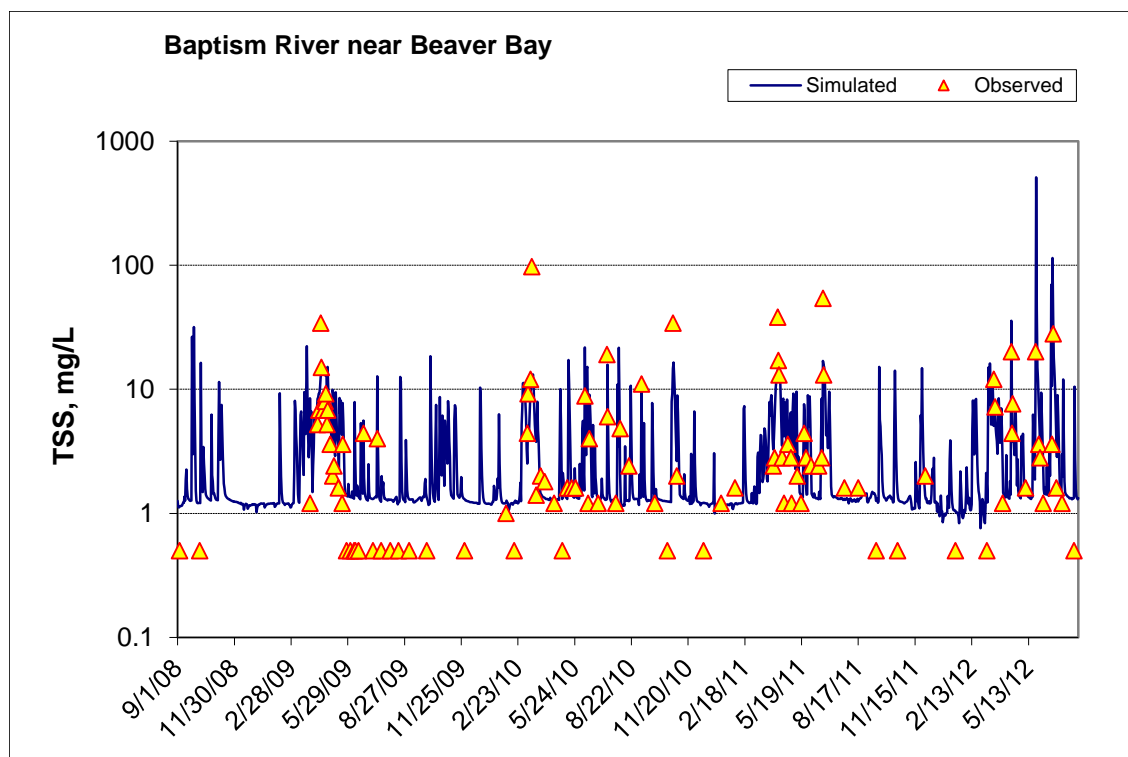


Figure 214. Time series of observed and simulated Total Suspended Solids (TSS) concentration at Baptism River near Beaver Bay

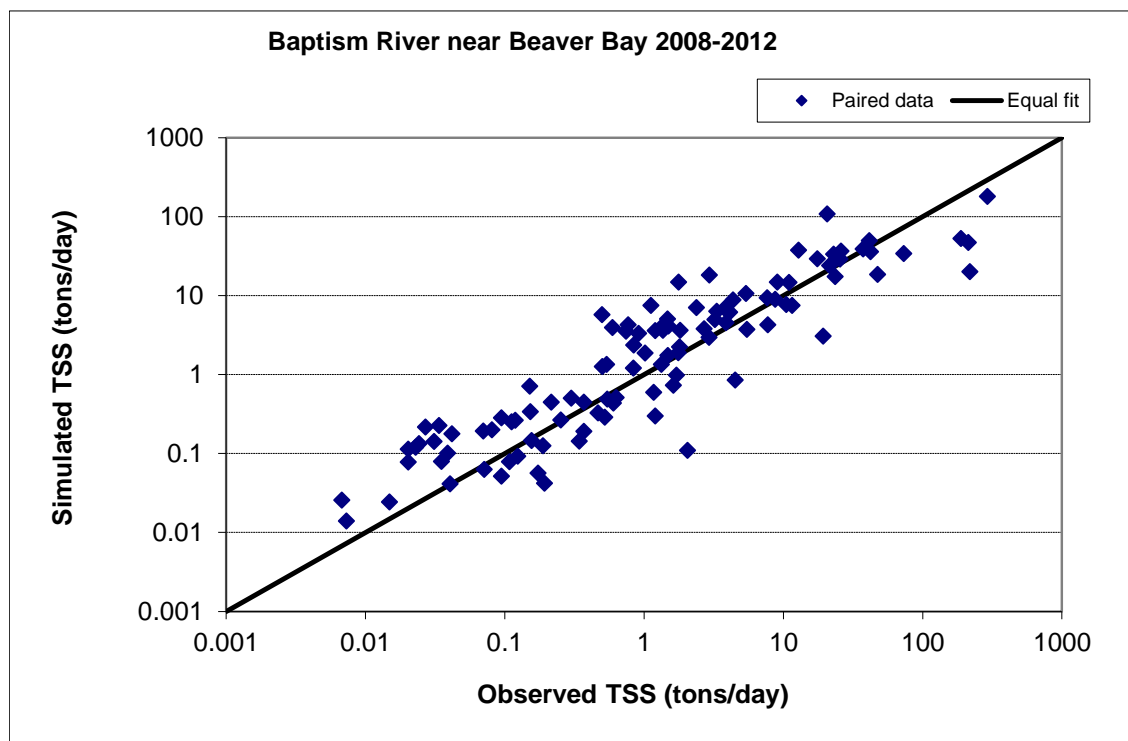


Figure 215. Paired simulated vs. observed Total Suspended Solids (TSS) load at Baptism River near Beaver Bay

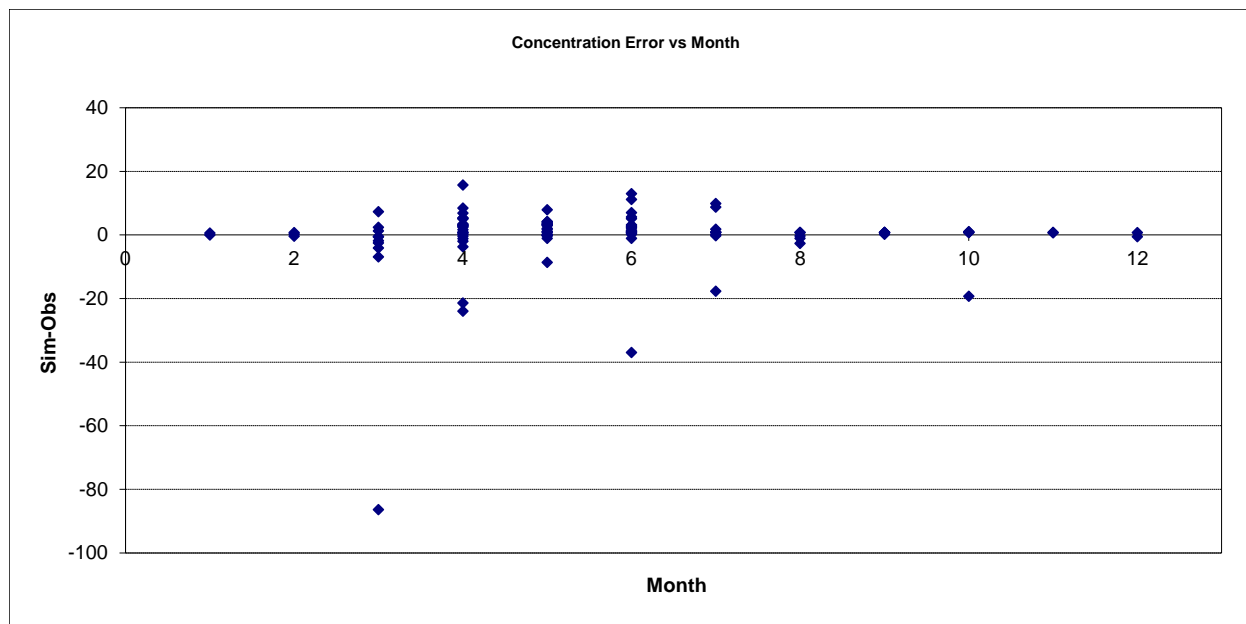


Figure 216. Residual (Simulated - Observed) vs. Month Total Suspended Solids (TSS) at Baptism River near Beaver Bay

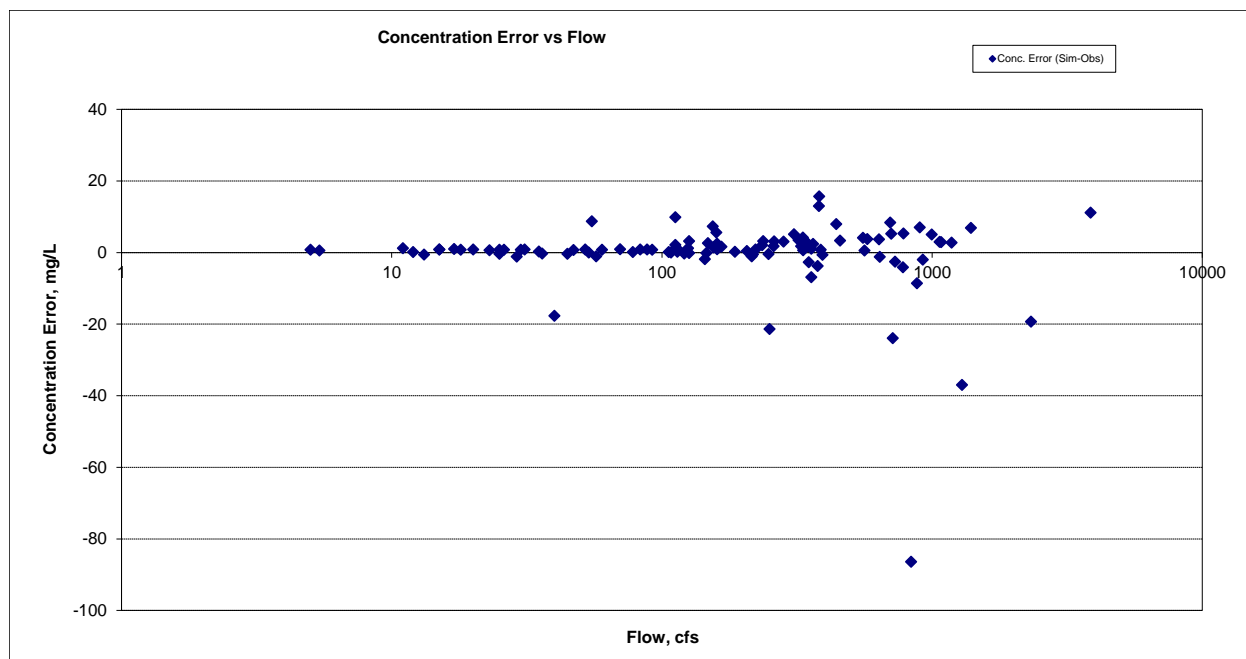


Figure 217. Residual (Simulated - Observed) vs. Flow Total Suspended Solids (TSS) at Baptism River near Beaver Bay

Ammonia Nitrogen (NH₃)

Table 42. Ammonia Nitrogen (NH₃) statistics

Count	19
Concentration Average Error	6.02%
Concentration Median Error	27.81%
Load Ave Error	38.31%
Load Median Error	5.58%
Paired t concentration	0.75
Paired t load	0.26

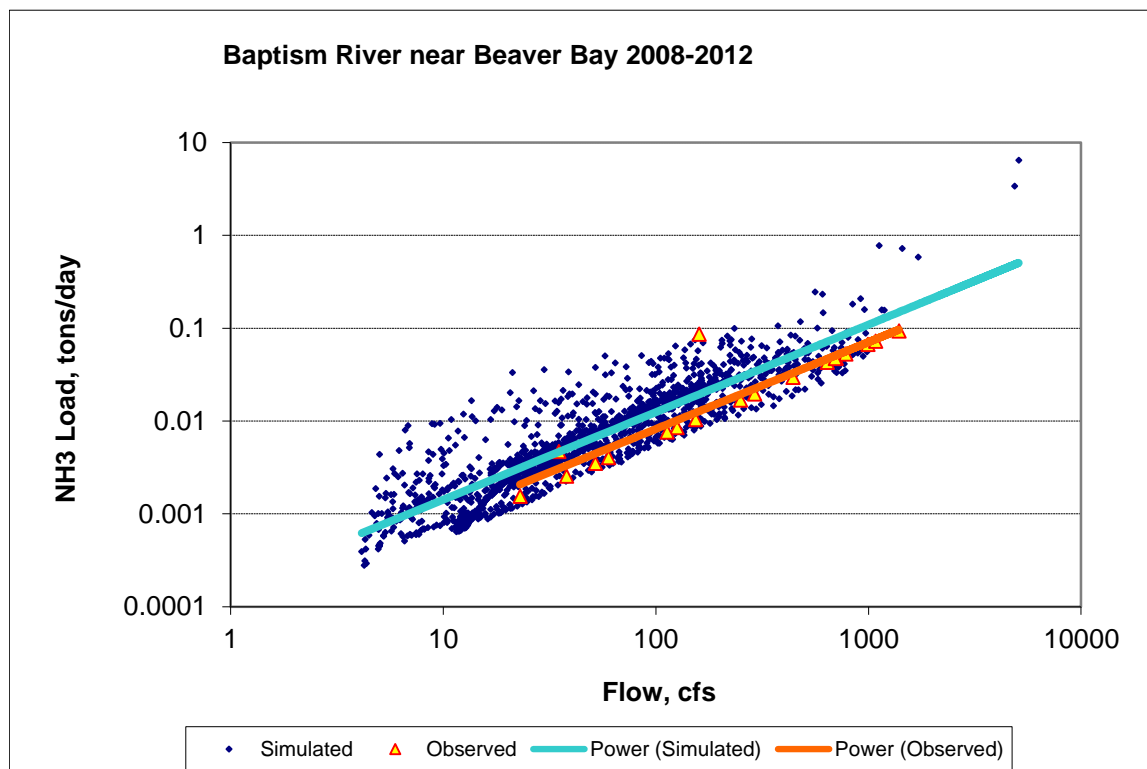


Figure 218. Power plot of simulated and observed Ammonia Nitrogen (NH₃) load vs flow at Baptism River near Beaver Bay

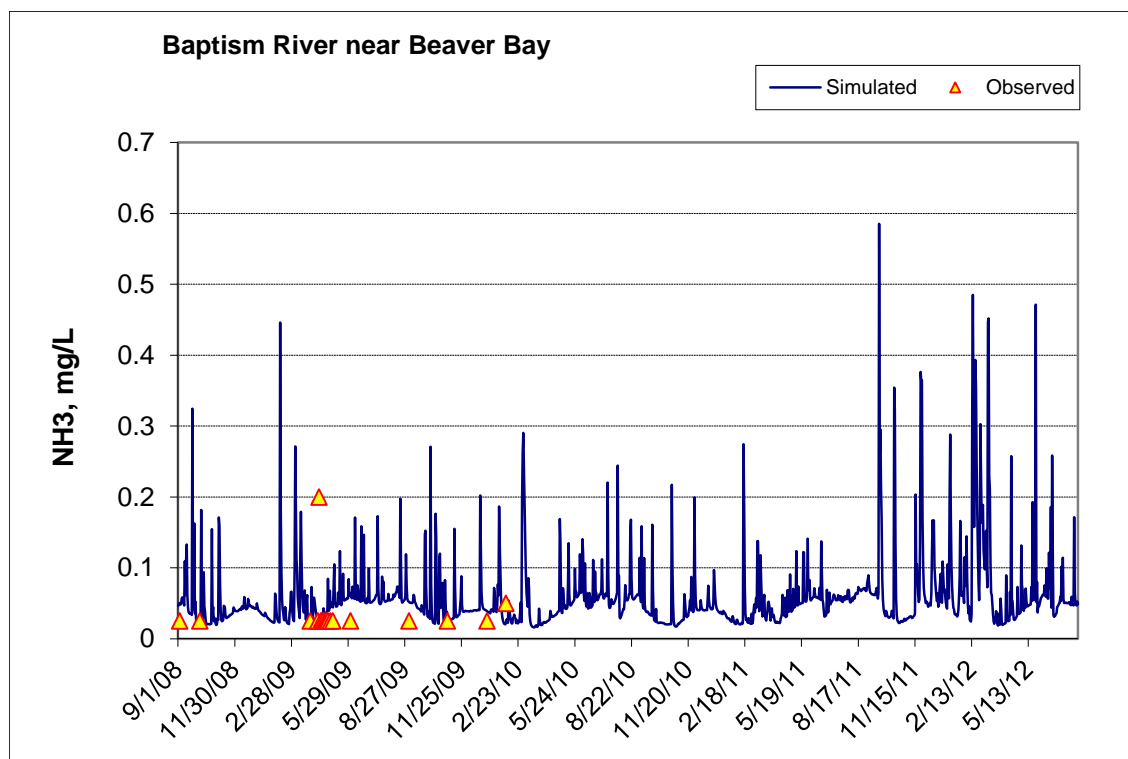


Figure 219. Time series of observed and simulated Ammonia Nitrogen (NH₃) concentration at Baptism River near Beaver Bay

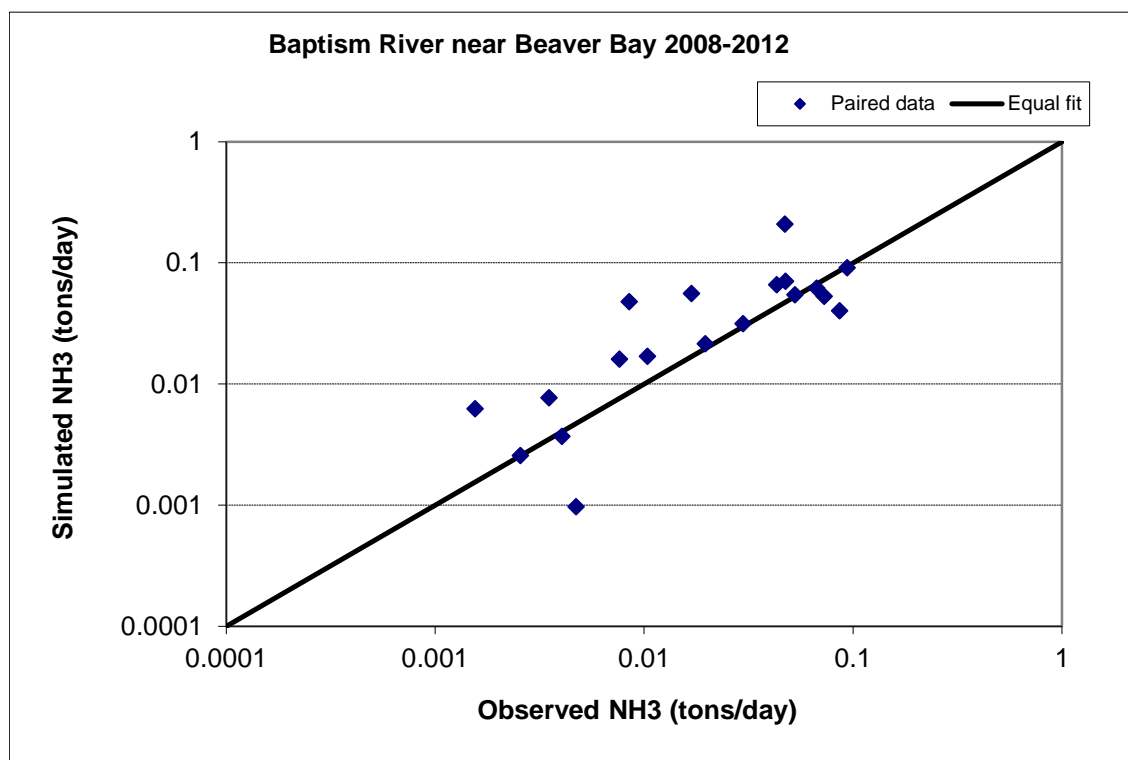


Figure 220. Paired simulated vs. observed Ammonia Nitrogen (NH₃) load at Baptism River near Beaver Bay

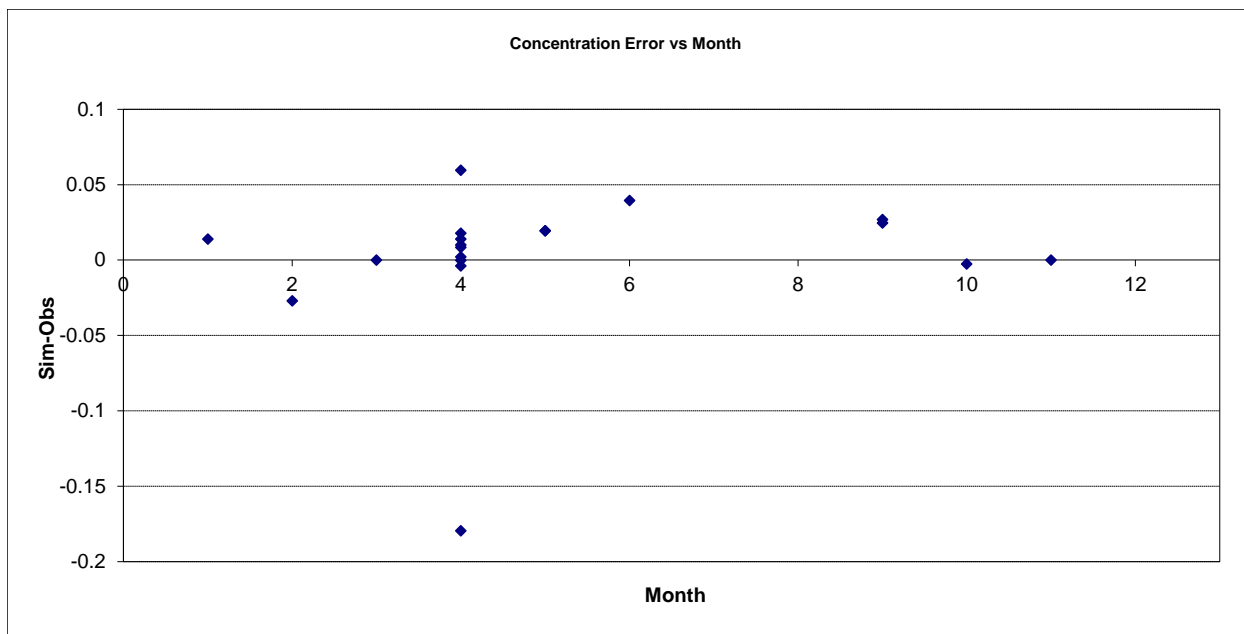


Figure 221. Residual (Simulated - Observed) vs. Month Ammonia Nitrogen (NH3) at Baptism River near Beaver Bay

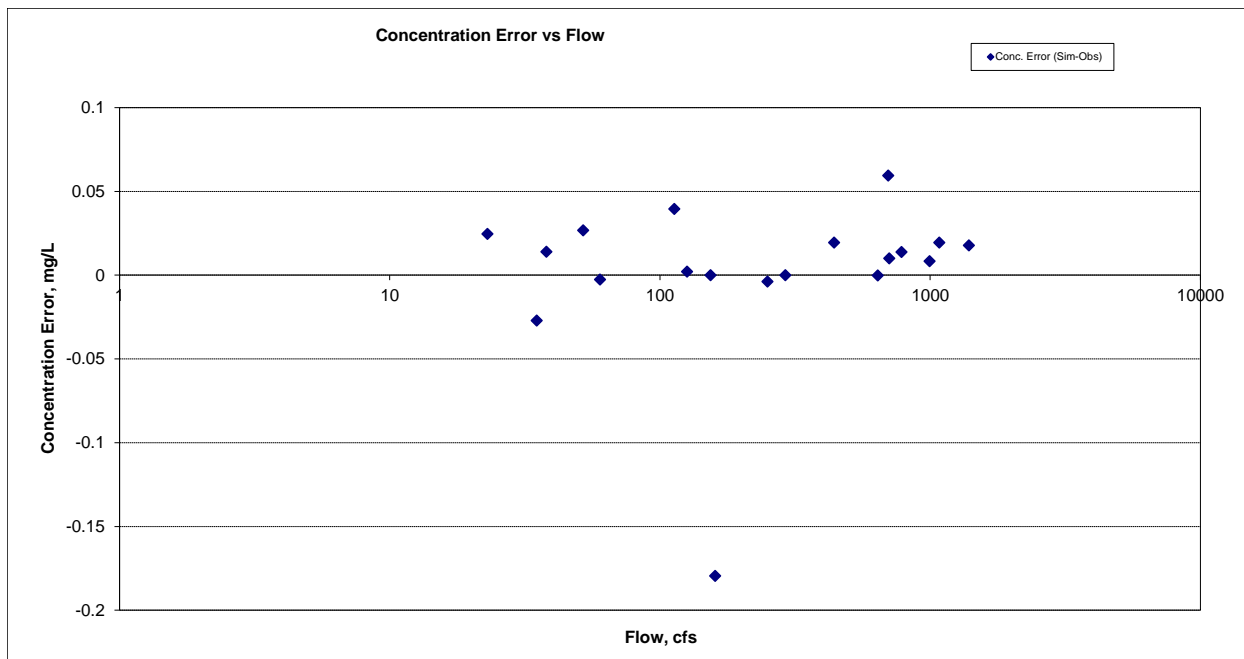


Figure 222. Residual (Simulated - Observed) vs. Flow Ammonia Nitrogen (NH3) at Baptism River near Beaver Bay

Organic Nitrogen (OrgN)

Table 43. Organic Nitrogen (OrgN) statistics

Count	19
Concentration Average Error	9.20%
Concentration Median Error	10.97%
Load Ave Error	37.31%
Load Median Error	-3.69%
Paired t concentration	0.93
Paired t load	0.26

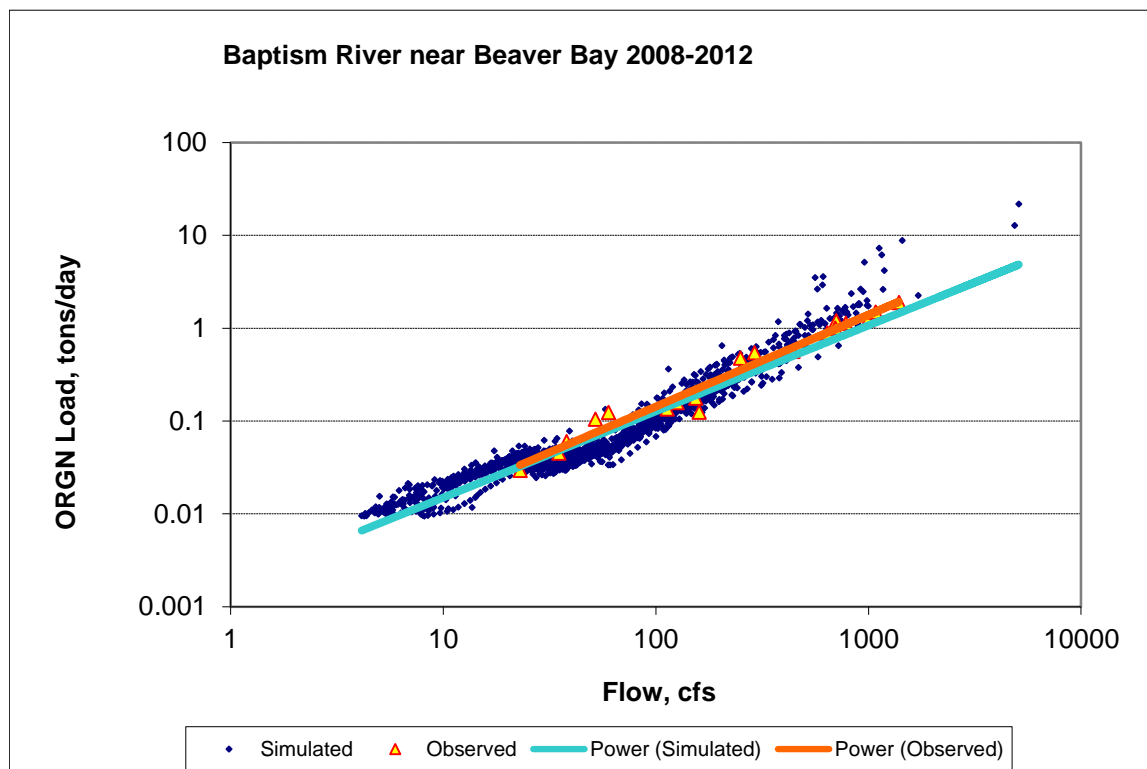


Figure 223. Power plot of simulated and observed Organic Nitrogen (OrgN) load vs flow at Baptism River near Beaver Bay

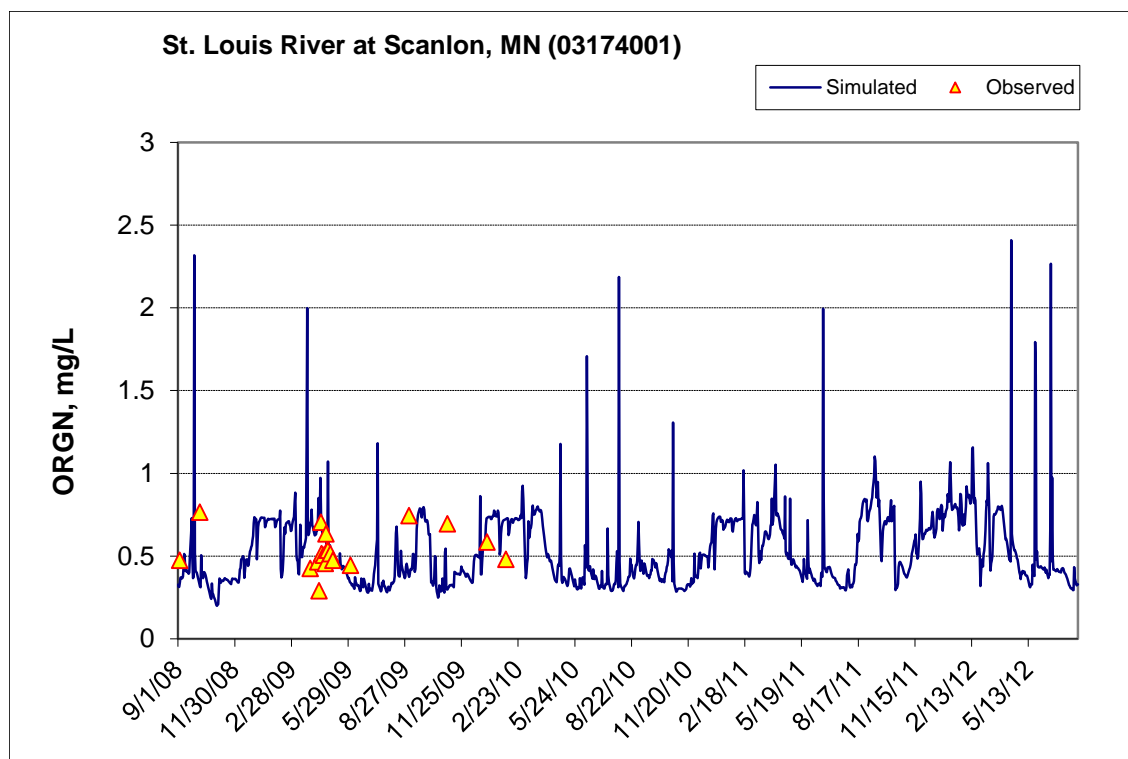


Figure 224. Time series of observed and simulated Organic Nitrogen (OrgN) concentration at Baptism River near Beaver Bay

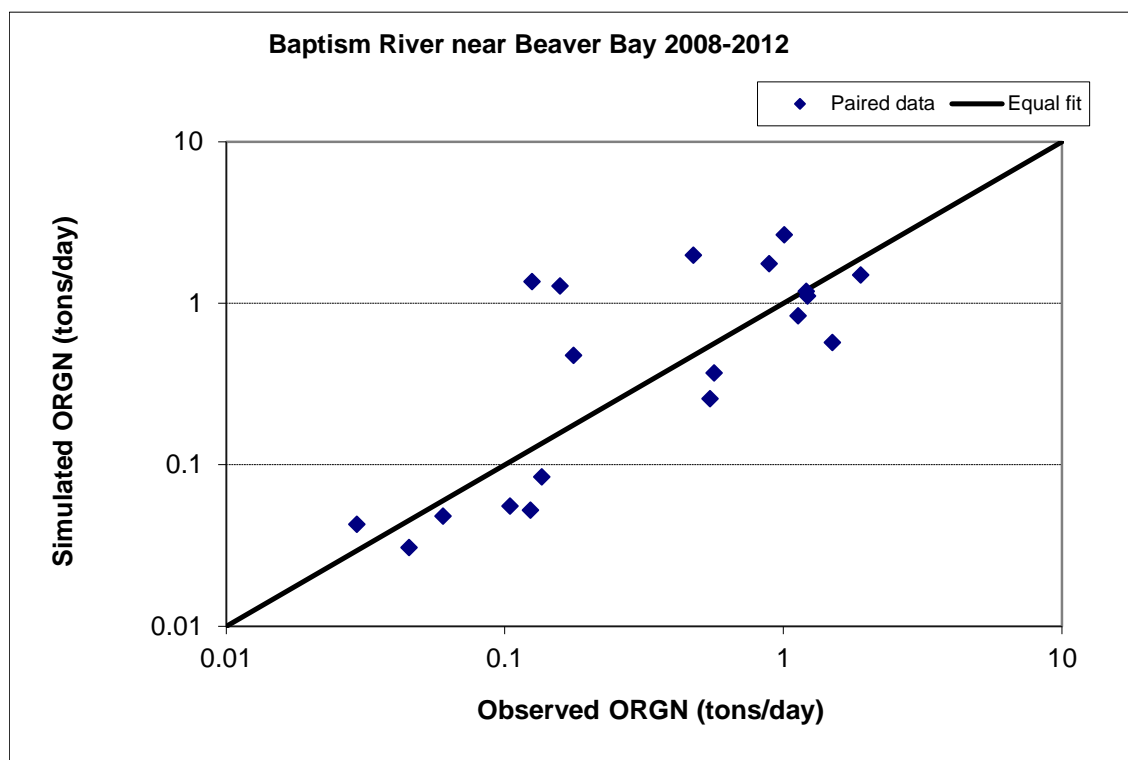


Figure 225. Paired simulated vs. observed Organic Nitrogen (OrgN) load at Baptism River near Beaver Bay

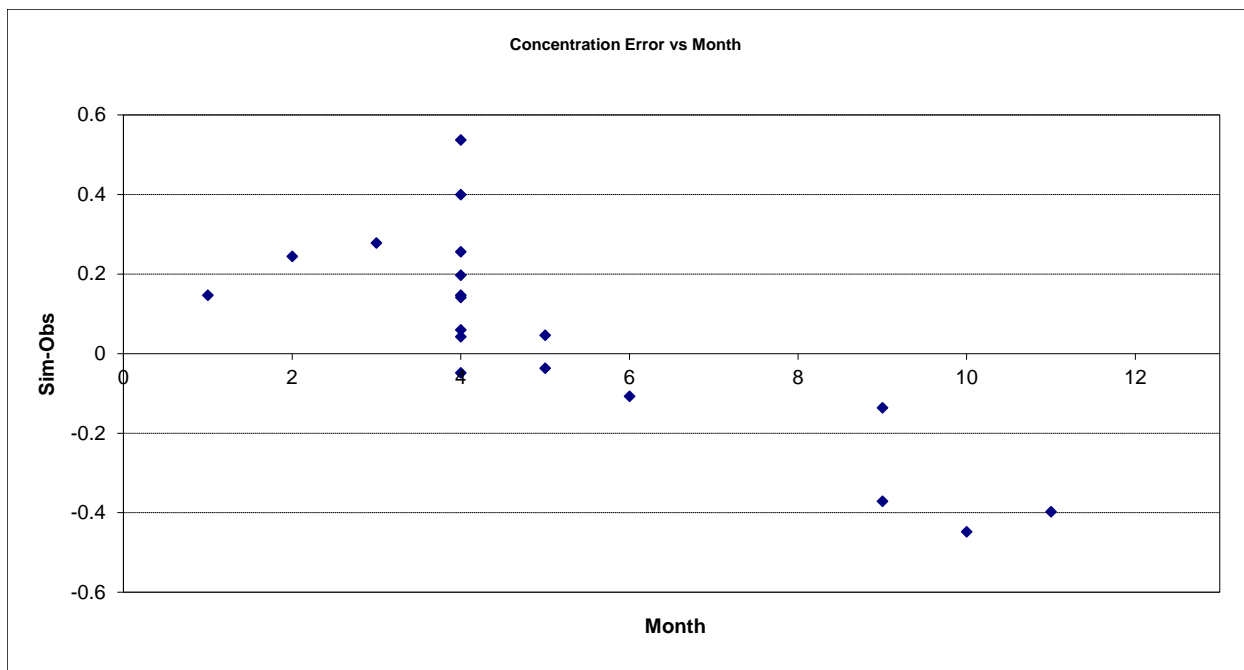


Figure 226. Residual (Simulated - Observed) vs. Month Organic Nitrogen (OrgN) at Baptism River near Beaver Bay

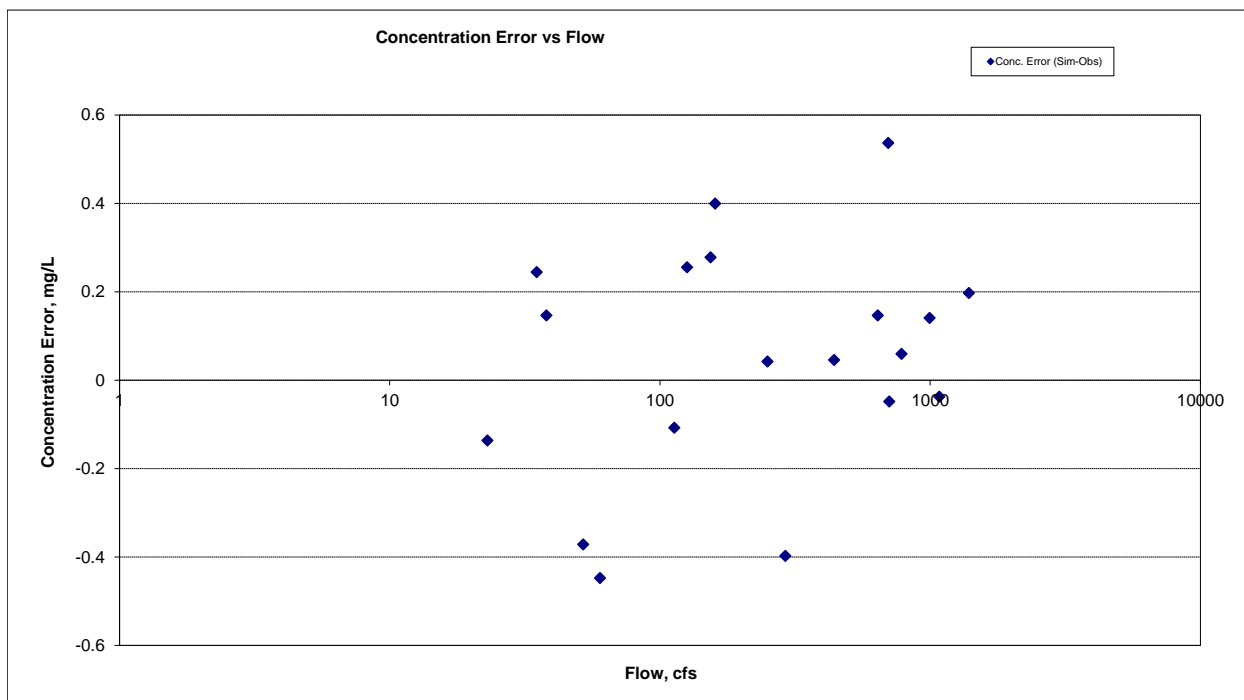


Figure 227. Residual (Simulated - Observed) vs. Flow Organic Nitrogen (OrgN) at Baptism River near Beaver Bay

Total Kjeldahl Nitrogen (TKN)

Table 44. Total Kjeldahl Nitrogen (TKN) statistics

Count	106
Concentration Average Error	-3.24%
Concentration Median Error	-7.17%
Load Ave Error	-4.15%
Load Median Error	-6.57%
Paired t concentration	1.00
Paired t load	0.83

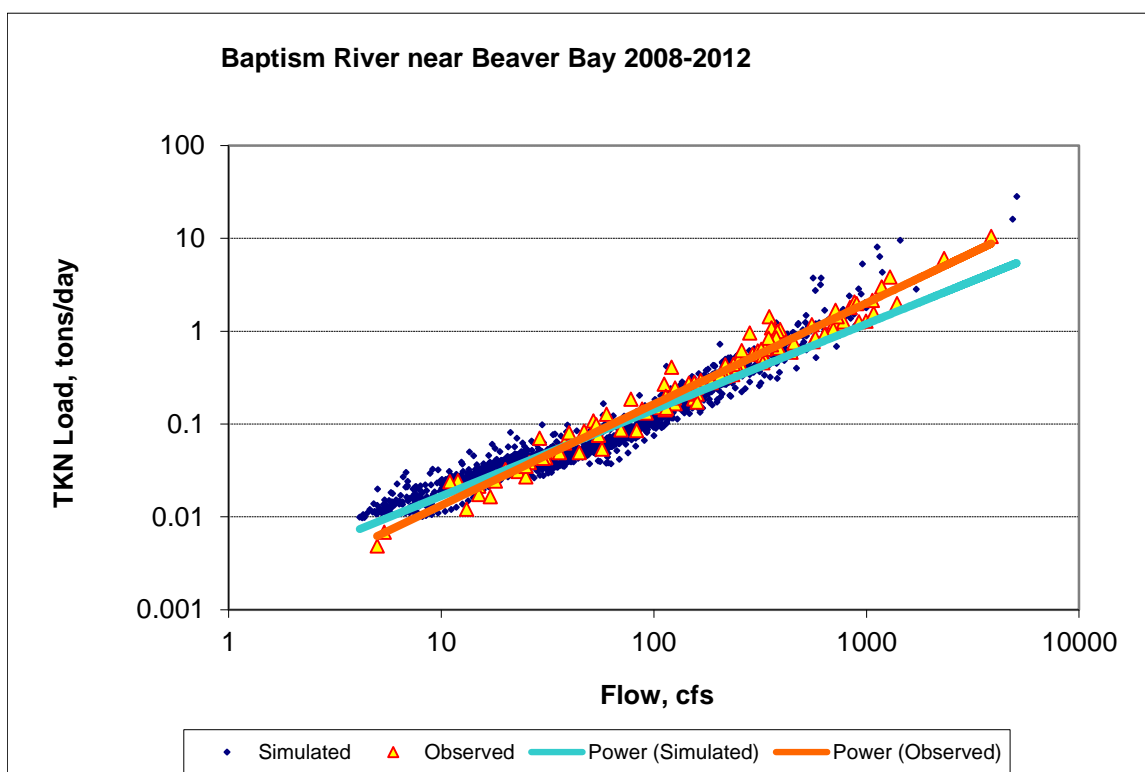


Figure 228. Power plot of simulated and observed Total Kjeldahl Nitrogen (TKN) load vs flow at Baptism River near Beaver Bay

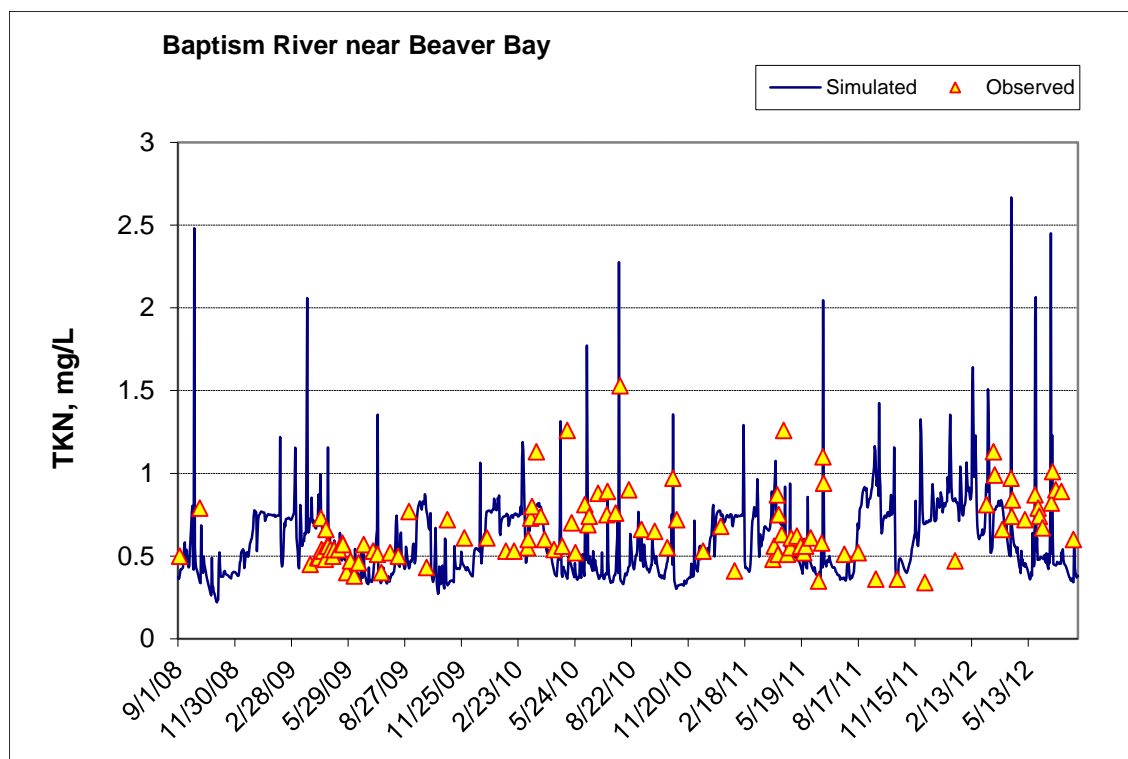


Figure 229. Time series of observed and simulated Total Kjeldahl Nitrogen (TKN) concentration at Baptism River near Beaver Bay

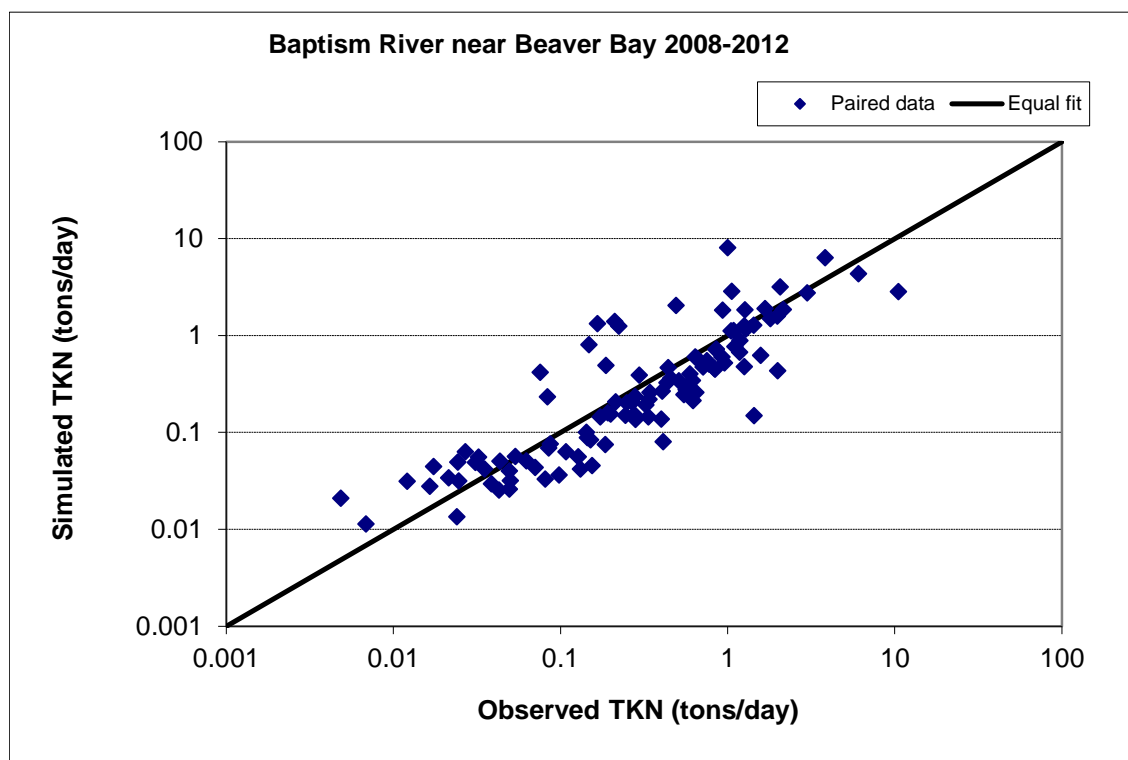


Figure 230. Paired simulated vs. observed Total Kjeldahl Nitrogen (TKN) load at Baptism River near Beaver Bay

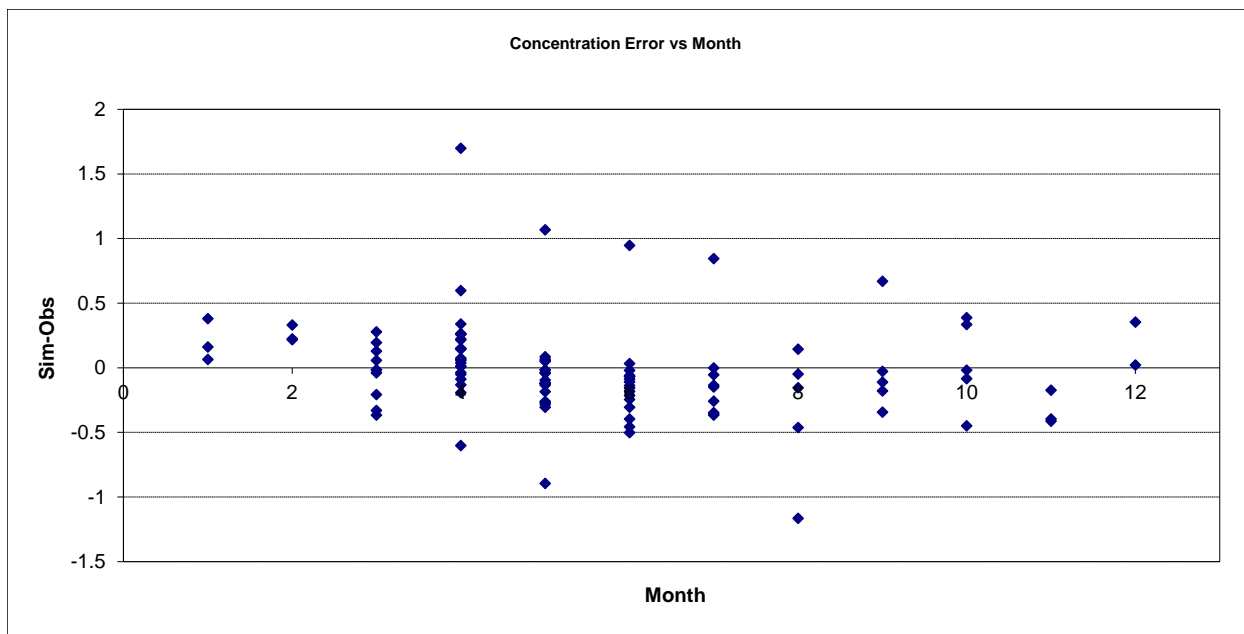


Figure 231. Residual (Simulated - Observed) vs. Month Total Kjeldahl Nitrogen (TKN) at Baptism River near Beaver Bay

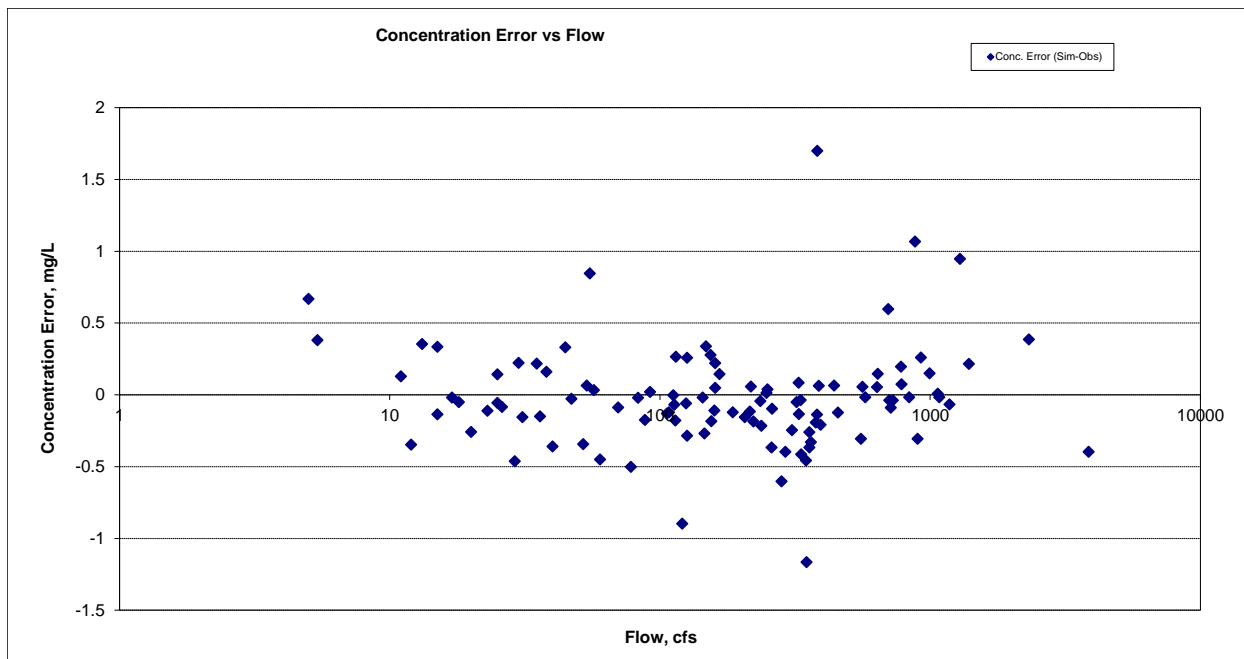


Figure 232. Residual (Simulated - Observed) vs. Flow Total Kjeldahl Nitrogen (TKN) at Baptism River near Beaver Bay

Nitrite+ Nitrate Nitrogen (NO_x)

Table 45. Nitrite+ Nitrate Nitrogen (NO_x) statistics

Count	106
Concentration Average Error	-13.97%
Concentration Median Error	-2.57%
Load Ave Error	-19.15%
Load Median Error	-0.71%
Paired t concentration	0.70
Paired t load	0.52

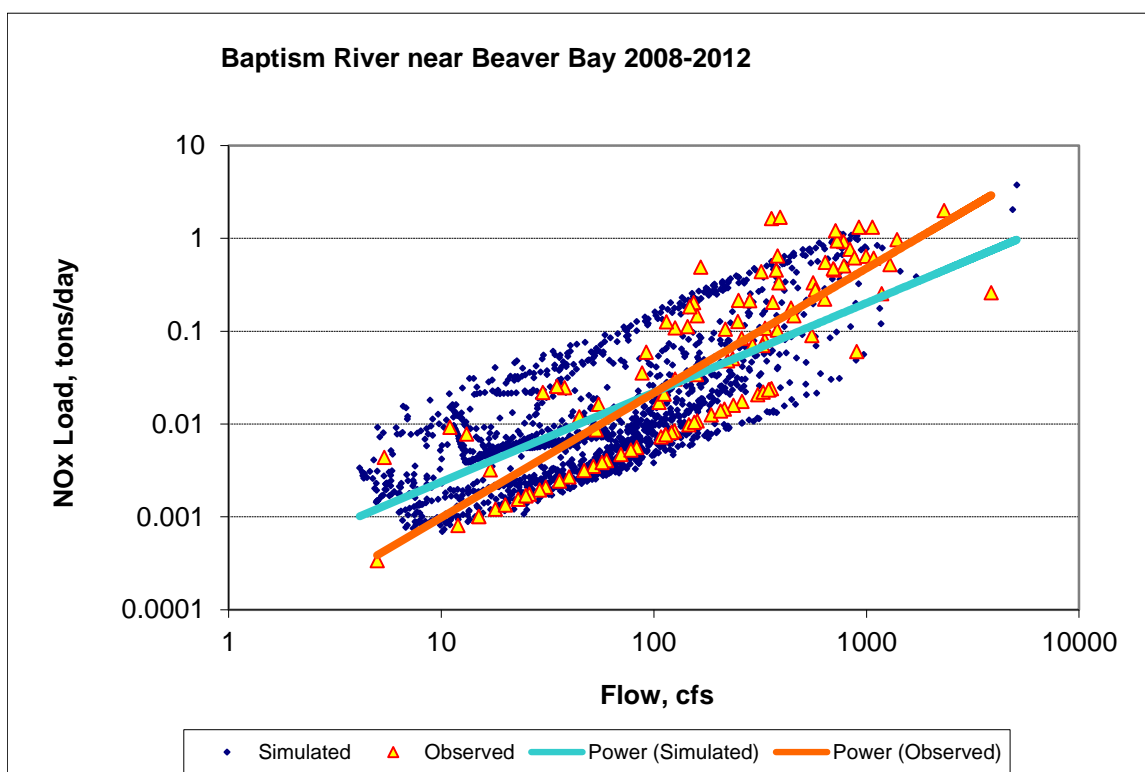


Figure 233. Power plot of simulated and observed Nitrite+ Nitrate Nitrogen (NO_x) load vs flow at Baptism River near Beaver Bay

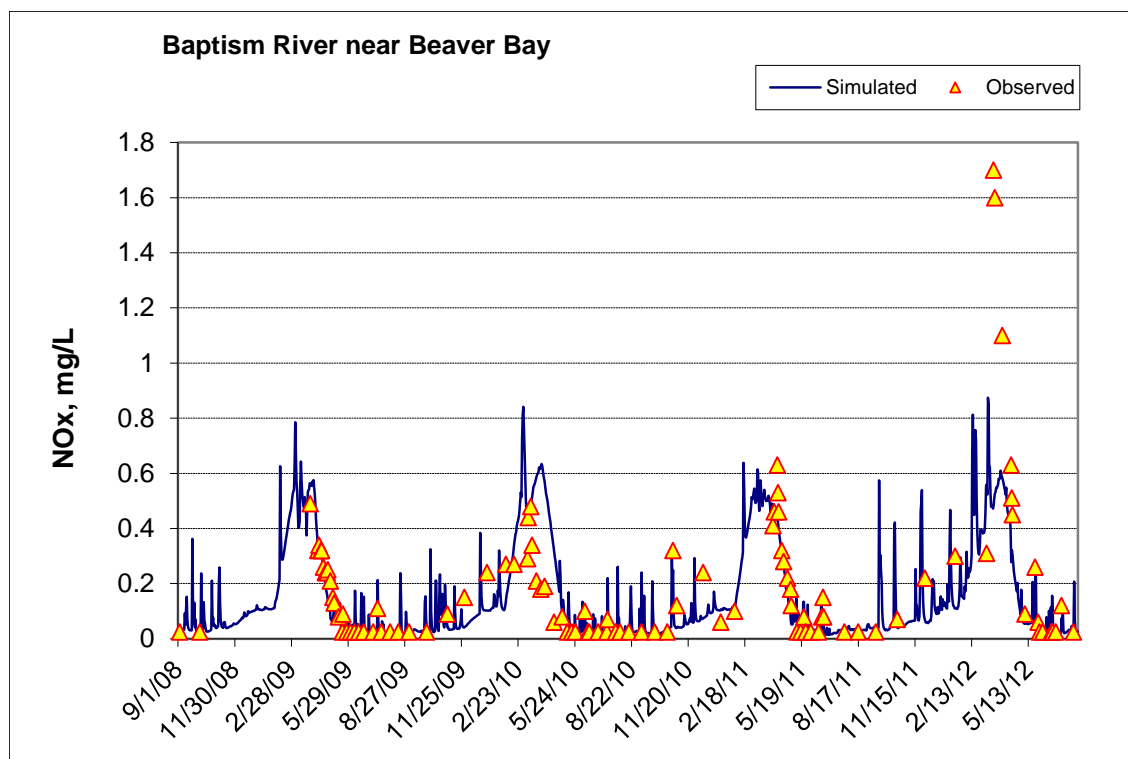


Figure 234. Time series of observed and simulated Nitrite+ Nitrate Nitrogen (NOx) concentration at Baptism River near Beaver Bay

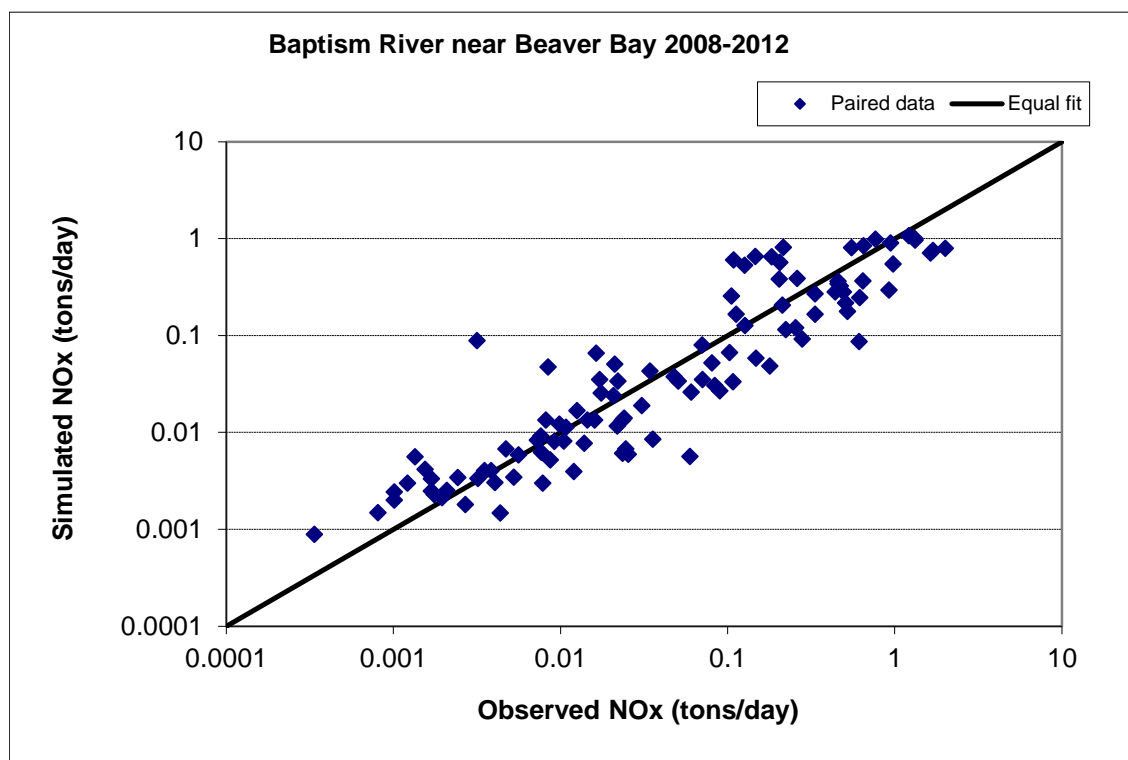


Figure 235. Paired simulated vs. observed Nitrite+ Nitrate Nitrogen (NOx) load at Baptism River near Beaver Bay

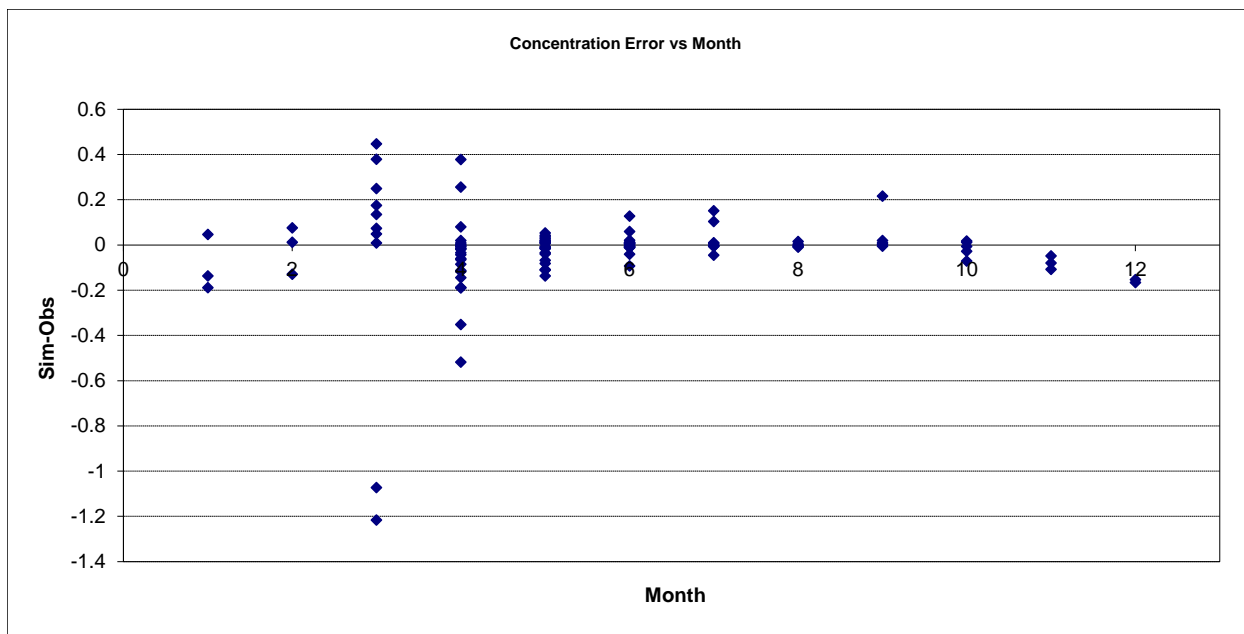


Figure 236. Residual (Simulated - Observed) vs. Month Nitrite+ Nitrate Nitrogen (NOx) at Baptism River near Beaver Bay

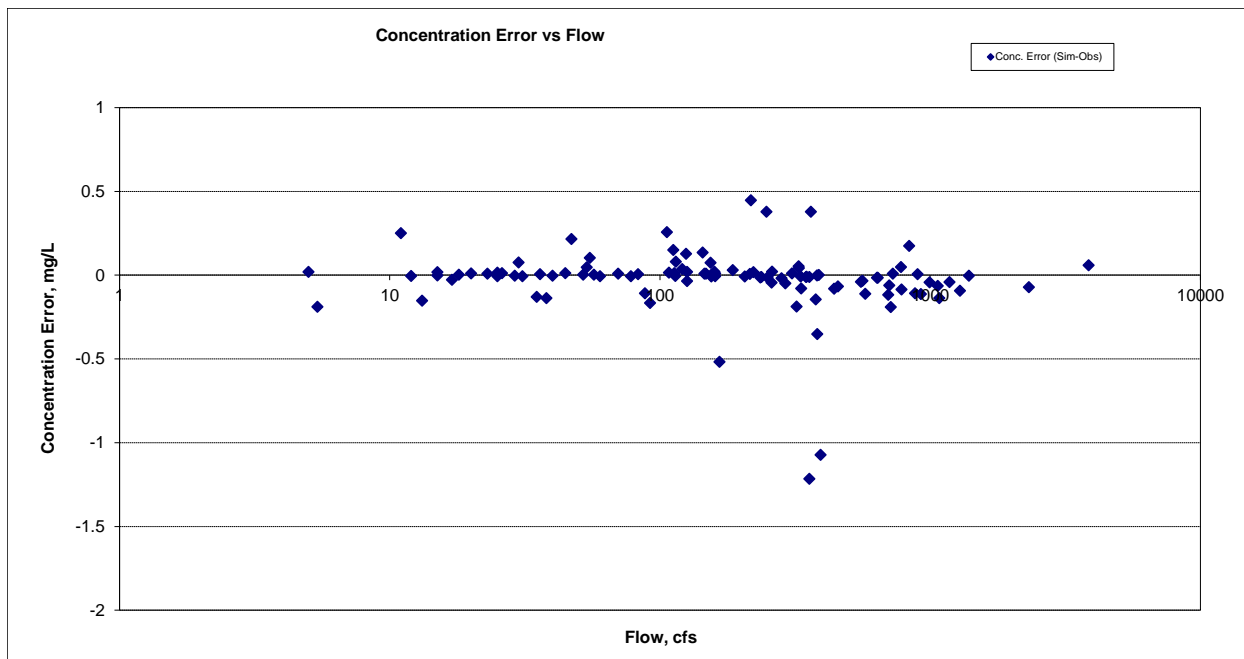


Figure 237. Residual (Simulated - Observed) vs. Flow Nitrite+ Nitrate Nitrogen (NOx) at Baptism River near Beaver Bay

Total Nitrogen (TN)

Table 46. Total Nitrogen (TN) statistics

Count	106
Concentration Average Error	-5.67%
Concentration Median Error	-7.15%
Load Ave Error	-7.77%
Load Median Error	-6.92%
Paired t concentration	1.00
Paired t load	0.79

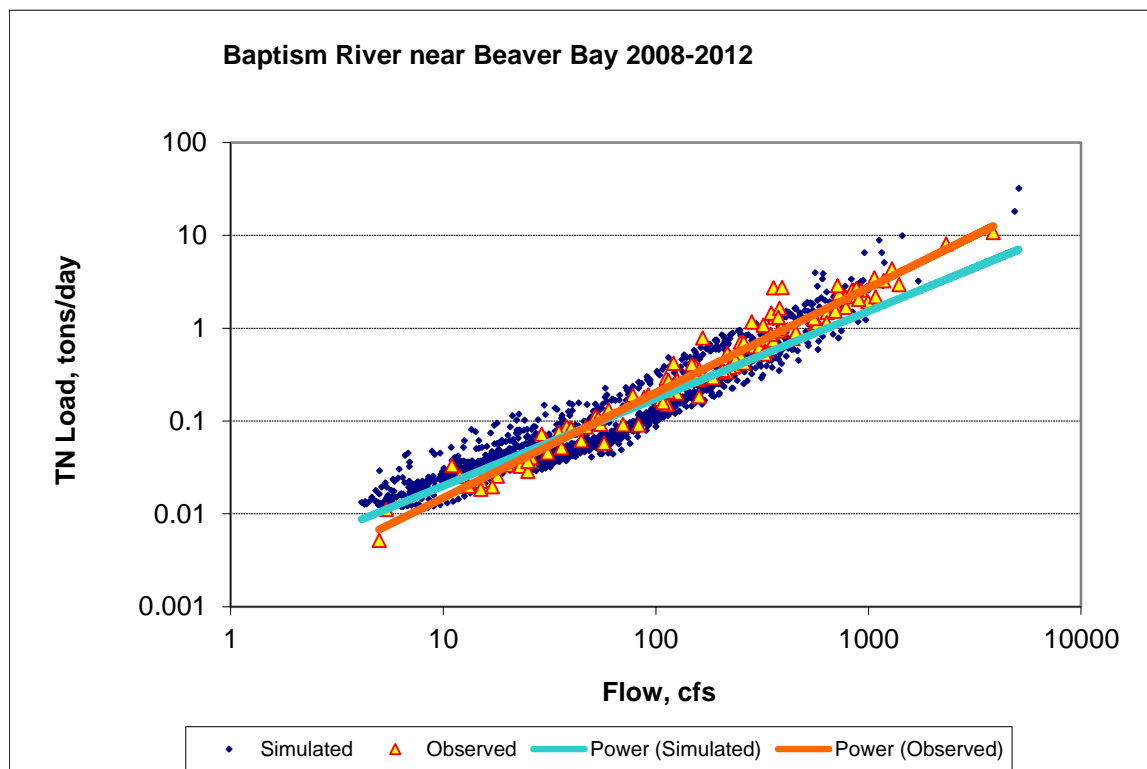


Figure 238. Power plot of simulated and observed Total Nitrogen (TN) load vs flow at Baptism River near Beaver Bay

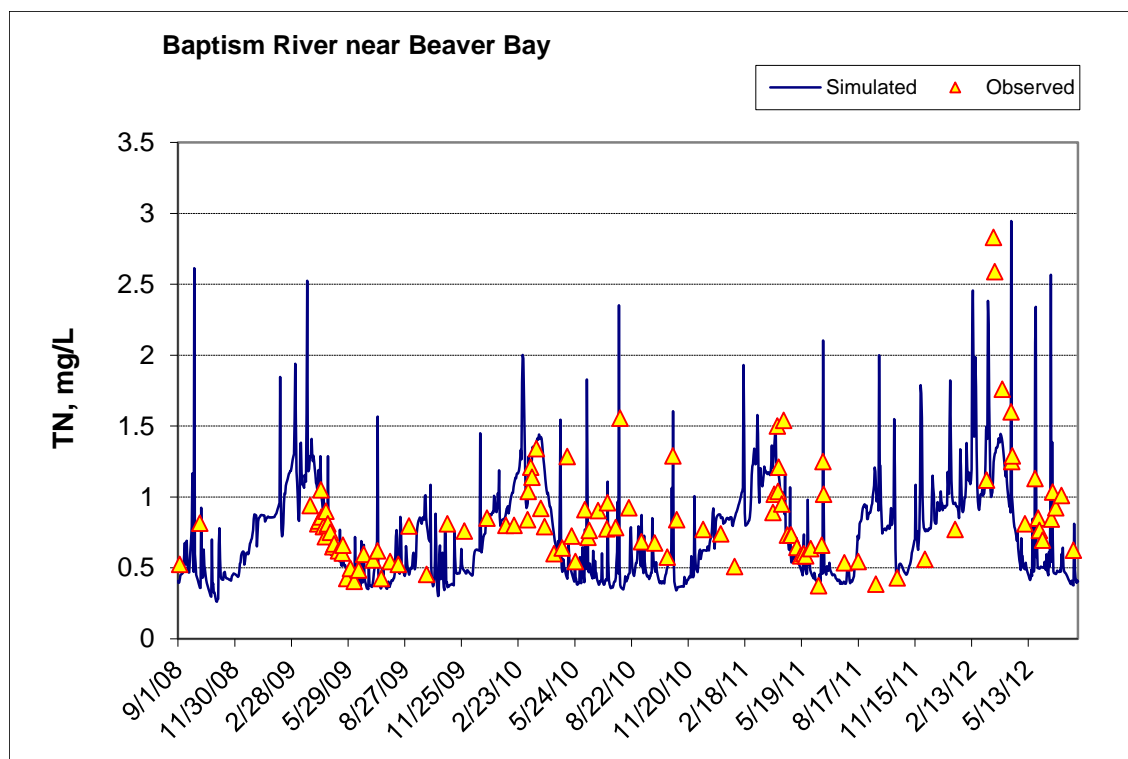


Figure 239. Time series of observed and simulated Total Nitrogen (TN) concentration at Baptism River near Beaver Bay

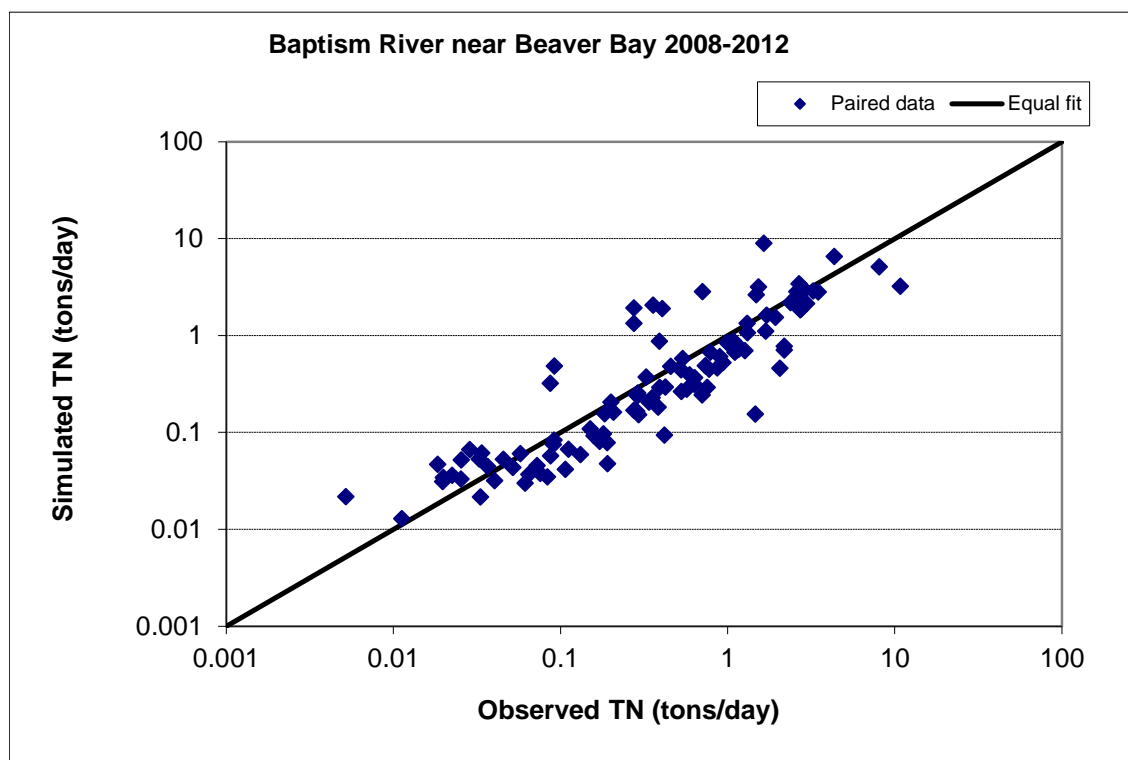


Figure 240. Paired simulated vs. observed Total Nitrogen (TN) load at Baptism River near Beaver Bay

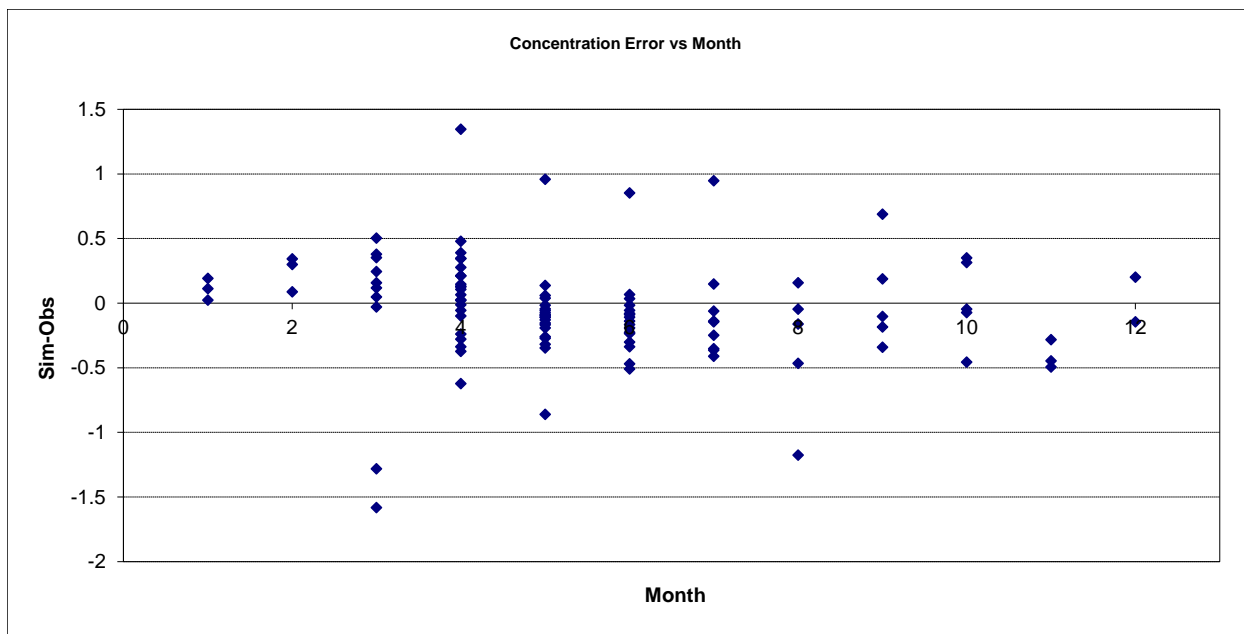


Figure 241. Residual (Simulated - Observed) vs. Month Total Nitrogen (TN) at Baptism River near Beaver Bay

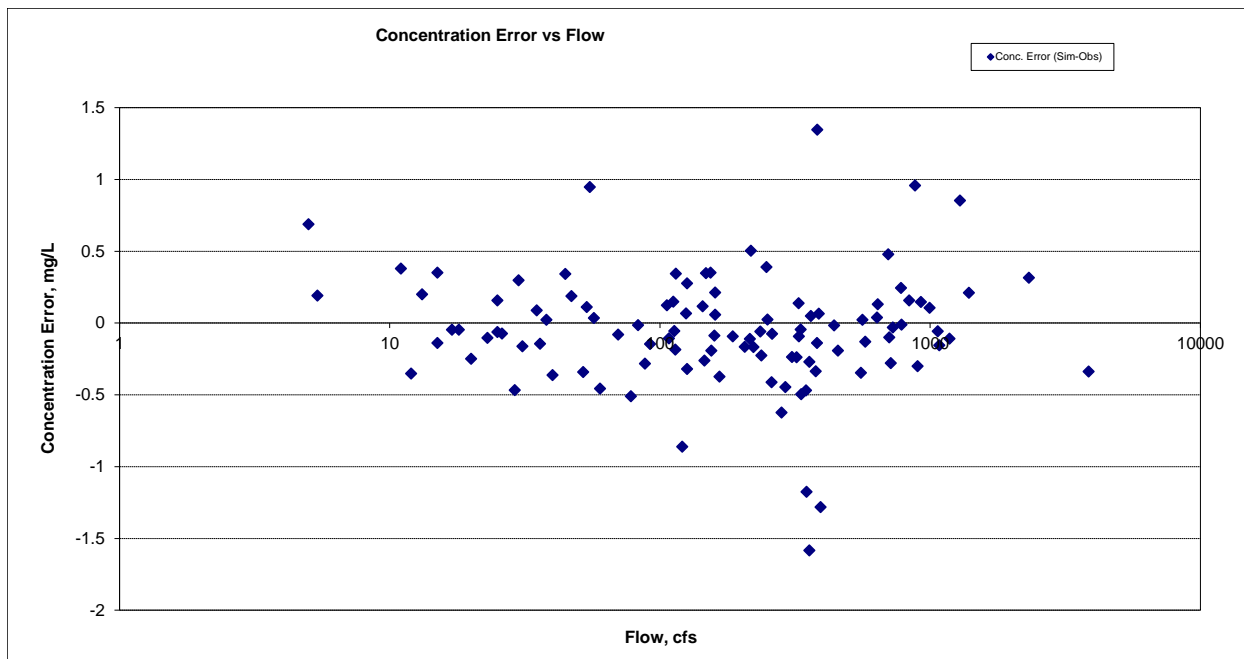


Figure 242. Residual (Simulated - Observed) vs. Flow Total Nitrogen (TN) at Baptism River near Beaver Bay

Soluble Reactive Phosphorus (SRP)

Table 47. Soluble Reactive Phosphorus (SRP) statistics

Count	106
Concentration Average Error	-3.35%
Concentration Median Error	4.43%
Load Ave Error	-28.22%
Load Median Error	-0.20%
Paired t concentration	0.99
Paired t load	0.34

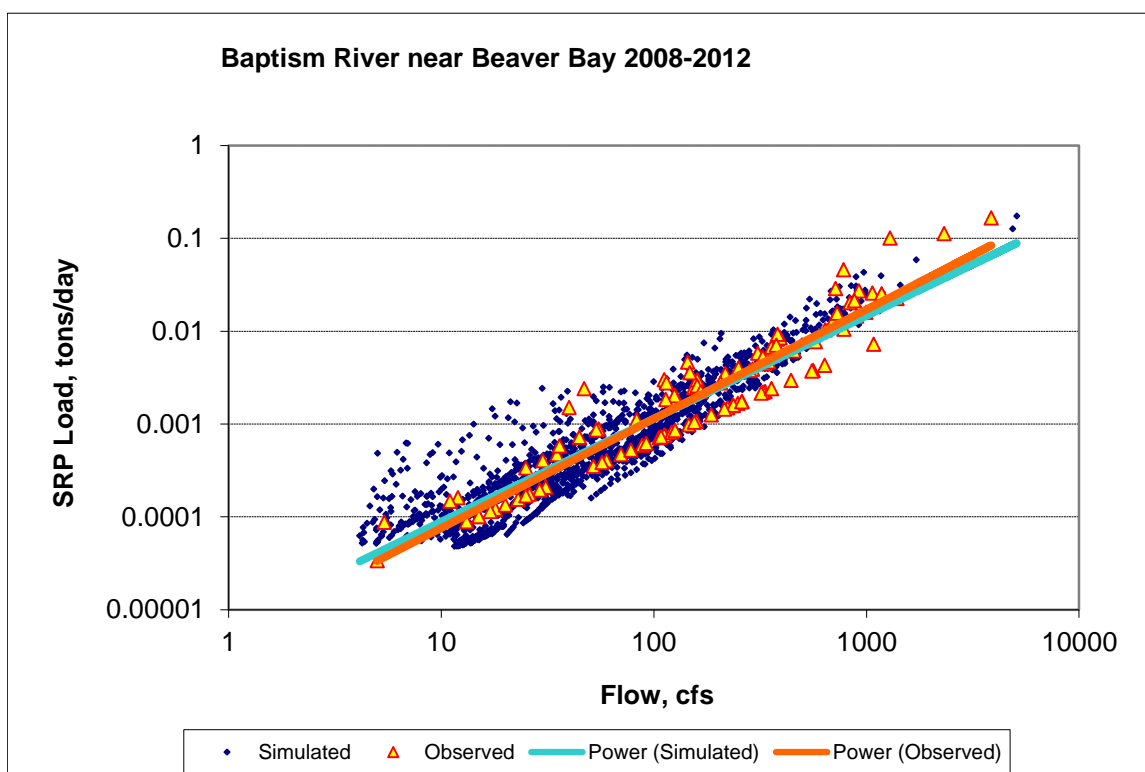


Figure 243. Power plot of simulated and observed Soluble Reactive Phosphorus (SRP) load vs flow at Baptism River near Beaver Bay

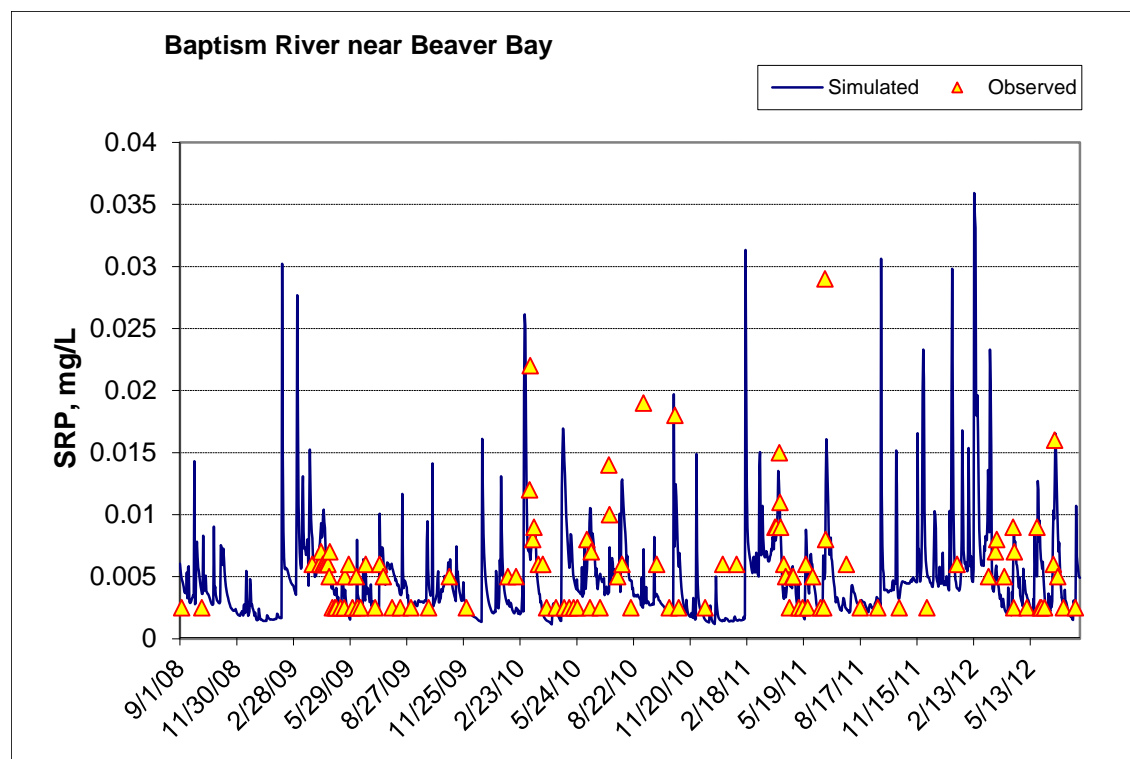


Figure 244. Time series of observed and simulated Soluble Reactive Phosphorus (SRP) concentration at Baptism River near Beaver Bay

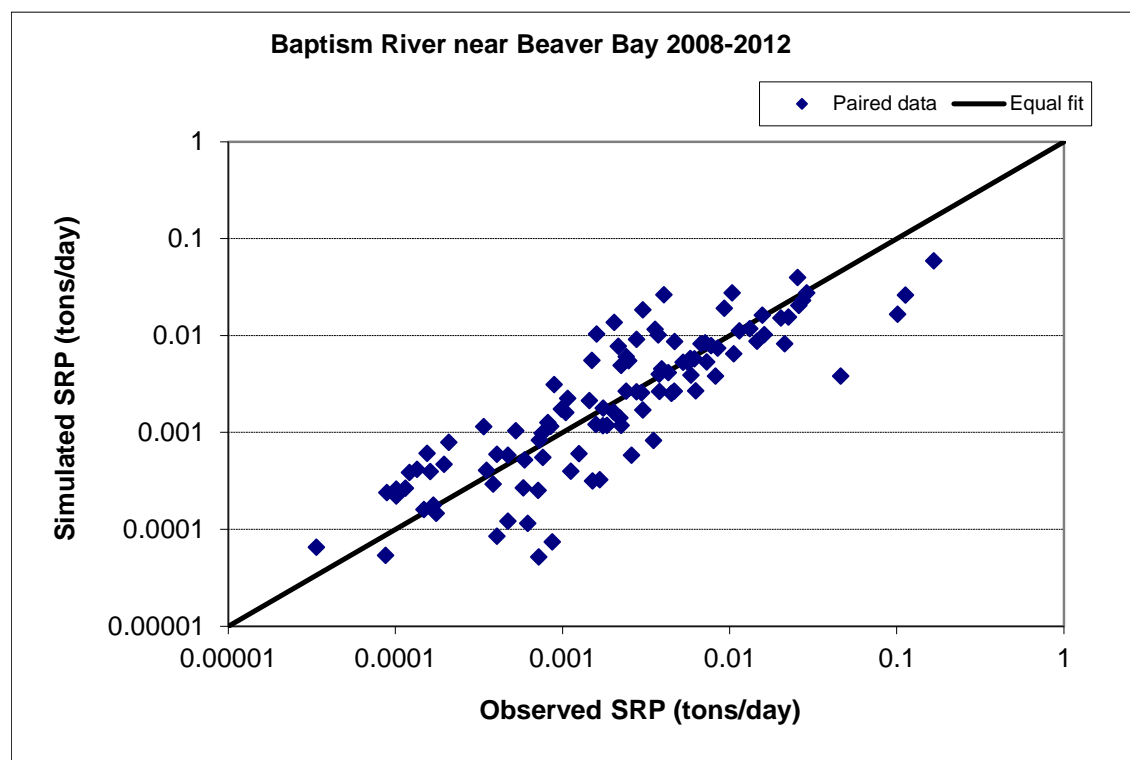


Figure 245. Paired simulated vs. observed Soluble Reactive Phosphorus (SRP) load at Baptism River near Beaver Bay

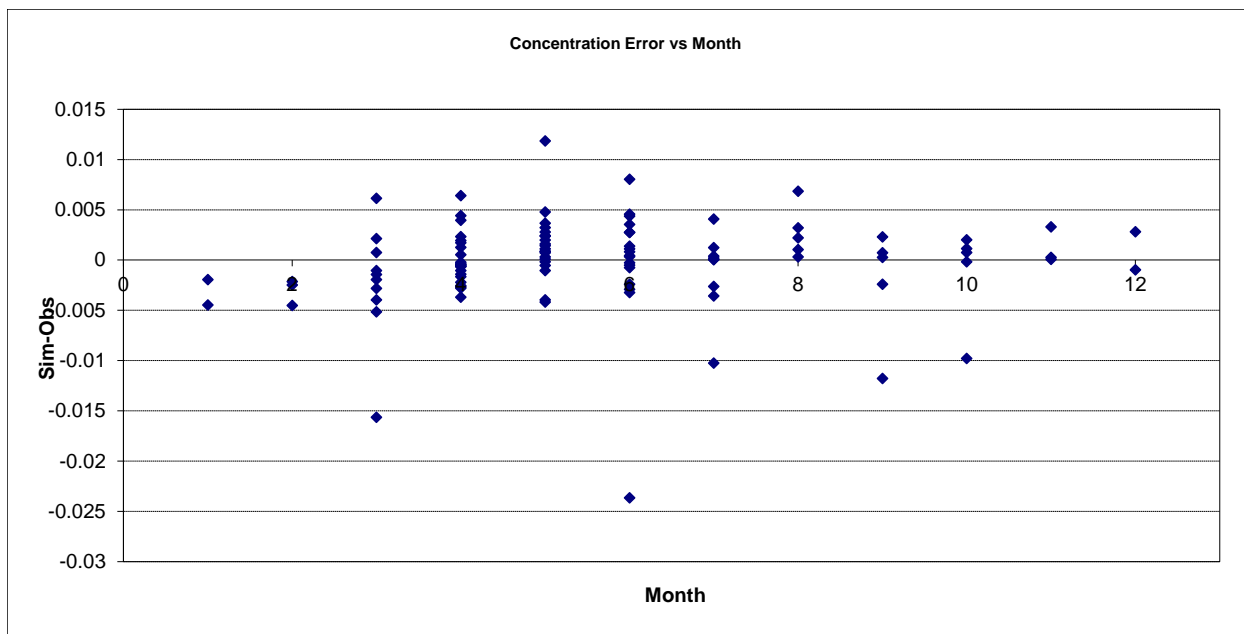


Figure 246. Residual (Simulated - Observed) vs. Month Soluble Reactive Phosphorus (SRP) at Baptism River near Beaver Bay

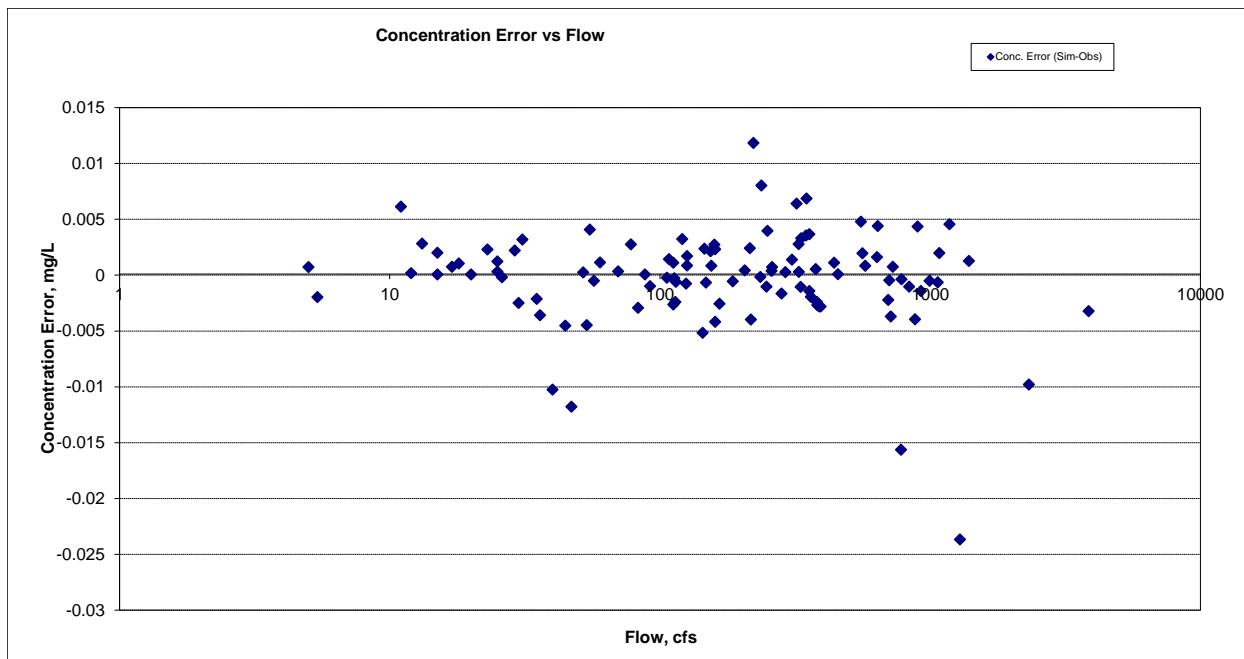


Figure 247. Residual (Simulated - Observed) vs. Flow Soluble Reactive Phosphorus (SRP) at Baptism River near Beaver Bay

Organic Phosphorus (OrgP)

Table 48. Organic Phosphorus (OrgP) statistics

Count	104
Concentration Average Error	13.11%
Concentration Median Error	1.43%
Load Ave Error	15.97%
Load Median Error	-3.20%
Paired t concentration	0.69
Paired t load	0.56

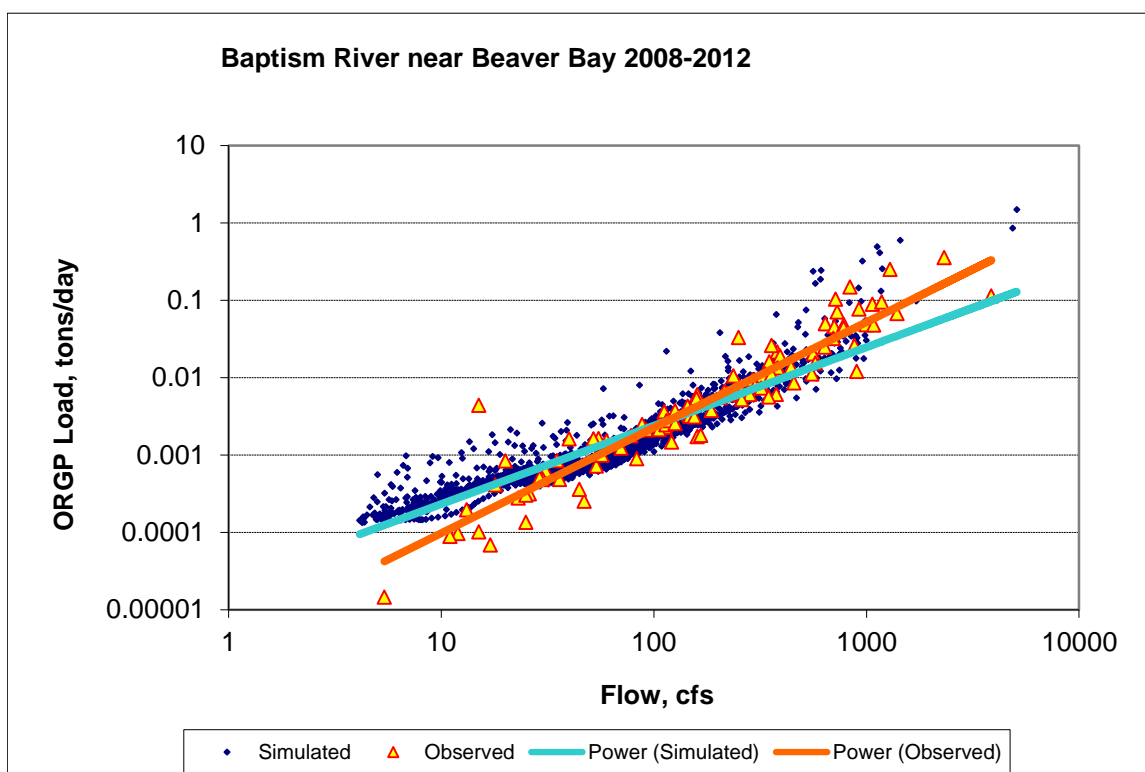


Figure 248. Power plot of simulated and observed Organic Phosphorus (OrgP) load vs flow at Baptism River near Beaver Bay

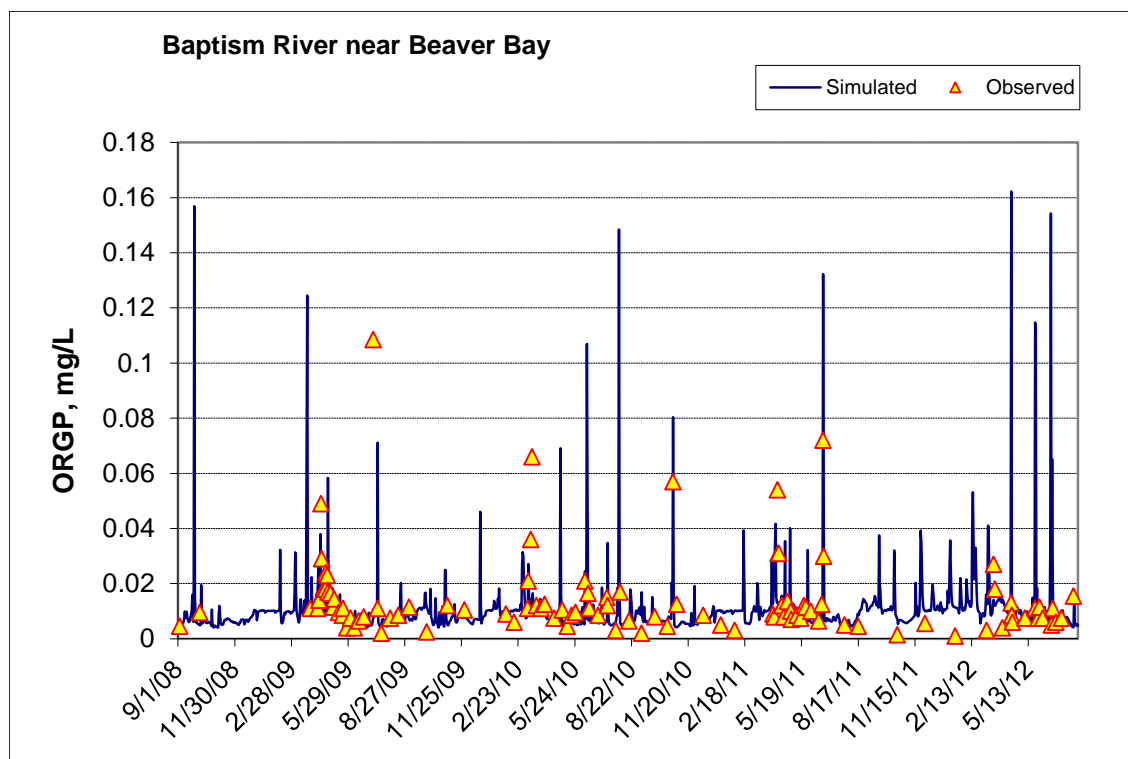


Figure 249. Time series of observed and simulated Organic Phosphorus (OrgP) concentration at Baptism River near Beaver Bay

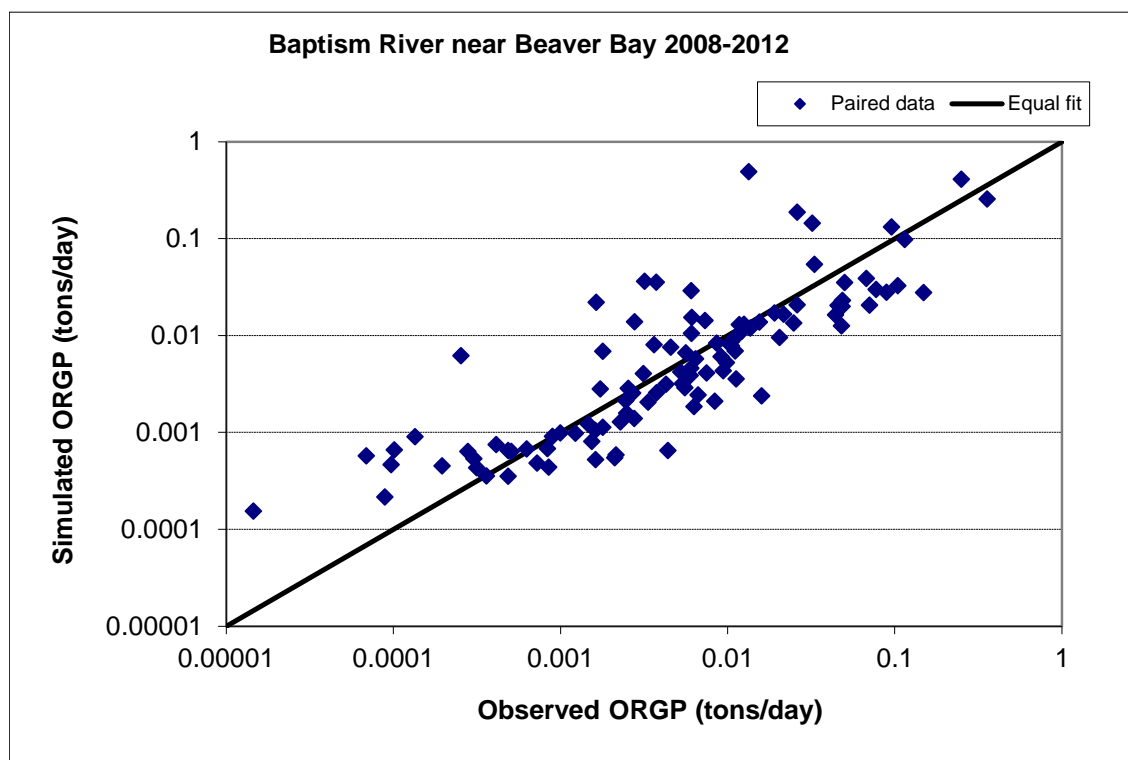


Figure 250. Paired simulated vs. observed Organic Phosphorus (OrgP) load at Baptism River near Beaver Bay

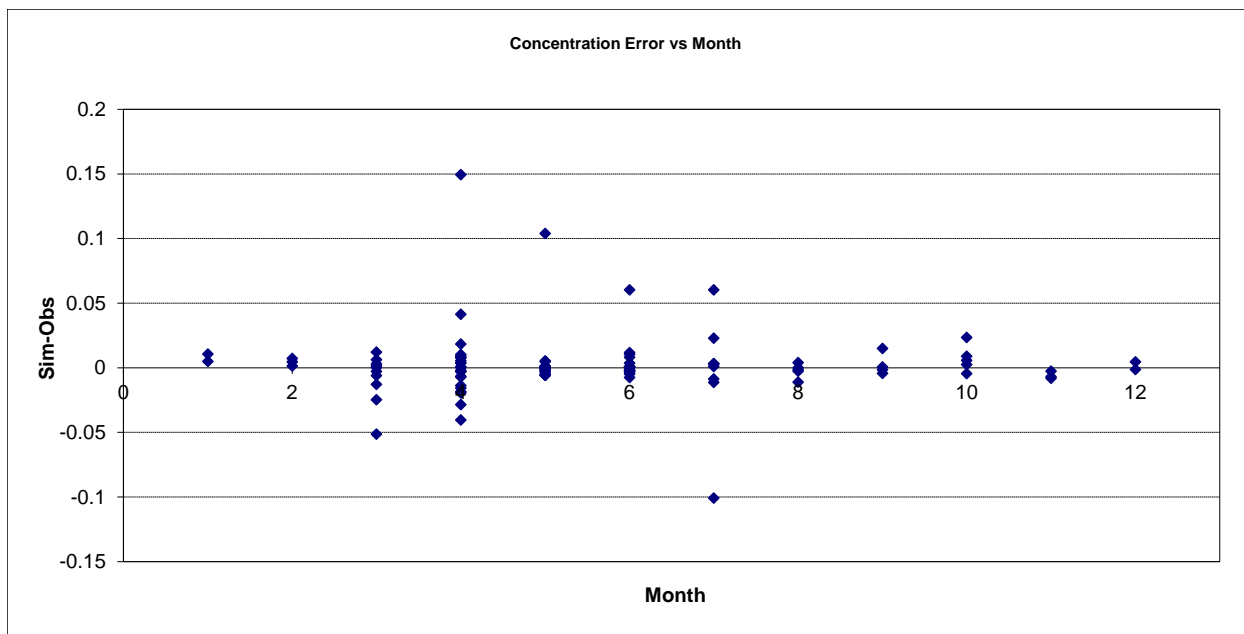


Figure 251. Residual (Simulated - Observed) vs. Month Organic Phosphorus (OrgP) at Baptism River near Beaver Bay

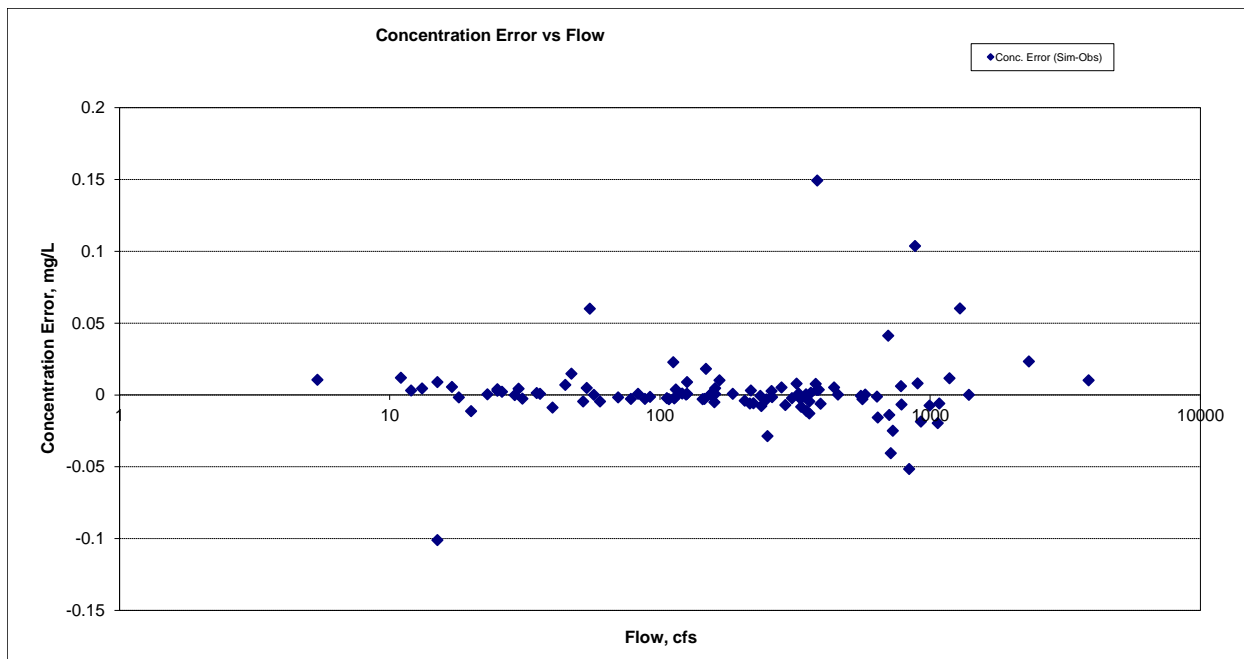


Figure 252. Residual (Simulated - Observed) vs. Flow Organic Phosphorus (OrgP) at Baptism River near Beaver Bay

Total Phosphorus (TP)

Table 49. Total Phosphorus (TP) statistics

Count	106
Concentration Average Error	8.86%
Concentration Median Error	1.37%
Load Ave Error	3.25%
Load Median Error	-2.30%
Paired t concentration	0.85
Paired t load	0.76

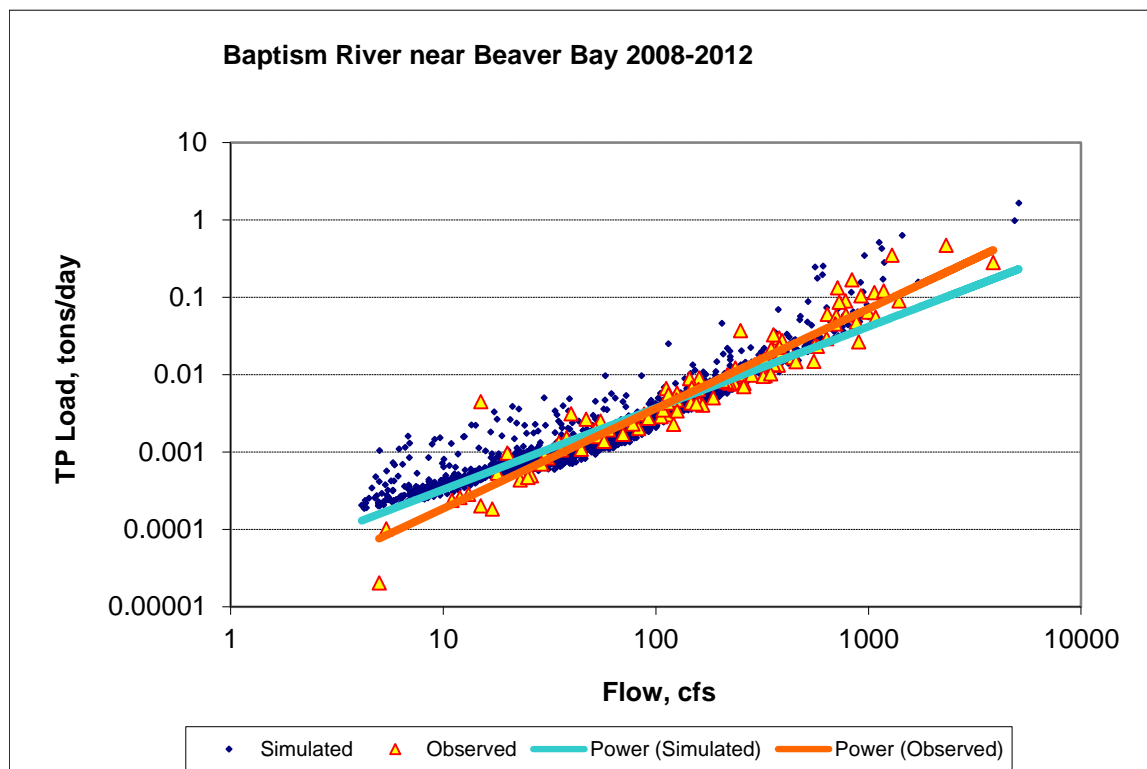


Figure 253. Power plot of simulated and observed Total Phosphorus (TP) load vs flow at Baptism River near Beaver Bay

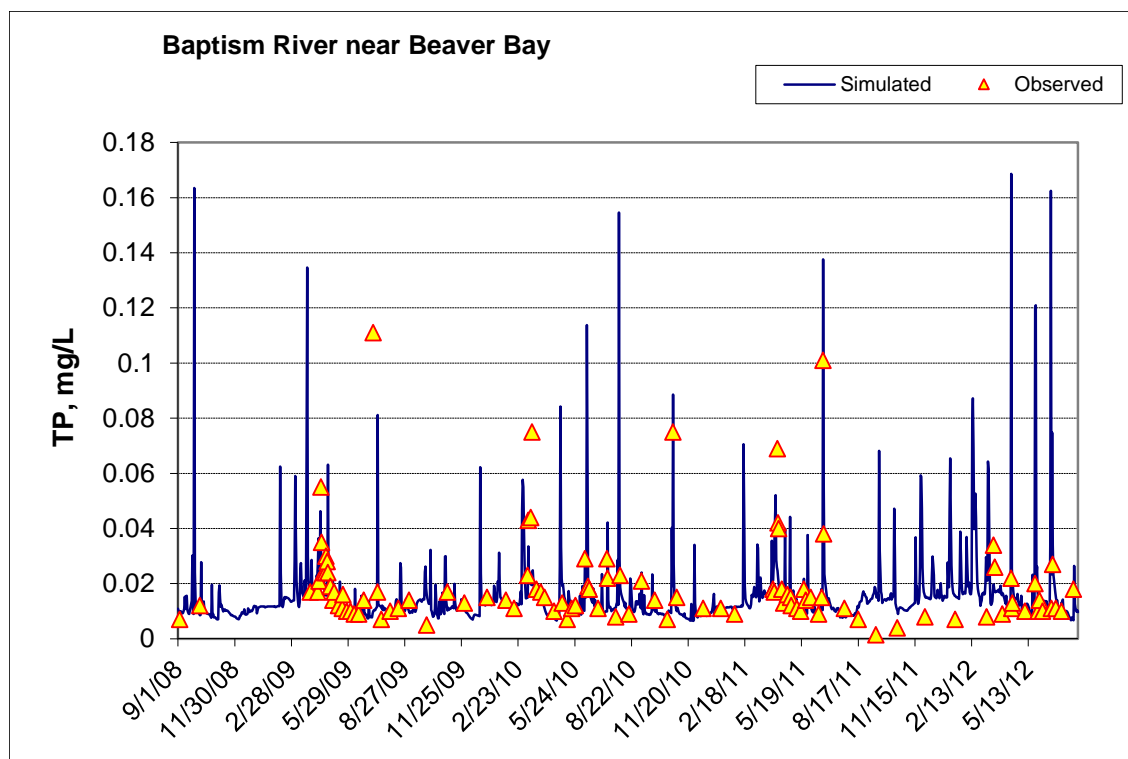


Figure 254. Time series of observed and simulated Total Phosphorus (TP) concentration at Baptism River near Beaver Bay

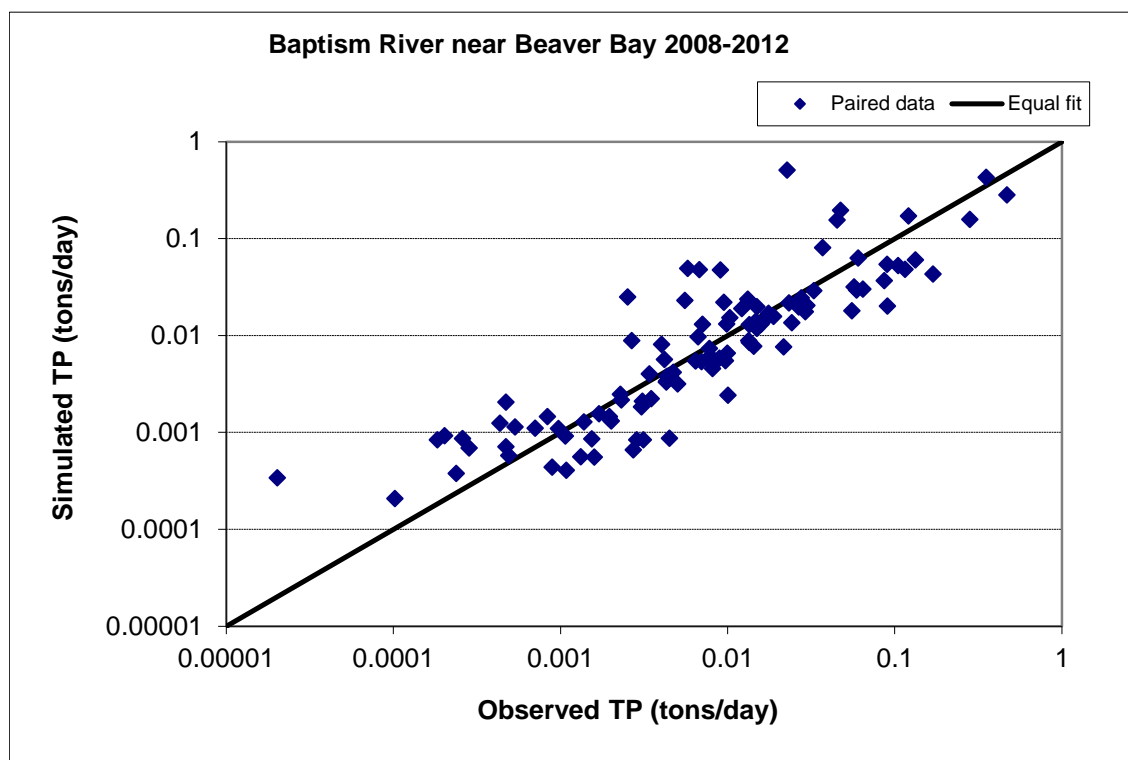


Figure 255. Paired simulated vs. observed Total Phosphorus (TP) load at Baptism River near Beaver Bay



Figure 256. Residual (Simulated - Observed) vs. Month Total Phosphorus (TP) at Baptism River near Beaver Bay

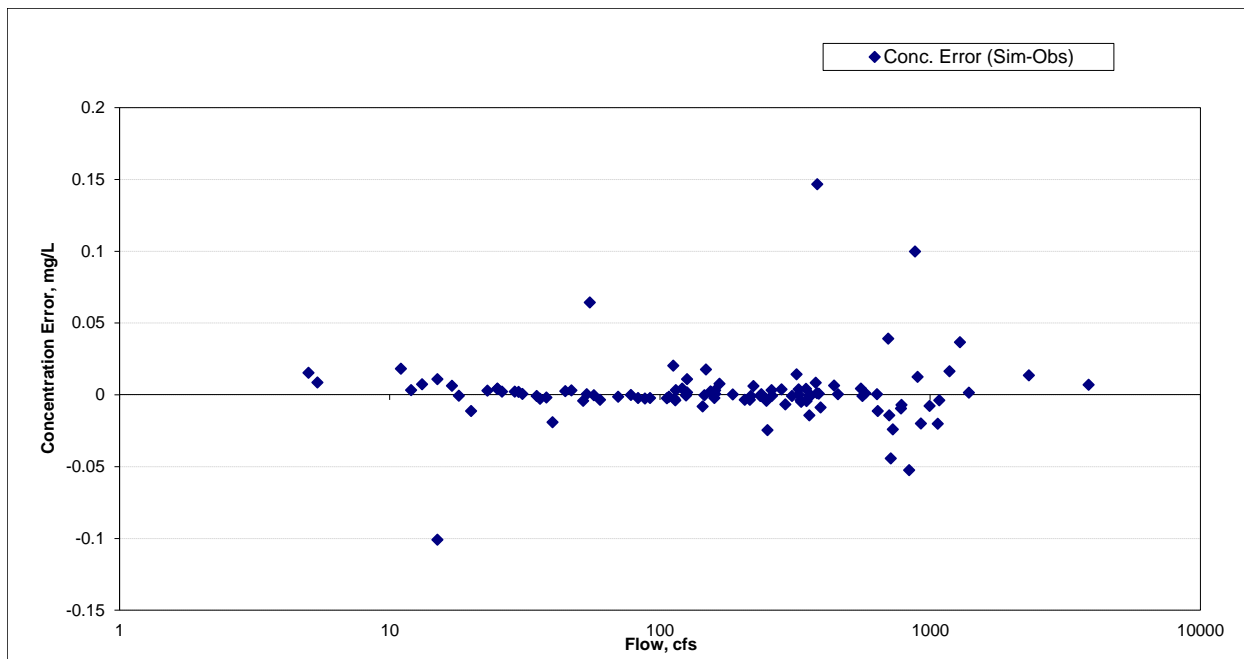


Figure 257. Residual (Simulated - Observed) vs. Flow Total Phosphorus (TP) at Baptism River near Beaver Bay

Poplar River near Lutsen (HYDSTRA 01063003)

Total Suspended Solids (TSS)

Table 50. Total Suspended Solids (TSS) statistics

Count	116
Concentration Average Error	2.18%
Concentration Median Error	8.18%
Load Ave Error	37.85%
Load Median Error	1.40%
Paired t concentration	0.90
Paired t load	0.29

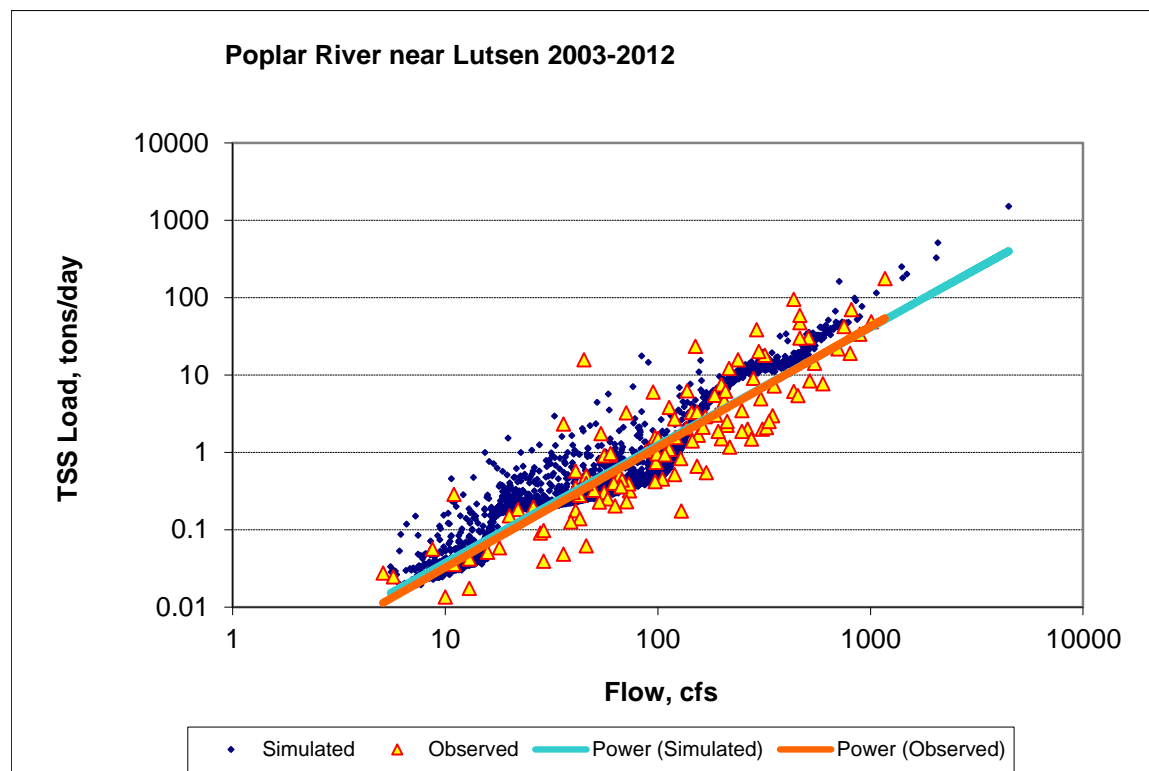


Figure 258. Power plot of simulated and observed Total Suspended Solids (TSS) load vs flow at Poplar River near Lutsen

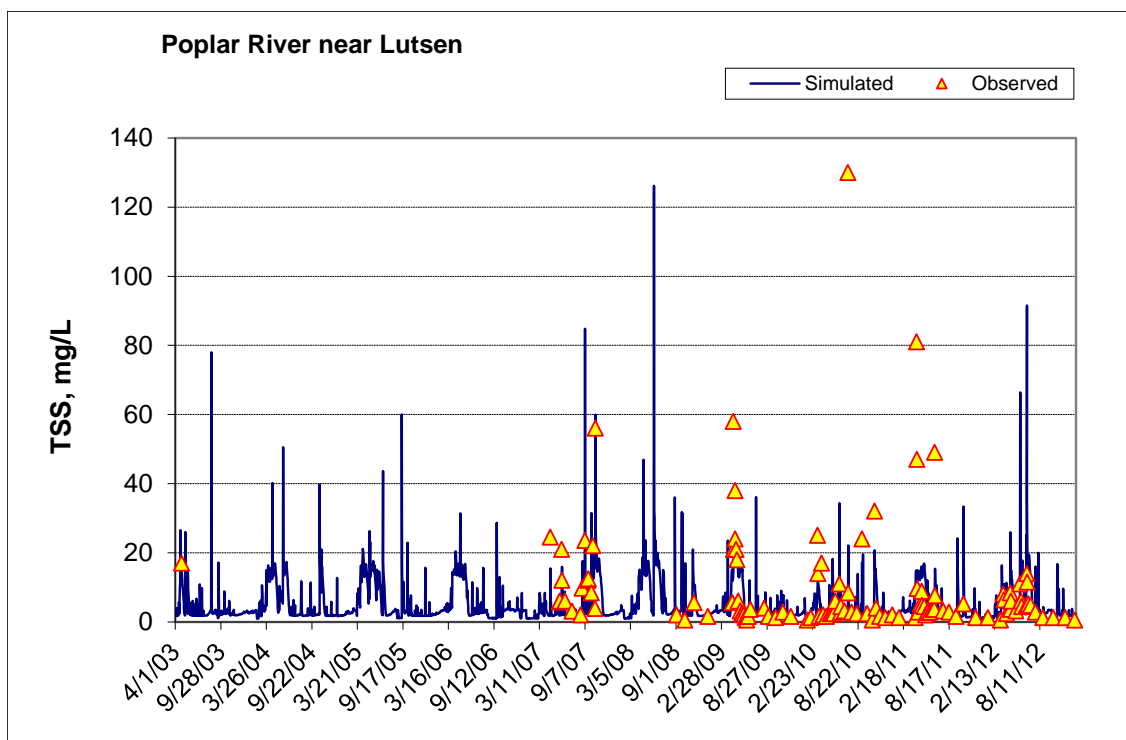


Figure 259. Time series of observed and simulated Total Suspended Solids (TSS) concentration at Poplar River near Lutsen

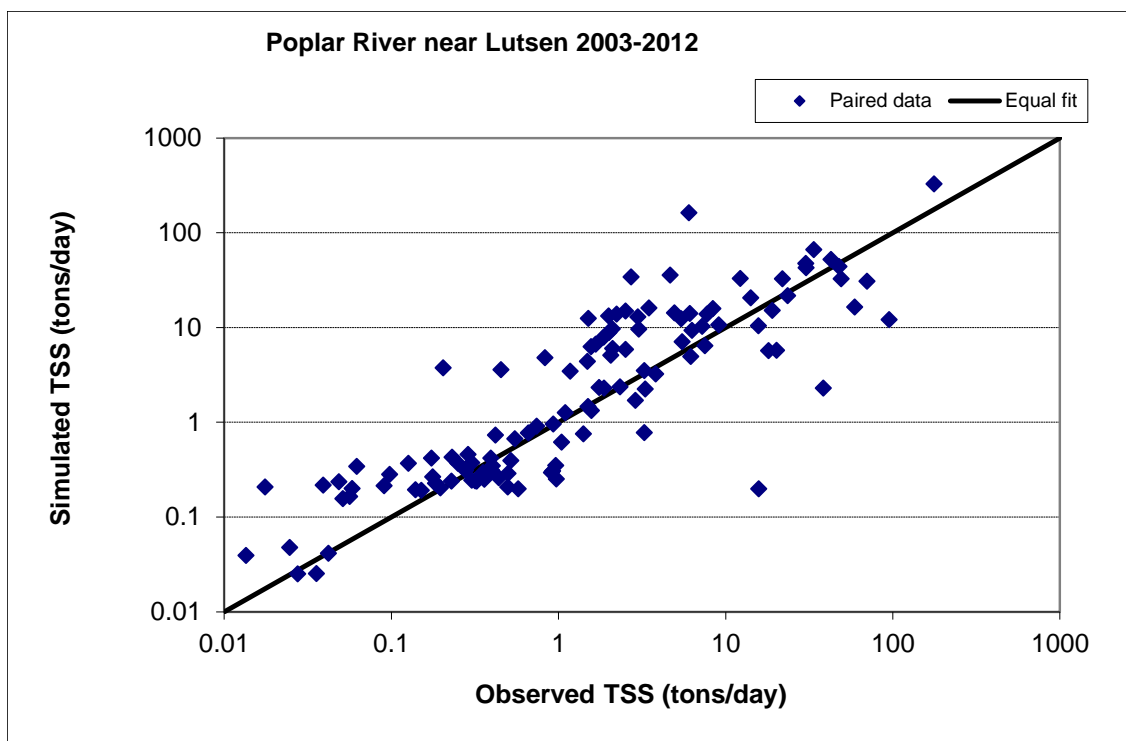


Figure 260. Paired simulated vs. observed Total Suspended Solids (TSS) load at Poplar River near Lutsen

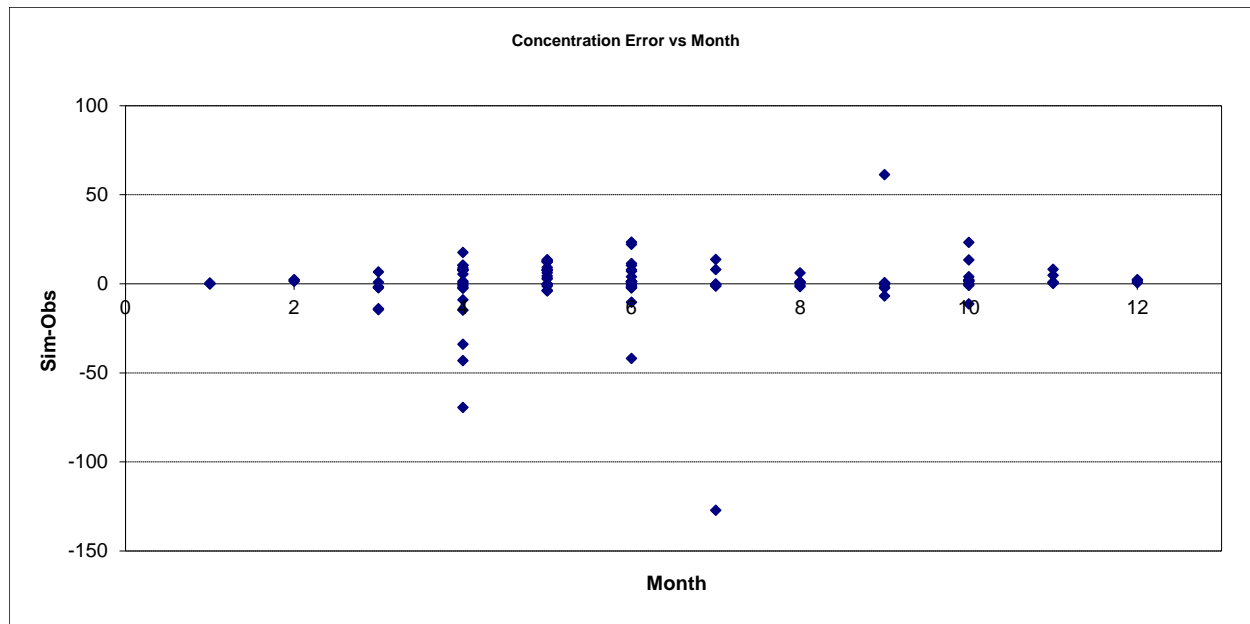


Figure 261. Residual (Simulated - Observed) vs. Month Total Suspended Solids (TSS) at Poplar River near Lutsen

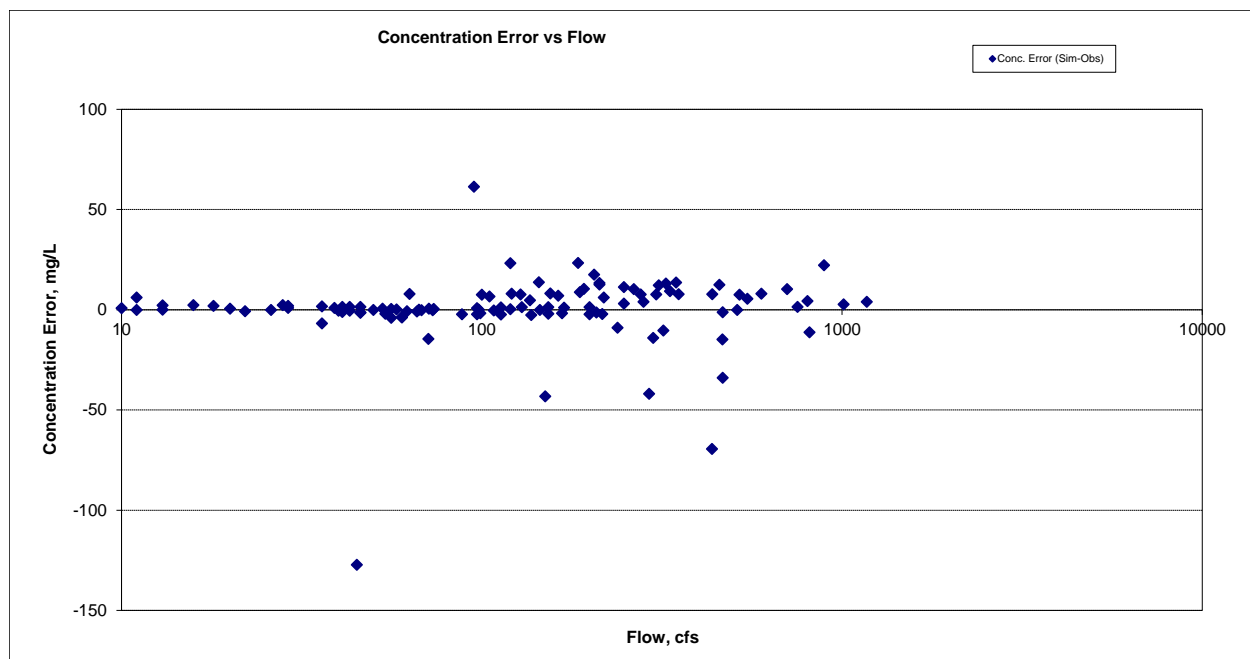


Figure 262. Residual (Simulated - Observed) vs. Flow Total Suspended Solids (TSS) at Poplar River near Lutsen

Ammonia Nitrogen (NH₃)

Table 51. Ammonia Nitrogen (NH₃) statistics

Count	16
Concentration Average Error	-1.59%
Concentration Median Error	-3.02%
Load Ave Error	46.98%
Load Median Error	22.16%
Paired t concentration	0.97
Paired t load	0.21

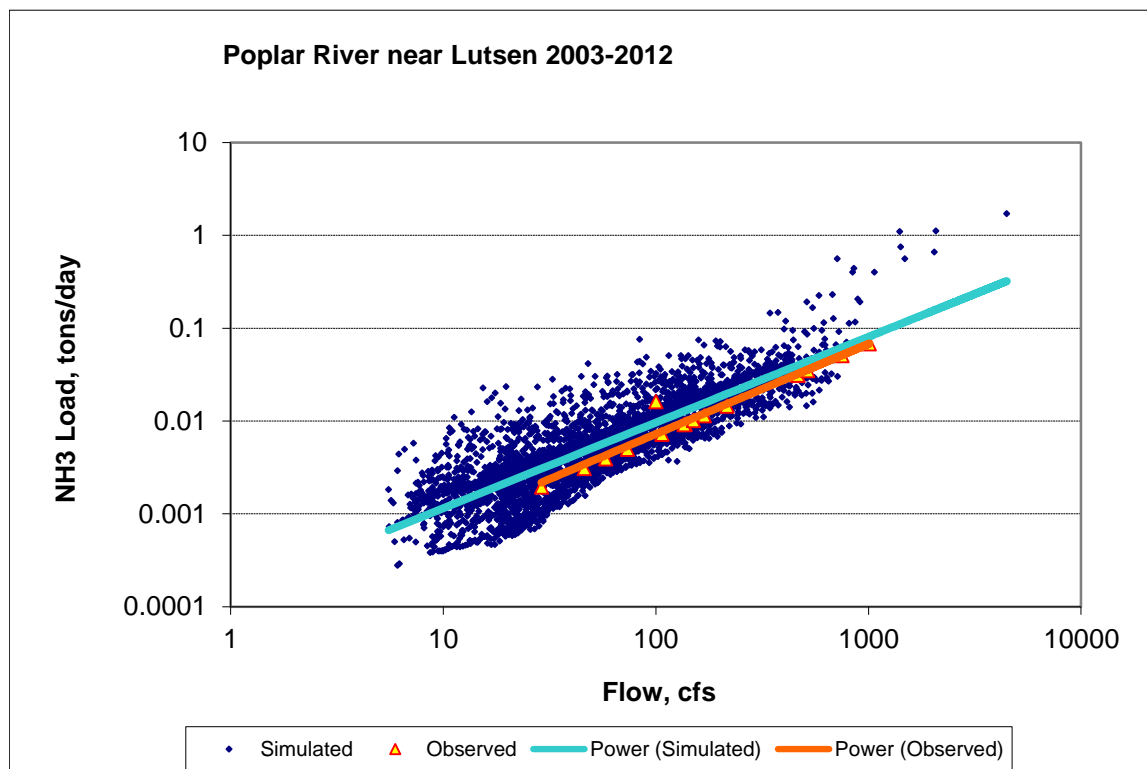


Figure 263. Power plot of simulated and observed Ammonia Nitrogen (NH₃) load vs flow at Poplar River near Lutsen

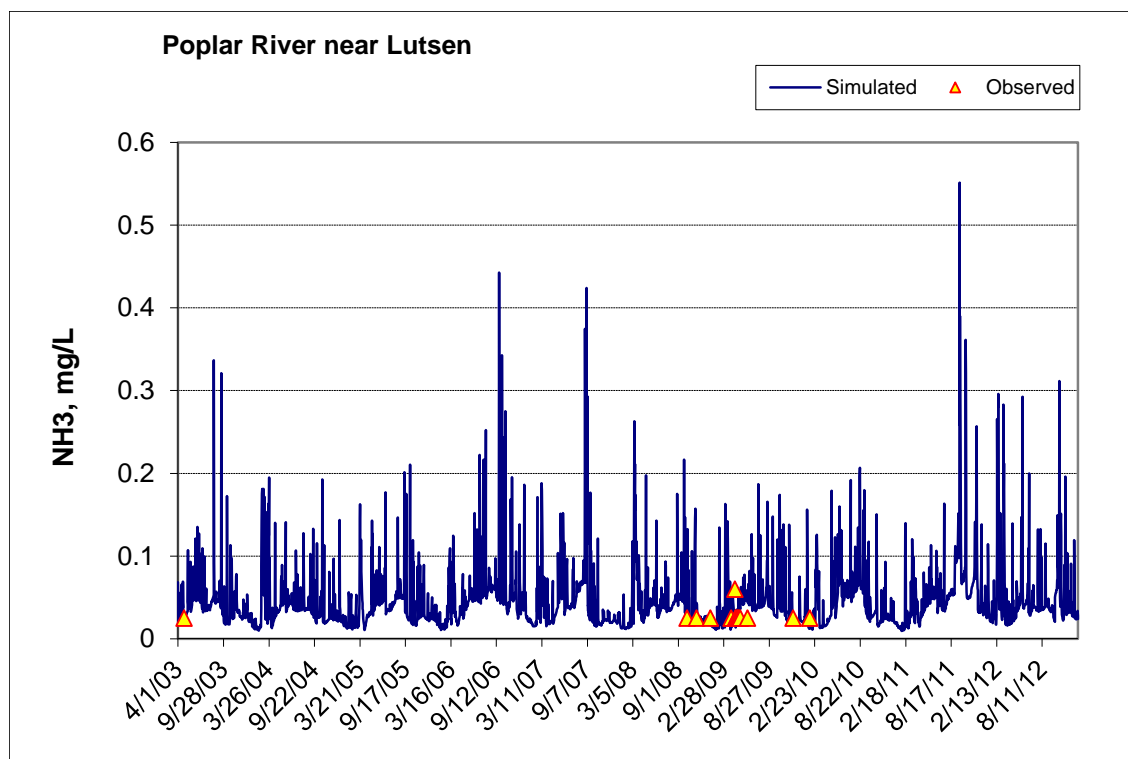


Figure 264. Time series of observed and simulated Ammonia Nitrogen (NH₃) concentration at Poplar River near Lutsen

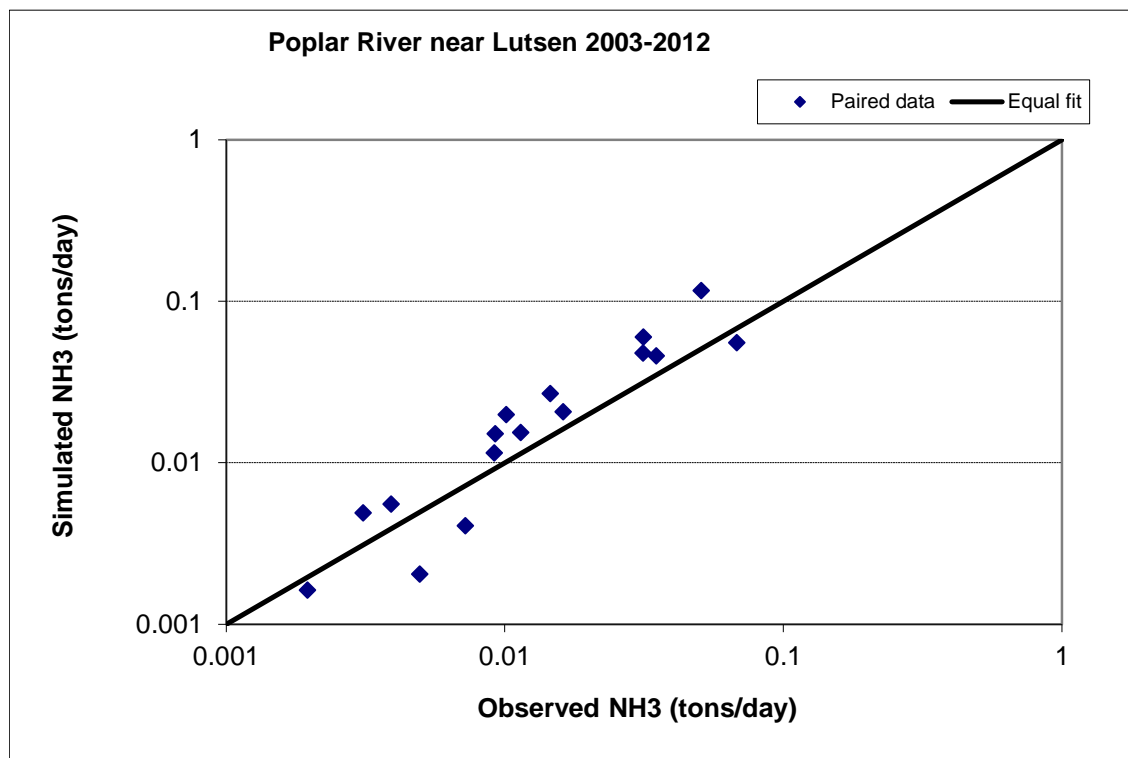


Figure 265. Paired simulated vs. observed Ammonia Nitrogen (NH₃) load at Poplar River near Lutsen

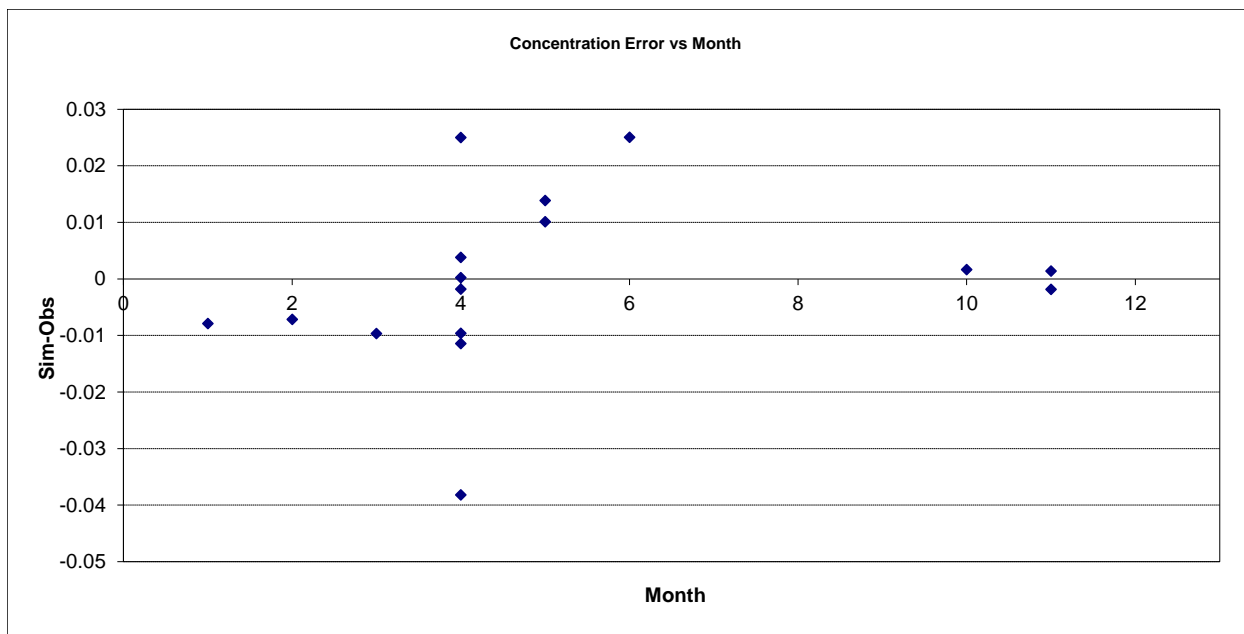


Figure 266. Residual (Simulated - Observed) vs. Month Ammonia Nitrogen (NH3) at Poplar River near Lutsen

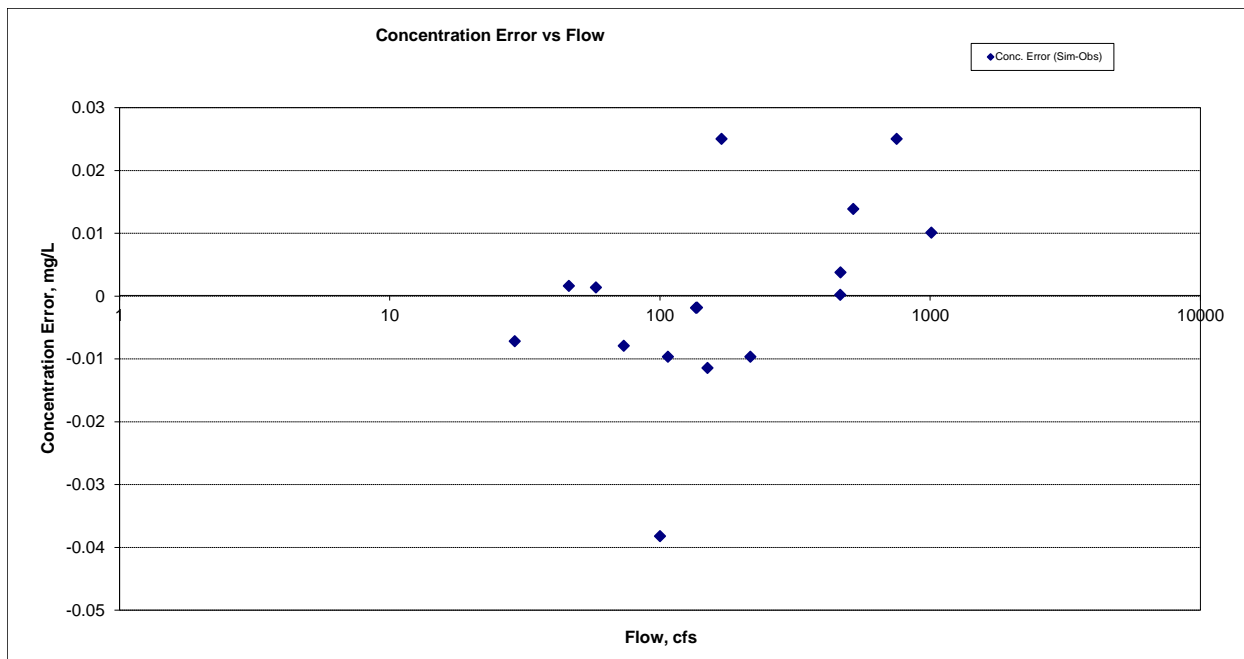


Figure 267. Residual (Simulated - Observed) vs. Flow Ammonia Nitrogen (NH3) at Poplar River near Lutsen

Organic Nitrogen (OrgN)

Table 52. Organic Nitrogen (OrgN) statistics

Count	16
Concentration Average Error	2.70%
Concentration Median Error	-3.43%
Load Ave Error	59.76%
Load Median Error	3.69%
Paired t concentration	0.98
Paired t load	0.13

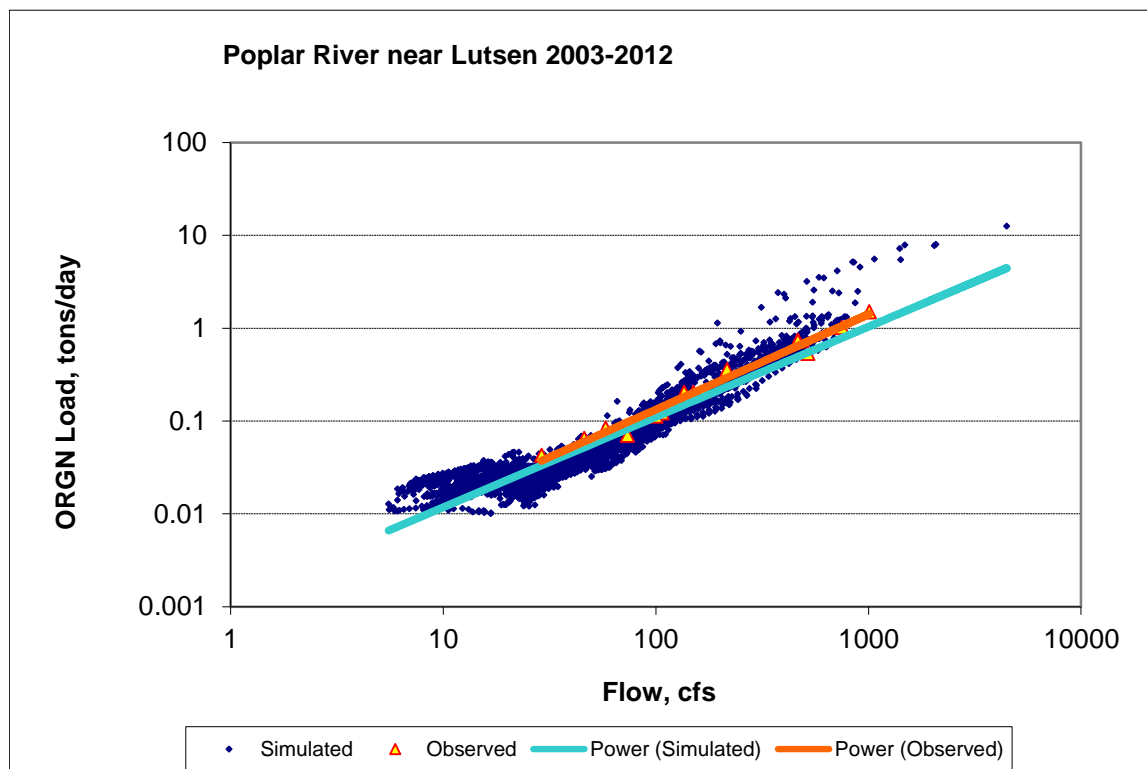


Figure 268. Power plot of simulated and observed Organic Nitrogen (OrgN) load vs flow at Poplar River near Lutsen

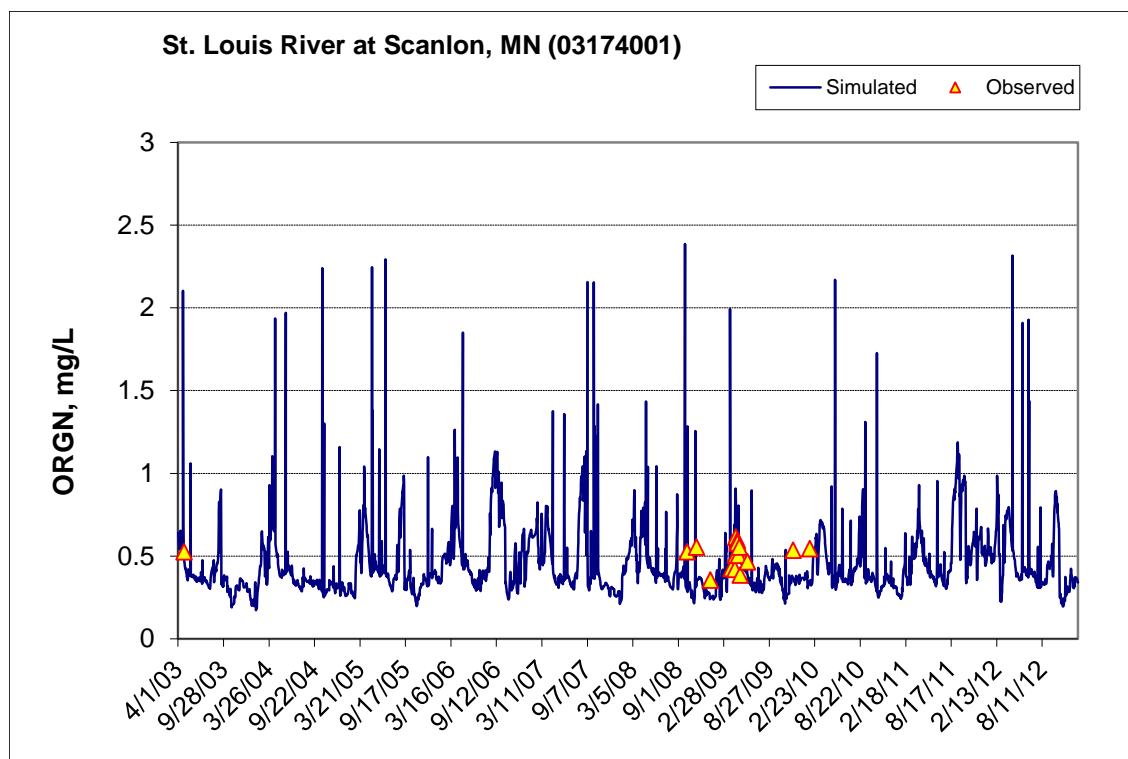


Figure 269. Time series of observed and simulated Organic Nitrogen (OrgN) concentration at Poplar River near Lutsen

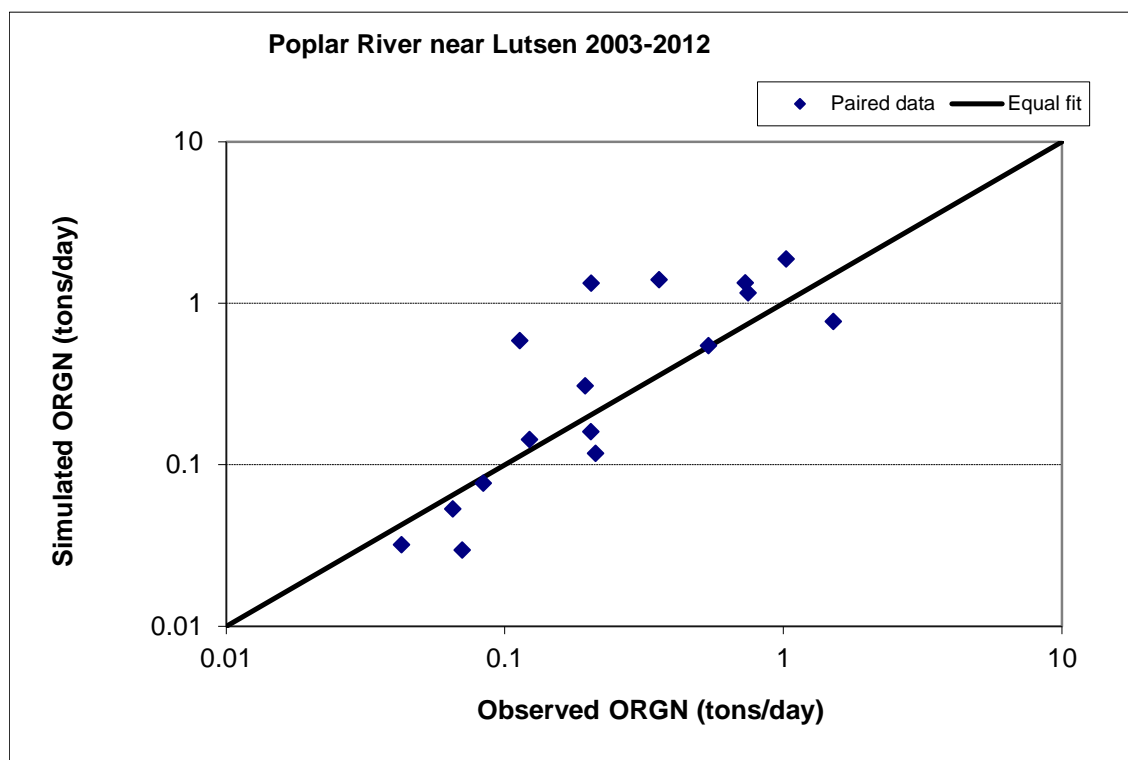


Figure 270. Paired simulated vs. observed Organic Nitrogen (OrgN) load at Poplar River near Lutsen

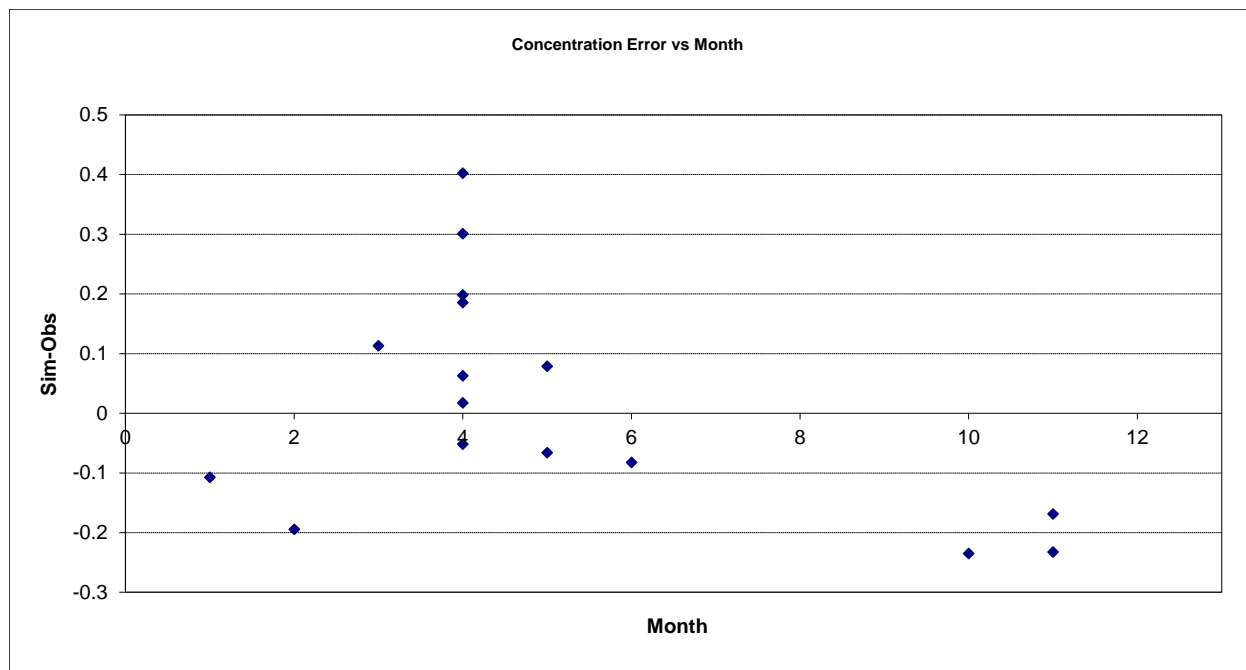


Figure 271. Residual (Simulated - Observed) vs. Month Organic Nitrogen (OrgN) at Poplar River near Lutsen

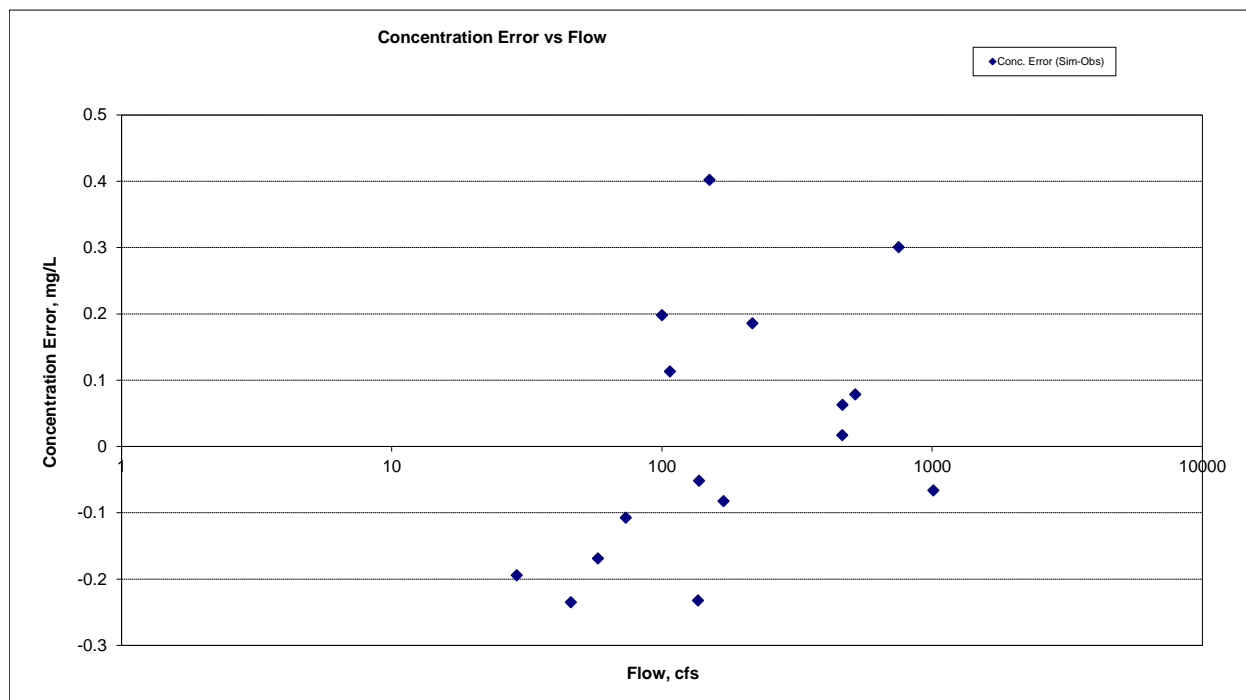


Figure 272. Residual (Simulated - Observed) vs. Flow Organic Nitrogen (OrgN) at Poplar River near Lutsen

Total Kjeldahl Nitrogen (TKN)

Table 53. Total Kjeldahl Nitrogen (TKN) statistics

Count	102
Concentration Average Error	-6.85%
Concentration Median Error	-8.83%
Load Ave Error	-0.46%
Load Median Error	-6.43%
Paired t concentration	1.00
Paired t load	0.92

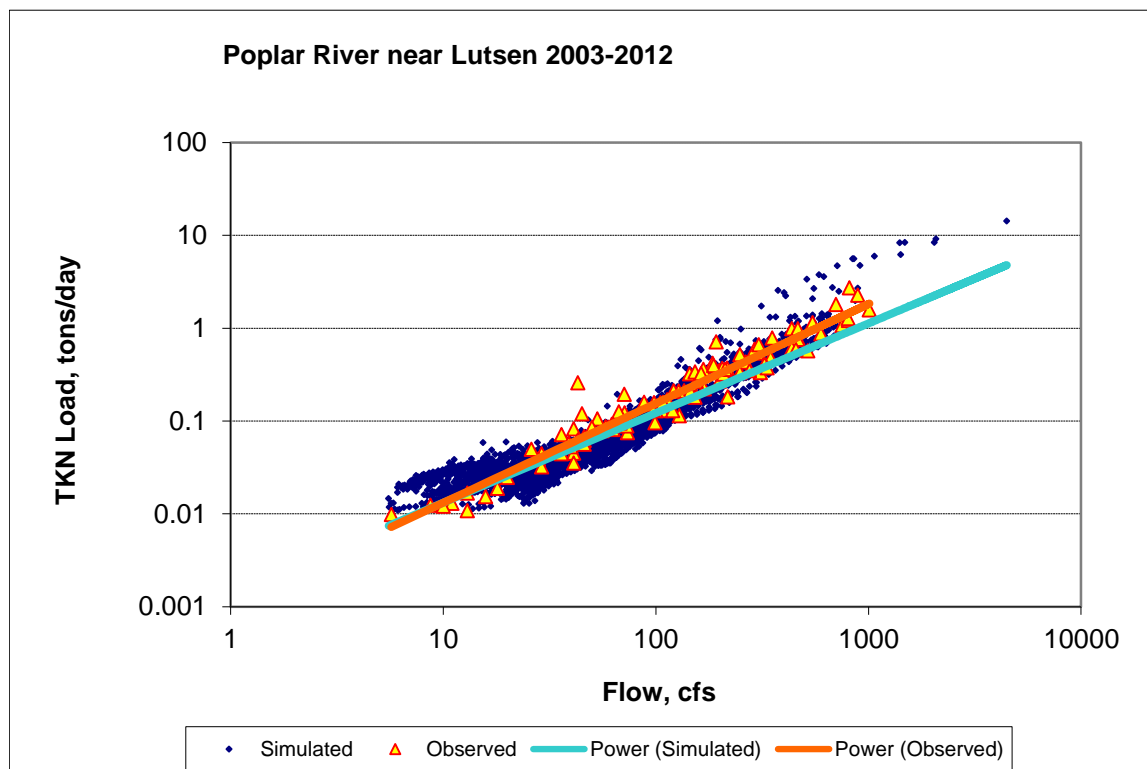


Figure 273. Power plot of simulated and observed Total Kjeldahl Nitrogen (TKN) load vs flow at Poplar River near Lutsen

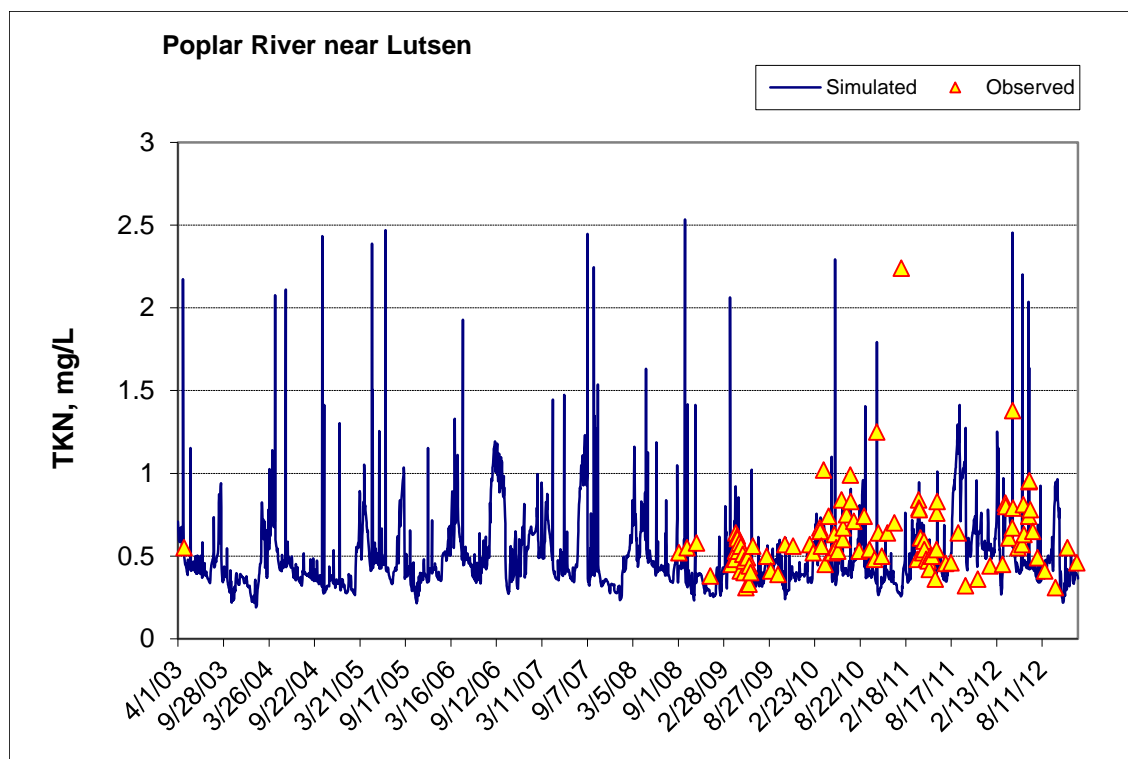


Figure 274. Time series of observed and simulated Total Kjeldahl Nitrogen (TKN) concentration at Poplar River near Lutsen

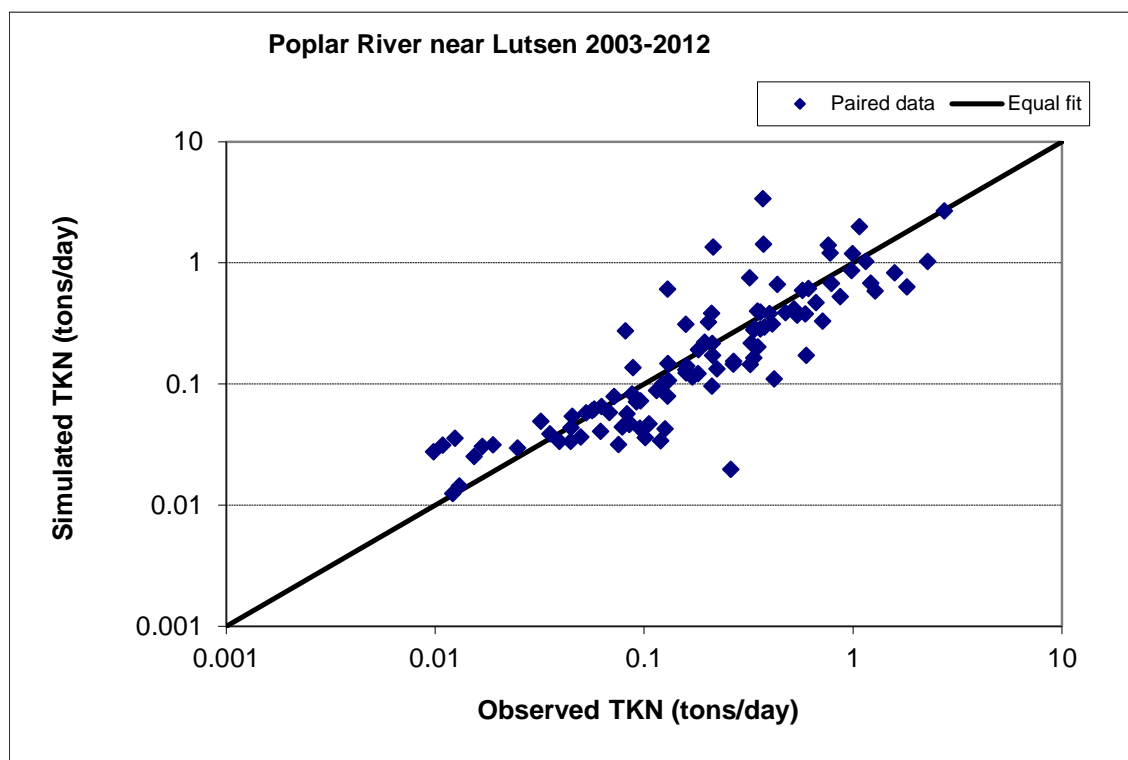


Figure 275. Paired simulated vs. observed Total Kjeldahl Nitrogen (TKN) load at Poplar River near Lutsen

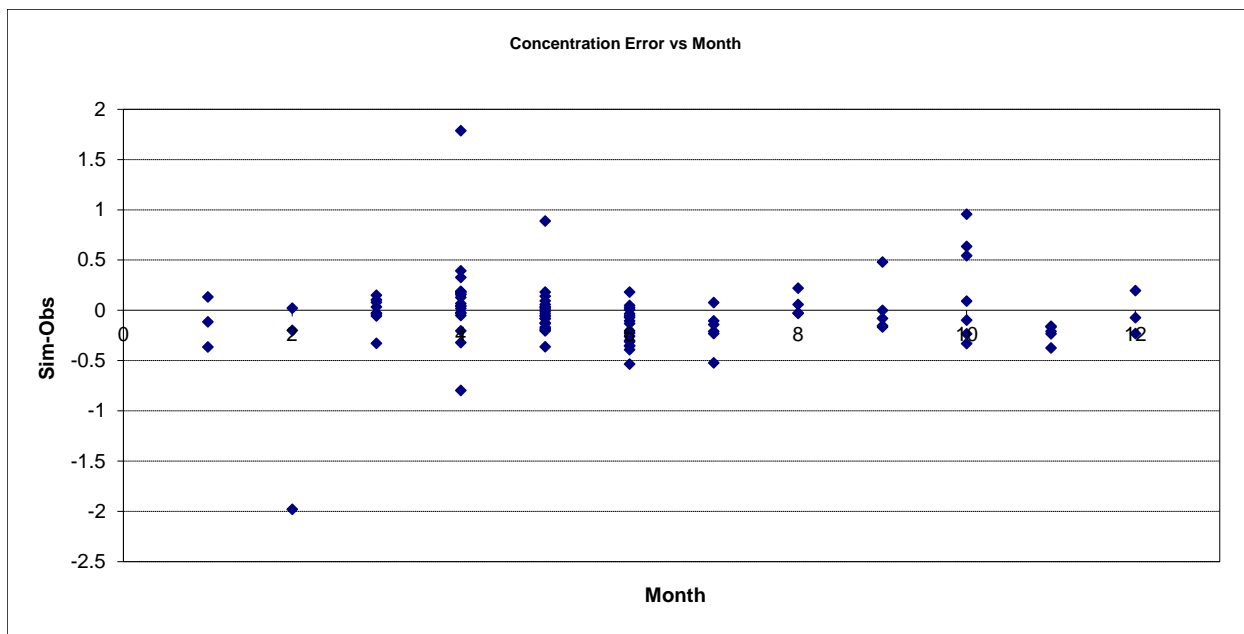


Figure 276. Residual (Simulated - Observed) vs. Month Total Kjeldahl Nitrogen (TKN) at Poplar River near Lutsen

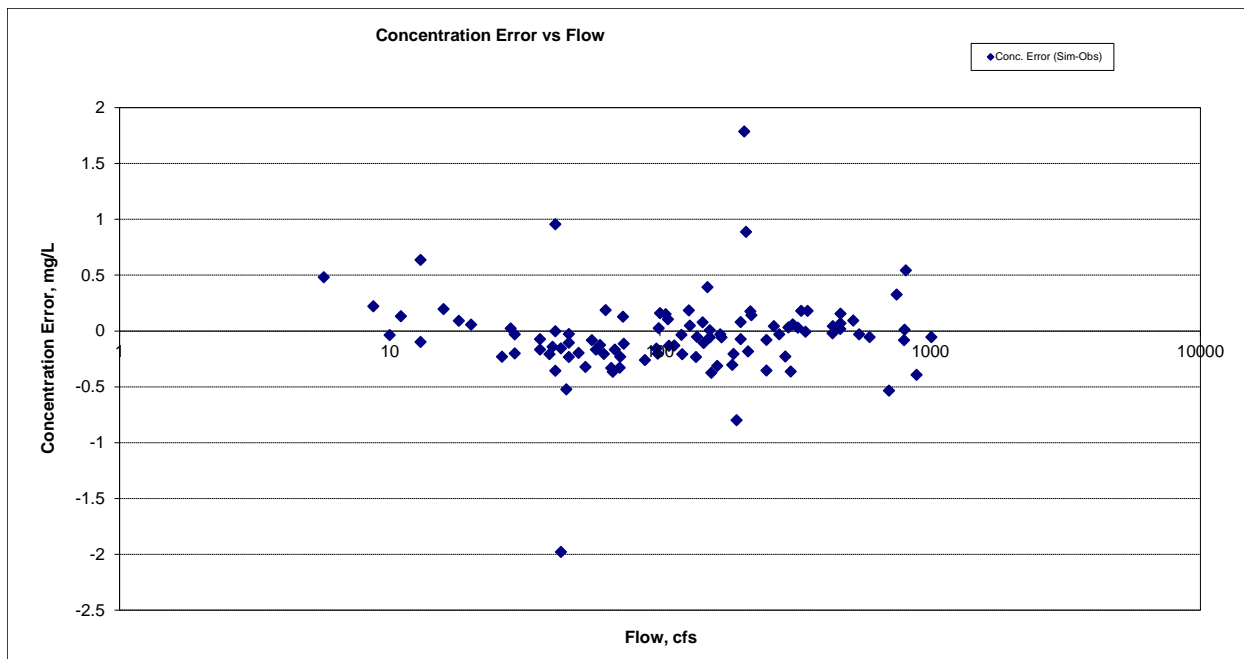


Figure 277. Residual (Simulated - Observed) vs. Flow Total Kjeldahl Nitrogen (TKN) at Poplar River near Lutsen

Nitrite+ Nitrate Nitrogen (NOx)

Table 54. Nitrite+ Nitrate Nitrogen (NOx) statistics

Count	102
Concentration Average Error	-11.06%
Concentration Median Error	12.98%
Load Ave Error	-34.50%
Load Median Error	3.17%
Paired t concentration	0.82
Paired t load	0.14

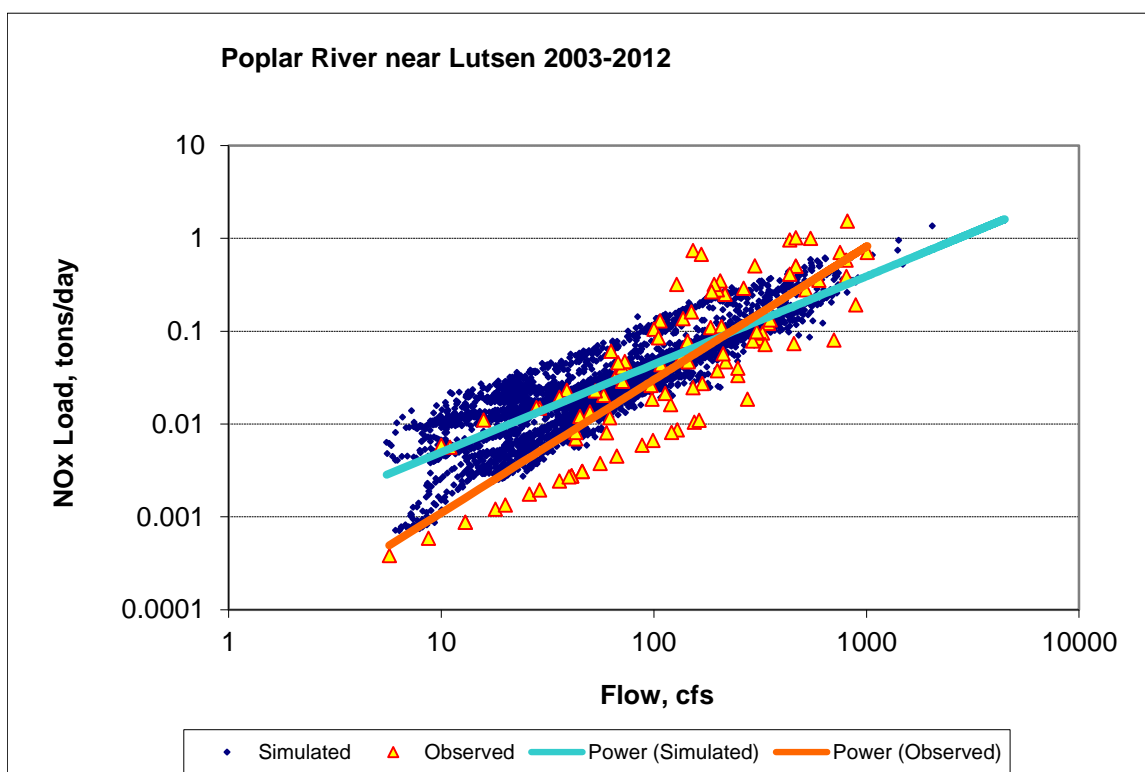


Figure 278. Power plot of simulated and observed Nitrite+ Nitrate Nitrogen (NOx) load vs flow at Poplar River near Lutsen

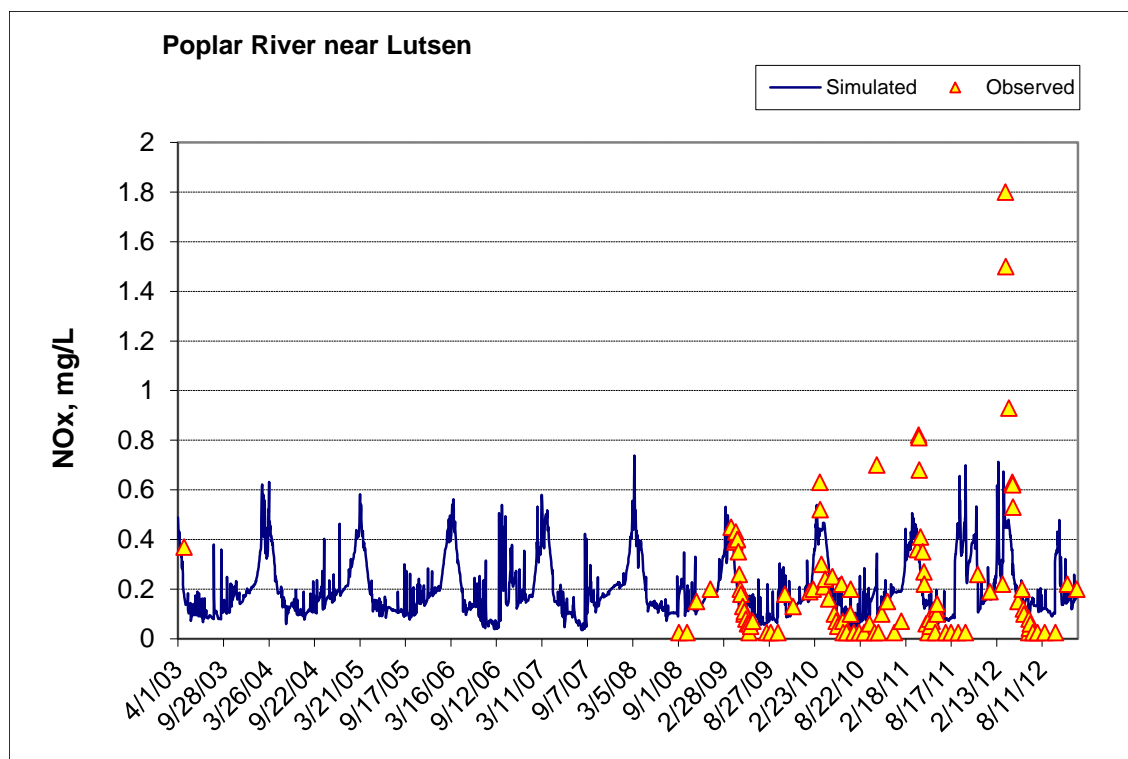


Figure 279. Time series of observed and simulated Nitrite+ Nitrate Nitrogen (NOx) concentration at Poplar River near Lutsen

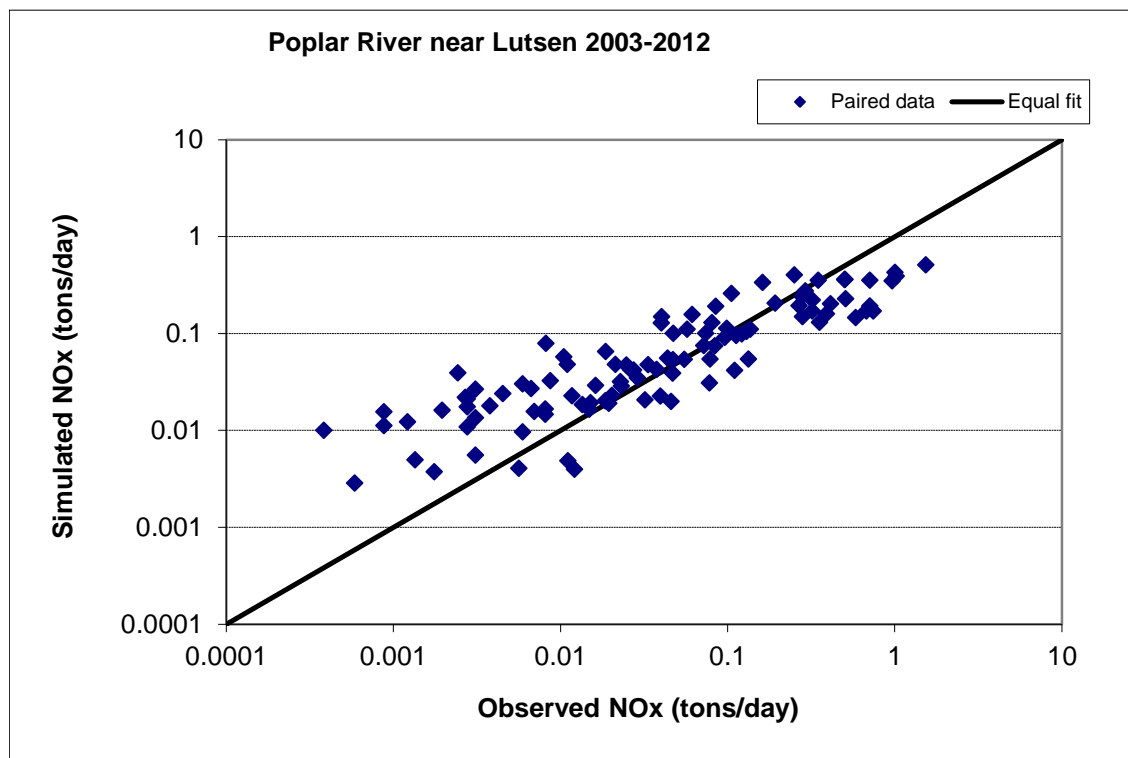


Figure 280. Paired simulated vs. observed Nitrite+ Nitrate Nitrogen (NOx) load at Poplar River near Lutsen

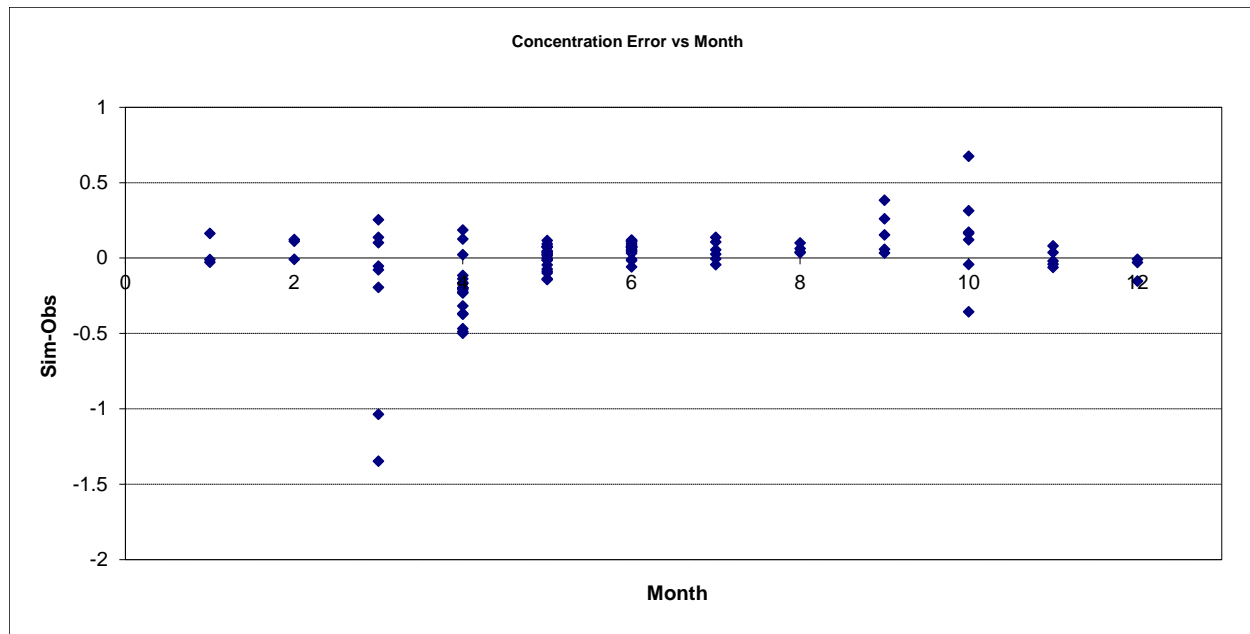


Figure 281. Residual (Simulated - Observed) vs. Month Nitrite+ Nitrate Nitrogen (NOx) at Poplar River near Lutsen

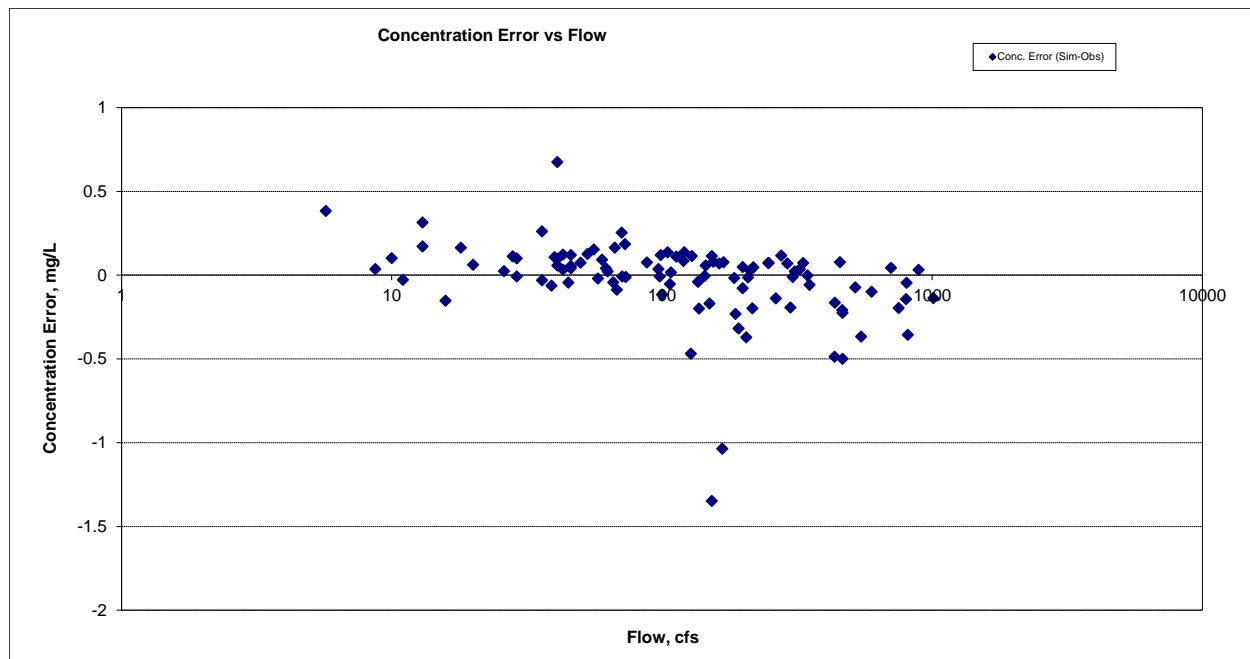


Figure 282. Residual (Simulated - Observed) vs. Flow Nitrite+ Nitrate Nitrogen (NOx) at Poplar River near Lutsen

Total Nitrogen (TN)

Table 55. Total Nitrogen (TN) statistics

Count	102
Concentration Average Error	-7.97%
Concentration Median Error	-7.53%
Load Ave Error	-10.85%
Load Median Error	-3.19%
Paired t concentration	0.99
Paired t load	0.76

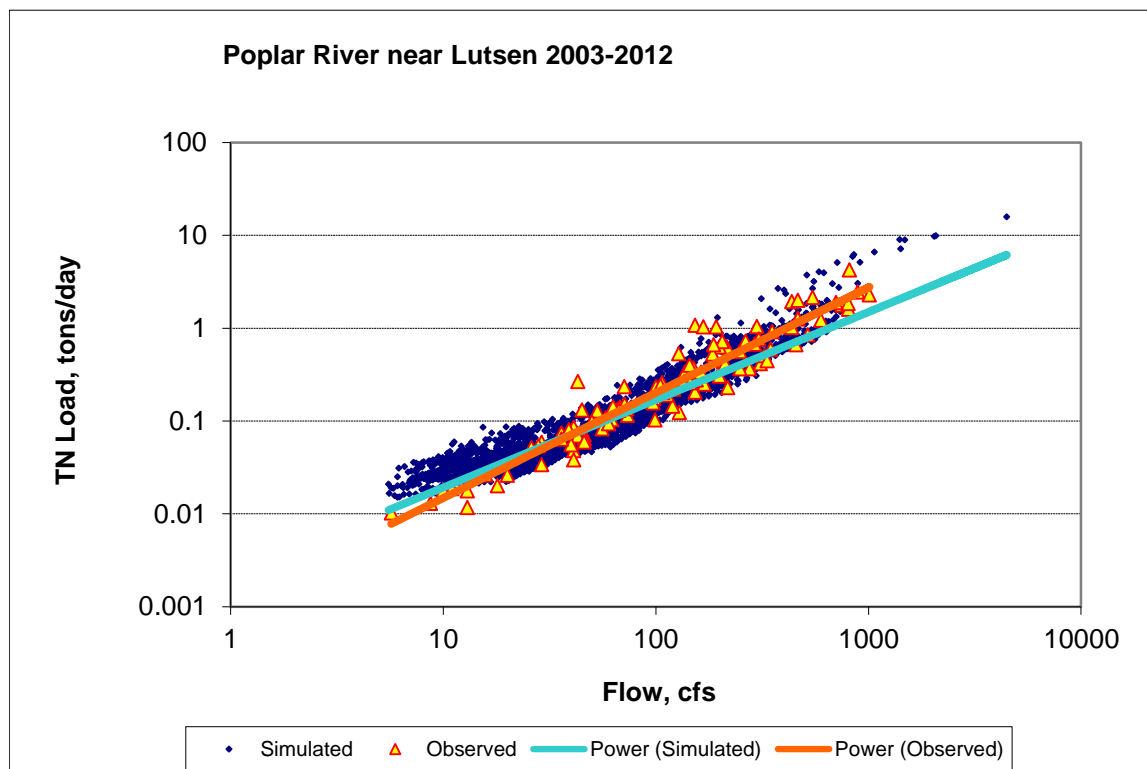


Figure 283. Power plot of simulated and observed Total Nitrogen (TN) load vs flow at Poplar River near Lutsen

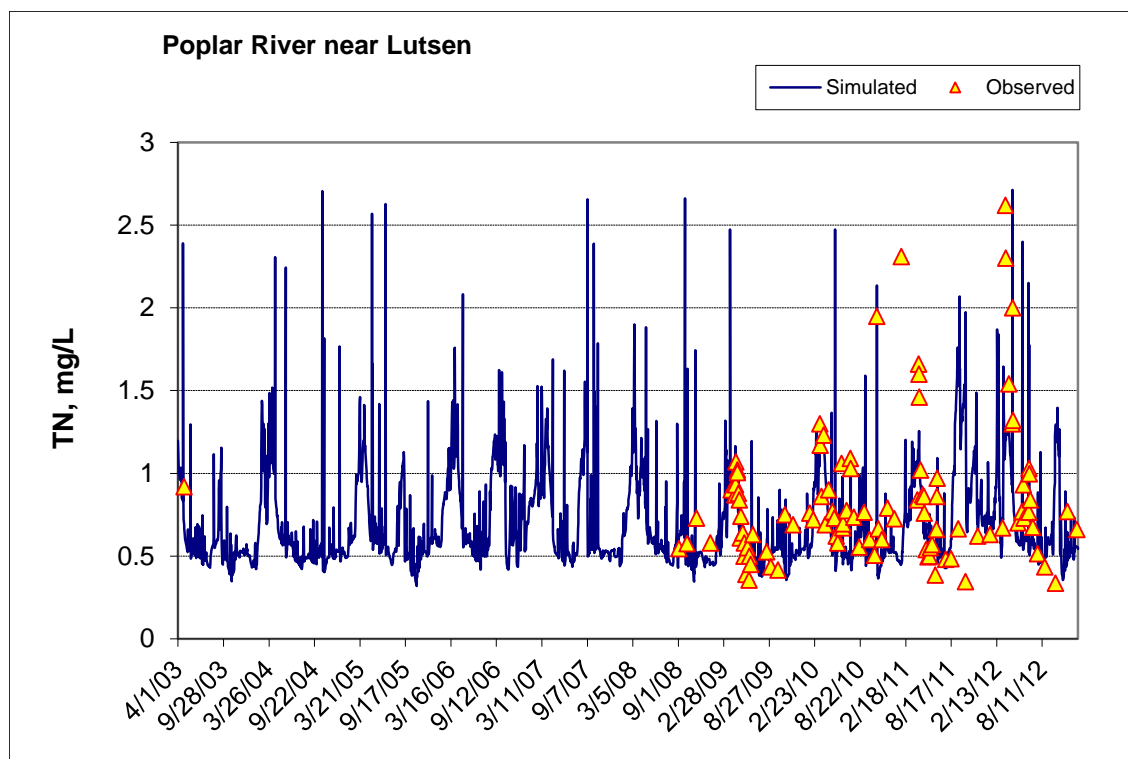


Figure 284. Time series of observed and simulated Total Nitrogen (TN) concentration at Poplar River near Lutsen

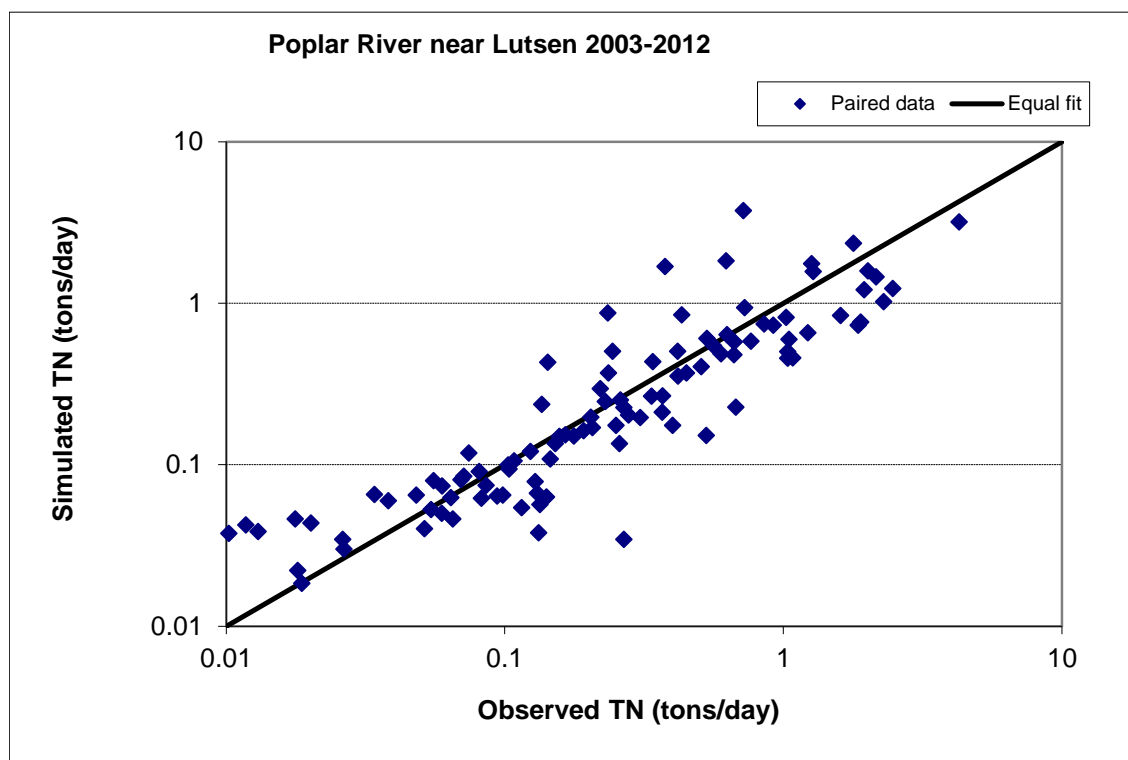


Figure 285. Paired simulated vs. observed Total Nitrogen (TN) load at Poplar River near Lutsen

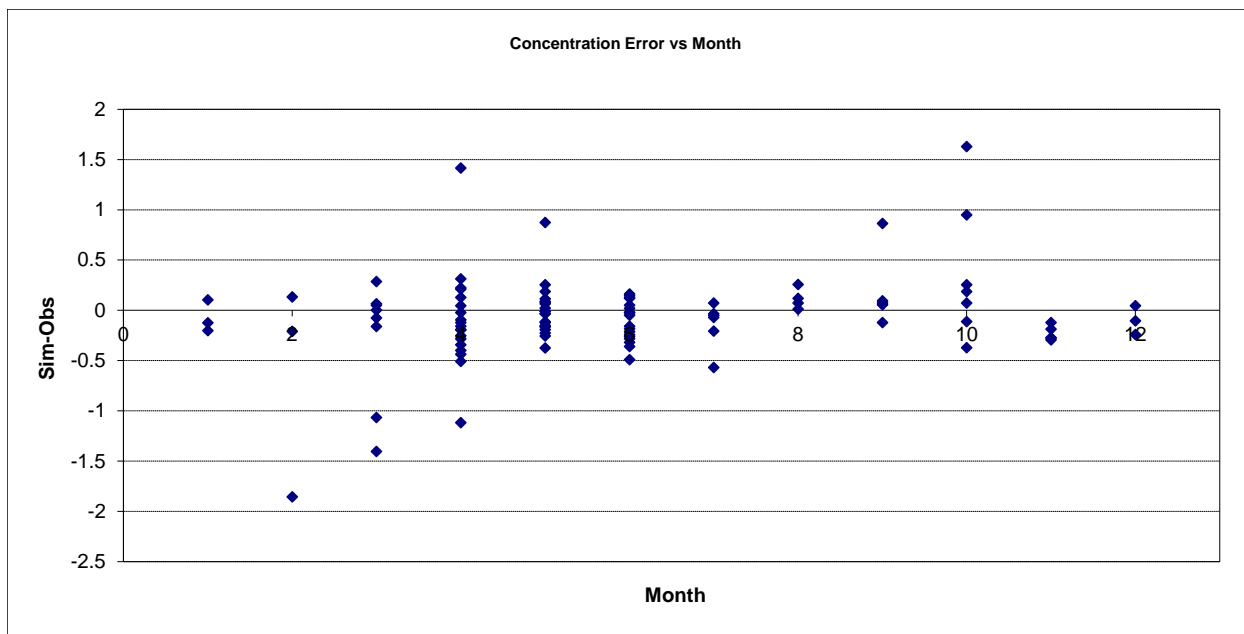


Figure 286. Residual (Simulated - Observed) vs. Month Total Nitrogen (TN) at Poplar River near Lutsen

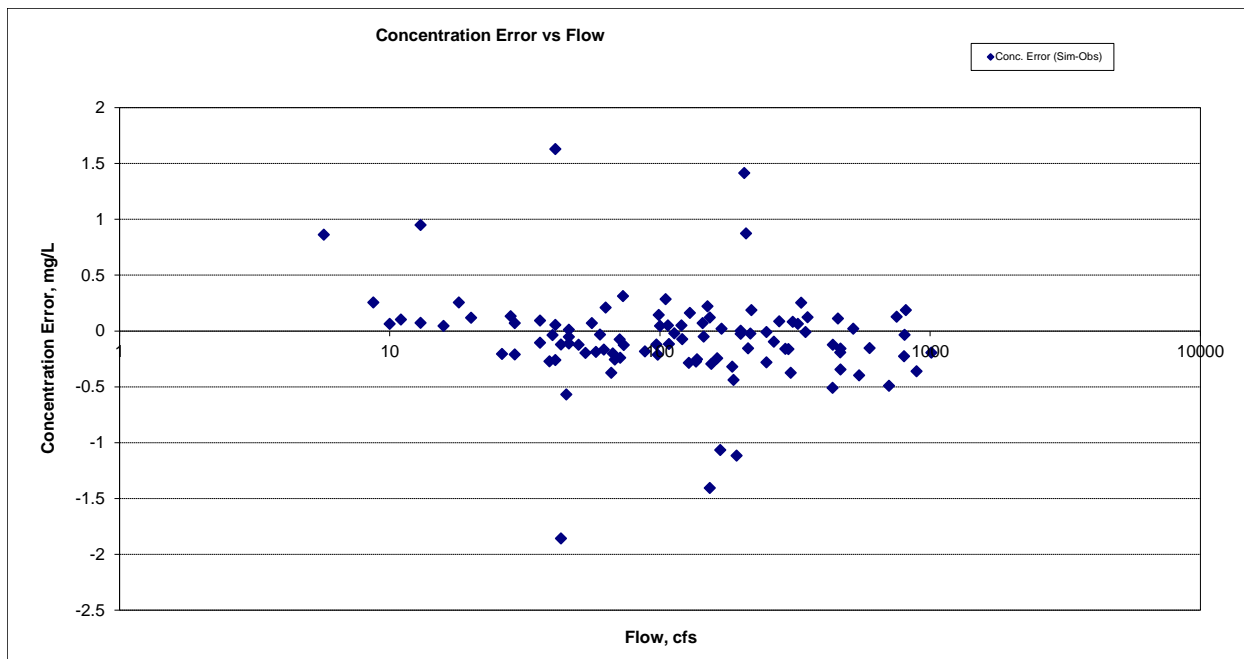


Figure 287. Residual (Simulated - Observed) vs. Flow Total Nitrogen (TN) at Poplar River near Lutsen

Soluble Reactive Phosphorus (SRP)

Table 56. Soluble Reactive Phosphorus (SRP) statistics

Count	101
Concentration Average Error	-27.43%
Concentration Median Error	-5.15%
Load Ave Error	-33.39%
Load Median Error	0.49%
Paired t concentration	0.27
Paired t load	0.16

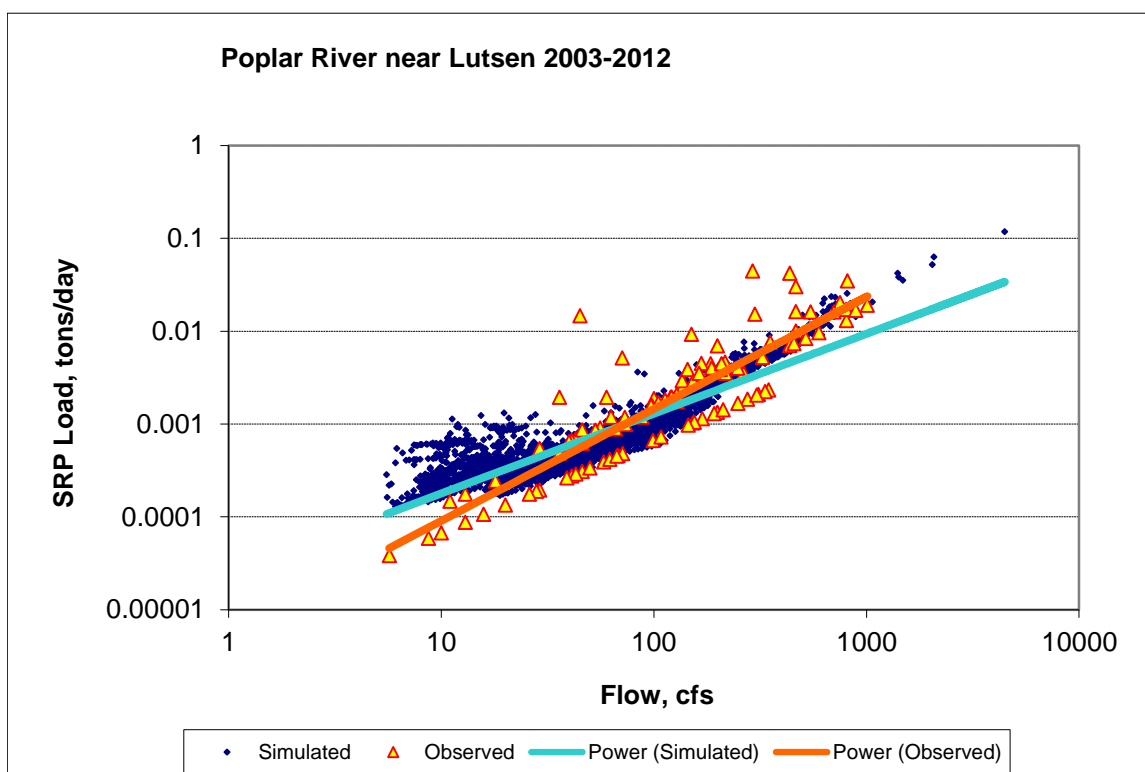


Figure 288. Power plot of simulated and observed Soluble Reactive Phosphorus (SRP) load vs flow at Poplar River near Lutsen

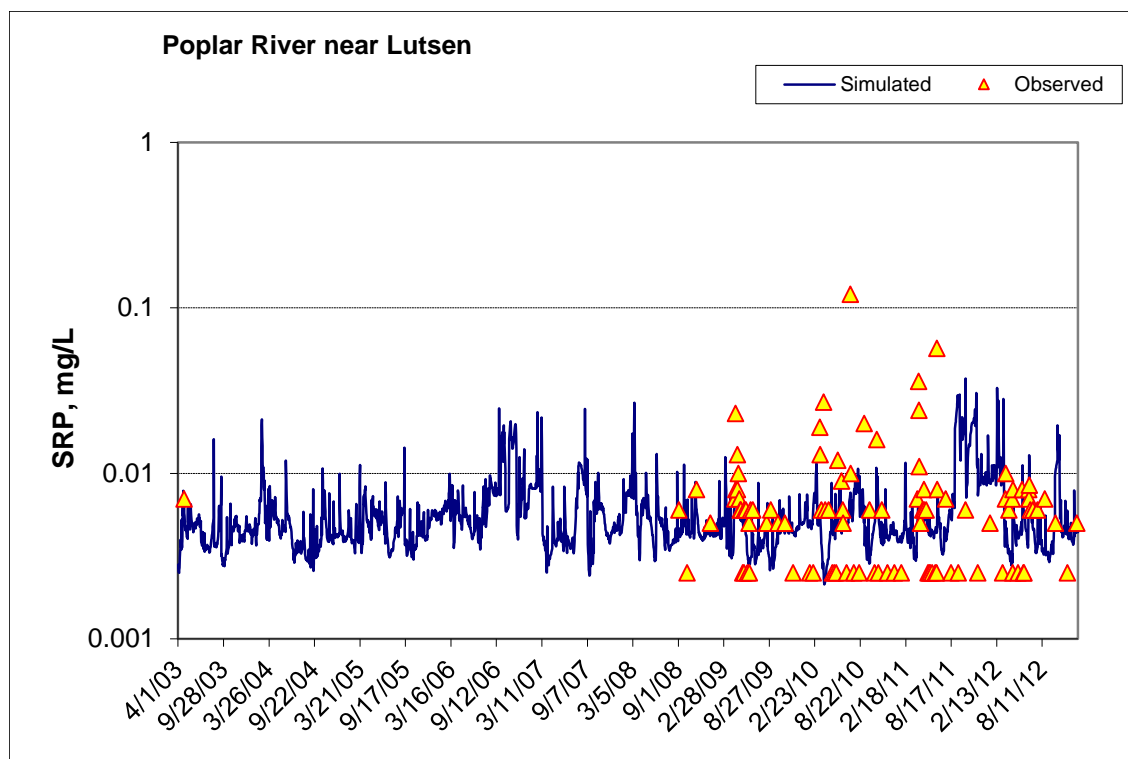


Figure 289. Time series of observed and simulated Soluble Reactive Phosphorus (SRP) concentration at Poplar River near Lutsen

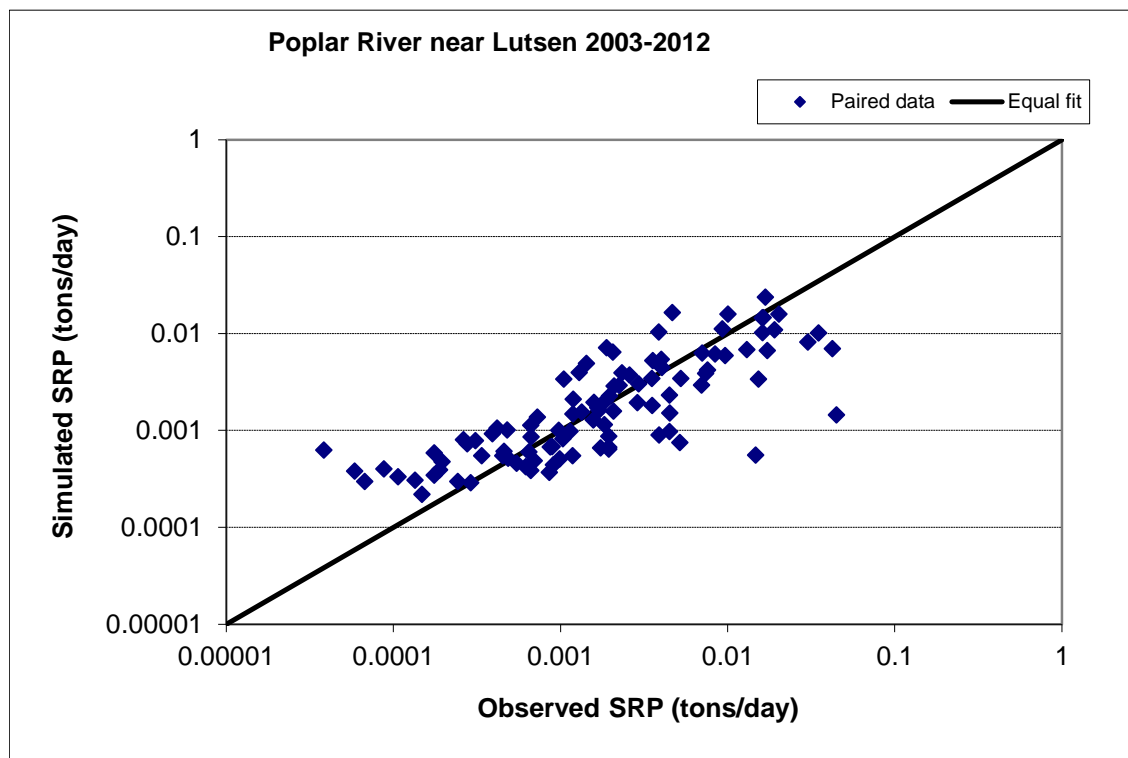


Figure 290. Paired simulated vs. observed Soluble Reactive Phosphorus (SRP) load at Poplar River near Lutsen

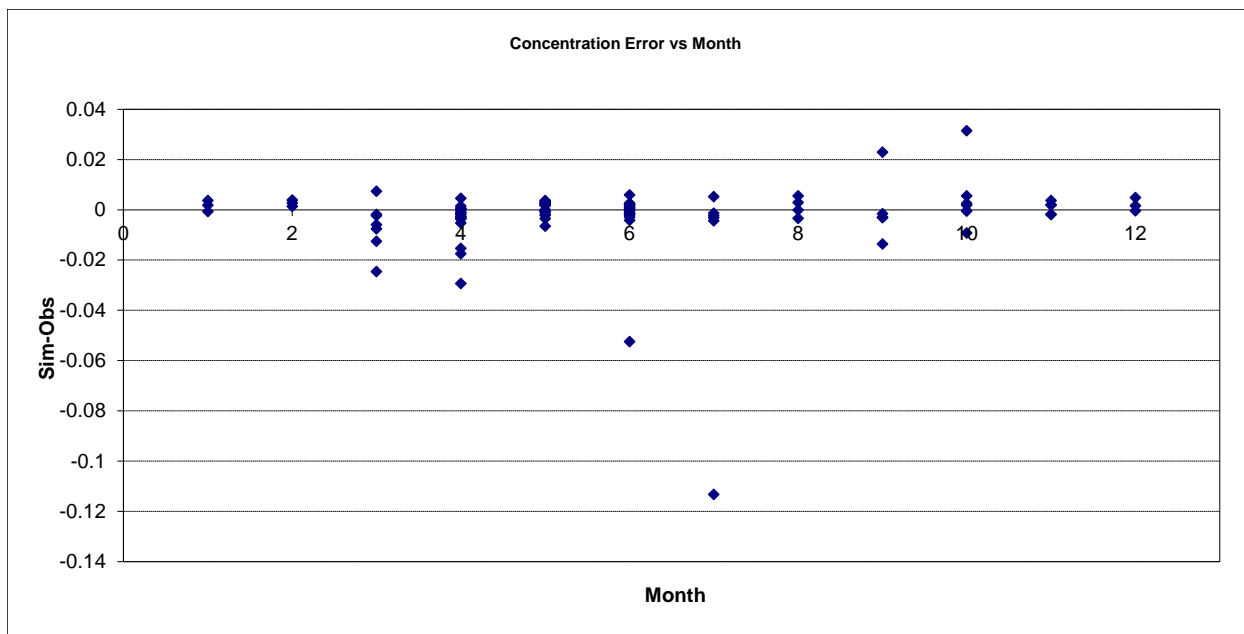


Figure 291. Residual (Simulated - Observed) vs. Month Soluble Reactive Phosphorus (SRP) at Poplar River near Lutsen

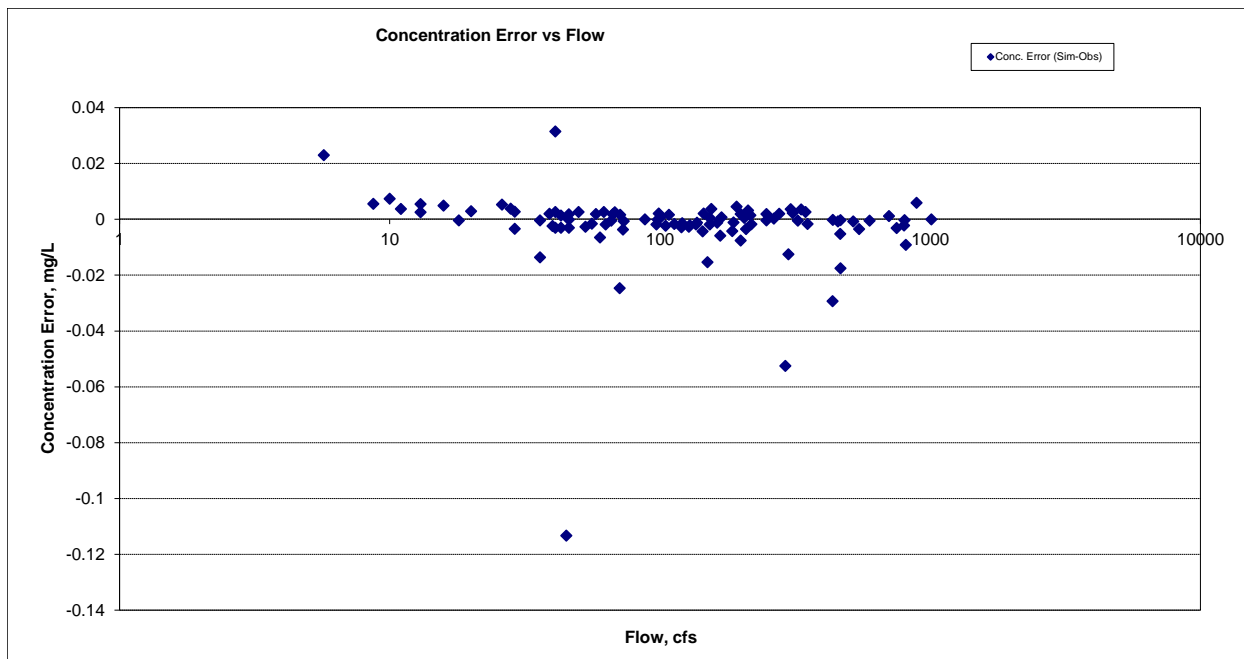


Figure 292. Residual (Simulated - Observed) vs. Flow Soluble Reactive Phosphorus (SRP) at Poplar River near Lutsen

Organic Phosphorus (OrgP)

Table 57. Organic Phosphorus (OrgP) statistics

Count	84
Concentration Average Error	-4.22%
Concentration Median Error	-10.27%
Load Ave Error	-9.98%
Load Median Error	-3.08%
Paired t concentration	0.95
Paired t load	0.69

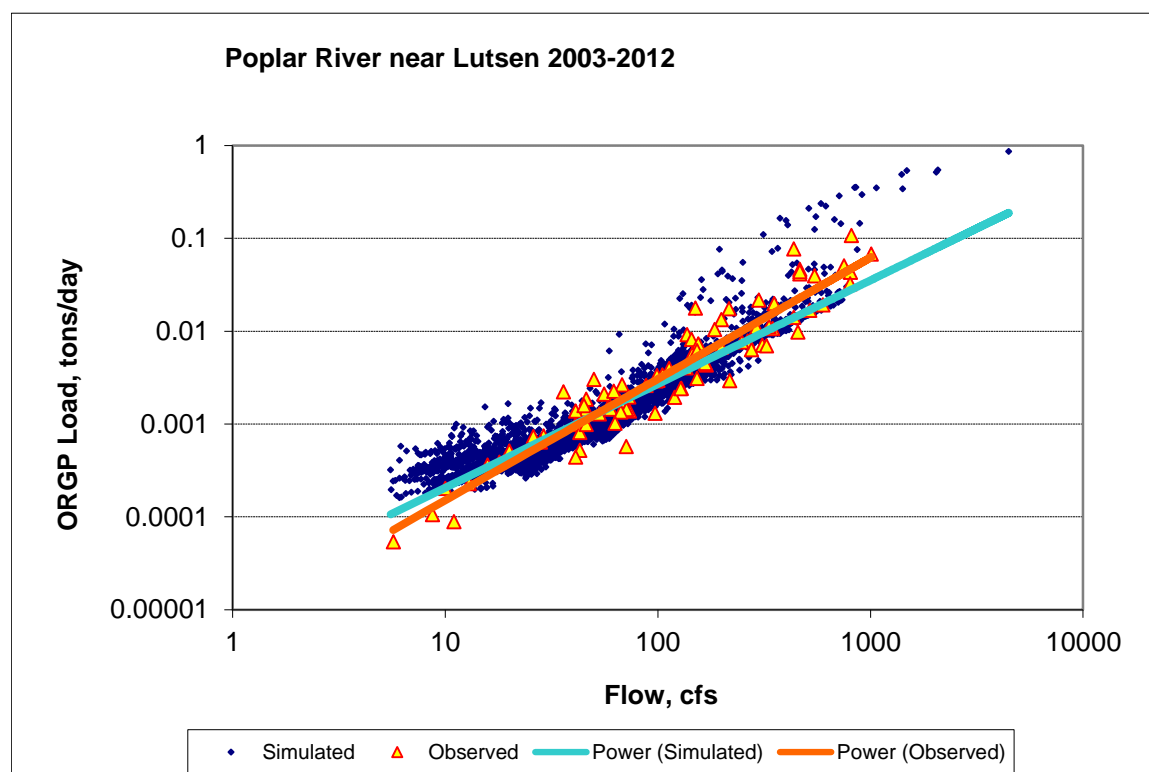


Figure 293. Power plot of simulated and observed Organic Phosphorus (OrgP) load vs flow at Poplar River near Lutsen

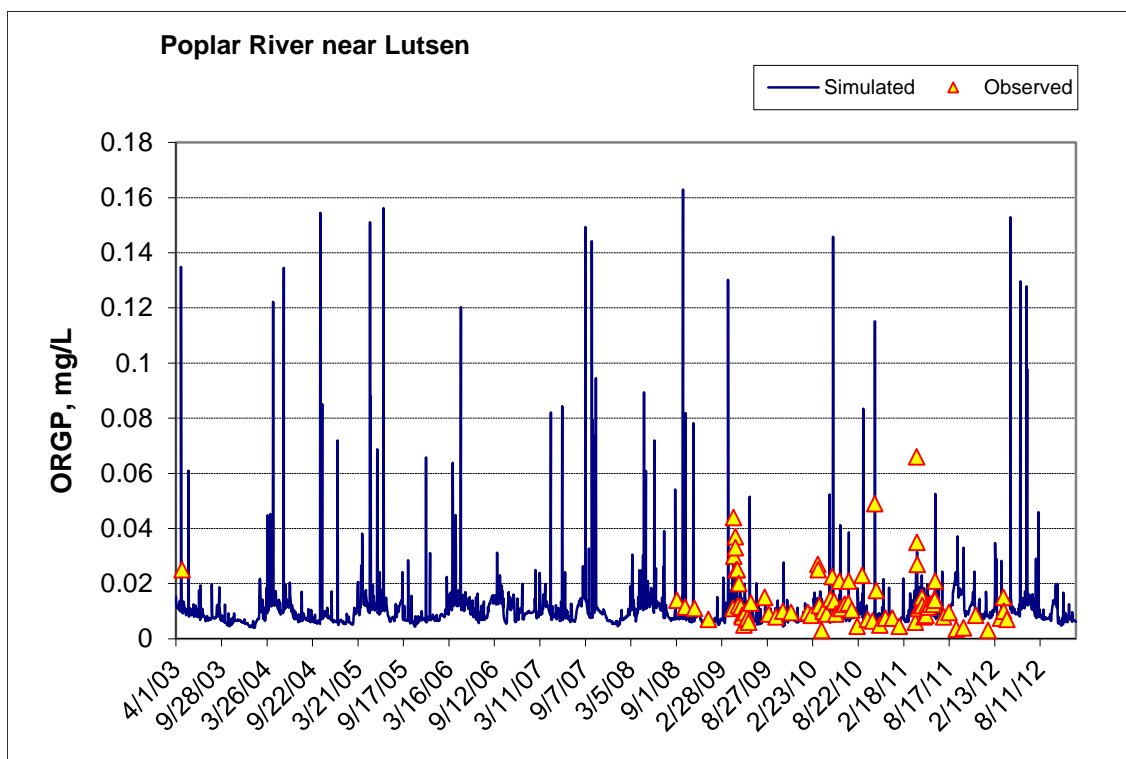


Figure 294. Time series of observed and simulated Organic Phosphorus (OrgP) concentration at Poplar River near Lutsen

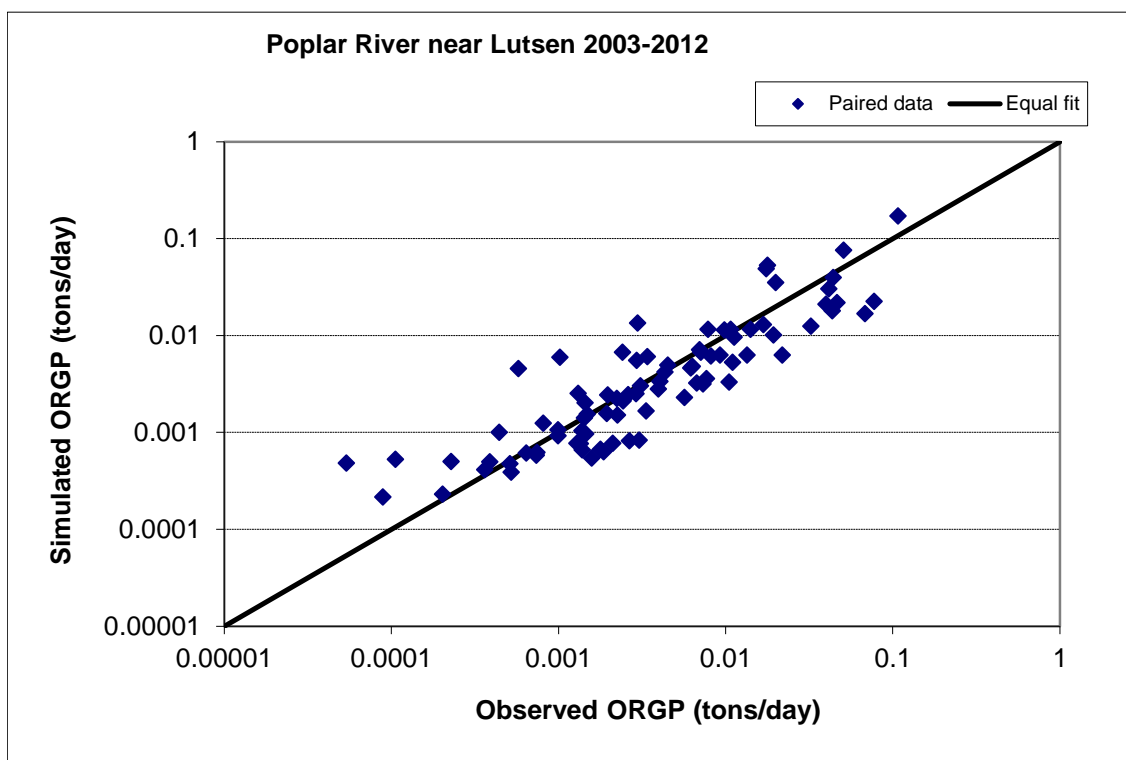


Figure 295. Paired simulated vs. observed Organic Phosphorus (OrgP) load at Poplar River near Lutsen

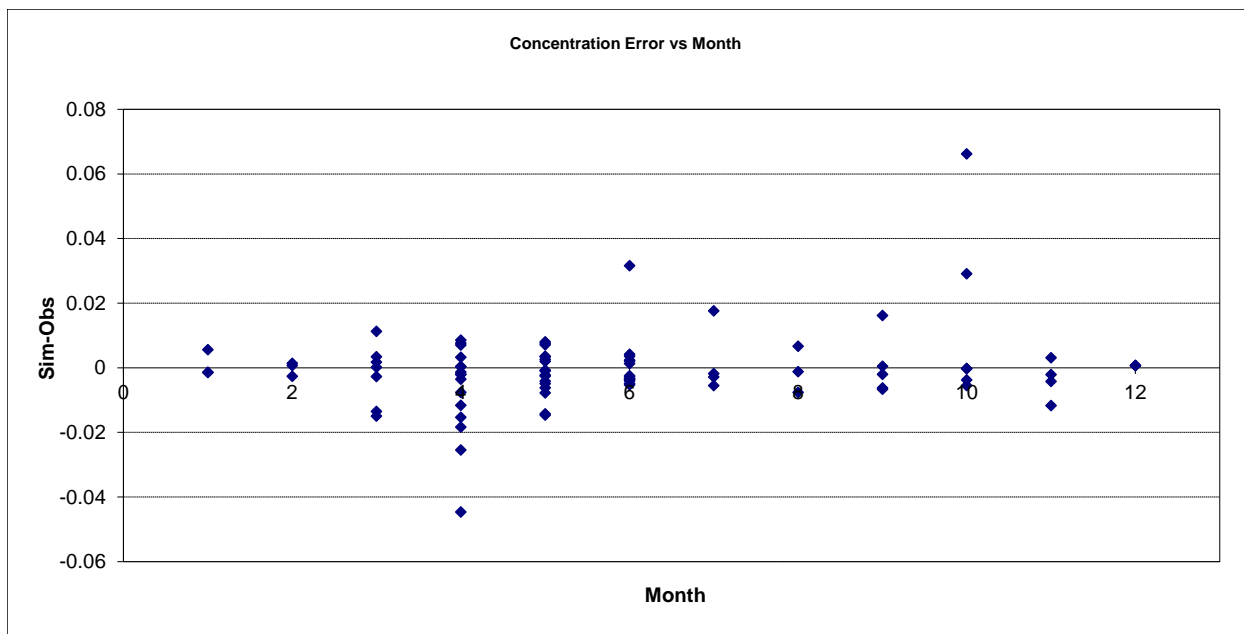


Figure 296. Residual (Simulated - Observed) vs. Month Organic Phosphorus (OrgP) at Poplar River near Lutsen

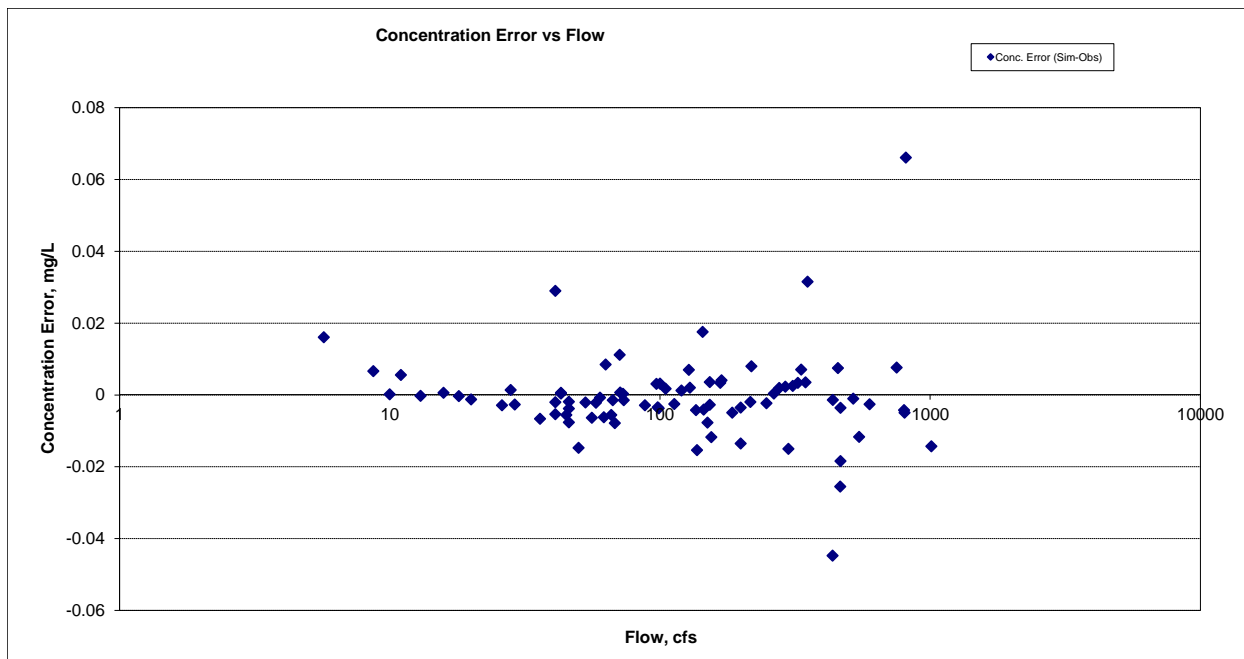


Figure 297. Residual (Simulated - Observed) vs. Flow Organic Phosphorus (OrgP) at Poplar River near Lutsen

Total Phosphorus (TP)

Table 58. Total Phosphorus (TP) statistics

Count	92
Concentration Average Error	-6.16%
Concentration Median Error	-7.10%
Load Ave Error	12.57%
Load Median Error	-1.83%
Paired t concentration	0.93
Paired t load	0.60

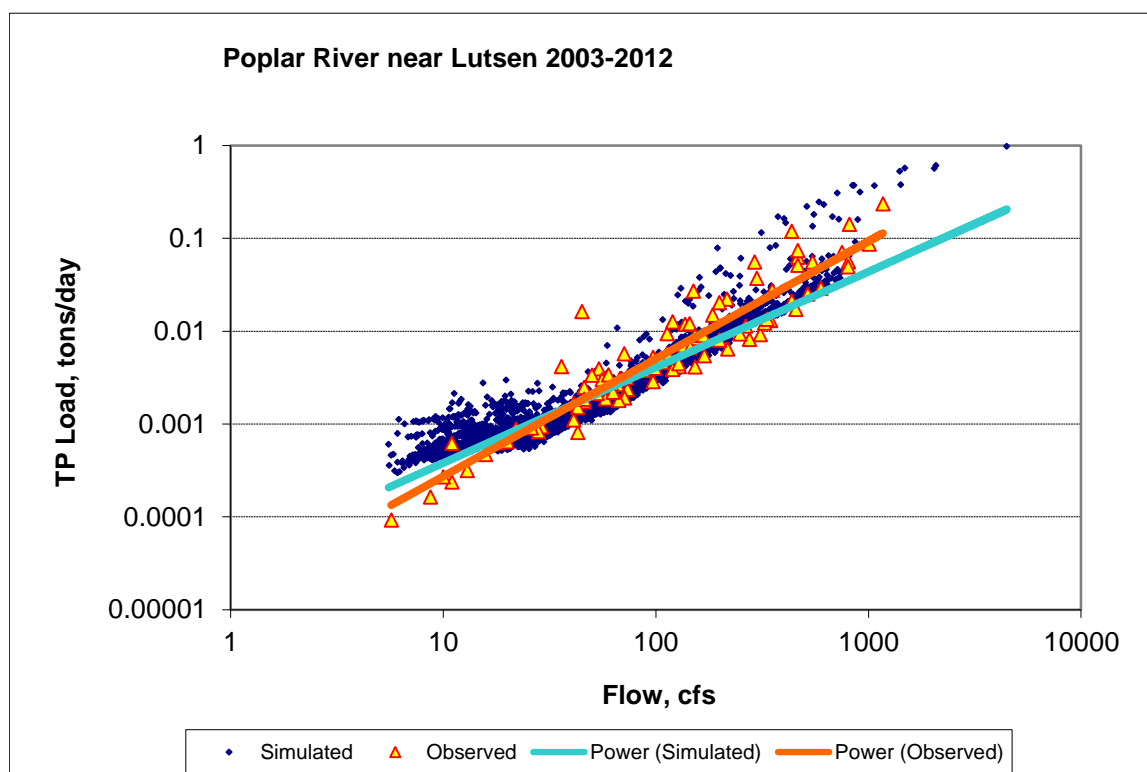


Figure 298. Power plot of simulated and observed Total Phosphorus (TP) load vs flow at Poplar River near Lutsen

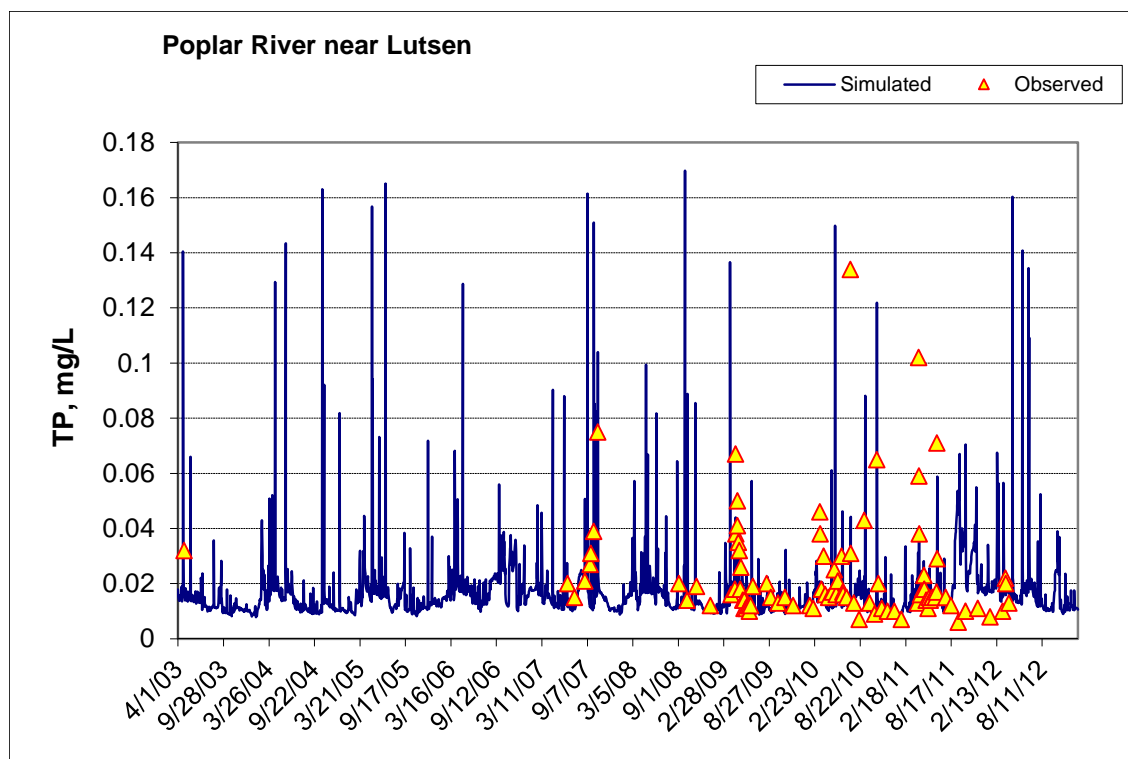


Figure 299. Time series of observed and simulated Total Phosphorus (TP) concentration at Poplar River near Lutsen

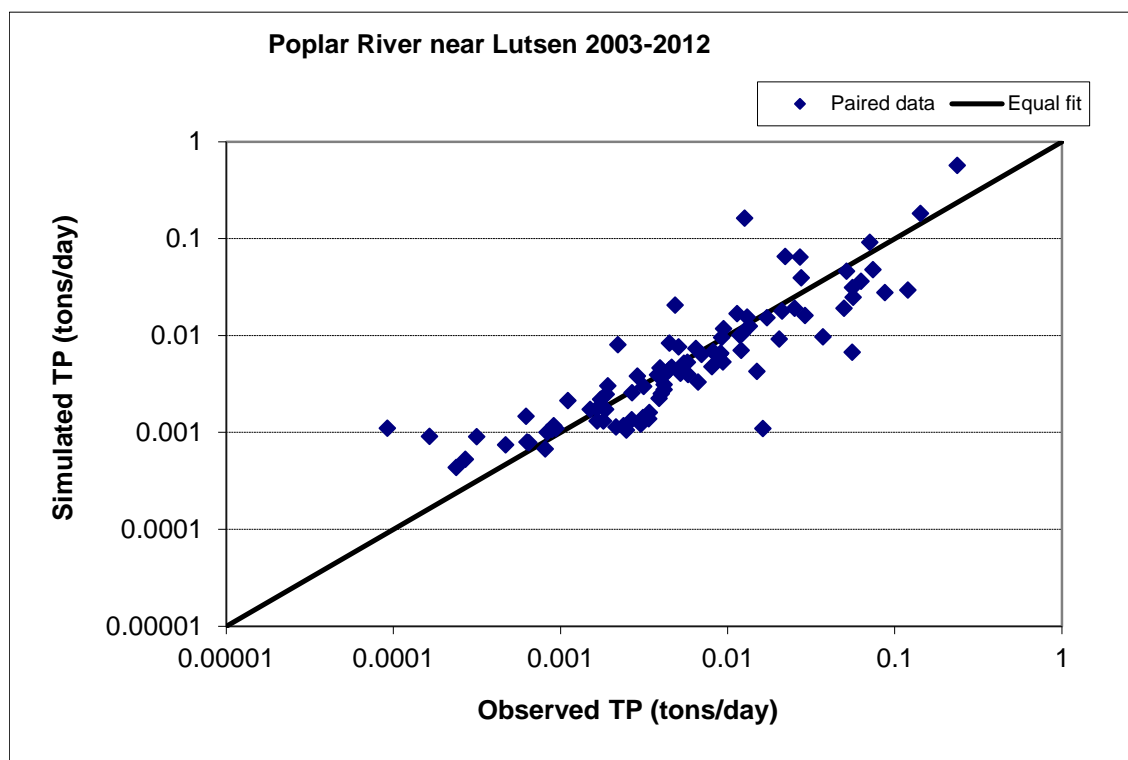


Figure 300. Paired simulated vs. observed Total Phosphorus (TP) load at Poplar River near Lutsen

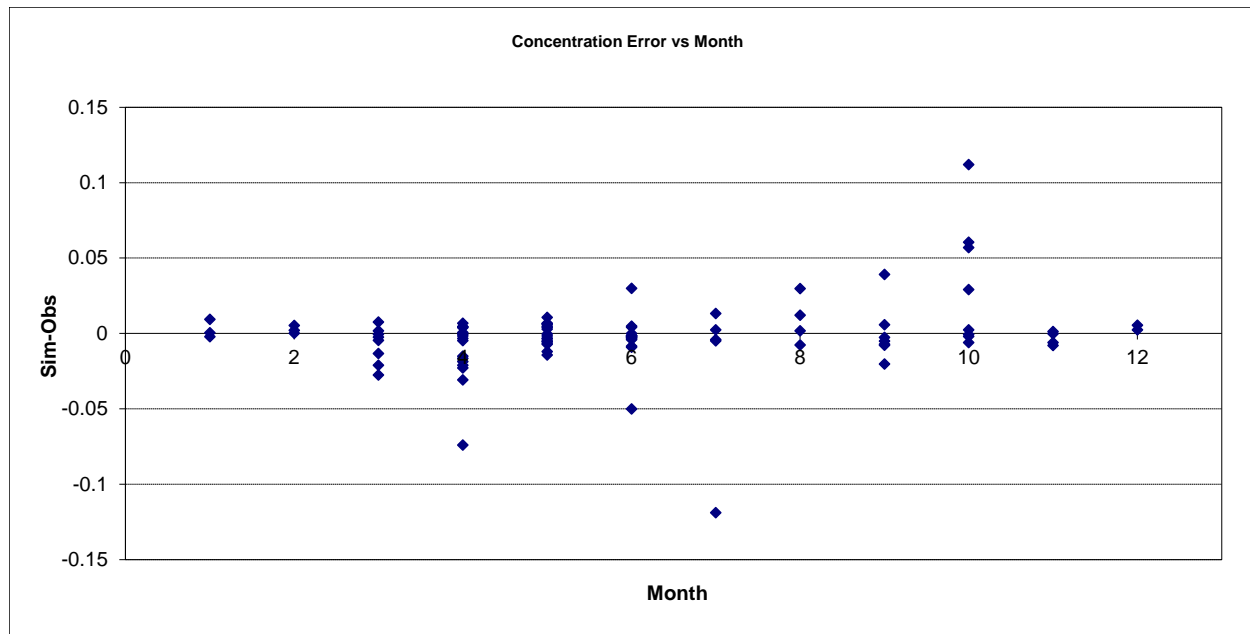


Figure 301. Residual (Simulated - Observed) vs. Month Total Phosphorus (TP) at Poplar River near Lutsen

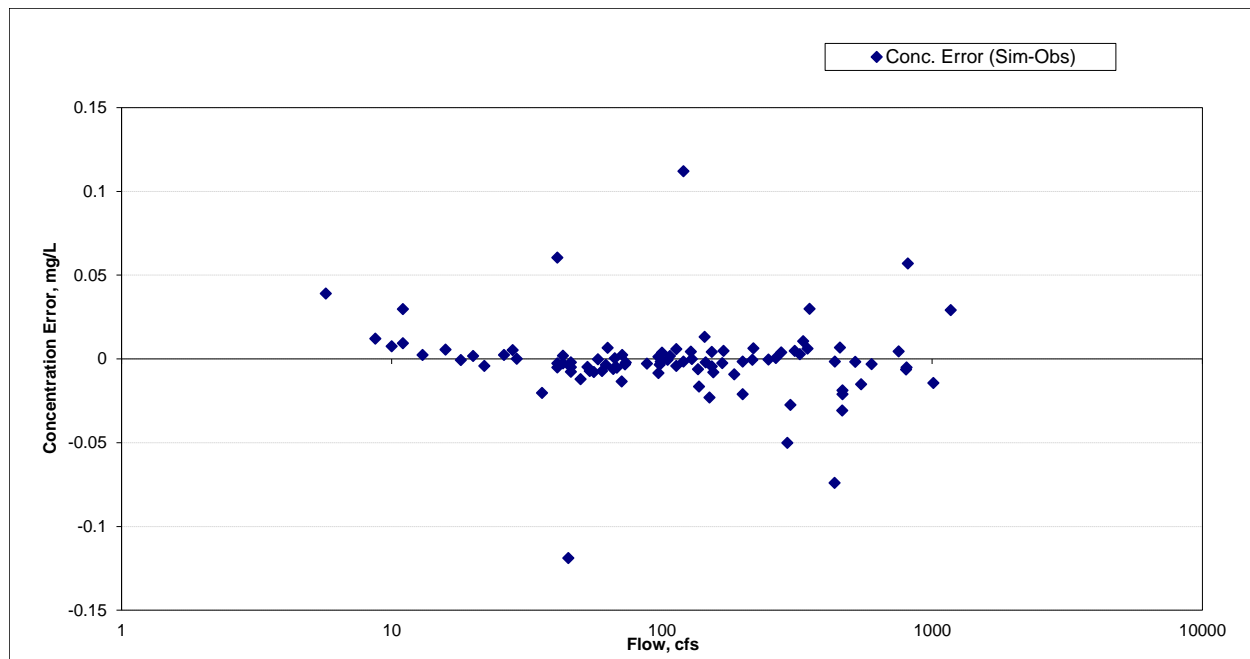


Figure 302. Residual (Simulated - Observed) vs. Flow Total Phosphorus (TP) at Poplar River near Lutsen

Brule River near Hovland (HYDSTRA 01022001)

Total Suspended Solids (TSS)

Table 59. Total Suspended Solids (TSS) statistics

Count	128
Concentration Average Error	-3.20%
Concentration Median Error	11.34%
Load Ave Error	-2.51%
Load Median Error	1.14%
Paired t concentration	0.92
Paired t load	0.74

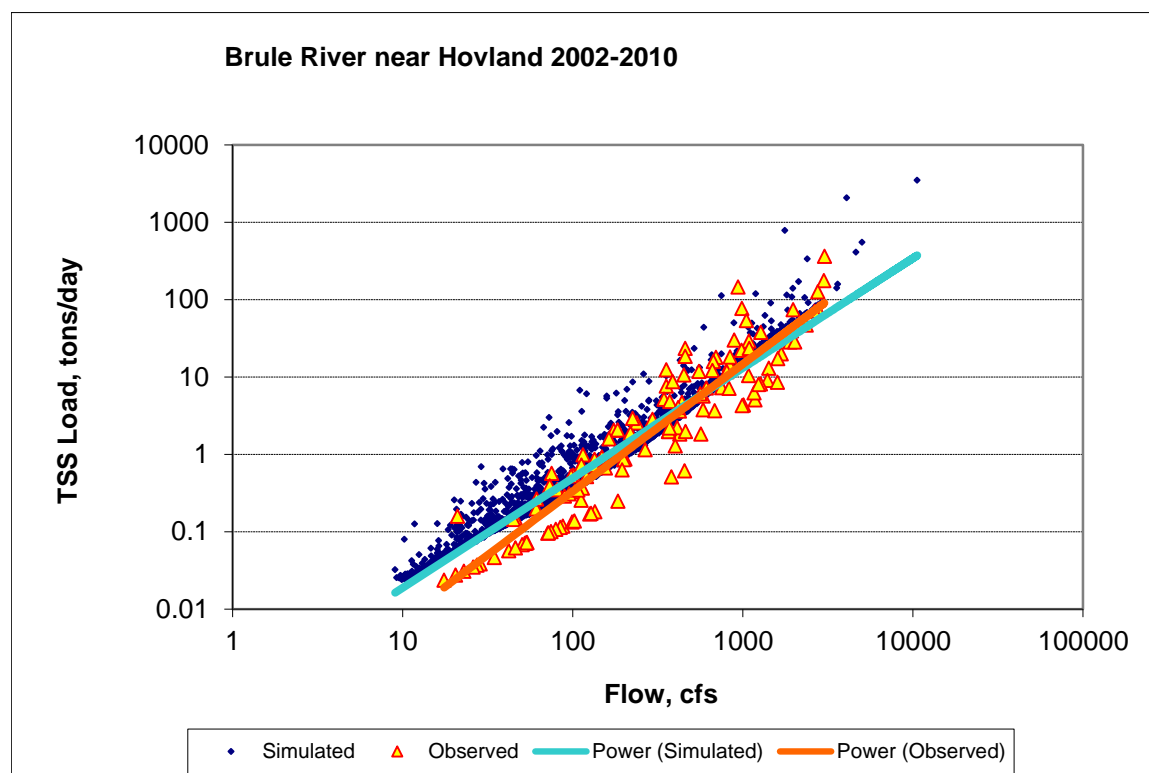


Figure 303. Power plot of simulated and observed Total Suspended Solids (TSS) load vs flow at Brule River near Hovland (validation period)

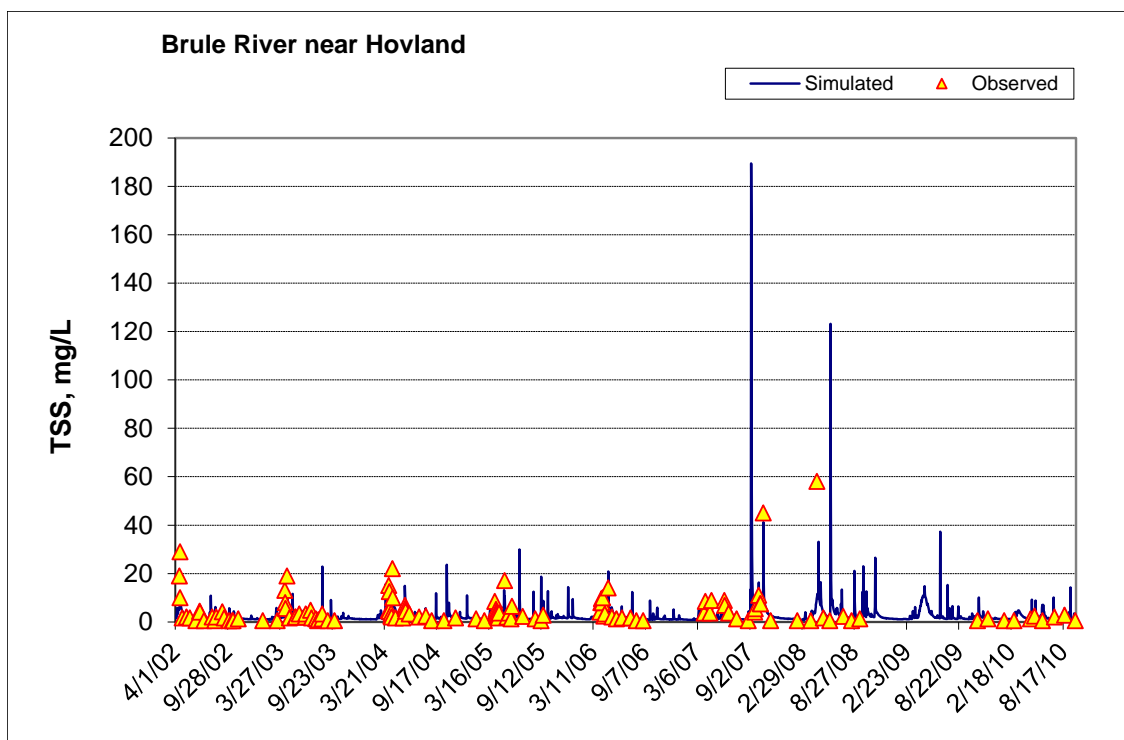


Figure 304. Time series of observed and simulated Total Suspended Solids (TSS) concentration at Brule River near Hovland

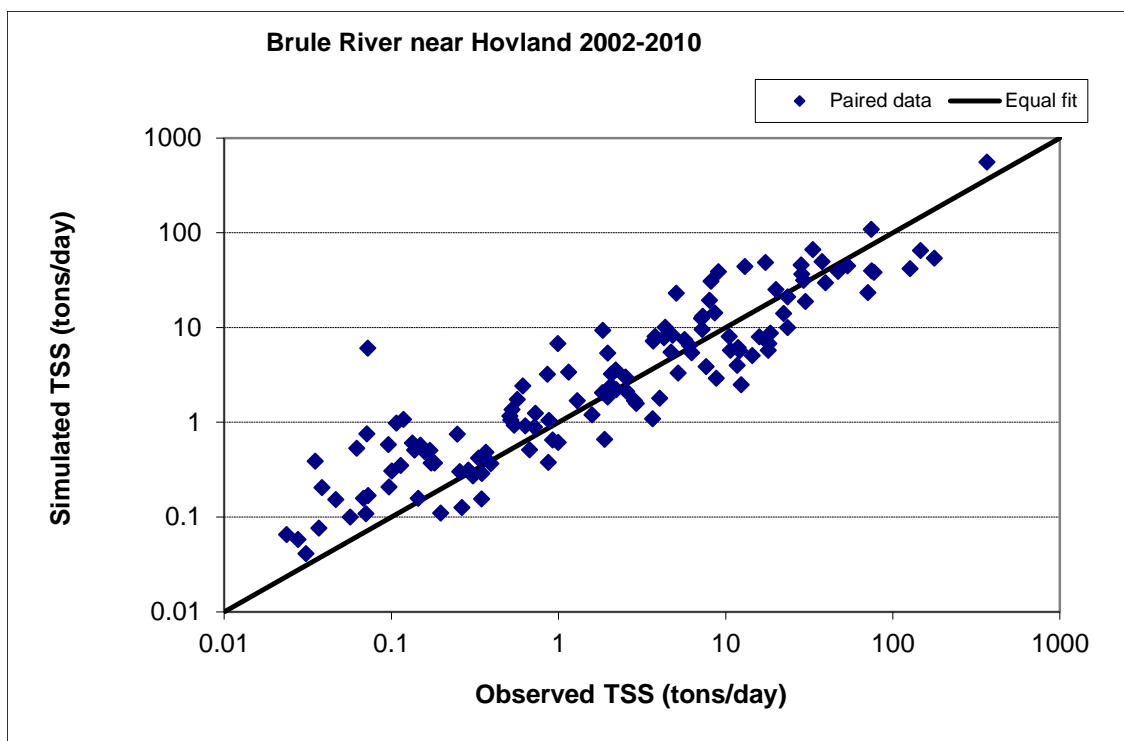


Figure 305. Paired simulated vs. observed Total Suspended Solids (TSS) load at Brule River near Hovland (validation period)

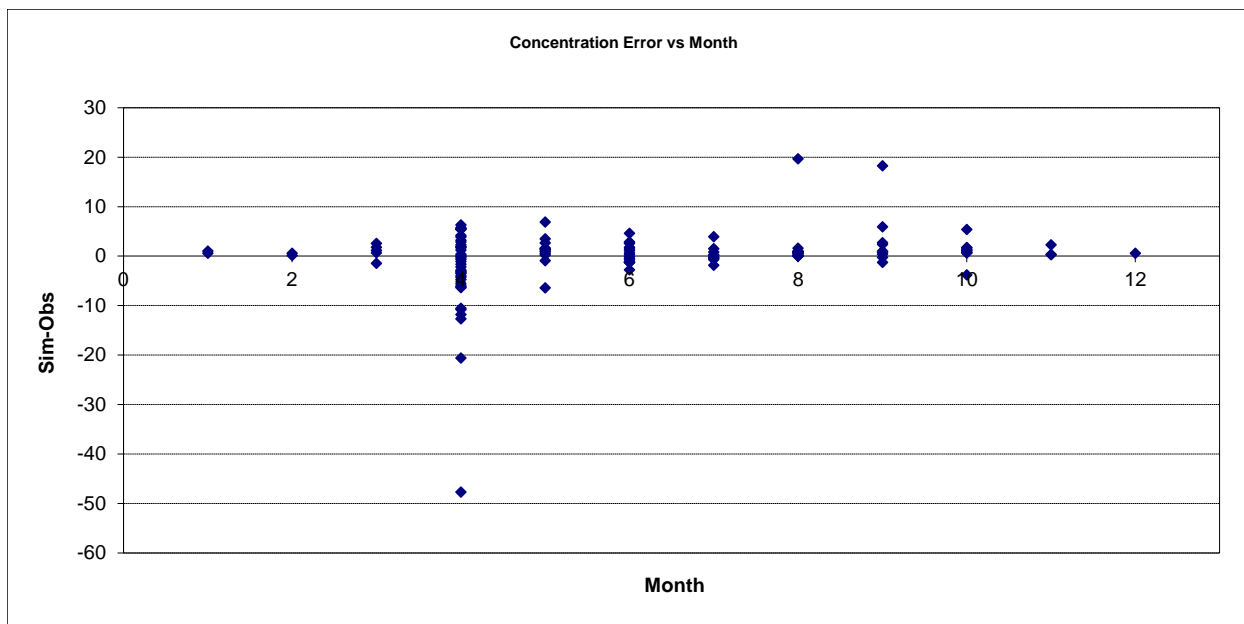


Figure 306. Residual (Simulated - Observed) vs. Month Total Suspended Solids (TSS) at Brule River near Hovland

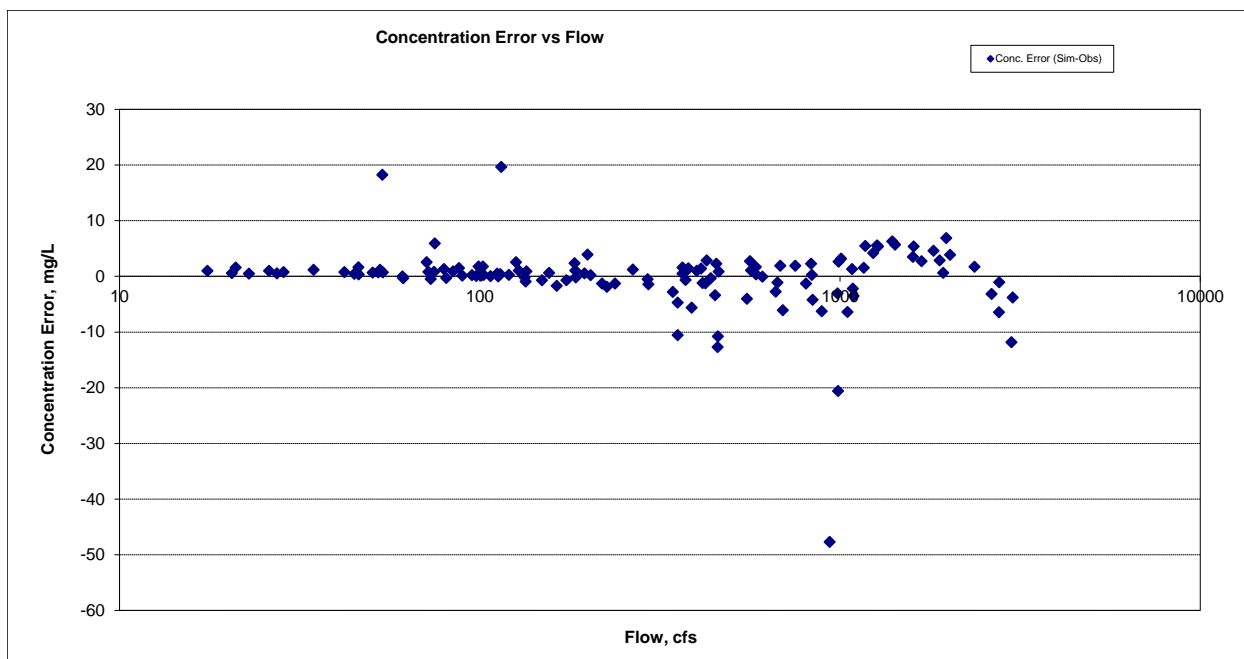


Figure 307. Residual (Simulated - Observed) vs. Flow Total Suspended Solids (TSS) at Brule River near Hovland

Ammonia Nitrogen (NH₃)

Table 60. Ammonia Nitrogen (NH₃) statistics

Count	39
-------	----

Concentration Average Error	-5.50%
Concentration Median Error	4.82%
Load Ave Error	-35.62%
Load Median Error	2.47%
Paired t concentration	0.86
Paired t load	0.30

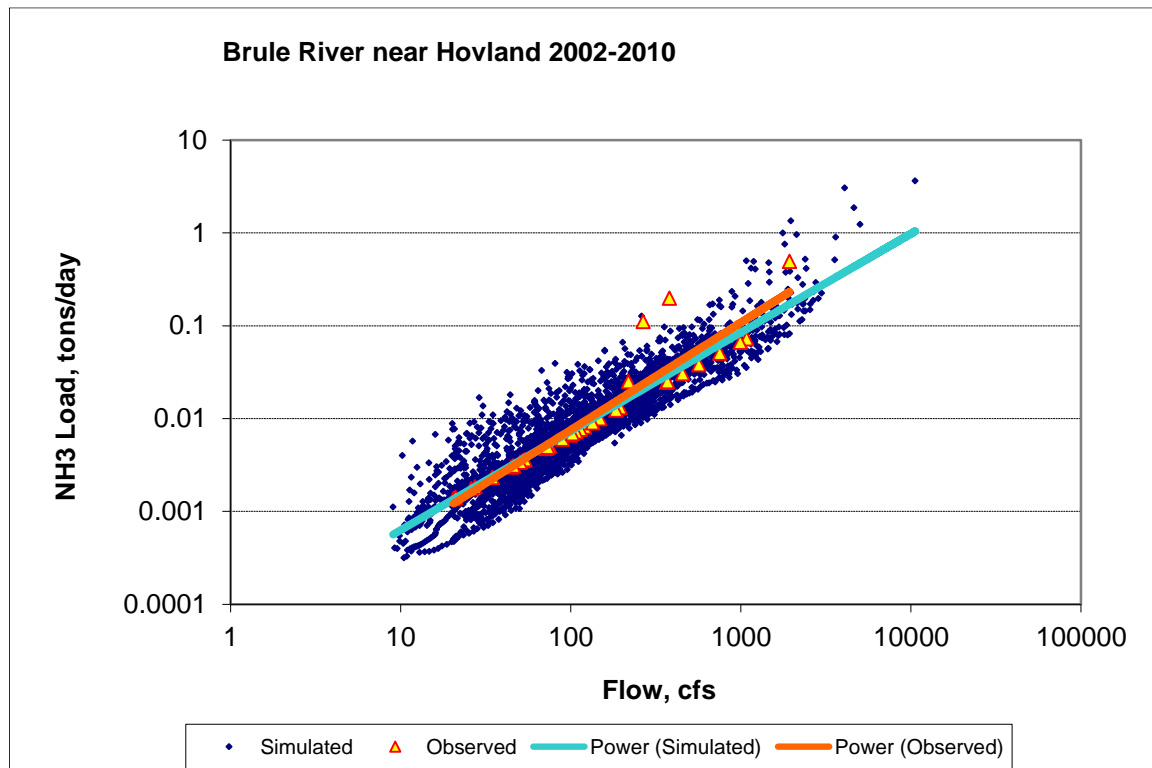


Figure 308. Power plot of simulated and observed Ammonia Nitrogen (NH₃) load vs flow at Brule River near Hovland (validation period)

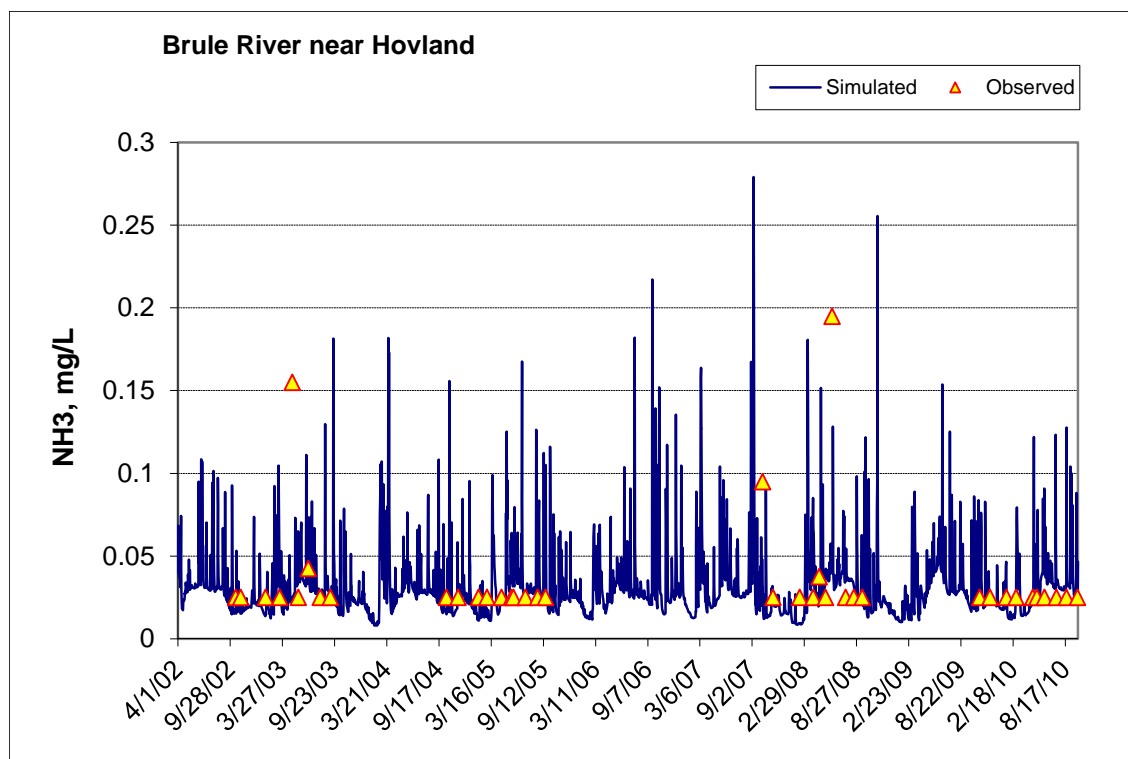


Figure 309. Time series of observed and simulated Ammonia Nitrogen (NH₃) concentration at Brule River near Hovland

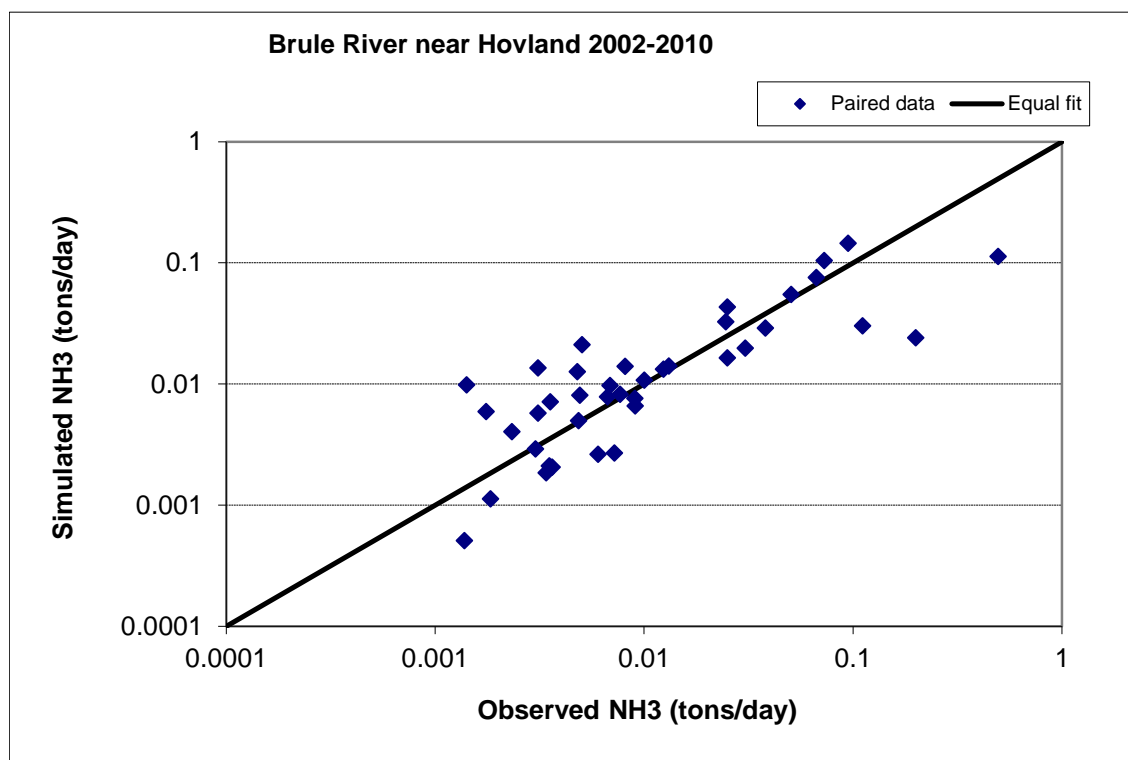


Figure 310. Paired simulated vs. observed Ammonia Nitrogen (NH₃) load at Brule River near Hovland (validation period)

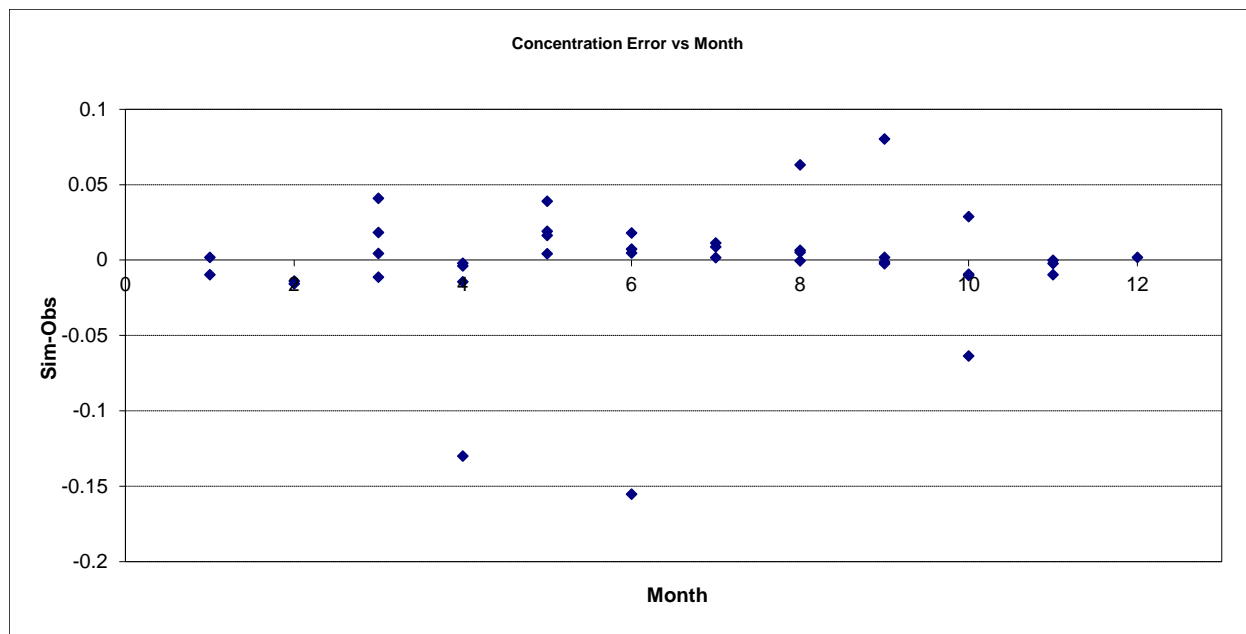


Figure 311. Residual (Simulated - Observed) vs. Month Ammonia Nitrogen (NH3) at Brule River near Hovland

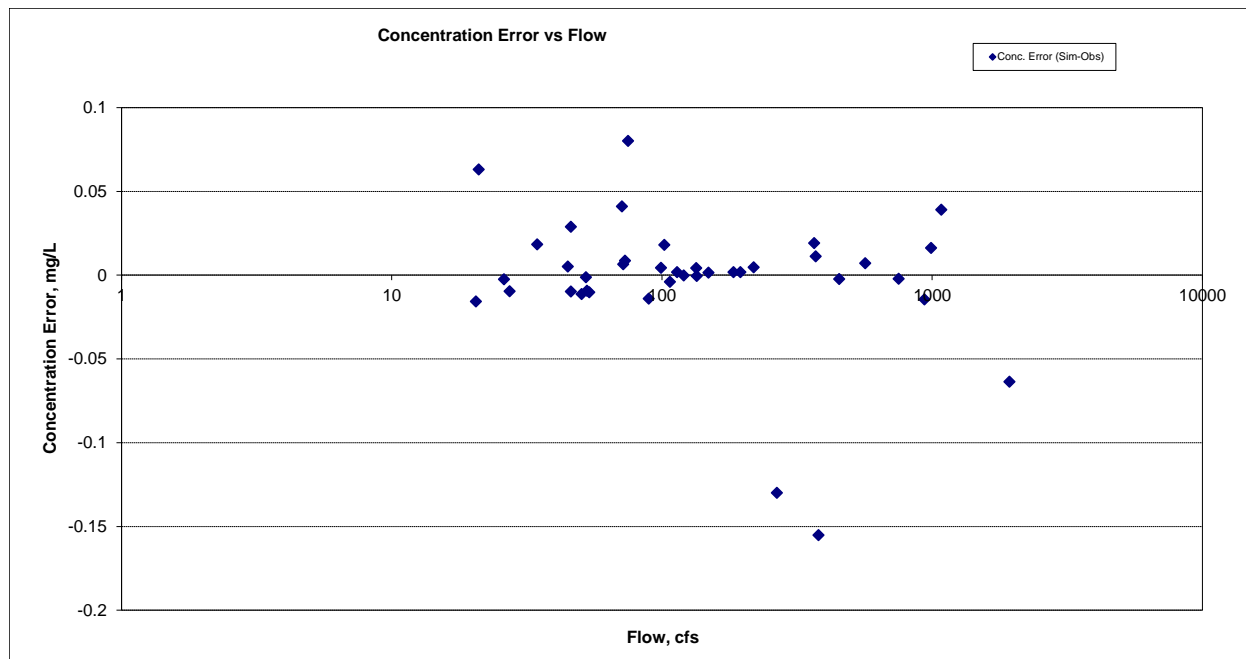


Figure 312. Residual (Simulated - Observed) vs. Flow Ammonia Nitrogen (NH3) at Brule River near Hovland

Organic Nitrogen (OrgN)

Table 61. Organic Nitrogen (OrgN) statistics

Count	6
-------	---

Concentration Average Error	-25.56%
Concentration Median Error	-11.05%
Load Ave Error	-31.98%
Load Median Error	-50.66%
Paired t concentration	0.31
Paired t load	0.30

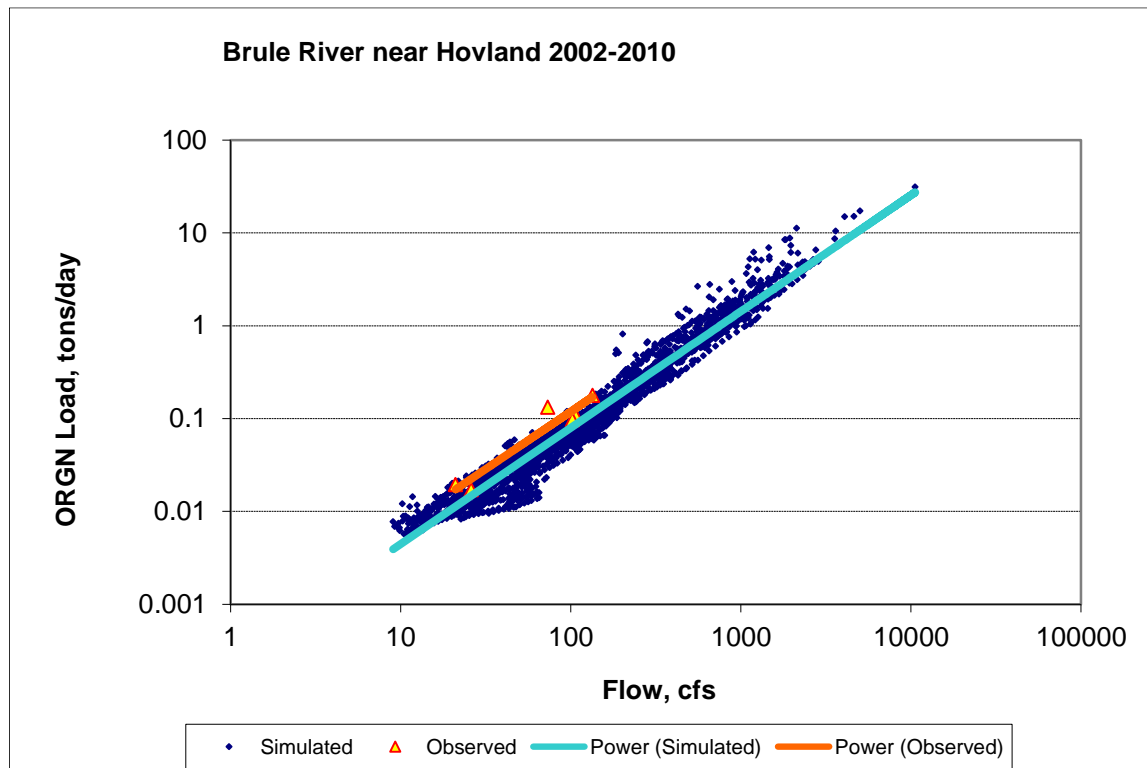


Figure 313. Power plot of simulated and observed Organic Nitrogen (OrgN) load vs flow at Brule River near Hovland (validation period)

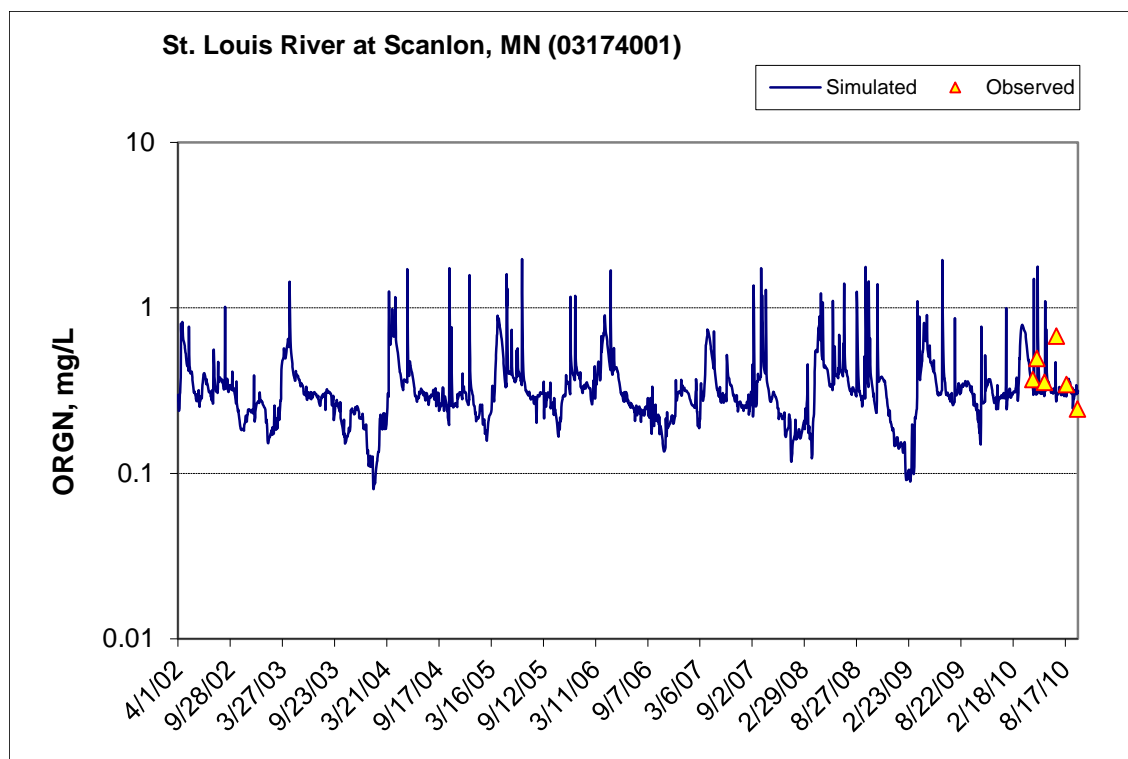


Figure 314. Time series of observed and simulated Organic Nitrogen (OrgN) concentration at Brule River near Hovland

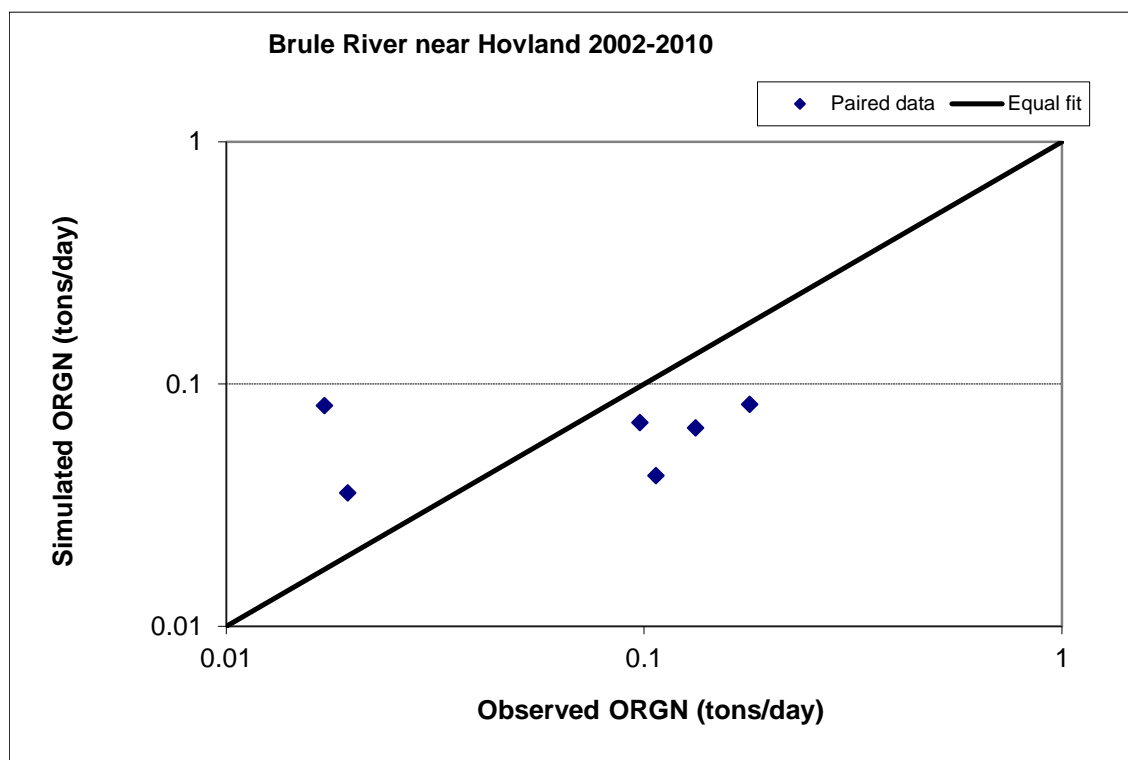


Figure 315. Paired simulated vs. observed Organic Nitrogen (OrgN) load at Brule River near Hovland (validation period)

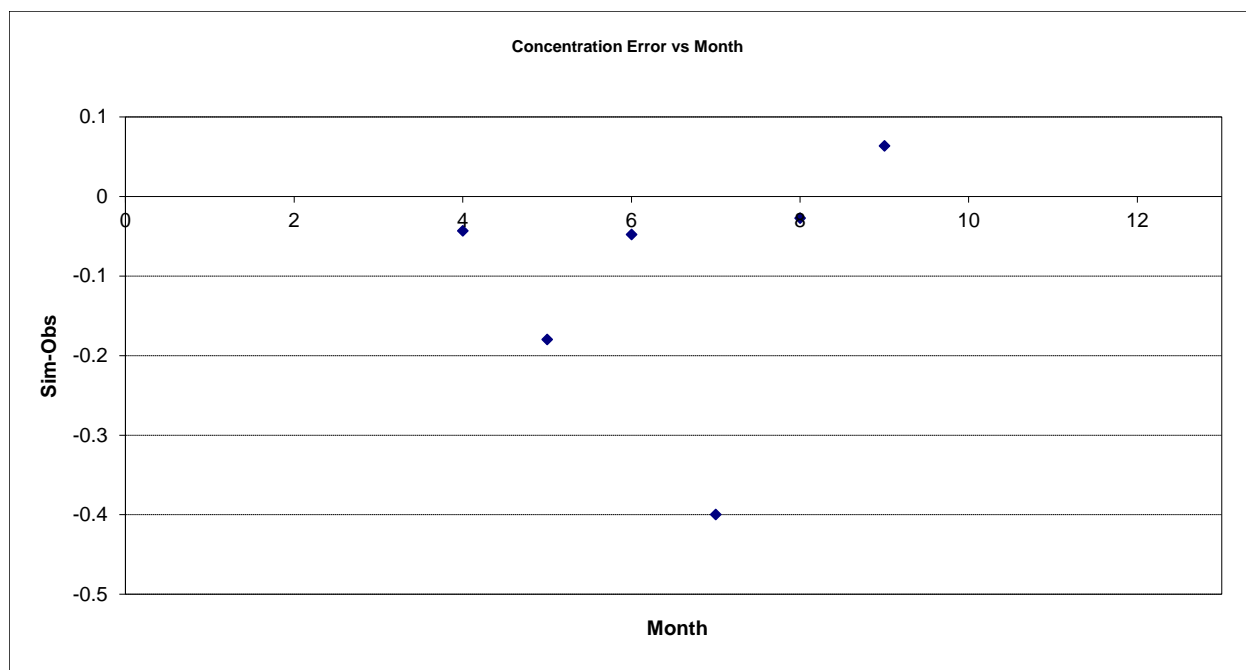


Figure 316. Residual (Simulated - Observed) vs. Month Organic Nitrogen (OrgN) at Brule River near Hovland

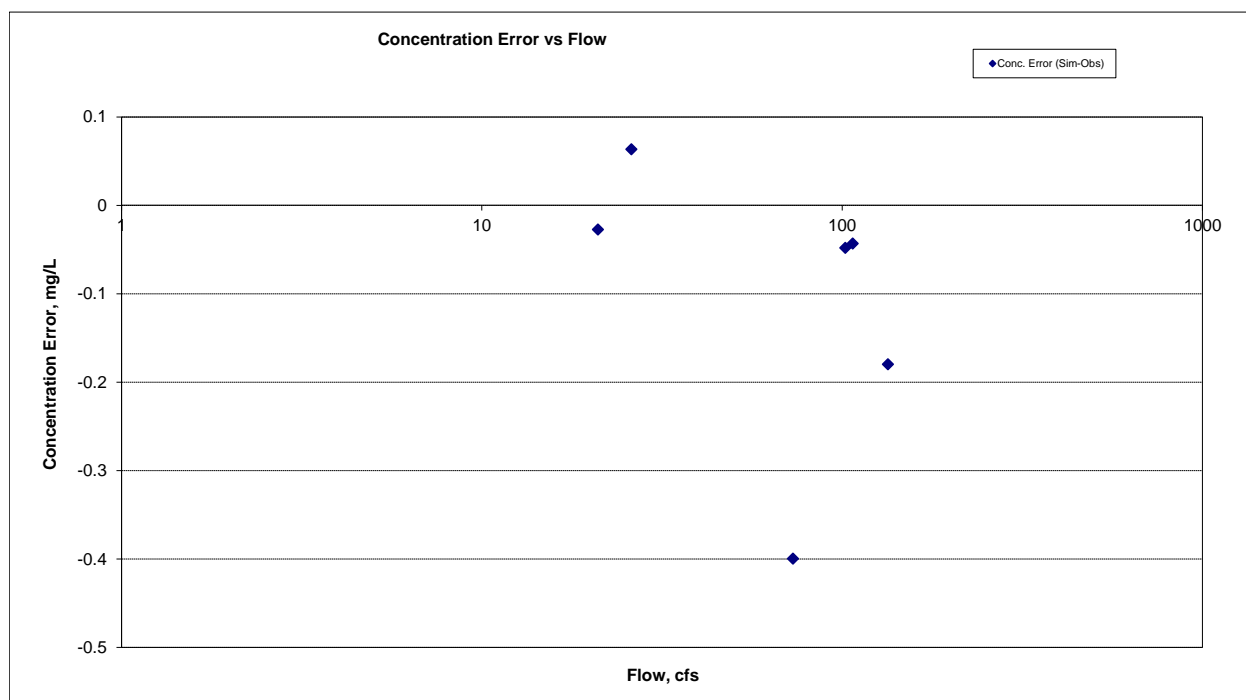


Figure 317. Residual (Simulated - Observed) vs. Flow Organic Nitrogen (OrgN) at Brule River near Hovland

Total Kjeldahl Nitrogen (TKN)

Table 62. Total Kjeldahl Nitrogen (TKN) statistics

Count	62
Concentration Average Error	6.54%
Concentration Median Error	5.26%
Load Ave Error	43.82%
Load Median Error	3.99%
Paired t concentration	0.99
Paired t load	0.11

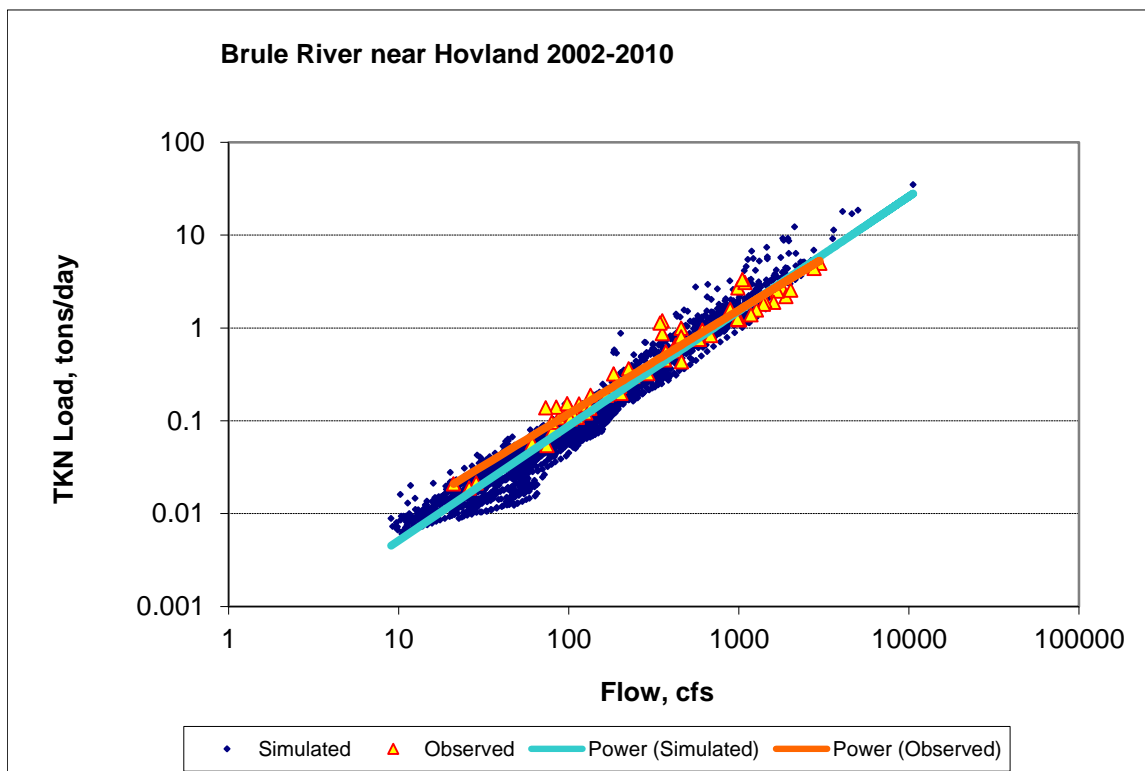


Figure 318. Power plot of simulated and observed Total Kjeldahl Nitrogen (TKN) load vs flow at Brule River near Hovland (validation period)

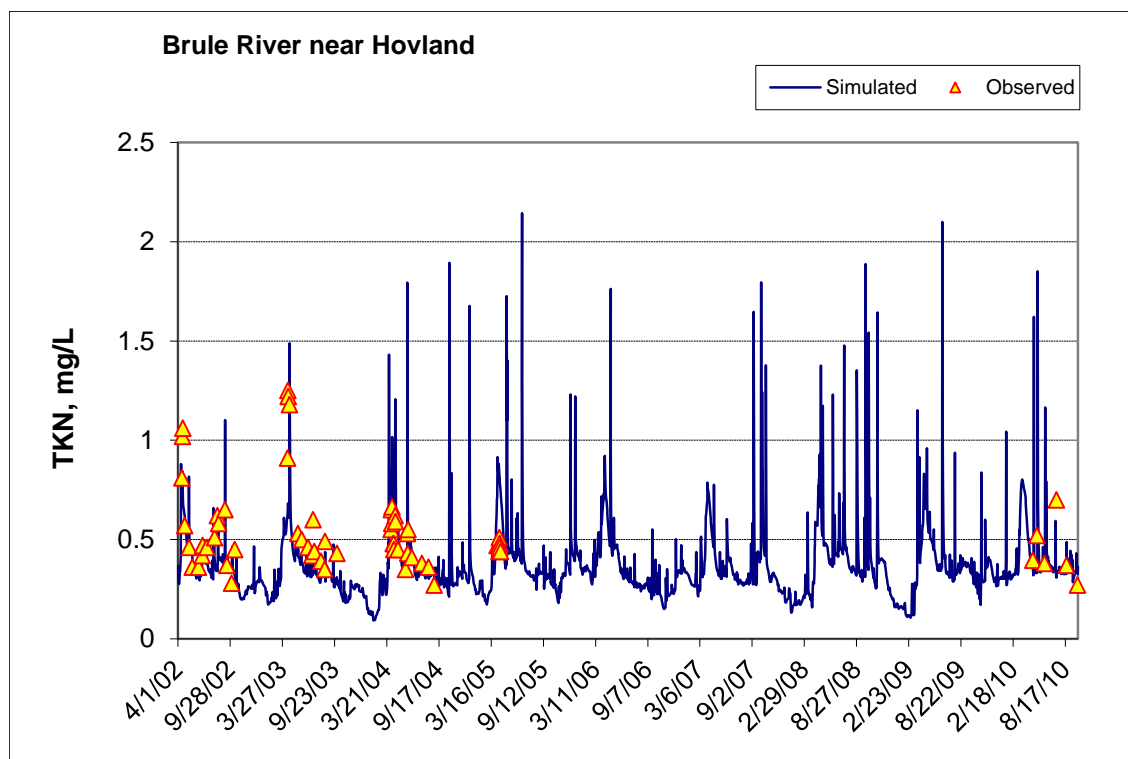


Figure 319. Time series of observed and simulated Total Kjeldahl Nitrogen (TKN) concentration at Brule River near Hovland

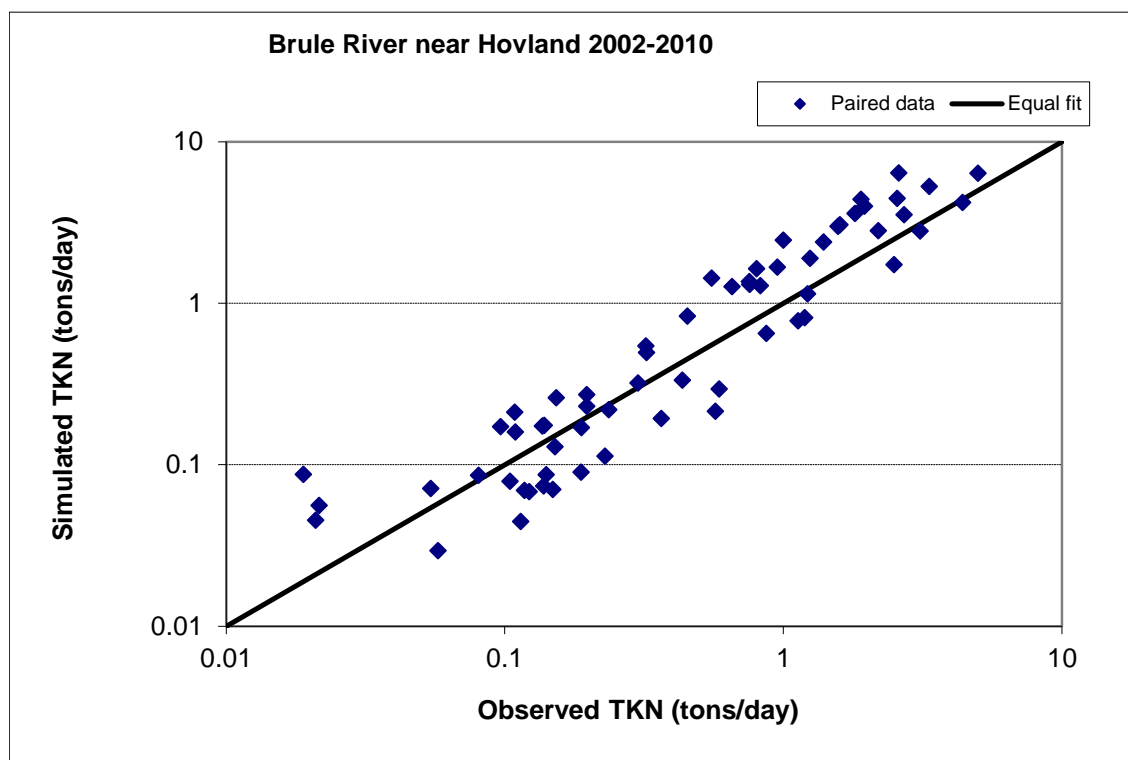


Figure 320. Paired simulated vs. observed Total Kjeldahl Nitrogen (TKN) load at Brule River near Hovland (validation period)

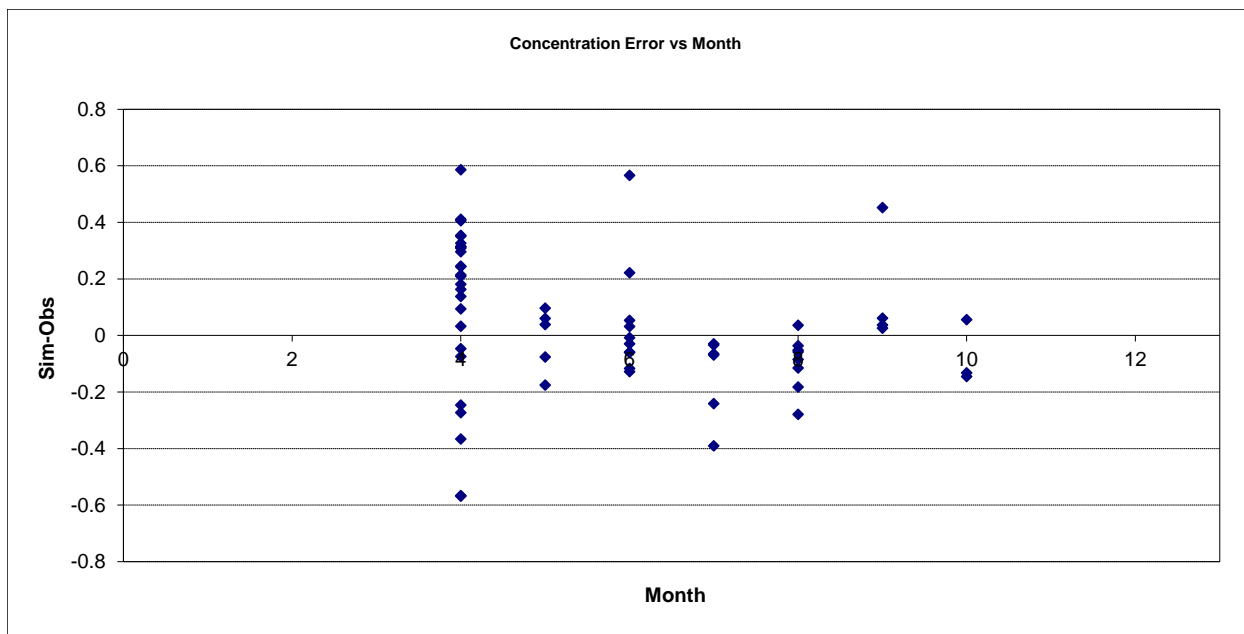


Figure 321. Residual (Simulated - Observed) vs. Month Total Kjeldahl Nitrogen (TKN) at Brule River near Hovland

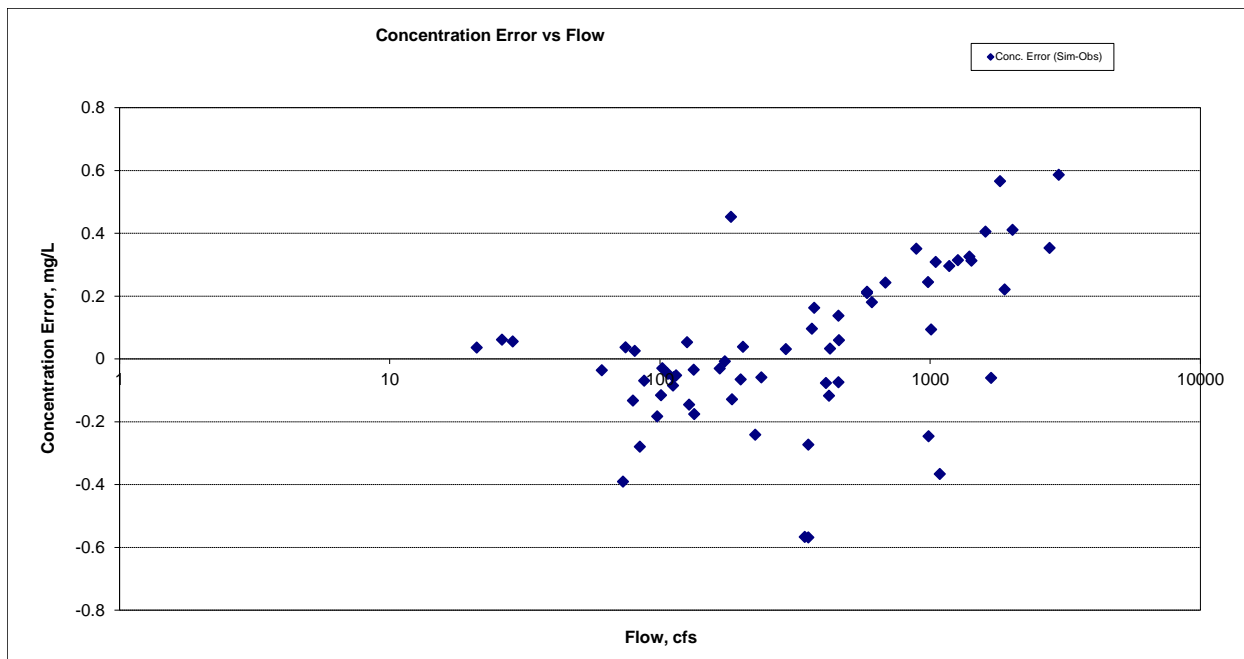


Figure 322. Residual (Simulated - Observed) vs. Flow Total Kjeldahl Nitrogen (TKN) at Brule River near Hovland

Nitrite+ Nitrate Nitrogen (NO_x)

Table 63. Nitrite+ Nitrate Nitrogen (NO_x) statistics

Count	94
-------	----

Concentration Average Error	39.58%
Concentration Median Error	54.38%
Load Ave Error	43.89%
Load Median Error	18.13%
Paired t concentration	0.01
Paired t load	0.09

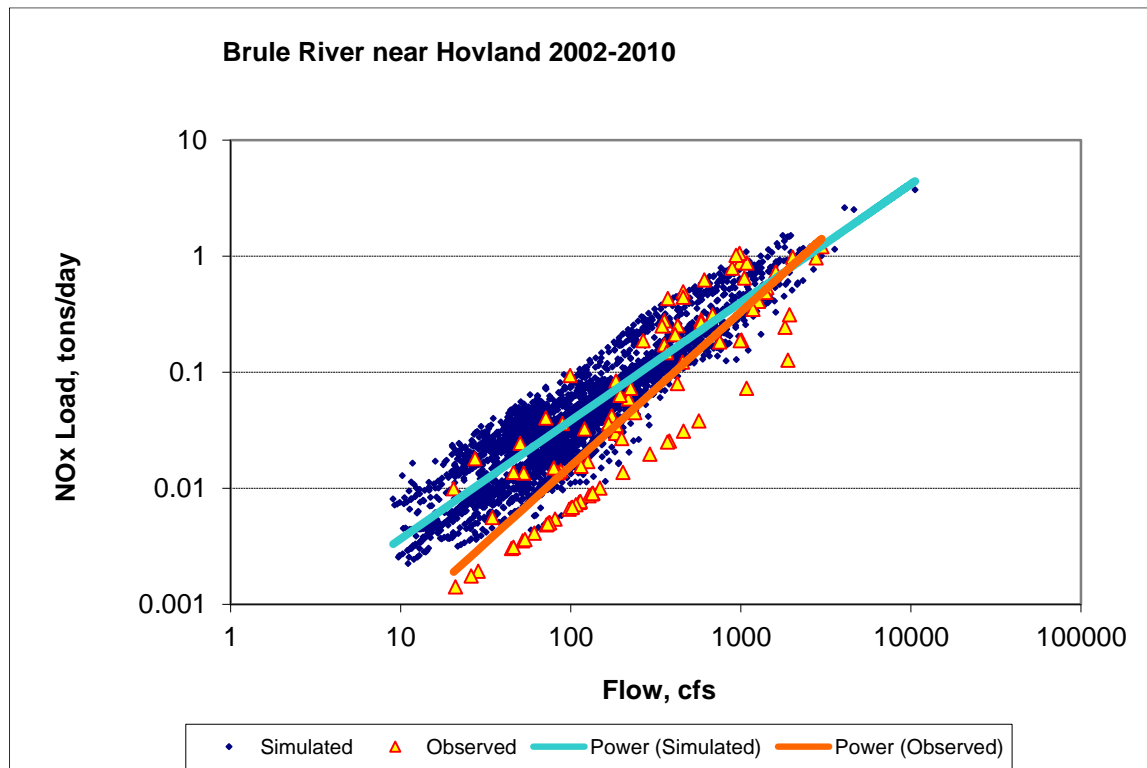


Figure 323. Power plot of simulated and observed Nitrite+ Nitrate Nitrogen (NOx) load vs flow at Brule River near Hovland (validation period)

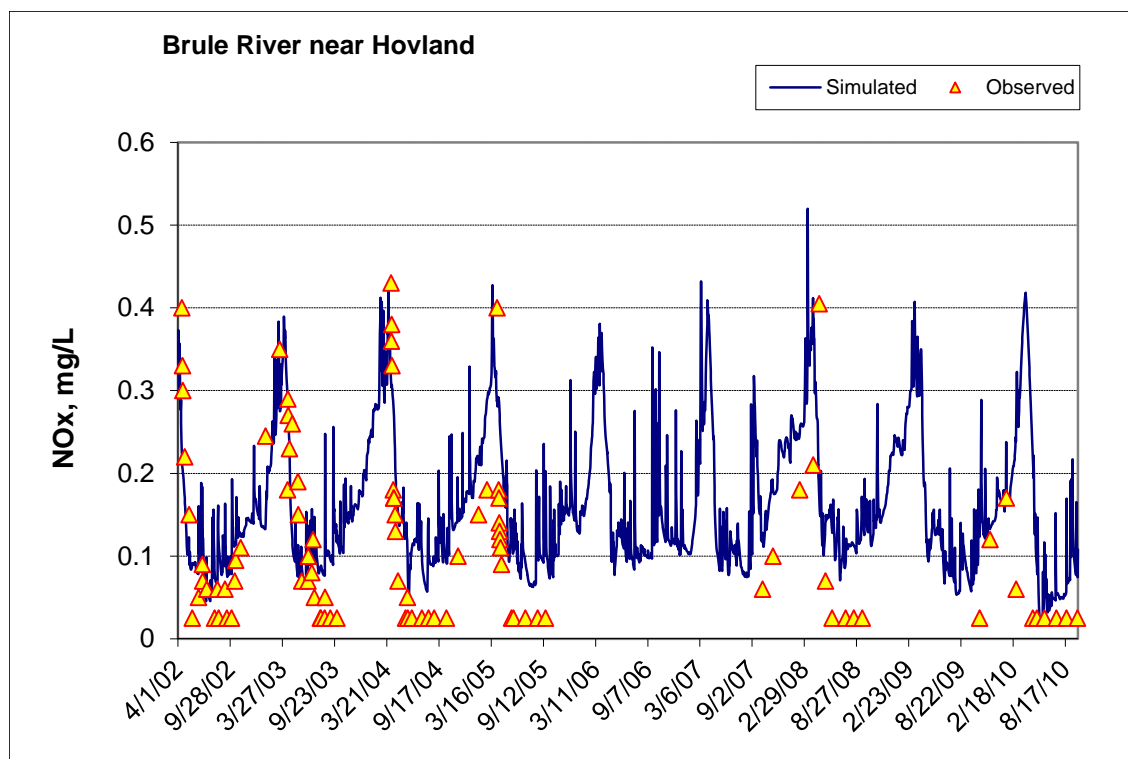


Figure 324. Time series of observed and simulated Nitrite+ Nitrate Nitrogen (NOx) concentration at Brule River near Hovland

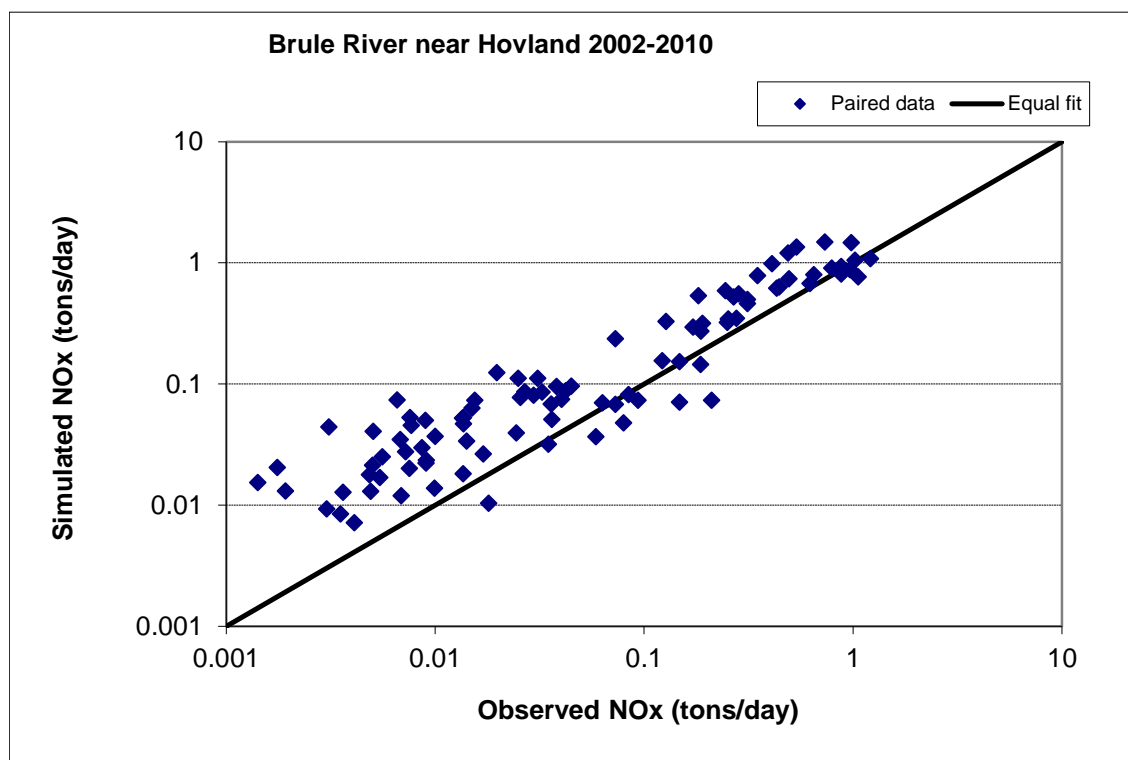


Figure 325. Paired simulated vs. observed Nitrite+ Nitrate Nitrogen (NOx) load at Brule River near Hovland (validation period)

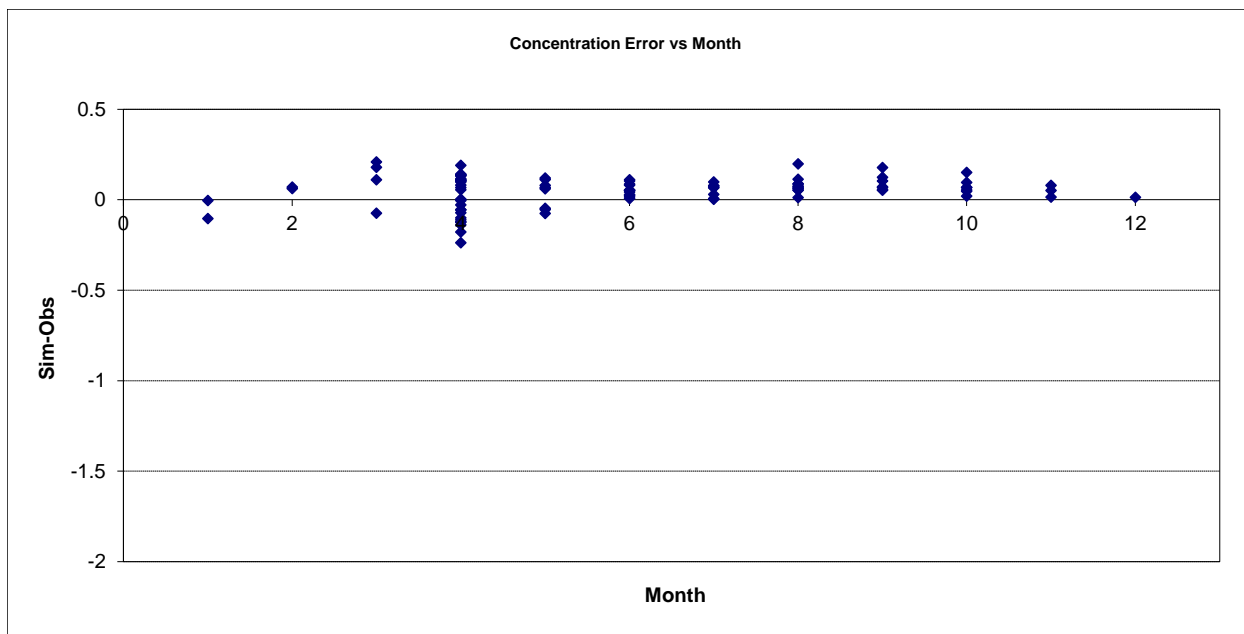


Figure 326. Residual (Simulated - Observed) vs. Month Nitrite+ Nitrate Nitrogen (NOx) at Brule River near Hovland

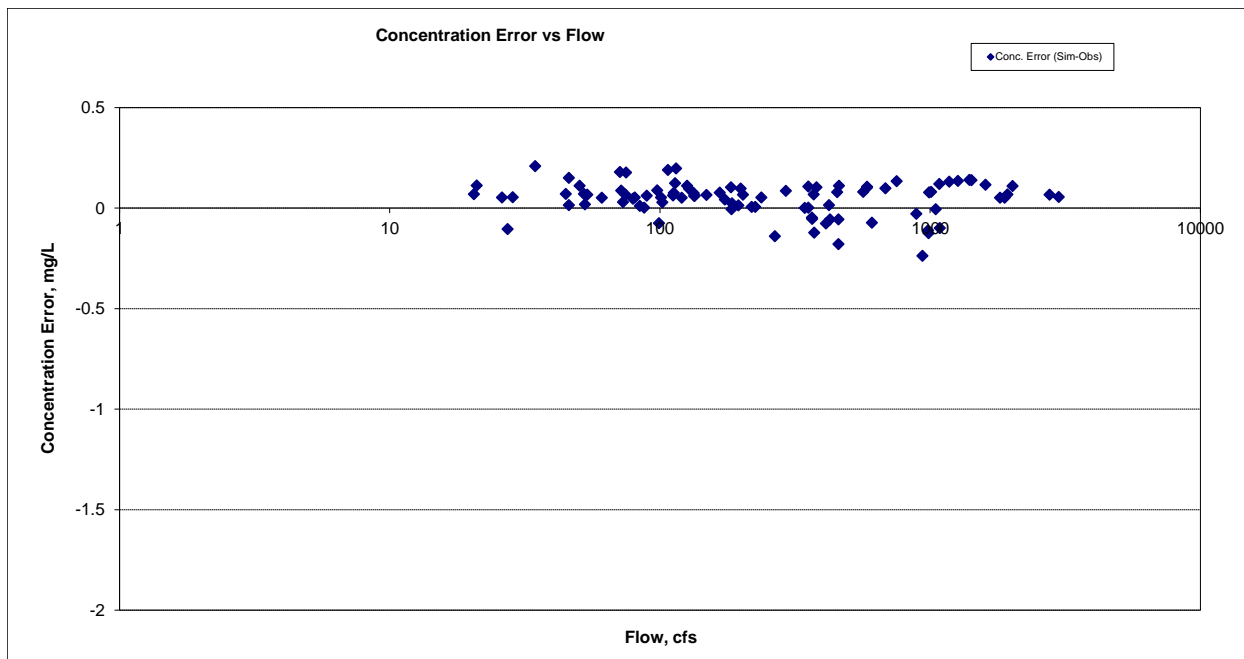


Figure 327. Residual (Simulated - Observed) vs. Flow Nitrite+ Nitrate Nitrogen (NOx) at Brule River near Hovland

Total Nitrogen (TN)

Table 64. Total Nitrogen (TN) statistics

Count	61
-------	----

Concentration Average Error	12.23%
Concentration Median Error	11.80%
Load Ave Error	46.50%
Load Median Error	6.81%
Paired t concentration	0.90
Paired t load	0.09

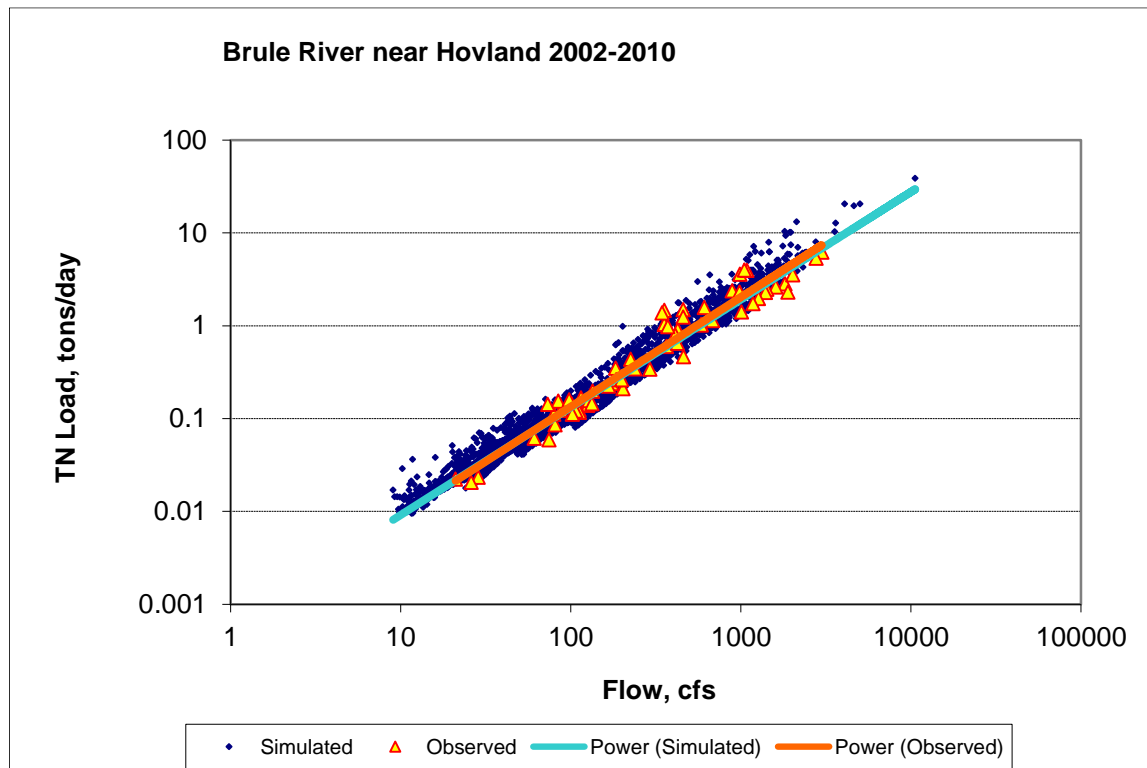


Figure 328. Power plot of simulated and observed Total Nitrogen (TN) load vs flow at Brule River near Hovland (validation period)

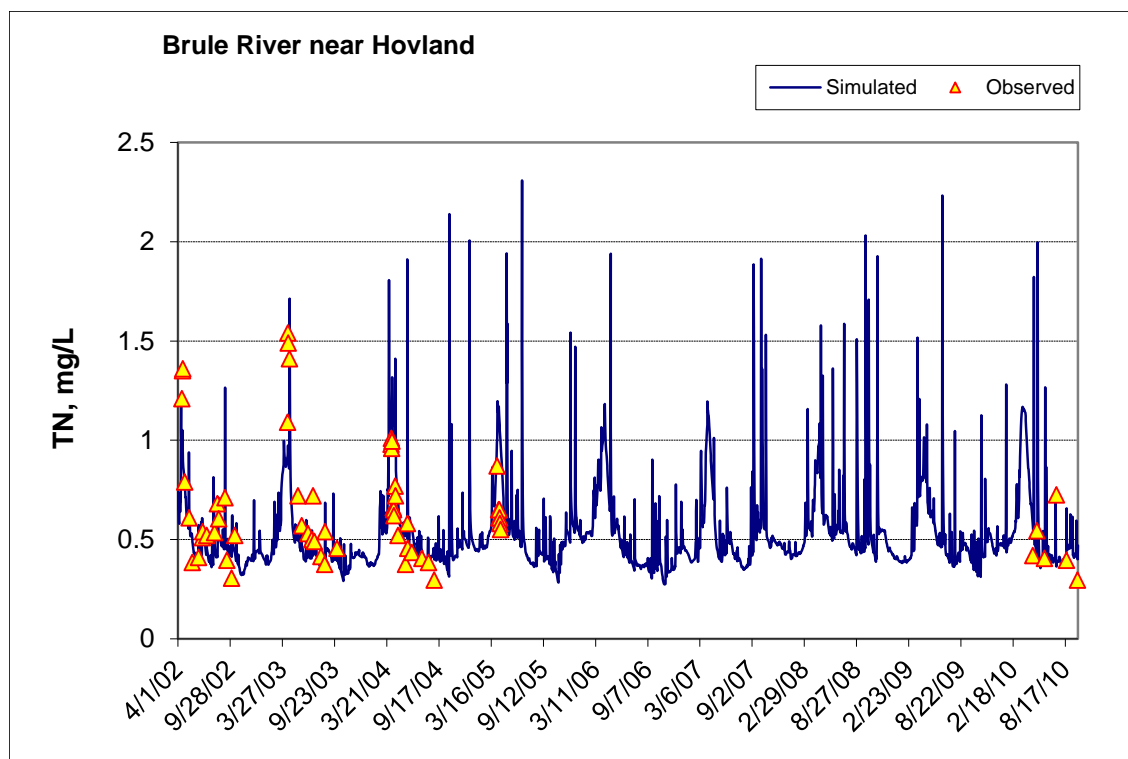


Figure 329. Time series of observed and simulated Total Nitrogen (TN) concentration at Brule River near Hovland

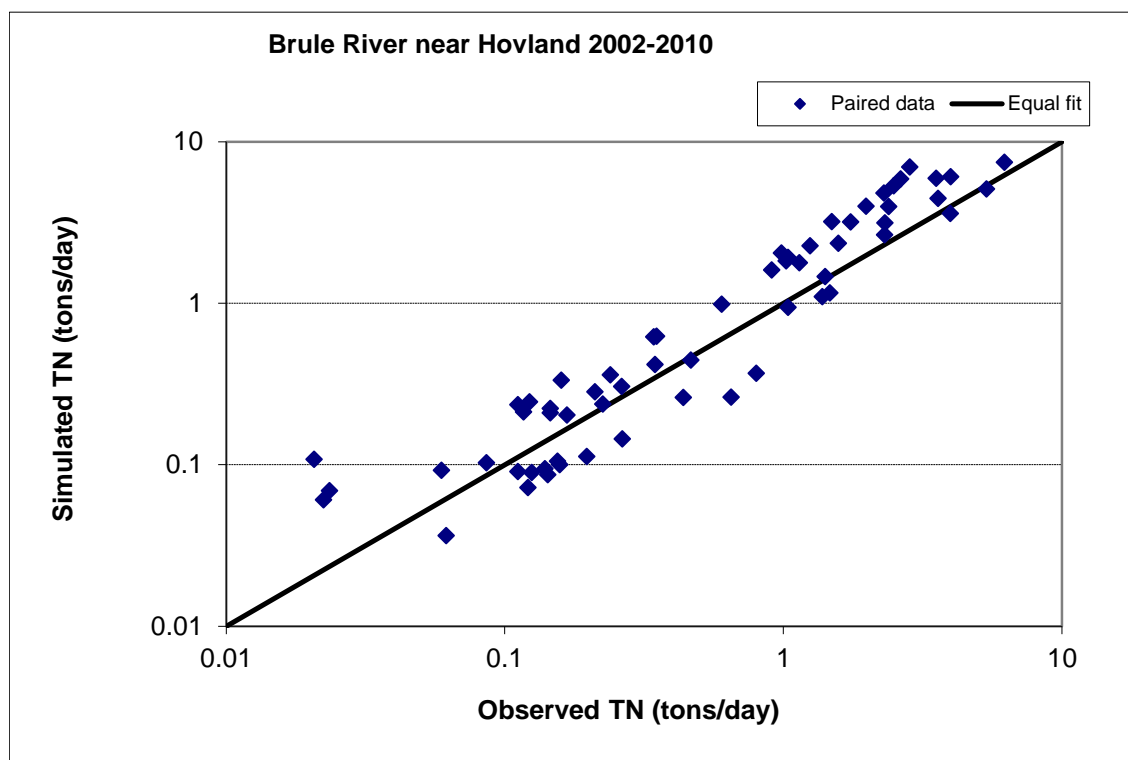


Figure 330. Paired simulated vs. observed Total Nitrogen (TN) load at Brule River near Hovland (validation period)

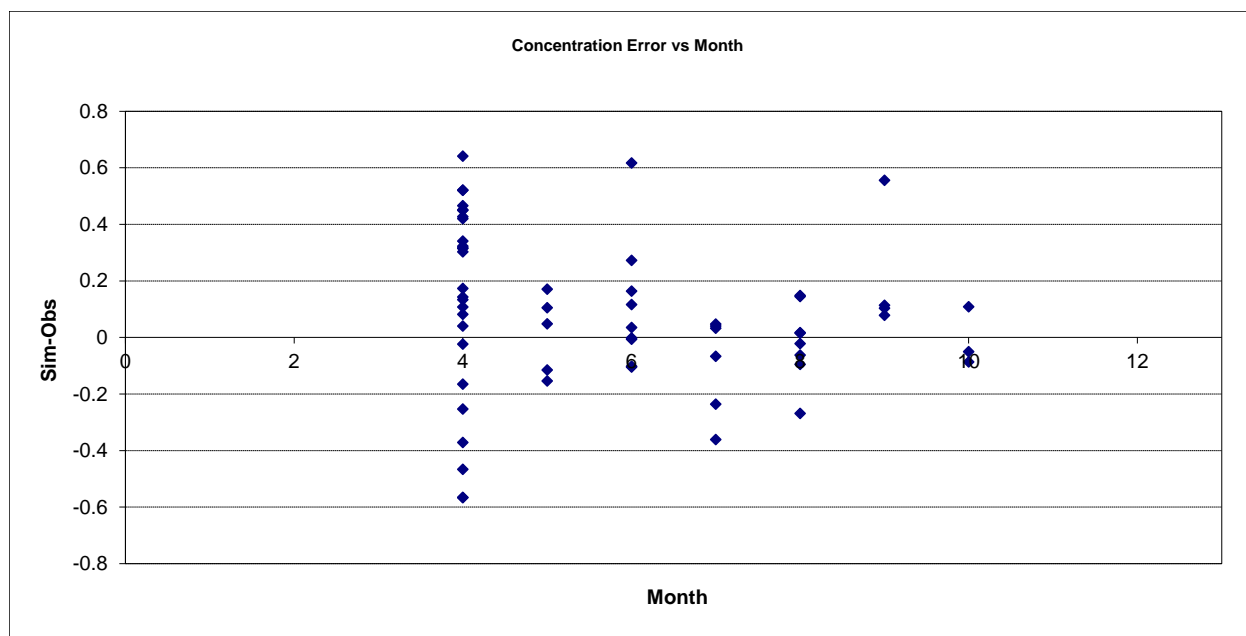


Figure 331. Residual (Simulated - Observed) vs. Month Total Nitrogen (TN) at Brule River near Hovland

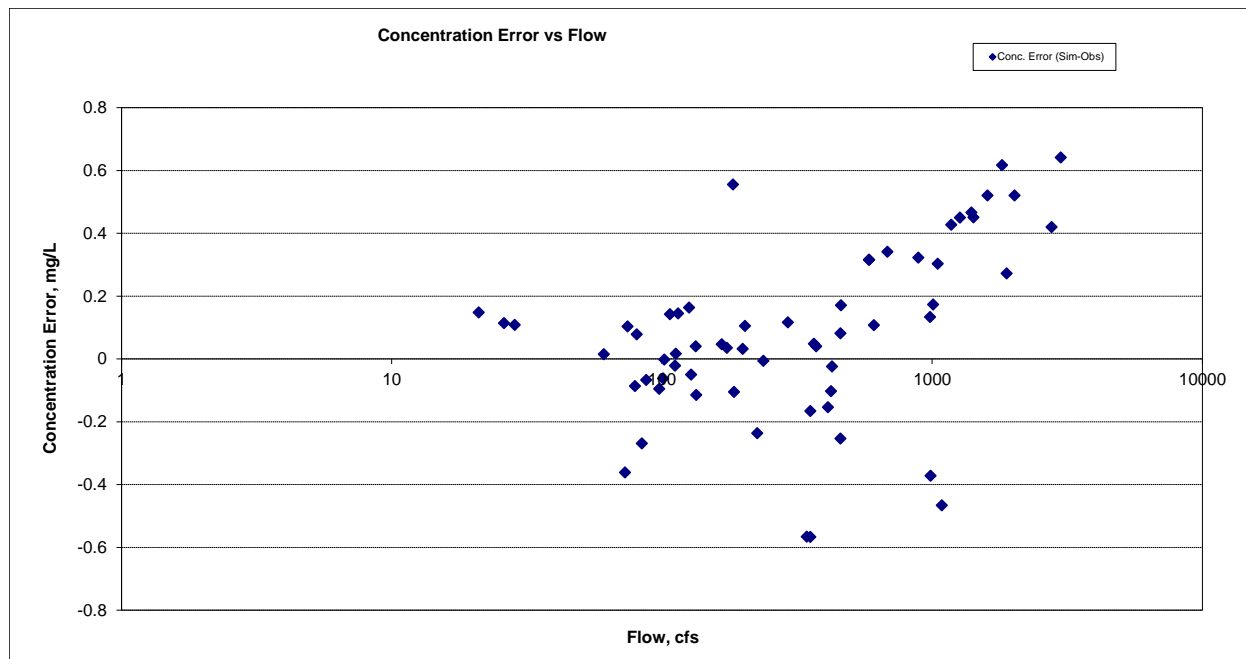


Figure 332. Residual (Simulated - Observed) vs. Flow Total Nitrogen (TN) at Brule River near Hovland

Soluble Reactive Phosphorus (SRP)

Table 65. Soluble Reactive Phosphorus (SRP) statistics

Count	48
-------	----

Concentration Average Error	36.07%
Concentration Median Error	8.41%
Load Ave Error	108.66%
Load Median Error	12.17%
Paired t concentration	0.06
Paired t load	0.01

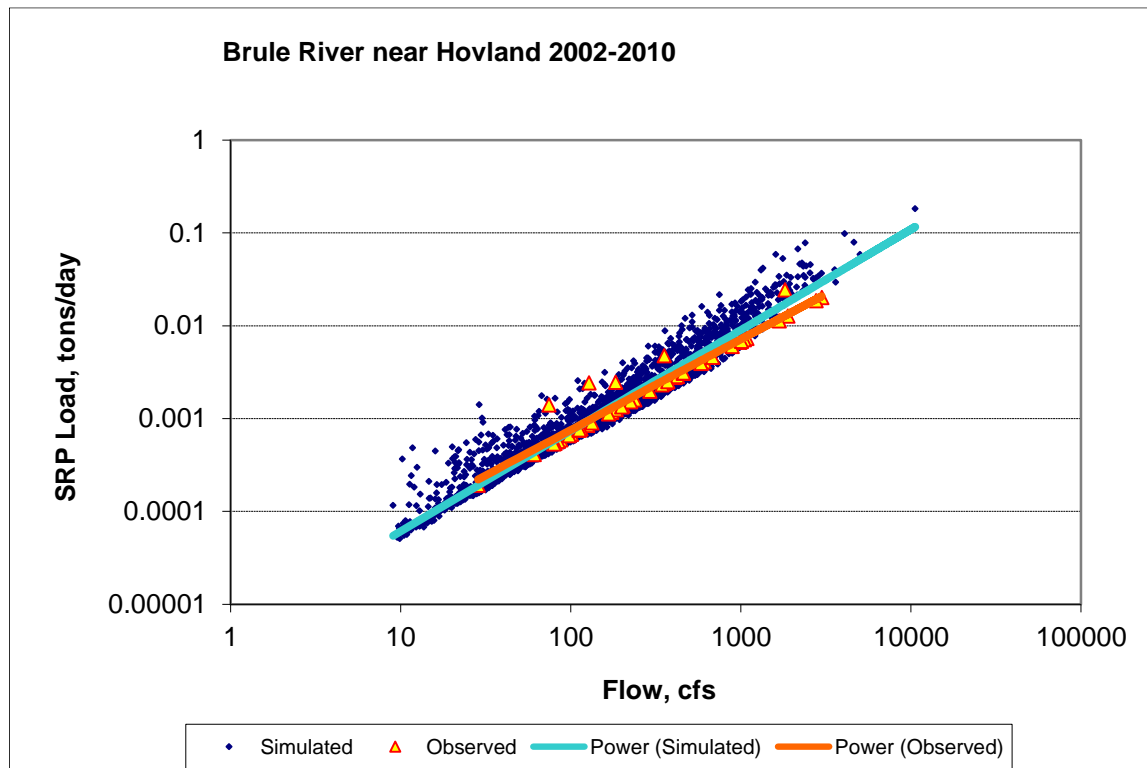


Figure 333. Power plot of simulated and observed Soluble Reactive Phosphorus (SRP) load vs flow at Brule River near Hovland (validation period)

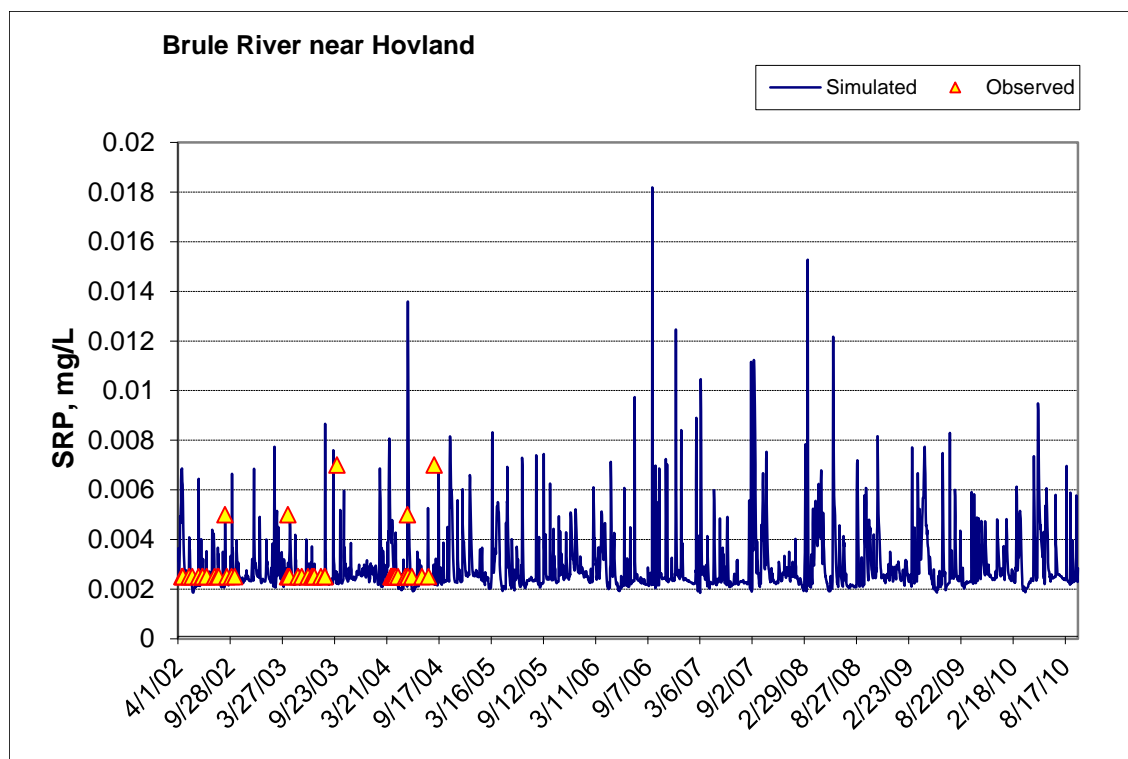


Figure 334. Time series of observed and simulated Soluble Reactive Phosphorus (SRP) concentration at Brule River near Hovland

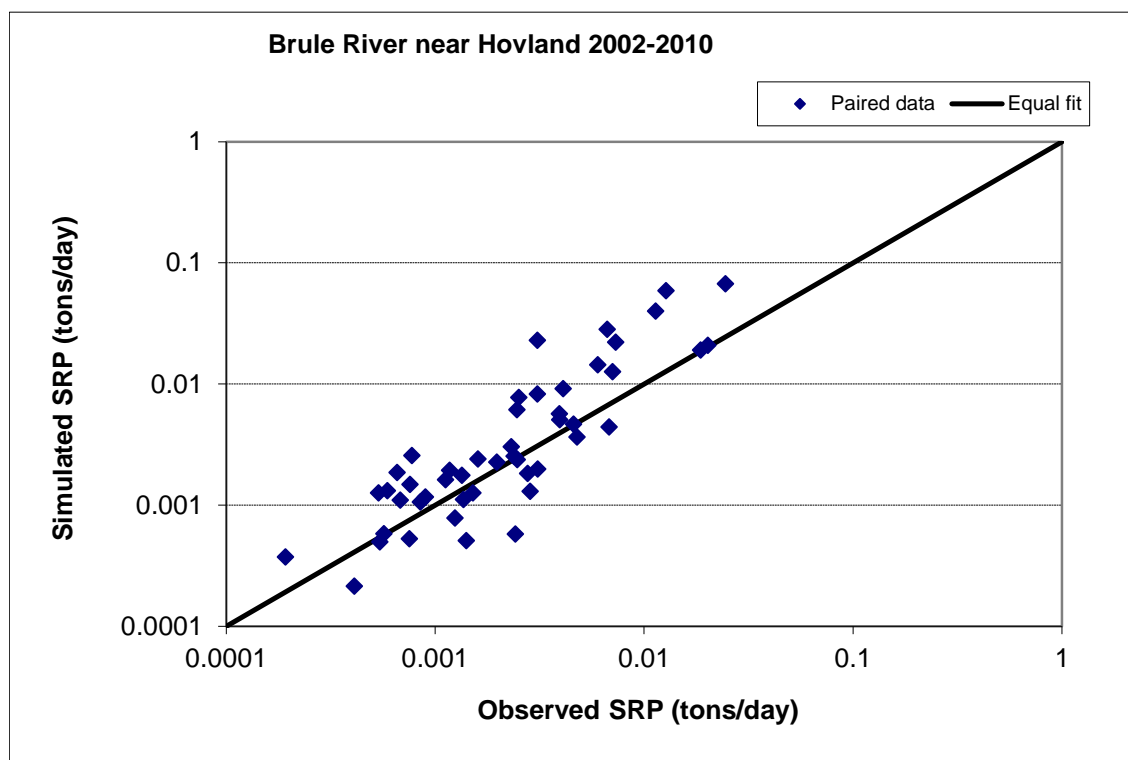


Figure 335. Paired simulated vs. observed Soluble Reactive Phosphorus (SRP) load at Brule River near Hovland (validation period)

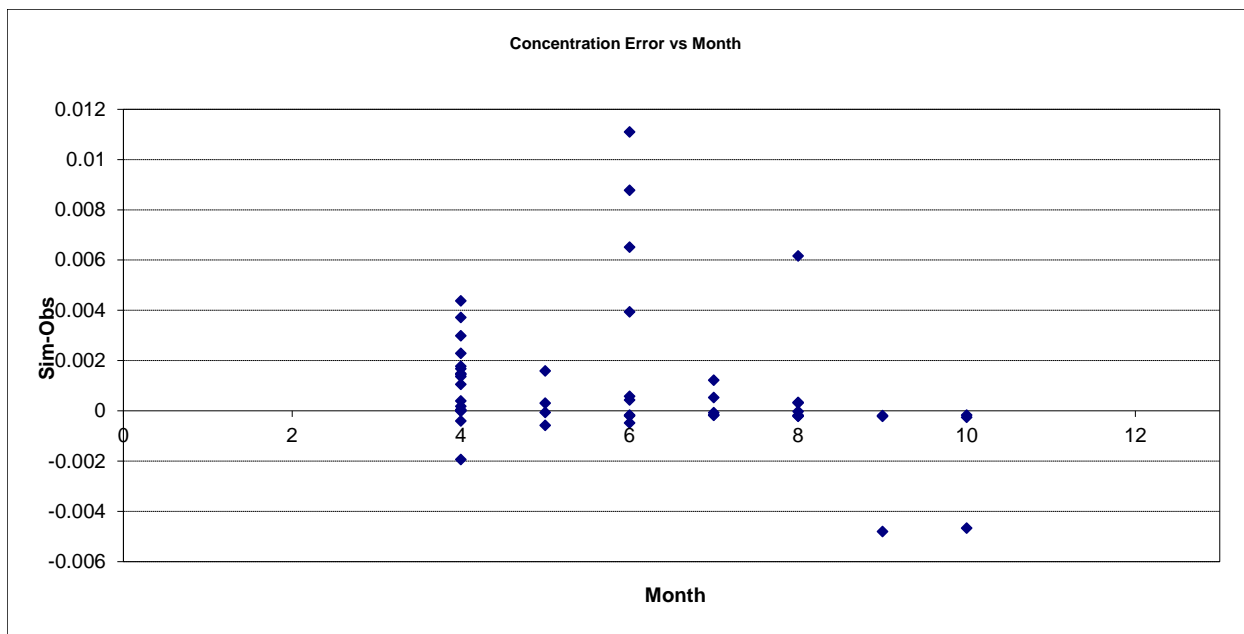


Figure 336. Residual (Simulated - Observed) vs. Month Soluble Reactive Phosphorus (SRP) at Brule River near Hovland

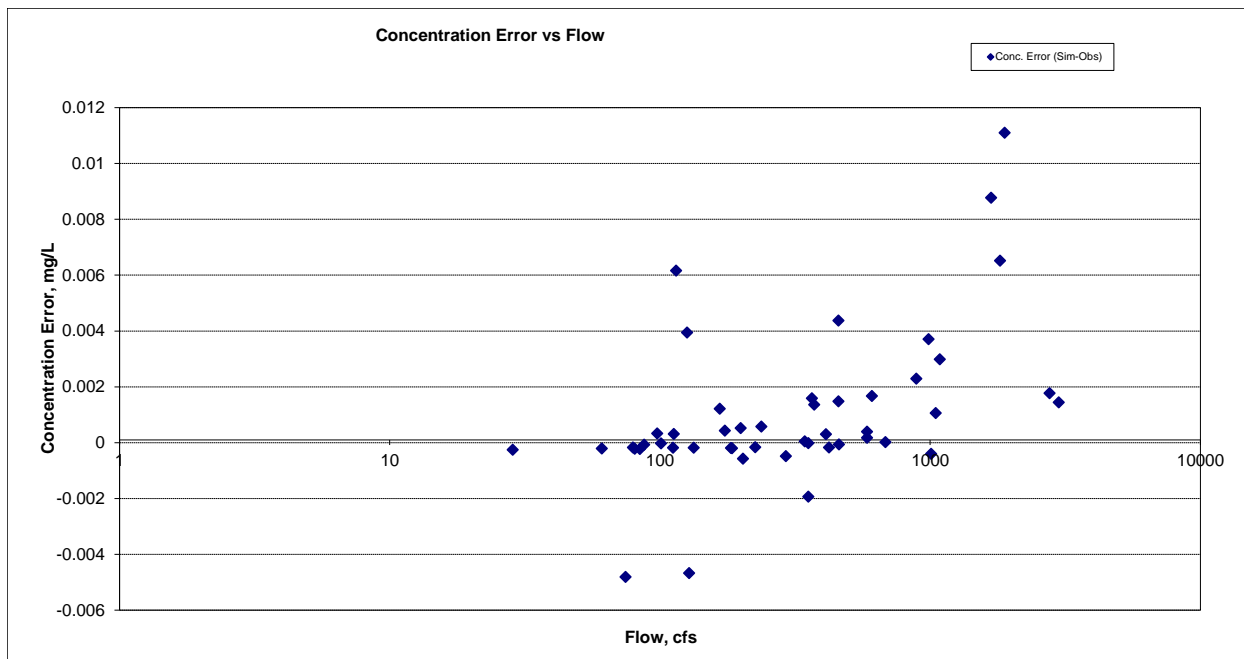


Figure 337. Residual (Simulated - Observed) vs. Flow Soluble Reactive Phosphorus (SRP) at Brule River near Hovland

Organic Phosphorus (OrgP)

Table 66. Organic Phosphorus (OrgP) statistics

Count	47
-------	----

Concentration Average Error	-25.14%
Concentration Median Error	-10.09%
Load Ave Error	-4.02%
Load Median Error	-1.74%
Paired t concentration	0.33
Paired t load	0.74

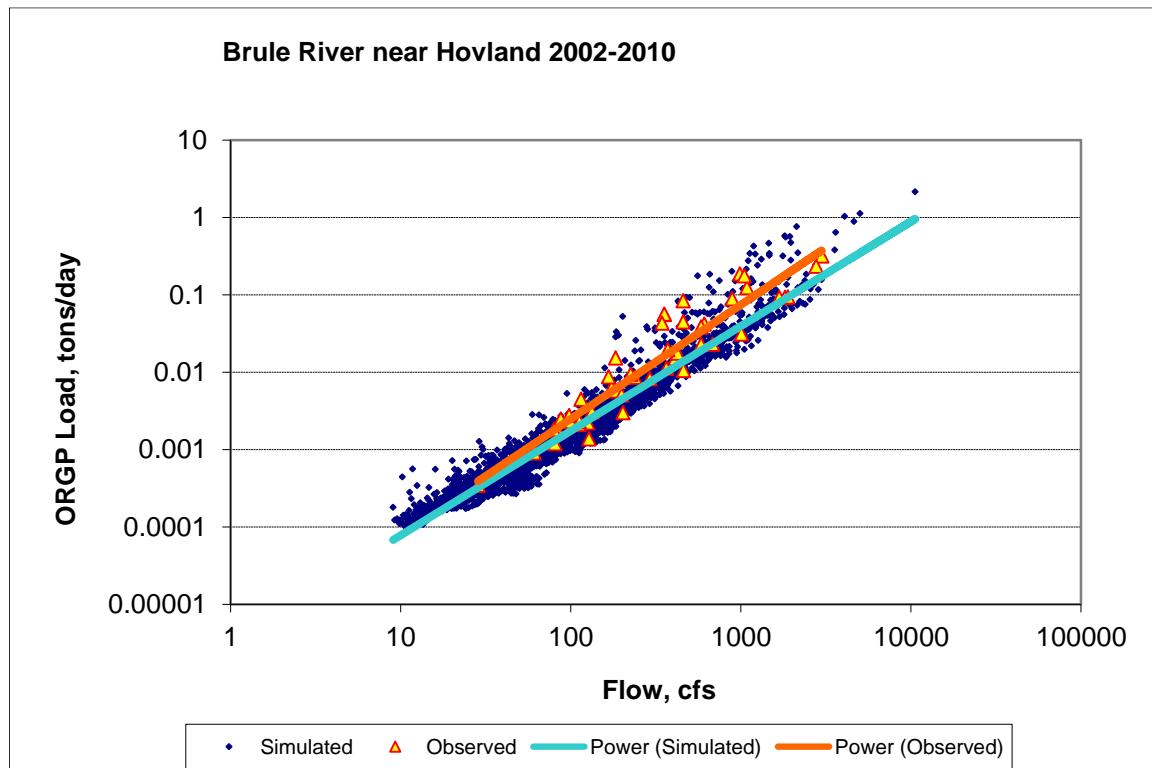


Figure 338. Power plot of simulated and observed Organic Phosphorus (OrgP) load vs flow at Brule River near Hovland (validation period)

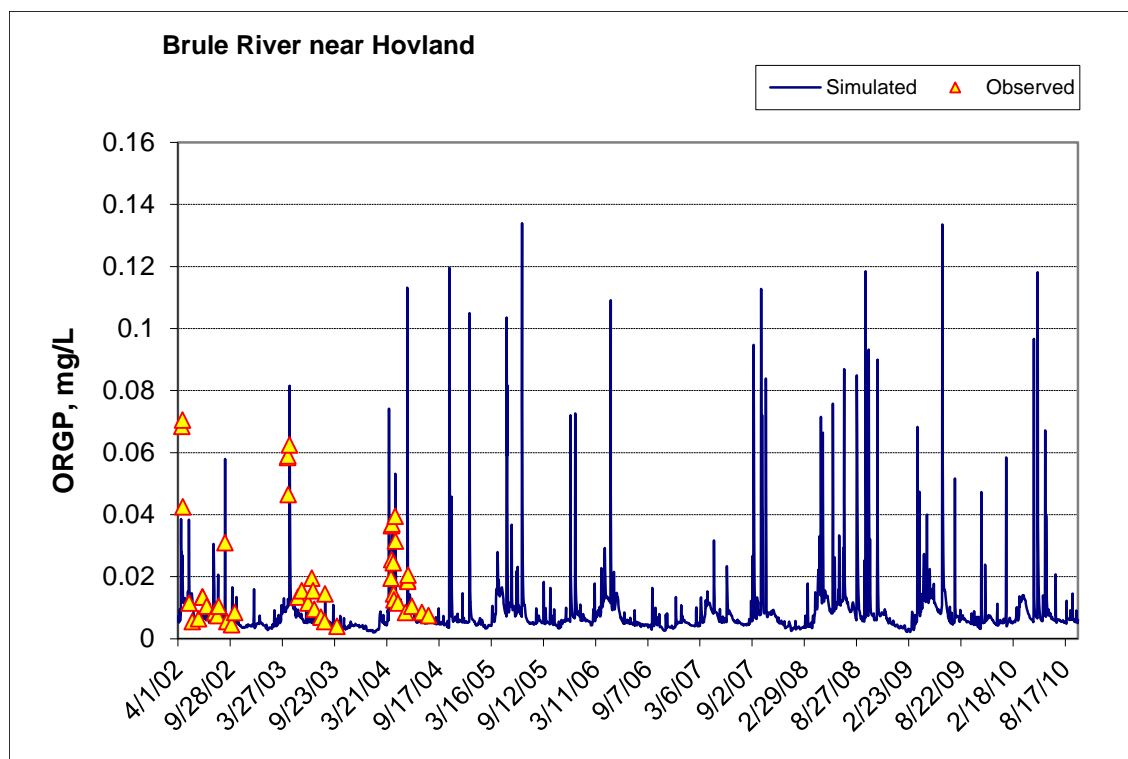


Figure 339. Time series of observed and simulated Organic Phosphorus (OrgP) concentration at Brule River near Hovland

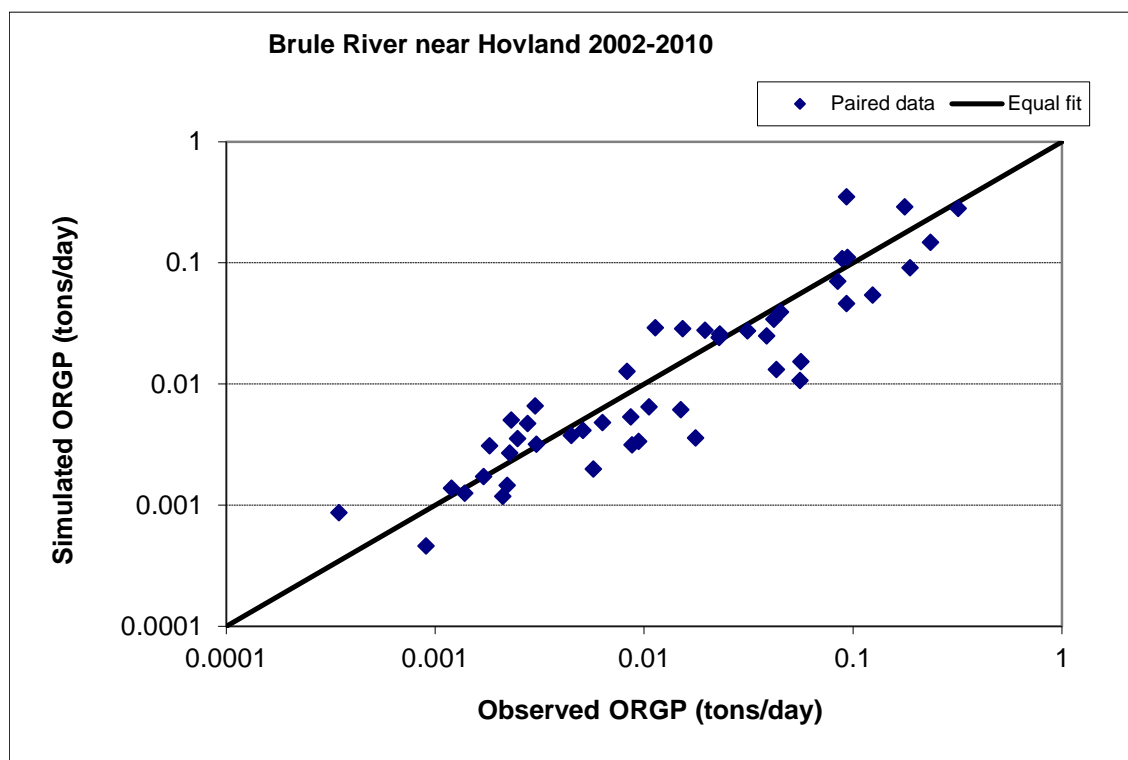


Figure 340. Paired simulated vs. observed Organic Phosphorus (OrgP) load at Brule River near Hovland (validation period)

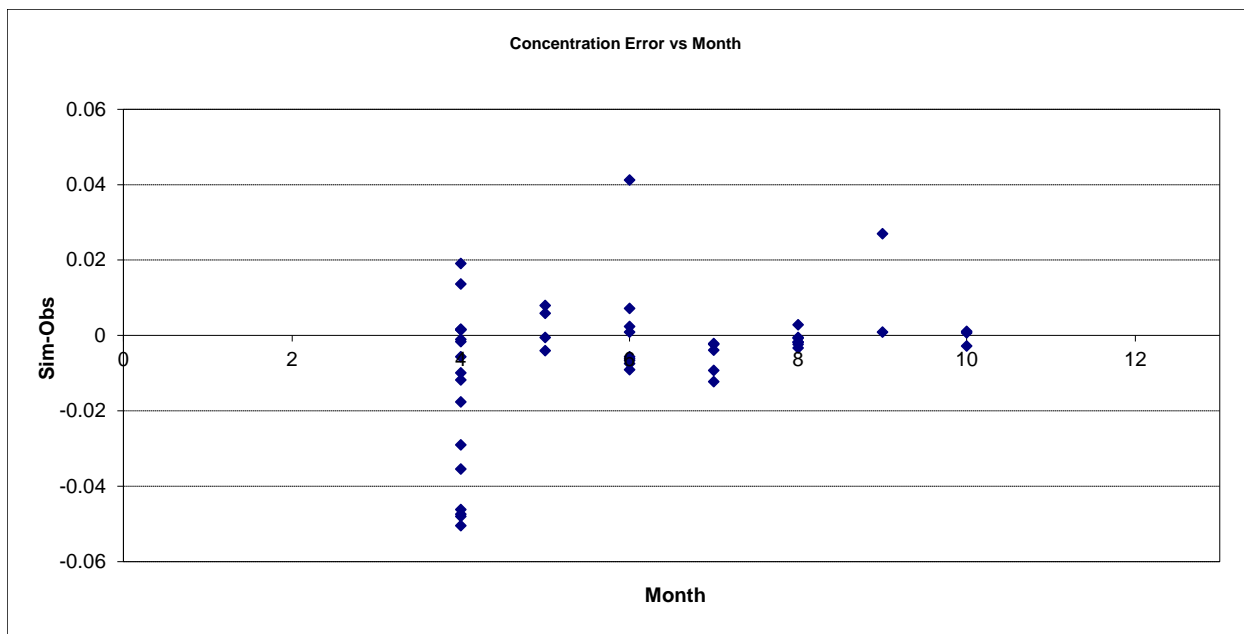


Figure 341. Residual (Simulated - Observed) vs. Month Organic Phosphorus (OrgP) at Brule River near Hovland

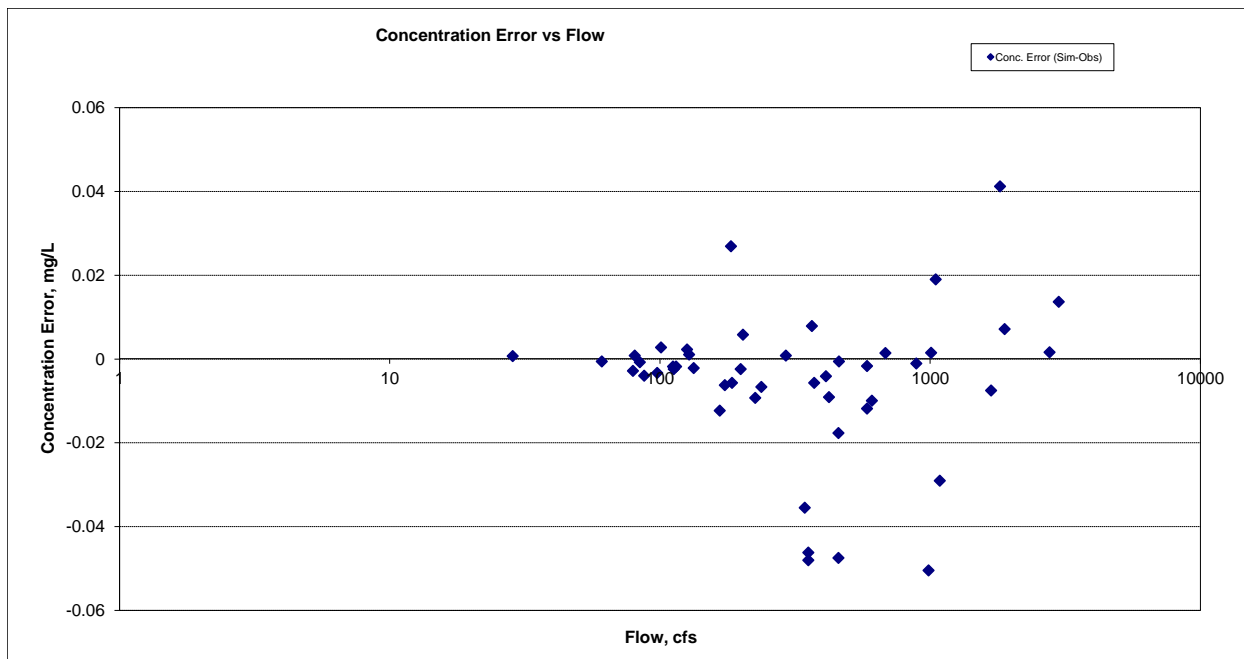


Figure 342. Residual (Simulated - Observed) vs. Flow Organic Phosphorus (OrgP) at Brule River near Hovland

Total Phosphorus (TP)

Table 67. Total Phosphorus (TP) statistics

Count	131
-------	-----

Concentration Average Error	-11.45%
Concentration Median Error	-12.24%
Load Ave Error	10.40%
Load Median Error	-2.37%
Paired t concentration	0.88
Paired t load	0.68

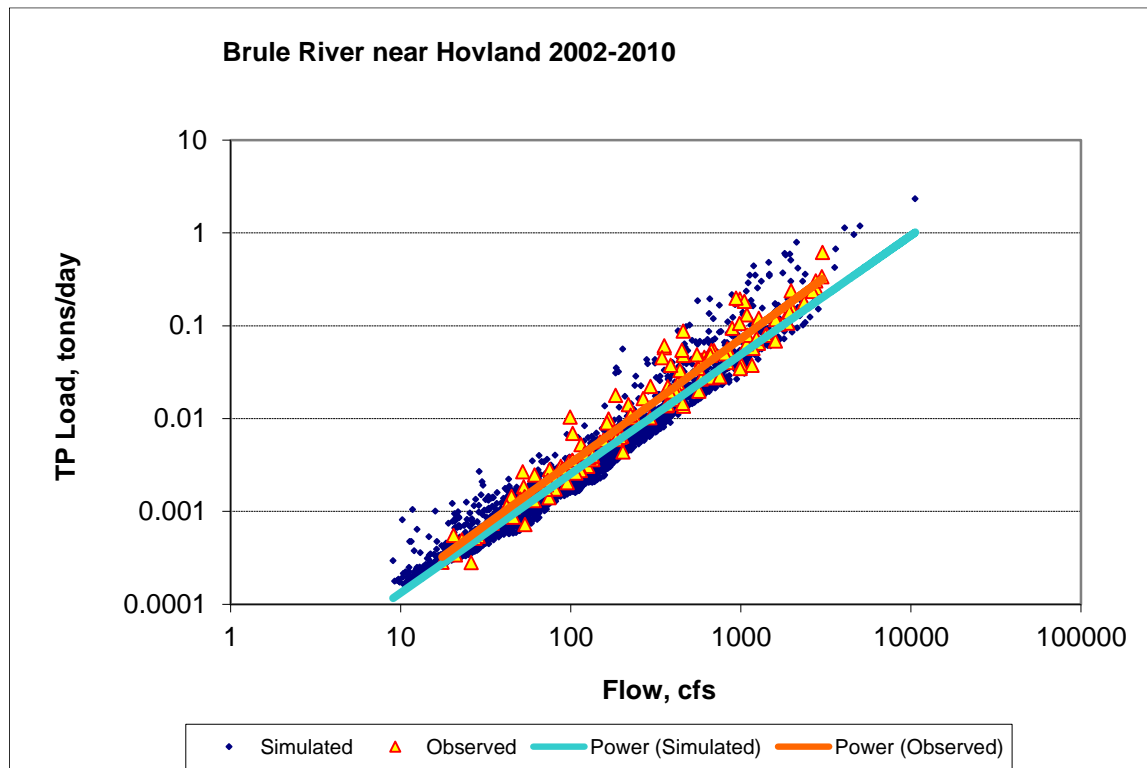


Figure 343. Power plot of simulated and observed Total Phosphorus (TP) load vs flow at Brule River near Hovland (validation period)

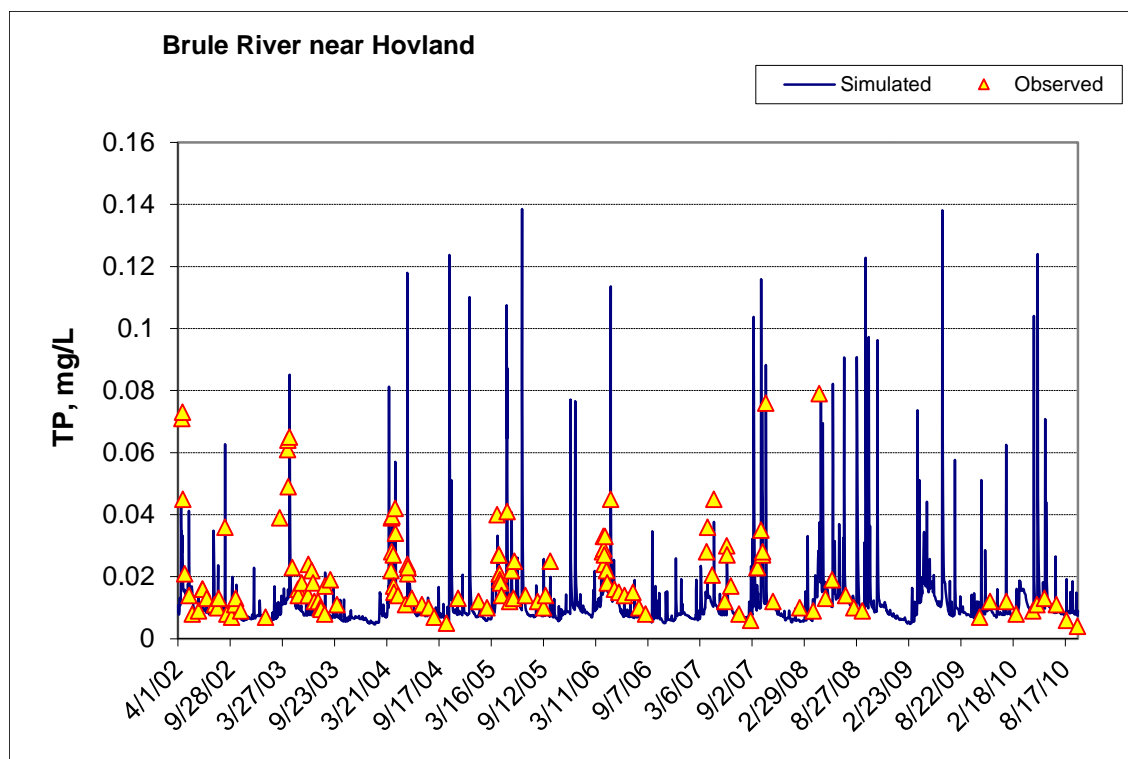


Figure 344. Time series of observed and simulated Total Phosphorus (TP) concentration at Brule River near Hovland

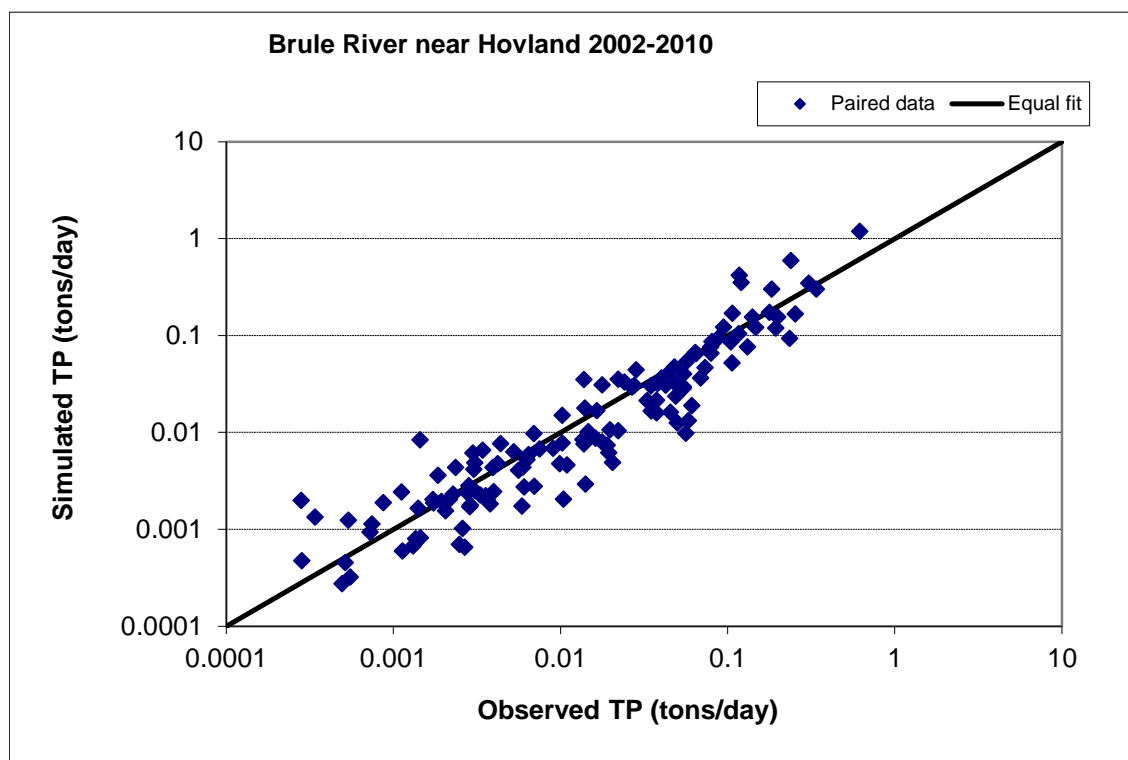


Figure 345. Paired simulated vs. observed Total Phosphorus (TP) load at Brule River near Hovland (validation period)

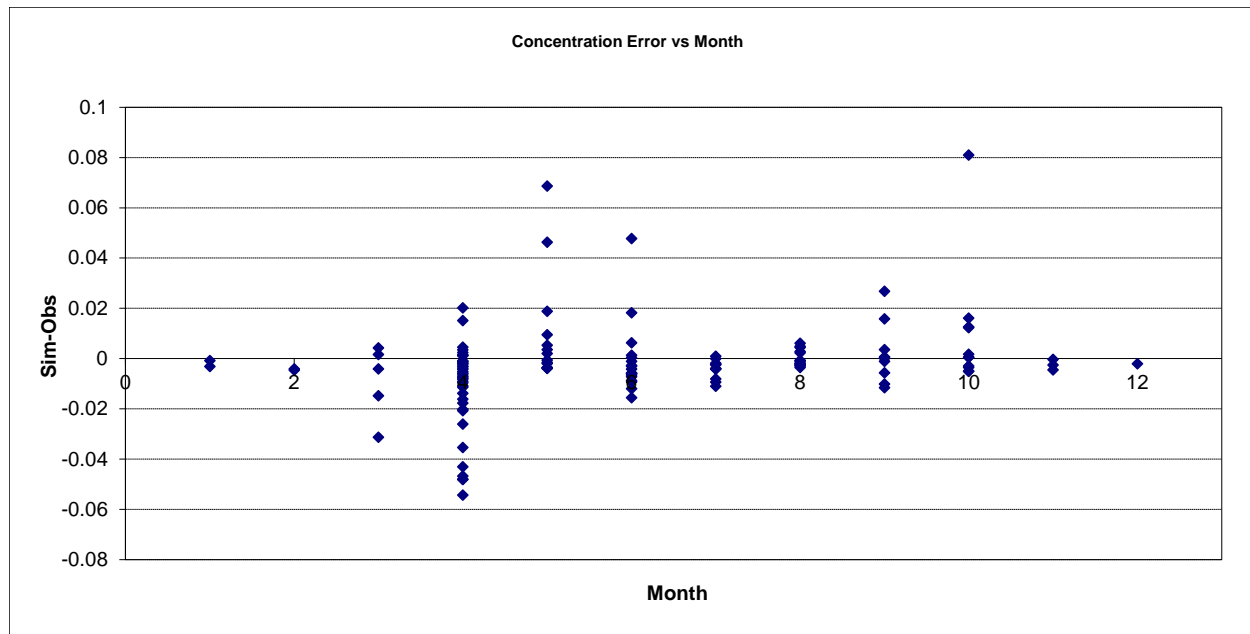


Figure 346. Residual (Simulated - Observed) vs. Month Total Phosphorus (TP) at Brule River near Hovland

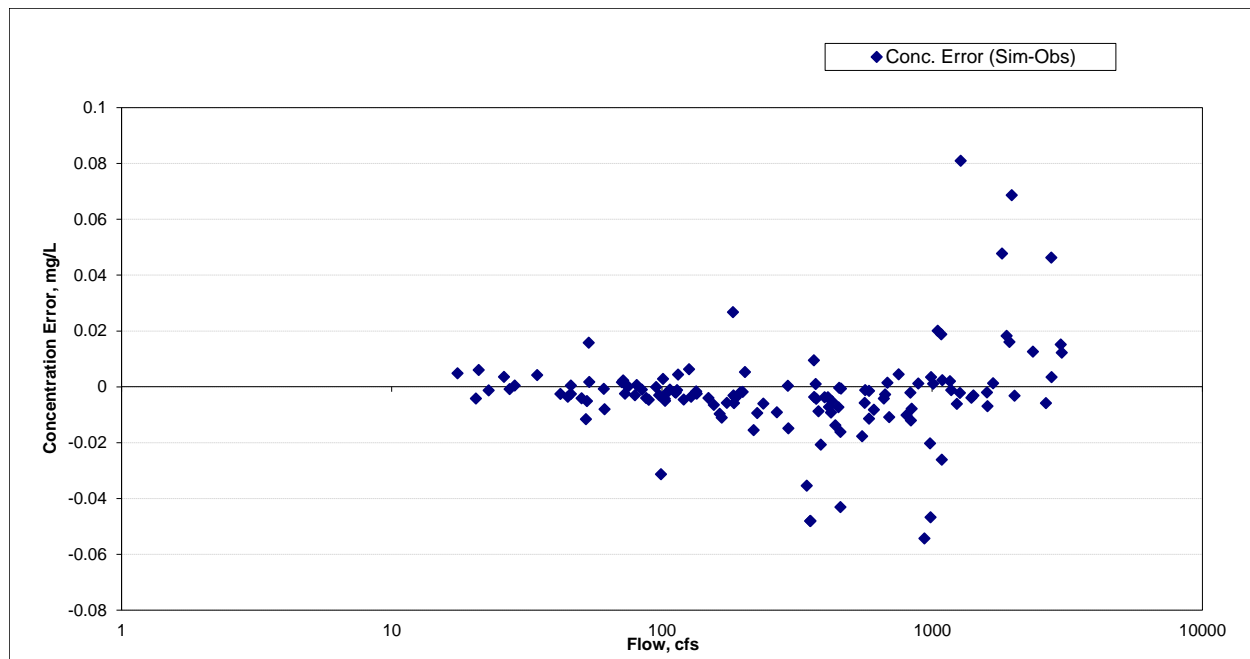


Figure 347. Residual (Simulated - Observed) vs. Flow Total Phosphorus (TP) at Brule River near Hovland

Caribou River (EQUIS S004-954)

Total Suspended Solids (TSS)

Table 68. Total Suspended Solids (TSS) statistics

Count	20
Concentration Average Error	-80.05%
Concentration Median Error	-24.21%
Load Ave Error	-77.45%
Load Median Error	-1.46%
Paired t concentration	0.04
Paired t load	0.18

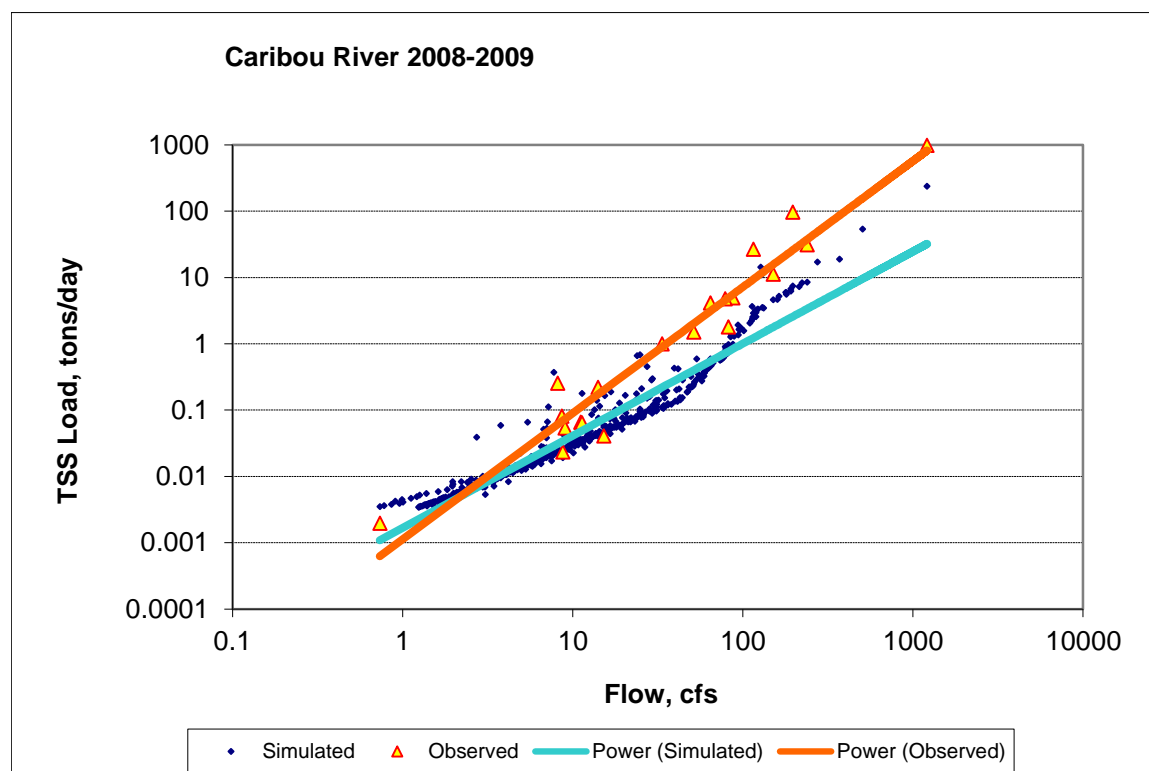


Figure 348. Power plot of simulated and observed Total Suspended Solids (TSS) load vs flow at Caribou River (validation period)

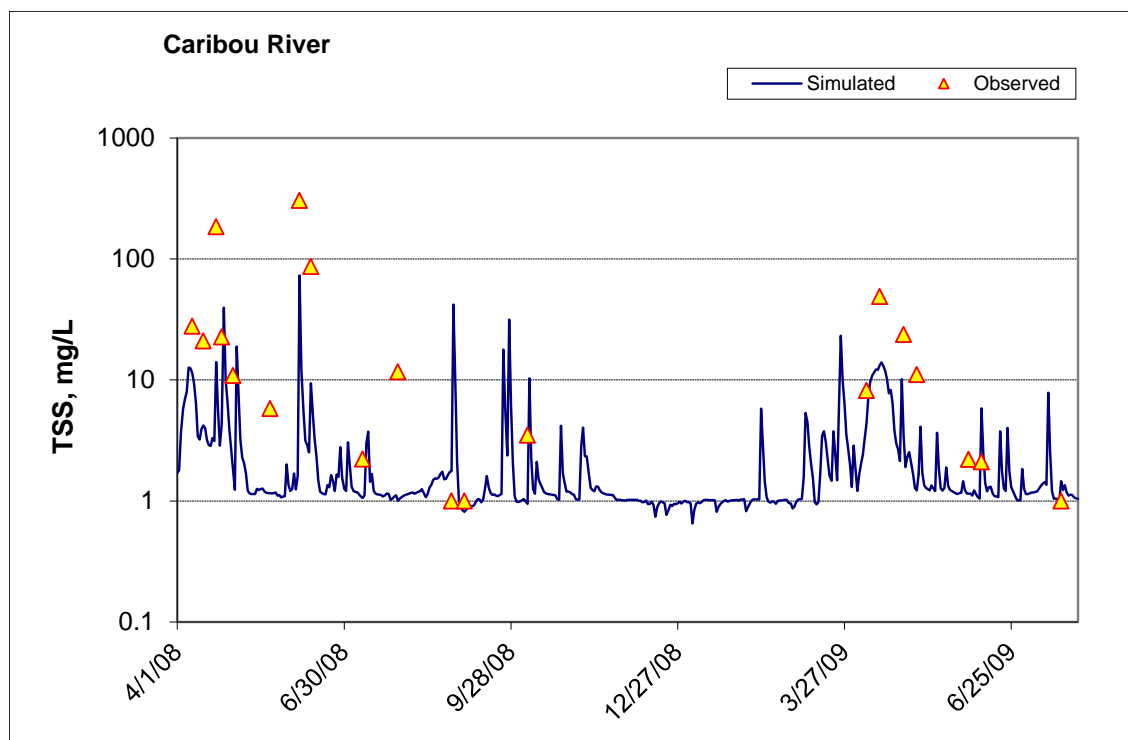


Figure 349. Time series of observed and simulated Total Suspended Solids (TSS) concentration at Caribou River

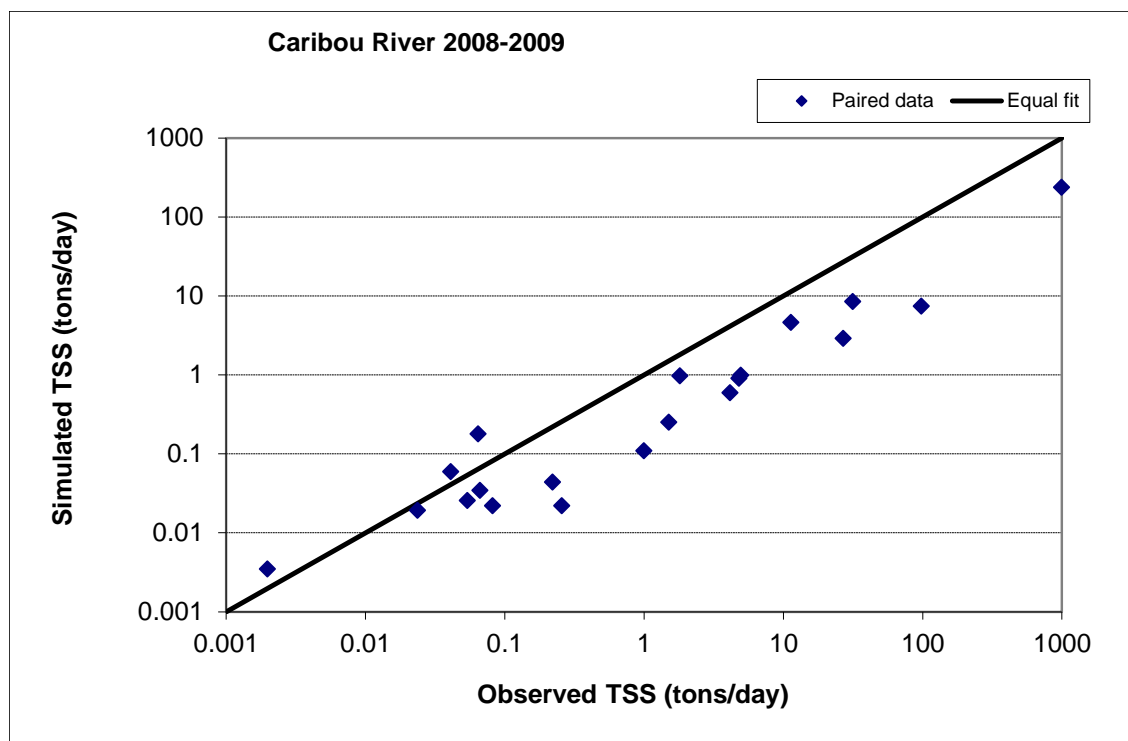


Figure 350. Paired simulated vs. observed Total Suspended Solids (TSS) load at Caribou River (validation period)

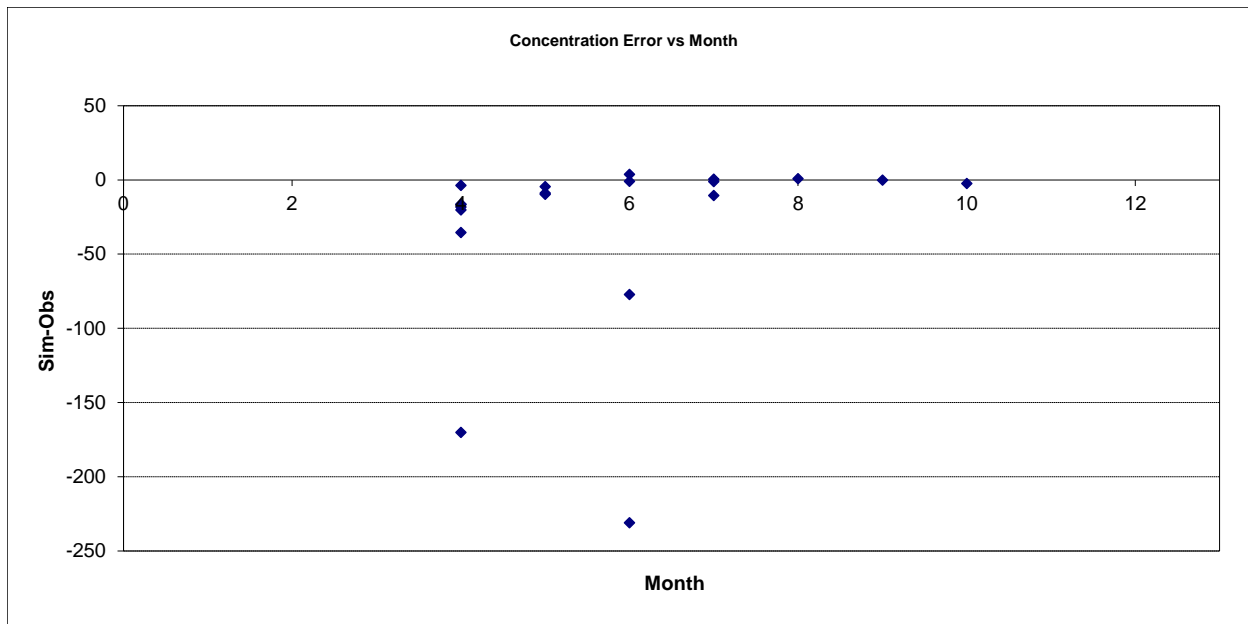


Figure 351. Residual (Simulated - Observed) vs. Month Total Suspended Solids (TSS) at Caribou River

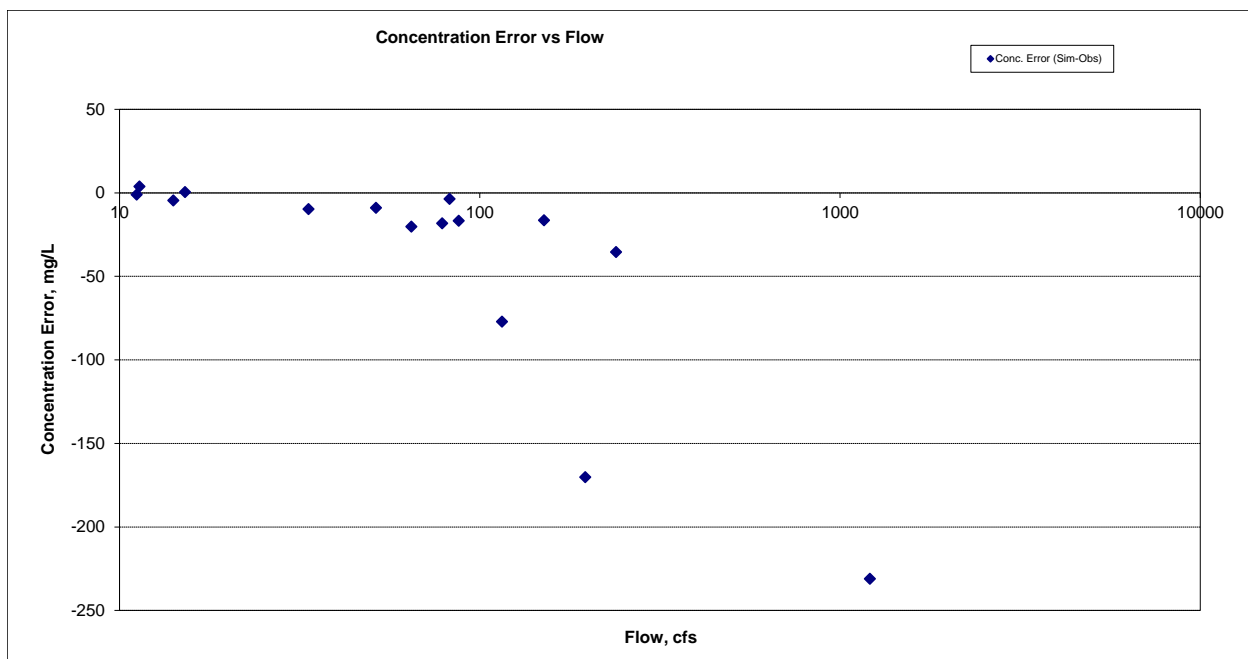


Figure 352. Residual (Simulated - Observed) vs. Flow Total Suspended Solids (TSS) at Caribou River

Nitrite+ Nitrate Nitrogen (NO_x)

Table 69. Nitrite+ Nitrate Nitrogen (NO_x) statistics

Count	20
Concentration Average Error	-47.39%
Concentration Median Error	-46.71%
Load Ave Error	-44.10%
Load Median Error	-8.35%
Paired t concentration	0.04
Paired t load	0.22

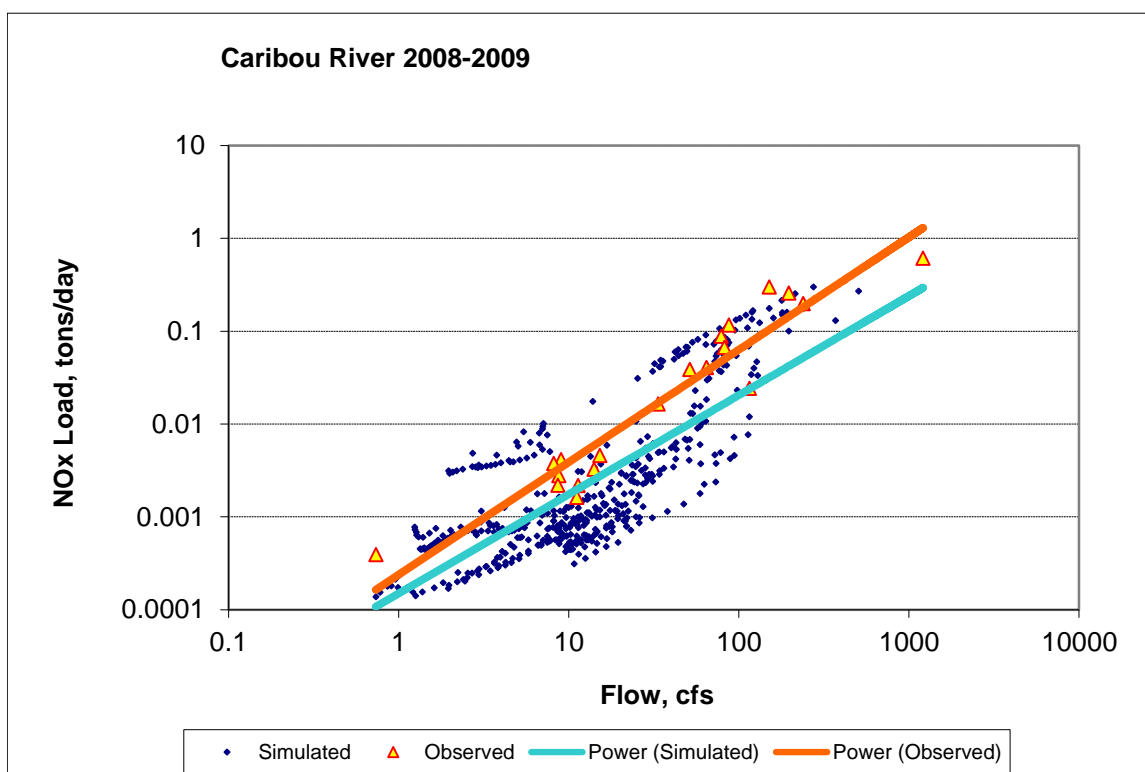


Figure 353. Power plot of simulated and observed Nitrite+ Nitrate Nitrogen (NO_x) load vs flow at Caribou River (validation period)

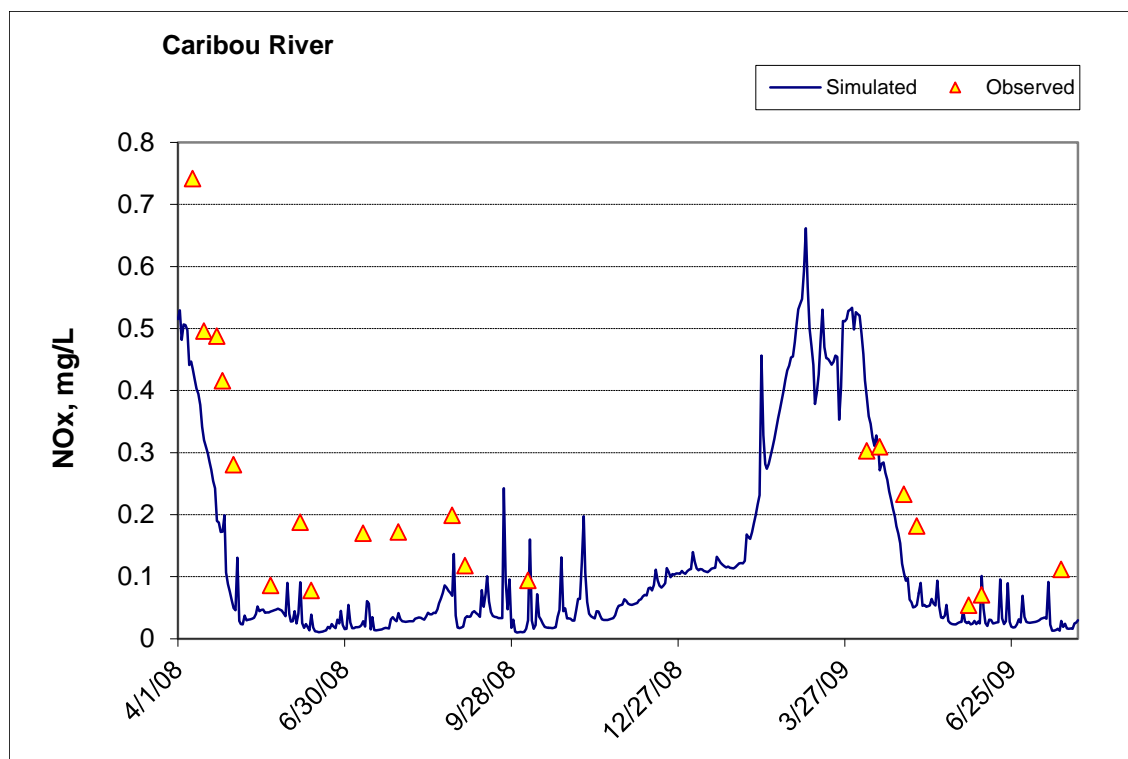


Figure 354. Time series of observed and simulated Nitrite+ Nitrate Nitrogen (NOx) concentration at Caribou River

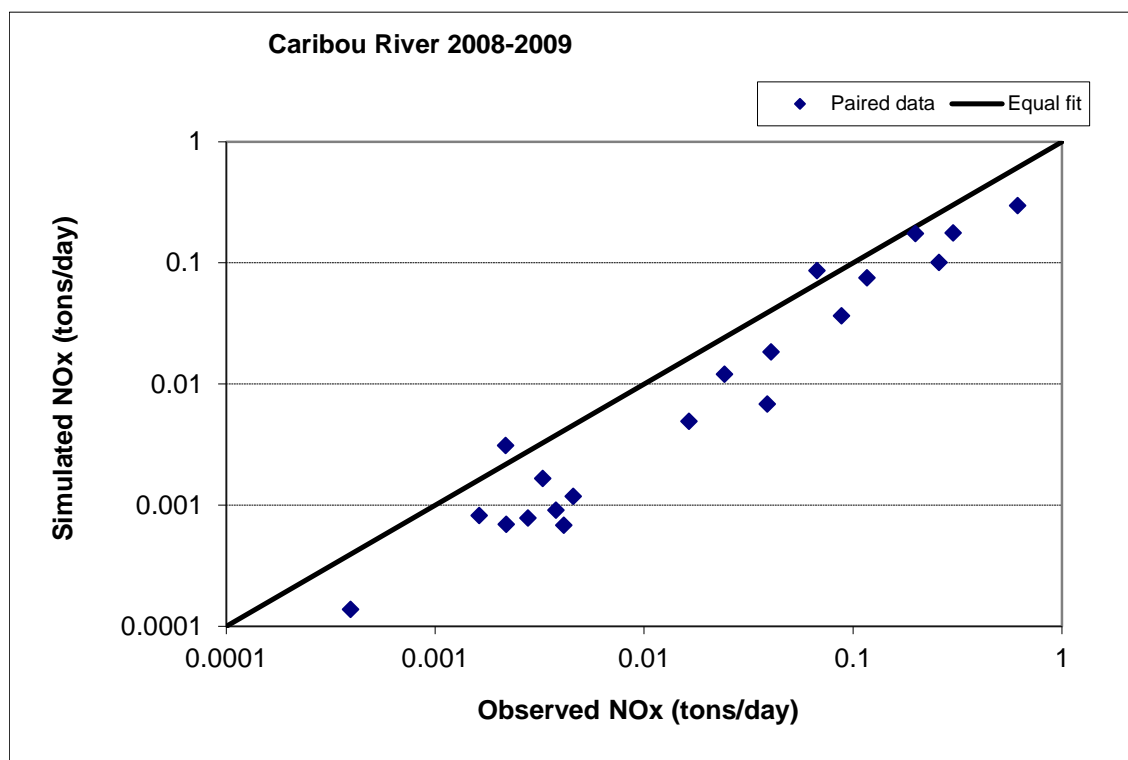


Figure 355. Paired simulated vs. observed Nitrite+ Nitrate Nitrogen (NOx) load at Caribou River (validation period)

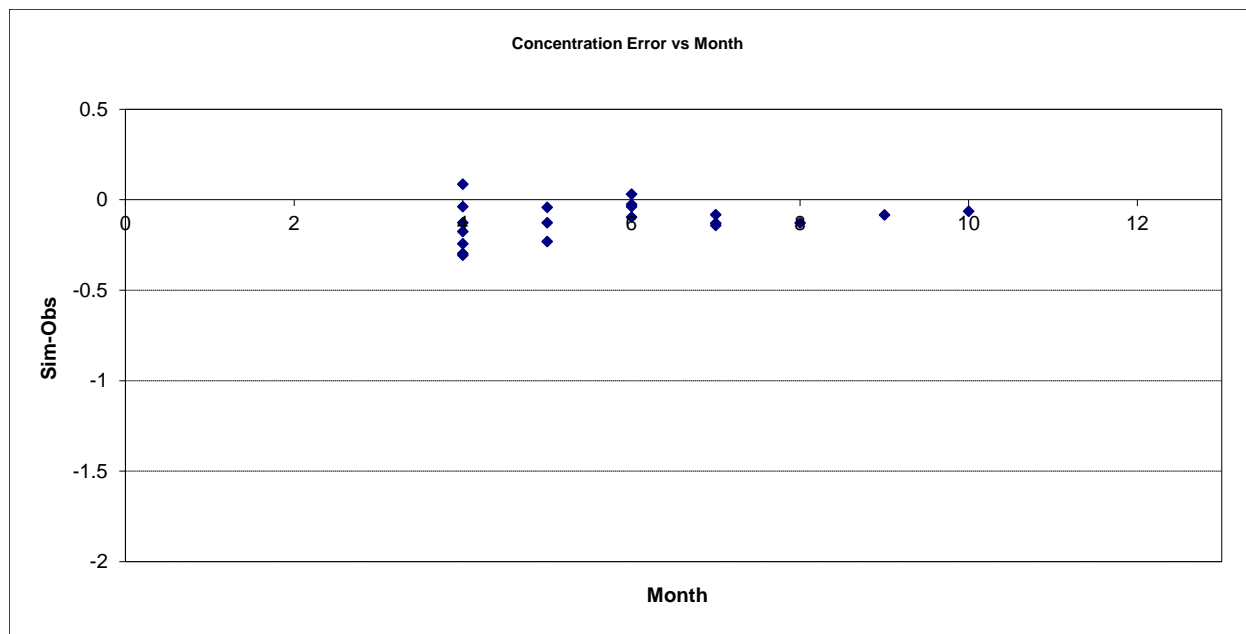


Figure 356. Residual (Simulated - Observed) vs. Month Nitrite+ Nitrate Nitrogen (NOx) at Caribou River

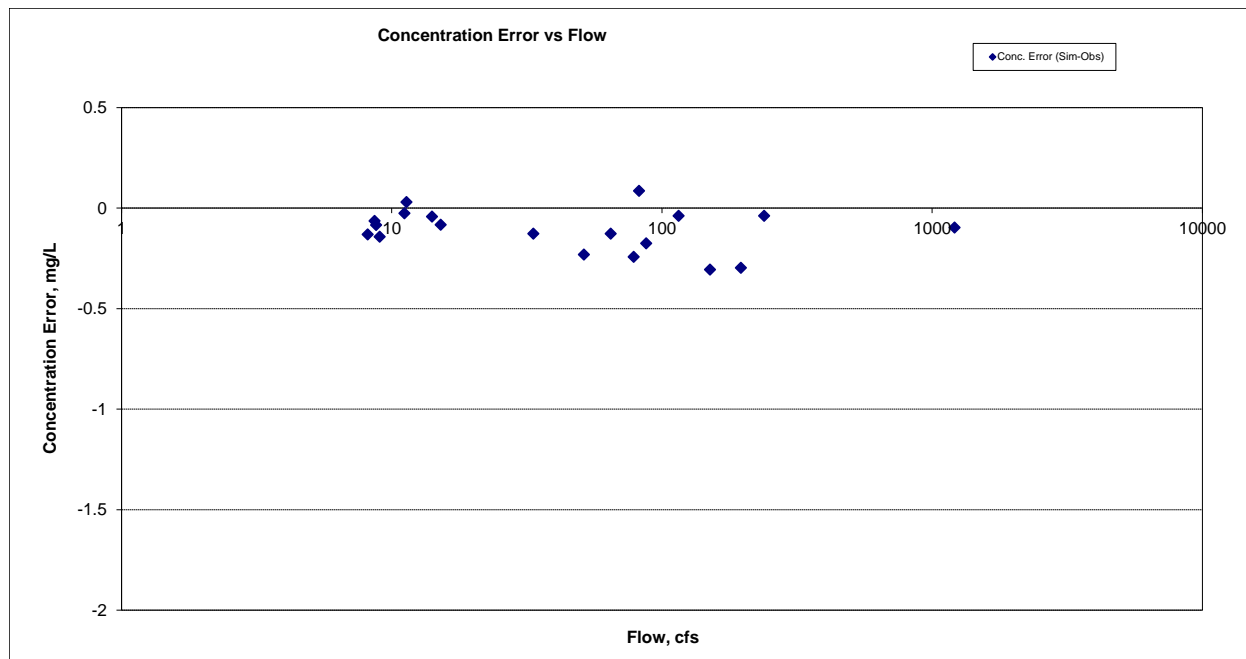


Figure 357. Residual (Simulated - Observed) vs. Flow Nitrite+ Nitrate Nitrogen (NOx) at Caribou River

Total Phosphorus (TP)

Table 70. Total Phosphorus (TP) statistics

Count	19
Concentration Average Error	21.76%
Concentration Median Error	18.77%
Load Ave Error	18.94%
Load Median Error	1.20%
Paired t concentration	0.47
Paired t load	0.51

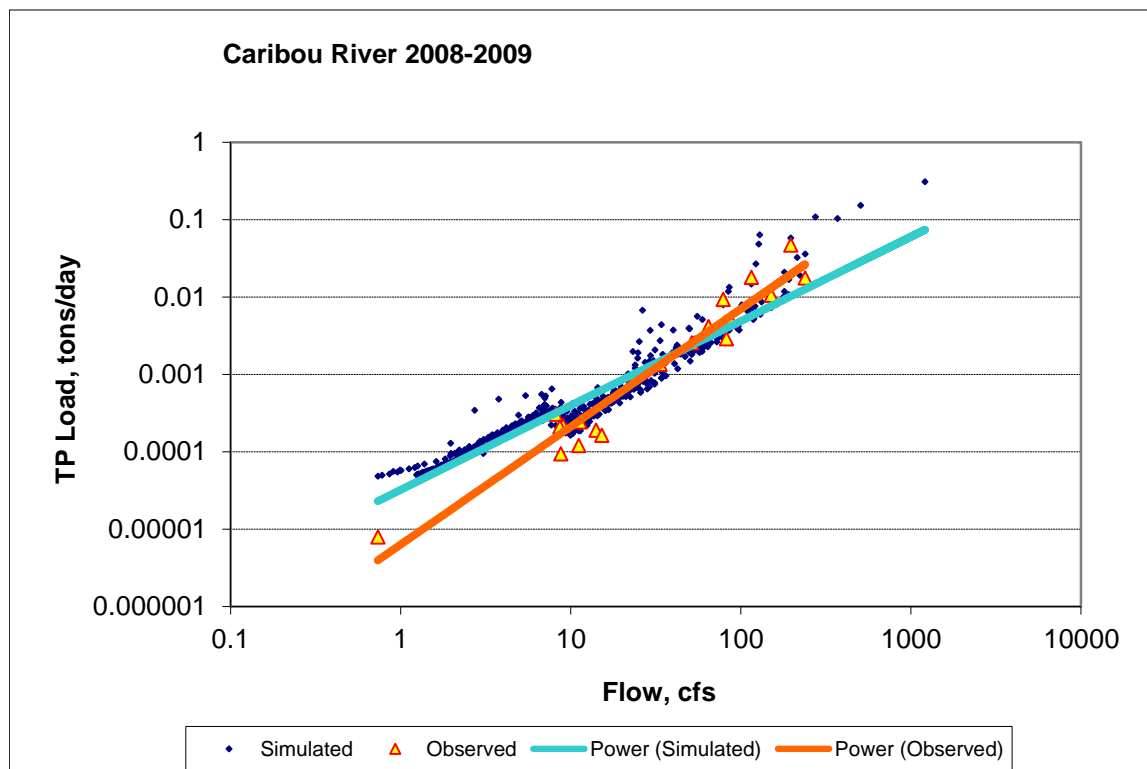


Figure 358. Power plot of simulated and observed Total Phosphorus (TP) load vs flow at Caribou River (validation period)

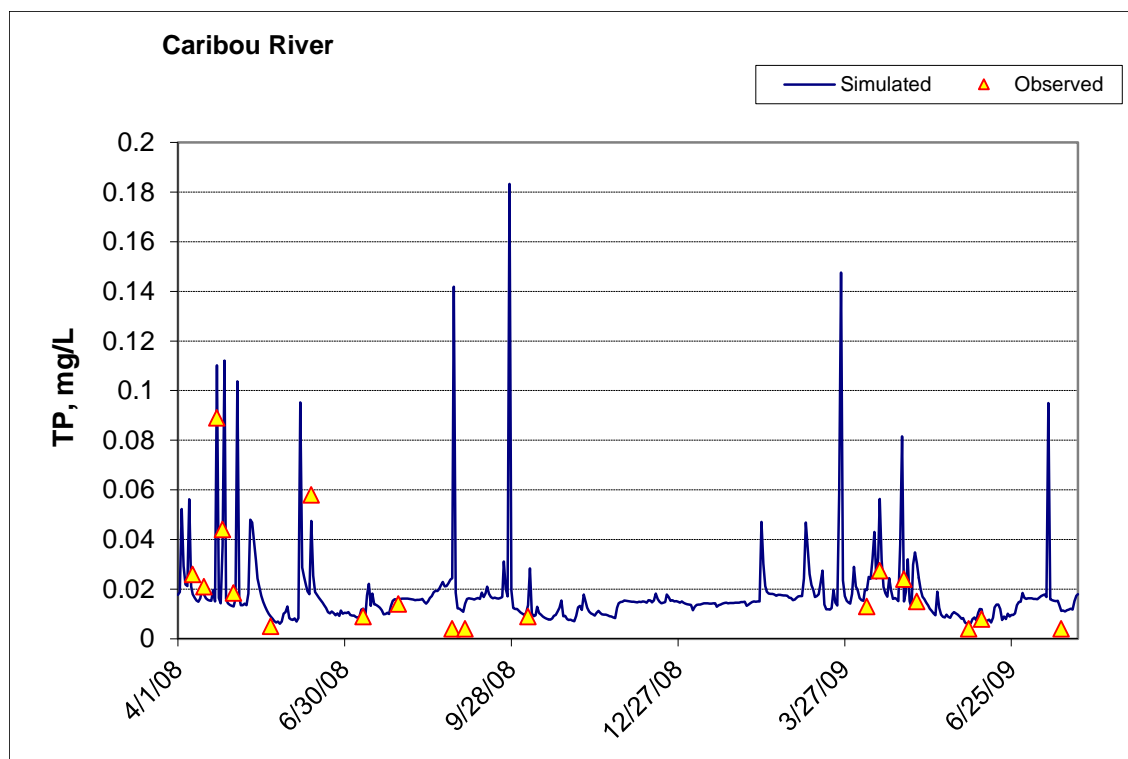


Figure 359. Time series of observed and simulated Total Phosphorus (TP) concentration at Caribou River

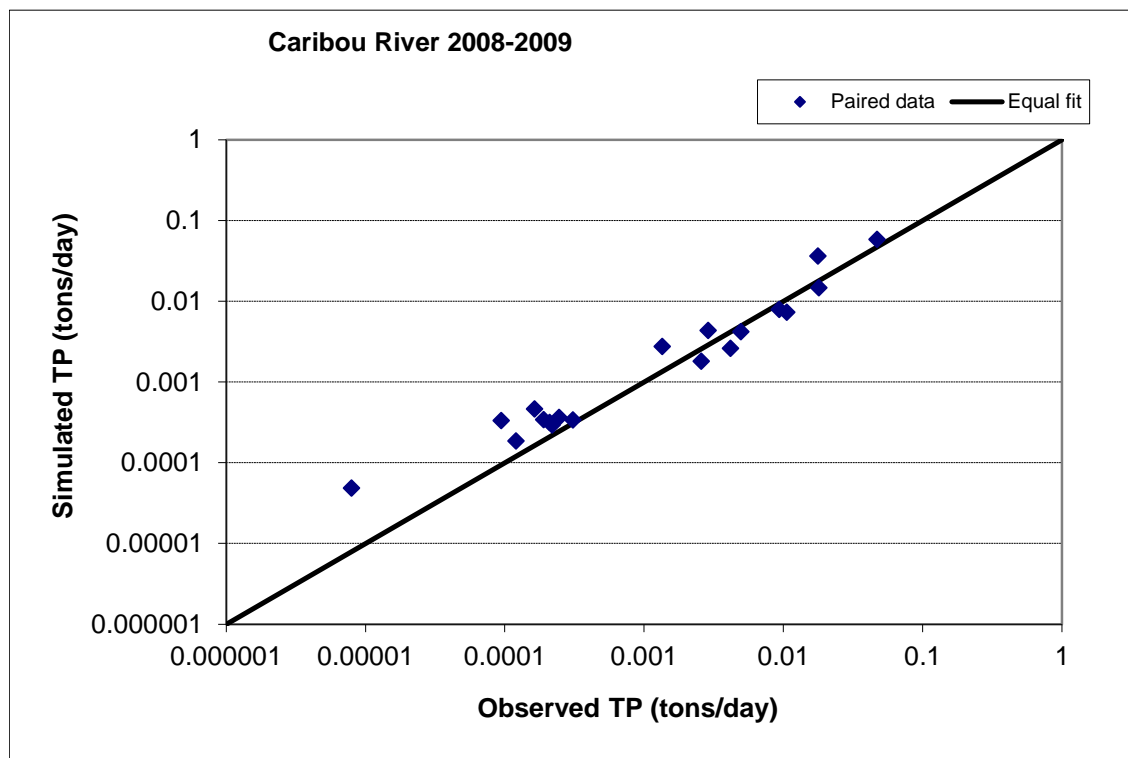


Figure 360. Paired simulated vs. observed Total Phosphorus (TP) load at Caribou River (validation period)

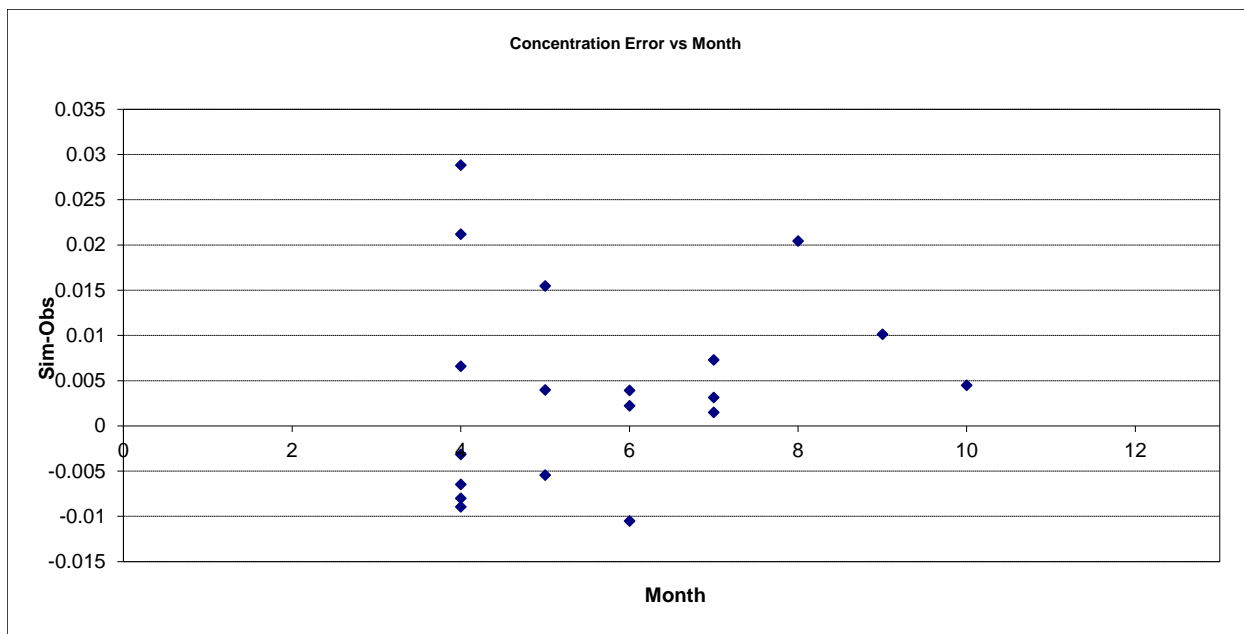


Figure 361. Residual (Simulated - Observed) vs. Month Total Phosphorus (TP) at Caribou River

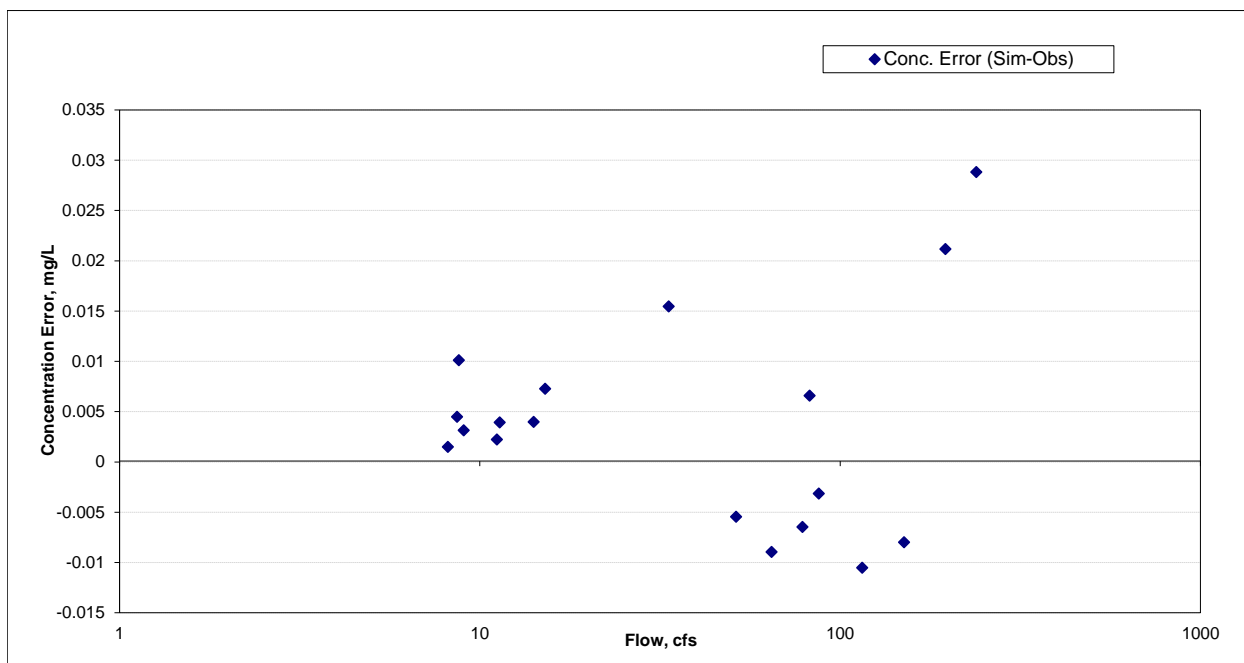


Figure 362. Residual (Simulated - Observed) vs. Flow Total Phosphorus (TP) at Caribou River

Cascade River (EQUIS S000-253)

Total Suspended Solids (TSS)

Table 71. Total Suspended Solids (TSS) statistics

Count	20
Concentration Average Error	-32.78%
Concentration Median Error	1.09%
Load Ave Error	-11.64%
Load Median Error	0.04%
Paired t concentration	0.38
Paired t load	0.54

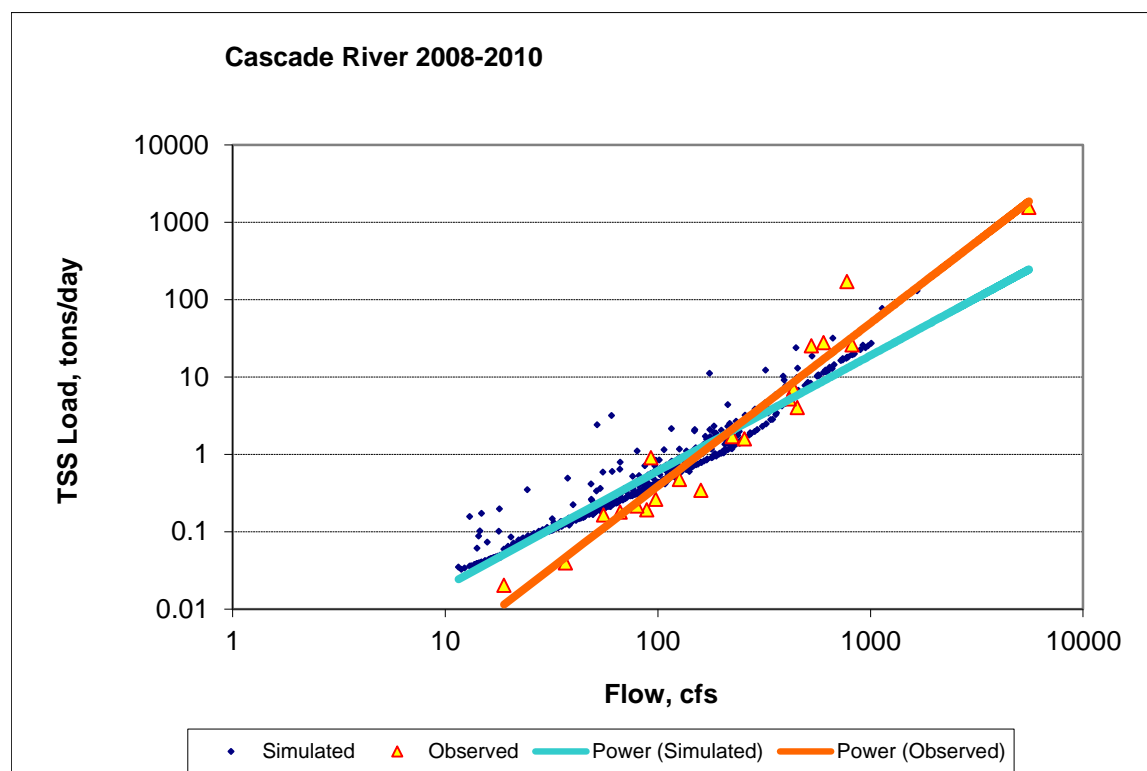


Figure 363. Power plot of simulated and observed Total Suspended Solids (TSS) load vs flow at Cascade River (validation period)

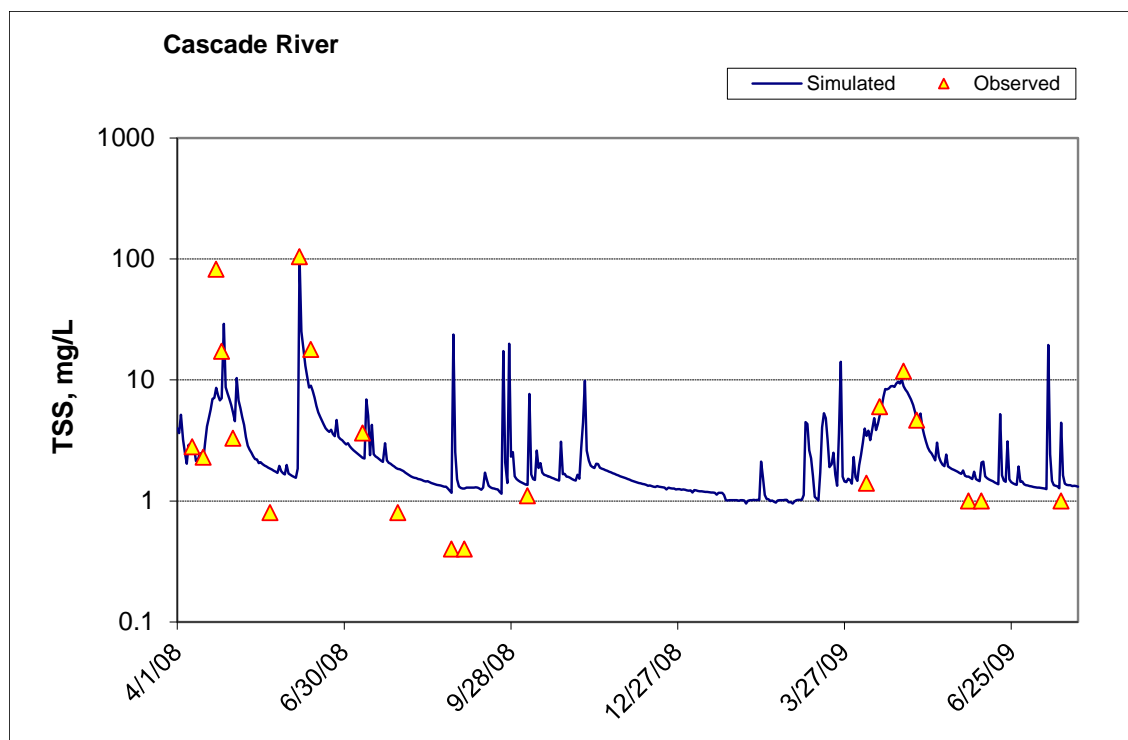


Figure 364. Time series of observed and simulated Total Suspended Solids (TSS) concentration at Cascade River

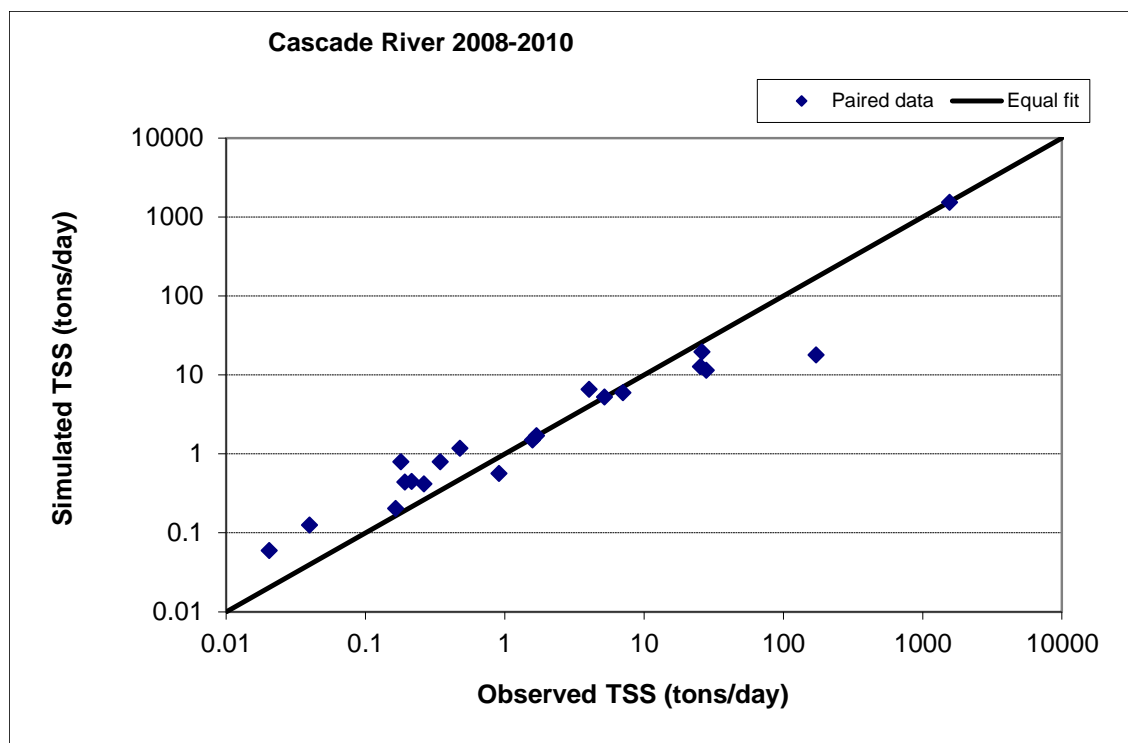


Figure 365. Paired simulated vs. observed Total Suspended Solids (TSS) load at Cascade River (validation period)

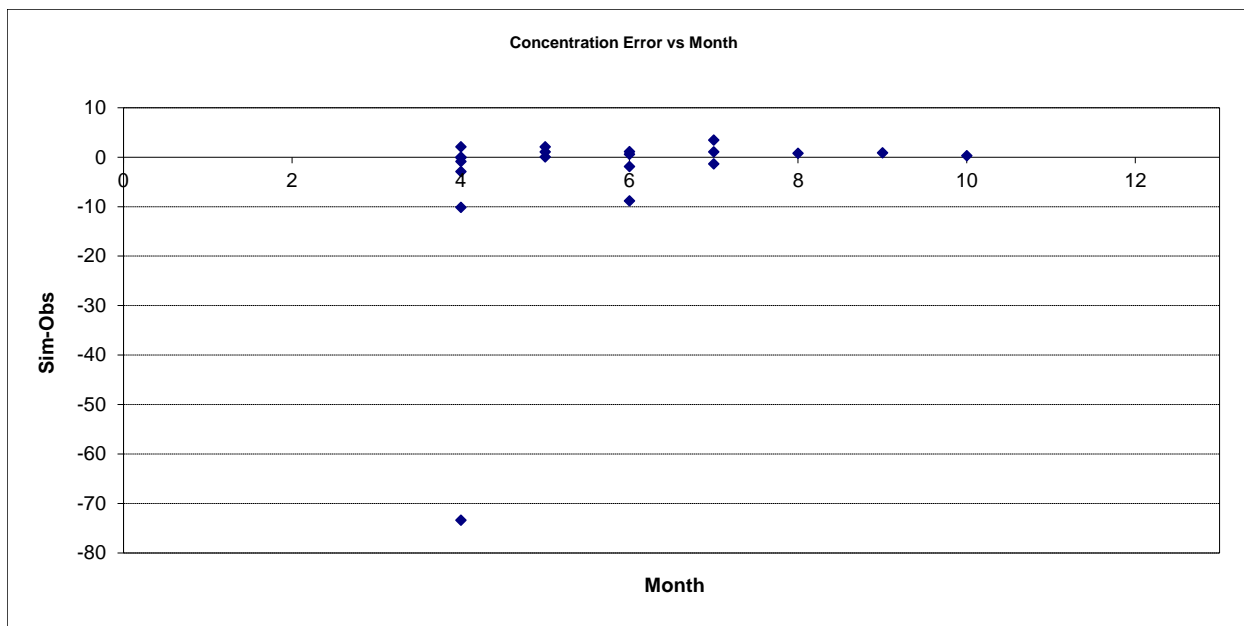


Figure 366. Residual (Simulated - Observed) vs. Month Total Suspended Solids (TSS) at Cascade River

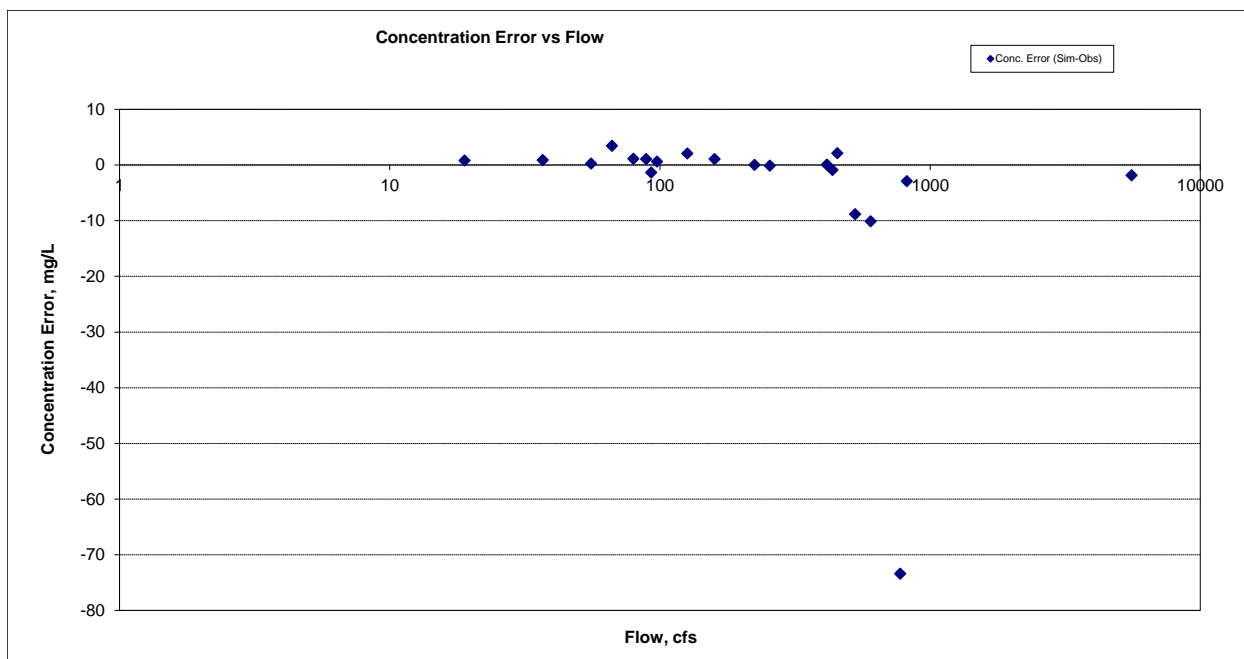


Figure 367. Residual (Simulated - Observed) vs. Flow Total Suspended Solids (TSS) at Cascade River

Nitrite+ Nitrate Nitrogen (NO_x)

Table 72. Nitrite+ Nitrate Nitrogen (NO_x) statistics

Count	20
Concentration Average Error	-39.72%
Concentration Median Error	-16.42%
Load Ave Error	-47.10%
Load Median Error	-2.52%
Paired t concentration	0.14
Paired t load	0.24

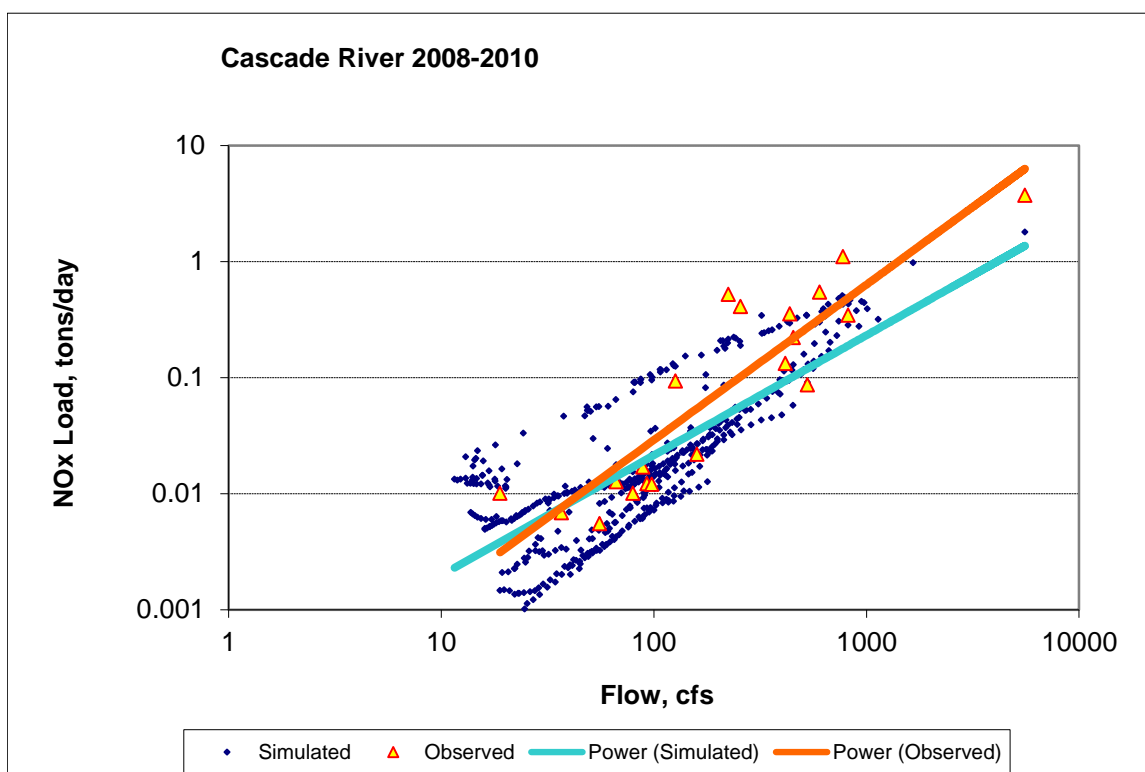


Figure 368. Power plot of simulated and observed Nitrite+ Nitrate Nitrogen (NO_x) load vs flow at Cascade River (validation period)

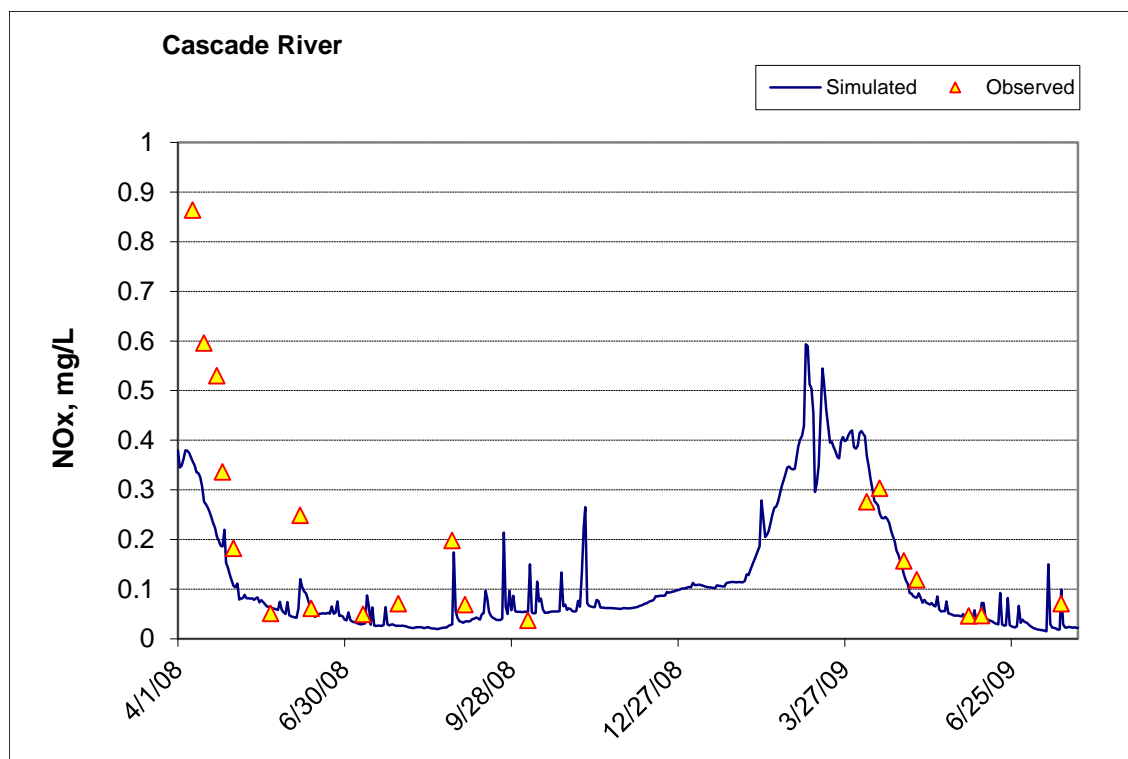


Figure 369. Time series of observed and simulated Nitrite+ Nitrate Nitrogen (NOx) concentration at Cascade River

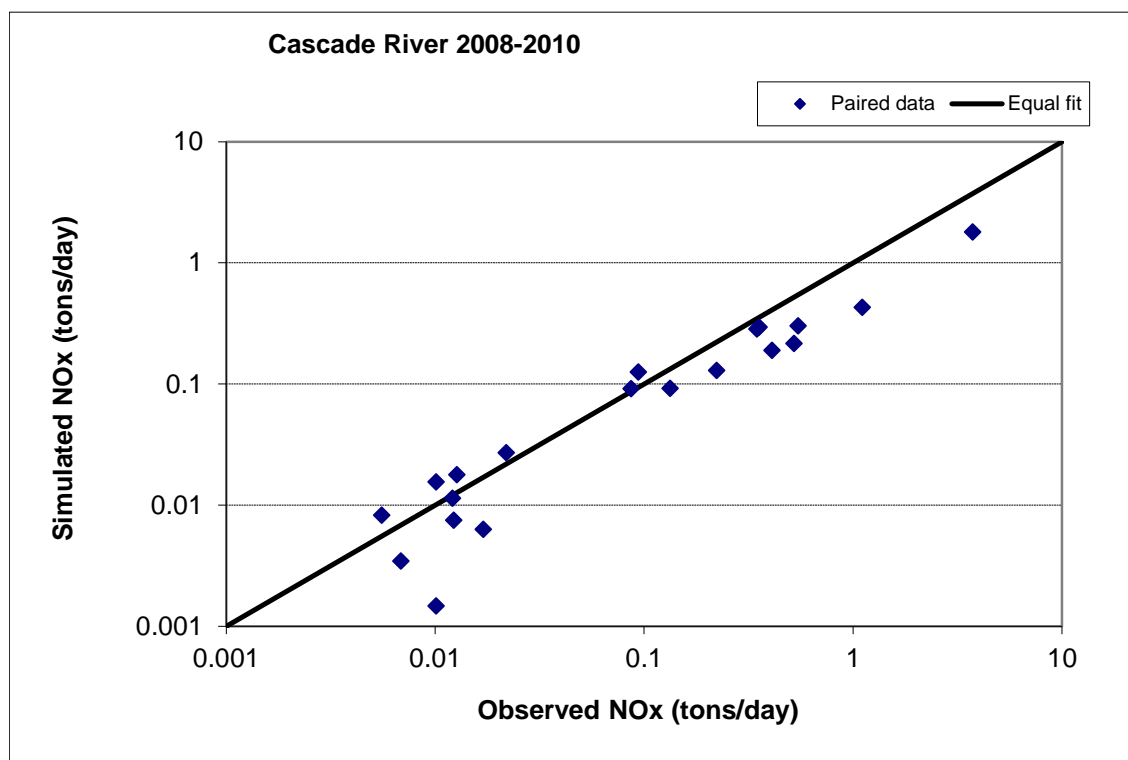


Figure 370. Paired simulated vs. observed Nitrite+ Nitrate Nitrogen (NOx) load at Cascade River (validation period)



Figure 371. Residual (Simulated - Observed) vs. Month Nitrite+ Nitrate Nitrogen (NOx) at Cascade River

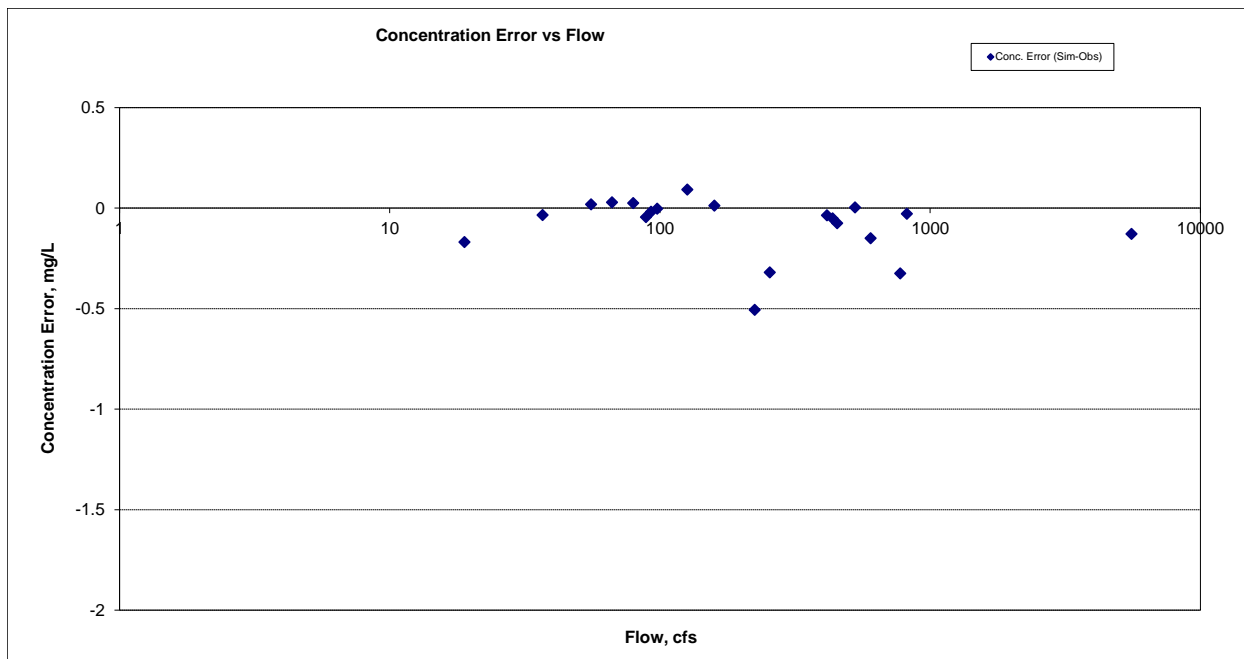


Figure 372. Residual (Simulated - Observed) vs. Flow Nitrite+ Nitrate Nitrogen (NOx) at Cascade River

Total Phosphorus (TP)

Table 73. Total Phosphorus (TP) statistics

Count	20
Concentration Average Error	-8.16%
Concentration Median Error	17.89%
Load Ave Error	-46.12%
Load Median Error	0.93%
Paired t concentration	0.68
Paired t load	0.34

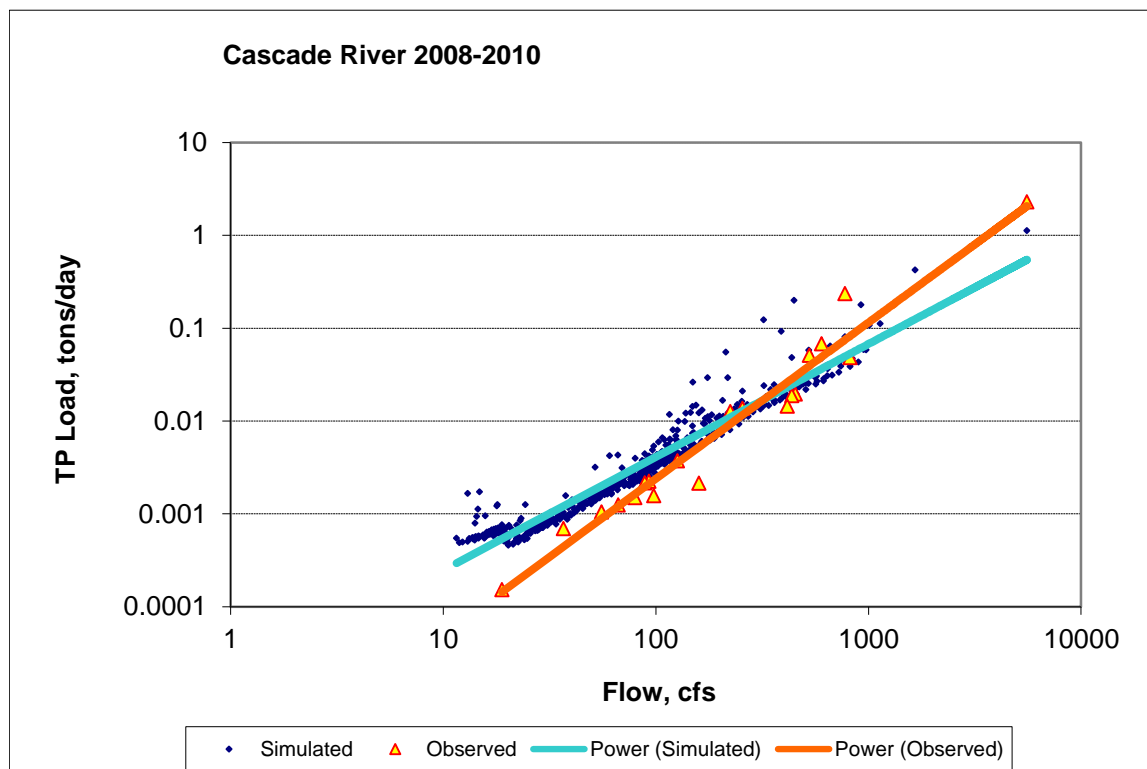


Figure 373. Power plot of simulated and observed Total Phosphorus (TP) load vs flow at Cascade River (validation period)

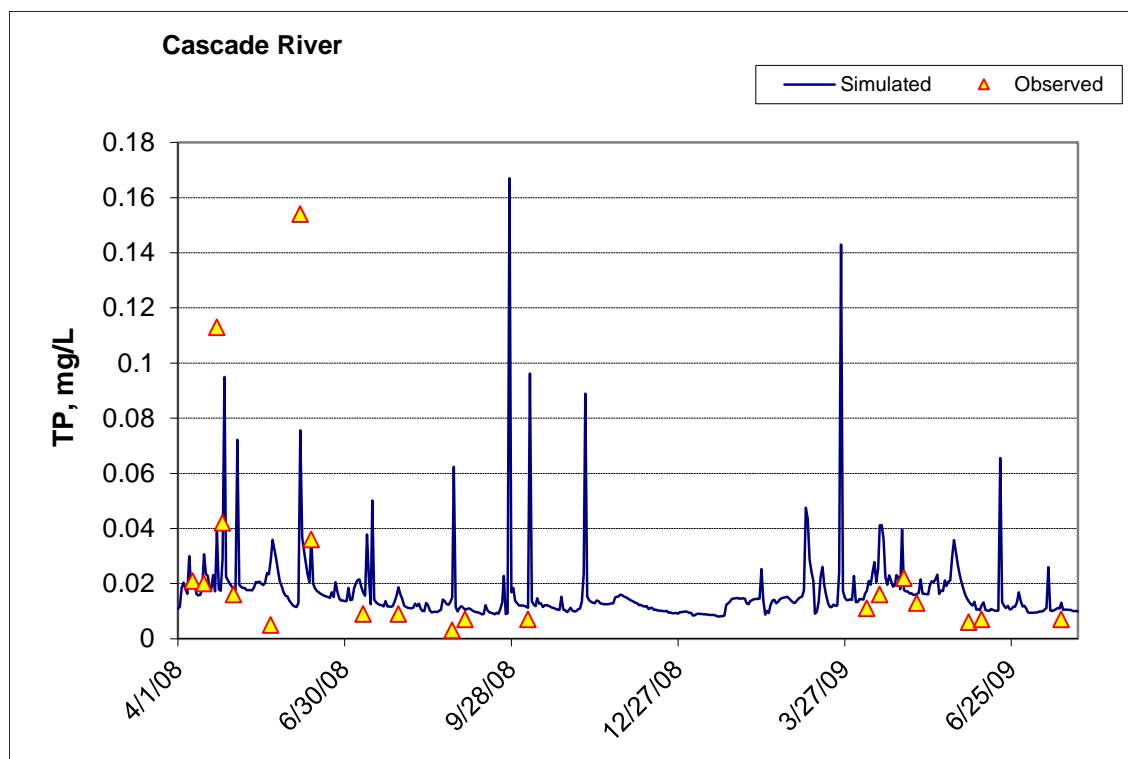


Figure 374. Time series of observed and simulated Total Phosphorus (TP) concentration at Cascade River

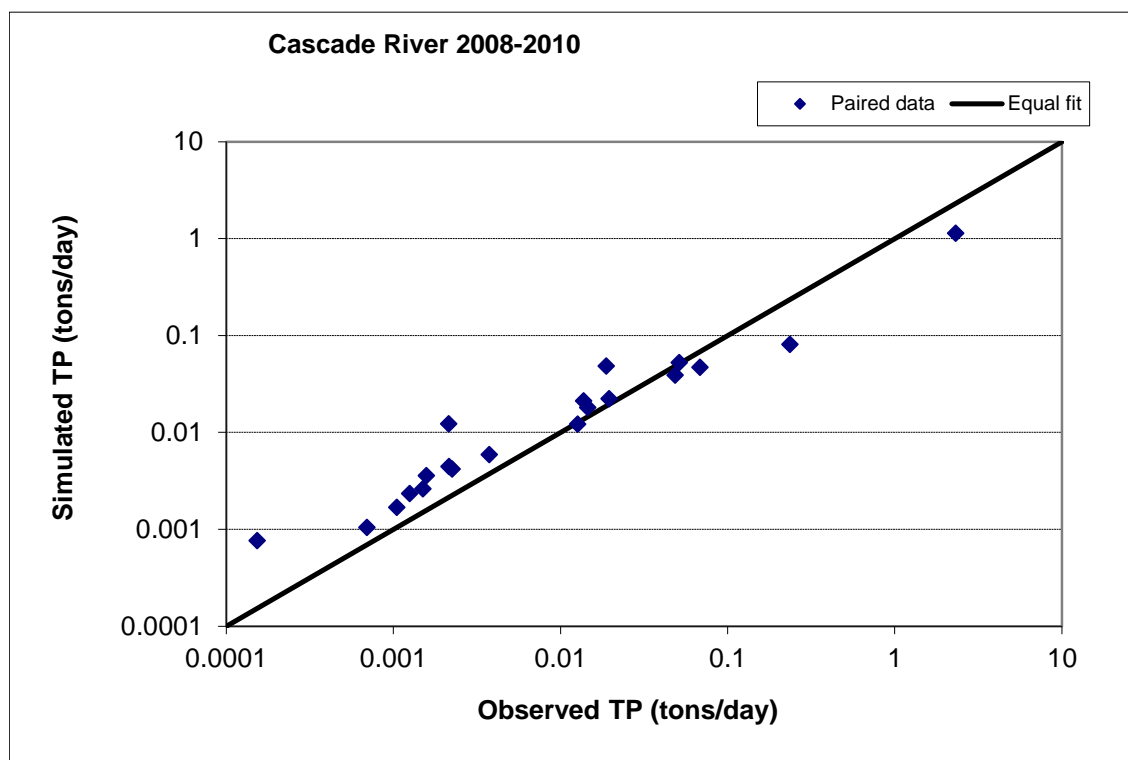


Figure 375. Paired simulated vs. observed Total Phosphorus (TP) load at Cascade River (validation period)



Figure 376. Residual (Simulated - Observed) vs. Month Total Phosphorus (TP) at Cascade River

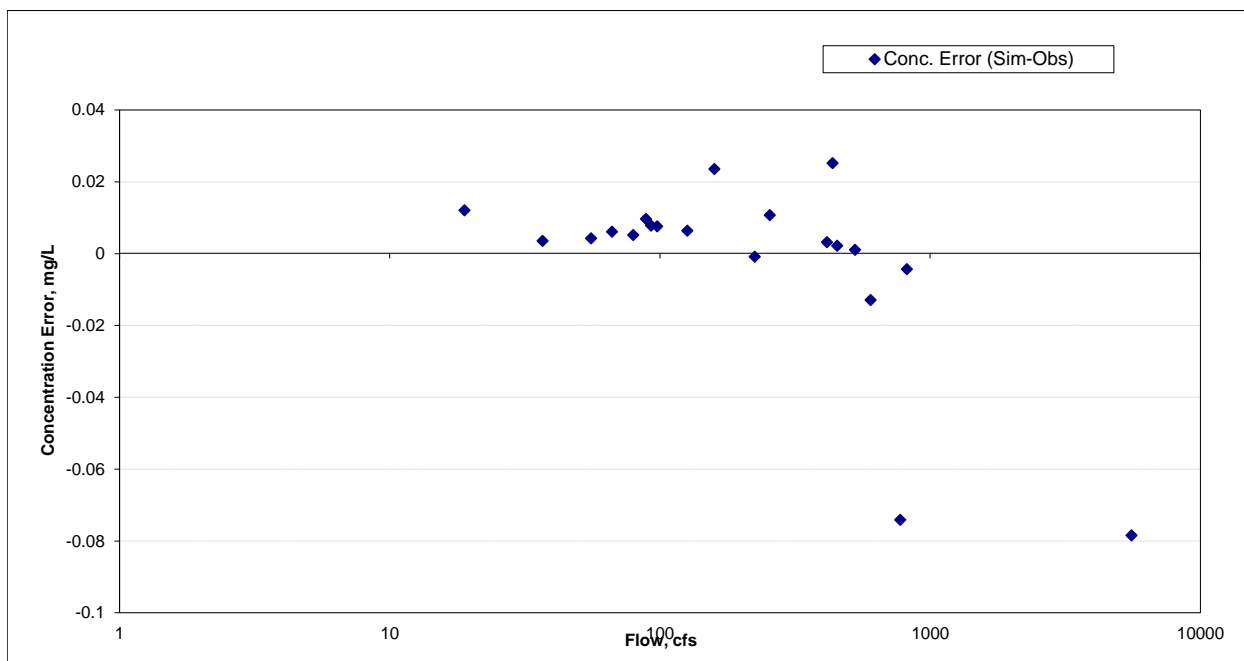


Figure 377. Residual (Simulated - Observed) vs. Flow Total Phosphorus (TP) at Cascade River

Flute Reed River (EQUIS S004-283)

Total Suspended Solids (TSS)

Table 74. Total Suspended Solids (TSS) statistics

Count	34
Concentration Average Error	-75.06%
Concentration Median Error	-16.10%
Load Ave Error	-85.35%
Load Median Error	-1.10%
Paired t concentration	0.03
Paired t load	0.04

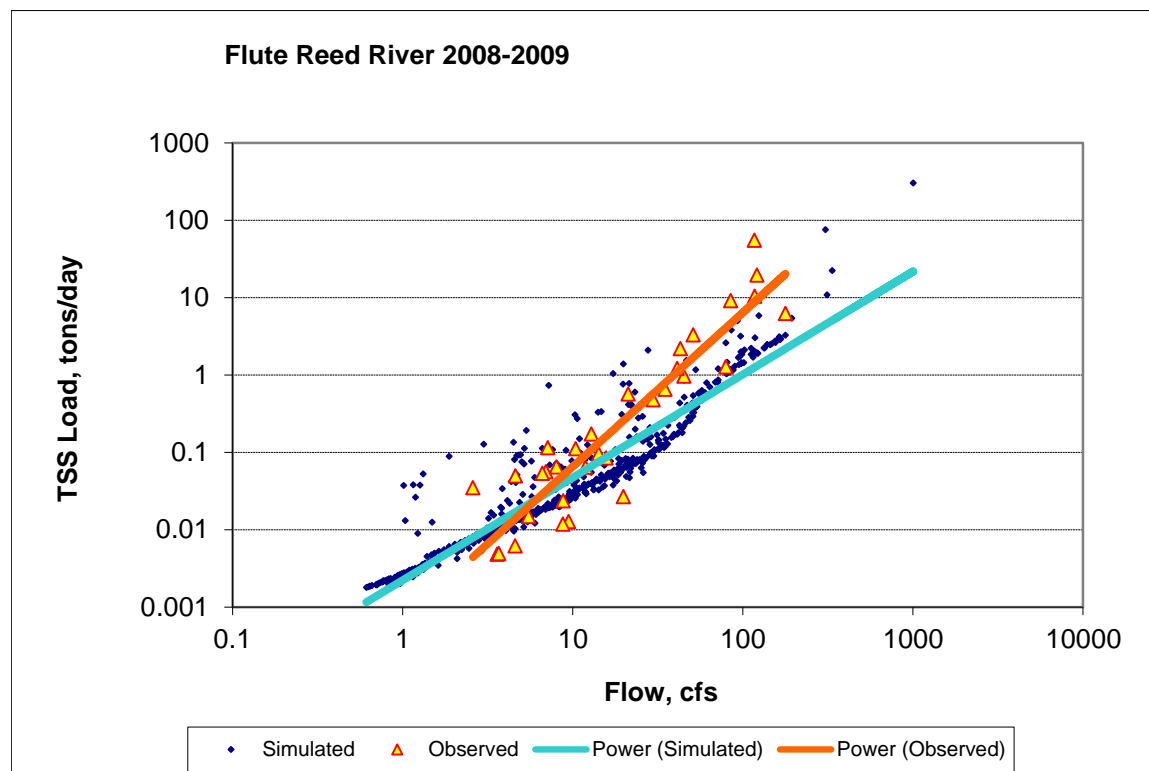


Figure 378. Power plot of simulated and observed Total Suspended Solids (TSS) load vs flow at Flute Reed River (validation period)

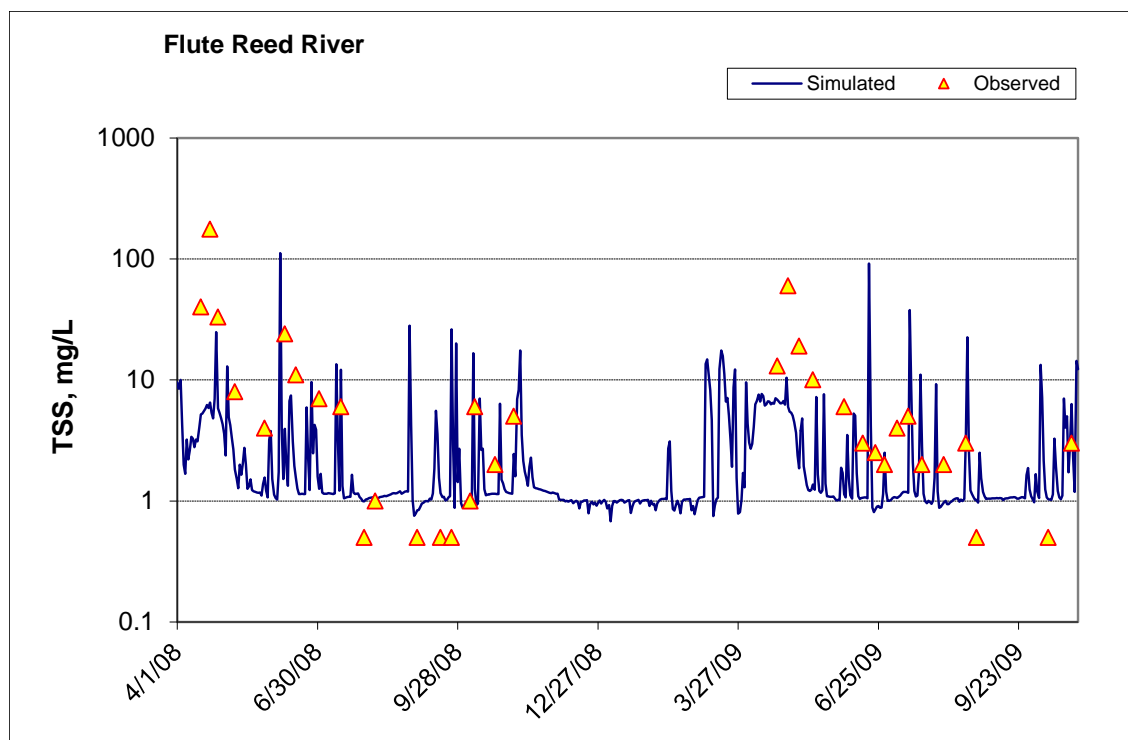


Figure 379. Time series of observed and simulated Total Suspended Solids (TSS) concentration at Flute Reed River

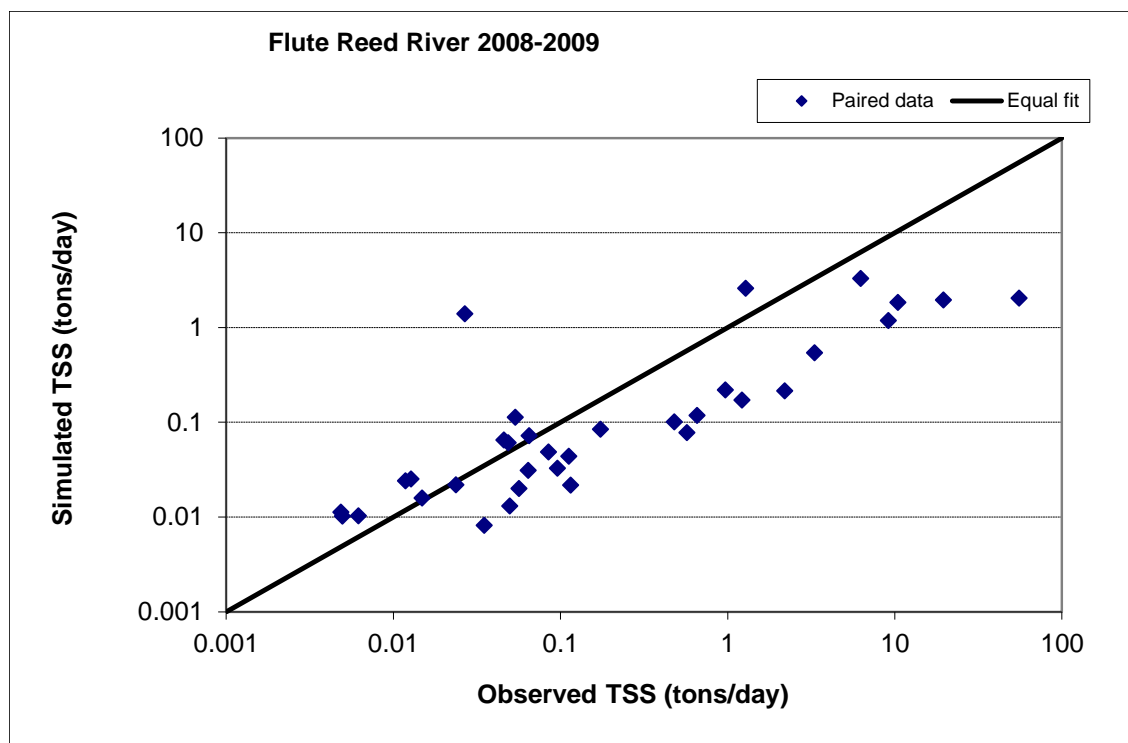


Figure 380. Paired simulated vs. observed Total Suspended Solids (TSS) load at Flute Reed River (validation period)

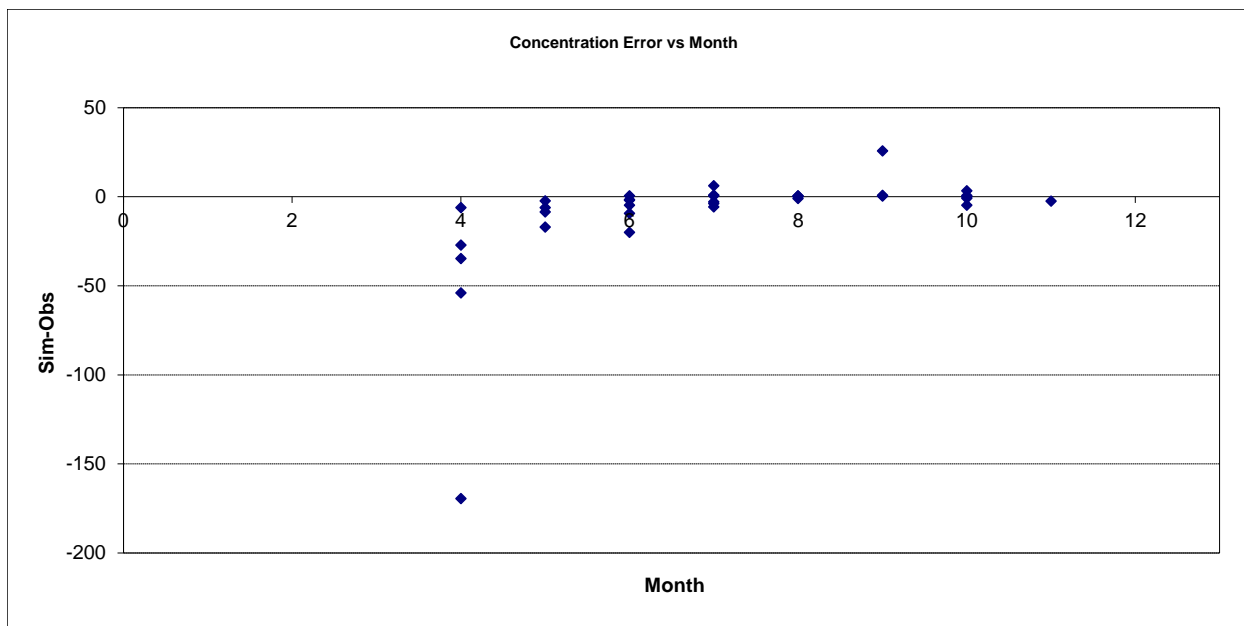


Figure 381. Residual (Simulated - Observed) vs. Month Total Suspended Solids (TSS) at Flute Reed River

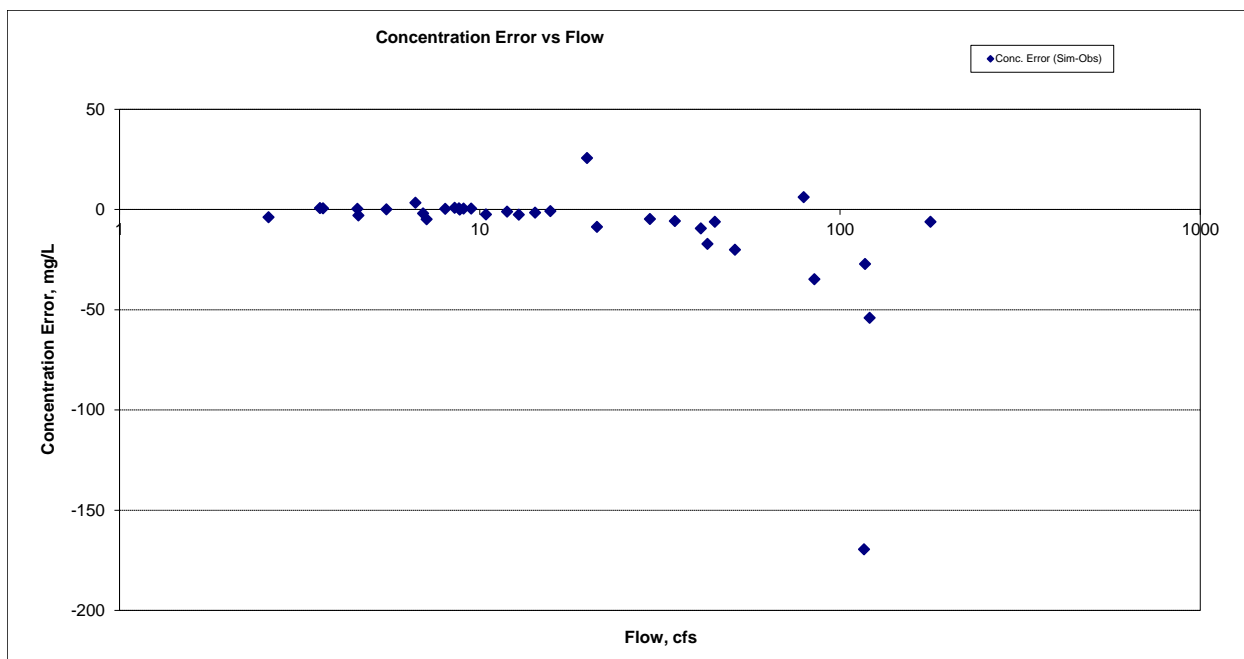


Figure 382. Residual (Simulated - Observed) vs. Flow Total Suspended Solids (TSS) at Flute Reed River

Nitrite+ Nitrate Nitrogen (NO_x)

Table 75. Nitrite+ Nitrate Nitrogen (NO_x) statistics

Count	35
Concentration Average Error	56.51%
Concentration Median Error	48.38%
Load Ave Error	1.84%
Load Median Error	4.10%
Paired t concentration	0.10
Paired t load	0.68

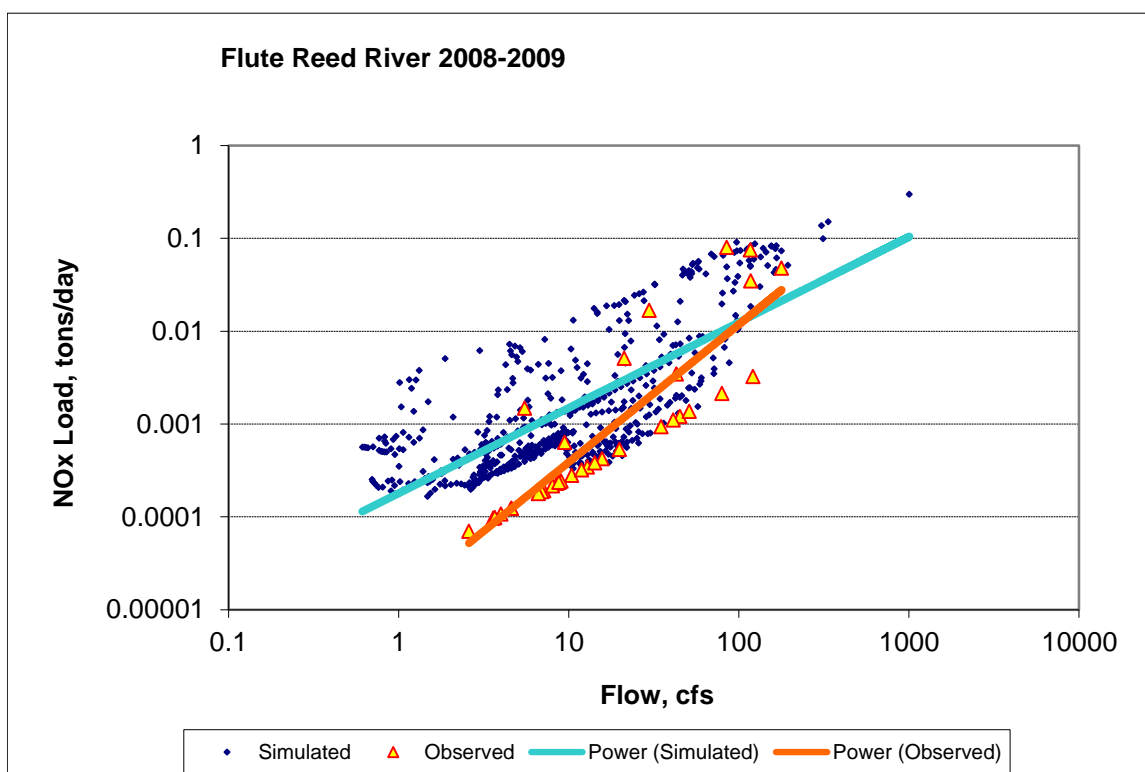


Figure 383. Power plot of simulated and observed Nitrite+ Nitrate Nitrogen (NO_x) load vs flow at Flute Reed River (validation period)

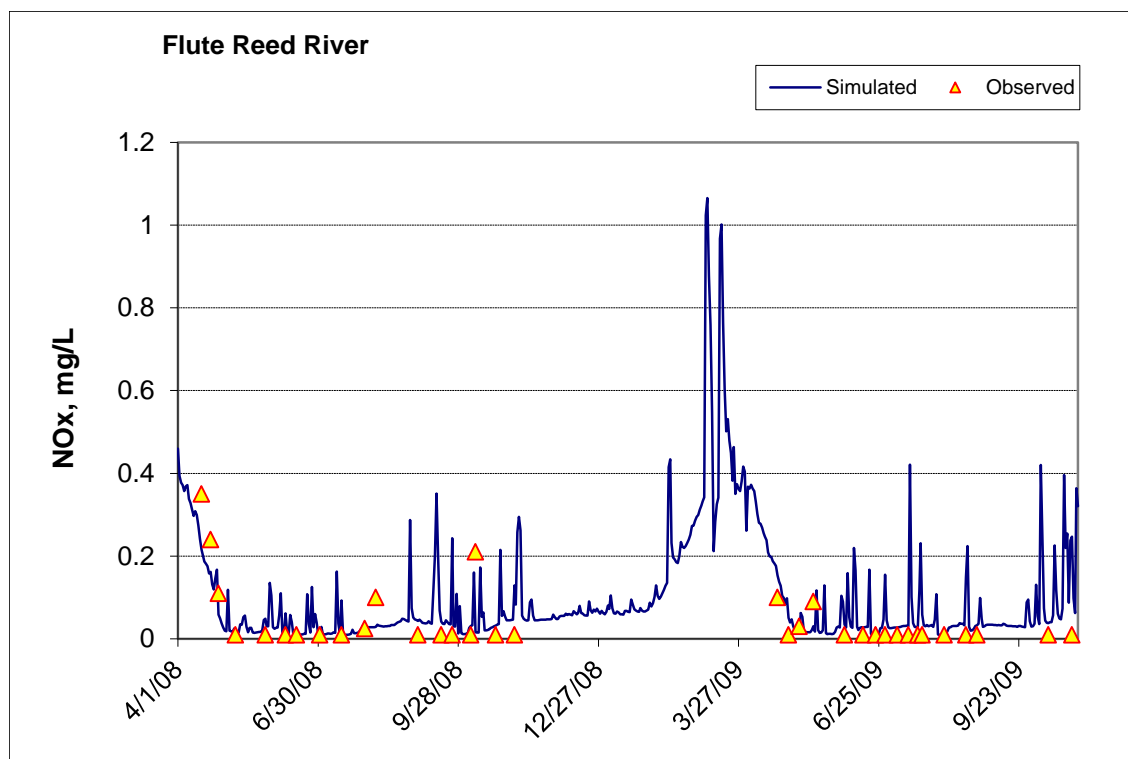


Figure 384. Time series of observed and simulated Nitrite+ Nitrate Nitrogen (NOx) concentration at Flute Reed River

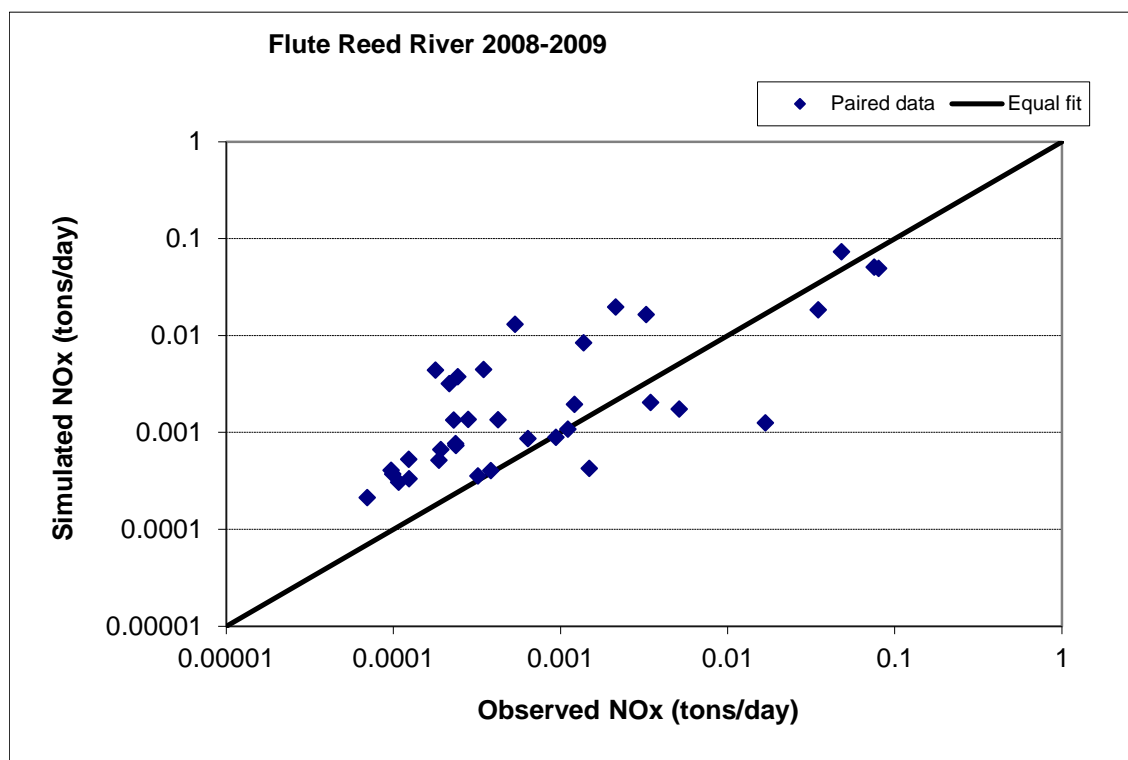


Figure 385. Paired simulated vs. observed Nitrite+ Nitrate Nitrogen (NOx) load at Flute Reed River (validation period)

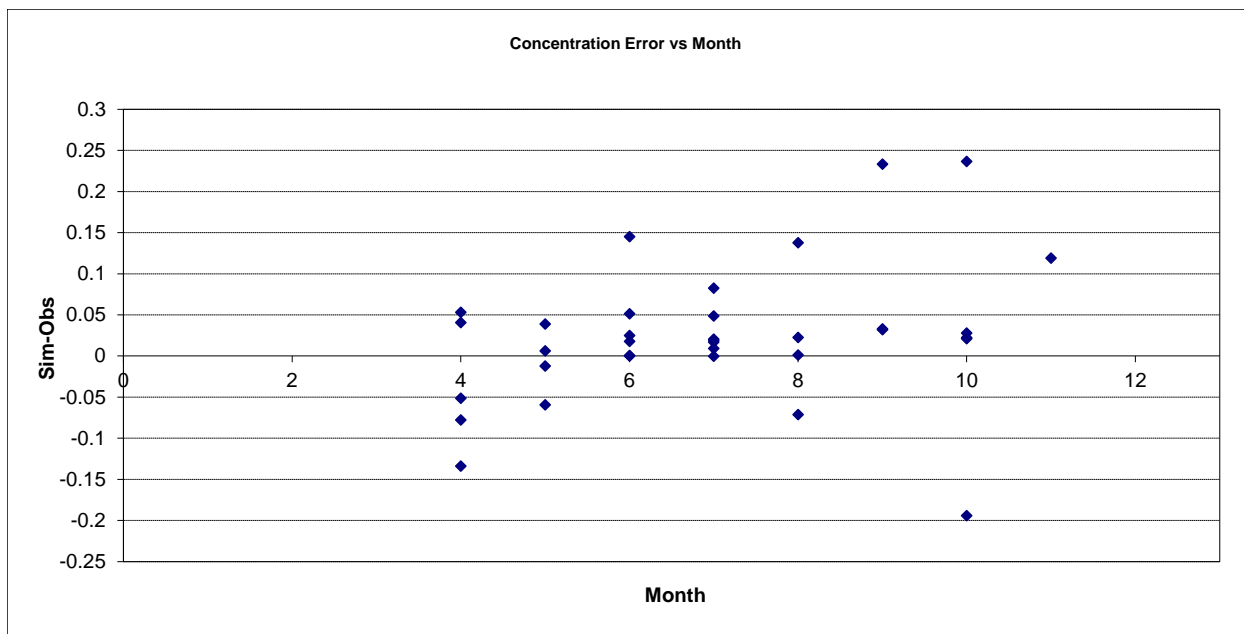
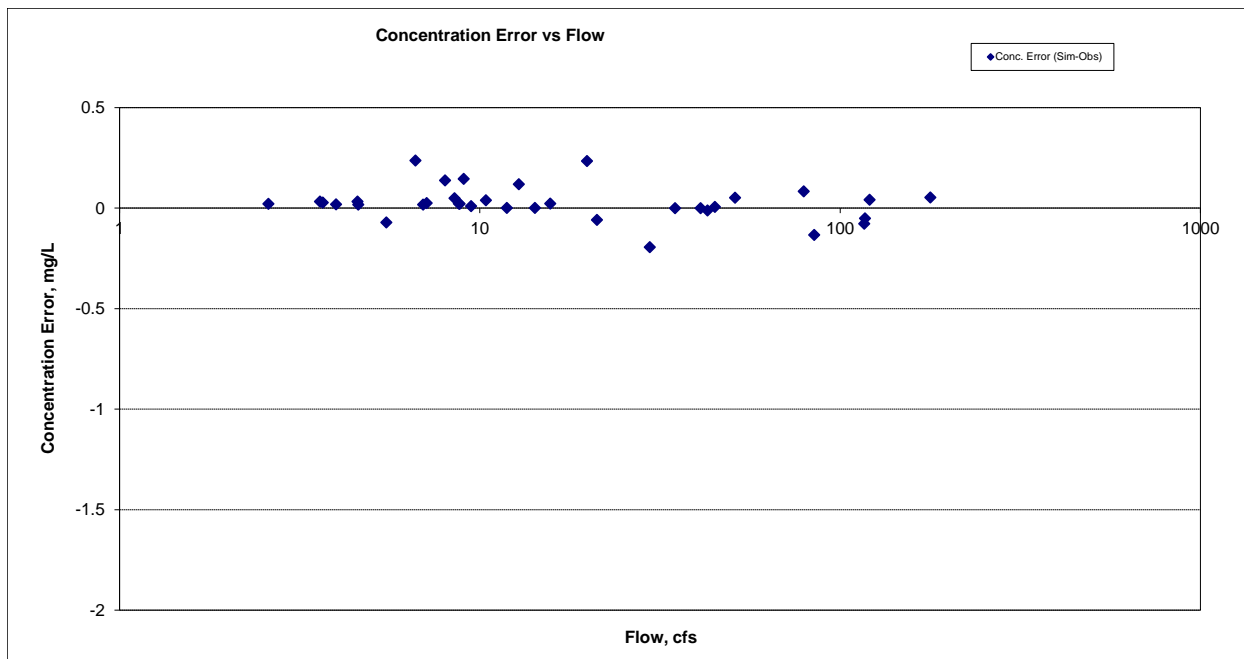


Figure 386. Residual (Simulated - Observed) vs. Month Nitrite+ Nitrate Nitrogen (NOx) at Flute Reed River



Total Phosphorus (TP)

Table 76. Total Phosphorus (TP) statistics

Count	35
Concentration Average Error	-30.20%
Concentration Median Error	-17.42%
Load Ave Error	-51.91%
Load Median Error	-2.55%
Paired t concentration	0.28
Paired t load	0.16

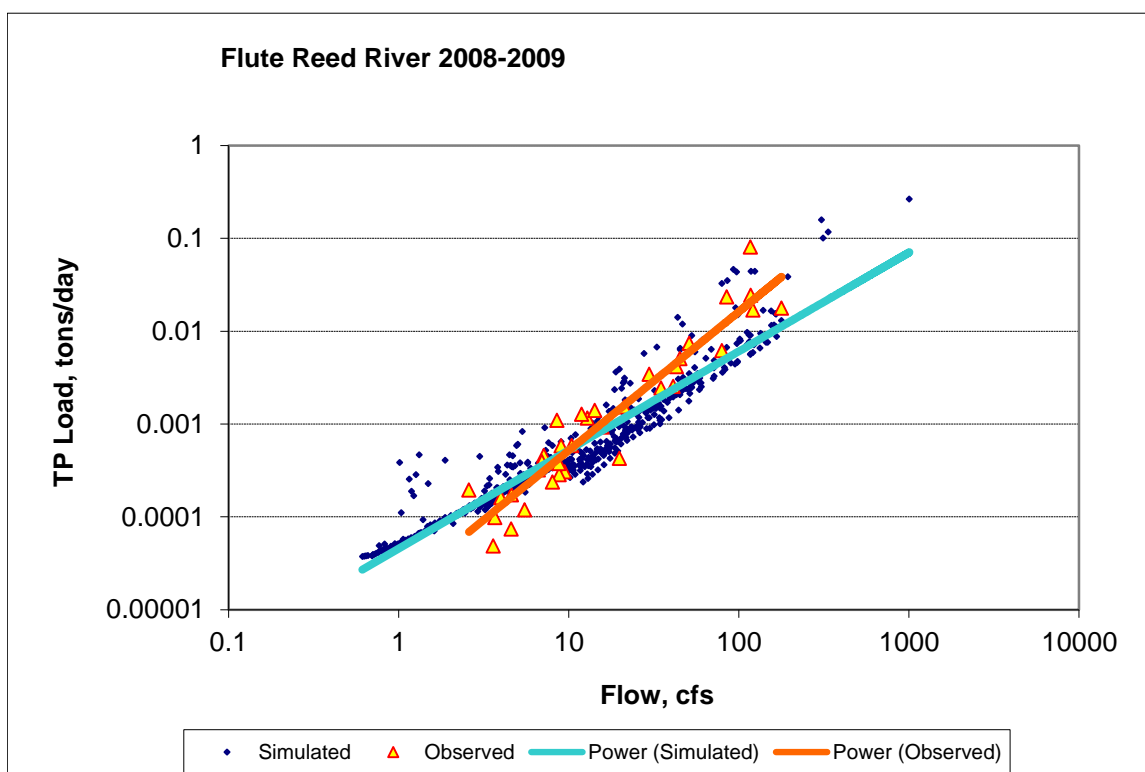


Figure 388. Power plot of simulated and observed Total Phosphorus (TP) load vs flow at Flute Reed River (validation period)

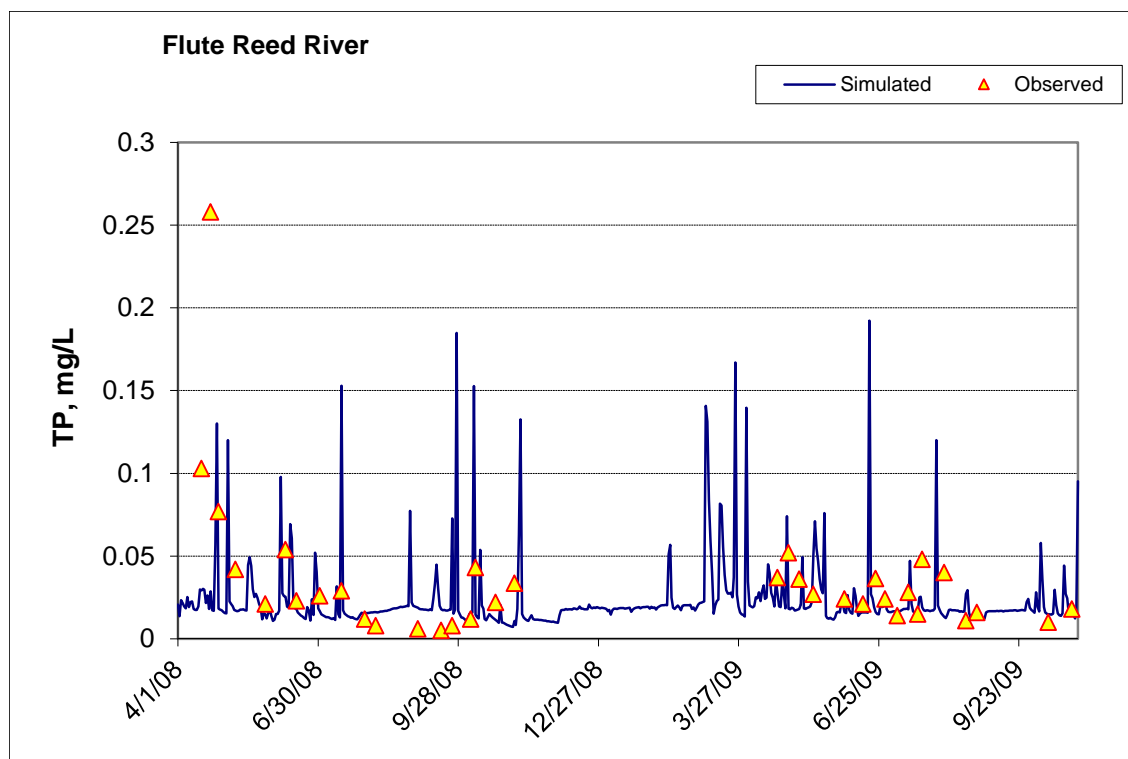


Figure 389. Time series of observed and simulated Total Phosphorus (TP) concentration at Flute Reed River

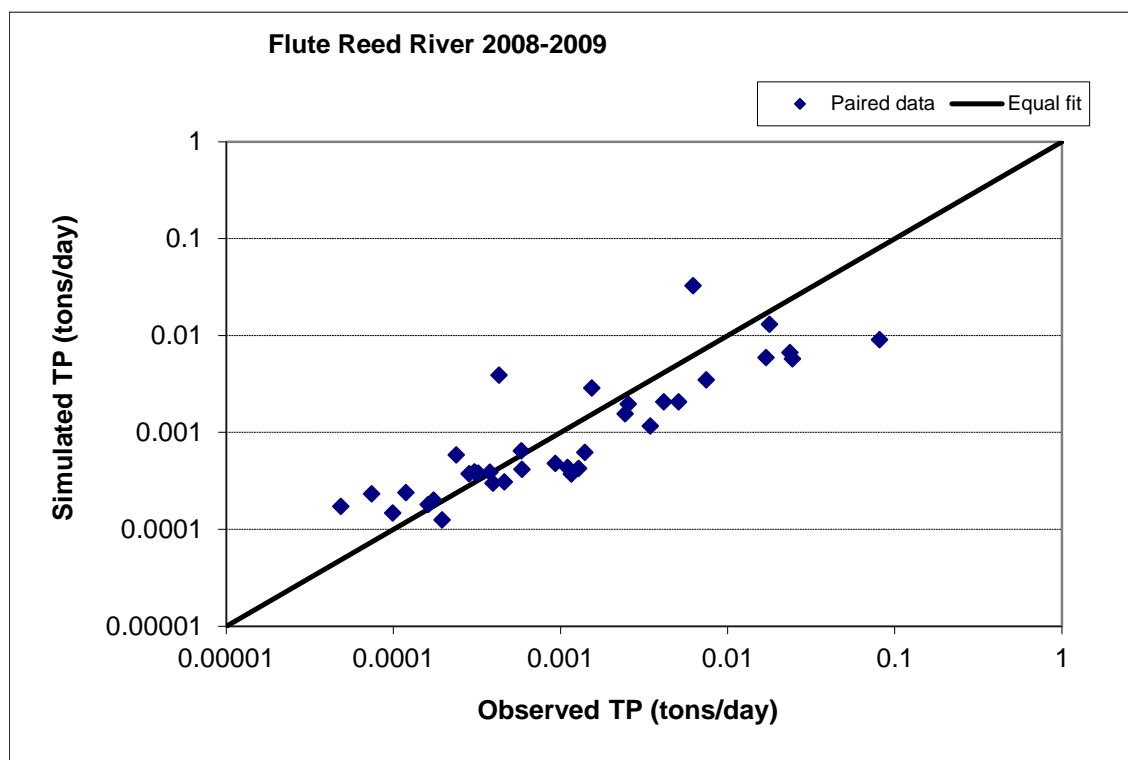


Figure 390. Paired simulated vs. observed Total Phosphorus (TP) load at Flute Reed River (validation period)

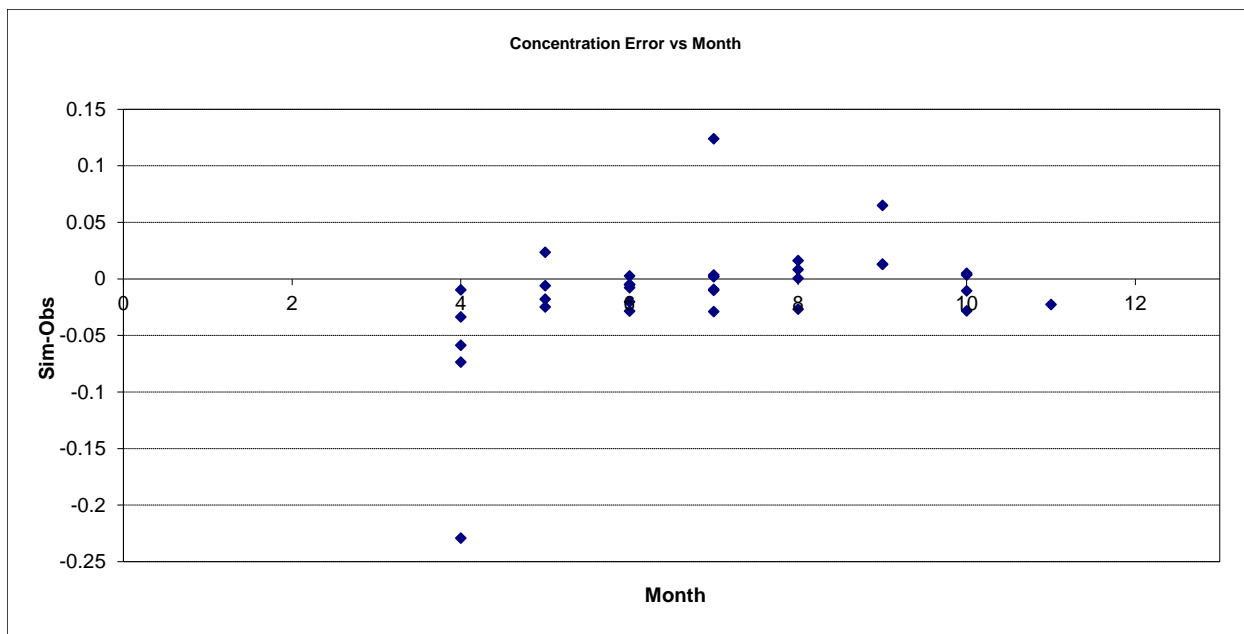


Figure 391. Residual (Simulated - Observed) vs. Month Total Phosphorus (TP) at Flute Reed River

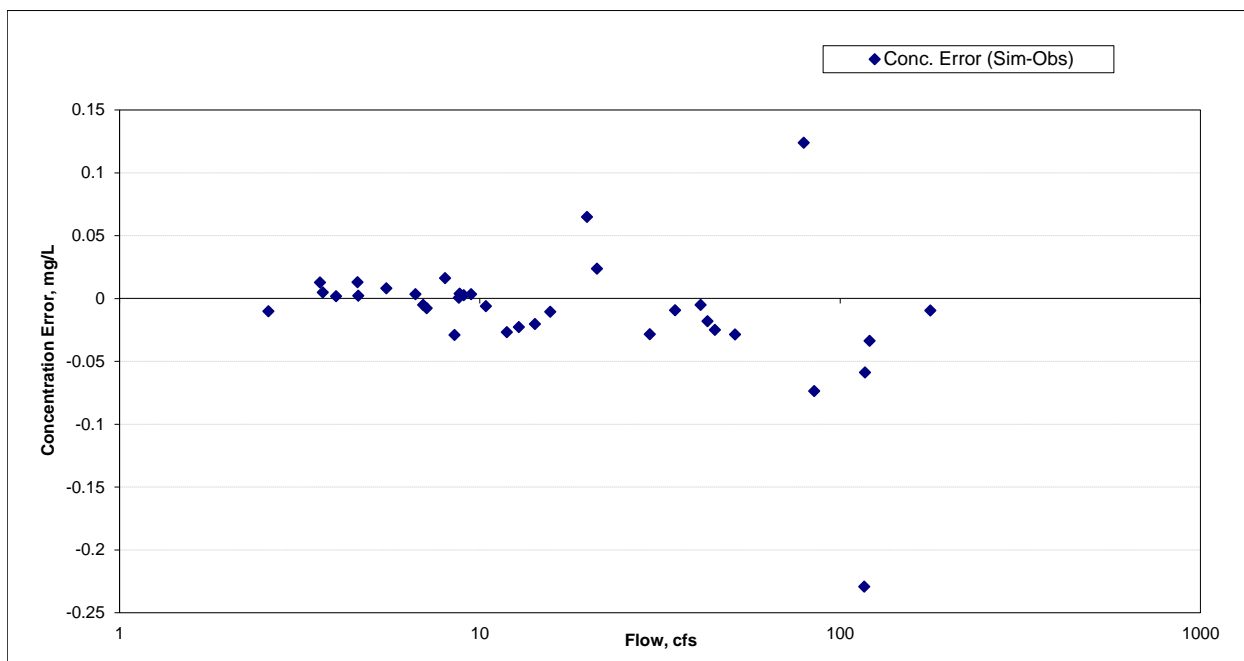


Figure 392. Residual (Simulated - Observed) vs. Flow Total Phosphorus (TP) at Flute Reed River



Lake Superior North and Lake Superior South Basins

Watershed Model Development Report

Prepared for
Minnesota Pollution Control Agency

Prepared by



One Park Drive, Suite 200 • PO Box 14409
Research Triangle Park, NC 27709

June 30, 2016

(This page left intentionally blank.)

Table of Contents

1	Introduction.....	1
2	Watershed Model Development	5
2.1	Upland Representation	5
2.1.1	Geology, Soils, and Slopes	5
2.1.2	Land Cover and Land Use	13
2.1.3	Development of Hydrologic Response Units.....	16
2.2	Meteorology	20
2.2.1	NLDAS and PRISM Data Processing.....	21
2.2.2	Auxiliary Weather Variables	25
2.3	Model Segmentation and Reach Network	26
2.3.1	Subwatershed Delineation	26
2.3.2	Stream Reach and Lake Delineation.....	30
2.3.3	Reach Hydraulics	35
2.4	Point Sources.....	41
2.5	Water Appropriations.....	42
3	Model Calibration and Validation Approach	45
3.1	Flow and Water Quality Data.....	45
3.2	Hydrology Calibration Approach	47
3.3	Sediment Calibration Approach	48
3.4	Water Quality Calibration Approach.....	51
4	Hydrology Calibration and Validation Results.....	55
4.1	Snow Calibration.....	55
4.2	Constraints on Soil Moisture Balance and Evapotranspiration	59
4.3	Flow Calibration.....	61
4.4	Flow Validation.....	64
4.5	Water Balance Summary	65
5	Sediment Calibration	67
5.1	Detached Sediment Storage.....	69
5.2	Upland Sediment Loading Rates	69
5.3	Reach Sediment Mass Balance.....	71
5.4	Calibration to Observed Suspended Solids Data	73
5.5	Comparison to FLUX Load Estimates	77

6	Nitrogen and Phosphorus Calibration.....	79
6.1	Nutrient Model Setup	79
6.1.1	Upland Sources	79
6.1.2	Channel Sources of Nutrients	83
6.1.3	Atmospheric Deposition	83
6.2	Nutrient Calibration.....	83
6.2.1	Comparison of Model to Observations	84
6.2.2	Comparison of Model to Flux Estimates of Delivered Load	89
6.2.3	Consistency with Lake Data	91
7	Water Temperature	93
8	Algae and Dissolved Oxygen	95
8.1	Algae	95
8.2	Dissolved Oxygen	97
9	Potential Model Enhancements	101
10	References	103

(The following appendices are included in a separate document.)

Appendix A.	Detailed Snow Calibration Results
Appendix B.	Detailed Flow Calibration Results
Appendix C.	Detailed Flow Validation Results
Appendix D.	Suspended Sediment and Water Quality Calibration and Validation

List of Tables

Table 2-1. Translation of Superior National Forest Terrestrial Ecological Unit Mapping into HSG	9
Table 2-2. Hydrologic Response Units for the Lake Superior Watershed Models	17
Table 2-3. Lakes Selected for Explicit Representation in Lake Superior South and North Watersheds.....	32
Table 2-4. Methods for Establishing Reach FTables.....	40
Table 2-5. Permitted Point Source Discharges in the Lake Superior South and North Models ..	41
Table 2-6. Permitted Surface Water Appropriations in the Lake Superior North and South Watersheds.....	43
Table 3-1. Selected HYDSTRA Flow Gage and EQUIS Water Quality Calibration Locations ..	45
Table 3-2. Water Quality Calibration Locations.....	46
Table 3-3. Performance Targets for HSPF Flow Simulation (Magnitude of Annual and Seasonal Relative Average Error; Daily and Monthly NSE)	48
Table 3-4. Performance Targets for HSPF Sediment Simulation (Magnitude of Annual and Seasonal Relative Average Error (<i>RE</i>) on Daily Values).....	51
Table 3-5. Performance Targets for HSPF Water Quality Simulation (Magnitude of Annual and Seasonal Relative Average Error (<i>RE</i>) on Daily Values).....	54
Table 4-1. HSPF Snow Calibration Parameter Values	55
Table 4-2. Summary of Snow Calibration Results	56
Table 4-3. Summary of Evapotranspiration Calibration Results	60
Table 4-4. Summary of Flow Calibration Results (Lake Superior South)	62
Table 4-5. Summary of Flow Calibration Results (Lake Superior North)	62
Table 4-6. Summary of Flow Validation Results	64
Table 4-7. Aggregated Water Balance for the Lake Superior South and North Watersheds (in/yr), based on 1993-2012 Simulations	65
Table 5-1. Average Upland Sediment Loading Rates (1993-2012) for Lake Superior South and North Watershed Models.....	70
Table 5-2. Summary of Sediment Calibration Results	76
Table 5-3. Comparison of Simulated and FLUX-Estimated Sediment Loads.....	78
Table 6-1. Reference Ranges for the Nutrient Loading Rates of Diverse Land Use Categories ..	80
Table 6-2. Summary Statistics for Total Phosphorus Calibration	86
Table 6-3. Summary Statistics for Total Nitrogen Calibration.....	86
Table 6-4. Summary Statistics for Total Nitrate+Nitrite-N Calibration	87

Table 6-5. MPCA FLUX Estimates and Model Simulated Annual Nutrient Loads, Calendar Years 2009-2011.....	91
Table 6-6. TP Concentrations in Explicitly Simulated Lakes of the Lake Superior South and Lake Superior North Watersheds	92
Table 8-1. Chlorophyll <i>a</i> Concentrations in Explicitly Simulated Lakes of the Lake Superior South and North Watersheds	96

List of Figures

Figure 1-1. Minnesota's Watershed Approach	1
Figure 1-2. Lake Superior North and Lake Superior South Watersheds	3
Figure 2-1. Bedrock Geology of the Lake Superior North Watershed	5
Figure 2-2. Bedrock Geology of the Lake Superior South Watershed	6
Figure 2-3. Digital Elevation Model of the Lake Superior North Watershed	7
Figure 2-4. Digital Elevation Model of the Lake Superior South Watershed	8
Figure 2-5. Hydrologic Soil Groups (HSG) for the Lake Superior North Watershed	11
Figure 2-6. Hydrologic Soil Groups (HSG) for the Lake Superior South Watershed	12
Figure 2-7. NLCD Land Cover for the Lake Superior North Watershed	14
Figure 2-8. NLCD Land Cover for the Lake Superior South Watershed	15
Figure 2-9. HRUs for the Lake Superior North Watershed	18
Figure 2-10. HRUs for the Lake Superior South Watershed	19
Figure 2-11. Snow Depth Normals (inches), 2002-2010	21
Figure 2-12. Weather Regions for the HSPF Model and Annual Precipitation Distribution	22
Figure 2-13. Comparison of EPA-BASINS and NLDAS Monthly Precipitation	23
Figure 2-14. Comparison of EPA-BASINS and PRISM Monthly Precipitation	24
Figure 2-15. Flow Gaging Locations in Lake Superior North and South Watersheds	27
Figure 2-16. Model Subwatershed Delineations for Lake Superior South Watershed	28
Figure 2-17. Model Subwatershed Delineations for Lake Superior South Watershed	29
Figure 2-18. Cumulative Distribution of Surface Area of Inline Lakes in the Lake Superior North and Lake Superior South Watersheds	30
Figure 2-19. Lakes Explicitly Represented in Lake Superior South Watershed	33
Figure 2-20. Lakes Explicitly Represented in Lake Superior North Watershed	34
Figure 2-21. Location of Permitted Point Source Discharges in the Lake Superior North and Lake Superior South Models	42
Figure 3-1. Shear Stress Distribution for Talmadge River (Reach 114)	50
Figure 4-1. Comparison of average monthly snow depth with SNODAS for Lake Superior South watershed	57
Figure 4-2. Comparison of Average Monthly Snow Depth to SNODAS for Lake Superior North watershed	57
Figure 4-3. Comparison of Average Monthly Snow Water Equivalents to SNODAS for Lake Superior South watershed	58

Figure 4-4. Comparison of Average Monthly Snow Water Equivalents to SNODAS for Lake Superior North watershed.....	58
Figure 4-5. Comparison of Average Monthly Simulated Evapotranspiration to MODIS Estimates for Lake Superior South Watershed.....	60
Figure 4-6. Comparison of Average Monthly Simulated Evapotranspiration to MODIS Estimates for Lake Superior North Watershed.....	61
Figure 4-7. Water Balance Distribution for the Lake Superior North Watershed	66
Figure 4-8. Water Balance Distribution for the Lake Superior South Watershed	66
Figure 5-1. Example Areas at High Risk of Bluff Collapse in the Amity Creek and Lester River Watersheds (http://www.nrri.umn.edu/coastalgis/newweb/html/bluffs.htm).....	68
Figure 5-2. Example Detached Sediment Storage (DETS) Series for Selected HRUs in the Lake Superior South Watershed	69
Figure 5-3. Reach Sediment Balance, Lake Superior South Watershed Model, 1993-2012.....	72
Figure 5-4. Reach Sediment Balance, Lake Superior North Watershed Model, 1993-2012.....	72
Figure 5-5. Simulated Average Annual Reach Scour and Deposition, Lake Superior South and North Watershed Models (tons/mi/yr), 1993-2012	73
Figure 5-6. Time Series Plot for Total Suspended Sediment Concentrations, Knife River near Two Harbors	74
Figure 5-7. Log-log Power Plot of Simulated Total Suspended Sediment Load and Load Inferred from Observed Concentration, Knife River near Two Harbors	75
Figure 5-8. Distribution of Concentration Error for Total Suspended Sediment, Knife River near Two Harbors	75
Figure 6-1. Average Simulated Total Nitrogen (TN) Unit Loading Rates for Land Use Categories in the Lake Superior South Watershed.....	81
Figure 6-2. Average Simulated Total Phosphorus (TP) Unit Loading Rates for Land Use Categories in the Lake Superior South Watershed.....	81
Figure 6-3. Average Simulated Total Nitrogen (TN) Unit Loading Rates for Land Use Categories in the Lake Superior North Watershed.....	82
Figure 6-4. Average Simulated Total Phosphorus (TP) Unit Loading Rates for Land Use Categories in the Lake Superior North Watershed.....	82
Figure 6-5. Example Calibration Plots for Total Phosphorus, Sucker River in the Lake Superior South Watershed.....	85
Figure 6-6. Comparison of Model to MPCA FLUX Estimates of Pollutant Load, Calendar Years 2009-2011, Sucker River near Palmers	89
Figure 6-7. Comparison of Model to MPCA FLUX Estimates of Pollutant Load, Calendar Years 2009-2011, Baptism River near Beaver Bay	90

Figure 6-8. Comparison of Model to MPCA FLUX Estimates of Pollutant Load, Calendar Years 2009-2011, Poplar River near Lutsen.....	90
Figure 7-1. Time-series of Simulated Average Daily Water Temperature Compared to Point-in-time Measurements in Amity Creek.....	94
Figure 8-1. Process Diagram for Oxygen Mass Balance in HSPF	97
Figure 8-2. Time-series plot of simulated average daily DO versus observed for Amity Creek	99

(This page left intentionally blank.)

1 Introduction

This report transmits and describes the hydrologic and water quality calibration of a watershed model of Minnesota's Lake Superior North (also known as Baptism-Brule) and Lake Superior South (also known as Beaver-Lester) basins (8-digit hydrologic unit codes [HUC8]: 04010101 and 04010102 - Figure 1-2), developed using the Hydrologic Simulation Program - FORTRAN or HSPF model (Bicknell et al., 2014). The MPCA is developing HSPF models for most HUC8 watersheds in Minnesota. These models are intended to provide information that supports total maximum daily load studies (TMDLs), watershed restoration and protection strategies, and comprehensive watershed planning under Minnesota's Watershed Approach (Figure 1-1). In addition to simulating hydrology, these models are designed to support biological stressor identification and analysis of pollution-related impairments such as elevated turbidity and the effects of elevated nutrient concentrations. The models are also useful to support analysis needed to develop TMDLs for dissolved oxygen and temperature, as well as to provide a tool for evaluating appropriate point source effluent limits for permitted facilities and evaluating management scenarios.

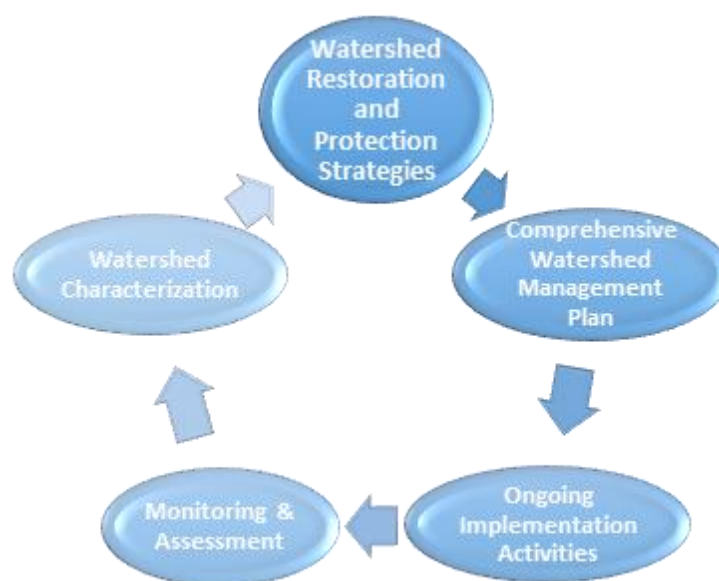


Figure 1-1. Minnesota's Watershed Approach

A watershed model is a tool to aid understanding of processes and consequences of human activities in a river basin, but is only one among a variety of tools. In particular, watershed models are not substitutes for the direct monitoring of physical and biological conditions. When properly calibrated to reproduce observed measurements, the models can, however, provide a reasonable mechanism for the extrapolation of monitoring data in space (to unmonitored locations) and in time (to unmonitored or future time periods). The watershed model also enables experiments to investigate how changes (such as changes in land use, management practices, or climate) may affect conditions in the watershed and allow stakeholders to plan accordingly. To be useful for these purposes the credibility of the model (and its associated level of uncertainty) must be established through comparison to real world data and through stakeholder input. This report is the initial step in that process.

Two meetings with stakeholders were held: October 2, 2014 and September 24, 2015. Meeting attendees represented the following organizations:

- Carlton Soil and Water Conservation District
- Cook Soil and Water Conservation District
- Fond du Lac Band of Lake Superior Chippewa
- Koochiching Soil and Water Conservation District
- Lake Soil and Water Conservation District
- Minnesota Department of Agriculture
- Minnesota Department of Natural Resources
- Minnesota Pollution Control Agency (Duluth and St. Paul offices)
- Minnesota Power
- Natural Resources Research Institute
- North St. Louis Soil and Water Conservation District
- South St. Louis Soil and Water Conservation District
- St. Louis County
- Superior National Forest, United States Forest Service
- United States Environmental Protection Agency
- United States Geological Survey
- University of Minnesota—Duluth
- Wisconsin Department of Natural Resources

At the first meeting, an overview of the project was provided, including the model structure, types of input and output data, and potential uses of the model. A data inventory was presented and stakeholders were asked to provide information on additional data that could be incorporated into the model development or calibration. At the second meeting, the model framework was presented, including the data used to develop and calibrate the model. Preliminary hydrology calibration graphics were presented. Potential approaches to model scenarios were discussed.

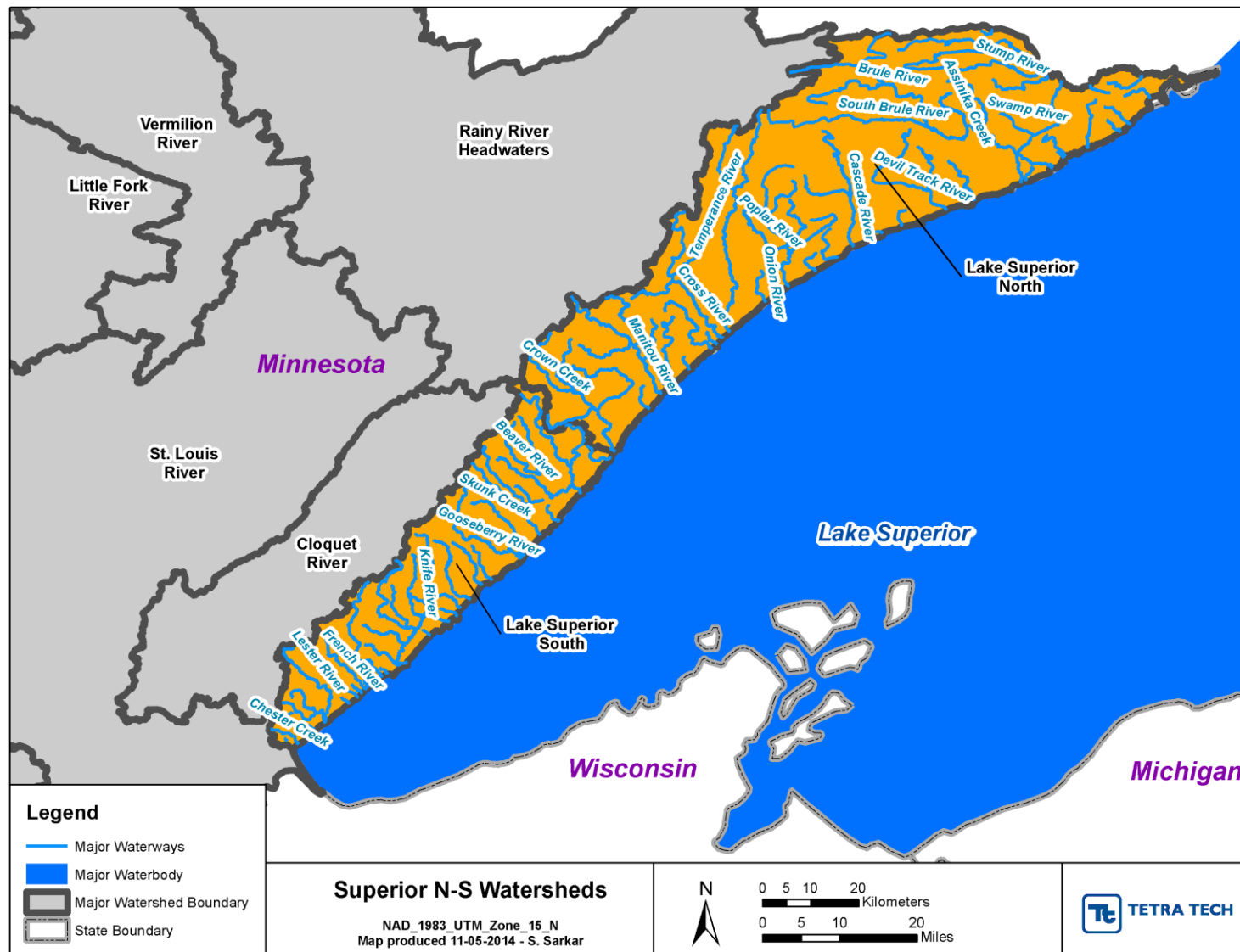


Figure 1-2. Lake Superior North and Lake Superior South Watersheds

(This page left intentionally blank.)

2 Watershed Model Development

2.1 UPLAND REPRESENTATION

The HSPF model was set up using a Hydrologic Response Unit (HRU) approach. The HRU concept provides a way to capture landscape variability into discrete units for modeling. In general, the HRU approach holds that landscapes possess an identifiable spatial structure, and that the corresponding patterns of runoff and stream chemistry are strongly influenced by climate, geology, and land use. An HRU is defined as a unit of land with relatively homogenous hydrologic properties determined by its underlying characteristics.

2.1.1 Geology, Soils, and Slopes

Geology is an important factor in the physical and chemical characteristics of soils in the Lake Superior North and Lake Superior South watersheds, and much of the area has thin soils with areas of exposed rock. Bedrock geology of these watersheds is shown in Figure 2-1 and Figure 2-2.

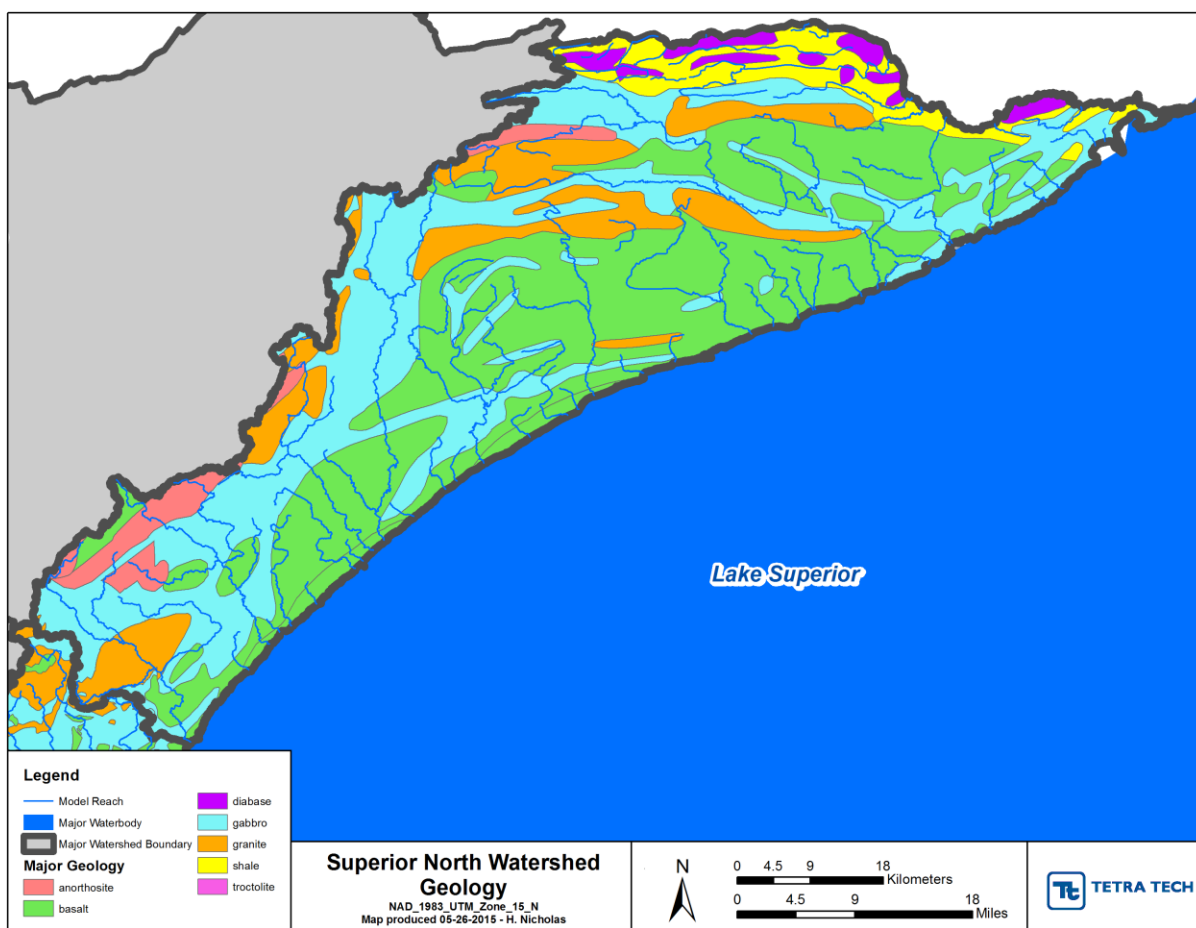


Figure 2-1. Bedrock Geology of the Lake Superior North Watershed

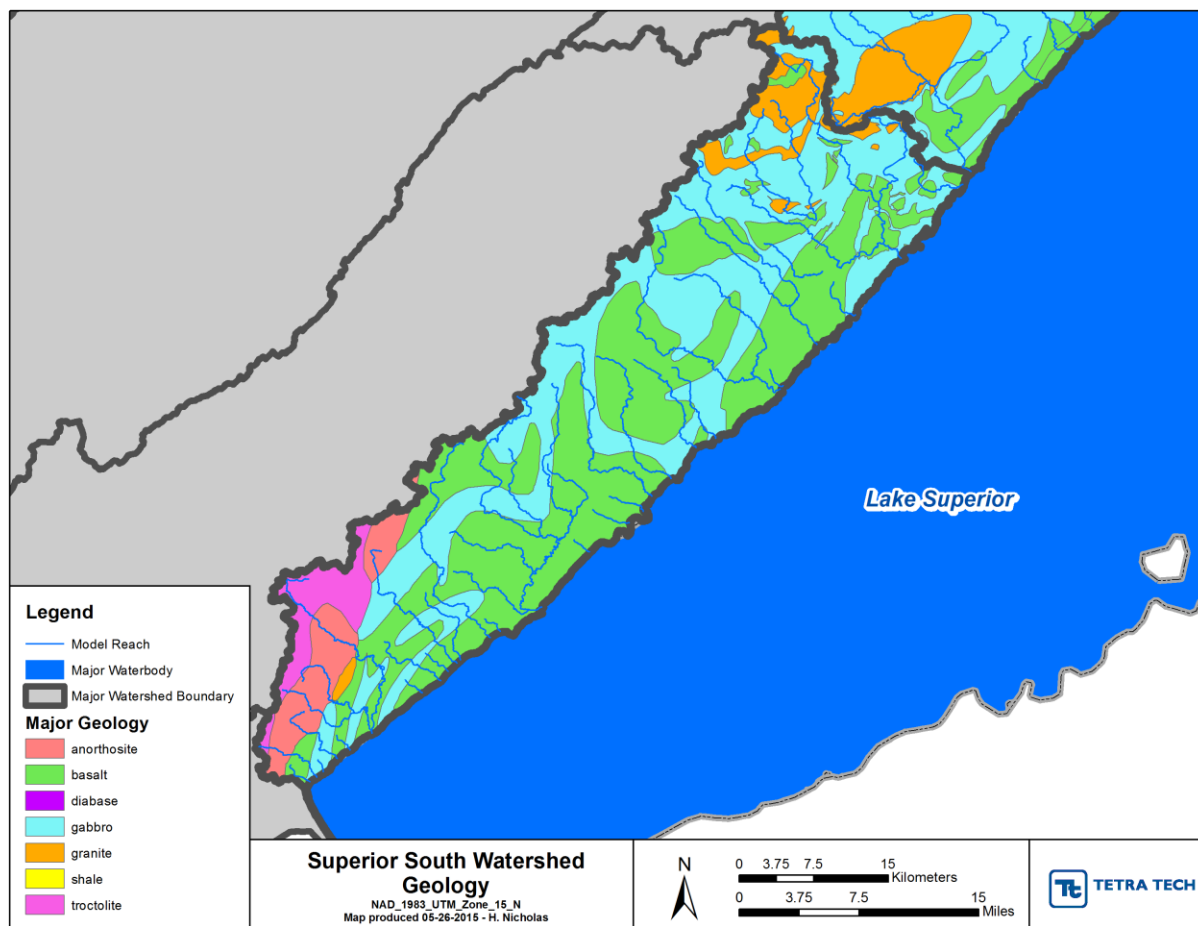


Figure 2-2. Bedrock Geology of the Lake Superior South Watershed

Topography of the watershed is dominated by the steep scarp between the uplands and the current extent of Lake Superior. Down-gradient of the scarp there are areas of lacustrine soils near the lake. Upstream and to the northwest of the scarp the landscape is characterized by relatively flat land with extensive swamps and glacial lakes, especially in the Lake Superior North watershed.

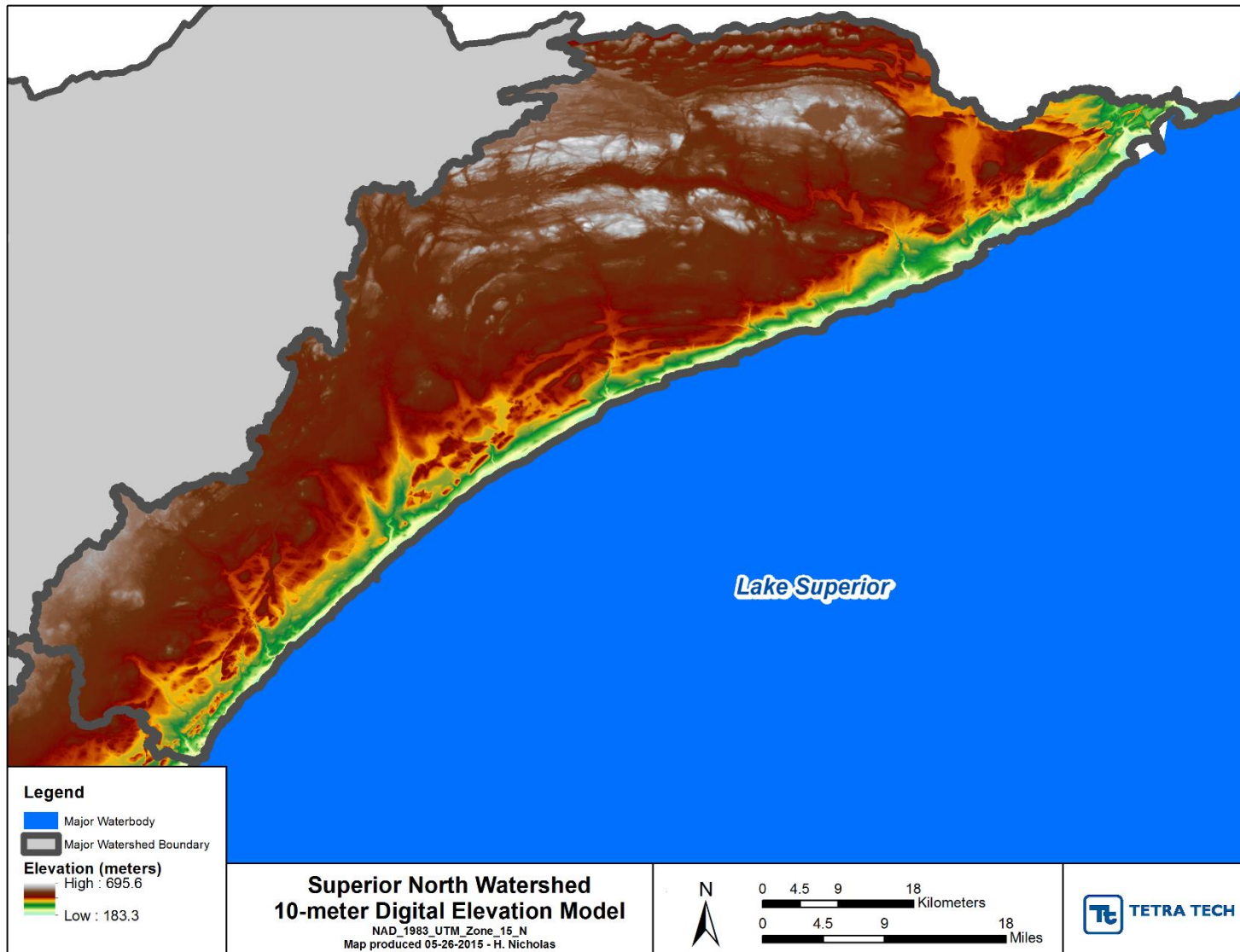


Figure 2-3. Digital Elevation Model of the Lake Superior North Watershed

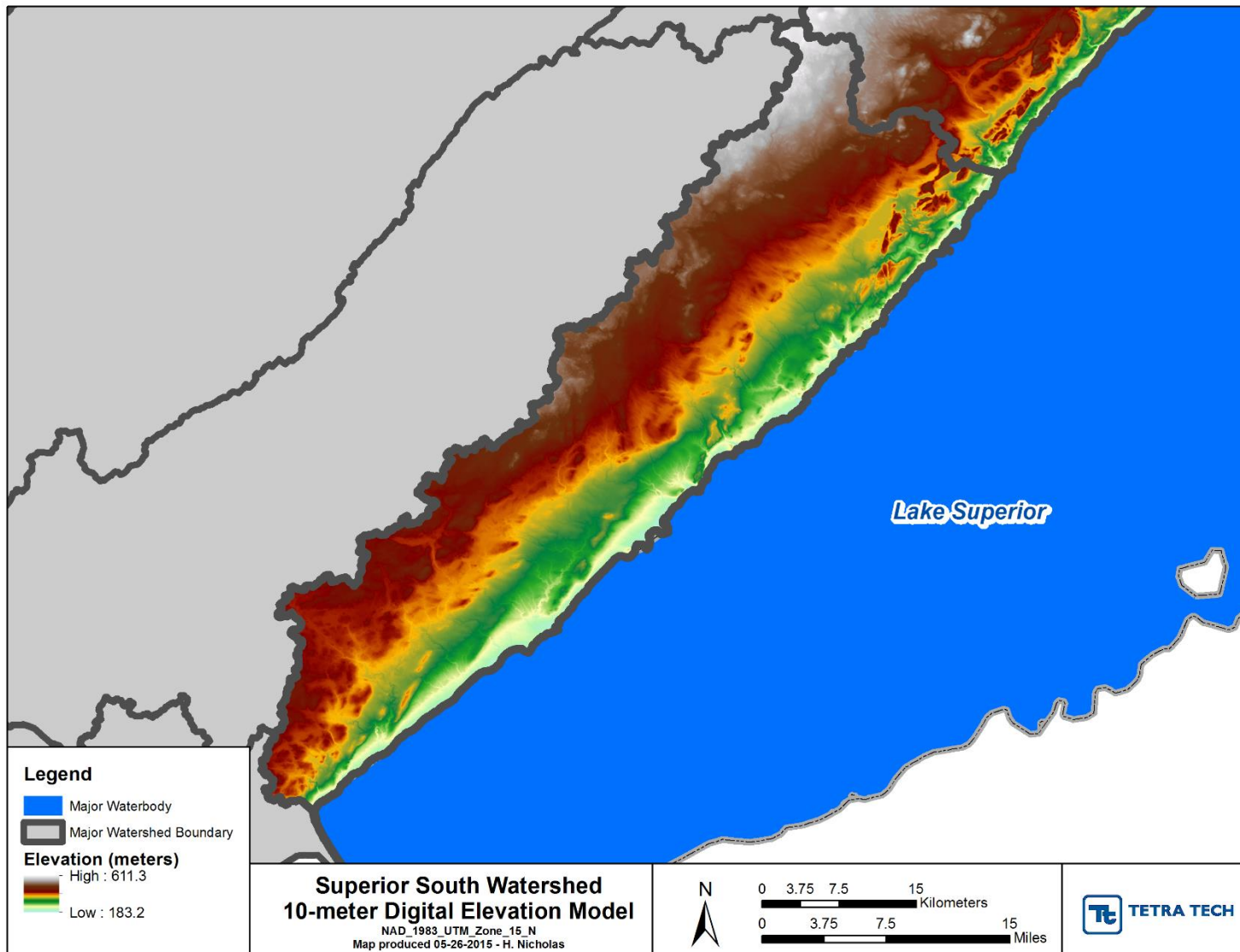


Figure 2-4. Digital Elevation Model of the Lake Superior South Watershed

For the purposes of hydrologic modeling, soils in the watershed were distinguished primarily by hydrologic soil group (HSG), which classifies soils according to infiltration potential. HSG was determined from the NRCS's Soil Survey Geographic Database (SSURGO). Where SSURGO data were not available, Superior National Forest Terrestrial Ecological Unit Mapping information provided by the U.S. Forest Service was translated into HSG (Table 2-1). Where neither SSURGO nor USFS data were available, HSG was determined from the NRCS's State Soil Geographic Database (STATSGO). Figure 2-5 and Figure 2-6 summarize the modeled HSGs.

Table 2-1. Translation of Superior National Forest Terrestrial Ecological Unit Mapping into HSG

Terrestrial Ecological Unit	Description	Translated HSG
8	Upland, well-drained sand and gravel soils with a water table at an estimated depth of five to eight feet and with plant communities having both upland and lowland species. Soils are susceptible to nutrient loss due to thinner surface organic layer and coarse textured soils.	A
9	Upland, droughty gravel and sandy soils with plant communities adapted to droughty conditions and a root zone dominated by gravels. Soils are susceptible to nutrient loss due to thinner surface organic layer and coarse textured soils.	A
11	Upland, well-drained sandy loam and loamy sand soils. Gravelly subsurface; plant communities adapted to dry sites. Soil susceptible to nutrient loss due to thin surface organic layer and coarse textured soils.	B
13	Upland, well-drained sandy loam and loamy sand soils with a gravelly subsurface and plant communities representative of dry uplands.	B
7	Upland, moderately well-drained sand and gravel soils with plant communities adapted to a fluctuating water table in a sandy root zone. Soils are susceptible to nutrient loss due to thinner surface organic layer and coarse textured soils	A
14	Upland, moderately well-drained, sandy loam to silt loam soils with a subsurface layer of dense soil that retains water for longer periods of time in some locations, and plant communities that have relatively high requirements for nutrients and moisture. Subsurface layer of dense soil will retain water long enough to create temporarily saturated soil in wet conditions and be more susceptible to rutting and compaction	C
15	Upland, well drained to moderately well-drained loam, clay loam and silt loam soils, and plant communities with a high requirement of nutrients and moisture. Silt and clay soils will retain water long enough to create temporarily saturated soil in wet conditions, more susceptible to rutting and compaction.	D
16	Upland, well-drained sandy loam or loam soils, 20 to 40 inches deep over bedrock. Plant communities have adapted to dry conditions and shallow soils depths to bedrock. Soils susceptible to nutrient loss due to thinner surface organic layer and shallow soil depth.	D
1	Lowland, moist loamy soils with plant communities that is transitional between uplands & lowlands. Somewhat poorly drained soils are susceptible to rutting and compaction when saturated.	C
10	Upland, moderately well-drained silty clay loam and clay soils with upland plant communities. Silty soils will retain water long enough to create temporarily saturated soil in wet conditions and be more susceptible to rutting and compaction.	D
12	Upland, poor to well-drained, bouldery, loamy soil. The ground is also covered with boulders. Plant communities have adapted to these site conditions. On some sites, the ground may be covered with boulders with very little vegetation. Soils are susceptible to nutrient loss due to lack of surface organic layer or organic layer underlain with boulders	C
2	Lowland, wet loamy and clayey soils with plant communities typical of wetlands. Can be forested or wetland shrub. Soils are susceptible to rutting and compaction due to continuous saturated conditions	D

Terrestrial Ecological Unit	Description	Translated HSG
3	Lowland, moist silty clay loam and clay soils with plant communities transitional between uplands and lowlands. Somewhat poorly drained soils are susceptible to rutting and compaction when saturated	D
4	Lowland, wet clay loam, silty clay, and clay soils with plant communities typical of clayey wetlands. Soils are susceptible to rutting and compaction due to continuous saturated conditions.	D
5	Lowland, acidic, poorly decomposed organic soils composed mainly of sphagnum and hyponym mosses with god plant communities adapted to permanently wet soils. Soils are susceptible to rutting and compaction due to continuous saturated conditions	D
6	Lowland, acidic to neutral organic soils composed of decaying woody plants and forbs with plant communities adapted to permanently wet soils. Soils are susceptible to rutting and compaction due to continuous saturated conditions.	D
17	Upland, well-drained sandy loam soils, 8 to 20 inches deep over bedrock. Plant communities have adapted to droughty conditions and shallow soil depths to bedrock. Soils are susceptible to nutrient loss due to thinner surface organic layer and shallow soil depth.	D
18	Upland, droughty loam and sandy loam soils less than eight inches deep over bedrock, with bedrock outcrops occurring on 5 to 30% of the ground surface. Plant communities have adapted to very dry conditions. Mosses commonly cover the ground. Soils are susceptible to nutrient loss due to the thinner surface organic layer and shallow soil depth.	D

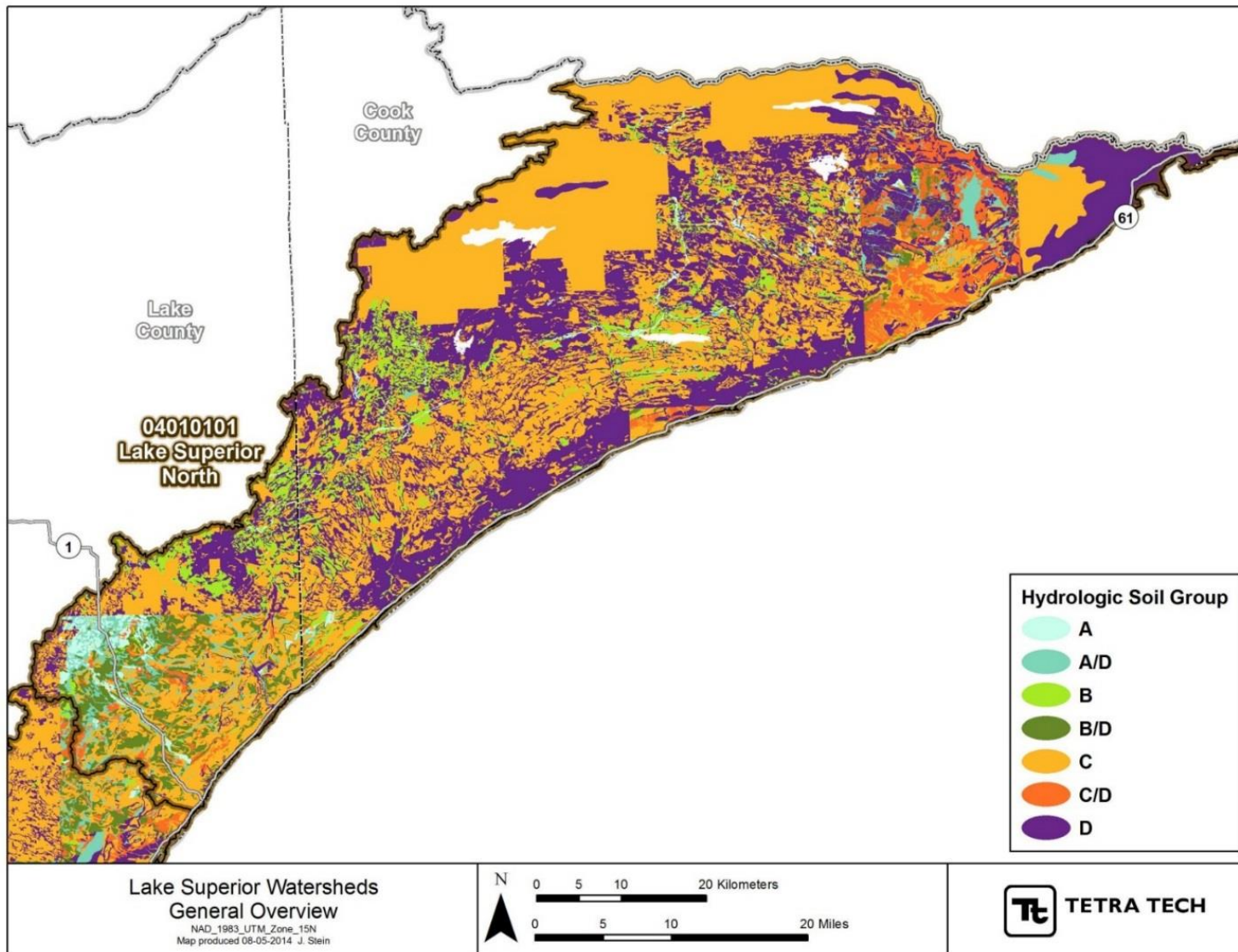


Figure 2-5. Hydrologic Soil Groups (HSG) for the Lake Superior North Watershed

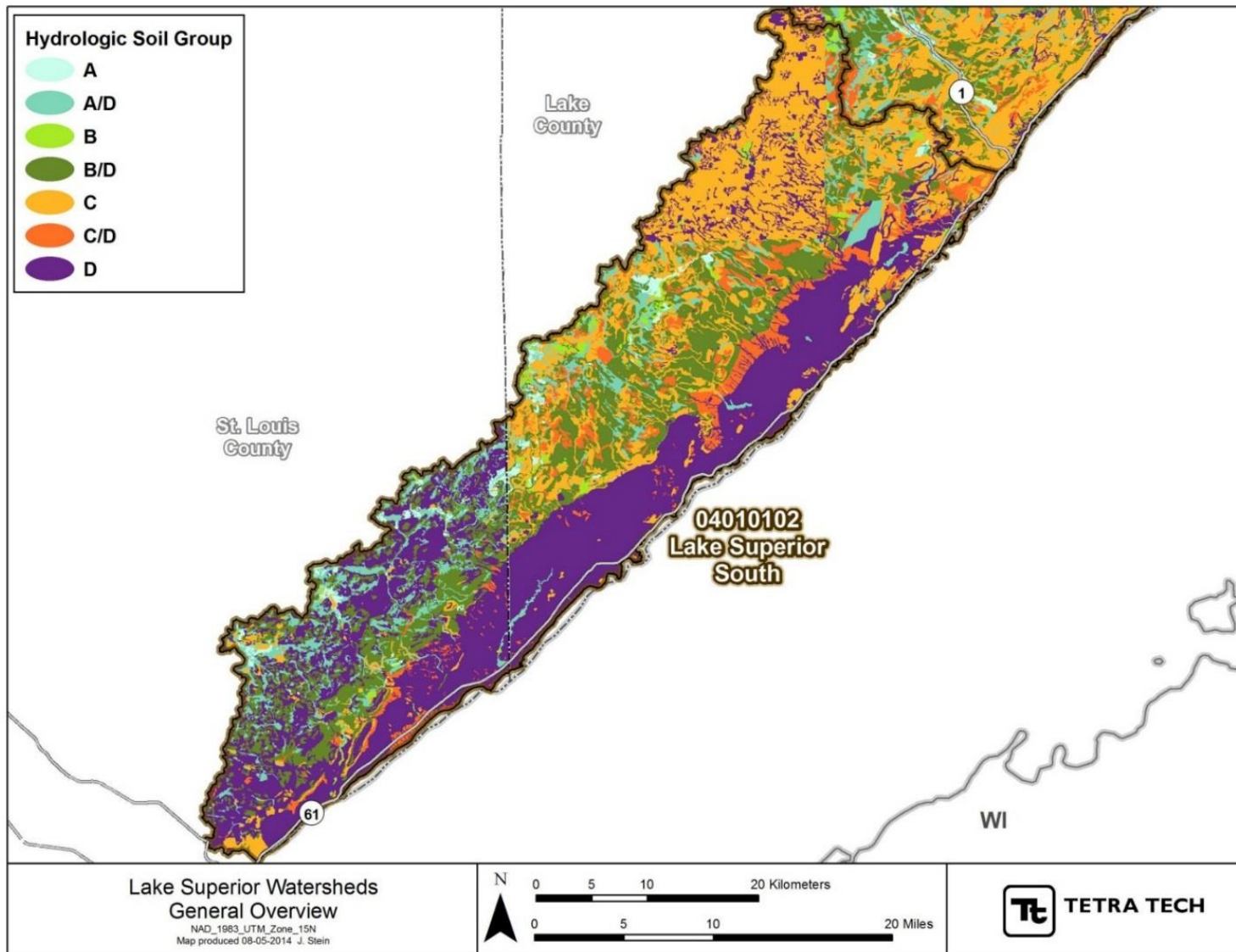


Figure 2-6. Hydrologic Soil Groups (HSG) for the Lake Superior South Watershed

2.1.2 Land Cover and Land Use

Forested areas and wetlands cover over 80% of the Lake Superior North and Lake Superior South watersheds (Figure 2-1 and Figure 2-2 and Table 2-2) according to the National Land Cover Database (NLCD) (MRLC, 2011). A portion of the City of Duluth is included in the Lake Superior South watershed and other small towns are present along Lake Superior including Two Harbors, Silver Bay, and Grand Marais. Developed land is approximately 6% of Lake Superior South and less than 2% of Lake Superior North.

Table 2-2. Land Cover Distribution in the Lake Superior North and Lake Superior South Watersheds

Land Cover Type	Lake Superior North		Lake Superior South	
	Acreage	% of Watershed	Acreage	% of Watershed
Deciduous Forest	235,456	23.2%	123,408	30.9%
Evergreen Forest	220,884	21.7%	42,595	10.7%
Mixed Forest	185,062	18.2%	72,420	18.1%
Shrub/Scrub	78,753	7.8%	29,924	7.5%
Grassland	9,322	0.9%	3,712	0.9%
Woody Wetlands	198,035	19.5%	84,321	21.1%
Emergent Herbaceous Wetlands	7,481	0.7%	5,882	1.5%
Developed, Open Space	16,148	1.6%	12,407	3.1%
Developed, Low Intensity	2,563	0.3%	6,438	1.6%
Developed, Medium Intensity	733	0.1%	3,505	0.9%
Developed, High Intensity	195	0.0%	812	0.2%
Hay/Pasture	279	0.0%	8,022	2.0%
Agriculture	188	0.0%	447	0.1%
Open Water	60,624	6.0%	4,088	1.0%
Barren Land	121	0.0%	1,401	0.4%
Unclassified	54	0.0%	0	0.0%
Total	1,015,898	100.0%	399,383	100.0%

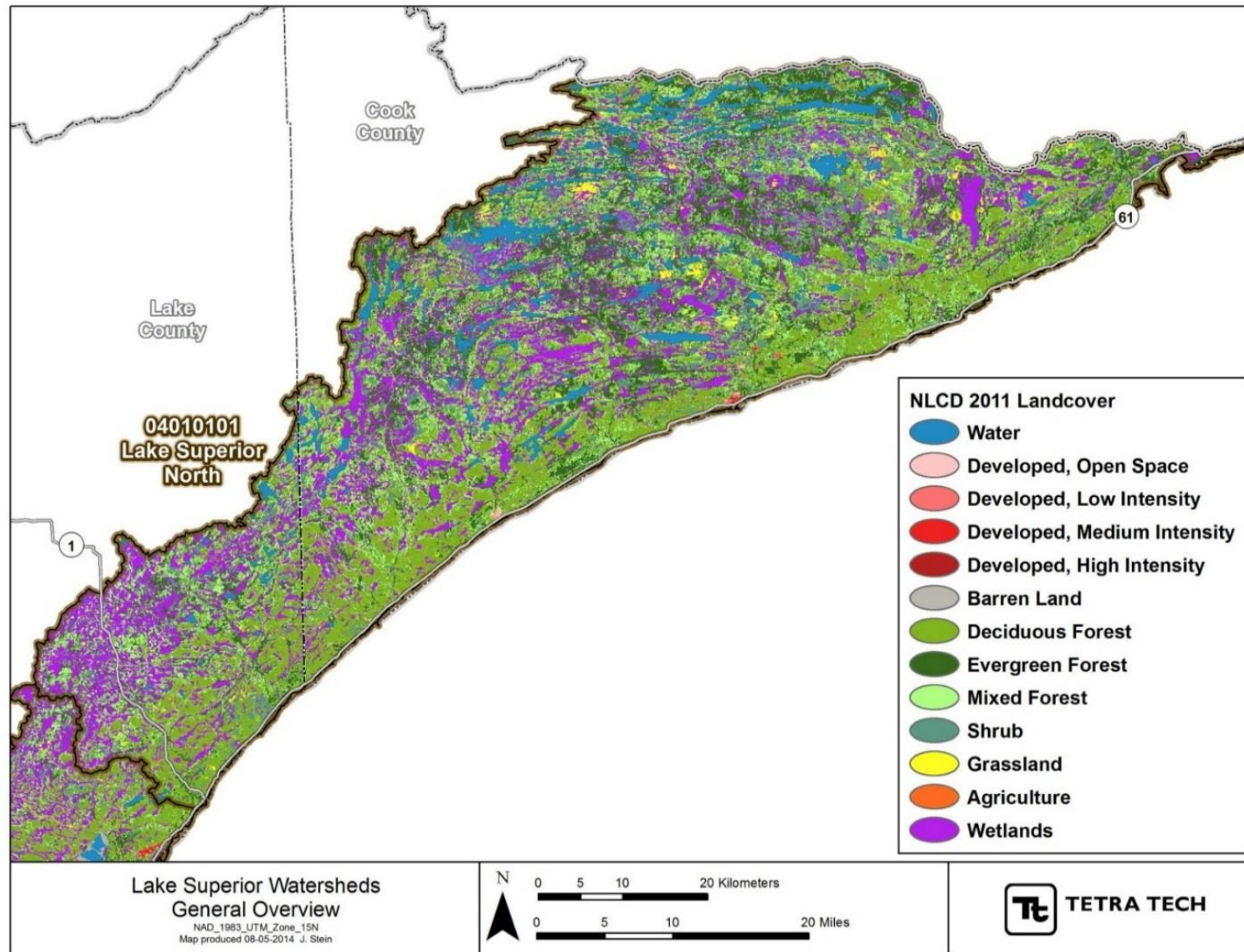


Figure 2-7. NLCD Land Cover for the Lake Superior North Watershed

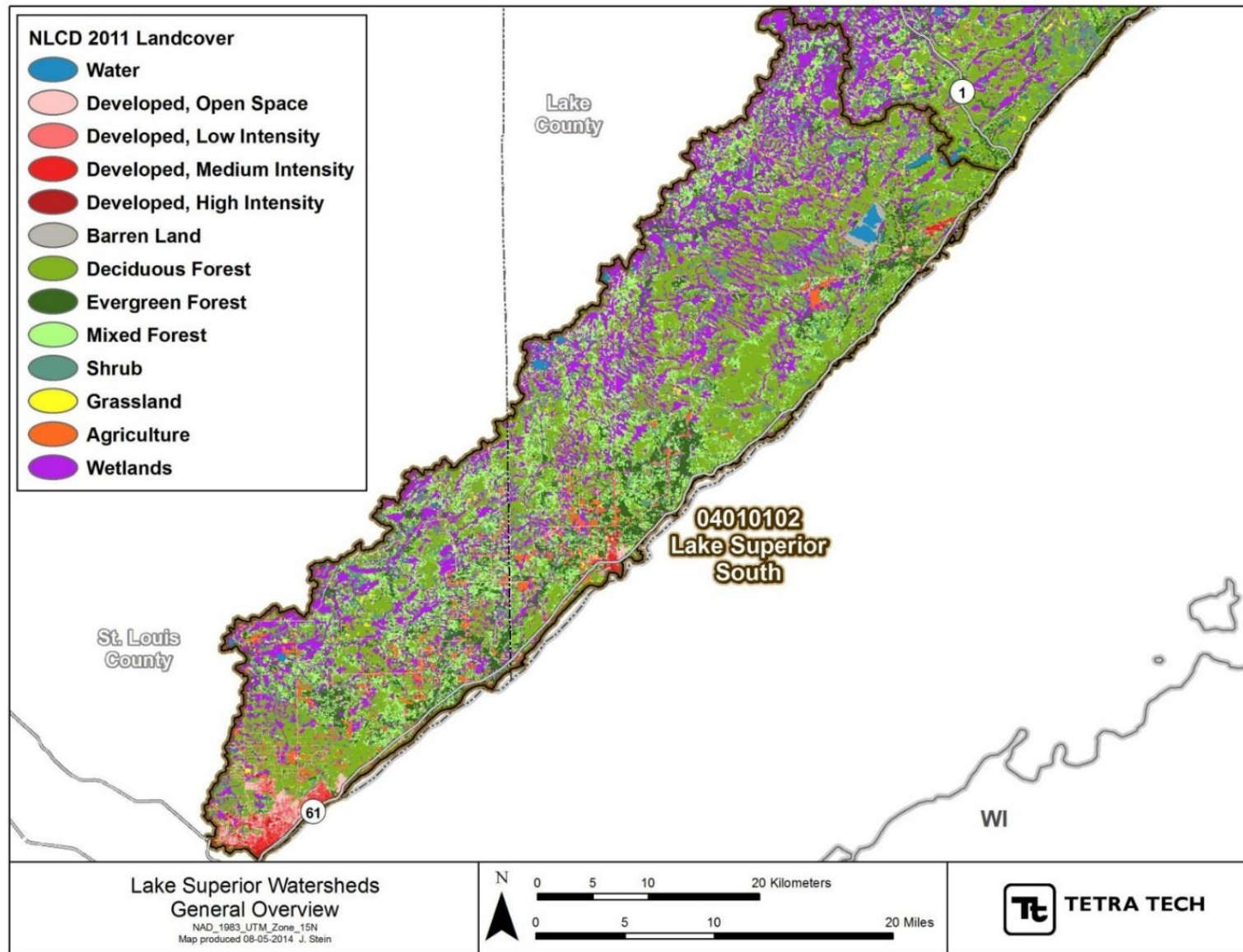


Figure 2-8. NLCD Land Cover for the Lake Superior South Watershed

2.1.3 Development of Hydrologic Response Units

The basic upland unit of the watershed model is the Hydrologic Response Unit or HRU, which represents a common set of characteristics for land use/cover and soil characteristics, along with weather station assignment. HRUs were developed consistent with the methods outlined in *Modeling Guidance for BASINS/HSPF Applications under the MPCA One Water Program* (AQUA TERRA, 2012).

Soils were distinguished primarily by HSG, which classifies soils according to infiltration potential (see Section 2.1.1). HRUs can also be characterized by slope classes where slope varies within a land use or soil type. Higher slopes in both the Lake Superior North and Lake Superior South watersheds occur on largely homogeneous land cover and soil types. These higher slopes occur on a scarp that extends inland along the north shore of Lake Superior, where igneous rocks from the Laurentian Plateau are exposed as the land surface descends to the lake surface (see Section 2.1.1). The land cover along the scarp is primarily deciduous forest. Therefore, separation into slope classes was deemed not necessary for these watersheds because the slope information is largely redundant with the land use and soil classes. High resolution is maintained among the forest classes due to their large area in these watersheds.

The National Land Cover Database (NLCD; MRLC, 2011) provides the basis for land use distribution (Figure 2-7 and Figure 2-8). NLCD classes were aggregated and combined with additional sources of information (Table 2-2). The initial land use analysis was performed using grid math in ArcGIS. LANDFIRE (Landscape Fire and Resource Management Planning Tools Project; LANDFIRE, 2013) spatial coverages were used to distribute NLCD “mixed forested” classifications into deciduous and evergreen forest based on dominant cover. Other land use types, such as barren, grass/shrub, and crop land use groups are a small fraction of the watershed area, and were not subdivided further.

Table 2-2 provides the sources of data used to refine the NLCD dataset land use categories. The NLCD and LANDFIRE coverages do a poor job of identifying roads, particularly in forested areas, and their road areas do not always align properly. Therefore, NLCD roads were dissolved back into the surrounding coverage and roads were re-evaluated based on TIGER (Topologically Integrated Geographic Encoding and Referencing) data. The TIGER roads datasets were overlain, or “burned into” the datasets listed above, which redistributed acreage from each unit. Road centerline data obtained at the county scale were compared with TIGER data. County centerlines not represented in the TIGER dataset consisted largely of narrow trails, which were burned into the land use as a component of the “barren” HRU.

The distribution of HSGs is shown above in Figure 2-5 and Figure 2-6. Hydrologic Soil Groups (HSG) for the Lake Superior South Watershed. Water, barren, and wetland HRUs are not subdivided by HSG, and HSG is not relevant for urban land covers due to disturbance and alteration of soil characteristics.

For the HSPF model, the pervious and impervious fractions of each developed land use class are separated. The Total Impervious Area (TIA) for each HRU was calculated based on NLCD impervious area coverages. NLCD grids were summed by impervious percentile and multiplied by that percentile to derive the impervious area, which was summed and divided by the total HRU area to derive the average impervious area for each HRU, as shown in Table 2-2. Effective impervious area (EIA) associated with each developed land use category was taken from Table 2.5 of AQUA TERRA (2012).

The final HRU distribution is shown in Figure 2-9 and Figure 2-10. Each land segment has as its base a three digit numeric code of the form *abc*, which represents the HRU-land use-HSG combination (Table 2-2). Different weather stations are assigned to HRUs by adding a multiple of 50 to the three digit numeric code for each weather station. This enables the land units to be grouped either by land use or weather station, which is useful for parameter entry.

The HRU numbering scheme summarized in Table 2-2 is applied directly to pervious land segments (PERLNDs). The same numbering scheme has been used for impervious land segments (IMPLNDs) associated with each pervious land segment. As evident from the table below, a percent imperviousness

is reported for all land covers and is generally small for all except the developed categories. As a result, impervious HRUs were only simulated for developed land cover classes. All road surfaces (both paved and unpaved, see Section 2.1.3) were simulated as impervious HRUs because unpaved roads are typically compacted and have minimal infiltration capacity; the adjacent road right of way is simulated as a pervious land use.

Table 2-2. Hydrologic Response Units for the Lake Superior Watershed Models

HRU Code	Description	HSG	Area (acres)	Percent Impervious	Data Source(s)
101	Water	C, D	64,300	0.0%	NLCD + HSG Overlay
102	Developed Open Space	-	27,510	8.5%	NLCD
103	Developed Low	-	6,541	32.3%	NLCD
104	Developed Med/High	-	2,216	58.1%	NLCD (Merge Med and High Density)
105	Barren/Trails	C, D	2,590	0.7%	NLCD + HSG Overlay + Narrow trails from county centerline data, DNR State Trails
106	Wetlands–Forested	A, B	282,831	0.1	NLCD + HSG Overlay
107	Wetlands–Herbaceous	C, D	11,234	0.1%	NLCD + HSG Overlay
108	Forest–Deciduous A,B	A, B	73,943	0.1%	NLCD Forest Codes + HSG Overlay + LANDFIRE
109	Forest–Deciduous C,D	C, D	338,054	0.1%	NLCD Forest Codes + HSG Overlay + LANDFIRE
110	Forest–Evergreen A,B	A, B	78,861	0.1%	NLCD Forest Codes + HSG Overlay + LANDFIRE
111	Forest–Evergreen C,D	C, D	373,323	0.1%	NLCD Forest Codes + HSG Overlay + LANDFIRE
112	Grassland/Shrubland A,B	A, B	27,242	0.1%	NLCD Herb/Shrub + HSG Overlay
113	Grassland/Shrubland C,D	C, D	101,905	0.1%	NLCD Herb/Shrub + HSG Overlay
114	Cropland/Pasture A,B	A, B	2,325	0.5%	NLCD + HSG Overlay
115	Cropland/Pasture C,D	C, D	6,919	0.5%	NLCD + HSG Overlay
116	Roads, Trails–Paved	-	10,804	10.6%	Roads: TIGER Primary, Secondary, and Local Streets (9m)
117	Roads–Unpaved	-	1,701	2.0%	TIGER Private Road and Vehicular Trail (9m)

NLCD: Land use data developed by The Multi-Resolution Land Characteristics (MRLC) consortium from decadal Landsat satellite imagery and other supplementary datasets. < <http://www.mrlc.gov/> >

DNR State Trails: Detailed spatial database of trails provided by MNDNR - Division of Parks and Trails. Includes information on trail usage, surface type, and width. < <http://www.dnr.state.mn.us/maps/index.html> >

LANDFIRE: a nationally complete, comprehensive, and consistent set of products that support fire and natural resource management organizations and applications. < <http://www.landfire.gov/datatool.php> >

TIGER: Spatial extracts from the Census Bureau's MAF/TIGER database, containing features such as roads, railroads, rivers, as well as legal and statistical geographic areas. < <https://www.census.gov/geo/maps-data/data/tiger-line.html> >

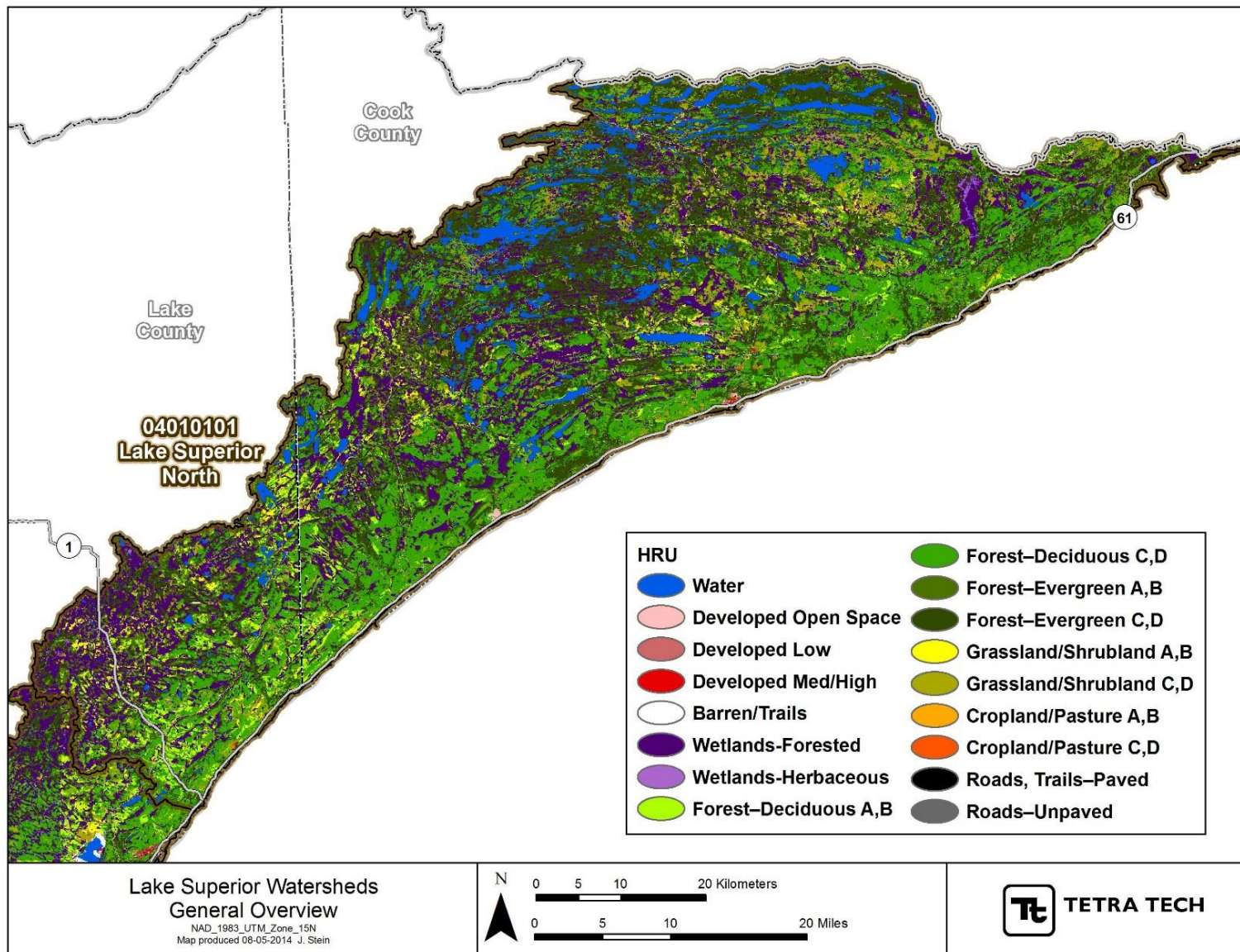


Figure 2-9. HRUs for the Lake Superior North Watershed

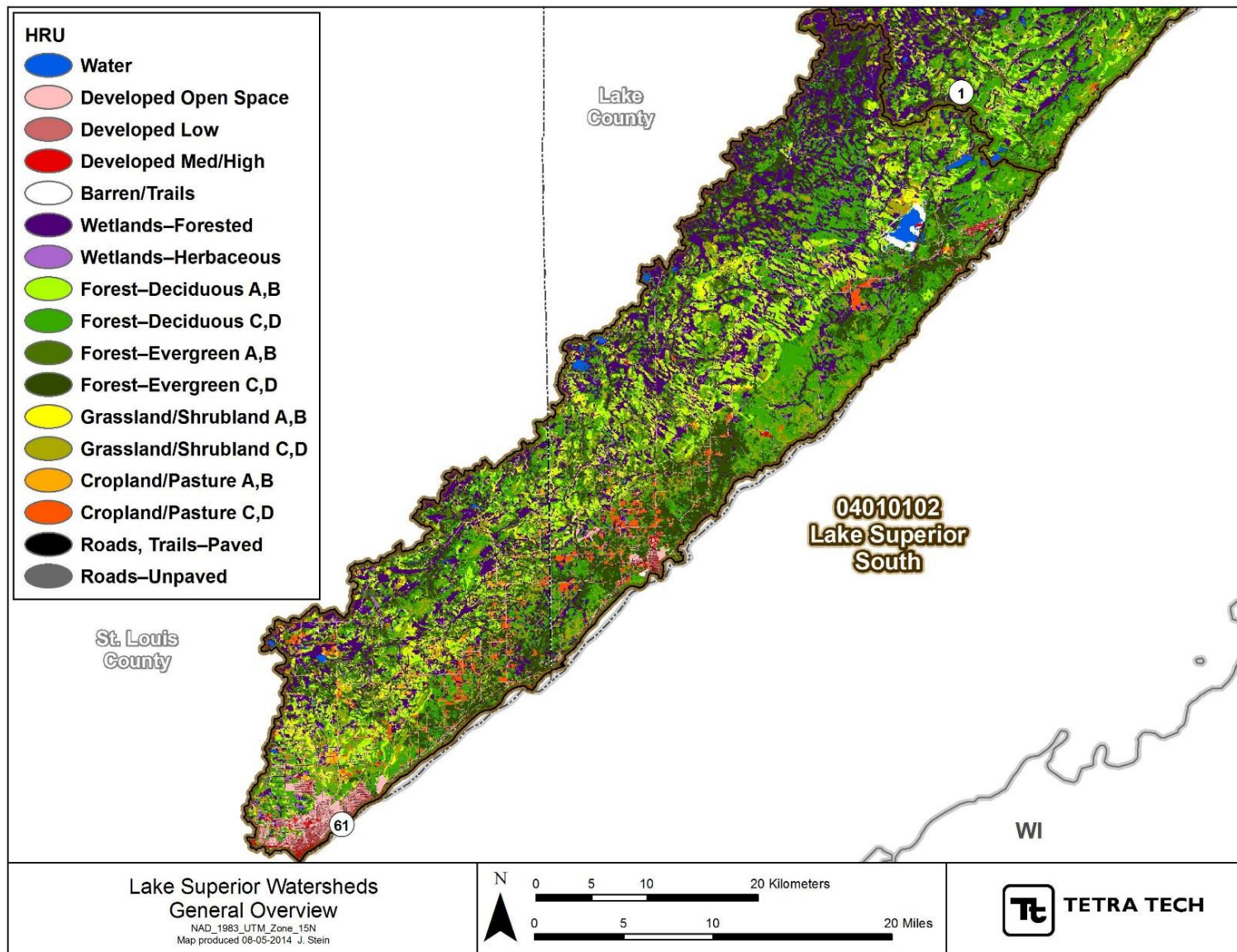


Figure 2-10. HRUs for the Lake Superior South Watershed

2.2 METEOROLOGY

Watershed responses are largely determined by meteorological inputs. Meteorological data required for an HSPF model consist of hourly precipitation (PREC), air temperature (ATEM), cloud cover (CLOU), dew point temperature (DEWP), solar radiation (SOLR), wind speed (WIND), and evapotranspiration (PEVT). MPCA has historically primarily relied on data available from the EPA-BASINS meteorological data set (USEPA, 2008) combined with local observed precipitation. However, the current version of the BASINS data extends only through 2009 necessitating analysis of newer data from the National Climatic Data Center (NCDC) and Minnesota State Climatologist for more recent periods, while significant QA work including patching missing observations is required for the local observer data. In addition, point-in-space monitoring records are often not representative of precipitation over a surrounding model area, especially during summer convective storms.

Weather in the Lake Superior North and South watersheds is strongly influenced by Lake Superior and the steep scarp that is present inland from the lake. These cause precipitation and temperature to vary strongly across short spatial scales – unlike most other Minnesota watersheds. This is evident, for example, in the spatial variation of snowfall across the watershed revealed by snowfall monitoring undertaken by the Minnesota Lake Superior Coastal Program (known as “Snow Rules!”) and supported by the State Climatology Office (<http://climate.umn.edu/snowrules/snowRules.htm>). Snow depth normals (Figure 2-11) show a region of peak snowfall inland of Wolf Ridge and a strong gradient from the lake. The pattern arises from changes in both elevation and the availability of moisture. Lake Superior is largely ice free in most winters and supplies moisture to cold, dry air flowing across its surface. The moisture is converted to snow when the air is re-cooled as it is lifted when it flows uphill as air crosses the shoreline. Similar patterns are seen for summer precipitation.

In recent years, several gridded meteorological products have been made available which have shown promise for water resources applications. Two such products were used for the development of the Lake Superior South and North watershed models. North American Land Data Assimilation System (NLDAS) provides continuous and gridded hourly data from 1979 to present and consists of all the meteorological forcing parameters required for an HSPF application. NLDAS was generally used for the development of meteorological time-series for the watershed models except for precipitation. The spatial resolution of NLDAS is however quite large (cell size approximately 12 km by 12 km) and may not represent spatial variation in precipitation over a small region well. As a result, another gridded dataset called PRISM was used for the development of precipitation time-series. PRISM provides continuous daily precipitation data from 1980 to present at a spatial resolution of 4 km by 4 km. Daily PRISM precipitation data were disaggregated to an hourly time-step using NLDAS hourly precipitation data as template.

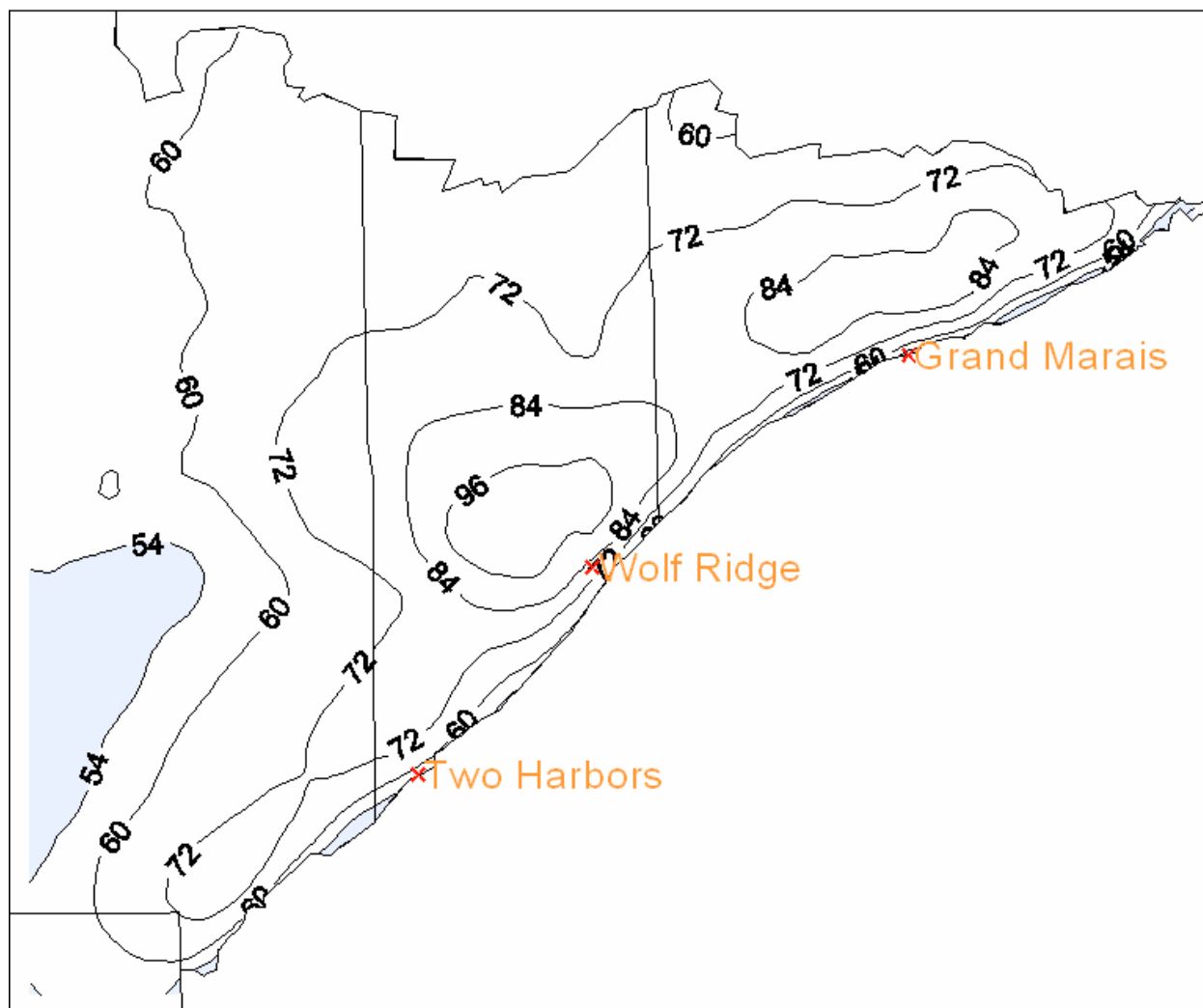


Figure 2-11. Snow Depth Normals (inches), 2002-2010

(<http://climate.umn.edu/snowrules/images/snow02-09.GIF>)

2.2.1 NLDAS and PRISM Data Processing

Daily PRISM precipitation files for the continental U.S. (CONUS) were downloaded and a Python script was developed to extract data for the grids intersecting the Lake Superior South and North watersheds. A total of 509 PRISM grid cells intersect the watersheds. In theory, each of these grid cells could be used to represent a weather station but that would result in the number of HRUs exceeding the upper bound of 999 for an HSPF application. As a result, these 509 grid cells were aggregated into regions of similar precipitation and snowfall. This methodology resulted in 18 weather regions (Figure 2-12). NLDAS files for the CONUS were also downloaded and a similar Python script was developed to extract data for the Lake Superior South and North watersheds. A total of 81 NLDAS grid cells intersect the watersheds.

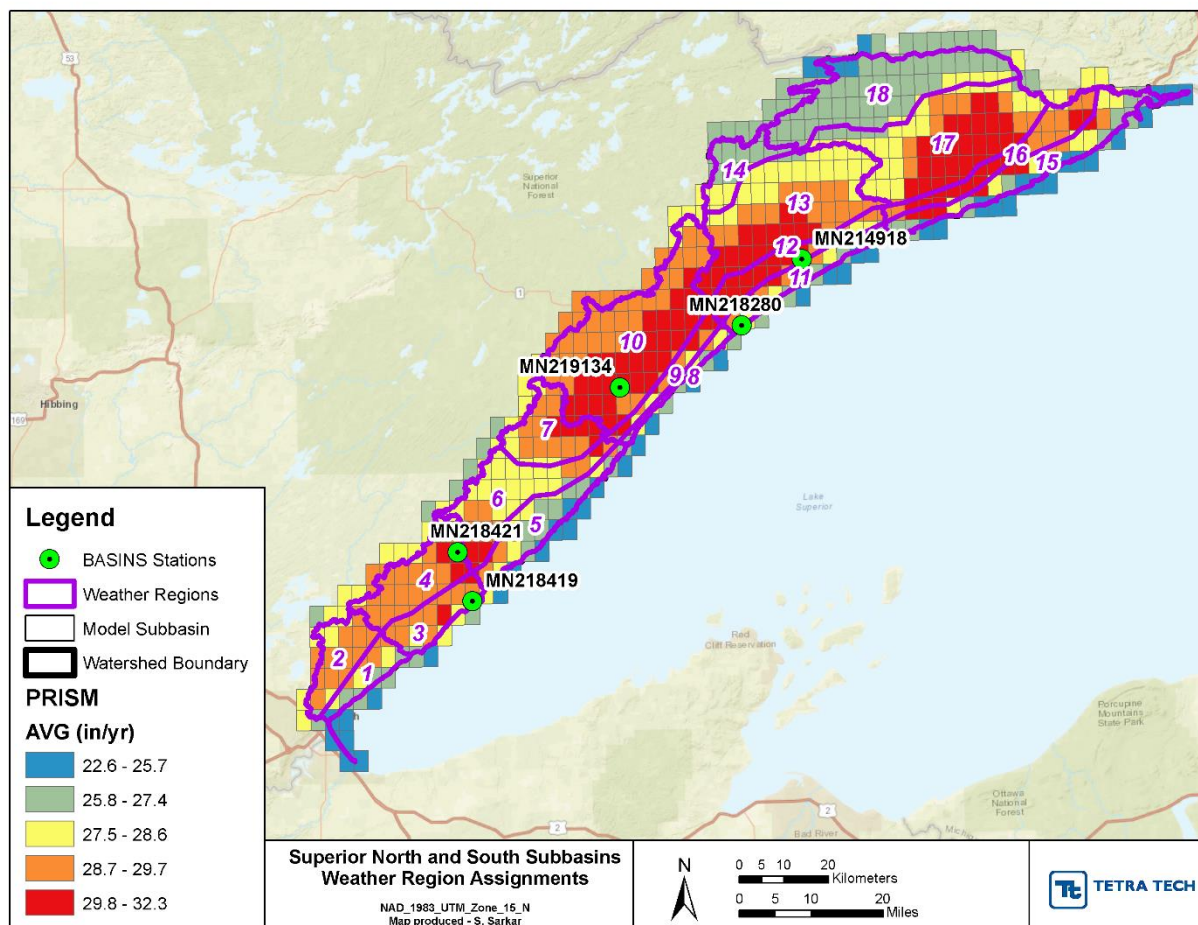


Figure 2-12. Weather Regions for the HSPF Model and Annual Precipitation Distribution

Both PRISM and NLDAS precipitation data were compared to rain gauge records in the BASINS meteorological data set to ensure that they were in general agreement. Comparisons were carried out for the following stations,

- MN218280 - Tofte Ranger Station
- MN219134 - Wolf Ridge ELC
- MN218419 - Two Harbors

An exact match is not expected, as totals at point gages can be affected by local convective storms and orographic effects. Monthly rainfall reported by NLDAS was generally found to be lower than that reported by BASINS (Figure 2-13). The total rainfall reported by NLDAS from 1993 to 2009 was found to be lower than reported by BASINS stations by 5% or more.

Figure 2-14 shows that the PRISM data generally correlates better with BASINS data. It was also found that the finer-resolution PRISM dataset generally represents the summer convective storm magnitudes better than the NLDAS dataset. PRISM precipitation is thus used in the watershed model. The differences in rainfall reported by PRISM and NLDAS are likely due to the differing interpolation techniques and spatial resolutions used by the two products. Other NLDAS meteorological parameters were also compared with BASINS and were generally found to be in agreement.

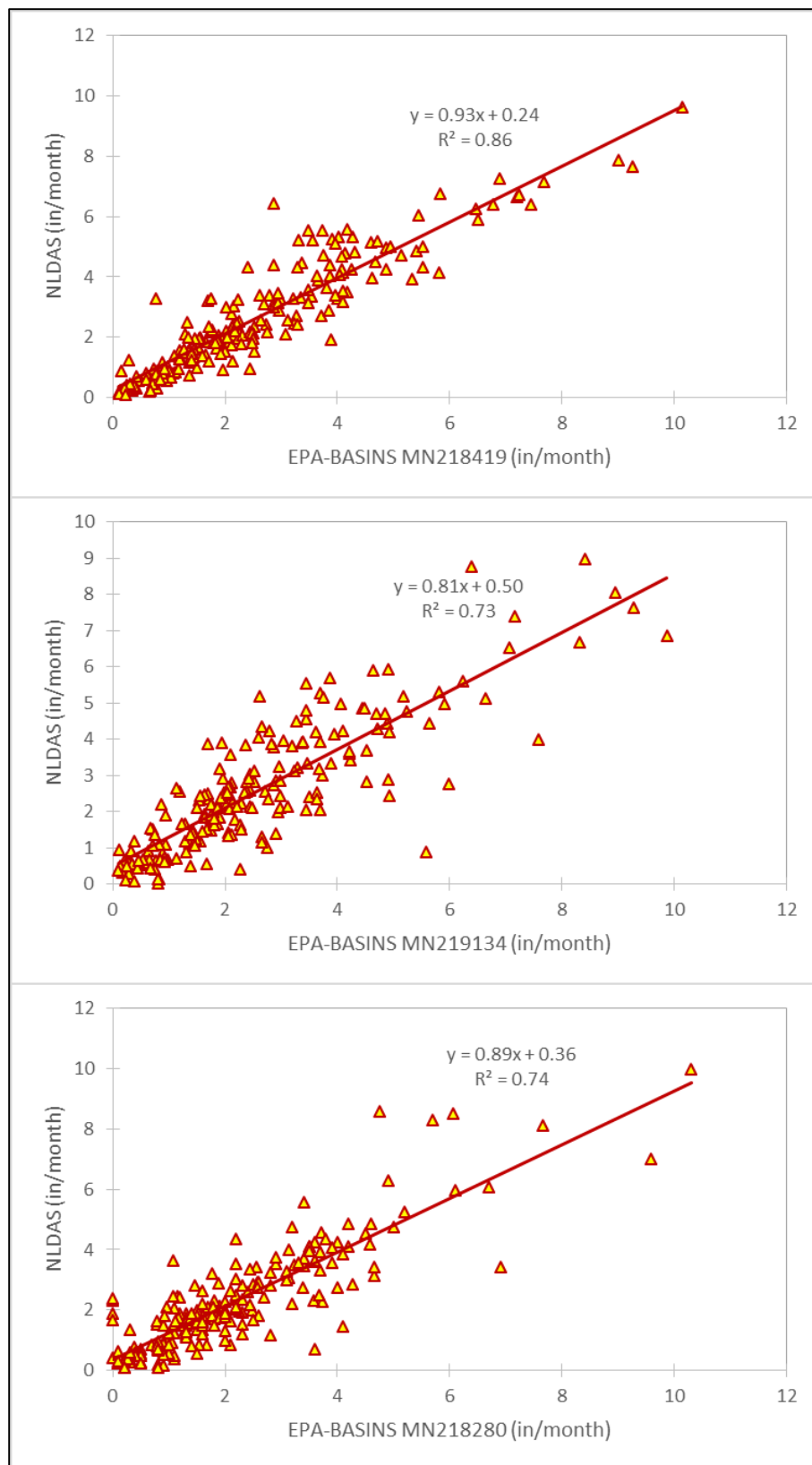
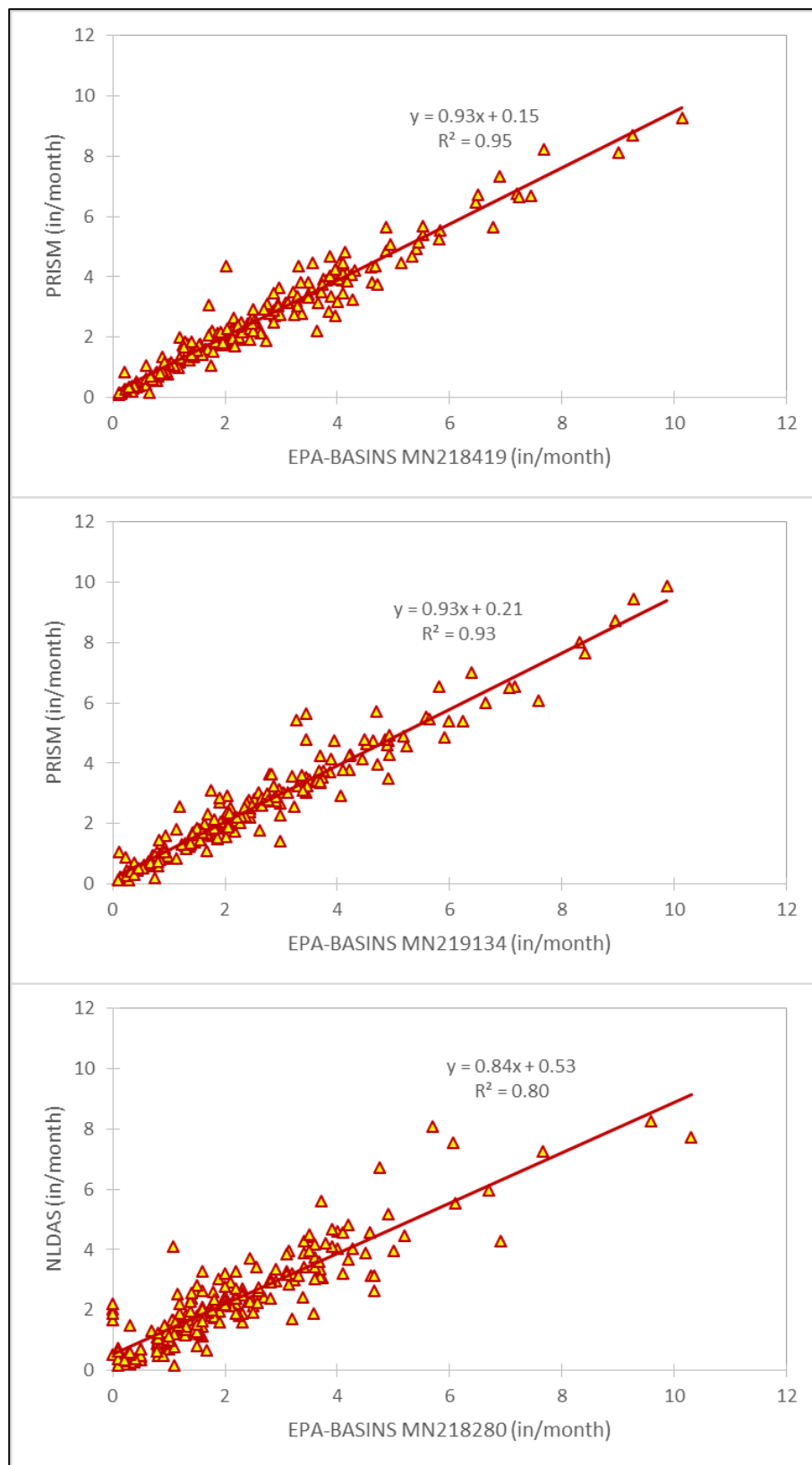


Figure 2-13. Comparison of EPA-BASINS and NLDAS Monthly Precipitation

**Figure 2-14. Comparison of EPA-BASINS and PRISM Monthly Precipitation**

2.2.2 Auxiliary Weather Variables

NLDAS directly provides matched and consistent estimates of air temperature, wind, and solar radiation. NLDAS also provides potential evapotranspiration (PET) calculated by a Penman energy balance method, although this is not directly used, as discussed below. Two variables required by HSPF – dewpoint temperature and cloud cover – are not directly available from NLDAS. These variables were calculated as follows:

Cloud cover is back calculated from the relationship of Davis (1997) describing the ratio of ambient solar radiation at the surface (E_{surf}) to radiation from a cloudless sky ($E_{cloudless}$):

$$\frac{E_{surf}}{E_{cloudless}} = 1 - 0.6740 C^{2.854},$$

where, C is the fractional cloud cover. $E_{cloudless}$ is a function of latitude and time of year and is calculated with the WDMUtil tool distributed with BASINS.

NLDAS does not provide dewpoint temperature, but does provide specific humidity. We estimate dewpoint by the following method:

1. Calculate vapor pressure (e , mb) as a function of atmospheric pressure (p , mb) and specific humidity (q) from definition of q as a function of the mixing ratio, yielding

$$e = \frac{q p}{0.622 + 0.378 q}$$

2. Use e to calculate dewpoint ($Td[C]$, °C) from e by solving the NOAA equation for e as a function of $Td[C]$:

$$Td[C] = \log_{10} \left(\frac{e}{6.11} \right) \times \left[\frac{237.3}{7.5 - e/6.11} \right]$$

3. Convert to dewpoint in °F:

$$Td[F] = 32 + Td[C] \times 9/5$$

4. Ensure consistency with local daily air temperature data minimum (T_{min} , °F):

$$Td[F] = \text{Max}(T_{min}, Td[F])$$

Dewpoint temperature is used in the calculation of PET, so some small inaccuracies in daily PET may be introduced, although these should average out over high and low pressure weather cycles. Dewpoint temperature is also used for the calculation of the effective temperature at which precipitation becomes snow ($\text{SNOTMP} = \text{TSNOW} + (\text{AIRTMP} - \text{DEWTMP}) \times (0.12 + 0.008 \times \text{AIRTMP})$).

As noted above, NLDAS provides an estimate of PET calculated by the modified Penman method of Mahrt and Ek (1984). However, PET is not a focus of NLDAS because NLDAS is designed to run a variety of Land Surface Models (LSMs; such as the NOAH model), most of which generate their own energy-based ET estimates. PET is provided in the NLDAS output only because one of the LSMs (SAC-SMA, the Sacramento soil moisture accounting model) does require it as an input (<http://ldas.gsfc.nasa.gov/nldas/NLDAS2forcing.php>; accessed 9/2/2015). On investigation it turns out that the PET that NLDAS reports is the PET calculated by the North American Regional Reanalysis (NARR) dataset (Mesinger et al., 2006). NARR is documented to have a large positive bias in the estimation of shortwave radiation (Xia et al., 2012). NLDAS corrects the NARR shortwave radiation estimates using satellite-based estimates, but the PET estimate ported from NARR is not corrected. In addition, NARR is at a coarser spatial scale than NLDAS and the PET estimates may be off in areas with strong edge effects.

Experiments conducted by Tetra Tech in the Lake Superior North and South HSPF models concluded that the NLDAS/NARR reported PET values were unreasonably high in some areas (due to the shortwave

radiation bias) and exhibited too great a variation from the coastline to the interior (in part this is likely due to the downscaling of coarser-grid NARR data). Further, the PET time series provided by NLDAS did not match the seasonal pattern of Penman Pan ET (Penman, 1948; Hummel et al., 2001) calculated at individual weather stations.

Based on these observations it was desirable to recalculate PET, rather than using the PET reported by NLDAS/NARR. We therefore calculated Penman Pan PET using inputs from NLDAS (including the corrected shortwave radiation) and applying the standard approach from BASINS that has been implemented in most other Minnesota HSPF models (AQUA TERRA, 2012). The Penman Pan ET calculated in this way does provide a reasonable match to the individual weather station results.

2.3 MODEL SEGMENTATION AND REACH NETWORK

2.3.1 Subwatershed Delineation

In accordance with MPCA guidance (AQUA TERRA, 2012), the Lake Superior North and Lake Superior South watershed models are constructed with subwatersheds that are generally at the scale of 12-digit Hydrologic Unit Code (HUC-12) subbasins, which are typically on the order of 10 to 100 square miles in size. Finer scale delineations may be needed to address specific local problems, such as impairments in small streams in the Duluth metropolitan area. Such a finer scale model is currently under construction for the Duluth area under a separate work assignment. That model overlaps a small portion of the Lake Superior South watershed (Tischer Creek, Amity Creek, and Lester River) and will provide better spatial resolution for this area of the basin-scale model.

The general objective of model segmentation for the Lake Superior North and Lake Superior South models was to follow HUC-12 boundaries to the extent practical with modifications to address special circumstances. The Minnesota Department of Natural Resources (MNDNR) HUC-12 boundaries polygon shapefile and MNDNR 24k Streams polyline shapefile served as the starting point for model subwatershed delineations.

Further sub-delineations of the MNDNR HUC-12 boundaries were made using supplemental spatial data to account for hydrological features such as control by impoundments and water quality monitoring and flow gaging station locations (Figure 2-15). The period of record and currency of HYDSTRA monitoring data were used to select locations to be used for HSPF model development, calibration, and validation as described in Section 3.1. Where needed, new subwatershed boundaries were created to allow easy inclusion of data gathered at these selected locations.

Sub-delineated HUC-12s were divided manually using ESRI ArcGIS Editor and followed the NHDPlus Version 2 Catchments boundaries (http://www.horizon-systems.com/NHDPlus/NHDPlusV2_home.php). Figure 2-16 and Figure 2-17 show the subbasin numbers and upstream-downstream routing.

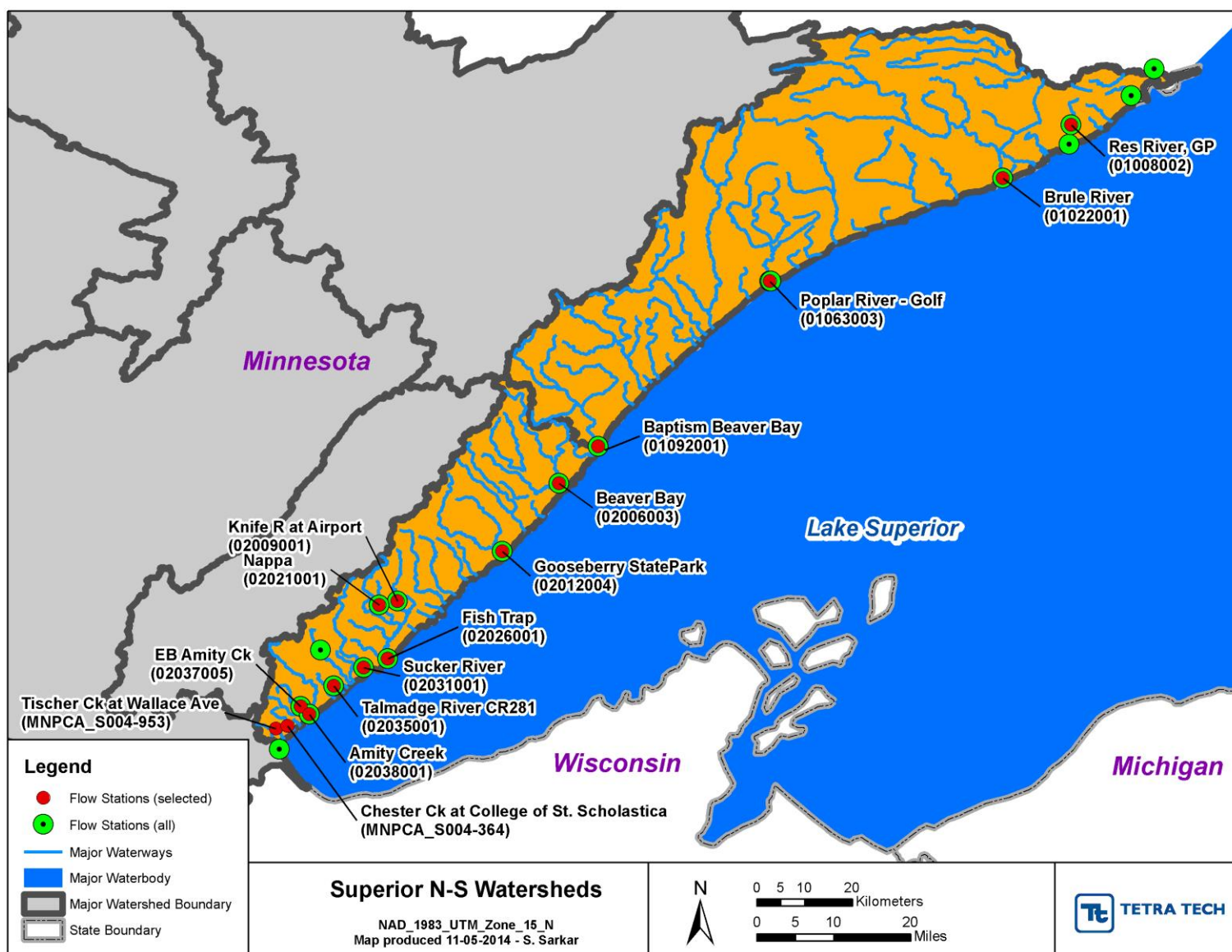


Figure 2-15. Flow Gaging Locations in Lake Superior North and South Watersheds

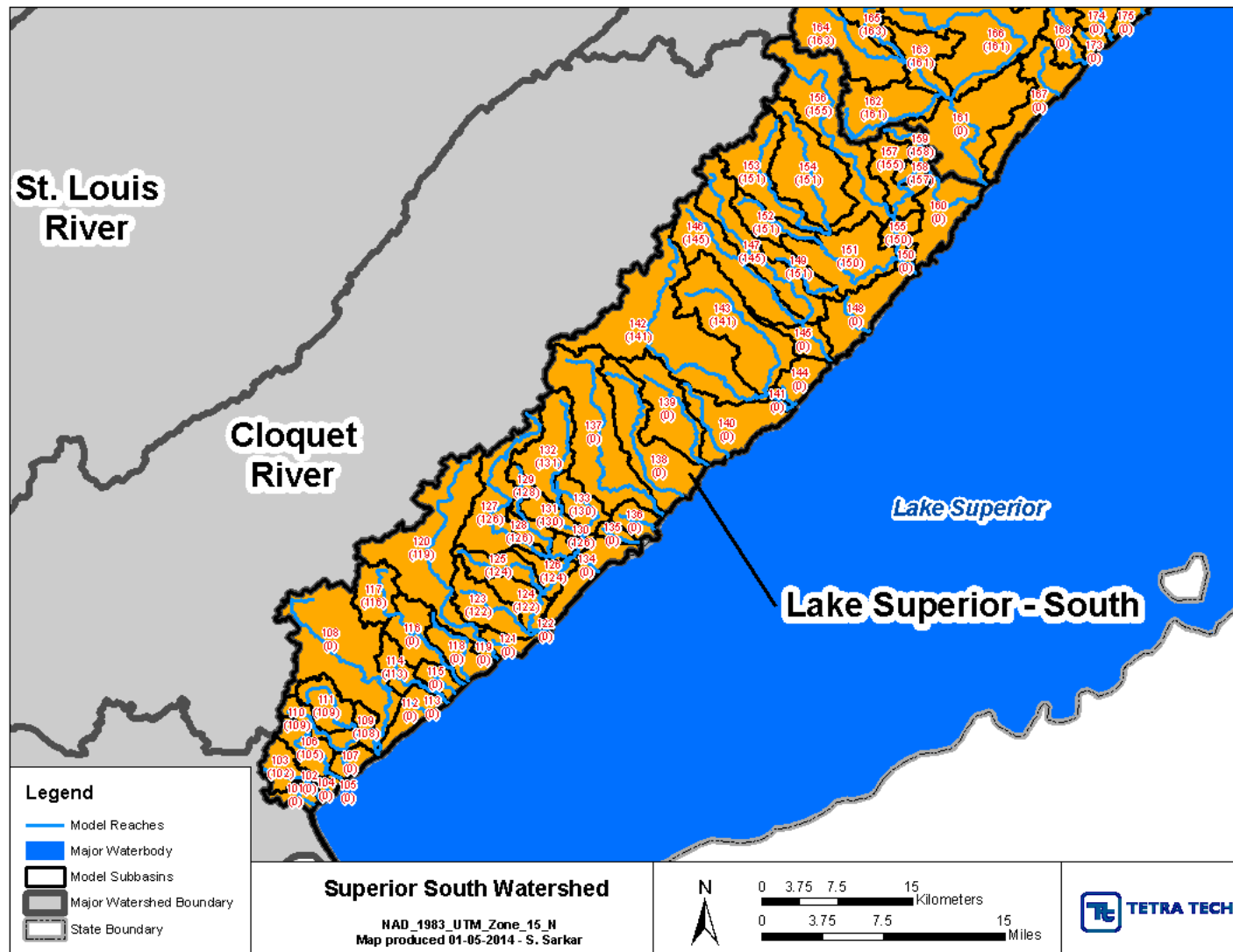


Figure 2-16. Model Subwatershed Delineations for Lake Superior South Watershed

Note: Numbers in parentheses indicate the downstream watershed. Subwatersheds with a downstream value of 0 drain to Lake Superior.

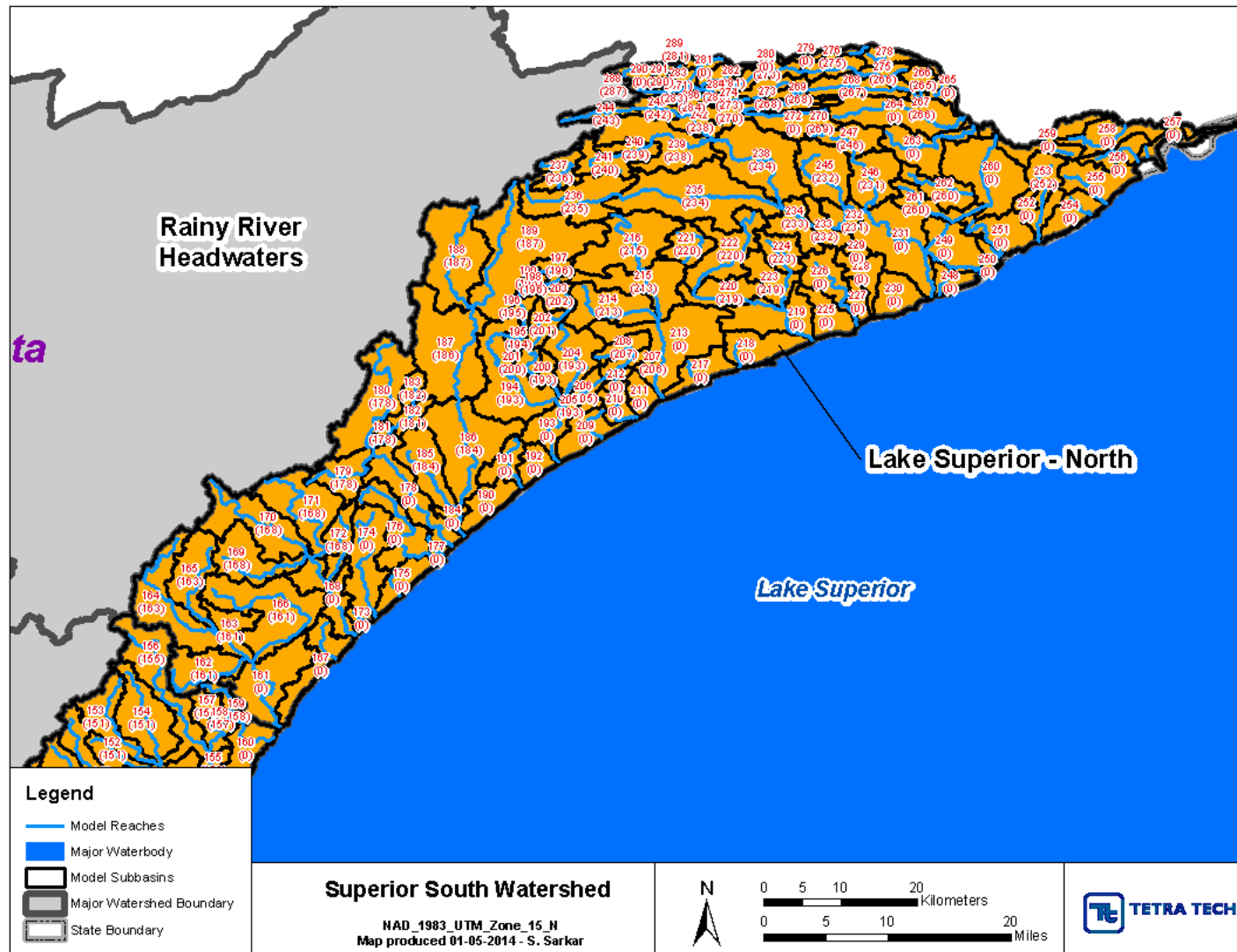


Figure 2-17. Model Subwatershed Delineations for Lake Superior South Watershed

Note: Numbers in parentheses indicate the downstream watershed. Subwatersheds with a downstream value of 0 drain to Lake Superior.

2.3.2 Stream Reach and Lake Delineation

HSPF represents a single main channel (reach) or lake waterbody for each model subbasin. These reaches carry the same identifying number as the subbasin. Lower order tributaries at finer spatial scales are not explicitly represented in the model and are accounted for implicitly in the upland simulation.

The study watersheds contain a large number of lakes, particularly in the Lake Superior North HUC8. Given the large number and lack of bathymetric data for many of the lakes, not all can be represented explicitly as lake segments in the model. (Those that are not will be represented as a water/wetland land use). Selection of lakes for explicit representation followed the general procedure outlined in AQUA TERRA (2012).

The process began with the 2008 MPCA Assessment lakes (197 lakes, excluding Lake Superior itself). NHD was then queried for lakes greater than 200 acres, which added another four lakes not assessed by MPCA. (One of these is the Swamp River wetland area, which is not classified by MPCA as a lake, but does appear to act as a shallow storage reservoir on a main reach). The Lake Superior North model does not include the Pigeon River mainstem (because much of the drainage area is in Canada); therefore, six inline lakes on the Pigeon River were eliminated.

The initial set included all current impaired lakes in the study watersheds. Lake listings are primarily for mercury derived from atmospheric deposition, which is addressed under a general TMDL and does not require explicit modeling of individual lakes. The only exception is Winchell Lake, which is listed for PCBs.

Lakes were next screened as to whether they are located in-line on a HUC 12-scale stream reach and the area cumulative distribution of these 84 lakes (including those on the Pigeon mainstem) was plotted (Figure 2-18). This distribution does not have a distinct inflection point, so we selected all lakes greater than 550 acres in area plus any lakes greater than 400 acres in area for which bathymetry was available.

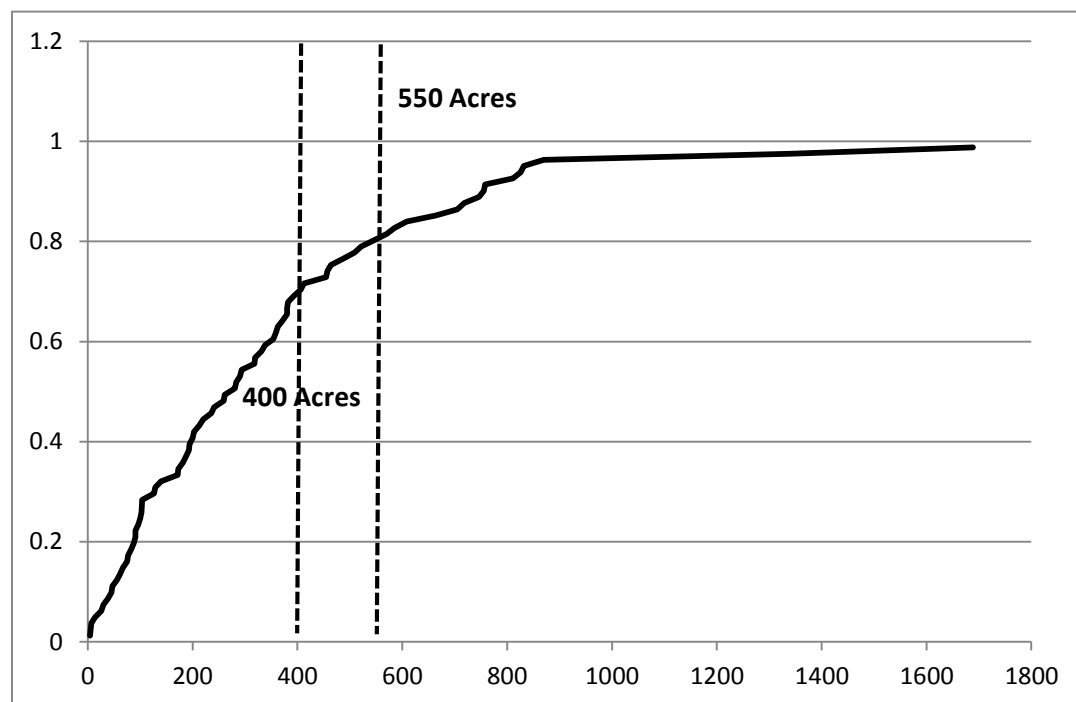


Figure 2-18. Cumulative Distribution of Surface Area of Inline Lakes in the Lake Superior North and Lake Superior South Watersheds

There are 117 lakes not in-line with HUC12 scale stream reaches. Many of these lakes are small and the inflection point of the distribution is approximately 150 acres. Contrary to the example shown in AQUA TERRA (2012), this is substantially smaller than the inflection point for the distribution of inline lakes. As it does not make sense to apply a smaller size criterion to lakes not in-line with reaches, the same size criteria (400 and 550 acres) were applied to this set of lakes. Finally, several additional small lakes were added to the selection because they occupy downstream positions where they are likely to exert a significant effect on flow in monitored rivers, or they are water bodies of particular interest for modeling (e.g., development pressure, popular recreation lakes). This resulted in selecting a total of 36 lakes for explicit simulation in the model. As a final step, lakes that were not selected but have bathymetry and occur in the same model subbasin as a selected lake were identified. Storage in these lakes will be aggregated with the selected lake in that subbasin.

The selected lakes are listed in Table 2-3, and shown in Figure 2-19 and Figure 2-20. Only one of these lakes (Lax) is in the Lake Superior South watershed.

Table 2-3. Lakes Selected for Explicit Representation in Lake Superior South and North Watersheds

Lake Name	Area (ac)	Bathymetry	Aggregated Lakes	Model Subbasin
Alder	509	Y		270 (N)
Alton	960	Y		182 (N)
Bearskin	487	Y		284 (N)
Brule	4,219	Y		236 (N)
Caribou	718	N		206 (N)
Cascade	467	Y		216 (N)
Clara	393	N		202 (N)
Clearwater	1,338	N		277 (N)
Crescent	746	Y		196 (N)
Deer Yard	338	Y		212 (N)
Devil Track	1,828	Y		280 (N)
Devilfish	412	Y	Chester	263 (N)
East Bearskin	570	Y	Aspen	271 (N)
East Pike	547	N		275 (N)
Elbow (nr Grand Marais)	380	N		224 (N)
Flour	323	Y		274 (N)
Four Mile (Fourmile)	586	Y		182 (N)
Gaskin	382	Y		240 (N)
Greenwood	2,026	Y		247 (N)
Hungry Jack	457	Y		285 (N)
Lax	291	Y		158 (S)
McFarland	380	Y		267 (N)
Northern Light	372	N		233 (N)
Pike	811	Y		208 (N)
Pine	2,111	N		268 (N)
Poplar	758	Y		243 (N)
Sawbill	826	N		188 (N)
Swamp River	1,688	N		260 (N)
Tait	354	Y		203 (N)
Tom	407	Y		261 (N)
Trout	258	Y		229 (N)
Two Island	750	Y		221 (N)
West Pike	756	N		276 (N)
White Pine	331	N		201 (N)
Wilson	652	Y	Elbow, Whitefish, Little Wilson	180 (N)
Winchell	870	N		241 (N)

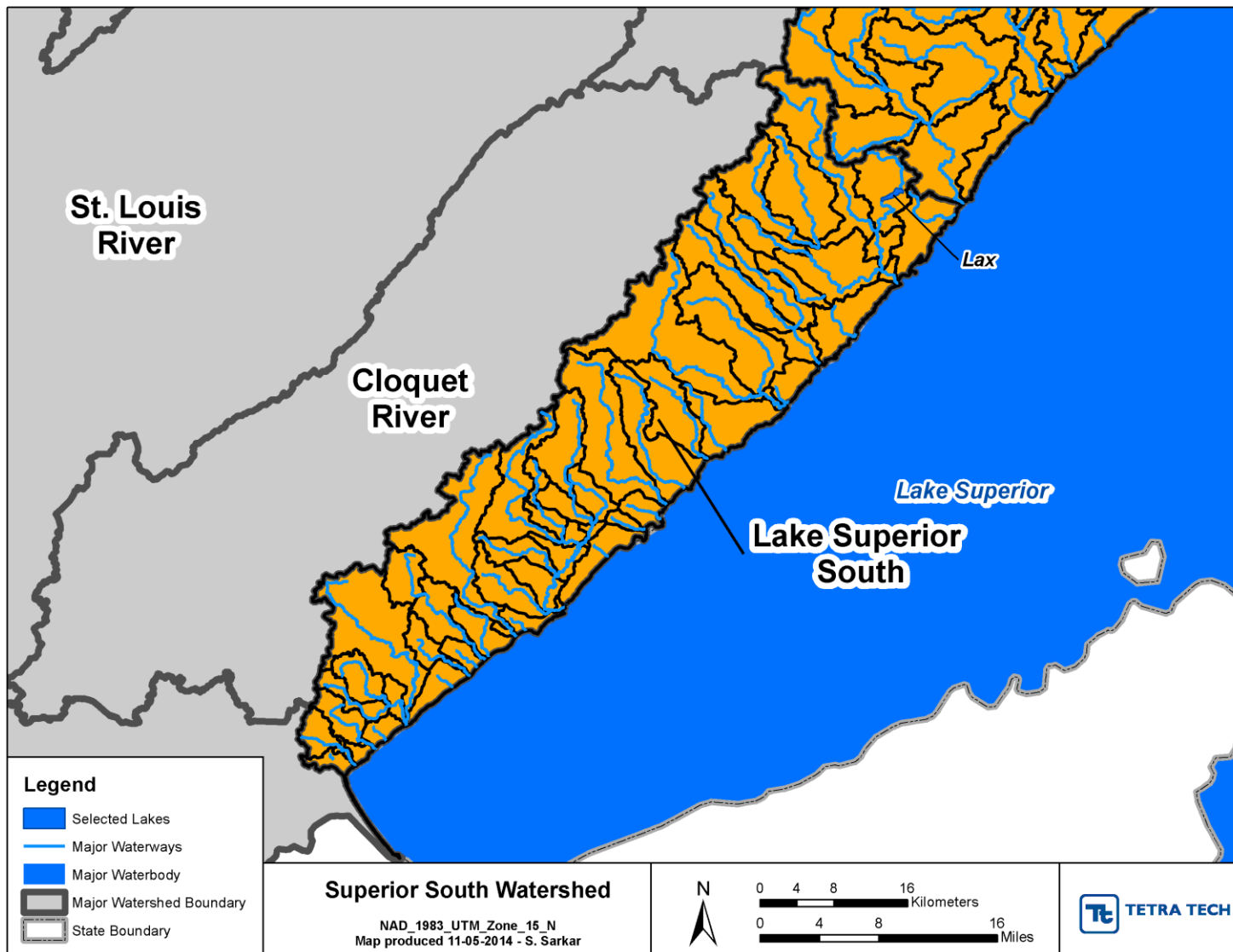


Figure 2-19. Lakes Explicitly Represented in Lake Superior South Watershed

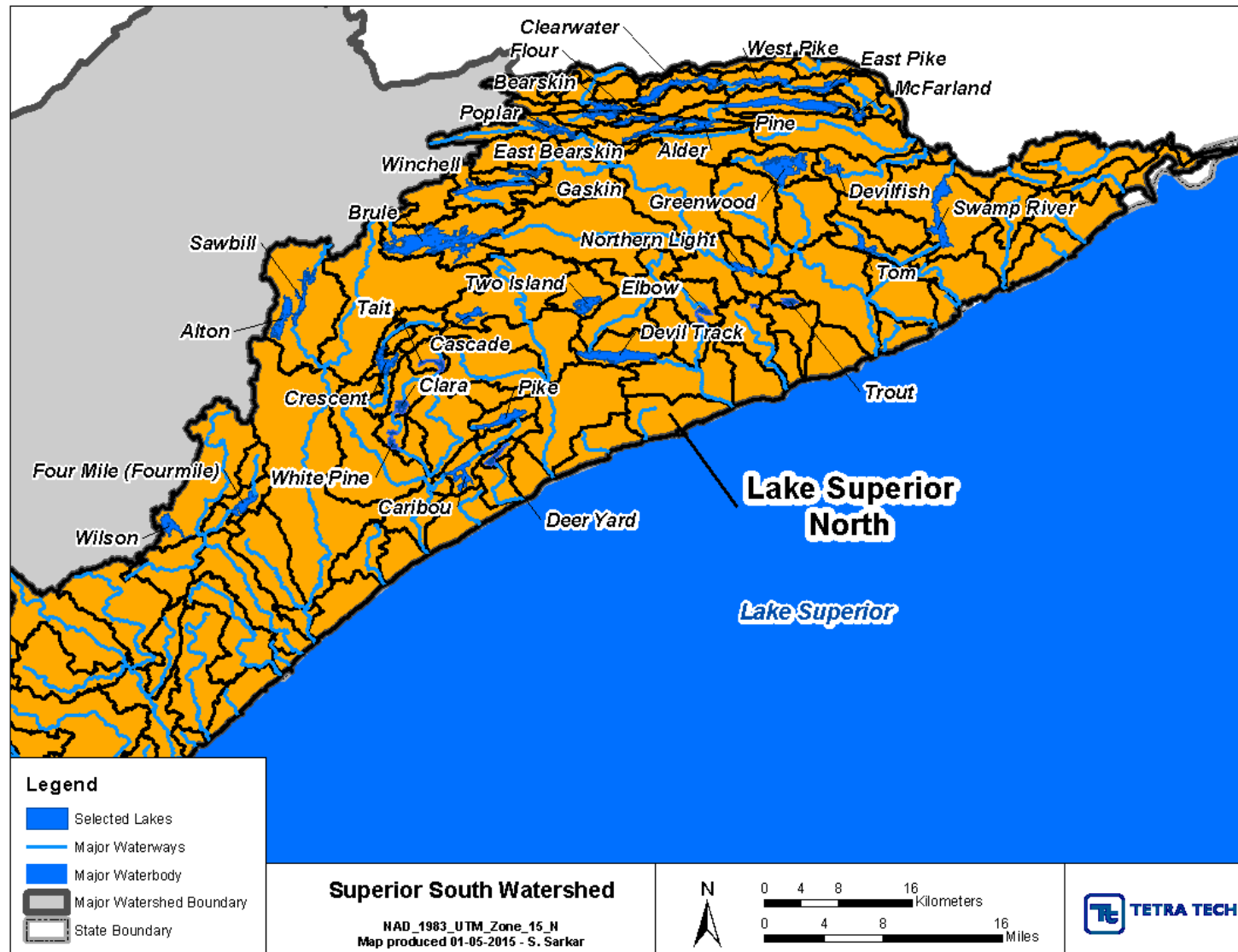


Figure 2-20. Lakes Explicitly Represented in Lake Superior North Watershed

2.3.3 Reach Hydraulics

Movement of sediment in stream networks, including transport, scour, and deposition rates, is determined by flow energy. HSPF does not directly solve hydraulic momentum equations for flow routing, but rather specifies information on the relationship between stage, discharge, and geometry through Functional Tables (FTables). The calculation of boundary shear stress from the FTable information is a key component of the simulation of sediment transport.

HSPF is a water balance (hydrologic) model and not a hydraulic model. HSPF represents stream reaches as one-dimensional fully mixed reactors and, while maintaining mass balance, does not explicitly conserve momentum. To simulate the details of hydrograph response to storm events HSPF relies on Function Tables (FTables) that describe the relationship of reach discharge, depth, and surface area to storage volume. At stable median flow conditions the model results are not particularly sensitive to the details of the FTable specification, as outflow tends to approximate the net inflows; however, the shape of the response to storm event peaks can be highly sensitive to FTable details. Given the interest of MNDNR in evaluating the distribution of flows in streams in Minnesota there is an increasing need to refine HSPF basin-scale model FTables.

By default, the BASINS version of HSPF estimates FTables by applying predetermined regressions against drainage area, but this approach does not take into account site-specific characteristics (such as obstructions) and is based on data from sites in ecoregions different from those found in Minnesota. Some local studies on the dependence of stream channel geometry on drainage area have been completed in our area of interest (e.g., Magner and Brooks, 2008 for the Nemadji River) and can be used; however, there are a variety of other approaches that are based on inputs ranging from completed hydraulic models to analysis based on individual cross sections. To optimize the HSPF models we need to incorporate as much hydraulic information as feasible; however, the available level of effort was also limited. The optimal approach for hydraulics in HSPF is to incorporate information from a detailed hydraulic model, such as HEC-RAS, but such models are generally not available for the Lake Superior North and South watersheds and creating such models is not part of the scope for this task. Therefore, we used a triage approach that seeks to optimize the best information available from a variety of sources at a feasible level of effort. The approaches are listed below in order of priority for application to this basin.

Note that the FTables primarily affect the details of the hydrograph shape. If we correctly characterize FTables for most reaches with monitoring the impact of FTable discrepancies in other, unmonitored reaches are likely to be small and can be improved in future iterations of the model without significant disturbance to the calibration.

2.3.3.1 Lake Storage and Outflow

Lakes and reservoirs typically have outflows that are determined by dam/weir characteristics or active management. Thus, lake FTables represent a different class of analyses than stream reach FTables, and essentially need to be addressed on a site-specific basis as a first priority. Site-specific FTables are calculated for lakes. These are based on specific characteristics of individual lakes/dams and take precedence over any other methods for creating FTables.

Where available, lake bathymetric data were used to characterize stage-storage relationships based on the elevation contour polylines contained in each dataset (MNDNR, 2002). Maximum or average depth data were obtained for the remaining lakes that lack bathymetry. The maximum depths (or inferred maximum depth consistent with the average depth) were used to estimate the lake volume at various stages based on the assumption that depth is a function of distance from the lake's shoreline. This was done by converting lake polygons to raster format and using the following linear transformation (Hollister and Milstead, 2010):

$$Z = D * Z_{\max} / D_{\max}$$

where Z is the depth for any given raster cell; D is the Euclidean distance from the shoreline, including islands; Z_{\max} is the measured maximum depth for a given lake; and D_{\max} is the maximum distance from the shoreline of a given lake. The lake depth raster dataset was then summed to calculate the lake volume:

$$\text{Lake volume} = \sum_{i=1, j=1}^n \text{Cell area} * \text{Depth } i, j$$

Storage volumes above the lake surface outlet level were estimated using LiDAR data. The outflows associated with various water depths were estimated using a rectangular weir equation. Lakes with natural outlets were approximated using a broad-crested weir assumption. The dimensions of the weir were determined from details provided by MNDNR hydrologists or, lacking direct information, from examination of aerial imagery.

2.3.3.2 Rating Table with Cross Section

Gage rating tables are available for some stream segments and can be used to develop detailed hydraulic relationships. A rating table is used to convert an observed measurement of gage height to an estimate of flow. Rating tables change over time as the channel shape changes in response to storm events. At the basin-scale of modeling, however, the details of elevation and cross-sectional area within individual stream segments are of less importance; rather, we need a reasonable representation of the stage-storage-discharge relationship. This can be obtained from recent rating tables with accompanying cross sections and will remain approximately valid for changing conditions over time (although the base level is likely to change) unless the channel form is extensively reworked.

To use rating tables with cross sections, we first calculate top width, cross sectional area, and wetted perimeter directly from the cross section. Volume and surface area at each rating table depth increment are then calculated by multiplying by the length of the reach within the subbasin. This implicitly assumes that the gage is located at a point that controls flow within the subbasin or is at least typical of flow in the subbasin. Where the gage does not fall at the subbasin mouth, assume depth and cross-sectional area remain constant over this relatively short distance, and use length of entire reach for calculation. We will not use rating tables from the middle of a subbasin if there is a significant proportional increase in drainage area from the gage to the subbasin pour point.

The HYDSTRA cross sections generally are to the water surface at the date of observation only. These cross sections are extended through use of the LiDAR elevation data flown in May 16 and 17 of 2011. In most cases, the water surface elevation at the date of the cross section is not the same as the water surface elevation in LiDAR. In the case where the cross section does not reach up to the LiDAR elevation the profile was interpolated between the two.

2.3.3.3 Rating Table without Cross Section

In this case a rating table provides a relationship between stream flow and gage height but information on cross section geometry is not available. For these gages we assume that the LiDAR provides the cross-section information above the water level on that date, while the sub-surface cross section is assumed to have a trapezoidal form. The gage height could be rather arbitrarily related to local geometry (e.g., installed in a deep pool or on the side of a bridge) and actual average channel depth. The USGS rating tables provide an offset value, which represents the elevation that should be subtracted from the gage height in evaluation of the stage-discharge relationships. The rating tables are thus converted by first adding any shift and then subtracting the offset before proceeding.

In the case of a gage where flow is reported for the date of the LiDAR coverage, back-solve Manning's equation to obtain average depth and top width at the observed flow condition under assumption that side slope of channel, m_c , is equal to 1.5 (see Section 2.3.3.7). The average depth – cross-sectional area – flow relationship up to this flow is calculated by scaling the rating table depths to the calculated average depth at the observed flow. Volume and surface area up to this depth are calculated by multiplying by reach length. Above this level flow as a function of depth increment is taken directly from the rating table, while surface area and incremental volume come from multiplying the LiDAR cross section area and top width (above the level at the LiDAR coverage data) times the reach length. If gaged flow is not available for the LiDAR date, a similar procedure is used except that the flow on the LiDAR date is estimated by comparison to nearby/similar gages as a function of drainage area.

2.3.3.4 Surveyed Cross Section Only (No Rating Table or Gaging)

Where there is information on cross-section geometry, but not a flow rating table, we use Manning's equation, as implemented in WinXSPRO (Hardy et al., 2005) for complex cross sections, to develop average depth – cross section area – top width – flow relationships. In many cases the cross section is divided into segments representing channel flow up to bank full and floodplain flow. These segments are assigned separate Manning's coefficients that can reflect site-specific conditions (where known). Default values are 0.04 for the channel and 0.06 for the floodplain. Volume and surface area are calculated by multiplying by reach length.

As the MNDNR cross sections typically do not include the overbank profile, these are supplemented by extending into the overbank using the LiDAR data as described in previous sections.

2.3.3.5 Road Culvert and Bridge Analysis

For cases where there is a bridge or road culvert either at the subbasin outlet or within the lower third of the subbasin without significant additional tributary inflows, it is reasonable to assume that the culvert controls the discharge rate, especially at higher flows. If culvert information is readily available, stage-discharge relationships can be based on culvert equations, plus analysis of overtopping of the road, represented as a broad-crested weir.

The Minnesota Department of Transportation (MNDOT) provided bridge and culvert information for major stream crossings of state and federal highways. Calculation of flow through a culvert is complicated because culverts are generally a significant constriction to flow and subject to a range of gradually varied and rapidly varied flow types that may be under either outlet control (in which the tailwater elevation has a significant influence) or inlet control (in which the headwater depth at the culvert inlet has a major influence). Culvert design calculations must simultaneously address both possibilities, leading to complex calculations. The Federal Highway Administration program HY8 (<http://www.fhwa.dot.gov/engineering/hydraulics/software/hy8/>), based on Schall et al., 2012, has been used for this purpose by MNDOT for many bridges. Where such results are available they are used to develop FTables.

2.3.3.6 Other Unsurveyed Reaches

A number of reaches do not have any of the information described in preceding sections. For these reaches it is possible to create cross sections using a combination of LiDAR and estimates of the magnitude and depth of flow on the LiDAR date; however, that is a labor intensive process that was beyond the current resources. Therefore, we define three cases. In the first case, the FTable for an adjacent subbasin is likely a good approximation for the candidate subbasin. In the second and third cases, we use default FTable calculation based on either the BASINS standard method that relates hydraulic geometry to drainage area or hydraulic geometry relationships developed for the Nemadji River basin.

Case 1: In this case the candidate reach is one subbasin upstream or downstream of a gaged reach, the incremental drainage area does not change by more than 25%, and no lake reaches intervene. In such cases, the adjacent FTable is assumed to be applicable with appropriate modifications. Modify the depth-cross sectional area-top width-discharge relationship based on the drainage area ratio. Multiply by reach length to obtain surface area and volume.

Case 2: When Case 1 does not apply, regressions between hydraulic geometry and drainage area are applied. For stream reaches that are predominantly on lacustrine clay substrate this makes use of the hydraulic geometry relationships developed for the lacustrine core of the Nemadji River basin. These equations are available in Magner and Brooks (2008) and accompanying files provided by Tim Larson of MPCA and describe bankfull cross-sectional area A_{bank} (ft²) and flow Q_{bank} (cfs) as a function of drainage area DA (mi²).

The following inputs are obtained from GIS.

DA	drainage area	mi ²
L	reach length	ft
W_m	stream width	ft
m_F	floodplain slope (inverse – expressed as run over rise)	
s	reach slope	

We also assume the following based in part on the standard method for FTables in BASINS Technical Note 2 (USEPA, 2007):

$W_F = W_{\text{bank}} = W_m$ (i.e., the bankfull width is the same as the observed width and the floodplain side width is assumed equal to the channel width)

$m_C = 1.5$ (channel side slope is assumed 1:1.5 due to somewhat incised nature of many streams in this area)

We then calculate:

A_{bank} (bankfull cross-sectional area in ft²) = $5.5209 \times DA^{0.7744}$ (Magner 15-sites equation, $R^2 = 0.9744$)

Q_{bank} (bankfull flow in cfs) = $41.913 \times DA^{0.7946}$ (Magner regression, $R^2 = 0.9001$)

Y_c (bankfull depth, ft) = A_{bank}/W_m

$Y_m = Y_c/1.25$ (standard method assumption)

We can use Q_{bank} to back-solve for the channel Manning's coefficient.

P_{bank} (bankfull wetted perimeter) = $W_m - 2 m_C Y_c + 2 Y_m (m_C^2 + 1)^{0.5} = b + 2 Y_m (m_C^2 + 1)^{0.5}$,

$n = A_{\text{bank}}/Q_{\text{bank}} \times 1.486 \times (A_{\text{bank}}/P_{\text{bank}})^{2/3} \times s^{0.5}$

The Manning's coefficient derived in this way should be constrained to be greater than or equal to 0.025 to protect against unreasonable solutions. A separate Manning's coefficient is assigned to overbank flow (0.06 in the absence of other information.)

This information obtained in this way can then be used in a modified version of Tetra Tech's FTables_Batch.xlsm, which calculates FTables based on hydraulic geometry.

Case 3: For other streams, FTables are developed using BASINS defaults for hydraulic geometry, in which bankfull width and depth are estimated by generalized equations such that:

Bankfull Width (m) = $1.29 DA(\text{km}^2)^{0.6}$; Bankfull Depth (m) = $0.13 DA(\text{km}^2)^{0.4}$.

The remainder of the hydraulic geometry and flow relationships are analyzed following the standard method given in USEPA (2007). We modified the default approach to use separate Manning's coefficients for the channel (default 0.04) and floodplain (default 0.06), and assume no friction loss between these two segments, as is done in WinXSPro. This approach is particularly appropriate for minor tributaries with no gaging or monitoring.

2.3.3.7 Back-Solving Manning's Equation

Several of the approaches described above for developing stream FTables require back-solving Manning's equation. Manning's equation for flow can be written in the following form (for English units; BASINS Technical Note 2):

$$Q = 1.486/n (by + m_c y^2)^{5/3} \times [b + 2y (m_c^2 + 1)^{0.5}]^{-2/3} \times S^{0.5},$$

where Q is flow in cfs, n is Manning's constant, b is the bottom width, m_c is the side slope of the channel expressed as the ratio of width to depth, y is the average depth, and S is the energy grade. We assume that $m_c = 1.5$ (consistent with the alternative method described in Technical Note 2) and S is approximated by the reach slope, so

$$Q = 1.486/n (by + 1.5 y^2)^{5/3} \times [b + 2y (2.5)^{0.5}]^{-2/3} \times S^{0.5}.$$

The channel Manning's coefficient can be specified based on site-specific data where available. A default channel value of 0.04 is used in other cases. The Excel Solver function is then used to estimate b given y.

2.3.3.8 FTable Development Summary

The methods applied to each reach in the current models are summarized in Table 2-4.

Table 2-4. Methods for Establishing Reach FTables

Superior N				
161: RTC	202: Lake	243: Lake	286: SFP	136: Mag
162: SFP	203: Lake	244: SFP	287: SFP	137: SFP
163: SFP	204: SFP	245: SFP	288: SFP	138: SFP
164: SFP	205: SFP	246: SFP	289: SFP	139: SFP
165: SFP	206: Lake	247: Lake	290: SFP	140: Mag
166: SFP	207: SFP	248: Culvert	Superior S	141: Mag
167: Mag	208: Lake	249: SFP	101: SFP	142: SFP
168: SFP	209: Mag	250: Mag	102: SFP	143: SFP
169: SFP	210: Culvert	251: Culvert	103: SFP	144: SFP
170: SFP	211: Mag	252: Mag	104: SFP	145: Culvert
171: SFP	212: Lake	253: SFP	105: SFP	146: SFP
172: SFP	213: SFP	254: Mag	106: SFP	147: SFP
173: Mag	214: SFP	255: SFP	107: SFP	148: Mag
174: SFP	215: SFP	256: Mag	108: SFP	149: SFP
175: Mag	216: Lake	257: Mag	109: RTC	150: Mag
176: Mag	217: SFP	258: SFP	110: SFP	151: SFP
177: SFP	218: Mag	259: SFP	111: SFP	152: SFP
178: SFP	219: Mag	260: Lake	112: SFP	153: SFP
179: SFP	220: Lake	261: Lake	113: Adj	154: SFP
180: Lake	221: Lake	262: SFP	114: RTC	155: SFP
181: SFP	222: SFP	263: Lake	115: Mag	156: SFP
182: Lake	223: SFP	264: SFP	116: SFP	157: SFP
183: SFP	224: Lake	265: SFP	117: SFP	158: Lake
184: Mag	225: Mag	266: SFP	118: Mag	159: SFP
185: SFP	226: SFP	267: Lake	119: Adj	160: Mag
186: SFP	227: Mag	268: Lake	120: RTC	Key:
187: SFP	228: SFP	269: SFP	121: Mag	Culvert: HY8 analysis
188: Lake	229: Lake	270: Lake	122: Mag	Adj: Extrapolate from adjacent FTable
189: SFP	230: Mag	271: Lake	123: SFP	Lake: Lake FTable
190: Mag	231: RTC	272: SFP	124: SFP	Mag: Magner hydraulic geometry regression
191: SFP	232: SFP	273: SFP	125: SFP	RTC: Rating table with cross section
192: Culvert	233: Lake	274: Lake	126: SFP	RTn: Rating table with no cross section
193: RTC	234: SFP	275: Lake	127: SFP	SFP: BASINS standard method
194: SFP	235: SFP	276: Lake	128: Adj	
195: SFP	236: Lake	277: Lake	129: RTn	
196: Lake	237: SFP	278: SFP	130: SFP	
197: SFP	238: SFP	279: SFP	131: Adj	
198: SFP	239: SFP	280: SFP	132: RTC	
199: SFP	240: Lake	281: SFP	133: RTn	
200: SFP	241: Lake	282: SFP	134: Mag	
	242: SFP	283: SFP	135: Mag	

2.4 POINT SOURCES

Seventeen permitted point source discharges are present in the Lake Superior South and North watersheds. Only eight of these discharge to streams within the model domain. The remaining discharge directly to Lake Superior and are therefore not included in the model.

There are ten permitted minor dischargers located within the Lake Superior South watershed, of which six discharge directly to Lake Superior. The Lake Superior North watershed has seven minor dischargers with three discharging to Lake Superior. There are no permits classified as major dischargers in the Lake Superior South and North watersheds. There is, however, a significant flow contribution of non-contact cooling water (derived from Lake Superior) in the Harbor Energy discharge to an un-named creek just upstream of the mouth, near Two Island Creek south of the Town of Schroeder.

MPCA researched the locations and discharge monitoring records for these dischargers, using the Delta system for the more recent records (generally from 1998 or 1999) and the EPA PCS system for earlier records. A total of eight point source discharges were quantified for inclusion in the models. The permit identifier, name, type (major/minor), HSPF model subbasin, and average flow of each discharge are summarized in Table 2-5 and their locations are shown in Figure 2-21.

Table 2-5. Permitted Point Source Discharges in the Lake Superior South and North Models

NPDES Code	Location Name	Type	Model Subbasin	Avg. Flow (MGD)
MN0040754	Beaver Bay	Minor - WWTP	150 (S)	0.052
MN0052230	Knife River	Minor -WWTP	122 (S)	0.017
MN0004413	French River	Minor - Industrial	116 (S)	0.693
MN0033731	Gooseberry State Park	Minor - WWTP	140 (S)	0.001
MN0053252	Caribou Highlands	Minor - WWTP	193 (N)	0.060
MN0060691	Lookout	Minor - WWTP	163 (N)	0.001
MN0057690	Tettegouche State Park	Minor - WWTP	161 (N)	0.0003
MN0002208	Harbor Energy	Minor – Non-contact cooling water	177 (N)	144

Nutrient and sediment load time series associated with each of these discharges are assigned based on reported monthly monitoring and, for unmonitored parameters, MPCA assumptions based on the type of discharger being represented. The Harbor Energy discharge is assumed to be a source of water and heat only.

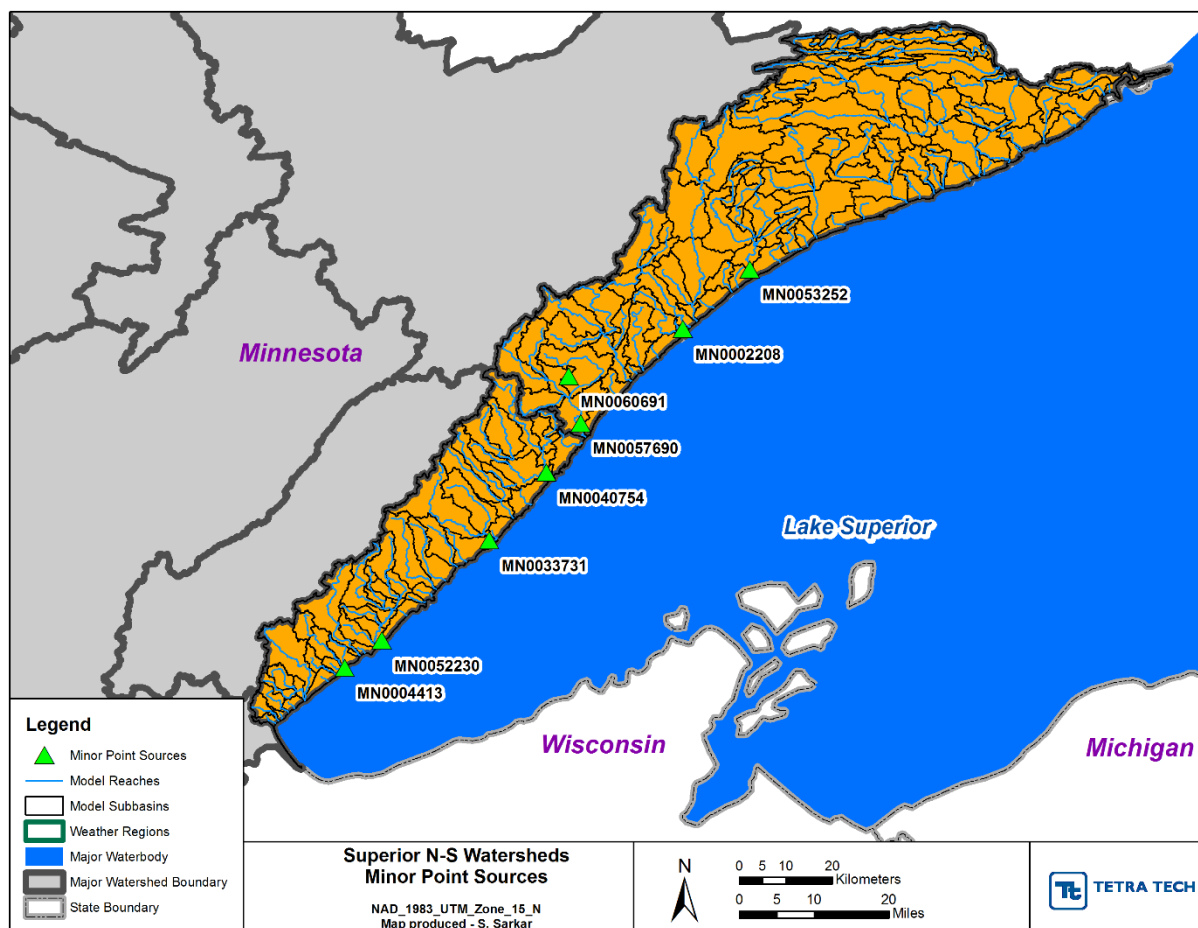


Figure 2-21. Location of Permitted Point Source Discharges in the Lake Superior North and Lake Superior South Models

Note: Discharges routed directly to Lake Superior are not shown.

2.5 WATER APPROPRIATIONS

Surface water is withdrawn from rivers and lakes for a variety of purposes, including municipal/domestic supply, industrial processing, and power plant cooling. Monthly or annual records of these appropriations are reported to MNDNR. There are two permitted surface water appropriations in the Lake Superior South basin and two in the Lake Superior North basin (Table 2-6). The largest appropriations, drawn from the Beaver River in the Lake Superior South basin, are for mine processing and golf course irrigation. An appropriation is also drawn from the lower Poplar River during winter for snowmaking at the Lutsen Mountain Resort.

Table 2-6. Permitted Surface Water Appropriations in the Lake Superior North and South Watersheds

Index	Permit Number	Name	Primary Use	Model Reach	Monthly Avg. Appropriation (MGD)	Period of Operation
1	1964-0846	Lutsen Mountains Corporation	Snow and Ice Making	193 (N)	0.159	1995 - 2012
2	2003-2074	City of Grand Marais	Golf Course Irrigation	219 (N)	0.011	2003 - 2012
3	1976-2052	Northshore Mining Company	Mine Processing	151 (S)	3.63	1995 - 2012
4	1971-0393	Silver Bay Country Club	Golf Course Irrigation	155 (S)	3.37	1995 - 2012

(This page left intentionally blank.)

3 Model Calibration and Validation Approach

3.1 FLOW AND WATER QUALITY DATA

Flow gaging in the Lake Superior North and South watersheds has been conducted by USGS and MNDNR. USGS gaging records were retrieved from the NWIS system and MNDNR gaging records from the HYDSTRA system. The majority of gages operate only on a seasonal basis (generally April through September) due to ice cover, which means that a large portion of the spring runoff may be missed, complicating efforts to fit an overall water balance.

The period of record and currency of HYDSTRA monitoring data was used to select locations to be used for HSPF model development, calibration, and validation. Only those gages with data available during the model simulation period (1993-2012) were selected for inclusion in the HSPF model. All gages with significant amounts of recent monitoring were included in the segmentation analysis with two exceptions: The Pigeon River gage is not considered because half of the Pigeon River watershed is in Canada and will not be modeled in this effort. The Duluth Ship Canal gage is in Duluth Harbor and not a part of the upland watershed model. HYDSTRA locations selected for use in the model are shown in Table 3-1; locations are shown above in Figure 2-15.

Table 3-1. Selected HYDSTRA Flow Gage and EQUIS Water Quality Calibration Locations

HYDSTRA/ EQUIS ID	STORET ID	USGS ID	Short Name	Start Date	End Date	Years	HUC8	Water Quality
02037005	S004-950		EB Amity Ck	4/10/2011	11/6/2012	1	South	
02038001	S001-757		Amity Creek	4/10/2002	12/31/2012	10	South	X
02035001	S001-755	04015368	Talmadge River CR281	4/18/2001	11/10/2008	7	South	X
02031001	S001-756	04015339	Sucker River	4/7/2001	12/31/2013	12	South	X
02009001	S003-670	04015325	Knife R. at Airport	5/14/2004	11/8/2010	6	South	X
02021001	S003-668	04015335	Nappa	10/1/2003	10/1/2007	4	South	
02026001	S003-642	04015330	Fish Trap	7/1/1974	8/27/2014	40	South	
02012004			Gooseberry State Park	3/30/2011	12/31/2012	1	South	
02006003	S004-955		Beaver R. at Beaver Bay	4/11/2011	11/12/2012	1	South	
01092001	S000-250	04014500	Baptism Beaver Bay	8/1/1928	12/31/2013	85	North	X
01063003	S004-406		Poplar River - Golf	10/1/2001	12/31/2013	12	North	X
01022001	S000-251	04011000	Brule River	4/15/2002	11/15/2012	10	North	X
01008002		04010528	Res River, GP	5/22/2003	6/2/2004	1	North	
<i>Gages not Selected</i>								
01001001		04010500	Pigeon River	6/1/1921	8/27/2014	93	North	
01063001		04012500	Poplar 0.1mi us MN61	10/1/1912	9/30/1961	49	North	
02002001		464646092-052900	Superior Bay, Duluth Ship Canal	10/1/1994	3/17/2012	18	South	
01008001		04010530	Reservation River, Hovland	4/1/1991	9/30/1992	1	North	
01005001		04010510	Grand Portage River	5/13/1991	9/30/1992	1	North	

Water quality data have been collected at many locations within the Lake Superior North and South watersheds. Most of these data are available in EQUIS, and MPCA provided a full download of all stations. Despite the volume of data, stations that have collected significant amounts of nutrient data over a time period coincident with the model simulation period are few and an even smaller number are at or near flow gaging stations, which allows verification of the flow simulation and calculation of loads in addition to concentrations. The model segmentation was designed to line up with available flow gage locations and monitoring sites known to have large amounts of water quality data; however, some stations with small to moderate amounts of monitoring data were not usable for calibration because they were on tributaries or lakes that were too small for explicit inclusion in the basin-scale models.

The seven locations with both flow and water quality data were selected as the primary model calibration locations in the Lake Superior South and Lake Superior North watersheds. These locations are summarized in Table 3-2. Additional stations that lack flow data, including various lake stations, were used for supplementary model calibration purposes.

Table 3-2. Water Quality Calibration Locations

Location	Model Reach	EQUIS Station(s)
Amity Creek near Duluth	109	S001-757
Talmadge River near Duluth	114	S001-755
Sucker River near Palmers	120	S001-756
Knife River near Two Harbors	123+124	S003-642
Baptism River near Beaver Bay	161	S000-250
Poplar River near Lutsen	193	S004-406
Brule River near Hovland	231	S000-251

During the early stages of the calibration process efforts focused on accurately portraying nutrient concentrations simultaneously at stations located on the major streams in the South and North watersheds. In the South watershed this included the stations on the Amity Creek, Talmadge River, Sucker River, and Knife River. (Note that Amity Creek will also be evaluated at a finer spatial resolution in the Duluth WRAPS model now under construction). The Lake Superior North watershed stations include Baptism River, Poplar River, and Brule River. Much of the Lake Superior South and North watersheds are dominated by wetlands and hardwood forests, and the dynamics in the wetlands and forests complicate the modeling effort. A literature review was completed to support the selection of parameters appropriate for northern, wetland and hardwood forest dominated watersheds (see Section 6). The water quality calibration consisted of refining parameters that control nutrient stoichiometry (P:C, and P:N), phytoplankton and benthic algae population dynamics, nutrient transport, deposition, and scour, and nitrogen transformations (e.g. ammonification rate).

Water quality was generally monitored during the calibration period for all the selected sites in the Lake Superior South and North watersheds. Sucker River and Poplar River were selected to demonstrate the water quality calibration for the HSPF models of the South and North watersheds, respectively. Organic and inorganic nitrogen and phosphorus components were calibrated simultaneously but are summarized independently in the following sections.

3.2 HYDROLOGY CALIBRATION APPROACH

The level of performance and overall quality of hydrologic calibration is evaluated in a weight of evidence approach that includes both visual comparisons and quantitative statistical measures. The calibration proceeds in a sequential manner through (1) general representation of the overall water balance, (2) calibration of snow depth, (3) assurance of consistency with satellite-based estimates of actual ET and soil moisture, and (4) detailed calibration relative to flow gaging for seasonal flows, shape of the flow duration curve, and hydrograph shape.

Key parameters for hydrologic calibration and information on their potential ranges are as described in *BASINS Technical Note 6* (USEPA, 2000). Initial values of key parameters were related to soil and climatological properties where appropriate. Specifically, infiltration rates (INFILT) were initialized (and subsequently varied by) HSG, while initial values of lower zone nominal soil storage capacity (LZSN), upper zone soil storage capacity (UZSN), and interflow inflow (INTFW) were set based on annual average rainfall, consistent with USEPA (2000). Seasonal patterns based on vegetative cover (MON-LZETPARM, MON-INTERCEP, and MON-MANNING) and snow simulations were initialized based on past experience with Minnesota models.

Given the inherent errors in input and observed data and the approximate nature of model formulations, absolute criteria for watershed model acceptance or rejection are not generally considered appropriate by most modeling professionals. In contrast, most decision makers want definitive answers to the questions—“How accurate is the model?” and “Is the model good enough for this evaluation?” Consequently, the current state of the art for model evaluation is to express model results in terms of ranges that correspond to “very good,” “good,” “fair,” or “poor” quality of simulation fit to observed behavior. These characterizations inform appropriate uses of the model: for example, where a model achieves a good to very good fit, decision-makers often have greater confidence in having the model assume a strong role in evaluating management options. Conversely, where a model achieves only a fair or poor fit, decision makers may assume a much less prominent role for the model results in the overall weight-of-evidence evaluation of management options.

For HSPF and similar watershed models, a variety of performance targets have been documented in the literature, including Donigian et al. (1984), Lumb et al. (1994), Donigian (2000), Moriasi et al. (2007), and Duda et al. (2012). Based on these references and past model experience, the HSPF performance targets for simulation of hydrology are summarized in Table 3-3. Model performance is generally deemed fully acceptable where a performance evaluation of “good” or “very good” is attained. It is important to clarify that the tolerance ranges are intended to be applied to mean values, and that individual events or observations may show larger differences and still be acceptable (Donigian, 2000).

The model calibration generally attempts to achieve a good balance between the relative error metrics and the Nash-Sutcliffe coefficient of model fit efficiency (NSE; Nash and Sutcliffe, 1970). Unlike relative error, NSE is a measure of the ability of the model to explain the variance in the observed data. Values may vary from $-\infty$ to 1.0. A value of $NSE = 1.0$ indicates a perfect fit between modeled and observed data, while values equal to or less than 0 indicate the model’s predictions of temporal variability in observed flows are no better than using the average of observed data. The accuracy of a model increases as the value approaches 1.0. Moriasi et al. (2007) suggest that achieving a relative error on total volume of 10 percent or better and an NSE of 0.75 or more on *monthly* flows constitutes a good modeling fit for watershed applications.

It should be noted that many of the available gage records in the Lake Superior North and South watersheds operate only on a seasonal basis, so that full evaluation of seasonal statistics (or, indeed, evaluation of the total water balance) is not possible. In addition, where winter gaging records are available they are typically imprecise due to interference from ice cover.

Table 3-3. Performance Targets for HSPF Flow Simulation (Magnitude of Annual and Seasonal Relative Average Error; Daily and Monthly NSE)

Model Component	Very Good	Good	Fair	Poor
1. Error in total volume	≤ 5%	5 - 10%	10 - 15%	> 15%
2. Error in 50% lowest flow volumes	≤ 10%	10 - 15%	15 - 25%	> 25%
3. Error in 10% highest flow volumes	≤ 10%	10 - 15%	15 - 25%	> 25%
4. Error in storm volume	≤ 10%	10 - 15%	15 - 25%	> 25%
5. Winter volume error (JFM)	≤ 15%	15 - 30%	30 - 50%	> 50%
6. Spring volume error (AMJ)	≤ 15%	15 - 30%	30 - 50%	> 50%
7. Summer volume error (JAS)	≤ 15%	15 - 30%	30 - 50%	> 50%
8. Fall volume error (OND)	≤ 15%	15 - 30%	30 - 50%	> 50%
9. NSE on daily values	> 0.80	> 0.70	> 0.60	≤ 0.60
10. NSE on monthly values	> 0.85	> 0.75	> 0.65	≤ 0.65

3.3 SEDIMENT CALIBRATION APPROACH

Sediment is one of the more difficult water quality parameters to calibrate in watershed models because observed instream concentrations depend on the net effects of a variety of upland and stream reach processes, only some of which are directly observed. Further, conditions in one stream reach may depend strongly on erosion and deposition patterns in the upstream reaches. Thus mass balance checks need to examine every reach in the model. Sediment calibration was undertaken in accordance with AQUA TERRA (2012) as well as the guidelines BASINS Technical Note 8: *Sediment Parameters and Calibration Guidance for HSPF* (USEPA, 2006). Sediment calibration required an iterative approach. The first step in calibration involves setting channel erosion to values that achieve a reasonable fit to observations when upland erosion is at rates consistent with the literature and soil survey data. The upland simulation is then further tuned. Next, the long-term behavior of sediment in channels is constrained to a reasonable representation in which degradation or aggradation amounts are physically realistic and consistent with available local information. Finally, results from detailed local stream studies are used to further ensure that the model provides a reasonable representation in specific areas.

The upland parameters for sediment were related to soil and topographic properties. HSPF simulates sediment yield to streams in two stages. First, HSPF calculates the detachment rate of sediment by rainfall (in tons/acre) as

$$DET = (1 - COVER) \cdot SMPF \cdot KRER \cdot P^{JRER}$$

where *DET* is the detachment rate (tons/acre), *COVER* is the dimensionless factor accounting for the effects of cover on the detachment of soil particles, *SMPF* is the dimensionless management practice factor, *KRER* is the coefficient in the soil detachment equation, *JRER* is the exponent in the soil detachment equation, which is recommended to be set to 1.81, and *P* is precipitation depth in inches over the simulation time interval. Direct addition of sediment (e.g., from wind deposition) is also added via

the parameter *NVSI*. Actual detached sediment storage available for transport (*DETS*) is a function of accumulation over time and the reincorporation rate, *AFFIX*.

The transport capacity for detached sediment from the land surface (*STCAP*) is represented as a function of overland flow:

$$STCAP = KSER \cdot (SURS + SURO)^{JSER}$$

where *KSER* is the coefficient for transport of detached sediment, *SURS* is surface water storage (inches), *SURO* is surface outflow of water (in/hr), and *JSER* is the exponent for transport of detached sediment.

DET is similar in concept to the Universal Soil Loss Equation (USLE; Wischmeier and Smith, 1978), which predicts sediment detachment as a function of is the rainfall erosivity, *RE*, a soil erodibility factor, *K*, a length-slope factor, *LS*, a cover factor, *C*, and a practice factor, *P*:

$$DET = RE \cdot K \cdot LS \cdot C \cdot P.$$

USLE predicts sediment loss from one or a series of events at the field scale, and thus incorporates local transport as well as sediment detachment.

There are two approaches that may be pursued from this point. One is to develop a formal approximation between the HSPF *KRER* and the USLE *K* factor as was done in Tetra Tech (2009). The other approach is to simply assume *KRER* = *K*, as is recommended in USEPA (2006). In theory, *KRER* ought to approximate the product of *K* and the *LS* factor, multiplied by a constant. However, slope is also a key factor in determining the depth of surface runoff and storage - and thus transport capacity - in HSPF, so the approach of deriving *KRER* from *K* and *LS* may encounter complications in practice. In areas of generally low slopes variation of *KRER* with slope is expected to be small and the relationship will tend toward linear. Therefore, it is sufficient to use the approach recommended in USEPA (2006) and equate *KRER* and *K*, as was done for this model. The major difference between the two approaches is in the practical definition of the reincorporation rate, *AFFIX*, which will assume different values in order to achieve a stable seasonal cycle of *DETS*.

Once *KRER* is established, the primary upland calibration parameter for sediment is *KSER*, which determines the ability of overland flow to transport detached sediment. HSPF can also simulate gully erosion in which sediment generated from the land surface is not constrained by rainfall detachment. Ravines and evidence of gully erosion are present throughout the Lake Superior South and North watersheds but specific locations are generally not known except for the GIS analysis of bluffs developed by the University of Minnesota – Duluth Natural Resources Research Institute (NRRI; <http://www.nrri.umn.edu/coastalgis/newweb/html/bluffs.htm>). Bluff loading was simulated by a separate method (described in Section 5). Limited gully erosion was simulated in areas with moderate to high slopes (greater than 5 percent).

Key parameters controlling channel erosion, deposition, and sediment transport within streams and rivers are as follows (USEPA, 2006):

KSAND: Sand transport is represented with a power function based on average velocity, such that carrying capacity for sand = *KSAND* x *AVVEL*^{*EXPSND*}. *KSAND* is set to 0.1 and *EXPSND* to 2 to start calibration and adjusted to improve the comparison between simulated and observed suspended sediment concentrations at flows where cohesive silt and clay sediments do not scour as well as to ensure a reasonable evolution of sand storage over time,.

TAUCD: HSPF calculates bed shear stress (*TAU*) during each model time step for each individual reach. The critical bed shear stress for deposition (lb/ft²) represents the energy level below which cohesive sediment (silt and clay) begins to deposit to the bed. Initial values of *TAUCD* for silt and clay were estimated by reach by examining the cumulative distribution function of simulated shear stress and setting

the parameter to a lower percentile of the distribution in each reach segment, as recommended by USEPA (2006). The 20th percentile was used for clay and the 25th percentile for silt.

TAUCS: The critical bed shear stress for scour (lb/ft^2) represents the energy level above which scour of cohesive sediment begins. Initial values of TAUCS were set, as recommended, at upper percentiles of the distribution of simulated shear stress in each reach (the 90th percentile for clay and the 95th percentile for silt). Values for some individual reaches were subsequently modified during calibration.

M: The erodibility coefficient of the sediment ($\text{lb}/\text{ft}^2\text{-d}$) determines the maximum rate at which scour of cohesive sediment occurs when shear stress exceeds TAUCS. This coefficient is a calibration parameter. It was initially set to 0.004 for silt, 0.003 for clay, and adjusted during calibration in some reaches.

An example of the distribution of shear stress versus flow for Talmadge River is shown in Figure 3-1. The notch that appears in the profile around 35 cfs represents the reduction in cross-section averaged shear stress that occurs when the flow spreads overbank into the flood plain.

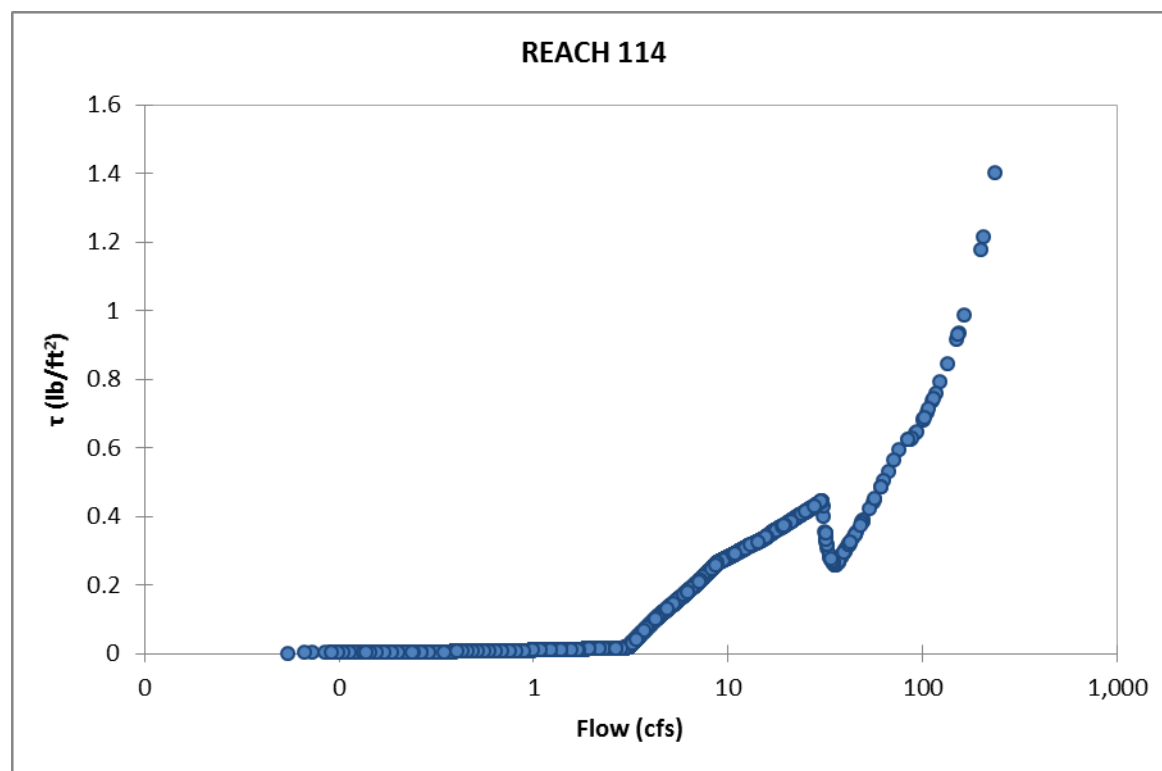


Figure 3-1. Shear Stress Distribution for Talmadge River (Reach 114)

Calibration for sediment and other water quality parameters differs from calibration for hydrology in that pollutant concentrations are in most cases not continuously monitored. Instead, observations typically provide measurements of conditions at a point in time and point in space via a grab sample. The discrete nature of these samples presents problems for model calibration: A sample that represents a point in time could have been obtained from a system where conditions are changing rapidly over time – for instance, the rising limb of a storm hydrograph. Such samples cannot be expected to be matched by a model prediction of a daily average concentration. On the other hand, there may be large discrepancies between dynamic model predictions of hourly concentrations and data that are a result of small timing errors in the prediction of storm event flow peaks. Spatially, grab samples reflect conditions in one part of a stream reach (which may or may not be composited over the width and depth of a cross section). HSPF model results, in contrast, represent average concentrations over the length of a stream reach which is assumed

to be fully mixed. Model predictions and field observations inevitably have some degree of mismatch in space and time and, even in the best models, will not fully match. Accordingly, a statistical best fit approach is needed.

Performance targets for sediment calibration, based on Donigan (2000), are summarized in Table 3-4. These performance targets are evaluated for both concentration and load, where load is estimated from concentration, on paired data, and should only be applied in cases where there are a minimum of 20 observations. Model performance is generally deemed acceptable where a performance evaluation of “good” or “very good” is attained.

Table 3-4. Performance Targets for HSPF Sediment Simulation (Magnitude of Annual and Seasonal Relative Average Error (RE) on Daily Values)

Model Component	Very Good	Good	Fair	Poor
Suspended Sediment	≤ 20%	20 - 30%	30 - 45%	> 45%

3.4 WATER QUALITY CALIBRATION APPROACH

Water quality simulation depends on the simulation of hydrology and sediment transport. This section addresses the calibration and validation of the model simulation of water temperature, dissolved oxygen, nutrients, and algae.

Although not a primary focus of the modeling effort, water temperature simulation is important in the watershed model for several reasons: water temperature affects many biologically mediated processes that influence water quality in the streams, and the temperature of the water determines how it will mix when it enters the lake.

Daily average water temperature in shallow flowing streams is largely controlled by air temperature. Temperature cycles within the day, however, may be strongly affected by heat gain from incoming solar radiation and heat loss due to longwave back radiation. Both of these effects are controlled by the extent of cover and shading on the stream in addition to meteorological variables such as solar radiation and cloud cover.

A detailed diel simulation of stream water temperature is a complex undertaking. The timing and magnitude of heat fluxes are controlled by a variety of factors such as stream orientation and vegetative and topographic shading angles that cannot be fully represented in a basin-scale HSPF model. For example, a stream oriented east-west is likely to be exposed to unshaded solar radiation for a longer part of the day than a stream oriented north-south. Stream shading varies over the course of the year as canopy density changes, and may also change over time as trees grow, are cut, fall due to ice and wind storms, or due to fire. HSPF approximates all these complex details through the assignment of a temporally constant “surface exposed” (CFSAEX) factor that represents the average fraction of tree-top solar radiation reaching the water surface. Given these issues, the stream temperature calibration was checked for reasonableness, but not constrained to achieve specific statistical targets.

Loading of nutrients that may support excess algal growth – either within the waterbodies of the Lake Superior North and South basins or in Lake Superior – is an important concern. The major nutrients controlling algal growth are phosphorus and nitrogen. Both are simulated in detail in the model. Minor nutrients (e.g., silica, iron) may also play a role in determining algal response but are not simulated in the watershed model. The first step in a sequential process for nutrient calibration is to verify that unit area loading rates were reasonable compared to literature values. Next, calibration to instream observations is carried out to refine the simulation. Plant growth has an important effect on nutrient balances during low

flow conditions and serves to convert inorganic nutrients into organic forms; therefore, nitrogen and phosphorus species must be calibrated simultaneously with algae.

In forested watersheds, much of the nutrient load moves as a constituent of organic matter (including leaf litter, other debris, and dissolved organic compounds, such as humic acids), while stream concentrations of inorganic nutrients remain low in these watersheds. In contrast, agriculture and fertilized lawns may export significant amounts of nutrients in inorganic forms. Point source discharges can contain a mix of organic and inorganic nutrient forms dependent on the treatment process.

The approach taken is to simulate three components in loading from the land surface as general quality constituents (GQUALs): inorganic nitrogen (nitrate, nitrite, and ammonia), inorganic phosphorus (total orthophosphate), and organic matter. Each of these constituents is then partitioned at the point of entry into the stream network:

- Inorganic nitrogen is partitioned into dissolved nitrate, dissolved ammonium, and sorbed ammonium. Fractions of the dissolved constituents are set to reproduce observed data, while sorption of ammonium is simulated using equilibrium partitioning assumptions (the model connects inorganic N from the land surface to dissolved N in the stream reach, but equilibrium partitioning to the sorbed form occurs instantaneously). Assignment of total inorganic nitrogen from the land surface to nitrate and ammonium at the point of entry to the stream is represented by a constant ratio throughout the model, but differs for agricultural land and impervious surfaces. Partitioning of ammonium between dissolved and sorbed forms depends on local suspended sediment concentrations. A small portion of the inorganic N is routed directly to organic N to represent uptake by heterotrophic organisms in low order streams (a process not explicitly simulated by the model).
- Inorganic phosphorus is partitioned into dissolved and sorbed fractions using equilibrium partitioning assumptions. As with ammonium, the fraction that becomes sorbed depends on the local suspended sediment concentration,
- Organic matter (biomass) is partitioned into labile and refractory organic carbon, organic nitrogen, and organic phosphorus components. Initial specifications were based on expected stoichiometry of forest litter, and then revised during calibration to achieve agreement with observed concentrations.

All three upland components (inorganic nitrogen, inorganic phosphorus, and organic matter) may be loaded through either surface flow or subsurface flow (interflow and groundwater discharge). The HSPF GQUAL algorithms do not maintain a full mass balance of subsurface constituents (which would require a groundwater quality model); rather, the user specifies concentration values, which may vary monthly, for interflow and groundwater. Surface washoff loading is considered from both pervious and impervious surfaces.

Inorganic phosphorus loading from pervious surfaces is simulated as a sediment-associated process because of the strong affinity of orthophosphate for soil particles. Surface loading of inorganic phosphorus is thus determined by a potency factor applied to sediment load, which may vary on a monthly basis to reflect changes in surface soil concentration associated with the annual growth cycle. (While this reflects the physical basis of surface loading of inorganic phosphorus, it does mean that any errors in the simulation of sediment loading will also affect estimates of inorganic phosphorus loading.) Subsurface flow pathways are assumed primarily to load small amounts of dissolved inorganic phosphorus. Organic matter is also simulated as a sediment-associated load from pervious surfaces, as this primarily represents the erosion of humus, leaf litter, and other detritus.

In contrast to phosphorus, inorganic nitrogen is highly soluble, and loading in surface runoff may occur independent of sediment movement (particularly where fertilizer is applied). Further, much of the nitrate

load in surface runoff represents input from atmospheric deposition. Therefore, inorganic nitrogen loading from pervious surfaces is represented via a buildup-washoff process in which the user specifies a rate of accumulation, an accumulation limit, and a flow rate sufficient to remove 90 percent of the accumulated material.

As noted above, representation of plant growth is a necessary part of the nutrient calibration process. HSPF contains routines for simulating planktonic (floating) and benthic (attached) algae. Growth, respiration, and death processes are affected and potentially limited by the availability of light, availability of inorganic nutrients, water depth, and water temperature. Because HSPF represents stream segments as one-dimensional, fully-mixed reactors, the predictions of algal response are averages throughout the stream segment volume. Planktonic and benthic algae simulations differ primarily in the way that the attenuation of light availability is calculated. For plankton light availability is calculated as the average over the euphotic depth, such that all phytoplankton are assumed to be mid-depth in the reach or the middle of the euphotic zone, whichever is smaller, then adjusted to the full volume of the reach. Benthic algae are assumed to be at the average depth of the reach. These simplifying assumptions can distort the actual response in some situations. For deeper reaches, especially lakes, the phytoplankton simulation results are an average over the reach volume, which does not match well with chlorophyll *a* observations collected from the photic zone. When the average depth is large relative to the light extinction rate benthic algal growth will be simulated as minimal, whereas significant growth may actually occur in the shallower edges of the lake or stream. The scheme does not include a representation of floating or emergent rooted macrophytes. While these can sometimes be successfully approximated with the benthic algae routines, the light availability calculations for benthic algae are not appropriate to these types of macrophytes and the program does not consider that floating/rooted macrophytes can exchange gases with the atmosphere and obtain nutrients from the sediment.

The dissolved oxygen simulation considers reaeration, the decay of organic matter (carbonaceous biochemical oxygen demand), oxidation of ammonia and nitrite N, sediment oxygen demand, and algal photosynthesis and respiration. In the slow-moving, wetland areas of the Lake Superior North and South watersheds, the DO balance is largely a factor of the interplay of algal growth and sediment oxygen demand exerted by the decay of settled organic matter.

For most water quality constituents, it is unreasonable to propose that the model predict all temporal variations in concentration and load. The model should, however, provide an accurate representation of long-term and seasonal trends in concentration and load, and correctly represent the relationship between flow and load. To ensure this, it is important to use statistical tests of equivalence between observed and simulated concentrations, rather than relying on a pre-specified model tolerance on difference in concentrations.

Ideally, average errors and average absolute errors should both be low, reflecting a lack of bias and high degree of precision, respectively. In many cases, the average error statistics will be inflated by a few highly discrepant outliers. It is therefore also useful to compare the median error statistics.

General performance targets for water quality simulation with HSPF are also provided by Duda et al. (2012) and are shown in Table 3-5. These are calculated from observed and simulated daily concentrations, and should only be applied in cases where there are a minimum of 20 observations.

Table 3-5. Performance Targets for HSPF Water Quality Simulation (Magnitude of Annual and Seasonal Relative Average Error (*RE*) on Daily Values)

Model Component	Very Good	Good	Fair	Poor
Temperature	≤ 7%	8 - 12%	13 - 18%	> 18%
Water Quality/Nutrients	≤ 15%	15 - 25%	25 - 35%	> 35%

Evaluation of water quality simulations presents a number of challenges because, unlike flow, water quality is generally not monitored continuously. Grab samples at a point in space and time may not be representative of average conditions in a model reach on a given day due to either spatial or temporal uncertainty (i.e., an instantaneous measurement in time may deviate from the daily average, especially during storm events, while a point in space may not be representative of average conditions across an entire model reach). Where constituent concentrations are near reporting levels, relative uncertainty in reported results is naturally high. Accurate information on daily variability in point source loads is also rarely available.

Evaluation of relative average error is recommended, but averages are prone to biasing by one or a few extreme outliers. Therefore, it is also useful to examine median relative errors, which are less influenced by outliers.

The performance targets for water quality simulation may be applied to either concentrations or loads. Concentrations provide the most natural metric, but error magnitude may be unduly influenced by variability at low flow conditions that has little effect on cumulative loading downstream. Loads are more meaningful for impacts in downstream lakes, harbors, and estuaries but are not directly observed and need to be estimated from flow and concentration – both uncertain. Tests on loads are performed in two ways: on paired data (observed and simulated daily average concentration multiplied by flow) and on complete time series of monthly loads. For the latter approach, “observed” monthly loads are estimated using the USACE FLUX32 program (a Windows-based update of the FLUX program developed by Walker, 1996), and are themselves subject to significant uncertainty.

Additional statistical tests are also applied as part of a weight-of-evidence examination of the water quality calibration. Two-sample *t*-tests are reported on the differences in mean concentration and mean load, with higher probability values indicating less chance that the measures are systematically different. A problem with the *t*-test is that the test is on a null hypothesis that the mean difference is exactly equal to zero, not whether the difference is physically meaningful. Therefore, a low value on the *t*-test (rejection of the null hypothesis) is generally considered of practical significance only when the mean difference is greater than 10 percent. Additional graphical tests are also performed to ensure that errors in the prediction of load and concentration do not exhibit strong correlations relative to flow magnitude and season.

4 Hydrology Calibration and Validation Results

4.1 SNOW CALIBRATION

Snow pack is a key component of the water balance of these northern watersheds and is particularly important for calibration when gage data are limited. Daily snow depth as simulated by the HSPF model was compared to snow depth and snow water equivalent available from the National Snow and Ice Data Center (NSIDC) and the “Snow Rules!” monitoring undertaken by the Minnesota Lake Superior Coastal Program (<http://climate.umn.edu/snowrules/snowRules.htm>). The NSIDC Snow Data Assimilation System (SNODAS) data products integrate snow data from satellites, ground observations and aircrafts to provide estimates of snow cover and associated parameters (Carroll et al., 2001). Snow depth and snow water equivalent are available from September 2003 to present at a spatial resolution of 1 km by 1 km and a temporal resolution of 1 day for the Continental United States (CONUS). HSPF simulated daily time-series were compared to SNODAS aggregated by weather regions.

During the snow depth calibration process values of parameters in the SNOW-PARM1 and SNOW-PARM2 blocks of the HSPF model were configured by weather regions. The calibrated values of these parameters are provided in Table 4-1. Summary statistics of snow calibration for depth and water equivalents are provided in Table 4-2. Graphical comparison of simulated and SNODAS snow cover are shown in Figure 4-1 to Figure 4-4.

The fit to snow depth and snow water equivalent is approximate as uncertainties exist in the interpretation of remotely sensed data in SNODAS. It is also important to note that snowfall and melt in the model are highly sensitive to ambient air temperature. Small inconsistencies in air temperatures may have potentially significant impacts on snow behavior, including whether precipitation is interpreted by the model as snow. As shown in Table 4-1, calibration for hydrology incorporated snow catch factors greater than one for half of the weather station areas. This compensates for the fact that precipitation gauges often under-estimate snow due to wind effects and was done to help achieve balance on total water yield, but may tend to over-estimate snow depth in mid-winter. Although the average errors are large for some weather regions, the errors in average snow depth and snow water equivalents spatially averaged over Lake Superior South and North watersheds are relatively lower (Figure 4-1 through Figure 4-4). Additional details of the snow calibration are provided in Appendix A.

Table 4-1. HSPF Snow Calibration Parameter Values

Parameter	Description	Calibrated Value	Recommended Range
SHADE	Fraction shaded from solar radiation	0.25 (Water)	0 - 0.8
		0.85 ^a (Evergreen forest)	
		0.85 ^a (Forested wetland)	
		0.5 (Deciduous forest)	
		0.5 (Herbaceous wetland)	
		0.1 (All other land-covers)	
SNOWCF	Snow gage catch correction factor	1.2 (WST 7)	1.0 - 2.0
		1.1 (WST 18)	

Parameter	Description	Calibrated Value	Recommended Range
		1.0 (All other WSTs)	
COVIND	Snowfall required to fully cover surface	0.1-0.5	0.1 - 10.0
RDCSN	Density of new snow	0.15	0.05 - 0.30
TSNOW	Temperature at which precipitation becomes snow	31.0-33.0	30.0 - 40.0
SNOEVP	Snow evaporation factor	0.10	0.0 - 0.5
CCFACT	Condensation/convection melt factor	0.1-0.5	0.5 - 8.0
MWATER	Liquid water storage capacity in snowpack	0.005	0.005 - 0.2
MGMELT	Ground heat daily melt rate	0.0001	0.0 - 0.1

a. The HSPF recommended value of SHADE is the fraction of forest cover that is coniferous or evergreen. For typical HSPF applications, forested land is not segregated into deciduous and evergreen forests. Since evergreen forest is modeled as a separate land use category in this application, the value of SHADE can theoretically be as high as 1.0.

Table 4-2. Summary of Snow Calibration Results

Weather Region #	Snow Depth			Snow Water Equivalent		
	Total Error ^a	Daily R ²	Daily NSE	Total Error	Daily R ²	Daily NSE
1	-18.8%	0.69	0.54	-20.0%	0.69	0.52
2	-13.7%	0.79	0.73	-9.0%	0.82	0.80
3	-13.1%	0.71	0.62	-12.4%	0.72	0.65
4	-11.3%	0.85	0.82	-8.9%	0.86	0.85
5	-6.6%	0.77	0.73	-1.9%	0.80	0.79
6	-5.3%	0.81	0.79	-1.6%	0.84	0.83
7	-0.2%	0.81	0.80	0.8%	0.85	0.84
8	-13.8%	0.59	0.30	-8.8%	0.59	0.41
9	-4.6%	0.71	0.68	-4.7%	0.74	0.72
10	10.6%	0.78	0.78	11.5%	0.82	0.81
11	6.0%	0.58	0.52	4.7%	0.59	0.53
12	-1.7%	0.65	0.61	-4.1%	0.67	0.64
13	4.2%	0.71	0.69	1.5%	0.73	0.72
14	13.0%	0.74	0.72	13.2%	0.75	0.74
15	-0.4%	0.62	0.58	-3.0%	0.63	0.60
16	-8.4%	0.63	0.56	-14.2%	0.63	0.55
17	-12.2%	0.69	0.63	-15.9%	0.71	0.66
18	-6.3%	0.70	0.65	-7.8%	0.71	0.67

a. Total error is calculated as the $\Delta = (\text{simulated} - \text{observed})/\text{observed}$

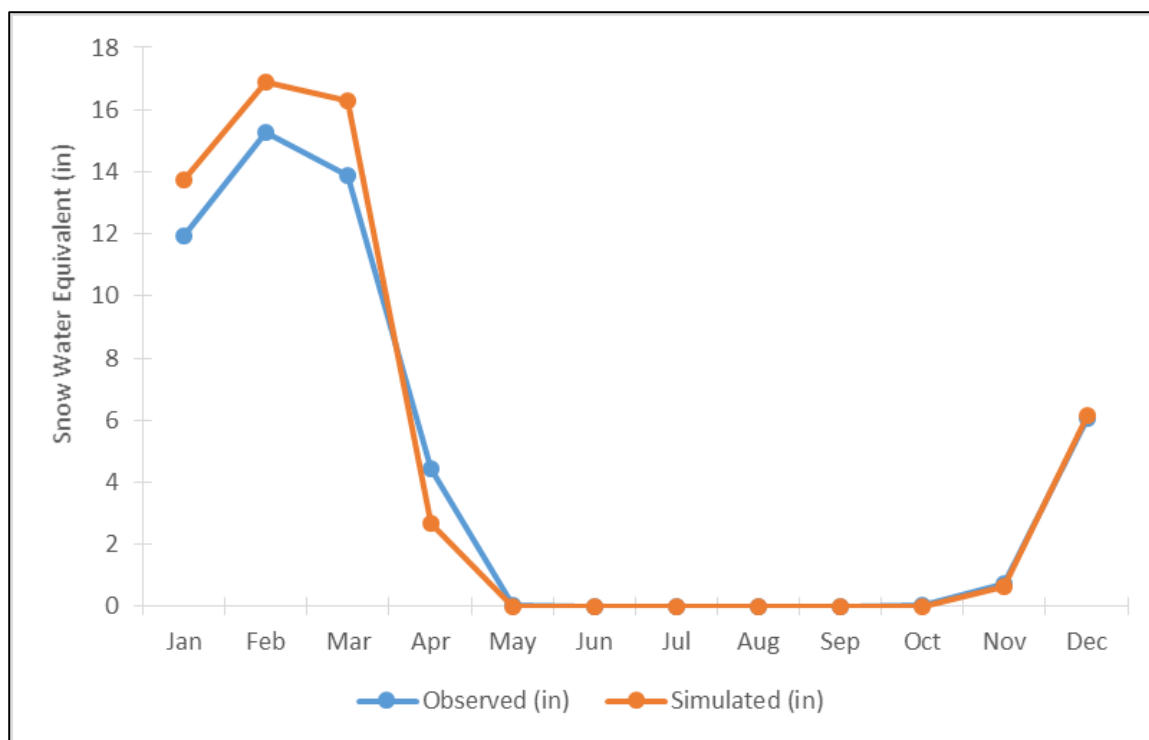


Figure 4-1. Comparison of average monthly snow depth with SNODAS for Lake Superior South watershed

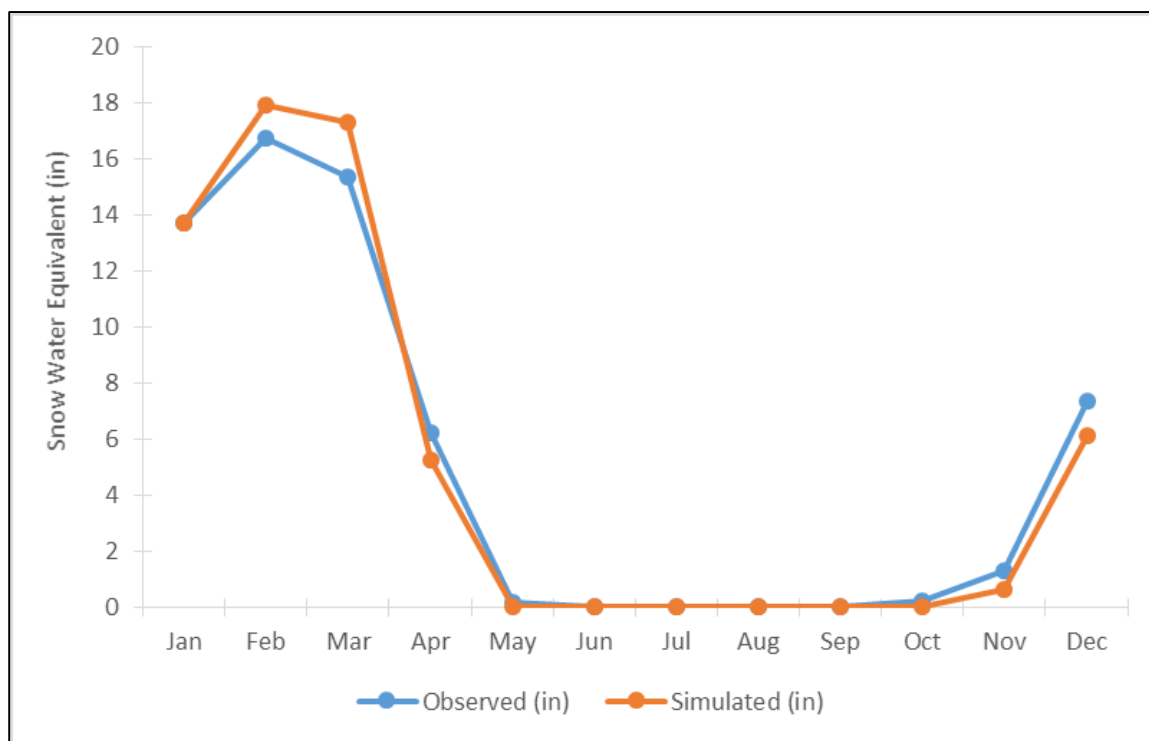


Figure 4-2. Comparison of Average Monthly Snow Depth to SNODAS for Lake Superior North watershed

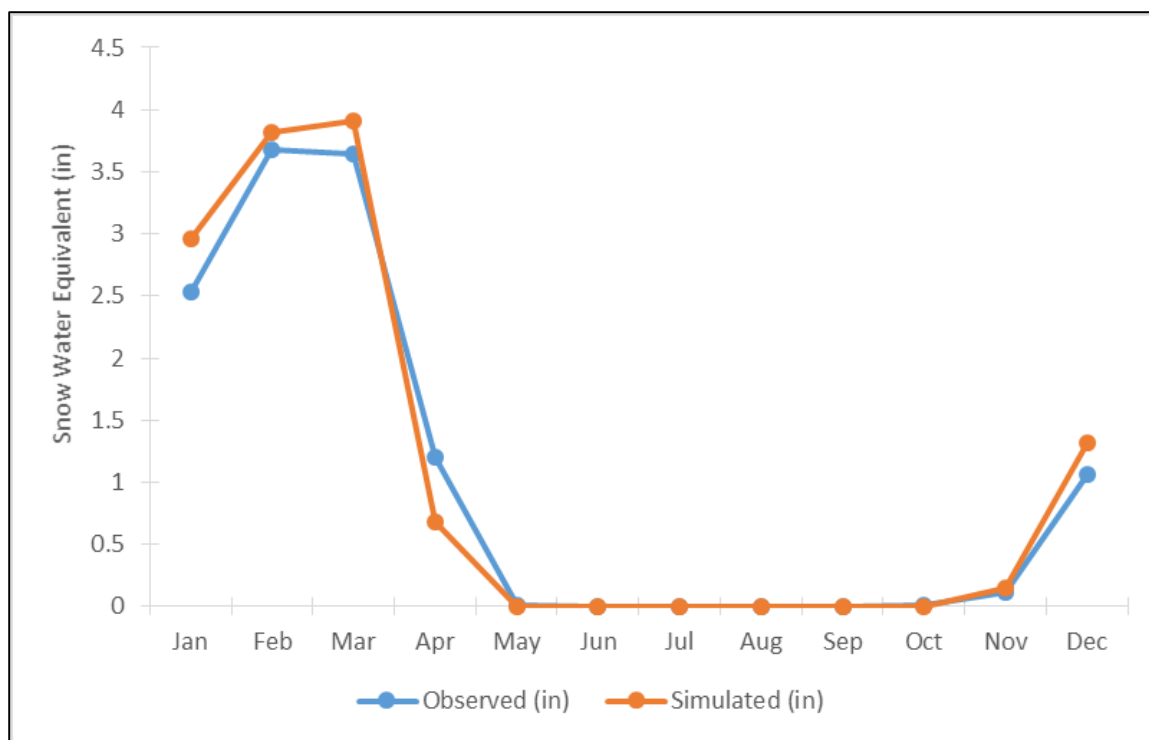


Figure 4-3. Comparison of Average Monthly Snow Water Equivalents to SNODAS for Lake Superior South watershed

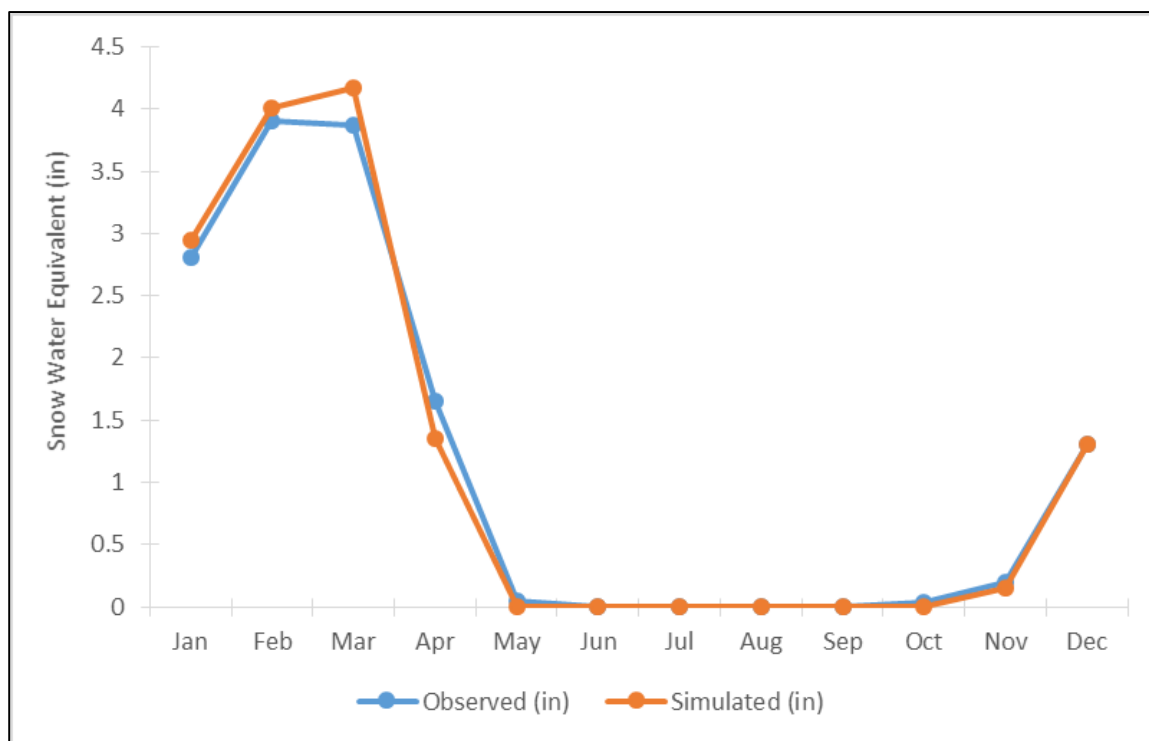


Figure 4-4. Comparison of Average Monthly Snow Water Equivalents to SNODAS for Lake Superior North watershed

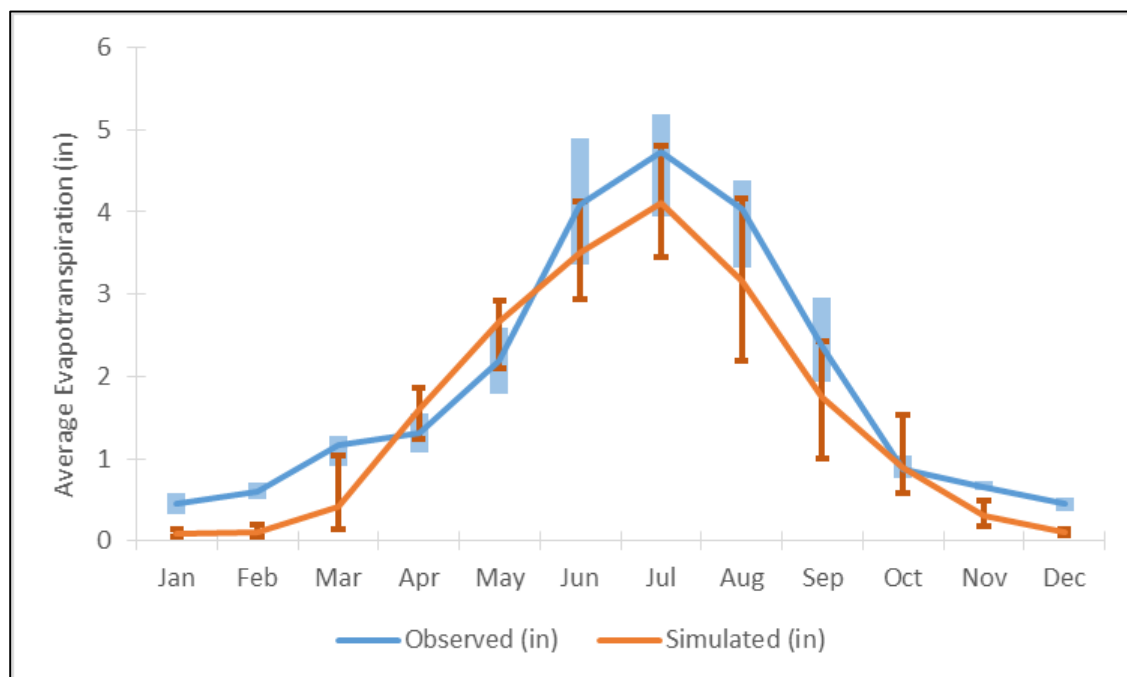
4.2 CONSTRAINTS ON SOIL MOISTURE BALANCE AND EVAPOTRANSPIRATION

Evapotranspiration (ET) is the largest component of the water balance and is thus crucial to hydrologic calibration. However, actual ET is often unconstrained in watershed models due to a lack of observed data. For the Lake Superior North and South models this issue was addressed through the use of remotely sensed ET data. The MODIS Global Evapotranspiration Project (MOD16) provides estimates of global terrestrial ET by using satellite remote sensing data at a spatial scale of 1 km² grid and at temporal scales of 8-days, months, and yearly totals from 2000 to 2010. It is important to recognize that MODIS does not directly measure evapotranspiration. Rather, an algorithm that considers MODIS land cover, albedo, leaf area index, and enhanced vegetation index is combined with daily meteorological data from NASA's Global Modeling and Assimilation Office reanalysis datasets using a Penman-Monteith type of approach (Mu et al., 2011). A validation study (Velpuri et al., 2013) showed that MODIS was able to estimate monthly ET within about 25 percent based on comparison to FLUXNET studies. These data are thus imprecise, but provide a useful reality check on the model formulation.

Monthly ET estimates for the Lake Superior North and South watersheds were extracted from the global MOD16 dataset. The gridded data were then aggregated to the level of the weather regions used in the model. The aggregated monthly data were compared to actual ET (TAET) simulated by the model and used to inform the pan coefficients used to convert Penman Pan PET to land surface PET in the model. The pattern of observed monthly evapotranspiration was also used to refine the MON-INTERCEP and MON-LZETPARM blocks in the HSPF model. Table 4-3 provides a summary comparison of simulated ET versus MODIS estimates. Figure 4-5 and Figure 4-6 show average monthly simulated evapotranspiration in comparison with MODIS estimates for Lake Superior South and North watersheds, respectively. In general, the simulated ET is similar to that estimated by MODIS, except in the winter months. MODIS estimates in the winter months are generally higher than that simulated by HSPF. It is not clear if this represents systematic over-estimation by MODIS or under-estimation by the HSPF snow sublimation algorithms; however, similar results have been observed in the St. Louis River watershed and other Minnesota HUC8 HSPF models. MODIS also predicts a slower ramp up of spring – early summer ET than is necessary to predict summer flows. This may be because the MODIS algorithm relies on leaf area whereas a significant portion of the total evaporation during early periods of plant growth may come directly from the soil surface.

Table 4-3. Summary of Evapotranspiration Calibration Results

Weather Region #	Total Error	Monthly R ²	Monthly NSE
1	26.2%	0.87	0.76
2	18.0%	0.89	0.84
3	21.2%	0.88	0.81
4	17.4%	0.90	0.85
5	22.8%	0.88	0.80
6	16.9%	0.89	0.84
7	12.7%	0.88	0.86
8	26.2%	0.88	0.78
9	22.3%	0.89	0.81
10	6.1%	0.89	0.88
11	25.3%	0.92	0.81
12	19.9%	0.92	0.85
13	4.5%	0.91	0.90
14	4.8%	0.89	0.84
15	25.4%	0.92	0.81
16	21.7%	0.91	0.84
17	9.8%	0.91	0.90
18	4.3%	0.90	0.87

**Figure 4-5. Comparison of Average Monthly Simulated Evapotranspiration to MODIS Estimates for Lake Superior South Watershed**

Note: The error bars on the chart show the range of observed and simulated monthly evapotranspiration while the solid lines represent the averages.

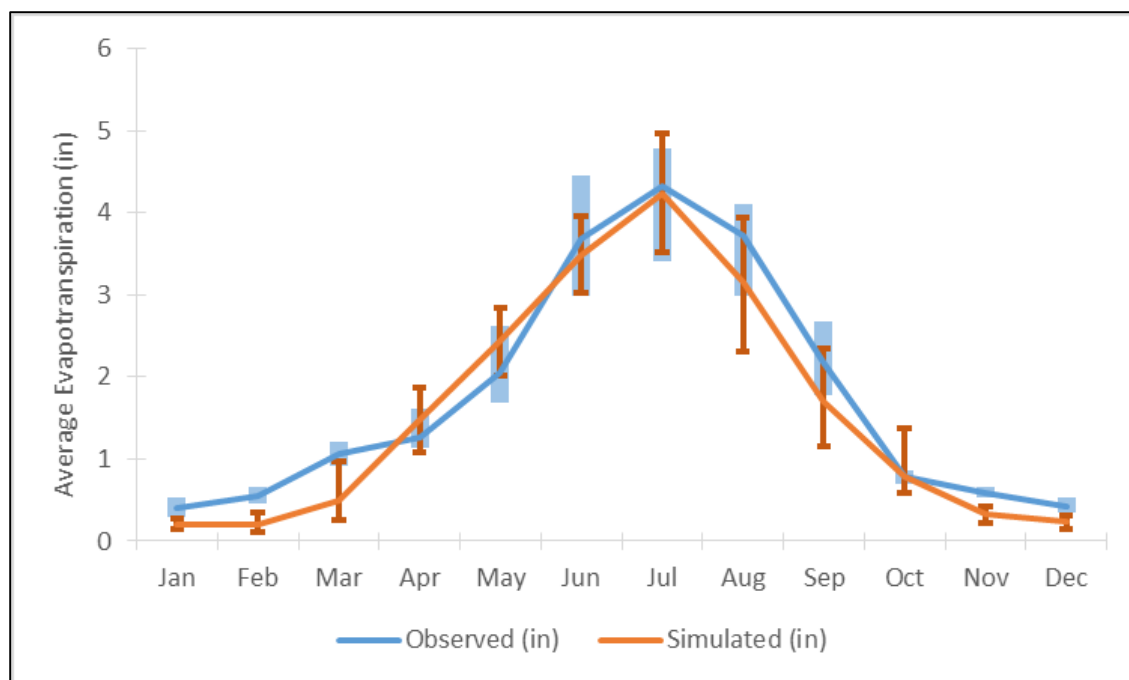


Figure 4-6. Comparison of Average Monthly Simulated Evapotranspiration to MODIS Estimates for Lake Superior North Watershed

Note: The error bars on the chart show the range of observed and simulated monthly evapotranspiration while the solid lines represent the averages.

4.3 FLOW CALIBRATION

Flow calibration and validation focused on the periods of 2002–2012 and 1993–2002, respectively. Calibration was completed by comparing time-series model results to gaged daily average flow. Key considerations in the hydrology calibration were the overall water balance, the high-flow to low-flow distribution, storm flows, and seasonal variations. The criteria in Table 3-3 are used to evaluate the quality of model fit.

The starting point for hydrologic parameters was provided by previous HSPF model applications in the adjacent St. Louis and Cloquet River watersheds. These starting values were then modified during calibration to optimize model fit while remaining within ranges recommended by USEPA (2000) and AQUA TERRA (2012).

Calibration results are ranked against the performance targets shown above in Table 3-3. Table 4-4 and Table 4-5 summarize the calibration results for gages in the Lake Superior South and North watersheds, respectively. Detailed analyses of all gages are provided in Appendix B.

While there are many gages in the watershed, the majority have only operated for a few years, and most report data only seasonally. Rating curves are also imprecise for many of these stations due to continual shifting of bed forms. This lends considerable uncertainty to the calibration. The short operational period of most gages also means that there are limited data for temporal validation. Hydrologist's notes accompanying the gage records show various periods in which there were equipment failures or the rating curve was suspect due to unstable channel conditions. Large percentage errors in low flows can arise in response to a small difference in actual flows in streams that have low summer flows, while highest flow errors can be unduly influenced by a single large event that requires extrapolation of the rating curve.

Table 4-4. Summary of Flow Calibration Results (Lake Superior South)

Statistic	Amity Creek	Talmadge River	Sucker River	Knife River	Gooseberry R	Beaver River
HYDSTRA gage number	02038001	02035001	02031001	02026001	02012004	02006003
Error in total volume	0.13%	-25.18%	3.35%	-1.10%	5.59%	-0.97%
Error in 50% lowest flows	17.69%	7.85%	-19.39%	40.79%	65.79%	20.05%
Error in 10% highest flows	-0.42%	-35.04%	12.11%	-13.45%	-1.37%	-3.57%
Seasonal volume error–Summer (J,A,S)	100.3%	56.66%	21.08%	85.56%	111.0%	44.08%
Seasonal volume error-Fall (O,N,D)	8.69%	-25.56%	-1.44%	8.89%	-4.59%	-2.71%
Seasonal volume error-Winter (J,F,M)	(1)	(1)	11.82%	8.15%	(1)	(1)
Seasonal volume error-Spring (A,M,J)	-10.92%	-36.58%	-0.11%	-14.53%	-0.08%	-4.20%
Error in storm volumes	15.95%	-24.82%	16.21%	-11.03%	1.06%	1.47%
Daily Nash-Sutcliffe Coefficient, NSE	0.65	0.53	0.75	0.79%	0.83	0.74
Baseline adjusted coefficient (Garrrick), E'	0.49	0.50	0.57	0.58%	0.67	0.64
Monthly NSE	0.71	0.57	0.87	0.87%	0.95	0.94

(1) Seasonal gage for which few winter measurements are available.

Note: Last three statistics formatted as fractions.

Table 4-5. Summary of Flow Calibration Results (Lake Superior North)

Statistic	Baptism River	Poplar River	Brule River
HYDSTRA gage number	01092001	01063003	01022001
Error in total volume	-4.35%	9.25%	-5.28%
Error in 50% lowest flows	-3.76%	17.97%	-1.28%
Error in 10% highest flows	-4.16%	4.39%	-8.81%
Seasonal volume error–Summer (J,A,S)	17.58%	28.19%	3.36%
Seasonal volume error-Fall (O,N,D)	-20.06%	28.85%	4.84%
Seasonal volume error-Winter (J,F,M)	2.31%	-8.67%	(1)
Seasonal volume error-Spring (A,M,J)	-4.48%	2.11%	-10.11%
Error in storm volumes	-10.43%	-3.07%	-7.52%
Daily Nash-Sutcliffe Coefficient, NSE	0.65	0.50	0.52
Baseline adjusted coefficient (Garrrick), E'	0.60	0.60	0.57
Monthly NSE	0.88	0.84	0.83

(1) Seasonal gage for which few winter measurements are available.

Note: Last three statistics formatted as fractions.

The modeled flow time-series matched well with the observed at the Amity Creek locations. The simulated March-April flows are generally lower than observed and could be due to under-representation of winter precipitation as to suspect observed data. The simulated low flow and summer volumes are larger than observed and maybe due to the under-representation of losses through conduits in bedrock stream channels or evapotranspiration losses during the summer months.

The model under-predicts total flow volume by more than 25% at the Talmadge River gage. A closer examination of the observed flow time-series shows that the average depth of flow on a unit area basis at this location is much larger compared to some of the neighboring watersheds despite similar landuse.

One reason could be under-estimation of precipitation over this watershed which is small compared to the relatively large weather regions over which the meteorological data are aggregated. There could also be other sources of inflow to the watershed that have not been identified.

The model performance at the Sucker and Knife River gages are generally good to very good. Over-estimation is however seen for low and summer flow volumes. Both these watersheds drain large wetland complexes in their headwaters. Some of the discrepancies observed during low flow conditions may be due to the complex hydrologic characteristics of these wetlands, which are affected by ice and seasonal plant growth, and likely not captured accurately by the model. It is also important to note that a large fraction of the observed data at the Sucker River gage is flagged as “Poor Archived Data Quality”. In addition, the gage was operated only seasonally prior to 2008. At the Knife River gage, although continuous, the fall and winter flow volumes are mostly estimated. The low flows at the Knife River gage are also influenced by fish ladder operations which are not explicitly simulated in the model.

The Gooseberry River and Beaver River gages essentially have data for two spring and summer seasons. The model performance, however, was good to very good for the short time-period of available data. Over-prediction of low and summer flow volumes are observed and are likely due to wetland influences as discussed earlier.

The landuse in the Lake Superior North watershed is similar to that in the South, consisting primarily of forests and wetlands, except that the Lake Superior South watershed has increased development near Duluth. Unlike the Lake Superior South streams, flows in many of the Lake Superior North streams are influenced by lakes. The largest of these lakes have been explicitly represented in the watershed model, but many smaller lakes are not.

The modeled flow time-series matched well with the observed at the Baptism River gage. All of the flow volume error statistics are rated as good or very good. Some of the peak flows events do appear to be over-estimated by the model and this reduces the daily Nash-Sutcliffe coefficient to 0.65 (fair). A closer examination of the observed flow time-series shows that a large number of the peak flows are flagged as “Poor Archived Data Quality”. The peak flow reported for 5/25/2012 should be particularly noted (which is flagged as poor). Taking this single data point out of model evaluation results in a daily NSE of 0.77 (“good”) compared to 0.65 when not removed.

Flow volume statistics for Poplar River and Brule River are also all good or very good, with the exception of flows below the median in Poplar River, which are rated as fair. In addition to large amounts of wetlands, lakes upstream of the Poplar and Baptism River gages are expected to have significant influence on streamflow, particularly during summer low flows. Further information on lake outlet dynamics would likely improve the simulation.

The model was generally able to capture the trends seen in the observed flow time-series in the Poplar and Brule River. The daily Nash-Sutcliffe coefficients for both rivers are in the neighborhood of 0.5 and rated as poor; however, the monthly NSEs are both good. The daily NSEs are reduced by the match between model and gage data for a few storm peaks, which may also be related to the simulation of lake discharges. Removing a few of these peaks from model evaluation greatly improves model performance on a daily time-step. Lake outflows in the model are simulated using simple weir equations (Section 2.3.3) that do not account for effects of ice and debris, which is a source of uncertainty in modeled flows.

A special note is needed regarding the Brule River, which flows through Judge C.R. Magney State Park. Various anecdotal evidence has suggested the possibility of significant loss from the river to subsurface pathways. The Wikipedia article on the park summarizes the issue as follows (https://en.wikipedia.org/wiki/Judge_C._R._Magney_State_Park; accessed 5/26/16):

“The park is best known for “The Devil’s Kettle”, an unusual waterfall located on the Brule River 1.5 miles (2.4 km) from its mouth. The river splits in two to flow around a mass of rhyolite rock. The eastern

flow goes over a two-step, 50-foot (15 m) waterfall and continues downstream. The western flow surges into a pothole, falling at least 10 feet (3.0 m), and disappears underground. It is believed the water rejoins the main channel of the river or has a separate outlet into Lake Superior, but it has never been located...[Johnson and Belanger, 2007.] Researchers have dropped brightly colored dyes, ping pong balls, and other objects into the Devil's Kettle without result. There is even a legend that someone pushed a car into the fissure, but given that the Devil's Kettle is wholly inaccessible by road, most commentators dismiss this as hyperbole.

“Not only is the outlet unknown, but there is currently no satisfactory geological explanation for the Devil's Kettle. Certainly riverbed potholes are known to form from rocks and grit swirling in an eddy with such force that they eventually drill a vertical shaft in the bedrock. How the flow is conducted away laterally, however, remains enigmatic. As geologist John C. Green [1996] writes:

‘One [theory] is that, after dropping down the pothole, the river runs along a fault underground, or as a variant, that it enters an underground channel and comes out somewhere under Lake Superior. Both of these ideas have one valid aspect in common: they recognize that water must move downhill! But the main problem is creating a channel or conduit large enough to conduct the impressive flow of half the Brule River! Faulting commonly has the effect of crushing and fracturing the rock along the fault plane. This could certainly increase the permeability of the rock — its capacity to transmit water — but the connected open spaces needed to drain half the river would be essentially impossible, especially for such a distance. Furthermore, there is no geologic evidence for such a fault at the Devil's Kettle. Large, continuous openings generally do not occur in rocks, except for caves in limestone terranes. The nearest limestone is probably in southeastern Minnesota, so that doesn't help... Maybe the Devil's Kettle bottoms out fortuitously in a great lava tube that conducts the water to the Lake... Unfortunately for this idea, they are not the right kind of volcanic rocks! Rhyolites, such as the great flow at this locality, never form lava tubes, which only develop in fluid basaltic lava. Even the basalts in this area may not be the "right kind", being flood basalts that spread laterally as a sheet from fissures, not down the slopes of a volcano. No lava tubes have been found in the hundreds of basalt flows exposed along the North Shore. Furthermore, the nearest basalt is so far below the river bed, and even if it did contain an empty lava tube (very unlikely after its long history of deep burial) the tube would have to be both oriented in the right direction (south) and blocked above this site so that it isn't already full of debris. And there are no reports of trees or other floating debris suddenly appearing at one spot offshore in Lake Superior. The mystery persists.’”

In our analyses of the Brule the HSPF model tends slightly to under-predict flows at the gage, downstream of the Devil's Kettle. This suggests that flow entering the Devil's Kettle most likely rejoins the mainstem of the river prior to reaching the gage.

4.4 FLOW VALIDATION

Only the Knife River gage had a long enough period of record to undertake separate validation tests. Results for the validation period are summarized in Table 4-6 and generally confirm the calibration results. The errors however suggest that the average simulated flows are lower than the observed flow. A closer look at the hydrograph shows that much of the under-prediction occurs during high flow periods from October to November 1998. This under-prediction could be due to inconsistencies in precipitation data. Detailed results are provided in Appendix C.

Table 4-6. Summary of Flow Validation Results

Statistic	Knife River
HYDSTRA gage number	02026001
Error in total volume	-8.17%
Error in 50% lowest flows	10.73%
Error in 10% highest flows	-21.20%
Seasonal volume error–Summer (J,A,S)	16.42%
Seasonal volume error–Fall (O,N,D)	-15.88%
Seasonal volume error–Winter (J,F,M)	-1.20%
Seasonal volume error–Spring (A,M,J)	-14.06%
Error in storm volumes	-21.17%
Daily Nash-Sutcliffe Coefficient, NSE	0.75
Baseline adjusted coefficient (Garlick), E'	0.62
Monthly NSE	0.78

4.5 WATER BALANCE SUMMARY

An additional check on the hydrologic calibration is provided in terms of an aggregated water balance for the combined land segments in each 8-digit HUC watershed. For the modeling period of record, the volume of precipitation on the watershed is compared to the sum of actual (simulated) ET, surface runoff, interflow, and active groundwater flow.

The results are summarized separately for the Lake Superior South and North watersheds (Table 4-7). The results are area-weighted across all hydrologic response units and weather stations. The South and North watersheds are covered primarily by forests and wetlands. Not surprisingly, evapotranspiration (TAET) and active groundwater outflow (AGWO) dominate the hydrology. The South watershed has a greater proportion of developed areas and a shallow clay till that limits infiltration to shallow groundwater, and thus converts a larger proportion of precipitation into surface runoff and interflow. Both basins are simulated with no losses to deep groundwater.

Table 4-7. Aggregated Water Balance for the Lake Superior South and North Watersheds (in/yr), based on 1993-2012 Simulations

	Precipitation (SUPY)	Surface Runoff (SURO)	Interflow (IFWO)	Active Ground Water Outflow (AGWO)	Loss to Deep Ground Water (IGWI)	Total Actual Evapo-transpiration (TAET)	Sum of Outputs	Storage Change
Lake Superior South	31.57	3.94	2.04	7.61	0.00	18.24	31.82	0.25
Lake Superior North	30.98	1.65	1.63	10.41	0.00	17.32	31.01	0.03

The percentage distributions for the aggregated water balance are shown in Figure 4-8 and Figure 4-7. In both watersheds about 43% of precipitation is converted to runoff; however, the direct surface (SURO) and interflow (IFWO) fraction is much greater, and the groundwater discharge baseflow (AGWO) component smaller, in the Lake Superior South watershed. This reflects the presence of a shallow clay

till approximately 6 to 8 inches below the ground surface throughout most of the Lake Superior South watershed that prohibits infiltration to the shallow aquifer. Estimates of actual ET for 1993-2012 are slightly higher than reported by Sanford and Selnick (2013) based on climate and land use regression equations, who suggest that the fraction of precipitation converted to ET is in the range of 50 to 59 percent in this region based on 1971-2000 meteorology. The percentage predicted in this study is on the higher end of this range and may reflect gradual trends of increasing temperature and precipitation in the model period of 1995-2012 relative to the earlier period reported by Sanford and Selnick (2013).

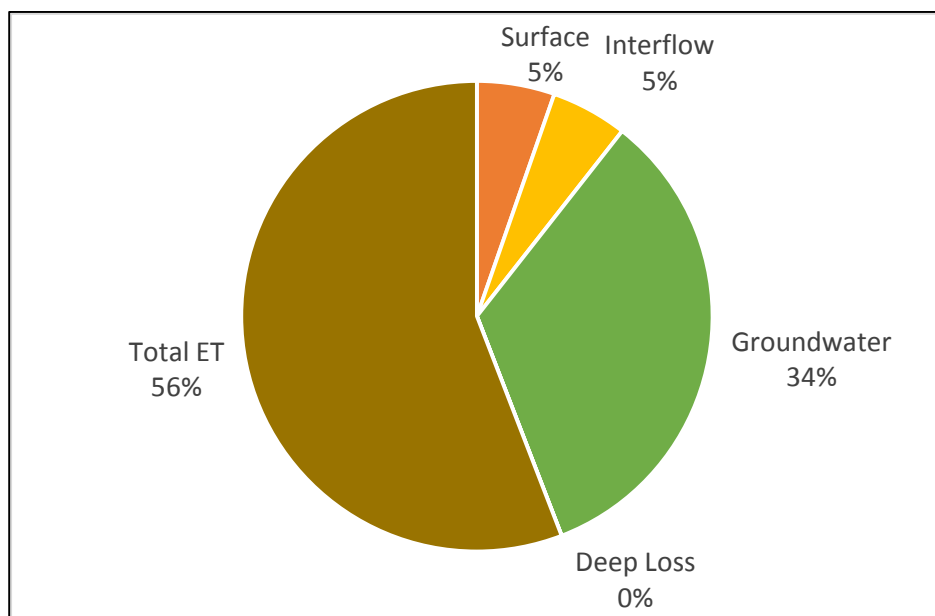


Figure 4-7. Water Balance Distribution for the Lake Superior North Watershed

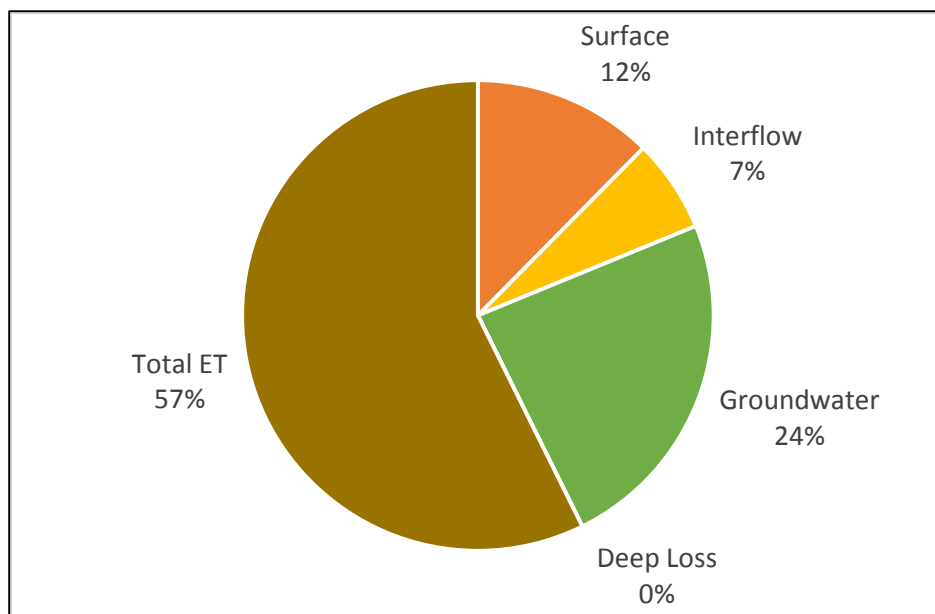


Figure 4-8. Water Balance Distribution for the Lake Superior South Watershed

5 Sediment Calibration

Sediment calibration follows the sequential procedure outlined in Section 3.3. The observed data sets for calibration are generally small and typically cover limited time periods (refer to Figure 2-15 for locations). More stations are available for the South watershed than the much larger North, although data were collected at many of these only briefly. There are insufficient data for a temporal validation exercise. Instead, all available data are used for calibration. The calibrated parameters yield reasonable representations of suspended sediment at multiple stations.

Sediment erosion and transport is of particular concern in many of the tributaries in the Lake Superior South and North watersheds. Extensive field work conducted on selected streams in the Lake Superior South watershed suggest that a large fraction of the sediment load originates from eroding banks and mass collapse of bluffs (Nieber et al., 2008; Neitzel, 2014). Nieber et al. (2008) conclude that approximately 90% of the sediment load in the Knife River watershed originates from bank erosion and bluff slumping. The estimates incorporate field observations and modeling using three different approaches, but are based on analysis of only three storms in 2005. Neitzel (2014) suggests that almost the entire sediment load in the Amity Creek watershed ultimately originates from slumping of bluffs near stream channels. The conclusions of the study are based on one year of observed data that overlaps the major floods of 2012. It is likely that the annual average load from bluff and a bank source is smaller.

HSPF is a one dimensional flow model and some of the complicated processes associated with bluff and bank erosion cannot be mechanistically simulated. The effects of shallow lateral flow on the mechanical strength of clay soils is a major factor in bluff collapse events, which partially decouples them from instream flow. In essence, bluff collapse events are quasi-random processes.

To simulate bluff contributions with HSPF in the Lake Superior North and Lake Superior South watersheds an approach similar to that adopted for the Minnesota River bluffs was used (Tetra Tech, 2009). In that approach, the load derived from bluffs (a succession of quasi-random events) is represented by adding a constant load to the bed sediment of reaches with identified high risk bluffs in the NRRI LiDAR analysis (<http://www.nrri.umn.edu/coastalgis/newweb/html/bluffs.htm>; see example in Figure 5-1). The transport of this additional load is then governed by the shear stresses acting on the reach bed, which enables these loads to be mobilized into the water column during high flows. Lower critical shear stresses and higher erodibility coefficients are used for the reaches receiving bluff loads to reflect the unconsolidated nature of the bluff contributions.

An important issue for sediment calibration is representing the correct division between sediment derived from uplands and sediment derived from reach scour. In some Minnesota watersheds, radiometric analysis using ^{210}Pb and ^{10}Be , both of which are derived from the atmosphere and decay over time into more stable forms, has been used to identify the fraction of sediment that derives from upland sources in recent contact with the atmosphere. Such information is not available for the Lake Superior North and South watersheds at this time, but could potentially be used to refine sediment calibration in the future.

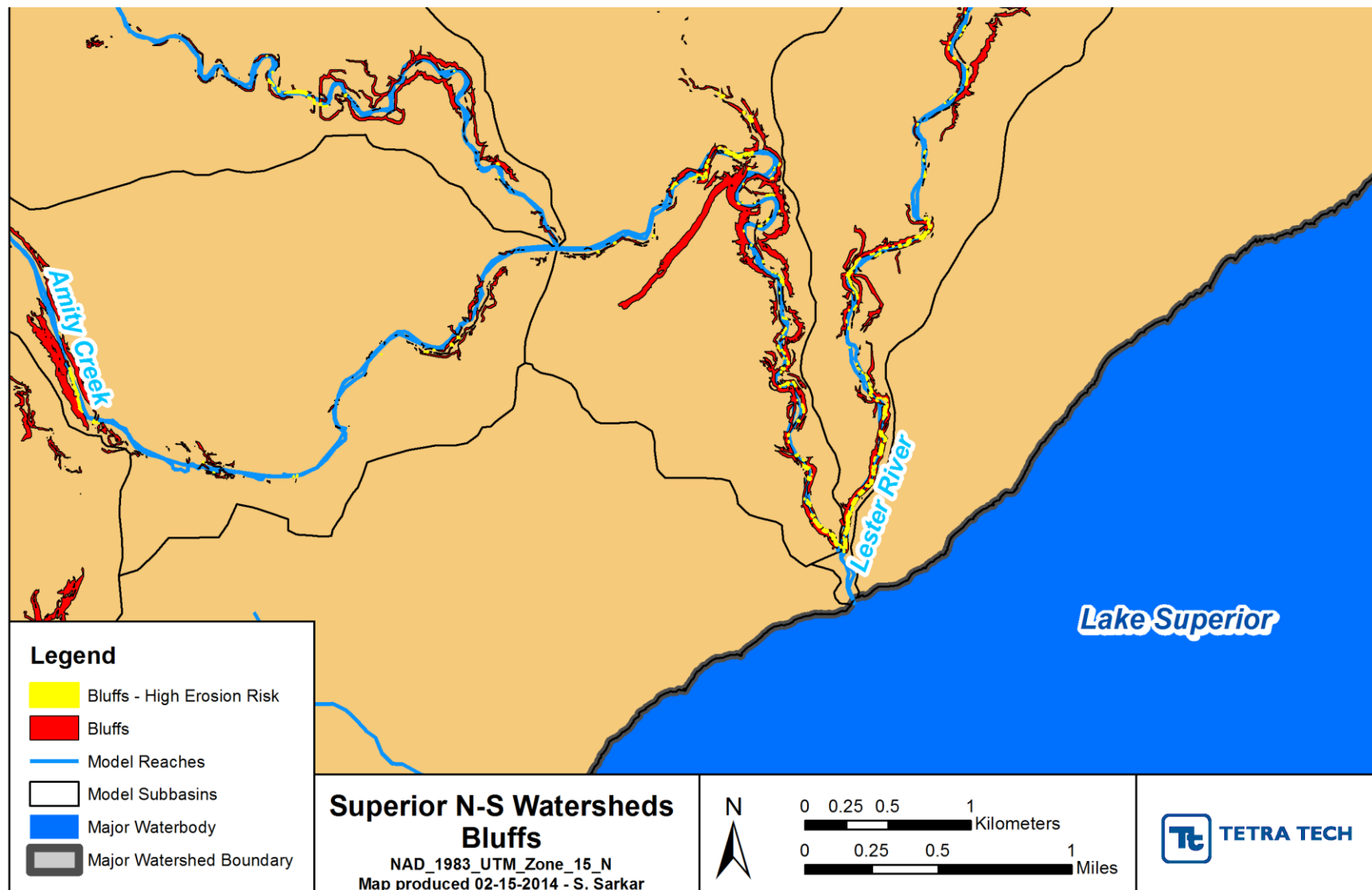


Figure 5-1. Example Areas at High Risk of Bluff Collapse in the Amity Creek and Lester River Watersheds
(<http://www.nrri.umn.edu/coastalgis/newweb/html/bluffs.htm>)

5.1 DETACHED SEDIMENT STORAGE

The sediment simulation begins on the uplands with simulation of the availability of detached sediment, which determines the sediment available for transport by surface sheet and rill flow processes. Time series of detached sediment storage (DETS) were checked for reasonableness, defined as exhibiting a quasi-stationary equilibrium with seasonal changes from wet to dry periods (USEPA, 2006). Example series from the Lake Superior South watershed are shown in Figure 5-2. The large peak at the right side of the plot shows the impact of the major storms in 2012.

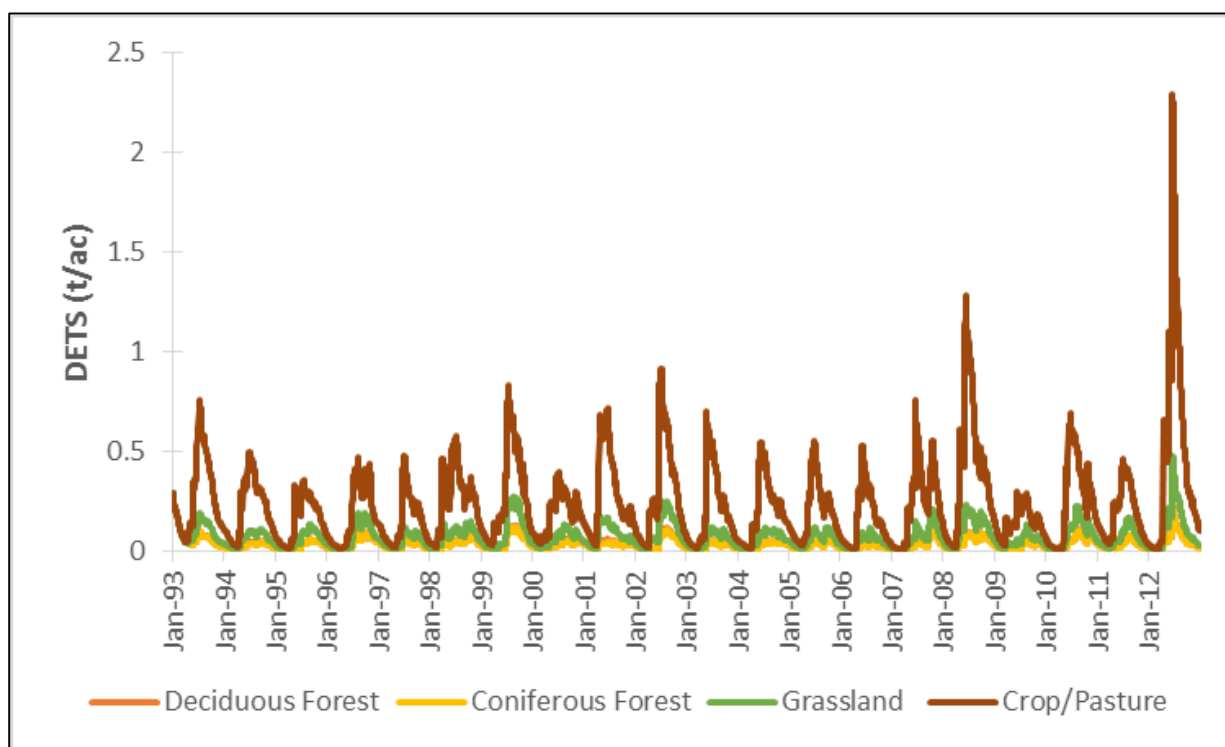


Figure 5-2. Example Detached Sediment Storage (DETS) Series for Selected HRUs in the Lake Superior South Watershed

Note: The DETS series for deciduous and coniferous forests are similar, with deciduous forest showing a slightly higher DETS in the summer-fall months. The deciduous time-series is plotted underneath the coniferous series and, because they are similar, is not readily visible on the figure.

5.2 UPLAND SEDIMENT LOADING RATES

The next step in sediment calibration is examination of the upland sediment loading rates. The Lake Superior North and South watershed models were calibrated separately for sediment. The differences in surface runoff and interflow volumes associated with the differing soils in the Lake Superior North and Lake Superior South watersheds result in different average upland sediment loading rates. Average upland sediment loading rates by land use (Table 5-1) show generally higher rates for the Lake Superior South than for the Lake Superior North watershed, consistent with the differences in runoff characteristics.

Table 5-1. Average Upland Sediment Loading Rates (1993-2012) for Lake Superior South and North Watershed Models

Landuse	Lake Superior South		Lake Superior North	
	Rate (t/ac/yr)	Load (t/yr)	Rate (t/ac/yr)	Load (t/yr)
Developed	0.067	0.667	0.038	0.312
Roads	0.103	0.262	0.129	0.480
Barren	0.289	0.234	0.182	0.090
Crop and Pasture	0.111	0.480	0.070	0.021
Forest	0.012	1.266	0.006	1.858
Grassland	0.029	0.715	0.016	0.643
Wetland	-	-	-	-
Water	-	-	-	-
Gully Erosion	0.011	2.188	0.004	1.958

Land use in both watersheds is dominated by forest and wetlands, with more developed land use in the South watershed. Few estimates of typical upland sediment loading rates in these watersheds are available in the literature. The upland loading rates shown in Table 5-1 for forest are lower than the typical range of 0.05 – 0.4 tons/ac/yr cited in Donigian and Love (2003) and Packer (1967), likely because harvested areas (represented as barren or shrub land) and roads, which contribute much of the forest upland sediment load, as well as channel erosion sources, are accounted for separately in our model. For comparison, Ellison et al. (2014) reported total sediment yield in the range of 0.04 - 0.08 tons/ac/yr for two largely forested northern Minnesota watersheds (Knife River and Little Fork River).

Loading rates for crop and pasture are also relatively low compared to typical national ranges cited in USEPA (2006); however, the intensity of these land uses is believed to be generally low compared to warmer climates. Pasture and crop are minor land uses in these watersheds and likely have very little impact on the overall sediment balance.

HSPF can also simulate gully or ravine erosion. This type of erosion depends on overland flow depth, but is independent of the detached sediment supply. Limited estimates exist on sediment loading from ephemeral gullies. A University of Minnesota study for the Lower Poplar River (Hansen et al., 2010; Nieber et al., 2013) suggests that ravines and upland channels contribute 243 and 312 t/yr of the total estimated 938 to 1,370 t/yr. This is approximately 59 to 41 % of the total sediment load from the Lower Poplar River. In the model, gully erosion was simulated for upland areas with slopes greater than 5% in both the South and North watersheds. Sediment loading simulated from gully erosion accounts for approximately 37% of the upland loading rate for both the South and North watershed models in total. This is smaller than the estimates from the study conducted on the Lower Poplar River, which has some of the steeper slopes in the model.

5.3 REACH SEDIMENT MASS BALANCE

Sediment scour and deposition was analyzed through tabulation on a reach by reach basis with the aim of ensuring that significant amounts of scour and deposition occur only in areas where reasonably expected. Summary analyses for the Lake Superior South and North watersheds are shown in Figure 5-3 and Figure 5-4, respectively. Because HSPF uses a one-dimensional representation of streams, all channel erosion sources are represented as changes in depth, whereas much of the channel erosion actually derives from stream banks. The majority of stream reaches have a simulated change in depth of less than plus or minus 0.1 feet over the 20-year period of simulation. A majority of reaches are simulated as exhibiting a small amount of net erosion. A few reaches have large amounts of deposition simulated and generally correspond to lakes explicitly simulated in the models where trapping of sediment is expected. The lake names are shown on the corresponding bars in the figures. Figure 5-5 shows the average annual net scour per unit length of each modeled reach for the simulation period.

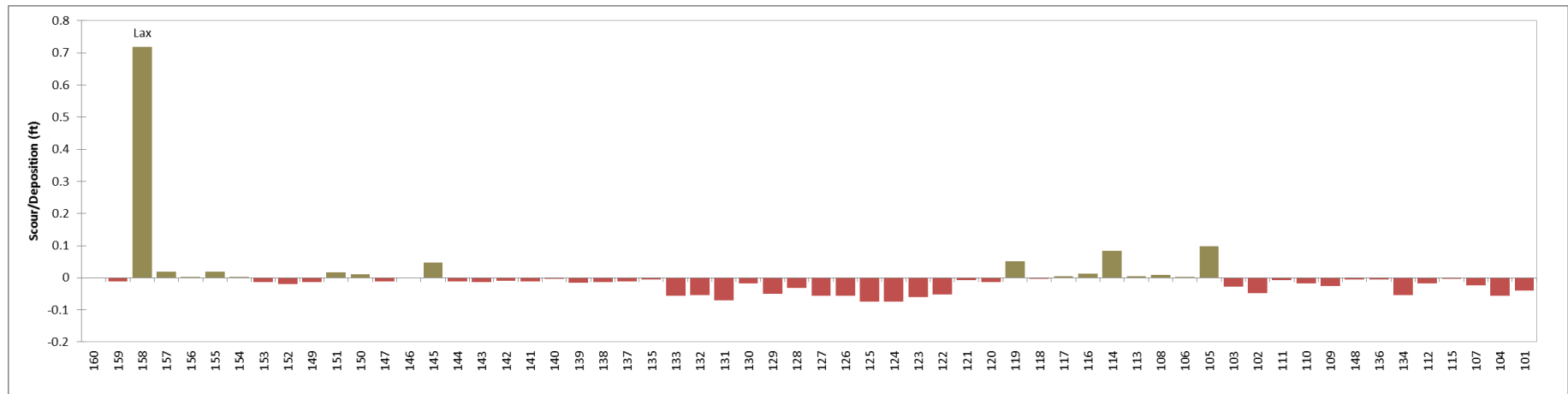


Figure 5-3. Reach Sediment Balance, Lake Superior South Watershed Model, 1993-2012

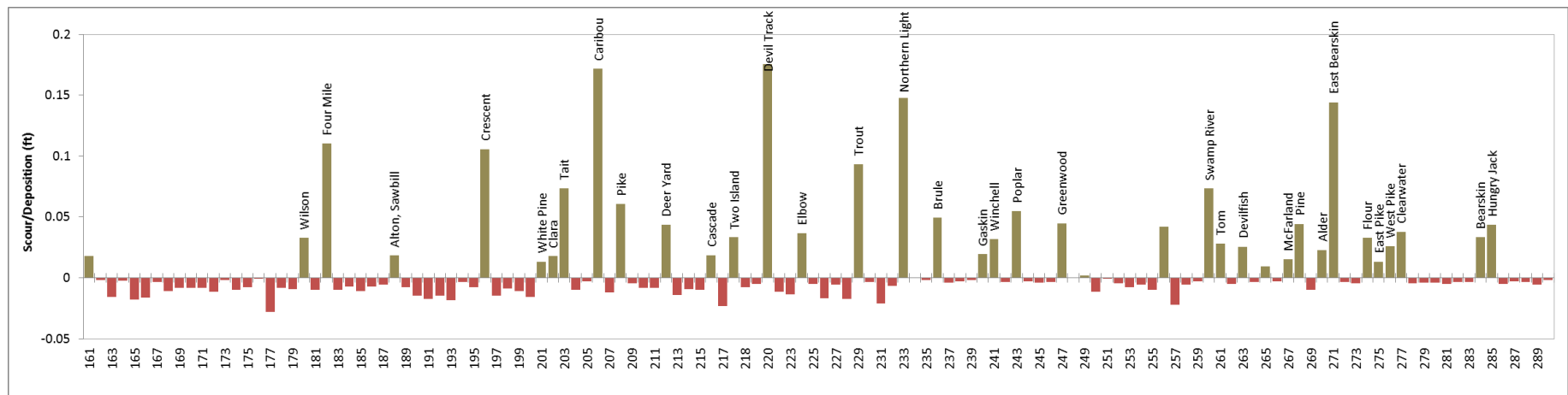


Figure 5-4. Reach Sediment Balance, Lake Superior North Watershed Model, 1993-2012

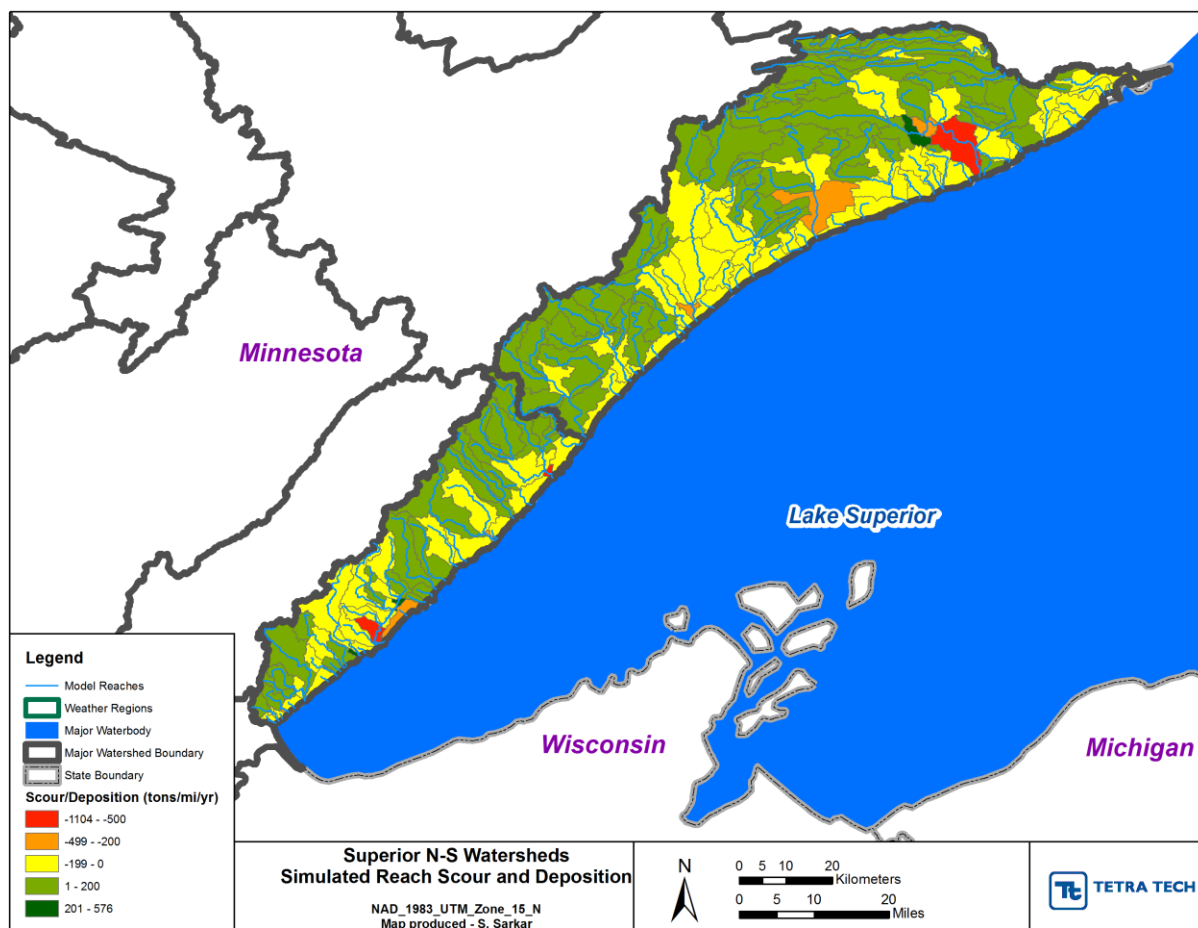


Figure 5-5. Simulated Average Annual Reach Scour and Deposition, Lake Superior South and North Watershed Models (tons/mi/yr), 1993-2012

5.4 CALIBRATION TO OBSERVED SUSPENDED SOLIDS DATA

Suspended sediment calibration took place at seven stations and used both visual and statistical approaches. We attempted to replicate the observed time series while at the same time minimizing relative errors associated with both concentration and load (as inferred from concentration and flow), as described in Section 3.3. Attention was paid to matching observed and simulated relationships between load and flow through the use of power plots, while also examining the distribution of error terms relative to both season and flow. It is not uncommon for relative error to be strongly leveraged by one or more outliers (especially for load, which tends to be determined by concentrations at high flows); therefore, the median error (which is not sensitive to outliers) is reported as well as the average error.

The detailed sediment calibration process is shown here through an example for the Knife River at Two Harbors. A complete set of graphical and statistical results for all calibration stations is provided in Appendix D. Four years of observations are available at the Knife River station. The model appears to track the observed data fairly well, although several very high observations are under-estimated (Figure 5-6). The average and median relative errors on concentration are good (-15% and 0.6%, respectively, comparing point-in-time observations to simulated flow-weighted average daily concentrations), while the average and median relative errors on load are -25.5% and 0.1%, suggesting some over-estimation at higher flows. A log-log power plot (Figure 5-7) shows that the observed and simulated loads have a

similar distribution relative to flow; however, the simulation has a “kink” in the middle flow range which deviates from the observed pattern. This is due to the simulation of channel shear stress versus flow, which is determined by the specification of the stream reach FTables, which may not be fully representative of actual channel dimensions. The distribution of prediction errors versus flow (Figure 5-8) also reveals this discrepancy in the region around flow of 175 cfs. Finally, several high concentration outliers are noticeable at high flows, leading to the inflated relative average error on load.

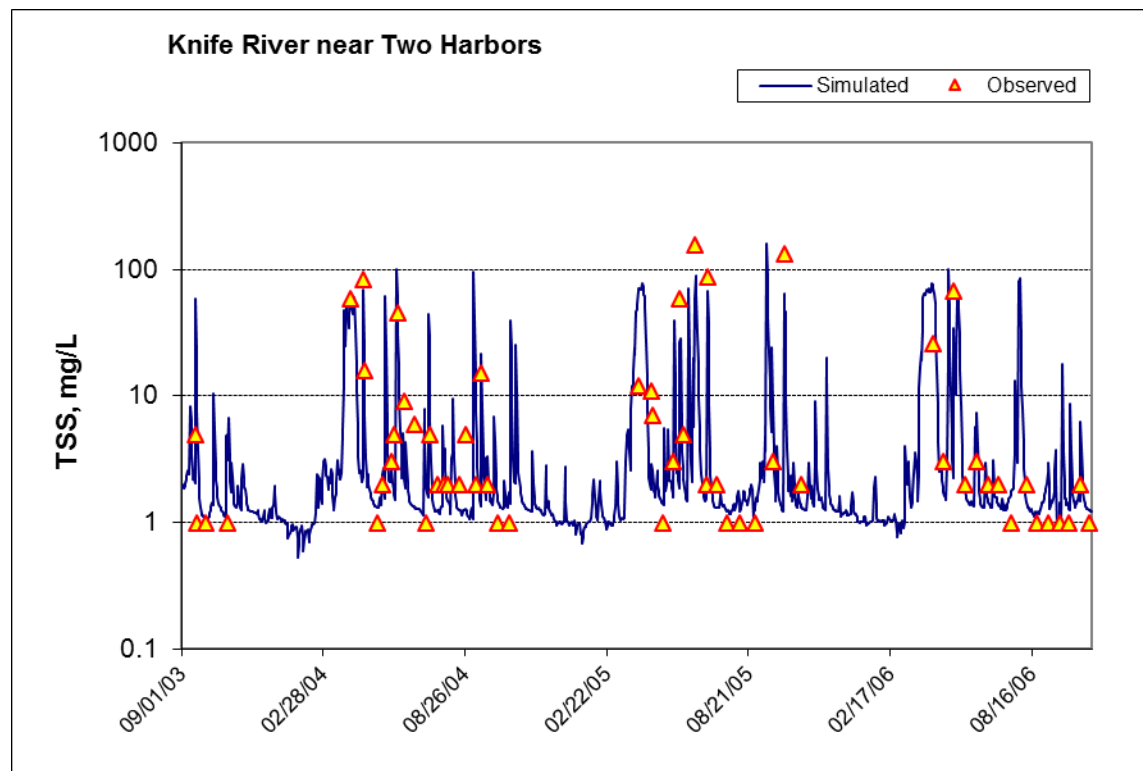


Figure 5-6. Time Series Plot for Total Suspended Sediment Concentrations, Knife River near Two Harbors

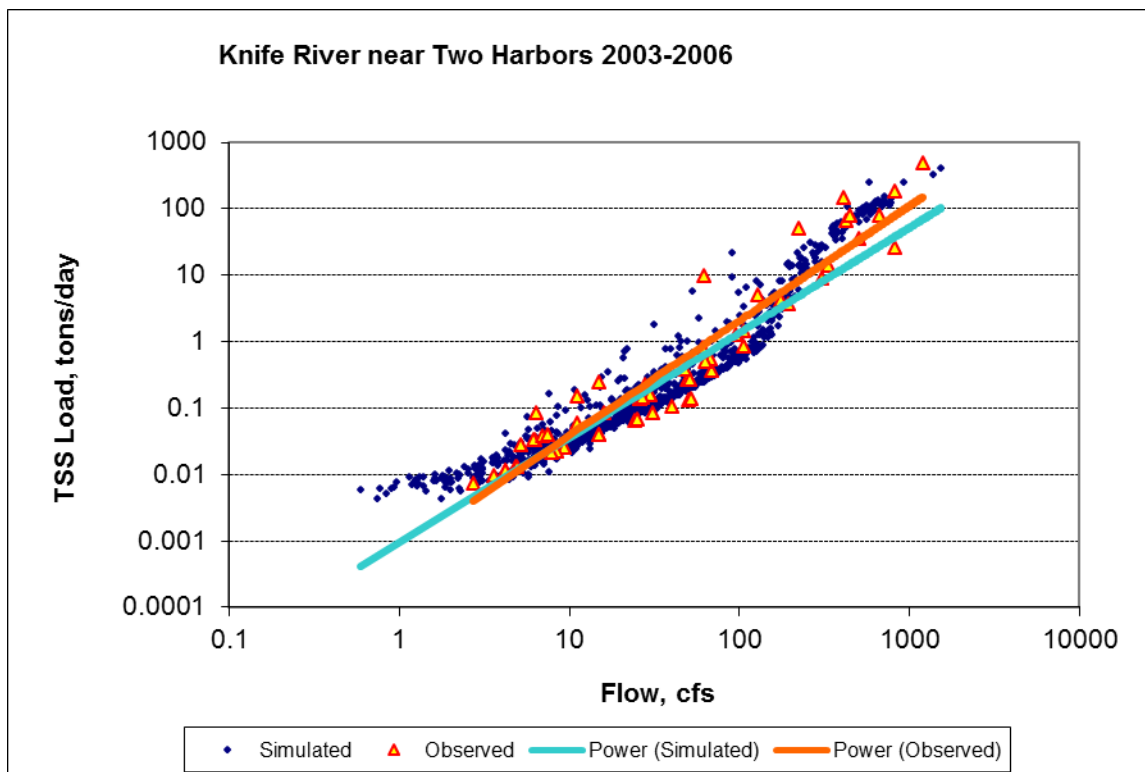


Figure 5-7. Log-log Power Plot of Simulated Total Suspended Sediment Load and Load Inferred from Observed Concentration, Knife River near Two Harbors

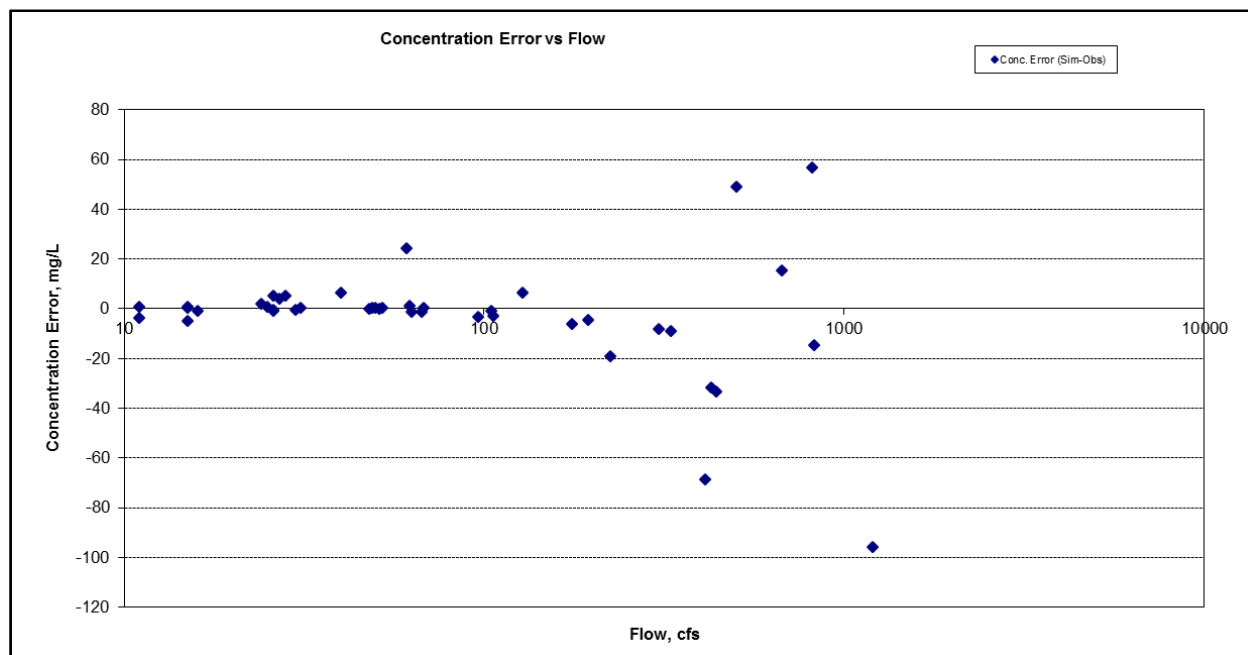


Figure 5-8. Distribution of Concentration Error for Total Suspended Sediment, Knife River near Two Harbors

Suspended sediment model fit statistics for all calibration stations are summarized in Table 5-2 (additional details and the accompanying graphics are in Appendix D). The fit for concentration is within the target range ($\pm 25\%$) for all the calibration stations. The magnitude of deviations associated with paired estimates of simulated load and “observed” load estimated from discrete concentration measurements frequently exceeds 25% at many of these locations. In part, this is a common issue for relatively small and flashy streams, for which point-in-time observations, especially at high flows, many not be representative of daily average concentrations. There are also a few large outliers that affect the average relative errors that could be associated with random bluff slumping events. In contrast, the median load errors are small. Some specific comments on results for individual stations are provided following Table 5-2.

Table 5-2. Summary of Sediment Calibration Results

Station	Dates	Relative Error on Concentration		Relative Error on Load	
		Average	Median	Average	Median
Lake Superior South Watershed					
Amity Creek at Duluth	2002-2010	3.2%	7.1%	68.8%	1.3%
Talmadge River near Duluth	2002-2008	23.5%	0.1%	-16.4%	0.0%
Sucker River near Palmers	2002-2012	-11.7%	-2.8%	-29.2%	-0.1%
Knife River near Two Harbors	2003-2006	-15.0%	0.6%	-25.5%	0.0%
Lake Superior North Watershed					
Baptism River near Beaver Bay	2008-2012	-5.2%	12.8%	-30.3%	1.0%
Poplar River near Lutsen	2003-2012	2.0%	8.1%	37.8%	1.4%
Brule River near Hovland	2002-2010	-3.2%	11.3%	-2.5%	1.1%

Notes regarding individual monitoring stations:

Amity Creek at Duluth (Reach 109): This station was monitored from 2002 to 2010 mostly during the summer and fall seasons. Amity Creek has extensive eroding bluffs. Some of the higher reported sediment concentrations are associated with moderate flows suggesting that they may be due to bluff slumping events. The high average relative error on load is mostly associated with a few outliers in the mid-range flows.

Talmadge River near Duluth (Reach 114): This station drains a relatively small area consisting primarily of forests and wetlands. The model simulates the peak concentrations well although the overall average is somewhat higher than the observed.

Sucker River near Palmers (Reach 120): This location has a moderate amount of data from 2002 to 2012. The simulated concentrations generally follow the trend seen in the observed data. A notch appears in the simulated concentration in the 70 cfs flow range and is consistent with the notch in the shear stress profile. The relatively large change in sediment concentration at this flow level is due to the increase in reach average shear stress up to bank full conditions, followed by a drop-off as flow expands into the floodplain. The FTable for this reach was developed based on a rating curve, associated in-channel cross section, and evaluation of the overbank profile from LiDAR at the specific location of the stream gage, which may not be representative of the reach as a whole. Uncertainties associated with the FTable development may have an impact on the hydraulic and sediment transport behavior of such reaches.

Knife River at Two Harbors (Reach 123+124): Data were collected at this location for a relatively short period of time from 2003 to 2006. The model represents the trend in observed data well. Some of the highest peaks are, however, under-estimated. As a result, the simulated average concentration is lower than the average from paired observations.

Baptism River near Beaver Bay (Reach 161): Data were collected at this location from 2008 to 2012. The model under-predicts some of the highest peaks. The model seems to have a high bias for the low flows but a closer examination of the observed data shows that a large number of these data points are non-detects and set as half the detection limit for model evaluation purposes. The concentration jump seen for the Sucker River gage is observed in this case as well and is likely related to the FTable, developed from the gage rating curve, not being representative of the reach as a whole.

Poplar River near Lutsen (Reach 193): Data at this location are available from 2003 to 2012 and may be affected by changes over time in development activities and improvements in management practices at the Lutsen Mountain Resort. Some of the highest observed concentrations occur at relative low flows suggesting random processes at work (bluff and bank slumping). The modeled concentration matches well with the trend in observed concentration. In addition, this sample site has a large number of lakes upstream that may have significant impacts on the sediment load.

Brule River near Hovland (Reach 231): Data at this location are available from 2002 to 2010. The modeled concentration matches well with the trend in observed concentration. Numerous lakes upstream of the gage likely have significant impacts on the sediment load.

5.5 COMPARISON TO FLUX LOAD ESTIMATES

The final check on the sediment calibration is comparison of long-term simulated loads to continuous loads estimated from interpolating observed flow and sparse concentration data. The “observed” loads can be estimated only where there is both flow and concentration monitoring. MPCA’s Watershed Pollutant Load Monitoring Network (WPLMN) is designed to obtain spatial and temporal pollutant load information from Minnesota’s rivers and streams and track water quality trends. As part of this program, MPCA releases estimates of annual pollutant loads for each 8-digit hydrologic unit code basin developed using the Corps of Engineers’ FLUX32 program (Walker, 1996).

MPCA provided FLUX analyses for 2009 – 2011 at three locations in the Lake Superior South and North. Comparisons to simulation results for the same time period are shown in Table 5-3. For each of these stations, the simulated load is similar to the FLUX-estimated load, with relatively small deviations.

Table 5-3. Comparison of Simulated and FLUX-Estimated Sediment Loads

Station	Date Range	Simulated Load (t/yr)	FLUX Load
Sucker River near Palmers	2009-2011	262	177
Baptism River near Beaver Bay	2009-2011	337	330
Poplar River near Lutsen	2009-2011	344	278

6 Nitrogen and Phosphorus Calibration

6.1 NUTRIENT MODEL SETUP

The nutrient simulation follows the same general approach used in other Minnesota HSPF models and recommended by AQUA TERRA (2012). Ammonia, nitrate nitrogen, orthophosphate, and generalized organic matter are simulated on the land surface, with the first two being represented by buildup-washoff processes and the second two simulated as sediment-associated using potency factors for pervious land (with a buildup-washoff approach for impervious land). Representation of point source loads of nutrients is described in Section 2.4. Full nutrient kinetics are represented instream, including the decay of organic matter, uptake by and release from planktonic and benthic algae, nitrification, denitrification, exchanges with the sediment bed, and sorption to sediment of ammonium and orthophosphate.

6.1.1 Upland Sources

The nutrient simulation for the uplands represents inorganic nitrogen, inorganic phosphorus, and organic matter as three distinct constituents. Inorganic phosphorus and organic matter on pervious surfaces are simulated using a sediment potency approach, while inorganic nitrogen on pervious surfaces and all three constituents on impervious surfaces are represented as a buildup/washoff process. Concentrations associated with subsurface flows are also included.

Within the stream reaches the model represents individual nutrient species (ammonia, nitrate, nitrite, organic nitrogen, orthophosphate, organic phosphorus, and organic carbon/BOD). The stream reach module is implemented with full nutrient simulation, including uptake by and release from plankton and benthic algae, decay of organic matter, oxidation of ammonium to nitrite and nitrite to nitrate nitrogen, bed exchanges of dissolved and sorbed nutrients, and ammonia volatilization.

The key parameters controlling the upland nutrient simulation are listed below:

MON-ACCUM: The monthly varying assignment of the build-up or accumulation of a constituent on a particular surface (lb/ac-d).

MON-SQOLIM: The monthly varying upper limit value beyond which a constituent can no longer accumulate on a surface (lb/ac).

MON-IFLW-CONC and **MON-GRND-CONC:** These parameters are used to assign the interflow and groundwater constituent concentrations on a monthly basis. The values for these parameters were estimated from the observed data with consideration of flow regime and then calibrated as necessary.

MON-POTFW: The monthly varying specification of constituent mass per sediment mass (lb/ton). For organic matter the assigned values were around 10^0 to 10^1 . The seasonal assignment for organic matter reflects the annual cycle of growth and then litter.

The sediment potency, build-up/washoff, and subsurface flow parameters for the Lake Superior North and Lake Superior South watersheds were initialized based on the St. Louis and Cloquet watersheds HSPF model and past experience. A literature review was conducted to establish appropriate ranges for unit-area loading rates of the diverse land use categories found in the watersheds (Table 6-1). The simulated unit-area loading rates were compared to the literature-based ranges and the surface and subsurface flow parameters were revised until reasonable loading estimates were established for TN and TP. Results for the Lake Superior South watershed are provided in Figure 6-1 and Figure 6-2. Results for the Lake Superior North watershed are shown in Figure 6-2 and Figure 6-3.

The average simulated TN unit loading rate for forest land segments in the Lake Superior South watershed is 3.7 lb-N/ac/yr, which is within but on the higher end of the reported range in Table 6-1. The

developed pervious and impervious average simulated values are 4.7 lb-N/ac/yr and 12.2 lb-N/ac/yr, respectively. These results are similar to the values reported by MPCA (2013), which range from 2 to 17 lb-N/ac/yr for mixed developed land use. The average simulated TN unit loading rate for wetlands is 1.2 lb-N/ac/year, within the literature-supported range of 0.5 to 5 lb-N/ac/yr (MPCA, 2004a). The cropland and pasture unit loading rate is near the lower limit of the reference range at 8.1 lb-N/ac/yr.

Reference TP unit loading rates for forest are as low as 0.05 lb-P/ac/yr (MPCA, 2004a) and as high as 0.5 lb-P/ac/yr (Loehr et al., 1989). The simulated TP unit loading rate for forest in the St. Louis and Cloquet watersheds aligns with the reference values at 0.27 lb-P/ac/yr. The TP unit loading rate from wetlands at 0.01 lb-P/ac/yr is slightly higher than reference values because subsurface flows contribute to the simulated load but generally are not considered in the literature-based values. The average simulated TP unit loading rate for cropland and pasture, 0.25 lb-P/ac/yr, aligns well with other studies that recommend loading rates of 0.11 to 1.7 lb-P/ac/yr for cropland (Dodd et al., 1992; Loehr et al., 1989) and 0.11 to 0.43 lb-P/ac/yr for pasture (Clesceri et al., 1986; McFarland and Hauck, 2001).

Table 6-1. Reference Ranges for the Nutrient Loading Rates of Diverse Land Use Categories

Land Use	TN (lb-N/ac/yr)	TP (lb-P/ac/yr)	Source
Forest	1.97 – 4.2	0.05 – 0.5	Clesceri et al., 1986; Loehr et al., 1989; MPCA, 2013; MPCA, 2004a; Reckhow et al., 1980
Wetland	0.5 – 5	0	MPCA, 2013; MPCA, 2004a
Pasture	6.1 – 23	0.11 – 0.43	Clesceri et al., 1986; McFarland and Hauck, 2001; MPCA, 2013; MPCA 2004a
Crop	7.5 – 23	0.11 – 1.7	Dodd et al., 1992; Clesceri et al., 1986; Loehr et al., 1989, MPCA, 2013; MPCA 2004a
Developed (pervious)	2 – 17	0.8 – 1.02	Loehr et al., 1989; MPCA, 2013; MPCA, 2004a; Reckhow et al., 1980
Developed (impervious)	2 – 17	0.8 -1.02	Loehr et al., 1989; MPCA, 2013; MPCA, 2004a; Reckhow et al., 1980
Barren	0.5 - 5	ND	MPCA, 2013
Shrub	0.5 - 5	0.05 – 0.12	MPCA, 2013; MPCA, 2004a

The loading rates for the Lake Superior North watershed by landuse were generally similar to those for the Lake Superior South watershed although some differences exist. The simulated unit area loads from the developed pervious category are larger for Lake Superior North than the simulated rates for the Lake Superior South watershed, although the amount of developed land in the Lake Superior North watershed is much smaller compared to the South. There are differences in slope and soil properties between the two basins that account for the higher rates. Phosphorus loading rates from forest are lower for Lake Superior North than for Lake Superior South. This was required to match the observed instream concentration data.

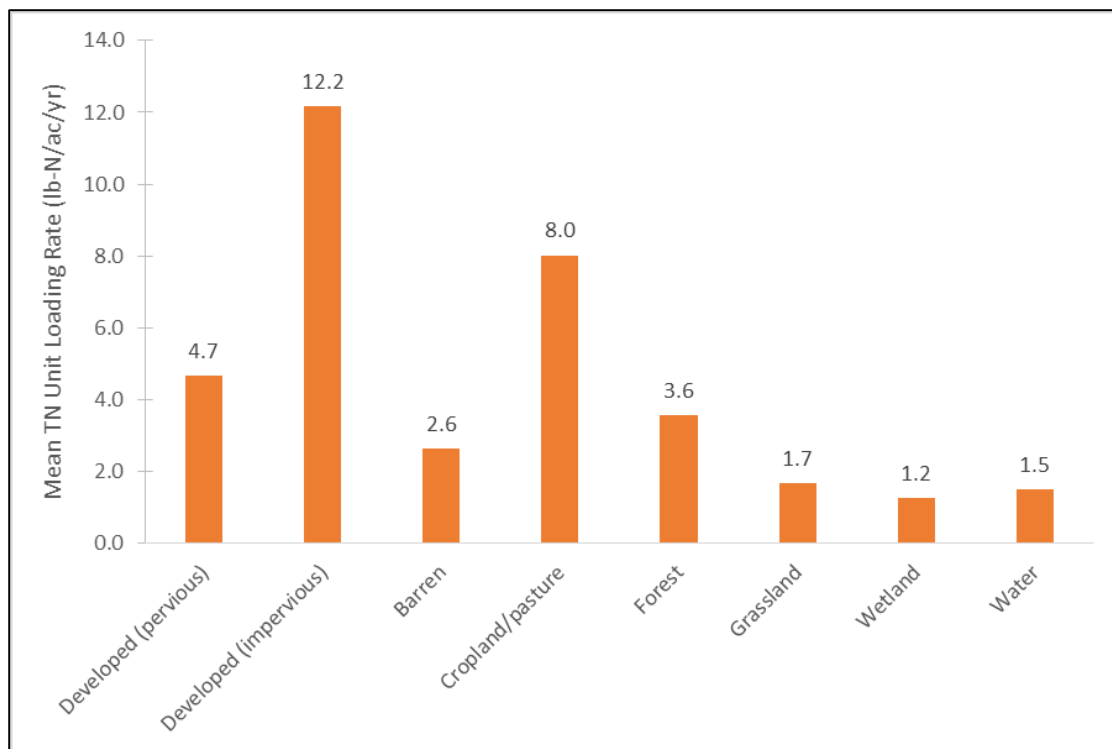


Figure 6-1. Average Simulated Total Nitrogen (TN) Unit Loading Rates for Land Use Categories in the Lake Superior South Watershed

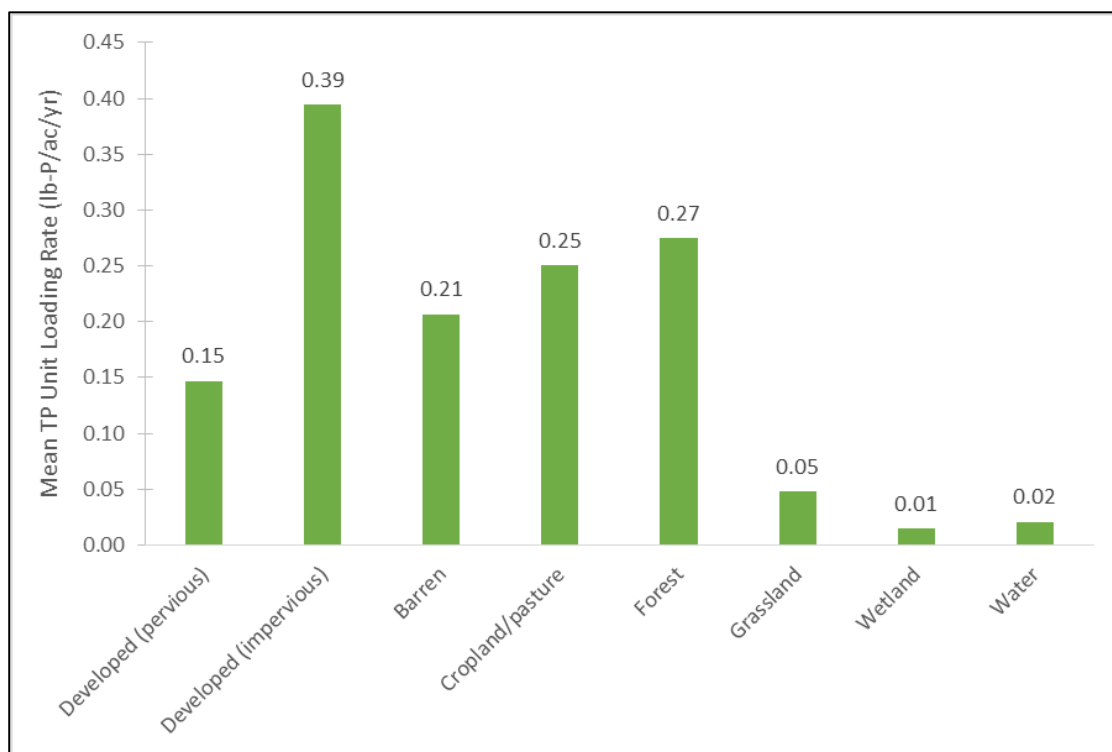


Figure 6-2. Average Simulated Total Phosphorus (TP) Unit Loading Rates for Land Use Categories in the Lake Superior South Watershed

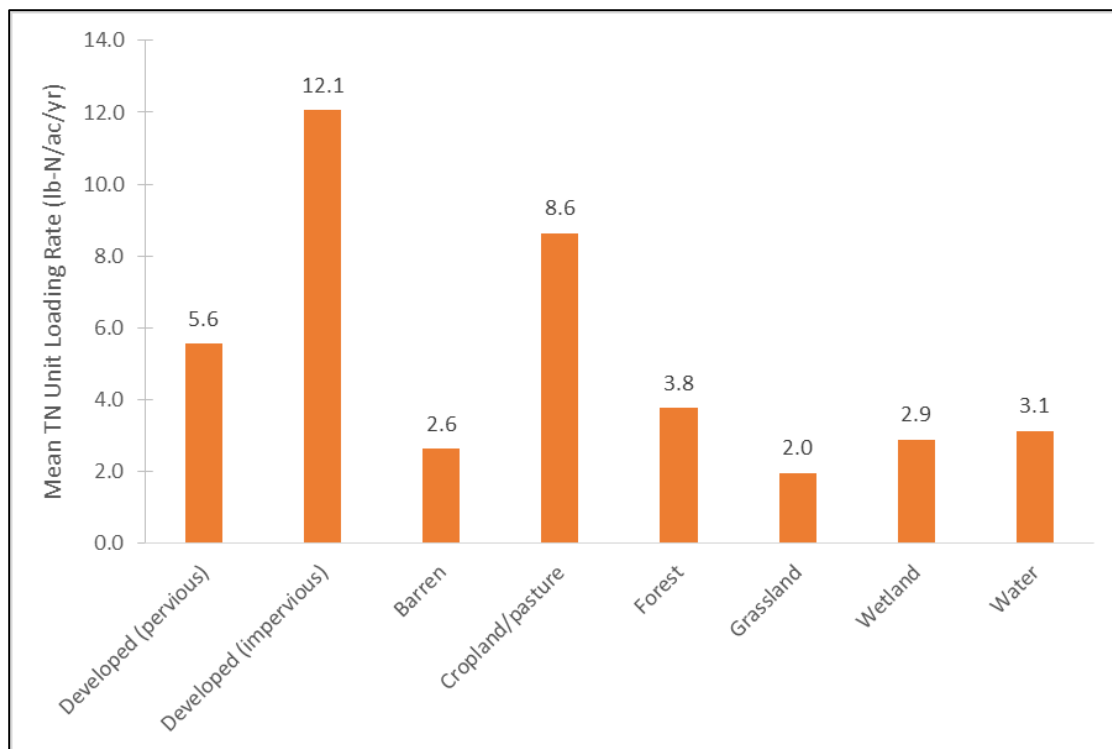


Figure 6-3. Average Simulated Total Nitrogen (TN) Unit Loading Rates for Land Use Categories in the Lake Superior North Watershed

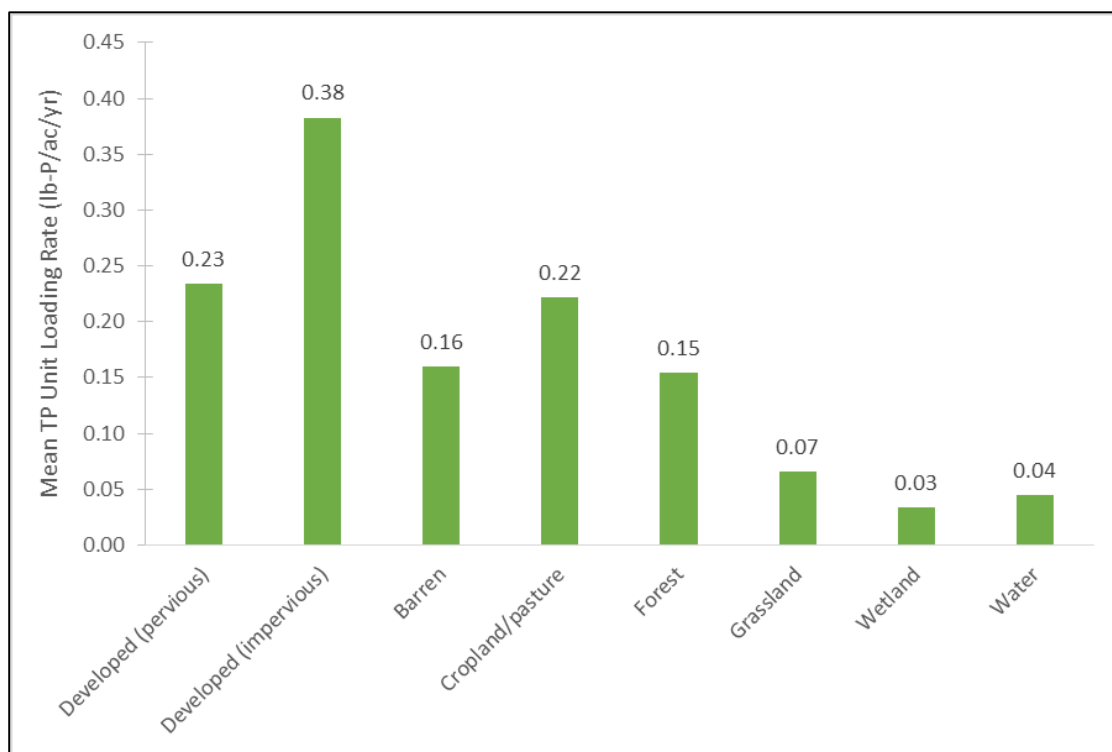


Figure 6-4. Average Simulated Total Phosphorus (TP) Unit Loading Rates for Land Use Categories in the Lake Superior North Watershed

6.1.2 Channel Sources of Nutrients

Nutrients can be gained or lost through exchanges with the sediment bed – either through releases in the dissolved form or by scour or deposition of nutrients that sorb to sediment. HSPF simulates ortho-phosphate and ammonia as sorbing to sediment and also represents release of dissolved ortho-phosphate, ammonia, and labile organic matter (as BOD, with associated nutrients) from the sediment.

Based on past experience with other Minnesota watershed models, adsorption coefficients were set for ortho-phosphate as P at 1,000 ml/g relative to silt and clay and 600 ml/g relative to sand; the corresponding numbers for total ammonia as N were 100 and 10 ml/g. Background sediment bed concentrations, which define the nutrient content of sediment scoured from the stream bed and banks, are set for ortho-phosphate at 300 mg-P/kg for silt and clay and 100 mg-P/kg for sand, and, for total ammonia N, 100 mg-N/kg for silt and clay and 10 mg-N/kg for sand.

The waters of these basins tend to contain ample amounts of iron, which can enhance the deposition of phosphorus in complexes with iron hydroxide under oxidized conditions. In oxygen-depleted sediment, this complexed phosphorus can be re-released in dissolved form. This is hypothesized as likely to be a significant process in lakes of the region that develop summer stratification and oxygen depletion in the hypolimnion, and also possibly in some slower-moving stream segments. The model is therefore set up to simulate releases of orthophosphate and ammonia N from sediment in lake segments. These releases are somewhat speculative and could be refined with detailed mass balance studies of individual lakes.

6.1.3 Atmospheric Deposition

The model simulates wet and dry deposition of ammonia-N and nitrate-N to pervious surfaces, impervious surfaces, and water bodies. In addition, both dry and wet deposition of phosphorus to water surfaces (explicitly simulated lakes and streams) is simulated. Atmospheric deposition of phosphorus to the uplands is not simulated because it is assumed to be implicit in the sediment potency representation of pervious land loading and the buildup/washoff representation of impervious land loading of phosphorus.

Wet deposition concentrations of ammonia and nitrate N (as mg-N/L) are taken from monthly data recorded at NADP stations MN05 (Fond du Lac) and MN99 (Wolf Ridge) for the South watershed. For the North watershed NADP stations MN99 (Wolf Ridge) and MN08 (Hovland) are used. These stations did not become operational until 1997. Input records for the time-period before 1997 were filled in using data from the NADP station MN18 (Fernberg). Dry deposition rates of ammonia and nitrate N (as lb-N/ac) are taken from CASTNET monitoring. There are no CASTNET stations within or particularly close to the watersheds studied here, so we use the station at Voyageurs National Park (VOY413) for the period after 1996, filling in earlier dates with monitoring from Perkinstown, WI (PRK134). In all cases, reported data were converted from molar units to mass or mass-based concentration as N.

Direct phosphorus deposition to surface water is represented in the model. The phosphorus deposition rate specified is the average estimated for the Lake Superior basin in the 2007 update to MPCA's phosphorus study (Twaroski, et al., 2007) of 0.115 kg-P/ha/yr. The wet deposition concentration for phosphorus is calculated as a seasonal time-series based on atmospheric deposition of calcium using a linear relationship. The average concentration using this approach is 10.5 µg-P/L.

6.2 NUTRIENT CALIBRATION

Nutrients from point and nonpoint sources are loaded to the stream reaches. Within the stream reaches the model represents the following nutrient species: ammonia-N, nitrite-N, nitrate-N, refractory organic nitrogen, orthophosphate-P, refractory organic phosphorus, and BOD. BOD represents the labile component of organic matter in the model and implicitly incorporates labile organic N and organic P, which are converted to inorganic forms as BOD decays. The stream reach module simulates instream

biogeochemical processes including nutrient uptake and release by plankton and benthic algae, decay of organic matter, nitrification/denitrification, absorption/desorption of nutrients on suspended sediment, and deposition and scour of sediment-stored nutrients.

The nutrient calibration and validation relies on a weight of evidence approach. Upland loading rates are constrained to be in general agreement with literature values (as described in 6.1.1), while point source discharges are based on monitoring or recommended assumptions for unmonitored parameters provided by MPCA (see Section 2.4). Model calibration then adjusts parameters to optimize the fit between model predictions and observations at multiple stations throughout the watershed and the robustness of the fit is checked with validation tests on a different time period. Model performance is then checked against other sources of information, including information developed by MPCA on delivered loads and lake phosphorus balances.

6.2.1 Comparison of Model to Observations

Comparisons between model predictions and sample observations are made in terms of both concentration and inferred load (concentration times simulated or observed flow). Complete graphical and tabular statistical results for each station are provided in Appendix D. Figure 6-5 provides an example of the primary types of calibration plots provided for each monitored nutrient parameter at each site, in this case showing the total phosphorus calibration for the Sucker River in the Lake Superior South watershed. The four panels in Figure 6-5 are:

- a. Standard time series plot, showing the observations and continuous model predictions of daily average concentrations. This shows general agreement, but can obscure biases in the simulation.
- b. A power plot comparing the relationship of observed and simulated loads versus flow. The objective here is that the relationship to flow (summarized by the power regression lines) should be similar for the model and observations. While generally true in this case, it will be noted that the simulated loads have a “hump” in the mid-range of flows. This in turn reflects the simulated relationship of flow and channel scour, derived from the channel form assumptions, which indicate a reduction in shear stress as flow spreads out onto the floodplain.
- c. A scatterplot of simulated versus observed concentrations shows the degree of spread or uncertainty about the 1:1 line.
- d. A plot of the residuals against flow is used to diagnose bias relative to the flow regime. In this example there is a reasonable balance between over and under-prediction across the range of flows, but some indication of a tendency to under-predict concentrations at the highest flows. A similar plot of residuals versus month is used to diagnose potential seasonal biases.

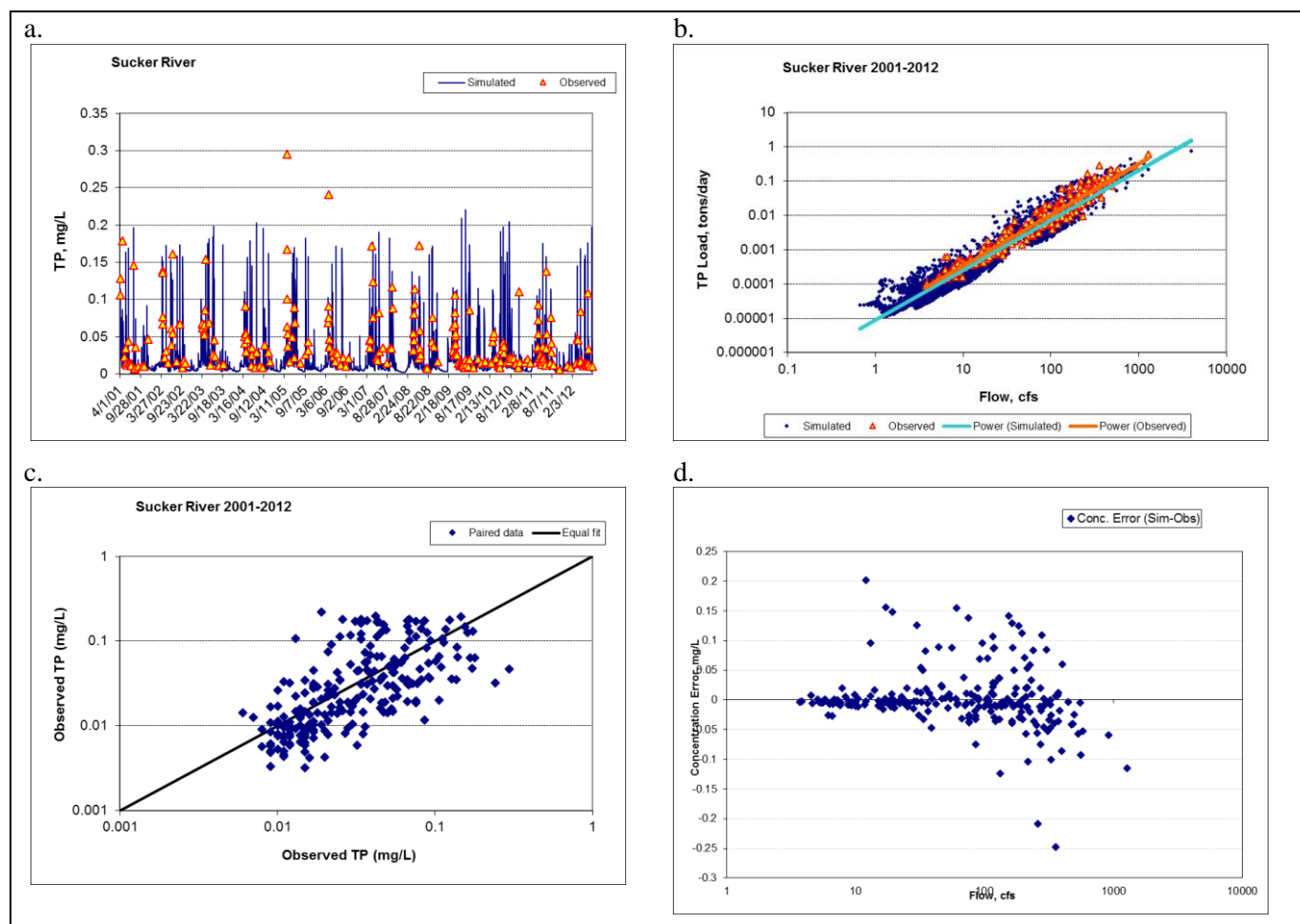


Figure 6-5. Example Calibration Plots for Total Phosphorus, Sucker River in the Lake Superior South Watershed

This section first provides an overview of the results with a focus on total phosphorus, total nitrogen, and nitrate nitrogen (nitrate nitrogen is included in the overview because it is often the predominant form of nitrogen and the number of observations for total nitrogen is limited at many stations). Results for individual nutrient species are then summarized, with full results provided in the appendices.

Summary statistics for the calibration of total phosphorus, total nitrogen, and nitrate nitrogen at all stations are provided in Table 6-2, Table 6-3, and Table 6-4, respectively. Discussion by watershed and parameter follows the tables. Data for the validation period was not available and therefore a validation exercise was not possible for the nutrient simulation.

Table 6-2. Summary Statistics for Total Phosphorus Calibration

Station	Calibration (2002-2012)					
	Count	Average Concentration (mg/L)	Concentration Average Relative Error (%)	Concentration Median Relative Error (%)	Paired Load Average Relative Error (%)	Paired Load Median Relative Error (%)
Lake Superior South						
Amity Creek near Duluth	127	0.072	-27%	-10%	-6%	-1%
Talmadge River near Duluth	108	0.054	-14%	-20%	-33%	-1%
Sucker River near Palmers	232	0.043	5%	-9%	10%	-1%
Lake Superior North						
Baptism River near Beaver Bay	106	0.020	9%	1%	3%	-2%
Poplar River near Lutsen	92	0.024	-6%	-7%	13%	-2%
Brule River near Hovland	131	0.021	-11%	-12%	10%	-2%

Note: Statistics calculated with non-detects set to one-half the detection limit.

* For Baptism River the calibration period is 2008-2012.

Table 6-3. Summary Statistics for Total Nitrogen Calibration

Station	Calibration (2002-2012)*					
	Count	Average Concentration (mg/L)	Concentration Average Relative Error (%)	Concentration Median Relative Error (%)	Paired Load Average Relative Error (%)	Paired Load Median Relative Error (%)
Lake Superior South						
Amity Creek near Duluth	59	0.961	-5%	-11%	15%	-1%
Talmadge River near Duluth	70	0.947	-12%	-20%	-24%	-3%
Sucker River near Palmers	175	0.789	-18%	-33%	8%	-5%
Lake Superior North						
Baptism River near Beaver Bay	106	0.855	-6%	-7%	-8%	-7%
Poplar River near Lutsen	102	0.835	-8%	-8%	-11%	-3%
Brule River near Hovland	61	0.662	12%	12%	46%	7%

Note: Statistics calculated with non-detects set to one-half the detection limit.

* For Baptism River the calibration period is 2008-2012.

Table 6-4. Summary Statistics for Total Nitrate+Nitrite-N Calibration

Station	Calibration (2002-2012)*					
	Count	Average Concentration (mg/L)	Concentration Average Relative Error (%)	Concentration Median Relative Error (%)	Paired Load Average Relative Error (%)	Paired Load Median Relative Error (%)
Lake Superior South						
Amity Creek near Duluth	71	0.178	14%	2%	-3%	0%
Talmadge River near Duluth	70	0.131	-7%	-4%	-39%	-1%
Sucker River near Palmers	175	0.099	-30%	-26%	-16%	-5%
Lake Superior North						
Baptism River near Beaver Bay	106	0.194	-14%	-3%	-19%	-1%
Poplar River near Lutsen	102	0.223	-11%	13%	-35%	3%
Brule River near Hovland	94	0.119	40%	54%	44%	18%

Note: Statistics calculated with non-detects set to one-half the detection limit.

* For Baptism River the calibration period is 2008-2012.

6.2.1.1 Lake Superior South Watershed

Ambient phosphorus concentrations in the Lake Superior South watershed streams tend to be relatively low, with most stations having an average concentration less than 0.05 mg/L. For the Sucker and Talmadge Rivers, the average relative errors on concentration for total phosphorus fall into the “Very Good” category ($\leq 15\%$). Results are rated only “Fair” for Amity Creek and likely associated with the under-estimation of some of the highest concentration. These observed high concentrations occur at relatively low flows and suggest that they could be linked to bluff slumping. Organic phosphorus contributions from bluff slumping are not simulated by HSPF. In terms of median relative error on concentration, the performance at all locations is rated “Good” to “Very Good”.

For average load error, Amity Creek and Sucker River are rated as “Very Good”. The model under-predicts load for Talmadge River and the performance is rated only “Fair”. This could be due to the under-estimation of a peak concentration in July 2002. The model performance is however rated as “Very Good” in terms of median load error.

For total nitrogen, the model performance in terms of average relative error on concentration is ranked “Very Good” for Amity Creek and Talmadge River and “Good” for Sucker River. In terms of median relative errors on concentration the performance for Amity Creek and Talmadge River are generally “Good” but only “Fair” for Sucker River. A closer look at the concentration errors versus flow (Appendix D) shows that the model under-predicts total Kjeldahl nitrogen (the sum of organic and ammonia nitrogen) concentrations associated with low to mid-range flows. A large area of the Sucker River is occupied by forested wetlands. It is likely that organic matter export from wetlands in this watershed is under-estimated.

It terms of load average relative error, Amity Creek and Sucker River are rated as “Very Good” while the performance for Talmadge River is “Good”. The model performance in terms of median load error is “Very Good” at all locations.

For nitrate+nitrite nitrogen (NO_x), the model performance was “Very Good” for Amity Creek and Talmadge River for average relative error on concentration. The performance was rated only “Fair” for Sucker River. The under-estimation at the Sucker River is associated with a negative bias during high flows and is largely associated with snow melt events. For relative median error on concentration, the model performance was “Very Good” for Amity Creek and Talmadge River but only “Fair” for Sucker River.

In terms of load average relative errors for NO_x, the model performance is “Very Good” for Amity Creek and Sucker River but is only “Fair” for Talmadge River. The model under-predicts some peak concentrations during snow melt events and this is the likely cause of an under-prediction in loads. Also note that the model under-predicts flow at the Talmadge River gage for unknown reasons which (as noted earlier) and has an impact on nutrient loads. The model performance in terms of median load errors is “Very Good” at all three locations.

6.2.1.2 Lake Superior North Watershed

Ambient phosphorus concentrations in the Lake Superior North watershed streams tend to be even lower than the South streams, with most stations having an average concentration less than 0.03 mg/L. For all three locations in the North watershed, the average relative errors on concentration for total phosphorus fall into the “Very Good” category ($\leq 15\%$). The model performance is also “Very Good” at all three locations in terms of median relative error on concentration. The model performance is “Very Good” in terms of load average error for Baptism River and “Good” for Poplar River and Brule River. The model performance in terms of load median error is “Very Good” at all three locations.

For total nitrogen, average relative error on concentration the model performance is rated “Very Good” for Baptism River and Poplar River and “Fair” for Brule River. It is important to note that total nitrogen is not directly reported and is calculated as sum of total Kjeldahl nitrogen (TKN) and nitrate+nitrite nitrogen (NO_x). A large number of NO_x samples collected at the Poplar and Brule River gages are reported as non-detect and thus influence the calculated total nitrogen concentration. If the non-detects are removed from the sample data set, the model performance for Brule River is “Good”.

In terms of average and median load errors, the model performance is “Very Good” at the Baptism and Poplar River gages. The performance at the Brule River gage is “Poor” for average load error and “Very Good” for median load error. The error magnitudes are also inflated by the presence of non-detects in the sample data for this location.

For nitrate+nitrite nitrogen, the model performance is rated “Very Good” for Baptism River in terms of average relative error on concentration. The performance for Poplar is “Fair” and “Poor” for Brule. Based on relative median error on concentration, the model performance is “Very Good” for Baptism River but “Poor” for Poplar and Brule. In terms of average and median load errors, the model performance is “Very Good” for Baptism and Poplar. The performance for Brule is “Poor” based on average load error and “Good” in terms of median load error. The errors are inflated by the presence of non-detects among the observed samples and the model performance improves greatly if these are removed from consideration. In addition to the presence of large areas of wetlands, there are also many lakes (especially in the Poplar and Brule River watersheds), which further complicates the nutrient dynamics in the Lake Superior North watershed.

There does appear to be a potential issue with the model representation of kinetic transformations among nitrogen species due to algal processes. In particular, the amount of different inorganic species is highly sensitive to the specification of the algal preference ratio for nitrate versus ammonia nitrogen. This is a fixed ratio in HSPF, but in reality may vary over the seasons as different planktonic and benthic algae/macrophytes predominate. This is of particular significance in the Lake Superior North watershed streams as a number of them are influenced by lakes.

6.2.2 Comparison of Model to Flux Estimates of Delivered Load

MPCA's Watershed Pollutant Load Monitoring Network (WPLMN) is designed to obtain spatial and temporal pollutant load information from Minnesota's rivers and streams and track water quality trends. As part of this program, MPCA releases estimates of annual pollutant loads for each 8-digit hydrologic unit code basin developed using the FLUX program, as described in Section 4. MPCA estimates at the gage station on the Sucker River, Baptism River and Poplar River are currently available for calendar years 2009-2011. Comparisons between the MPCA FLUX estimates and model simulated results are shown in Figure 6-6 through Figure 6-8 and Table 6-5.

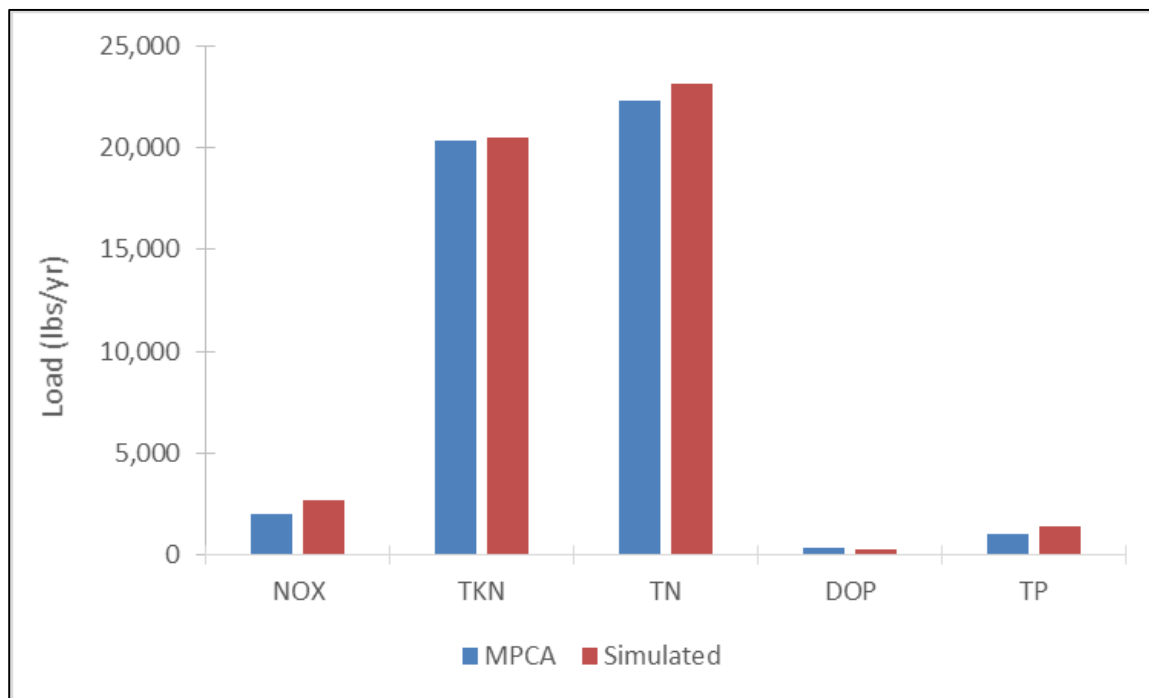


Figure 6-6. Comparison of Model to MPCA FLUX Estimates of Pollutant Load, Calendar Years 2009-2011, Sucker River near Palmers

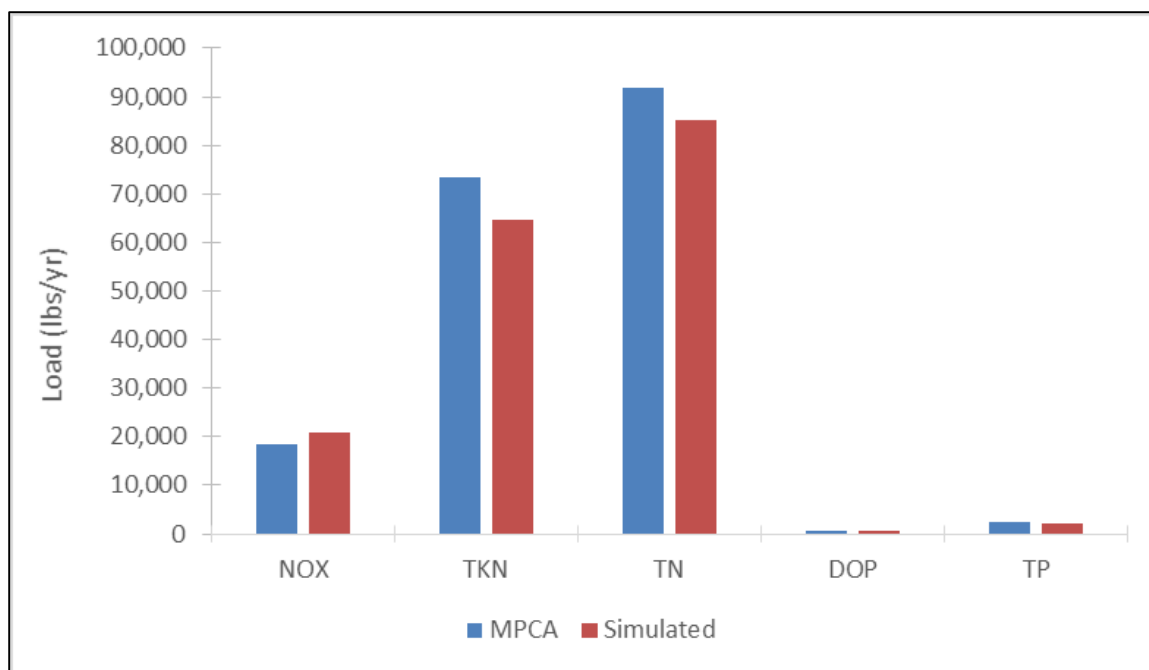


Figure 6-7. Comparison of Model to MPCA FLUX Estimates of Pollutant Load, Calendar Years 2009-2011, Baptism River near Beaver Bay

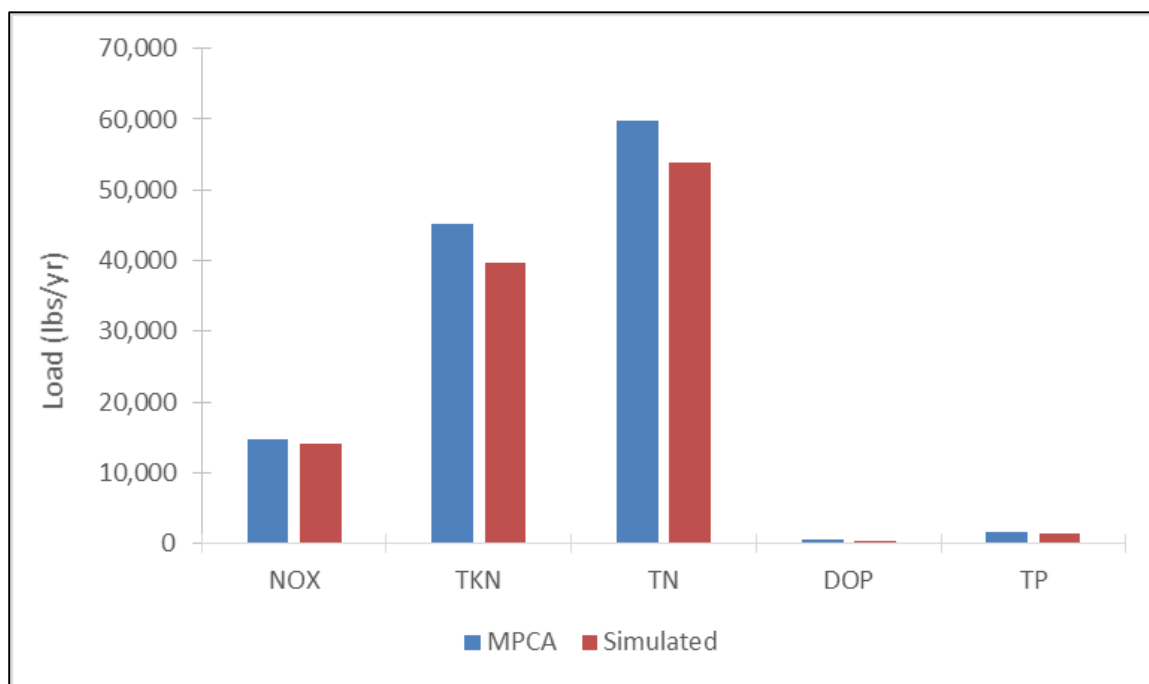


Figure 6-8. Comparison of Model to MPCA FLUX Estimates of Pollutant Load, Calendar Years 2009-2011, Poplar River near Lutsen

Table 6-5. MPCA FLUX Estimates and Model Simulated Annual Nutrient Loads, Calendar Years 2009-2011

Station		Nitrate + Nitrite N	Total Kjeldahl N	Dissolved Ortho-P	Total P	Total N
Sucker River near Palmers	MPCA FLUX	1,977	20,327	305	1,051	22,304
	Simulated	2,669	20,482	260	1,420	23,151
	Difference	25.9%	0.8%	-17.3%	26.0%	3.7%
Baptism River near Beaver Bay	MPCA FLUX	18,523	73,413	638	2,343	91,936
	Simulated	20,774	64,525	639	2,268	85,299
	Difference	10.8%	-13.8%	0.2%	-3.3%	-7.8%
Poplar River near Lutsen	MPCA FLUX	14,664	45,133	520	1,605	59,797
	Simulated	14,095	39,739	414	1,401	53,835
	Difference	-4.0%	-13.6%	-25.8%	-14.6%	-11.1%

For total nitrogen, the match between FLUX and model simulations is rated “Very Good” for Sucker, Baptism, and Poplar Rivers. The model does appear to over-predict total phosphorus load in the Sucker River (although the total load is small). Improving this would likely require a better understanding and representation of processes in the wetland complex in the headwaters of the Knife and Sucker River watersheds.

Model performance is also “Very Good” for total Kjeldahl nitrogen, which is the dominant fraction of nitrogen load (primarily as organic nitrogen). The match is not as good for nitrate + nitrite nitrogen or dissolved ortho-phosphorus. Both of these constituents are very sensitive to plant/algal uptake of inorganic nutrients and release of organic nutrients, much of which occurs in wetlands. HSPF does not provide detailed simulation of kinetic processes in wetlands. The nutrient dynamics are further complicated by the presence of a large number of lakes in the Lake Superior North watershed.

6.2.3 Consistency with Lake Data

The Lake Superior North watershed has a large number of lakes. In contrast, the Lake Superior South watershed has only a few lakes with small watersheds. Detailed nutrient balance studies are not available for most, if any, of these lakes. MPCA has, however, conducted screening analyses of many of these lakes using the MINLEAP protocol (Wilson and Walker, 1989; MPCA, 2005). MINLEAP is designed to predict eutrophication in Minnesota lakes based on watershed area, lake depth, and ecoregional phosphorus concentrations. It is a scoping tool designed to estimate lake condition based on minimal data that calculates water and phosphorus balance and in-lake predicted phosphorus and chlorophyll *a* concentrations, which are compared to observed concentrations.

TP predictions in 24 explicitly simulated lakes in the Lake Superior South and North models are compared to available growing season average concentrations in Table 6-6. Given the small sample sizes, the model and observations are reasonably in agreement for most of the monitored lakes. It is important to note that HSPF predicts the nutrient content of the entire water volume, whereas the observations for most lakes are summer results from the surface water, suggesting that much of the TP input to these lakes

may settle and be sequestered in the bottom water during summer stratification. This is especially true for certain deeper lakes (> 100 ft.) like Trout (MPCA, 2011) and Clearwater (MPCA, 2004b) that regularly stratify. A different analytical tool that incorporates a two-dimensional analysis may be needed to interpret nutrient concentrations in these and other stratified lakes (see discussion in Section 9).

Table 6-6. TP Concentrations in Explicitly Simulated Lakes of the Lake Superior South and Lake Superior North Watersheds

Lake	Model Reach	Monitored Average and Range (1995-2012)	Simulated Seasonal Average and Range (1995-2012)
Wilson	180	0.019 (0.009 - 0.087)	0.017 (0.012 - 0.033)
Four Mile (Fourmile)	182	0.029 (0.019 - 0.039)	0.026 (0.019 - 0.041)
Crescent	196	0.019 (0.015 - 0.026)	0.019 (0.014 - 0.032)
White Pine*	201	0.018 (0.016 - 0.022)	0.014 (0.009 - 0.04)
Clara	202	0.021 (0.013 - 0.026)	0.018 (0.011 - 0.044)
Tait	203	0.015 (0.007 - 0.028)	0.015 (0.01 - 0.027)
Caribou	206	0.018 (0.003 - 0.121)	0.02 (0.016 - 0.029)
Pike	208	0.01 (0.005 - 0.024)	0.011 (0.009 - 0.017)
Deer Yard	212	0.016 (0.009 - 0.05)	0.015 (0.01 - 0.028)
Cascade*	216	0.013 (0.011 - 0.014)	0.019 (0.01 - 0.061)
Devil Track	220	0.013 (0.008 - 0.023)	0.016 (0.012 - 0.024)
Elbow	224	0.019 (0.012 - 0.026)	0.014 (0.008 - 0.059)
Trout	229	0.01 (0.004 - 0.027)	0.012 (0.01 - 0.017)
Northern Light	233	0.014 (0.01 - 0.025)	0.016 (0.007 - 0.136)
Poplar	243	0.01 (0.005 - 0.023)	0.013 (0.011 - 0.023)
Greenwood	247	0.009 (0.003 - 0.019)	0.013 (0.011 - 0.016)
Tom	261	0.013 (0.008 - 0.022)	0.015 (0.011 - 0.03)
Devilfish*	263	0.011 (0.008 - 0.015)	0.016 (0.01 - 0.038)
East Bearskin	271	0.01 (0.007 - 0.014)	0.014 (0.01 - 0.026)
Flour	274	0.03 (0.007 - 0.25)	0.026 (0.014 - 0.042)
Clearwater	277	0.006 (0.004 - 0.025)	0.009 (0.008 - 0.015)
Bearskin	284	0.025 (0.004 - 0.254)	0.021 (0.013 - 0.03)
Hungry Jack	285	0.009 (0.002 - 0.028)	0.012 (0.01 - 0.024)
Lax	158	0.018 (0.013 - 0.026)	0.016 (0.008 - 0.048)

* Observed data available for 2013 only

7 Water Temperature

Water temperatures are of interest in their own right for habitat evaluation. Water temperature also has an important influence on the simulation biochemical transformations. The HSPF modules used to represent water temperature include PSTEMP (soil temperature) and HTRCH (heat exchange and water temperature).

Simulation of soil temperature is accomplished using three layers: the surface soil layer, upper subsurface layer, and groundwater subsurface layer. The surface layer is the portion of the land segment that determines the overland flow water temperature. The upper subsurface layer determines interflow temperature while the groundwater subsurface layer determines the temperature of discharging ground water. Surface and upper subsurface layer temperatures are estimated in HSPF by applying a regression equation relative to observed air temperature. The groundwater subsurface temperatures are supplied as slowly varying monthly time series that reflect average groundwater temperatures for the region and season. Initial parameters for the Lake Superior North and Lake Superior South watershed models are based on recommendations in the Long Prairie example file provided as part of MPCA's HSPF modeling guidance (AQUA TERRA, 2012).

Once water enters a stream, temperature is impacted by processes that increase or decrease the heat content of the water. Mechanisms that can increase the heat content of the water are absorption of solar radiation, absorption of long-wave radiation, and conduction-convection exchange with the atmosphere. Mechanisms that decrease the heat content are emission of long-wave radiation, conduction-convection, and evaporation. Heat exchanges between the water and stream bed are also simulated.

Stream temperature follows diel cycles and is strongly affected by the pattern of shading over the course of the day and the local microclimate, as well as specific locations of cooler groundwater discharges to streams. Local-scale variations in hydraulics can also influence temperature readings: for instance, temperatures are likely to be different in a part of a reach impounded by a beaver dam than in a free-flowing riffle. A watershed-scale HSPF model can typically match observed daily *average* water temperature but is limited in its ability to simulate the daily cycles of water temperature at specific locations. This is because HSPF represents stream segments as one-dimensional, fully-mixed reactors. These segments are typically in the range of 3 to 15 miles in length in models built at a HUC12 scale, as is the case here, and variations within the segment are averaged out. For instance, a single average value represents shading over the whole stream segment and the model does not consider the orientation or aspect of the stream segment relative to the position of the sun. HSPF, as a one-dimensional model, also does not address vertical variation in temperature, which is especially important in deeper lakes and reservoirs. HSPF also turns off the simulation of instream heat exchange processes when water depth falls below 2 inches. In contrast, a detailed water temperature model for a stream reach (e.g., the QUAL2K model) would typically specify segments with lengths on the order of a tenth of a mile and include a detailed analysis of shading from vegetation and topography in relation to solar position throughout the day and year. For the HSPF application we used an empirical approximation fit during calibration in which the shading factor (i.e., CFSAEX, the fraction of light not shaded out) is scaled relative to the fraction of forest cover in a subwatershed as $1 - 0.73 \cdot \text{fraction forest}$.

While water temperature is reported along with most water quality observations, scattered point in time measurements are of limited use for adjusting the temperature calibration due to strong diel patterns. Continuous stream temperature data are available for several Lake Superior South streams; however, calibration to continuous water temperature data has not been pursued at this time. Modeled water temperature was compared to grab sampling at several MPCA flow gaging locations and was found generally to conform to the trends in the observed dataset. An example time-series plot for Amity Creek at Duluth is shown in Figure 7-1.

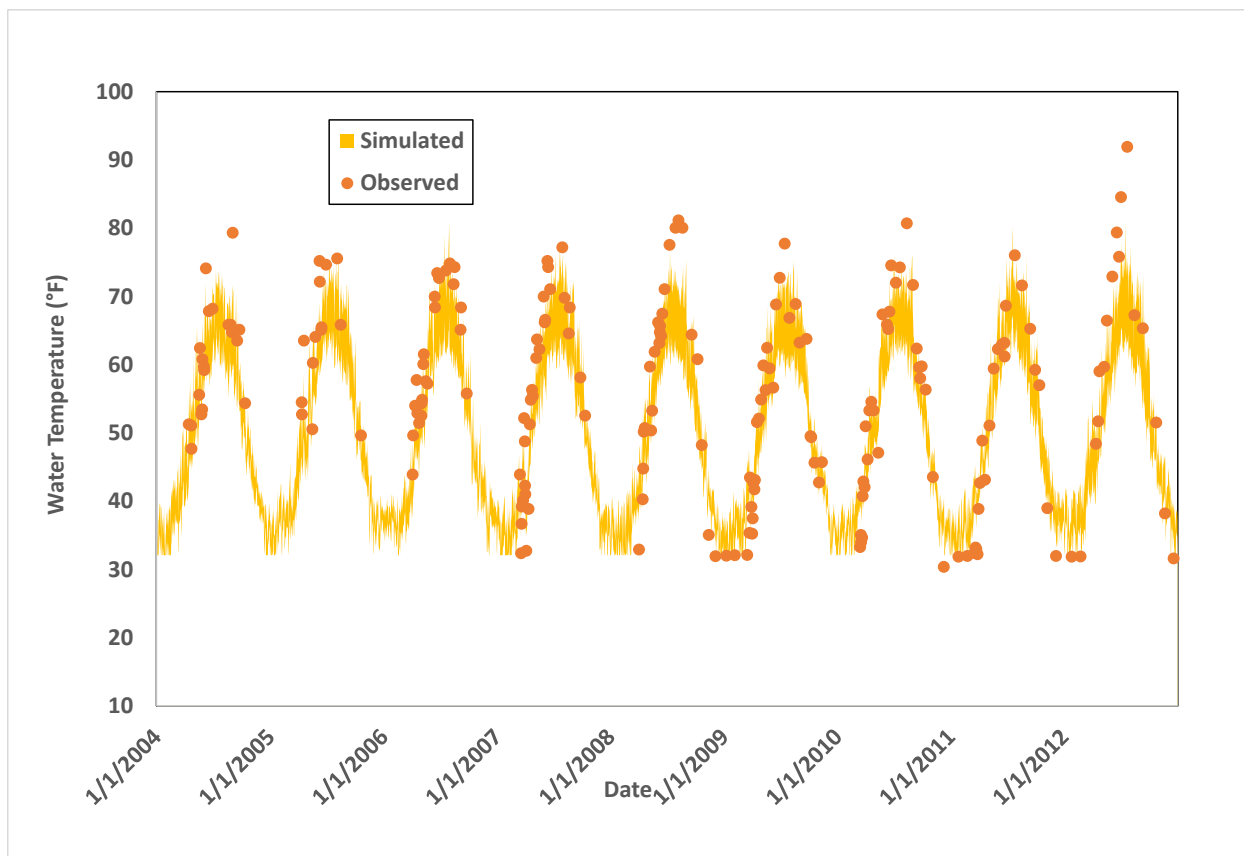


Figure 7-1. Time-series of Simulated Average Daily Water Temperature Compared to Point-in-time Measurements in Amity Creek

The current model predicts the general trend in water temperature in Amity Creek, but under-predicts point measurements during the summers of 2005 and 2006. These represent daytime temperatures on hot summer days that are elevated above the daily average. Detailed simulation of water temperature in this and other streams in the region would likely require a finer-scale model and a detailed analysis of shading. The basin-scale HSPF model could provide boundary conditions for such analyses of specific reaches of interest.

8 Algae and Dissolved Oxygen

The current development of the Lake Superior North and Lake Superior South watershed models does not focus on calibration for algae and dissolved oxygen (DO); however, these must be addressed because they interact with other processes that control nutrient kinetics. The influence of algae/macrophyte photosynthesis and respiration on DO means that DO and algae must be calibrated simultaneously.

8.1 ALGAE

Only very limited data are available on algae and macrophytes in flowing streams and wetlands of the Lake Superior South and Lake Superior North watersheds. Observations of chlorophyll *a*, the primary photosynthetic pigment in most algae, are available for many lakes and serve as an indicator of planktonic algae density – but do not provide information on benthic algae and macrophytes. However, many of the monitored lakes are of small size and not explicitly simulated in the basin-scale model. Given the relative paucity of information on algal density, model calibration focused on ensuring that planktonic chlorophyll *a* concentrations were in a reasonable range.

For the Lake Superior South and Lake Superior North watersheds, the lakes assessed with MINLEAP modeling by MPCA (MPCA, 2014 for Lake Superior South and a series of earlier, individual lake monitoring reports for Lake Superior North) had average observed (growing season) chlorophyll *a* concentrations ranging from 0.8 to 10 µg/L. While more data are available for lakes than streams, much of the available data do not cover the entire model simulation period (1993-2012). Chlorophyll *a* predictions in 24 explicitly simulated lakes in the Lake Superior South and North models are compared to growing season average concentrations for the simulation period contained in the EQUIS database or in earlier MINLEAP reports (for the Lake Superior North watershed) in Table 8-1. Given the small sample sizes, the model and observations are close to the expected range for most of the monitored lakes. The model under-predicts observations in some lakes which appear to be shallow headwater lakes with small drainage areas. The model also over-predicts observations in some, mostly deeper lakes. HSPF is a one-dimensional reach model that predicts the algal content of the entire water volume, whereas the observations are summer results near the surface. A different analytical tool that incorporates a two-dimensional analysis may be needed to interpret nutrient concentrations in these and other stratified lakes (see discussion in Section 9).

Table 8-1. Chlorophyll a Concentrations in Explicitly Simulated Lakes of the Lake Superior South and North Watersheds

Lake	Model Reach	Monitored Average and Range (1995-2012)	Simulated Seasonal Average and Range (1995-2012)
Wilson	180	3.6 (0.6 - 11.5)	2.9 (0.5 - 6)
Four Mile (Fourmile)	182	5.9 (1.2 - 15.4)	5 (1 - 9.2)
Crescent	196	5.6 (2.9 - 9.6)	4.9 (3 - 6.4)
White Pine*	201	8 (4 - 12)	0.1 (0.1 - 0.3)
Clara	202	3.8 (1.9 - 7.5)	0.1 (0.1 - 3.3)
Tait	203	3.7 (1.4 - 6.8)	3.3 (0.7 - 5.8)
Caribou	206	7.3 (1 - 32)	5.5 (2.3 - 9.8)
Pike	208	1.9 (1 - 4)	2.2 (1.3 - 3.6)
Deer Yard	212	4.7 (1 - 23)	4 (1.3 - 10.7)
Cascade*	216	4 (3 - 5)	3.6 (1.3 - 10.1)
Devil Track	220	3.7 (1 - 7.6)	2.6 (0.8 - 7.5)
Elbow	224	5.7 (2 - 11)	0.1 (0.1 - 1.6)
Trout	229	1.5 (0.4 - 4.4)	1.9 (0.7 - 3.5)
Northern Light	233	1.1 (0.6 - 1.8)	0.3 (0.1 - 7)
Poplar	243	3.6 (1 - 6)	2.6 (0.3 - 4.9)
Greenwood	247	2.3 (1 - 4.7)	1.9 (1 - 3.9)
Tom	261	4.3 (2 - 6)	3.3 (2 - 6.5)
Devilfish*	263	5.5 (3 - 10)	3.4 (1.4 - 7)
East Bearskin	271	3.4 (2 - 6)	2.9 (0.3 - 4)
Flour	274	2.1 (0.6 - 4)	2.7 (0.6 - 8)
Clearwater	277	1.5 (0.3 - 5)	1.3 (0.7 - 2.3)
Bearskin	284	1.9 (0.6 - 3.8)	2.6 (0.2 - 6.1)
Hungry Jack	285	2.3 (1 - 5)	2.1 (0.2 - 8.6)
Lax	158	6.8 (2.3 - 10.3)	2.1 (0.1 - 9.5)

* Observed data available for 2013 only.

8.2 DISSOLVED OXYGEN

Simulation of DO in waterbodies depends on a complex interaction between reaeration, algal production and respiration, and BOD (Figure 8-1). Many of these processes also affect nutrient balances, so the DO calibration must be achieved consistent with the nutrient calibration. The oxygen balance is also strongly dependent on water temperature simulation, which affects reaction rates and determines the saturation DO concentration.

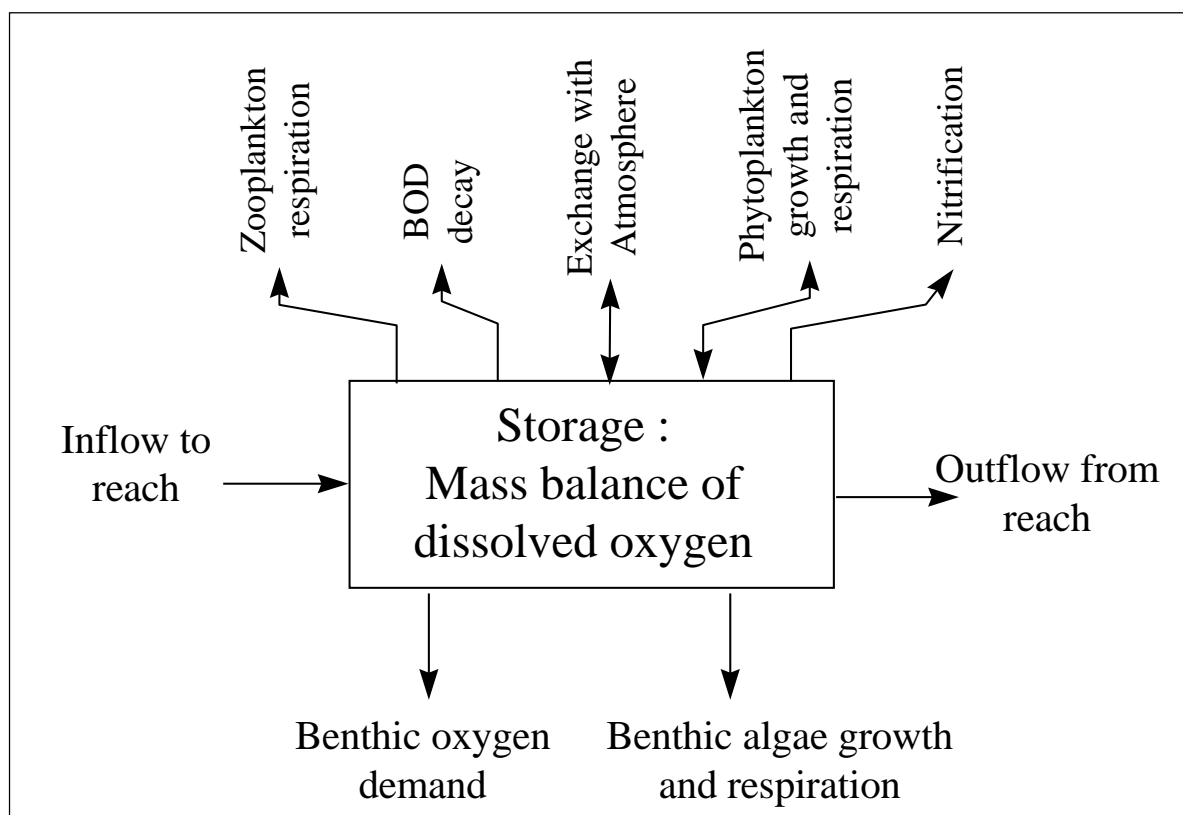


Figure 8-1. Process Diagram for Oxygen Mass Balance in HSPF

The impact of plant photosynthesis/respiration and diel cycles of water temperature on DO result in a situation where grab sample measures of DO are not very informative for model calibration. Many of the components of the oxygen mass balance in the Lake Superior South and North watersheds have little or no available monitoring data. Specifically, there are no known monitoring data for reaeration rates, benthic oxygen demand, or benthic algal or zooplankton densities. As noted in Section 8.1, monitoring for planktonic algae in streams is very limited. While biochemical oxygen demand (BOD) data exist for many locations, the majority of observations are for 5-day total BOD, whereas HSPF uses ultimate carbonaceous BOD. Total BOD includes the nitrogenous component and may also be affected by the presence of reduced iron. As a result, the model parameters must be specified based on best professional judgment and experience with other, similar sites. The model can then be tested on its ability to reproduce observed DO concentrations.

Reaeration: When oxygen concentrations are reduced below saturation, oxygen tends to move from the atmosphere to the water, a process known as reaeration. The rapidity of reaeration depends on how well the water is mixed and the turbulence present at the water surface. HSPF provides several options for

simulating stream reaeration. For the watershed models the Tsivoglou energy dissipation method (Tsivoglou and Wallace, 1972) is used (with default parameters) for stream segments, while reaeration in lake segments is a function of wind speed and surface area (Bicknell et al., 2014).

Biochemical Oxygen Demand: HSPF simulates nitrogenous and carbonaceous components of biochemical oxygen demand separately, with the nitrogenous component being determined by concentrations of reduced inorganic nitrogen species (ammonium and nitrite). Carbonaceous biochemical oxygen demand (CBOD) loading from the watershed is simulated as the labile fraction of total organic carbon, as described in Section 6.1. As the decay of CBOD results in the conversion of labile organic matter to inorganic nutrients, the representation of CBOD is largely constrained by the nutrient calibration.

The CBOD decay rate (k_d) is expected to be relatively low due both to the nature of organic carbon derived from forest and wetland vegetation, except immediately downstream of point sources. A k_d value of 0.0035 per hour (0.084 per day) appears to provide reasonable results. This is near the low end of the range of values reported nationally for streams without untreated waste input (USEPA, 1997).

Benthic Interactions. Organic soils and sediment associated with northern wetlands affect the oxygen balance. These may both release BOD into the stream and exert a sediment oxygen demand (SOD) at the sediment-water interface. No direct measurements of SOD were identified, and these components are at this time a calibration adjustment factor. Note that in parts of the watershed the oxidation of reduced iron or sulfide could exert a significant oxygen demand. As HSPF does not explicitly address these components in the oxygen balance they are treated as part of the SOD.

Algal Dynamics: The activities of floating (planktonic) and attached (benthic) algae also affect the oxygen balance in streams. Algae produce oxygen as a byproduct of photosynthesis during sunlight hours, but are net consumers of oxygen through respiration at night. Algae can also die off, contributing to the biochemical oxygen demand.

Calibration for dissolved oxygen presents some of the same challenges as the temperature calibration as there is likely to be significant diel variability due to the influence of algal photosynthesis and respiration that limits the information value of scattered grab samples. There may also be significant spatial variability at scales smaller than the reaches in the basin-scale model due to local changes in light availability, substrate composition, and reaeration capacity.

Continuous timeseries of DO observations coincident with the modeling time period were not identified for streams in the Lake Superior South and Lake Superior North watersheds. As a result, calibration checks for DO consisted of ensuring that simulated time-series followed the trends in the observed grab sampling data. An example time-series plot for Amity Creek at Duluth is shown in Figure 8-2. As with temperature, summer grab samples show DO concentrations higher than simulated daily averages. This reflects the influence of daytime photosynthesis, which can result in supersaturation of DO in the water column.

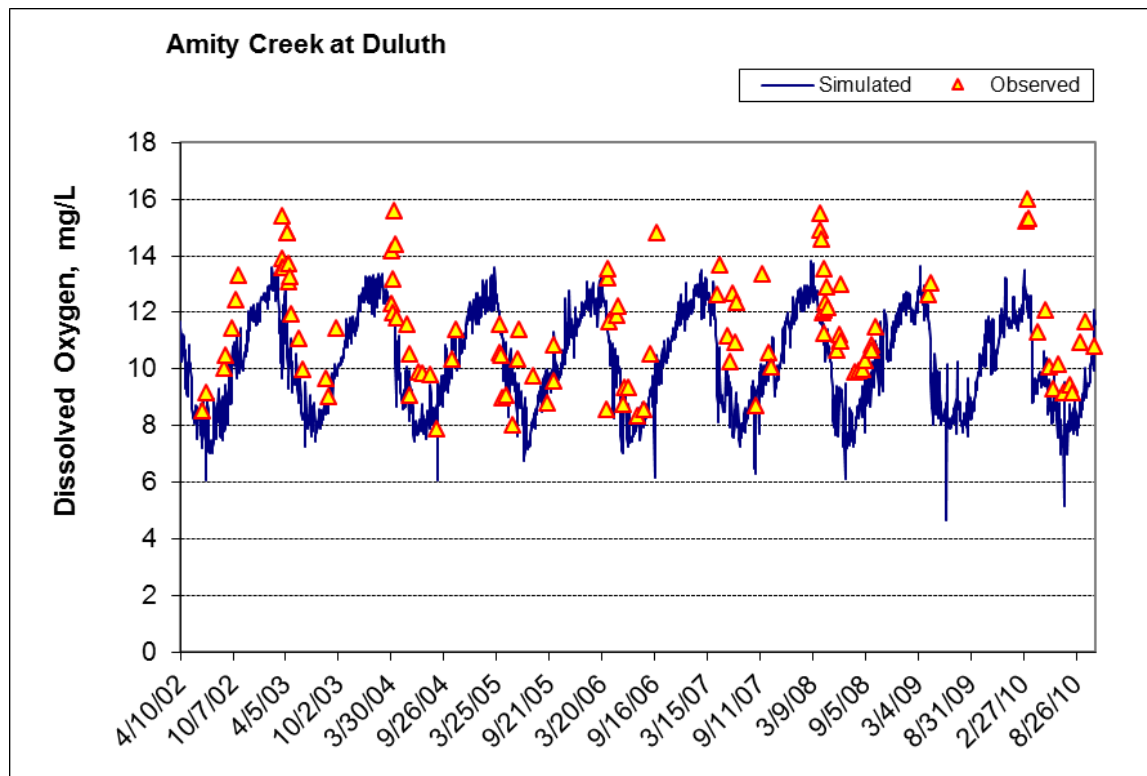


Figure 8-2. Time-series plot of simulated average daily DO versus observed for Amity Creek

(This page left intentionally blank.)

9 Potential Model Enhancements

The model calibration results presented in this report are based on simulations and comparisons to observed data through the end of 2012. Data collection in the watershed has continued and intensified since 2012, especially in the Lake Superior South watershed. Some streams that lack observed data within the modeling time-frame have subsequently had monitoring data collected, as well as detailed stressor identification surveys. Extension of the models past 2012 could make use of these newer data and would likely result in adjustments and improvements to the model calibration. Some additional refinements to model segmentation may be needed to make full use of data collected on smaller tributaries or at locations in the stream network not currently demarcated in the model.

One area of hydrology to which additional attention may be needed is the representation of wetlands. For instance, the wetland complex in the headwaters of the Knife and Sucker rivers has a significant impact on the simulated streamflow downstream, and seasonal variations in wetland hydrology due to winter ice damming and summer vegetation growth may have important consequences. In the current models, seasonal changes in water storage in wetlands are implemented through the use of seasonally variable upper soil zone storage capacities. Other approaches to wetland simulation, such as specification of large wetlands as reaches (rather than upland land uses) or use of pervious land FTables to describe storage discharge relationships should be evaluated to improve the seasonal behavior of wetlands in the models. Scant monitoring is available for direct evaluation of the representation of wetland hydrology in these watersheds at this time. Targeted data collection on selected large wetlands could greatly improve our understanding of this aspect of basin hydrology.

For model hydraulics, further analysis of channel cross sections and road culverts and, possibly, development of full hydraulic models for streams of high interest, would improve the simulation of the hydrograph shape. Such refinements would primarily affect the simulation of the high flow conditions that have an important impact on sediment processes. Additional FTable development could be pursued using culvert information on county road crossings (e.g., Beaster and Andersen, 2009). Changes in stream channel geometry caused by the 2012 floods should also be evaluated in more detail. The geomorphic classifications of stream types developed for the Duluth area (Fitzpatrick et al., 2006) may be useful in this process.

Elevated suspended sediment concentrations and turbidity are a concern in a number of the streams in the Lake Superior North and Lake Superior South watersheds. Accurate quantification of sediment loading sources is of high importance for developing implementation options and would benefit from additional detailed study. Work has already been done on the Knife River, Amity Creek, and Poplar River watersheds to this end, and has been used as a guide to configure the sediment component of the HSPF models. More such studies in other streams that are prone to problems associated with sediment will be helpful to refine the model further. Radiometric studies have been used in other Minnesota watersheds to constrain the fraction of instream sediment load derived from upland sources. Such data are not currently available for the Lake Superior North and Lake Superior South, watersheds, but could be used to refine the models further if they become available in the future.

Eroding bluffs have been identified as a major source of sediment in several of the Lake Superior North and South streams. Loadings from bluffs in the watershed models are currently specified using a constant rate of replenishment to the bed sediment storage in affected streams and are based on high risk erosion areas identified in a GIS dataset of bluffs. In addition to the high risk erosion areas the dataset also has a full coverage of bluff areas. It may be useful to refine the model to represent bluffs as a separate land use type that has its own hydrologic characteristics and is subject to surface gully erosion in addition to bluff collapse.

Simulation of nutrient balances and algal concentrations in most lakes appears reasonable, although monitoring data are limited in many cases. There are, however, limitations to the ability of HSPF to simulate lake processes as HSPF represents waterbodies as one-dimensional, fully mixed reactors. This makes HSPF a useful tool for representation of nutrient balances in fully mixed lakes; however, the effects of stratification of the water column cannot be directly represented in the model. This suggests that an optimal approach for evaluating eutrophication issues in lakes in the Lake Superior North and Lake Superior South watersheds would be to link the HSPF watershed model to lake models that are better able to represent these processes. A wide variety of lake models exist, at varying levels of complexity. For some stratified lakes of high importance, use of a complex two-dimensional lake model with a short time step (such as the USACE-supported CE-QUAL-W2) model may be appropriate. However, a complex modeling approach is likely to be infeasible for all of the lakes present in the watershed – yet some representation of seasonal mixing in each stratifying lake is desirable to represent seasonal mixing processes. One more parsimonious and less expensive alternative would be to use a simple model such as BATHTUB (Walker, 1996) to estimate the seasonal average distribution of nutrients and algae in surface and bottom waters, driven by the cumulative loads estimated by HSPF. In addition to providing a tool to evaluate conditions within individual lakes, the BATHTUB results could be used to constrain the reasonable range of concentrations of nutrients and algae in the outflow from each lake in the basin-scale HSPF model.

Summer water temperatures and dissolved oxygen conditions are an important concern in the streams that support cold water and high quality fisheries in this region. The current model development includes limited calibration to water temperature, primarily to assure that temperatures are in the correct range; this calibration could be extended and improved. While limited continuous water temperature data are available for some of the streams represented in the models, these continuous data have not yet been used in detailed calibration of water temperature in the models. In addition, there were no available continuous dissolved oxygen measurement during the model time period. As discussed in Section 7, the basin scale watershed models aggregate stream reaches into segments in the range of 3 to 15 miles in length, and variations within the segment are averaged out. In contrast, continuous temperature monitoring addresses water temperature at a single, discrete location that is affected by local riparian cover, topographic shading, and the orientation or aspect of the stream segment relative to the position of the sun, all of which have strong impacts on energy inputs and exchanges over the course of a day, so the HSPF model is best suited to produce daily averages over a whole stream length, not hourly patterns at a specific cross section. A detailed examination of temperature and dissolved oxygen (e.g., for TMDL development) would best be served through the development of finer-scale models for reaches of interest, using a tool such as the QUAL2K model. The basin-scale HSPF model can be used to provide boundary conditions for a detailed model of this type.

10 References

- AQUA TERRA. 2012. Modeling Guidance for BASINS/HSPF Applications under the MPCA One Water Program. Prepared for Minnesota Pollution Control Agency by AQUA TERRA Consultants, Mountain View, CA.
- Beaster, T., and K. Anderson. 2009. Inventory and Assessment of Coastal Zone Stream Crossings on County Roads in Cook County, Minnesota. Cook County Soil and Water Conservation District.
- Bicknell, B.R., J.C. Imhoff, J.L. Kittle, Jr., T.H. Jobes, P.B. Duda, and A.S. Donigian, Jr. 2014. HSPF Version 12.4 User's Manual. National Exposure Research Laboratory, Office of Research and Development, U.S. Environmental Protection Agency, Athens, GA.
- Carroll, T., D. Cline, G. Fall, A. Nilsson, L. Li, and A. Rost. 2001. *NOHRSC Operations and the Simulation of Snow Cover Properties for the Conterminous U.S.* Proceedings of the 69th Annual Meeting of the Western Snow Conference, pp. 1-14.
- Donigian, A.S., J.C. Imhoff, B.R. Bicknell, and J.L. Kittle. 1984. Application Guide for the Hydrologic Simulation Program - FORTRAN. EPA 600/3-84-066. U.S. Environmental Protection Agency, Athens, GA.
- Clesceri, N.L., S.J. Curran, and R.I. Sedlak. 1986. Nutrient loads to Wisconsin lakes: Part I. Nitrogen and phosphorus export coefficients. *Water Resources Bulletin*, 22(6), 983-989.
- Davis, R.F. 1997. Comparison of modeled to observed global irradiance. *Journal of Applied Meteorology*, 35: 192-201.
- Dodd, R., G. McMahon, and S. Stichter. 1992. Watershed Planning in the Albemarle-Pamlico Estuarine System: Report 1 – Annual Average Nutrient Budgets. Report 92-10, U.S. Environmental Protection Agency, Center for Environmental Analysis, Raleigh, NC.
- Donigian, A.S. Jr. 2000. *HSPF Training Workshop Handbook and CD*. Lecture #19. Calibration and Verification Issues, Slide #L19-22. U.S. Environmental Protection Agency, Washington Information Center, January 10–14, 2000. Presented to and prepared for U.S. Environmental Protection Agency, Office of Water, Office of Science and Technology, Washington, DC.
- Donigian, A.S., Jr., J.C. Imhoff, B.R. Bicknell, and J.L. Kittle, Jr. 1984. Application Guide for Hydrological Simulation Program – FORTRAN (HSPF). EPA-600/3-84-965. U.S. Environmental Protection Agency, Environmental Research Laboratory, Athens, GA.
- Donigian, A.S. Jr., and J.T. Love. 2003. Sediment Calibration Procedures and Guidelines for Watershed Modeling. Presented at the Water Environment Federation Total Maximum Daily Load Conference, November 16–19, 2003, Chicago, IL.
- Duda, P.B., P.R. Hummel, A.S. Donigian, Jr., and J.C. Imhoff. 2012. BASINS/HSPF: Model use, calibration, and validation. *Transactions of the ASABE*, 55(4): 1523-1547.
- Ellison, C.A., B.E. Savage, and G.D. Johnson. 2014. Suspended-Sediment Concentrations, Loads, Total Suspended Solids, Turbidity, and Particle-Size Fractions for Selected Rivers in Minnesota, 2007 through 2011. Scientific Investigations Report 2013–5205. U.S. Geological Survey, Reston, VA. <http://dx.doi.org/10.3133/sir20135205>.
- Fitzpatrick, F.A., M.C. Peppler, M.M. DePhilip, and K.E. Lee. 2006. Geomorphic Characteristics and Classification of Duluth-Area Streams, Minnesota. Scientific Investigations Report 2006–5029. U.S. Geological Survey.
- Green, J.C. 1996. Geology on Display: Geology and Scenery of Minnesota's North Shore State Parks. Minnesota Department of Natural Resources, St. Paul, MN.

- Hardy, T. P. Panja, and D. Mathias. 2005. WinXSPRO, A Channel Cross-Section Analyzer, User's Manual, Version 3.0. Gen. Tech. Rep. RMRS-GTR-147. USDA Forest Service Rocky Mountain Research Station, Stream Systems Technology Center, Fort Collins, CO.
http://www.fs.fed.us/rm/pubs/rmrs_gtr147.pdf.
- Hollister, J., and W.B. Milstead. 2010. Using GIS to estimate lake volume from limited data. *Lake and Reservoir Management*, 26(3): 194-199.
- Hummel, P., J. Kittle Jr., and M. Gray. 2001. WDMUtil Version 2.0, A Tool for Managing Watershed Modeling Time-Series Data, User's Manual. Prepared for U.S. Environmental Protection Agency by AQUA TERRA Consultants, Decatur, GA.
- Johnson, S., and K. Belanger. 2007. *Minnesota Waterfalls*. Trails Books. Madison, WI.
- LANDFIRE. 2013. LANDFIRE Existing Vegetation Type Layer. U.S. Department of Interior, Geological Survey. <http://landfire.cr.usgs.gov/viewer>, accessed 12/2014.
- Loehr, R. C., S.O. Ryding, and W.C. Sonzogni. 1989. Estimating the nutrient load to a waterbody. *The Control of Eutrophication of Lakes and Reservoirs, Volume I, Man and the Biosphere Series*, S. O. Ryding and W. Rast, ed., Parthenon Publishing Group, 115-146.
- Lumb, A.M., R.B. McCammon, and J.L. Kittle, Jr. 1994. User's Manual for an Expert System (HSPEXP) for Calibration of the Hydrological Simulation Program – FORTRAN. Water-Resources Investigation Report 94-4168. U.S. Geological Survey, Reston, VA.
- Magner, J.A., and K.N. Brooks. 2008. Predicting stream channel erosion in the lacustrine core of the upper Nemadji River, Minnesota (USA) using stream geomorphology metrics. *Environmental Geology*, 54:1424-1434, doi:10.1007/s00254-007-0923-3.
- Mahrt, L., and M. Ek. 1984. The Influence of atmospheric stability on potential evapotranspiration. *Journal of Climate and Applied Meteorology*, 23: 222-234.
- McCuen, R.H., Z. Knight, and A.G. Cutter. 2006. Evaluation of the Nash-Sutcliffe efficiency index. *Journal of Hydrologic Engineering*, 11(6): 597-602.
- McFarland, A. M. S., and Hauck, L. M. 2001. Determining nutrient export coefficients and source loading uncertainty using in stream monitoring data. *Journal of the American Water Resources Association*, 37(1), 223-236.
- Mesinger, F. et al. 2006. North American regional reanalysis. *Bulletin of the American Meteorological Society*, doi:10.1175:BAMS-87-3-343.
- Minnesota Department of Natural Resources (MNDNR). 2002. Lake Bathymetric Contours, Ecological Services and Fisheries Divisions. <http://deli.dnr.state.mn.us/>, accessed 1/29/2015.
- Minnesota Pollution Control Agency (MPCA). 2004a. Detailed Assessment of Phosphorus Sources to Minnesota Watersheds. Minnesota Pollution Control Agency, St. Paul, MN.
- Minnesota Pollution Control Agency (MPCA). 2004b. Citizen Lake-Monitoring Program (CLMP+): Advanced Volunteer Lake Monitoring in Cook County. Minnesota Pollution Control Agency, St. Paul, MN.
- Minnesota Pollution Control Agency (MPCA). 2005. Minnesota Lake Water Quality Assessment Report: Developing Nutrient Criteria (Third Edition). Minnesota Pollution Control Agency, St. Paul, MN.
- Minnesota Pollution Control Agency (MPCA). 2011. Sentinel Lake Assessment Report, Trout Lake (16-0049), Cook County, Minnesota. Minnesota Pollution Control Agency, St. Paul, MN.

- Minnesota Pollution Control Agency (MPCA). 2013. Nitrogen in Minnesota Surface Waters: Conditions, Trends, Sources, and Reductions. Minnesota Pollution Control Agency, St. Paul, MN.
- Minnesota Pollution Control Agency (MPCA). 2014. Lake Superior – South Watershed Monitoring and Assessment Report. Minnesota Pollution Control Agency, St. Paul, MN.
- Moriasi, D.N., J.G. Arnold, M.W. Van Liew, R.L. Bingner, R.D. Harmel, and T.L. Veith. 2007. Model evaluation guidelines for systematic quantification of accuracy in watershed simulations. *Transactions of the ASABE*, 50(3): 885-900.
- MRLC. 2011. National Land Cover Database. Multi-Resolution Land Characteristics. <http://www.mrlc.gov/about.php>, accessed 1/2015.
- Mu, Q., M. Zhao, and S.W. Running. 2011. Improvements to a MODIS global terrestrial evapotranspiration algorithm. *Remote Sensing of Environment*, 115:1781-1800.
- Nash, J. E., and J. V. Sutcliffe. 1970. River flow forecasting through conceptual models: Part 1: A discussion of principles. *Journal of Hydrology*, 10(3): 282-290.
- Neitzel, G.D. 2014. Monitoring Event-Scale Bluff Erosion with Repeat Terrestrial Laser Scanning, Amity Creek, Duluth, MN. A thesis submitted to the faculty of the graduate school of the University of Minnesota in partial fulfillment of the requirements for the degree of Master of Science. http://conservancy.umn.edu/bitstream/handle/11299/163326/Neitzel_umn_0130M_14795.pdf.
- Nieber, J.L., B.N. Wilson, J.S. Ulrich, B.J. Hansen, and D.J. Canelon. 2008. Assessment of Streambank and Bluff Erosion in the Knife River Watershed. Report to Minnesota Pollution Control Agency. Dept. of Bioproducts and Biosystems Engineering, University of Minnesota, St. Paul, MN. <http://www.lakesuperiorstreams.org/archives/knife/assessment%20of%20streambank%20and%20bluff%20erosion%20in%20the%20knife%20river%20watershed.pdf>.
- Packer, P. E. 1967. Forest Treatment Effects on Water Quality. In *Forest Hydrology*, eds. W. E. Sopper and H. W. Lull. Pergamon Press, New York.
- Penman, H.L. 1948. Natural evaporation from open water, bare soil, and grass. *Proc. Royal Society of London A*, 193:120-146.
- Reckhow, K.H., M.N. Beaulac, and J.T. Simpson. 1980. Modeling Phosphorus Loading and Lake Response under Uncertainty: A Manual and Compilation of Export Coefficients. EPA-440/5-80-011. Office of Water Regulations, Criteria and Standards Division, U.S. Environmental Protection Agency, Washington, DC.
- Sanford, W.E, and D.L. Selnick. 2013. Estimation of evapotranspiration across the conterminous United States using a regression with climate and land-cover data. *Journal of the American Water Resources Association*, 49(1): 217-230.
- Schall, J.D., P.L. Thompson, S.M. Zerges, R.T. Kilgore, and J.L. Morris. 2012. Hydraulic Design of Highway Culverts, Third Edition. Hydraulic Design Series # 5, FHWA-NHI-12-029. Federal Highway Administration, Washington, DC.
- Tetra Tech. 2009. Minnesota River Basin Turbidity TMDL and Lake Pepin Excessive Nutrient TMDL: Model Calibration and Validation Report. Prepared for Minnesota Pollution Control Agency by Tetra Tech, Inc., Research Triangle Park, NC.
- Tsivoglou, E.C., and J.R. Wallace. 1972. Characterization of Stream Reaeration Capacity. EPA-R3-72-012. U.S. Environmental Protection Agency, Washington, DC.

- Twaroski, C., N. Czoschke, and T. Anderson. 2007. Detailed Assessment of Phosphorus Sources to Minnesota Watersheds – Atmospheric Deposition: 2007 Update. Prepared for Minnesota Pollution Control Agency by Barr Engineering, Minneapolis, MN.
- USEPA. 1997. Technical Guidance Manual for Developing Total Maximum Daily Loads, Book II: Streams and Rivers, Part 1: Biochemical Oxygen Demand / Dissolved Oxygen and Nutrients / Eutrophication. EPA 823-B-97-002. Office of Science and Technology, U.S. Environmental Protection Agency, Washington, DC.
- USEPA. 2000. Estimating Hydrology and Hydraulic Parameters for HSPF. BASINS Technical Note 6, EPA-823-R00-012. Office of Water, U.S. Environmental Protection Agency, Washington, DC.
- USEPA. 2006. BASINS Technical Note 8: Sediment Parameter and Calibration Guidance for HSPF. Office of Water, U.S. Environmental Protection Agency, Washington, DC.
- USEPA. 2007. Two Automated Methods for Creating Hydraulic Function Tables (FTABLES). BASINS Technical Note 2. Office of Water, U.S. Environmental Protection Agency, Washington, DC.
- USEPA. 2008. Using the BASINS Meteorological Database—Version 2006. BASINS Technical Note 10. Office of Water, U.S. Environmental Protection Agency, Washington, DC. Available online at http://water.epa.gov/scitech/datait/models/basins/upload/2009_04_13_BASINSs_tecnote10.pdf.
- Velpuri, N.M., G.B. Senay, R.K. Singh, S. Bohms, and J.P. Verdin. 2013. A comprehensive evaluation of two MODIS evapotranspiration products over the conterminous United States: Using point and gridded FLUXNET and water balance ET. *Remote Sensing of Environment*, 139: 35-49.
- Walker, W.W. 1996. Simplified Procedures for Eutrophication Assessment and Prediction: User Manual. Instruction Report W-96-2. U.S. Army Engineer Waterways Experiment Station, Vicksburg, MS.
- Wilson, C.B., and W.W. Walker, Jr. 1989. Development of lake assessment methods based upon the aquatic ecoregion concept. *Lake and Reservoir Management*, 5(2): 11-22.
- Xia, Y., K. Mitchell, M. Ek, J. Scheffeld, B. Cosgrove, E. Wood, L. Luo, C. Alonge, H. Wei, J. Meng, B. Livneh, D. Lettenmaier, V. Koren, Q. Duan, K. Mo, Y. Fan, and D. Mocko. 2012. Continental-scale water and energy flux analysis and validation for the North American Land Data Assimilation System Project Phase 2 (NLDAS-2). 1. Intercomparison and application of model products. *Journal of Geophysical Research*, 117, DO3109.